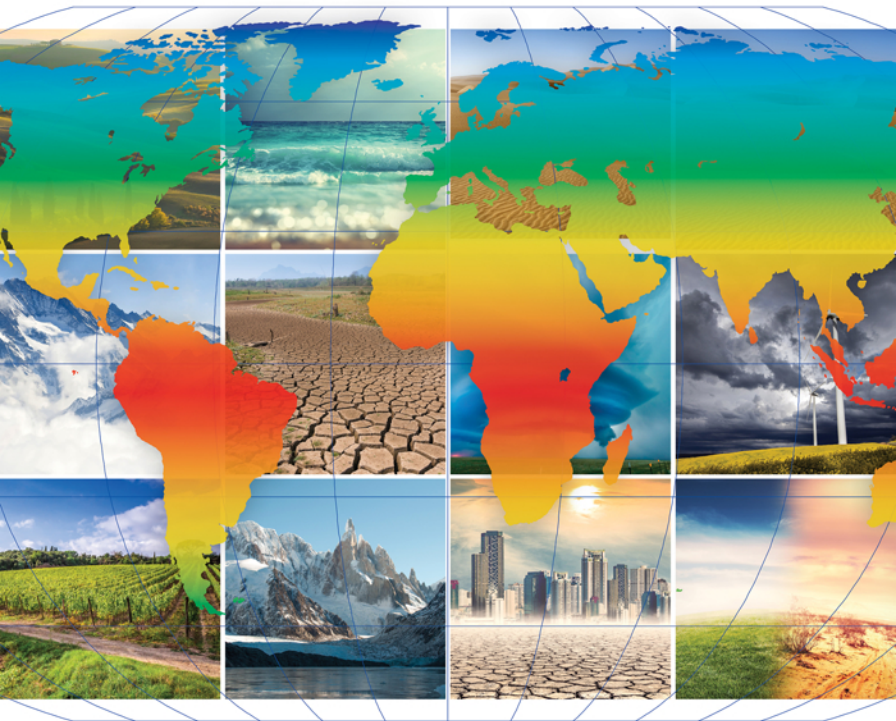


CLIMATOLOGY

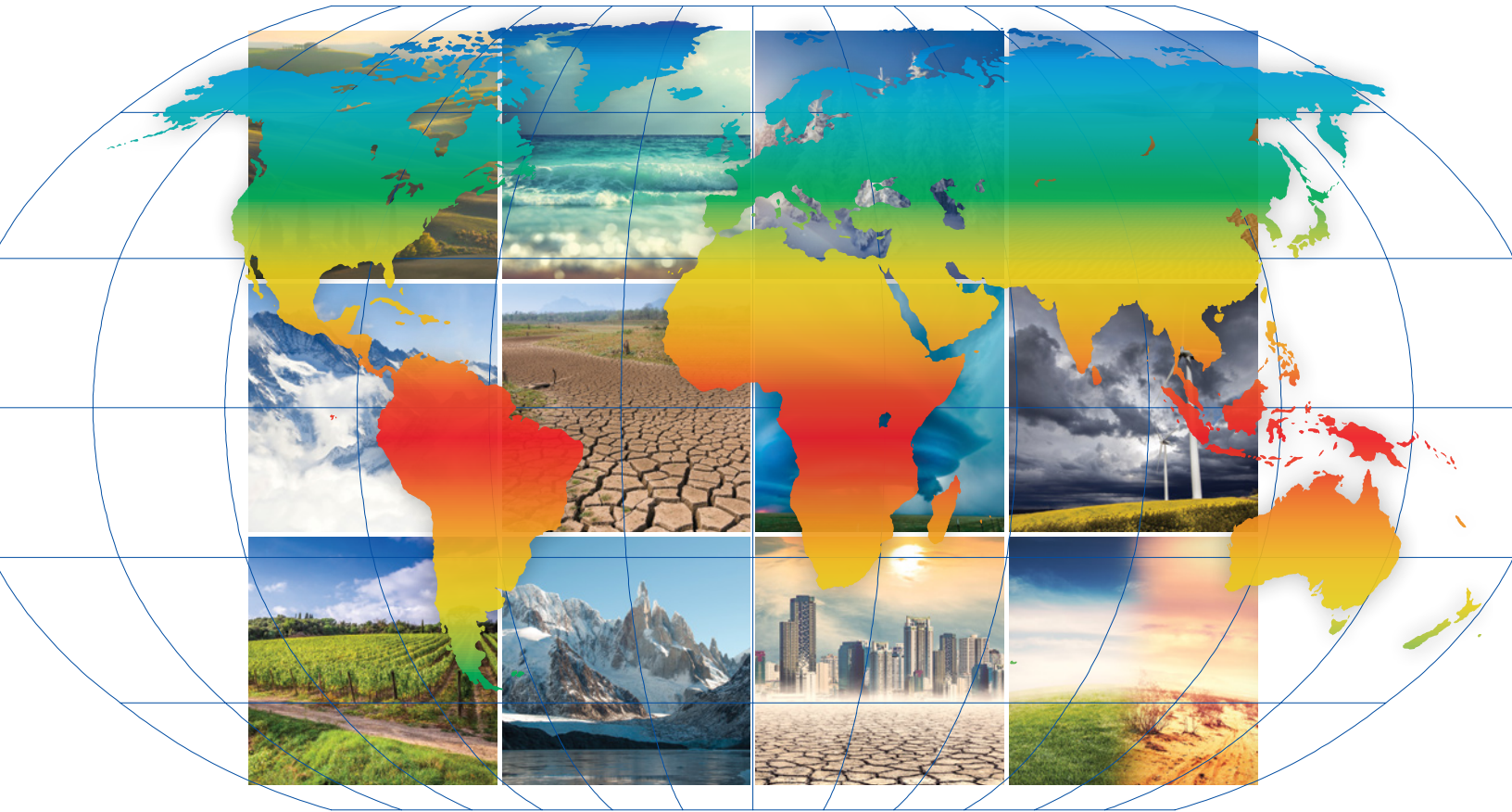
FOURTH EDITION



ROBERT V. ROHLI
ANTHONY J. VEGA

CLIMATOLOGY

FOURTH EDITION



ROBERT V. ROHLI

Louisiana State University

ANTHONY J. VEGA

Clarion University of Pennsylvania



JONES & BARTLETT
LEARNING



World Headquarters

Jones & Bartlett Learning
5 Wall Street
Burlington, MA 01803
978-443-5000
info@jblearning.com
www.jblearning.com

Jones & Bartlett Learning books and products are available through most bookstores and online booksellers. To contact Jones & Bartlett Learning directly, call 800-832-0034, fax 978-443-8000, or visit our website, www.jblearning.com.

Substantial discounts on bulk quantities of Jones & Bartlett Learning publications are available to corporations, professional associations, and other qualified organizations. For details and specific discount information, contact the special sales department at Jones & Bartlett Learning via the above contact information or send an email to specialsales@jblearning.com.

Copyright © 2018 by Jones & Bartlett Learning, LLC, an Ascend Learning Company

All rights reserved. No part of the material protected by this copyright may be reproduced or utilized in any form, electronic or mechanical, including photocopying, recording, or by any information storage and retrieval system, without written permission from the copyright owner.

The content, statements, views, and opinions herein are the sole expression of the respective authors and not that of Jones & Bartlett Learning, LLC. Reference herein to any specific commercial product, process, or service by trade name, trademark, manufacturer, or otherwise does not constitute or imply its endorsement or recommendation by Jones & Bartlett Learning, LLC and such reference shall not be used for advertising or product endorsement purposes. All trademarks displayed are the trademarks of the parties noted herein. *Climatology, Fourth Edition* is an independent publication and has not been authorized, sponsored, or otherwise approved by the owners of the trademarks or service marks referenced in this product.

There may be images in this book that feature models; these models do not necessarily endorse, represent, or participate in the activities represented in the images. Any screenshots in this product are for educational and instructive purposes only. Any individuals and scenarios featured in the case studies throughout this product may be real or fictitious, but are used for instructional purposes only.

12656-3

Production Credits

VP, Executive Publisher: David D. Cella
Executive Editor: Matthew Kane
Associate Editor: Audrey Schwinn
Editorial Assistant: Loren-Marie Durr
Senior Production Editor: Nancy Hitchcock
Marketing Manager: Lindsay White
Production Services Manager: Colleen Lamy

Manufacturing and Inventory Control Supervisor: Amy Bacus
Composition: S4Carlisle Publishing Services
Cover Design: Kristin E. Parker
Rights & Media Specialist: Meredith Tumas
Media Development Editor: Shannon Sheehan
Printing and Binding: LSC Communications
Cover Printing: LSC Communications

Cover Credits: Alps: © vichie81/Shutterstock; Tuscany: © Taiga/Shutterstock; Desert: © Denis Burdi/Shutterstock; Cityscape: © Mrs_ya/Shutterstock; Wind turbines: © Pablo Prat/Shutterstock; Ocean: © Iakov Kalinin/Shutterstock; Drought: © 24Novembers/Shutterstock; Snow-covered trees: © Creative Travel Projects/Shutterstock; Frozen lake: © Hugo Brizard – YouGoPhoto/Shutterstock; Global warming: © alphaspirt/Shutterstock; Vines in Tuscany: © Shaiith/Shutterstock; Tornado: © Minerva Studio/Shutterstock; Climate map: © freesoulproduction/Shutterstock.

Library of Congress Cataloging-in-Publication Data

Names: Rohli, Robert V. | Vega, Anthony J.
Title: *Climatology* / Robert V. Rohli, Louisiana State University, Anthony J. Vega, Clarion University of Pennsylvania.
Description: Fourth edition. | Burlington, Massachusetts : Jones & Bartlett Learning, [2018] | Includes index.
Identifiers: LCCN 2017010380 | ISBN 9781284126563
Subjects: LCSH: Climatology--Textbooks.
Classification: LCC QC981 .R649 2018 | DDC 551.5--dc23
LC record available at <https://lccn.loc.gov/2017010380>

6048

Printed in the United States of America

21 20 19 18 17 16 15 14 13 12 11 10 9 8 7 6 5 4 3 2 1



Brief Contents

PART 1	The Basics	1
	Chapter 1	Introduction to Climatology 3
	Chapter 2	Atmospheric Structure and Composition 11
PART 2	Climatological Processes	23
	Chapter 3	Controls on the Climate System 25
	Chapter 4	Atmospheric Interactions with the Other “Spheres” 53
	Chapter 5	Energy, Matter, and Momentum Exchanges near the Surface 79
	Chapter 6	Global Hydrologic Cycle and Surface Water Balance 107
	Chapter 7	General Circulation and Secondary Circulations 131
PART 3	Climates Across Space	155
	Chapter 8	Climatic Classification 157
	Chapter 9	Extratropical Northern Hemisphere Climates 179
	Chapter 10	Tropical and Southern Hemisphere Climates 229

PART 4	Climates Through Time	271
Chapter 11	Climatic Change and Variability: A Paleoclimatic Overview.....	273
Chapter 12	Modern Climatic Change.....	301
Chapter 13	Linking Spatial and Temporal Aspects of Climate Through Quantitative Methods	325
PART 5	Relationships Between Climate and Other Endeavors	345
Chapter 14	Applied Climatology, Climate Impacts, and Climatic Data.....	347
Chapter 15	Future of Climatology	365



Contents

Preface	ix
The Student Experience	x
Teaching Tools	xii
Acknowledgments	xiii

PART 1 The Basics **1**

Chapter 1 Introduction to Climatology **3**

Meteorology and Climatology	4
Scales in Climatology	6
Subfields of Climatology	6
Climatic Records and Statistics	7
Summary	9

Chapter 2 Atmospheric Structure and Composition **11**

Origin of the Earth and Atmosphere	12
Atmospheric Composition	13
Carbon Cycle	13
Constant and Variable Gases	15
Faint Young Sun Paradox	16
Atmospheric Structure	17
Summary	21

PART 2 Climatological Processes **23**

Chapter 3 Controls on the Climate System .. **25**

Latitude	26
Earth–Sun Relationships	28
Revolution	28
Rotation	28
Axial Tilt and Parallelism	28
Combined Effect of Revolution, Rotation, and Tilt ..	29
Distance to Large Bodies of Water	32
Circulation	33
Pressure	34
Wind	36

Surface Versus Upper-Level Winds	41
Vertical Motion	41
Cyclones and Anticyclones	42
Oceanic Circulation	44
Topography	46
Local Features	46
Putting It All Together: Spatial and Seasonal Variations in Energy	47
Summary	49

Chapter 4 Atmospheric Interactions with the Other “Spheres” **53**

Ocean Circulation	54
Surface Currents	54
Deep Ocean Thermohaline Circulations	57
El Niño–Southern Oscillation Events	59
Walker Circulation	60
Historical Observations of ENSO	62
El Niño Characteristics	63
La Niña Characteristics	64
Global Effects	65
Effects in the United States	67
Relationship to Global Warming	69
Climatic Feedbacks in the Ocean	69
Volcanic Activity and Climate	70
General Effects	70
Aerosol Indices	71
Deforestation and Desertification	71
Cryospheric Changes	73
Ice on the Earth’s Surface	73
Feedbacks in the Cryosphere	74
Summary	75

Chapter 5 Energy, Matter, and Momentum Exchanges near the Surface **79**

Properties of the Troposphere	80
Near-Surface Troposphere	80
Energy in the Climate System	81
Sun as Energy Source	81
Measuring Radiant Energy	87

Radiation Balance	90
Turbulent Fluxes	92
Substrate Heat Flux	92
Energy Balance	93
Local Flux of Matter: Moisture in the Local	
Atmosphere	93
Atmospheric Moisture	93
Moisture in the Surface Boundary Layer	95
Measuring Evapotranspiration	96
Atmospheric Statics, the Hydrostatic	
Equation, and Stability	97
Statics and the Hydrostatic Equation	97
Atmospheric Stability	98
Assessing Stability in the Local Atmosphere	99
Momentum Flux	102
Putting It All Together: Thermal and Mechanical	
Turbulence and the Richardson Number	102
Summary	104

Chapter 6 Global Hydrologic Cycle and Surface Water Balance 107

Global Hydrologic Cycle	108
Surface Water Balance	110
Potential Evapotranspiration	111
Evapotranspiration	114
Precipitation	114
Soil Moisture Storage	121
Deficit	122
Surplus and Runoff	122
Putting It All Together: A Worked Example	
of the Surface Water Balance	124
Types of Surface Water Balance Models	125
Water Balance Diagrams	126
Drought Indices	126
Summary	128

Chapter 7 General Circulation and Secondary Circulations 131

Circulation of a Nonrotating Earth	132
Idealized General Circulation on a Rotating Planet ..	133
Hadley Cells	133
Polar Cells	134
Planetary Wind Systems	134
Modifications to the Idealized General Circulation:	
Observed Surface Patterns	137
Land–Water Contrasts	137
Locations and Strength of Features	
in the Hadley Cells	138
Locations and Strength of Features	
in the Polar Cells	139

Locations and Strength of Surface	
Midlatitude Features	141
Putting It All Together: Surface Pressure	
Patterns and Impacts	141
Modifications to the Idealized General Circulation:	
Upper-Level Airflow and Secondary Circulations ..	142
Vorticity	143
Constant Absolute Vorticity Trajectory	145
Flow Over Mountainous Terrain	146
Baroclinicity	147
Rossby Wave Divergence and Convergence	147
Rossby Wave Diffluence and Confluence	148
Polar Front Jet Stream	149
Mean Patterns of Rossby Wave Flow	151
Summary	153

PART 3 Climates Across Space 155

Chapter 8 Climatic Classification 157

Early Attempts at Global Climatic Classification ..	158
Classical Age of Climatic Classifications	159
Modified Köppen Climatic Classification System ..	159
Thornthwaite Climatic Classification System	164
Other Global Classification Systems	166
Genetic Classifications	167
Air Masses and Fronts	169
Classification of Fronts	171
Local and Regional Classifications	173
Quantitative Analysis to Derive Climatic Types ..	174
Eigenvector Analysis	174
Cluster Analysis	175
Hybrid Techniques	176
Summary	176

Chapter 9 Extratropical Northern Hemisphere Climates 179

Climatic Setting of North America	180
General Characteristics	180
Severe Weather	180
Role of the Gulf of Mexico and the	
Low-Level Jet	182
Effect of Mountain Ranges	182
Effect of the Great Lakes	183
Ocean Currents and Land–Water Contrast	184
Climatic Setting of Europe	185
General Characteristics	185
Effect of Ocean Currents	185
Effect of Mountain Ranges	186
Blocking Anticyclones	186

Climatic Setting of Asia	187
General Characteristics	187
Monsoonal Effects	187
Effect of Mountain Ranges	188
Effect of Coastal Zones on Climate	189
Regional Climatology	189
B—Arid Climates	189
C—Mesothermal Climates	198
D—Microthermal Midlatitude Climates	211
E—Polar Climates	222
H—Highland Climates	223
Summary	224

Chapter 10 Tropical and Southern Hemisphere Climates 229

Contrasts Between Extratropical and Tropical Atmospheric Behavior	230
Contrasts Between Northern and Southern Hemisphere Atmospheric Behavior	230
Climatic Setting of Africa	231
General Characteristics	231
Intertropical Convergence Zone	231
Air Mass and General Circulation Influences	232
Indian Ocean Dipole	234
Climatic Setting of Australia and Oceania	234
General Characteristics	235
El Niño–Southern Oscillation Influences	235
South Pacific Convergence Zone	236
Madden-Julian Oscillation	237
Quasi-Biennial Oscillation	238
Climatic Setting of Latin America	238
ENSO Contributions	239
Climatic Setting of Antarctica	240
Regional Climates	242
A—Tropical Climates	242
B—Arid Climates	253
C—Mesothermal Climates	256
E—Polar Climates	262
H—Highland Climates	265
Summary	267

PART 4 Climates Through Time 271

Chapter 11 Climatic Change and Variability: A Paleoclimatic Overview 273

Climatic Changes in Geological History	276
Temperature	276
Ice Ages and Sea Level	280
Recent Trends	280

How Do We Know What We Know About Past Climatic Changes?	283
Basic Principles	283
Radiometric Dating	284
Lithospheric and Cryospheric Evidence	285
Biological Evidence	288
Historical Data	289
Converging Proxy Evidence	290
Natural Causes of Climatic Change and Variability	290
Continental Drift and Landforms	290
Milankovitch Cycles	291
Volcanic Activity	293
Variations in Solar Output	294
El Niño–Southern Oscillation Events	296
Summary	297

Chapter 12 Modern Climatic Change 301

Global Warming	302
Greenhouse Effect	302
Greenhouse Gases	302
Urban Heat Island	307
Direct and Indirect Effects of Global Warming	309
Global Warming: The Great Debate	309
Atmospheric Pollution	312
Global Dimming	313
Atmospheric Factors Affecting Pollution Concentrations	313
Air Quality Legislation in the United States	314
Classifying Air Pollutants	314
By Response	314
By Source	315
Reactions and Attitudes to Climatic Change	319
Prevention	319
Mitigation	319
Adaptation	320
Continued Research	320
Summary	320

Chapter 13 Linking Spatial and Temporal Aspects of Climate Through Quantitative Methods 325

Computerized Climate Models	326
Types of GCMs	327
Representing the Earth–Ocean–Atmosphere System in GCMs	327
Data for GCMs	330
Seven Basic Equations	330
Navier-Stokes Equations of Motion	330
Thermodynamic Energy Equation	332
Moisture Conservation Equation	333
Continuity Equation	333

Equation of State.....334

Similarities and Differences Between GCMs
and Weather Forecasting Models.....335

Limitations of Model Results336

Statistical Techniques..... 336

Atmospheric Teleconnections 337

Extratropical Teleconnections in the Pacific:
The Pacific Decadal Oscillation.....337

Extratropical Teleconnections in the
Atlantic Ocean.....339

Teleconnections over North America.....342

Summary..... 342

**PART 5 Relationships Between
Climate and Other
Endeavors 345**

**Chapter 14 Applied Climatology, Climate
Impacts, and Climatic Data 347**

Climate Impacts 348

Impacts on Natural Systems.....348

Impacts on Societal Systems349

Impacts on Human Health and Comfort.....350

Climate Vulnerability, Adaptability,
and Resilience350

Climatological Data Sources 351

Data Collection Agencies351

Primary Versus Secondary Data.....352

Secondary Data Sources for Applied Synoptic
and Dynamic Climatological Studies352

Secondary Sources for Applied Studies
of the Climate System359

Secondary Sources Well Suited to Studies
in Paleoclimatology and Climate Change359

Secondary Sources Well Suited to Studies
in Physical Climatology359

Summary..... 362

Chapter 15 Future of Climatology 365

Relationship Between Climatology and
Meteorology 365

Interdisciplinary Work with Other Scientists 366

Interaction Between Climate Scientists and
Nonscientific Professionals..... 366

Improved Atmospheric Data Availability
and Display..... 367

Recognition of the Possibility for
Rapid Climate Change368

Climatology as Part of the Ultimate Goal
of Sustainability 368

Summary..... 370

Glossary 371

Index..... 398



Preface

Welcome to an exciting journey to learn more about one of the most widely discussed sciences today. It would be rare to browse newsfeeds in any form for more than a few minutes without a story that pertains in some way to climate. Congratulations on taking the responsibility for being a well-informed citizen on some of the most important environmental issues of our time.

We remain indebted to our family, friends, colleagues, and especially our students who have provided constructive comments to prepare us for undertaking this *Fourth Edition*. We collected those comments and made substantial content-related changes to this edition in nearly every chapter. Some changes involved merely updating data on graphs and maps, whereas others amounted to a complete revision or addition of a chapter section. Some additions reflect the emergence of new prevailing thought as it relates to issues already discussed in previous editions, such as the 2016 survey of global warming opinions among professional atmospheric scientists (Chapter 12). Other additions, such as the notion of climate vulnerability, broaden the scope of the book in parallel to the broadening scope of climatology. We remain invigorated by the rapid developments in our chosen field, but at the same time we feel frustrated that these developments mean that *Climatology* is never quite complete!

The comments we heard motivated us to retain the format and level of the *Third Edition*. This text continues to serve the upper-level undergraduate or introductory-level graduate student. We are aware that users come from

a wide array of topical backgrounds. For students lacking a background in basic atmospheric science, the fundamentals are covered in Chapters 1 (“Introduction to Climatology”), 2 (“Atmospheric Structure and Composition”), 3 (“Controls on the Climate System”), and 4 (“Atmospheric Interactions with the Other ‘Spheres’”). More experienced readers will be challenged by the “Questions for Thought” at the end of each chapter and by the level of detail of some topics, particularly those in the later chapters. Clarity of explanations, breadth and depth of content, flexibility in instructor-determined chapter assignments, suitability for wide audiences, and timeliness of topical coverage continue to be the principles upon which this book is based.

Although all chapters can be covered in a 3-hour-per-week, semester-length course, some chapters (particularly Chapters 5, 13, and 14) remain self-contained; skipping them would result in little loss of the book’s main message. However, these chapters, which cover the basics of boundary layer climatology, climate modeling, and applied climatology, respectively, also form the building blocks for a deeper level of understanding that is expected in more specialized advanced courses and in graduate-level research.

We believe that an improved understanding of the climate system should contribute to a student’s development toward improvements in three core outcomes in their education: (1) critical-thinking ability, (2) communication skills, and (3) sense of social responsibility. We hope that the *Fourth Edition* remains true to these goals to an even greater extent than the previous editions.

The Student Experience

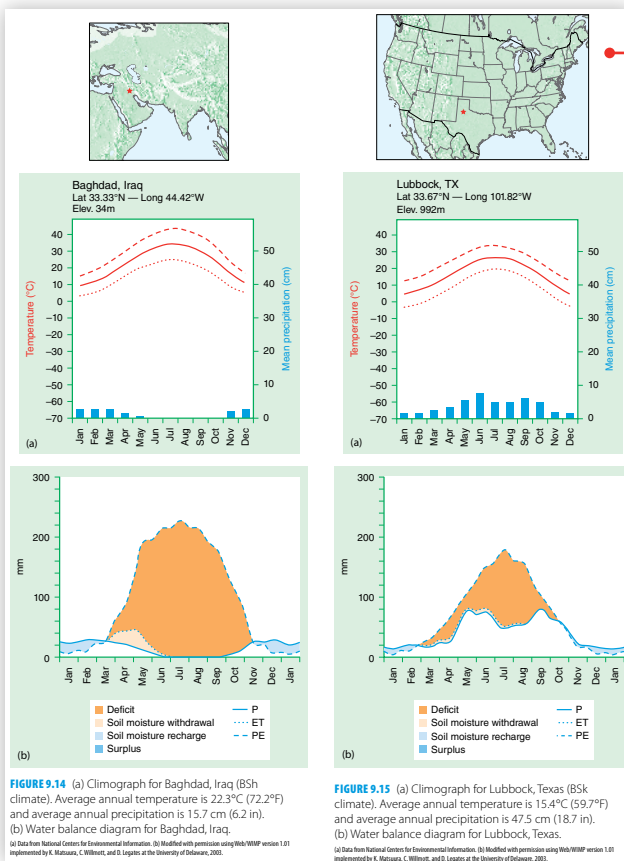
Beginning a new course in climatology can be a daunting experience for many students. *Climatology, Fourth Edition*, therefore, incorporates several pedagogical elements to help with comprehension and retention while also generating enthusiasm about the topic. The pedagogical aids that appear in every chapter include the following:

Chapter at a Glance provides instructors and students with a snapshot of the key concepts they will encounter in each chapter and serves as a checklist to help guide and focus study.

CHAPTER AT A GLANCE

- Properties of the Troposphere
- Near-Surface Troposphere
- Energy in the Climate System
 - Sun as Energy Source
 - Measuring Radiant Energy
 - Radiation Balance
 - Turbulent Fluxes
 - Substrate Heat Flux
 - Energy Balance
- Local Flux of Matter: Moisture in the Local Atmosphere
 - Atmospheric Moisture
 - Moisture in the Surface Boundary Layer
 - Measuring Evapotranspiration
- Atmospheric Statics, the Hydrostatic Equation, and Stability
 - Statics and the Hydrostatic Equation
 - Atmospheric Stability
 - Assessing Stability in the Local Atmosphere
- Momentum Flux
- Putting It All Together: Thermal and Mechanical Turbulence and the Richardson Number
- Summary
- Key Terms
- Review Questions
- Questions for Thought

The completely **revised art program**, in full color for the first time, offers enhanced clarity and gradation of all maps, climographs, and images to better illustrate and help students fully understand the diversity of climate within varying climate types.



Key Terms listed at the end of each chapter and bolded throughout aid in students' review of the material. For further help with learning the vocabulary, students are encouraged to use the **Glossary** at the end of the book, as well as the interactive glossary, animated flashcards, and crossword puzzles on the Navigate Companion Website.

Key Terms

Absolute zero	Ideal gas law	Plane of the ecliptic
Adret slope	Inertia	Pressure
Advection	Inertial period	Pressure gradient force (PGF)
Aerosol	Insolation	Prime meridian
Antarctic Circle	Isobar	Radiant energy
Anticyclone	Isotherm	Refraction
Aphelion	Joule	Revolution
Arctic Circle	June solstice	Rotation
Attenuation	Kelvin temperature scale	<i>Second law of thermodynamics</i>
Autumnal equinox	Kinetic energy	Sensible energy
Axial tilt	Lake effect snow	September equinox
Backing	Latent energy	Solar declination
Beam spreading	Latitude	Solar noon
Centrifugal acceleration (CA)	Leeward	Specific heat
Circle of illumination	Longitude	Summer solstice
Continental	March equinox	Thermohaline circulation
<i>Convection</i>	Maritime effect	Time zone
Coriolis effect (CE)	Midlatitude (frontal) wave	Tropic of Cancer
Cyclone	cyclone	Tropic of Capricorn
December solstice	Millibar (mb)	Tropical cyclone
Downdraft	<i>Momentum</i>	<i>Troposphere</i>
Ekman spiral	<i>National Weather Service</i>	Ubac slope
Equation of state	Navier-Stokes equations	Updraft
<i>Evaporation</i>	of motion	Upwelling
Flux	Newton (N)	<i>Urban heat island</i>
Free atmosphere	Newton's laws of motion	Veering
Friction	North Atlantic Drift	Vernal equinox
Geostrophic balance	Orographic effect	Wind
Geostrophic wind	Parallelism	Windward
Gulf Stream	Pascal (Pa)	Winter solstice
Heat index	Path length	
<i>Hydrostatic equilibrium</i>	Perihelion	

Terms in italics have appeared in at least one previous chapter.

Review Questions

1. Explain how Earth and its atmosphere formed.
2. How is today's atmosphere similar to and different from early Earth's atmosphere?
3. Describe how oxygen came to comprise almost 21% of the atmosphere today.
4. Given that solar output has increased over the past 4.6 billion years, how have Earth's temperatures remained fairly constant over that same time?
5. What is residence time and why is it important?
6. What is the carbon cycle and how does it operate?
7. Describe the thermal structure of the atmosphere.
8. What causes the thermal characteristics associated with each thermal layer of the atmosphere?
9. Compare and contrast the heterosphere and the homosphere.
10. Why is there no defined top to the atmosphere?

Review Questions ensure that students have assimilated the most important concepts of the chapter. These questions challenge students to describe, discuss, explain, compare, and contrast the material they just read. Answers to the even-numbered review questions can be found on the Navigate Companion Website.

Questions for Thought take learning a step further, asking students to think critically and apply theory to reality. These questions can be used for independent study, in homework assignments, or to stimulate class discussion.

Questions for Thought

1. After studying the chapters discussing climates around the world, discuss the climatic accuracies and inaccuracies portrayed in three popular movies. Would the plot of the movie have changed if the climates had been portrayed more accurately?
2. Assume that a 7000-m (23,000-ft) mountain suddenly appears at your current location. Using

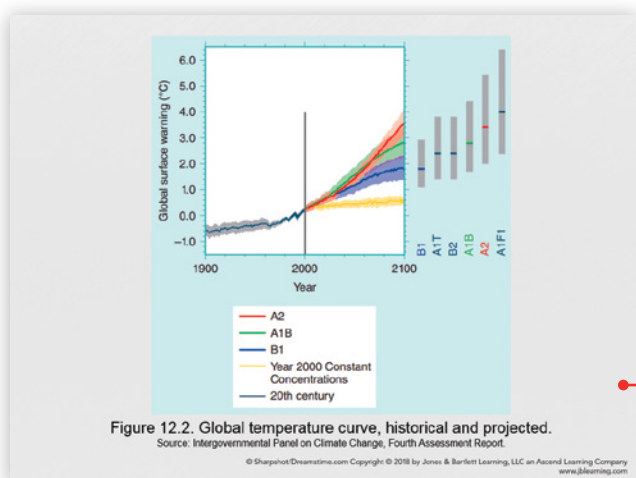
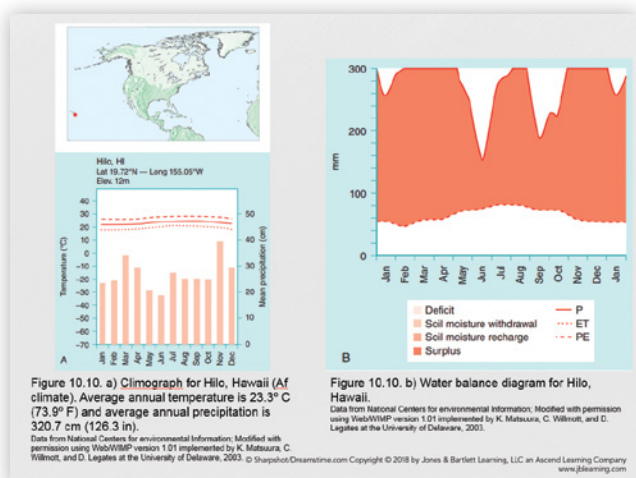
the normal environmental lapse rate, calculate the vertical average temperature from your current elevation to the mountain peak. Based on that temperature, calculate which climatic zones would appear on the mountain, and where they would be located both vertically and horizontally (assuming shading influences, etc.).

Additional Online Resources are available for students and instructors, including practice quizzes, an interactive glossary, answers to even-numbered review questions, and flashcards.

Teaching Tools

A variety of Teaching Tools are available for qualified instructors to assist with preparing for and teaching their courses. These resources are accessible via digital download and multiple other formats.

The **Image Bank in PowerPoint format** contains all of the illustrations, photographs, and tables (for which Jones & Bartlett Learning holds the copyright or has permission to reproduce electronically). These images are not for sale or distribution but may be used to enhance your existing slides, tests, and quizzes or other classroom material.

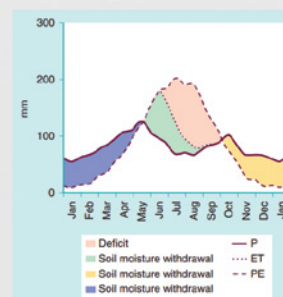


The comprehensive and time-saving **Test Bank** has been updated and expanded to include more than 1,000 exam questions.

xii

Water Balance Diagrams

- Show actual and mean conditions
- The PE curve always mimics temperature curve
- Soil moisture recharge is the difference between P and PE when $P > PE$
- Surplus is when $P > PE$ and soil moisture is at capacity



Climatological Data Sources: Secondary Data Sources for Applied Synoptic and Dynamic Climatological Studies (continued)

- NOAA produces several publications including:
 - Hourly Precipitation Data (HPD)
 - Daily Synoptic Series
- The World Meteorological Organization (WMO) also publishes data

TABLE 14.5 Information Contained in Hourly Precipitation Data

Section	Data Included
Daily precipitation totals by station	Precipitation by station, including the type of gauge used
Hourly precipitation totals by station	Precipitation totals at each hour, ending on the hour
Monthly precipitation maxima by station	Maximum for measurement periods of 15, 30, and 45 minutes and 1, 2, 3, 6, 12, and 24 hours, with the date and time of occurrence

© Sharpshot/Dreamstime.com Copyright © 2018 by Jones & Bartlett Learning, LLC in Accord Learning Company www.jblearning.com

The **Lecture Outlines in PowerPoint format** provide lecture notes and images for each chapter of *Climatology*. Instructors with the Microsoft PowerPoint software can customize the outlines, art, and order of presentation.



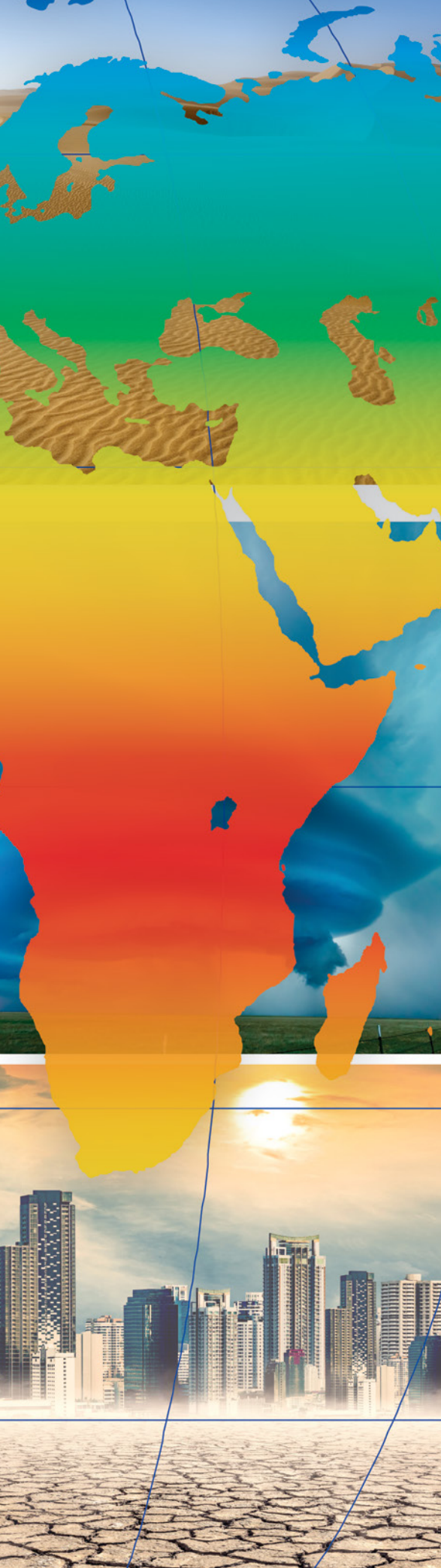
Acknowledgments

Once again, we thank all of our mentors, colleagues, friends, students, and family who have offered advice and encouragement. We also are most appreciative of the staff at Jones & Bartlett Learning for their hard work in improving this edition. We are particularly grateful for the investment in top-notch graphics and a four-color presentation in this edition. We also appreciate all of the suggestions and input from reviewers who have provided feedback over this and previous editions of this text:

Matthew F. Bekker, Brigham Young University
Tianna A. Bogart, Frostburg State University
Andrew Carleton, Pennsylvania State University
Paul J. Croft, Kean University
Kimberly DeBiasse, University of Wisconsin–
Milwaukee
Daniel L. Druckenbrod, Rider University
Dorothy Freidel, Sonoma State University
Brent C. Hedquist, Texas A&M
University–Kingsville
Chad Kauffman, California University of
Pennsylvania
Steve LaDochy, California State University,
Los Angeles

Charles W. Lafon, Texas A&M University
Kevin Law, Marshall University, West Virginia
State Climatologist
Stephen E. MacAvoy, American University
Bryan G. Mark, The Ohio State University
Corene Matyas, University of Florida
Melvin L. Northup, Grand Valley State
University
Robert Pellenbarg, College of the Desert
Robert Mark Simpson, University of Tennessee at
Martin
Bohumil M. Svoma, University of Missouri
Stephen Tsikalas, Jacksonville State University
Lensyl Urbano, University of Memphis
Timothy J. Wallace, Mississippi State University
Lin Wu, California State Polytechnic University,
Pomona
Hengchun Ye, California State University,
Los Angeles

As always, we welcome and appreciate comments from anyone, but especially students, on how subsequent editions can be improved.



PART 1

The Basics

CHAPTER 1 Introduction to Climatology

- Meteorology and Climatology
- Scales in Climatology
- Subfields of Climatology
- Climatic Records and Statistics
- Summary
- Key Terms
- Review Questions
- Questions for Thought

CHAPTER 2 Atmospheric Structure and Composition

- Origin of the Earth and Atmosphere
- Atmospheric Composition
- Faint Young Sun Paradox
- Atmospheric Structure
- Summary
- Key Terms
- Review Questions
- Questions for Thought





CHAPTER 1

Introduction to Climatology

CHAPTER AT A GLANCE

- Meteorology and Climatology
- Scales in Climatology
- Subfields of Climatology
- Climatic Records and Statistics
- Summary
- Key Terms
- Review Questions
- Questions for Thought

Climatology may be described as the scientific study of the behavior of the **atmosphere**—the thin gaseous layer surrounding Earth’s surface—integrated over time. Although this definition is certainly acceptable, it fails to capture fully the scope of climatology. Climatology is a holistic science that incorporates data, ideas, and theories from all parts of the Earth–ocean–atmosphere system, including those influenced by humans, into an integrated whole to explain atmospheric properties.

The Earth–ocean–atmosphere system may be divided into a number of zones, with each traditionally studied by a separate scientific discipline. The part of the solid Earth nearest to the surface (to a depth of perhaps 100 km) is called the **lithosphere** and is studied by geologists, geophysicists, geomorphologists, soil scientists, vulcanologists, and other practitioners of the environmental and agricultural sciences. The

part of the system that is covered by liquid water is termed the **hydrosphere**; it is considered by those in the fields of oceanography, hydrology, and limnology (the study of lakes). The region comprising frozen water in all its forms (glaciers, sea ice, surface and subsurface ice, and snow) is known as the **cryosphere** and is studied by those specializing in glaciology, as well as specialized physical geographers, geologists, and oceanographers. The biosphere, which crosscuts the lithosphere, hydrosphere, cryosphere, and atmosphere, includes the zone containing all life forms on the planet, including humans. The **biosphere** is examined by specialists in the wide array of life sciences, along with physical geographers, geologists, and other environmental scientists.

The atmosphere is the component of the system studied by climatologists and meteorologists. Holistic interactions between the atmosphere and

TABLE 1.1 Examples of Interactions Between the Atmosphere and the Other “Spheres” and Impacts on Thermal Receipt/Climate

Sphere Interacting with Atmosphere	Example of a Potential Impact
Lithosphere	Large volcanic eruptions can create a dust and soot cloud that can reduce the receipt of solar radiation, cooling the global atmosphere for months or years.
Hydrosphere	Changes in ocean circulation can cause global atmospheric circulation shifts that produce warming in some regions and cooling in others.
Cryosphere	Melting of polar ice caps can cause extra heating at the surface where ice was located because bare ground reflects less of the solar energy incident upon the surface than ice.
Biosphere	Deforestation increases the amount of solar energy received at the surface and alters atmospheric chemistry by returning carbon dioxide stored in living plant matter to the atmosphere.

each combination of the “spheres” are important contributors to the climate (TABLE 1.1), at scales from local to planetary. Thus, climatologists must draw on knowledge generated in several natural and sometimes social scientific disciplines to understand the processes at work in the atmosphere. Because of its holistic nature of atmospheric properties over time and space, climatology naturally falls into the broader discipline of geography.

Over the course of this book we shall see that these processes can be complex. The effects of some of these interactions cascade up from local to planetary scales, and the effects of others tend to cascade down the various scales to ultimately affect individual locations over time. The processes are so interrelated with other spheres and with other scales that it is often difficult to generalize by saying that any particular impact begins at one component of the system or side of the scale and proceeds to another.

We can state that the scope of climatology is broad. It has also expanded widely from its roots in ancient Greece. The term “climatology” is derived from the Greek word “klima,” which means “slope,” and reflects the early idea that distance from the equator alone (which causes differences in the angle or slope of the Sun in the sky) drove climate. The second part of the word is derived from “logos,” defined as “study” or “discourse.” Modern climatology seeks not only to describe the nature of the atmosphere from location to location over many different time scales but also to explain why particular attributes occur and change over time and to assess the potential impacts of those changes on natural and social systems.

► Meteorology and Climatology

The two atmospheric sciences, meteorology and climatology, are inherently linked. **Meteorology** is the study of **weather**—the overall instantaneous condition of the atmosphere at a certain place and time. Weather is described through the direct measurement of particular atmospheric properties such as temperature, precipitation, humidity, wind direction, wind speed, cloud cover, and cloud type. The term “weather” refers to tangible aspects of the atmosphere. A quick look or walk outside may be all that is needed to describe the weather of your location. Of course, these observations may be compared with the state of the atmosphere at other locations, which in most cases is different.

Because meteorology deals with direct and specific measurements of atmospheric properties, discussion of weather centers on short-duration time intervals. Weather is generally discussed over time spans of a few days at most. How is the weather today? How does this compare with the weather we had yesterday? What will the weather be like tomorrow or toward the end of the week? All of these questions involve short-term analysis of atmospheric properties for a given time and place. So meteorology involves only the present, the immediate past, and the near future.

But a much more important component of meteorology is the examination of the forces that create the atmospheric properties being measured. Changes in the magnitude or direction of these forces over time and changes in the internal properties of the matter being affected by these forces create differences in weather conditions over time. Although many meteorologists

are not directly involved with forecasting these changes, meteorology is the only natural science in which a primary goal is to predict future conditions. Weather forecasting has improved greatly with recent technological enhancements that allow for improved understanding of these forces, along with improved observation, data collection, and modeling of the atmosphere. Currently, weather forecasts produced by the **National Weather Service** in the United States are accurate for most locations over a period of approximately 72 hours.

By contrast, **climate** refers to the state of the atmosphere for a given place over time. It is important to note that climatologists are indeed concerned with the same atmospheric processes that meteorologists study, but the scope is different. Meteorologists may study the processes for their own sake, while climatologists study the processes to understand the long-term consequences of those processes. Climatology, therefore, allows us to study atmospheric processes and their impacts far beyond present-day weather.

There are three properties of climatic data to consider: normals, extremes, and frequencies. These are used to gauge the state of the atmosphere over a particular time period as compared with atmospheric conditions over a similar time period in the past. **Normals** refer to average weather conditions at a place. Climatic normals are typically calculated for 30-year periods and give a view of the type of expected weather conditions for a location through the course of a year. For example, climatologically normal conditions in Crestview, Florida, are hot and humid during the summer and cool but not cold in winter.

Two places could have the same average conditions but with different ranges of those conditions, in the same way that two students who both have an average of 85% in a class may not have acquired that average by earning the same score on each graded assignment. Therefore, **extremes** are used to describe the maximum and minimum measurements of atmospheric variables that can be expected to occur at a certain place and time, based on a long period of observations. For example, a temperature of 0°C (32°F) at Crestview in April would fall outside of the range of expected temperatures.

Finally, **frequencies** refer to the rate of incidence of a particular phenomenon at a particular place over a long period of time. Frequency data are often important for risk assessment, engineering, or agricultural applications. For instance, the frequency of hailstorms in a city is a factor in determining a homeowner's insurance premium. Or if an engineer designs a culvert to accommodate 8 cm (3 in.) of rain in a 5-hour period but that frequency is exceeded an average of two times per year, this rate of failure may or may not be acceptable to the citizens affected by the culvert. A farmer may

want to know how many days on average exceed 1.5 cm (0.6 in.) of rain in October because October rains are problematic for any crop harvested during that month.

We can say then that both meteorologists and climatologists study the same atmospheric processes but with three primary and important differences. First, the time scales involved are different. Meteorologists are primarily concerned with features of the atmosphere at a particular time and place—the “weather”—whereas climatologists study the long-term patterns and trends of those short-term features—the “climate.” Second, meteorologists are more concerned with the processes for their own sake, while climatologists consider the long-term implications of those processes. Third, climatology is inherently more intertwined with processes happening not only in the atmosphere but also in the other “spheres” because the interactions between the atmosphere and the other spheres are more likely to have important consequences over longer, rather than shorter, time scales. This is particularly true if those processes occur over large areas, because the impacts usually take longer to develop in such cases. For instance, if the Great Lakes were to totally evaporate, such a process would necessarily take place over a long time period. The difference in water level in the Great Lakes between today and tomorrow would not cause much impact on tomorrow's weather as compared with today's. A meteorologist would not need to take this atmosphere–hydrosphere interaction into account when considering tomorrow's weather. However, the difference in water content between the Great Lakes over centuries is more likely to have a noticeable and dramatic impact on climate during that time period. Interactions between the atmosphere and other spheres, such as in this example, thus must be considered when evaluating climate.

Regardless of the differences between meteorology and climatology, it is important to recognize that the distinction between the two is becoming increasingly blurred over time. A successful climatologist should have a firm grounding in the laws of atmospheric physics and chemistry that dictate the instantaneous behavior of the atmosphere. An effective meteorologist should recognize the importance of patterns over time and the impacts of those and other patterns on the Earth–ocean–atmosphere system.

The holistic perspective of climatology also carries over to include interactions between the atmosphere and social systems. The impact of people on their environment is a theme in climatology that has become more prevalent in recent years. It is being increasingly recognized that many features of the human condition are related to climate. This is especially true of climatic “extremes” and “frequencies,” because it is the

“abnormal” events, and conditions exceeding certain thresholds, that generally cause the greatest impact on individuals and society.

► Scales in Climatology

Just as temporal scale is important, climatology also involves the study of atmospheric phenomena along many different spatial scales. There is usually a direct relationship between the size of individual atmospheric phenomena and the time scale in which that phenomenon occurs (FIGURE 1.1). The **microscale** represents the smallest of all atmospheric scales. Phenomena that operate along this spatial scale are smaller than 0.5 km (0.3 mi) and typically last from a few seconds to a few hours. A tiny circulation between the underside and the top of an individual leaf falls into this category, as does a tornado funnel cloud, and everything between. A larger scale is the **local scale**, which operates over areas between about 0.5 and 5 km (0.3 to 3 mi)—about the size of a small town. A typical thunderstorm falls into this spatial scale.

The next spatial scale is the **mesoscale**, which involves systems that operate over areas between about 5 and 100 km (3 to 60 mi) and typically last from a few hours to a few days. Such systems include those you may have encountered in earlier coursework, such as the mountain/valley breeze and land/sea breeze circulation systems, clusters of interacting thunderstorms known as mesoscale convective complexes, a related phenomenon associated with cold fronts termed “mesoscale convective systems,” and the central region of a hurricane.

Moving toward larger phenomena, we come to the **synoptic scale**, a spatial scale of analysis that functions over areas between 100 and 10,000 km (60 to 6000 mi). Systems of this size typically operate over periods of days

to weeks. Entire tropical cyclone systems and midlatitude (frontal) cyclones with their associated fronts fall into the synoptic scale. Because these phenomena are quite frequent and directly affect many people, the synoptic scale is perhaps the most studied spatial scale in the atmospheric sciences.

Finally, we can also study and view climate over an entire hemisphere or even the entire globe. This represents the largest spatial scale possible and is termed the **planetary scale**, because it encompasses atmospheric phenomena on the order of 10,000 to 40,000 km (6000 to 24,000 mi). Because in general the largest spatial systems operate over the longest time scales, it is no surprise then that planetary-scale systems operate over temporal scales that span weeks to months. Examples of planetary-scale systems include the broad wavelike flow in the upper atmosphere and the major latitudinal **pressure** and **wind** belts that encircle the planet.

► Subfields of Climatology

Climatology can be divided into several subfields, some of which correspond to certain scales of analysis. For instance, the study of the microscale processes involving interactions between the lower atmosphere and the local surface falls into the realm of **boundary-layer climatology**. This subfield is primarily concerned with exchanges in energy, matter (especially water), and **momentum** near the surface. Physical processes can become complex in the near-surface “boundary layer” for two reasons. First, the decreasing effect of **friction** from the surface upward complicates the motion of the atmosphere and involves significant transfer of momentum downward to the surface. Second, the most vigorous exchanges of energy and moisture occur in this layer because solar radiant

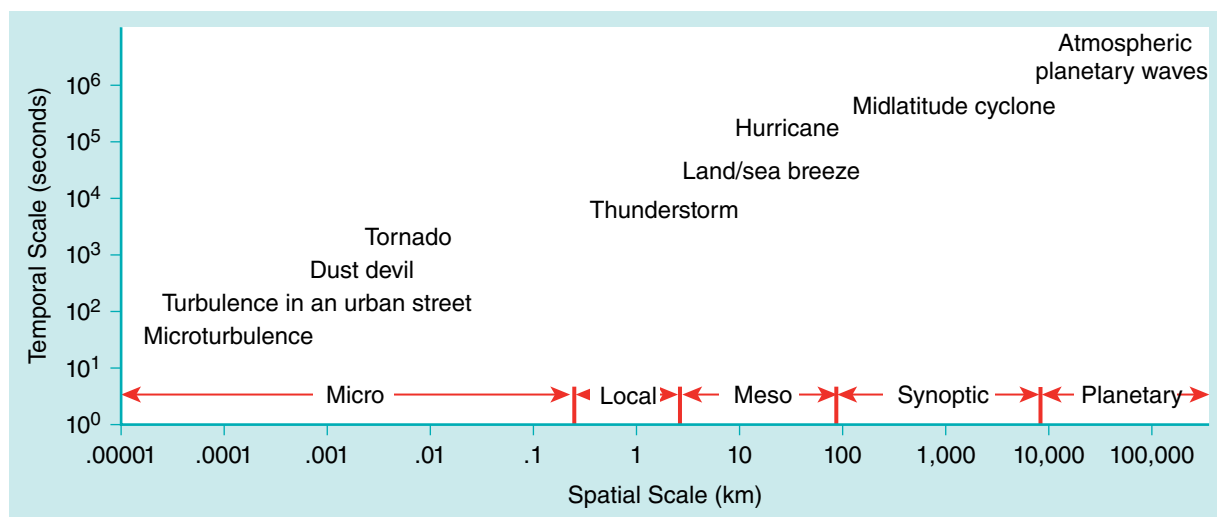


FIGURE 1.1 Spatial–temporal relationships for selected atmospheric features.

energy striking the ground warms it greatly and rapidly compared with the atmosphere above it and because the source of water for **evaporation** is at the surface. Boundary-layer climatology may be further subdivided into topics that examine surface–atmosphere interactions in mountain/alpine regions, urban landscapes, or various vegetated land covers.

Physical climatology is related to boundary-layer climatology in that it studies energy and matter. However, it differs in that it emphasizes the nature of atmospheric energy and matter themselves at climatic time scales, rather than the processes involving energy, matter, and momentum exchanges only in the near-surface atmosphere. Some examples include studies on the causes of lightning, atmospheric optical effects, microphysics of cloud formation, and air pollution. Although meteorology has traditionally emphasized this type of work to a greater extent than climatology, climatologists have contributed to our understanding of these phenomena. Furthermore, the convergence of meteorology and climatology as disciplines will likely lead to more overlap in these topics of research in the future.

Hydroclimatology involves the processes (at all spatial scales) of interaction between the atmosphere and near-surface water in solid, liquid, and gaseous forms. This subfield analyzes all components of the **global hydrologic cycle**. Hydroclimatology interfaces especially closely with the study of other “spheres,” including the lithosphere, cryosphere, and biosphere, because water is present in all of these spheres and interactions readily occur between them.

Another subfield of climatology is **dynamic climatology**, which is primarily concerned with general atmospheric dynamics—the processes that induce atmospheric motion. Most dynamic climatologists work at the planetary scale. This differs from the subfield of **synoptic climatology**, which is also concerned with the processes of circulation but is more regionally focused and usually involves more practical and specific applications than those described in the more theoretical area of dynamic climatology. According to climatologist Brent Yarnal, synoptic climatology “studies the relationships between the atmospheric circulation and the surface environment of a region.” He goes on to state that, “because synoptic climatology seeks to explain key interactions between the atmosphere and surface environment, it has great potential for basic and applied research in the environmental sciences.” Synoptic climatology may act as a keystone that links studies of atmospheric dynamics with applications in various other disciplines.

Synoptic climatology is similar in some ways to **regional climatology**, a description of the climate of a particular region of the surface. However, synoptic

climatology necessarily involves the explanation of process, whereas regional climatology may not.

The study of climate can extend to times before the advent of the instrumental weather record. This subfield of climatology is termed **paleoclimatology** and involves the extraction of climatic data from indirect sources. This **proxy evidence** may include human sources such as books, journals, diaries, newspapers, and artwork to gain information about preinstrumental climates. However, the field primarily focuses on biological, geological, geochemical, and geophysical proxy sources, such as the analysis of tree rings, fossils, corals, pollen, ice cores, striations in rocks, and sediment deposited annually on the bottoms of lakes (**varves**).

Bioclimatology is a diverse subfield that includes the interaction of living things with their atmospheric environment. **Agricultural climatology** is the branch of bioclimatology that deals with the impact of atmospheric properties and processes on living things of economic value. **Human bioclimatology** is closely related to the life sciences, including biophysics and human physiology.

Applied climatology is different in its orientation from the other subfields of climatology. While the others seek to uncover causes of various aspects of climate, applied climatology is primarily concerned with the effects of climate on other natural and social phenomena. This subfield may be further subdivided. One area of focus involves attempts to improve the environment. Examples include using climatic data to create more efficient architectural and engineering design, generating improvements in medicine, and understanding the impact of urban landscapes on the natural and human environment. Other examples involve the possibility of modifying the physical atmosphere to suit particular human needs, such as with the practice of **cloud seeding**, which attempts to extract the maximum amount of precipitation from clouds in water-scarce regions.

In general, each subfield overlaps with others. We cannot fully understand processes and impacts relevant to any subfield without touching on aspects important for others and at least one other nonclimatology field. For example, an agricultural climatologist interested in the effect of windbreaks to reduce evaporation rates in an irrigated field must understand the near-surface wind profile and turbulent transfer of moisture, along with soil and vegetation properties.

► Climatic Records and Statistics

Because climatology deals with aggregates of weather properties, statistics are used to reduce a vast array of recorded properties into one or a few understandable numbers. For instance, we could calculate the **daily mean temperature**—the average temperature

for the entire day—for yesterday at a particular location through a number of methods. First, we could take all recorded temperatures throughout the day, add them together, and then divide by the total number of observations.

A much simpler (but less accurate) method of calculating the daily mean temperature is actually the one that is used: A simple average is calculated from the maximum and minimum temperatures recorded for the day. This method is the most common because in the days before computers were used to measure and record temperature, special thermometers that operated on the principle of a “bathtub ring” were able to leave a mark at the highest and lowest temperature experienced since the last time that the thermometer was reset. Each day, human observers could determine the maximum and minimum temperature for the previous 24 hours, but they would not know any of the other temperatures that occurred over that time span. For most of the period of weather records, we knew only the maximum and minimum daily temperatures.

Of course, the numerical average calculated by the maximum–minimum method differs somewhat from the one obtained by taking all hourly temperatures and dividing by 24. Even though we have automated systems now that can measure and record temperatures every second, we do not calculate mean daily temperatures using this more accurate method because we do not want to change the method of calculating the means in the middle of our long-term weather records. What would happen if the temperatures began to rise abruptly at the same point in the period of record that the method of calculating the mean temperature changed? We would not know whether the “change” represented an actual change in climate or was just an artifact of a change in the method of calculating the mean temperature.

But what about that average temperature? Is it actually meaningful? Let’s say that yesterday we recorded a high temperature of 32°C (90°F) and a low of 21°C (70°F). Our calculated average daily temperature would be about 27°C (80°F). This number would be used to simply describe and represent the temperature of the day for our location. But the temperature was likely to have been 27°C (80°F) only during two short periods in the day, once during the mid-day hours when climbing toward the maximum and again as temperatures decreased through the late afternoon. So the term “average temperature” is actually a rather abstract notion. Most averages or climatic “normals” are abstract notions, but the advantage from a long-term (climatic) perspective is that they provide a “mechanism” for analyzing long-term changes and variability.

“Extremes” are somewhat different. As we saw earlier in this chapter, climatic extremes represent the most unusual conditions recorded for a location. For example, these may represent the highest or lowest temperatures during

a particular time period. Extremes are often given on the nightly news to give a reference point to the daily recorded temperatures. We might hear that the high temperature for the day was 33°C (92°F), but that was still 5°C (8°F) lower than the “record high” of 38°C (100°F) recorded on the same date in 1963. As long as our recorded atmospheric properties are within the extremes, we know that the atmosphere is operating within the expected range of conditions. When extremes are exceeded or nearly exceeded, then the atmosphere may be considered to be behaving in an “anomalous” manner. The frequency with which extreme events occur is also important. Specifically, if extreme events occur with increasing frequency, the environmental, agricultural, epidemiological, and economic impacts will undoubtedly increase.

Why are climatic records important? During the 1980s and 1990s the rather elementary notion that climate changes over time was absorbed by the general public. Before that time many people thought that climate remained static even though weather properties varied considerably around the normals (averages). With heightened understanding of weather processes came the realization that climate varies considerably as well. Climatic calculations and the representation of climate for a given place over time became exceedingly important and precise. The problems associated with the calculation of various atmospheric properties still existed, however, and the methods of calculating these properties could have far-reaching implications on such endeavors as environmental planning, hazard assessment, and governmental policy.

With today’s technology we would assume that calculating a simple average temperature for Earth, for instance, would be easy. However, data biases and methodological differences complicate matters. Many of these issues have been mathematically corrected in recorded data. Given the corrections, it is generally accepted that Earth’s average annual temperature has risen by about 0.85°C (1.53°F) since the widespread instrumental record began in 1880.

Another factor that complicates the interpretation of the observed warming is the increasingly urban location of many weather stations as urban sprawl infringes on formerly rural weather stations. Early in the twentieth century many weather stations in the United States and elsewhere were located on the fringe of major cities. This was especially true toward the middle part of the century with the construction of major airports far from the urban core. Weather observations could be recorded at the airport in a relatively rural, undisturbed location. As cities grew, however, these locations became swallowed up by urban areas. This instituted considerable bias into long-term records as artificial heat from urban sources, known as the **urban heat island**,

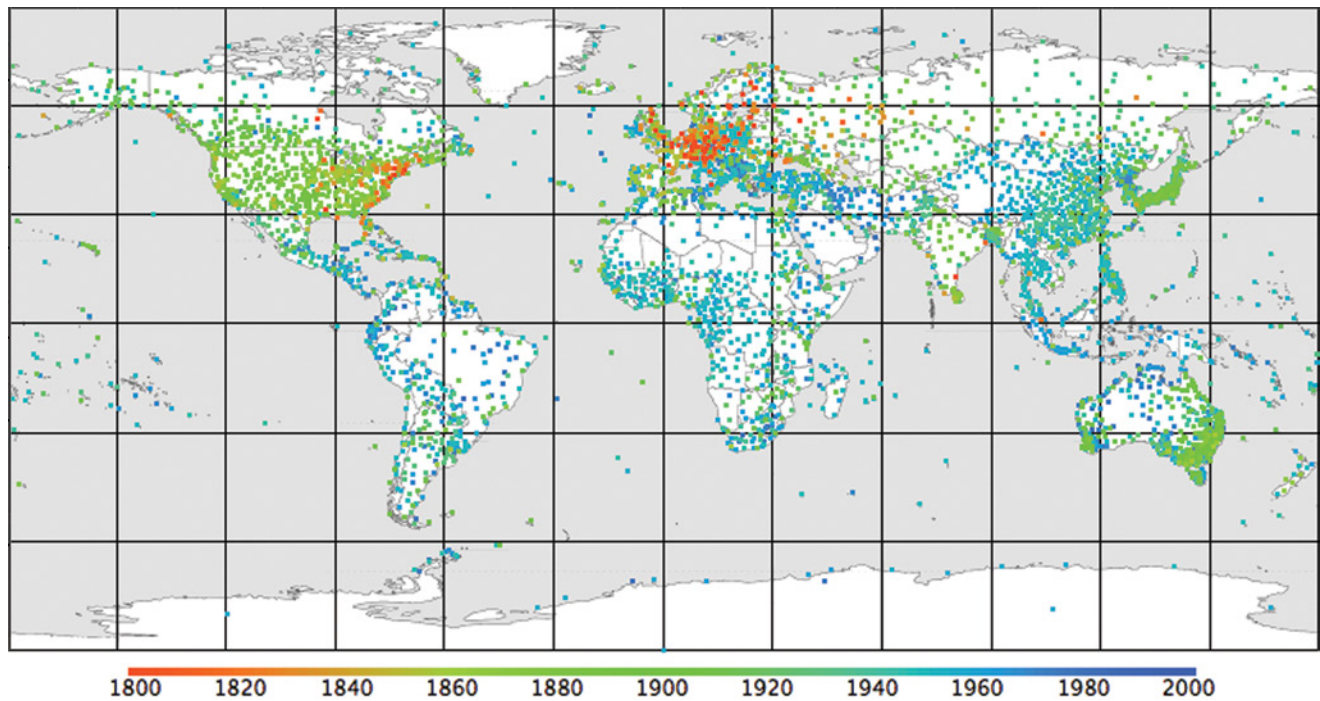


FIGURE 1.2 Location of global surface observations in the Global Historical Climatology Network at various years.

Courtesy of Kevan Hashemi. © 2015. Retrieved from: www.hashemifamily.com/Kevan/Climate/#Global%20Surface.

became part of the climatic record. Various properties, such as the abundance of concrete that absorbs solar energy effectively, the absence of vegetation and water surfaces, and the generation of waste heat by human activities contribute to the heat island. The urban heat island provides an excellent example of how humans can modify natural climates and can complicate the calculation and analysis of “natural” climatic changes.

In addition, the long-term recordings themselves may be plagued by other problems. Consider that most weather records for the world are confined to more-developed countries and tend to be collected in, or near, population centers. Developing countries, rural areas, and especially the oceans are poorly represented in the global weather database, particularly in the earlier part of the record (**FIGURE 1.2**). Oceans comprise over 70% of the planet’s surface, yet relatively few long-term weather records exist for these locations. Most atmospheric recordings over oceans are collected from ships, and these recordings are biased by inconsistencies in the height of the ship-mounted weather station, the type of station used, the time of observation, and the composition of ship materials. Furthermore, ocean surface temperatures are derived in a variety of ways, from inserting a thermometer into a bucket of collected ocean water to recording the temperature of water passing through the bilge of the ship (with the heat generated by the ship included in the recording). Vast tracts of ocean were largely ignored until the recent

arrival of satellite monitoring and recording technology, because the representation of surface and atmospheric properties was greatly limited to shipping lanes.

Even records taken with rather sophisticated weather stations may be biased and complicated to some degree by rather simple issues. Foremost among these are station moves. Moving a station even a few meters may ultimately bias long-term recordings as factors such as differing surface materials and solar exposure occur. Also of note is **time of observation bias**, which involved data bias based on the time of day when measurements are recorded at different stations. Finally, systematic biases and changes in the instrumentation may cause inaccuracies in measurements. The result of these, and a host of other biases, is that considerable data “correction” is required. Both the biases and the correction methods fuel debate concerning the occurrence of actual atmospheric trends.

► Summary

This chapter introduces the field of climatology. It describes the scope of climatology, the inherent differences between meteorology and climatology, and the associated notions of weather and climate. Meteorology studies changes in weather, the state of atmospheric properties for a given location over a relatively short period of time, while climatology examines weather properties over time for a location. Climatology is a holistic science in that it involves understanding the

interaction of the atmosphere with other aspects of the Earth–ocean–atmosphere system using many different spatial and temporal scales. Each scale partially defines the many interlocking subfields of climatology, including boundary-layer, physical, hydro-, dynamic, synoptic, regional, paleo-, bio-, and applied climatology. Interactions occur between the atmosphere, lithosphere,

hydrosphere, cryosphere, and biosphere. All are important to the establishment of global, hemispheric, and regional climates.

Climatic data and calculations also are described, with particular emphasis on climatic normals, extremes, and frequencies. Some causes of spurious climatic data, such as the urban heat island, are also introduced.

Key Terms

Agricultural climatology	Frequencies	Paleoclimatology
Applied climatology	Friction	Physical climatology
Atmosphere	Global hydrologic cycle	Planetary scale
Bioclimatology	Human bioclimatology	Pressure
Biosphere	Hydroclimatology	Proxy evidence
Boundary-layer climatology	Hydrosphere	Regional climatology
Climate	Lithosphere	Synoptic climatology
Climatology	Local scale	Synoptic scale
Cloud seeding	Mesoscale	Time of observation bias
Cryosphere	Meteorology	Urban heat island
Daily mean temperature	Microscale	Varve
Dynamic climatology	Momentum	Weather
Evaporation	National Weather Service	Wind
Extremes	Normals	

Review Questions

1. Why is the science of climatology inherently holistic?
2. Briefly describe Earth's "spheres." Give examples of how each of the spheres is connected.
3. Compare and contrast the notions of weather and climate.
4. Compare and contrast the sciences of meteorology and climatology.
5. Describe the various spatial and temporal scales of climatology.
6. Discuss the different subdisciplines within climatology. How are they different from/similar to one another?
7. How are mean temperatures calculated? Discuss the problems inherent in the calculation methods.
8. What is the urban heat island and why is it relevant to temperature assessment?

Questions for Thought

1. Think of several examples of how advancements in science and technology may have helped climatology to evolve as a science since 1950.
2. In today's age of specialization, is climatology's interdisciplinary nature an advantage or a disadvantage?
3. To what extent are "extreme events" a matter of perspective?
4. In what sense might the occurrence of noncatastrophic events cause catastrophic events to occur?

CHAPTER 2

Atmospheric Structure and Composition

CHAPTER AT A GLANCE

- Origin of the Earth and Atmosphere
- Atmospheric Composition
 - Carbon Cycle
 - Constant and Variable Gases
- Faint Young Sun Paradox
- Atmospheric Structure
- Summary
- Key Terms
- Review Questions
- Questions for Thought

The *atmosphere* is a collection of gases held near the Earth by gravity. It is also pulled away from the Earth because a vacuum exists in the harsh conditions of space. One of the most fundamental properties of the universe—the **second law of thermodynamics**—states that energy (and, therefore, mass, because energy and mass are related by Einstein's theory of relativity) moves from areas of higher concentration (in this case, Earth's lower atmosphere) to areas of lower concentration (outer space). The atmosphere thus represents a place where a balance is generally achieved between the downward-directed gravitational force and

the upward-directed force of buoyancy. This balance is termed **hydrostatic equilibrium**. This extremely thin and delicate zone known as the atmosphere makes life as we know it possible on the planet. When you look in the sky the atmosphere appears to continue infinitely, but if Earth were the size of an apple, the atmosphere would have the thickness of the apple's skin.

Technically, the atmosphere is a subset of the air because it is composed solely of gases. By contrast, air contains not only gases but also **aerosols**—solid and liquid particles suspended above the surface that are too tiny for gravity to pull downward. Solid aerosols include

ice crystals, volcanic soot particles, salt crystals from the ocean, and soil particles; liquid aerosols include clouds and fog droplets.

Because the atmosphere is composed of the lightest elements gravitationally attracted to the Earth, many assume that it has little or no mass. Compared with the mass of the solid Earth (6×10^{24} kg; or 6×10^{21} metric tons) and oceans (1.4×10^{21} kg; or 1.4×10^{18} metric tons), the atmosphere is indeed light. But the atmosphere has a substantial total mass of 5×10^{18} kg (5×10^{15} metric tons)!

The mass of the air is in constant motion, giving considerable impact to the surface environment. For example, a tornado can cause catastrophic devastation to a location. In the case of a tornado, the mass of air has substantial acceleration. According to **Newton's second law of motion**, force is the product of mass and acceleration. The two factors combine, in this situation, to produce a force capable of devastation.

The atmosphere is an extremely complex entity that must be viewed simultaneously on many levels, both temporally and in three spatial dimensions (west–east, north–south, and vertical). Atmospheric processes can be difficult to understand. To appreciate the nature of the atmosphere properly, we must first understand the origins of the atmosphere and its changes since the origin of the planet.

► Origin of the Earth and Atmosphere

According to the best scientific information, the universe is thought to have begun 13.8 billion years ago. At that time all matter in the universe was confined to a single space. An explosion of unimaginable proportion sent this matter—mostly hydrogen—outward in all directions. Over time, gravity caused matter to collect in various areas of space to form galaxies. Within the galaxies smaller amounts of matter condensed gravitationally into stars. Star formation began to occur when hydrogen was compressed under its own gravitational weight. If the mass involved was sufficiently large, **nuclear fusion**—a process that converts lighter elements (principally hydrogen) into heavier elements (primarily helium)—began. Such reactions released amazing quantities of radiant energy while creating (fusing) all matter heavier than hydrogen.

Occasionally, a star exploded, sending heavier elements outward through the galaxy. Vast clouds of dust, called **nebula** (FIGURE 2.1), formed, and the original gravitational accumulation process began anew. Our solar system is believed to have formed from a nebula approximately 5 billion years ago. The Sun gravitationally



FIGURE 2.1 The Orion Nebula.

Courtesy of NASA, ESA, M. Robberto (Space Telescope Science Institute/ESA), and the Hubble Space Telescope Orion Treasury Project Team.

attracted the bulk of the elements that composed the nebula. Planets formed as balls of dust gravitationally collected over various orbits about the primitive Sun. Earth was one such ball of dust. As it grew the elements fused together and collapsed under their own weight and gravity. As Earth grew in size, its gravity increased proportionately. Friction caused the Earth materials to melt. Melting was also encouraged by frequent impacts with large **planetesimals**, which were essentially small planets of condensed debris moving over wildly eccentric orbits about the Sun. These planetesimals contributed heavier elements and mass to the growing Earth while shattering and melting its hot surface. A collision between Earth and a planetesimal is thought to have created the Moon. Remnants of early solar system planetesimals are present today in the vast asteroid field between Mars and Jupiter. The **Oort cloud**—a collection of icy comets and dust that surrounds the outer edges of our solar system—also acts as a relic of conditions present in the early stages of solar system formation.

In these early times Earth's atmosphere is believed to have consisted of light and inert (noble) gases such as hydrogen, helium, neon, and argon. These gases were effectively swept away as the **solar wind**—radioactive particles from the Sun moving through space at nearly the speed of light—developed. Today, Earth is largely devoid of noble gases as a result. So how did the atmosphere that we know today form?

The composition of the atmosphere can be explained by looking at volcanic activity, which is rather limited over Earth's surface today but was apparently widespread

billions of years ago as the early Earth cooled slowly from its primordial molten state. As volcanic material cooled, gases were released through the process of **outgassing**, which primarily involved diatomic nitrogen (N_2) and carbon dioxide (CO_2), with lesser amounts of water vapor, **methane** (CH_4), and sulfur. The **condensation** of water vapor into liquid water in the cool atmosphere formed clouds and precipitation. Precipitation collected in low-elevation areas of the planet and accumulated over time to form the oceans.

Our planet is unique in the solar system because of the presence of liquid water. This is a consequence of many related, and interacting, factors—some of which include distance to the Sun and atmospheric composition. Because water is essential to life, it is not surprising that Earth is the only planet known to support life.

► Atmospheric Composition

Today, the dry atmosphere consists primarily of N_2 and diatomic oxygen (O_2). Diatomic nitrogen is a stable gas that comprises 78% of the present-day atmospheric volume (**TABLE 2.1**). The abundance of N_2 has increased as a percentage of the total atmospheric volume primarily because it is not removed as effectively from the atmosphere as are most other atmospheric gases. The **residence time**—the mean length of time that an individual molecule remains in the atmosphere—of N_2 is believed to be approximately 16.25 million years.

The next-most abundant gas in the present-day dry atmosphere is oxygen, comprising approximately 21% of the atmospheric volume. About 0.93% of the remaining 1% of the dry atmosphere is composed mostly of argon (Ar), and a wide array of atmospheric trace gases constitute the remainder. Of these, CO_2 is the fourth-most abundant gas in the dry atmosphere, representing 0.041% of the dry atmosphere, or 407 parts per million (ppm), as of June 2016. It plays an especially important

role in maintaining the temperature of the planet at a level comfortable for life in its present form. Earth's early atmosphere apparently contained far more CO_2 than today's and little or no O_2 . So where did most of the CO_2 go after outgassing in the primitive atmosphere, and how did O_2 come to replace it?

The evolution of Earth's atmospheric composition (including O_2) involves significant interactions with the *biosphere*, *hydrosphere*, and *lithosphere*. About 3.5 billion years ago an interesting development occurred in the extensive waters of primordial Earth that profoundly affected the evolution of the atmosphere. Single-celled organisms, called **prokaryotes**, began to appear. These simple ancestors of bacteria and green algae absorbed nutrients directly from the surrounding environment. Prokaryotes released CO_2 to the atmosphere as a by-product of **fermentation**, the process by which simple organisms acquire energy through the breakdown of food. The evolution of prokaryotes led to more complex, often multicellular, organisms called **eukaryotes**, which contain more complex internal structures and release even more CO_2 into the atmosphere in the process of **respiration**. Most life on Earth is believed to have evolved from the further development of eukaryotes. Prokaryotes and eukaryotes would have had to develop in the oceans, however, because without oxygen in the atmosphere the protective **ozone** (O_3) layer could not have formed to protect terrestrial life from the harmful **ultraviolet (UV) radiation** emitted by the Sun. Over time, CO_2 continued to accumulate, as it became a larger and larger component of the atmospheric volume.

By about 3 billion years ago another major development in the history of life on Earth apparently caused another major change to the atmospheric composition. The early evolution of eubacteria, and later, protists, and eventually aquatic green plants led to a significant extraction of CO_2 from the atmosphere in **photosynthesis**—the process by which green plants use sunlight to synthesize food. O_2 is released into the atmosphere as a byproduct of photosynthesis. As green plants began to populate Earth, first in the oceans and later on land after the presence of O_2 gradually led to the formation of ozone (O_3) and the O_3 layer—atmospheric CO_2 decreased in concentration while atmospheric O_2 simultaneously increased. Today most of the atmospheric CO_2 is stored in vast quantities of sedimentary rock, originally extracted from the atmosphere by living things. The amount of atmospheric O_2 present today represents a similar percentage to that of CO_2 in the early atmosphere.

TABLE 2.1 Composition of the Dry Atmosphere

Gas	Percentage of Air	
Nitrogen (N_2)	78.08	} 99.03
Diatomic oxygen (O_2)	20.95	
Argon (Ar)	0.93	
Carbon dioxide (CO_2)	0.041	
All others	0.003	

Carbon Cycle

The process described above essentially represents the atmospheric component of the **carbon cycle**, the

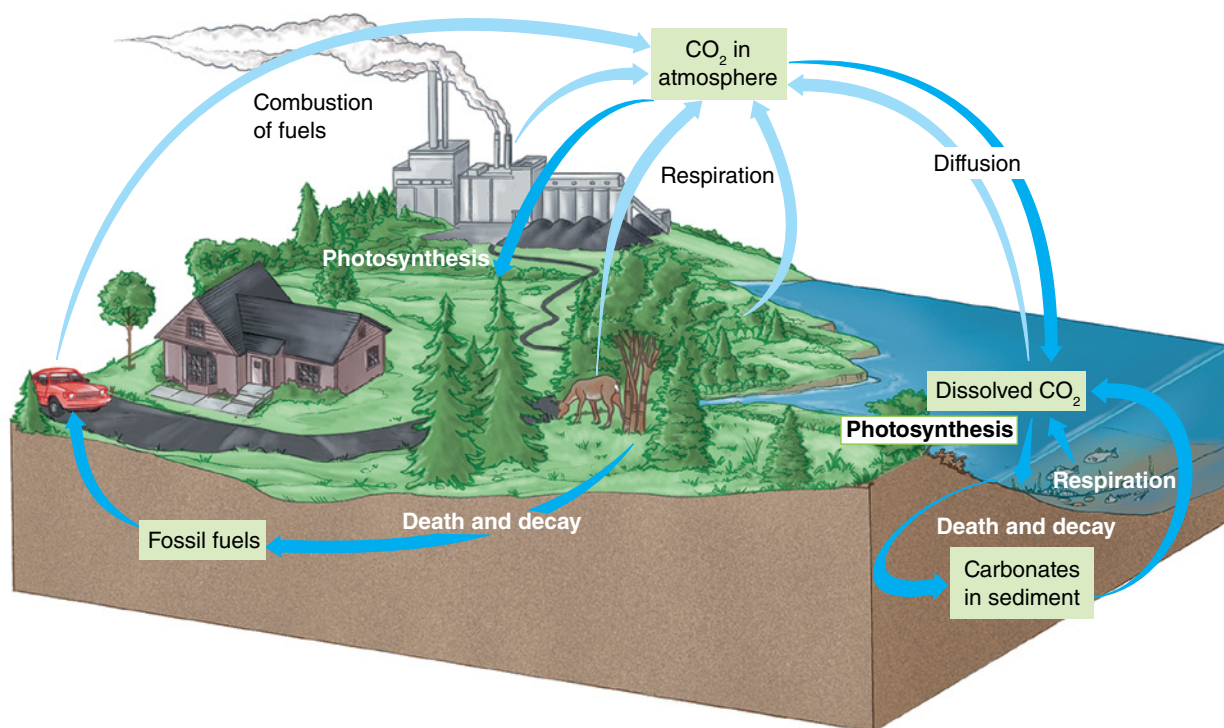


FIGURE 2.2 The global carbon cycle.

continuous movement of carbon through the Earth–ocean–atmosphere system. Carbon can exist in various Earth–ocean–atmosphere **reservoirs**—the components of a system that effectively store matter and/or energy for a certain period of time, after which they allow for the movement (**flux**) of that matter and/or energy to another component of the system. Carbon reservoirs include the atmosphere, which houses CO₂; the biosphere, which comprises all living matter; and the oceans, which include dissolved carbonates (FIGURE 2.2). Over time carbon cycles among these various reservoirs. The carbon residence time is different for each reservoir, with the rates of exchange directly related to the size of the reservoir. The largest carbon reservoir, comprising the vast majority of carbon in the Earth–ocean–atmosphere system, is sedimentary rock, which may store carbon for billions of years.

The second-largest reservoir is the oceans, which act as a **sink** for atmospheric CO₂ by absorbing many gigatons of CO₂ from the atmosphere each year. Over time CO₂ is transported from the atmosphere into the deep ocean layers in a slow process. Once the CO₂ is transported into the deep ocean, it may remain there for many thousands of years.

The biosphere (including soil) is also a reservoir that acts as a sink for CO₂ from the atmosphere. It is then transported and stored elsewhere in the system. For example, the vast majority of carbon in the rock reservoir was extracted from the atmosphere through

biological processes. Residence time associated with the biosphere may be examined on a number of levels. Carbon is held directly in the biosphere as long as the living organism remains alive. Once the organism dies, carbon exits this sink as the remains of the organism decay. Some of this carbon may become buried naturally and transported into the rock reservoir. This process is effective in marine environments where an abundance of organic matter filters to the ocean floor, building huge layers of organic matter over time. Some of the decaying carbon dissolves directly into water, becoming part of the oceanic carbon reservoir, and some reenters the atmosphere through **diffusion**. Much oceanic biomass eventually solidifies into sedimentary rock. Finally, the atmosphere represents the smallest carbon sink, and the carbon exchange rate to this reservoir is rapid—only about 100 years.

The natural carbon cycle is being disrupted by human activities. Since the dawn of the Industrial Revolution in the late 1700s, people have been burning ever-increasing quantities of **fossil fuels**—deposits of carbon primarily in the form of coal, oil, and natural gas. Fossil fuels contain carbon that was removed from the atmosphere long ago through natural processes and stored in the vast rock reservoir. Normally, this carbon would be re-released back to the atmosphere over millions of years. However, humans are extracting and releasing this material back to the atmosphere in very short periods of time. The atmospheric quantity of CO₂ increased from 270 ppm

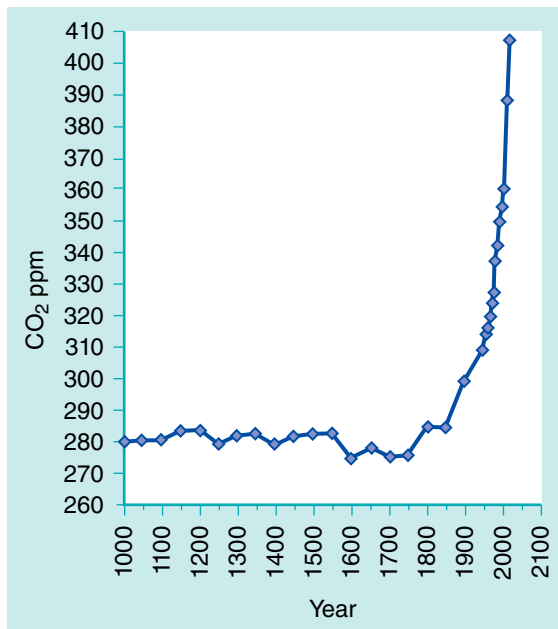


FIGURE 2.3 Exponential rise in atmospheric carbon dioxide over the past 1000 years.

in 1800 to 407 ppm today, with the bulk of the increase occurring since 1950 (**FIGURE 2.3**).

Whereas clues of the atmospheric concentration of CO_2 in the distant past come from chemical analysis of air bubbles trapped in ice, CO_2 concentration has been measured directly since 1957 atop Mauna Loa in Hawaii—a site as far removed as possible from local sources of pollution. The time series of atmospheric CO_2 since 1957 is known as the **Keeling curve** (**FIGURE 2.4**), named for Charles Keeling, the climatologist who showed that CO_2 released from fossil fuel combustion would accumulate significantly in the atmosphere.

The Keeling curve not only verifies the rapid increase since 1957, but it also reveals the seasonal cycle of CO_2 . Maximum concentrations occur in early spring in the northern hemisphere, where most of the world's middle- and high-latitude forests are located. The relative lack of photosynthetic activity during the dormant northern winter months causes a buildup of atmospheric CO_2 into March. Likewise, minimum atmospheric CO_2 in northern hemisphere autumn results from the buildup of biomass throughout the northern hemisphere's spring and summer months.

The long-term exponential growth in the atmospheric CO_2 concentration concerns most climatologists and environmental scientists. Carbon dioxide is an integral component of Earth's energy balance because it absorbs energy that is radiated from the Earth and then reemits energy back downward to the Earth, thereby keeping the surface warmer than it would be if the CO_2 were not present. This phenomenon is known as the **greenhouse effect**. The rapid increase in the quantity

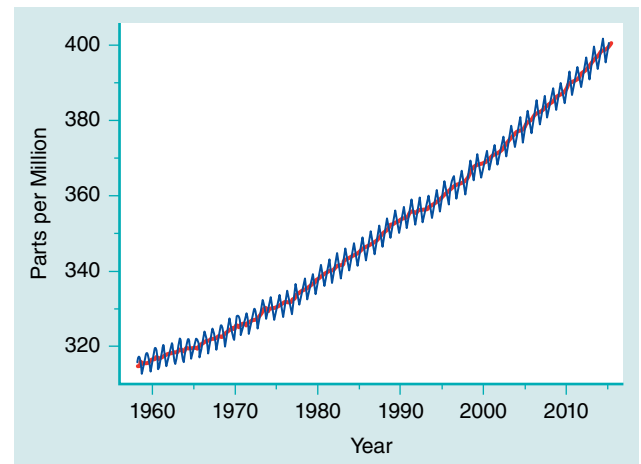


FIGURE 2.4 The Keeling curve—atmospheric CO_2 at Mauna Loa Observatory.

Data from: Scripps Institution of Oceanography and NOAA Earth System Research Laboratory.

of atmospheric CO_2 is considered the culprit for the observed increases in temperature of Earth's surface in the last several decades.

Constant and Variable Gases

Constant gases are those that have relatively long residence times in the atmosphere and that occur in uniform proportions across the globe and upward through the bulk of the atmosphere. These gases include nitrogen, oxygen, argon, neon, helium, krypton, and xenon.

Variable gases are those that change in quantity from place to place or over time (**TABLE 2.2**). They generally have shorter residence times than constant gases, as various processes combine to cycle the gases through reservoirs. The most abundant variable gas is water vapor, which can occupy as much as 4% of the lower atmosphere by volume. Higher percentages of water vapor are impossible because atmospheric processes (cloud formation and precipitation) limit the amount that may be present in the atmosphere for any location. The atmosphere is efficient in ridding itself of excess water vapor.

The amount of water vapor in the atmosphere varies widely across space because water and energy must be available at the surface for *evaporation* to occur. Water vapor content is maximized over locations with abundant energy and surface water, so the wettest atmospheres occur over tropical waters and rain forest regions. In addition, water vapor is largely limited to the lower atmosphere because as height increases, atmospheric water vapor is increasingly likely to condense to liquid water in the cooler, high-altitude conditions.

Surprisingly, some locations that experience little precipitation may have abundant water vapor in the atmosphere. The maximum amount of water vapor that may exist in the atmosphere is directly related to air

TABLE 2.2 Concentrations of Variable Gases of the Atmosphere

Gas	ppm of Air
Water vapor (H_2O_v)	0.1–40,000
Carbon dioxide (CO_2)	~407
Methane (CH_4)	~1.8
Hydrogen (H_2)	~0.6
Nitrous oxide (N_2O)	~0.31
Carbon monoxide (CO)	~0.09
Ozone (O_3)	~0.4
Fluorocarbon 12 (CCl_2F_2)	~0.0005

temperature. When high temperatures combine with a nearby surface water source, high amounts of water vapor are usually present. For example, the Red Sea region tends to have high quantities of atmospheric water vapor despite the lack of precipitation. This region is dry not because water vapor is unavailable but because the region lacks a means by which the precipitation process can occur easily.

As implied by the Red Sea example, deserts are generally not the regions of lowest atmospheric water vapor content. Instead, polar regions are normally the driest locations on Earth. This is because little energy is present in cold air to evaporate water. Furthermore, as air cools, water vapor readily condenses to form clouds and perhaps precipitation, thereby minimizing the mass of water vapor in the atmosphere. So the regions with the least water vapor tend to be the coldest locations on Earth. Over such locations in winter, the water vapor content may approach zero. The total will never actually reach zero because there is always at least some water vapor present in the lower atmosphere, but the total reaches about 0.00001% of the atmospheric volume in central Antarctica.

Several other variable gases are important. Among these, CO_2 is most abundant. As stated earlier, the variable nature of CO_2 stems from its increasing quantity over time, since the late 1700s. The rate of increase is about 0.4% per year or by about 35% since 1800. Other notable variable gases include CH_4 , nitrous oxide (N_2O), carbon monoxide (CO), tropospheric ozone (O_3), and a family of chemicals known as **chlorofluorocarbons**

(**CFCs**). Humans have had at least some influence in the concentration of all these gases, and CFCs are entirely human derived. Collectively, these gases make up only a small amount of the atmosphere, but they can have important implications for some processes.

► Faint Young Sun Paradox

Evidence contained in sedimentary rocks and sediments, ice sheets, and fossils reveals that Earth's average temperature has remained within a range of about 15°C (27°F) for most, if not all, of its geological history. This implies that even global-scale shifts in mean environmental conditions, from ice ages to ice-free conditions on Earth, have occurred within a range of temperature variability that is smaller than the summer to winter temperature difference at most locations outside the tropics.

This fact has caused considerable consternation for many climate scientists because of an apparent contradiction between what is known about energy released during the evolution of stars, such as our Sun, and evidence of Earth's temperature through geological time. Stars obtain energy through the constant nuclear fusion of hydrogen into heavier elements. These reactions cause stars to expand gradually and grow hotter and brighter over time. Eventually, stars expend their sources of energy and extinguish themselves. We can assume that energy emitted from the early Sun was about 25% to 30% less than that emitted today, because this pattern is observed throughout the life cycle of other stars like the Sun. We also know that even small changes in solar output can induce drastic climatic changes on Earth. If solar output today were decreased by 25% to 30%, temperatures would quickly plummet to a point whereby Earth would be entirely frozen. Because the young Sun must have been weak, at first glance it would appear that Earth must have been frozen for the first 3 billion years of its history. But evidence does not support the notion that Earth was ever below freezing on a global annual average basis. Furthermore, little credible evidence has been found for widespread glaciation during the first half of Earth's existence. This apparent contradiction between a weak Sun but relatively warm global conditions is the **faint young Sun paradox**.

How could temperatures have been above freezing during the early times of geological history? How could Earth maintain a small variance in temperature over time if the Sun were much weaker in the early history of the planet? How could temperatures maintain themselves over time as the Sun grew hotter?

The most logical answer to these questions is that the Earth–ocean–atmosphere system must have some

type of internal regulator that keeps temperatures within a reasonable range regardless of changes to solar output over time. This regulator must have been present in the early atmosphere. How would this have happened? Examining the radiation balance of Earth today reveals that surface temperatures are only indirectly caused by incoming solar radiation—**insolation**—being absorbed at the surface. If surface receipt of solar radiation alone determined temperatures, average Earth temperatures would be about -18°C (0°F). Instead, the transfer of energy (either from the Sun or Earth) absorbed in the atmosphere down to the surface augments radiation received at the surface directly from the Sun. Certain gases in the atmosphere, such as H_2O and CO_2 , are known to be efficient absorbers of energy escaping the surface. Much of this energy is then reemitted back down to reheat the surface. This process—the greenhouse effect—is responsible for the life-supporting temperatures we enjoy today. The net result is that the average temperature of Earth is raised from -18°C (0°F) to a more comfortable 15°C (59°F).

So which **greenhouse gases** could have helped the early Earth to remain relatively warm? The two most abundant greenhouse gases in today's atmosphere are water vapor and CO_2 . As far as we can tell, the quantity of water vapor has remained relatively constant since primordial times. Until recently it was assumed that the wide fluctuations of CO_2 over time caused Earth's temperature to remain relatively stable via the greenhouse effect. That argument suggests that during times in Earth history when the Sun was relatively weak, such as in Earth's early atmosphere, the high concentrations of CO_2 may have effectively absorbed large amounts of radiation emitted from Earth and reemitted much of that radiation back downward in the greenhouse effect. Just as the solar output began to increase, the onset of plant evolution and proliferation would have been removing enough atmospheric CO_2 to keep the insolation and temperatures on Earth fairly constant.

But if excessive levels of CO_2 indeed caused Earth to remain warm despite a weak Sun, such concentrations probably would have been too high to allow the generation of organic molecules, so life could not have existed easily. Furthermore, no geological evidence has been found to suggest that CO_2 concentrations were ever large enough to have created such a strong greenhouse effect. Specifically, in an oxygen-free atmosphere such as early Earth would have had, CO_2 levels of about eight times today's concentrations would have produced the mineral **siderite** (FeCO_3) in the top layers of the soil as iron reacted with the CO_2 , but not enough FeCO_3 has been found in relic soils to support this hypothesis. Better explanations for the faint young Sun paradox were sought.

A second explanation is that ammonia (NH_3) caused the early greenhouse effect. This hypothesis was proposed by Carl Sagan and George Mullen of Cornell University in the late 1970s and was based on the observation that NH_3 behaves as a strong greenhouse gas. The problem with this argument is that experiments have shown that NH_3 is easily broken up by UV radiation in oxygen-free conditions, such as in the atmosphere before the arrival of photosynthesis. Nevertheless, the NH_3 explanation is still plausible because shielding by other gases may have allowed NH_3 to accumulate in the lower atmosphere and be an important greenhouse gas.

A third explanation, proposed by Harvard scientists in the early 2000s, is that in the pre-photosynthesis Earth, the planet's oxygen-devoid atmosphere made conditions ideal for oxygen-intolerant microbes called **methanogens**. These methanogens (so-named because they release CH_4 as a waste product) likely allowed CH_4 to produce a strong greenhouse effect, which would have warmed Earth even though the Sun emitted less radiation at the time. It is well known that CH_4 is a highly effective greenhouse gas. Once oxygen entered the atmosphere from photosynthesis, the methanogens began to die off and CH_4 became less important as a greenhouse gas. In today's oxygen-rich atmosphere the concentration of CH_4 is extremely minute—an average of only 1.8 ppm in the atmosphere. Some geoscientists surmise that the demise of the methanogens caused Earth's first global ice age and perhaps contributed to subsequent ice ages.

Regardless of the explanation, most of Earth's history is thought to have been dominated by somewhat higher temperatures than exist today, or at least temperatures that are not far below those now. The debate over the explanation of the faint young Sun paradox lingers on.

► Atmospheric Structure

The atmosphere may be divided into a series of layers based on thermal qualities (**FIGURE 2.5**). The lowest layer of the atmosphere is called the **troposphere**. This is a very thin zone confined to the first 8 to 20 km (5 to 12 mi) above Earth's surface, yet this atmospheric layer contains approximately 75% of the mass of the atmosphere. The compressibility of air allows its weight to exert a downward force on, and compress, the lower atmosphere. This layer therefore also contains air of the greatest mass per unit volume: **density**.

The term “troposphere” is derived from the Greek word meaning “to turn.” This indicates that the troposphere is a region in which mass is constantly overturning, largely as a result of thermodynamic (heat-driven) processes. Most insolation passes through the atmosphere

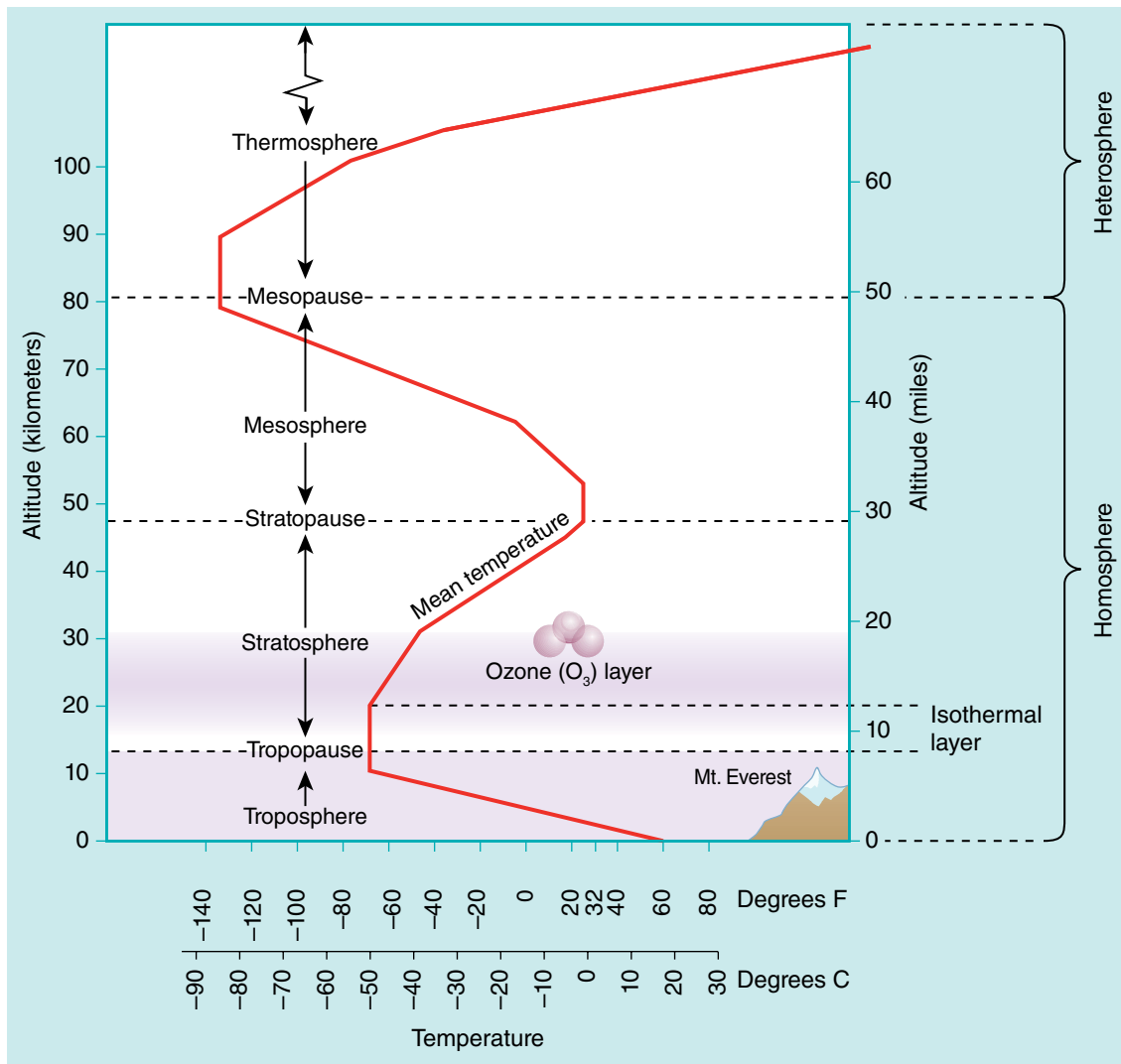


FIGURE 2.5 The vertical structure of the atmosphere.

before being absorbed by the Earth's surface. The heated surface then warms the air directly above it through the process of **conduction**. This gives the lowest layers of the atmosphere buoyancy and causes the air to rise in a process known as **convection**. Eventually this air cools and sinks. Because this vertical movement is integral to the development of most weather-related processes, the troposphere is sometimes referred to as the "weather sphere."

Because the atmosphere is heated primarily from Earth's surface and because the compression of atmospheric gas decreases with height (as the weight of the atmosphere above it decreases), a decrease of temperature usually occurs with increasing height through the troposphere. This decrease is known as the **environmental lapse rate**. Through the troposphere, air cools at an average rate of $6.5^{\circ}\text{C}/\text{km}$ (or $3.5^{\circ}\text{F}/1000\text{ ft}$), although this value may vary widely from place to place and from day to day, and even on an hourly basis.

According to one form of **Charles' law**, in an ideal gas (which the atmosphere approximates), density decreases as temperature increases if pressure remains constant. Air that is warmer than surrounding air thus rises. Because Earth is not heated equally and relatively warm air rises, the troposphere does not have a uniform depth. Instead, the troposphere is thicker near the equator than near the poles. Near the equator the layer is approximately 20 km (12 mi) thick, whereas near the poles in winter the thickness is only about 8 km (5 mi). Roughly the same amount of atmospheric mass exists over the two locations, but the density of that air is less over the equator and greater over the poles.

The top of the troposphere is called the **tropopause**. This feature marks the boundary between the troposphere below and the next layer of the atmosphere above (Figure 2.5). The average temperature at the tropopause is about -57°C (-70°F), which represents quite

a decrease from the 15°C (59°F) average temperature of the surface.

The layer above the troposphere is the **stratosphere**. Temperatures remain somewhat constant from the tropopause upward into the stratosphere for about 10 km (6 mi). Any zone of relatively constant temperature with height, such as this one, is called an **isothermal layer**. Above the isothermal layer temperatures actually increase with height through the rest of the stratosphere. This increase of temperature with height—a **temperature inversion**—is caused by the absorption of UV radiation by the triatomic form of oxygen (O_3), or ozone.

The so-called ozone layer in the stratosphere occurs because of several processes that have important implications for terrestrial life on the planet. To understand the workings of the ozone layer we must first review the nature of radiation reaching Earth from the Sun. Insolation arrives in Earth's atmosphere in a wide range of **wavelengths**, which are measured in **micrometers** (millionths of a meter [μm]). Shorter wavelengths are associated with more intense (and therefore more harmful to living things) energy than longer wavelengths. The Sun emits more energy at a wavelength of about 0.5 μm than at any other wavelength, with successively less energy emitted at successively shorter and longer wavelengths (**FIGURE 2.6**). By convention, energy from solar origin shorter than 4.0 μm is usually referred to as **shortwave radiation** in the atmospheric sciences. Wavelengths of the peak amounts of shortwave radiation occur in the visible part (0.4 to 0.7 μm) of the **electromagnetic spectrum**—the full assemblage of all possible wavelengths of electromagnetic energy.

Any insolation with wavelengths less than 0.4 μm is too intense to allow terrestrial life to exist. UV radiation falls between wavelengths of 0.01 and 0.40 μm , making UV radiation harmful to living organisms. Fortunately, N_2 absorbs electromagnetic radiation of wavelengths below 0.12 μm . But how does the ozone layer protect us from UV radiation at wavelengths between 0.12 and 0.40 μm ?

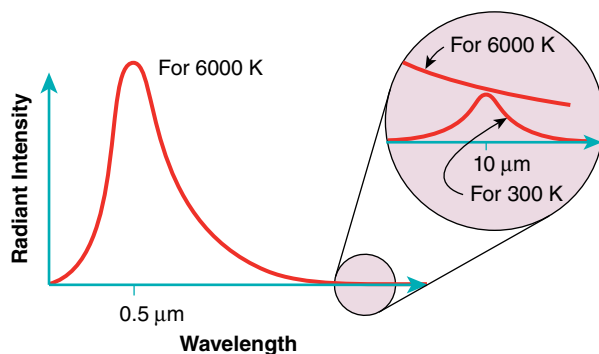


FIGURE 2.6 Emitted energy by wavelength for the Sun and Earth, assuming a surface temperature of 6000 K for the Sun and 300 K for the Earth.

Some of the diatomic oxygen (O_2) that enters the atmosphere from photosynthesis near the surface reaches the stratosphere over time. Because O_2 molecules effectively absorb UV radiation at wavelengths between 0.12 and 0.18 μm , the O_2 reaching the stratosphere is exposed to incoming harmful radiation. When this radiant energy strikes O_2 molecules, a chemical reaction in the presence of light that splits the molecular bonds—**photodissociation**—is triggered and two monatomic oxygen (O) atoms are liberated. Because O is inherently unstable, it bonds quickly and easily with other atoms and molecules. Some of these O atoms chemically bond with an O_2 molecule to form an O_3 molecule that effectively absorbs UV radiation at wavelengths between 0.18 and 0.34 μm . But in the absorption process the O_3 becomes photodissociated into O and O_2 , and the O then bonds with another O_2 to form O_3 . The process then repeats endlessly, ensuring that oxygen is continuously being reworked into O_3 in the stratosphere. UV radiation at wavelengths between 0.18 and 0.34 μm is effectively “absorbed”—actually used in chemical processes with emitted heat as a byproduct—such that only the UV radiation at wavelengths between 0.34 and 0.40 μm filters to Earth's surface. This harmful radiation can cause skin cancer, cataracts, and other problems if we are exposed to it in large doses, but at least we are protected from the much more harmful shorter UV wavelengths.

Early in geological history, the first organisms must have formed in murky waters because no O_2 (and, therefore, no O_3) existed to protect them from UV radiation. By the time life evolved into shallow water areas and onto land surfaces, O_2 released from photosynthesis had built a stratospheric O_3 layer. Life has never been exposed to excessive amounts of UV radiation and has never adapted to it. Increasing exposure to UV radiation is damaging to terrestrial life.

Humans have contributed to thinning the fragile O_3 layer over the past half-century by producing CFCs. Most general uses for CFCs involved refrigeration both as a gas (Freon) and as an insulating substance (foam and Styrofoam). CFCs were also used as a propellant for aerosol sprays. When chlorine from CFCs and bromine are released to the atmosphere, they can make their way upward to the stratosphere where they readily bond with monatomic oxygen atoms. Such a bond does not allow the O to bond with O_2 to produce the O_3 that would absorb UV radiation. The result is that increased amounts of UV radiation reach the surface, where adverse effects on organisms occur. Although O_3 is found throughout the stratosphere, if all stratospheric ozone were compressed to the surface it would create a layer only 3 mm thick. Since the U.S. ban on CFC production took effect on January 1, 1996, the ozone layer has shown some signs of recovery.

The ozone formation process is responsible for the temperature inversion in the stratosphere. As O_3 molecules absorb UV radiation, they acquire energy. The O_3 at the top of the stratosphere has the first opportunity to gain energy (and, therefore, temperature, because temperature is a measure of the energy or heat content of matter) from incoming UV radiation. Its temperature, therefore, is higher than for molecules lower in the stratosphere. The process of O_3 production and dissociation happens in the stratosphere because this is the uppermost layer for which atmospheric density is high enough to allow O and O_2 to meet and bond quickly enough so that incoming UV radiation is absorbed effectively. Temperatures rise to approximately -18°C (0°F) at the **stratopause**, which is about 48 km (29 mi) above the surface. The stratopause is the boundary between the stratosphere and the layer above it.

The layer above the stratosphere is the **mesosphere**, from the Greek prefix *meso-*, which means “middle.” Although this layer does sit near the middle of the atmosphere from an altitude perspective—in the region between the stratopause and about 80 km (50 mi) above the surface—the low-density mesosphere does not represent the middle of the atmosphere by density or volume. Because of the compressibility of gases, the middle of the atmosphere by density and volume is only about 5.5 km (3.4 mi) above the surface—well within the troposphere.

Similar to the troposphere, temperatures in the mesosphere decrease with height. The temperature inversion characteristic of the stratosphere is not present in the mesosphere because it is too high for photodissociated O_2 to encounter other oxygen atoms or molecules to bond with quickly enough to absorb the incoming UV radiation. Instead, the increased density and proximity to the surface and stratospheric heat sources below the mesosphere make the lower mesosphere warmer than the top of this layer. Temperatures at the **mesopause** average approximately -84°C (-120°F).

Few processes of consequence to weather and climate are known to occur in the mesosphere in part because so little atmospheric mass exists in this zone. Charged particles from the Sun that are captured by Earth’s magnetic field in the mesosphere can disrupt telecommunications during their release of energy. These same charged particles are also responsible for the northern lights (*aurora borealis*; **FIGURE 2.7**) and southern lights (*aurora australis*). But even these processes have minimal effect on Earth’s weather and climate.

From the surface up through the mesosphere, the proportion of atmospheric gases is about the same as that at the surface, except for the greater concentration of O_3 in the stratosphere. The first three “spheres” of the atmosphere are thus sometimes collectively known as the **homosphere**, which means “same sphere.” Above



FIGURE 2.7 The *aurora borealis*.

© Roman Krochuk/Shutterstock.

the mesosphere gases stratify into layers according to their atomic weights because there is so little mass to “stir them up.” That region is termed the **heterosphere**.

The heterosphere corresponds to the final thermal layer of the atmosphere, the **thermosphere**. Like the stratosphere, the thermosphere is characterized by temperatures that increase with height—a temperature inversion. Unlike the stratosphere, however, where the inversion exists because of O_3 absorption of insolation, the thermospheric temperature inversion occurs because the uppermost N_2 and O_2 molecules have the first opportunity to absorb insolation. Their position allows them to attain extraordinarily high temperatures because Earth’s magnetic field captures charged high-energy particles from the Sun.

The number of those molecules with such high temperatures is miniscule, however, because of the sparseness of the atmosphere at such heights. The total mass of the thermosphere accounts for only about 0.01% of the total atmospheric mass. The decrease of density, mass, and volume of the atmosphere can be expressed by the **mean free path** of a molecule—the distance an individual molecule must travel before encountering another molecule. The mean free path at the surface is on the order of a micrometer. By contrast, in the thermosphere the mean free path is on the order of a kilometer or more. Despite the fact that the individual molecules have very high amounts of energy, there are so few molecules to contain the heat that even if you could somehow survive for more than a fraction of a second at those heights, you would freeze to death instantly even at temperatures above 1100°C (2000°F)!

A thermopause does not exist; instead, the atmosphere simply merges slowly into interplanetary space. Individual gas molecules may be gravitationally attracted to the planet for quite a distance into space. Most agree, however, that the atmosphere extends no higher than about 1000 km (600 mi) above the Earth’s surface.

► Summary

The atmosphere is a fragile and complex collection of gases gravitationally attracted to Earth. It originated early in the history of the planet as volcanic materials cooled and outgassed. The early atmosphere is believed to have been composed primarily of N_2 and CO_2 , but O_2 gradually replaced CO_2 as the second-most abundant gas since the evolution and proliferation of simple organisms and green plants, which have stored carbon in their biomass and released O_2 into the atmosphere over the past 3 billion years.

Carbon is stored for certain periods of time within a number of reservoirs such as rock layers, the ocean, biomass, and the atmosphere. This cycle of carbon is important in the history of Earth. Its importance has been challenged recently, however, by evidence suggesting that methane-emitting microbes may have played a greater role than previously believed in Earth’s early history by absorbing energy emitted by Earth via the greenhouse effect. This methane may have kept Earth’s temperatures within a narrow range of variability, despite a weaker solar output.

The troposphere is the lowest layer of the atmosphere and is where nearly all weather and climate processes of importance occur. Temperatures in the troposphere usually decrease with height because of the increased density in the most compressed part of the atmosphere—the part nearest to the surface—and because of proximity to the surface, which absorbs insolation more effectively than the air above it. The stratosphere is the second layer from the surface and is characterized by increases in temperature with height—a temperature inversion—because of ozone absorption. In the mesosphere temperatures decrease with height for the same reason they do in the troposphere. The final thermal layer of the atmosphere is the thermosphere, which is characterized by a temperature inversion because of the direct absorption of incoming radiation by N_2 and O_2 .

Key Terms

Aerosol
Atmosphere
Biosphere
Carbon cycle
Charles’ law
Chlorofluorocarbon (CFC)
Condensation
Conduction
Constant gas
Convection

Density
Diffusion
Electromagnetic spectrum
Environmental lapse rate
Eukaryote
Evaporation
Faint young Sun paradox
Fermentation
Flux
Fossil fuel

Greenhouse effect
Greenhouse gas
Heterosphere
Homosphere
Hydrosphere
Hydrostatic equilibrium
Insolation
Isothermal layer
Keeling curve
Lithosphere

Mean free path	Ozone (O ₃)	Sink
Mesopause	Photodissociation	Solar wind
Mesosphere	Photosynthesis	Stratopause
Methane (CH ₄)	Planetesimal	Stratosphere
Methanogen	Prokaryote	Temperature inversion
Micrometer	Reservoir	Thermosphere
Nebula	Residence time	Tropopause
Newton's second law of motion	Respiration	Troposphere
Nuclear fusion	Second law of thermodynamics	Ultraviolet (UV) radiation
Oort cloud	Shortwave radiation	Variable gas
Outgassing	Siderite	Wavelength

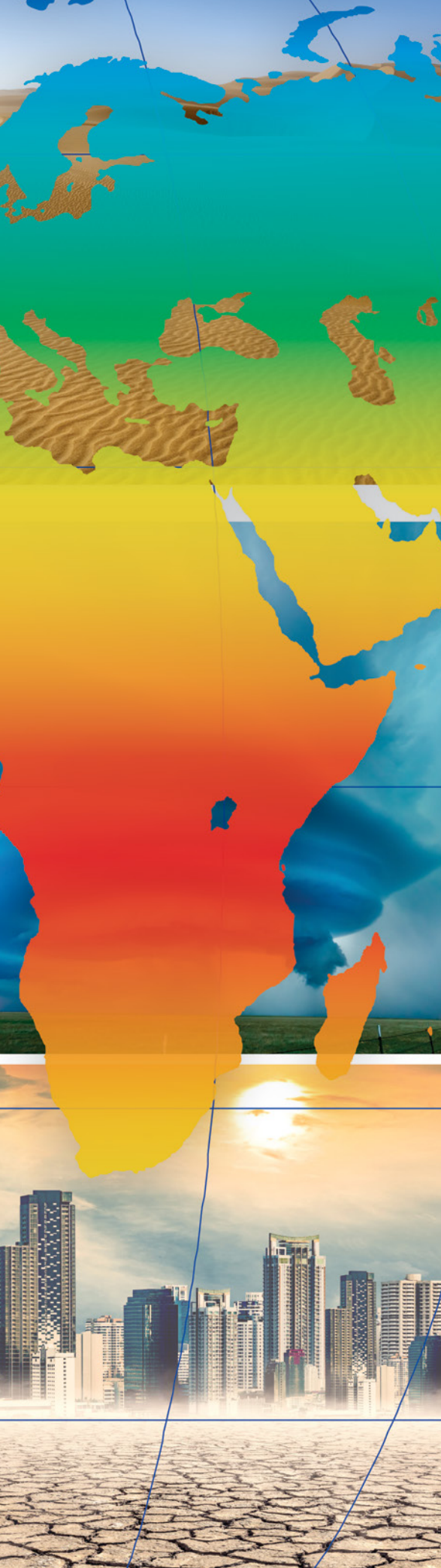
Terms in italics also appeared in Chapter 1.

Review Questions

1. Explain how Earth and its atmosphere formed.
2. How is today's atmosphere similar to and different from early Earth's atmosphere?
3. Describe how oxygen came to comprise almost 21% of the atmosphere today.
4. Given that solar output has increased over the past 4.6 billion years, how have Earth's temperatures remained fairly constant over that same time?
5. What is residence time and why is it important?
6. What is the carbon cycle and how does it operate?
7. Describe the thermal structure of the atmosphere.
8. What causes the thermal characteristics associated with each thermal layer of the atmosphere?
9. Compare and contrast the heterosphere and the homosphere.
10. Why is there no defined top to the atmosphere?

Questions for Thought

1. Give as many examples of the second law of thermodynamics as you can think of, both related to and not related to the atmosphere.
2. Why do the *aurora borealis* and *aurora australis* occur in the mesosphere and not elsewhere in the atmosphere?
3. Why are the auroras not visible in the tropical parts of the Earth?



PART 2

Climatological Processes

CHAPTER 3 Controls on the Climate System

- Latitude
- Earth–Sun Relationships
- Distance to Large Bodies of Water
- Circulation
- Topography
- Local Features
- Putting It All Together: Spatial and Seasonal Variations in Energy
- Summary
- Key Terms
- Review Questions
- Questions for Thought

CHAPTER 4 Atmospheric Interactions with the Other “Spheres”

- Ocean Circulation
- El Niño–Southern Oscillation Events
- Volcanic Activity and Climate
- Deforestation and Desertification
- Cryospheric Changes
- Summary
- Key Terms
- Review Questions
- Questions for Thought

CHAPTER 5 Energy, Matter, and Momentum Exchanges near the Surface

- Properties of the Troposphere
- Near-Surface Troposphere
- Energy in the Climate System
- Local Flux of Matter: Moisture in the Local Atmosphere

Atmospheric Statics, the Hydrostatic Equation, and Stability
Momentum Flux
Putting It All Together: Thermal and Mechanical Turbulence and the Richardson Number
Summary
Key Terms
Review Questions
Questions for Thought

CHAPTER 6 Global Hydrologic Cycle and Surface Water Balance

Global Hydrologic Cycle
Surface Water Balance
Putting It All Together: A Worked Example of the Surface Water Balance
Types of Surface Water Balance Models
Water Balance Diagrams
Drought Indices
Summary
Key Terms
Review Questions
Questions for Thought

CHAPTER 7 General Circulation and Secondary Circulations

Circulation of a Nonrotating Earth
Idealized General Circulation on a Rotating Planet
Modifications to the Idealized General Circulation: Observed Surface Patterns
Putting It All Together: Surface Pressure Patterns and Impacts
Modifications to the Idealized General Circulation: Upper-Level Airflow and Secondary Circulations
Summary
Key Terms
Review Questions
Questions for Thought



CHAPTER 3

Controls on the Climate System

CHAPTER AT A GLANCE

- Latitude
- Earth–Sun Relationships
 - Revolution
 - Rotation
 - Axial Tilt and Parallelism
 - Combined Effect of Revolution, Rotation, and Tilt
- Distance to Large Bodies of Water
- Circulation
 - Pressure
 - Wind
 - Surface Versus Upper-Level Winds
 - Vertical Motion
 - Cyclones and Anticyclones
 - Oceanic Circulation
- Topography
- Local Features
- Putting It All Together: Spatial and Seasonal Variations in Energy
- Summary
- Key Terms
- Review Questions
- Questions for Thought

Several factors control the general state of the atmosphere for a given location and, therefore, govern weather and climate. For instance, we expect locations in the midlatitudes to experience pronounced differences in temperature throughout the year. Most

tropical locations show much less seasonal change in temperature, but they may have seasonal precipitation changes. These differences are due in part to the influence of the various climatic controls. This chapter details how and why the climatic “site” of a place is dictated by its

latitude, location relative to solar radiation receipt, and local factors. The climatic “situation” of a place relative to other features, such as water bodies and major atmospheric circulation features, is also presented because it impacts the types and distribution of climates that we see on Earth.

► Latitude

To understand the importance of location on Earth relative to the Sun’s direct rays, we must first review the concept of **latitude**—a set of imaginary lines that run from west to east around the Earth, paralleling the equator and each other (FIGURE 3.1). They are therefore usually referred to as “parallels.” Latitude lines are named for the angle they make between their location, the center of the Earth, and the equator. The latitude of the equator itself must therefore be 0° and the North and South Poles have latitudes of 90° . We always indicate whether a latitude coordinate is north or south of the equator (0°) by using the letter “N” or “S” after the angle. For instance, Kent, Ohio, lies at approximately 41°N latitude, or almost half the angular distance between the equator and the North Pole. Parallels of latitude provide an indicator of the location of a place relative to the equator. More specifically, the location of any place can be expressed in terms of how far north or south of the equator the place lies, with one degree of latitude corresponding roughly to 111 km (69 mi) on Earth’s surface.

Longitude is defined as a set of imaginary north–south lines running through the North and South Poles perpendicular to the equator and every other parallel of

latitude (Figure 3.1). Longitude lines are also referred to as “meridians.” Unlike lines of latitude, meridians of longitude are not parallel to each other; they converge toward the poles, even though they may not appear to converge because of the way that some maps are constructed. The longitude coordinate actually measures the angle created between the point of interest, the center of the Earth at the same parallel of latitude, and a point on that latitude along the arbitrarily defined **prime meridian**—the meridian running through Greenwich, England, which is at 0° longitude. Each degree of angle east or west of Greenwich represents one degree east or west longitude, with the direction designated by “E” or “W” after the angle. The maximum longitude coordinate is 180° , or halfway around the world from the prime meridian. The combination of a latitude and longitude coordinate in this grid system allows us to pinpoint any location on the surface of the Earth accurately.

But why does latitude have anything to do with climate? Quite simply, as latitude increases beyond the tropics, solar energy—*insolation*—on a given day strikes the surface at a decreasing angle, from 90° (where the ray is directly overhead) to 0° (where the Sun is on the horizon; FIGURE 3.2). The lower the Sun’s angle (i.e., the closer to 0°) above the horizon, the less intense the insolation, because the ray can undergo **attenuation**—the depletion of solar rays—more effectively by interacting with more atmospheric particles when it reaches Earth from a lower angle. When the Sun is directly overhead (i.e., at a 90° Sun angle), solar rays pass through the atmosphere most efficiently because they strike the surface perpendicular to it and have fewer opportunities to be attenuated. The result is that the rays are more intense when they hit the surface.

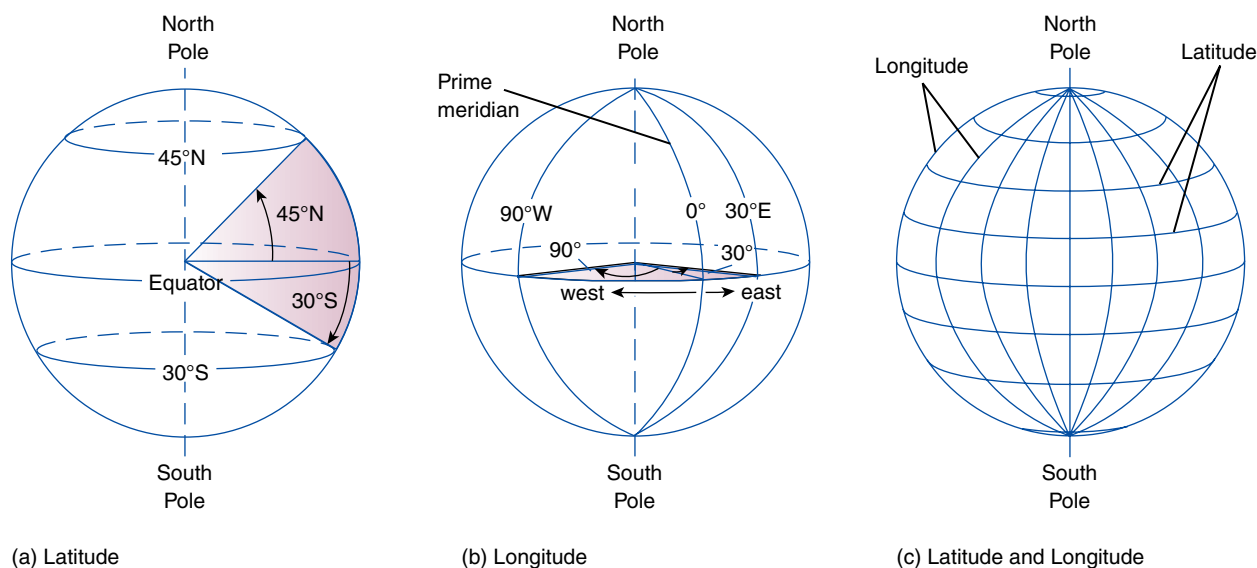


FIGURE 3.1 Lines of latitude and longitude.

Gases, liquid and frozen water, water vapor, dust, and other *aerosols* floating in the air absorb, reflect, and scatter away insolation. Attenuation increases as concentrations of particles in the air and the **path length** of radiant energy increase through the depth of the atmosphere. The more attenuation there is in the atmosphere, the less intense the insolation will be when it strikes Earth's surface. Imagine using a flashlight to illuminate the sidewalk at night. Then imagine the same flashlight on a foggy day shining on the sidewalk or the same flashlight atop a skyscraper attempting to illuminate the same sidewalk. The greater number of water molecules on the foggy day or the greater distance atop the skyscraper allows for more attenuation, thereby reducing the amount of light striking the sidewalk. Increased attenuation, therefore, leads to decreased surface

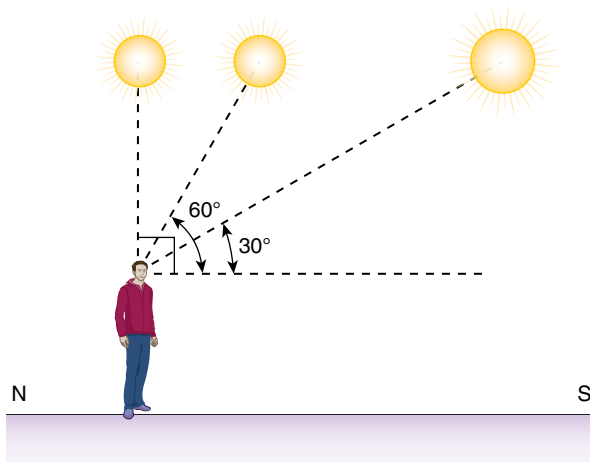


FIGURE 3.2 Variation in local sun angle.

heating power. By contrast, a relatively short path length through the atmosphere to the surface allows for the energy to be more concentrated per unit of surface area, with less attenuation by atmospheric aerosols.

Beam spreading is also a concept of importance relative to surface energy receipt. To illustrate this notion, imagine you are holding a flashlight that is pointed straight down at the floor. The beam of energy is focused and the illuminated area will likely approximate the actual area of the shining face of the flashlight. Energy is concentrated through a small area on the floor in that situation. Now imagine you shine the flashlight across the floor some meters away from you. The illuminated region now expands and elongates, even though the same battery is producing the same amount of light from the flashlight. The same amount of energy is now spread across a larger area. In the same way, when the Sun is shining on a location at a low angle, warming is less intense than if the Sun were shining from a high angle because its energy is dispersed across a wider region of Earth's surface.

Earth's spherical shape causes areas receiving lower solar angles to see higher attenuation and beam spreading rates because of long path lengths through the atmosphere to the surface. To illustrate this concept, imagine two lines, A and B, as shown in **FIGURE 3.3**. Line A passes from the Sun through the atmosphere to the surface in the equatorial region; we say that this path length equals 1. Line B passes from the Sun through the atmosphere and touches the Earth at the North Pole. For solar energy to reach the surface of a high-latitude location, it must travel a much longer distance through the atmosphere. Specifically, the path length

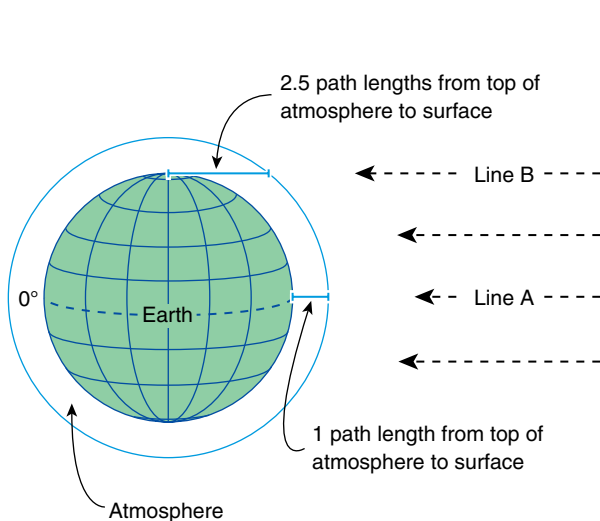
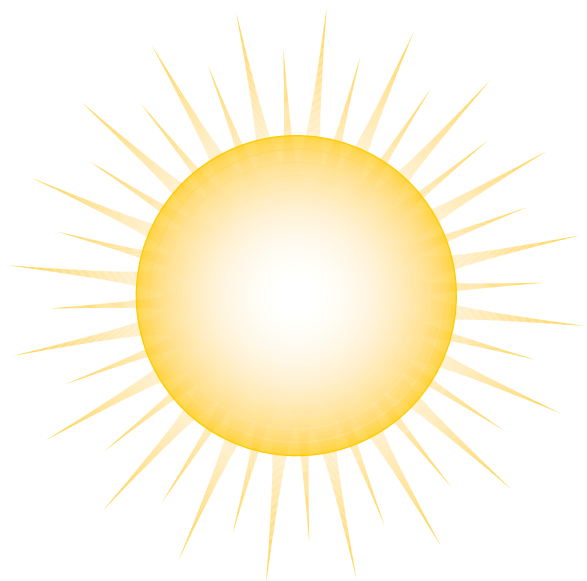


FIGURE 3.3 Atmospheric path length due to Earth's curvature.



increases approximately 2.5 times simply because of Earth's curvature. Because of the great distances between the Sun and Earth, for this and all other discussions of insolation we can assume that solar energy travels in parallel lines to Earth's system. If Earth were shaped like a block rather than a sphere, the path length of the Sun's rays through the atmosphere would be essentially the same for lines A and B. But the spherical nature of Earth makes it curve away from the Sun and gives much greater path lengths and subsequent beam spreading to locations at higher latitudes.

The parallel of latitude experiencing the direct rays of the Sun—the rays that fall perpendicular to the surface, or 90° above the horizon—on a given day always has the shortest path length. That latitude is termed the **solar declination**, and it varies only between 23.5°N and 23.5°S latitude. So, for locations north of 23.5°N latitude or south of 23.5°S latitude, the Sun is never directly overhead (i.e., at a 90° angle). For a given time of day, the higher the latitude outside the tropics, the lower the Sun's angle will be. So because of their differences in latitude alone, we would expect Vancouver, British Columbia, to have a lower Sun angle, more attenuation, more beam spreading, and less intense sunlight than San Diego, California. Latitude affects climate because it affects the Sun angle of a location, which in turn affects the intensity of radiation received at the surface, which in turn affects temperature.

As we will see shortly, latitude also impacts day length throughout the year. The greater the number of hours of daylight, the more time exists for the surface to heat up. Variations in both solar declination and day length occur because of the changing relationships between Earth's surface and the Sun through the year. Such relationships are responsible for creating distinct seasons.

► Earth–Sun Relationships

In combination with latitude, Earth–Sun relationships contribute heavily to the characteristics of climatic “sites” on Earth. These influences occur because of Earth's revolution around the Sun, rotation on its axis, and its axial tilt. Together, these factors produce daily and seasonal cycles of energy and temperature.

Revolution

Earth's **revolution**—its orbit around the Sun—creates a distinct impact on temperature on Earth when combined with other factors. The orbit itself is not circular, and its elliptical path is not even perfectly centered about the Sun. The average distance from Earth to the Sun throughout the year is 149.67 million km (92.96 million mi). Given this distance, and the constant speed of

light through the vacuum of space ($299,338 \text{ km s}^{-1}$ or $186,000 \text{ mi s}^{-1}$), it takes approximately 8.3 minutes for light emitted from the Sun to enter Earth's atmosphere. When you see the Sun, you are actually seeing the Sun as it was 8.3 minutes ago!

The Earth–Sun distance varies from about 147.09 million km (91.36 million mi) on or about January 3—termed **perihelion**—to about 151.92 million km (94.36 million mi) on or about July 4—termed **aphelion**. Obviously, given the dates at which the perihelion and aphelion occur (during northern hemisphere winter and summer, respectively), the distance from the Sun must play little role in controlling intraannual surface temperature variations. If the Earth–Sun distance were the most important factor producing the seasons, January would be summer in both the northern and southern hemispheres, because it is the month when the Earth is closest to the Sun, and July would be winter in both hemispheres.

Rotation

Rotation—the spin of the Earth on its axis—causes differing longitudes to experience the most direct ray of the Sun they receive on a given day at different times. The direction of rotation is from west to east, or counterclockwise when viewed from above the North Pole. One complete rotation (i.e., 360° of longitude) occurs every 24 hours, which is equivalent to motion through 15° of longitude every hour.

Because of rotation, the Earth is divided into **time zones**, 24 longitudinally-based regions across the Earth's surface. They are approximately 15° of longitude in width, with the “official” time set 1 hour apart in each adjacent time zone. When one time zone is receiving the most direct ray of sunshine (i.e., is situated in direct sunlight), others are on the fringe of the illuminated part of Earth, while others are in darkness. Exactly one-half of Earth is illuminated at any given time. The **circle of illumination** is the line, as viewed from space, which separates the illuminated and dark halves of Earth. It is constantly changing in position across Earth's surface.

Axial Tilt and Parallelism

To understand the cause of seasonality, we must examine the concepts of axial tilt and parallelism. The **plane of the ecliptic** represents the plane that bisects both Earth and the Sun (**FIGURE 3.4**). It is the plane on which Earth revolves around the Sun. Imagine a perpendicular line passing through Earth, through the plane of the ecliptic. This line does not pass through the poles, but instead the angle between this line and Earth's axis represents Earth's **axial tilt**. The axis of rotation (which passes through both

poles) lies 23.5° from the perpendicular line through the plane of the ecliptic. Likewise, the equator is tilted 23.5° from the plane of the ecliptic. If the Earth had no axial tilt, the equator would align along the plane of the ecliptic and the poles would align along the perpendicular line through the plane of the ecliptic.

This 23.5° axial tilt can be thought of as being “fixed.” No matter where Earth is in its revolution around the Sun, the axis still points in the same direction and remains at the same angle. This principle is known as **parallelism**. The northern hemisphere’s axis of rotation has a convenient reference point in space—Polaris, or the North Star. If you were standing on the North Pole through the course of the year, you would always see Polaris at a 90° angle above the horizon, or directly over your head. The other stars would rotate around you throughout the year as Earth orbits the Sun, but Polaris would appear as a fixed point. The axis of Earth is always parallel to itself for every position in its orbit (**FIGURE 3.5**). In reality, Earth’s axial orientation and angle of tilt do vary slightly

through geological time, and this variance is believed to contribute to global climatic changes. On time scales important in the context of contemporary weather and climate, we can think of the axis as remaining unchanged in orientation and angle of tilt.

Combined Effect of Revolution, Rotation, and Tilt

With the exception of the equator, the proportion of each line of latitude inside the circle of illumination changes throughout the course of the year, as demonstrated in Figure 3.5. In June more than half of any parallel of latitude in the northern hemisphere is in the daylight sector and more than half of any parallel of latitude in the southern hemisphere is in darkness. But for Earth as a whole exactly half is illuminated at any time. In December more than half of any parallel of latitude in the northern hemisphere is in darkness, while more than half is in daylight in the southern hemisphere. The closer to the pole the line of latitude is (in either hemisphere), the greater the difference in day length from June to December.

The number of hours each day during which a given parallel of latitude is inside the circle of illumination is the same as the day length at that latitude on that day. Day length changes throughout the year as the proportion of a parallel of latitude inside the circle of illumination changes. These changes have profound impact on the heating of Earth throughout the year and cause the seasons to exist. To understand how these processes work, we must put together what we have learned about revolution, rotation, and tilt.

The changing orientation of Earth’s axis of rotation with respect to the Sun throughout the year causes these relationships to exist. Orientation changes because of Earth’s revolution. Remember

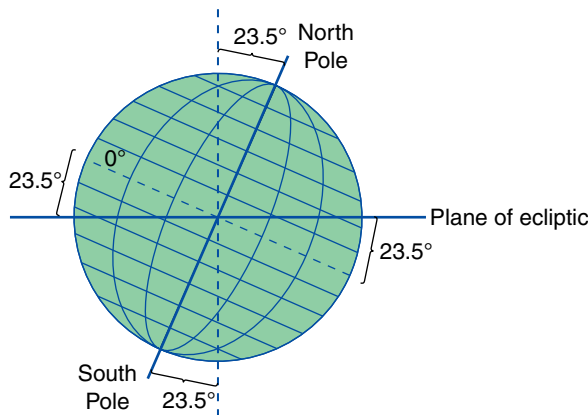


FIGURE 3.4 Earth’s tilt is 23.5° from a perpendicular line through the plane of ecliptic.

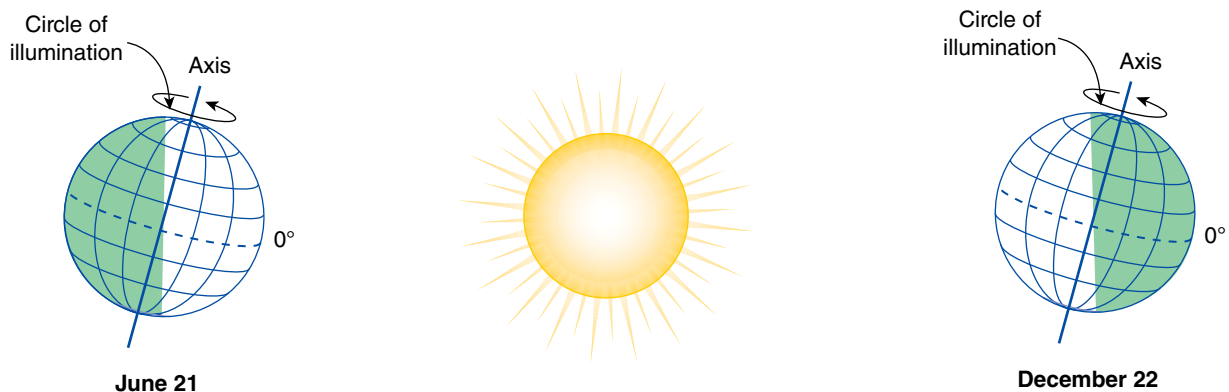


FIGURE 3.5 Unequal division of lines of latitude into day and night by the circle of illumination with change in orbital position.

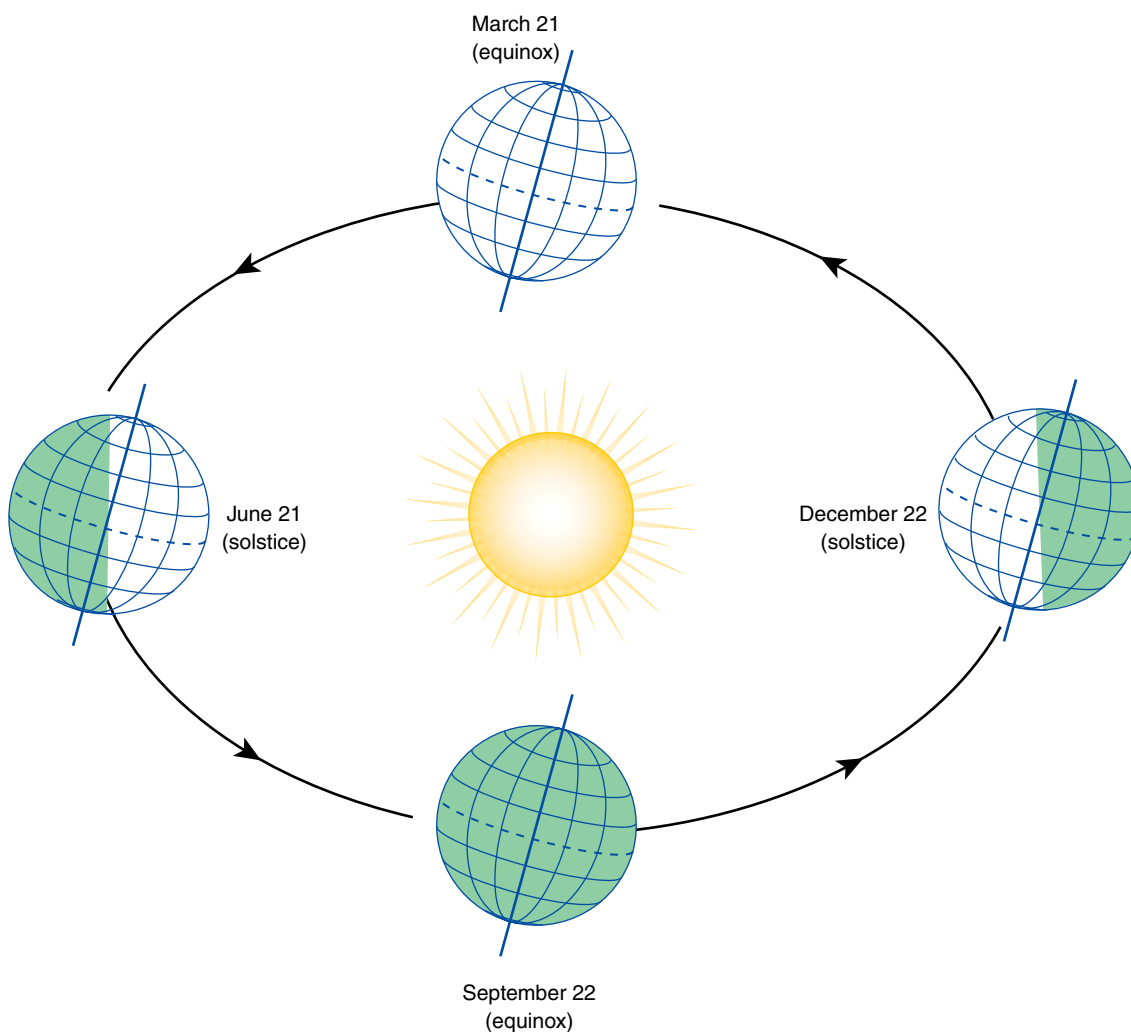


FIGURE 3.6 Relationships between Earth's axis and the circle of illumination during the course of the year.

that Earth's axis maintains parallelism throughout its orbit (**FIGURE 3.6**). So at one point in Earth's orbit, on or about June 21 (depending upon a leap year; this book uses the most common dates), the northern hemisphere axis is pointed maximally toward the Sun (this is termed the **June solstice**—or **summer solstice** in the northern hemisphere). This concept is shown on the far left side of Figure 3.6, where we see evidence for the northern hemisphere's long summer days and short nights and generally warmer conditions in the northern hemisphere and colder conditions in the southern hemisphere (which faces away from the Sun) at the corresponding latitude. On all days from March 21 through September 22 the northern hemisphere is pointed toward the Sun, but the pointing is most direct on June 21. On that day the tilt of Earth causes the solar declination to be at 23.5°N latitude—the **Tropic of Cancer**.

It is also clear from Figure 3.6 that on June 21 more than half of any line of latitude in the northern hemisphere

is in daylight and less than half of that parallel of latitude is in darkness. Furthermore, the farther north the line of latitude, the greater the percentage of that parallel is in daylight on June 21. Days are longer than nights in the northern hemisphere from March 21 to September 22 (centered on June 21), because the pointing of the axis toward the Sun in the northern hemisphere during that period would leave any line of latitude in daylight for a longer period of time than it would be in darkness as Earth rotates on its axis.

In the northern hemisphere, day length increases from the equator to the **Arctic Circle** (66.5°N) on any given day from March 21 through September 22 as a higher percentage of each line of latitude sits within the illuminated half of Earth as latitude increases.

On June 21, day length increases from 12 hours at the equator to 24 hours at the Arctic Circle. Every location north of the Arctic Circle receives constant daylight through this 24-hour solstice period, and for longer periods of time as one continues north, until

day length reaches 6 months (from March 21 through September 22) at the North Pole! The position of the Sun does little to indicate when it is time to sleep or eat—it merely circles around the horizon rather than dipping beneath it.

In the southern hemisphere, nights are longer than days from March 21 to September 22 (centered on June 21), because the South Pole is tilted away from the Sun during that interval, with the most direct tilt away from the Sun occurring on June 21 (the winter solstice in that hemisphere). On any given day from March 21 through September 22, day length decreases from the equator to the **Antarctic Circle** (66.5°S) as the parallels of latitude become less and less included within the circle of illumination as latitude increases. Again, the maximum effect occurs on June 21, when day length ranges from 12 hours at the equator to zero at the Antarctic Circle. A total absence of daylight exists for even longer periods successively south from the Antarctic Circle to a maximum of 6 consecutive months of darkness (from March 21 through September 22) at the South Pole. The effect of the tilt away from the Sun is cold conditions for the southern hemisphere. Because Earth is simultaneously farthest from the Sun (aphelion) near the June solstice, the southern hemisphere's winter season is even colder than it would be because of the effect of tilt alone. Because the equator is neither in the northern nor the southern hemisphere, days and nights are of equal length on June 21 (as on every other day of the year).

On the right side of Figure 3.6 we can see that December 22 marks the opposite point in the Earth's revolution around the Sun. That day, termed the **winter solstice** in the northern hemisphere, or, generically, the **December solstice**, sees conditions that are the same as those that occur on June 21, but the hemispheres are reversed. Parallels of latitude in the northern hemisphere have a decreasing day length from the equator to the Arctic Circle (12 hours to 0 hours, respectively) on that day, while in the southern hemisphere day length increases from the equator to the Antarctic Circle (12 hours to 24 hours, respectively). On all days from September 22 through March 21 the northern hemisphere is pointed away from the Sun and the southern hemisphere is pointed toward the Sun, but the effect is most direct on December 22. On that day the tilt of the Earth causes the solar declination to be at 23.5°S latitude—the **Tropic of Capricorn** (Figure 3.6).

Because of these conditions, significant differences in insolation are received at the surface during the course of a year, except near the equator. There are also significant latitudinal differences in insolation received at any given day of the year. The northern hemisphere as a whole experiences an energy surplus in June, July, and August that accounts for warm conditions throughout the

hemisphere. The southern hemisphere is in the opposite situation during those months, with a net energy deficit and resulting cold conditions. In December the situation is reversed as the northern hemisphere axis is pointed away from the Sun and the southern hemisphere axis is pointed toward it. The hemispheres are then in a net energy deficit and surplus, respectively.

Between the extremes represented by the solstices, Earth moves through the transition seasons. At the midpoints between the two solstices, Earth's axis is pointed neither directly toward nor away from the Sun. Instead, the axis of rotation is pointed in a "neutral" direction on March 21 (the **March equinox**, or **vernal equinox** in the northern hemisphere) and September 22 (the **September equinox**, or **autumnal equinox** in the northern hemisphere). In the southern hemisphere the autumnal equinox occurs on March 21 and the vernal equinox occurs on September 22, because the seasons are reversed from those in the northern hemisphere. On the equinoxes, the solar declination is at the equator. So, to see the Sun directly over your head (90°) on March 21 or September 22, you would have to be located along the equator at **solar noon**—the time when the Sun is at its highest point in the sky on a given day.

On the equinoxes, the circle of illumination bisects each parallel of latitude because the axis is pointed neither toward nor away from the Sun. The result is that each parallel location in the world experiences 12 hours of daylight and 12 hours of darkness on those days. Even though every location has virtually the same day length on the equinoxes, not every location receives the same intensity of radiation because of differences in solar angle. The angle at solar noon decreases with increasing latitude from 90° at the equator on the equinoxes. This decreasing solar angle causes greater beam spreading and attenuation with increasing path length. Local factors, such as cloudiness, may also complicate the relationship between solar angle and intensity of energy receipt.

The only parallel of latitude that has virtually unchanging day length throughout the year is the equator. It should be noted that day length does fluctuate slightly during the course of the year even at the equator. This is because day length is determined by the time between sunrise (when the leading edge of the Sun's disk—not the middle of it—reaches above the horizon) and sunset (when the trailing edge of the Sun's disk slips below the horizon). At times of the year when the solar declination is more distant from the equator (e.g., the solstices), at least part of the solar disk remains above the horizon for slightly longer than 12 hours at the equator. Furthermore, **refraction**—bending of light as it moves through air of varying density—causes sunlight to appear above the horizon for a few minutes before and after the Sun is actually above the horizon. So, at all locations day

length is generally a few minutes longer than would be expected; it exceeds 12 hours by a few minutes even at the equator, with the difference slightly greater at times of the year when solar declination is farthest away.

The equator lies at the middle of the “tropics,” the latitudes between the Tropics of Cancer and Capricorn. Tropical locations see the vertical rays of the Sun pass overhead twice a year. Realistically, the vertical rays of the Sun at solar noon would never be far from any tropical location. As a result, the tropics generally have high solar angles at noon throughout the year. Day length also does not vary much from 12 hours in tropical locations. The absence of short days, along with the short path length through the atmosphere and lack of significant beam spreading and attenuation, both as a result of consistently high noon solar angles, causes energy surpluses and high temperatures throughout the year.

► Distance to Large Bodies of Water

Another major control on climate is a “situation” variable known as **continentality**—location relative to large bodies of water (especially oceans). Such large bodies are capable of storing huge quantities of energy during high-energy times (summer) and releasing this energy slowly to the atmosphere during low-energy times (winter). These energy *fluxes* can have a significant effect on the climate of a location adjacent to the water body. Assuming that all other factors are equal, summers over or near oceans are not as warm as they are in the interiors of continents. Likewise, winters in coastal and oceanic locations are generally not as severe as they are in inland locations. In addition, the onset of seasons is delayed significantly over and near oceans because of the oceanic absorption of the energy through the summer and slow release of it to the atmosphere from autumn through winter.

To determine the relative importance of this climate control, let’s negate the impact of latitude and Earth–Sun relationships. To do this we compare the climates of three cities that lie near the same line of latitude but in various regions of North America. Choosing cities near the same line of latitude ensures that all three cities are subjected to roughly the same amount of energy because of latitude (and, therefore, the effects of path length, attenuation, beam spreading, and sphericity are similar). Would all the cities have the same climate?

The three cities we use in our example are San Francisco, California; St. Louis, Missouri; and Washington, DC. All three cities lie between 37° and 39°N (**FIGURE 3.7**). In winter St. Louis is coldest of the three cities, on average, but St. Louis also has the highest summer temperatures.

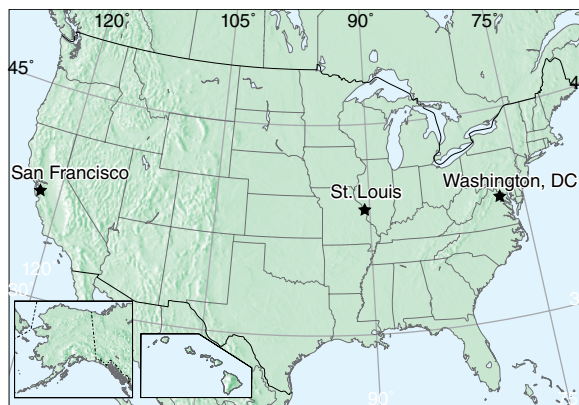


FIGURE 3.7 Continental position of San Francisco, St. Louis, and Washington, DC.

This wide annual temperature range occurs because of the distance from St. Louis to a large water body. The oceanic storage of radiant energy during summer and release of that energy to the atmosphere during winter do not provide much relief from the summer warmth and winter cold for St. Louis. Instead, interior areas of continents, such as the location of St. Louis, warm significantly during summer and cool substantially during winter. This creates more seasonal extremes in temperature and a larger seasonal temperature range for affected locations. St. Louis experiences this effect of continentality on its seasonal climate.

On the other hand, the warmest of the three cities in winter and the coolest in summer is San Francisco, which is downwind from the largest body of water on Earth and, therefore, has the most significant **maritime effect**—a moderating influence on temperatures by bodies of water. We will see shortly why Washington, DC has less of a maritime effect than San Francisco, even though both cities are coastal.

The slow response of water bodies to inputs of energy and the slow rate of release of energy that is input through insolation can be represented by a quantity known as **specific heat** or thermal capacity—the amount of heat (energy) required to raise the temperature of a 1-g mass by 1 °C. Specific heat for various substances is shown in **TABLE 3.1**. The specific heat of water is about five times greater than that of land. This means that, given the same mass of water and a sample of solid Earth, the water requires about five times more energy to heat to the same temperature as the solid. Furthermore, energy is easily distributed in a water column through **convection**—the vertical transfer of energy or matter through a fluid—and horizontally through **advection** in the form of ocean currents. This redistribution helps to maintain relatively constant surface temperatures over the seasons. Another factor contributing to consistency of temperature in the oceans is water transparency, which

TABLE 3.1 Specific Heat Values for Various Substances at 0°C

Substance	Specific Heat (Joules kg ⁻¹ K ⁻¹)
Mercury	139
Granite	190
Sand	835
Glass	840
Dry air	1005
Saturated air	1030
Water	4187

allows insolation to penetrate to a depth of up to about 100 m (330 ft). Because insolation is spread vertically down the water column, the surface temperature does not change appreciably.

Continental versus maritime effects are important contributors to the climate of any location. Globally, the greatest seasonal extremes occur over the largest land masses. Not surprisingly, Asia experiences the greatest continentality on Earth. But the effect of continentality may even manifest itself over relatively short distances from a large water body.

Smaller water bodies such as lakes, swamps, and marshes can also cause important temperature variations. Locations that are **windward** (upwind) of a lake tend to have more extreme variations in temperature than those that are **leeward** (downwind). A good example is Toronto, Ontario, which lies on the windward side of Lake Ontario for much of the year. Toronto has lower winter temperatures and higher summer temperatures than Watertown, New York, which is located on the downwind side of the lake.

An additional factor contributing to the continentality and maritime effects involves the use of insolation at the surface. When water is present, some insolation is required to evaporate water rather than to heat surfaces. To evaporate a bucket of water, a sufficient amount of insolation must be present, and this **radiant energy** is converted to **latent energy** during *evaporation*. This latent energy cannot simultaneously be used for heating air (**sensible energy**). Swimmers may feel cold after getting out of a swimming pool even on a hot summer day because of latent heating at the expense of sensible heating on their skin during the evaporation process. This

also explains why rubbing alcohol feels cold even though the alcohol is stored at room temperature. Alcohol is an easily evaporated substance, which means that latent heating is occurring at the expense of sensible heating on the skin as the alcohol evaporates. We can think of evaporation as a “cooling” process; evaporation involves the absorption of energy and conversion of it to latent form. It is important to note that at least some evaporation occurs in any unfrozen water body, regardless of the overlying air temperature. As such, the water body surface experiences some amount of evaporative cooling.

When the atmosphere is nearly saturated with water vapor (as is often the case in humid climates), little additional evaporation (and, therefore, little cooling) can occur. Perspiration cannot evaporate easily if the atmosphere is nearly saturated, and little evaporative cooling can occur. This “stickiness,” created by high humidity, increases the **heat index**—a contrived “temperature” based on how the temperature “feels” for people. This creates rather unpleasant conditions. By contrast, dry places such as Arizona generally do not feel as uncomfortable in high temperatures because the low humidity allows freer evaporation (and subsequent cooling) through perspiration.

Water in the form of clouds also plays a significant role in daily temperature variations. This is especially true for most tropical locations and in midlatitude locations during the summer months. Typically, these clouds are generated through convection, so they often become most prominent during the late afternoon when warm, humid air near the surface rises and its water vapor condenses into liquid water. Once formed, the clouds absorb, scatter, and reflect significant amounts of insolation, which may lead to a respite from the high temperatures. Often, the clouds generate precipitation, and this precipitation also cools the surface both directly (by adding cool water to the surface) and indirectly (through the cooling effect of evaporation of the surface water after the precipitation ends).

Given the accumulated properties of water, a large water body sees relatively little temperature variance over the course of the year, particularly if it is in the tropical part of Earth where day length and solar angles remain similar throughout the year. Because water temperatures remain nearly constant through the year, associated coastal locations such as San Francisco also see more constant temperatures through the year than inland locations such as St. Louis.

► Circulation

Climate is also affected by location relative to atmospheric circulation features. The mission of the atmospheric circulation is to balance energy inequalities across the

latitudes in accordance with the *second law of thermodynamics*. This mission is never accomplished, however, because of the constant inequalities in the amount of insolation being received across the latitudes. Most of this imbalance is initiated by the Earth–Sun relationships and position on the continent relative to oceans, as discussed previously. But other effects, including atmospheric circulation characteristics, also play important roles.

Even if two locations have the same latitude, the same distance to the ocean, and Earth–Sun relationships affect them in the same way (i.e., they are in the same hemisphere), they still may not have the same climate. One location may be affected by atmospheric circulation from a certain direction more often than another. To clarify this notion let's go back to an earlier example. Which of the three cities mentioned previously would experience the second-coldest winter?

On initial glance it may seem that Washington, DC and San Francisco would have the same moderating maritime effect because each city lies adjacent to a large ocean. But the maritime effect for Washington is much less than for San Francisco because of the direction of the prevailing winds. Because the prevailing wind direction in the midlatitude part of Earth is from the west, Washington is windward rather than leeward of the moderating influence of the ocean, unlike San Francisco. We say that the prevailing wind direction in the midlatitudes is westerly because in the atmospheric sciences wind direction is always named for the direction from which the wind is blowing.

In winter the westerly prevailing winds chill considerably over the cold North American continent. In summer the prevailing winds tend to have a south-westerly component, which adds low-latitude energy. Further heating occurs as the air blows over the warmed continental surface. Moisture originating from the Gulf of Mexico and/or the southwestern North Atlantic Ocean evaporates into the air, creating hot and humid conditions for Washington. The proximity of the North Atlantic does impart some maritime effect on Washington, DC; the maritime effect provides Washington with conditions that are a bit warmer in winter and a bit cooler in summer than they should be, given the energy receipt at its latitude. Nevertheless, Washington, DC is significantly colder in winter and warmer in summer than San Francisco because of the effect of circulation. By contrast, prevailing circulation advects—transfers horizontally—moderate Pacific air from the westerly winds to San Francisco.

The relatively high winter temperatures and low summer temperatures of San Francisco caused by the maritime effect led Mark Twain to his famous quip that “the coldest winter I ever spent was the summer I spent

in San Francisco.” The pronounced maritime effect is caused by circulation features not only in the atmosphere but also in the ocean. In addition to the westerly winds discussed above, the nearby cold ocean current provides a circulation regime that prevents the summer temperatures from rising too much. The prevailing westerly summer winds are chilled over the cool ocean waters before blowing onshore. Because the ocean's surface temperature changes relatively little over the course of the year, San Francisco enjoys a relatively constant temperature through the year. High temperatures are often in the low 20s°C (70s°F), while lows dip into the teens (10s°C; ~50s°F). The air is also relatively moist, giving it an added chilling effect, even during summer.

Pressure

Circulations that result in climates differing across space are caused by horizontal inequalities in atmospheric pressure. To understand this process of wind generation fully, we first need to understand the concept of pressure and pressure imbalances (pressure gradients).

Pressure is simply a measure of the amount of force applied to a given surface area. If we imagine a closed volume of air, the amount of air pressure is proportional to the frequency of molecular collisions of the matter composing the air. In such a case there are two ways that pressure could increase. The first is to decrease the volume. Putting the same number of molecules in a smaller volume increases the frequency of collisions. Because density is mass divided by volume, decreasing the volume is the same as increasing the density if mass is held constant. Pressure and density are directly proportional to each other.

A second way to increase pressure is to increase the speed at which the molecules move in the closed container. Faster-moving molecules inherently collide with one another more readily. Temperature is a measure of the **kinetic energy**, or energy of motion, of molecules in a substance. Kinetic energy is present in all matter. According to kinetic theory, motion may cease only if the theoretical **absolute zero** (0 K, -273°C , or -460°F) temperature is reached. Although scientists at the Massachusetts Institute of Technology recently created conditions in a laboratory at which absolute zero was approached to a few billionths of a degree, all naturally occurring substances have kinetic energy, and increasing the temperature of matter increases the speed of molecules comprising that matter.

We therefore can also say that pressure and temperature are directly proportional if we hold volume (and, thus, density) constant. Likewise, a decrease in pressure is associated with an increase in volume, decrease in density, and/or decrease in temperature, as

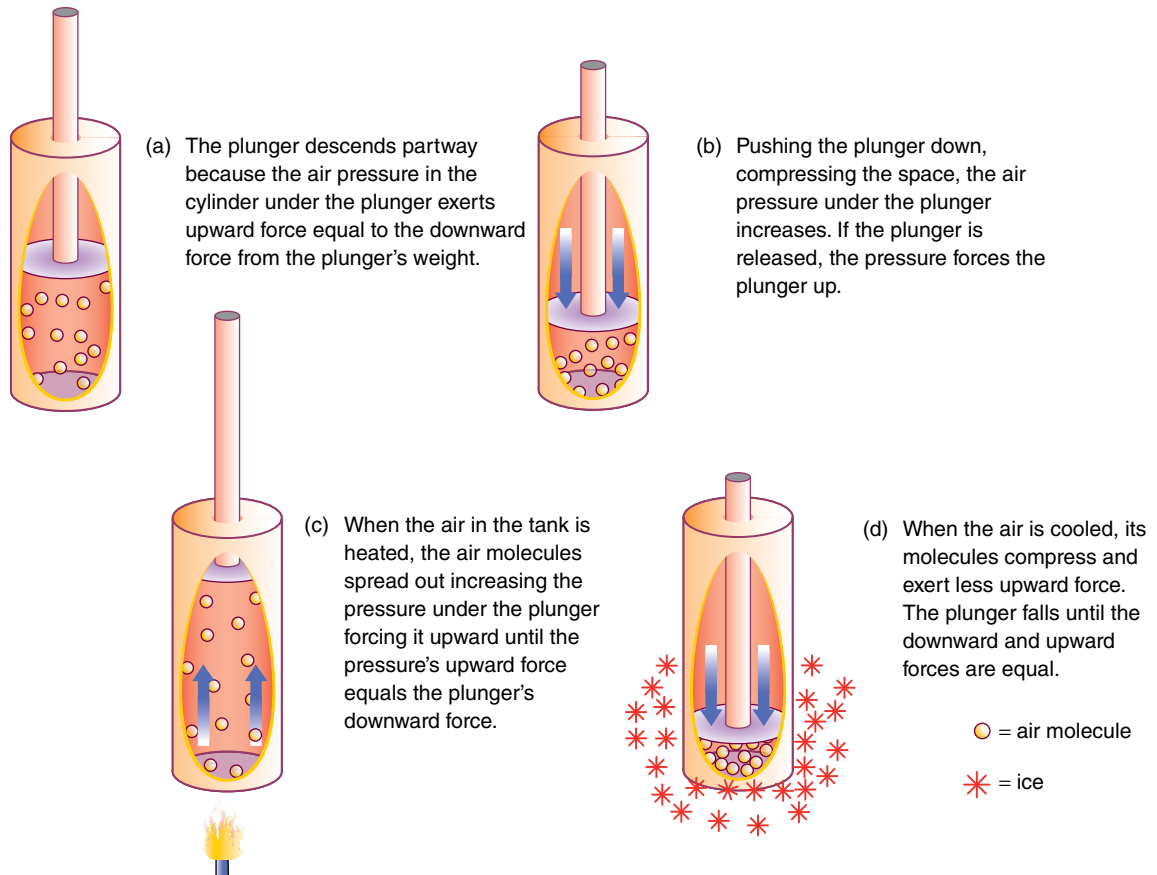


FIGURE 3.8 Pressure in a hypothetical pump with no outlet.

shown in **FIGURE 3.8**. These relationships are expressed quantitatively in the **equation of state** for an ideal gas (also known as the **ideal gas law**). For perfectly dry air (which approximates an ideal gas), the equation of state is

$$P = \rho R_d T$$

where P represents pressure, ρ is density, R_d is the dry gas constant ($287 \text{ Joules kg}^{-1} \text{ K}^{-1}$), and T is the temperature using the **Kelvin temperature scale**—a means of representing temperature such that it is proportional to the amount of energy contained by the molecules composing the matter. The **Joule** is the metric unit of energy or work, with units of $\text{kg m}^2 \text{ s}^{-2}$. If these units seem to be cumbersome, keep in mind Einstein's theory of relativity, $E = mc^2$, where E represents energy, m is mass, and c is the speed of light. Mass has units of kilograms and speed squared must be in units of $\text{m}^2 \text{ s}^{-2}$. The equation above also suggests that if pressure remains constant, warmer air is less dense than colder air.

Air pressure is sometimes expressed as the number of pounds of force exerted on a square inch of Earth's surface. Expressed this way the average sea level pressure of Earth is 14.7 lb in^{-2} . This means that for every square inch of surface area, the "weight" of the atmospheric

column on it is about the same as the weight of a bowling ball. If we were to add up all the square inches of surface area on the human head, the total atmospheric weight pushing downward would be about 600 lbs. If we were to lie down, we would experience over 5 tons of atmospheric pressure bearing down on us at sea level. So why are we not crushed by this pressure? It is because the pressure force is exerted in all directions—not just downward. Our bodies (and those of other creatures) also have internal fluid pressures that exert themselves outward against this pressure. We are in equilibrium with our physical surroundings.

If we were to increase pressure on our bodies, we would feel the negative effects of this "excess" pressure. For instance, divers readily experience an increase of pressure because of the increasing mass of water pushing downward onto their bodies as they dive deeper and deeper into the water. Eventually, they would reach a point where the fluids and gases of their bodies could not offset the increasing pressures and they would implode. Pressure increases with depth within a fluid. The atmosphere is a fluid, and we lie at the bottom of a gaseous ocean of air. The weight of the atmosphere represented by its pressure is, therefore, maximized at the surface or, more generally, at sea level. Even though

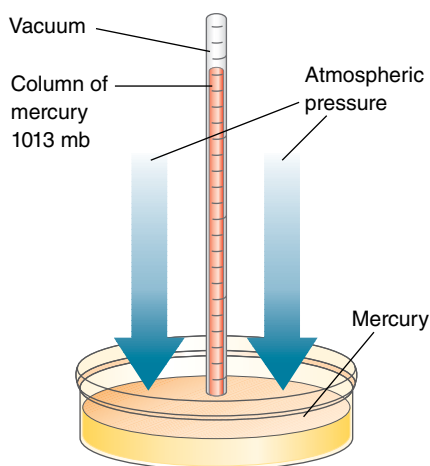


FIGURE 3.9 Schematic representing a mercury barometer.

pressure may be expressed in terms of pounds per square inch, this notation is rarely used in the atmospheric sciences. Other pressure notations are preferred. The first measurements of pressure used the height of a fluid in a vacuum tube. The downward pressure (force) of the atmosphere actually pushed the fluid up the vacuum tube. This experiment was initially done with water, and huge tubes were needed. It was found that a more conveniently sized tube containing mercury was more useful, and the invention of the mercury barometer in 1643 is credited to Evangelista Torricelli. To determine atmospheric pressure, one needed only to note the number of “inches of mercury” in the tube (**FIGURE 3.9**).

Today, atmospheric scientists seldom use the number of inches of mercury to represent pressure. Instead, even in the United States they represent pressure using the **Newton (N)**—a metric unit that measures force per square meter. One Newton of force per square meter is termed a **Pascal (Pa)** and 100 Pascals equal 1 **millibar (mb)**. The top of the atmosphere has a pressure reading of 0 Pa (or 0 mb), because no overlying mass exists to exert pressure, whereas sea level has an average pressure of 101,325 Pa or 1013.25 mb.

Pressure varies greatly in the vertical; as one ascends through the atmosphere there is less mass above and, therefore, a reduction in pressure. Of course, this makes comparisons of pressure between locations of different elevations meaningless. To alleviate this problem the actual recorded pressure at each weather station is mathematically “corrected” to that which would occur if that location were at sea level. This reduction to sea level equivalent allows for the role of elevation to be effectively eliminated. With pressures undergoing a reduction to sea level equivalent, it is possible to compare pressures at any stations directly, regardless of elevation differences.

Comparison of pressures on a map is usually done by connecting locations that have the same sea

level-corrected pressure using **isobars**—lines of equal pressure. An isobaric map of the United States is shown in **FIGURE 3.10**. The interpretation of isobars is intuitive. All locations on one side of a given isobar have pressure values above that represented by the isobar, and all areas to the other side of an isobar have pressure values below that which is represented by the isobar. For example, in Figure 3.10 the highest pressures are located in northwestern North America and off the east coast of North America. The lowest pressures on that day are found in the northeast, around Hudson Bay. By convention, on all surface weather maps only every fourth millibar is represented by an isobar. This convention allows a user to compare how closely packed the isobars are on any two maps; the closer the isobars, the greater the variation in pressure across space.

In general, “high pressure” indicates pressures above that of mean sea level, while “low pressures” are considered to be those below that of mean sea level. But pressure systems can also be considered to be “high” or “low” relative to one another. For instance, we might note a low-pressure system migrating across the country, but that “low” pressure could actually have a central pressure reading in excess of mean sea level pressure if this pressure is lower than other pressure readings surrounding it.

Wind

Now that we have an understanding of atmospheric pressure, we can begin to understand winds and circulation. *Wind* is simply air in motion; stated another way, it is the transfer of atmospheric mass from one location to another. The transfer occurs because there is an excess of atmospheric mass in one location and a lack of mass in another. Places where there is “extra” air have higher pressure, and places that have less air have lower pressure. Air moves in relation to pressure imbalances in either the vertical or the horizontal. Fluids always move from areas of higher concentration to areas of lower concentration, in accordance with the second law of thermodynamics, unless acted on by some other force.

Imagine a cup of coffee. If the level of coffee happens to be higher on one side of the cup than the other (i.e., the mass or pressure of a “column” of coffee from top to bottom is not the same across the cup), you would expect the coffee to slosh back across the cup to even out the level, unless some other force is maintaining the imbalance (such as your hand tilting the cup). Similarly, the atmosphere also always attempts to equal out imbalances of mass or pressure.

Because an area with low pressure actually has less atmospheric mass than surrounding locations, it may be compared with a hole. The word “depression” is often used to describe an area of low pressure. If a fluid exists

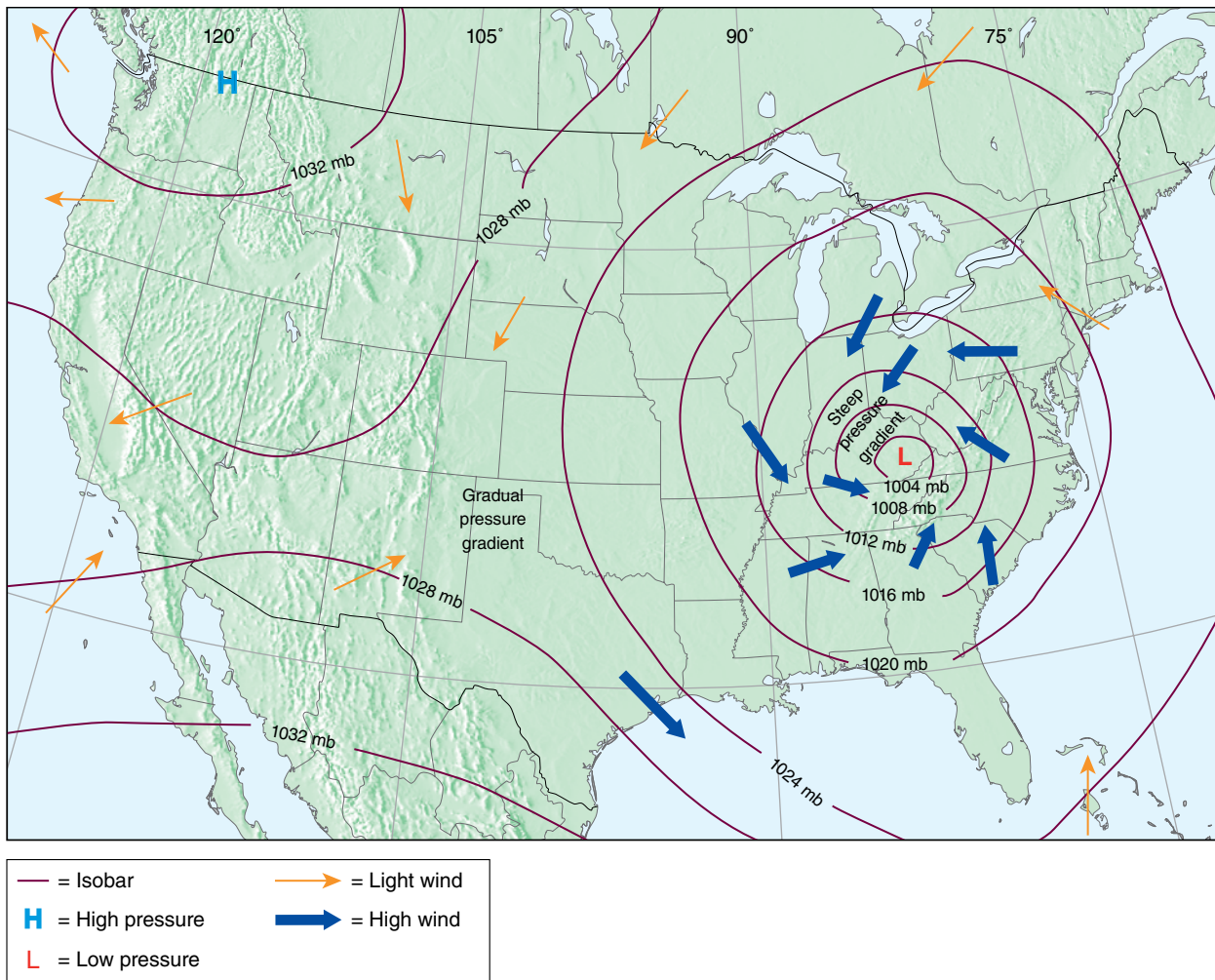


FIGURE 3.11 The pressure gradient force.

between the high-elevation and low-elevation points on the landscape. The larger the elevation difference across a particular distance (or the smaller the distance between points that have the same elevation difference), the steeper the slope and the higher the speed of the moving water.

In the same way, wind speed is proportional to the pressure difference between the high- and low-pressure areas. If there is a large difference between two pressure centers across a given distance, air will move faster than if the pressure differences were smaller. Likewise, if the pressure difference is the same across two pairs of points but the distance between one pair of points is less than the distance between another pair, air will move faster between the first pair of points, and we would say that the pressure gradient is greater. If there is no difference in pressure across a distance (i.e., no pressure gradient), the air will not move.

The Coriolis Effect

Once air is in motion, other forces may change its trajectory and speed. One “force” that causes considerable

change on the trajectory of air in motion is the **Coriolis effect (CE)**—a force caused by differences in Earth’s angular velocity about the local vertical. To understand the concept of the local vertical, imagine a person standing at the equator and another person standing at the North Pole, as in **FIGURE 3.12**. As you can see, the person at the equator rotates because she is riding on the Earth, but her rotation is not about her local vertical at all. On the other hand, the person standing at the North Pole is rotating completely about his local vertical.

To make the point clearer, hold a pen in your outstretched hand parallel to the floor and turn yourself around, as if you are the Earth rotating. The pen is rotating because you are rotating, but the pen is not spinning about its local vertical at all because you are not turning the pen itself. Now hold the pen in your hand while reaching up vertically and begin rotating yourself around. If there is writing or some other mark on the pen, notice how it constantly faces a different direction. We can say that the entire component of the pen’s rotation is about its local vertical. In reality, most of us do not live either at the equator or at the poles, so our rotation is somewhat

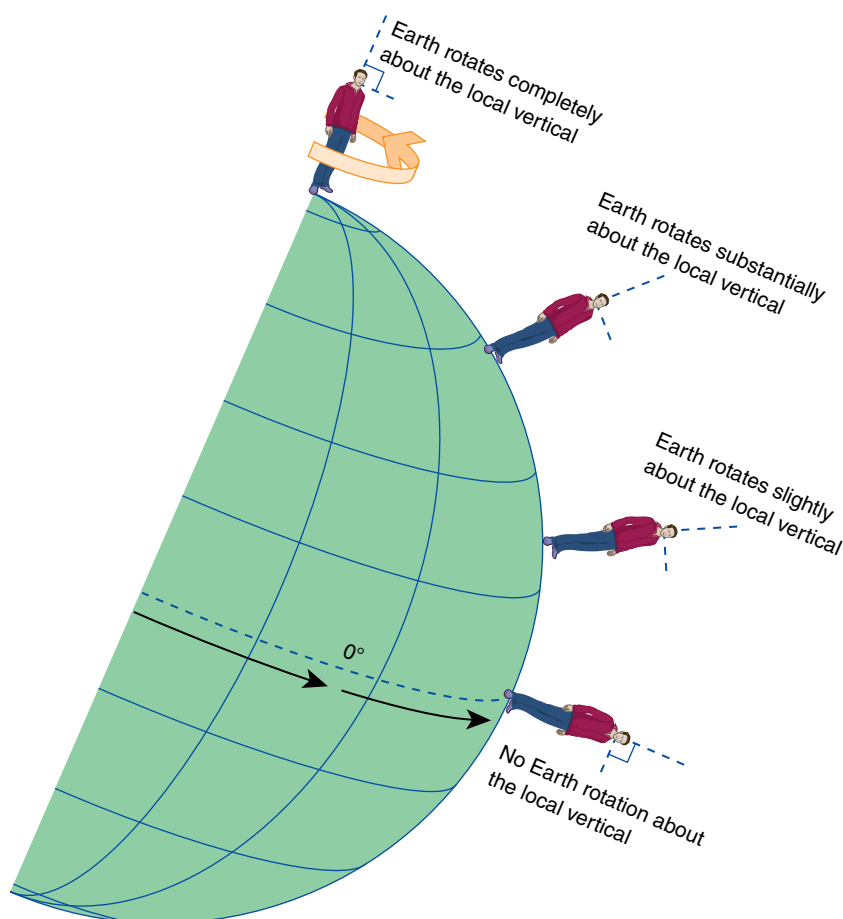


FIGURE 3.12 Earth rotation and the local vertical.

about the local vertical, with the proportion increasing with latitude, as shown in Figure 3.12.

In short, then, the CE is an apparent force that causes deflection of a fluid in motion when it is rotating at least somewhat about the local vertical. If Earth did not rotate, there would be no rotation about any local vertical, and the CE would not exist. Because there is no rotation about the local vertical at the equator, there is no CE there either. The CE increases in strength with latitude because the proportion of the rotation about the local vertical increases with latitude.

The CE is expressed mathematically as

$$CE = 2\Omega (\sin\phi) v$$

where Ω (omega) equals the angular velocity of Earth (a constant), ϕ (phi) is the latitude at which the object is moving, and v represents the wind speed. Because Earth rotates through 360° (or 2π radians) in 24 hours (or 86,400 seconds), Ω is actually equal to $2\pi/86,400$ s or $7.27 \times 10^{-5} \text{ s}^{-1}$.

From the previous equation we can see quantitatively that the Coriolis deflection of a moving object is directly proportional to both the latitude and the wind speed. All

other factors being equal, as latitude increases, CE increases. Likewise, the equation shows that a greater speed produces an increased CE. If the latitude is zero (i.e., at the equator), we can see that CE is zero, as suggested previously.

But which way will a moving object appear to be deflected? The west-to-east direction of Earth's rotation causes objects in motion in the atmosphere to be deflected to the right in the northern hemisphere and to the left in the southern hemisphere. To understand this, assume that a rocket is launched from the North Pole to a point on the equator. The rocket initially travels in a straight line along, say, 0° longitude. Will the rocket actually hit the equator at that line of longitude? No! The reason is that once it is launched, the rocket travels in a perfectly straight line from north to south. As the rocket travels above Earth, however, Earth actually spins underneath it from west to east because Earth must rotate faster on its axis as latitude decreases, to move through a greater number of kilometers of circumference in the same 24 hours as it needs to rotate at higher latitudes (where Earth has a smaller circumference). The rocket thus hits to the west of the intended target or, if you faced the direction of initial movement of the rocket in flight, to the *right* of the intended target.

Now imagine that you are launching the same rocket from the South Pole. Again, Earth moves from west to east underneath the rocket. This places the landing west of the intended target once again. The deflection in the southern hemisphere is now to the *left*, however, if you are facing the direction of initial movement while standing at the pole.

As implied above, the amount of deflection changes with the latitude of the moving object because of differences in Earth's rotational speed at different latitudes. In 24 hours a person standing at the equator would have to travel the entire circumference of the planet to arrive back at the same point relative to a point in space. So over 24 hours a person at the equator would travel 40,075 km (24,901 mi) in a circle. By contrast, a person at the pole would simply spin around the same point in a circle over 24 hours. A person at the equator is moving about 1609 km hr^{-1} (1000 mi hr^{-1}), while a person at the poles does not even leave the point at which he or she started. This difference creates a rotational pull on objects and fluids in motion. The increasing amount of curvature of Earth toward the poles also plays a role in deflection. An object's apparent trajectory is deflected to the right of the initial direction of motion in the northern hemisphere and to the left in the southern hemisphere (no matter the direction of motion), with the amount of deflection proportional to both speed and latitude.

This apparent force is the subject of misunderstandings concerning the flow of water in bathtubs. Such rotating motions are not initiated by Coriolis deflection. An object must be in motion (have **inertia**) for a particular length of time, varying by latitude, for the CE to be important. This **inertial period** is one half of the pendulum day—the time required for the plane of a freely suspended pendulum to complete an apparent rotation about a local vertical. A fluid would have to be in motion for some number of hours (in most cases) before Coriolis deflection would occur. Water movement in a bathtub cannot meet those requirements. The spin induced on water moving into a drain is actually influenced by the dimensions, shape, and configuration of the basin itself, plus other factors including the water input direction, velocity of fluid input, and size and location of the drain. In general, the CE is negligible at small temporal and spatial scales. It would be an exaggeration to blame a missed putt on the rotation of the Earth!

If inertial period is so important, why do the atmosphere and oceans experience CE deflection instantly when set in motion? This is because such fluids are always in motion and have been since their formation. Their inertial periods have been surpassed billions of years ago and the deflective response is continuous.

Centrifugal Acceleration

Centrifugal acceleration (CA) is an apparent outward-directed force on an object moving along a curved trajectory. CA is simply a manifestation of inertia. Although some physicists argue that there really is no such force (there is simply inertia), atmospheric equations express this force quite frequently.

To understand the influence of CA, imagine air moving from a high- to low-pressure area. Initially, the PGF causes the air to move in a straight line toward the low-pressure core at a particular speed as determined by the pressure gradient. But as soon as the air begins moving, the CE causes it to curve to the right (in the northern hemisphere) with the amount proportional to the speed and latitude of the moving air. At that point the trajectory shows curvature, and CA begins altering the trajectory by pulling the air to the outside of the curve. The faster the wind movement and the tighter the curve, the greater the centrifugal pull. An air stream has its initial trajectory altered first by CE and then again by CA. It is this centrifugal pull that allows tornadoes to maintain their spin, particularly because the wind speeds are so fast and the circulation is very tight in a tornado.

Mathematically, CA can be expressed as $CA = v^2/r$, where v is the linear wind velocity and r represents the radius of curvature of motion. For perfectly straight flow, r would be infinite and CA would approach zero. For tighter circulations, such as a tornado, r is small and winds are large, and CA is extremely strong.

The concept of CA can be used to provide entertainment. Virtually every amusement park ride uses CA to stimulate sensors in the inner ear. The spinning cage, which plasters riders to the cage with such force they cannot even lift an arm, is a particularly good example. Simple experiments such as placing water in a bucket and spinning it about the body in a vertical circle also demonstrate the principle of CA. The water does not fall out of the bucket even when the bucket is upside down if the bucket is spun quickly enough. In this case CA exceeds the force of gravity. Of course, if the bucket is slowed beyond a critical point, the bucket spinner will be doused in water. Another example occurs in a washing machine. The spin cycle spins the internal basin. CA forces the clothing and water to the outside of the basin. Small holes in the basin allow water to escape the basin and drain from the machine, partially drying the laundry.

Friction

Friction is another force that affects wind. It is also the most difficult component to quantify mathematically. As a force of opposition, friction works to decrease the speed of moving objects. In the atmosphere, friction is maximized near the surface and decreases with height

until it becomes negligible in the **free atmosphere** (also termed the “friction-free zone”) that characterizes most of the atmosphere.

The amount of friction applied to overlying moving air depends on the nature of the surface. Air flowing over smooth surfaces, such as water bodies, encounters much less friction than air moving over mountainous surfaces. Likewise, vegetation, hills, pastures, buildings, and roads all impart varying amounts of friction to moving air. With such variety it is impossible to describe and understand the precise effects of friction across even small spaces. This makes it impossible to account fully for friction and all its effects in mathematical equations that are used to forecast future air motions.

Friction must be accounted for in forecasts because it not only slows air, but it also indirectly alters the trajectory. Remember that both the CE and the CA alter wind trajectories and both depend on wind speed. Faster-moving objects experience greater Coriolis and centrifugal deflection. If friction is applied, speed is reduced. If speed is reduced, so is the amount of trajectory deflection from those two forces. The varying amount of friction with height thus causes wind direction to shift with height. For this reason many equations used in forecasting future conditions are solved for the free atmosphere where friction is negligible.

So wind is a combination of interactions between four forces:

- PGF, which determines initial air speed and direction
- CE, which alters trajectory by deflecting moving air to the right (in the northern hemisphere) and is a function of speed and latitude
- CA, which pulls the Coriolis-influenced curving air slightly back toward the initial trajectory (to the outside of the curve) as a function of speed and curvature
- Friction, which slows the air, thus affecting the speed and reducing the amount of deflection from both CE and CA

We can simply state that

$$\text{Surface wind} = \text{PGF} + \text{CE} + \text{CA} + F$$

where F is friction. All forces are interacting with each other to produce a wind moving in a particular direction at a particular speed.

Mathematical equations are capable of quantifying all aspects of air motion accurately except friction. The three **Navier-Stokes equations of motion** (for west–east, south–north, and down–up directions) form the ABCs of numerical weather forecasting. Data are collected at

various weather observation sites around the world and input into computers that apply the equations to the initial data to forecast motion a few minutes into the future. The equations are reapplied using the “new” data as input and the process is repeated until forecasts of 6 hours, 12 hours, and each 12-hour increment afterward out to a few days are generated.

Surface Versus Upper-Level Winds

The varying effect of friction with height creates great differences in the representation in computer models of winds at the surface compared with those in the free atmosphere. But how are the equations applied if friction cannot be accounted for properly? The answer is rather simple: We greatly oversimplify the friction term in the equations. Because much of the focus in the computer models is on upper-air circulation, where friction is assumed to be negligible, the harm caused by inaccuracies in the oversimplified friction equations is minimized. Automated forecasts also use surface data, but these often are not used to forecast large-scale motion. But if they are, they are more likely to be erroneous because of the poorly handled friction terms.

In the contiguous United States, “official” upper-air weather data are collected from only 74 locations twice a day. By comparison, surface data are available from thousands of stations, with many providing minute-by-minute data. But large spatial gaps occur between the upper-air observations, and large temporal gaps (12 hours) exist between readings. Many conditions change within the atmosphere that cannot be detected in the computer-based forecast because of the coarse set of input observations across both space and time. It is rather amazing that from such scant observations any forecast holds any degree of accuracy, yet the *National Weather Service* forecasts are generally accurate out to 3 days.

Vertical Motion

Air also moves vertically in the atmosphere. An upward-directed pressure gradient always exists on Earth because pressure (and atmospheric mass) decreases rapidly with height. The tendency for air to rise from the surface to lower-pressure regions aloft (buoyancy) is balanced by the downward force of gravity. In all, a large-scale equilibrium exists between buoyancy and gravity, and the atmosphere remains permanently adjacent to the surface of Earth, a situation known as *hydrostatic equilibrium*. But local imbalances can occur between the gravitational force and upward-directed PGF. Storm systems, particularly thunderstorms, represent situations in which local hydrostatic imbalances occur. In such cases a net transfer of atmospheric mass occurs from

the surface upward and of *momentum* from the upper atmosphere downward. **Updrafts** carry air aloft, while **downdrafts** move air toward the surface.

Cyclones and Anticyclones

A **cyclone** is simply an enclosed area of relatively low pressure. If the cyclone exists at the surface, it is characterized by a convergence of winds into that low-pressure center, which initiates rising motions. These rising motions trigger cloud and precipitation-forming processes. Surface cyclones are, therefore, associated with storms. Many in the United States refer to tornadoes as “cyclones,” whereas in parts of Asia a “cyclone” indicates a storm of tropical origin such as a hurricane. Any storm system in which surface air spirals about and into a low-pressure core is technically a cyclone. In general, there are three main types of cyclonic storms: the **midlatitude (frontal) wave cyclone**, the **tropical cyclone** (tropical storm/hurricane), and the tornado.

The term “cyclone” technically refers to the type of air motion involved. The PGF dictates that air move toward the low-pressure core at a speed proportional to the pressure gradient minus friction. However, the CE deflects that airflow to the right (in the northern hemisphere) at some angle corresponding to the speed of airflow and

the latitude of the system. The result is a system that spins counterclockwise in the northern hemisphere (**FIGURE 3.13**) and clockwise in the southern hemisphere. At some point in the upper *troposphere*, air diverges to compensate for the convergence near the surface.

Because of friction near the surface, air crosses closed isobars at some angle in a surface cyclone. In the free atmosphere, however, air flows parallel to the isobars in a counterclockwise motion above the cyclone (**FIGURE 3.14a**). The wind direction therefore changes with height, from a counterclockwise (in the northern hemisphere) and inward motion at the surface to a counterclockwise motion that parallels the isobars aloft. Another way of stating this is that the wind direction is deflected more and more to the right (in the northern hemisphere) with height—through a process called **veering**—until it parallels the isolines. Veering can be thought of as a clockwise change in wind direction with height. In the southern hemisphere, the winds around a surface cyclone move clockwise (because CE pulls winds to the left as they move into the low-pressure center) and inward, whereas winds aloft would simply move clockwise. In the southern hemisphere, then, winds turn more and more to the left, with a counterclockwise change in wind direction with height—through a process called **backing**.

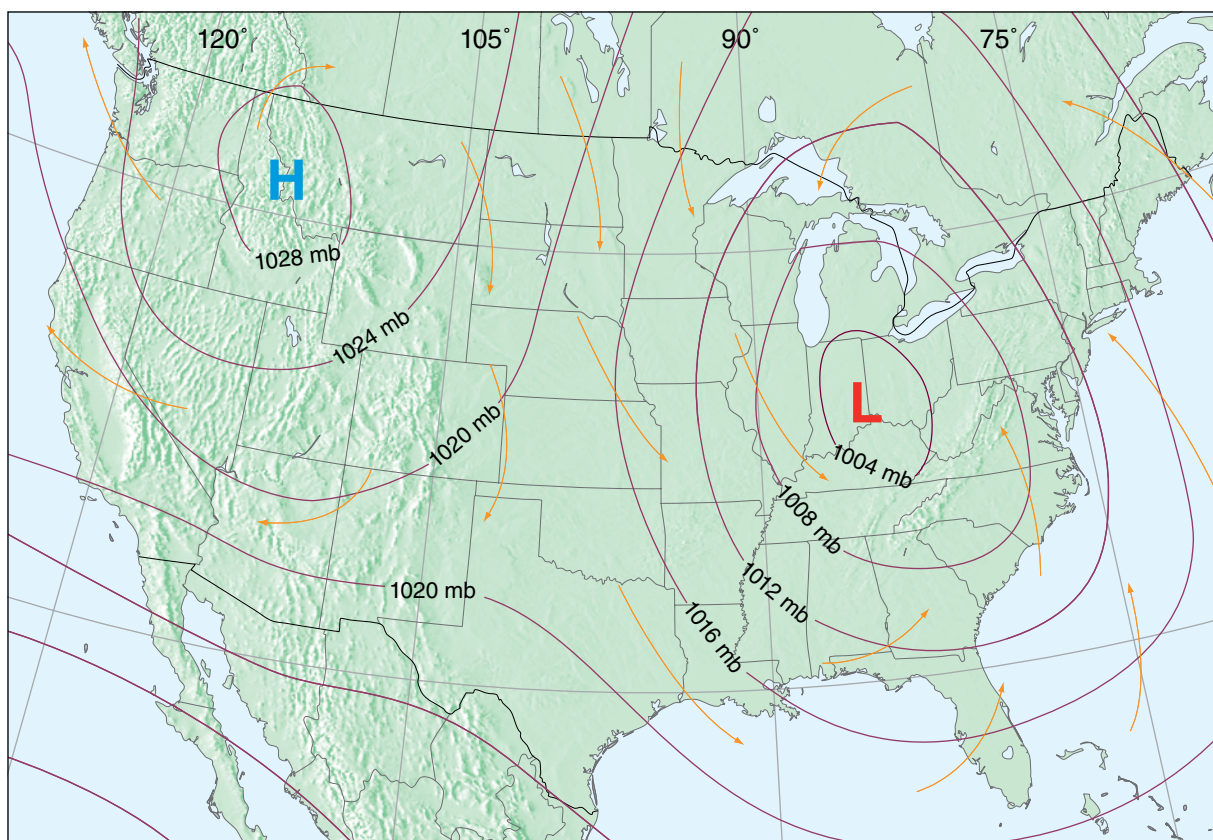


FIGURE 3.13 Northern hemisphere surface cyclone and anticyclone airflow patterns.

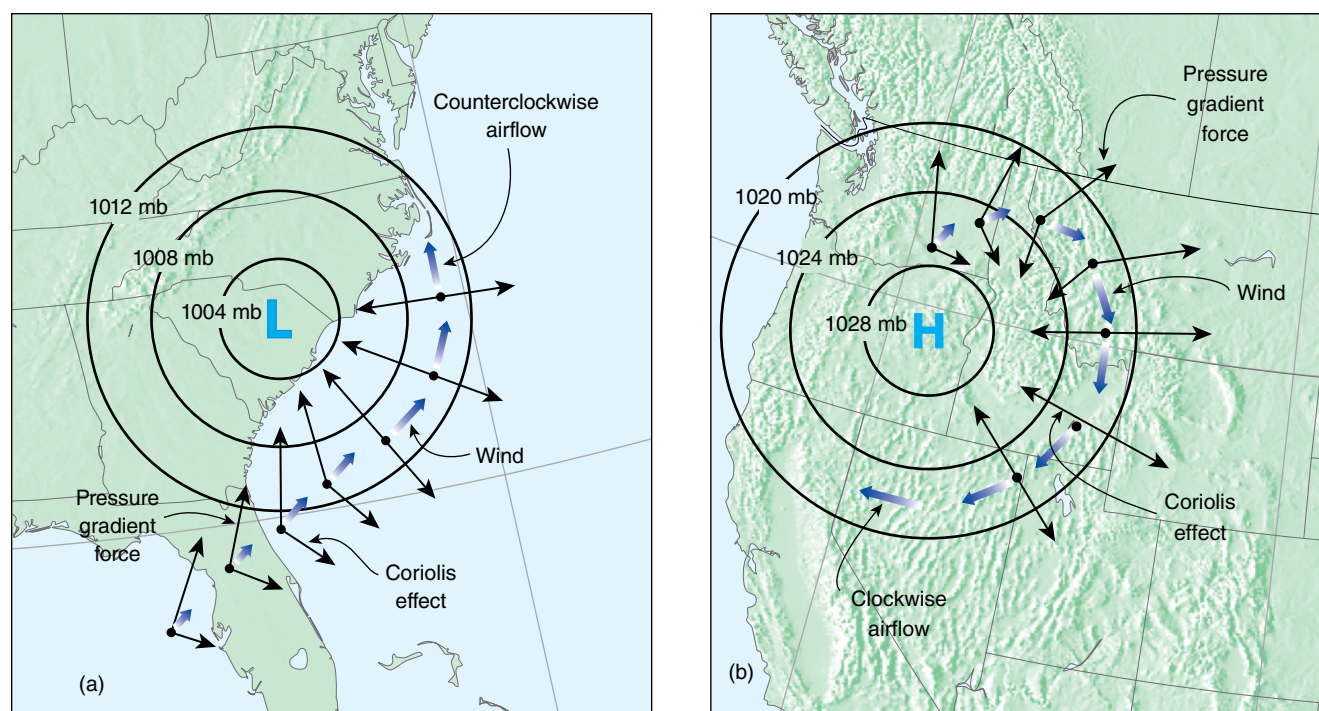


FIGURE 3.14 Northern hemisphere upper airflow: (a) cyclone; (b) anticyclone.

If the flow is sufficiently straight that CA can be ignored and is sufficiently high above the surface that friction can be ignored, we can say that the veering or backing ends when there is a balance between the PGF and the CE, a condition known as **geostrophic balance**. Airflow in geostrophic balance is termed the **geostrophic wind** and flows along constant pressure surfaces instead of across them.

Anticyclones—enclosed areas of high pressure—have opposite circulation patterns from cyclones (**FIGURES 3.13** and **3.14b**). These systems are characterized by surface divergence because the PGF initially pulls air outward away from the high-pressure core in an effort to eliminate the pressure gradient. But as the air moves from the central core toward lower-pressure regions extending in all directions, the airflow is deflected by the CE. Again, deflection is to the right in the northern hemisphere, resulting in a clockwise and outward spin at the surface and clockwise flow aloft. Southern hemisphere anticyclones spin in an opposite manner: counterclockwise and outward at the surface and counterclockwise aloft.

How can airflow outward from a central point near the surface be sustained for any length of time? The air must be coming from somewhere. Again, an anticyclone shows opposite conditions from a cyclone. An anticyclone has air moving toward a central location in the upper atmosphere to compensate for the divergence of air from the central core at the surface. This air converges at the upper levels, forcing sinking motions at the

central core and then outward motions from a central surface region. Sinking motions reduce or eliminate the possibility for cloud formation. Without clouds, the chances of precipitation are obviously nonexistent. Therefore, anticyclones are generally characterized by relatively clear conditions (**FIGURE 3.15**).

As with cyclones, the upper-air characteristics of anticyclones are opposite those at the surface. In anticyclones, upper-air convergence is associated with the surface divergence below it. As we have seen, in cyclones surface convergence is linked to upper-air divergence. So where does rising air go in the cyclones and where does sinking air come from in the case of the anticyclones? If viewed independently, these questions are difficult to answer. We must instead view the atmosphere as an integrated whole in a three-dimensional sense to understand interactions between seemingly disparate systems.

After surface air rushing toward the low-pressure core of a cyclone is deflected en route to the core, it converges with air streams entering from other directions and spirals upward. This air expands and cools on its ascent, forming clouds and possibly precipitation. At some level aloft, the air diverges and continues to move laterally across the upper troposphere until convergence once again occurs elsewhere, in a location associated with the upper-level features of a surface anticyclone. There, the air is forced to sink back toward the surface. Once the air reaches the surface, it spirals outward toward

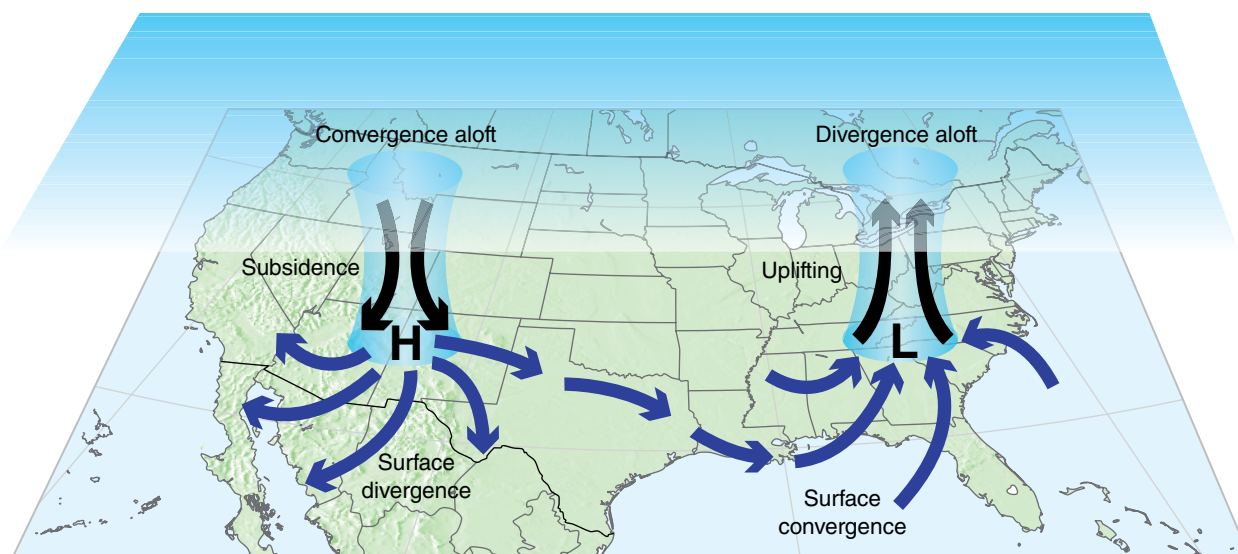


FIGURE 3.15 Surface and upper airflow characteristics of northern hemisphere cyclones and anticyclones.

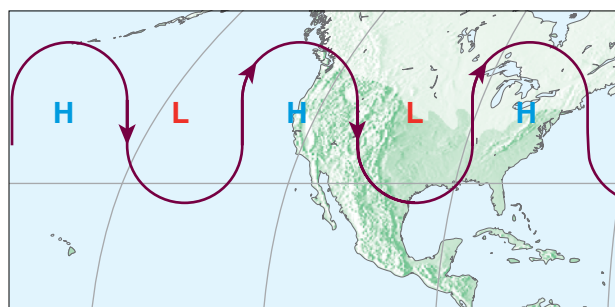


FIGURE 3.16 Synergistic relationship between circulation around cyclones and anticyclones (northern hemisphere example).

surrounding lower pressure and the process continues with air again rising in those locations.

The motion associated with cyclones and anticyclones is integrated. Imagine looking down at the surface from a point in space. Now imagine that you see two spheres, each spinning clockwise over an area of the northern hemisphere. Now imagine another ball located between the two larger ones. That ball would spin in a counterclockwise direction, like gears in a machine, in opposition to the surrounding larger ones (**FIGURE 3.16**). This situation describes the surface interactions between two anticyclones with a cyclone sandwiched between them. The anticyclones feed the cyclone with surface air streams that converge and rise. The cyclone then feeds the anticyclones with upper-airflow that converges and sinks. Such interactions occur continuously.

Oceanic Circulation

We have seen that the purpose of the atmospheric circulation is to balance inequalities of energy incident

on the surface, in fulfillment of the second law of thermodynamics. Besides atmospheric circulation, another mechanism for mitigating some of Earth's energy imbalances is the "situation" created by oceanic circulation. Although the ocean is a denser fluid than the atmosphere, it nevertheless has the same "mission" as the atmosphere. Most oceanic circulation characteristics are created by the same energy inequalities present in the atmosphere. Ocean movement follows **Newton's laws of motion**—the same laws that govern atmospheric motions.

Surface ocean currents are considered to be those that extend to approximately 100 m (330 ft) below the surface; they are driven primarily by surface winds. Frictional drag occurs between air moving over a water surface and the water at the surface. This energy causes motion in the water surface. The momentum is then transferred downward into the water column. Surface-generated energy below about 100 m (330 ft) approaches zero. Deeper ocean motions are initiated by processes outside of the atmosphere's direct influence.

Water motion does not correspond as closely to surface airflow as one might expect. Instead, the water surface may be viewed as being a stationary fluid when air begins to move above it. Frictional drag transfers to the ocean, and the water begins to move. Once the surface water begins moving, it is subject to Coriolis deflection. Surface water immediately deflects to the right of the airflow (in the northern hemisphere). Again, deflection is proportional to the speed of motion and the latitude. At the surface a deflection of about 45° to the right (in the northern hemisphere) of the airflow trajectory occurs, but this deflection only affects a column of water a few meters in thickness. The momentum involved in moving that surface column of water is then

transferred downward to the next few meters of water. That band of water is disturbed and—like the surface water—is subjected to Coriolis deflection. The speed of the second layer is slightly slower, resulting in an offset drag to the trajectory of the water column above it. This action spurs successive layers of deeper waters to curve, which in turn respond with additional Coriolis deflection, until friction between layers slows the final layer of water to stillness.

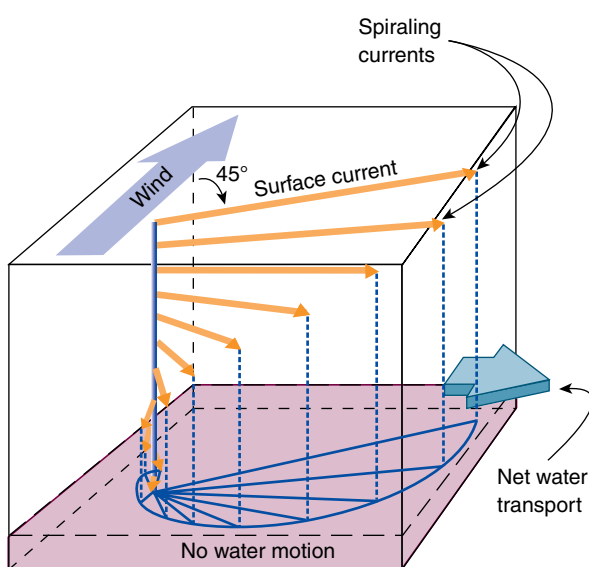
The result is the **Ekman spiral**—a spiral of water motion extending from the surface downward to a depth of approximately 100 m (330 ft). Identified and quantified in 1902 by the Swedish oceanographer Walfrid Ekman, it causes the bulk of water flow to move at a right angle to the initiating wind stress (**FIGURE 3.17**). The Ekman spiral is important in climatology because this phenomenon is

partly responsible for **upwelling**—an ascending current of cold water from depths of about 1000 m (3300 ft) to the surface in certain locations. When surface waters move offshore because of the Ekman spiral, the cold water from the depths moves upward to replace it. In addition to providing a mechanism for nutrients to be returned to the surface, upwelling greatly contributes to the climatology of the coastal zones affected because of the cold water that is brought upward.

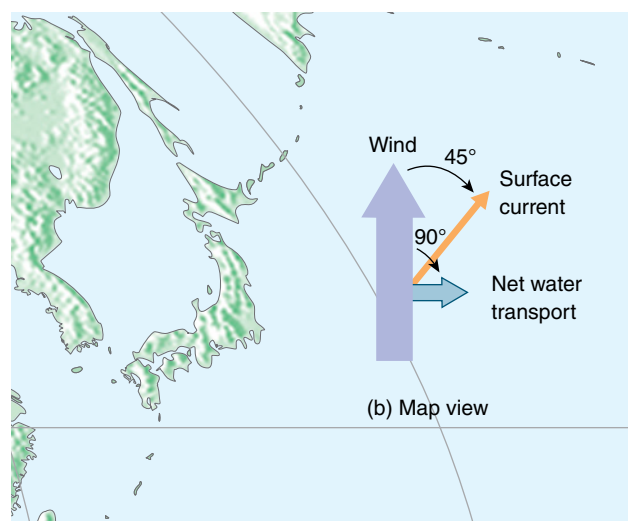
Deeper ocean currents are initiated by temperature and salinity inequalities across space. Because cold water is denser than warmer water, this density characteristic affects three-dimensional motion of water in an attempt to achieve an ocean of homogeneous density. Likewise, differences in salinity also set deep waters into three-dimensional motion to accomplish the mission of the oceans, as denser saltier waters move below less dense fresher waters as they flow laterally. Areas with cold, salty water, such as the northern North Atlantic near Iceland, see particularly pronounced sinking motions as near-surface water is eventually carried to the ocean floor. This northern Atlantic water moves equatorward as it sinks, eventually crossing the equator and moving into the Indian Ocean. The water is forced to rise in the western North Pacific near Indonesia where a surface current is initiated that carries the water back to the North Atlantic. This resembles a deep ocean conveyor belt that results in **thermohaline circulation**, a slow energy transportation system that greatly affects global climatic conditions. “Thermo” refers to differences in thermal characteristics in the deep ocean; “haline” refers to salinity characteristics.

In general, the most important and immediate oceanic circulation effects on climates are the surface currents. These currents generally follow the winds produced by semipermanent pressure zones that exist in the atmosphere. Clockwise (in the northern hemisphere) or counterclockwise (in the southern hemisphere) circulation associated with semipermanent subtropical anticyclones exists in each ocean basin around 30° latitude. These features impart the most influence on oceanic surface circulation, partially because the oceans are so vast at the subtropical latitudes. These circulations cause cold ocean currents on the eastern sides of the ocean basins as cold water migrates from higher latitudes toward lower latitudes. The western ocean basins are dominated by warm surface currents moving from the equatorial areas poleward and transferring excess energy from low latitudes toward higher ones. Cold and warm surface currents greatly affect climates located near the eastern and western coastlines of continents.

Europe provides an excellent example of the influence of surface ocean currents on climates. Lisbon, Portugal is positioned at a similar parallel of latitude as New York



(a) Ekman spiral in the northern hemisphere



(b) Map view

FIGURE 3.17 Ekman spiral.

City (about 42°N), but Lisbon is climatologically warmer than New York. Likewise, much of Norway exists at latitudes equivalent to northern Canada and Siberia, but, again, the temperatures in Norway are much higher in winter, on average, than those locations. The strong maritime effect in Europe and prevalence of the warm **Gulf Stream** current keep much of Europe relatively warm during winter. That ocean current originates in the Caribbean and travels northward past the Atlantic seaboard of the United States before moving away from North America toward Europe. As it traverses the North Atlantic, it is renamed the **North Atlantic Drift**. This warm current brings large supplies of energy to Europe. As the current wraps northward around Scandinavia, it keeps Murmansk, a port city in Russia, ice free despite being north of the Arctic Circle.

► Topography

Topography also affects climates. Temperature in the troposphere generally decreases with height, at an average rate of 6.5 °C/km. If a location is mountainous, the climate varies widely across short distances because of rapid changes in altitude (and, therefore, temperature) and the amount of exposure to the Sun through the year. If a location is relatively flat, that area responds to energy changes more uniformly.

The rapid decrease in atmospheric mass (and, therefore, density) with height also affects conditions in rugged terrain. One-half of the mass of the atmosphere lies within only 5 km (3 mi) of the surface. In high elevations the decreased mass of the atmosphere can cause human health implications such as oxygen deprivation, resulting in shortness of breath, headaches, nosebleeds, and even death.

Because of decreases in mass and density, it is common to see high diurnal temperature ranges at high elevations compared with other locations that are lower in elevation but along the same parallel of latitude. This contrast is caused by differences in the transfer of energy through a “thin” versus a “thick” atmosphere. The thicker atmosphere at low elevations stores heat far longer and more effectively than one that contains less mass because the matter composing the dense, thick atmosphere absorbs a relatively large amount of insolation. By contrast, at high elevations less matter is available in the thin, sparse atmosphere to absorb radiation. The result is that mountain peaks have warmer daytime surfaces than one might expect because of differences in pressure alone. At night the sparse high-altitude atmosphere allows the surface to radiate its energy back to space quickly and effectively, causing temperatures to plummet.

Mass and density changes also affect the behavior of fluids such that at high elevations water evaporates

more quickly than in a denser atmosphere. This occurs because individual water molecules can “break free” from the surrounding water more easily under lower pressure and convert into a vapor more easily. Increased pressure associated with a denser atmosphere tends to hold the individual water molecules more firmly together as a liquid. We can see a manifestation of this concept by examining the boiling point of water at various elevations. As elevation increases, the temperature at which water boils decreases. At sea level water boils at a temperature of 100°C (212°F). But at approximately 2.75 km (9000 ft) above sea level, the boiling point of water is roughly 9.2 °C (16.5 °F) lower.

Topography also influences the distribution of precipitation. When air is forced up the side of a slope, it is likely to become saturated, because air saturates more easily as it cools moving uphill. This **orographic effect** may cause a cloud to be created and perhaps produce precipitation. The windward side of a slope often experiences significantly more precipitation than the leeward side. The leeward side is often quite dry, because as the air sinks downhill it warms, which stifles cloud and precipitation processes.

In the extratropical northern hemisphere, the south-facing slope often experiences much higher temperatures than locations at the same elevation on the north-facing slope, because of direct exposure to solar radiation. The southern hemisphere’s north-facing slopes tend to be warmer for the same reasons. The side facing the Sun is known as the **adret slope**; these are typically more useful for agriculture and range activities than the side of the mountain confined in the shadow of sunlight—the **ubac slope**. Adret slopes are also more likely to be dotted with villages as a result of the economic activities occurring on them. The ubac slope is not only colder but is also often damper and more likely to be forested, because evaporation rates are slower, but if the mountain is high enough, trees cannot grow in the frigid upper reaches of the mountain. In locations where the western side of the adret, which experiences the hot afternoon Sun, receives little orographic precipitation, the mountain can have especially large moisture differences from the adret to the ubac slope. In locations with a pronounced orographic effect, however, the leeward versus windward sides will usually show a stronger moisture contrast than the adret versus ubac sides.

► Local Features

The last climatic control is collectively described as local features. This catch-all term refers to isolated influences on the climate of a particular small area adjacent to those influences. Such factors include the

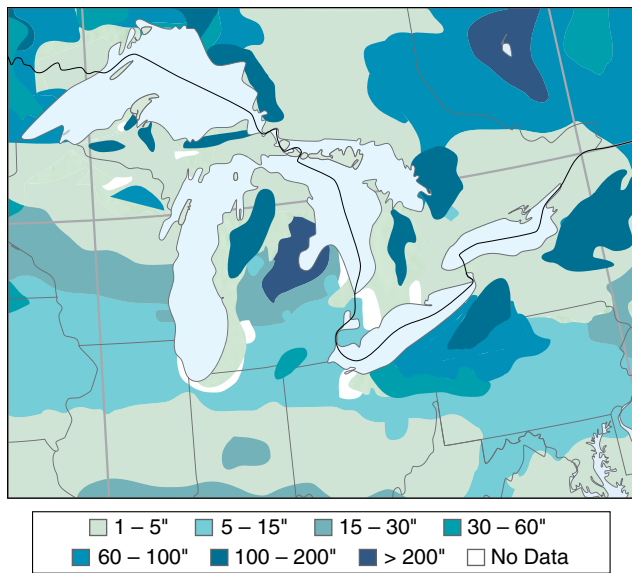


FIGURE 3.18 Average annual snowfall totals (inches) along the Great Lakes.

Data from Morgan, M. D., and J. M. Moran. 1997. *Weather and People*. (Upper Saddle River, NJ: Prentice Hall).

presence of lakes, wetlands, forests, agricultural areas, and urban areas.

A notable example of a feature's influence on local climate involves the Great Lakes. During winter, **lake effect snows** occur as the relatively warm lake waters evaporate into much colder, drier air masses blowing over them from the northwest. The moisture quickly condenses in the cold air, creating clouds and snowfall for the downwind locations (**FIGURE 3.18**).

Another notable example of a local influence on climate involves the extra warmth associated with cities, a phenomenon known as the *urban heat island*. Urban areas heat more than the surrounding rural regions because of a combination of impervious surfaces, lack of vegetation, building geometry, the presence of glass and steel structures, and machines (including air conditioners and cars) that emit waste heat into the local environment. In some cases urban areas may be as much as 6 to 8 C° (10 to 15 F°) warmer than the surrounding rural environment.

Pollution can also contribute to local energy and temperature variations because it interacts with some radiation streaming toward the surface. Pollution needs to be severe for one to notice an appreciable decrease in surface temperatures. Recent conflicting research calls into question the net effect of pollution, as the absorption of insolation and subsequent extra radiation emitted downward to Earth by some types of pollutants may create a net warming effect. We simply do not have a deep enough understanding of the effects of pollution on temperature to reach a firm conclusion on its impact.

▶ Putting It All Together: Spatial and Seasonal Variations in Energy

A location's climate results from the culmination of all climatic controls working cumulatively. Some factors contribute to wide energy variations over the globe through the course of the year, despite the fact that circulation is constantly working to even out these energy imbalances. The result is that temperature varies from one location to another across Earth and at any particular location through the course of the year.

Isotherms—lines connecting points that have the same temperature—can be used to map the influence of the various controls on climate. **FIGURE 3.19** shows that July isotherms extend poleward over the warm continents of the northern hemisphere as a direct result of continentality influences. The most significant warming occurs over Asia, where continental influences are most pronounced. By comparison, ocean temperatures show a somewhat even and gradual temperature decline with increasing latitude. Figure 3.19 also shows that the longer July days in the high latitudes of the northern hemisphere lead to relatively mild temperatures, while the southern hemisphere's high latitudes (over Antarctica) show extremely low temperatures. In general, a decline in temperatures with increasing latitude is discernible for both hemispheres. Nevertheless, significant alterations occur because of maritime and continentality effects.

In January the northern hemisphere shows pronounced continental impacts as isotherms dip dramatically toward the equator over the continents (**FIGURE 3.20**). The pattern is caused by rapid and intense cooling of the land surfaces during this time of net energy deficits. Again, Asia has especially strong effects because of the size of that land mass. The southern hemisphere shows a rather simplistic, latitudinally driven temperature pattern because of the lack of continental effects in that hemisphere. But some continentality is still evident as isotherms shift poleward over the continents in the southern hemisphere summer.

The effects of ocean currents may be seen as well. Isotherms dip equatorward along the eastern ocean edges as cold, high-latitude water is pulled toward the equator, in July (Figure 3.19), in January (Figure 3.20), and in all other months. A further influence stems from coastal upwelling because of the net transport of surface waters by the Ekman spiral away from the coast. Likewise, the western ocean basins show poleward bumps in the isotherm patterns as warm, low-latitude waters migrate poleward. The Gulf Stream is a prime example.

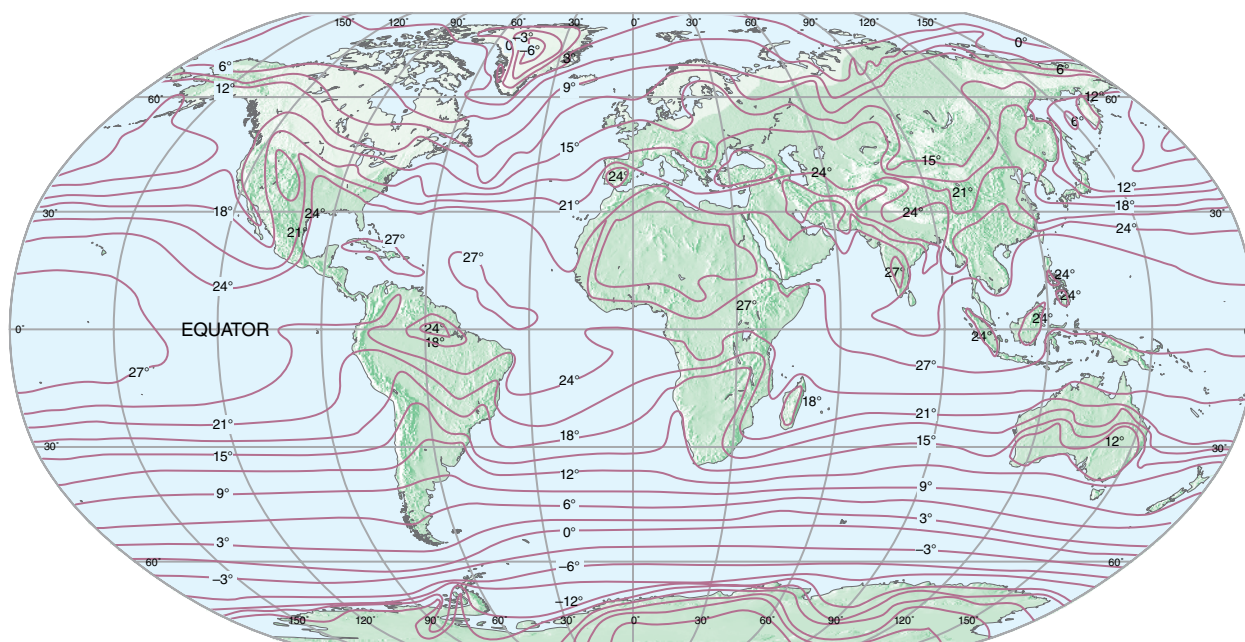


FIGURE 3.19 July surface air temperatures ($^{\circ}\text{C}$).

Data from: National Oceanic and Atmospheric Administration.

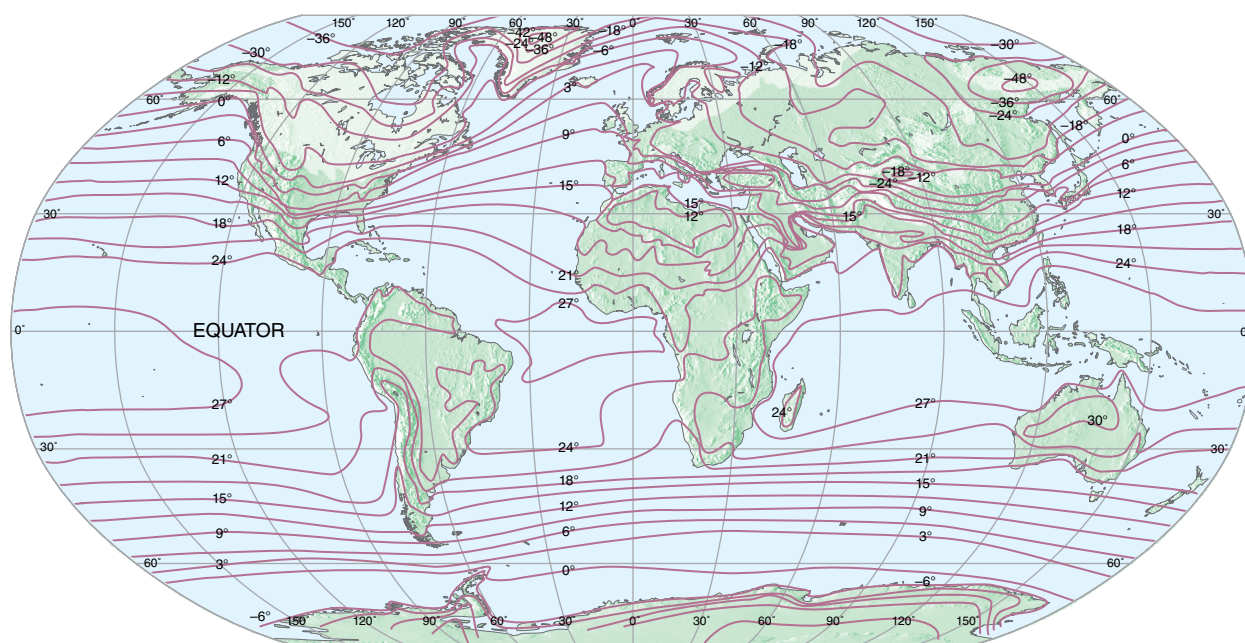


FIGURE 3.20 January surface air temperatures ($^{\circ}\text{C}$).

Data from: National Oceanic and Atmospheric Administration.

Continental and maritime effects are easily seen on a map depicting the difference between mean January and July temperatures. **FIGURE 3.21** shows these differences. Large continental regions exhibit significant differences, whereas maritime locations depict more thermal consistency throughout the year. The largest land masses show the widest range of mean monthly temperature through the year. Central Asia experiences an astonishing 60°C (108°F) or more temperature change, while the high latitudes of

North America record a maximum change of about 45°C (81°F) throughout the year. Because of its low latitude, Africa reports a maximum monthly range of only about 20°C (36°F) between the extreme seasons, whereas South America and Australia record peak ranges on the order of 15°C (27°F). The continent that sees the least amount of intraannual temperature change is Antarctica. This is caused largely by the continuous ice coverage, which effectively reflects summer's insolation.

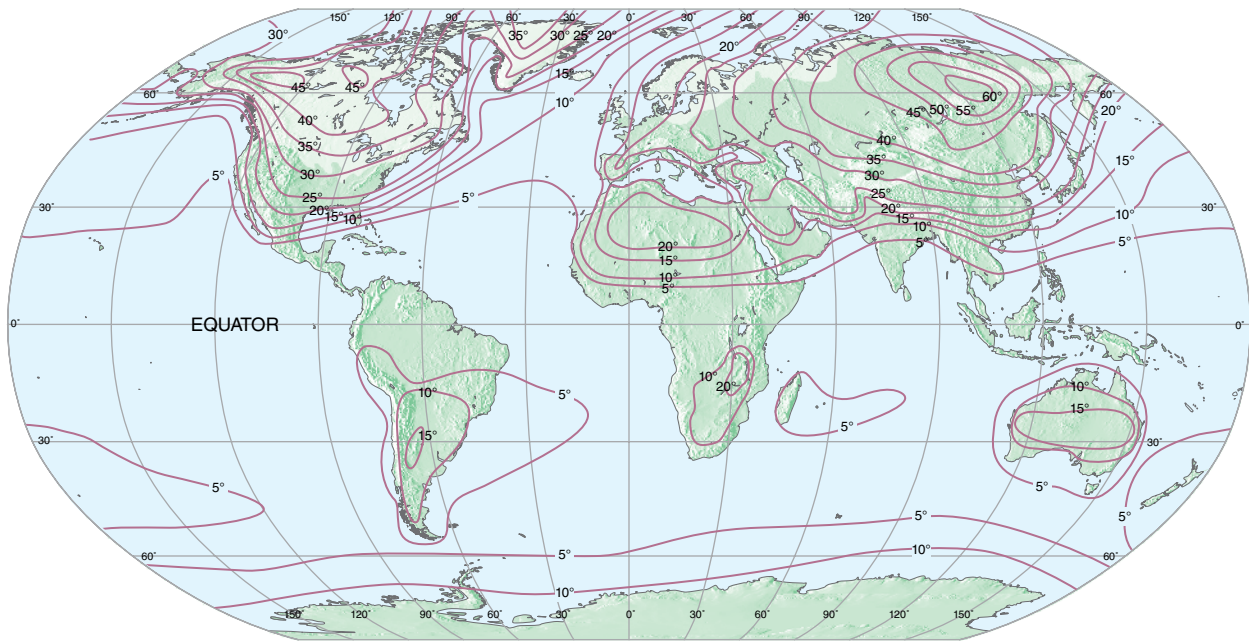


FIGURE 3.21 Temperature differences between January and July (°C).

Data from: National Oceanic and Atmospheric Administration.

► Summary

Six factors cause the climate of a location to have its fundamental characteristics: latitude, Earth–Sun relationships, position in the continent, atmospheric and oceanic circulation, topography, and local features. Latitude is the position of a location on Earth relative to the equator. Assuming that all other factors are equal, locations with higher latitudes (i.e., more poleward locations) generally experience lower temperatures than locations at lower latitudes. The Sun’s rays strike at a 90° angle only at the meridian of longitude that is experiencing solar noon and the parallel of latitude at the solar declination on a given day. All other lines of latitude (and longitude) experience solar angles that are less than 90°. The solar declination thus changes with the day of the year, as Earth revolves around the Sun, and the longitude of the Sun’s direct rays changes with the time of day, as Earth rotates on its axis.

Earth–Sun relationships play an important role as controls on climate. Earth’s orbit is not circular, and the Sun is not at the center of the orbit. Instead, Earth is closest to the Sun during January and farthest from it during July. Earth–Sun distance does not cause the seasons, but it does affect the severity of the winter and summer seasons. Instead, the changing orientation of Earth’s tilt relative to the position of the Sun as Earth revolves around the Sun is the cause of the seasons. The tilt and revolution cause all lines of latitude to receive differing amounts of solar radiation throughout the year and the direct rays of the Sun to strike at latitudes

varying from 23.5°N (the Tropic of Cancer) to 23.5°S (the Tropic of Capricorn). Tilt and revolution also cause day length to vary over the course of the year for each line of latitude, except at the equator.

Continental position is also an important climatic control. Interior continental locations are more affected by variations in energy through the course of the year than coastal locations. This difference occurs largely because large water bodies are capable of storing large quantities of energy during warm periods and releasing that energy during colder periods. This imparts a moderating maritime effect on coastal locations, while interior locations experience a wider temperature range through the year as part of a continentality effect.

Atmospheric and oceanic circulation factors play a role in the climate of particular locations as well. The mission of both the atmospheric and the oceanic circulation is to balance inequalities in input energy received from the Sun. Persistence of motion of these fluids leads directly to prevailing winds and ocean currents, thereby affecting climates. Wind is simply a transfer of atmospheric mass between two locations, and it is the atmospheric mechanism behind the circulations that affects climate. Wind speed and direction result from several interacting forces, including the PGF, the CE, CA, and friction. Surface winds are affected most strongly by friction, which changes the speed and trajectory of the initial wind. Upper-level winds are affected by friction only negligibly, so air motion in the free atmosphere is quite different from that near the surface. Pressure

differences in the atmosphere lead to the development of cyclones and anticyclones.

Topography and local features also play significant roles in the development of the climate of a location.

All controls on climate cause variations in energy across Earth's surface. The influence of these controls across space is evident on a map of isotherms.

Key Terms

Absolute zero	Ideal gas law	Plane of the ecliptic
Adret slope	Inertia	<i>Pressure</i>
Advection	Inertial period	Pressure gradient force (PGF)
<i>Aerosol</i>	<i>Insolation</i>	Prime meridian
Antarctic Circle	Isobar	Radiant energy
Anticyclone	Isotherm	Refraction
Aphelion	Joule	Revolution
Arctic Circle	June solstice	Rotation
Attenuation	Kelvin temperature scale	<i>Second law of thermodynamics</i>
Autumnal equinox	Kinetic energy	Sensible energy
Axial tilt	Lake effect snow	September equinox
Backing	Latent energy	Solar declination
Beam spreading	Latitude	Solar noon
Centrifugal acceleration (CA)	Leeward	Specific heat
Circle of illumination	Longitude	Summer solstice
Continentality	March equinox	Thermohaline circulation
<i>Convection</i>	Maritime effect	Time zone
Coriolis effect (CE)	Midlatitude (frontal) wave	Tropic of Cancer
Cyclone	cyclone	Tropic of Capricorn
December solstice	Millibar (mb)	Tropical cyclone
Downdraft	<i>Momentum</i>	<i>Troposphere</i>
Ekman spiral	<i>National Weather Service</i>	Ubac slope
Equation of state	Navier-Stokes equations	Updraft
<i>Evaporation</i>	of motion	Upwelling
<i>Flux</i>	Newton (N)	<i>Urban heat island</i>
Free atmosphere	Newton's laws of motion	Veering
<i>Friction</i>	North Atlantic Drift	Vernal equinox
Geostrophic balance	Orographic effect	<i>Wind</i>
Geostrophic wind	Parallelism	Windward
Gulf Stream	Pascal (Pa)	Winter solstice
Heat index	Path length	
<i>Hydrostatic equilibrium</i>	Perihelion	

Terms in italics have appeared in at least one previous chapter.

Review Questions

1. Discuss the role of latitude as a climate control.
2. How does position on a continent affect the climate of a location?
3. Compare and contrast the maritime effect and continentality by examining the climate of various cities located along the same line of latitude.
4. Discuss the important characteristics of Earth's orbit.
5. What is the axial tilt of Earth and why is this important?
6. How does parallelism play a role in seasonality?
7. Compare and contrast Earth-Sun relationships during the equinoxes and solstices.

8. How do Earth–Sun relationships affect the spatial and temporal distribution of energy through the year for each hemisphere?
9. What roles do day length, attenuation, aerosols, and path length play in seasonality?

Questions for Thought

1. Given what you have learned in this chapter, can a hurricane track from the northern to the southern hemisphere, or vice versa? Why or why not?
2. What forces are most important in producing a tornado?
3. How does specific heat compare between water and land surfaces?
4. What is the surface wind equation and how do the forces involved interact to produce wind?
5. How are winds, and the forces involved, in the free atmosphere similar to/different from those at the surface?
6. Compare and contrast characteristics of cyclones and anticyclones.
7. What role do surface ocean currents play in climate?
8. What is the Ekman spiral and how does it develop?
9. How are thermohaline currents important to climate?
10. What is the role of topography and altitude on the climate of a particular location?
11. What local features may influence the climate of a location? How?



CHAPTER 4

Atmospheric Interactions with the Other “Spheres”

CHAPTER AT A GLANCE

- Ocean Circulation
 - ▶ Surface Currents
 - ▶ Deep Ocean Thermohaline Circulations
- El Niño–Southern Oscillation Events
 - ▶ Walker Circulation
 - ▶ Historical Observations of ENSO
 - ▶ El Niño Characteristics
 - ▶ La Niña Characteristics
 - ▶ Global Effects
 - ▶ Effects in the United States
 - ▶ Relationship to Global Warming
 - ▶ Climatic Feedbacks in the Ocean
- Volcanic Activity and Climate
 - ▶ General Effects
 - ▶ Aerosol Indices
- Deforestation and Desertification
- Cryospheric Changes
 - ▶ Ice on the Earth’s Surface
 - ▶ Feedbacks in the Cryosphere
- Summary
- Key Terms
- Review Questions
- Questions for Thought

In addition to the major controls on the climate system, such as the effects of *latitude*, Earth–Sun relationships, *continentality*, atmospheric and oceanic circulation, elevation, and general local features, interactions between the *atmosphere*, *hydrosphere*, *lithosphere*, and *biosphere* must also be considered. This chapter explains the role of other important components on the climate system. These contributors may be thought of as internal components because they affect the system already set in place by the aforementioned climate controls. The features discussed in this chapter work to influence and change the already-established climate system. The oceans warrant further scrutiny in this regard. Because over 70% of Earth’s surface is covered by oceans, processes occurring in the oceans play an important role in climate and climatic variations. The chapter concludes with other examples of interactions between the various “spheres” that affect climate.

► Ocean Circulation

Surface Currents

Atmospheric Effects

Oceanic surface currents are driven by overlying winds that on the broadest scale are dictated by the great global atmospheric **subtropical anticyclones**—large, semipermanent high-pressure cells that exist in each

ocean basin approximately centered on the 20° to 30° parallel of latitude. These subtropical anticyclones wax and wane in strength and position seasonally, but they are always present. The clockwise circulation of the anticyclones in the northern hemisphere and the counterclockwise circulation of the systems in the southern hemisphere initiate corresponding surface water motions in the oceans. Of course, the near-surface waters are also moved by the *Coriolis effect* inducing the *Ekman spiral*, but for a large section of the oceans, near-surface waters move in a general clockwise pattern in the northern hemisphere and counterclockwise in the southern hemisphere because of these subtropical anticyclones (FIGURE 4.1). These circular flows, caused by a coupling of the atmospheric and surface oceanic circulations, are termed **gyres**.

The large-scale motions of the oceanic surface ensure that cold currents occupy the eastern sides of the ocean basins and warm currents are found along the western edges of the basins. This spatial pattern is caused by mass *advection*—lateral movement—of warm waters traveling from relatively low latitudes along the western ocean edge, while cold water from the high latitudes is advected along the eastern edge, in both hemispheres. The effect is that low surface temperatures on the eastern ocean basins (with warmer air above the cold air adjacent to the cold water) tend to stabilize the atmosphere. A **stable atmosphere** is one in which vertical motions are discouraged because the colder, denser air exists below

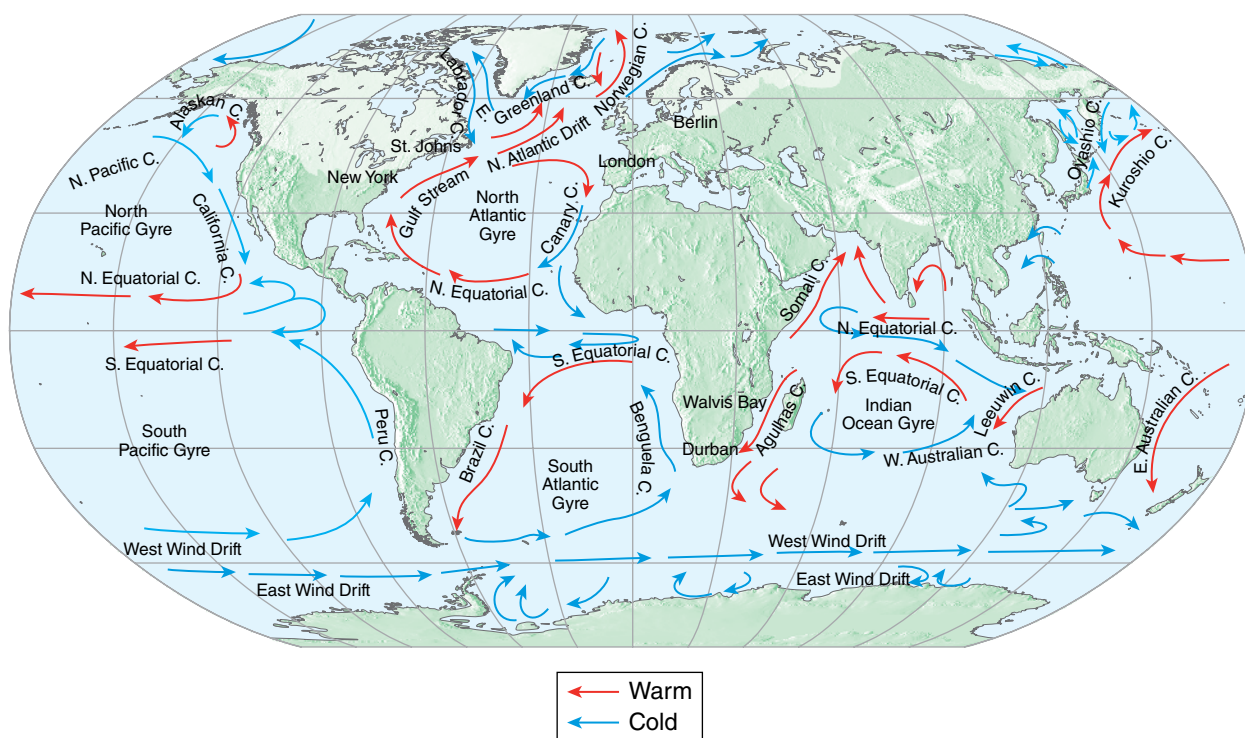


FIGURE 4.1 Surface currents.

warmer, less dense air. A stable atmosphere promotes net sinking motions in the atmosphere, which discourages cloud formation processes. For this reason some of the most enjoyable climates on Earth are located along the eastern ocean margins (and, therefore, the western coasts of continents) where pleasant temperatures, abundant sunshine, and little precipitation occur.

By contrast, the western ocean basins are dominated by warm waters that destabilize the overlying atmosphere. In this situation warm, moist air adjacent to the warm ocean currents becomes buoyant and rises. Such an **unstable atmosphere** is generally conducive to cloud formation and precipitation. The western ocean basins (and the adjacent eastern coasts of continents) therefore typically have abundant precipitation that is usually distributed fairly evenly throughout the year. During summers the subtropical and tropical midlatitude regions on the east coasts of continents become hot and humid because abundant water vapor usually exists from the *maritime effect*. In winter the effect is less pronounced, at least in the middle and subtropical latitudes, as westerly wind systems dominate the mid-latitudes, promoting more continental temperatures along the eastern coasts.

Upwelling, Downwelling, and Mass Advection

Upwelling reinforces the effect of the cold currents along the eastern ocean basins. When offshore surface winds parallel a coastline for some distance, with the coastline to the left of the direction of flow in the northern

hemisphere (and to the right of the flow in the southern hemisphere), the net water advection near the surface is directed away from the coastline by the Ekman spiral. Upwelling results from the Ekman spiral's deflection of surface water to the right (in the northern hemisphere) with depth. Examples of locations around the world where upwelling is particularly effective because of the coastline shape and consistency of the winds are shown in **FIGURE 4.2**. Upwelling also can occur in areas where two currents diverge, allowing water from the depths to rise to replace the surface water that has been moved away laterally. Regardless of the cause of the upwelling, departing surface waters are replaced by cold deep water from beneath. In such situations an already cold surface current becomes even colder.

Perhaps the best example of upwelling is associated with the **Humboldt** (also known as the **Peru**) **current** located off the western coast of South America (**FIGURE 4.3**). The South Pacific subtropical anticyclone is particularly well established and strong, because of the size of the South Pacific Ocean and the lack of interfering land masses. A strong and persistent counterclockwise circulation results and forces very cold surface waters to move equatorward from the Antarctic. As this water parallels the South American coast, the Ekman spiral forces it westward. The upwelling results in one of the coldest ocean currents on Earth. The low surface temperatures (even at tropical latitudes) stabilize the overlying atmosphere, causing cool, dry climates to dominate the western edge of the continent. The Atacama Desert of coastal Peru and Chile is the driest desert on Earth.

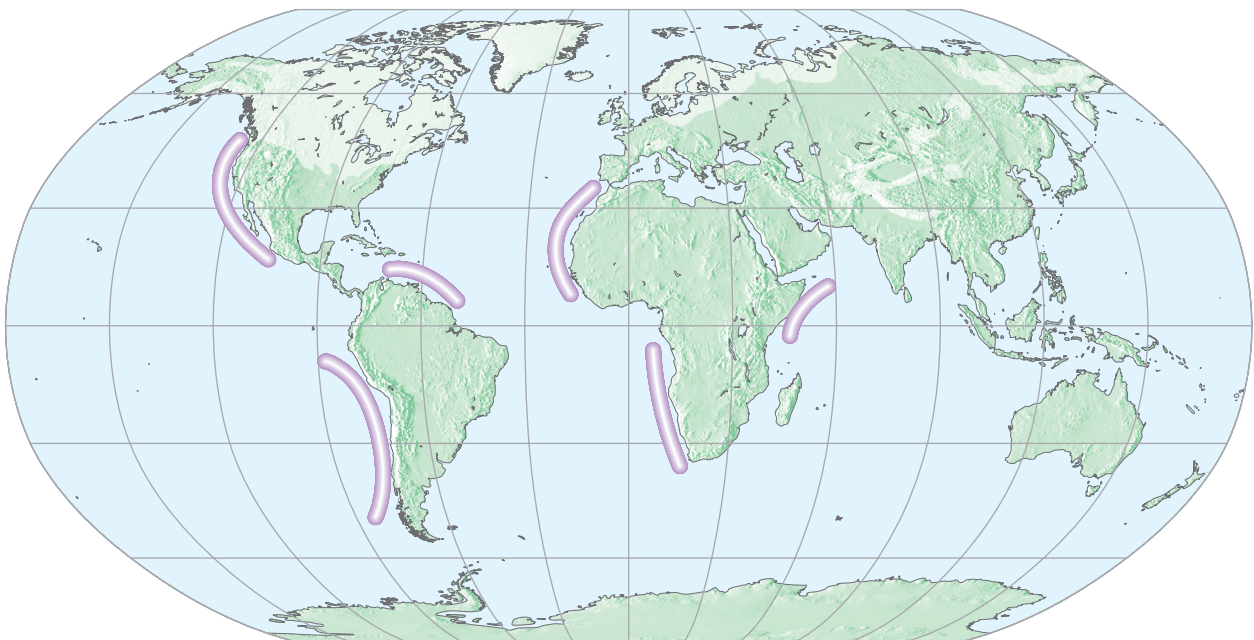


FIGURE 4.2 Major regions of upwelling in the world ocean.

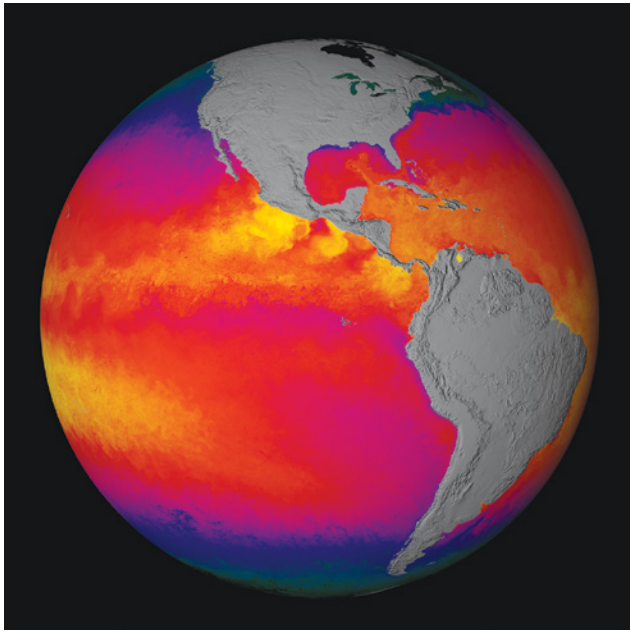


FIGURE 4.3 Cold water upwelling (in purple) along the western South American coast.

Courtesy of NASA Goddard Space Flight Center.

On the western sides of ocean basins, **downwelling** may occur. This oceanic process is the reverse situation in which surface airflow pushes water against a coast-line where it is forced to sink. In addition, in locations where two surface ocean currents converge, the pile-up of surface water can induce downwelling. Downwelling typically supports high ocean temperatures as sinking warm waters push the cold water to deeper levels. An example occurs along the equatorial western Pacific Ocean where easterly (east to west) winds push waters westward toward Indonesia. This water warms significantly along its westward journey across the tropics. On the western side of the equatorial Pacific, the water is forced to sink. The Ekman spiral does not affect the bulk of this water because the Coriolis effect does not occur along the equator. Without Coriolis deflection the current maintains its straight course. The **Maritime Continent**—the Indonesia–Philippines–Australia region—is, therefore, dominated by high ocean surface temperatures that promote low-level atmospheric instability. Such situations support cloud formation and precipitation. Locations on the western sides of ocean currents (eastern sides of continents) in the subtropics are usually dominated by warm, wet climates.

In the North Atlantic Ocean, for example, the subtropical anticyclone forces a clockwise circulation that supports the cold water **Canary current** off the coast of southern Europe and northern Africa, the **North Equatorial current** near the equator, the warm **Gulf Stream** along the eastern coast of North America, and the **North Atlantic Drift**, which completes the northern

gyre circulation. Again, the circulation regime is initiated by the atmospheric anticyclone and mimicked by the ocean in a corresponding gyre. Similar oceanic circulations occur in all other ocean basins.

Because of the deflection of the Ekman spiral, water tends to pile beneath the subtropical anticyclones in each ocean basin. As the gyre circulates, the Ekman spiral dictates that mass advection occurs 45° to 90° to the right (in the northern hemisphere) of the initial water motion. Equatorward-moving surface water, the Canary current in this example, is forced toward the central ocean region. Water moving from east to west across the low latitudes in association with the North Equatorial current is also forced by the Ekman spiral toward the middle of the basin. Surface waters associated with the Gulf Stream and portions of the North Atlantic Drift, which moves essentially west to east, are also forced toward the ocean center. The result is a mound of water located roughly in the middle of the North Atlantic Ocean basin near the center of the atmospheric subtropical anticyclone. The mound supports sea levels exceeding those of surrounding locations.

At the same time, gravity acts on the mound, pulling it downward toward the lower sea level on the periphery. The water within this mound thus is constantly affected by offsetting forces. The Coriolis effect (manifested as the Ekman spiral) pushes water inward, whereas gravity pulls water outward (downward). As the water circulates clockwise (in the northern hemisphere) along this mound, it reaches an equilibrium between the two forces. An oceanic version of **geostrophic flow** occurs when these forces are in balance (**FIGURE 4.4**).

An exactly opposite condition occurs for waters flowing counterclockwise (in the northern hemisphere) in association with semipermanent low atmospheric pressure regions, normally centered around 60° latitude. An oceanic depression occurs at these locations and waters swirl around the depression in geostrophic balance.

The central axes of these mounds and depressions are not perfectly centered beneath the atmospheric highs and lows but instead are offset toward the west of the centers. This is because Coriolis deflection

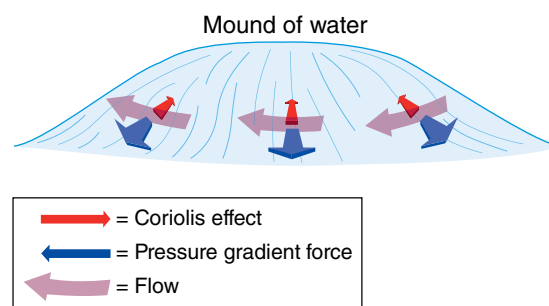


FIGURE 4.4 Geostrophic balance in the ocean.

increases with latitude, affecting the amount of water transported via the Ekman spiral along the gyre. Poleward-moving currents have increasing amounts of water advected toward the center of the basin, while equatorward-moving currents have decreasing amounts of net transport along their trajectory. The result is a pile of water with its axis offset to the west of the central ocean basin.

The offset central axis causes poleward-moving waters (i.e., on the western sides of ocean basins in both hemispheres) to be squeezed in a relatively narrow zone between the continent and the mound axis. When a moving fluid converges, as in this case, a speed change is initiated because the fluid is forced through a smaller space over a constant time period. This type of speed change may be seen when placing a finger partially over the opening of a hose. Once the opening constricts, water, under pressure, is forced to increase in velocity. In the ocean the response results in **western-boundary intensification**, a deep and swift western ocean basin current (FIGURE 4.5). The Gulf Stream is a perfect example of western-boundary intensification, because it is a deep, fast-moving western ocean basin current. On the opposite side of the ocean basin, the cold water current (in this case, the Canary current) is typically shallow and slow-moving and is spread across a larger surface area. These properties affect the climates of adjacent locations.

Another way to view western-boundary intensification is relative to the slope of the sea surface. Because the central axis of the water mound is offset to the west, the corresponding slope in sea surface is steeper in that location. This results in water moving along a steeper pressure gradient, which increases the speed of water motion. On the opposite side of the ocean basin, the colder water flows over a much gentler sea surface slope, resulting in a slower rate of flow (Figure 4.5).

Deep Ocean Thermohaline Circulations

Surface currents are not the only currents that influence climate. Deep ocean currents are driven by *thermohaline*

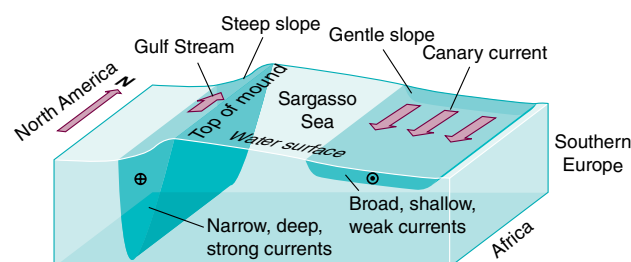


FIGURE 4.5 Western-boundary intensification.

circulation. **Thermohaline currents** flow in response to temperature (“thermo”) and/or salinity (“haline”) characteristics through the deep ocean. Just as density differences (cold versus warm) in air drive atmospheric motions, deep ocean thermohaline differences establish net pressure gradients. The fluids of the deep ocean respond, because denser waters tend to sink beneath less dense waters. Because colder, saltier water is denser than warmer, fresher water, net downward motions occur where waters become colder and/or saltier. Warmer and/or fresher waters are more buoyant and rise. Any situation in which colder water underlies warmer water represents **stable stratification**, the oceanic equivalent to a stable atmosphere (FIGURE 4.6). Further *convection* (vertical motion) is suppressed unless another force or energy source initiates it.

Deep ocean currents are actually driven by surface processes because seawater gains its thermohaline characteristics from surface sources. Intense solar heating in low-latitude regions warms the water surface sufficiently to decrease its density. The reduced solar input and heat loss (to the frigid atmosphere) in high-latitude regions favor a denser ocean surface because of its colder surface characteristics. Precipitation characteristics of both the ocean and the surrounding land masses also influence the density of ocean waters. Some oceanic areas have abundant precipitation; water in such areas

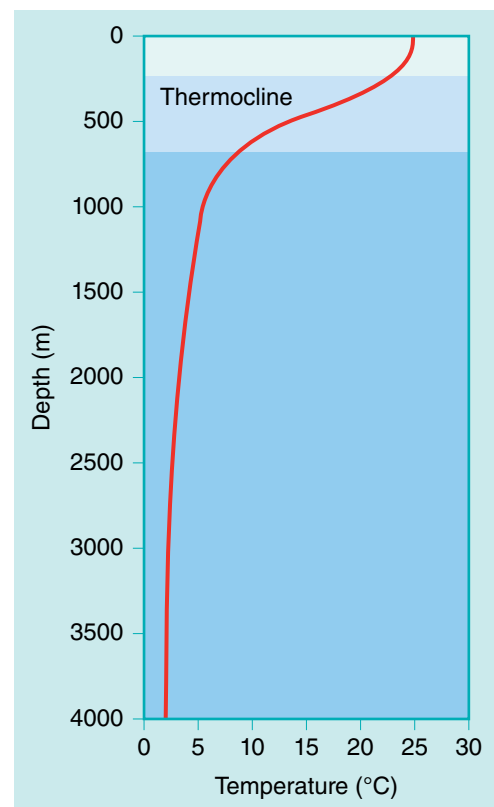


FIGURE 4.6 Deep water stratification.

is less dense because of this high input of fresh water. Likewise, oceanic areas near coastlines in humid climates typically have fresher water because of abundant input of stream discharge. By contrast, marine areas that receive less precipitation than *evaporation* and/or have input only from a few small streams typically have dense, salty water. Somewhat surprisingly to most students, a high percentage of the global ocean falls into this “dry” category.

The freshest ocean waters on Earth are typically found near the equator, where high temperatures and abundant precipitation support low-density waters. High salinities usually occur near the centers of the subtropical anticyclones (30° latitude), where abundant sunshine evaporates large quantities of surface water, leaving behind salts. When these salty waters are advected to higher latitudes, the high salt content combines with lower temperatures to create the densest ocean waters. These waters sink to the deep layers of the ocean where they are forced to move along thermohaline gradients.

Source areas are locations near the surface that provide water to the ocean depths. These are located in relatively high-latitude regions of the Atlantic and Pacific Oceans (**FIGURE 4.7**). In the North Atlantic, deep water originates at the surface near Iceland, where it sinks and moves equatorward. The South Atlantic also acts as a source area for deep water near Antarctica and in the area east of the tip of South America. In the North

Pacific, deep water sinks near the tip of the Aleutian Islands and moves equatorward. The South Pacific deep-water source area is located near 65°S latitude.

Many deep-water thermohaline currents exist, but the main one in the Pacific moves deep water from the North Pacific southward across the equator and then loops in the extreme South Pacific back toward the equator. In the Atlantic Ocean the main body of deep water also begins in the northern hemisphere near Iceland. It travels equatorward largely beneath the Gulf Stream, crosses the equator off the eastern coast of South America, and then continues toward Antarctica. Once in the high latitudes the deep water turns eastward before moving back toward the equator. The deep water travels northward near its opposing equatorward-flowing counterpart, before completing the loop near Iceland.

Deep waters travel at varying depths relative to each other. This makes it possible for different deep-water currents to occupy similar regions. The deepest waters in the Atlantic Ocean are those arriving from the **Antarctic Bottom Water**, the coldest ocean current, which forms near Antarctica (Figure 4.7). The **Antarctic Deep Water**, which is slightly warmer, moves over that layer as it flows northward and gently upward, eventually flowing beneath the current known as the **North Atlantic Deep Water**. The progression continues upward to the surface.

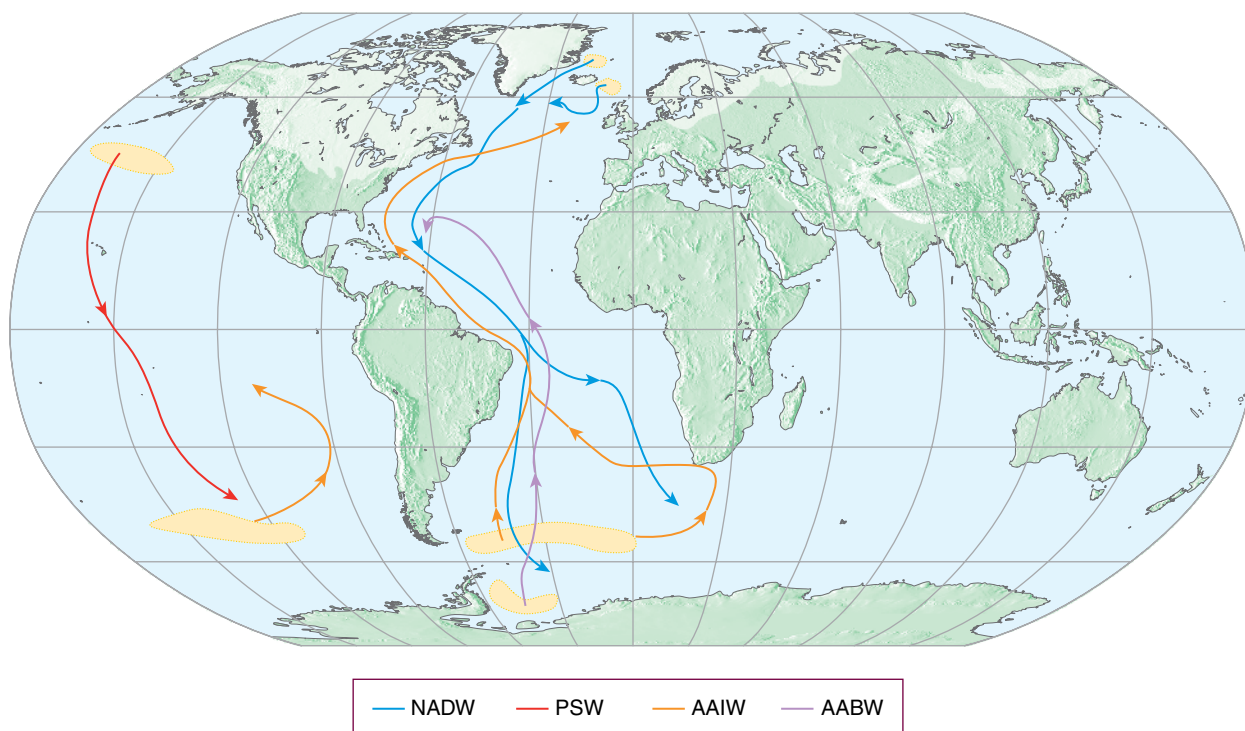


FIGURE 4.7 Deep ocean currents of the world with source areas depicted in yellow.

Data from Gordon, A. L., Lamont-Doherty Geological Observatory Report 1990–91.

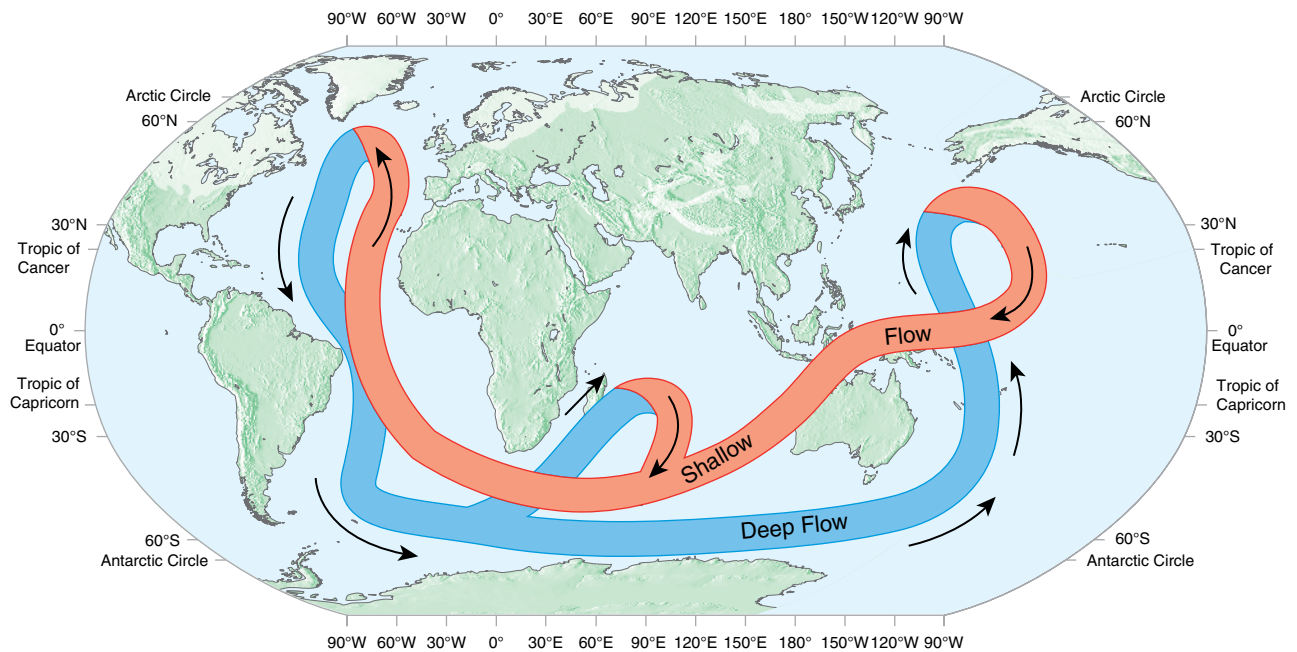


FIGURE 4.8 The Stommel deep water conveyor model.

In the Pacific, two currents—the **Common Water**, initiated again near Antarctica, and the **Pacific Subarctic Water**—occupy the lowest layers of the ocean. These currents are overridden by the **Antarctic Intermediate Water** and the **North Pacific Intermediate Water**. Surface waters override those layers. Thermohaline currents in the Indian Ocean are dominated by Common Water arriving from the region of Antarctica and Antarctic Intermediate Water.

Coexisting with these individual thermohaline currents is a massive conveyor current that connects all the ocean basins on Earth except the Arctic. Much of what is known concerning this deep-water thermohaline conveyor comes from the work of Henry Stommel. In 1958 Stommel devised the simplified model of deep ocean circulation, basing water motions on similar forces that drive western-boundary intensification. The **Stommel model** indicates that net sinking motions are initiated in the North Atlantic near Iceland (**FIGURE 4.8**). This water sinks to the floor of the North Atlantic as it moves equatorward. After crossing the equator the conveyor moves toward Antarctica, where Antarctic Bottom Water is added. Then, it turns eastward to move between Africa and Antarctica. The deep water continues eastward but forks into two branches, one progressing equatorward through the Indian Ocean and the other moving eastward into the Pacific. The Indian Ocean branch rises toward the surface near the equator south of India. This water then turns southward and moves as a warmer shallow layer back toward the Atlantic. The southern deep-water branch progresses into the South Pacific before moving northward east of Australia. This

water stream crosses the equator and rises in the central North Pacific. It then loops back and moves near the Maritime Continent as shallow water. This current ultimately joins the shallow water stream in the Indian Ocean. Both branches then move back around the tip of Africa and into the Atlantic, where the conveyor moves northward, ultimately sinking again near Iceland.

This deep-water conveyor is capable of transporting huge amounts of oxygen and energy from one side of the planet to the other. The oxygen provides a mechanism by which oceanic life is supported. The energy is capable of influencing climate for centuries, as signatures of past climatic variations are present in the slow-moving water itself. Reintroduction of this stored energy into the present or future atmosphere can alter climate, particularly where the conveyor approaches the surface and can transfer the energy back into the atmosphere easily. Likewise, present-day atmospheric changes, most notably **global warming**, can provide additional storage of energy in the conveyor belt and elsewhere in the oceans. This additional energy is likely to cause future changes both to the hydrosphere in the form of surface currents, thermohaline circulation, and conveyor belt and to other “spheres” in the climate system. The impacts are uncertain.

► El Niño–Southern Oscillation Events

The **El Niño–Southern Oscillation (ENSO) event** is perhaps one of the most misunderstood of all atmospheric processes. ENSO events affect global weather in a

profound way. Only Earth–Sun relationships exert more of an influence on the global climate system than ENSO.

The term **El Niño**, translated from Spanish as “the boy,” originally referred to the annual warming of the equatorial ocean current off the western coast of South America during the Christmas season (**FIGURE 4.9a**). This sea surface warming is associated with the change of seasons—the beginning of winter in the northern hemisphere and summer in the southern hemisphere. For most of the year in the tropics, strong winds, known as **trade winds**, push the warm surface waters of the tropical Pacific westward, allowing upwelling of cold, deep ocean waters in the eastern tropical Pacific. As the seasonal atmospheric circulation pattern becomes established during the transition of autumn and spring, trade winds along the equator weaken, allowing the warm water in the western equatorial Pacific to migrate back toward the east. This annual migration warms the Pacific’s eastern equatorial rim, typically around December.

Over the years the meaning of the term El Niño has changed from its original reference to the normal annual event described above. It is now used to refer only to the unusually extreme increases in sea surface temperatures (SSTs) occurring for several months approximately every 3 to 7 years in the central and eastern equatorial Pacific Ocean. By contrast, **La Niña**—the opposite of El Niño—refers to a strengthened “normal” situation, which typically reinforces cold water conditions in the eastern equatorial Pacific and warm water conditions in the western tropical Pacific near the Maritime Continent (**FIGURE 4.9b**).

The **Southern Oscillation**, recognized by the climatologist Sir Gilbert Walker in the 1930s, refers to a seesaw effect of surface atmospheric pressure between

the eastern and western equatorial Pacific Ocean in which higher-than-normal pressure in one of these two regions is coincident with lower-than-normal pressure in the other. Climatologist Jacob Bjerknes realized in 1969 that these pressure changes resulted from SST variations in the equatorial Pacific, establishing the link between El Niño and La Niña events and the Southern Oscillation.

Today, most climatologists refer to the entire phenomenon as El Niño–Southern Oscillation, or ENSO. The variations in atmospheric pressure associated with extremes in the Southern Oscillation and the changes in the oceans during extreme phases of ENSO (El Niño or La Niña events) cause unusual global atmospheric circulation features and impacts. Because it is associated with a reversal of the typical Pacific pressure patterns rather than an intensification of them, the El Niño phase usually has wider and stronger impacts than the La Niña phase.

Walker Circulation

In 1969 Bjerknes coined the term **Walker circulation** to describe the connection between the atmospheric pressure centers in the equatorial Pacific associated with the Southern Oscillation, the SSTs, and the tropical trade winds that blow from east to west near the surface across the Pacific Ocean (and other regions of the Earth within the tropics). The Walker circulation exists to balance the normally observed pressure gradients over the tropical Pacific Ocean. The Walker circulation represents “normal” or “ENSO-neutral” atmospheric and oceanic conditions in the equatorial Pacific Ocean, characterized by high surface atmospheric pressure in the east and relatively low surface

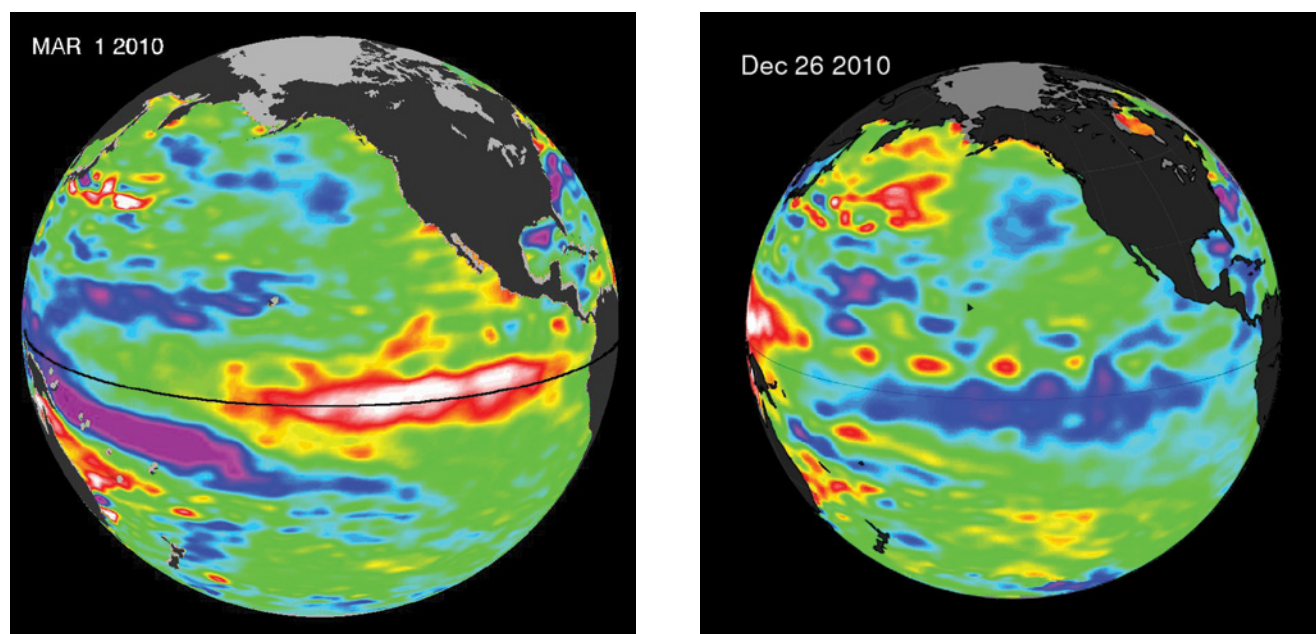


FIGURE 4.9 (a) Satellite image of sea surface temperatures in the Pacific Ocean during an El Niño event. (b) Satellite image of sea surface temperatures in the Pacific Ocean during a La Niña event.

Courtesy of JPL/NASA.

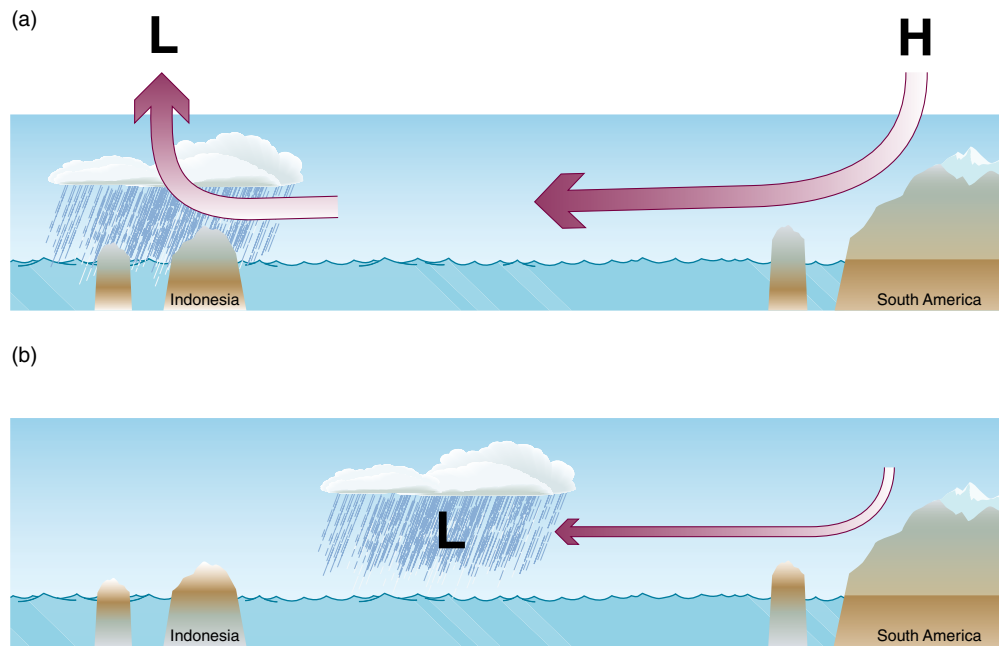


FIGURE 4.10 “Normal” (or “ENSO-neutral”) Walker Circulation (a), and El Niño-related atmospheric circulation (b).

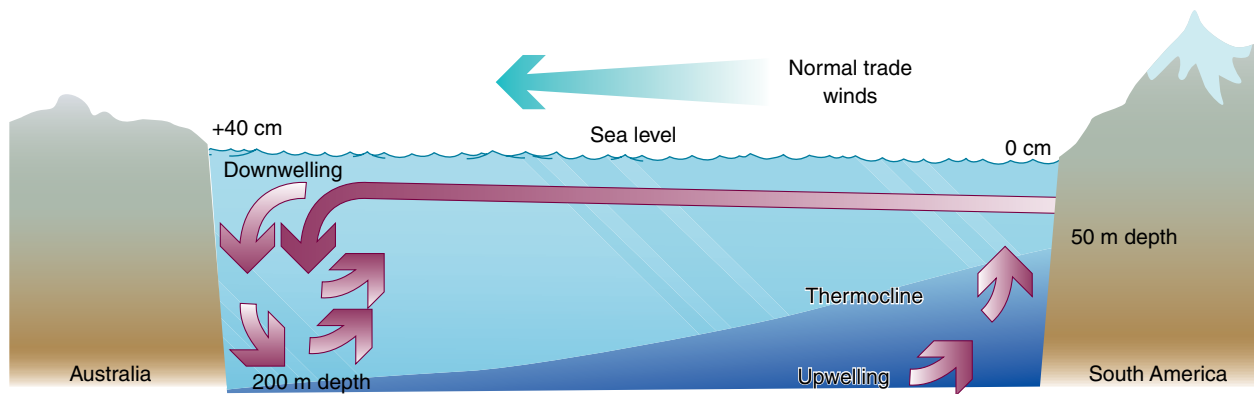


FIGURE 4.11 Warm water piling in the western equatorial Pacific during “normal” or “ENSO-neutral” conditions.

pressure in the west (**FIGURE 4.10**). A pressure gradient forms in an east-to-west direction at the surface with atmospheric mass (winds) working to “fill the low.” Thus, surface winds normally blow strongly from the east toward the west in this region. Known as the **northeast trade winds** (or northeast trades) in the northern hemisphere and the **southeast trade winds** in the southern hemisphere, these winds comprise a major part of the global atmospheric circulation and are simply the equatorward extensions of the STHs (gyres).

The frictional dragging of the sea surface by these winds causes the North and South Equatorial currents to occur along the equator, approximating the atmospheric circulation pattern, flowing from east to west in both hemispheres. The currents push the surface waters warmed by the Sun westward. This results in an accumulation of

warm water in the western tropical Pacific Ocean near Australia and the Maritime Continent. Average sea level may be as much as 40 cm (16 in) higher and water temperatures 4° to 8 C° (7° to 14 F°) higher in the western tropical Pacific than at the same latitude in the eastern Pacific near South America (**FIGURE 4.11**). The reduced sea surface temperatures (SSTs) in the east are caused both by the cold surface current of the eastern South Pacific and by upwelling of colder, deep water replacing the warmer surface waters that were displaced to the west by the equatorial currents.

These “normal” or ENSO-neutral ocean temperatures control the Walker circulation along the equator. Lower SSTs in the east chill the overlying air, which in turn increases the air density, reducing its buoyancy. The sinking air causes high atmospheric pressure and

usually restricts precipitation because cool air is less likely than warm air to rise vertically so that its moisture can condense and form vertical clouds. The eastern equatorial Pacific is normally dry as a result, and the extension of this dry area on the land surface is the dry Atacama Desert. Warm waters in the western tropical Pacific cause the density of overlying air to decrease. The rising air leads to lower atmospheric pressure and buoyancy that produces frequently cloudy and wet conditions over the region.

A simple index was devised to describe the atmospheric pressure variations in the tropical Pacific Ocean. The **Southern Oscillation Index (SOI)** is derived from sea level pressure differences between the eastern and western Pacific. The SOI is found by subtracting the air pressure at sea level in Darwin, Australia, from that in Tahiti. This value is often standardized statistically so that a value of zero represents ENSO-neutral conditions, values exceeding +1 may be considered to coincide with La Niña in the ocean, and values below −1 may be considered to represent El Niño conditions. Another means of identifying El Niño and La Niña events involves monitoring SSTs in various regions of the equatorial Pacific Ocean. A temperature departure of ± 1 C° away from normal conditions for 3 consecutive months constitutes a major event. In more recent years, the so-named **Niño 3.4 Index** is often used as a means of representing the averaged SST values over a combination of Regions 3 and 4 (as defined by an international team of geoscientists) of the tropical

Pacific Ocean. The Niño 3.4 Region is bounded by 120°W–170°W and 5°S–5°N (**FIGURE 4.12**). Positive values of the index for a given time period indicate warmer than normal SSTs (El Niño) in the 3.4 region, and negative numbers represent colder than normal SSTs (La Niña) (**FIGURE 4.13**). Climatologists also define the state of ENSO by incorporating multiple variables, including sea level pressure, surface wind vectors, SSTs, surface air temperatures, and cloud cover, into a single index. This **Multivariate ENSO Index** is also positive during El Niño and negative during La Niña. “Official” historical monthly ENSO indices are available online.

Historical Observations of ENSO

Direct information about ENSO events first came from accounts of Spanish explorers in South America during the 1500s. Indirect data sources such as tree rings, flood frequency, sediment cores, and coral reef growth suggest that anomalous weather events associated with ENSO events have been occurring for at least many thousands of years. The earliest written records of impacts believed to be related to extreme El Niño phases extend from the Chimú Dynasty (AD 1100) in the Moche Valley of Peru and indicate periodic extreme flooding, now known as **Chimú Floods**, extending as far back as 2500 years before present. Other solid evidence suggests that the ENSO phenomenon has existed for at least 5000 years, and other research suggests that it may have existed for far longer into the geologic past.

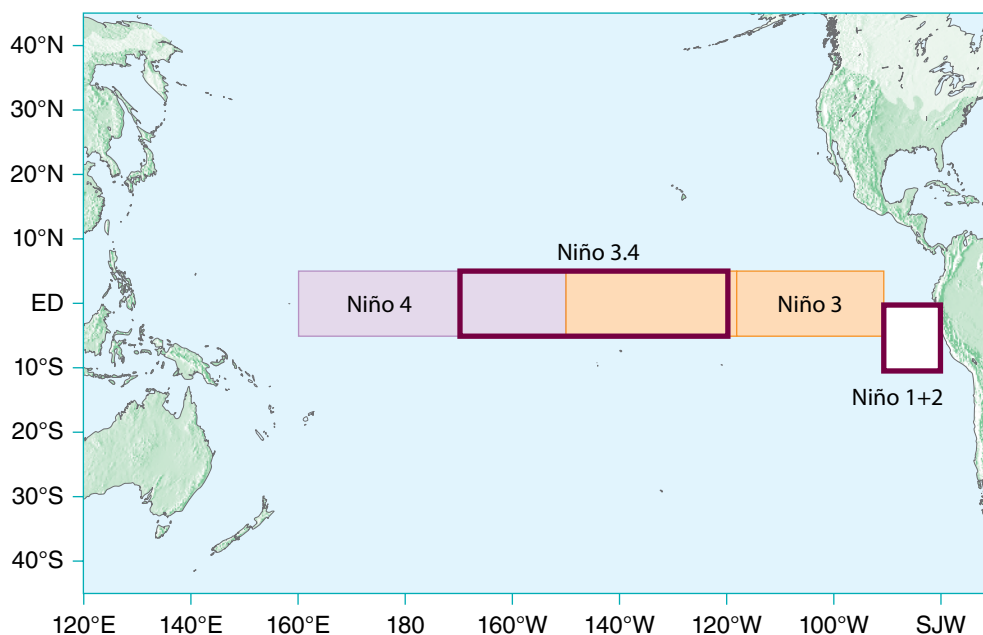


FIGURE 4.12 Niño 3.4 region.

Data from National Centers for Environmental Information/NESDIS/NOAA.

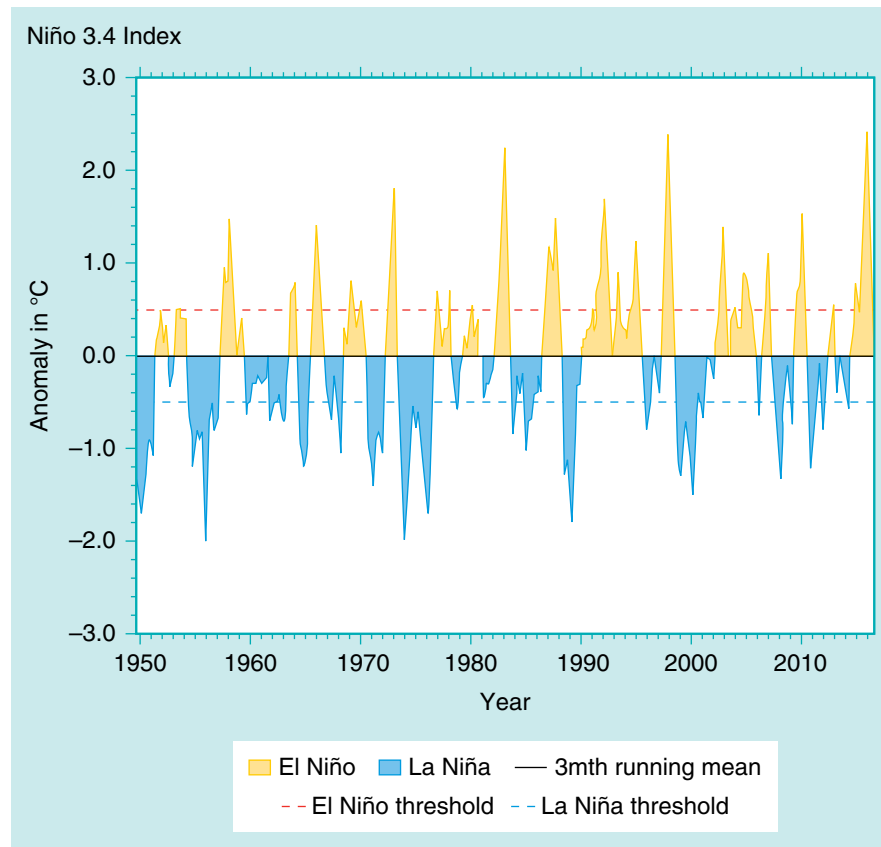


FIGURE 4.13 Niño 3.4 Index over time.

Data from National Centers for Environmental Information NESDIS NOAA.

Most accounts are not direct observations of atmospheric or oceanic conditions but indirectly suggest the possible presence of ENSO extremes. Sources include ship logs in addition to writings by clergy members who reported unusual natural phenomena in great detail. These records became more detailed between 1600 and the mid-1800s, when South American events were chronicled in European literature. Accounts from historians, explorers, geographers, pirates, and engineers became more detailed toward the end of the 1800s. Some of these types of evidence are listed in **TABLE 4.1**.

El Niño Characteristics

An El Niño event in the ocean coincides with a reversal of the normal Walker circulation. Trade wind flow weakens along the equator, allowing the pool of warm water piled up in the western Pacific to flow back toward the east. Because ENSO-neutral and (especially) La Niña conditions pile warm water in the west, the ocean is simply regaining a somewhat uniform sea surface level when the trade wind flow weakens.

TABLE 4.1 Indirect Evidence for El Niño Events in Historical Sources

- Variations in travel times from sailing vessels
- Ship logs noting unusual weather and sea conditions
- Presence of “aguaje” or red tide, a bloom of toxic marine plankton
- Abnormally warm waters along the South American coast
- Severe and unusual weather events, such as heavy rains and flooding
- Property damage caused by floods
- Travel obstructions from washed-out roads or mudslides
- Agricultural destruction
- Increases in sea levels along the South American coast
- Mass mortality of marine sea life caused by a decrease in the upwelling of nutrients
- Death and/or departure of birds
- Reductions in productivity in coastal fisheries

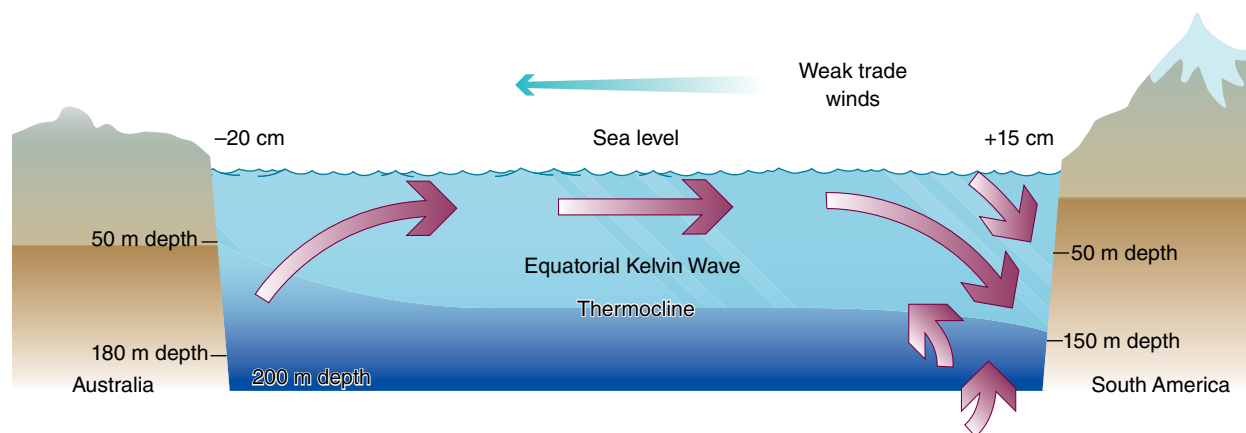


FIGURE 4.14 Ocean response to El Niño.

As the warm water migrates eastward, the overlying atmospheric low-pressure center follows the warm water migration eastward as well. By the time the warm water pool reaches the eastern boundary of the tropical Pacific Ocean, reduced atmospheric pressures and increased precipitation are well established. At the same time, colder than normal water conditions become established in the western tropical Pacific. Higher pressures build over that area as a result, and precipitation is far below normal in the region around the Maritime Continent. El Niño, then, simply coincides with a reversal of the “normal” or “neutral” equatorial Pacific air/sea conditions set up by the Walker circulation (**FIGURE 4.14**).

Movement of the warm water pool from west to east during El Niño, usually taking about 4 months, appears in the form of an **equatorial Kelvin wave**—a pool of warm water moving eastward while surface waves propagate westward. The surface waves are initiated by overlying winds that continue to blow from east to west as a part of the normal trade wind flow. During El Niño events, however, the trade winds are weaker than normal, which allows the warm water pool to move eastward as an equatorial Kelvin wave.

When the warm water pool reaches the eastern boundary, it splits into three primary components. The main component is the **equatorial Rossby wave**, which sloshes back westward along the equator, typically reaching the starting point within 6 to 8 months, ending the El Niño event. Movement of the return flow in this wave is slower than the original Kelvin wave. These oceanic Rossby waves differ from Kelvin waves in that the bulk of water motion is in the same direction as the surface waves.

The remainder of the original eastward-moving equatorial Kelvin wave splits into **coastal Kelvin waves**—smaller warm water pools that migrate north and south along the North and South American coasts—displacing cold currents off the west coasts of both continents.

These waves are responsible for many regional climate abnormalities such as increased storminess.

The warm water pool in the eastern equatorial Pacific causes a downward movement of the **thermocline**—the boundary between warm surface waters and colder deep waters. Oceanic upwelling still occurs in the eastern ocean during El Niño events, but because of the deeper thermocline the cold water involved in upwelling is confined to the deeper layers. Because of these abnormally warm waters near the American coast, El Niño events are sometimes referred to as warm-ENSO events. In its entirety an El Niño event usually lasts between 10 and 14 months.

Because so much energy is transported across such a large distance regardless of the ENSO phase, disruptions to the ENSO-neutral situation have worldwide atmospheric consequences. The most direct effects occur in the tropics during the El Niño phase (**FIGURE 4.15**). The reversal of the usual atmospheric pressure and SST patterns during El Niño events causes atmospheric and oceanic circulation systems on the planetary scale to readjust. These anomalous circulation patterns cause seemingly chaotic weather conditions worldwide. Normally dry regions, such as western North and South America and western Australia, become much wetter than normal, while characteristically wet regions such as northeastern Brazil, eastern Australia, and the Maritime Continent become excessively dry. Such disruption of normal atmospheric and oceanic conditions leads to some devastating ecological and economic problems.

La Niña Characteristics

During the La Niña phase the trade wind flow along the equatorial Pacific Ocean becomes even stronger than normal, which increases warm water accumulation in the western equatorial Pacific and cold water upwelling in the east. This causes a deeper thermocline in the western tropical Pacific and a shallower than normal thermocline

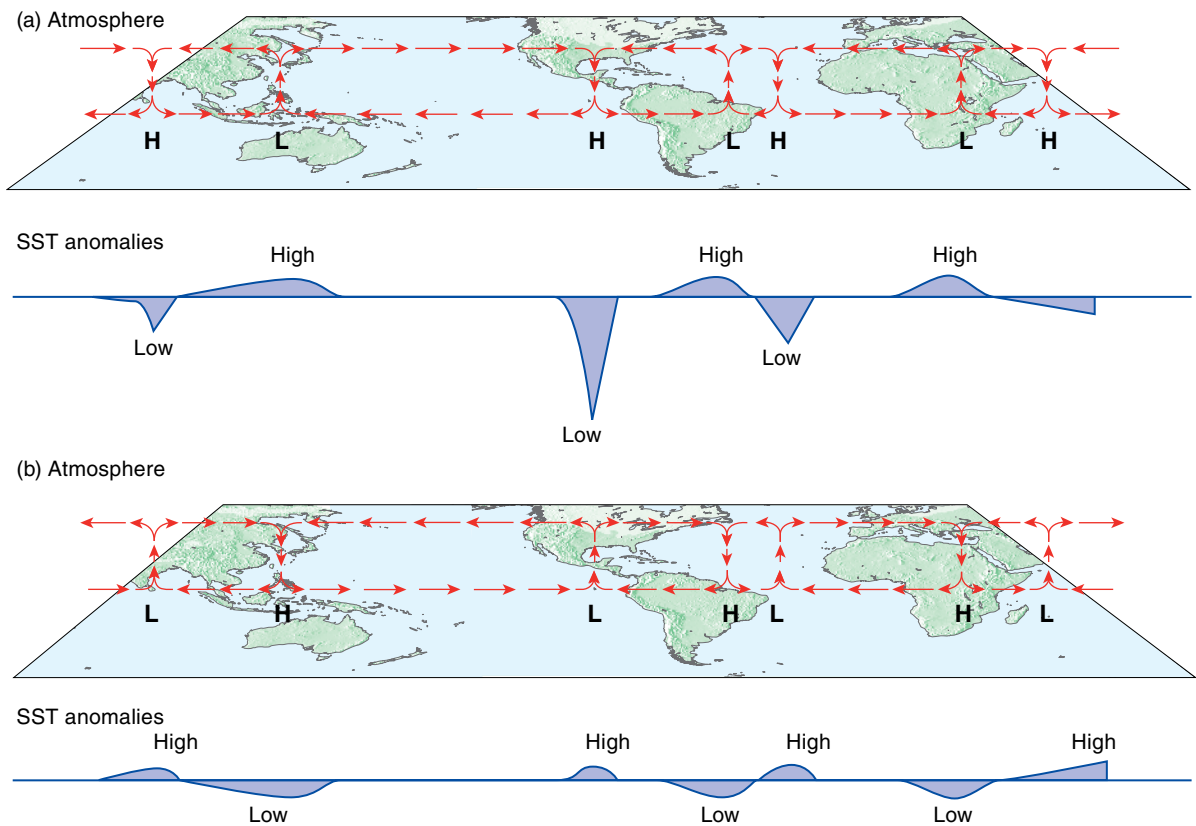


FIGURE 4.15 Equatorial air circulation/ocean temperature anomalies during ENSO-neutral (a) and El Niño periods (b).

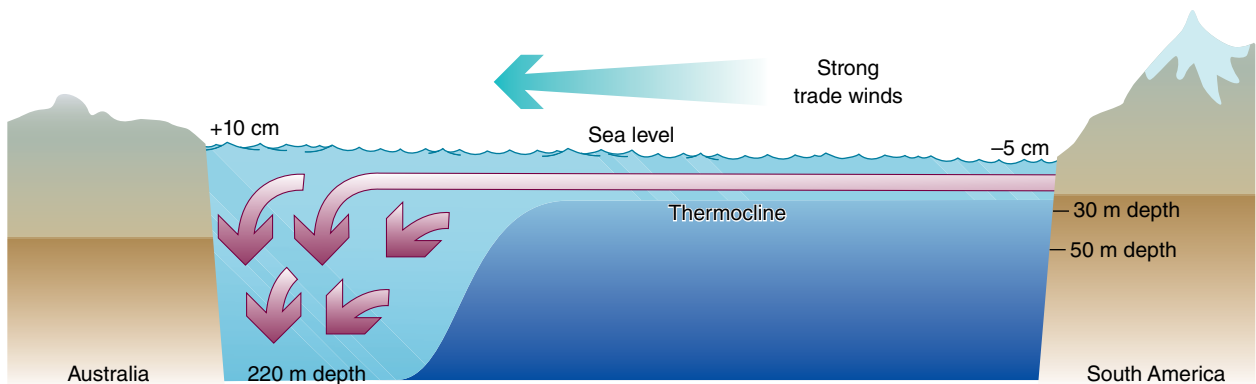


FIGURE 4.16 Ocean response to La Niña.

in the east (**FIGURE 4.16**). Sea levels respond accordingly, as the west records higher than normal sea levels and temperatures, while in the east lower than normal sea levels and temperatures occur. The enhanced cold water upwelling near the Americas has given La Niña another name in recent years—"cold-ENSO events."

Global Effects

As suggested above, the consequences of ENSO events do not stop with the equatorial Pacific Ocean. A closer inspection of Figure 4.15 reveals that the effects of warm-ENSO events carry through the downstream

circulation patterns of the entire tropics. Because lower pressure builds over the western portion of South America during negative phases of the Southern Oscillation, the circulation regime of eastern South America is altered. Normally, eastern South America is dominated by low atmospheric pressure associated with the abundant heat and humidity from the Amazon rain forest. During the El Niño phase the western South American low disrupts the usual circulation over the eastern portion of the continent. As a result, higher than normal air pressure and subsiding airflow is initiated over tropical eastern South America, bringing drought to much of the rain forest region.

Just as the circulation is altered in South America during warm-ENSO events, the circulation regimes of other tropical locations are affected. The relatively high-pressure regime that normally prevails over southwestern Africa flips to lower atmospheric pressure and the region becomes anomalously wet. This in turn reverses the normally low pressures that occur near southeastern Africa, resulting in higher air pressures and drought near Madagascar. This induces a low-pressure region over the

equatorial Indian Ocean, which is normally dominated by higher pressures, and the region becomes wetter than normal. Finally, the circulation is linked to the western side of the Walker circulation over eastern Indonesia and northeastern Australia, which experiences El Niño-induced above-normal air pressures and the drought conditions discussed previously. The effect is that the atmosphere seesaws to an opposite regime from normal. **FIGURE 4.17a** shows the El Niño winter climate anomalies for the globe.

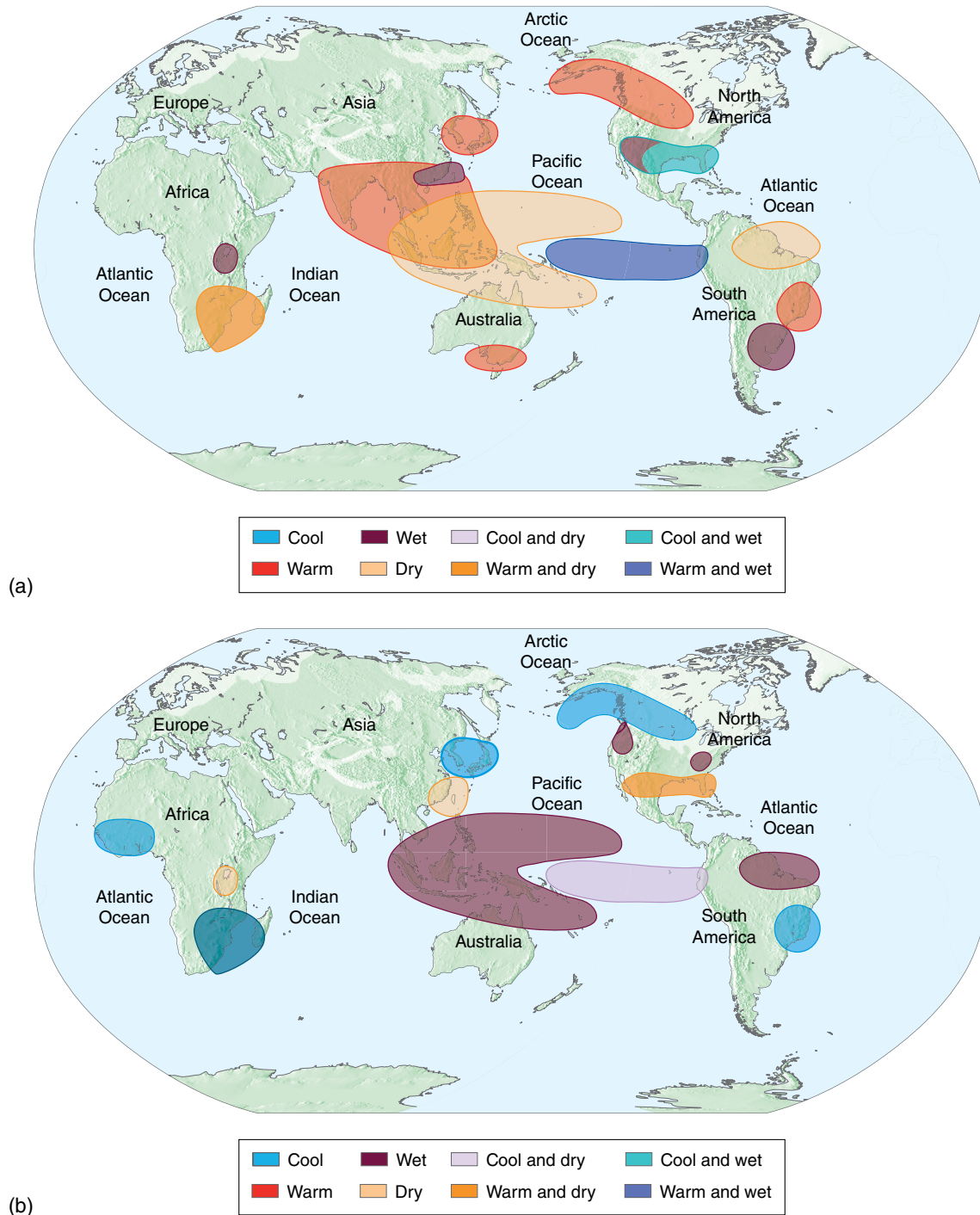


FIGURE 4.17 Global climate anomalies. (a) El Niño winter. (b) La Niña winter.

Courtesy of NOAA. Retrieved from: www.pmel.noaa.gov/elnino/impacts-of-el-nino.

TABLE 4.2 Persistent Global Effects of El Niño

Condition	Areas Affected
Drier than normal	Maritime Continent; southeastern Africa and Madagascar; east central Africa; eastern South America (Brazil)
Wetter than normal	Central equatorial Pacific Ocean; eastern equatorial Pacific Ocean and western South America (Ecuador, Peru); southeastern South America (southern Brazil, Argentina); southeastern United States
Warmer than normal	Japan, eastern Asia (China/Manchuria); northwestern North America (southern Alaska through U.S. Pacific Northwest into central North America); eastern Canada (Labrador, Nova Scotia)

Energy transfers during warm-ENSO events also alter temperate climates, as indicated in **TABLE 4.2**. Such interactions originate from increased energy and moisture transport from the equatorial Pacific into the midlatitudes. Much of this energy transport is accomplished by the poleward-moving coastal Kelvin waves. These warm water pools displace cold currents along the west coasts of North and South America, overriding the colder, denser currents normally present in those locations. This position allows the abundant stored oceanic energy to be transferred easily into the atmosphere, particularly under the conditions of unusually low atmospheric pressure, initiating rising motions in the atmosphere. Such conditions are capable of energizing storms that then migrate across the normally dry western continental locations.

As a general rule, La Niña situations strengthen normal atmospheric circulation patterns across the tropics. A normally dry region becomes exceedingly dry; a normally wet region becomes exceedingly wet, as depicted in **FIGURE 4.17b**. Such conditions may have as many negative ecological and economic consequences as an El Niño event in some locations.

Extreme phases of the Southern Oscillation stress ecosystems in several ways. Large-scale animal migrations and die-outs occur in the affected regions. These factors in turn stress humans as food sources are affected and landscapes are degraded. For instance, western South America has seen widespread famine as a result of fish migrations during warm-ENSO events. As fish move away from the coast in search of prey, birds that feed

on the fish are affected. In addition, human populations are affected directly, because seafood serves as a prime source of nutrition in these coastal cultures affected by El Niño. At the same time, dry western South American regions may experience heavy rains that cause widespread floods in a landscape barren of vegetation and without natural stream drainage capable of handling the sudden downbursts. Mudslides become common on hill slopes and occasionally destroy entire villages. Roads become blocked and bridges collapse. In short, widespread ruin may occur during particularly strong ENSO events.

Effects in the United States

Relationships between El Niño and the U.S. climate have been fairly well documented. Because the **jet streams**—fast currents of air in the upper troposphere—are most active during the cool season (November to March), the region sees most ENSO-related changes during that time. In particular, southern and central U.S. precipitation and southwestern U.S. temperatures appear strongly tied to warm-ENSO events. Increased energy and moisture are transported from the tropics to North America as the equatorial Kelvin wave and the smaller coastal Kelvin wave warm pools override cold currents along North and South America. Increased precipitation and storm activity thus are also typical effects of El Niño in much of the southern, central, and southwestern United States. The small, northward-migrating coastal Kelvin pool displaces the usual cold **California current** off the U.S. Pacific coast, destabilizing the overlying atmosphere and causing an adjustment in the North American jet streams.

The two major rivers of air in the high troposphere—the **polar front jet stream** (over midlatitude locations) and the **subtropical jet stream**—transport energy and moisture in a generally west-to-east direction. During warm-ENSO events, the **amplitude**—the north–south and south–north component of motion—of the polar front jet stream tends to increase across the United States. Jet amplitude dictates where storms form, their intensity, and direction of migration.

During the El Niño phase the polar front jet is altered from normal as a **trough**—an equatorward dip in the flow—overrides the eastern North Pacific Ocean (**FIGURE 4.18**). Midlatitude storm systems form just to the east of trough regions. The trough is accompanied by a **ridge**—a poleward shift in the jet flow—downstream (toward the east). For La Niña, the jet amplitude increases such that western North America underlies a more pronounced ridge while the eastern continent experiences a deep trough (Figure 4.18b).

During warm-ENSO events the polar front jet may split into two distinct branches—one north, one

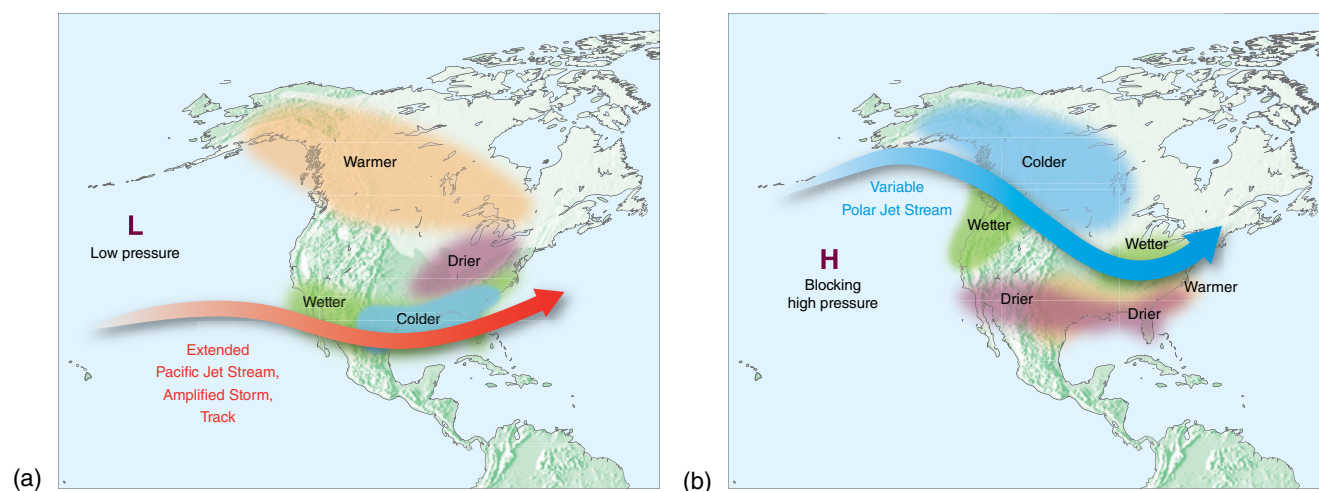


FIGURE 4.18 The North American climatic response to jet stream alterations. (a) El Niño and (b) La Niña.

Courtesy of National Oceanic and Atmospheric Administration. www.climate.gov.

south—over the eastern North Pacific Ocean. This situation greatly alters normal jet flow across North America and affects the climate of many associated regions. The northern branch of the polar front jet tends to remain farther to the north than the usual polar front jet and prevents the coldest Canadian air from penetrating southward into the United States during most warm-ENSO events. Warm-ENSO winters thus are usually warmer than normal in the northern United States and southern Canada. The southern branch of the polar front jet during warm-ENSO events flows across the northern Gulf of Mexico, as shown in Figure 4.17a, and tends to steer midlatitude storm systems into the Gulf Coast states, after allowing them to acquire moisture over the Gulf of Mexico. The subtropical jet still exists in its normal form, south of the southern branch of the polar front jet, even when the polar front jet bifurcates.

Because some El Niño events can trigger increases in jet amplitude across North America, a trough in the northern branch of the polar jet can cause colder air to infiltrate the eastern United States as far as the Gulf Coast. Northern states are not impacted with extreme events under these conditions because this cold air would have been present whether or not the dip in the jet stream existed. This trough also causes an increase in precipitation for the southern United States.

The northeastern United States shows a weaker relationship between El Niño and temperature and precipitation patterns. One explanation for the lack of relationship is that the polar front jet exits the continent over the Northeast regardless of jet flow amplitude. It should be noted, however, that any particular warm-ENSO event can cause drastic changes in northeastern U.S. weather. Each ENSO event changes the jet flow

pattern somewhat differently, and strong El Niño events occasionally change the jet pattern substantially. The response to El Niño in the northeastern United States is usually slightly higher temperatures along with slightly drier conditions caused by a net reduction in snowfall.

Recent research indicates that cold-ENSO events have as much influence on precipitation in the southern United States as warm-ENSO events. Recent La Niña years have been accompanied by pronounced drought throughout the southern and south-central United States, even in summer, if La Niña persists through the summer. Additionally, cold-ENSO periods are associated with temperature increases throughout the Southwest as the polar front jet stream pushes northward over the western United States. Slight temperature increases also occur in the north-central area of the United States. La Niña periods also see heightened Atlantic hurricane activity if the event is in force into late summer and autumn, as was evidenced by the very active 2004 and 2005 seasons. Incipient El Niño conditions in late summer and autumn 2006 and early summer 2009 were associated with a much quieter Atlantic hurricane season.

The El Niño event of 2014–2016 was one of the most notable on record. Among its many impacts were oppressive heat and drought in the western tropical Pacific and parts of Africa, with decreases in food production contributing to hunger, malnutrition, and disease. In addition, tropical cyclone activity was affected, with a suppression of Atlantic basin frequency, increased frequencies in the North Pacific basin, and an eastward displacement of South Pacific tracks in response to the eastward migration of the warm pool. Some are attributing the record-breaking globally averaged temperatures in 2014 and 2015 to this El Niño event.

Relationship to Global Warming

Although much research has been done on ENSO events, additional work is still needed. Many mechanisms thought to trigger ENSO events must be explained further. One such mechanism that has gained recent publicity is global warming. Current global warming is exacerbated by human emission of pollutants known as *greenhouse gases*. The recent speculation that global warming triggers extreme ENSO events was generated by a higher incidence of intense ENSO events during recent years of high global temperatures. Since 1970 warm-ENSO events have occurred with a periodicity of about 2.8 years. This significantly exceeds the frequency of the long-term average of 4.7 years. In time, relationships between a warmer atmosphere and El Niño events may prove valid; however, the reverse may be equally true: that a higher incidence of intense warm-ENSO events may be forcing, at least in part, higher global temperatures. Such a realization may be substantiated given the slow response of oceans to atmospheric forcing in addition to the long-term heat storage capability of oceans.

Recent research supports a more plausible explanation for the increase in extreme ENSO events since 1970. An oceanic phenomenon known as the **Pacific Decadal Oscillation (PDO)** is directly tied to ENSO strength and frequency. The PDO is similar to the Southern Oscillation in that warm and cold phases occur over time. As the name implies, variability associated with the PDO occurs much more slowly than that associated with the Southern Oscillation. A PDO regime may last 20 to 30 years, during which one phase of the oscillation tends to dominate. During times when the Southern Oscillation and the PDO are in phase (i.e., both in a “warm phase” or in a “cold phase”), the impacts of the Southern Oscillation tend to be magnified. When the phases offset the Southern Oscillation effects tend to be dampened.

A PDO warm phase occurred from the early 1970s until the late 1990s. This situation supported frequent and strong El Niño events. For about 5 years beginning with the winter of 1997 and 1998 the PDO showed signs of shifting phases every 5 years or so. This shift seems to be rather unusual in the last century. The cold phase, which has been in place since around 2008, is believed to support and magnify the effects of La Niña.

Clearly, continued research on the causes and effects of extreme ENSO events becomes more important with the increasing demands made by humans upon the natural environment. Given the abnormalities in the temperature and precipitation regimes during El Niño and La Niña events, heightened understanding of these

events is important for planning purposes in a wide array of environmental and societal applications.

Climatic Feedbacks in the Ocean

An important role in the climate system is played by the **positive feedback system**—an input that creates change to a system in such a way that it triggers additional, similar changes in the system. A small snowball rolling down a hill—picking up more snow on its trek, thereby gaining *momentum* and rolling faster and faster as it gains more mass—is an effective example of a positive feedback. Another example is the suggestion planted by seeing a person in your climatology class yawn; within seconds several classmates yawn, despite the interesting course material.

By contrast, a **negative feedback system** involves an input to the system that decreases the likelihood of further changes of the same type to the system. An example of a negative feedback system might be your study habits. If you study hard and do well on the first exam, you may then be tempted to study less and then do poorly on the second exam. But then you are likely to study harder and do better on the third exam. The net effect is that your overall grade is average. Negative feedbacks lead to stabilization of a system.

In the Earth–ocean–atmosphere system, feedback loops are well established. Any change in the energy balance of the planet, through increased input of energy into the system, or changes in the release of stored energy to space will initiate a series of positive and negative feedbacks. Offsets will result but, overall, a change will ultimately result as Earth processes reach a new equilibrium.

Media attention has focused considerably on the role of greenhouse gases in the atmosphere and the subsequent increases in stored energy in the Earth–ocean–atmosphere system. The situation involves increased concentrations of gases that absorb radiation emitted upward from Earth’s surface and reemit some of it back downward, which in turn creates warmer surface temperatures. This oversimplified notion does not account for the myriad positive and negative feedback mechanisms involved. For example, early research focused on a possible positive feedback involving clouds caused by increased evaporation and subsequent *condensation* rates in a warmer surface environment. This increased cloud cover would effectively absorb more outgoing radiation and increase surface temperatures in a “run-away” *greenhouse effect*. The hypothesis predicted rapid and strong increases in surface temperature. Research ultimately revealed that the opposite was true; a negative feedback would result due to increases in cloud albedo reflecting more incoming solar radiation. The net effect

would be cooling of the surface, and at least somewhat of a balance in the system.

Another potential negative feedback has drawn interest. The **CLAW hypothesis** (so-named based on the first letter of the surname of each of the scientists formulating the hypothesis) refers to a biologically-induced energy loop that could either exaggerate or moderate increased surface temperatures. Research has revealed that photosynthesizing oceanic microorganisms called **phytoplankton** increase in abundance either as a result of increased water temperatures or increased *photosynthesis* as a result of increased energy. In addition to providing about half of the atmospheric oxygen (O_2) released by plants, phytoplankton produce **dimethyl sulfide [DMS; $(CH_3)_2S$]** through their growth cycles. As DMS increases in ocean waters, it is transferred to the atmosphere where it oxidizes to form **sulfur dioxide (SO_2)** and sulfate aerosols. The sulfate aerosols then may act as **condensation nuclei** by encouraging the condensation of water vapor around them, which in turn stimulates the number and thickness of clouds. The increased cloudiness then reflects more *insolation* from the cloud tops, which may regulate the original cause of higher ocean temperatures—increased energy at the surface.

On the other hand, one of the proposers of the CLAW hypothesis, James Lovelock, subsequently posited that a positive feedback may be at work at the same time or instead of a negative feedback loop. This so-called **anti-CLAW hypothesis** posits that increased ocean surface warming would increase the stable stratification within the ocean, with even warmer water overlying the cold bottom waters. The increased stability would reduce the upwelling necessary to restore nutrients to the surface from the depths. Without as many nutrients, phytoplankton population growth would be curtailed, DMS production and transfer to the atmosphere would decrease, less cloud cover would result, and amplification of the warming would occur.

Which hypothesis is correct? Clearly, more research is needed. Moreover, we do not know if other unknown biological or nonbiological processes associated with the global sulfur cycle may be as important as or more important than the known components.

► Volcanic Activity and Climate

General Effects

As Earth’s crustal plates move very slowly (at about the same rate at which your fingernails grow), volcanic activity occurs in certain locations. This volcanism contributes to both short- and long-term climatic fluctuations. The primordial atmospheric composition

resulted from the *outgassing* of molten rock as the Earth cooled and the molten material hardened. This led to an atmosphere rich in N_2 and CO_2 . Water vapor was also initially introduced to the atmosphere through outgassing processes. The atmosphere shed excessive water vapor in the form of precipitation, which eventually cooled and solidified the crust and formed the oceans of today. The composition of the atmosphere is, therefore, linked to volcanic activity.

Evidence indicates that the early landscape of Earth was marked by rather frequent volcanism as the volatile Earth cooled from the surface inward. Over time, volcanic activity decreased. Still, volcanism is an important contributor to the Earth–ocean–atmosphere system. We typically do not hear about active volcanism unless a particular volcanic event directly threatens humans or the event is of such magnitude as to invite attention. Many cases of active volcanism are associated with “cracks” in the oceanic crust that are widening—midoceanic ridges—deep beneath the ocean surface, whereas others are associated with rather remote locations such as the Aleutian Island chain of Alaska. Others, such as Kilauea, Hawaii, are tourist attractions.

Volcanic activity today contributes 1.2 to 2.1×10^{11} kg (130 to 230 million tons) of CO_2 to the atmosphere each year. Volcanoes also add between 3.3 and 6.6×10^{12} kg (3.6 and 7.3 billion tons) of SO_2 to the atmosphere annually. Significant amounts of water vapor are also ejected into the atmosphere. Of the gases emitted by volcanoes, the one that produces the most significant climatic signal is SO_2 . The amount of CO_2 emitted by volcanic activity is low compared with the amount already present in the atmosphere. The additional amount is quickly absorbed into biomass and/or the oceans. Water, of course, exits the atmosphere quickly as precipitation. But SO_2 presents a different problem.

SO_2 and atmospheric *aerosols* of volcanic origin can trigger either net surface cooling or warming, depending on individual eruption characteristics. SO_2 typically combines in the atmosphere with water, dust, and sunlight to produce **vog**, or volcanic smog. Vog can have both local- and planetary-scale impacts. At the local scale vog may form near the surface, where it may hinder loss of longwave radiation back to space, leading to warming. On the island of Hawaii, vog is persistent because of the continuous effusive (gentle) eruption of Kilauea since 1986. The volcano contributes about 1.8 million kg (2000 tons) of SO_2 to the local atmosphere daily.

Vog becomes a planetary-scale problem when a major explosive eruption ejects sulfur compounds into the *stratosphere*. Once there, the sulfur compounds can linger up to 4 years, in part because the stratosphere is higher than most precipitation clouds, which would

rinse aerosols and SO₂ from the atmosphere. SO₂ combines with the limited amounts of water found in the stratosphere, dust particles, and sunlight to form vog. In that situation the vog is capable of producing a haze that has a rather high **albedo**—the percentage of incoming energy from the Sun that is reflected off an object. The result is that the haze directly reduces surface air temperatures.

Long-term climatic changes are not initiated by single volcanic events. Instead, volcanoes lead to significant long-term climatic changes only during prolonged periods of above-normal activity. Persistent volcanism is thought to help maintain Earth's rather steady climate state, with temperatures that have varied by less than 15 C° (27 F°) over its 4.6-billion-year history. Individual volcanoes are, however, capable of altering hemispheric and global climates over relatively short time periods. When volcanoes erupt, gases and solid aerosols (**particulates**) are ejected into the atmosphere. Most of the aerosols fall back to the surface over short periods of time. Particles that are sand sized or larger fall back to the surface within minutes of an eruption. Smaller aerosols are capable of being suspended in the atmosphere for much longer periods. This is especially true of dust-sized and smaller particles, which may reach the stratosphere if the volcano is high and the eruption is especially explosive. Large eruptions have an average recurrence of about 30 years over recorded history (**TABLE 4.3**).

Aerosol Indices

Two indices have been designed to estimate the amount of aerosols, especially those of volcanic origin, in the atmosphere. The **Dust Veil Index** is based on the amount of material dispersed into the atmosphere. It uses surface air temperatures and the amount of insolation reaching the surface, among other variables, to estimate the total amount of particulates in the atmosphere. This index is most useful in the midlatitudes because it has been calibrated in predominantly middle-latitude locations. Its major weakness is that by using temperature to estimate the Dust Veil Index it is impossible to assess the impact of volcanic activity on temperature accurately.

The **Volcanic Explosivity Index** is based only on volcanic criteria. The data used are derived from the magnitude, intensity, dispersion, and destructiveness of individual volcanic events. A scale between 1 and 8 is used for each event, with 8 being the strongest volcanic event. An event with a Volcanic Explosivity Index exceeding 4 is assumed to produce emissions into the stratosphere, but atmospheric composition is not taken into account in the derivation of the Volcanic Explosivity Index.

Similar short-term effects are believed to be caused by meteor impacts. One example is Barringer Crater

TABLE 4.3 Major Volcanic Eruptions of the Past 200 Years

Volcano, Location	Year	Average Resulting Global Temperature Decline (C°)
Tambora, Indonesia	1815	0.4–0.7
Krakatau, Indonesia	1883	0.3
Santa Maria, Guatemala	1902	0.4
Katmai, Alaska	1912	0.2
Agung, Indonesia	1963	0.3
El Chichón, Mexico	1982	0.5
Mount Pinatubo, Philippines	1991	0.5
Eyjafjallajökull, Iceland	2010	believed to be negligible



FIGURE 4.19 Barringer Crater near Winslow, Arizona.

Courtesy of D. Roddy (U.S. Geological Survey), Lunar and Planetary Institute/NASA.

near Winslow, Arizona (**FIGURE 4.19**), where the impact of a meteor of 40 to 50 m (130 to 160 ft) in diameter is likely to have provided global dust-related cooling some 50,000 years ago.

▶ Deforestation and Desertification

Humans play a role in climatic variation through a number of ways. Most **anthropogenic** (human-induced) climatic effects relate to changes in atmospheric composition

through the combustion of *fossil fuels* and the manufacture of certain gases and solids. Human land-use activities also can contribute to variation and changes in the climate system. Many of these involve the processes of deforestation and desertification.

Deforestation refers to the systematic and widespread clearing of forested regions. Although most associate deforestation with tropical locations, the most widespread deforestation actually occurred in Europe and North America a few hundred years ago. Entire forests were cleared for fuel and/or building materials during the early part of the Industrial Revolution, beginning in the late 1700s. Today, the most widespread deforestation occurs in tropical rain forests, where large tracts of land are deforested to support either individual subsistence farms or grazing areas.

Because soils in the rain forest regions are leached of their nutrients by the abundant rainfall, they are not well suited to agriculture. As a result, farmers must continually move from location to location because agriculture is usually successful for only a few years before the soil's nutrients become depleted. This type of migratory farming in which forests are continually cleared, often by burning, is called **slash and burn agriculture**. This method became widespread once it was discovered that burning vegetation adds nutrients to the upper soil layers. These nutrients are capable of supporting crops for only a few extra years.

If small plots of land are deforested in this manner, no long-term damage is done because the surrounding forest is quick to recapture the “slashed and burned” plot. The problem today involves large deforested plots of land, especially when the activity leaves only small patches of rain forest surrounded by much larger deforested areas. These small plots are not sufficient to maintain their existence, and they become more susceptible to disease and other problems with such a high percentage of the trees near the fringe of the forest. The result is that the isolated plots die off. Human activities then move farther into the forest, taking more and more trees out of existence.

In many areas the rain forests have been totally decimated in this manner. Deforestation of old growth forests within the past few centuries in many locations in Central America has left only a tiny percentage of rain forest undisturbed, and total annihilation looms in the near future. Currently, the worst deforestation of tropical rain forests is occurring in South America, especially northeastern Brazil, and in Indonesia. At present rates of clear cutting, it is estimated that all rain forests will be eliminated within the next 100 to 200 years, if not sooner. This deforestation has dire ecological consequences. Tropical rain forests represent the most diverse ecosystems on Earth's land surface. Elimination

of these regions will directly lead to massive extinctions of plants and animals, many of which may be useful for medicinal and economic purposes.

Large-scale deforestation causes numerous impacts on climate. Most of the precipitation water in rain forests is generated locally through the process of **transpiration**—the constant recycling of rainwater through uptake through tree roots and out through the leaves. Tropical rain forests have been referred to as the **rain machine** for that reason. Once the trees are removed, precipitation is more likely to run downslope and leave the area. Temperatures after deforestation increase abruptly, in part because of the loss of shade but also because removal of forests will reduce the transpiration which would have allowed the insolation to evaporate water (*latent energy*) rather than heat up the local environment (*sensible energy*).

An additional climatic problem is that deforestation involves the removal of one of the planet's primary carbon *sinks*. In 1 year a single acre of trees can store as much CO₂ as is released by driving 26,000 miles. The discontinuation of photosynthesis when the trees die decreases the rate at which CO₂ can be removed from the atmosphere. This has large-scale consequences because increased atmospheric CO₂ is a primary cause of global warming. Furthermore, the burning of the trees returns CO₂ that was sequestered in the biomass to the atmosphere, directly increasing atmospheric CO₂ concentrations. Finally, photosynthesis in the tropical rain forests produces a large share of the planet's atmospheric oxygen. Obviously, elimination of the planet's “lungs” would be disastrous.

While deforestation of tropical rain forests receives the most news coverage, it is becoming increasingly recognized that the loss of the vast slow-growing, coniferous subarctic forests of the northern hemisphere called **boreal forests** is also of grave concern. These trees store even more CO₂ than tropical rain forests. In addition to the role of the trees themselves as a CO₂ sink, the boreal forest also binds carbon and *methane* in peat and permanently frozen terrain—**permafrost**—beneath it. Removal of even modest sections of the forest, in response to economic pressures of logging and mineral and fossil fuel extraction, has been estimated to release enough CO₂ and CH₄ to accelerate global warming noticeably.

Another human land-use effect that can modify large-scale climate changes is **desertification**—the expansion of deserts into semiarid regions, largely through the impact of human activities such as ranching and overuse of water. The domestication of grazing animals has expanded in many semiarid regions of the world, where grasslands are dominant. When these activities become too concentrated, they can quickly



FIGURE 4.20 The Sahel region of Africa.

strip a region of vegetation, deplete and contaminate water, and compact the soil, leading to a rapid drying of the landscape.

Semiarid regions typically display wide variability in the precipitation regime. Wet periods may persist for many years or decades, only to be offset by years or decades of exceedingly dry conditions. Humans typically move into the regions during wet periods and establish grazing practices. But during the dry periods that inevitably follow, they are reluctant to leave. Their continued activities quickly compound the problem, leading to further expansion of the surrounding desert.

Perhaps the most prevalent example of desertification is the **Sahel**—a region of Africa that borders the southern rim of the Sahara Desert that has undergone widespread degradation over the recent past (**FIGURE 4.20**). Much of the problem began in the early twentieth century, when wet conditions brought people into the region. This settlement, combined with natural population growth and the demise of transient herders in favor of more permanent herding establishments, created a situation with far too many grazing animals in the region. During the 1970s widespread drought in the region caused the animals to strip far too much vegetation in a short period of time before succumbing to the drought themselves. The concurrent water and food shortages led to tragic famine and death throughout the region. The consequent impact on the landscape was rapid desertification and southern expansion of the Sahara Desert. The region has

yet to recover and remains one of the primary regions of food and water shortages on the planet.

Once the desert expands into a semiarid region, it is difficult for vegetation to reclaim the region because the local water and energy balances are disrupted. The removal of vegetation changes the color and texture of the landscape. The generally dark and rough vegetated surface is replaced by lighter and smoother surfaces, which in turn support higher albedoes, reflecting away a higher percentage of insolation. But this effect is more than compensated by a decrease in water availability after the vegetation is removed. Like a deforested landscape, an unvegetated landscape allows water to run off the surface more quickly, causing less evaporative cooling and a higher percentage of energy devoted to sensible heating rather than latent heating. The results are increased temperatures, reduced water availability, and larger sections of land being converted to desert.

Several other land cover changes affect climates, particularly at the local scale. For example, irrigation and construction of dams and reservoirs tend to alter the local water and energy budget by producing sudden, periodic, and drastic increases in water availability at the surface. Drainage of swamps tends to have the opposite impact. In all these cases, although local evaporation rates and humidity are likely to be affected, the scale is usually too small to see significant changes in local precipitation totals. And, of course, the most dramatic land cover change on the planet—urbanization—has the distinct and irrefutable global impact of warming the climate in the form of the *urban heat island*, affecting the availability of water at the Earth's surface, and altering atmospheric circulation.

► Cryospheric Changes

Ice on the Earth's Surface

The *cryosphere*—the region consisting of all seasonal and “permanent” ice on the planet—is both a direct consequence of and an influence on the climate system. It may exist as a part of continental ice sheets, semipermanent alpine glaciers, seasonal sea ice, and/or seasonal snowpack. During cold periods of the year, all forms of ice accumulate from precipitation and/or **deposition**—the direct conversion of atmospheric water vapor to ice, bypassing the liquid water phase.

In the case of glaciers, the bulk of the ice body remains in below-freezing temperatures throughout the year. A portion, however, does exist in areas where temperatures exceed the freezing point for at least part of the year, so parts of glaciers are continually melting. Glacial advances occur during cooler and/or wetter periods when the rate of snow/ice **accumulation** in the

colder part of the glacier exceeds the rate of **ablation** (which includes melting and **sublimation**—the conversion of ice directly to water vapor, bypassing the liquid water phase) in the warmer part of the glacier. Glacial retreat occurs during times when the rate of ablation exceeds accumulation. In the case of a retreating glacier the ice merely melts or sublimates back from its most equatorward or downhill extent—the glacier does not physically move backward. A net mass balance point exists at the **equilibrium line**—a point within the body of glacier where the rate of accumulation equals the rate of ablation. As this line moves equatorward and/or downhill, the glacier is “healthy,” indicating growth, and when it retreats poleward and/or uphill, ablation exceeds accumulation for the system.

Earth has undergone several periods when most glaciers and ice sheets simultaneously advanced over many thousands of years. These glacial advances—intervals of 50,000 to 150,000 years or so—are separated by **interglacial phases**, warmer periods of approximately 8,000 to 12,000 years when net glacial retreat occurs in most glaciers. Summer temperatures generally determine whether glacial advance or retreat is occurring, because even abnormally high winter temperatures are below freezing in most glacial environments. Cool, short summers with snowy transition seasons generally provide the optimal conditions for glacial advance. Long, warm, dry summers cause the high rates of ablation coincident with interglacial phases.

Regardless of whether a glacial or interglacial phase is occurring, any time in geological history when semipermanent ice exists somewhere on Earth’s surface is termed an **ice age**. We are in an ice age today, because permanent ice exists on the planet—in Antarctica, Greenland, the north polar ocean, and on the tops of the world’s highest mountains at any latitude. The present ice age may have begun as many as 40 to 50 million years ago, but evidence shows that it became more intense some 1.6 million years ago. The last major glacial advance in the present ice age peaked between 12,000 and 18,000 years ago. This advance is known as the **Wisconsin Glacial Phase**, which occurred during the **Pleistocene Epoch**, a generally cold period that occurred from about 1.8 million years ago until about 10,000 years ago. Because planetary temperatures have generally increased for the last 10,000 years or so, most of the ice has been retreating poleward and/or uphill, and we are currently in the **Holocene Interglacial Phase**, an interglacial phase within the present ice age that corresponds to the **Holocene Epoch**, the present epoch in geological time. In recent years, the Holocene Epoch has also been referred to as the **Anthropocene Epoch**, to emphasize the impact of humans on the climate.

Feedbacks in the Cryosphere

An important positive feedback in the cryosphere is caused by surface albedo changes when the ice- and snow-covered area expands or contracts. The surface of the terrestrial Earth is, for the most part, dark. Expansion of bright white continental ice sheets across continents increases hemispheric and global albedo. In such instances a larger percentage of insolation is reflected from the surface to space. As a result, a decrease in the amount of absorbed insolation occurs at the surface, triggering a reduction in temperature, which in turn supports further growth of the ice sheets.

A similar positive feedback system occurs during periods of slight warming, such as at the beginning of an interglacial phase. Slightly elevated temperatures trigger increased icepack ablation. The albedo then decreases slightly, as the darker surface beneath the ice is exposed. This in turn initiates increased absorption of insolation. The net energy gains then cause increased atmospheric temperatures, which cause further increases in ablation and further albedo decreases.

It is apparent from the discussion above that the cryosphere is intricately linked to the atmosphere over long time scales. But the cryosphere can also influence the atmosphere (and vice versa) on short time scales. For example, a region may be hit with a heavy snowfall event in autumn. In such a case the snow may effectively change the regional albedo. After the event, the surface albedo changes may cause the region to grow colder, which in turn may cause the polar jet stream to shift farther equatorward than normal, because it exists near the boundary between cold and warm air. Because the jet steers midlatitude storm systems, displacement of the jet may initiate even more snowstorms over the affected regions. In this way a positive feedback system is set up, causing even more snowpack and higher albedo rates even farther equatorward, leading to further cooling.

Given such direct relationships between the cryosphere and the atmosphere, it is important that researchers examine and understand processes involving changes in the cryosphere. Such changes may lead to feedback systems that could influence the planetary-scale atmosphere. These atmospheric changes may then cause further feedbacks in the cryosphere and the other “spheres” in the climate system.

Researchers studying regional ice packs have found that the spring melt in western Canada has occurred earlier in more recent years than before, changing by as much as a half-day per year since 1955. These findings support computer modeling studies that suggest widespread reduction in snow cover could occur over the next 50 to 100 years as concentrations

of greenhouse gases such as CO₂ increase in the atmosphere. But this trend is not solely dependent on greenhouse warming, as extreme ENSO events, shifts in major circulation patterns, and other factors also play important roles.

Some researchers now estimate that the Greenland ice sheet, the largest in the northern hemisphere, could lose as much as one-half of its mass over the next thousand years, leading to an increase in global sea level of about 2.7 m (9 ft). Adjacent summer sea ice has decreased markedly over the past few decades, and some expect that within the next century the Arctic Ocean could be largely ice-free. Alpine (mountain) glaciers are in active retreat worldwide, with only a few regional exceptions.

Temperatures over the West Antarctic Ice Sheet have increased by approximately 4 C° (7 F°) over the past half century. A decrease in adjacent sea ice extent has also resulted, and two large collapses of major ice shelves have occurred over the past decade. The East Antarctic Ice Sheet appears to have remained stable during the same time period. If all permanent continental ice were to melt, sea levels would rise by approximately 67 m (220 ft).

A common misconception is that the melting of sea ice would not affect sea level because the ice displaces the same volume of seawater as its water equivalent. But because fresh water is less dense than saltwater, freshwater ice floats higher over the salty seawater and does not displace quite as much seawater as it would if the two had the same density. So when freshwater floating ice melts, it increases sea level by a small amount because of an increased amount of meltwater compared with the amount of seawater originally displaced.

Both this extra water and (especially) melted continental ice would greatly affect populations, because many of the world's major cities would be inundated by the sea level increases. Fortunately, even in the worst-case scenarios, the entire cryosphere is not expected to melt completely in a short time. But the (unknown) feedback mechanisms involved would determine whether any initial warming and melting would be counteracted (a negative feedback) or accelerated (a positive feedback). Positive feedbacks would further warm the climate system, which itself could have major global consequences. Observations generally confirm that the polar parts of the Earth have warmed more than tropical regions. This notion is termed **Arctic amplification**.

► Summary

This chapter explores the effects of several phenomena in the nonatmospheric “spheres” of the climate system

on climate. Surface ocean currents derived from atmospheric circulation in turn affect the adjacent climate of affected locations. The subtropical anticyclones centered in each ocean basin play an especially important role in the strength, direction, and variability of these currents. The anticyclones and corresponding semipermanent low-pressure cells—*cyclones*—located poleward of the anticyclones support cold ocean currents in the eastern ocean basins and warm ocean currents in the western basins in each hemisphere. The Ekman spiral, combined with latitudinal differences in Coriolis deflection, causes an accumulation of water to the west of the central ocean basin, which leads to western-boundary intensification—strong, deep, warm ocean currents in the western ocean basins—and shallow, slower cold currents in the eastern basins. Deep ocean currents also influence the broad-scale climate. Deep-water motions are described for each ocean basin, with particular attention paid to the Stommel model deep-water circulation, which stores and releases large quantities of energy into the climate system over long time periods.

El Niño–Southern Oscillation events represent the greatest single source of variability in the climate, excluding Earth–Sun-related seasonality. El Niño events occur when a warm water pool that normally occurs in the western equatorial Pacific Ocean migrates eastward during times of reduced trade wind flow. The water pool brings changes to typical atmospheric stability patterns. Specifically, clouds and precipitation occur in the normally clear, dry eastern Pacific region. Because of the immense amount of energy carried by the pool, global climatic regimes are affected. The opposite phenomenon—La Niña—is associated with the “normal” (ENSO-neutral) directions of oceanic and atmospheric flow but with increased intensities of that flow and effects. Biological effects in the ocean, such as the role of phytoplankton in the production of dimethyl sulfides, clearly have a role to play in global climate, but we are uncertain of whether the impacts produce a net dampening (negative feedback) or amplification (positive feedback) of warming.

Processes in the lithosphere and biosphere can also impact the climate system. Times of heightened volcanic activity may produce both short-term and even long-term climate variation. Human activities such as deforestation and desertification alter local to regional energy and water balances, which can ultimately affect hemispheric and global climate regimes. Finally, the cryosphere was discussed as an element of the climate system. Positive and negative feedback systems, especially in the cryosphere, are likely to dictate the severity of impacts of climatic change caused by human and natural forces.

Key Terms

Ablation	Equatorial Rossby wave	Permafrost
Accumulation	Equilibrium line	Peru current
<i>Advection</i>	<i>Evaporation</i>	<i>Photosynthesis</i>
<i>Aerosol</i>	<i>Fossil fuel</i>	Phytoplankton
Albedo	Geostrophic flow	Pleistocene Epoch
Amplitude	Global warming	Polar front jet stream
Antarctic Bottom Water	<i>Greenhouse effect</i>	Positive feedback system
Antarctic Deep Water	<i>Greenhouse gas</i>	Rain machine
Antarctic Intermediate Water	<i>Gulf Stream</i>	Ridge
Anthropocene Epoch	Gyre	Sahel
Anthropogenic	Holocene Epoch	<i>Sensible energy</i>
Anti-CLAW hypothesis	Holocene Interglacial Phase	<i>Sink</i>
Arctic amplification	Humboldt (Peru) current	Slash and burn agriculture
<i>Atmosphere</i>	<i>Hydrosphere</i>	Source area
<i>Biosphere</i>	Ice age	Southeast trade winds
Boreal forest	<i>Insolation</i>	Southern Oscillation
California current	Interglacial phase	Southern Oscillation Index (SOI)
Canary current	Jet stream	Stable atmosphere
Chimú Floods	La Niña	Stable stratification
CLAW hypothesis	<i>Latent energy</i>	Stommel model
Coastal Kelvin wave	<i>Latitude</i>	<i>Stratosphere</i>
Common Water	<i>Lithosphere</i>	Sublimation
<i>Condensation</i>	Maritime Continent	Subtropical anticyclone
Condensation nuclei	<i>Maritime effect</i>	Subtropical jet stream
<i>Continentality</i>	<i>Methane</i>	Sulfur dioxide (SO ₂)
<i>Convection</i>	<i>Momentum</i>	Thermocline
<i>Coriolis effect</i>	Multivariate ENSO Index	<i>Thermohaline circulation</i>
<i>Cryosphere</i>	Negative feedback system	Thermohaline current
<i>Cyclone</i>	Niño 3.4 Index	Trade winds
Deforestation	North Atlantic Deep Water	Transpiration
Deposition	<i>North Atlantic Drift</i>	Trough
Desertification	North Equatorial current	Unstable atmosphere
Dimethyl sulfide (DMS)	North Pacific Intermediate	<i>Upwelling</i>
Downwelling	Water	<i>Urban heat island</i>
Dust Veil Index	Northeast trade winds	Vog
<i>Ekman spiral</i>	<i>Outgassing</i>	Volcanic Explosivity Index
El Niño	Pacific Decadal Oscillation	Walker circulation
El Niño–Southern Oscillation	(PDO)	Western-boundary intensification
(ENSO) event	Pacific Subarctic Water	Wisconsin Glacial Phase
Equatorial Kelvin wave	Particulates	

Terms in italics have appeared in at least one previous chapter.

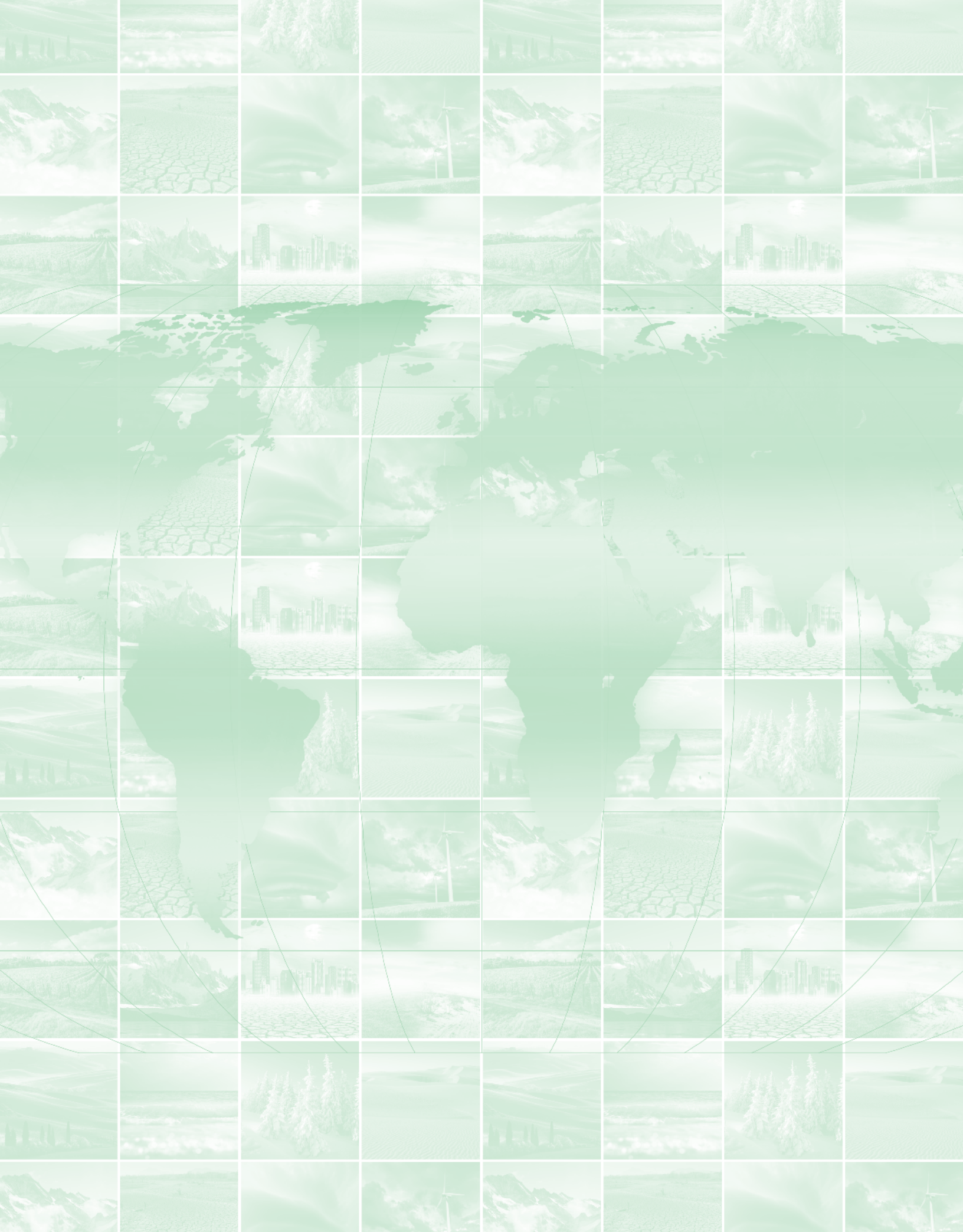
Review Questions

- Discuss the role of atmospheric circulation in creating and maintaining surface currents in the oceans.
- Discuss the role of surface ocean currents on climate.
- What is geostrophic balance in the oceans and why is it important?
- Describe the importance of western-boundary intensification.
- What are thermohaline currents and how and why are they maintained?
- How are thermohaline currents tied to the atmosphere and how can these currents affect climatic variations in the future?

7. Discuss the importance of the Stommel model of deep-water motion.
8. What is the Walker circulation?
9. Describe ENSO-neutral conditions along the equatorial Pacific Ocean.
10. What is El Niño and how is it initiated?
11. Discuss changes in the sea surface circulation and the thermocline of the Pacific Ocean during an El Niño event.
12. Describe the changes in the overlying atmosphere during an El Niño event.
13. Discuss the global climatic significance of an El Niño event.
14. What is a La Niña event and why is it significant?
15. Compare and contrast deforestation and desertification and their impacts on the climate system.
16. How do atmospheric changes drive processes in the cryosphere?
17. How can changes in the cryosphere lead to changes in the climate system?

Questions for Thought

1. Think of an example of a possible negative feedback mechanism that might result in a minimization of the global warming problem in the cryosphere.
2. How might a warmer atmosphere alter surface and deep ocean currents, and what effect would such changes have on the general atmospheric circulation?
3. How might continued human-related tropical deforestation alter regional and even global climate?





CHAPTER 5

Energy, Matter, and Momentum Exchanges near the Surface

CHAPTER AT A GLANCE

- Properties of the Troposphere
- Near-Surface Troposphere
- Energy in the Climate System
 - ▶ Sun as Energy Source
 - ▶ Measuring Radiant Energy
 - ▶ Radiation Balance
 - ▶ Turbulent Fluxes
 - ▶ Substrate Heat Flux
 - ▶ Energy Balance
- Local Flux of Matter: Moisture in the Local Atmosphere
 - ▶ Atmospheric Moisture
 - ▶ Moisture in the Surface Boundary Layer
 - ▶ Measuring Evapotranspiration
- Atmospheric Statics, the Hydrostatic Equation, and Stability
 - ▶ Statics and the Hydrostatic Equation
 - ▶ Atmospheric Stability
 - ▶ Assessing Stability in the Local Atmosphere
- Momentum Flux
- Putting It All Together: Thermal and Mechanical Turbulence and the Richardson Number
- Summary
- Key Terms
- Review Questions
- Questions for Thought

In addition to the role of “site” and “situation,” which includes *latitude*, land–sea distribution, circulation, topography, and local features on climates, interactions involving the *hydrosphere*, *lithosphere*, *biosphere*, and *cryosphere* also affect climate. These factors and their impacts can be felt on a variety of spatial scales. The scales range from the **microscale** to the **planetary scale**. This chapter describes the influence of these and other factors on near-surface climates. It also introduces the effect of energy, matter, *momentum*, and *friction* on local climates.

► Properties of the Troposphere

As we have seen, the atmosphere can be subdivided into various layers based on the expected change in temperature with height. In this chapter we keep the discussion focused on the lower part of the *troposphere*, the layer from the surface up to 8 to 20 km (5 to 13 mi) high (the *tropopause*). The troposphere is thickest over the tropics, where warm air tends to expand, stretching the distance vertically, and thinnest over the polar areas in winter, where the intense cold air compresses.

The troposphere is characterized by temperatures that normally decrease with height, both because of the decreasing compression of atmospheric gases with increasing height and because of the increasing distance from the (indirect) heat source—the surface. In general, the atmosphere tends to transmit most of the *shortwave radiation*—electromagnetic radiation at *wavelengths* between about 0.4 to 4.0 micrometers (μm)—from the Sun through it. The surface (particularly the land surface) absorbs most of the shortwave energy incident upon it. This causes the surface to emit **longwave radiation** (electromagnetic radiation at wavelengths greater than 4.0 μm) upward. The near-surface atmosphere is more likely to absorb longwave radiation than locations higher in the troposphere, because more atmospheric mass is concentrated near the surface.

Although it varies across space and time, the average rate of cooling with height in the troposphere is 6.5 °C/km. This rate is known as the *environmental lapse rate* (ELR, or λ). As we see later in this chapter, ELR is a critical determinant of whether vertical motion occurs easily in the troposphere. The root word “tropo” means “turning,” and the troposphere is so-named because it is often characterized by *convection*—vertical motions that are caused by hotter air near the surface rising while cooler air aloft sinks, or **turbulence**—vertical motions caused by surface friction on advecting air.

Because about 75% of the atmosphere’s mass and nearly all its water vapor are located in the troposphere, this

layer is sometimes referred to as the “weather and climate layer.” The lowest part of this layer, which contains an even more disproportionate share of the atmosphere’s mass and water and an even greater tendency for vertical motion, is the site of the most vigorous and intense exchanges of energy, matter, and momentum in the climate system.

► Near-Surface Troposphere

Four subdivisions within the troposphere can be defined, as shown in **FIGURE 5.1**: (1) laminar layer, (2) roughness layer, (3) transition layer, and (4) *free atmosphere*. The **laminar layer** is the part of the atmosphere that is nearest to the surface or elements on the surface, such as a leaf, roof, or wave on the sea. This layer is only a few millimeters thick, at most. By definition, the laminar layer is characterized by smooth flow that parallels the features of the surface over which it moves. Several laminar layers may even exist vertically when the shape of the surface feature is complicated. For example, every leaf on a tree has a laminar layer adjacent to its surface. The features of this layer are most important in plant physiology applications, because the atmospheric flow across the leaves is an important factor affecting the loss of water from the plant’s surface.

Above the laminar layer is a zone of strong convection or turbulence, called the **roughness layer**, characterized by a large component of vertical motion compared with horizontal motion. The turbulence in this layer is almost entirely mechanical in origin. **Mechanical turbulence** is motion caused by the friction, irregular

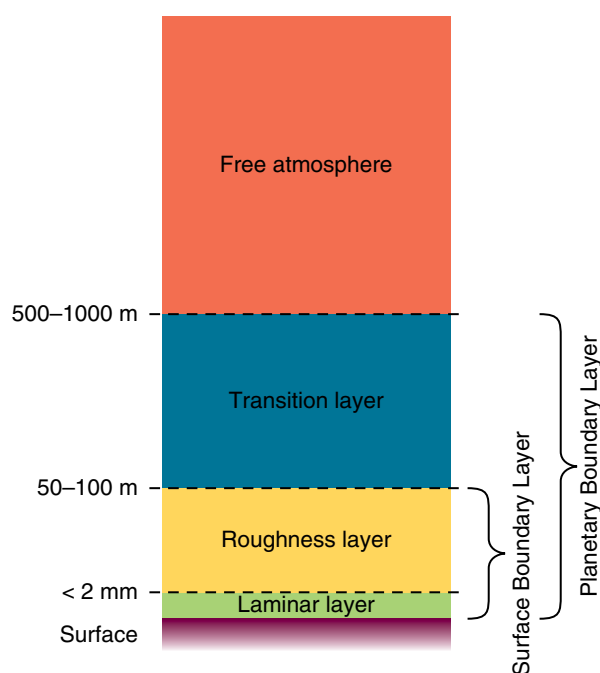


FIGURE 5.1 The near-surface troposphere.

flow, and vertical gradients of momentum associated with the roughness elements, such as trees in a forest, buildings, mountains, or crops.

Less important in the roughness layer, particularly within a dense plant canopy, is **thermal turbulence** resulting from unequal heating of the surface, because differences in surface heating are small when shading occurs from the roughness elements. The roughness layer may extend up to one to three times the height of the individual roughness elements (to perhaps 50 to 100 m). It is thicker by day than by night because of the increased differences of surface heating across space during daylight hours. The maximum height of the roughness layer occurs with a medium density of roughness elements. Interestingly, if the roughness elements become too closely packed and uniform in height, the top of the roughness elements may mimic a smooth surface and show relatively little mechanical or thermal turbulence and more laminar-like flow.

The roughness layer is important from an energy perspective. The vertical motion that dominates this zone transports energy used to drive atmospheric processes between the surface and the atmosphere above this layer. In most cases, especially in daylight hours, the surface is warmer than the atmosphere above it and energy is transported upward via the **turbulent flux (flow) of sensible heat**—also known as the **sensible heat flux (Q_H)**. The most intense turbulence is associated with situations when the temperature difference between the surface and the air above it is very large.

The upward transport of matter is also important in the roughness layer. The type of matter that is of most concern to climatologists is water. The **turbulent flux of latent heat**—also known as **latent heat flux (Q_E)**—transports water vapor, usually in an upward direction also, from the surface where oceans, soil moisture, streams, and lakes evaporate liquid water to the atmosphere. From there, the turbulent flow may allow clouds to form.

Unlike the fluxes of heat (energy) and matter (i.e., water), the **vertical flux of horizontal momentum (τ)** or **shearing stress** is usually transported downward, from the atmosphere to the surface. This is because winds usually strengthen with increasing height, as friction decreases. The net *flux* of horizontal momentum is downward as turbulence carries air with greater momentum downward and air with lesser momentum upward.

The laminar layer and the roughness layer combined are sometimes referred to as the **surface boundary layer (SBL)**. In the SBL the turbulent fluxes and the momentum flux are generally considered to be constant with height, but not over time. According to **Fick's law**, the flux of any entity is proportional

to the gradient of that entity in the fluid (liquid or gas) through which the flux occurs. The gradient of energy or moisture from the surface upward or the gradient of momentum downward hence must also be constant to the top of the SBL at any given place and time. We can take this logic one step further by saying that the rate at which the energy, water, or momentum is moved vertically is constant from one height to another within the SBL at one moment in time. Because the energy and momentum fluxes are constant with height, wind direction theoretically cannot change within the SBL.

The **transition layer** extends from the top of the SBL to approximately 500 to 1000 m above the surface. Again, this layer extends farther upward by day than by night, as convective processes thrive in the afternoon heat. In the transition layer turbulent features from the SBL remain important. Some of the characteristics of the free atmosphere above this layer, however, also have some importance. The shearing stress gradually decreases with height in the transition layer until it becomes zero, which defines the top of the layer, at which a negligible vertical flux of horizontal momentum occurs. The decrease in friction with height in the transition layer causes winds to change direction in a “spiral staircase” pattern; this is the *Ekman spiral* in the atmosphere. For instance, a balloon that is released changes direction in a rather predictable pattern (**FIGURE 5.2**). Collectively, the laminar, roughness, and transition layers comprise the **planetary boundary layer**.

In the free atmosphere friction is generally assumed to be negligible. In that layer, flow is governed by the *pressure gradient force*, the apparent horizontal deflective force known as the *Coriolis effect*, *centrifugal acceleration*, and *geostrophic balance*.

► Energy in the Climate System

Sun as Energy Source

The Sun is the source of essentially all energy that drives atmospheric and oceanic circulations. Without the Sun's unequal heating of Earth, there would be no need for the atmosphere or oceans to circulate, because no differences in heat (energy) would be received from one place to another on Earth's surface. Because the differences in local energy received from the Sun are so important in the climate system, many applications rely on knowing the position of the Sun in the sky. For example, agricultural models rely on the intensity of *insolation* to determine the rate at which *photosynthesis* allows a crop to grow. Architects design buildings so the overhang over a window is short enough to let the winter Sun (which is relatively low in the sky) into the

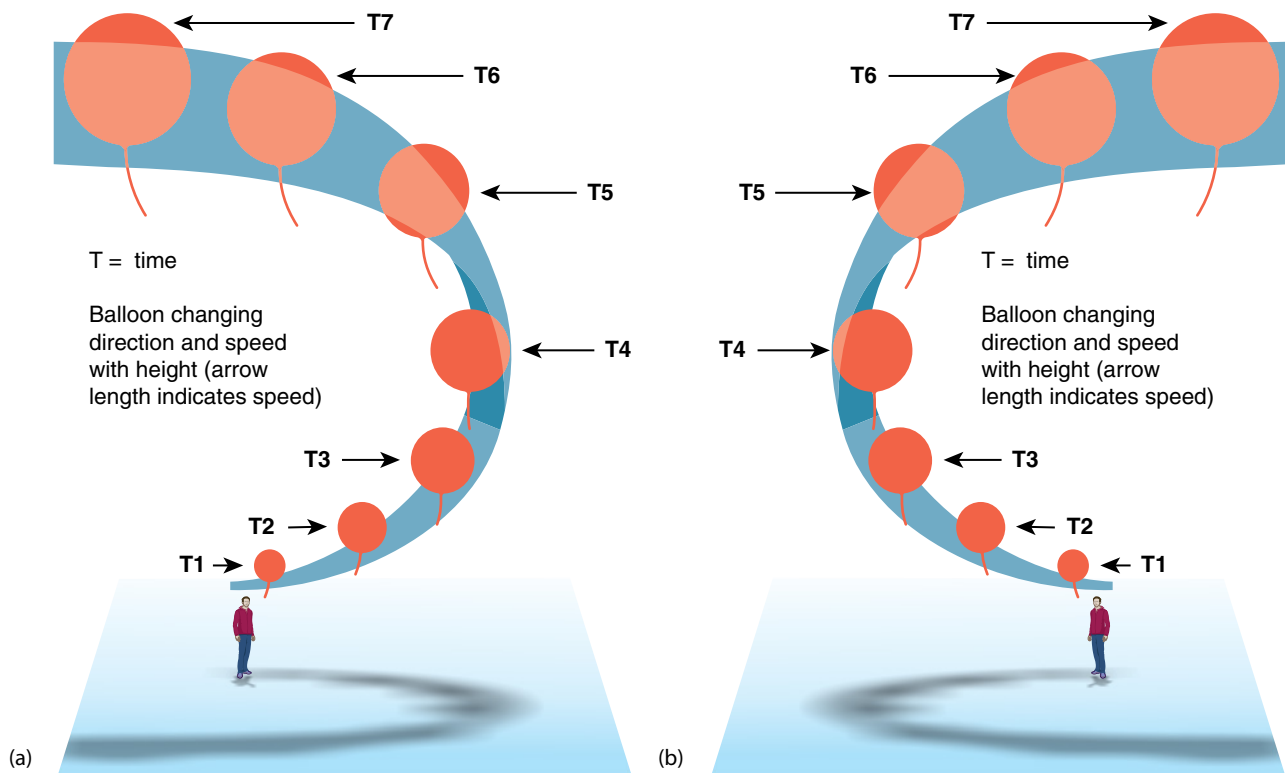


FIGURE 5.2 Change of wind direction with height in the Ekman layer in the (a) northern hemisphere and (b) southern hemisphere.

room yet is long enough to keep the hot summer Sun (which is higher in the sky) out of the room (**FIGURE 5.3**). Traffic engineers know that at certain times of the day and certain times of the year the Sun will be situated directly behind a traffic light, making the signal especially difficult to see. Additional traffic signals should be installed in more visible parts of the intersection.

All these applications require the precise calculation of the position of the Sun. The position of the Sun also largely governs the receipt of shortwave radiation input on a surface. When the Sun is high in the sky, such as near noon around 23.5°N or 23.5°S around the *summer solstice*, its radiation reaches the surface more effectively because it does not have to pass through a great distance of atmosphere (**FIGURE 5.4**). So we can say that the **optical air mass**—the ratio of the distance that a beam travels through the atmosphere (*path length*) to the minimum distance that it could possibly have to travel to reach the surface—is near 1.0. Conversely, when the Sun is low in the sky, such as around the *winter solstice* in the high latitudes or near sunrise and sunset at any latitude, the long path of radiation through the atmosphere allows a significant amount of the radiation to undergo *attenuation*—which includes the **absorption** of energy by air particles and **scattering** away from the surface—before it reaches the surface. In such a situation the optical air mass is likely to be much greater than 1.0.

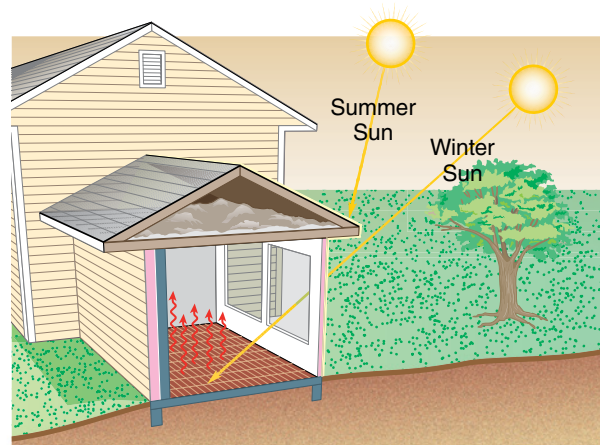


FIGURE 5.3 Effect of Sun angle on building design: An overhang.

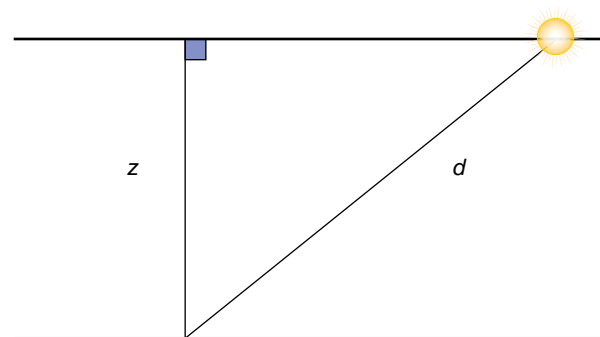


FIGURE 5.4 The optical air mass would be the ratio of d to z .

Sun Path Diagrams

Although the equations used to describe these positions are not presented here, the position of the Sun in the sky at any day of the year and any time of the day, for any latitude, can be plotted on a **Sun path diagram**. Just as a position on a map has coordinates in angular degrees of latitude and *longitude*, we can describe the Sun's location in the sky using the coordinates of **zenith angle** and **azimuth angle**. The zenith angle expresses how many degrees the Sun is located away from the local vertical (**FIGURE 5.5**). So when the Sun is directly overhead at a given location, its zenith angle is 0° . At sunrise and sunset the zenith angle is 90° .

The azimuth angle represents the number of degrees that the Sun is located away from north (**FIGURE 5.6**). For example, if the Sun is in the northern sky (as it is for locations in the southern hemisphere's extratropical

areas near noon), its azimuth angle would be 0° , but if the Sun is exactly in the eastern sky at a given location (as it is near sunrise on some days of the year), it would have a 90° azimuth. Likewise, a 180° azimuth angle suggests that the Sun is in the southern sky (as it is near noon in the extratropical northern hemisphere). And a 270° azimuth angle implies that the Sun is in the western sky.

FIGURE 5.7 shows Sun path diagrams for locations at various latitudes. When using Sun path diagrams, the *solar declination* must be known for the day of interest. The declination is $23^\circ 27'$ N latitude on June 21, 0° on the **equinoxes**, and $23^\circ 27'$ S latitude on December 22.

Notice that the Sun tracks increasingly toward the southern sky at solar noon as latitude increases in the northern hemisphere. Nevertheless, the position of the Sun at sunrise and sunset at a given day of the year increasingly

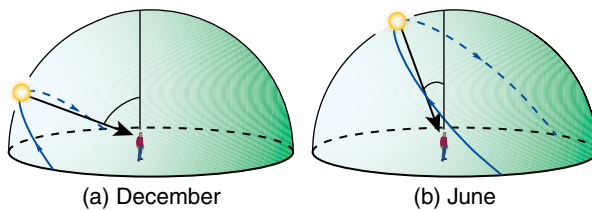


FIGURE 5.5 Zenith angle.

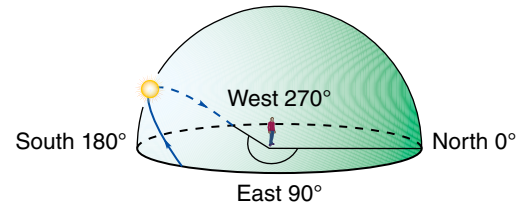


FIGURE 5.6 Azimuth angle.

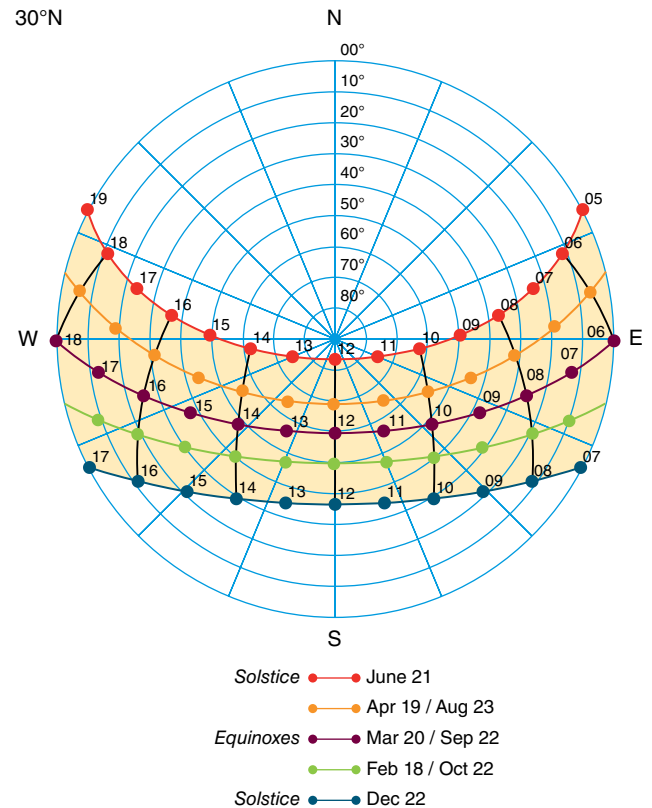
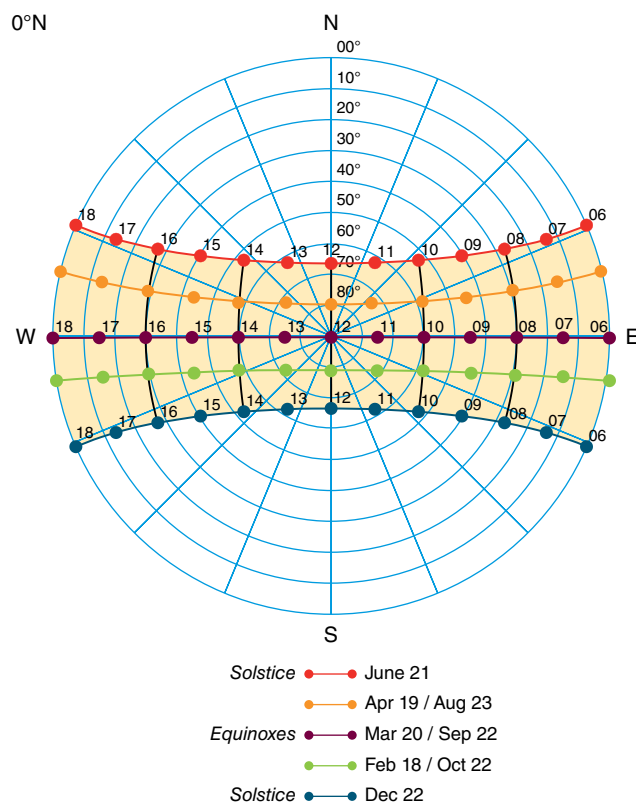


FIGURE 5.7 Sun path diagrams for latitudes 0° , 30°N , 45°N , 60°N , 80°N , 30°S , 45°S , 60°S , and 80°S : the number at the points indicates the hour of the day.

Courtesy of A. Christen, University of British Columbia.

(Continues)

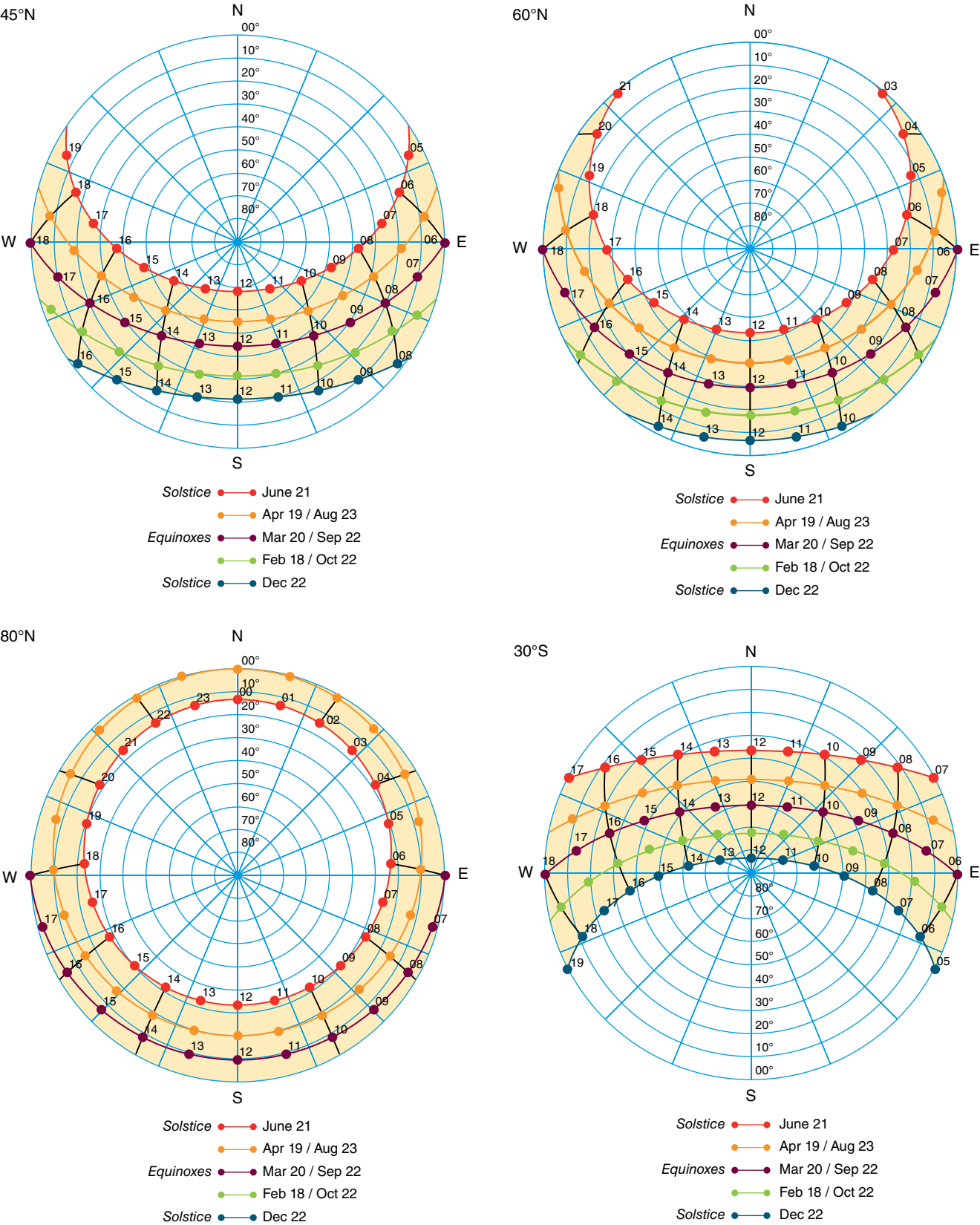


FIGURE 5.7 Continued

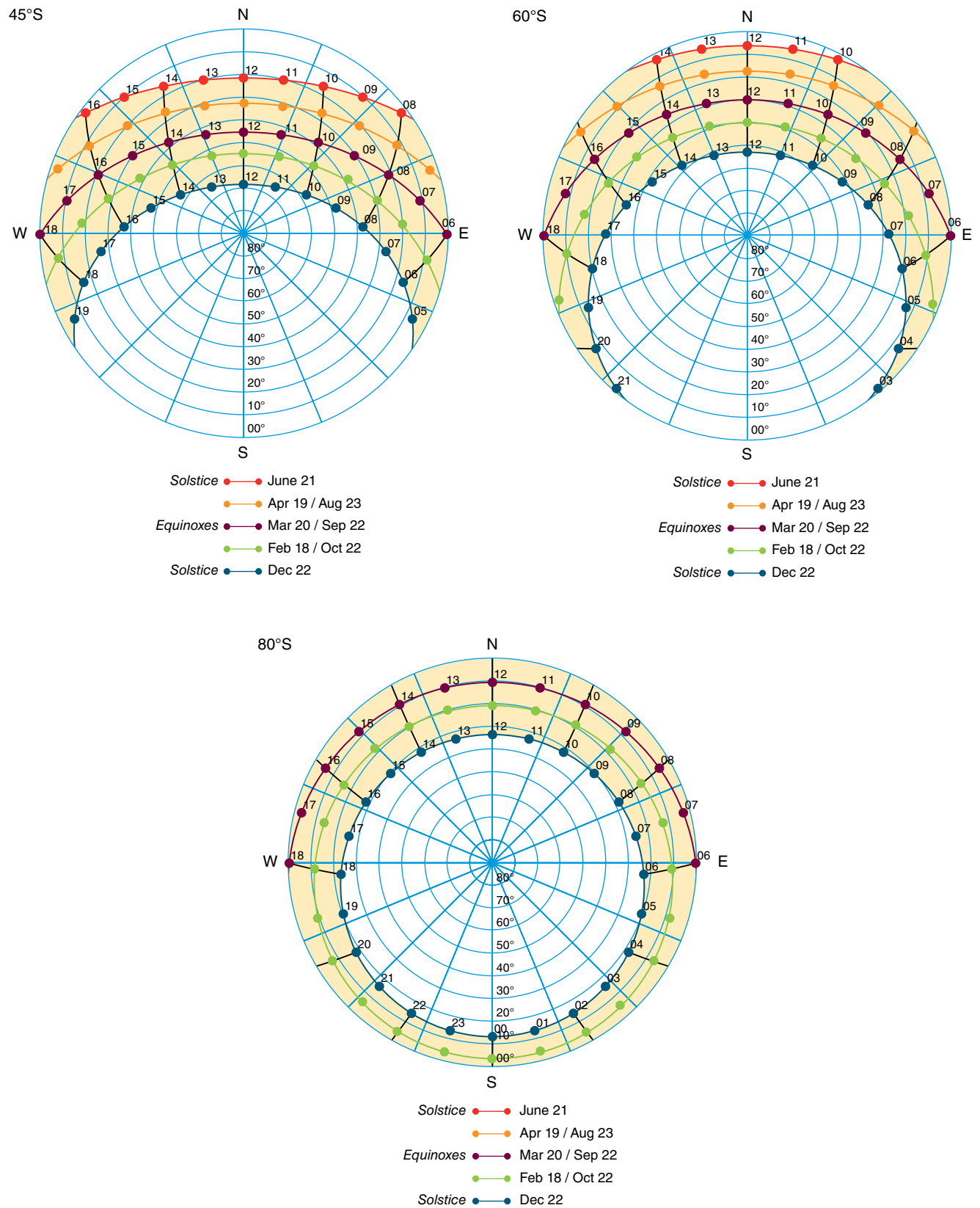


FIGURE 5.7 Continued

acquires a northerly component as latitude increases in the northern hemisphere too, until inside the *Arctic Circle*, where sunrise and sunset do not exist for at least 1 day of the year. It is indeed an oversimplification to say that the Sun rises in the east and sets in the west.

Solar Time

Solar time is the “true” time at a location based on the location’s position with respect to the Sun. Specifically, *solar noon* at a given meridian of longitude occurs when the Sun is at the highest position that it will achieve on a given day at that meridian. Put another way, solar noon at any meridian of longitude occurs when the *rotation* of Earth puts that particular meridian directly in front of the Sun. Note, though, that on a given day only one parallel of latitude along that meridian—the solar declination on that day—receives the direct rays of the Sun (and, therefore, would have a zenith angle of zero at solar noon). If we used solar time to represent the time shown on our clocks, locations along every meridian of longitude would have different times on their clocks. This would create undue confusion for everyone when communicating with others across long (or even short) distances.

To remedy this problem we use a simplification called **zone mean time**—a system in which the “clock time” is synchronized across a range of longitudes so that no adjustment is necessary except when crossing from one *time zone* to another. Twenty-four time zones are arranged longitudinally, with the “clock time” set 1 hour apart at each zone (FIGURE 5.8). The zone mean

time actually corresponds to the solar time only at the **principal meridians**—24 longitudinal designations around the world. The principal meridians are located at 0° and at 15°, 30°, 45°, 60°, 75°, 90°, 105°, 120°, 135°, 150°, and 165° east and west longitude along with 180° longitude, which roughly corresponds to the **international date line**. For example, because New Orleans, Louisiana, is located at 90°W longitude, the zone mean time is equal to the solar time, and no adjustment is necessary to compute the solar time at that location.

But most locations are not on principal meridians, so an adjustment is required to use a Sun path diagram correctly. Earth rotates through 360° of longitude every 24 hours, so it rotates through 15° every hour (which explains why the principal meridians are 15° apart and have times that are 1 hour apart from adjacent principal meridians). Taken further, we can say that Earth rotates through 1° of longitude every 4 minutes. Because Earth rotates from west to east, locations east of a principal meridian have solar noon before the solar noon of their principal meridian, and locations west of a principal meridian experience solar noon after their principal meridian. In either case the offset is by 4 minutes for every degree of longitude separating a location from the principal meridian in its time zone (FIGURE 5.9).

In actuality, slight variations in Earth’s orbital velocity throughout the year cause Earth to have to rotate slightly more or less than 360° to reach the next successive solar noon. This imperfection necessitates another adjustment called the **equation of time**. This adjustment varies not by location (in contrast to the correction for the zone mean time) but by time of year. FIGURE 5.10 shows that

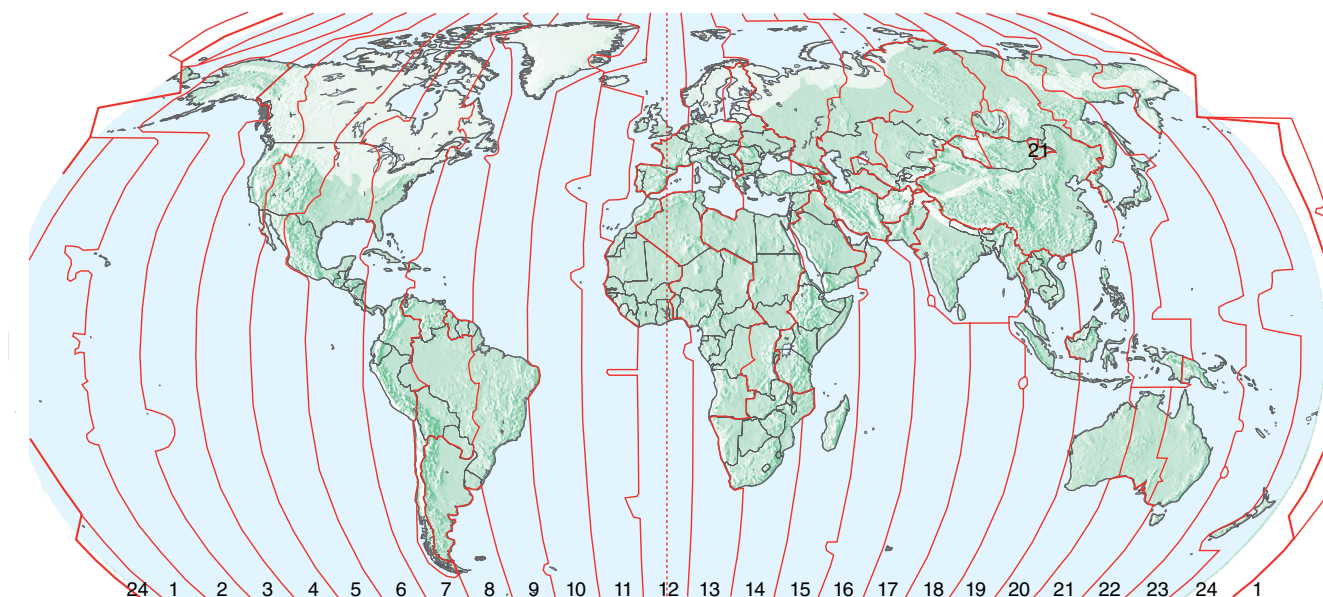


FIGURE 5.8 Time zones of the world.

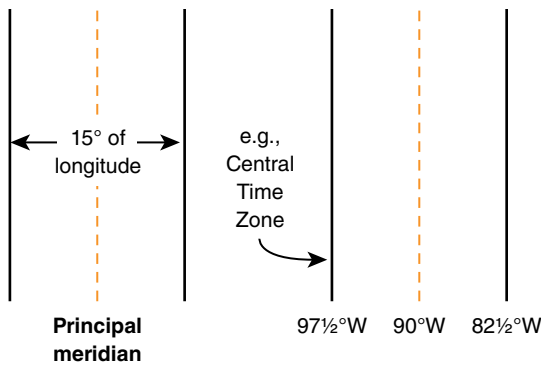


FIGURE 5.9 Relationship of principal meridian to time zone.



FIGURE 5.10 The position of the Sun in the sky at a given location and time of day through the course of the year.

Courtesy of Anthony Ayiomamitis.

at the same time each day, the Sun is located in a different position throughout the year, and the path that the Sun takes at the same time of day during the course of a year assumes the form of a figure eight. The equation of time adjustment may add up to 16 minutes and 23 seconds (on or about November 5) or take away up to 14 minutes and 20 seconds (on or about February 13) to the zone mean time to compute the solar time. The adjustment necessary for the equation of time can be shown with an **analemma**—a graph in the general shape of a figure eight (**FIGURE 5.11**). It can also be shown as a graph (**FIGURE 5.12**), or in tabular form (**TABLE 5.1**).

The term “**local apparent time**” is sometimes used as a synonym for solar time to describe the “true” time

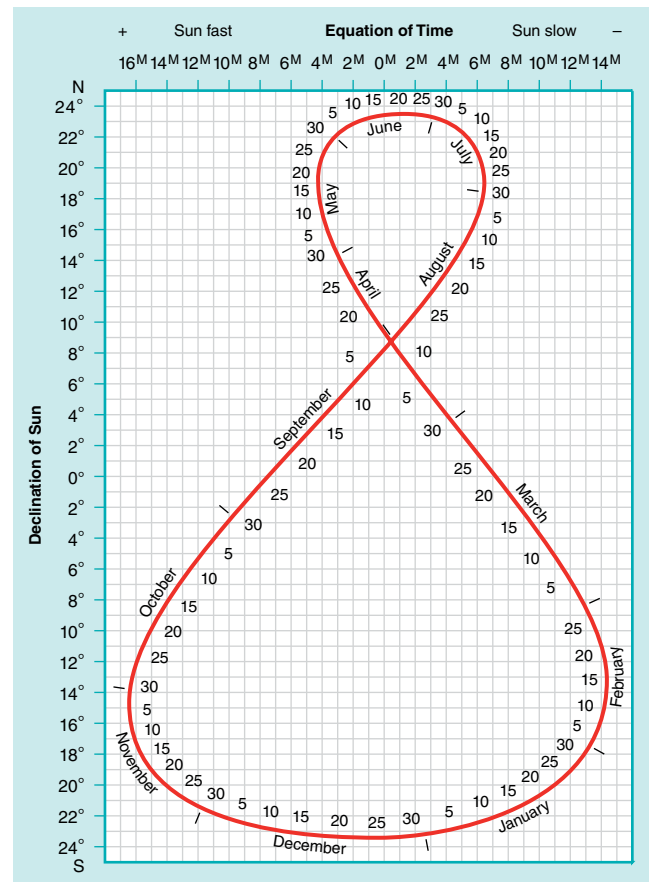


FIGURE 5.11 An analemma.

Data from: U.S. Coast and Geodetic Survey.

after the zone mean adjustment and equation of time adjustment are incorporated.

Theoretically then, no location should have clocks that differ from local apparent time by more than about 46 minutes (7.5° of longitude east or west of the principal meridian times 4 minutes per degree of longitude, plus 16 minutes for the equation of time adjustment on November 5). But for convenience and economic advantage some locations are included in time zones beyond 7.5° east or west of a given principal meridian. For example, Cincinnati, Ohio, (84.5°W longitude) is closer to the 90°W principal meridian than to the 75°W principal meridian, even though it uses Eastern Time (for which the 75°W meridian is the standard meridian). This means that Cincinnati actually has solar time that is 38 minutes earlier in the day than clock time, if no equation of time adjustment is necessary (which occurs on or about April 16, June 14, September 1, and December 26). Solar noon on those 4 days occurs at about 12:38 pm on the clock in Cincinnati.

Measuring Radiant Energy

Any instrument that measures the flux of radiation over a unit area of the surface (in Watts per square meter) is termed a **radiometer**. Most radiometers operate on

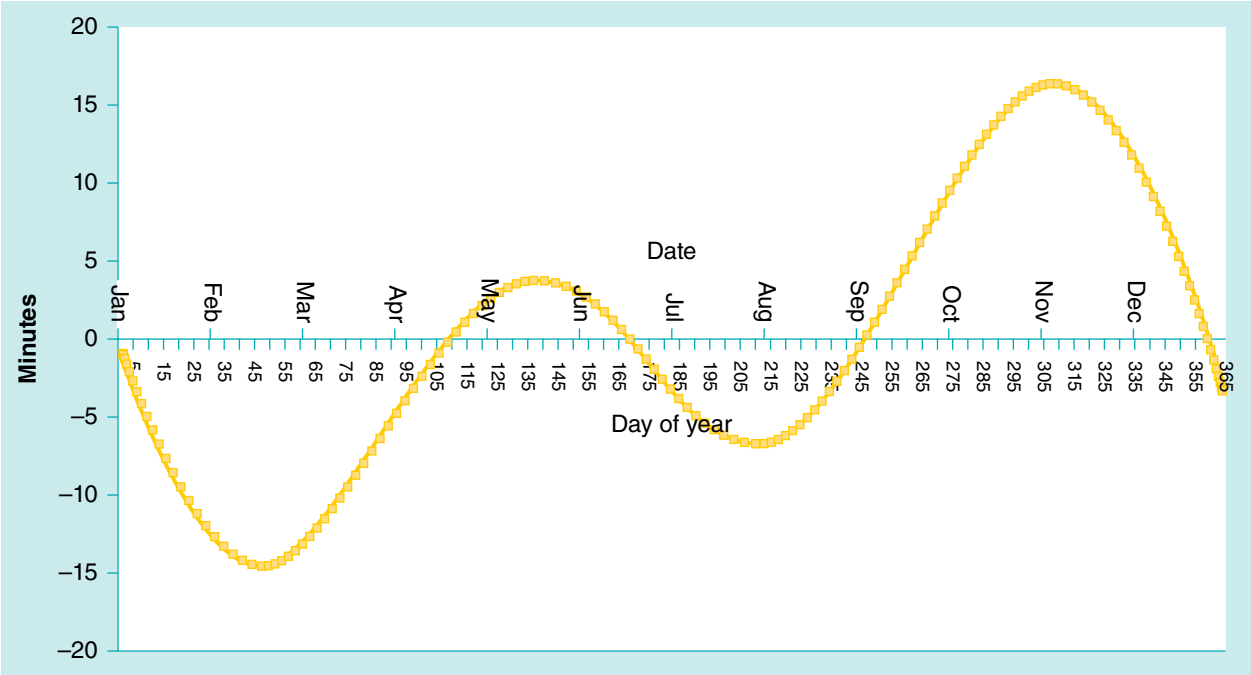


FIGURE 5.12 An “Equation of Time” graph.

TABLE 5.1 Equation of Time Adjustment by Day of Year, in Minutes								
	Day of Year	Minutes		Day of Year	Minutes		Day of Year	Minutes
Jan 1	1	−3.23	Feb 21	52	−13.8	Apr 13	103	−0.78
Jan 5	5	−5.1	Feb 25	56	−13.3	Apr 17	107	0.217
Jan 9	9	−6.83	Mar 1	60	−12.6	Apr 21	111	1.1
Jan 13	13	−8.45	Mar 5	64	−11.8	Apr 25	115	1.883
Jan 17	17	−9.9	Mar 9	68	−10.9	Apr 29	119	2.55
Jan 21	21	−11.2	Mar 13	72	−9.82	May 1	121	2.833
Jan 25	25	−12.2	Mar 17	76	−8.7	May 5	125	3.283
Jan 29	29	−13.1	Mar 21	80	−7.53	May 9	129	3.583
Feb 1	32	−13.6	Mar 25	84	−6.33	May 13	133	3.733
Feb 5	36	−14	Mar 29	88	−5.12	May 17	137	3.733
Feb 9	40	−14.3	Apr 1	91	−4.2	May 21	141	3.567
Feb 13	44	−14.3	Apr 5	95	−3.02	May 25	145	3.267
Feb 17	48	−14.2	Apr 9	99	−1.87	May 29	149	2.85

	Day of Year	Minutes		Day of Year	Minutes		Day of Year	Minutes
June 1	152	2.45	Aug 13	225	−4.95	Oct 25	298	15.77
June 5	156	1.817	Aug 17	229	−4.2	Oct 29	302	16.17
June 9	160	1.1	Aug 21	233	−3.32	Nov 1	305	16.35
June 13	164	0.3	Aug 25	237	−2.3	Nov 5	309	16.38
June 17	168	−0.55	Aug 29	241	−1.17	Nov 9	313	16.2
June 21	172	−1.42	Sep 1	244	−0.25	Nov 13	317	15.78
June 25	176	−2.28	Sep 5	248	1.033	Nov 17	321	15.17
June 29	180	−3.12	Sep 9	252	2.367	Nov 21	325	14.3
July 1	182	−3.52	Sep 13	256	3.75	Nov 25	329	13.25
July 5	186	−4.27	Sep 17	260	5.167	Nov 29	333	11.98
July 9	190	−4.93	Sep 21	264	6.583	Dec 1	335	11.27
July 13	194	−5.5	Sep 25	268	8	Dec 5	339	9.717
July 17	198	−5.95	Sep 29	272	9.367	Dec 9	343	8.017
July 21	202	−6.25	Oct 1	274	10.03	Dec 13	347	6.2
July 25	206	−6.4	Oct 5	278	11.28	Dec 17	351	4.283
July 29	210	−6.38	Oct 9	282	12.45	Dec 21	355	2.317
Aug 1	213	−6.28	Oct 13	286	13.5	Dec 25	359	0.333
Aug 5	217	−5.98	Oct 17	290	14.42	Dec 29	363	−1.65
Aug 9	221	−5.55	Oct 21	294	15.17			

the basis of thermoelectricity—that is, the amount of radiation received is proportionate to the temperature increase on the sensor. This temperature increase is then converted back to the intensity of radiation that would have caused such a temperature change.

A **pyranometer** is a radiometer that measures only shortwave (solar) radiation, and a **pyrgeometer** detects only longwave radiation (i.e., radiation emitted from the atmosphere or Earth). Pyranometers and pyrgeometers work by allowing only shortwave radiation (or longwave radiation for the pyrgeometer) to be transmitted through a dome and heat the surface of a sensor. A **pyrradiometer** measures all-wave radiation. In actuality, the use

of two of these three types of instruments simultaneously allows the deduction of the third (unmeasured) radiation variable, because the pyrradiometer's reading should be the sum of the shortwave and longwave radiant fluxes.

Any of the above types of instruments with “net” preceding its name implies that the instrument subtracts the energy lost from the energy gained at the surface. For example, a net pyrradiometer measures the amount of all-wave energy incident on a surface less the amount of all-wave energy emitted by the surface. Net radiometers usually require two sensors—one pointing upward and one pointing downward—to measure the net flux of energy both toward and away from the surface.

Radiation Balance

The **net radiation** (Q^* , pronounced “Q-star”) received at any given point on Earth varies tremendously over time. Sometimes the net radiant flux is negative. This occurs whenever the local surface is losing more radiant energy than it gains. Such a situation is common over an ice sheet or in any location where a near-surface *temperature inversion*—an increase in temperature with height—is occurring. At other times, strongly positive values of Q^* occur at a place, such as on a hot summer afternoon, when the surface receives insolation faster than it can emit longwave radiation back up to the atmosphere. The global amount of shortwave radiation received by Earth’s entire surface from the Sun (termed $K\downarrow_{\text{sfc}}$ and pronounced “K down at the surface”) at any one moment in time is essentially constant, however.

Solar radiation that enters the atmosphere is involved in various processes, including atmospheric absorption (retention by a particle and conversion to internal energy), scattering in all directions by the atmosphere, and **reflection** from the tops of clouds or the surface. In recent years satellite data have made it possible for us to determine the amount of energy involved in each of the processes of absorption, scattering, and reflection (**FIGURE 5.13**). On a global annual average basis, approximately 30% of $K\downarrow$ descending to the top of the atmosphere is reflected by cloud tops, scattered by atmospheric particles back to space, or reflected from the surface all the way out to space. Collectively, shortwave energy that exits the atmosphere upward in such a manner is termed $K\uparrow$ (pronounced “K up”). This 30% is sometimes referred

to as the **planetary albedo**, but the term “*albedo*” in its strictest sense refers only to energy that is reflected from a surface as a proportion of the total energy incident upon that surface. Of course, cloudy locations tend to experience a greater planetary albedo than places with clear skies, because of increased reflection from cloud tops and scattering by cloud droplets back to space. Typical albedo values for various surfaces are shown in **TABLE 5.2**.

Insolation that is not part of the planetary albedo may be absorbed in the atmosphere, scattered downward, or transmitted through the air. On a global annual average basis approximately 25% of $K\downarrow$ at the top of the atmosphere is absorbed by atmospheric gases and *aerosols*. Again, this value varies by several percentage points at any given place and time. On a global annual average basis only the remaining approximately 45% of $K\downarrow$ that reaches the top of the atmosphere is transmitted to the surface.

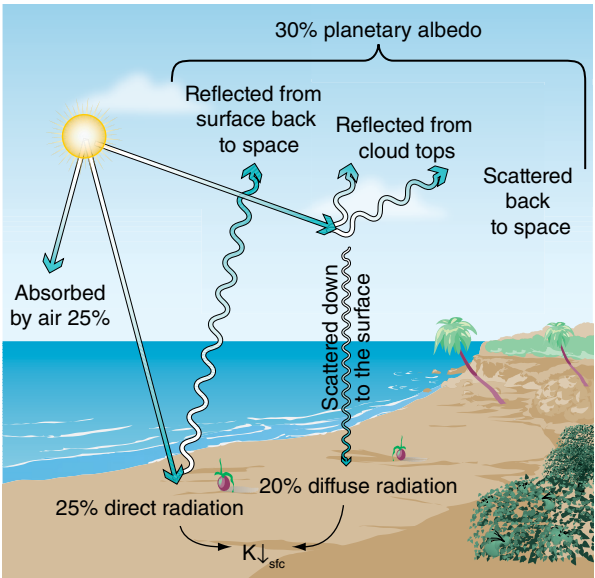


FIGURE 5.13 Schematic representing the global shortwave radiation budget.

TABLE 5.2 Common Albedo Values for Various Surfaces

Surface	Albedo Value
Fresh snow	75–90
Thick cloud	50–80
Ocean with high zenith angle	50–70
Old snow	50–60
Thin cloud	40–60
Earth–ocean–atmosphere system	30
Dry soil	15–35
Meadow	15–30
Cropland (depending on stage of growth)	10–35
Forest	5–15
Urban land	5–15
Wet soil	5–15
Ocean with low zenith angle	3–5

Insolation that reaches the surface without being absorbed or scattered downward is termed **direct radiation**, whereas **diffuse radiation** is radiant energy that reaches the surface only after being scattered downward. On a global annual average slightly more of the energy that reaches the surface occurs in the form of direct radiation than diffuse radiation, with a higher percentage of diffuse radiation occurring in cloudy and polluted atmospheres. Diffuse radiation—along with *advection*, the lateral movement of mass or energy—is the reason that the temperature difference between a sunny location and a nearby shady location is not greater than it is, and it also explains why a sunburn is possible even while sitting in the shade.

At a given location even though shortwave energy is being received only between sunrise and sunset, the radiation budget is not “dead” at night. Any object with a temperature above *absolute zero* (which includes every object found so far!) emits radiant energy all the time—day and night. If such an object does not have a temperature that is as hot as the Sun, its emitted radiant energy can be characterized as longwave. Thus Earth and its atmosphere emit longwave energy at all times of the day and night, with the intensity and wavelength of radiant energy emitted depending on the temperature of the emitter. In reality, as explained elsewhere in the text, Earth emits radiation at a wide range of wavelengths but with the vast majority at so-called longwave ranges. Likewise, the Sun’s emission spectrum includes a wide range of wavelengths focused on the so-called shortwave range.

For Earth as a whole, on a global annual average most longwave energy emitted by the surface (termed $L\uparrow$ and pronounced “L up”) is absorbed by the air. Only a small fraction (perhaps 7% to 15%) of $L\uparrow$ is transmitted completely through the air and escapes to space unimpeded. Most of this $L\uparrow$ has wavelengths that fall in the **atmospheric window**—the range in the *electromagnetic spectrum* between 8 and 13 μm in which a low percentage of longwave radiation is absorbed, at least under clear-sky conditions. The proportion of $L\uparrow$ that is absorbed by the air is greater in cloudy, humid, and low-elevation environments and less in dry and highland environments because water and water vapor are efficient absorbers of longwave radiation. Any longwave energy from the surface that is absorbed by the air is then reemitted by the air in all directions. Although some of this energy is emitted out to space, more of it is emitted downward (termed $L\downarrow$ and pronounced “L down”) and absorbed near the surface, because most of the atmospheric mass is concentrated closer to the surface rather than near the “top” of the atmosphere. $L\downarrow$ is sometimes termed **counter-radiation**.

A simple **radiation balance equation** can be created. We can say that

$$Q^* = (K\downarrow - K\uparrow) + (L\downarrow - L\uparrow)$$

The equation shows that net radiation is the sum of the net shortwave radiant energy (K^*) received at the surface and the net longwave radiant energy (L^*) received at the surface. K^* is the difference between the shortwave radiant energy that reaches the surface ($K\downarrow$) and that which is reflected from the surface ($K\uparrow$), while L^* represents the difference between the longwave radiant energy that reaches the surface as counter-radiation ($L\downarrow$) and that emitted by the surface ($L\uparrow$).

At night $K\downarrow$ is zero, and $K\uparrow$ must also be zero because no shortwave energy can be reflected if none is incident on the surface. In such a case the first term on the right side of the equation (K^*) is zero. Most of the time, at most locations, $(L\downarrow - L\uparrow)$ is slightly negative, because as we saw already the Sun tends to heat the surface more effectively than it heats the air (45% of the incident energy absorbed at the surface versus 25% absorbed in the air, on a global annual average basis). So most of the time, the longwave energy emission should be greater in the upward direction from the surface than in the downward direction from the air. So at night the typical scenario is for Q^* to be slightly negative. On a sunny summer afternoon, $(K\downarrow - K\uparrow)$ is generally a large positive number at the surface, because only a small percentage of the shortwave energy from the Sun is reflected upward. This term is usually more strongly positive than the $(L\downarrow - L\uparrow)$ term is negative. The typical situation on a summer day hence is for Q^* to be positive until late afternoon.

Q^* is inherently tied to temperature changes at the surface. If Q^* is positive at a location (as it is from morning until at least mid-afternoon on most days), there is a surplus of energy and the temperature is likely to rise, unless the extra energy is advected away from that location or is sent vertically via turbulent fluxes. If Q^* is negative (as it is from late afternoon until just after sunrise on most days), then there is a deficit of radiant energy at that location and the temperature falls as a result, unless energy from elsewhere is advected into the location.

We might expect that if we computed Q^* at the surface for many locations all around the world at a given instant in time, they should all average out to zero. Some places are experiencing night whereas others are experiencing day, and some are having the opposite season from others. However, if we calculated surface Q^* for a whole range of locations around the world, we would find a surplus of energy. Likewise, if we calculated Q^* for the air for a large number of

locations around the world, we would observe a deficit. The deficit in the air would be equal in magnitude to the surplus at the surface. If energy transfer occurred by radiation alone, Earth's surface as a whole would warm over time, while the atmosphere above it (for Earth as a whole) would be constantly cooling. Another mechanism must exist to transfer energy from the surface up to the air, to keep the Earth–ocean–atmosphere system in an energetic equilibrium (even though local places on Earth do indeed warm and cool at different times).

Turbulent Fluxes

Convection is the mechanism by which energy is transferred vertically from the surface to the air. This process occurs when more-energized molecules in a heated fluid rise and less-energized molecules in a cooler fluid sink. In the “real” world this flux of energy can take the form of turbulent or convective fluxes introduced earlier in this chapter.

The first convective flux is known as the turbulent (or convective) flux of sensible heat or, more simply, the sensible heat flux (Q_H). This flux is manifested in the atmosphere by the familiar observation that warmer air rises. For Earth as a whole, Q_H transfers only a relatively small percentage of the excess energy from the surface upward because relatively little Earth is covered by land, particularly at tropical latitudes where abundant surface heating occurs.

Nearly all the remainder of the energy is transferred by the turbulent (or convective) flux of latent heat or, more simply, the latent heat flux (Q_E). In Q_E excess radiant energy at the surface is used to evaporate water or to melt or sublime ice (convert it from solid directly to vapor). In the processes of melting, *sublimation*, and *evaporation* this energy absorbed by the water molecules is stored in latent (“hidden”) form. Later, when the evaporated water undergoes *condensation* (changing phase from vapor to liquid form) or when the liquid water freezes or even undergoes *deposition* (changing phase from water vapor directly to ice, bypassing the liquid stage altogether; the opposite of sublimation), the same amount of energy that was required to evaporate, melt, or sublime the water is then released. **FIGURE 5.14** depicts the energy involved in these phase changes.

In the tropical part of Earth, where a surplus of radiant energy exists, water is even more abundant than in the rest of Earth, so Q_E is large. As evaporated water from the tropical oceans is circulated poleward by winds, some of it condenses or deposits. These processes cause the release of latent heat in the cloud-formation process. It is this latent heat (energy) release that can be converted to the *kinetic energy*—energy of motion—that powers winds in storms.

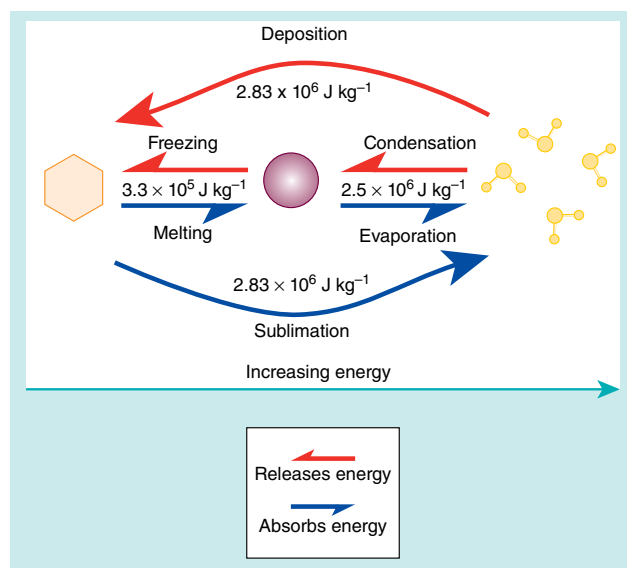


FIGURE 5.14 Schematic representing phase changes of water.

Substrate Heat Flux

A tiny percentage of the excess radiant energy at the surface is also transferred through *conduction*—the transfer of energy through solids from one molecule to another. Conduction occurs in solids due to the close packing of molecules. Because the atmosphere is not a solid, conduction is negligible there. The flux of energy by conduction is known as the **substrate heat flux (Q_G)**.

Even in solids Q_G is inefficient and slow. For example, the transfer of energy downward from the surface on a hot summer day may occur only down to perhaps 1 m from the surface. If you planted a thermometer at a depth of 1 m and could monitor its readings, you probably would not notice a spike in temperature in the afternoon and a temperature minimum in the early morning shown on that thermometer. Of course, the depth at which the diurnal cycle of temperature becomes negligible does vary depending on the mineral composition and moisture content of the soil. Dogs are well aware that conduction is not an efficient process; on a hot summer day they dig holes in the yard because they know the inefficiency of conduction means the ground is much cooler only a few centimeters below the surface. And after they dig a small hole, the new surface warms quickly, which means they must dig a deeper hole!

At a depth of perhaps 15 m (50 ft), the inefficiency of conduction means that even summer and winter temperatures are indistinguishable. By the time the summer insolation penetrates to such depths via Q_G , the heat gradient moves back upward because the subsurface layer is warmer than the air as summer ends. The temperature beneath such an equilibrium

depth remains constant. If you have ever been in a subsurface cave, you know the temperature inside that cave is not dependent on the outside temperature on the day when you visited. Instead, the cave's temperature is always equal to the mean annual temperature at that location.

Despite the fact that conduction is a far smaller component of the global atmospheric energy budget than convection, Q_G can sometimes play an important role locally (particularly at short time scales) in transferring energy from the surface downward (when the surface is being warmed) or from beneath the surface upward (when the surface is colder than the ground beneath it). For example, conduction allows snow to melt relatively quickly after a relatively warm period when ample energy has been stored in the ground. Nevertheless, Q_G is usually small and becomes negligible at relatively shallow depths.

Q_G can be measured relatively easily using **soil heat flux plates**. But because Q_G varies greatly in magnitude over very small distances due to differences in moisture and mineral composition of the soil, measured values should be averaged at several locations in an area for assessing the magnitude of Q_G and its relative importance compared to radiation and convection.

Unlike Q_H and Q_E , by convention Q_G is positive when in the downward direction. All three fluxes can be thought of as positive when directed away from the surface and negative when directed toward the surface. During most of the daytime hours into late afternoon the fluxes are usually positive, and at night they are often negative (**FIGURE 5.15**).

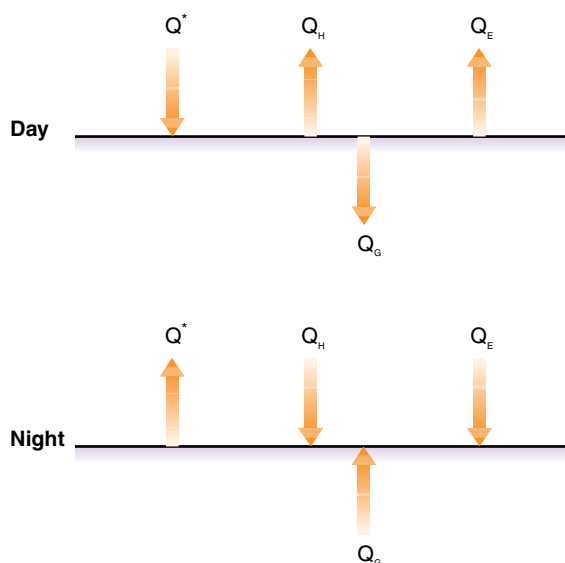


FIGURE 5.15 Typical direction of the turbulent fluxes by day and by night.

Energy Balance

After including the effects of the **energy balance**, the relationship between the radiant flux received at the surface and the convective and conductive fluxes can be expressed as

$$Q^* = Q_H + Q_E + Q_G$$

So we can say that the net radiation received at a point on the surface must be “used” by some combination of sensible heating, latent heating, and heating of the subsurface layer. Earlier we saw that the radiation balance is

$$Q^* = (K\downarrow - K\uparrow) + (L\downarrow - L\uparrow)$$

so we can substitute to produce another form of the energy balance equation:

$$(K\downarrow - K\uparrow) + (L\downarrow - L\uparrow) = Q_H + Q_E + Q_G$$

The equation above states that the sum of the net shortwave and net longwave radiation receipt at the surface must be balanced by the convective loss of energy from the surface upward through Q_H and Q_E and the conductive loss downward through Q_G . On a hot summer afternoon when $K\downarrow$ is high, some combination of a net loss of energy through longwave radiation and convective and/or conductive fluxes must occur to offset this input of energy locally, or the local temperature will increase. Of course, in most cases a high input of insolation cannot be balanced by the radiative, convective, and conductive fluxes, so the temperature does increase. But unlike the radiation balance for Earth's surface as a whole, at any instant in time the total energy balance would theoretically be zero. Some places on Earth gain energy (and, therefore, warming), and others lose energy (and cooling). At longer temporal scales (years to millennia), however, other factors might cause long-term warming or cooling of the entire Earth–ocean–atmosphere system.

Local Flux of Matter: Moisture in the Local Atmosphere

Atmospheric Moisture

The second entity of importance in the near-surface atmosphere is matter, and moisture is the most important type of matter in dictating climate. There are several ways to represent moisture in the atmosphere.

Vapor pressure (e) is the atmospheric pressure exerted by water vapor. This is divided by **saturation vapor pressure (e_s)**—the atmospheric pressure exerted by water vapor when the air is at saturation—to calculate **relative humidity**.

Because e and e_s both have units of pressure—the *Pascal (Pa)* or *millibar (mb)*—relative humidity is simply a ratio. The amount of moisture in the air at saturation depends on temperature. The higher the temperature, the greater the amount of water vapor in the atmosphere when the atmosphere reaches saturation; e_s is a function of temperature. The **Clausius-Clapeyron equation**, one of the most fundamental equations in all of atmospheric thermodynamics, shows that e_s can be considered solely a function of temperature at the range of temperatures and pressures experienced on Earth. Mathematically, the Clausius-Clapeyron equation is

$$e_s = 611 \text{ Pa} \exp \left[\frac{L_v M_v}{R^* \left(\frac{1}{273} - \frac{1}{T} \right)} \right]$$

where L_v is the latent heat of vaporization ($2.5008 \times 10^6 \text{ Joules kg}^{-1}$ at 0°C and changing minimally over the range of Earth temperatures), M_v represents the molecular weight of water vapor ($0.018015 \text{ kg mol}^{-1}$), R^* is the universal gas constant ($8.314 \text{ J mol}^{-1} \text{ K}^{-1}$), and T is in the *Kelvin temperature scale*. It should be noted that over an ice surface L_v is substituted by the latent heat of sublimation (L_s , or $2.8345 \times 10^6 \text{ J kg}^{-1}$ at 0°C).

If we plot e_s as a function of T using the Clausius-Clapeyron equation, the relationship between these variables is an exponential curve, as shown in **FIGURE 5.16**. A look at the e_s curve confirms that as the temperature

falls (during the course of a “normal” evening, for example), e_s decreases. But a decrease in e_s causes relative humidity to increase, even if the actual amount of vapor in the air (e) remains constant.

To see why, suppose the temperature is 20°C (68°F) and the air has 12 mb of water vapor in it. Figure 5.16 shows that at that temperature the air would be saturated if it had 24 mb of water vapor in it. The relative humidity in this case would be 50%. If the temperature began to fall until e equals e_s (as shown by the line from A to B in Figure 5.16), saturation will be reached, and the relative humidity will be 100%. The temperature at which saturation occurs at a given place and time is known as the **dewpoint temperature (T_d)**. This is shown by the temperature at B in Figure 5.16. To be more precise, whenever T_d is below 0°C it is termed the **frostpoint temperature**. In Figure 5.16 it is evident that if $e = 12 \text{ mb}$ (shown at A), then the air would have to cool from 20°C to about 9°C (48°F) before it would become saturated. T_d in this case would therefore be 9°C .

If T_d is reached, condensation or deposition begins, releasing latent energy during the phase change. The same amount of solar radiant energy that was required to evaporate a certain volume of water (540 calories per gram, at 100°C) would be released when that volume of water then condensed. The amount of energy released during deposition would equal the sum of the energy released when the same volume of water condensed (vapor to liquid) and when it froze (liquid to solid), plus the amount of energy released in cooling the liquid water from the temperature at which it became a liquid to the freezing point.

The energy transformation described above is one manifestation of the **first law of thermodynamics**—an important principle stating that energy can never be simply created or destroyed in nature; it can only change from one form to another. This concept pervades all the natural sciences. Insolation is converted from a radiant form of energy to a latent form during the evaporation process, and then this energy is released when the vapor returns to a liquid or solid state. This released energy cannot simply vanish; it must be converted to another form. It is this released energy that appears as kinetic energy. Ultimately, then, the energy to drive winds in a storm comes from the Sun.

As we have seen, although T_d is expressed in units of temperature, it is actually a measure of humidity. The closer the dewpoint temperature is to the air temperature, the more humid the air, because in such a case the temperature would have to fall only slightly for it to become saturated. During the course of a day T_d changes little, unless the actual amount of vapor in the air (e) changes. One scenario that could cause e to change is

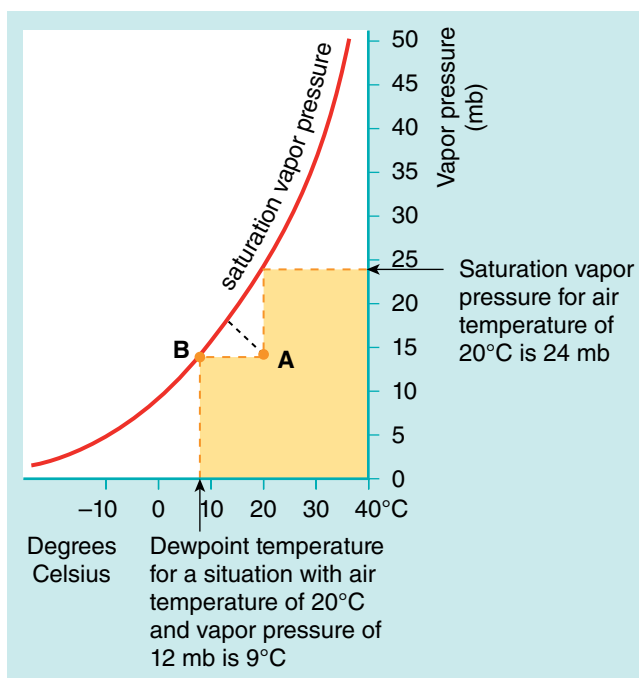


FIGURE 5.16 Saturation vapor pressure as a function of temperature.

a shift in wind direction that introduces advection of moisture from an oceanic surface into an area. A small increase in T_d would also occur in the morning if there is dew or frost on the ground. In that case when the Sun rises, its radiation evaporates the dew or melts or sublimates the frost.

In actuality, changes in air temperature do change the dewpoint temperature a bit—about one-sixth of a Celsius degree per Celsius degree of temperature change—even if the amount of water vapor in the air (e) remains constant. But this change is slight compared with the change in relative humidity with temperature. Dewpoint temperature is actually a more useful and meaningful measure of atmospheric humidity than relative humidity, which only states how close air is to saturation regardless of vapor content.

Another quantity that may be used to represent the amount of vapor in the air is **absolute humidity**—the mass of water vapor per cubic meter (a volume) of air. Because its units are actually those of *density*, absolute humidity is sometimes known as vapor density. This quantity is seldom used in climatological work because a cubic meter of air may contain a drastically different amount of mass at two different vertical heights in the atmosphere. Indeed, as you go up a mountain there is bound to be less water vapor per cubic meter of air because there is less of every type of molecule with height. It is, therefore, usually impractical to use absolute humidity to compare the moisture content of air from one place to another at a different elevation.

Another means of expressing moisture in the atmosphere is by **specific humidity** (usually abbreviated as q)—the ratio of the mass of water vapor to the mass of the air. Because there are no units for q , we say that it is a **dimensionless quantity**—a ratio or constant that has no units associated with it. In this case the units are kilograms per kilogram, which cancel out. Specific humidity is an effective variable for comparing the moisture characteristics across geographic distances because it is not temperature dependent (as are relative humidity and, to a lesser extent, dewpoint temperature) and it does not inherently change because of elevation (as does absolute humidity).

Because specific humidity is so useful, the important question is, “How is it measured?” The answer is that it is not measured directly for most applications. Instead, it can be computed by a relationship derived from atmospheric thermo-dynamics:

$$q = \frac{e\varepsilon}{p}$$

where p is atmospheric pressure and ε is the ratio of the molecular weight of water vapor to the molecular weight

of dry air—a dimensionless constant of 0.622. But how can we measure e ? Because relative humidity is the ratio of e to e_s , and e_s is a known function of temperature via the Clausius-Clapeyron equation, measurement of temperature (with a thermometer) and relative humidity (with a **hygrometer**) can allow us to compute e , which can then be used to compute q , provided that atmospheric pressure is known.

Moisture in the Surface Boundary Layer

Because of the practicality of specific humidity, it is often the variable used to represent moisture in the SBL. Highly precise and accurate thermoelectric sensors can derive q from surrogate variables. As we will see, this is a convenient means of estimating the flux of water from the surface to the air through the combined processes of evaporation and transpiration.

Less familiar than evaporation, *transpiration* is the process by which vegetation loses water from its leaf surface that had moved from the soil through its roots and stem. The loss of water occurs through the **stomates** (also known as stomata)—tiny pores in the leaf tissue. An analogous process in humans is perspiration, where water stored in the biomass of humans is lost through pores in the epidermis.

Unlike humans, vegetation can regulate the loss of water through transpiration. During drought and at other times when water is scarce, reductions in this rate reduce water losses. This happens because the lack of soil moisture decreases the water circulated to the **guard cells**—leaf cells that are adjacent to the stomates. When the guard cells receive water, they expand and widen the stomatal openings. The absence of water in guard cells causes them to shrink and decrease the size of the stomatal openings, thereby allowing less water to escape to the air. This natural regulation process allows vegetation to pump excess water to the air during wet times and to conserve water during dry periods, providing them a greater possibility for survival during periods of environmental stress.

The transpiration process is driven by the Sun, in the same way that the Sun provides radiant energy to drive the evaporation process. Transpiration rates are generally greatest on a dry, sunny day when abundant water is available in the soil. This scenario creates a strong gradient of water from the surface to the air and a tendency for the vapor to be moved upward toward drier areas. At night, transpiration decreases to an insignificant rate.

Climatologists are usually not concerned with distinguishing the amount of water that is lost from the surface to the air via the evaporation and transpiration processes individually. Instead, they usually lump the quantities of atmospheric moisture attributable to evaporation and transpiration together to form a variable

known as **evapotranspiration (ET)**. Because of its significance in hydrological, biological, agricultural, and economic applications, ET is an important variable in many environmental monitoring applications. Unfortunately, the measurement of ET is often substandard, and high-quality data usually are available only through a sparse network of sites. As a result, simpler but less accurate means of estimating ET are often used and reported in historical data sets as ET.

Measuring Evapotranspiration

The *National Weather Service* determines ET through the use of a **Class A Evaporation Pan**, an instrument that consists of a metal pan 1.2 m (4 ft) in diameter that sits on a short wooden platform and is exposed to the elements (**FIGURE 5.17**). Inside the pan is a heavy, cylindrical metal tube reaching the bottom of the pan, and inside this cylinder is an analog gauge with the appearance of a fishhook. Water is placed in the pan up to about 8 cm (3 in) from the top, and the analog “fishhook” gauge is positioned vertically with a caliper so that it barely breaks the plane of the water. The next day, after some water has evaporated, the fishhook gauge is repositioned, and the vertical displacement distance read on the caliper represents the centimeters or inches of water that have evaporated since the previous reading. Of course, if precipitation has fallen since the last measurement period, the evaporation reading must take into account the amount of precipitation (measured in an adjacent gauge) that was added to the pan.

In the “real world,” water is not always as readily available in the environment as it is in the evaporation pan. The use of an evaporation pan, therefore, provides an estimate of **potential evapotranspiration (PE)**—the maximum amount of ET that would occur if water were not a limiting factor. If this value is less than the amount of precipitation that has fallen over that interval, water is abundant.



FIGURE 5.17 A Class A Evaporation Pan.

Courtesy of NWS/NOAA.

However, the pan even overestimates the “true” PE, for three important reasons: (1) the metal pan is heated much more than a natural area is heated, allowing more energy to be available to evaporate water than is present in a natural environment; (2) cohesion between liquid water drops and soil particles in the natural environment slows the evaporation rate as compared with the higher evaporation rates inherent in the pan; and (3) PE is overestimated in the pan because the presence of wind moving across the pan provides a continual source of relatively dry air into which water readily evaporates. By comparison, if a large field in the real world were saturated with water, some water would evaporate and then move over another part of the field that already was saturated with evaporated water. The new area, therefore, would not evaporate any new water from that part of the field. As a result of these factors, a **pan adjustment coefficient** is typically used to estimate PE from pan evaporation. It varies spatially but averages about 0.7, suggesting that PE occurs at a rate of about 70% of the evaporation rate in the pan.

Another means of determining ET rates is by means of a **lysimeter**, an instrument installed beneath the surface that weighs the soil and vegetation on top of it (**FIGURE 5.18**). By knowing the mass of dry soil and vegetation along with the density of water



FIGURE 5.18 Installation of a lysimeter at St. Joseph Research Station, St. Joseph, Louisiana.

Courtesy of Ernest Clawson.

(1000 kg m^{-3}), the water content of the volume can be determined. Although highly accurate, lysimeters are far more expensive to install and maintain than evaporation pans, and the network of lysimetric data is particularly sparse.

Far more sophisticated methods exist for measuring ET, but because these require precise and expensive equipment they are usually done only experimentally and not on a routine, ongoing basis. An example is **eddy covariance**, where theoretical equations are derived based on the measurement of covariance of fluctuations between vertical wind velocity (for vertical fluxes) and changes in temperature, specific humidity, and horizontal wind speed. These equations allow the estimation of turbulent transfer of energy, moisture, and momentum, respectively. For example, measurement of Q_E , the energy equivalent of evaporation, by eddy covariance or by other means can be used to derive ET. This is based on the premise that the ET rate (in meters of precipitation equivalent per second, which can then be converted to mm hr^{-1}) is a function of Q_E as follows:

$$ET = \frac{Q_E}{L_v \rho_l}$$

where L_v is the latent heat of vaporization ($2.5008 \times 10^6 \text{ J kg}^{-1}$ at 0°C) and ρ_l represents the density of water (1000 kg m^{-3}).

Eddy covariance systems have been deployed in recent years for varying surface types. Unfortunately, despite decreasing costs of equipment in recent years, eddy covariance equipment remains expensive and is not readily available at many locations.

► Atmospheric Statics, the Hydrostatic Equation, and Stability

The ease with which moisture (along with energy, momentum, and other forms of matter) can move vertically in the air at a given time and place is governed by **stability**—local atmospheric conditions that describe the likelihood of a local mass or “parcel” of air to rise or sink spontaneously. The vertical distribution of absorbed energy in the local near-surface air is extremely influential in determining the stability conditions. If the air parcel has a tendency to rise, the vertically directed force of **buoyancy** pulls it upward in opposition to the downward-directed gravitational force. In other situations the downward-directed gravitational force exceeds the upward-directed buoyancy force and the

parcel of air sinks. Stability conditions impact weather and climate greatly, because upward motion is important in enhancing convection and generating clouds and precipitation.

Statics and the Hydrostatic Equation

The **hydrostatic equation** expresses the relationship between the upward-directed buoyancy force and the downward-directed acceleration caused by gravity (9.8 m s^{-2}). It relates the pressure change (Δp) in a static atmosphere to height differences (Δh) over which those pressure changes are observed, as follows:

$$g = -\frac{1}{\rho} \frac{\Delta p}{\Delta h}$$

where ρ is atmospheric density. The hydrostatic equation shows that the mean density of a layer of the atmosphere can be calculated if we know the pressure at two known heights—the top and the bottom of that layer. Because the gravitational acceleration is essentially constant near Earth’s surface, it is apparent from the equation above that as density increases, the difference in pressure with height must also increase. Pressure decreases quickly with height near the ground (where density is highest), but higher up in the atmosphere (where density is less) pressure does not decrease so quickly with height. We have already seen that the *equation of state* shows that cold air is denser than warm air at a given pressure. So now the hydrostatic equation can be used to verify a simple feature of atmospheric motion: Cold (dense) air has a tendency to sink and create a large vertical difference in pressure (high pressure at the bottom and much lower pressure above—the location from which the air left).

The hydrostatic equation thus describes vertical motion in the atmosphere, and it is this vertical motion that is associated with stability. A parcel of air cools as it rises. It is tempting to believe that if it cools it must sink, but this is not necessarily the case. Even as it cools, if it remains warmer than the surrounding air, the parcel continues to rise—positive buoyancy. If its ascent causes the parcel to cool to the dewpoint temperature, the condensation process would begin to create a cloud, which may produce some form of precipitation. In humid locations there is often enough moisture in the air that the parcel does not have to rise far to cool enough to become saturated, so the cloud-formation process happens relatively easily. For this reason the cloud base tends to be relatively near the surface in humid areas. In arid locations a parcel has to rise to great heights before it cools to the dewpoint temperature and forms clouds. This leads to

high cloud bases, thinner clouds, and less likelihood of precipitation.

Atmospheric Stability

In a *stable atmosphere* if a parcel of air is forced to rise for any reason, it will sink once the lifting force is removed. The buoyancy force therefore cannot overcome the gravitational force in stable conditions. If the atmosphere is stable at a given place and time, it is difficult for energy and moisture to move vertically from the surface, and little of the moist air can be cooled to the dewpoint temperature, making cloud formation difficult or impossible. Stable conditions are usually associated with fair weather. The downward motion associated with stable conditions allows momentum to be transferred relatively easily from aloft (where friction is relatively low) toward the near-surface atmosphere (where friction is higher). The lack of vertical motion under stable conditions can also have less pleasant effects. For example, pollutants are difficult to disperse from surface point sources under stable conditions.

By contrast, in an *unstable atmosphere* the parcel of air continues to rise even after the lifting force is removed. The buoyancy force exceeds the gravitational force under unstable conditions. Such conditions enhance the upward movement of energy and moisture from the surface and often allow the vertical growth of thunderstorm clouds and the dispersion of local pollutants.

Stability conditions involve a continuum rather than a simple stable/unstable dichotomy. At certain places and times the atmosphere may be extremely unstable, whereas in other situations it may be slightly unstable, slightly stable, or extremely stable. A hypothetical case is the **neutral atmosphere**—an atmosphere where the parcel neither rises nor sinks once the lifting force is removed. It maintains its position no matter where it is placed in the atmosphere because its internal temperature is always equal to the temperature of the ambient (surrounding) atmosphere.

So how do we know the degree of stability (or instability) of a local atmosphere? To understand what determines the stability conditions, it is important to understand the concept of **lapse rate**—the rate at which temperature changes (decreases usually, in the troposphere) with height. By convention, a positive lapse rate is said to occur when the temperature decreases with increasing height. A negative lapse rate is known as a temperature inversion because the temperature profile is “inverted” from what we normally expect in the troposphere; that is to say, in an inversion temperature increases as height increases.

If a parcel of air rises (or sinks) quickly enough that it does not have enough time to exchange any energy

with the surrounding air, it is said to have **adiabatic motion**, which implies that the cooling of the parcel with increasing elevation is caused solely from within the parcel itself. If a parcel rises adiabatically, it cools at a totally predictable lapse rate, because it can expand under the decreasing pressure exerted by the (decreasing) column of air above it. It cools as it expands because one implication of the first law of thermodynamics is that energy is used in some combination of either maintaining the parcel’s temperature or doing work (i.e., expanding the parcel’s area). Because the total amount of energy in the parcel remains constant in an adiabatic process (by definition) and the amount of pressure exerted on the parcel from above decreases as it rises, the use of its energy to expand becomes preferable at the expense of maintaining the temperature of the parcel.

On the other hand, as the parcel sinks adiabatically, it must warm at a totally predictable lapse rate because it must compress under the increasing column of air exerting increasing pressure on it from above. Work is done on the parcel from above in this case, and the energy is used to increase the parcel’s temperature. The rate of warming for sinking motion is exactly the same as the rate of cooling for rising motion, in fulfillment of the first law of thermodynamics.

This rate of cooling with ascent and warming with descent is termed the **unsaturated adiabatic lapse rate (UALR)**. The UALR—also represented by Γ_u and pronounced “gamma sub u”—is approximately 9.8 °C/km (or about 1 °C/100 m) and is the rate at which the parcel of air cools with ascent (or warms with descent) at every location on Earth, every day of the year, as long as it remains unsaturated.

If at any point on the parcel’s ascent it becomes saturated, the UALR is no longer in effect, even if the motion remains adiabatic. The reason for this difference is that at saturation, latent energy is released to other air molecules inside the parcel in the condensation, freezing, or deposition process. This release of latent energy prevents the parcel from cooling as rapidly as it could cool under unsaturated conditions.

As the parcel continues to rise, less water vapor exists in it at the decreasing temperatures and greater distance from the surface. Consequently, successively less latent energy can be released in the condensation, freezing, or deposition processes, and the parcel can cool more rapidly with its continued ascent than initially upon saturation. Eventually, it cools at nearly the same rate as if it were not saturated. But the net effect of adiabatically rising motion will still always be cooling because the effect of reduction of pressure from above will more than compensate for the effect of the latent heat release. The rate of cooling with ascent, however, will never be as great as in unsaturated conditions. With sinking motion,

adiabatic warming will always occur at Γ_u because even a minuscule increase in pressure from above will warm the parcel to the extent that it is no longer saturated (because e_s always increases with temperature).

From this discussion, then, it is apparent that unlike the UALR, the **saturated adiabatic lapse rate (Γ_s)** is not a constant value. Instead, it varies according to the amount of moisture in the air to be condensed, frozen, or deposited. In the tropics the high temperatures allow abundant moisture to exist in the air (i.e., high e_s). Under conditions of saturation (such as over the tropical oceans), condensation, freezing, and deposition cause abundant latent energy release, hindering the parcel's cooling on its initial ascent. On the other hand, over polar regions in winter, where e_s is very low under such frigid temperatures, little moisture exists to change phase and release latent energy. The SALR in such conditions is only slightly less than the UALR.

Is the adiabatic assumption valid? The answer is that it is never completely valid, but sometimes it is more valid than at other times. Regardless, we have to make the adiabatic assumption because there is no way to monitor the temperature change of every parcel of air that rises or sinks at all times across the entire Earth. So this is a necessary assumption, but one that can sometimes be invalid. Weather forecasts are likely to fail when the assumption is not reasonably valid.

The third lapse rate has already been introduced: the ELR (γ)—the temperature profile of the static (ambient) atmosphere surrounding an adiabatically moving parcel of air. The ELR varies daily and across space (FIGURE 5.19). It may be negative (in the case of a temperature inversion), strongly positive (when temperature decreases rapidly with increasing height), or slightly positive (when temperature only decreases slowly with height). On a global, annual average basis γ is about $6.5^\circ\text{C}/\text{km}$ ($3.5^\circ\text{F}/1000\text{ ft}$). So if we neglect

all other factors, we could expect that a location at 1.5 km (5000 ft) in elevation would, on average, be approximately 9.7°C (17.5°F) cooler than it would be if it were at sea level.

The ELR can be measured by sending up a **radiosonde**—an instrument package that ascends with weather balloons. At 74 different sites in the contiguous United States, the National Weather Service launches weather balloons synchronously at 0000 UTC and 1200 UTC (i.e., at midnight and noon, respectively, in Greenwich, England). These radiosondes electronically report the temperature, pressure, and dewpoint temperature from many different heights to ground-based computers. The data are then sent to a central computer near Washington, DC where they are used in weather analysis and prediction.

So three different lapse rates are important for assessing atmospheric stability. If a parcel of air is moving adiabatically, its tendency to rise or sink is determined simply by comparing its temperature (which is governed by Γ_u or Γ_s , as the case may be) with the temperature of its surrounding environment (represented by γ). If the parcel of air is warmer than its surrounding environment at a given height, it tends to rise (as in the unstable atmosphere shown in FIGURE 5.20 and FIGURE 5.21).

If the air parcel is colder than its surrounding environment at any height, it sinks (as in the stable atmosphere shown in Figures 5.20 and 5.21). But if an air parcel is in a situation in which it encounters colder (denser) air, it rises even if it is statically stable.

It is not uncommon at all for γ to fall between Γ_u and Γ_s . When $\Gamma_s < \gamma < \Gamma_u$ the air parcel in an unsaturated atmosphere is cooler than its surrounding environment and the atmosphere is stable. When $\Gamma_s < \gamma < \Gamma_u$ and the air is saturated, the air parcel is warmer than its surrounding environment at a given height and the atmosphere is unstable. By increasing the amount of moisture in the air to saturation, upward motion is encouraged and the atmosphere is destabilized. This **conditional instability**—with the atmosphere's stability “condition” determined by whether or not the air is saturated—is important because it facilitates the precipitation-formation process because saturated air can rise more easily than unsaturated air.

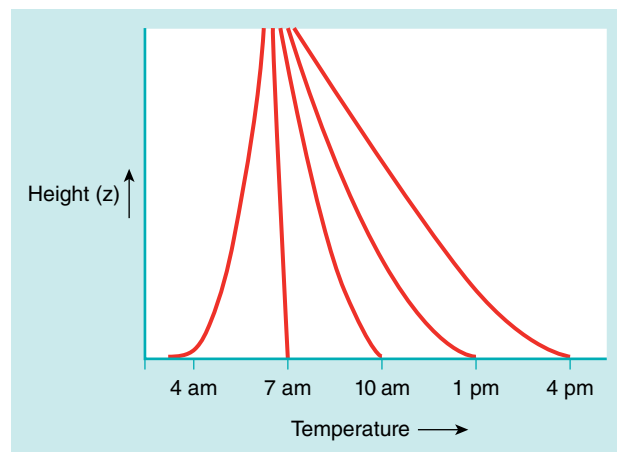


FIGURE 5.19 Typical variation of the ELR throughout the course of a day.

Assessing Stability in the Local Atmosphere

Thermodynamic Diagrams

The stability conditions of a local atmosphere are identified easily using a **thermodynamic diagram**—a tool that can be used by atmospheric scientists to make a quick determination about whether or not air at a given place

and time is likely to rise spontaneously. **FIGURE 5.22** shows the most common type of thermodynamic diagram used in the United States—the **Skew T-Log P diagram**. The medium zigzagging purple solid line on the right represents the temperature profile of the static atmosphere from the surface upward to over 16 km (9.9 mi) high—the ELR.

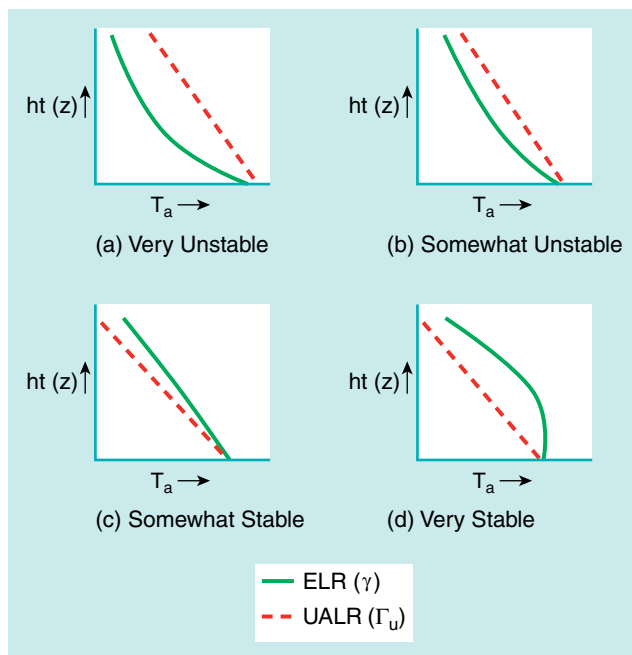


FIGURE 5.20 Unsaturated adiabatic lapse rates under various atmospheric conditions: (a) very unstable, (b) somewhat unstable, (c) somewhat stable, and (d) very stable.

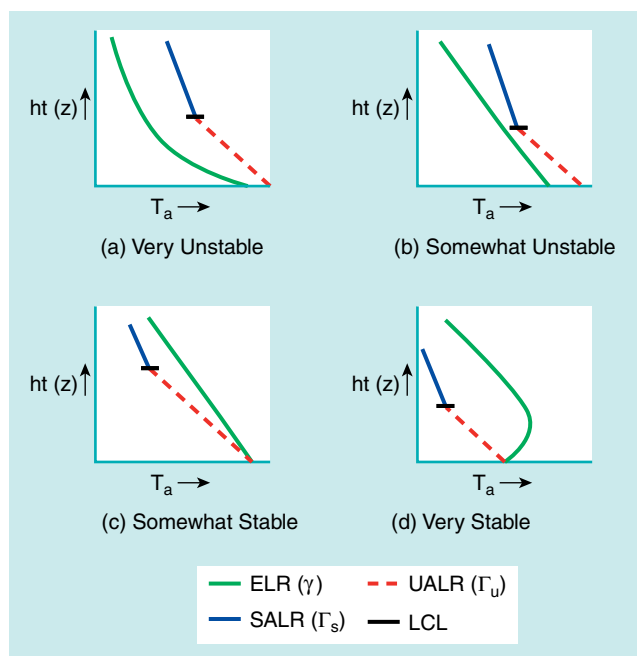


FIGURE 5.21 Saturated adiabatic lapse rates under various atmospheric conditions: (a) very unstable, (b) somewhat unstable, (c) somewhat stable, and (d) very stable.

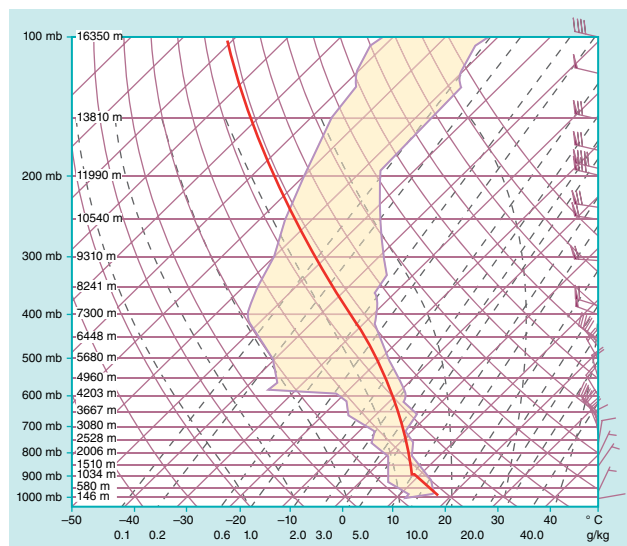


FIGURE 5.22 Thermodynamic diagram for Washington, DC at 8:00 am local time, 31 May 2005.

Data from: National Weather Service/NOAA.

The lines representing the temperature are slanted, or “skewed,” upward from left to right. The medium zigzagging purple solid line on the left side of the diagram represents the dewpoint temperature at any height. Pressure is shown by the horizontal lines, which increase in spacing vertically. The “log P” reminds us that only the logarithm of pressure increases at equal intervals on the graph.

Figure 5.22 shows that at a height of 7300 m, the temperature of the static atmosphere is approximately -35°C . In atmospheric layers where the two medium solid lines are near each other (such as in the lower troposphere in Figure 5.22), the atmosphere is more moist, and in layers where the two medium solid lines are far apart, the air is drier. The thick orange solid line in Figure 5.22 represents the **adiabat**—the temperature profile of an adiabatically moving parcel of air. Notice how the air parcel’s temperature abruptly shifts at an elevation of about 1050 m in Figure 5.22. This represents the **lifting condensation level**—the level at which the air becomes saturated and the air parcel no longer cools at the UALR but begins cooling instead at the SALR.

Now look at the example shown in **FIGURE 5.23**. In this case it is obvious that the air is far more humid than in the previous example, because the ELR and dewpoint plots are near each other. We can see from comparing the position of the adiabat with that of the ELR that the adiabatically moving air parcel is warmer than its surrounding environment in the lower to middle troposphere. The vertical distance for which the adiabatically moving air parcel trajectory is warmer than γ represents the depth of the unstable layer. The area between the parcel’s trajectory and temperature profile is approximately proportional to the intensity

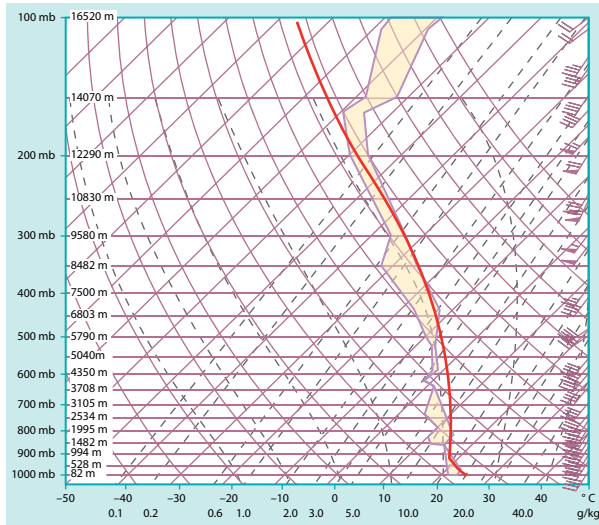


FIGURE 5.23 Thermodynamic diagram for Tallahassee, Florida, at 8:00 am local time on 1 June 2005.

Data from: National Weather Service/NOAA.

of the instability. The same rules hold in cases of stable atmospheres.

Potential Temperature

From the discussion above, it follows that in an unsaturated atmosphere, stability is related to the vertical gradient of environmental temperature across some height z as follows: For a stable atmosphere:

$$\frac{\Delta T}{\Delta z} > -9.8 \text{ C}^\circ/\text{km}$$

For an unstable atmosphere:

$$\frac{\Delta T}{\Delta z} < -9.8 \text{ C}^\circ/\text{km}$$

For a neutral atmosphere:

$$\frac{\Delta T}{\Delta z} = -9.8 \text{ C}^\circ/\text{km}$$

where Δ represents the difference in the value of the variable at two measurement heights. Notice that the negative signs are necessary because temperature would decrease with increasing height at the UALR.

It is convenient to define a new variable at this point to simplify the calculations necessary to determine local stability using the equations above. By definition, **potential temperature (θ)** is the temperature that a parcel of air would have if moved dry adiabatically from its height (z) in the atmosphere to the 1000-mb level. For example, we know that if the parcel were at the 850-mb

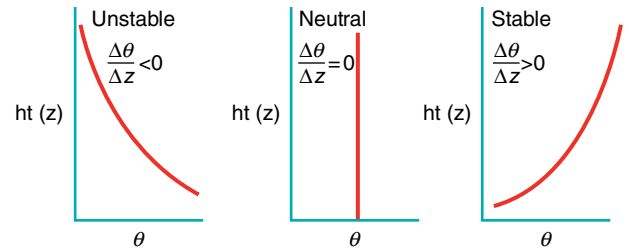


FIGURE 5.24 A typical gradient of potential temperature with height under unstable, neutral, and stable conditions.

level, it would have to warm at Γ_u from the height of the 850-mb level down to the height of the 1000-mb level. Mathematically, we can say that

$$\theta = T + \Gamma_u (z - z_{1000 \text{ mb}})$$

Using differential calculus we could differentiate the equation above and show that a stable atmosphere (or layer of the atmosphere) is one in which θ increases with height. Likewise, unstable conditions are characterized by θ that decreases with height, and a neutral atmosphere is one in which θ is constant with height (**FIGURE 5.24**).

In analyses in the SBL, θ is often replaced by T because the difference between the gradient of temperature with height and the gradient of θ with height is so slight in near-surface, local-scale applications. Recall that because $\Gamma_u = 9.8 \text{ C}^\circ/\text{km}$, this only amounts to approximately $0.01 \text{ C}^\circ/\text{m}$. You can see from the previous equation that the difference between θ and T is negligible at such scales. But for synoptic- and global-scale analysis, the difference between θ and T is usually significant.

The concept of potential temperature can also be explained graphically (**FIGURE 5.25**). In the left side of the figure, a hypothetical air parcel (dashed line representing γ) that begins at the surface (near 1000 mb of pressure) with a temperature of 10°C cools with height to a temperature of about 6°C at height A, to about 5°C at height B (of 0.5 km), to about 4°C at height C, and then warms in a temperature inversion from height C to height D. For reference, Γ_u is also shown in the left graph of Figure 5.25, with the solid line. At any point in the air parcel's temperature/height graph, the air parcel's potential temperature (θ) could be determined by following a line paralleling Γ_u from that point in the trajectory to the 1000-mb level—which is near the surface if near sea level. The temperature at the surface shown by that parallel line is θ . For example, on the left side of Figure 5.25, the potential temperature would be about 7.5°C at A (dotted black line in Figure 5.25), 10°C at B, about 12°C at C, and about 15°C at D. The right side of Figure 5.25 plots θ as a function of height.

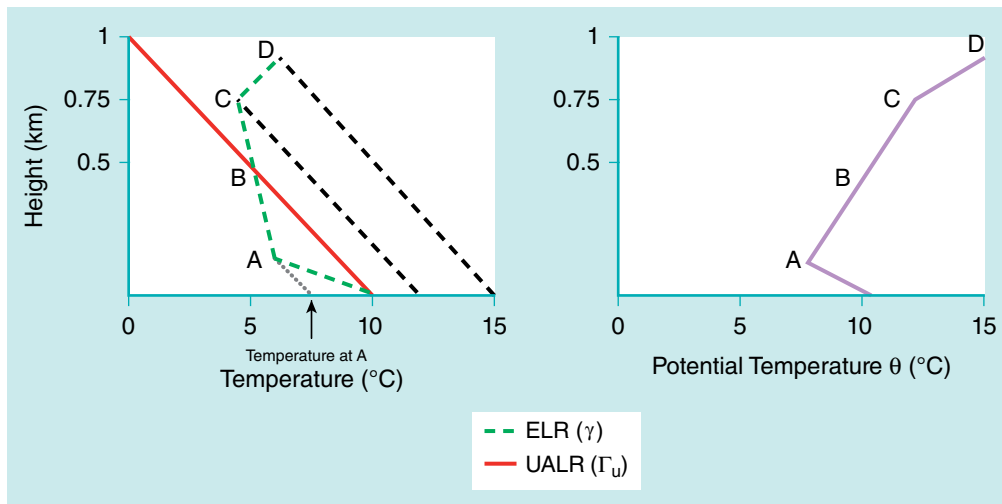


FIGURE 5.25 Relationship between temperature profile and potential temperature profile, for a hypothetical air parcel and environmental lapse rate.

Any place where this plot slants upward to the left (i.e., θ decreases with height, as from the surface to A in the example shown) represents an unstable atmosphere. We already knew that the atmosphere was unstable in this level, because in the left side of the figure the dashed line (representing γ) is to the left of the solid line (representing Γ_u). But in places where the right figure slopes upward to the right (i.e., θ increases with height), the atmosphere is stable.

► Momentum Flux

In addition to energy, matter (particularly water vapor), and stability, another important feature of the local atmosphere is momentum. For example, when wind speed is much greater at 2 m above the surface than at 0.5 m above the surface, momentum transport is enhanced because the extra momentum associated with the faster winds must be transported downward to satisfy Fick's law. You experience this momentum flux whenever you feel a gust of wind. Whenever winds increase with height, horizontal momentum is transferred downward to locations where less momentum is present. Natural systems always work to eliminate gradients of natural entities, such as pressure, moisture, and momentum. The gust that you feel in a thunderstorm is probably the result of efficient momentum exchange under very unstable conditions.

As we noted at the beginning of this chapter, unlike the gradient of energy and matter (i.e., water vapor), the momentum flux (usually represented by τ) is usually downward rather than upward, because wind

speed (and, therefore, momentum) usually increases with height in the troposphere as friction decreases. As was the case for energy and moisture, the sharpest vertical gradient of momentum is found in the SBL, but in the SBL this flux is constant with height at any given instant. Unlike the effect of friction in the free atmosphere, the vertical difference in momentum is important for any two heights in the SBL separated even by short vertical distances.

► Putting It All Together: Thermal and Mechanical Turbulence and the Richardson Number

As introduced earlier, both thermal turbulence and mechanical turbulence can produce rising motion in a local atmosphere. Upward motion associated with thermal turbulence occurs when the atmosphere is unstable, which occurs when θ decreases with height ($\Delta\theta/\Delta z < 0$). You may have noticed a bird take off from a locally warm spot, such as a bare rock, because the hot air at the surface of the bare rock provides sufficient thermal turbulence to aid in lift for takeoff. Thermal turbulence is sometimes referred to as **free convection** because vertical motion results spontaneously from differences in energy content between an adiabatically moving air parcel and its surrounding environment.

On the other hand, mechanical turbulence occurs independently of stability conditions. Rather, it

is **vertical wind shear**—the change of wind speed with height ($\Delta u/\Delta z$)—that produces the momentum gradient associated with mechanical turbulence. Mechanical turbulence is sometimes referred to as **forced convection** because the vertical motion results from dynamic rather than thermodynamic causes. Even when the atmosphere is stable, mechanical turbulence can cause uplift through forced convection.

The **gradient Richardson number (Ri)** provides a convenient index for describing the relative importance of thermal and mechanical turbulence in the local near-surface atmosphere. It is also useful for assessing local stability conditions. Mathematically, in a vertical layer of the atmosphere,

$$Ri = \frac{g}{\bar{\theta}} \frac{(\Delta \bar{\theta}/\Delta z)}{(\Delta \bar{u}/\Delta z)^2}$$

where g is the gravitational acceleration (9.8 m s^{-2}) and $[\bar{\theta}]$ represents the mean potential temperature in the layer.

Notice several features of the preceding equation. First, the mechanical turbulence term (in the denominator) is squared, so it cannot be negative (though even before squaring the term it would rarely be negative because we usually expect wind speed to increase with height). The only term that can be negative is the thermal turbulence term (in the numerator). It follows that under unstable local conditions (when, by definition, $\Delta \bar{\theta}/\Delta z$ is negative), Ri must be negative. As the atmosphere becomes more unstable, $\Delta \bar{\theta}/\Delta z$ becomes more negative and Ri approaches $-\infty$. By contrast, in a stable local atmosphere (when, by definition, $\Delta \bar{\theta}/\Delta z$ is positive), Ri must be positive. As the atmosphere becomes more stable, $\Delta \bar{\theta}/\Delta z$ becomes more positive and Ri approaches ∞ . Looking at the equation another way, we can say that at a small vertical wind shear $\Delta \bar{u}/\Delta z$, $|Ri|$ is large, and the atmosphere tends to be strongly stable or strongly unstable. In its most extreme case, at $\Delta \bar{u}/\Delta z = 0$ (as when there is no wind or no vertical gradient of wind), $|Ri|$ approaches $-\infty$.

In nonneutral conditions both thermal and mechanical turbulence are present unless the winds are calm or constant with height. In an unstable local atmosphere, vertical motion resulting from mechanical turbulence is enhanced by the thermal profile of the atmosphere. In stable conditions the thermal structure dampens vertical motion generated by mechanical turbulence.

The case of a neutral atmosphere is both interesting and important. Under neutral conditions $\Delta \bar{\theta}/\Delta z$ is zero by definition. In other words, there is no thermally induced turbulence, and Ri must be zero. So for a neutral atmosphere any turbulence must be mechanical in origin, and the source of energy for all turbulence is the kinetic energy of the wind from the free atmosphere. Stated

another way, regardless of the sign of Ri , for a given $\Delta \bar{\theta}/\Delta z$, $|Ri|$ decreases as wind shear (i.e., mechanical turbulence) increases. Neutral conditions are best met under cloudy skies and strong winds in the lowest 1 to 2 m of the atmosphere.

Much theory in boundary layer climatology rests on the assumption that mechanical turbulence dominates thermal turbulence (i.e., that near-neutral conditions exist). For example, if the wind speed at only one height is known, then it is much easier and more accurate to estimate the wind speed at any other height in the SBL under neutral rather than nonneutral conditions. This **logarithmic wind profile** is an important manipulation because climatological data sources usually measure wind at only one height in the atmosphere. **FIGURE 5.26** shows the plot of wind speed versus the natural logarithm of height under varying stability conditions. Notice that, theoretically, wind speed approaches zero at some height z_0 —the **roughness length**—which is approximately 10% of the height of the dominant features on the ground (such as blades of grass, trees in a forest, or houses). In neutral conditions, thus a straight line can be drawn on semilogarithmic graph paper to connect the points represented by measured wind speed at one known height (u_z) and z_0 for a given land cover (where wind speed is zero). This line allows us to estimate the wind speed at any known height. The slope of this line varies; it is inversely related to τ .

Under stable or unstable conditions, measurement of wind speed at one height alone is not as useful for estimating wind speeds at other heights, because, as is shown in Figure 5.26, the profile is not linear under such conditions. The validity of making an assumption of neutral stability should always be checked.

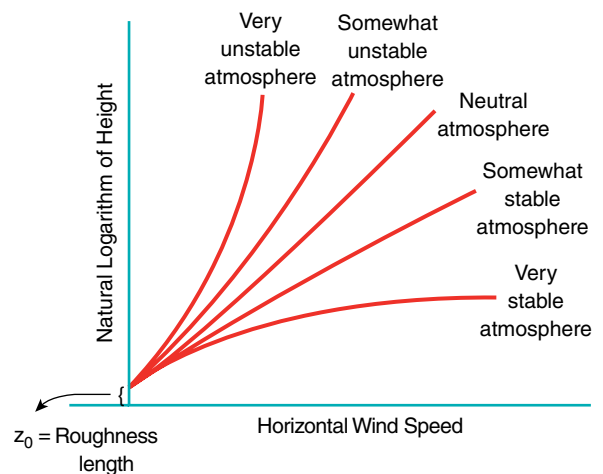


FIGURE 5.26 The logarithmic wind profile, and variations of wind profile with stability.

Modified from: Oke, T. R., *Boundary Layer Climates*, 2nd ed. New York: Routledge, 1987.

► Summary

The lower troposphere is a very complicated as well as important part of the atmosphere because it lies closest to people and Earth's surface. The laminar layer occupies the lowest few millimeters of the atmosphere, and the roughness layer, where the most vigorous exchanges of energy, matter, and momentum occur through mechanical and thermal turbulence, lies above it. Collectively, these two layers are termed the SBL. In the SBL turbulent fluxes of sensible heat (which generally transport energy upward in the local atmosphere), latent heat (which usually transports moisture upward), and shearing stress (which usually transports momentum downward) are considered to be constant. Above the SBL lies the transition layer, where the influence of friction is present but decreasing with height, and above that layer is the free atmosphere, where friction can be considered to be negligible.

Calculations of local energy transport begin with understanding the position of the Sun in the sky at a location. This depends on the time of day and the time of year. A Sun path diagram can be used to map the Sun for a given latitude and solar declination according to its zenith angle and azimuth angle, once the local apparent time is determined based on the distance of the location from the principal meridian and the time of year.

Radiant energy from the Sun is determined by using radiometers. Special types of radiometers measure only shortwave radiation, only longwave radiation, or all-wave radiation. Shortwave energy from the Sun may be absorbed, scattered, or reflected before it reaches the surface. It may also be scattered down to the surface as diffuse radiation. Direct radiation is transmitted through the atmosphere all the way to the surface. Although some longwave radiant energy emitted from Earth's surface escapes into space, most tends to be absorbed by the atmosphere at most locations and is then largely reradiated back downward in the form of counter-radiation. The net radiation at a given place and time refers to the difference between the amount of all-wave radiant energy absorbed and the sum of shortwave energy reflected and longwave energy emitted.

The transfer of radiant energy alone is not sufficient to make the shortwave energy receipt at the surface balance the loss of energy from the surface through longwave fluxes. Instead, convection is important at all scales to complete the energy balance, and conduction may also be important locally. Convection is accomplished through the turbulent fluxes of sensible heat and latent heat. Conduction occurs through the substrate heat flux. The radiative, convective, and conductive fluxes collectively comprise the energy balance of a location. When the energy balance is positive the local temperature is

increasing, and when the energy balance is negative the local temperature is decreasing. But for the whole Earth–ocean–atmosphere system the energy balance theoretically remains at zero on short time scales. At longer time scales other factors (both natural and human induced) may cause long-term changes to the system's energy receipt and temperature.

Atmospheric moisture is the most important component of mass in the SBL. Moisture can be expressed either by vapor pressure, relative humidity, dewpoint temperature, or absolute humidity, but in many microclimatological studies of atmospheric moisture, specific humidity affords some advantages as the variable of interest. Moisture may be transported upward either directly by evaporation or transpiration through vegetation, but climatologists usually simply consider the combined effect of ET. Most higher-level plants can control the loss of moisture through transpiration to some extent because the stomates on their leaves may partially close during dry periods. Such plants can affect their local atmospheric environments by accelerating the loss of water to the atmosphere during times of waterlogged soils (as long as the atmosphere is not saturated) and slowing the transpiration rates as the soil begins to dry out. ET may be measured using a lysimeter, and potential ET may be estimated with a Class A Evaporation Pan.

The vertical movement of energy and moisture within and beyond the SBL is an important feature of the local circulation. The hydrostatic equation describes the balance of forces between the downward-directed gravitational acceleration and the upward-directed buoyancy effect. Atmospheric stability conditions play a major role in the tendency for energy and moisture to move vertically through the SBL to the free atmosphere.

In an unstable atmosphere vertical motion is enhanced, turbulent fluxes are encouraged, and a rising parcel of air that does not exchange energy with surroundings (i.e., moving adiabatically) may cool to its dewpoint temperature on its ascent, whereupon its moisture condenses and forms a cloud. In a stable atmosphere vertical motion is suppressed, dispersion of pollutants is minimized, turbulent fluxes are more likely to be reduced, and an adiabatically moving air parcel will not be likely to rise to the point at which it reaches its dewpoint temperature unless it is forced to rise by some other mechanism.

Stability conditions at a specific place and time can be assessed by comparing the ELR with the unsaturated (or saturated if saturation has been reached) adiabatic lapse rate. If the adiabatically moving parcel of air is warmer than its surrounding environment, the atmosphere is unstable at that height, and if it is cooler than its surrounding environment, the atmosphere is stable

at that level. Stability can be assessed relatively easily using a thermodynamic diagram such as the Skew T–Log P diagram.

The replacement of temperature with potential temperature simplifies calculations of stability. Any situation in an unsaturated atmosphere in which the potential temperature increases with height is stable, whereas unstable conditions occur when potential temperature decreases with height. In the lowest few meters of the atmosphere, the difference between the gradient of temperature with height and the gradient of potential temperature with height is negligible.

Unlike the transfer of energy and matter, momentum is typically transferred downward because wind speed usually increases with height. This momentum flux (or shearing stress) is represented by the degree of vertical wind shear or the difference in horizontal wind speed

across a vertical length. This flux is much greater in the SBL than in the free atmosphere. The ratio of thermal turbulence (which is a function of potential temperature and indicates stability conditions) to mechanical turbulence (a function of vertical wind shear and representing vertical momentum transfer) is known as the gradient Richardson number. The atmosphere is stable when that number is positive and unstable when negative. The latter case is sometimes termed “free convection.” The atmosphere is in a neutral stability condition when the gradient Richardson number approaches zero, and in such a case all vertical motion results from mechanical forcing, also known as “forced” convection. Neutral conditions are often assumed in much boundary layer theory, including the logarithmic wind profile. Thus when such assumptions are made, their validity should be checked.

Key Terms

Absolute humidity	Eddy covariance	Lapse rate
<i>Absolute zero</i>	<i>Ekman spiral</i>	<i>Latitude</i>
Absorption	<i>Electromagnetic spectrum</i>	Lifting condensation level
Adiabatic motion	Energy balance	<i>Lithosphere</i>
<i>Advection</i>	<i>Environmental lapse rate (ELR)</i>	Local apparent time
<i>Aerosol</i>	<i>Equation of state</i>	Logarithmic wind profile
<i>Albedo</i>	Equation of time	<i>Longitude</i>
Analemma	Equinox	Longwave radiation
<i>Arctic Circle</i>	<i>Evaporation</i>	Lysimeter
Atmospheric window	Evapotranspiration (ET)	Mechanical turbulence
<i>Attenuation</i>	Fick's law	Microscale
Azimuth angle	First law of thermodynamics	<i>Millibar (mb)</i>
<i>Biosphere</i>	<i>Flux</i>	<i>Momentum</i>
Buoyancy	Forced convection	<i>National Weather Service</i>
<i>Centrifugal acceleration</i>	<i>Free atmosphere</i>	Net radiation
Class A Evaporation Pan	Free convection	Neutral atmosphere
Clausius-Clapeyron equation	<i>Friction</i>	Optical air mass
<i>Condensation</i>	Frostpoint temperature	Pan adjustment coefficient
Conditional instability	<i>Geostrophic balance</i>	<i>Pascal (Pa)</i>
<i>Conduction</i>	Gradient Richardson	<i>Path length</i>
<i>Convection</i>	number (Ri)	<i>Photosynthesis</i>
<i>Coriolis effect</i>	Guard cell	Planetary albedo
Counter-radiation	<i>Hydrosphere</i>	Planetary boundary layer
<i>Cryosphere</i>	Hydrostatic equation	Planetary scale
<i>Deposition</i>	Hygrometer	Potential evapotranspiration (PE)
<i>Density</i>	<i>Insolation</i>	Potential temperature (θ)
Dewpoint temperature (T_d)	International date line	<i>Pressure gradient force</i>
Diffuse radiation	<i>Joule</i>	Principal meridian
Dimensionless quantity	<i>Kelvin temperature scale</i>	Pyranometer
Direct radiation	<i>Kinetic energy</i>	Pyrgeometer
	Laminar layer	Pyrradiometer

Radiation balance equation	Specific humidity	Turbulence
Radiometer	Stability	Turbulent flux of latent heat (latent heat flux) (Q_E)
Radiosonde	<i>Stable atmosphere</i>	Turbulent flux of sensible heat (sensible heat flux) (Q_H)
Reflection	Stomate	Unsaturated adiabatic lapse rate (UALR)
Relative humidity	<i>Sublimation</i>	<i>Unstable atmosphere</i>
<i>Rotation</i>	Substrate heat flux (Q_G)	Vapor pressure (e)
Roughness layer	<i>Summer solstice</i>	Vertical flux of horizontal momentum (shearing stress) (τ)
Roughness length (z_0)	Sun path diagram	Vertical wind shear
Saturated adiabatic lapse rate (Γ_s)	Surface boundary layer (SBL)	<i>Wavelength</i>
Saturation vapor pressure (e_s)	<i>Temperature inversion</i>	<i>Winter solstice</i>
Scattering	Thermal turbulence	Zenith angle
<i>Shortwave radiation</i>	Thermodynamic diagram	Zone mean time
Skew T–Log P diagram	<i>Time zone</i>	
Soil heat flux plate	Transition layer	
<i>Solar declination</i>	<i>Transpiration</i>	
<i>Solar noon</i>	<i>Tropopause</i>	
Solar time	<i>Troposphere</i>	

Terms in italics have appeared in at least one previous chapter.

Review Questions

- Describe the properties of the sublayers in the near-surface part of the troposphere.
- What is the difference between mechanical turbulence and thermal turbulence?
- Describe the two convective or turbulent fluxes in the near-surface atmosphere.
- Describe the conductive flux that is important near the surface.
- What is shearing stress and how/why does it occur?
- What does a Sun path diagram tell us and how is it interpreted?
- How can solar time be calculated from zone mean time?
- Describe the different types of radiometers and their functions.
- Describe the variables that can be used to represent atmospheric humidity.
- How can evapotranspiration be measured?
- Why is a pan adjustment coefficient necessary when evaluating potential evapotranspiration?
- How is atmospheric stability evaluated?
- What is the adiabatic assumption and why is it critical to assessing atmospheric stability?
- What is potential temperature and how can it be used to simplify the evaluation of stability in the atmosphere?
- What does the gradient Richardson number tell us about the condition of the near-surface atmosphere?

Questions for Thought

- Review the Sun path diagrams presented in Figure 5.7. Does day length change linearly across the year? Does the answer to that question depend on latitude?
- If you have had a course in differential calculus, differentiate the equation [$\theta = T + \Gamma_u(z - z_{1000\text{ mb}})$] with respect to z to show that in a neutral atmosphere, potential temperature does not change with height.
- Show that the hydrostatic equation and the gradient Richardson number are dimensionless.



CHAPTER 6

Global Hydrologic Cycle and Surface Water Balance

CHAPTER AT A GLANCE

- Global Hydrologic Cycle
- Surface Water Balance
 - ▶ Potential Evapotranspiration
 - ▶ Evapotranspiration
 - ▶ Precipitation
 - ▶ Soil Moisture Storage
 - ▶ Deficit
 - ▶ Surplus and Runoff
- Putting It All Together: A Worked Example of the Surface Water Balance
- Types of Surface Water Balance Models
- Water Balance Diagrams
- Drought Indices
- Summary
- Key Terms
- Review Questions
- Questions for Thought

Local moisture is moved from Earth's *hydrosphere* up to the atmosphere through the combined processes of *evaporation* and *transpiration*—*evapotranspiration (ET)*. Although climatologists do not usually distinguish between whether water was evaporated directly from the surface or only evaporated after being transpired, most water loss from vegetated surfaces is through transpiration. The **latent heat flux**

is the energetic process that moves energy involved in phase changes of water from the surface up into the atmosphere. This chapter focuses on these and related processes in more detail and on a broader scale, as components of the climatic water balance.

The *condensation*, freezing, or *deposition* of every water molecule in the atmosphere and subsequent precipitation of all that water at any moment in time would

produce about 2.5 cm (1 in) of **precipitable water**—the depth of water (in centimeters) in a column of atmosphere if all water molecules in that column condensed and precipitated and it were distributed evenly across Earth's surface. In reality, however, the distribution of atmospheric moisture is uneven. Tropical, oceanic locations average about 5 cm (2 in) of precipitable water, while less than 0.5 cm (0.2 in) exists in polar latitudes. The major reason for the difference is that the colder air near the poles has lower *saturation vapor pressure* and therefore lower humidity values.

The unevenness of the distribution of precipitable water invites two other important implications. First, because most places on Earth receive well more than 5 cm of precipitation per year, the same water molecules are continually recycled throughout the Earth–ocean–atmosphere system. It has been estimated that the average water vapor molecule spends only approximately 8 days in the atmosphere—its *residence time*—before it is precipitated back down to the surface. The water you used this morning to brush your teeth may be the same water a dinosaur drank 65 million years ago! Second, the movement of water on Earth must be intricately tied to the planetary atmospheric circulation such that it is accumulated in some places more easily than in others.

The constant cycling of this water (in all its forms) throughout the Earth–ocean–atmosphere system—the *global hydrologic cycle*—is the first major topic of this chapter. Subsequently, the chapter examines the climatic

water balance as a means of accounting for the abundance of local water in various components of the hydrologic cycle at a given instant.

▶ Global Hydrologic Cycle

The global hydrologic cycle is illustrated in **FIGURE 6.1**. The left side of the diagram represents the hydrologic cycle for the terrestrial part of Earth, while the right side depicts the oceanic surface and adjacent atmosphere. Saltwater in the ocean dominates all other *reservoirs* of water in the Earth–ocean–atmosphere system.

Figure 6.1 also shows that over 73% of the total reservoir of fresh water is in the form of solid water in the *cryosphere*. Nearly all the rest, about 26%, lies in the form of **groundwater**—water stored beneath the soil (**FIGURE 6.2**). About 95% percent of the remaining 1% of Earth's fresh water lies near the surface in the form of freshwater lakes, soil moisture, and all surface streams. At any given time only a minuscule amount of water—perhaps only 0.05% of the fresh water on Earth—is present in the terrestrial and marine atmosphere. It is not surprising that the marine atmosphere contains more water than the terrestrial atmosphere, both because most of the Earth is covered by water and because water is more readily available for evaporation over the oceans.

Figure 6.1 also shows the relative magnitudes of the *fluxes* of water in all its forms via precipitation,

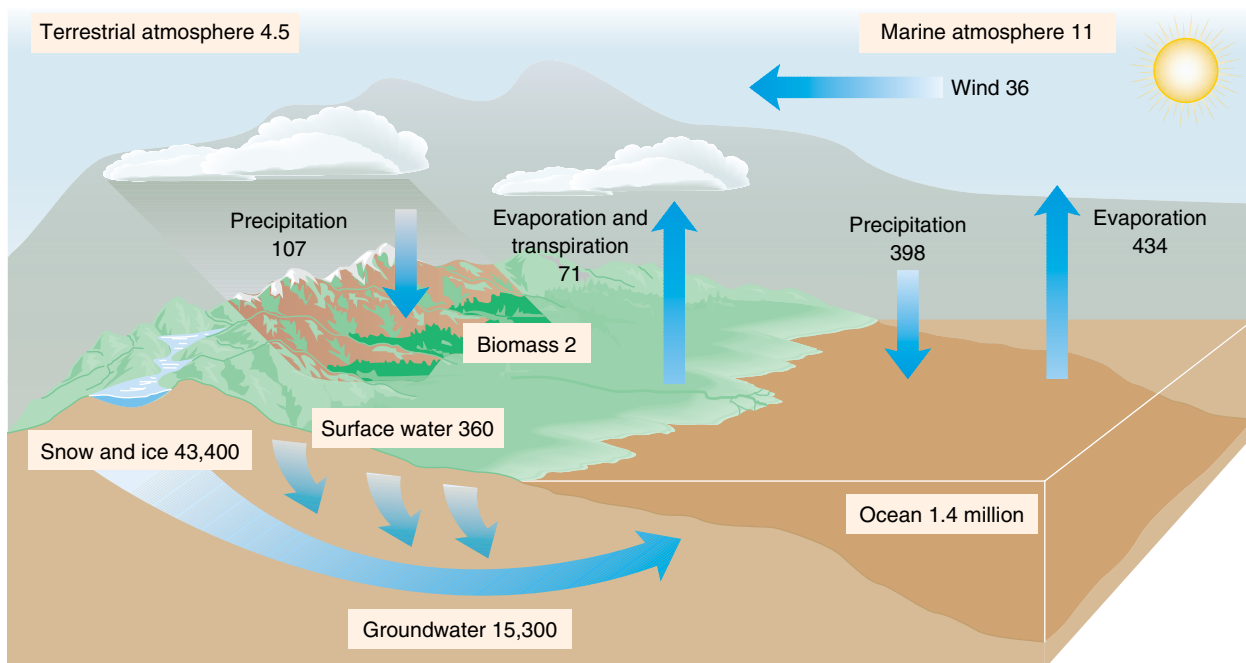


FIGURE 6.1 Schematic of the global hydrologic cycle. Reservoirs are shown in boxes and fluxes are shown with arrows. Values represent volume in thousands of km³, with fluxes calculated on an annual basis.

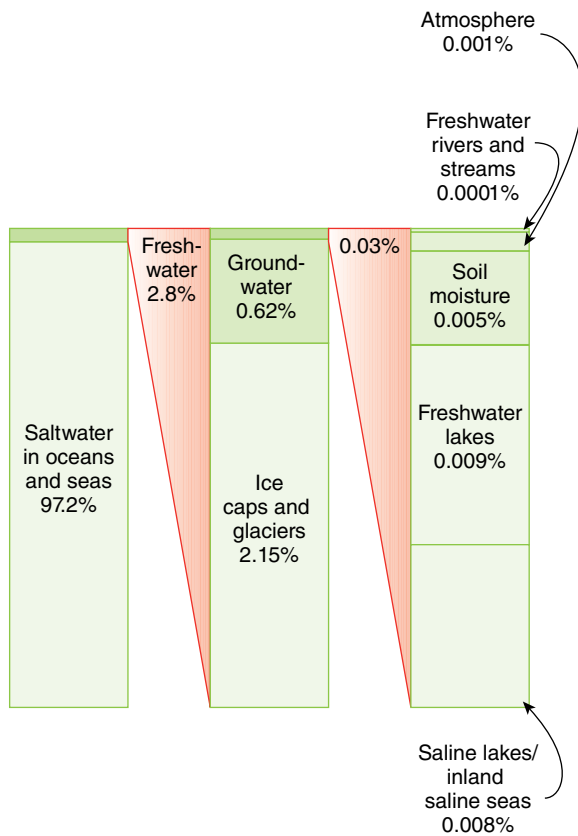


FIGURE 6.2 Global distribution of water on Earth.

advection, and ET. Once again, because most of the Earth is covered by water, the bulk of the fluxes occur over the oceans. Notice also that more water is lost from the ocean through evaporation than is gained by precipitation; the difference is $36,000 \text{ km}^3 \text{ yr}^{-1}$. In the terrestrial atmosphere the opposite occurs. The process of ET moves less water up to the terrestrial atmosphere than is returned to the surface in the form of precipitation. The difference is once again $36,000 \text{ km}^3 \text{ yr}^{-1}$. Without any other fluxes to compensate, this implies that the oceans are drying up and the continents are becoming more and more waterlogged over time. But, of course, other fluxes do compensate. Because nearly all the terrestrial Earth lies above sea level, the excess water ($36,000 \text{ km}^3 \text{ yr}^{-1}$) from precipitation flows downhill, into streams, and out to sea via **runoff**. And this $36,000 \text{ km}^3 \text{ yr}^{-1}$ of water is constantly replenished by being advected from the marine atmosphere to the terrestrial atmosphere via winds (Figure 6.1). The global hydrologic cycle results in nearly constant amounts of water on the continental and oceanic parts of Earth over short time periods.

At geological time scales, however, the global hydrologic cycle is slightly different. For example, meltwater from continental ice sheets and glaciers runs off to the sea, and a new equilibrium is established as a result. At

shorter time scales, the loss of biomass in the form of *deforestation* or other removal decreases terrestrial ET. Although this decrease may be slight on a global basis because biomass returns only $2000 \text{ km}^3 \text{ yr}^{-1}$ of water to the atmosphere, it could be significant on local and regional scales where a higher percentage of the precipitation comes from water returned to the atmosphere locally by ET. Once again, though, a new equilibrium is established globally after the process restabilizes.

FIGURES 6.3 and 6.4 show the North American and global, respectively, mean annual distribution of runoff. In general, locations that receive abundant precipitation tend to have large natural waterways to remove the excess water. The classic example of such a situation is the Amazon River in South America, which flows almost entirely through wet climates. Runoff is so significant in the Amazon that this river produces more than four times the discharge (in $\text{m}^{-3} \text{ s}^{-1}$) than that of the river with the second-highest runoff rate in the world. The Amazon discharges more than 10 times the volume of water than the Mississippi River. In wet areas such as those found in the Amazon basin, runoff carries excess water out to sea, minimizing impacts of flooding and preventing saline water from the ocean from intruding inland. In arid areas runoff may even be seen as wasted fresh water—people are reluctant to “waste” fresh water by letting it reach the sea.

Although other fluxes of water do occur on Earth, these values are relatively small and are not shown in Figure 6.1. Some surface water seeps downward through **percolation**—a very slow process through the *lithosphere* that replenishes groundwater supplies. In many locations the rate of removal of this groundwater for industrial, agricultural, and domestic uses far exceeds the rate of replacement by percolation. In addition, a relatively small flux from the groundwater to the ocean also occurs, perhaps offsetting the rate of percolation on a global basis. Another flux not shown in Figure 6.1 because it is subsumed within a larger process is **infiltration**—the downward movement of water from the surface into the soil and plant rooting zone. Infiltration differs from percolation in that it occurs nearer to the surface. On a long-term, global basis much of the infiltrated water is moved from the soil back to the atmosphere through ET.

A simple calculation known as the **global water balance equation** can be used to express the balance between the input and the output of water to and from the surface on a global basis. If we neglect the output fluxes that are small, we can say that,

$$P = ET + R$$

where P represents precipitation, ET is evapotranspiration, and R is runoff.

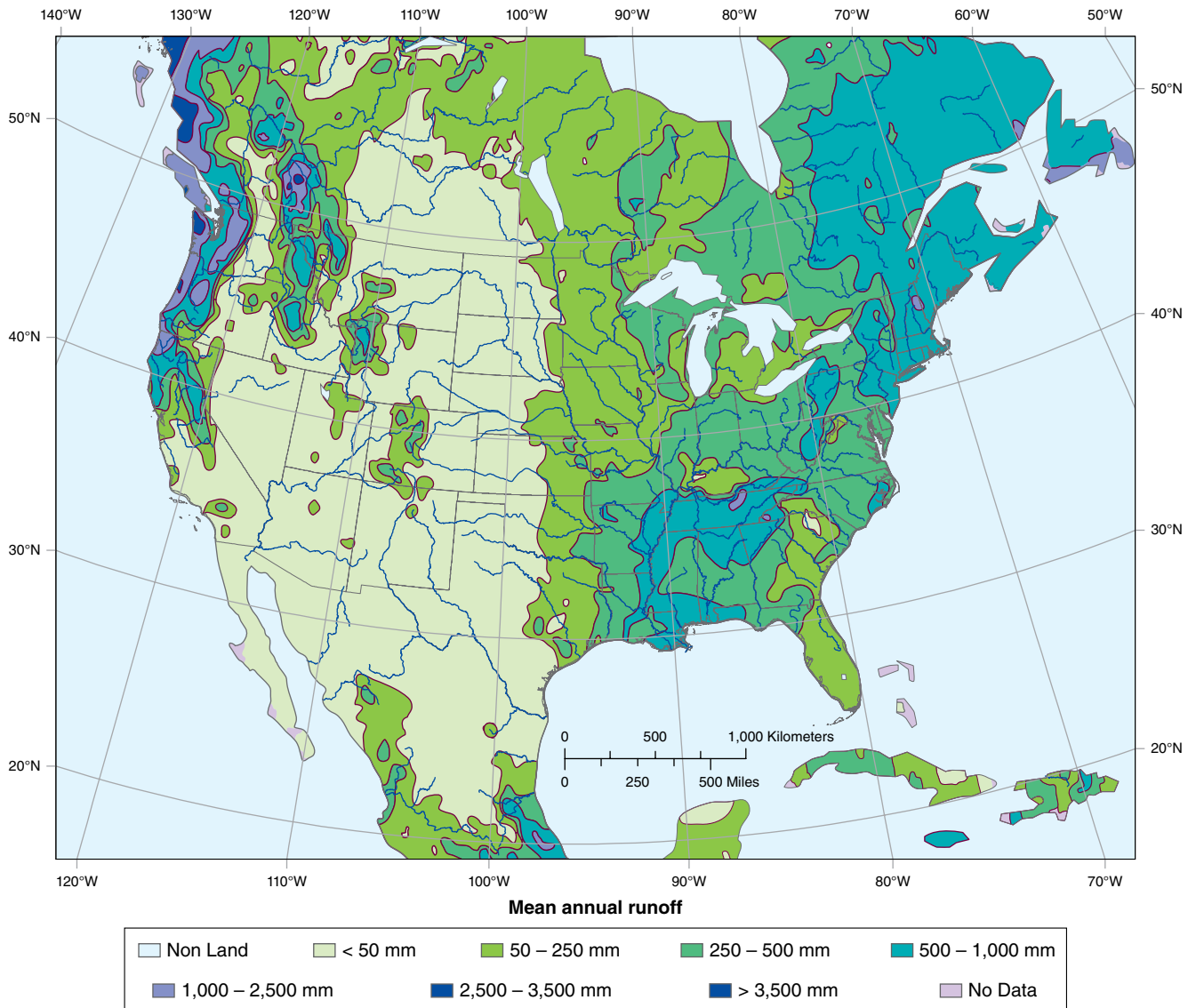


FIGURE 6.3 Mean annual runoff in North America, 1980–2015.

Courtesy of Sara A. Ates. Data from: Fekete, B. M., C. J. Vörösmarty, and W. Grabs (2000 & 2002).

Two interesting observations of the global water balance equation emerge if we compare it with the energy balance equation. First, the only term that is shared between the two equations is ET. Recall that the energy equivalent of ET is Q_E , and the two terms are related by,

$$ET = \frac{Q_E}{L_v \rho_\ell}$$

where L_v is the latent heat of vaporization ($2.5008 \times 10^6 \text{ J kg}^{-1}$) and ρ_ℓ represents the density of water (1000 kg m^{-3}). ET thus affects both the energy balance and the water balance simultaneously. It is no wonder, then, that this is such a critical concept in climatology.

The second observation from the global water balance equation is that, like the energy balance equation, this equation balances on a global, annual-average basis. At any one local place on Earth's surface,

however, neither equation may be balanced. Just as the *net radiation* (Q^*) may be positive or negative locally, precipitation may exceed, or be exceeded by, the rate of removal of water from the surface via ET and runoff at a given time and place. Local surface moisture content changes constantly, but in the global system the budget must balance.

► Surface Water Balance

Because the global water balance need not balance locally, it is useful for climatological and environmental monitoring applications to estimate how much water is involved in each of the reservoirs and fluxes at a given place and time. For example, if we can model the amount of water in the soil, foresters may have a better idea of whether the poor health of a tree stand is

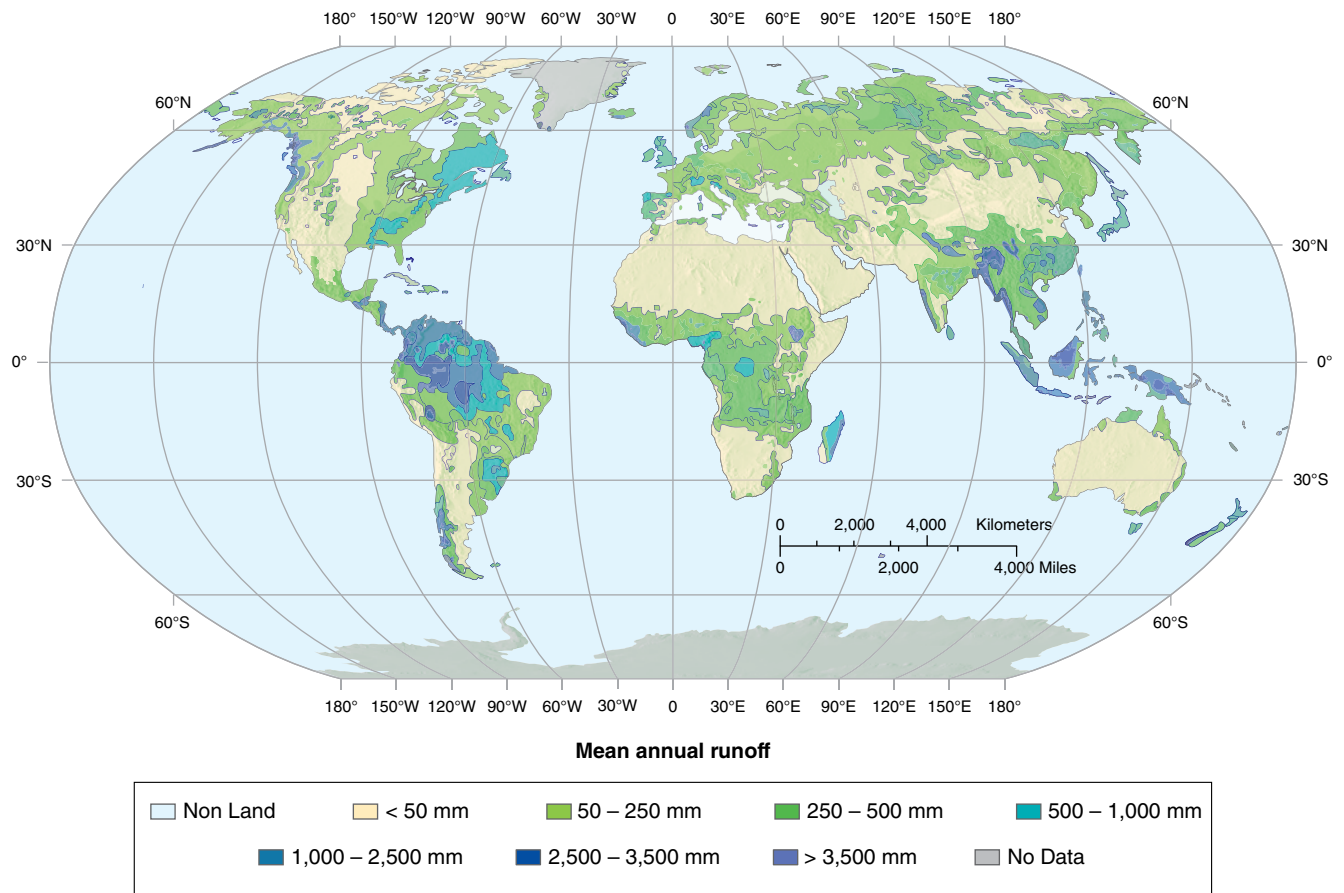


FIGURE 6.4 Global distribution of mean annual runoff, 1980–2015.

Courtesy of Sara A. Ates. Data from: Fekete, B. M., C. J. Vörösmarty, and W. Grabs (2000 & 2002).

caused by inadequate moisture supplies. The **surface water balance** represents an environmental systems approach to understanding the hydrological cycle on a local level. It emphasizes the input, output, and storage of water and its interactions with the available energy and moisture at Earth's surface. The modern surface water balance was developed by American climatologist C. W. Thornthwaite in the 1940s for the purpose of climatic classification based on the degree of availability of surface water on a climatological basis.

Potential Evapotranspiration

The surface water balance largely depends on the calculation of *potential evapotranspiration (PE)*—an energy term that represents the climatic demand for water from the landscape driven by the amount of *insolation* at the surface. It is theoretically the maximum amount of evaporation and transpiration in centimeters or inches of precipitation equivalent that solar radiant energy could set in motion over a given period of time. It almost always peaks in summer, when the most energy is available to drive the ET process. We can consider PE to represent the maximum amount of ET that would occur over a waterlogged short grass field or the “water need” of the

atmosphere. **FIGURES 6.5** and **6.6** show the annual average PE in North America and in the world, respectively.

PE can be estimated by using a correction factor to the measured amount of evaporation from a pan of water, or (preferably) by using a *lysimeter*. But evaporation pans and lysimeters are available at few locations, and most have not been in continuous operation for a sufficiently long period of time to develop reliable climatologies of PE. Therefore, it is advantageous to estimate PE based on available data collected both currently and in the historical records.

Although others have devised alternative means of estimating PE, Thornthwaite developed what became known as **Thornthwaite potential evapotranspiration**—a set of empirical equations to estimate PE based only on the temperature and *latitude* of the location of interest. The purpose of including latitude in this calculation is that latitude determines Sun angle and day length, and these, along with temperature, represent the amount of energy availability to drive the ET process. But why did Thornthwaite choose only these variables, when ET rates also are affected by wind speed, atmospheric *stability*, cloud cover, and humidity characteristics? He decided that even though other variables are also important for determining ET, the lack of data for most

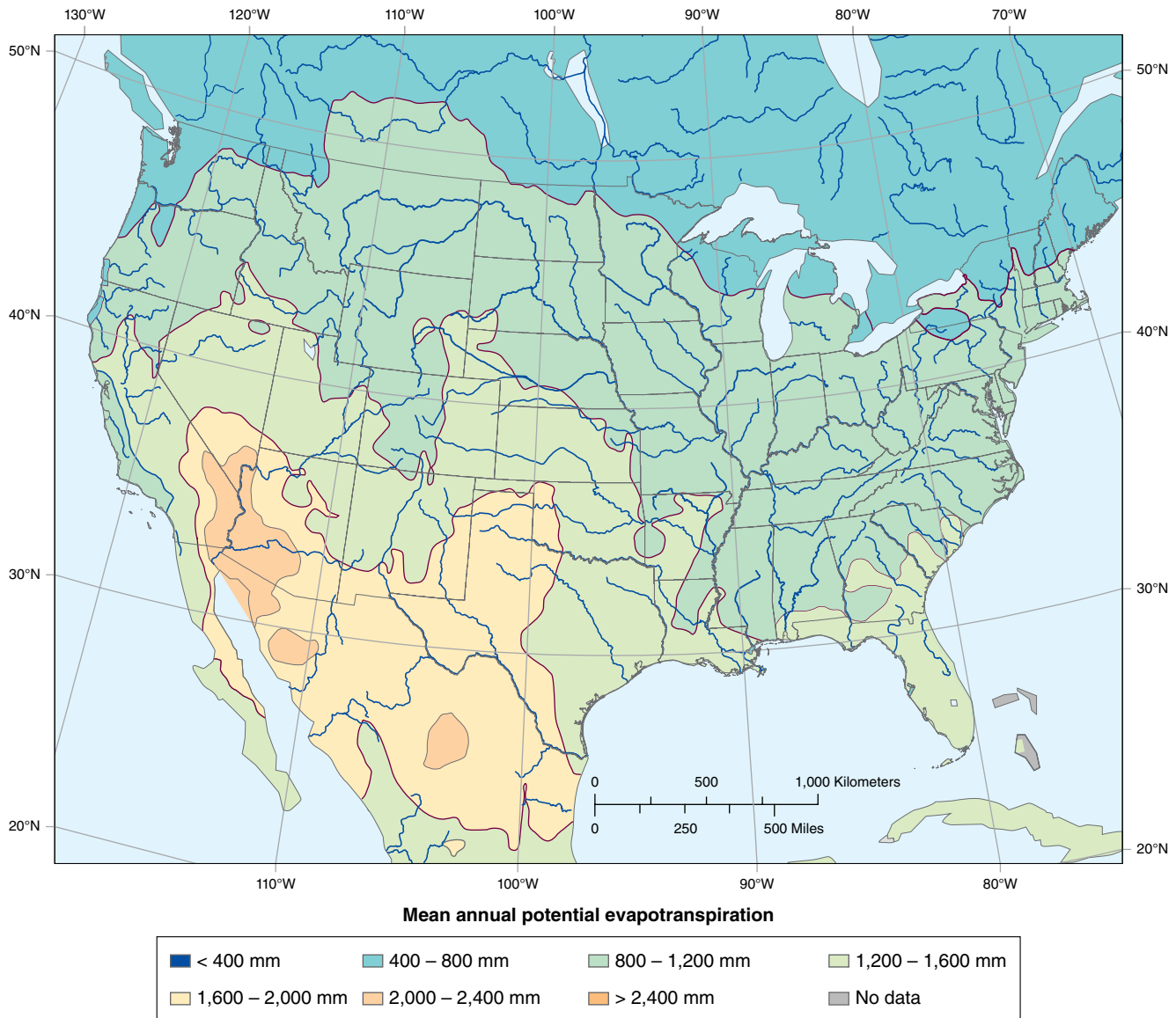


FIGURE 6.5 Mean annual PE in North America, 1980–2015.

Courtesy of Sara A. Ates. Data from: University of East Anglia Climatic Research Unit; Jones, P.D.; Harris, I.C. (2008).

EQUATION 6.1
$$\text{PE}_{\text{unadjusted}} (\text{mm month}^{-1}) = \begin{cases} 0 & \text{if } T_i < 0^\circ\text{C} \\ 16 \left(\frac{10T_i}{I} \right)^a & \text{if } 0^\circ\text{C} \leq T_i < 26.5^\circ\text{C} \\ -415.85 + 32.24T_i - 0.43T_i^2 & \text{if } T_i \geq 26.5^\circ\text{C} \end{cases}$$

locations on Earth would limit the utility of the surface water balance to the few places where data were available for all these variables. For this reason he chose to introduce a simpler but more applicable model.

Cort Willmott and colleagues at the University of Delaware modified Thornthwaite’s original PE by first computing an “unadjusted” PE, as shown in **EQUATION 6.1**, where T_i is the mean monthly air temperature in degrees Celsius and $i = 1$ for January, 2 for February, and so on. In addition,

$$I = \sum_{i=1}^{12} \left(\frac{T_i}{5} \right)^{1.534}$$

and

$$a = 6.75 \times 10^{-7} I^3 - 7.71 \times 10^{-5} I^2 + 1.79 \times 10^{-2} I + 0.49$$

But, because different months have different numbers of days, PE can be adjusted such that,

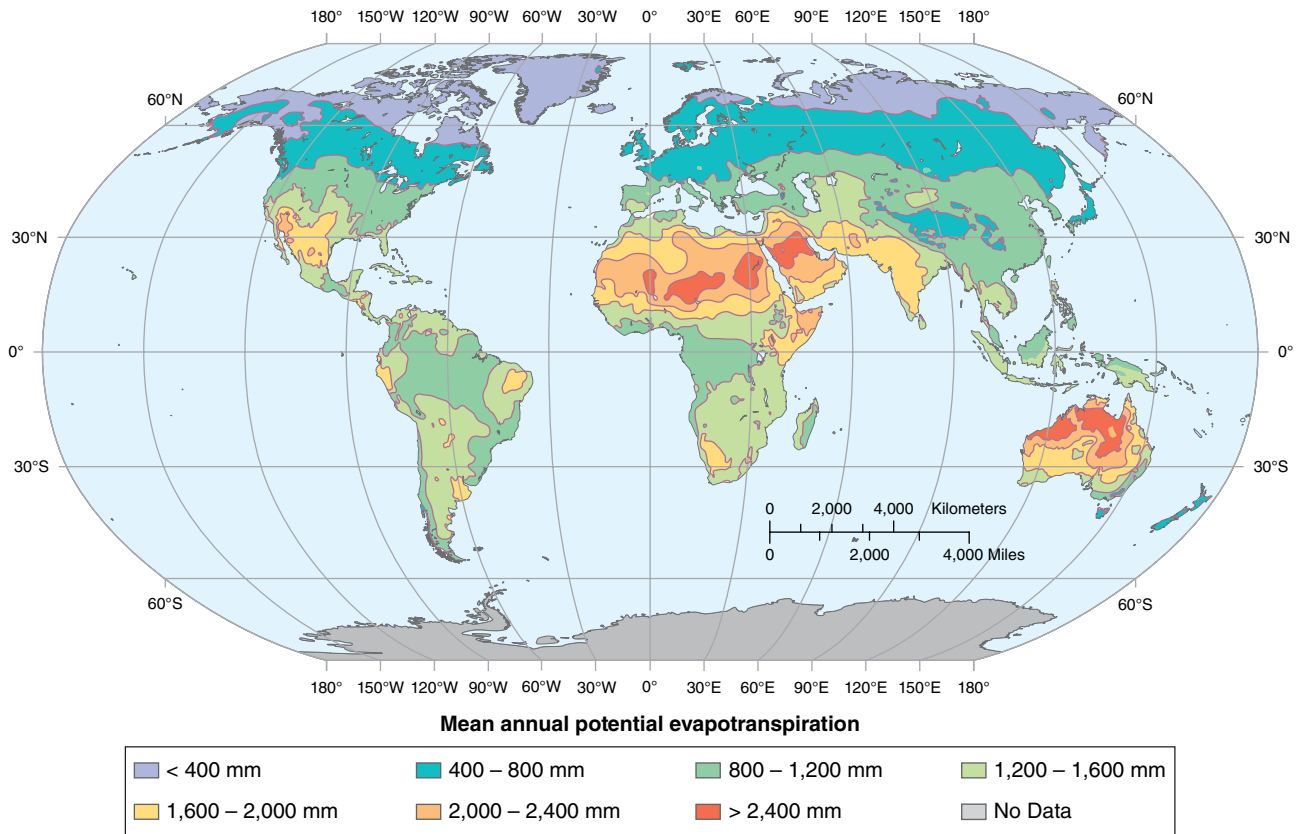


FIGURE 6.6 Mean annual PE globally, 1979–2015.

Courtesy of Sara A. Ates. Data from: University of East Anglia Climatic Research Unit; Jones, P.D.; Harris, I. (2008).

$$PE_{\text{unadjusted}} (\text{mm month}^{-1}) = PE_{\text{unadjusted}} \frac{n}{30} \frac{h}{12}$$

where n is the number of days in the month and h is the number of hours of daylight on the 15th day of the month. This set of statistically derived equations was developed in humid environments of the eastern United States. It tends to overestimate PE in arid, non-midlatitude environments and in arid conditions in normally humid environments.

Over the years other researchers have offered alternate methods of calculating PE. Most notably, the British climatologist H. L. Penman's method and several variants of it frequently appear in the climatology research literature. Although some believe the Penman family of methods—what has become known as the **Penman-Monteith equation**—is more accurate because the equation is derived from physical laws rather than statistical relationships (as is Thornthwaite's equation), the multitude of input data required often presents a problem for application. For example, to calculate the PE based on this model, net radiation (Q^*), *substrate heat flux* (Q_G), *vapor pressure* (e , or some humidity measurement that can be converted to vapor pressure), temperature, and **resistance** must be measured or estimated. Resistance is a component of force exerted by the air that works in the opposite direction of the flux

(so it is generally directed downward in opposition to the latent and **sensible heat fluxes**) and has units of seconds per meter. In general, resistance is higher during times of atmospheric stability and lower during times of instability. This is a cumbersome quantity to measure accurately, and several other quantities required in the Penman-Monteith equation are not measured routinely at weather stations.

One version of the Penman-Monteith equation is:

$$ET = \frac{S}{S + \gamma} \frac{(Q^* - Q_G)}{L_v \rho_\ell} - \frac{\rho C_p \Delta D}{L_v \rho_\ell r_a}$$

where S represents the slope of the saturation vapor curve as a function of temperature (Pa K^{-1} , calculated using the *Clausius-Clapeyron equation*); γ is the psychrometric constant (65.5 Pa K^{-1}); L_v is the latent heat of vaporization ($2.5008 \times 10^6 \text{ Joules kg}^{-1}$ at 0°C and changing minimally over the range of Earth temperatures); ΔD is the difference in **wet bulb depression**—the difference between the air temperature and temperature after being cooled by evaporation when measuring *relative humidity*—at two heights in the surface boundary layer (in the *Kelvin temperature scale*); and r_a represents aerodynamic resistance (s m^{-1}).

The most critical assumption of the Penman equation is that S is constant. In other words, the ratio of the difference between the vapor pressure and the saturation vapor pressure at that temperature to the difference between air temperature and *dewpoint temperature* is constant. Because this condition occurs near saturation, Penman's ET often is taken to represent PE.

Evapotranspiration

Another fundamental variable in the calculation of the surface water balance is ET. This variable is distinguished from PE because PE estimates only the maximum possible ET that could occur from a waterlogged grass field. By contrast, ET estimates the actual amount of water transpired through plants or evaporation that does occur. ET does not represent the demand for water but what actually transpires and evaporates. Therefore, ET must always be less than or equal to PE. Perhaps a useful analogy is the amount of money you spend shopping compared with the maximum amount you could possibly spend if money were not a limiting factor. For most of us these values are not the same.

Although ET can be determined using more complicated methods, several researchers have developed simple equations to estimate ET based only on available data. A relatively simple ET equation that offers some advantages, particularly in the arid western United States, has been the **Blaney-Criddle model** formulated by soil conservation scientists H. F. Blaney and W. D. Criddle. The original version of this model is:

$$ET = kf$$

where ET is in mm/month, k is a crop-specific coefficient, and f is a consumptive use factor given by:

$$f = \frac{TP}{100}$$

where T is the mean monthly temperature (in °F) and P represents the monthly percentage of annual daylight hours.

Another technique is the **Turc method**, which was developed for western Europe but has provided reasonable results in some other locations. This method can be expressed as:

$$ET = a_T 0.013 \frac{T_{\text{mean}}}{T_{\text{mean}} + 15} \frac{23.8856K \downarrow + 50}{L_v}$$

where ET is in mm day⁻¹, T_{mean} is the mean daily temperature (in °C), and $K \downarrow$ is the mean solar radiation (MJ m⁻² day⁻¹, where MJ represents "megajoules," or millions of Joules). The coefficient a_T is a humidity-based

value such that if the mean daily relative humidity is greater than or equal to 50%, then $a_T = 1.0$. If the mean daily relative humidity is less than 50%, then a_T has the value of:

$$a_T = 1 + \frac{50 - RH_{\text{mean}}}{70}$$

In addition, many other techniques for evaporation estimation are available. Some have been shown to be more useful in certain geographical areas, while others have been more appropriate estimators in other regions.

Precipitation

Precipitation (P) is the "input" water to the surface in the surface water balance. It represents the atmospheric delivery of moisture to Earth's surface. This delivery occurs in widely varying totals from place to place (**FIGURES 6.7 and 6.8**). Precipitation is simply compared with PE for the place and time of interest to determine the moisture conditions. In a wet month, $P - PE$ is positive because more precipitation is input to the surface than can be removed from it by the atmosphere. In a dry month, $P - PE$ is negative because there is a greater atmospheric demand for water than is delivered by precipitation. Thornthwaite created a climatic classification system that uses a moisture index based on this concept. In this system, whenever P exceeds PE, the moisture index values are positive. Magnitudes of the positive or negative moisture indices are used to delineate climatic boundaries in the Thornthwaite system.

Although PE peaks in summer for almost all locations, precipitation can peak at different times of the year at different locations. In climates that have precipitation peaking in summer, floods and droughts may not be as common as in places where precipitation peaks in winter. In the former case precipitation arrives at the same time that the atmospheric demand for water is high so neither too much nor too little water remains on the surface. In the latter case, droughts and wildfires are common in summer and floods and/or mudslides may be common in winter, because the atmosphere's demand for water is coming precisely at the time when moisture is unavailable through precipitation, and the water arrives when insufficient energy exists for the atmosphere to remove it easily. Vegetative cover (or lack thereof) and land use can affect the severity of the droughts, wildfires, floods, and landslides in such landscapes.

Although precipitation at some sites is measured using technologically advanced equipment, the vast majority of the 13,000 official precipitation reporting stations in the continental United States relies on the

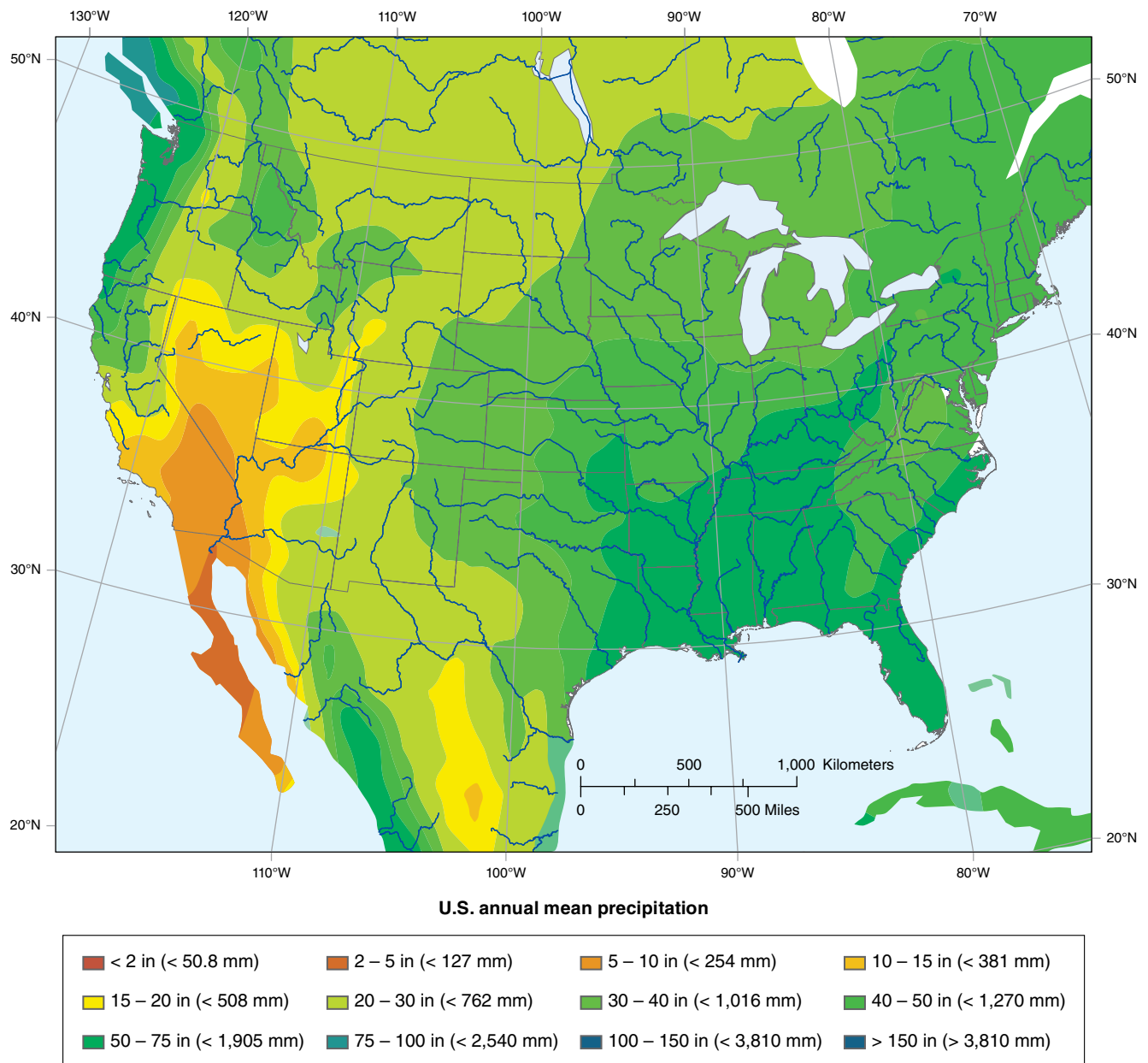


FIGURE 6.7 Mean annual precipitation in North America, 1979–2015.

Courtesy of Sara A. Ates. Data from: Japan Meteorological Agency/Japan, 2013, updated monthly. JRA-55: Japanese 55-year Reanalysis, Daily 3-Hourly and 6-Hourly Data.

collection of precipitation from a simple, nonrecording cylindrical container with a diameter of 20 cm (8 in; [FIGURE 6.9](#)). Inside the cylinder sits a funnel that opens into a smaller cylindrical tube. The smaller tube collects up to 5 cm (2 in) of rainfall before the precipitation overflows into the larger tube. Because the inner tube collects precipitation from an opening that is 10 times the area of the opening in the smaller tube, a special stick with “centimeters” or “inches” set apart at increments of 10 cm (or 10 in) is used to measure the precipitation. The purpose is to facilitate the precision of measurement down to a millimeter or hundredth of an inch. When the stick is wet, it leaves a temporary “wetness” mark on it, so that the stick can be placed through the opening in the funnel, removed, and then precipitation can be

measured easily. If more than 5 cm (2 in) of precipitation falls, the collected precipitation in the larger tube can then be poured back into the smaller tube for measurement. Other nonrecording rain gauges have graduated markings on the inner tube itself that also lengthen each “inch” 10 times; these collect 1 inch of precipitation in the inner tube before spilling into the larger tube that accommodates 5 inches of precipitation.

Measurement of precipitation in the form of snow is only slightly more complicated. Most snow gauges have flanges surrounding the gauge to minimize the impact of blowing snow ([FIGURE 6.10](#)). Snow collected in the gauge is then simply melted and converted to centimeters (or inches) of rainfall equivalent. Heavy, wet snow may have two to three times the depth of its rainfall equivalent,

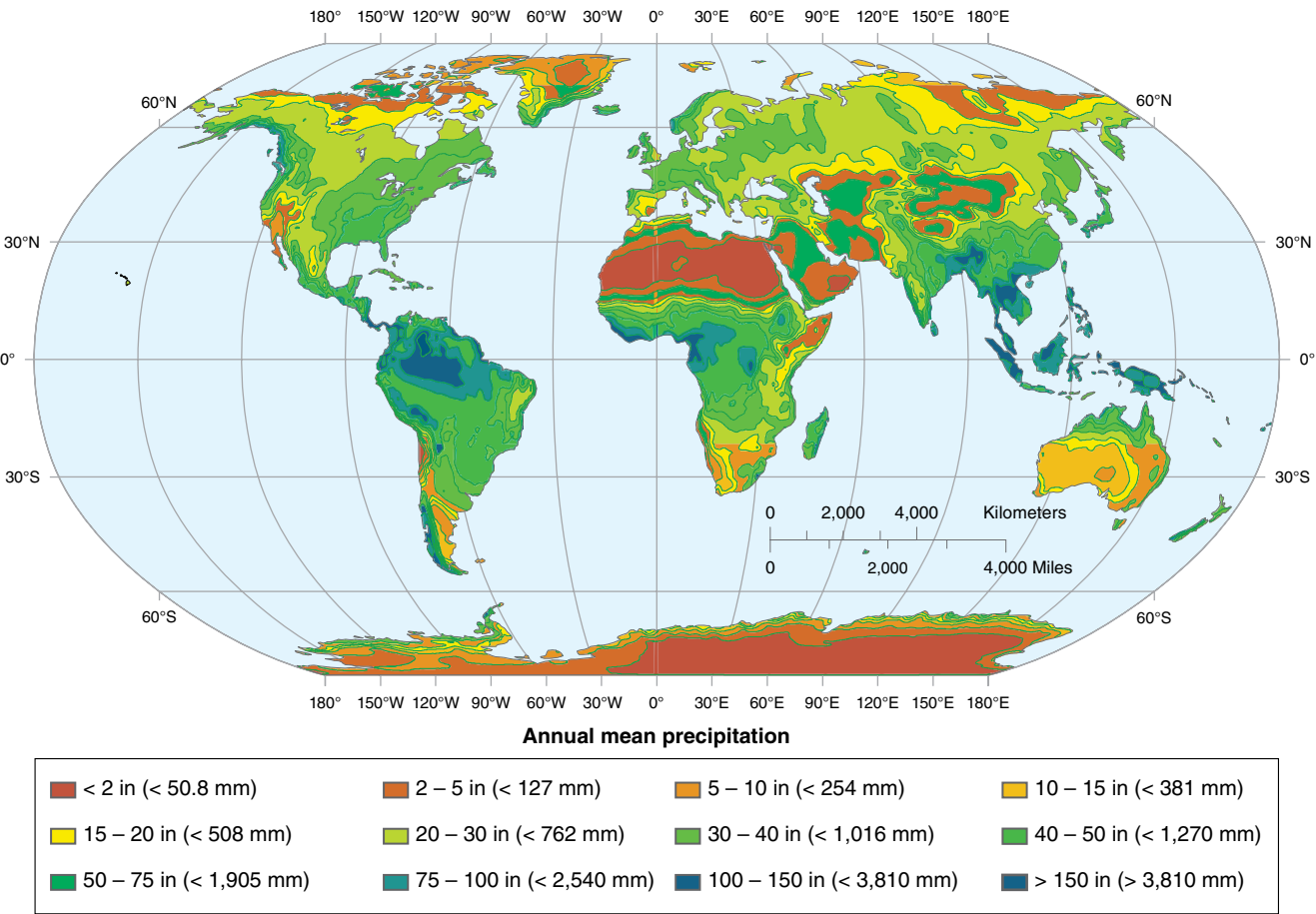


FIGURE 6.8 Mean annual precipitation globally, 1979–2015.
Courtesy of Sara A. Ates. Data from: Japan Meteorological Agency/Japan, 2013, updated monthly. JRA-55: Japanese 55-year Reanalysis, Daily 3-Hourly and 6-Hourly Data.



FIGURE 6.9 A standard nonrecording rain gauge used in the United States.
Courtesy of High Sierra Electronics, Inc.



FIGURE 6.10 A snow gauge.
Courtesy of Alan Sim.

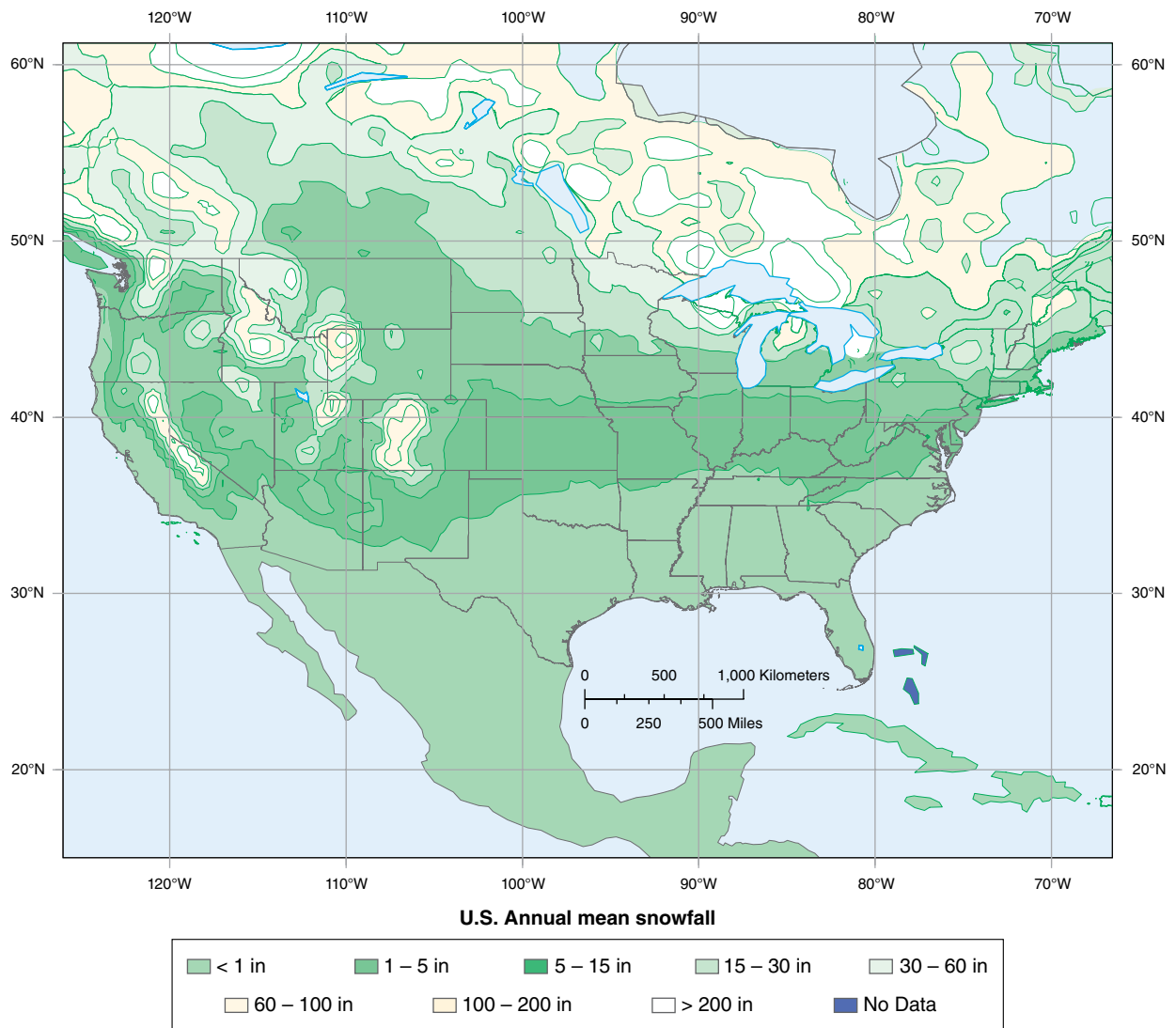


FIGURE 6.11 Mean annual snowfall (in water equivalent) in North America, 1979–2015.

Courtesy of Sara A. Ates. Data from: Annual Average Water equivalent of accumulated snow depth 1979–2015; Japan Meteorological Agency/Japan.

and dry, powdery snow may be 25 times as deep as its rainfall equivalent. A reasonable (though not always accurate) rule of thumb is to assume that, on average, 10 to 12 cm of snow equals 1 cm of water equivalent. Average annual snowfall totals for North America are shown in **FIGURE 6.11**, and those for the world are shown in **FIGURE 6.12**. Snow can detract from the water balance model's accuracy, because in some areas snow precipitation may remain on the surface for months before it melts. Therefore, snow may be counted as an input of precipitation months before it can actually be used or runs off from the surface. However, many water balance models do take into account the "storage" of water in solid form when it falls as snow and its delayed capability to become runoff.

Even though it sounds as if 13,000 rain gauges would provide high-quality coverage of precipitation across the United States, this coverage amounts to an average of only one gauge per 723 km² (284 mi²) in

the continental United States. This equates to one rain gauge for every 27 × 27 km (17 mi × 17 mi) plot of land, although the spatial distribution is not uniform. You have certainly observed situations where rain and snow events can differ drastically across such a large area. The network of gauges across the United States is especially inadequate in summer, when localized, intense thunderstorms are commonplace. Nevertheless, the United States remains much better served by precipitation data than most other parts of the world. As a result of the lack of high-quality data, current research involves the application of radar- and satellite-derived measurement of precipitation to supplement the existing network of stations.

Aside from the problem of having too few observations of precipitation, data from the stations that do exist are prone to reporting inaccurate results. Because the vast majority of precipitation stations are operated and maintained by humans, errors exist

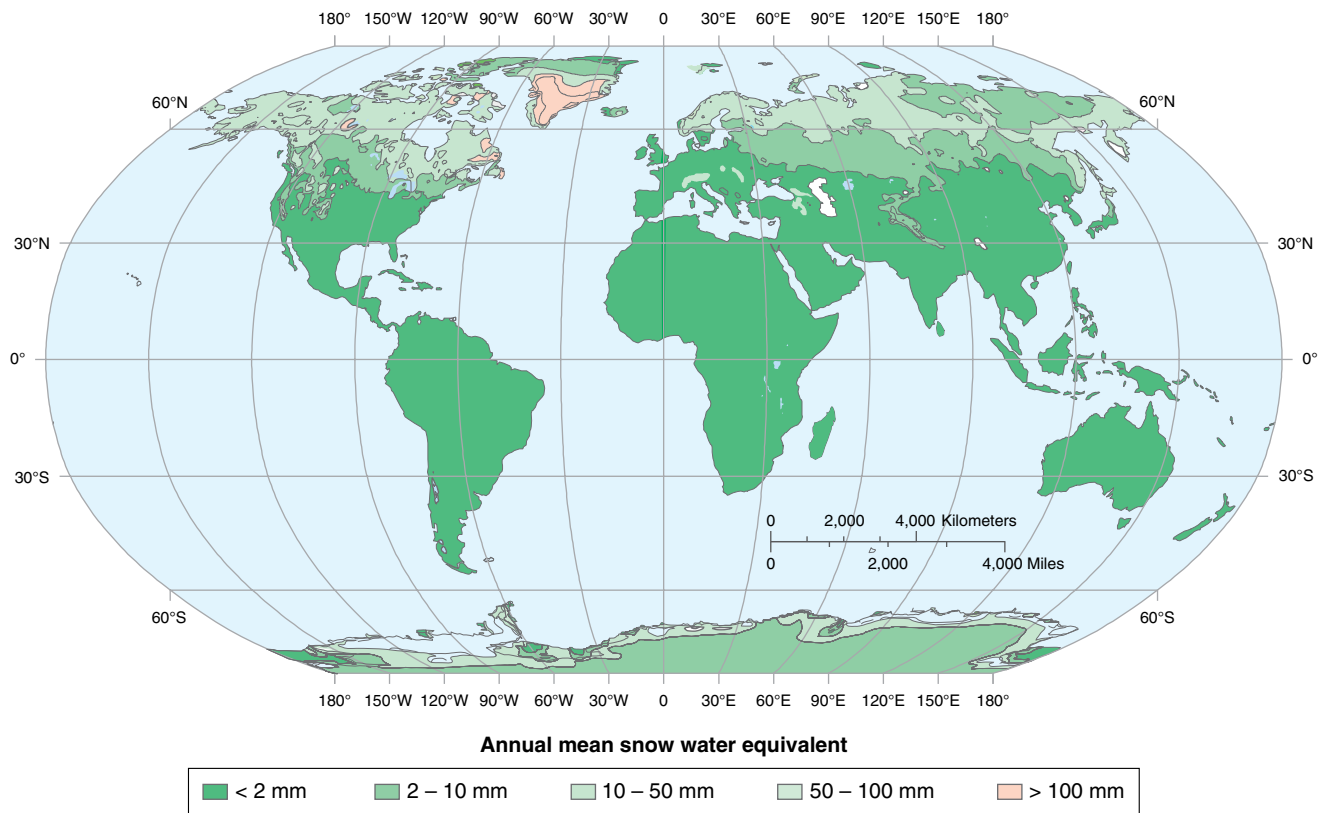


FIGURE 6.12 Global annual mean snow-cover depth (mm equivalent water), 1979–2015.

Courtesy of Sara A. Ates. Data from: Annual Average Water equivalent of accumulated snow depth 1979–2015; Japan Meteorological Agency/Japan. 2013.

that cause problems with the precipitation data. Some stations report missing observations more frequently than others.

In addition, there are systematic, instrumental errors in the precipitation gauges. According to estimations by climatologist David Legates, several factors constitute an **undercatch** of approximately 11%. First, the movement of wind across the gauge creates a **Bernoulli effect**, a phenomenon whereby the increase in wind speed with height over the gauge causes a decrease in air pressure above the gauge. This decreases the likelihood that a drop of precipitation will fall into the gauge and instead causes precipitation to fall away from the gauge. Winds around rain gauges have been estimated to cause an average undercatch of perhaps 8%, with higher values in windy conditions and lower values in calm conditions. In addition, the presence of water “stuck” on the side of the gauge, termed the “wetted perimeter” (which escapes measurement), and evaporation of collected water inside the gauge collectively may amount for another 3% of undercatch. Despite these errors, precipitation data in the United States are of relatively high quality, but these potential errors should be considered when using precipitation data to evaluate the “true” amount of precipitation that has fallen.

In the absence of radar-derived precipitation data (which provides continuous precipitation

measurement across an area), the precipitation measured at a point must be converted to an areal estimate for use in hydrologic modeling, flood analysis, and water conservation planning. For example, four precipitation stations exist in Hancock County, Illinois. The sites measure 5.0, 1.0, 1.5, and 4.0 cm of rainfall for a particular rainfall event (**FIGURE 6.13a**). Is it fair to simply average these four and say that 2.9 cm of rain fell across the county? This number could be multiplied by the area of the county (2061 km², or 2.061×10^{13} cm²) and then converted to cubic meters to provide an estimated total volume of water supply that fell as precipitation in Hancock County (59.7 million m³). But as you can see in Figure 6.13, the stations are not distributed evenly across the county. So a simple average of the four precipitation totals may not be a fair way to assess the total volume of water that fell.

Automated spatial analysis methods such as the isohyetal method, Thiessen polygon method, gridpoint technique, and kriging have been used to handle problems such as the one described above. The **isohyetal method** uses **isohyets**—lines of constant precipitation totals, analogous to the *isotherms* for temperature. These are drawn across Hancock County, as in **FIGURE 6.13b**. Then, **geographic information systems** or graphical methods could be used to determine that 3.9% of the

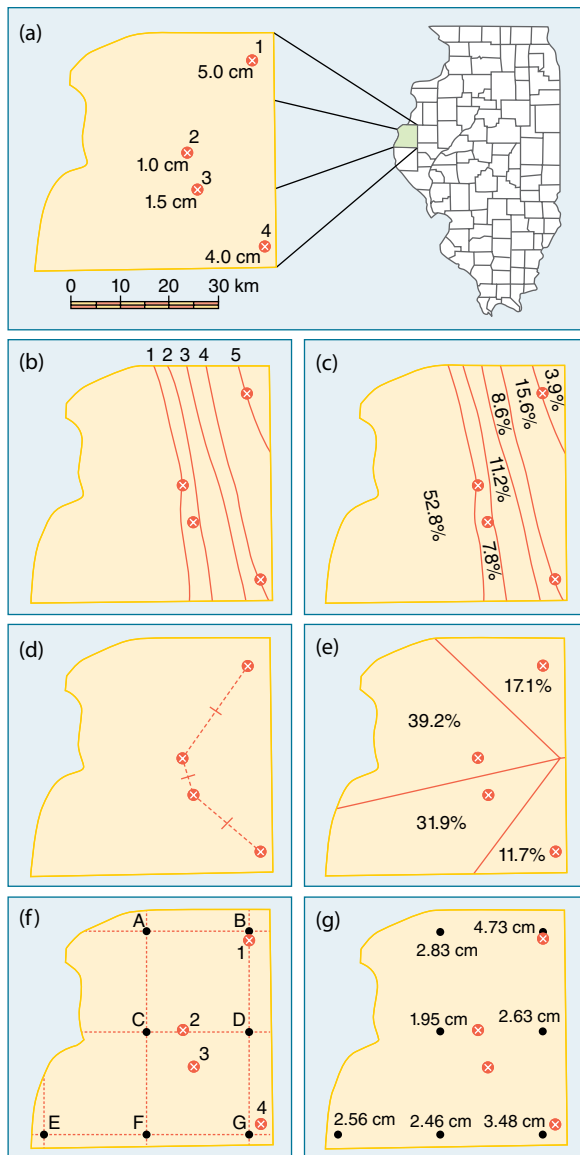


FIGURE 6.13 Spatial methods of estimating rainfall totals in Hancock County, Illinois. (a) Measured precipitation at the four weather stations. (b) Isohyets of precipitation, in centimeters. (c) Percentage of the county's area between each isohyet, for calculation of the isohyetal method. (d) Connecting the lines that connect each adjacent weather station and drawing perpendicular bisectors for those lines. (e) Calculating the area enclosed within each polygon formed by the perpendicular bisectors, for the Thiessen polygon method. (f) Superimposing a grid over the county. (g) Estimating the precipitation at each gridpoint, for the gridpoint technique.

county's area had precipitation exceeding 5 cm, 15.6% of the county was between 4.0 and 5.0 cm, 8.6% was between 3.0 and 4.0 cm, 11.2% was between 2.0 and 3.0 cm, 7.8% was between 1.0 and 2.0 cm, and 52.8% was below 1.0 cm (**FIGURE 6.13c**). For the part of the county with totals exceeding 5.0 cm, we might assume a uniform total of 5.5 cm. This is reasonable because if any station had measured as much as 6 cm, another isohyet would have been drawn. Likewise, uniform totals of 4.5 cm are assumed for the locations between 4.0 and 5.0 cm, 3.5 cm is used for the part of the county between 3.0 and 4.0 cm, 2.5 cm is used for the area between 2.0 and 3.0 cm, 1.5 cm is assumed for the area between 1.0 and 2.0 cm, and finally, 0.5 cm is assumed for that part of the county with totals below 1.0 cm of rainfall. We then multiply the total by the percentage of area having that assumed total and sum the parts (**EQUATION 6.2**). This technique produces a county-averaged precipitation of 1.88 cm, a total considerably below that calculated by simply averaging the four measured values.

The **Thiessen polygon method** is also a spatial or graphical method, but it operates differently. In this method a person or a computer draws perpendicular bisectors for the lines connecting each adjacent station in the study area, as shown in **FIGURE 6.13d**. These perpendicular bisectors are then extended until they meet, as shown in **FIGURE 6.13e**. This procedure ensures that any location in the county falls within the same polygon as the nearest precipitation measuring station. Then, the point-based totals are weighted by these percentages to determine an overall precipitation total for the county (**EQUATION 6.3**). In this example the Thiessen polygon method gives a result of 2.19 cm across the county, somewhat more than the 1.88 cm computed by the isohyetal method.

Another strategy that can be implemented is the **gridpoint technique**, a method in which an artificial grid is superimposed over the study region, with the coarseness of the grid dependent on the amount of computing power and sophistication necessary. The precipitation totals derived for each of the gridpoints are calculated according to an inverse-distance-weighting function of the precipitation at each of the known stations. For example, in **FIGURE 6.13f**, the total distance between gridpoint A and all four stations is 118 km,

$$\text{EQUATION 6.2} \quad \text{County Average Precipitation} = (5.5 \text{ cm} \times 0.039) + (4.5 \text{ cm} \times 0.156) + (3.5 \text{ cm} \times 0.086) + (2.5 \text{ cm} \times 0.112) + (1.5 \text{ cm} \times 0.078) + (0.5 \text{ cm} \times 0.528)$$

EQUATION 6.3

$$\text{County Average Precipitation} = (5.0 \text{ cm} \times 0.171) + (1.0 \text{ cm} \times 0.392) \\ + (1.5 \text{ cm} \times 0.319) + (4.0 \text{ cm} \times 0.117)$$

EQUATION 6.4

$$\text{Precip. at Point A} = \frac{\frac{118}{21}(\text{Precip. at Station 1}) + \frac{118}{22}(\text{Precip. at Station 2}) + \frac{118}{29}(\text{Precip. at Station 3}) + \frac{118}{46}(\text{Precip. at Station 4})}{\frac{118}{21} + \frac{118}{22} + \frac{118}{29} + \frac{118}{46}}$$

with 21 km to station 1, 22 km to station 2, 29 km to station 3, and 46 km to station 4. The distance-weighting scheme provides a derived precipitation at gridpoint A of 2.83 cm, calculated from **EQUATION 6.4**. Once precipitation is estimated in this manner at all gridpoints in the county (**FIGURE 6.13g**), a simple average of the derived precipitation totals can be used to estimate the countywide precipitation. In this example, the county-averaged precipitation is 2.95 cm, far more than either the isohyetal or the Thiessen polygon methods. Interestingly, in this case the gridpoint method produces a value that is very close to the simple arithmetic mean of the four stations.

Which technique is best? This question is difficult to answer, because no technique seems to work most effectively in all locations at all times of year. Of the three techniques, the isohyetal method is considered by some to be most accurate in a higher percentage of cases because the effect of local features, such as topography, water bodies, and land cover, should implicitly influence the weighting scheme. For example, if a mountain is causing a local *orographic effect*, then the region with high precipitation should have a small area. The Thiessen polygon method and the gridpoint technique weigh the stations merely on distance, with no implicit ability to distinguish local features that influence the values at those station points. Conversely, each storm event would require the calculation of new isohyets and weighting systems, whereas for the Thiessen polygon and gridpoint methods, weightings could be established one time and always be the same, as long as no stations appeared or disappeared from the network.

A final technique known as **kriging** uses advanced geostatistical techniques, with the assumption of some uncertainty in the model, to estimate the value at a collection of locations that are not measured. There are various types of kriging that account for the distribution of the modeled data, and kriging allows for both exact and inexact or smoothed interpolations. Inexact interpolations are useful when outliers may

exist that adversely impact the modeled surface, thus eliminating the “bulls-eye” effect. In kriging, a graph called a **variogram** is used to express the relationship between the distance of any two points in the study area and the squared variation in the value between them—in this case, precipitation. The properties of the variogram, including variability in the squared differences used to create it, determines the values at unmeasured locations. Then, one of the other three methods can be used to compute areal-weighted values based on more data points.

Other more advanced twists on the kriging concept exist. For example, the variogram can be modeled as an ellipse to account for directional trends that may exist, such as increased precipitation along a long, narrow mountain range. **Co-kriging** considers the effect of other variables on the spatial interpolation of the variable being mapped using a kriging procedure. And **empirical Bayesian kriging** allows for multiple variograms to be created for subsets of the data during modeling instead of assuming that a singular variogram fits the entire surface. The variograms are then used to create a single surface during the final step of modeling.

So again the question arises—“But which spatial interpolation technique is best?” A common approach for evaluating the relative effectiveness of each spatial interpolation method is to withhold data from one station, while including all of the other station data in interpolating the value of that one “missing” station, using each of the various spatial interpolation techniques. Then the analysis is repeated multiple times, with each station in the dataset being withheld, one at a time, while repeating the same analyses. Then when the actual measured data from each “missing” station is compared to the interpolated data for that station, using each different spatial interpolation technique, the technique that can “predict” the “missing” stations’ data most precisely could be considered as the best technique, at least for that study area, for the variables being considered at that period of time.

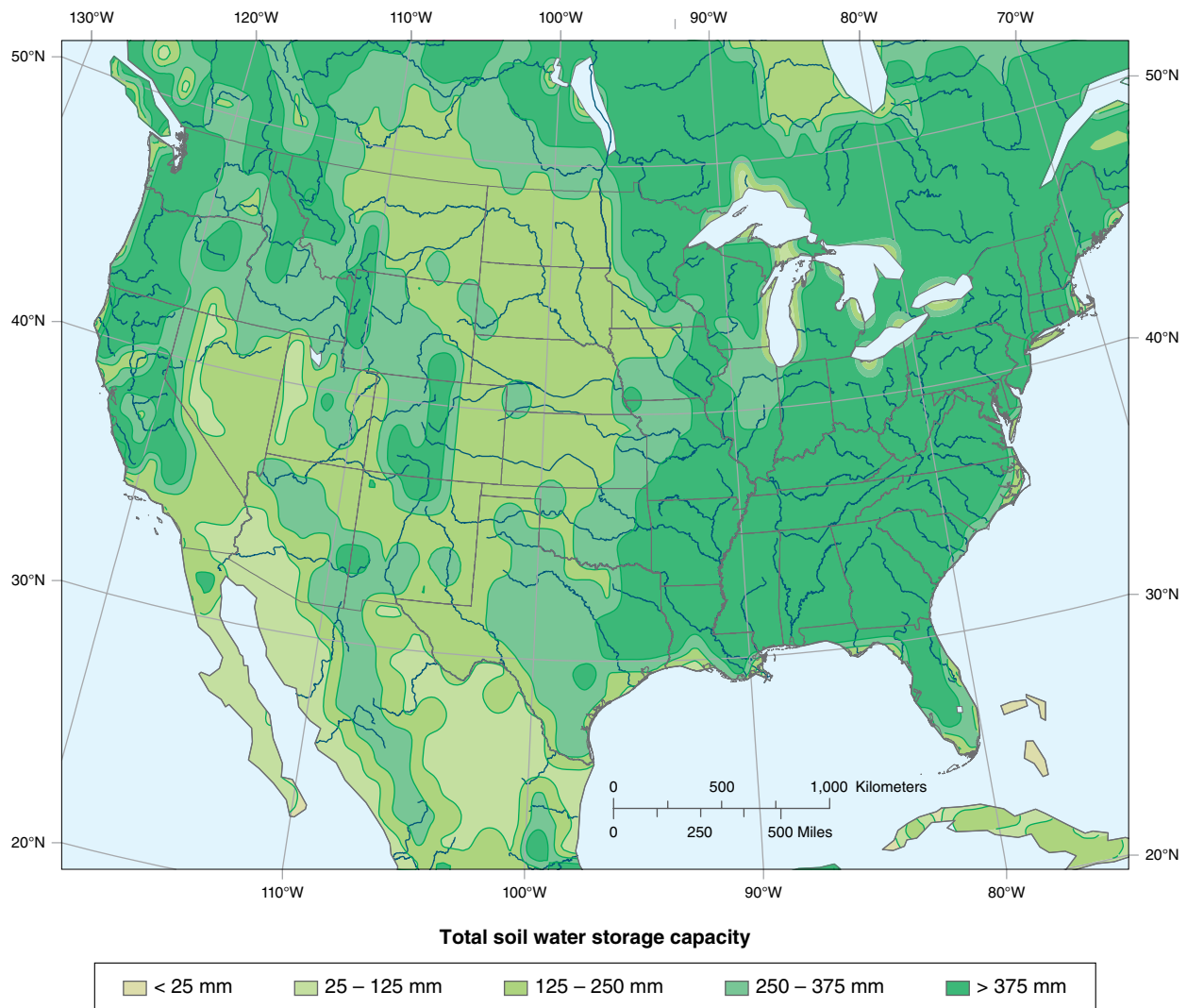


FIGURE 6.14 Soil moisture storage capacity in North America (mm).

Courtesy of Sata A. Ates. Data from: Webb, Robert W., Cynthia E. Rosenzweig, and Elissa R. Levine. 2000. *Global Soil Texture and Derived Water-Holding Capacities*.

Soil Moisture Storage

Soil moisture storage consists of the water available within the rooting zones of plants for transpiration and evaporation. North American and global mean annual soil moisture are shown in **FIGURES 6.14** and **6.15**, respectively. Even though this quantity is a ratio of the volume of water to the volume of Earth in which it sits, this number is converted into equivalent centimeters or inches of precipitation, for easy comparison with PE, ET, and precipitation. Just as a sponge has a limit of water that it can store, the soil also becomes saturated if too much water is present.

The amount of water (in centimeters or inches of precipitation equivalent) that saturated soil can retain against gravity is known as **field capacity** or **soil moisture storage capacity**. This quantity varies locally with the texture, shape, and uniformity of soil particles and the depth of soil.

Porosity—the ratio of the volume of all the pore spaces in a soil to the volume of the whole—is related

to the texture, shape, and uniformity of the soil and also to soil moisture storage. In general, because grains are bigger in sandy soils than in silty or clayey soils, the pore spaces are usually largest. However, porosity may be greater in silty soils because of the high number of pore spaces. On average, perhaps 25% of the volume of a soil may be pore space. If a soil of 25% porosity extends 60 cm (24 in) into the subsurface, then 15 cm (6 in) of water can be held in storage.

Just as soils have a threshold of the maximum amount of water that they can hold, there is also a minimum. Although zero moisture is the theoretical minimum, in actuality even when there is some moisture present in the soil, it may be useless to plants because the **surface tension** of water may be high, which could prohibit it from being usable. Small isolated water drops may adhere well enough to the soil particles that plants cannot pull them upward for transpiration, and they cannot be evaporated. This minimum amount of water (in centimeters or inches of precipitation equivalent) that is necessary in

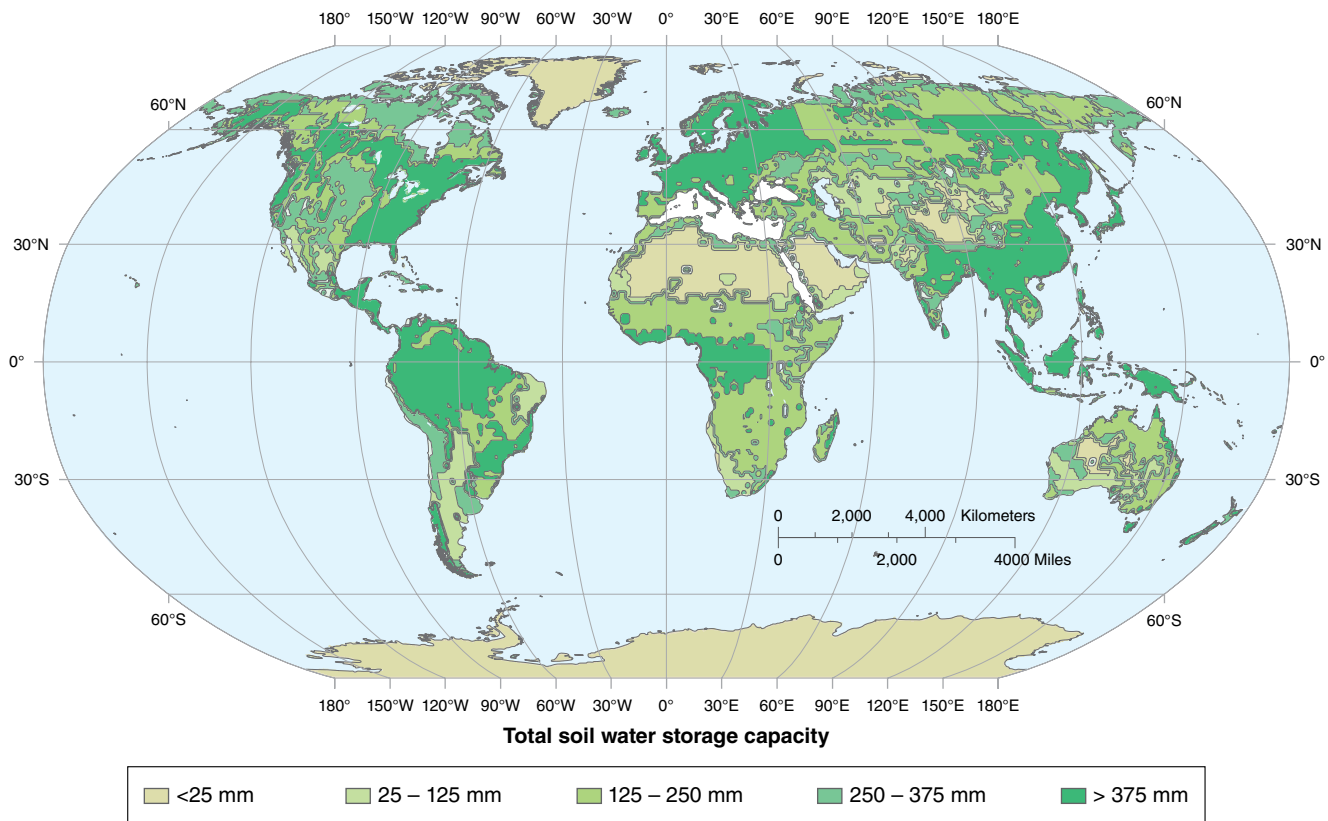


FIGURE 6.15 Soil moisture storage capacity globally (mm).

Courtesy of Sata A. Ates. Data from: Webb, Robert W., Cynthia E. Rosenzweig, and Elissa R. Levine. 2000. Global Soil Texture and Derived Water-Holding Capacities.

the rooting zone to allow extraction by plants is known as the **wilting point**. As the name suggests, any amount of water in the soil less than the wilting point is unable to nourish plants. In most cases a farmer wants to provide sufficient irrigation water to avoid allowing the soil water to decrease to the wilting point.

Deficit

Moisture is not always available in the soil when it is needed. Anytime the atmospheric demand for moisture from the surface (PE) is not fulfilled by some combination of precipitation and by water withdrawn from storage in the soil (**soil moisture withdrawal**), a **deficit** results. By analogy, if the demand for your money (the bills) cannot be paid either by your paycheck (the input) or by your savings in the bank (storage withdrawal), you are said to be in deficit as well. Deficit can be considered to represent the part of PE that is not available to be transmitted to the atmosphere. It is the result of a situation in which the atmosphere has the energy to evaporate more water than it can acquire from the surface either through ET of precipitation or water stored in the soil.

Deficit may be considered as an indicator of environmental stress, and, therefore, it is an important concept for climatologists and those who use climatological data. The lack of precipitation alone may not always represent

the onset of drought; instead, a drought occurs whenever serious deficit occurs, whether or not precipitation has been falling recently. A week without rainfall may produce deficit conditions in summer (when PE is high) but not in winter (when PE is low).

Surplus and Runoff

At the other extreme, during periods of sufficient precipitation we may have a situation of excess water even after PE is satisfied and soil moisture is at field capacity. Any water that is not needed for ET or **soil moisture recharge**—the process of bringing the soil moisture storage to its field capacity—becomes **surplus** water. The rate of recharge depends on the soil's **permeability**—the property that describes the ability of water to flow between soil particles (or rock, in the case of groundwater recharge). Permeability depends on the shape and orientation of the soil (or rock) grains. If the pore space between individual grains is small and/or poorly connected, the permeability is low and falling precipitation generally will not provide fast recharge rates. Note that despite a low permeability, porosity may still be high if there are many small, poorly connected spaces, so soil moisture storage in such a case would be high even though the recharge rate would be slow. On the contrary, a situation in

which there are large and/or well-connected pore spaces allows for high permeability and facilitates the recharge of the soil or groundwater.

Surplus occurs only after precipitation falls on saturated soils. On a watershed basis, the surplus term gives a good estimate of streamflow volumes by applying a statistical relationship, often by estimating that 50 to 60% of the surplus eventually becomes runoff to streamflow. What happens to the remaining surplus? Some becomes **interception**—water that is held on surfaces other than the soil, such as tree leaves and rooftops—until it eventually evaporates. Other water becomes **depression storage**—water that is stored in puddles, gutters, and other natural or artificial “depressions” on the landscape. Still other water percolates to replenish groundwater supplies. These sources generally are not considered separately in the surface water balance—a simple ratio is usually chosen that relates the amount of surplus to the amount of runoff.

Runoff is an important output of the water balance model for numerous reasons. Too much runoff may cause

floods and also makes river navigation hazardous. Too little runoff can cause other types of navigation hazards, and it can also threaten drinking and irrigation water supplies. In addition, the lack of sufficient runoff near the mouths of rivers can cause **saltwater intrusion** from the open ocean up into normally freshwater areas. During the drought of 1988 in the United States, saltwater intrusion into the Mississippi River penetrated over 160 km (100 mi) upriver from the mouth, endangering coastal habitats and ecosystems and threatening drinking water supplies.

In the United States the 13 River Forecast Centers operated by the **National Oceanic and Atmospheric Administration** are responsible for using the precipitation forecasts from the *National Weather Service* as input to water balance models for predicting the streamflow on the nation's waterways (**FIGURE 6.16**). This precipitation must be area-weighted using one or more of the schemes described previously. Then, the water balance model is used to predict not only the **crest**—the peak volume of streamflow—but also the time of peak streamflow after a precipitation event at various points

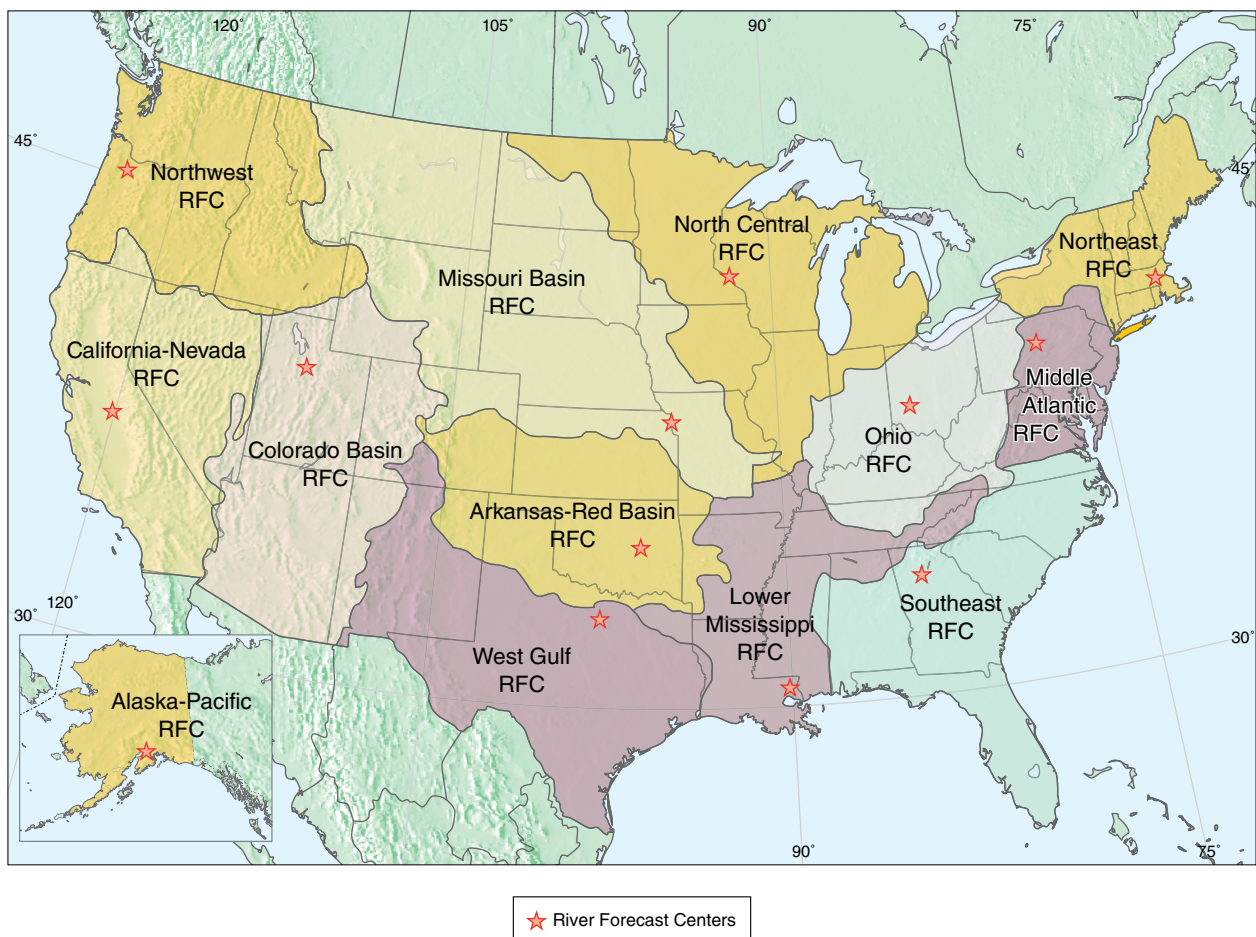


FIGURE 6.16 The 13 River Forecast Centers (RFC) in the United States operated by the National Oceanic and Atmospheric Administration.

Data from NOAA.

along the stream resulting from either local and/or upstream precipitation. The quality of the forecasts depends on both the accuracy of the National Weather Service precipitation forecasts and the accuracy of the water balance results for upstream regions produced by other river forecast centers. Errors in either step cause errors in the stream forecasts. Accurate stream forecasts can be of great societal and economic benefit, because floods claim more lives and property losses in the United States and the world than any other form of weather-related hazard.

▶ Putting It All Together: A Worked Example of the Surface Water Balance

The best way to understand how the surface water balance operates is to work through an example. **TABLE 6.1** shows a mean monthly water balance for Baton Rouge, Louisiana. The mean monthly PE (in centimeters, based on the modified Thornthwaite calculations) and

TABLE 6.1 Mean Monthly Water Balance in (a) Centimeters and (b) Inches for Baton Rouge, Louisiana

[illegible]

precipitation values (based on 30-year averages of rain gauge measurements) are given. These represent the data needed to complete the rest of the calculations.

From these data and the assumption that the balance begins with a saturated soil, we can do some simple arithmetic to calculate the water balance. Specifically, we can see that in January mean precipitation exceeds PE by 9.4 cm (3.7 in). But because the soil is already at field capacity at the beginning of January (by assumption), all this extra water goes to surplus. The same situation occurs in February, March, and April, with 9.9, 8.9, and 5.4 cm, respectively (3.9, 3.5, and 2.1 in), going into surplus. May is the first month of the year when mean PE exceeds mean precipitation. The 0.7 cm (0.3 in) that the atmosphere demands but does not receive from precipitation is accommodated by soil moisture withdrawal. This results in a change in soil moisture storage (ΔST) of -0.7 cm (-0.3 in) and a total ST of 14.3 cm (5.7 in). Likewise, in June, July, and August the amount of water that the atmosphere needs but cannot receive through precipitation is also available in storage. So neither surplus nor deficit exists for the period of May through August. Continual soil moisture withdrawal through these months results in only 1.2 cm (0.5 in) of precipitation in storage by the end of August. This water is not adequate to accommodate the 2.7 cm (1.1 in) demand for water in September that is not provided by precipitation. Therefore, a deficit of 1.5 cm (0.6 in) is accumulated in September. Likewise, a deficit of 0.5 cm (0.2 in) occurs in October. But the decreasing PE values cause precipitation to exceed the atmospheric demand for water in November and December. Soil moisture recharge in Baton Rouge occurs until the soil has returned to field capacity (15 cm, or 6.0 in) by the end of December.

When working through a continuous surface water balance simulation, the calculations should begin at least a year before the time for which data are needed. The reason is that an “adjustment” time is needed so that calculations can begin at an accurate initial amount of soil moisture storage. By including a year or two before the “actual” period, the chances are more likely that at some point in that initial period (particularly in winter, when PE is lowest), the simulation will correctly indicate that soil moisture is at field capacity. From that point forward, the results will be “correct.” Of course, in drier climates it may be necessary to use a much longer initial period to ensure that at some point before the “actual” data are computed the simulation became calibrated correctly.

When performing any water balance analysis, two equations can be used to verify that the calculations are correct:

$$P = ET + S \pm \Delta ST$$

$$PE = ET + D$$

where S is surplus, ST is soil moisture storage, and D is deficit. If either of these equations does not balance, then an error has been made. Conceptually, the first equation suggests that the input of precipitation must be balanced by some combination of the three places that the water can be assumed to go: ET, surplus, and soil moisture recharge/withdrawal. The second equation states that the amount of water that the atmosphere could use must equal the amount of water that the atmosphere receives plus the amount that it could use but does not receive. These equations verify that the calculations shown in Table 6.1 are correct for each of the 12 monthly totals and for the annual sum.

Finally, it should be noted that a surface water balance model may be run for time intervals other than monthly. Some applications require daily water balance conditions, whereby daily estimates of PE and measurements of precipitation are used to simulate moisture conditions in the soil. Agriculturalists may use daily water balance models along with daily weather forecasts to determine the optimal amount and timing of irrigation to use for a crop.

► Types of Surface Water Balance Models

Some surface water balance models, such as the one just described, are **equal availability water balance models**. These assume that soil water is equally available to be evapotranspired regardless of the amount of storage in the soil. In applications for which more precision is needed, a **decreasing availability water balance model** may be implemented. Such models assume that as soil moisture withdrawal increases, the water becomes increasingly more difficult to be moved upward via ET. This is done through a new variable called **accumulated potential water loss**, which is usually given in a tabular format, based on the field capacity of a given soil, following work done by Thornthwaite and his colleague John Mather. The accumulated potential water loss is a running total of the $P - E$ value (provided it is a negative number). In principle, the decreasing availability model mimics the “real world” because as the soil begins to dry out, *guard cells* begin to resist the loss of moisture through the *stomates* of plants via ET. Furthermore, as the soil dries an increasingly higher percentage of water in the soil is “stuck” by surface tension to soil and rock particles and cannot be lost to the atmosphere easily.

Another modification that may be made to the surface water balance is to divide the surface zone into two or more layers. The model may be tweaked to allow water to be lost more freely from the top layer but more stringently from successively lower layers. For example, an equal availability assumption may be made in the top layer but a decreasing availability model may be implemented for the bottom layer.

► Water Balance Diagrams

Because of the difficulty of ascertaining a general impression of the hydroclimatology by simply examining a table of numbers, a **water balance diagram** provides a helpful way of evaluating the water balance of a location. In this book, all water balance diagrams are generated using WebWIMP, courtesy of the University of Delaware. **FIGURE 6.17** shows an example of a mean monthly water balance diagram for Dallas, Texas. Note, however, that water balance diagrams need not be for mean hydroclimatic conditions but may also depict actual moisture conditions over any period of time desired.

In the water balance diagram, the PE curve always mimics the temperature curve, because PE is a function of temperature and the number of daylight hours. In Figure 6.17 PE is represented as a dashed line. The precipitation line for Dallas (the solid line in Figure 6.17) shows a fairly even distribution throughout the year, with a slight peak in spring and a secondary peak during autumn. The graph for Dallas shows that for the

period of October through May, precipitation exceeds PE, resulting in an abundance of water at the surface.

Soil moisture recharge is represented by the area between the precipitation and the PE curves when precipitation exceeds PE and the soil is not yet at field capacity. This happens climatologically in Dallas from October through late January (Figure 6.17). On the water balance diagram, surplus is represented by the area between the precipitation and the PE curve when precipitation exceeds PE and the soil is at soil moisture capacity. The graph also shows that by the end of January the soil is at field capacity in Dallas, and all excess water from that point until the end of May becomes surplus. In the water balance diagrams throughout this book, surplus includes surface runoff, subsurface runoff below the plant root zone, interception, and depression storage.

In June, $P - E$ is negative in Dallas, and soil moisture withdrawal commences. Soil moisture withdrawal is represented by the area between the precipitation curve and the ET curve (the dotted line in Figure 6.17), when precipitation is less than PE. The ET curve also usually peaks in summer, as it does in Dallas, but unless the soil is so wet that the atmosphere is always getting enough water (which does not happen in Dallas), this curve is not always as high as the PE curve.

Between June and October in Dallas, some of the water demanded by the atmosphere cannot be fulfilled by the amount of water in storage. The graph shows this deficit as the area between the PE and ET curves. Thus, the period of July through September tends to accumulate the largest deficits in Dallas on a climatological basis. By October the return of “wet” (positive $P - E$) conditions puts an end to the deficit.

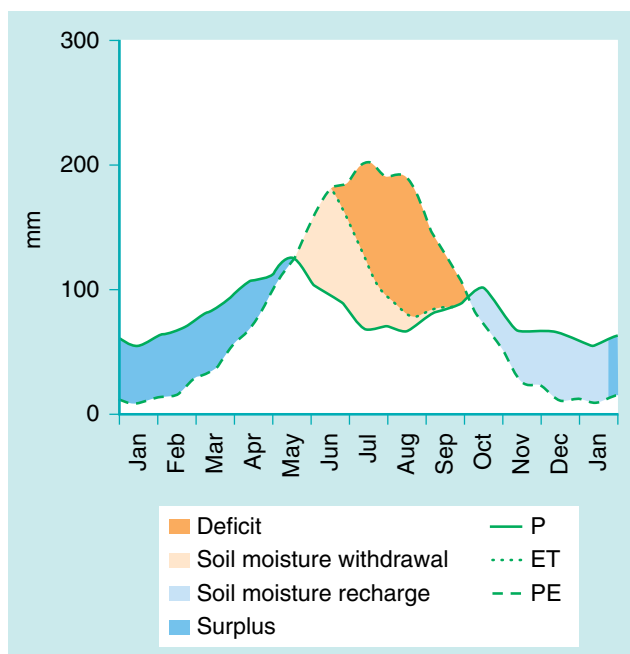


FIGURE 6.17 Mean water balance diagram for Dallas, Texas.

Modified with permission using WebWIMP version 1.01 implemented by K. Matsuura, C. Willmott, and D. Legates at the University of Delaware in 2003.

► Drought Indices

Several drought indices based on the water balance model have been developed to provide a sense of the severity of flood or drought conditions in the United States. Maps of several drought indices are available on the Internet on a near-real-time basis. For example, the **Palmer Drought Severity Index (PDSI)** provides an assessment of long-term moisture conditions on a weekly basis by climate division across the United States (**FIGURE 6.18**). The PDSI is produced by the Climate Prediction Center and is derived by comparison with normal conditions for a **climate division**, with zero representing average soil moisture conditions at that climate division for that time of year. Likewise, positive values represent above-normal moisture conditions for that location and negative values are used for drier-than-normal soil moisture. Notice in Figure 6.16 that in some cases the lack of abundant data in sparsely populated areas may make for interesting spatial

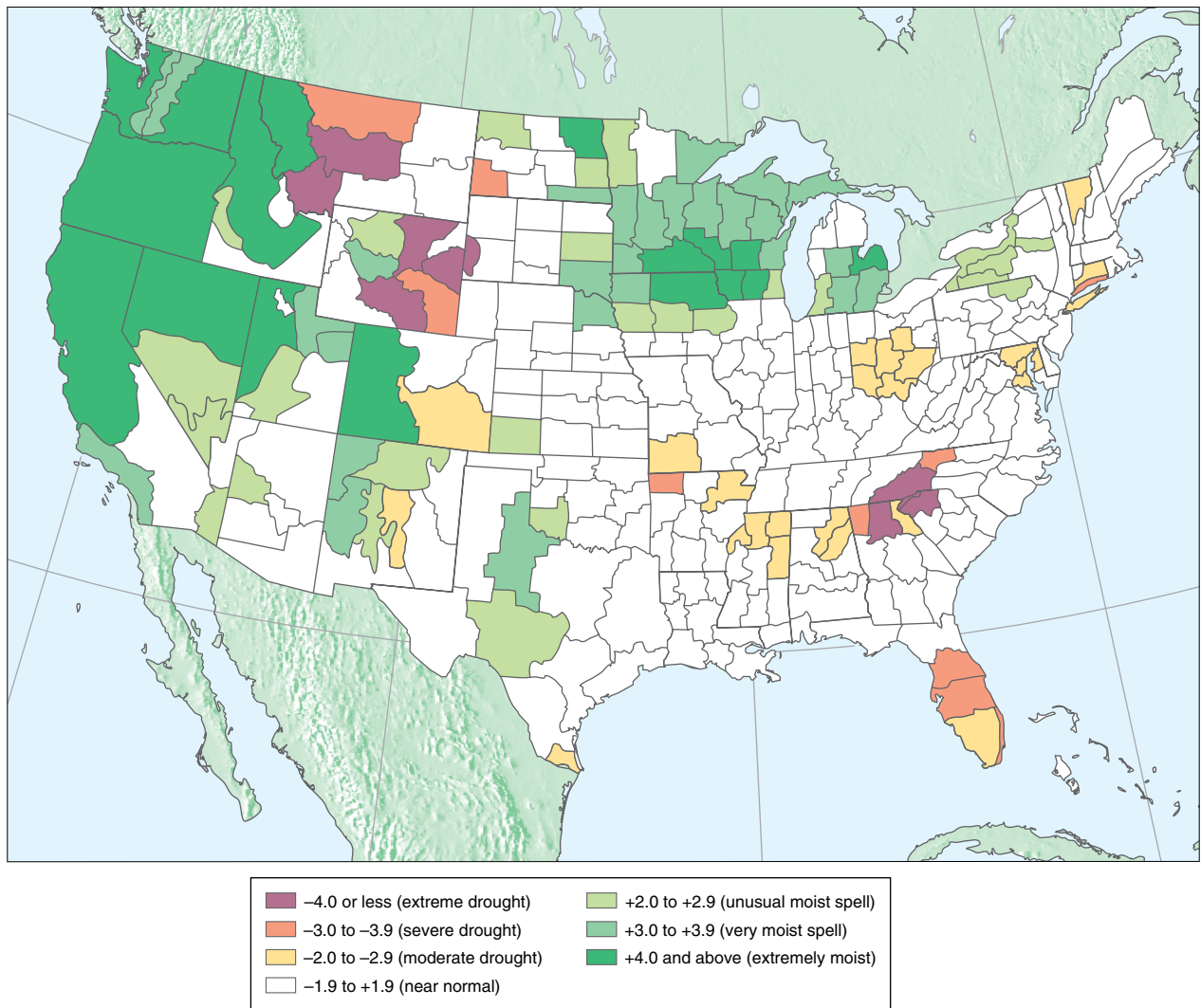


FIGURE 6.18 Palmer Drought Severity Index for the week ending February 11, 2017.

Data from NOAA.

patterns. For example, northwestern Nevada's PDSI values contrast with those in adjacent states.

Because the calculations for PDSI involve relatively deep soil moisture conditions, PDSI is often considered to represent long-term moisture. A modest rain event or two is unlikely to end dry conditions at a location, and a few rainy days are unlikely to instigate flood conditions. For some applications the lag between the onset of a wet or dry period and the appearance of a PDSI that corresponds to these moisture conditions is too long to provide adequate warning. This index should therefore be used only when assessing long-term moisture conditions. For example, water resource planners are likely to use the PDSI to assist in policy related to long-term water budgeting. Similar to the PDSI is the **Palmer Hydrological Drought Index**, a measure used for even longer-term analysis than the PDSI that reflects conditions relating to groundwater availability and reservoir supplies.

Another commonly used tool based on the water balance is the **Crop Moisture Index (CMI)**, which is also produced for the United States by the Climate Prediction Center. Like the PDSI, the CMI is customized for comparison with climatological conditions at a location, with positive values representing moist conditions for that location at that time of year and negative indices representing successively drier conditions (**FIGURE 6.19**). Unlike the PDSI, the CMI is weighted heavily in the uppermost soil layers, which causes changes in soil moisture conditions to appear relatively quickly compared with the PDSI. Thus, a rain event or two, or a few dry days, can strongly impact the CMI at a particular location. This index is more useful for short-term agricultural interests because most crops require the presence of moisture in the near-surface soil so that it can be easily accessed by the crops.

A final important index is the **Keetch-Byram Drought Index**—a measure designed by the U.S. Forest Service to assess the risk of fire potential by examining

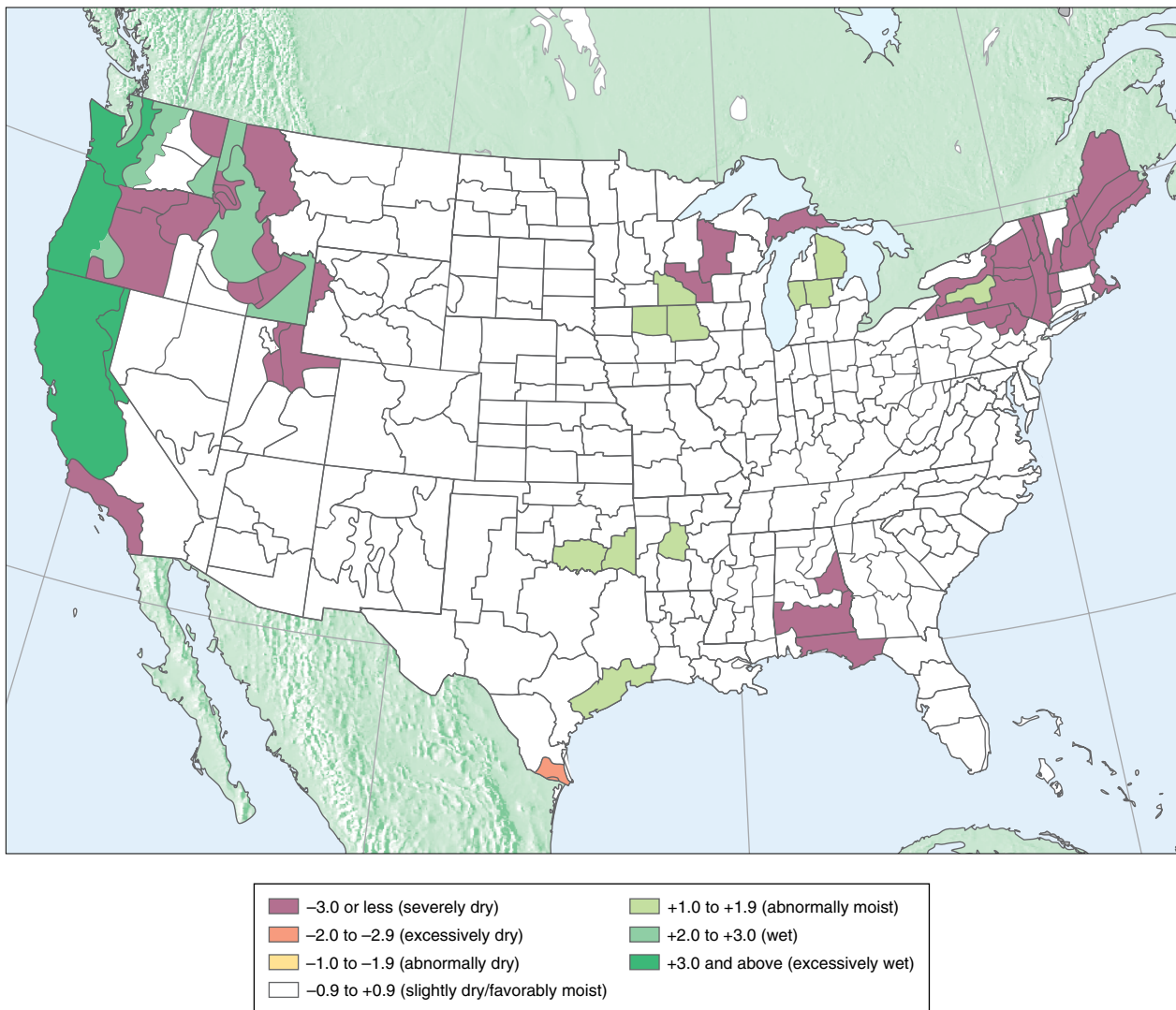


FIGURE 6.19 Crop Moisture Index for the week ending February 11, 2017.

Data from NOAA.

the relationship between ET and precipitation in the organic matter on a forest floor and in the uppermost soil layers. Like the PDSI and CMI, the Keetch-Byram Drought Index is run continuously and is available on a near-real-time basis. Values range from 0, representing no fire hazard, to 800, representing the most severe hazard potential (**FIGURE 6.20**).

► Summary

The global hydrologic cycle involves both reservoirs and fluxes. Reservoirs are dominated by the world ocean and the cryosphere, but the most accessible water for human consumption is in small and unevenly distributed reservoirs across Earth, including ground and soil moisture, streams, freshwater lakes, and the atmosphere. Net fluxes in the global hydrologic cycle circulate water

from the ocean surface to the marine atmosphere, to the terrestrial atmosphere, to the land surface, and back to the ocean via runoff. Although these fluxes seem robust, they are affected by human activities, particularly on climatological time scales. The global water balance equation can be used to describe the major fluxes, but it ignores locally important features such as infiltration, percolation, interception, and depression storage.

Hydroclimatic conditions at a location can be modeled using the surface water balance. In this technique PE is calculated—for example, by using a variation of Thornthwaite's method or by the Penman-Monteith method—and is compared with precipitation during the time period of interest. Precipitation is measured via a network and, like any of the other water balance variables, can be areally weighted to convert point estimates to an areal estimate. If excess water is available at the surface after PE is fulfilled, soil moisture recharge occurs, and if

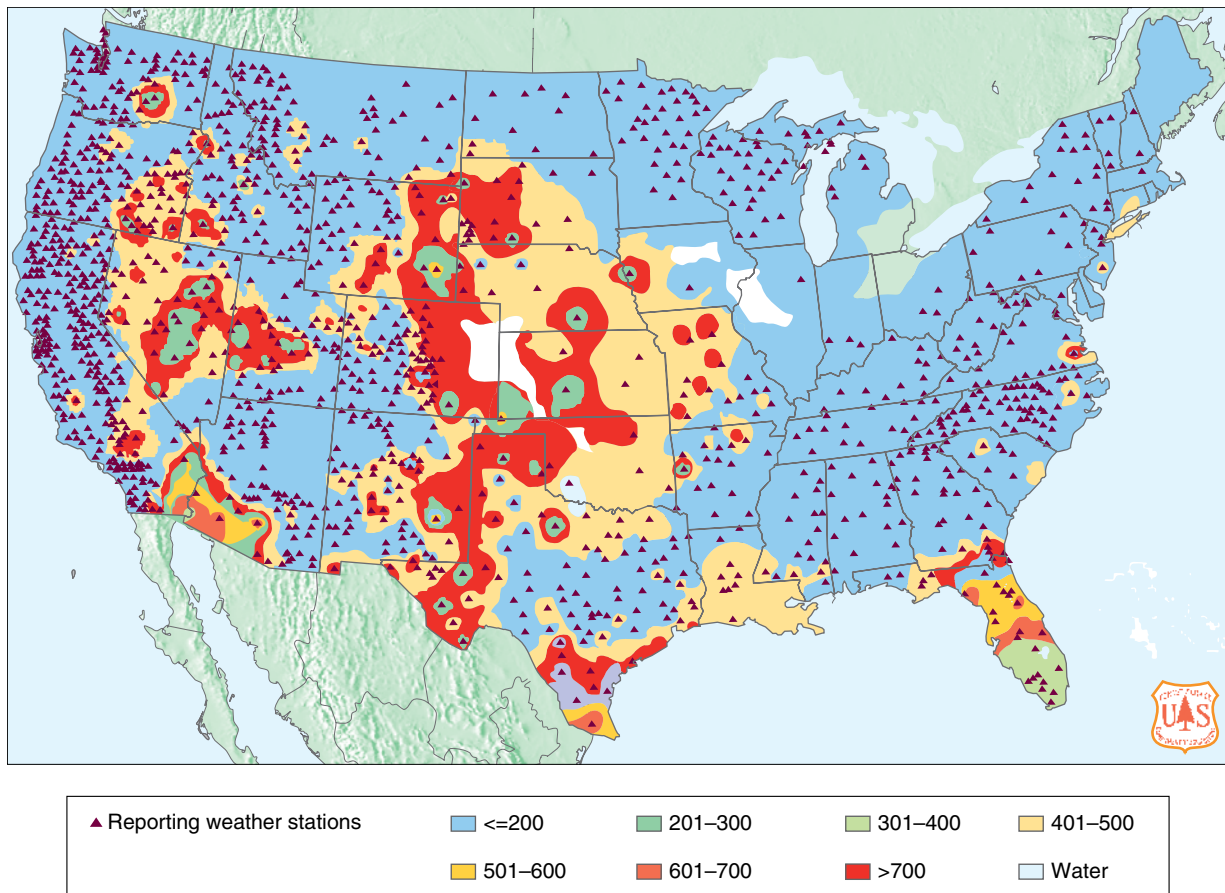


FIGURE 6.20 The Keetch-Byram Drought Index for February 15, 2017.

Data from the U.S. Forest Service/Wildland Fire Assessment System, Missoula, MT.

the soil reaches field capacity, surplus and runoff result. On the other hand, if insufficient moisture is available through precipitation to satisfy the atmospheric demand for water (represented by PE), soil moisture withdrawal occurs. If the soil moisture is inadequate to supply the necessary water to the atmosphere, the actual ET is less than the PE and deficit results.

Equal availability water balance models assume that regardless of soil moisture content, water is withdrawn equally easily during wetter and drier periods, whereas

decreasing availability water balance models assume that the loss of moisture is hindered when it becomes limiting, because of resistance from vegetation. Water balance diagrams represent a relatively simple means of assessing moisture conditions at a place graphically, either on a mean climatological basis or for a particular duration of time. Likewise, drought indices based on water balance models, such as the PDSI and the CMI, have been developed to provide a near-real-time assessment of hydroclimatic conditions across the United States.

Key Terms

Accumulated potential water loss

Advection

Bernoulli effect

Blaney-Criddle model

Clausius-Clapeyron equation

Climate division

Co-kriging

Condensation

Crest

Crop Moisture Index (CMI)

Cryosphere

Decreasing availability water
balance model

Deficit

Deforestation

Deposition

Depression storage

Dewpoint temperature

Empirical Bayesian kriging

Equal availability water balance
model

Evaporation

Evapotranspiration (ET)

Field capacity

<i>Flux</i>	National Oceanic and	Sensible heat flux
Geographic information systems	Atmospheric Administration	Soil moisture recharge
<i>Global hydrologic cycle</i>	<i>National Weather Service</i>	Soil moisture storage capacity
Global water balance equation	<i>Net radiation (Q^*)</i>	Soil moisture withdrawal
Gridpoint technique	<i>Orographic effect</i>	<i>Stability</i>
Groundwater	Palmer Drought Severity Index	<i>Stomate</i>
<i>Guard cell</i>	(PDSI)	<i>Substrate heat flux (Q_G)</i>
<i>Hydrosphere</i>	Palmer Hydrological Drought	Surface tension
Infiltration	Index	Surface water balance
<i>Insolation</i>	Penman-Monteith equation	Surplus
Interception	Percolation	Thiessen polygon method
Isohyet	Permeability	Thornthwaite potential
Isohyetal method	Porosity	evapotranspiration
<i>Isotherm</i>	<i>Potential evapotranspiration (PE)</i>	<i>Transpiration</i>
<i>Joule</i>	Precipitable water	Turc method
Keetch-Byram Drought Index	<i>Relative humidity</i>	Undercatch
<i>Kelvin temperature scale</i>	<i>Reservoir</i>	<i>Vapor pressure</i>
Kriging	<i>Residence time</i>	Variogram
Latent heat flux	Resistance	Water balance diagram
<i>Latitude</i>	Runoff	Wet bulb depression
<i>Lithosphere</i>	Saltwater intrusion	Wilting point
<i>Lysimeter</i>	<i>Saturation vapor pressure</i>	

Terms in italics have appeared in at least one previous chapter.

Review Questions

- Where are the major reservoirs and fluxes in the global hydrologic cycle? What are their relative sizes?
- Explain the difference between percolation and infiltration.
- What are some of the major advantages and criticisms of the Thornthwaite method of calculating PE?
- How does the Penman-Monteith method of calculating PE differ from Thornthwaite's method?
- How does the depth of snow in a gauge compare with the equivalent amount of liquid precipitation?
- What is undercatch? How and why does it occur?
- How can point-based estimates of rainfall be converted to areal estimates?
- What advantages does the isohyetal method offer over the Thiessen polygon method and the gridpoint technique?
- Under what circumstances is ET less than PE in the natural environment?
- How does porosity relate to soil moisture storage capacity?
- Why is the wilting point an important measure of moisture content in the soil?
- Which of the surface water balance variables is most indicative of drought? Why?
- In the surface water balance, why is runoff only a part of the total surplus value?
- What is the difference between an equal availability and a decreasing availability water balance model?
- When should the Palmer Drought Severity Index be used instead of the Crop Moisture Index to assess environmental moisture conditions?

Questions for Thought

- What effect does a large soil moisture storage capacity have on a location as compared with another location that has the same precipitation and PE totals but a lower soil moisture storage capacity?
- How do impervious surfaces such as parking lots impact the water balance terms?
- Why is it so complicated to estimate the potential impacts of global warming on the surface water balance at a location?



CHAPTER 7

General Circulation and Secondary Circulations

CHAPTER AT A GLANCE

- Circulation of a Nonrotating Earth
- Idealized General Circulation on a Rotating Planet
 - Hadley Cells
 - Polar Cells
 - Planetary Wind Systems
- Modifications to the Idealized General Circulation: Observed Surface Patterns
 - Land–Water Contrasts
 - Locations and Strength of Features in the Hadley Cells
 - Locations and Strength of Features in the Polar Cells
 - Locations and Strength of Surface Midlatitude Features
- Putting It All Together: Surface Pressure Patterns and Impacts
- Modifications to the Idealized General Circulation: Upper-Level Airflow and Secondary Circulations
 - Vorticity
 - Constant Absolute Vorticity Trajectory
 - Flow Over Mountainous Terrain
 - Baroclinicity
 - Rossby Wave Divergence and Convergence
 - Rossby Wave Diffluence and Confluence
 - Polar Front Jet Stream
 - Mean Patterns of Rossby Wave Flow
- Summary
- Key Terms
- Review Questions
- Questions for Thought

Collectively, the processes occurring within the various components of the climate system contribute to the “real-world” atmospheric circulation and its variations. This chapter explains **general circulation**—the overall, prevailing pattern of winds on large spatial and temporal scales. Certainly, some circulations are local and unusual compared with the overriding, prevailing patterns. At broad spatial scales over a long period of time, however, the atmosphere’s preferred directions of circulation are particularly noticeable. These patterns steer energy, matter (especially water and solid *aerosols*), and *momentum* from one part of Earth to another.

Circulation results from fulfillment of the *second law of thermodynamics*. One form of this law states that energy tends to be moved from areas of greater concentration to areas of lesser concentration. Because the Sun heats Earth’s surface unequally, a circulation must exist in the atmosphere and oceans that attempts to equalize this energy imbalance. But the energy can never be balanced perfectly because as the general circulation of the atmosphere and the oceans continuously attempts to redistribute the energy, the Sun continuously warms different parts of the Earth at different rates.

Specifically, the general circulation redistributes heat (energy) that arrives at the Earth in greater quantities near the equator than near the poles. Factors such as the unequal distribution of land mass with *latitude* and variation of landforms and land cover types across the terrestrial Earth have concomitant implications for the radiation balance, thereby complicating the general circulation. Specific climate types result from this general circulation.

In addition to general circulation, this chapter focuses on **secondary circulations**—smaller circulation systems that are characterized by traveling high- and low-pressure systems that affect climate. These circulations are influenced in the midlatitudes by their position relative to planetary-scale waves of motion. This chapter also examines the relationship between these waves and surface *anticyclones* and *cyclones*.

► Circulation of a Nonrotating Earth

Before we can understand the atmosphere’s general circulation on the “real” Earth, let us first consider the properties of the circulation if Earth did not rotate. The British meteorologist Sir George Hadley first postulated the general atmospheric circulation in 1735. His studies centered on a simple model of hemispheric *convection*. He posited that air should warm, become less dense,

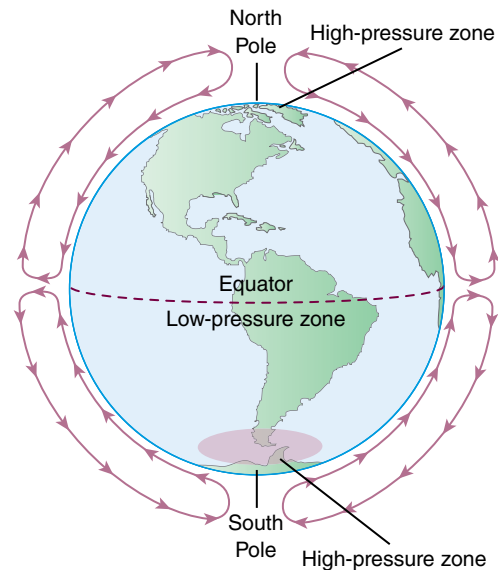


FIGURE 7.1 The simple hemispheric convection cell model of atmospheric circulation proposed by Hadley.

and rise in the area near the equator (**FIGURE 7.1**). Following the model of a convection cell, he thought that this rising equatorial air would then travel poleward far above the surface (in both the northern and southern hemispheres), ultimately cooling and sinking in the polar areas. This air stream would then diverge at the surface in the vicinity of the poles and move back equatorward across the surface to begin the process anew. The sinking air at the poles from this circulation would produce a permanent surface anticyclone at each pole. A belt of low pressure would exist in the equatorial region, with the lowest pressure along the *longitude* that was being heated most directly—experiencing *solar noon*—at that particular time of day.

The major problem with Hadley’s view of atmospheric circulation was that it did not match observed data of wind patterns reported from sailing vessels across the globe. The circulation of the planet is more complex than the simple single hemispheric convection cell pattern suggested by Hadley. Still, Hadley’s work was the first to include the upper atmosphere in thoughts centered on the general circulation of the atmosphere, and for that it gains merit.

There are two main complications that Hadley did not consider. The first is that Earth’s surface is not uniform. Rather, it has many different topographic and land/water surface variations that upset the formation of a single hemispheric convection cell in each hemisphere. Because these variations are often local or regional, they tend to contribute even more to local and synoptic circulation patterns than to changes in the “general” circulation. The second complication—the rotation of Earth—exerts a more direct influence on the general

circulation. This rotation initiates trajectory changes in moving fluids through the *Coriolis effect*.

► Idealized General Circulation on a Rotating Planet

Hadley postulated correctly that, in general, air near the equator gains thermal buoyancy because of its warmth. He was also correct to infer that the cold air near the poles has a tendency to sink. We have already seen that rising air is generally associated with atmospheric low-pressure situations, whereas sinking air is typically linked to high-pressure systems. A broad belt of low surface pressure dominates the equatorial region, whereas higher surface pressures exist over the poles.

Hadley Cells

Hadley also proposed that air rising near the equator begins moving toward the poles in the upper *troposphere*. This upper-level poleward motion occurs because of an upper atmospheric pressure gradient that pushes

air away from the equator (where there is an excess of pressure aloft caused by the “extra” air that rose from the surface). **FIGURE 7.2** shows a model of the general circulation on a rotating planet.

Unlike the model originally proposed by Hadley, most of the air aloft flowing away from the equator does not actually travel all the way to the poles. Instead, much of it cools while it is high above the surface and sinks in the vicinity of 30° latitude (both north and south of the equator). A small amount of air does continue poleward though, and provides the mechanism by which heat and matter are circulated and redistributed poleward beyond 30° latitude. The air that sinks near 30° latitude diverges from the point of impact at the surface near 30° latitude, forming the *subtropical anticyclones*, or subtropical highs, which are centered at approximately 30° latitude in each hemisphere. As we see later, the highs are situated over each major ocean basin.

The region of the subtropical anticyclones also is known as the **horse latitudes**—a term derived from the days of European exploration when sailors are said to have discarded horses overboard when they found themselves under the stagnant regions beneath the

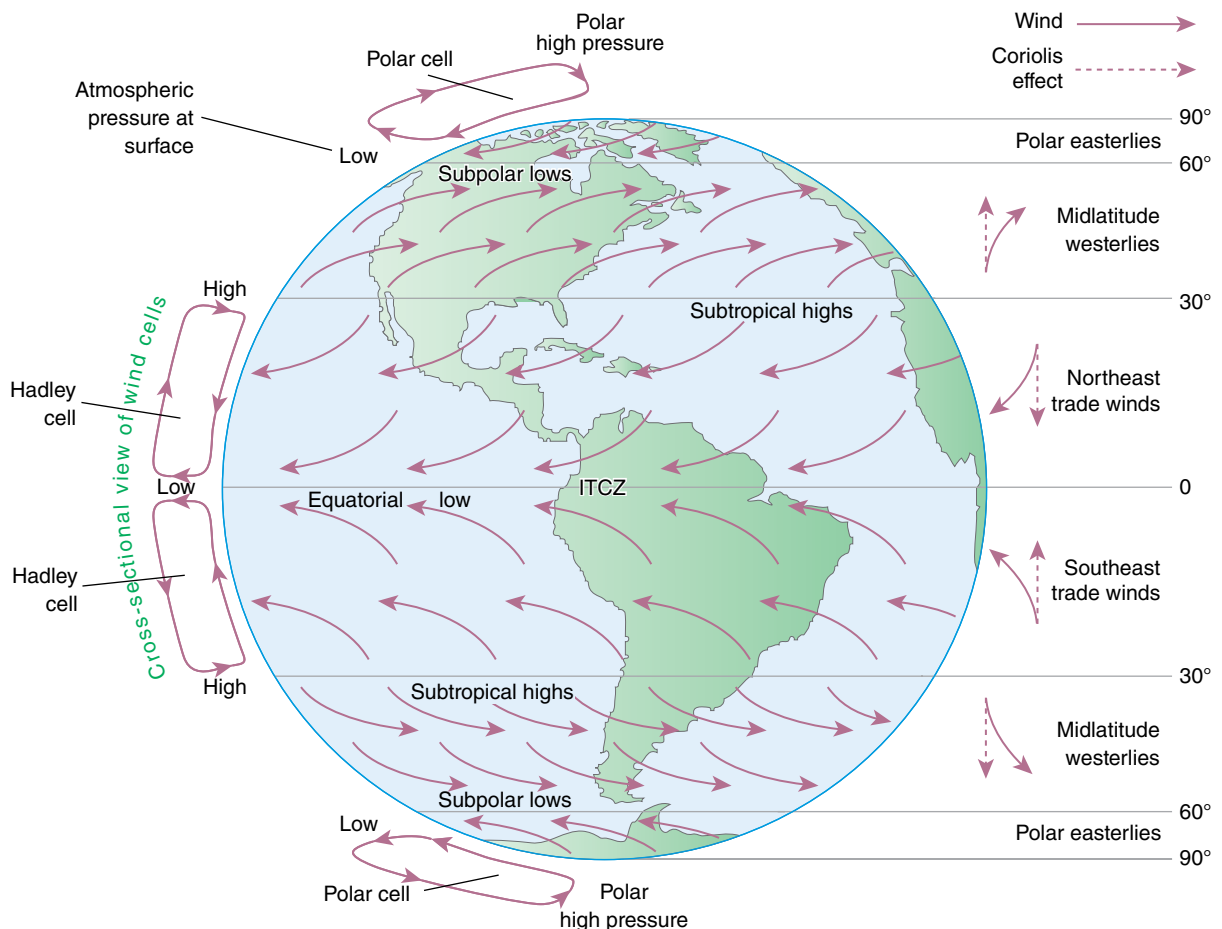


FIGURE 7.2 Pressure and wind belts of the three-celled general circulation model.

high-pressure zones. The weak descent of air through the atmosphere in these regions provides little in the way of steering currents necessary to push sailboats across vast distances. Sailing vessels frequently stalled in these areas. Water shortages ensued, which sealed the fate of horses onboard. The subtropical anticyclone region of the North Atlantic Ocean where the **Bermuda-Azores high** is located is also known as the **Sargasso Sea** because of the prevalence of the sargasso seaweed that accumulates seasonally in the rather calm, stagnant waters under sunny skies.

This circulation between the equator and 30° latitude is largely convective, as vertical motions within it are driven solely by *sensible heating*. This convection cell, with rising motion near the equator and sinking motion near 30° latitude, is termed a **Hadley cell**; one Hadley cell exists in each hemisphere.

Polar Cells

Near the poles the net energy deficits reinforced by high *attenuation* rates, increased *beam spreading*, and the high *albedo* of snow and ice in polar areas cause the air to increase in *density*, which initiates sinking motions through the atmosphere. This air diverges at the surface, inducing the permanent high atmospheric pressure at the surface—the **polar highs** (one at each pole). The polar high is also termed the “polar vortex,” a name that has gained recent media attention, especially during winter when expansion carries very cold air to lower latitudes.

Upon reaching the surface, the diverging air travels equatorward toward lower latitudes, is deflected by the Coriolis effect, and eventually converges at approximately 60° latitude with air that was diverging from the subtropical anticyclones at 30°. The converging air near 60° latitude is forced to rise. As we have seen, rising air motions are associated with low atmospheric pressures. The convergence creates **subpolar lows**—areas of relatively low surface pressure centered on 60° latitude in each hemisphere. Most of the air aloft over the subpolar lows continues back poleward, resulting in one circulation system in each hemisphere known as the **polar cells**. A small amount of the atmospheric mass does continue equatorward aloft; this air contributes to the equator-to-pole redistribution of energy and matter.

Planetary Wind Systems

As we have seen, starting at the poles and moving toward the equator at 30° intervals of latitude are surface oscillations of high (near 90°), low (near 60°), high (near 30°), and low (near 0°) pressure in each hemisphere (Figure 7.2). These differences in pressure across space

set up differences in atmospheric mass, because pressure is a function of force (which is the product of mass and acceleration according to *Newton’s second law*). Because mass is transferred from areas of higher concentration to areas of lower concentration, this general surface pressure distribution sets up the planetary wind systems. Winds are simply the transfer of atmospheric mass between an area of excess mass and an area containing less mass. Because pressure differences define winds, let’s begin our discussion with an examination of the influence of the major pressure features on surface wind patterns.

Surface Wind Systems

As with all surface anticyclones, air in the subtropical anticyclones at approximately 30° latitude in each hemisphere sinks and diverges across the surface in all directions. The *pressure gradient force* pushes air directly toward lower pressure areas—namely, toward 0° and 60° latitude in each hemisphere, the equatorial and subpolar lows, respectively. Because of the rotation of the planet, the Coriolis effect deflects these surface winds to the right in the northern hemisphere. This causes air diverging from the northern hemisphere’s subtropical highs to flow clockwise (anticyclonically) as it moves outward. Likewise, air diverging from the southern hemisphere’s subtropical highs flows counterclockwise—also anticyclonically for that hemisphere—as it moves outward away from the high, as the Coriolis effect deflects motion to the left in that hemisphere (Figure 7.2).

Surface winds moving between 30°N and the equator therefore take on a motion that is from the northeast. As we saw elsewhere in the text, winds are always named for the direction from which they blow. These winds are, therefore, appropriately called the *northeast trade winds* (or northeast trades). They are termed “trade winds” because they constituted the primary sailing trade route between southern Europe and Spanish America across the North Atlantic Ocean. The northeast trade winds steered Christopher Columbus from his point of departure in Spain toward his unintended destinations in the Caribbean, Central America, and northern South America. A strong argument can be made that Spanish is the primary language spoken in Latin America and the Caribbean because of the northeast trade winds!

The southern hemisphere also has trade winds, but the leftward deflection of the Coriolis effect causes air flowing out of the subtropical anticyclones to move counterclockwise and surface winds to move primarily from the southeast between 30°S latitude and the equator. These are called the *southeast trade winds* (or southeast trades). It should be easy to remember that the northeast trades occur in the northern hemisphere, whereas the southeast trade winds occur in the southern hemisphere.

Because the northeast and southeast trade winds converge into the low-pressure equatorial low, the equatorial low is sometimes known as the **Intertropical Convergence Zone (ITCZ)**. Although the name appears rather imposing, it is quite explanatory as it describes surface airflow across the tropics that converges in a zone across the low latitudes. The ITCZ also carries another name—the **doldrums**, a belt of relatively stagnant winds that form as air rises from the surface because of trade wind convergence from both hemispheres. Sailing ships venturing into this area would often stagnate for long periods. Being “stuck in the doldrums” achieved colloquial status, signifying a depression of some sort. Interestingly, the doldrums became the region of many mutinies, including the famous mutiny of Captain Bligh on the *HMS Bounty*.

On the poleward sides of the subtropical anticyclones, the surface pressure gradient force pushes air from the high-pressure core toward the subpolar lows. This air is then deflected to the right (in the northern hemisphere) or the left (in the southern hemisphere) on its trek to fill in the subpolar low. In this case, though, the latitude is higher than in the case of the tropical trade winds, so the Coriolis deflection is stronger. Recall that the magnitude of the Coriolis deflection is proportional to latitude. This strong deflection causes the general circulation between 30°N and 60°N latitude to be approximately from west to east near the surface. This surface wind belt is known as the **midlatitude westerlies**. The southern hemisphere also has westerlies between 30°S and 60°S latitude. Even though the Coriolis deflection in that hemisphere is from the opposite direction, the fact that the midlatitude zone is south of the subtropical anticyclone rather than north of the high (as in the northern hemisphere) causes surface westerly winds to exist in the southern hemisphere as well.

Air sinking to the surface and diverging equatorward at the polar highs also undergoes Coriolis deflection. As the air travels from the region of the North Pole toward lower latitudes, it is deflected strongly (because of the high latitude) to the right. This creates the surface wind belt known as the **polar easterlies**, as near-surface prevailing air is generally from the east. Surface air moving from the region of the South Pole is deflected to the left as it moves toward that hemisphere's subpolar low. Coriolis deflection to the left also creates polar easterlies near the surface for that hemisphere between 90° and 60°S latitude.

To summarize, moving from the region of the poles toward the equator, the following surface wind belts occur:

- Polar easterlies (90–60°N latitude)
- Midlatitude westerlies (60–30°N)

- Northeast trades (30°N–0°)
- Southeast trades (0–30°S)
- Midlatitude westerlies (30–60°S)
- Polar easterlies (60–90°S)

Upper-Level Winds in the Hadley and Polar Cells

Upper-level winds overlaying the surface wind patterns are also an important component of the general circulation. As is shown in Figure 7.2, the upper-level pressure gradient force pushes air in the opposite direction from that at the surface in both the Hadley cells and the polar cells. At the surface the pressure gradient force is directed from the subtropical anticyclones to the equatorial low in the Hadley cells. But aloft, the upper-level pressure gradient force pushes air from the equatorial region toward the poles, therefore moving air over the subtropical anticyclones. Over the polar cell the upper-level pressure gradient force pushes the air from the area over the subpolar lows to the area over the polar highs, a direction opposite to that at the surface. Of course, in both the Hadley cells and the polar cells, the Coriolis effect causes a deflection of these winds generated by the pressure gradient force. The deflection is less in the Hadley cell than in the polar cell because of the lower latitudes. The result is upper-level southwesterlies over the northern hemisphere Hadley cell, northwesterlies over the southern hemisphere Hadley cell, and westerlies over the polar cells in both hemispheres (**FIGURE 7.3**). These polar westerlies aloft advected the tephra from the Eyjafjallajökull volcanic eruptions in Iceland eastward toward Europe in the spring of 2010, causing redirected air travel over northern Europe and the North Atlantic.

As air aloft in the Hadley cell continues to move poleward (the southwesterlies aloft in the northern hemisphere and the northwesterlies aloft in the southern hemisphere), the Coriolis effect increases in strength. The deflection to the right of the flow (or to the left of the flow in the southern hemisphere) increases poleward, and flow becomes increasingly westerly near the poleward edge of the Hadley cell in each hemisphere. Winds at these positions are often strong, in large part because of **conservation of angular momentum**—an important property of curved motion in a fluid on Earth. Anything that is “conserved”—in this case, angular momentum—remains constant.

Like any type of momentum, angular momentum is the product of a mass and a velocity. Angular momentum simply includes an additional variable—the radius of curvature. The “tighter” the curve, the smaller is the radius of curvature. An infinitely large radius of

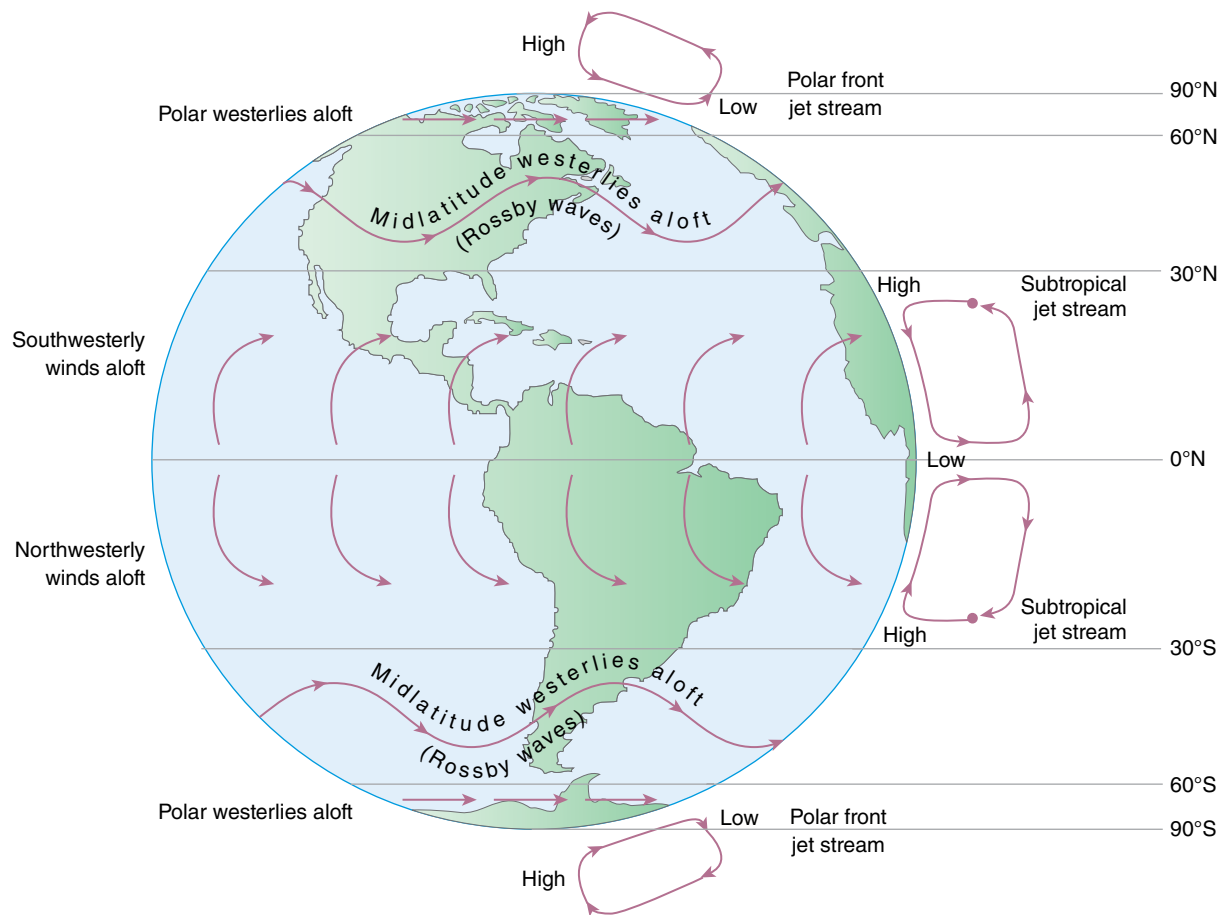


FIGURE 7.3 Global upper-level wind systems.

curvature occurs for straight-line flow. The conservation of angular momentum can be expressed quantitatively as

$$mvr = \text{constant}$$

where m is mass, v represents velocity, and r is the radius of curvature. In the atmosphere, mass is virtually constant. The equation above therefore suggests that as r decreases, v increases in order to maintain a constant angular momentum. Ice skaters know that to spin faster (increase velocity), they must become “thinner” by moving their arms inward to reduce their radius of curvature. In the atmosphere, westerly winds moving around the hemisphere at higher latitudes have smaller radii of curvature (the distance between the westerly wind and the north Earth’s axis) than westerly winds moving around the hemisphere at lower latitudes. As air moves poleward, its radius of curvature decreases (i.e., it goes from the wider part of Earth near the equator to the narrower part of Earth near the poles) and begins to curve increasingly to the right (in the northern hemisphere) because of the increasing Coriolis effect. Its velocity must increase simultaneously as r decreases to ensure that angular momentum is conserved. The result is the westerly *subtropical jet stream* that exists near 30°N and 30°S latitude (Figure 7.3). The variability

of this fast-moving river of air in the upper troposphere exerts a significant impact on weather and climate in subtropical latitudes.

Upper-Level Winds in the Midlatitudes

To understand the upper-level winds overlying the midlatitude surface westerlies, upper-level pressure gradients can be considered in terms of **geopotential height**, which is simply the altitude (in meters above sea level) of a given pressure surface over a particular location at a certain time. For example, the 500-mb geopotential height represents the altitude at which 500 mb of pressure is being exerted by the weight of the atmosphere in an atmospheric column. Because mean sea level pressure is 1013.25 mb, the 500-mb geopotential height also represents the approximate middle of the atmosphere from a mass perspective; roughly half of the atmospheric mass is above and the other half is below the 500-mb geopotential height level.

In relatively warm air, such as in the equatorial part of Earth, the surplus of heat increases the molecular *kinetic energy* of the gases in the air column. As this energy causes molecules of air to expand upward, the warm air becomes less dense than the colder air as

the gases occupy more volume and, therefore, weigh less per unit volume than when pushed closer together near the surface. We would expect that the 500-mb level (and other constant-pressure levels) over the equatorial part of Earth would be relatively high. In a warm column of atmosphere the elevation that divides the total mass of the atmosphere in half is relatively high because the molecules are spread out more vertically in the column. In the polar part of Earth, the high density of cold air occurs because molecular kinetic energy in the individual gas molecules is relatively low. This causes a contraction of the air column and a downward movement of the constant-pressure levels.

In the real world, then, the net energy surplus within the tropics causes tropospheric thermal expansion in that area, and the net energy deficit at the poles causes tropospheric contraction. The equatorial *tropopause* averages approximately 19 km (12 mi) above the surface, but the polar tropopause averages only about 10 km (6 mi) above the surface. A steady decrease in upper-level geopotential heights tends to occur from the equator toward each pole as colder conditions prevail (FIGURE 7.4). Furthermore, the difference in a given geopotential height level between the equator and pole increases with increasing height in the troposphere. It is apparent from Figure 7.4 that the 850-mb geopotential height is somewhat higher over the tropics than over the poles. But above the 850-mb level, the tropics are also warmer than the poles (particularly in winter), so the 700-mb geopotential height difference between the equator and the pole is compounded on the difference that already occurred at the 850-mb level. The latitudinal slope in geopotential heights creates a pressure gradient that pushes air horizontally from areas with higher heights (lower latitudes) to areas with lower

geopotential heights (higher latitudes). Because the gradient steepens and friction weakens with increasing height, we expect the winds to strengthen with height. In the Hadley and polar cells, these upper-level winds cannot strengthen as much as in the midlatitudes because they are constrained by the flow in the rest of the cell, including that at the surface.

When upper-tropospheric air moves poleward in response to this midlatitude height gradient, the Coriolis effect deflects it. Ultimately, a balance is gained between the pressure gradient force and Coriolis effect, which results in upper-level westerly winds in both hemispheres from the tropics all the way to the poles. The midlatitude region is the only one of the three zones per hemisphere (Hadley, polar, and midlatitude) in which upper-level winds occur in the same direction as the mean surface winds.

► Modifications to the Idealized General Circulation: Observed Surface Patterns

Land–Water Contrasts

The model described above is an idealized conception of the circulation system of Earth. It assumes that there are no surface variations—the model applies only to a planet composed solely of water. But in the real world, land–water contrasts complicate circulation in the climate system. Large water bodies maintain relatively constant temperatures through the course of a year compared with inland areas, assuming that all other factors are equal. The consistency is caused by a combination of water transparency, high *evaporation* rates, vertical and horizontal currents, and a high *specific heat* in water, all of which dampen fluctuations in temperature near the water surface.

On the other hand, continents show wide temperature variations across the seasons because their opaque surfaces absorb *insolation* in a tiny surface layer and then readily transfer that energy back to the atmosphere. Inland surfaces also have relatively low evaporation rates (causing a relatively high percentage of energy to be devoted to sensible heat), virtually no convective/advective motion to redistribute energy within the surface, and a low specific heat. These factors produce surfaces that heat quickly when energy is present and cool quickly during periods of energy deficit.

Given these factors and variations in surface elevations associated with continents, it is no surprise that including continents into the idealized model causes disruptions to the general circulation features. But the

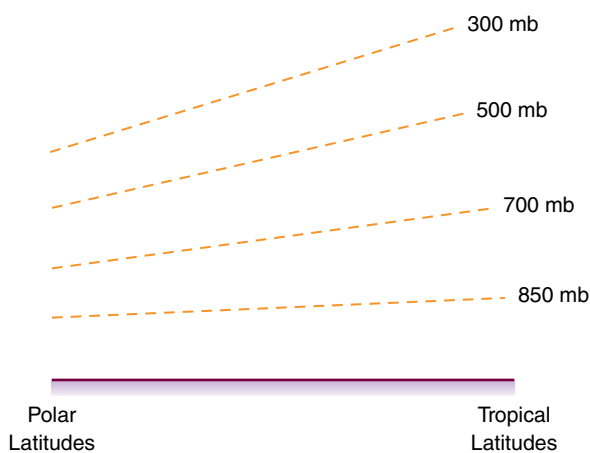


FIGURE 7.4 The slope of geopotential height surfaces from the equator to the North Pole. A similar slope would occur in the southern hemisphere, as heights decrease toward the South Pole.

idealized model does provide a useful starting point to a better understanding of the more complex real-world features.

Locations and Strength of Features in the Hadley Cells

ITCZ and Trade Winds

The ITCZ exists in a similar form in the real world as in the idealized pattern (FIGURE 7.5). It may be thought of as a constantly moving convective thunderstorm chain that follows the migration of the vertical solar ray across varying longitudes through the course of a day and between the tropical latitudes through the course of the year. But the ITCZ is much more physically constrained by surface temperature characteristics than the faster-moving solar rays. It therefore lags considerably behind the solar radiation maximum in its latitudinal migration. Also, it never reaches the maximum latitudinal position of the 90° vertical ray, which is at the *Tropic of Cancer* (on June 21) and the *Tropic of Capricorn* (on December 22; FIGURE 7.6). Instead, the ITCZ tends to migrate only approximately $10\text{--}20^\circ$ of latitude away from the equator in most locations, lagging behind the *solar declination*. The ITCZ moves poleward into the summer hemisphere in response to

the displacement of the vertical solar rays. The ITCZ does not migrate much over places affected by cold ocean currents, such as the tropical west coast of South America, even if these locations are in the path of the Sun's vertical rays.

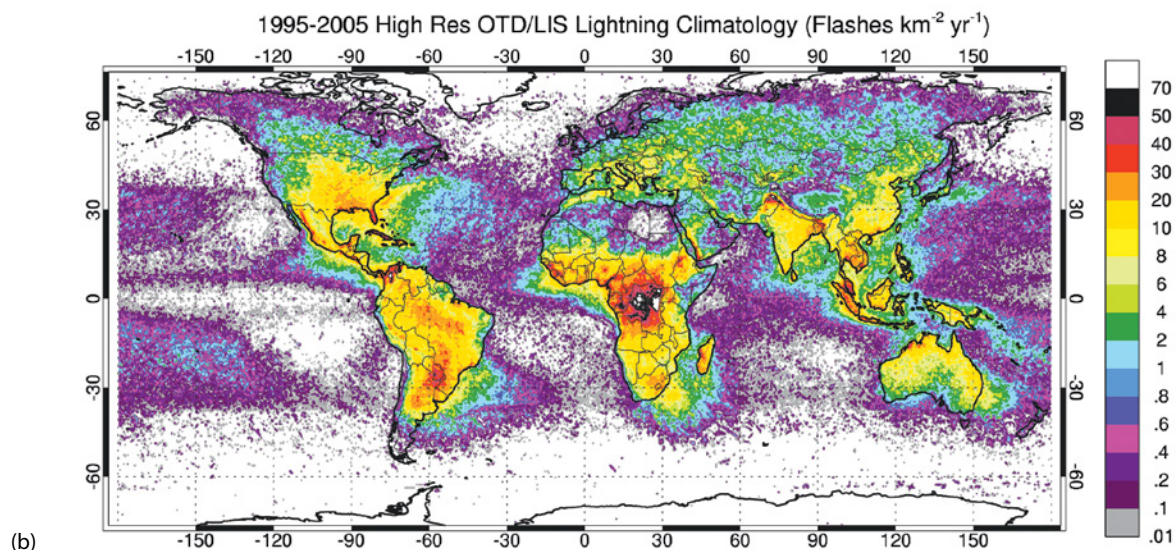
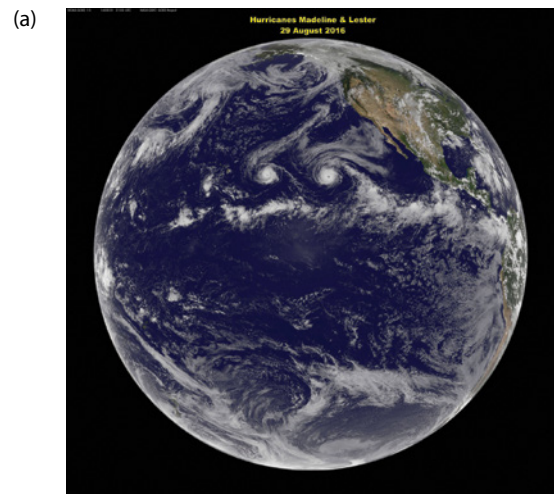
As the ITCZ migrates seasonally, the trade winds also migrate—to their northernmost extent in northern hemisphere summer and to their southernmost extent in northern hemisphere winter. Some locations on Earth may experience the trade winds for only part of the year. This migration can have a significant influence on the seasonal climate of tropical locations.

Subtropical Anticyclones

The idealized model suggests that a continuous belt of surface high pressure should exist across the planet near 30°N and 30°S —the subtropical anticyclones. In reality, however, these anticyclones occur only over the ocean basins near 30° latitude, and they are larger and

FIGURE 7.5 Global view of ITCZ represented by (a) the line of low-latitude clouds on 1 September 2016 (notice Hurricanes Madeline and Lester in the central tropical North Pacific) and (b) the most concentrated lightning flashes.

(a) Courtesy of NASA GOES Project Science. (b) Courtesy of Global Hydrology Resource Center/NASA.



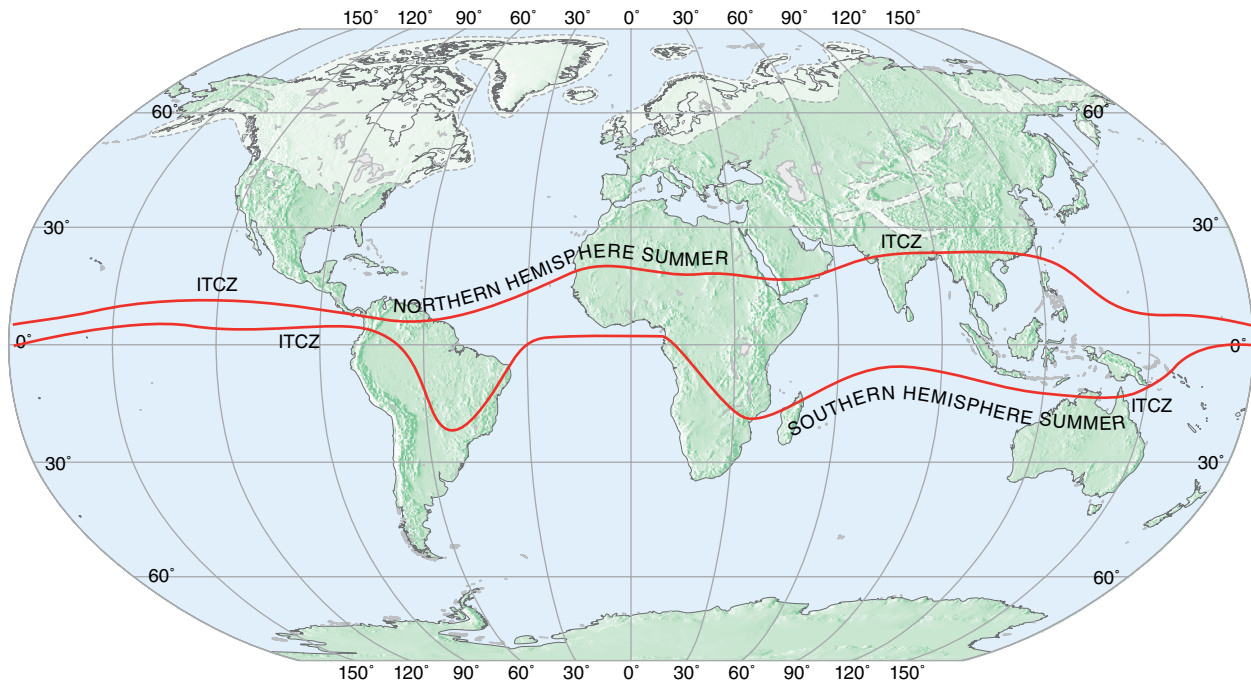


FIGURE 7.6 Migration of the ITCZ through the year.

Data from NOAA/GOES.

stronger in summer than in winter (**FIGURE 7.7**). The reason is that the tendency for high pressure at 30°N and 30°S is reinforced by the *relatively* cool summer conditions (compared with the adjacent land surfaces) over the oceans. The relatively cool ocean surface chills the overlying air, increasing low-level atmospheric *stability*. During that time internal pressure in the subtropical anticyclones reaches a maximum. The subtropical anticyclones are strongest when and where the ocean surface is much colder than the continental surface in the subtropics. The sinking air that results diverges at the surface, spilling toward lower-pressure locations in all directions before experiencing Coriolis deflection.

By contrast, the subtropical land surfaces heat effectively under long day lengths and high solar angles in summer. They tend to encourage rising motion (and lower surface pressure) that offsets the general circulation's tendency for sinking motion and high surface pressure. The subtropical continents are, therefore, typically too warm in summer to support the development and maintenance of semipermanent surface high-pressure cells.

The subtropical anticyclones migrate somewhat from their summer position, latitudinally with solar declination and longitudinally depending on where the coolest water lies, within the subtropical oceans. They also weaken in winter because the ocean surface is *relatively* warm compared with the land surfaces at similar latitudes. This relative warmth induces rising

motion that tends to offset the tendency for sinking air at 30°N and 30°S , as suggested by the idealized general circulation model. Instead, pressure tends to increase over the relatively cold terrestrial atmosphere.

The major surface-based, semipermanent, high-pressure cells located near 30°N latitude are the Bermuda-Azores high in the North Atlantic Ocean and the **Hawaiian high** (also known as the **North Pacific high**) in the North Pacific Ocean (Figure 7.7). Southern hemisphere subtropical anticyclones include the **South Pacific high**, the **South Atlantic high**, and the **Indian Ocean high**.

Locations and Strength of Features in the Polar Cells

Surface pressure features in the polar cells also strengthen and weaken seasonally. During winter the lack of insolation in the high latitudes causes intense surface chilling, which greatly increases low-level atmospheric stability. The frigid, dense air sinks and moves equatorward vigorously. The sinking air creates high surface pressure in the vicinity of the poles—the polar highs. These permanent anticyclones—one in each hemisphere—reach their maximum strength during winter and weaken somewhat in summer as the long summer days provide a bit of warming even at the poles. The intensification of the polar high in the winter hemisphere extends the entire polar cell equatorward, including the subpolar low-pressure zones, to approximately 55°N and 55°S .

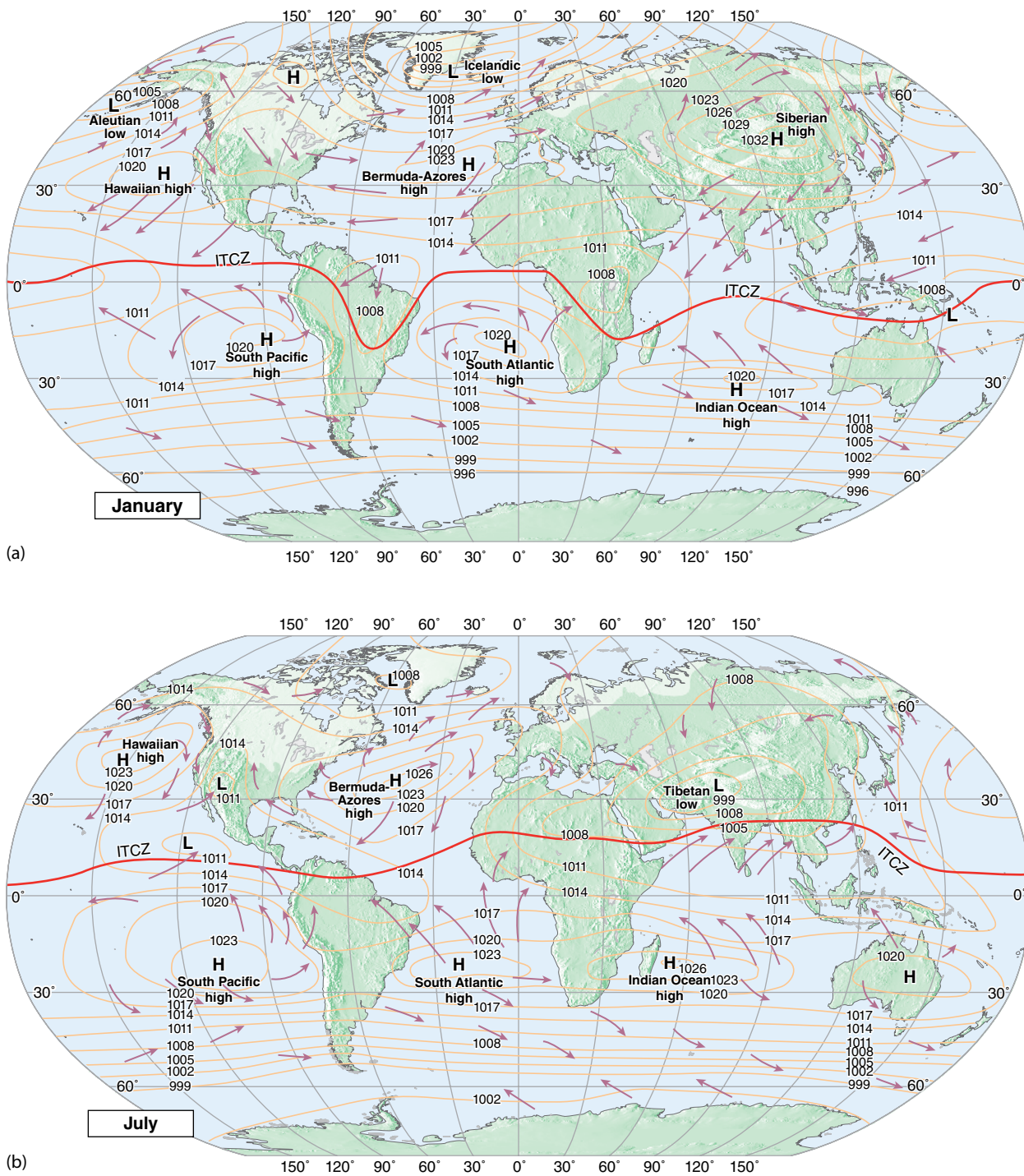


FIGURE 7.7 Mean surface isobars, positions of the semipermanent surface pressure cells, and associated winds, during (a) January and (b) July.

Data from January Pressure and Predominant Winds, and July Pressure and Predominant Winds, 1995. *Goode's World Atlas*, 19th ed. Edited by E.B. Espenshade. Skokie, IL: Rand McNally and Co., 1995.

latitudes. The weakening of the polar high in the summer hemisphere contributes to the contraction of the polar cell to approximately 65°N and 65°S latitude, coincident with the poleward migration of the subtropical anticyclones.

Like the subtropical anticyclones, the subpolar lows are confined to the ocean basins rather than being a continuous feature across the globe as depicted in the

idealized model. The subpolar lows are also similar to the subtropical anticyclones in that their existence is tied to surface temperature variations between land and sea. In winter, oceanic regions at the subpolar latitudes are generally warmer than the adjacent continental locations, both because of the thermal storage properties of water and because of warm ocean currents that transport energy from lower latitudes. The relatively

warmer ocean surface promotes low-level atmospheric instability, thereby reinforcing the tendency for rising motion as suggested by the idealized general circulation. This supports the development and maintenance of semipermanent surface cyclonic cells, particularly in winter—the subpolar lows. Buoyant air in the subpolar lows is associated with strong pressure gradients, windiness, and storminess, particularly during winter. The semipermanent North Atlantic subpolar cyclone is known as the **Icelandic low** and that in the North Pacific is referred to as the **Aleutian low** (Figure 7.7). Southern hemisphere subpolar lows are weak and exist only in a broad, continuous belt, because of fairly consistent surface ocean temperatures across the latitudes.

Continental areas at approximately 55–60°N latitude are frigid in winter. These cold land surfaces support sinking motion, which counteracts the general circulation's tendency for having rising motion at these latitudes. During winter, the *continentality* over the massive Asian continent sometimes causes the lowest surface temperatures for the northern hemisphere to exist over Siberia rather than at the North Pole. This high surface pressure expands over Asia, even into the zone where the idealized general circulation suggests that rising motion should occur. This surface anticyclone is known as the **Siberian high**. In the southern hemisphere, no such continental areas exist at 55–60°S latitude, so there is no equivalent to the Siberian high.

During summer, the long day lengths in high-latitude locations increase continental surface heating substantially, particularly in the northern hemisphere. Under such conditions the thermal gradient between the land masses and the oceans in the vicinity of 60° latitude decreases, weakening the pressure gradient. With *relatively* cooler oceans in summer (compared with adjacent land surfaces), the tendency for rising motion over the subpolar low regions is reduced, and the semipermanent surface oceanic subpolar lows weaken and shrink, as shown in Figure 7.7. At the same time, the Asian land mass heats considerably, once again because of continentality, and the Siberian high disappears. Instead, a semipermanent zone of low pressure occurs over south-central Asia—the **Tibetan low**. The flip-flop of pressure over the Asian land mass between the Siberian high in winter and the Tibetan low in summer as a result of continentality is the primary cause of a monsoon circulation in Asia.

Regardless of season, the subpolar lows are generally located where the cold surface air moving equatorward from the polar high meets the much warmer poleward-moving air diverging from the subtropical anticyclones. As we have seen, this convergence is displaced poleward in summer and equatorward in winter. The convergence of these two surface air streams causes rising

motion that is enhanced by the temperature differences between the two streams, with the warmer tropical air pushed upward over the colder polar air. This region is the boundary between cold, dense, polar air and warm, less dense, tropical air and is often termed the **polar front**. Storm formation (or **cyclogenesis**) frequently occurs along this band of latitudes because the steep thermal gradient supports the development and motion of migratory cyclones as secondary circulation features.

Locations and Strength of Surface Midlatitude Features

The seasonal fluctuation in strength of the subpolar lows and subtropical anticyclones works in tandem. In the winter hemisphere the subpolar lows are strengthened and displaced equatorward, while the subtropical anticyclones are relatively weak and pushed equatorward also. In the summer hemisphere the subtropical highs are strengthened and displaced poleward, whereas the subpolar lows simultaneously shrink and retreat poleward. The areas between the subpolar lows and the subtropical highs—the midlatitudes—are affected differently throughout the year by these pressure patterns.

Both the subpolar lows and the subtropical highs are affected more by the changing thermal surface characteristics of the northern hemisphere than by those in the southern hemisphere. The increased concentration of land area in the northern hemisphere promotes stronger land–sea contrasts than in the southern hemisphere. Likewise, the semipermanent subtropical highs and subpolar lows are more consistent in their presence and strength in the southern hemisphere because of the lack of large land masses at the subtropical and (especially) subpolar latitudes. This allows the southern hemisphere to exhibit circulation that is much closer to the idealized model than the northern hemisphere.

▶ Putting It All Together: Surface Pressure Patterns and Impacts

To summarize, the summer hemisphere sees weakening and contraction of the polar high and subpolar lows and expansion of the subtropical highs. The ITCZ pushes poleward through the tropical part of the summer hemisphere at the same time. This migration of the ITCZ contributes heavily to tropical precipitation regimes. The winter hemisphere sees expansion and strengthening of the polar high and the oceanic subpolar lows into lower latitudes, while the subtropical anticyclones weaken and retreat equatorward.

The waxing and waning of these pressure systems affect and are affected by the changing of the seasons in the high and midlatitudes. The changes in the semi-permanent circulation cells trigger direct precipitation regime changes for many high and midlatitude locations. In lower latitudes, precipitation changes directly define the seasons because thermal changes are minimal or nonexistent because of day length consistency through the course of the year. There, the ITCZ is the primary precipitation-forcing mechanism. When the ITCZ migrates over or near a region, it brings thunderstorms and associated precipitation. This occurs during the high-Sun period of “summer,” which is defined not so much by higher temperatures as by direct rays of sunshine falling in the same hemisphere as the point of interest. During the lower-Sun season, the ITCZ migrates to the opposite hemisphere, taking with it the primary precipitation-forcing mechanism. This causes a distinct wet/dry seasonal regime for many locations.

► Modifications to the Idealized General Circulation: Upper-Level Airflow and Secondary Circulations

As we have seen, flow in the upper-level midlatitudes is primarily westerly. These upper-atmospheric air currents typically exhibit flow characteristics that meander northward and southward, however, as they move in the general west-to-east direction. We may characterize the broad-scale, upper-level atmospheric flow at a

given time based on the *amplitude* or “waviness” of the flow pattern. If the upper airflow exhibits a relatively deamplified, or nearly straight, west-to-east pattern on a given day, the atmospheric pattern is classified as having a **zonal flow** (FIGURE 7.8a). If significant latitudinal amplification occurs in the midlatitude flow pattern on a given day, then the atmospheric pattern is said to have a **meridional flow** (FIGURE 7.8b).

Virtually all airflow has at least some meridional component, meaning that the flow pattern is at least somewhat wavy. Because some amplitude is present in all flow regimes, any upper-airflow pattern may be broken into wave segments. Any portion of the midlatitude wave pattern in either hemisphere that “bumps” poleward is termed a *ridge*—an elongated zone of high pressure (as opposed to an *enclosed* area of high pressure, which is an anticyclone). The elongation of high pressure refers to the fact that where the midlatitude flow moves poleward, the high pressure of the subtropical anticyclones can be elongated poleward as well. A ridge at the 300-mb level is shown in Figure 7.8b centered over the upper Mississippi Valley.

Any portion of the flow pattern that “dips” equatorward is termed a *trough*—an elongated area of low pressure. By contrast, a cyclone is an *enclosed* zone of low pressure. In Figure 7.8b a 250-mb trough is situated over the central United States. When the midlatitude flow dips equatorward, the relatively low pressure associated with the subpolar lows also can be elongated toward the equator.

Interestingly, ridges in the southern hemisphere appear the same as troughs in the northern hemisphere, and vice versa. This is because a dip *southward* of midlatitude flow in the southern hemisphere represents a

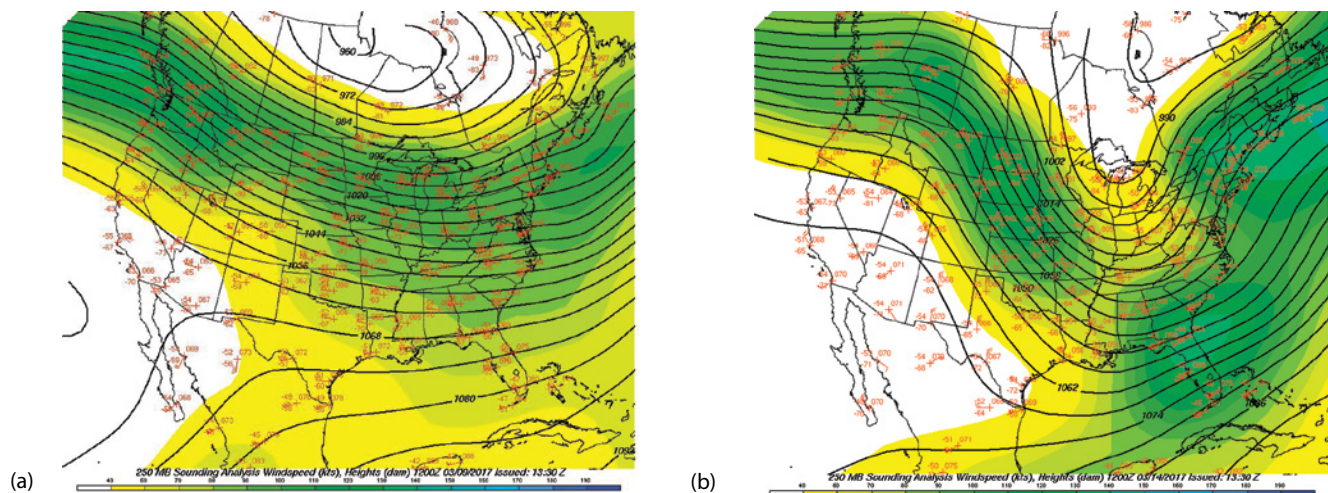


FIGURE 7.8 (a) This map of the 250-mb geopotential height field from 9 March 2017 shows zonal flow over much of the eastern United States. The isohypses are labeled in meters at which the 300-mb geopotential height surface existed on that day. (b) A 250-mb map of the United States on a day (14 March 2017) characterized by meridional flow across much of the nation.

Data from The Ohio State University WWW Weather Server, courtesy of the Department of Geography/Atmospheric Sciences Program.

place where the subtropical anticyclones to the *north* can be elongated, creating a ridge. Likewise, a jog to the north in the southern hemisphere represents a location where the subpolar low-pressure systems can be elongated equatorward, thereby forming a trough.

Like other types of waves, atmospheric waves can be described according to *wavelength*—the distance from one wave crest (ridge) to an adjacent wave crest (or the distance from one wave trough to an adjacent wave trough). Typically, midlatitude atmospheric waves that have wavelengths of hundreds of kilometers are simply called **long waves**, or **Rossby waves**, named after the atmospheric physicist Carl Rossby, who was instrumental in explaining upper-atmospheric dynamics during the first half of the twentieth century. Rossby waves are continuous around the hemisphere, circumnavigate each pole, and define the polar vortex.

During winter the northern hemisphere usually has three or four long waves. The latitudinal thermal gradient is maximized during winter when the polar areas receive little to no insolation and the low latitudes still receive nearly as much energy as they receive in summer. Rossby waves must have some amplification to redistribute this energy imbalance latitudinally in an attempt to equalize the differences. In summer the number of long waves increases to as many as six, but the amplitudes decrease because the latitudinal thermal gradient decreases when the high latitudes warm up under long day lengths. Through all seasons, Rossby waves tend to be less meridional in the southern hemisphere than in the northern hemisphere. Instead, the near-continuous ocean in the southern hemisphere plays a greater role in the redistribution of energy than it does in the northern hemisphere.

Because these upper-air Rossby waves result from latitudinal thermal inequalities, the ridges and troughs are essential in the energy balance of a hemisphere. The trough-to-ridge sides of these waves allow warm, and often moist, low-latitude air masses to move poleward, and the ridge-to-trough sides of Rossby waves allow cold and often drier air to move equatorward. Without these long waves helping to redistribute energy across the midlatitudes, energy differences would continuously increase between the tropics and the poles. This would result in the poles becoming increasingly colder while the equator increasingly warmed, and soon life would be restricted to the narrow zone where a thermal balance was achieved.

Vorticity

An important feature of upper-atmospheric Rossby wave flow in climatology is **vorticity**—the rotation, or spin, of any object. Although seemingly simplistic, vorticity

may be viewed in a number of ways. The vorticity of an object such as a person, a particle in the atmosphere, or a storm system can occur either because the object itself is rotating or because it is situated on or in another object that is rotating (i.e., Earth), or both. **Relative vorticity** (usually denoted by ζ , the lowercase Greek letter zeta) is the spin that occurs because the object itself is turning. If you hold your pen vertically and twirl it between your fingers, you impart relative vorticity on the pen. If you hold your pen stationary but instead *you* begin rotating, your pen is still rotating but for a different reason.

Particles in the atmosphere are always rotating because they possess **planetary vorticity** (f)—the spin they acquire because of the rotation of Earth. The amount of this vorticity is proportional to the Coriolis effect, which as we have seen is itself proportional to latitude and speed of motion. Specifically, in the expression of the Coriolis effect,

$$CE = 2\Omega (\sin \phi) v$$

the term $2\Omega(\sin \phi)$, where Ω is the angular velocity of Earth and ϕ represents latitude (with negative values for southern hemisphere latitudes), is sometimes referred to as the **Coriolis parameter**, but it really represents f .

Earth rotates on its axis in such a way that if we were to look down from space directly on the North Pole we would see counterclockwise rotation (from west to east). But when viewed from below the South Pole, Earth is simultaneously rotating clockwise. By convention, any rotation in the same direction as Earth's rotation in that hemisphere is termed **positive vorticity**. Thus, counterclockwise-spinning objects in the northern hemisphere and clockwise-spinning objects in the southern hemisphere (both of which include cyclones in their respective hemispheres) are said to exhibit positive or “cyclonic” vorticity. So for residents of either hemisphere, “positive vorticity advection” suggests the approach of a storm. Objects spinning in a clockwise manner in the northern hemisphere (or counterclockwise in the southern hemisphere) are said to have **negative vorticity**, because this rotation opposes that of Earth itself. Anticyclones in either hemisphere have negative vorticity.

In the northern hemisphere air flowing around ridges also has negative vorticity, because it is moving clockwise around the ridge, while air moving around troughs has positive vorticity. In the southern hemisphere ridges are also associated with negative vorticity (as the air moves counterclockwise through the ridge) and troughs are linked to positive (clockwise) vorticity.

Usually, vorticity in the middle atmosphere (i.e., the 500-mb geopotential height level) is considered to

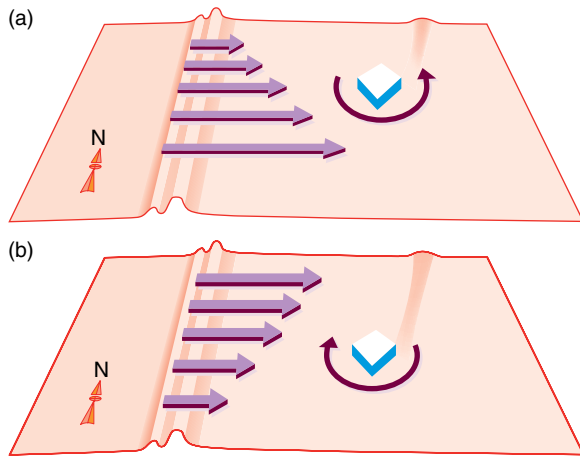


FIGURE 7.9 Transverse wind shear. In (a), the transverse wind shear will produce counterclockwise rotation, or positive ζ . In (b), the transverse wind shear will produce clockwise rotation, or negative ζ .

be most important for weather forecasting and analysis. If positive (or negative) vorticity is occurring halfway up the mass of the atmosphere, that same spin is likely to be propagated upward and downward to encompass most of the mass of the atmosphere over that location. If that vorticity is positive, the likelihood for storminess is enhanced. If it is negative, storm development is less likely.

The shearing motions that result from variations in wind speed across a horizontal surface are described as **transverse wind shear**, a force that is responsible for much of the ζ in air and can lead to positive or negative vorticity (FIGURE 7.9). To understand how transverse wind shear can cause ζ to exist in the Rossby waves, imagine a fast-meandering core of air, represented as a place where the pressure gradient is steeper than elsewhere in an upper-level weather map (FIGURE 7.10a). As this *jet stream* moves across a horizontal surface in the midtroposphere in the area approaching a ridge, the air is pushed poleward. If we place a giant ball on the inside of the curve in the jet stream at the ridge, it would rotate against the spin of Earth's surface—in a clockwise direction in the northern hemisphere. This is because transverse shear is created from the north side of the ball in the northern hemisphere (where air is moving quickly) to the south side of the ball (where air is moving slower). Thus, the ridge area is characterized by negative ζ (regardless of hemisphere). Now imagine a position downstream from the ridge. There the jet stream meanders such that the belt dips equatorward. If we place a giant ball on the inside of this trough at the jet, the ball would spin in a counterclockwise manner in the northern hemisphere. This causes positive ζ (regardless of hemisphere) as a result of transverse wind shear.

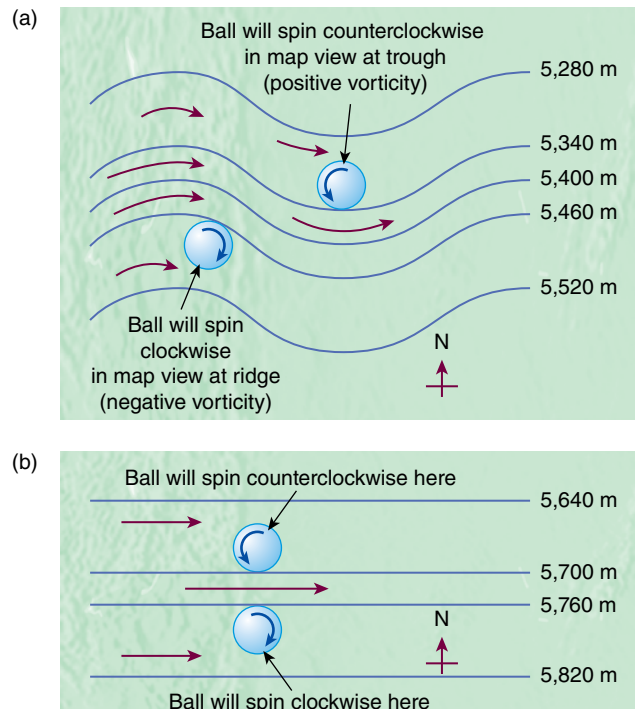


FIGURE 7.10 An example of the impact of transverse wind shear on relative vorticity (a) in a Rossby wave and (b) in a zonal flow.

If we track a parcel of air moving from a ridge to an adjacent downstream trough, we find that ζ increases as the air parcel moves downstream, regardless of hemisphere. Air near the ridge axis experiences the strongest negative ζ (in either hemisphere) because the parcel spins maximally in a clockwise (or counterclockwise in the southern hemisphere) manner at that location. Air near the trough axis experiences the maximum amount of positive ζ because a parcel spins maximally in a counterclockwise (or clockwise in the southern hemisphere) manner at that location. Between the ridge and the trough, air parcels show a ζ increase from negative to positive values in either hemisphere.

As the parcel continues toward the next downstream ridge, ζ begins to decrease as the air moves from a positive ζ region (the trough axis) toward a negative ζ region (the ridge axis) in either hemisphere. Again, this ζ change is caused by transverse wind shear. At the midway point between the trough axis and the ridge axis, the parcel of air experiences zero ζ , after which the rotation reverses.

Because ζ is a function of airflow curvature, strongly meridional patterns show the greatest ζ changes between ridges and troughs. Zonal patterns have only small ζ changes between the ridge and trough axes if the pressure gradient is constant. However, changes in the latitudinal pressure gradient cause transverse wind shear even if the flow is zonal (FIGURE 7.10b). Rossby

wave patterns provide both favorable and unfavorable zones for cyclogenesis, which requires counterclockwise rotation (in the northern hemisphere) or positive ζ (in either hemisphere). Deamplified or zonal flow provides neither strong support for nor resistance to cyclogenesis, except when differing wind speeds across space cause transverse shear.

Changes in ζ as air moves also impact the development and life cycles of weather systems. If the air acquires positive ζ , the formation of low pressure and cyclogenesis is encouraged. Surface anticyclones are supported by negative ζ in either hemisphere. This occurs at 500-mb ridges. Surface cyclones, such as those manifested as midlatitude storm systems, are supported by 500-mb troughs. The greater the amount of positive and negative ζ present aloft, the greater the spin of air through the column of air between the middle troposphere and the surface. This is associated with the strength of the individual surface systems and their resulting atmospheric features.

The characteristics of ζ are so closely related to surface system characteristics that most weather forecasters examine a map of 500-mb geopotential heights and ζ to determine initial forecasting scenarios. In the case of midlatitude storminess, low geopotential heights combined with positive vorticity advection (in either hemisphere) indicate the position of the core of a cyclone in the secondary circulation. Numerical models project changes in ζ and positions of the ζ maxima over time. If the ζ in the region shows signs of maintaining itself or strengthening in the computer models, then the surface cyclone is likely to either maintain its strength or increase in strength accordingly. If the midtropospheric ζ in a region shows signs of weakening, then so will the surface system, ultimately to the point of dissipation. The future trajectory of the surface system may be forecasted by using computer-projected 500-mb vorticity characteristics. Similar analyses are conducted at climatological time scales for forecasting potential impacts of long-term changes in the general circulation on precipitation and storminess across space. Analogous modeling endeavors have estimated climatic conditions in the distant past.

The climate of a region is determined by the frequency and types of weather systems (and, therefore, vorticity) passing over it. However, ζ is only one component of the total vorticity. Even in the total absence of transverse wind shear (hypothetically a perfectly zonal pattern with no changes in pressure gradients), f is present in the moving atmosphere, except at the equator where the Coriolis effect is zero. **Absolute vorticity** (denoted by N , the uppercase Greek letter nu) is the sum of the relative and planetary vorticity. Expressed quantitatively,

$$N = \zeta + f$$

the most important feature of N is that it is conserved—that is, it remains constant—in the atmosphere. This property has important ramifications for planetary-scale atmospheric flow.

Constant Absolute Vorticity Trajectory

As we have seen, cyclones have converging air motions at the surface but offsetting diverging air motions aloft (regardless of the hemisphere). Anticyclones have diverging air motions at the surface but have offsetting converging air motions aloft. The upper-air level where atmospheric motions oppose those near the surface maximally is typically located just beneath the tropopause. Somewhere between the two zones is the **level of nondivergence**, where neither convergence nor divergence occurs. Although the level of nondivergence may vary, the 500-mb geopotential height surface is often a good approximation of the level of nondivergence, because it is located where about half of the mass of the atmosphere is above it and half is below it.

Carl Rossby showed that at the level of nondivergence air motion follows a **constant absolute vorticity trajectory**. A parcel of moving air simply follows a path that conserves N over time. Imagine a parcel moving laterally in the midlatitude westerlies along the level of nondivergence. If it begins to move higher in latitude at all—say from southwest to northeast in the northern hemisphere (or northwest to southeast in the southern hemisphere)—Coriolis deflection is increasing (**FIGURE 7.11**). At the same time f is increasing, to conserve N the amount of ζ must decrease as it moves poleward. This causes it to acquire negative ζ (clockwise flow in the northern hemisphere), thereby creating a ridge (in either hemisphere). When the parcel reaches the area of maximum negative vorticity (and maximum f)—the ridge axis—its clockwise (in the northern hemisphere) flow begins to take it toward the southeast (or northeast in the southern hemisphere). N is conserved.

As the parcel continues to move southeastward (northeastward in the southern hemisphere), its f

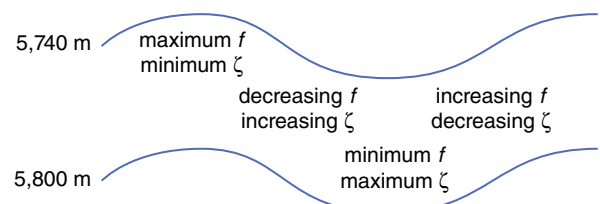


FIGURE 7.11 Relative and planetary vorticity features associated with midtropospheric Rossby waves.

decreases; so ζ must increase. This increasing ζ manifests itself as counterclockwise flow in the northern hemisphere (clockwise in the southern), and continued counterclockwise flow (clockwise in the southern hemisphere) eventually takes the parcel to a point at which it is as far equatorward as it will go. That point is the one at which f is at a minimum and ζ is at its maximum—the trough axis. Again, N is conserved. Continued motion toward the next downstream ridge once again sees increasingly positive f and increasingly negative ζ in either hemisphere.

Changes in ζ and Coriolis deflection cause adjustment in motion throughout the entire wave train of air around the hemisphere. For instance, as air moves into a ridge axis, Coriolis deflection increases as the parcel moves into higher latitudes. Even though there is an offset of ζ , the Coriolis deflection to the right in the northern hemisphere (left in the southern) causes the air parcel to turn equatorward on exiting the axis. The parcel moves toward lower latitudes along a northwest to southeast trajectory (or southwest to northeast trajectory in the southern hemisphere). At the trough axis f is at its weakest point, while the amount of ζ is maximized. This ζ overshadows the Coriolis deflection such that the parcel now turns to the left in the northern hemisphere (right in the southern), causing the air to move along a southwest to northeast trajectory (northwest to southeast in the southern hemisphere). The result is that a ridge of a particular amplitude is associated with downstream adjustments that affect the development of a trough. The process continues with N being conserved as a function of ever-changing Coriolis deflection and ζ values. A series of long waves circumnavigating the entire hemisphere results.

Because N is conserved, any change in airflow at any location along the wave pattern is “felt” by all points upstream and downstream. For instance, if air were to speed up over a trough-to-ridge side of the Rossby wave in a meridional flow pattern, the Coriolis effect would increase because it is proportional to wind speed (and because f has increased). This increased pull to the right (in the northern hemisphere) would be instantly offset by a decrease in ζ to conserve N . Such a situation would amplify the ridge. The flow would then readjust (again) because increasingly meridional motion would cause more extreme decreases in f with equatorward flow, initiating rapid increases in ζ to conserve N . This would cause the downstream trough to deepen, and meridional flow would be further intensified. Adjustments in this area would trigger further readjustments in the next downstream ridge and so on, leading to an increasingly meridional pattern over time. Any adjustment of airflow in one location is propagated downstream until the entire longwave pattern fully readjusts to the new stimulus.

At some point a critical maximum is reached when sufficient energy has been redistributed meridionally. At

that time the pattern readjusts to a more zonal pattern. Such a situation often creates closed migratory low- and high-pressure areas, which represent airflow regions similar to cutoff meanders in streams.

When we view Rossby wave patterns over time, we see preferred geographical areas where flow adjustments occur. Pairs of locations where ridging and troughing or opposite pressure anomalies frequently occur simultaneously are termed **action centers**. Any adjustment in the pressure pattern in an action center triggers an offsetting adjustment at the other action center. Likewise, changes over time occur in climatologically preferred locations of ridge–trough pairs along the longwave pattern.

The correlated atmospheric flow patterns resulting from a “seesaw” pattern of pressure and ridging/troughing at action centers are termed **teleconnections**. Because teleconnections are associated with adjustments in midtropospheric patterns, they are responsible for driving climatic variations at the surface for many regions.

Flow Over Mountainous Terrain

Changes in flow pattern characteristics can occur for reasons other than conservation of N during conditions of constant absolute vorticity trajectory. For instance, in mountainous areas the atmosphere constricts vertically. This occurs as the space between the surface and the tropopause (h) decreases as surface elevation increases (FIGURE 7.12). When a moving fluid constricts to a smaller vertical space, a rotational change occurs because, like N , **potential vorticity** is conserved. Potential vorticity (PV) can be expressed as

$$PV = \frac{\zeta + f}{\Delta h} \quad \text{or} \quad PV = \frac{N}{\Delta h}$$

Consider the case of air moving from west to east in the midlatitude westerlies across western North America, when it encounters the Rocky Mountains. As air moves upslope Δh decreases, so N must also decrease. But if the air is flowing from west to east in the midlatitude westerlies, f is unchanging because f is a function of latitude, which does not change in west-to-east flow. For potential vorticity (PV) to be conserved, ζ must decrease as the air moves upslope. As we have seen, decreasing ζ is associated with increasingly anticyclonic (clockwise in the northern hemisphere) flow. This encourages a ridge to form immediately west of a high mountain range that is oriented perpendicular to the direction of the flow.

By contrast, as air flows downslope on the *leeward* side of the mountains, Δh increases, so N must also increase (Figure 7.12). But again, f is constant for westerly flow, so for potential vorticity to be conserved, ζ must increase.

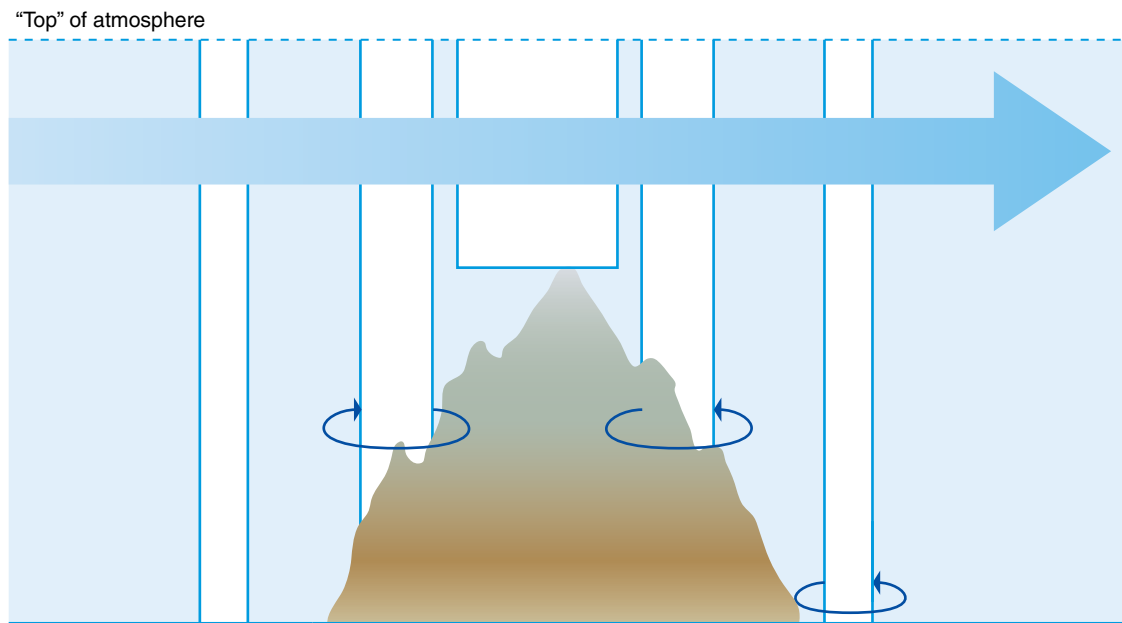


FIGURE 7.12 Prevailing airflow encountering a mountain range conserving potential vorticity.

Increasing ζ is associated with cyclonic (counterclockwise in the northern hemisphere) flow. This encourages a trough to form downstream from the peaks in the midlatitudes in each hemisphere. Cyclogenesis is common leeward of major midlatitude mountain ranges.

Baroclinicity

Another situation that leads to changes in Rossby wave flow involves **baroclinicity**—the intermixing of steep thermal gradients across small regions. Such gradients often occur at coastlines, where there is a differential heating of land masses versus ocean surfaces at a given line of latitude. The most pronounced thermal gradients occur on the leeward side of midlatitude continents during winter as the continents chill substantially while the ocean temperatures remain relatively mild. This effect is reinforced by the warm ocean currents that dominate the western sides of ocean basins (eastern sides of continents) as low-latitude waters move poleward in the oceanic gyres. During winter the thermal gradient across the eastern coasts of continents is maximized.

Any region (at the surface or aloft) where air is being advected into a region with a drastically different temperature is termed a **baroclinic zone**. Baroclinic zones are regions of active and sometimes severe weather systems in the midlatitudes. Geographical areas where baroclinic zones are preferred have frequently stormy climates. Low-level baroclinicity generally causes wind speed to strengthen with elevation as the heights of constant upper-air pressure surfaces attempt to even out over a small region. These changes manifest themselves through the longwave pattern. In general, if a baroclinic

zone occurs in association with an upper-level trough, the development of surface cyclones is strongly encouraged. Baroclinic zones are apparent on a map where *isotherms* are packed closely together, especially when they are nearly perpendicular to the Rossby wave flow. The latter indicates that efficient thermal advection is occurring. In **FIGURE 7.13**, notice how the 500-mb baroclinic zone focused over sections of the Atlantic Coast is associated with the longwave trough. As air moves through that trough, it acquires counterclockwise rotation (i.e., positive vorticity) and supports cyclonic development.

Rossby Wave Divergence and Convergence

Surface cyclones require diverging air aloft to sustain surface convergence. Such air is found on the trough-to-ridge side of the Rossby waves (**FIGURE 7.14**). To see why, imagine air moving around the trough aloft (in the northern hemisphere). In such a case it must turn to the left to remain parallel to the **isohypses**—lines of constant geopotential height. Flow in the upper-level maps generally parallels the isohypses because *geostrophic balance*—a balance between the pressure gradient force and the Coriolis effect—occurs aloft. To turn against the direction induced by the Coriolis effect, the speed must be slow enough to reduce the Coriolis effect sufficiently.

On the other hand, as air moves through a ridge (in the northern hemisphere) it turns to the right to remain parallel to the isohypses. Because this is the direction that the Coriolis effect deflects the air, the speed increases coincident with the strengthening of the Coriolis effect. Note the Coriolis effect weakens

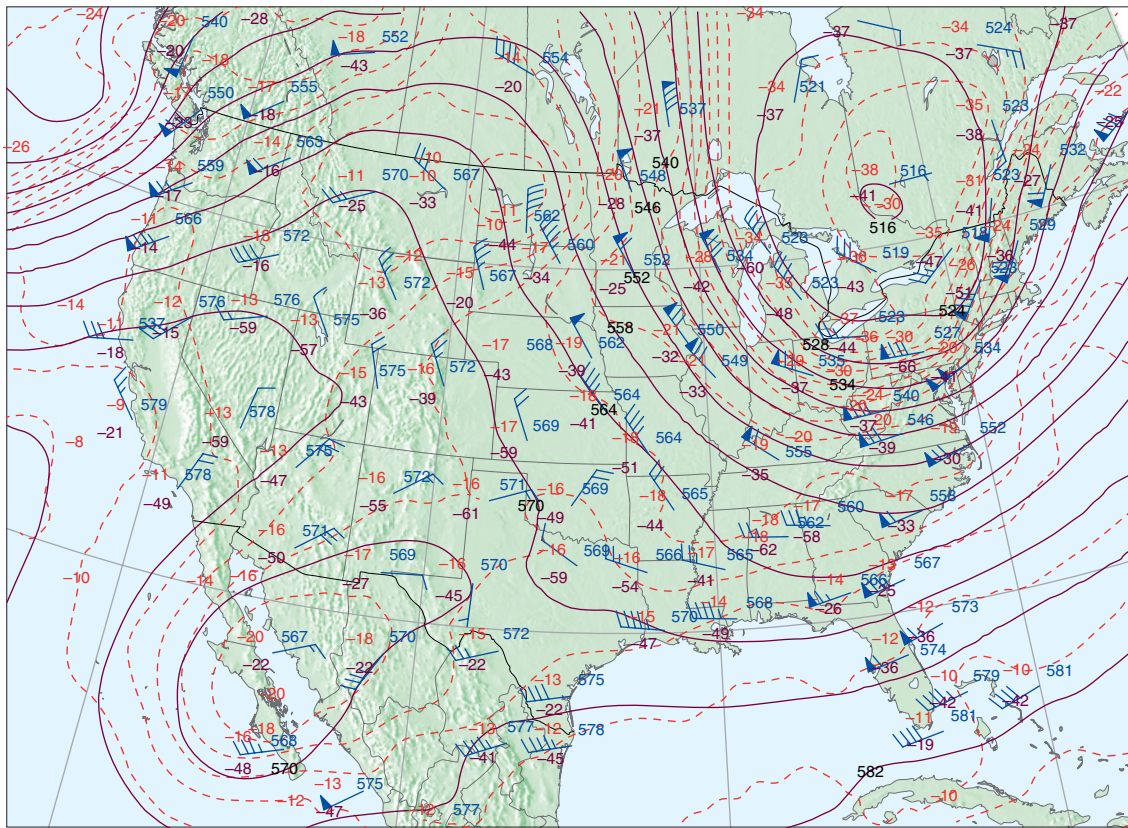


FIGURE 7.13 A 500-mb weather map for February 16, 2017. Notice how the isotherms (dashed lines) are packed closely together over the Pacific Northwest and over and east of the Great Lakes on this day, coinciding with the closely packed isohypses (solid lines). This indicates strong baroclinic zones, deep troughs, and strong surface cyclones in both locations. By contrast, few isotherms appear over the southwestern United States and Mexico, where lighter 500-mb winds occur in association with a pronounced midcontinent ridge and a coinciding surface anticyclone.

Courtesy of National Weather Service/NOAA.

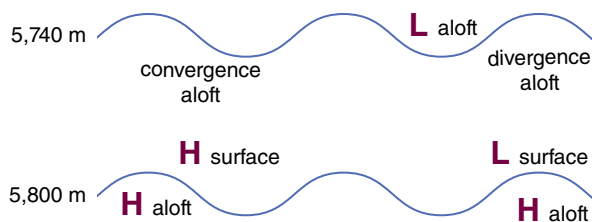


FIGURE 7.14 Areas of favorable surface cyclone and anticyclone formation relative to the Rossby wave pattern.

at the trough and strengthens at the ridge (in either hemisphere) because latitude is relatively low at the trough and higher at the ridge.

Air therefore diverges on the trough-to-ridge side of the Rossby wave aloft, moving relatively slowly around the trough and then relatively fast around the downstream ridge (assuming that the isohypse gradient is the same for both). This divergence on the trough-to-ridge side of the upper-level Rossby wave induces rising motion to replace the air that has “spread out” aloft. Air cannot approach laterally because it must remain parallel to the isohypses to ensure the balance of forces suggested by geostrophic flow.

The rising motion is supportive of surface low pressure—a cyclone. So surface cyclones are found on the trough-to-ridge side of the wave in either hemisphere (Figure 7.14).

By contrast, the ridge-to-trough side of the wave is associated with convergence aloft (in either hemisphere) as air slows down and “piles up.” This abundance of air aloft induces a sinking motion on the ridge-to-trough side of the wave and surface high pressure. Surface anticyclones therefore are located beneath the ridge-to-trough side of the Rossby wave in either hemisphere.

Rossby Wave Diffluence and Confluence

Additionally, areas of diffuence and confluence in the upper-level Rossby waves can create rising and sinking motion. **Diffuence** refers to the horizontal spreading of air streams at a given height, and **confluence** involves areas where air is converging horizontally (**FIGURE 7.15**). Upper-level diffuence supports rising air motions by developing an upper-air vacuum as air parcels spread away from each other. Air rushes into the vacuum from below, which initiates and maintains surface low-pressure centers.

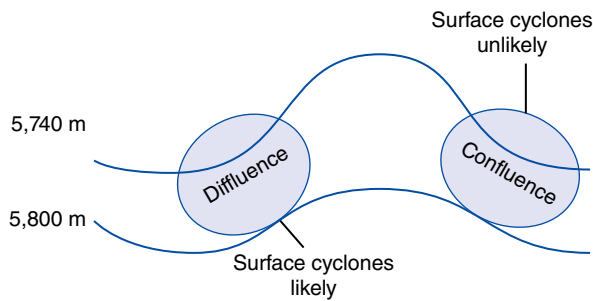


FIGURE 7.15 Areas of favorable surface cyclone and anticyclone formation relative to the Rossby wave pattern: Diffluence and confluence.

Confluence consists of air streams that converge horizontally toward each other. At upper levels the “pile up” of air associated with such motions causes air to slow down. Gravity prevents this “extra” air from moving out to space, so the only place the air can move is downward. Thus, sinking motions result. These motions initiate and support the development of surface anticyclones.

Polar Front Jet Stream

Embedded within the upper-level midlatitude westerlies are cores of extremely fast airflow. These places are indicated on upper-level maps by isohypses that become closely spaced (but, of course, isohypses can never intersect each other). If we examine a map with the North (or South) Pole in the center, as in **FIGURE 7.16**, an enclosed area of closely spaced isohypses would be apparent some distance from the pole over the midlatitudes. Airflow through these closely spaced isohypses is continuous around the hemisphere. The enclosed region represents the **circumpolar vortex**, an area of strong winds aloft that encircles the surface polar high. The *polar front jet stream*, which marks the periphery of the circumpolar vortex, is a core of fast-moving air that meanders through the upper troposphere. There is one polar front jet in the northern hemisphere and another in the southern hemisphere. The strongest wind speeds occur just beneath the tropopause in the 300-mb to 200-mb height field area where the geopotential height gradient is strongest and friction is minimal.

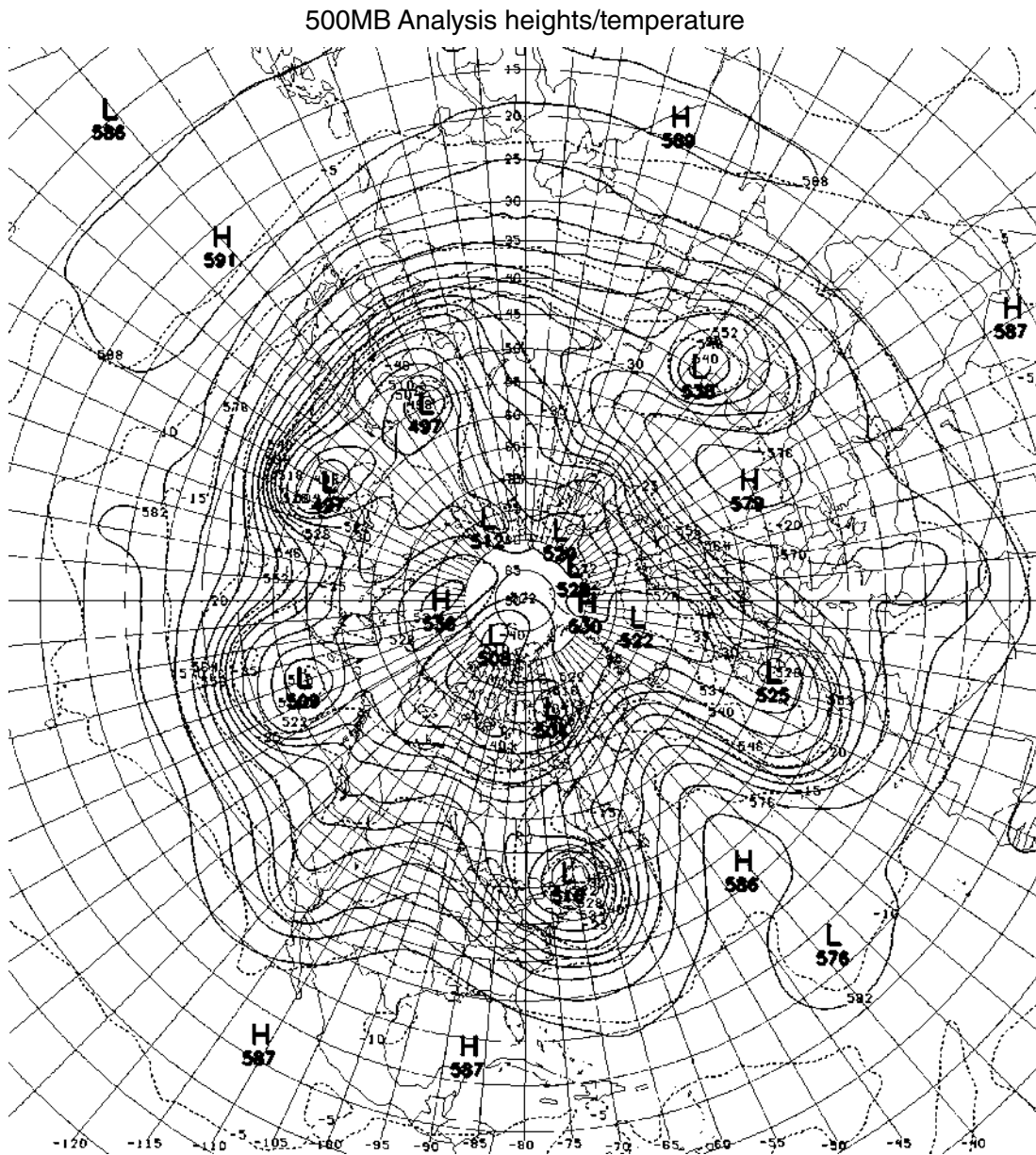
The region of greatest wind speed within the polar front jet stream—the **jet streak**—occurs over the primary baroclinic zones, which exist at the boundary between cold air of polar origin and equatorially derived air. The speed of the polar front jet stream is directly proportional to the latitudinal thermal gradient, with steeper thermal gradients and baroclinic zones inducing steeper geopotential height gradients and a faster jet. Baroclinicity supports and maintains jet stream flow characteristics.

If a jet streak is divided into quadrants, such as in **FIGURE 7.17**, the upwind or “back” two quadrants are

termed the “entrance” region and the downwind or “front” two quadrants are termed the “exit” region. In the midlatitudes, airflow would have an entrance on the west side and an exit on the east side of the jet streak, regardless of hemisphere. In the entrance region, the upper-level air is accelerating, so the Coriolis effect will be increasing as the air accelerates. However, the inertia associated with the slower-moving air as it enters the entrance region does not allow the increased bending associated with a strengthening Coriolis effect to manifest itself immediately. Thus, a momentary imbalance of forces in the entrance region of the jet streak exists, such that the effect of the pressure gradient force is slightly greater than the manifestation of the Coriolis effect. In other words, the flow is not geostrophic in the entrance region; instead, air flows across the isobars a bit, toward the lower isohypses (pressure) on the poleward side of the jet streak (regardless of hemisphere). This upper-level convergence on the poleward side of the jet streak’s entrance region is associated with sinking air and surface storm suppression. By contrast, the equatorward side of the entrance region would have experienced a bit of upper-level divergence as the air flows across the isohypses towards the poles, and this upper-level divergence would be compensated by rising motion, lower surface pressure, and surface convergence. Storms tend to be enhanced on this (equatorward) side of the entrance region.

In the exit region of the jet streak, the winds are decelerating rapidly in a short distance. This deceleration is linked to a decreasing magnitude of the Coriolis effect. But in reality, the forces are momentarily out of balance, with the bending of the winds by the Coriolis effect remaining more intense than would be expected by the decreased wind speeds, because of inertia. The result is a momentary imbalance of forces in the exit region of the jet streak, with the manifestation of the Coriolis effect exceeding the effect of the pressure gradient force and moving air equatorward slightly. The pile-up of air aloft on the equatorward side and the divergence of air on the poleward side of the exit region means that air beneath the poleward side of the jet streak is likely to rise and be associated with lower surface pressure, while air is likely to sink on the equatorward side of the exit region.

In addition, the fact that the winds move faster at the jet streak axis means that there will generally be counterclockwise shear on the northern side and clockwise shear on the southern side of the exit region. This counterclockwise shear in the northern hemisphere and clockwise shear in the southern hemisphere (i.e., positive ζ) magnifies the effect of the storm development in the exit region. So the left front (northern hemisphere) and right front (southern hemisphere) tend to be the quadrants of the jet streak that experience the greatest likelihood of storms. But the right rear (northern hemisphere)



11/21/2016 12UTC 000HR FCST Valid Mon 11/21/2016 12UTC NCEP/NWS/NOAA

FIGURE 7.16 The northern hemisphere's circumpolar vortex at the 500-mb level on 20 April 2013. The locations where the isohypses are packed closely together represent the extent of the northern hemisphere's circumpolar vortex.

Courtesy of National Weather Service/NOAA.

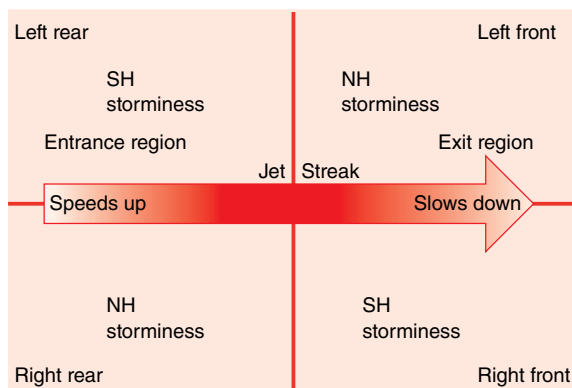


FIGURE 7.17 Characteristic atmospheric features in the area of a jet streak.

and left rear (southern hemisphere) quadrants can also experience storm enhancement despite the negative ζ associated with those areas.

Air of tropical and polar origin meets in the midlatitudes to produce active baroclinic zones. The tropical air is usually also humid because a large geographical area of the tropical Earth is over oceans and because warm air has high *saturation vapor pressure*. The polar air is often also dry because relatively more of the polar Earth is either covered by land or sea ice and because the saturation vapor pressures decrease with decreasing temperatures. The boundary between the tropical and polar air pools produces a distinct thermal–moisture boundary through the vertical profile of the atmosphere. Air temperatures

change significantly over small areas near the boundary. The location of this thermal gradient at a given time determines the location and shape of the circumpolar vortex and the location of the polar front jet stream in the zone between the subpolar lows and the subtropical highs.

The height of geopotential pressure surfaces is directly related to the thermal properties of air, in fulfillment of the *equation of state*, also known as the *ideal gas law*, for dry air:

$$P = \rho R_d T$$

where P represents pressure (in *Pascals*), ρ represents density, R_d is the dry gas constant, and T is in the *Kelvin temperature scale*. If we were to examine the 500-mb geopotential height field (an unchanging pressure value), we would notice that the density of that pressure surface decreases over areas of higher temperature and increases over areas of lower temperature, in fulfillment of the equation of state. Density decreases when air rises, so warmer areas must have higher constant pressure surfaces than colder areas (Figure 7.4). This is a direct result of thermal expansion (warming conditions) and contraction (cooling conditions) of a fluid, as described by the equation of state.

A sharp thermal gradient occurs between warm and cold air at the surface with the boundary extending through a vertical profile of the atmosphere. In the vicinity of the 300-mb geopotential height layer and extending to about the 200-mb layer (just beneath the tropopause), geopotential heights slope sharply across the thermal boundary. Remember that air in the upper atmosphere flows down the geopotential thermal gradient from equatorward to poleward latitudes. The pressure gradient force is always pulling air toward the poles as the geopotential height fields are lower in height (thermally contracted) than over lower latitudes (thermally expanded). This creates a steep geopotential height slope above the thermal boundary between warm and cold air.

As air begins to flow across this gradient, it accelerates. This increase in slope provides energy to the jet stream. However, air does not simply flow over the sloping heights toward the pole. As we already know, Coriolis deflection pushes air to the right in the northern hemisphere, allowing for geostrophic balance to be reached with the pressure gradient force, which is pulling air toward the pole. This results in a rapidly moving stream of air flowing generally from west to east above the warm–cold air boundary. The same situation (heights sloping poleward) occurs in the southern hemisphere, which also results in a west-to-east-flowing jet stream as air is pulled to the left by Coriolis deflection.

The polar front jet stream's location varies as the flow of air travels along the area of constant N . The jet stream as identified on upper-air weather maps can be used to

identify ridges and troughs, and corresponding Rossby waves, in the upper troposphere. The jet is also important in governing surface weather, because it represents the boundary between cold and warm air and it tends to govern the development and movement of midlatitude storm systems. Analysis of the polar front jet stream and prediction of its future motions are essential for short-term and long-term atmospheric prediction and analysis.

The thermal boundary associated with the polar front jet stream is generally much more prominent in winter because the latitudinal thermal gradient is much greater during that season than during the summer. Wind speeds typically reach 160 km hr^{-1} (100 mi hr^{-1}) in winter but drop to about 80 km hr^{-1} (50 mi hr^{-1}) in summer.

Mean Patterns of Rossby Wave Flow

Climatological analysis of the polar front jet stream is often done by examining average patterns, even though variability and extremes are also important components of climatology. The jet stream's position varies substantially from day to day, but analysis of the position and intensity of the jet over long time scales shows distinct monthly and seasonal patterns.

As explained above, the sharp surface thermal gradients associated with coastal locations produce baroclinic regions that generally correspond to the location of the polar front jet. The constraint of upper airflow by conservation of absolute vorticity results in rather distinct atmospheric teleconnections. The polar front jet is located maximally equatorward during the coldest part of the year. This results from the expansion of the polar anticyclone and subtropical lows and contraction of the subtropical anticyclones during winter. In summer the semipermanent pressure cells reverse from their winter tendencies. This causes the polar jet to retreat maximally poleward.

The presence of topographical barriers and baroclinic zones causes persistence in the long-term jet pattern. For instance, air motion over North America is typically characterized by a ridge over the western mountain cordillera and a trough over the east. This pattern is associated with the conservation of potential vorticity as the height of the air parcel decreases as it moves upslope and then decreases as it moves downslope. The amplitude of the jet changes in association with vorticity and thermal characteristics as described above. A reverse flow—a trough in the west and ridge in the east—does occur, but it is rather infrequent. Recent studies show that once the reverse pattern establishes itself, it can be quite persistent.

Climatological averages of middle-tropospheric patterns for the northern hemisphere reveal many of the principles discussed above. **FIGURE 7.18** shows that 500-mb geopotential heights are generally higher in

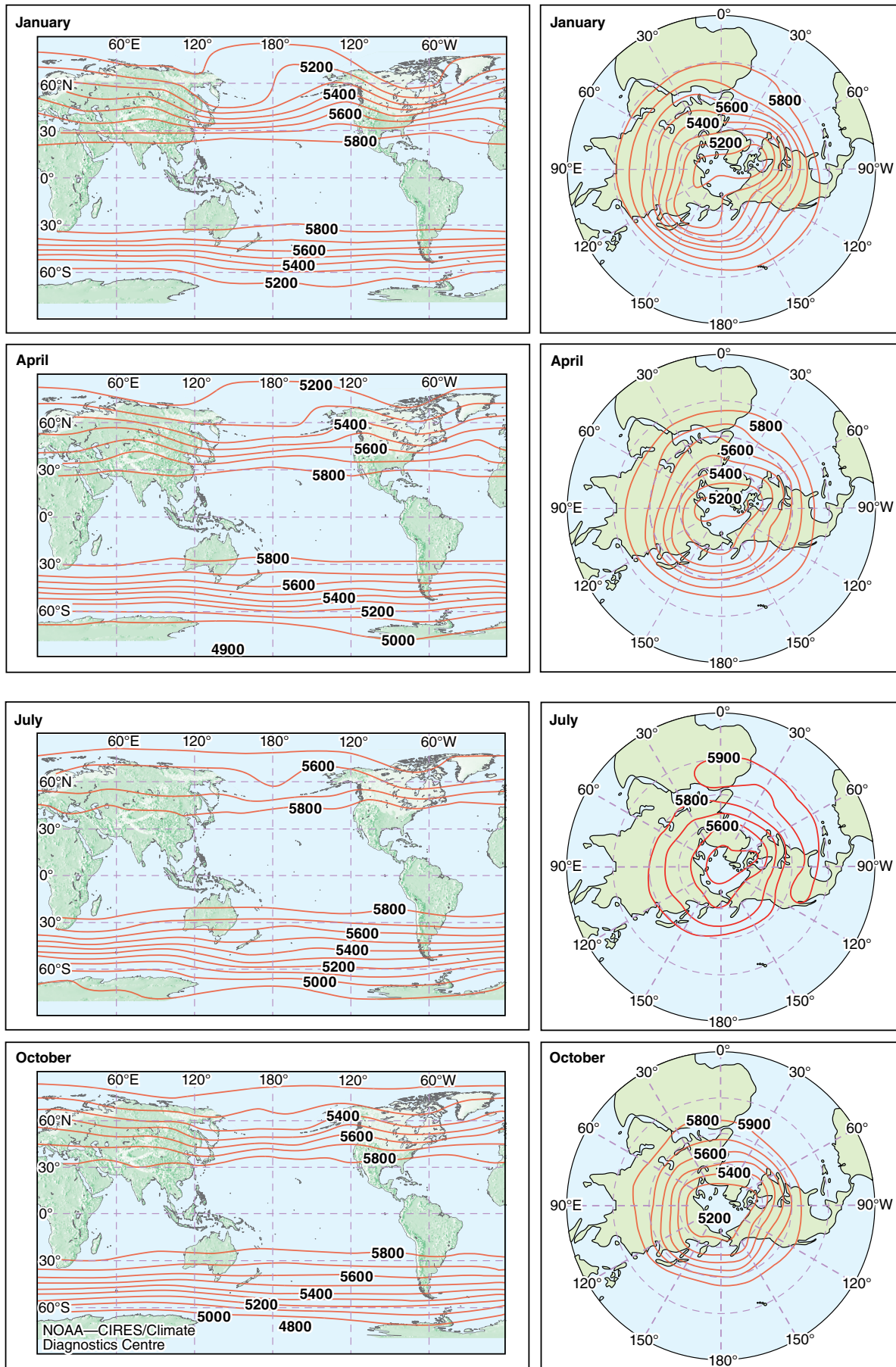


FIGURE 7.18 Mean 500-mb geopotential heights in the northern hemisphere, for January, April, July, and October.

Data from NOAA/CIRES Climate Diagnostics Center and the University of Colorado at Boulder.

summer than in winter over any given location and that the 500-mb geopotential height gradients are steeper in winter than in summer. The equatorial areas have weak 500-mb geopotential height gradients year-round. In contrast, few major seasonal changes occur in the southern hemisphere. The dominant presence of water, resulting in a fairly stable latitudinal thermal gradient in the southern hemisphere, keeps the patterns fairly constant throughout the year.

► Summary

General circulation exists to redistribute energy that arrives at Earth in greater quantities near the equator than near the poles. Because of the rotation of Earth, this circulation is characterized by a Hadley cell and a polar cell in both the northern and the southern hemispheres. Air in the Hadley cell moves upward near the equator at the Intertropical Convergence Zone, with a poleward motion to about 30°N and 30°S latitude; sinks at the subtropical anticyclones; and then moves equatorward again in the form of the northeast trade winds (northern hemisphere) and the southeast trade winds (southern hemisphere). The subtropical jet stream exists aloft at the poleward edge of the Hadley cell in each hemisphere as angular momentum is conserved, and it exerts significant influences on the subtropical atmosphere, many of which are poorly understood.

The polar cell is characterized by sinking air at the pole, equatorward surface motion to about 60°N or 60°S (deflected by the Coriolis effect to become the polar easterlies), rising air at the subpolar lows, and then poleward motion (deflected to become westerlies) aloft. Between the Hadley and polar cells in each hemisphere are surface westerly winds, with stronger westerlies aloft. Within the midlatitudes atmospheric flow aloft takes the form of Rossby waves, which pull air toward the pole (ridge) and toward the equator (trough) as it moves generally from west to east embedded in the westerlies.

Vorticity is an important feature of atmospheric motion. Air flowing in upper-level Rossby waves conserves its absolute vorticity, thereby ensuring that ridges and troughs remain confined to the middle latitudes. Because potential vorticity is conserved, air moving upslope in the midlatitude westerlies acquires anticyclonic (negative) vorticity, while that moving down the leeward slope acquires positive vorticity. The trough-to-ridge side of the wave and any areas of diffluence along the wave support surface cyclones and cyclogenesis. The ridge-to-trough side of the wave and any areas of confluence along the wave support surface anticyclones and anticyclogenesis.

The circumpolar vortex and in particular the polar front jet stream exist over the zone of the sharpest temperature contrasts and the strongest baroclinic zone. This feature is embedded within the Rossby waves and can exert a significant influence on the weather and climates beneath it.

Key Terms

Absolute vorticity

Action center

Aerosols

Albedo

Aleutian low

Amplitude

Anticyclone

Attenuation

Baroclinic zone

Baroclinicity

Beam spreading

Bermuda-Azores high

Circumpolar vortex

Confluence

Conservation of angular momentum

Constant absolute vorticity trajectory

Continental

Convection

Coriolis effect

Coriolis parameter

Cyclogenesis

Cyclone

Density

Diffluence

Doldrums

Equation of state

Evaporation

General circulation

Geopotential height

Geostrophic balance

Gyre

Hadley cell

Hawaiian high

Horse latitudes

Icelandic low

Ideal gas law

Indian Ocean high

Insolation

Intertropical Convergence Zone (ITCZ)

Isohypse

Isotherm

Jet streak

Jet stream

Kelvin temperature scale

Kinetic energy

Latitude

Leeward

Level of nondivergence

Long wave

Longitude

Meridional flow

Midlatitude westerlies	Relative vorticity	Subpolar low
<i>Momentum</i>	<i>Ridge</i>	<i>Subtropical anticyclone</i>
Negative vorticity	Rossby wave	<i>Subtropical jet stream</i>
<i>Newton's second law</i>	Sargasso Sea	Teleconnection
North Pacific high	<i>Saturation vapor pressure</i>	Tibetan low
<i>Northeast trade winds</i>	<i>Second law of thermodynamics</i>	Transverse wind shear
<i>Pascal</i>	Secondary circulation	<i>Tropic of Cancer</i>
Planetary vorticity	<i>Sensible heat</i>	<i>Tropic of Capricorn</i>
Polar cell	Siberian high	<i>Tropopause</i>
Polar easterlies	<i>Solar declination</i>	<i>Troposphere</i>
Polar front	<i>Solar noon</i>	<i>Trough</i>
<i>Polar front jet stream</i>	South Atlantic high	Vorticity
Polar high	South Pacific high	<i>Wavelength</i>
Positive vorticity	<i>Southeast trade winds</i>	Zonal flow
Potential vorticity	<i>Specific heat</i>	
<i>Pressure gradient force</i>	<i>Stability</i>	

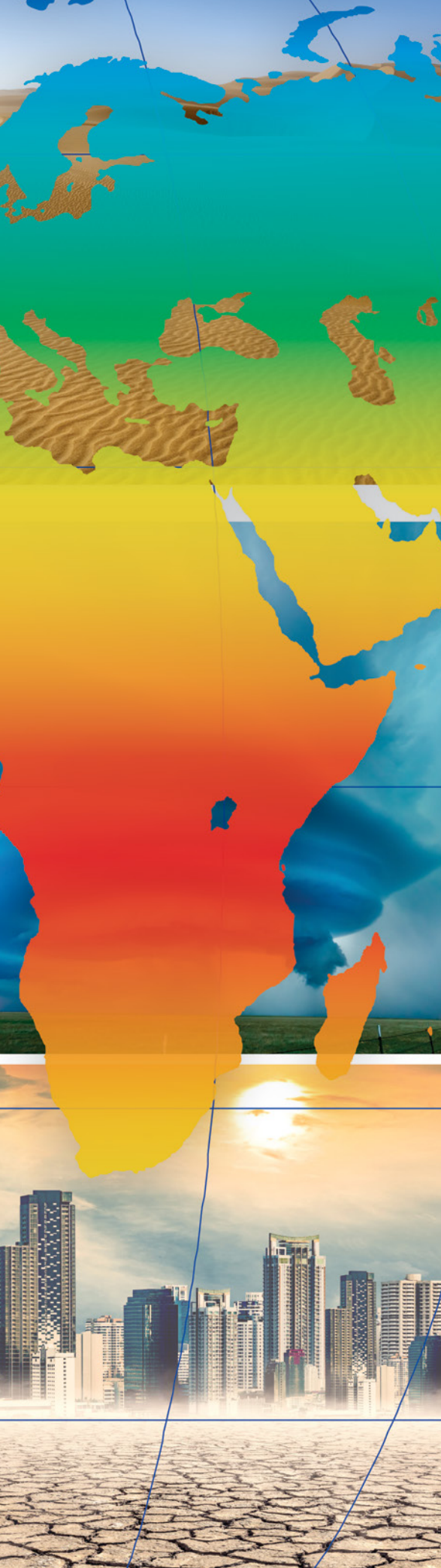
Terms in italics have appeared in at least one previous chapter.

Review Questions

- Discuss the primary atmospheric circulation features present on a nonrotating planet with a continuous, uniform surface.
- Describe the key pressure and wind features in the idealized circulation model.
- Compare and contrast the idealized circulation model to reality. Why are they different?
- Does the idealized global circulation model adequately describe upper-atmospheric motions? If not, then why not?
- Describe the waxing and waning of the semi-permanent pressure cells through the course of the year.
- Discuss the annual migration of the semipermanent pressure cells.
- Identify and compare relative and absolute vorticity.
- Discuss the role of positive and negative vorticity in association with ridges and troughs.
- Describe the role of vorticity in the development of zonal and meridional Rossby wave patterns.
- Why is absolute vorticity important? Of what is it a function?
- Discuss the role of constant absolute vorticity trajectory relative to atmospheric motions aloft.
- What are teleconnections and teleconnection action centers and why are they important to upper-atmospheric flow patterns?
- Discuss the role of baroclinicity in the development of upper-atmospheric flow patterns.
- What is the polar front jet stream, how does it form, and why is it an important feature of mid-latitude upper airflow?

Questions for Thought

- The text says that the Rossby waves in the southern hemisphere tend to be less meridional than those in the northern hemisphere. Why do you believe that this might be the case?
- If the Earth were to warm up, what do you believe might happen to the various semipermanent pressure features around the world?
- Assume an Earth surface comprised solely of water. Describe midlatitude jet stream characteristics for this Earth. Would troughs and ridges develop? Why or why not?



PART 3

Climates Across Space

CHAPTER 8 Climatic Classification

- Early Attempts at Global Climatic Classification
- Classical Age of Climatic Classifications
- Genetic Classifications
- Local and Regional Classifications
- Quantitative Analysis to Derive Climatic Types
- Summary
- Key Terms
- Review Questions
- Questions for Thought

CHAPTER 9 Extratropical Northern Hemisphere Climates

- Climatic Setting of North America
- Climatic Setting of Europe
- Climatic Setting of Asia
- Regional Climatology
- Summary
- Key Terms
- Review Questions
- Questions for Thought

CHAPTER 10 Tropical and Southern Hemisphere Climates

- Contrasts Between Extratropical and Tropical Atmospheric Behavior
- Contrasts Between Northern and Southern Hemisphere Atmospheric Behavior
- Climatic Setting of Africa
- Indian Ocean Dipole
- Climatic Setting of Australia and Oceania
- Climatic Setting of Latin America
- Climatic Setting of Antarctica
- Regional Climates
- Summary
- Key Terms
- Review Questions
- Questions for Thought



CHAPTER 8

Climatic Classification

CHAPTER AT A GLANCE

- Early Attempts at Global Climatic Classification
- Classical Age of Climatic Classifications
 - Modified Köppen Climatic Classification System
 - Thornthwaite Climatic Classification System
 - Other Global Classification Systems
- Genetic Classifications
 - Air Masses and Fronts
 - Classification of Fronts
- Local and Regional Classifications
- Quantitative Analysis to Derive Climatic Types
 - Eigenvector Analysis
 - Cluster Analysis
 - Hybrid Techniques
- Summary
- Key Terms
- Review Questions
- Questions for Thought

If you were given a list of 500 cities around the world and were asked to divide that list into categories based on the climates those cities experience, how would you do it? You would probably not put Seoul, South Korea, in the same category as Bogotá, Colombia, simply because the temperature regime is too different between those cities to be listed in the same category. Similarly, Cairo, Egypt, and Kuala Lumpur, Malaysia, probably do not belong in the same category because

the former city is arid and the latter is wet. But what categories are the most logical?

Because climate represents the integrated total of weather, and weather represents a great variety of individual atmospheric phenomena such as temperature, precipitation amount and type, seasonality, humidity, wind direction and speed, and cloud type, many different atmospheric variables can be used to categorize climate. All these variables are important contributors to the

overall climate of a location. For certain applications, however, some variables are more important than others. If you were conducting your climatic classification as an employee of a giant energy conglomerate that was investigating the feasibility of installing hundreds of wind turbines around the world to generate wind power, the most logical atmospheric variables to include might be wind speed and direction and seasonal variability of wind. Perhaps some stations have consistently strong winds from a similar direction year-round, another set of stations may have light winds from variable directions in summer but strong winds from the same direction in winter, and so forth. In short, the criteria used in the classification of climates depend on the use of the classification.

A characteristic of all sciences, classification is used to simplify our conception of a complicated process. Biologists have an elaborate, hierarchical classification of life, with kingdom at the broadest level and species (and variety) at the most specific. Similarly, geologists classify rocks and minerals, and chemists classify elements. Even in everyday life we use classification as a shortcut to describing things. When you hear the word “chair,” you understand that the person speaking with you may be conveying information about anything from a recliner to a beanbag chair, to a throne, to a device for execution.

Effective classifications can be helpful, but ineffective classifications can be more confusing than helpful. The number of classes is also important. Classifications that have too many categories can be cumbersome and difficult to implement, but those that have too few categories group items together that have little in common. Any effective classification procedure, including those in climatology, minimizes the *within-group variability* of the variables being considered and maximizes the *between-group variability*.

Tens of thousands of weather stations around the world record at least some meteorological information on a regular basis. Much of these data are reported to national and/or worldwide climate centers on monthly to annual time scales. Climatic classification systems were devised to summarize the overwhelming amount of atmospheric data that can accumulate even over a short time period and to simplify the climatic characteristics of any location.

Regionalization of climate is useful for several reasons. First, it is an effective tool to gauge the expected pattern of weather for particular locations. Expected weather over the course of the year may be used as an initial forecasting tool. Second, regionalization of weather can identify useful *extremes* and climatic *normals* to which daily meteorological variables may be compared even if no data are available at the exact point of interest. Third,

long-term shifts in the boundaries of climatic regions as indicated by climatic classifications may provide an indicator of the degree of climatic variability and change shown over time, which could be manifested as shifts in bioclimatic and agricultural zones, domains of diseases, and weather-related human mortality.

Planetary-scale climatic classification schemes allow for the identification of generalized climatic regions. Although local and regional-scale classifications can be extremely useful in resolving particular climate-related problems, more generalized climatic information at broader scales can also be useful in aiding understanding of climatic variation across space. Generalized planetary-scale climatic classification schemes are usually devised using the most widely needed and readily available atmospheric variables: temperature and precipitation and seasonality of those variables. As noted previously, however, they may require other data, depending on the intended application.

► Early Attempts at Global Climatic Classification

Early attempts by the ancient Greeks at classifying climate resulted in the identification of three principal climate regions: the Frigid Zone, the Temperate Zone, and the Torrid Zone. The **Frigid Zone** obviously represented the polar *latitudes* of the planet, an area once thought to be uninhabited due to excessive cold. The **Torrid Zone** also was deemed uninhabitable because of the extreme heat thought to occur within the tropics. The **Temperate Zone**, representing the supposedly only habitable portion of the planet, lay between the other two latitudinal extremes. Not surprisingly, Greece fell in the Temperate Zone. This identification scheme was devised around 500 bc by Paramenides, sometimes known as the Father of Logic. It represents an early attempt to classify climate based solely on logic, in the total absence of climatic data.

Other climatic classification schemes followed, including one by Hipparchus who updated the Paramenides classification by including information on the calculated day length for particular locations. Calculations about day lengths were based on solar angle on the spherical Earth's surface (yes, early Greek scholars knew that Earth was a sphere and were able to calculate its circumference). According to this classification the zones were renamed *klimata*—a word referring to slope, which in this case represents the inclination of the noon Sun at a point on Earth.

Logic-based climatic classification systems persisted until the development and proliferation of weather

recording instrumentation. Of particular importance was the development of the thermoscope by Galileo in 1593, which led to the development of the first thermometer created by Santorre in 1612 and the barometer by Evangelista Torricelli, a student of Galileo, in 1643. Once these and updated forms of the instruments were dispersed worldwide, the formal analysis of weather and climate became a realistic possibility.

► Classical Age of Climatic Classifications

Because of relatively short data records (most weather records persist for less than 100 years) and the massive amount of atmospheric data collected from individual weather stations, the identification of true climatic regions is a relatively recent endeavor. The classical age of climatic analysis began with the mathematical and vegetation-based **Köppen Climatic Classification System** devised by the botanist Vladimir Köppen in 1870. It was Köppen who coined the term “climatic classification.” The Köppen system uses monthly temperature and precipitation data in making the calculations.

The **Thornthwaite Climatic Classification System**, formulated by C. Warren Thornthwaite in 1931 and completed in 1948, represents an alternative to the Köppen system. The Thornthwaite system is built on the physical interactions between local precipitation and temperature rather than only the moisture and temperature data. It represents a more sophisticated and precise scheme of classification based on local surface water availability.

The Köppen system is the most widely used system, largely because of its simplicity and its strong correspondence between climatic regions, natural vegetation communities called **biomes**, and soil types. The Thornthwaite system is preferred by physical scientists in need of precise climate information, particularly when moisture availability is of critical importance, as it is in agricultural, hydrological, and environmental planning applications.

Modified Köppen Climatic Classification System

Not coincidentally, the Köppen system is largely based on dominant vegetation types, because the botanist recognized that most vegetation types respond directly to climatic inputs, especially temperature and moisture variations. Believing that natural vegetation could be used as a rough indicator of generalized climatic regions, he determined that the same mean value of the

atmospheric variable (e.g., temperature, precipitation) that separates two biomes should also separate two climatic types.

Over the years the Köppen climatic classification has undergone some revisions, most notably by the climatologists Rudolf Geiger in 1961 and Glenn Trewartha and Lyle Horn in 1980, to provide more accurate correspondence between climatic zones and biomes. The modified Köppen climatic regions in this book use the Geiger modification and are shown in **FIGURE 8.1**. While neither Köppen, Geiger, Trewartha, nor Horn intended for the climates to be delineated over the oceans, the availability of gridded global data sets of variables that were used in calculating the biomes allows the equivalent oceanic climatic types to be included in Figure 8.1. Although the system does have some inherent drawbacks, the fundamental attraction lies in the simplicity and accuracy of the system.

Köppen observed and mapped the **ecotone**—the transition zone between two biomes—and then used temperature and precipitation data to derive equations to define the climatic boundary between those two biomes. Using such criteria Köppen identified five main climatic groups: A (tropical), B (arid), C (**mesothermal** or midlatitude mild), D (**microthermal** or midlatitude cold), and E (polar). With some exceptions the A, C, and D climates support the growth of trees, whereas the B and E climates generally do not, being either too dry or too cold, respectively. Later, an additional group, H (highland), was added to account for the extreme climatic variations across short distances in mountainous locations. Note that Figure 8.1 is shown at a resolution that is too coarse to allow for H climates to be shown. The main types were further subdivided into additional second- and third-order subdivisions to classify regional climates more precisely. **TABLES 8.1, 8.2, and 8.3** detail the Köppen-Geiger climate system.

Specific Köppen-Geiger climatic types are derived by combining appropriate first-, second-, and third-order subdivisions. In the case of A, C, and D climates the second-order subdivision refers to the precipitation seasonality (with “f” representing climates that are wet year-round, “m” representing tropical monsoon conditions, “s” indicating dry summer climates, and “w” representing dry winter climates). For B climates the second-order subdivision is “W” if the dry climates are true deserts and “S” if the dry climates are only semi-arid. Notice the capitalization on this and only some of the other second-order letters. Because German nouns are always capitalized, the capital letters represent their equivalent nouns in German. In the case of “E” climates, the second-order subdivision is “T” for **Tundra climate**, a milder polar subtype, while “F” (frozen) is used to represent the Ice Cap subtype.

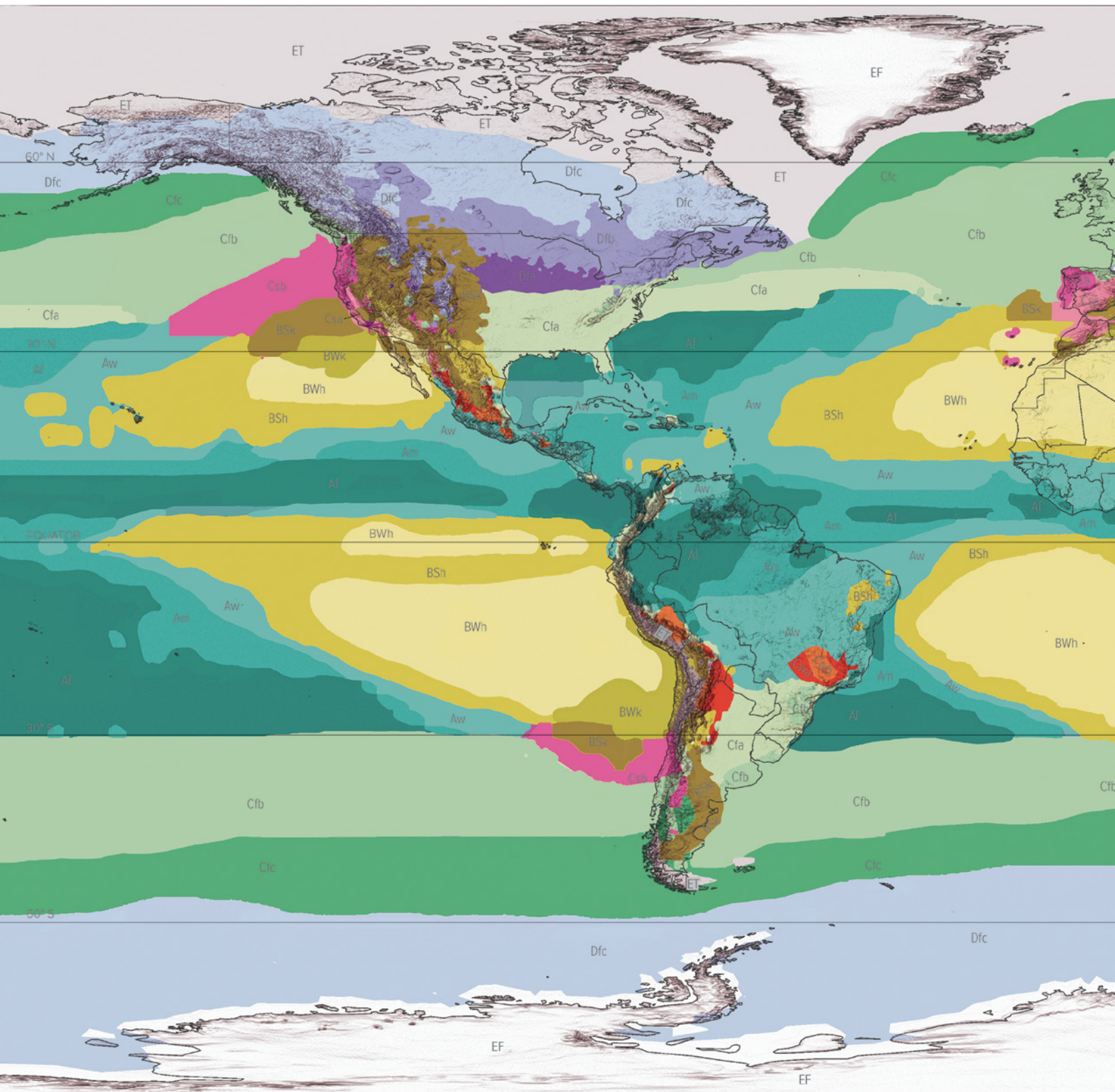


FIGURE 8.1 Köppen-Geiger climate regions of the world.

Reproduced from McGraw-Hill Education, S.J. Reynolds, R.V. Rohli, J.K. Johnson, P.R. Waylen, and M.A. Francek, *Exploring Physical Geography*, Second Edition © McGraw-Hill Education.

TABLE 8.1 First-Order Köppen-Geiger Climatic Classification Division

Subtype	Classification	Criteria Specifics
A	Tropical	Coolest month $> 18^{\circ}\text{C}$ (64°F)
B	Dry	See specifics bulleted in text
C	Mesothermal	Coldest month $> 0^{\circ}\text{C}$ (32°F) but $< 18^{\circ}\text{C}$ (64°F) Warmest month $> 10^{\circ}\text{C}$ (50°F)
D	Microthermal	Coldest month $< 0^{\circ}\text{C}$ (32°F) Warmest month $> 10^{\circ}\text{C}$ (50°F)
E	Polar	Warmest month $< 10^{\circ}\text{C}$ (50°F)
H	Highland	Undifferentiated highland climates

TABLE 8.2 Major First-Order Köppen-Geiger Climatic Classification Subdivisions

Subtype	Classification	Criteria Specifics
BW	Desert	True desert
BS	Steppe	Semiarid
ET	Tundra	Warmest month $< 10^{\circ}\text{C}$ (50°F) but $> 0^{\circ}\text{C}$ (32°F)
EF	Ice Cap	Perpetual frost, all months $< 0^{\circ}\text{C}$ (32°F)

For the mesothermal and microthermal climates, third-order subdivisions identify the characteristics of summer temperatures, with “a” used for hot summers, “b” for warm summers, “c” for mild summers, and the rare “d” for cool summers. Arid climates have a third-order subdivision of “h” and “k,” which denote “hot” and “cold” arid or semiarid regions, respectively.

For example, Atlanta, Georgia’s Cfa climatic type indicates a mild midlatitude climate (C) featuring an even distribution of precipitation through all months of the year (f) and hot summers (a). The system yields 13 major climatic types with additional subtypes. **TABLE 8.4** describes the major climate types in the Köppen-Geiger system. Although many other second- and third-order subdivisions have been identified, those listed in the tables are the most commonly used.

TABLE 8.3 Partial Listing of Köppen-Geiger Second- and Third-Order Subdivisions

Second Order	Third Order	Criteria Specifics
	a	Warmest month $> 22^{\circ}\text{C}$ (72°F)
	b	Warmest month $< 22^{\circ}\text{C}$ (72°F)
	c	Fewer than 4 months $> 10^{\circ}\text{C}$ (50°F)
	d	Same as c but coldest month $< -38^{\circ}\text{C}$ (-36°F)
f		Constantly moist. Rainfall through all months of year
m		Monsoon rain, short dry season. Total rainfall sufficient to support rain forest
s		Summer dry season
w		Winter dry season
W or S	h	Hot and dry year-round Average annual temperature $> 18^{\circ}\text{C}$ (64°F)
W or S	k	Cold and dry year-round Average annual temperature $> 18^{\circ}\text{C}$ (64°F)
	n	Frequent fog
	n'	Infrequent fog but high humidity and low rainfall

Because natural vegetation boundaries are ambiguous in most locations, they should be viewed as broad transition zones rather than absolute boundaries between dissimilar climates. This is especially true of tropical climates, which are delineated by natural vegetation boundaries that are governed by annual precipitation variations.

Midlatitude climates tend to be separated by temperature thresholds. Specifically, mesothermal climates have a mean temperature of the coldest month above 0°C (32°F) but below 18°C (64°F), with the mean temperature of the warmest month above 10°C (50°F). Such conditions sustain midlatitude broadleaf and mixed

TABLE 8.4 Major Climatic Types of the Köppen-Geiger System

Class Type	Description
Af	Tropical rainy
Am	Tropical monsoon
Aw	Tropical wet/dry
BW	Desert (truly arid)
BS	Steppe (semiarid)
Cf	Midlatitude rainy, mild winter
Cw	Midlatitude wet/dry, mild winter
Cs	Mediterranean
Df	Midlatitude rainy, cold winter
Dw	Midlatitude wet/dry, cold winter
ET	Tundra
EF	Ice Cap
H	Highland (variable, mountainous)

forests, temperate rain forests—including the redwoods and sequoia of California—and in one subcategory, tall grasslands. Microthermal climates are those in which the mean temperature of the coldest month is below 0°C (32°F), while the mean temperature of the warmest month lies above 10°C (50°F). These climates support hardier broadleaf, mixed, and needleleaf forests. In essence, these two may be considered to represent warm extratropical and cool/cold extratropical (but nonpolar) climates, respectively.

The warmest month in polar climates has a mean temperature below 10°C (50°F). The ecotone between subtypes of E climates is delineated by whether any months in the year have an average temperature above freezing. If so, the ET (Tundra) designation is used. Tundra includes various types of shrubs and successively shorter vegetation in the poleward direction, including Arctic grasses, hardy species of mosses, and lichens (a symbiotic combination of fungus and algae that clings to rock), but no trees. The **treeline** separates the D from the E climates in the Köppen-Geiger system. EF climates are characterized by limited, highly specialized life forms—if any at all.

Virtually all the climates discussed thus far are derived from only a few input variables. Dry climates (B) are a bit more involved, however. A “dry” climate is one in which mean *evapotranspiration* tends to exceed mean precipitation during most months. These two interacting variables must be accounted for and quantified using a simplified *surface water balance* approach. A region in which most precipitation occurs during the cool (winter) season shows a markedly different water balance from one in which the majority of precipitation falls during the warm (summer) season. These climatic differences present themselves in the type and distribution of vegetation given that summer evapotranspiration rates are much higher than those during winter. Likewise, a similar annual precipitation total at the two locations may produce completely different ecosystems built around the timing of the precipitation and the resultant water balance.

A notable feature of Figure 8.1 is the strong (and surprising to many) presence of B climates over the subtropical oceans. The lack of fresh water prohibits inhabitation of many subtropical islands and restricts it to areas with local orographic enhancement on other islands.

Dry (B) climates occur if any one of the following three sets of criteria is completely true, where P represents annual precipitation in centimeters and T is mean annual Celsius temperature:

- More than 70% of the annual precipitation occurs in the summer half of the year *and* $P < 2(T + 14)$.
- More than 70% of the annual precipitation occurs in the winter half of the year *and* $P < 2T$.
- Less than 70% of the annual precipitation occurs in the summer half of the year, less than 70% occurs in the winter half of the year, *and* $P < 2(T + 7)$.

One of the most noteworthy features of B climates is their prevalence over oceans. As shown in Figure 8.1, a substantial part of the world's subtropical oceans experience the combination of high temperatures and little precipitation.

A given B climate is classified as a true desert climate (BW) if any of the following are completely true:

- More than 70% of the annual precipitation occurs in the summer half of the year *and* $P < (T + 14)$.
- More than 70% of the annual precipitation occurs in the winter half of the year *and* $P < T$.
- Less than 70% of the annual precipitation occurs in the summer half of the year, less than 70% occurs in the winter half of the year, *and* $P < (T + 7)$.

Otherwise, the B climate is classified as BS—a semi-arid or **steppe climate**. Notice that to distinguish BW from BS climates in each case above, the term on the

TABLE 8.5 True Desert (BW) and Steppe (BS)
Köppen-Geiger Climatic Subdivisions

Subdivision	Description
h	Mean annual temperature > 18°C (64°F)
k	Mean annual temperature < 18°C (64°F)
k'	Mean temperature of warmest month < 18°C (64°F)
s	Receives less than 30% of precipitation during warm season (summer)
w	Receives less than 30% of precipitation during cool season (winter)

right is halved from the criteria to distinguish B climates from the humid climates. The BW and BS climates can be further subdivided as shown in **TABLE 8.5**; multiple subdivisions are possible, such as BW_{hs}.

Although the Köppen-Geiger classification may seem complex, in reality it is quite simple. The system is fairly accurate at presenting generalized climatic regions, but it is not ideal if specific local and short-term climatic influences are important. Regional climatic boundaries may shift over short periods of time given the annual variability of both temperature and precipitation at particular locations. The system is inaccurate in places where climate is not the primary reason for the distribution of particular natural vegetation types; soil type, topographical relief, and other factors can play more significant roles than subtle climate differences in some places. There is, therefore, not an exact correspondence between climatic type and vegetation distribution. Finally, the system does not explain why the climatic types exist and is instead solely based on the broad-scale results of climate—the data. This makes it difficult to quantify specific attributes that cause particular climatic types. Despite these drawbacks the system is widely regarded as the most useful broad-scale climatic classification system. The Köppen-Geiger system is, therefore, used in this book to discuss regional climatic types. But first we examine some other commonly used systems.

Thornthwaite Climatic Classification System

In the 1930s C. Warren Thornthwaite devised a precise climatic classification system. Thornthwaite thought that climate could be ultimately classified by the interactions

between the amount of energy present at a location over the course of the year and the amount of available moisture. These interactions between energy and moisture are the keys to identifying individual climatic zones in this system.

To complete the system, Thornthwaite devised a number of specific indices to quantify necessary climatic components. The **moisture index (MI)** is based on the precipitation amount and the *potential evapotranspiration (PE)* rate for a location. PE refers to the number of centimeters of equivalent precipitation that could be lost from the surface to the atmosphere from both surface *evaporation* and plant *transpiration* from a short grass field given a nonlimiting supply of soil moisture. The Thornthwaite method of calculating PE differs from others, but regardless of the system of estimating PE this variable can be used to calculate a simple water balance for a location. The MI is calculated from,

$$MI = \frac{100 (S - D)}{PE}$$

where S is the *surplus* water amount and D represents the *deficit* water amount, both in centimeters of precipitation equivalent.

For any period when PE meets or exceeds the precipitation amount, the surplus is zero. In such a scenario the equation above shows that the MI is zero or negative, indicating aridity. The opposite scenario—a precipitation amount that exceeds PE—is associated with $S > 0$ and $D = 0$, suggesting humid conditions and a positive MI. Using the MI, Thornthwaite calculated nine climatic moisture regimes. This classification is detailed in **TABLE 8.6**.

Thornthwaite also derived a **thermal efficiency index**—the ratio of temperature to a calculated evapotranspiration value. Again, nine thermal climatic types are identified (Table 8.6). In addition to the MI and temperature-to-evapotranspiration ratio, Thornthwaite calculated a **dryness index (DI)** and a **humidity index (HI)** to identify the times of the year with water deficit or surplus. Calculations for each are as follows:

$$DI = 100 \frac{D}{PE}$$

$$HI = 100 \frac{S}{PE}$$

The DI and HI delineate additional climatic sub-categories, as shown in **TABLE 8.7**. A final subdivision of the system comes from the examination of **summer thermal efficiency concentration**—the ratio of PE in the summer months to total annual PE in the surface water balance at a location. This is shown in **TABLE 8.8**.

TABLE 8.6 Major Moisture and Temperature Divisions of the Thornthwaite Classification System

Moisture Divisions			Temperature Divisions		
	Climatic Type	Moisture Index	T/ET (cm)	Climate	Type
A	Very humid	≥ 100	14.2	E'	Ice
B ₄	Humid	80–99	28.5	D'	Tundra
B ₃	Humid	60–79	42.7	C' ₁	Microthermic
B ₂	Humid	40–59	57.0	C' ₂	Microthermic
B ₁	Humid	20–39	71.2	B' ₁	Mesothermic
C ₂	Moist subhumid	0–19	85.5	B' ₂	Mesothermic
C ₁	Subarid	–33–0	99.7	B' ₃	Mesothermic
D	Semiarid	–66 to –32	114	B' ₄	Mesothermic
E	Arid	–110 to –65	> 114	A'	Megathermic

TABLE 8.7 Thornthwaite Climatic Classification Subcategories

	Humid Climates (A, B, C ₂)	DI
R	Little or no little deficit	0–16.7
S	Moderate summer deficit	16.7–33.3
W	Moderate winter deficit	16.7–33.3
s ₂	Large summer deficit	> 33.3
w ₂	Large winter deficit	> 33.3
	Dry Climates (C, D, E)	HI
D	Little or no water surplus	0–10
S	Moderate winter surplus	10–20
W	Moderate summer surplus	10–20
s ₂	Large winter surplus	> 20
w ₂	Large summer surplus	> 20

TABLE 8.8 Summer Thermal Efficiency Subdivisions of the Thornthwaite Classification System

Subtype	Summer Thermal Efficiency Concentration (%)
a'	< 48.0
b' ₄	48.0–51.9
b' ₃	51.9–56.3
b' ₂	56.3–61.6
b' ₁	61.6–68.0
c' ₂	68.0–76.3
c' ₁	76.3–88.0
d'	> 88.0

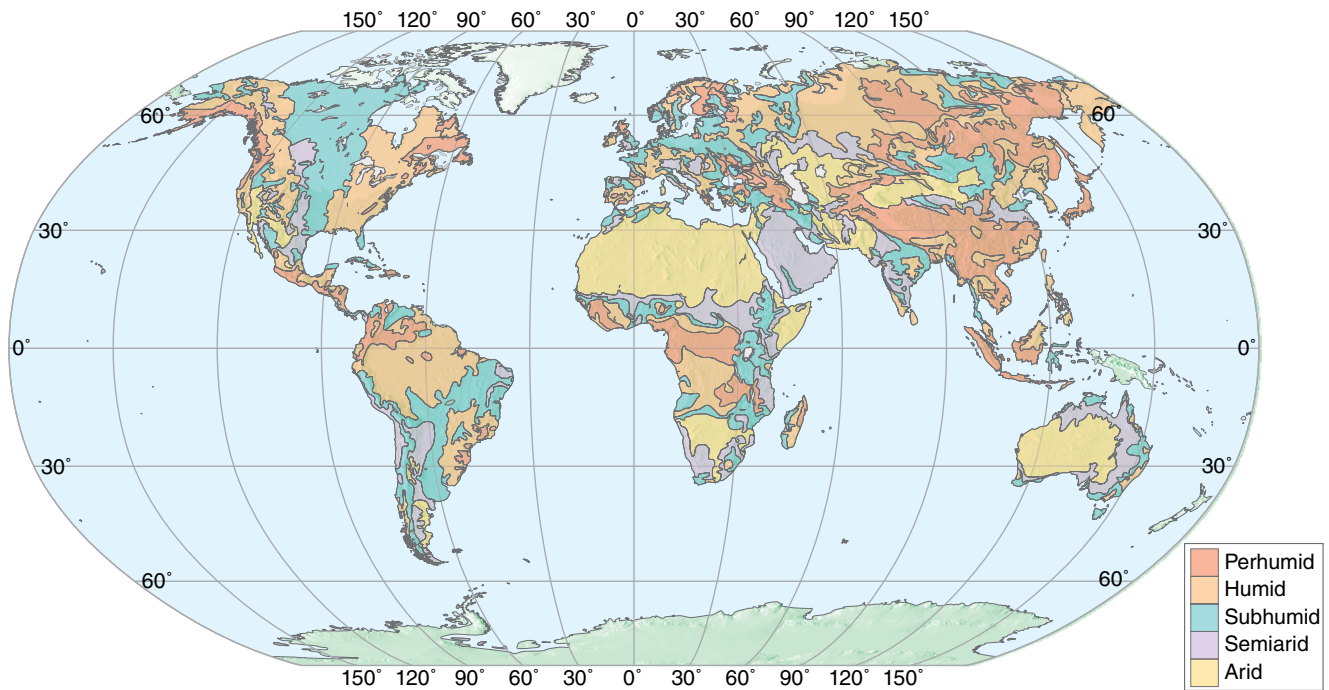


FIGURE 8.2 Generalized Thornthwaite climate regions.

Data from Carter, D. B. and J. R. Mather. 1966. Climatic classification for environmental biology. *Publications in Climatology* 19(4): 304–395.

Similar to the Köppen-Geiger classification system, individual climatic types are denoted by the combination of letters produced by the four indices.

The major Thornthwaite climate regions are shown in **FIGURE 8.2**. This system provides more detail than the Köppen-Geiger system. It also expresses climatic regions by incorporating the synergistic impacts of energy and moisture availability for examined locations. The classification system also implicitly links the energy balance to the water balance through the concept of PE. On the other hand, the Thornthwaite classification is complex, perhaps to the point of becoming cumbersome. **FIGURE 8.3** shows the results of an overlay of the generalized Köppen and Thornthwaite classifications for the contiguous United States.

Other Global Classification Systems

In 1947 American botanist and climatologist L. R. Holdridge devised a similar classification system that came to be known as the **Holdridge Life Zones Climatic Classification System**. Although it was intended to be for global application, it became most widely used in tropical areas, where it has proved useful in ecological and alpine applications. One version of the Holdridge system is shown in **FIGURE 8.4**. The Holdridge system defines **biotemperature** as an adjusted temperature

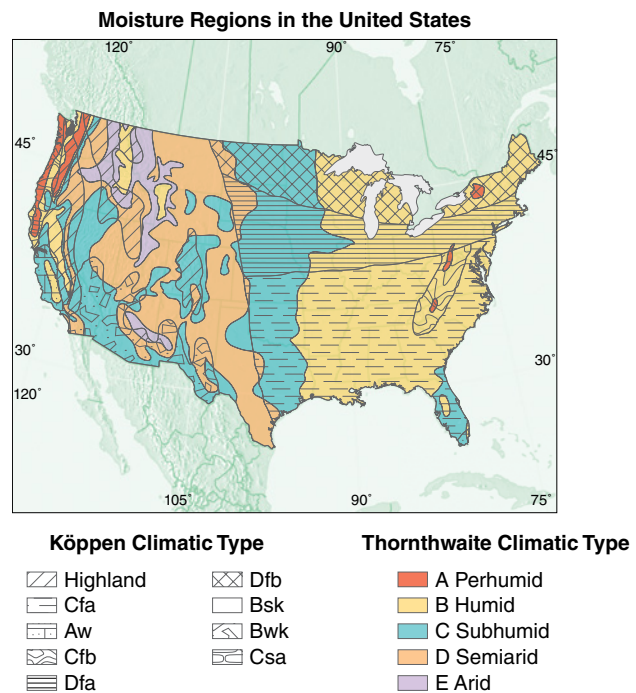


FIGURE 8.3 An overlay of the Köppen-Geiger and Thornthwaite climate regions in the United States.

Courtesy of Timothy Melançon.

that considers temperatures below freezing or above 30°C to be noncontributors to the proliferation of life (i.e., to have a biotemperature of zero), because plants

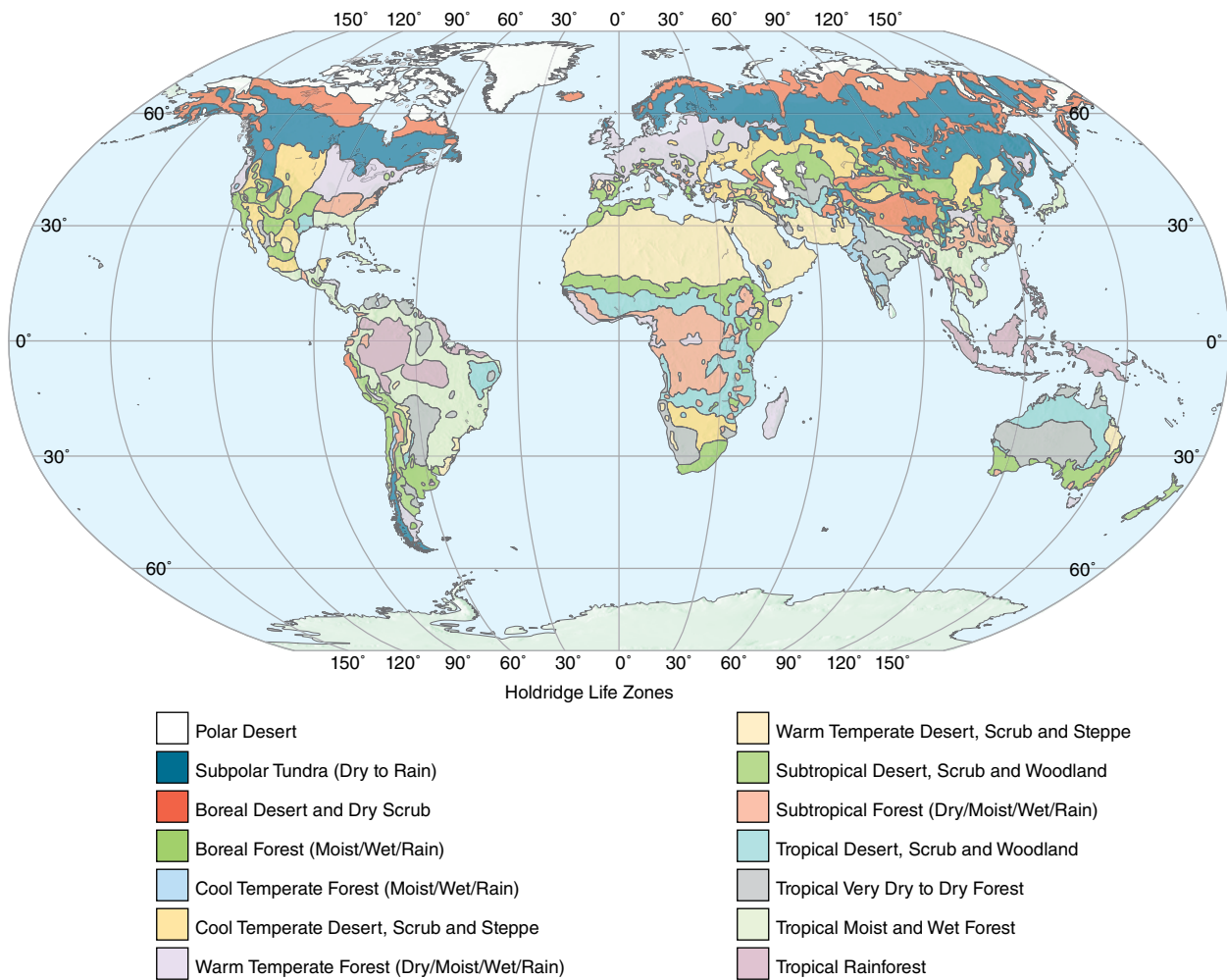


FIGURE 8.4 World map of Holdridge climate types.

Data from Leemans, R. 1990. Holdridge Life Zones of the World. Global data sets collected and compiled by the Biosphere Project, Working Paper, IIASA-Laxenburg, Austria. Adapted from Oak Ridge National Laboratory Distributed Active Archive Center, Oak Ridge, Tennessee, U.S.A. [http://daac.ornl.gov/NPP/html_docs/hold2_npp.html].

are dormant whether the temperature is freezing, far below freezing, or above 30°C. The Holdridge model also includes annual precipitation and the ratio of PE to precipitation, but Holdridge's method of calculating PE differs from Thornthwaite's. Ratios above 1.0 represent arid climates and ratios below 1.0 suggest humid climates. Holdridge's "triangular" approach to climatic classification results in 36 different possible climatic types (**FIGURE 8.5**).

Other researchers, such as the Russian climatologist (born in what is now Belarus) M. I. Budyko, also used the concept of evaporation in classifying climate. The **Budyko Climatic Classification System** uses an energy budget approach to classifying climates. In Budyko's system the ratio of *net radiation* (Q^*) to the energy required to evaporate a unit volume of local precipitation is calculated. Excess energy results in increasingly dry climates. The wet–dry climate boundary occurs where the **Budyko ratio** is 1.0.

► Genetic Classifications

The classification systems discussed above are all driven by data, operating on the premise that locations sharing similar climatic data are grouped into the same climatic type. In the Köppen-Geiger system the data involve monthly temperature and precipitation and the seasonal variations of each. The Thornthwaite and Holdridge systems rely on the computation of PE based on monthly temperature and precipitation data—a surface water balance approach. Budyko includes a radiation variable in his system.

A system that requires the input of data to calculate the climatic type based on predetermined class boundaries, such as those discussed above, is termed an **empirical climatic classification system**. Such systems have the advantage of being easy to implement in locations where high-quality and abundant climatic data are available. They also ensure that two locations

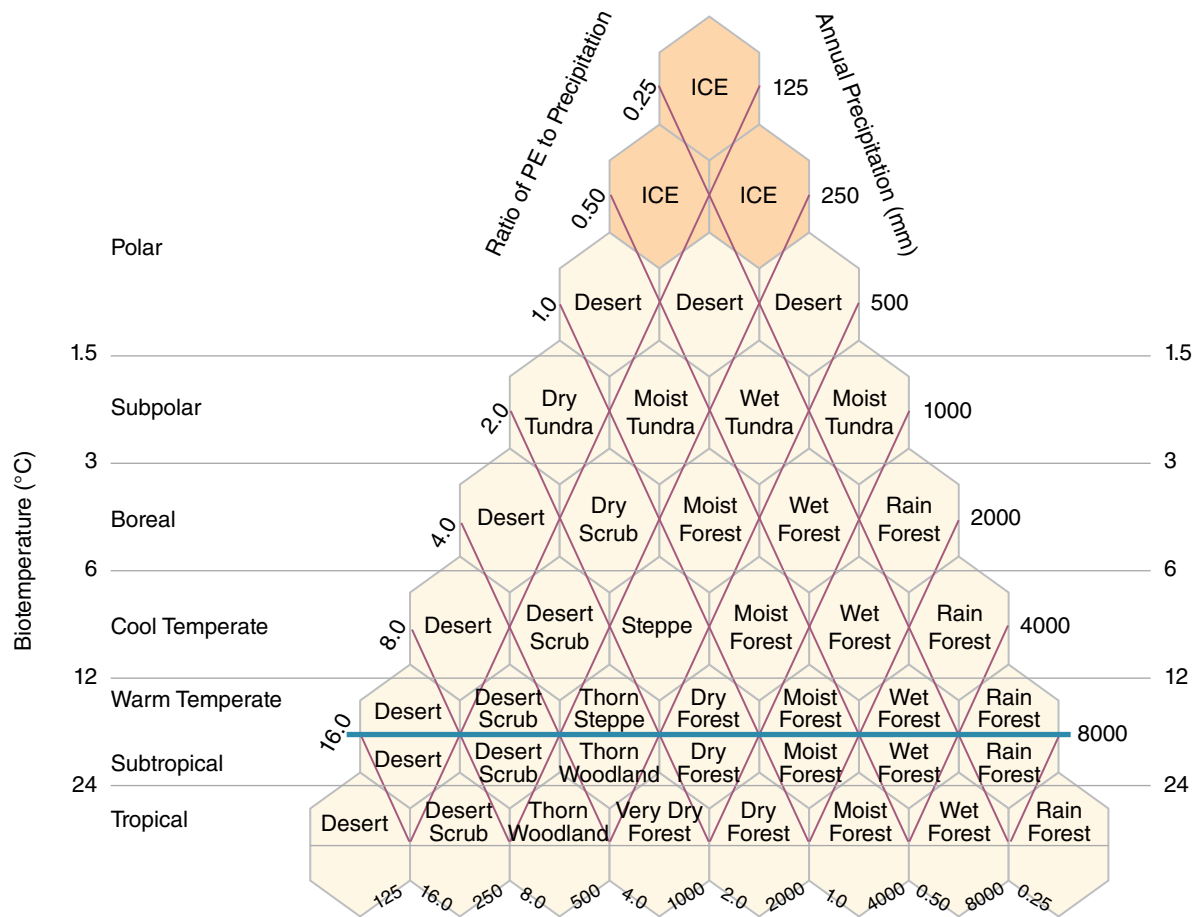


FIGURE 8.5 The Holdridge life zones pyramid.

Source: The Holdridge Life Zones Pyramid. Cuming, Michael J. and Barbara A. Hawkins, 1981. "TERDAT: The FNOC System for Terrain Data Extraction and Processing." Technical Report M-254, 2nd ed. Prepared for USN/FNOC and published by the World Meteorological Organization.

with similar climatic attributes for the variables in question are categorized in the same group.

A **genetic classification system** is used to categorize climates solely on the basis of the major forcing mechanisms that make climate the way that it is. For example, the proximity of the *subtropical anticyclone* in summer but not winter is a forcing mechanism that is shared by San Diego, California, and Cape Town, South Africa. A genetic classification system would, therefore, probably consider these two cities to be in the same category.

In this case it just so happens that the temperature and precipitation features of San Diego and Cape Town are similar enough to be categorized in the same Köppen category also. By contrast, let's consider the case of Reno, Nevada, and Spokane, Washington. The climates of both cities are influenced by their position on the *leeward* side of the major mountain ranges—the Sierra Nevada in the case of Reno and the Cascades in the case of Spokane (**FIGURE 8.6a**).

A **climograph** is a representation of the monthly mean temperature (using a line) and precipitation (using

bars) for each month of the year at a place. Climographs can be efficient for characterizing the general climatological features of a location. The climograph in **FIGURE 8.6b** shows that Reno is warmer, drier, and better radiated than Spokane. A position on the leeward side of the slope does not necessarily provide the same conditions to both locations, but the climates of both locations are dictated largely by their positions on leeward slopes.

Genetic classifications do not compare the absolute numbers that represent the effect of the forcing mechanisms. Rather, they simply consider the causes involved. They are inherently more subjective than empirical methods, which can use rigid rules to classify the climates. How can we be sure that being on the leeward side of the mountain is a more important forcing mechanism than location with respect to common storm tracks, elevation, or any other potential forcing mechanism?

The **Bergeron Climatic Classification System**, devised by Swedish meteorologist Tor Bergeron in 1928, is one early-modern genetic classification system. This system categorizes the climate at a location based on

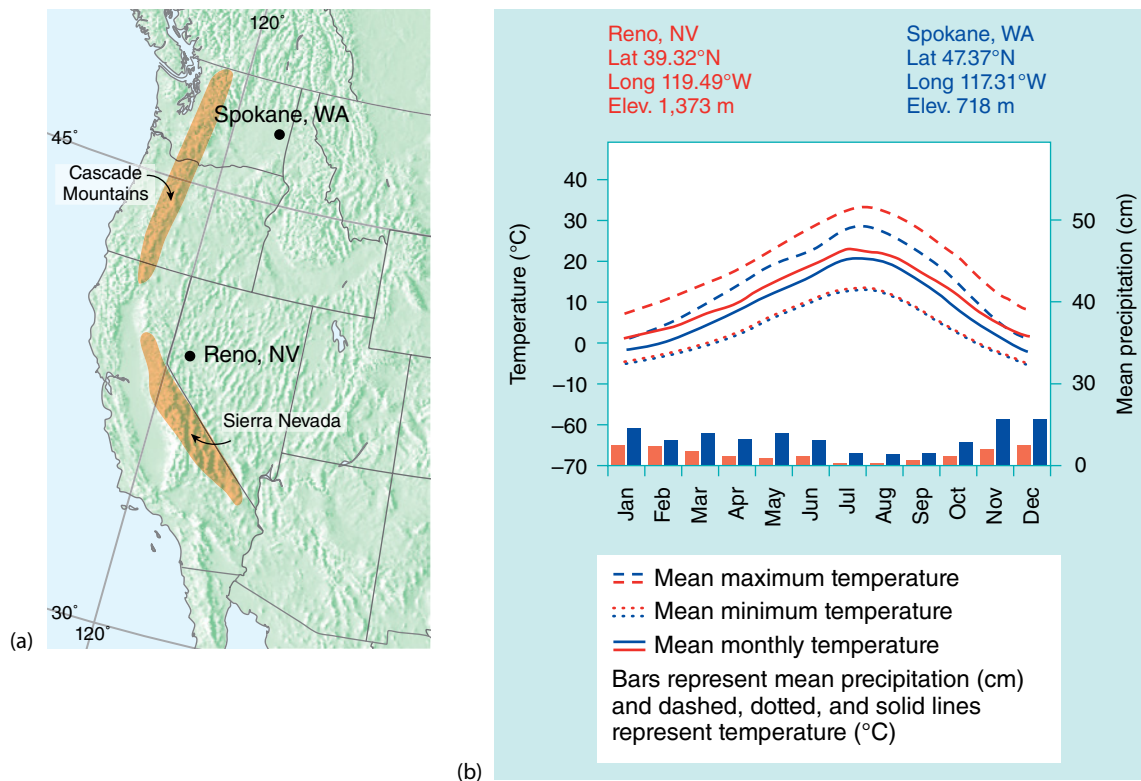


FIGURE 8.6 (a) Reno, Nevada, and Spokane, Washington, in relation to the Sierra Nevada and Cascade Mountains, respectively. (b) Climograph for Reno, Nevada, and Spokane, Washington.

the manual and somewhat subjective determination of frequency with which it is dominated by certain types of weather. Improvements on this system were suggested by several climatologists, most notably by the German-American Helmut Landsberg. These genetic classification strategies evolved during the time that the important concepts in the science of meteorology described below were developing in the United States.

Air Masses and Fronts

As discussed above, classification schemes have been used to denote major types of atmospheric conditions. Simple classifications became the focus of weather forecasting early on in the development of meteorology as a separate scientific discipline. These classification schemes were based on absolute and relative temperature and moisture characteristics, and they proved somewhat useful until Jacob Bjerknes showed, in 1922, that the development of frontal storm systems was of critical forecasting importance.

The Bjerknes model classified areas of a surface midlatitude *cyclone* and associated pressure features into specific sectors, with each section exhibiting particular weather characteristics. Forecasting the motion of the migratory cyclone became the new focus, allowing forecasters to anticipate specific weather characteristics over

time for a location as a cyclone tracked over a region. This classification scheme improved the accuracy of weather forecasting and is still used today. Knowledge of air masses and the Bjerknes model, which applies only to midlatitude systems, is necessary to fully understand the midlatitude regional climates around the world.

Air Masses

An **air mass** is a body of air that is relatively uniform in its characteristics for distances of hundreds to thousands of square kilometers. The characteristics of an air mass result largely from the properties of the **source region**—the place where the air mass forms—usually a relatively broad, homogeneous region where air may stagnate. **FIGURE 8.7** shows the major air mass source regions for the globe. Remember that air gains its temperature and moisture properties directly from the surface through the absorption of terrestrial radiation and the evapo-transpiration of moisture, respectively. Source regions that are cold and dry—such as those occurring over high-latitude continental regions—produce cold, dry air masses. By contrast, air stagnating over a large, warm ocean surface likely gains the properties of that surface, resulting in a warm, moist air mass. The transfer of the source region's thermal and moisture characteristics to the air mass overlying it is enhanced through *turbulence*.

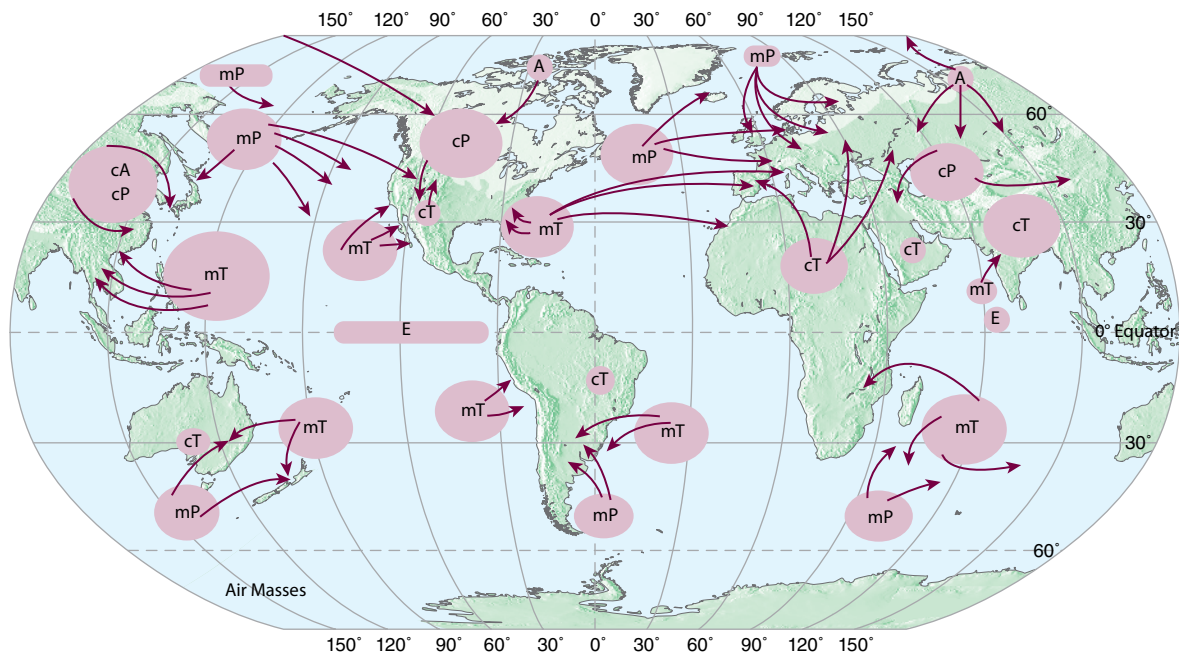


FIGURE 8.7 Major air masses and their source regions.

The more unstable the atmosphere, the more rapidly the atmospheric properties of the source region can be transferred to the air mass over it. The longer an air mass remains over its source region, the more likely the air mass is to attain the properties of its source region.

Source regions are typically flat because such areas attain fairly uniform energy and moisture characteristics, as opposed to a mountainous terrain where those factors change appreciably across small spaces. Source regions tend to be tropical and high-latitude ocean regions and broad, flat continental regions. Most mid-latitude regions are poor source regions because in the midlatitudes different air masses converge and weather changes rapidly.

The air mass classification system typically uses only two variables—moisture and temperature characteristics (TABLE 8.9). The moisture indicator appears first in the designation system. The lowercase letter “c” represents air of continental origin and, therefore, dry atmospheric conditions, and “m” indicates moist air of maritime origin. Temperature characteristics follow with uppercase designators. The uppercase letter “T” denotes warm air of tropical origin, “A” denotes bitter cold air of Arctic origin, and “P” indicates somewhat less severe cold air of polar origin.

Classifying the various air mass types is simply a matter of combining the moisture and temperature designators. Two cold, dry air mass types affect the northern sections of the northern hemisphere. These are the intensely cold and dry **Arctic (A) air masses** and the slightly warmer and more humid **continental polar (cP) air masses**. Likewise, high-latitude oceans produce

TABLE 8.9 Air Mass Classification System

Temperature	Moisture Characteristics	
	Dry	Humid
Cool/cold	A, cP	mP
Warm/hot	cT	mT, E

cool, humid air masses called **maritime polar (mP) air masses**. Portions of the northern hemisphere extratropics are affected by tropical air masses as well. Tropical oceanic source regions generate **maritime tropical (mT) air masses**, while inland tropical source regions produce the hot, dry **continental tropical (cT) air masses**. The system also includes a category for the **equatorial (E) air mass**—a more extreme version of the mT air mass type. Note that A and E air mass types only need to have one letter because A air masses are inherently dry (as so water is available to evaporate and so little energy is available to evaporate water in such latitudes) and E air masses are inherently moist (because of the abundance of moist source regions and the abundant energy to evaporate water at these latitudes). It is important to distinguish the *air mass* classification system from the Köppen *climatic* classification system—in the latter “A” represents a tropical climate and “E” represents a polar climate! The midlatitude, upper-tropospheric

Rossby waves transfer air masses away from their source regions. Arctic and polar air masses migrate equatorward on the ridge-to-trough side of the wave, whereas tropical air masses undergo *advection* in a poleward direction on the trough-to-ridge side of the wave. These waves exist as a mechanism to even out the imbalance between energy receipt at the poles and equator. These continuous motions of air, which respond to energy inequalities across the latitudes, represent the primary mission of the atmosphere. But because the Sun is, of course, constantly sending more intense energy to the equator than to polar regions, this mission of achieving thermal balance across the latitudes can never be achieved. The result is a warmer polar area and a cooler equatorial area than would exist without the Rossby wave activity, but polar areas remain colder than the tropical parts of Earth.

Classification of Fronts

Cold, Warm, and Stationary Fronts

Because the midlatitude part of Earth is the region where cold air and warm air masses usually converge, this is the area where vigorous exchanges of energy occur. A **front** is a narrow zone of perhaps 100 km (60 mi) where air masses of different temperature and humidity meet. A **cold front** represents a situation in which a colder air mass is pushing a warmer air mass back toward its source region. Cold fronts are represented on surface weather maps by blue lines, with blue triangles pointing in the direction in which the cold air is moving (**FIGURE 8.8a**). The warm air at a cold front is pushed upward at an angle of perhaps 2° above the horizontal. Although this angle may seem gentle, it is actually steep. The atmosphere is thin enough that if air moves upward at a 2° slope and we assume that the tropopause is 12 km (7.5 mi) above the surface, the horizontal distance required to reach all the way up to the tropopause (x) could be calculated as,

$$\tan 2^\circ = \frac{12 \text{ km}}{x}$$

or only 344 km (213 mi)! This relatively narrow zone is sufficient to ensure that cloud cover at cold fronts is vertically oriented. This produces **cumuliform clouds** and includes the severe weather-producing **cumulonimbus clouds**. Cumuliform clouds generally produce intense precipitation of short duration. “Cumuli-” means “piled up” and originates from the same root that produces words such as “accumulation” and “cumulative.”

A **warm front** is a region where a warmer air mass is displacing a colder one poleward. These are represented on surface weather maps by red lines with red semicircles pointing in the direction that the warmer

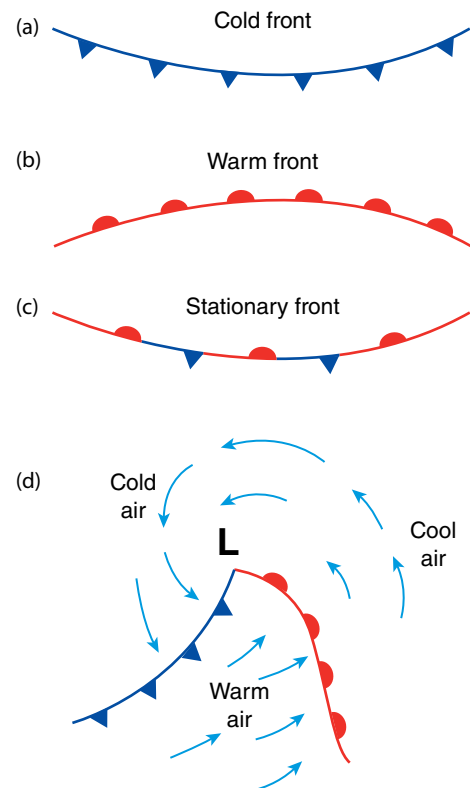


FIGURE 8.8 Fronts. (a) Cold front. (b) Warm front. (c) Stationary front. (d) The midlatitude wave cyclone.

air is moving (**FIGURE 8.8b**). The ascent of relatively warm air at the warm front proceeds only at perhaps an angle of 1° . At this rate of steepness the air would take 687 km (427 mi) to reach a 12-km-high tropopause. This gentler angle ensures the formation of more horizontally oriented **stratiform clouds**, which are widespread and associated with precipitation of only light or moderate intensity that lasts for long periods of time. Precipitation intensity is directly proportional to cloud thickness and is thus less in stratiform clouds, which are much thinner than cumuliform clouds. Warm fronts may produce convective clouds if the air is particularly unstable, but this is a less common phenomenon.

For periods of up to several hours the cold and warm air masses may temporarily meet at a **stationary front**—a stalemate in which neither air mass is pushing the other backward. Stationary fronts are depicted on a weather map by an alternating red and blue line, with blue triangles pointing in the direction that the colder air would move if it could move and red semicircles pointing in the direction that the warmer air would move if it could move (**FIGURE 8.8c**).

When referring to fronts it is important to note that the temperatures are relative ones. The air behind a cold front may be 0°C (32°F) in winter but 30°C (86°F) in summer. It is also colder in higher latitudes than in lower latitudes, as the air masses warm as they move equatorward.

Midlatitude Wave Cyclone

Fronts do not typically occur in isolation. Instead, they are usually part of a larger system known as the *midlatitude wave cyclone* (FIGURE 8.8d). These cyclones are the largest storm systems on the planet, with diameters between 1600 and 3200 km (1000 and 2000 mi). Because weather conditions vary across space depending on location with respect to the midlatitude wave cyclone, such a cyclone provides an ideal model for classification systems. At the core of the midlatitude wave cyclone is a cyclonic (i.e., low-pressure) center. The rotation of air around the cyclone (counterclockwise in the northern hemisphere) causes colder air to be pushed equatorward behind (i.e., to the west of) the cyclone. This is the cold front. Likewise, ahead of (i.e., to the east of) the cyclonic center, the counterclockwise rotation pushes tropical air poleward. This is the warm front.

Midlatitude wave cyclones are sometimes referred to as *secondary circulations* because they are embedded within the larger general circulation. Specifically, air associated with a midlatitude wave cyclone rotates cyclonically (counterclockwise in the northern hemisphere) while it is also moving in a general west-to-east direction as dictated by the general circulation (i.e., the midlatitude westerlies). Such circulation is common in nature; a river has a general circulation downslope toward sea level, with smaller eddies spinning while embedded within that general circulation.

Migratory anticyclones also may act as secondary circulations by spinning about within the broader-scale general circulation. Unlike midlatitude wave cyclones, midlatitude anticyclones cannot be associated with trailing fronts, because the sinking air in an anticyclone does not provide adequate energy via the release of *latent heat* to develop the pressure gradients required to move fronts poleward or equatorward.

Occluded Fronts

In general, a cold front progresses around a midlatitude cyclone faster than a warm front as the entire system moves eastward in the midlatitude circulation. The reason is that colder air can displace warmer air relatively easily because it is denser than the warmer air. Warm fronts migrate relatively slowly because it is more difficult for the less dense, warmer air to displace the colder air. Also, the midlatitude cyclone migrates in the same general direction of warm front propagation, so the warm front does not radically change its position relative to the core of the system. After a few days of traveling eastward in the midlatitude westerlies, the cold front actually catches up with the warm front near the cyclonic center, where the two

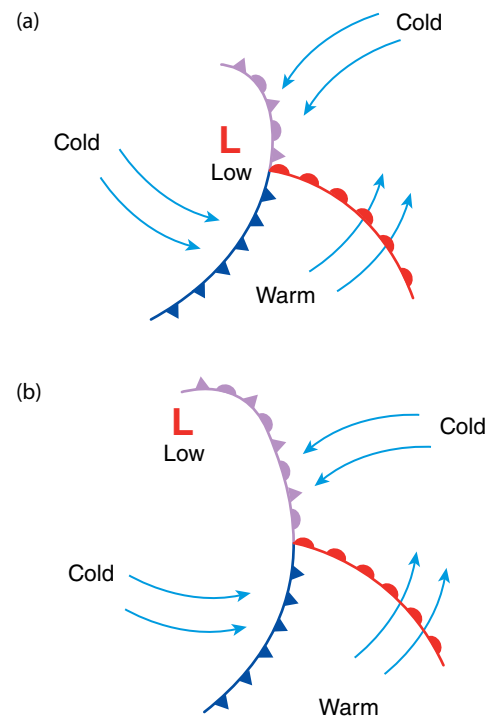


FIGURE 8.9 The occlusion process. (a) Occlusion begins nearest to the low pressure center (b) and then proceeds away from the center over time.

fronts are closest to each other (FIGURE 8.9a). The result is an **occluded front**, which is depicted on a weather map by a purple line with alternating purple triangles and semicircles both pointing in the direction that the colder air is moving after having caught up with the warm front. Over time, the occlusion proceeds farther away from the cyclonic center (FIGURE 8.9b) as the **warm sector**—the area between the fronts—closes. At occluded fronts, both cumuliform clouds associated with the (former) cold front and stratiform clouds associated with the (former) warm front are present. By the time occlusion occurs, most of the storm's moisture has precipitated and most of its energy has been spent. The entire system will have also moved into an area of decreasing upper-air *absolute vorticity* as it approaches the upper-level *ridge*, altering the motion of air through the vertical. This causes the system to decay. Occluded fronts are usually associated with abundant clouds but neither intense precipitation nor severe weather activity.

At an occluded front the warmer air mass is lifted over the surface by both the cold and the warm fronts. This results in a *stable stratification* of air, with colder, denser air lying beneath warmer, less dense air. This vertical lifting is also superimposed on the horizontal mixing of air induced by the cyclonic circulation of the entire system. Overall, the system worked to push colder

air equatorward and warmer air poleward while lifting the less dense air over denser air. The system extracts energy from the differences between contrasting air masses. The occlusion represents the point when vertical and horizontal mixing has been accomplished. The temperature contrast between the air masses wanes and the fronts disappear, coincident with vorticity changes in the overlying atmosphere. Occlusion can be considered to be the end of the midlatitude wave cyclone's life.

► Local and Regional Classifications

The **Lamb Weather Types** and **Muller Weather Types** are two climatic classification systems based on the midlatitude wave cyclone model. Although at their core they represent meteorological classification systems, these two systems can be used in climatic classification by tabulating daily frequencies of predefined weather patterns observed over the British Isles and the U.S.

Gulf coast, respectively, in calendar form. These two systems are based on the position of a location relative to major secondary circulation features, including mid-latitude cyclones and anticyclones. **FIGURE 8.10** provides an example of the Muller Types. Other similar manual climate classification systems have followed these by requiring manual analysis of weather maps to produce the classification.

The Lamb and Muller Weather Types are genetic attempts to classify climates at local and regional scales. Of the many climatic classification schemes, the majority address specific climatic topics for particular locations or regions. For example, **FIGURE 8.11** shows a regionalization of temperature across the south-central United States, devised for analyzing changes in extreme temperature events across regions. When temperature is anomalously high (or low) at one location in Figure 8.11, it also tends to be anomalously high (or low) at all other locations within the same region. Meanwhile, temperatures in other delineated regions have as little in common as possible with concurrent temperatures in the group in question.

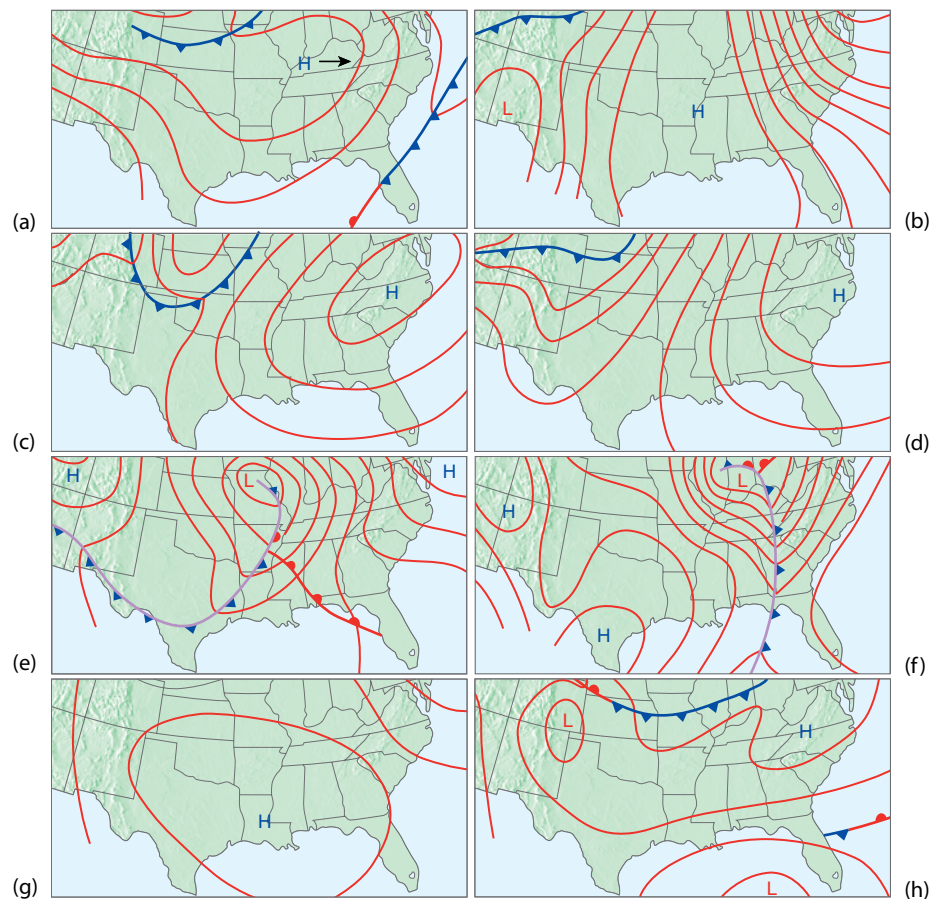


FIGURE 8.10 An example of the Muller Weather Types for the Central Gulf of Mexico coast–Pacific High type. This anticyclone centered over Arkansas, Texas, Oklahoma, and Louisiana was pushed eastward from the Pacific region.

Data from the National Weather Service, NOAA.

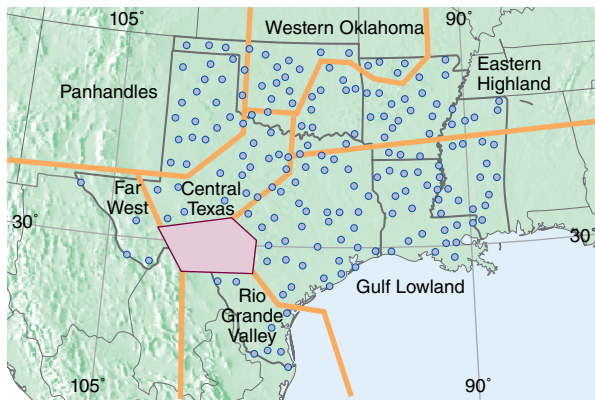


FIGURE 8.11 A climatic classification of temperature in the south-central United States. The light gray area in southwestern Texas indicates a region where lack of data precluded cluster assignment.

Modified from Bohr, G. S. 2005. Trends in extreme daily temperature events in the south-central United States. Dissertation, Louisiana State University.

► Quantitative Analysis to Derive Climatic Types

Eigenvector Analysis

The technique used to delineate the temperature regions in the south-central United States in Figure 8.11 is one of a family of multivariate mathematical techniques called **eigenvector analysis**. The technique allows for relationships between two different sets of variables to be analyzed simultaneously. Climatologists are usually concerned with three types of variables: atmospheric data (which may include variables such as surface temperature, 500-mb *geopotential height*, wind speed, and humidity), spatial variables (represented by weather stations), and temporal variables (such as monthly data from 1895 through 2013).

To date, no mathematician has identified a way to analyze all three sets of variables simultaneously while considering the variables as part of each respective set. But eigenvector analysis allows us to find relationships between any two sets of variables simultaneously while holding the third set constant. For example, a common type of eigenvector analysis (including the temperature study for the south-central United States discussed previously) examines how one atmospheric variable (not a set of variables) varies across space and time. Such an analysis allows the climatologist to map the spatial distribution of that variable (such as surface air temperature) while simultaneously considering the temporal variation in that variable. Where in the study area is the greatest temporal variability in (say) surface temperature, and how does this variability change over time? This is a powerful analytic tool, because no other

family of quantitative techniques allows for simultaneous analysis across space and time. The only alternatives are visualization techniques, which could show a “movie” of how (say) temperature changes across space and time, but such changes would be difficult to quantify.

Alternatively, we could examine how a set of atmospheric variables (such as surface temperature, 500-mb geopotential height, humidity, and wind speed) interacts holistically at one station over time. This type of eigenvector analysis would hold space constant while examining the variability of atmospheric variables through time. Of course, such analysis would not allow for the mapping of the results *per se*, but if separate analyses were conducted, one station at a time, then atmospheric and temporal variables could be analyzed simultaneously at each site. Locations where similar characteristics of the atmosphere tend to occur simultaneously would be categorized as being dominated by the same air mass type at that time. This is the premise behind the **Spatial Synoptic Classification System** designed by climatologists Laurence Kalkstein, Scott Sheridan, and others.

Time is seldom the entity held constant in climatology, because climatology is inherently concerned with conditions across time. However, multiple analyses could be conducted, perhaps one analysis per day (where time is held constant on each iteration). The distribution of synoptic types (represented by the various atmospheric variables) across space (represented by the weather stations) then can be mapped for each day, with temporal changes in the pattern noted.

In climatology the specific eigenvector technique that is most typically used is **principal components analysis (PCA)**. For reasons beyond the scope of this discussion, this analytical tool is preferred over other related types of eigenvector techniques: common factor analysis, singular value decomposition, and empirical orthogonal function analysis. In each of the three types of examples described previously, PCA can identify **components**—the main modes of variability in the data set.

Returning to the example shown in Figure 8.11, in analyses such as this one that examine spatial and temporal differences in only one atmospheric variable, the PCA technique provides coefficients for each spatial variable (called **loadings**) and each temporal variable (called **scores**) on the component. The loadings are proportional to the degree to which the eigenvector model represents each of one type of variable (say, temperatures at various stations) collectively for all temporal observations in the data set. The scores are proportional to the degree to which the model represents variability in each of the other type of variable (in this case, each temporal observation) collectively for the

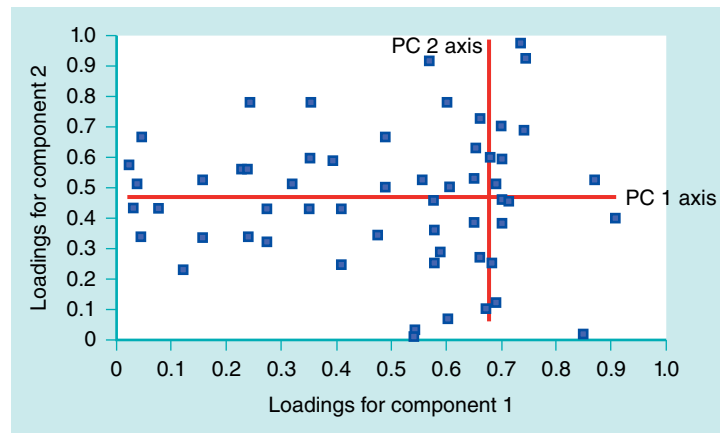


FIGURE 8.12 Schematic of a hypothetical data set with loadings of the first two principal components plotted. The first regression line maximizes explained variance in the data set, and a second perpendicular regression line maximizes the explanation of residual variance.

first variable (temperature collectively, undistinguished by station). The PCA model (and all other eigenvector techniques) maximizes the relationship between the component and as many locations and times as possible. Then the eigenvector technique generates a second component solution that attempts to provide the strongest relationship possible between the atmospheric variable of interest (temperature) across the other two entities (space and time, in this example) that remains unaccounted for by the first component.

By analogy, imagine a series of data points in two-dimensional space (**FIGURE 8.12**). A **regression line** can be drawn to pass as closely as possible to as many points as possible, so as to minimize the squared sum of the vertical distances between each point and the line. If the line passes close to many points, then the model represented by the line effectively “explains” the variance in the data points. By contrast, if the data points are scattered all over the graph, as they are in Figure 8.12, the regression line would not explain as much variance. If a second line is drawn that is perpendicular to the first line, it may explain the **residual**—“new” variance that remains unexplained by the first component. PCA uses eigenvectors in this manner to “draw lines” as near as possible to as many points as possible, represented in this case by spatial and temporal data. Each of these lines corresponds to a certain amount of variance present in the data set. Eventually there will be as many lines drawn through the data set as there are data points in the set so that 100% of the data set variance is explained.

Loadings and scores also are associated with the second component (line), which is perpendicular to the first component and accounts for a particular amount of the remaining data set variance (but less than the first component, which passes through the greatest concentration of data points). If a third component is

also calculated, it is represented by a line that is perpendicular to both the first and the second lines. The process can again be repeated, but we cannot even imagine this line, because it would occur in three dimensions. Mathematically, and in a multidimensional space of a computer, drawing this line is possible, and it is “drawn” in such a way that it explains as much of the remaining (or residual) variance in the data set as possible. The process is again repeated with each successive component explaining less variability than the one before, as the unloaded (unrelated) data points are farther from the interior cluster. But it is, of course, impossible to visualize these perpendicular lines because they, too, exist in more dimensions than our brains can process.

Cluster Analysis

The actual classification process in any eigenvector analysis (including PCA) comes when the matrix of loadings or scores (which usually represents the spatial and temporal variability, respectively, in the data set) is subjected to a **cluster analysis**. In the example of temperatures across the south-central United States, cluster analysis could be used to categorize the loadings across space. Each station in the analysis would have a loading for each of the n components retained for analysis. We could plot the loadings of each station (at whatever the spatial scale of analysis was) in n -dimensional space. Obviously, because it is impossible to visualize more than three dimensions, this is a highly abstract concept. So let’s just imagine a two-dimensional solution (**FIGURE 8.13**). If the loadings for the first two components are plotted as shown, a clustering procedure can group the resulting points into a manageable number of clusters, with the points (stations) whose loadings are closer to each other in the same group. Then boundaries can be drawn to

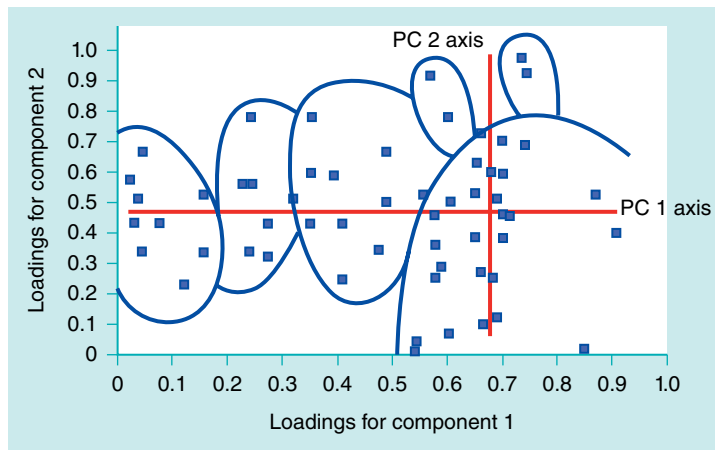


FIGURE 8.13 A cluster-based solution using the data shown in Figure 8.12.

separate the stations that fall into different categories. Just as the loadings can be clustered to delineate spatial regions, scores can be clustered to identify months (or days, or whatever the temporal scale of analysis) that have similar temporal properties of the atmospheric variable being analyzed (in this case, temperature).

Several types of cluster analysis can be used, and each gives a slightly different classification result. However, all have the common goal of selecting the groups so that the distance in n -dimensional space between the points within the cluster (within-group variability) is minimized. Likewise, the distance between points that lie in different clusters (between-group variability) should be maximized. The researcher may select the number of clusters to be created, either by using a preselected value or by looking for natural “break points” in the data. This could be determined by plotting the **eigenvalues**—the total variance accounted for by a component—for each component on a chart called a **scree plot**. At some point a break in the eigenvalue curve appears, as in **FIGURE 8.14**. The researcher should examine all components up to the break point while discarding all components that appear after that point. So, for example, if the division of a data set into seven clusters does not minimize the distances between points within each cluster much better than a six-cluster solution, then the researcher may simply opt for the six-cluster solution because it is simpler to use.

Hybrid Techniques

In recent years some researchers have made use of **hybrid climatic classification techniques**—methods of climatic categorization that have the advantages of manual techniques such as the Lamb or Muller Weather Types and those of automated eigenvector analysis. Hybrid methods typically require the investigator to identify “prototype” atmospheric circulation patterns manually—a “textbook” case of each particular genetic

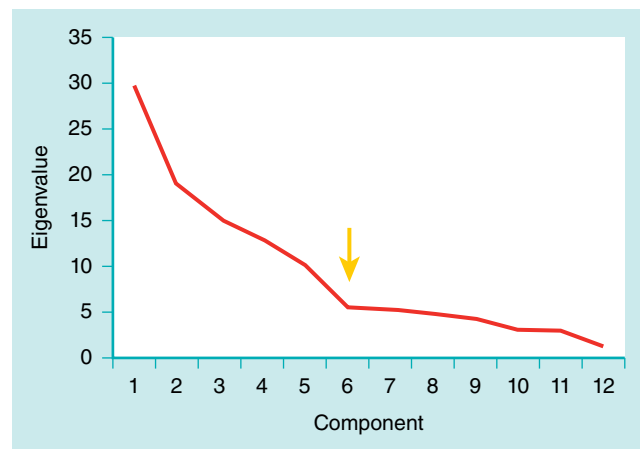


FIGURE 8.14 Hypothetical scree plot with “break in slope” denoted.

category, perhaps. Then a computerized cluster analysis is used to categorize all other days (or months, if monthly mean data are used) automatically into the group with the prototype day (or month) that the weather map for the day (or month) in question most resembles. This is done by comparing the pressure or geopotential height value at each data point on the map to the corresponding value at each analogous point on each of the prototype maps. Such a map provides the smallest sum of differences for all pairs of data points with the day to be classified and is the circulation type for the day in question.

Summary

Climatologists classify climates for the same reason as other scientists—that is, to summarize and simplify our conception of a myriad of unique climates. The ancient Greeks divided Earth into three zones, based on their perception of habitability in those zones. In

modern times Vladimir Köppen's classification system has become the most widely used system, largely because of its strong correspondence to vegetation and soil realms. Thornthwaite developed a classification system based on the surface water balance, thereby implicitly incorporating energy as a driver of evaporation. Thornthwaite's system is more detailed and precise than Köppen's classification, but the complexity of deriving the moisture indices has limited its utility, particularly among nonscientists. Other notable classifications have been derived by Holdridge and Budyko.

Genetic classifications are based on the causes of the climate rather than on the results as shown by climatic data. Such genetic classifications in the extratropical world often rely on the position of a location relative to air masses, fronts, and midlatitude wave cyclones. Air masses can be characterized as Arctic, continental polar, maritime polar, maritime tropical, continental tropical, and equatorial.

When dissimilar air masses meet, fronts are formed, and these fronts represent parts of a midlatitude wave cyclone. At a cold front the colder air mass displaces a warmer air mass. Cold fronts are characterized by cumuliiform cloudiness and possibly intense precipitation and severe weather. The warm front is the site of warmer

air that is displacing colder air, and it is characterized by stratiform cloud cover and precipitation of light to moderate intensity across a widespread area. Eventually, the occlusion process ends the midlatitude wave cyclone's life span. Notable among the cyclone-based genetic classification systems are weather-typing schemes such as those devised by Lamb and Muller that can be adapted for use in regional climatological analysis.

Eigenvector-based techniques in combination with cluster analysis can be used to automate the classification process for the analysis of data across space and time. The Spatial Synoptic Classification is a notable example of such a classification. Eigenvector analysis can also be used to identify the major climatic types represented in the data set. This is done by manipulating a data matrix containing two types of entities (some combination of locational variables, temporal variables, and atmospheric variables) so that the major modes of variability in the data set are extracted. The resulting loadings and scores matrix can then be clustered to categorize the major climatic types in the data set. In recent years human observers can select the "prototype" of the major types, and then automated clustering techniques can be used to find the prototype to which a given day or month corresponds most closely.

Key Terms

Absolute vorticity

Advection

Air mass

Arctic (A) air mass

Bergeron Climatic Classification System

Biome

Biotemperature

Budyko Climatic Classification System

Budyko ratio

Climograph

Cluster analysis

Cold front

Component

Continental polar (cP) air mass

Continental tropical (cT) air mass

Cumuliform cloud

Cumulonimbus cloud

Cyclone

Deficit

Dryness index (DI)

Ecotone

Eigenvalue

Eigenvector analysis

Empirical climatic classification system

Equatorial (E) air mass

Evaporation

Evapotranspiration

Extreme

Frigid Zone

Front

Genetic classification system

Geopotential height

Holdridge Life Zones Climatic Classification System

Humidity index (HI)

Hybrid climatic classification technique

Köppen Climatic Classification System

Lamb Weather Types

Latent heat

Latitude

Leeward

Loading

Maritime polar (mP) air mass

Maritime tropical (mT) air mass

Mesothermal

Microthermal

Midlatitude wave cyclone

Moisture index (MI)

Muller Weather Types

Net radiation (Q^)*

Normal

Occluded front

Potential evapotranspiration (PE)

Principal components analysis (PCA)

Regression line

Residual

Ridge

Rossby wave

Score

Scree plot

<i>Secondary circulation</i>	Summer thermal efficiency	<i>Transpiration</i>
Source region	concentration	Treeline
Spatial Synoptic Classification	<i>Surface water balance</i>	Tundra climate
System	<i>Surplus</i>	<i>Turbulence</i>
<i>Stable stratification</i>	Temperate Zone	Warm front
Stationary front	Thermal efficiency index	Warm sector
Steppe climate	Thornthwaite Climatic	
Stratiform cloud	Classification System	
<i>Subtropical anticyclone</i>	Torrid Zone	

Terms in italics have appeared in at least one previous chapter.

Review Questions

1. What purpose does climatic classification serve?
2. What is the goal of any climatic classification system?
3. How did the ancient Greeks classify the climates of Earth?
4. What is the goal of the Köppen Climatic Classification System?
5. What is the basis of the Thornthwaite Climatic Classification System?
6. In the Köppen system, what does the third letter usually represent?
7. What is the treeline and how is it used in the Köppen system?
8. How did Köppen define “dry” when he devised the arid or “B” climatic type?
9. What is the moisture index in the Thornthwaite system and how is it derived?
10. In what part of the world is the Holdridge Life Zones Classification most applicable? Why?
11. On what is the Budyko Climatic Classification System based, and how is it best used?
12. How does a genetic classification system differ from an empirical classification system?
13. Discuss how and why air masses form over source regions.
14. What are the four types of fronts? How does each form and what are the general characteristics of each?
15. Briefly describe the midlatitude wave cyclone model.
16. How would weather conditions (winds, temperature, moisture, clouds, and precipitation) change for a location if a midlatitude cyclone tracked over it with the core of the system passing to the north of the location?
17. What are the three entities that can be evaluated only two at a time in climatological classification using eigenvector analysis?
18. Why is it necessary to use cluster analysis after doing eigenvector analysis for climatic classification?

Questions for Thought

1. In what sense could the argument be made that the Budyko Climatic Classification System is both empirical and genetic?
2. Draw a midlatitude cyclone model, complete with warm and cold fronts, for the southern hemisphere.
3. Do you believe that manual methods are better than the computer-generated eigenvector techniques for classifying climates? Why or why not?
4. Design a climatic classification system for tourists interested in outdoor urban sculpture.



CHAPTER 9

Extratropical Northern Hemisphere Climates

CHAPTER AT A GLANCE

- Climatic Setting of North America
 - General Characteristics
 - Severe Weather
 - Role of the Gulf of Mexico and the Low-Level Jet
 - Effect of Mountain Ranges
 - Effect of the Great Lakes
 - Ocean Currents and Land–Water Contrast
- Climatic Setting of Europe
 - General Characteristics
 - Effect of Ocean Currents
 - Effect of Mountain Ranges
 - Blocking Anticyclones
- Climatic Setting of Asia
 - General Characteristics
 - Monsoonal Effects
 - Effect of Mountain Ranges
 - Effect of Coastal Zones on Climate
- Regional Climatology
 - B—Arid Climates
 - C—Mesothermal Climates
 - D—Microthermal Midlatitude Climates
 - E—Polar Climates
 - H—Highland Climates
- Summary
- Key Terms
- Review Questions
- Questions for Thought

Have you ever wondered whether some other place on Earth, perhaps thousands of miles away, has the exact same type of climate as your hometown? Because the fundamental forcing properties—such as day length, Sun angle, storm passages, elevation, *continentality*, and cloud cover—exert an influence everywhere on Earth, it is possible that distant locations may have the same fundamental climatic properties. This chapter describes and explains the major aspects of the climatic setting of the extratropical northern hemisphere, with a focus on the Köppen-derived climates of North America, Europe, and Asia. Tropical climates that occur in North America and Asia are discussed elsewhere in the text.

► Climatic Setting of North America

General Characteristics

The climates of North America may be described as diverse. Conditions range from extremely dry to exceedingly wet and from bitterly cold to oppressively hot. The extreme range of *latitudes* in North America, from the tropics to well within the *Arctic Circle*, causes a wide array of temperatures. In addition, the continent spans longitudinally from approximately 170°E to about 30°W, or from the western edge of the Aleutian Islands to the eastern shores of Greenland. Although the *international date line* is situated at approximately 180° longitude, it zigzags around the Aleutians so that all of Alaska is on the same calendar day even though the westernmost part of the state is actually in the eastern hemisphere.

With such an expansive latitudinal and longitudinal span, one would expect a considerable continental influence. Although continentality is an important factor in the climatology of North America, the presence of the Gulf of Mexico and the North Atlantic Ocean gives the eastern half of North America a significant *maritime tropical (mT) air mass* influence as well. Furthermore, the north–south mountain chain alignment in North America allows mT air masses to infiltrate deep into the continental interior east of the Rockies, thus reducing the effect of continentality in comparison with Asia.

The most densely populated parts of North America lie within the northern hemisphere's midlatitudes and subtropics. The northern hemisphere's midlatitudes can be defined as the region between 30°N and approximately 60°N. The climate of this area is dominated by the *midlatitude westerlies*. The midlatitudes represent a zone of transition between the warm, moist tropics and the cold, dry polar region. Pronounced seasonality and a wide range of weather phenomena occur across this part of the continent.

Severe Weather

The midlatitude part of North America is the site of some of the most impressive severe weather on the planet. No other area of the world experiences such frequent juxtaposition of radically different *air masses* as midlatitude North America. This variety of air masses occurs primarily because of the orientation of the major north–south mountain ranges (**FIGURE 9.1**). This arrangement allows for *continental polar (cP)* and *Arctic (A)* air masses to penetrate to fairly low latitudes, where they mix freely with mT air masses that migrate deep into the continental interior. The resulting *baroclinicity*—the intermixing of different air masses—leads to the development of strong *midlatitude wave cyclones*. Frequently, along the warm and (especially) the *cold front* region of these storm systems, tornadoes, hail, strong winds, heavy precipitation (rain, snow, hail, sleet, and/or freezing rain), and/or lightning occur.

In mid- to late-fall, the Atlantic coast of North America may also occasionally experience a midlatitude wave cyclone that interacts and merges with an approaching *tropical cyclone*. Such a situation can intensify the combined system to the level of a major **hurricane**. This occurs when the low pressure cores of each system merge and deepen such that the tropical system takes on midlatitude cyclone characteristics near landfall. The storm system essentially becomes a severe **Nor'easter**. Such an event is sometimes termed a **superstorm** and can have drastic consequences. Hurricane/Superstorm Sandy of October 2012 is the most noteworthy recent event. Sandy was the largest

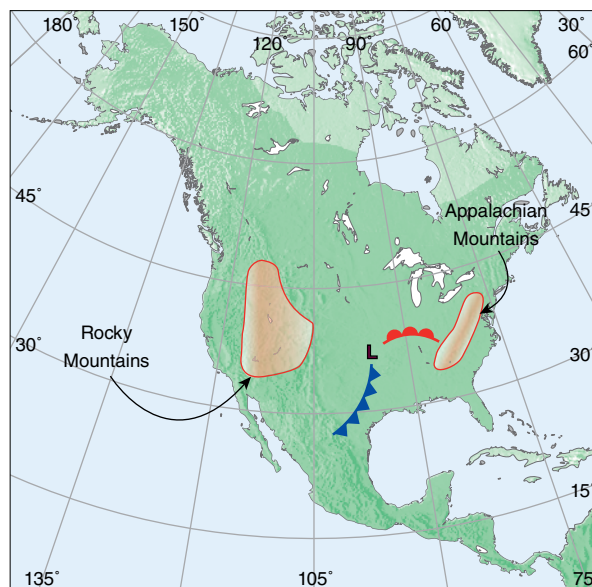


FIGURE 9.1 Selected physiographic features of North America.

Atlantic hurricane on record in terms of the diameter of its wind field, and was surpassed only by Hurricane Katrina of 2005 in property damage estimates among Atlantic tropical cyclones. In addition, Sandy exhibited retrograde motion, traveling east-to-west against the normal west-to-east storm trajectories common in the midlatitudes. This placed the storm over major cities such as New York and Philadelphia and affected the Atlantic coast from Cuba to the Maritime Provinces of Canada.

While Sandy was unusual in size, strength, and motion characteristics, the merging of such systems is not uncommon. Another example of such a merging of storm systems was the 1991 Halloween Nor'easter, nicknamed "The Perfect Storm." That storm caused widespread destruction along the coastline of the U.S. Northeast, but its trajectory carried the system over the Grand Banks region of the Canadian North Atlantic, sparing major populated areas in both the United States and Canada.

Because of the high frequency and magnitude of severe frontal *cyclones* and tropical cyclones, the United States leads the world in tornado frequency, recording an average of approximately 1000 per year. Tornadoes typically develop in the large *cumulonimbus clouds* that accompany a cold front, in association with a tropical cyclone, or (most frequently) in advance of a cold front along a **squall line**.

Squall line thunderstorms are set up as mT air meets a *continental tropical (cT) air mass* within the warm sector of a midlatitude wave cyclone, at a location termed the **dryline**. When these two warm air masses meet, the mT air is forced above the drier cT air because moist air is less dense and more buoyant than dry air. If this fact is surprising, recall that most of the dry atmosphere is composed of N_2 and O_2 , while H_2O consists of two atoms of the lightest element and only one of oxygen (which is only slightly heavier than nitrogen). A molecule of water therefore has a lower atomic mass than a molecule in dry air, even if the air masses are of the same temperature. As the moist air rises, it is often unstable because of the greater amount of energy associated with air in the warm sector. Cold front thunderstorms create a cold downdraft of air—the **outflow boundary** or **gust front**—that wedges beneath warmer air in advance of the cold front line. The combination of lifting caused by the dryline and the outflow boundary leads to rapid uplift of the warm air in the warm sector near the cold front convergence area. This can result in squall line thunderstorms that may be severe enough to spawn tornadoes.

Many of the most impressive tornadoes are generated by severe frontal cyclones in the continental interior from south-central Canada southward through central

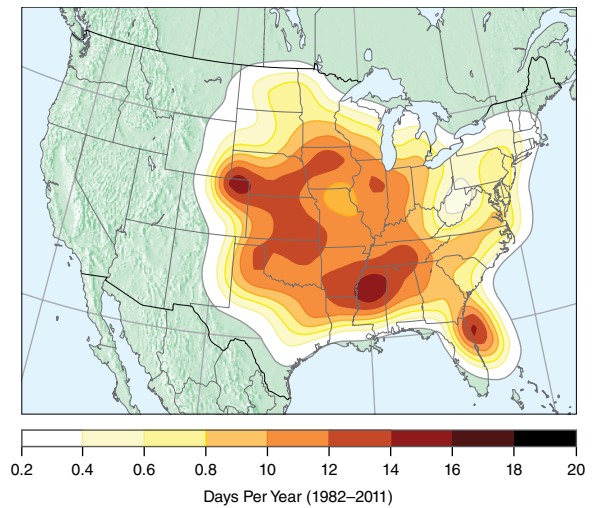


FIGURE 9.2 Average number of days per year with a tornado within 25 miles.

Courtesy of Patrick Marsh, NOAA.

Texas. This region has the greatest frequency of major tornadoes on Earth and is dubbed **Tornado Alley**. But, in actuality, the high-frequency region of North American tornadoes extends eastward in a broad area from the northern and southern sectors of the "alley," giving it a "C" shape, somewhat overlapping densely populated areas (**FIGURE 9.2**). These eastern extensions include the Midwest and the Gulf South of the United States. The highest rate of tornado-related casualties in the United States is found in **Dixie Alley**—a region in the Gulf South ranging from Texas to Florida. This pattern is due to a combination of factors, including complex forested terrain, low visibility from severe thunderstorm rainfall, and a relatively high percentage of residents in dwellings that lack stability and the safety of basements.

The preference for tornadoes in the central United States is often explained by the "clashing" of very different air masses above terrain that does little to prevent the coldest and warmest air masses from meeting in the midlatitudes. However, research in 2014 by meteorologist David Schultz and colleagues suggests that the "clash of air masses" explanation for tornadogenesis is oversimplified and incorrect. Instead, they suggest that the air mass contrast is important for tornadogenesis insofar as it encourages *vertical wind shear*, or an abrupt increase in horizontal wind speed with height, and that tornadoes are most likely in locations where sufficiently strong (though not necessarily the strongest) vertical wind shear overlies an intensely *unstable atmosphere*.

Surface conditions may play a significant role as greater evapotranspiration rates in association with soil and vegetation enhance low-level instability. For this

reason, tornadoes may occur more regularly over some areas than others. Specifically, tornado frequencies can increase downwind of a sharp land-use/vegetation/soil boundary change if the surface augments instability.

Role of the Gulf of Mexico and the Low-Level Jet

The Gulf of Mexico is of particular importance to North American climates. The Gulf represents the *source region* for the mT air masses that are so important east of the Rocky Mountains. The effect of Gulf moisture is augmented by the **low-level jet (LLJ) stream**, a river of air at approximately the 800- to 900-mb level, moving at perhaps 40–110 km hr⁻¹ (25–70 mi hr⁻¹). The LLJ advects copious amounts of moisture into the southern Great Plains.

The LLJ occurs either nocturnally from diurnal pressure changes associated with daily heating of the continent or through interactions with a cyclone. In the former case, the difference in elevation from west to east across North America plays a role in its formation (**FIGURE 9.3**). Specifically, as radiative cooling occurs nocturnally in the lower-elevation eastern part of North America, the *longwave radiation* lost from the surface is gained by the atmosphere at approximately the same height as the surface of the western United States. At the same time, the loss of surface radiation in the western

United States is occurring. This situation induces sinking of cold air over the western United States, while the relatively warm air at the same height over the eastern United States rises. This causes a *geopotential height* gradient from east to west (Figure 9.3). But as the air begins to move from east to west (against the midlatitude westerlies), the *Coriolis effect* turns the air stream to the right. The result is a southerly flow of air into the southern Great Plains. Atmospheric *stability* and an associated midlevel *temperature inversion* increase wind speeds through the *surface boundary layer* by restricting vertical fluid motion.

The effect happens at night because daytime *shortwave radiation* receipt from the Sun reduces the tendency for the surface cooling and sinking air in the western United States. However, the LLJ can occur during the daytime or nighttime in association with a midlatitude wave cyclone to the northwest of the Gulf of Mexico. In such cases the counterclockwise rotation around the cyclone draws moist air northward ahead of the cold front. The presence of the LLJ enhances the development of severe frontal cyclones and associated tornadoes.

Effect of Mountain Ranges

The high western cordillera of North America creates direct modifications to the climate. First, it effectively

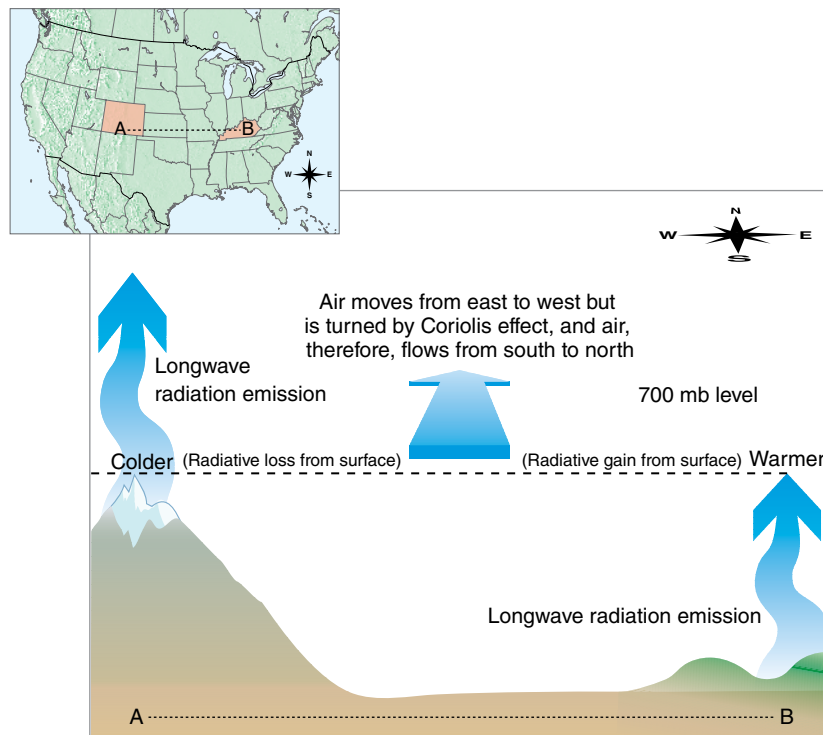


FIGURE 9.3 The formation of the LLJ in the United States.

prevents warm, moist Gulf air from being pushed by the large semipermanent *Bermuda-Azores high* west of the Rocky Mountains. It also prevents cP and A air masses from spilling westward against the flow of the midlatitude westerlies. As a result, air mass contrast is weak west of the Rocky Mountains, which means that powerful fronts and associated severe weather are relatively rare in extreme western North America. Certainly, midlatitude wave cyclones occur west of the Rockies, but these are generally *occluded fronts* that move in the westerlies from the western Pacific and Asia. They are characterized by weak frontal uplift, cloudiness, and light precipitation. During *El Niño* events the mean storm track is displaced equatorward and is termed the **Pineapple Express** because of its origins closer to Hawaii. The Pineapple Express provides abundant moisture for snowpack on the *windward* (western, in this case) side of the Sierra Nevada Mountains, which subsequently provides the water supply for densely populated southern California.

The Rocky Mountains also provide the mechanism for *ridges*—elongated areas of high pressure—to be locked in place over them. Furthermore, because of conservation of *potential vorticity*, air that descends the *leeward* sides of high mountains such as the Rockies is likely to acquire *positive vorticity* on its descent. The resulting storms often are vigorous and may spawn tornadoes, particularly if associated with the dryline.

Cyclogenesis is frequent on the leeward sides of the Rockies, particularly when abundant moisture is present. This occurs most noticeably during the transition seasons of autumn and spring. Midlatitude wave cyclones that form in this region are called **Colorado wave cyclones** or, farther north, **Alberta clippers**. The arrangement of a trough-to-ridge side of the *Rossby wave* east of the mountain cordillera also generally provides these surface storms with adequate upper-level divergence needed to sustain them as they traverse eastern North America. Such a situation, aided by the topography, promotes the intermingling of contrasting air masses. These interactions help create the most violent weather on Earth as the atmosphere works to equalize energy and moisture inequalities.

Air moving downslope from high mountains warms at the *unsaturated adiabatic lapse rate* along its descent. As a result, mountains create a situation where air can be very dry and warmer on their leeward sides. Such winds are capable of evaporating snow or water quickly. In western North America these downslope winds are known as the **Chinook winds** (the word “Chinook” is derived from a Native American term for “snoweater”). *Evaporation* and melting caused by Chinooks can destabilize slopes, causing avalanches. They can also

trigger extremely rapid changes in weather, as air may shift from northerly (cold) to westerly (warming Chinook winds) in only a matter of minutes to hours. The greatest 2-minute temperature change ever recorded on Earth, an astonishing 27 C° (49 F°), occurred in Spearfish, South Dakota, on January 23, 1943, in association with a Chinook wind.

Downslope winds also occur often on the western side of the Pacific coastal mountain ranges when a surface *anticyclone* is situated over Nevada or Utah. In such cases the clockwise flow of air around the anticyclone lifts air up the eastern sides of the slopes and down the western sides in southern California, where it dries because of adiabatic warming. On descent this air may be so dry, particularly in the late summer/autumn dry season, that forest fires and water shortages are a typical occurrence. These **Santa Ana winds** are a major hazard to life and property.

In some synoptic situations the alignment of mountains in North America also causes **cold air damming**—a condition whereby low-level cold air becomes trapped on the upwind side of highlands. This occurs from either a midlatitude surface anticyclone or cyclone forcing surface air toward a mountain range, often along the sides of both the Rocky and the Appalachian mountains when synoptic-scale systems migrate eastward (**FIGURE 9.4**). This synoptic situation pushes air from these secondary circulations against the windward side of the mountains, sometimes for days. Warm, moist air overruns the colder, denser air, enhancing cloudiness and precipitation. The damming event may cause a variety of precipitation types as the moist air is pushed upslope, with rain in lower elevations and freezing rain, sleet, and snow at successively higher elevations. Furthermore, in a damming event the affected region sees persistent cold for longer than would occur if the mountains were not present. Adiabatic cooling of the air mass moving upslope further decreases associated temperatures.

Effect of the Great Lakes

The Great Lakes are a significant source of moisture and energy in the continental interior. The presence of the lakes offsets some of the continental influence, as the lakes store energy throughout the summer and release it to the atmosphere slowly during winter. In the cold season the region surrounding the lakes, especially on the leeward areas to the south and east, remains milder than comparable regions upwind of the lakes.

During summer the opposite situation occurs. The downwind areas remain cooler and more humid than their continental position would indicate, as the lakes

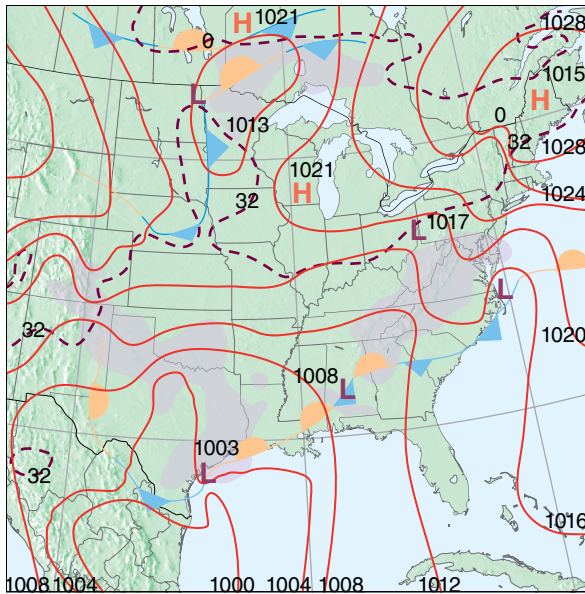


FIGURE 9.4 Typical scenario of cold air damming east of the Appalachians. Note how the clockwise circulation around the anticyclone in the northeastern United States and the counterclockwise circulation associated with the cyclone over the southeastern United States pin cold air against the Appalachian Mountains. Fortunately, the freezing line (purple dashed line) remained north of the area of most intense cold air damming, thereby preventing a more serious weather hazard.

Courtesy of NOAA.

store energy and allow for a higher percentage of *latent heat* at the expense of *sensible heat*.

Similar to any other large body of water, the lakes also delay the onset of the seasons. Fruit trees and grape vines flourish adjacent to the lakes because the delayed onset of spring protects the fruits from early budding, which would leave them more susceptible to damage from late spring frosts. The Great Lakes also prolong the frost-free period in fall, which aids fruit ripening before the first frost.

The Great Lakes also cause significant precipitation modifications. *Lake effect snows* occur leeward of the lakes in autumn through spring, as the still-warm lake waters evaporate into A and cP air masses being advected over the region from the northwest. This induces rapid cloud and precipitation formation processes that cause significant snowfall along the leeward shores. Many leeward regions receive nearly continuous snow and cloud coverage for long periods during the cold season. These phenomena frequently occur with the trailing cold fronts from Alberta clippers, but they also occur when migratory anticyclones cause northwesterly airflow across the lake surfaces. Lake effect snows alter the local *surface water balance* of near-shore locations

as affected regions record some of the highest snowfall totals on the continent. Mean annual snowfall totals typically decrease in the leeward direction away from the lakes by over 1.6 cm km^{-1} (1 in mi^{-1}). In other instances (especially in association with Lakes Superior and Michigan) snowfall is maximized in snowbelts farther inland because of topographic enhancement. The “snow machine” weakens if the lakes begin to freeze. Because of its shallowness, Lake Erie is more likely than the other lakes to freeze in winter, despite its more southerly location.

Ocean Currents and Land–Water Contrast

The eastern side of North America is affected by the warm oceanic *Gulf Stream* that results from the clockwise circulation around the Bermuda-Azores high. In winter, cP or A air masses, particularly those affected by cold air damming, are sometimes positioned adjacent to this warm, moist air near the Atlantic coast. This meeting of cold and warm air with accompanying moisture provides the ingredients necessary for strong northeast-moving storms known as nor'easters. These winter storms exert a significant impact on the extreme event climatology of the northeastern United States because they form and intensify quickly, and they may drop copious amounts of snowfall on a densely populated region. Slight differences in a nor'easter's track can cause major differences in both the amount and the type of precipitation. A track to the east-northeast provides little or no snow on the United States, but a nor'easter with a track that is slightly more south-to-north in orientation may produce more than 90 cm (3 ft) of snow in New England and New York. Widespread areas may undergo changes in precipitation from rain to freezing rain to sleet and finally snowfall, depending on the exact location and trajectory of the storm and its associated fronts. Such a sequence of precipitation types may effectively halt transportation and cause massive power outages through much of the most densely populated region of the continent.

Farther north, the Gulf Stream curves eastward away from the continent, and the cold **Labrador current** replaces the departing Gulf Stream, at times reaching as far south as Maryland. This cold current often chills the warmer air overlying it, resulting in frequent coastal fogs in the Atlantic Provinces of New Brunswick, Nova Scotia, Prince Edward Island, and Newfoundland and in northern New England. This cold water may either stabilize the local atmosphere, trapping the fog near the surface, or produce storminess along the margins between the air over the cold water and the warmer air adjacent to it.

Ocean currents also exert significant climatic effects elsewhere in North America. For example, the **Loop current** branches off from the warm Gulf Stream, which originates in the Caribbean Sea, flowing west of the Florida coast, where it “loops” across a section of the Gulf of Mexico. It then moves into the Atlantic between Florida and Cuba, contributing its energy to the Gulf Stream. One effect of this warm water is the energy that it provides to developing tropical cyclones. The position of the warm water also influences tropical cyclone trajectories, with increased likelihood of intensification and occurrence over the Loop current.

The 2005 Atlantic hurricane season provides an excellent example of the influence of the Loop current. Although most Gulf–Atlantic tropical cyclones do not strike the U.S. mainland, with only about 25% striking the U.S. Gulf coast and slightly less striking the Atlantic coast, multiple strikes may occur in the same season, particularly when the Loop current is advecting warm water into the Gulf of Mexico. Hurricanes Katrina, Rita, Wilma, and others of 2005 show the influence of anomalously high Gulf sea surface temperatures associated with the Loop current during the height of the hurricane season. All three of these storms contained 280 km hr^{-1} (175 mi hr^{-1}) winds at some point in their life cycle.

In winter the usually warm Gulf of Mexico waters sometimes meet with frigid cP air masses at the coastal zone, which can trigger nor'easter-like storms that originate in the northwestern Gulf of Mexico continental shelf. Like nor'easters, these **Gulf Coast cyclones** can be dangerous, because they are nearly always accompanied by abundant moisture from which latent heat can be released to power the quickly intensifying storm. An example of an intense Gulf low was the March 1993 “Blizzard of the Century” that impacted most of the Gulf and Atlantic coasts. An extremely rapid drop in core pressure, termed a meteorological bomb, occurred over a warm Gulf of Mexico eddy that spun from the warm Loop current in the eastern part of the basin.

The cold *California current* produced by the flow around the *Hawaiian high* near the U.S. Pacific coast exerts a more benign influence on the North American climate. This current stabilizes the surface atmosphere by reducing the *environmental lapse rate*, often even creating a surface temperature inversion. The result is a low frequency of severe weather on the Pacific coast, increased frequencies of fog as moisture is trapped near the surface, and increased air quality problems in heavily populated areas such as Los Angeles.

► Climatic Setting of Europe

General Characteristics

Europe’s climate may be described as milder than it should be, given the relatively high latitude of the continent. Latitudinally, the bulk of Europe exists near or poleward of the U.S.–Canadian border (**FIGURE 9.5**). Yet, by comparison, most of Canada experiences a harsher climate than most of Europe. For example, the southernmost region of Europe (southern Spain, Italy, and Greece) lies at a latitude similar to New York City. Images of these southern European locales usually include warm, sunny days. This is hardly an image that one would have of New York’s climate, especially during winter.

Europe is generally not an ideal source region for bitter cold air masses, except for the inland areas of Russia and other eastern European countries in winter. Instead, *maritime polar (mP)* air masses of Atlantic origin are advected eastward in the midlatitude westerlies, south of the *Icelandic low*. These air masses dominate most of Europe, but occasionally mT and cT air masses can penetrate the southernmost sections of the continent. Two primary factors explain the relative mildness of European climates considering its latitude.

Effect of Ocean Currents

The first reason that Europe’s climate is relatively mild involves the warm *North Atlantic Drift*—a warm surface ocean current that flows across the North Atlantic basin to the Arctic Ocean north of Scandinavia and into the Barents Sea as an extension of the Gulf Stream. As the Gulf Stream travels northward along the U.S. Atlantic coast, it slowly curves away from North America toward the mid-ocean basin. In the mid-ocean region the Gulf Stream is renamed the North Atlantic Drift. The bulk

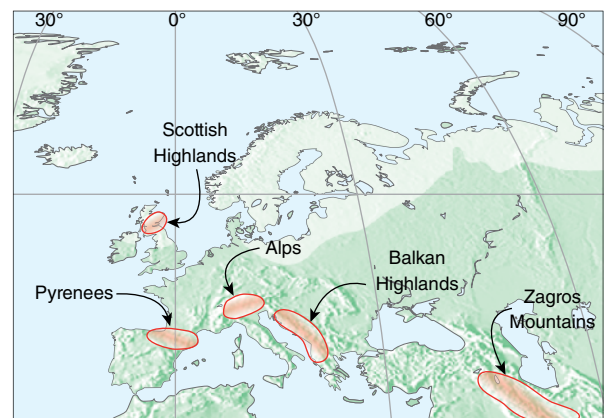


FIGURE 9.5 Selected physiographic features of Europe.

of the water in the North Atlantic Drift originates in the low-latitude *North Equatorial current*. Most of the remainder originates from the warm Caribbean Sea and the Gulf of Mexico via the Loop current.

The North Atlantic Drift is the northern extension of the circulation gyre that occupies the North Atlantic basin. This gyre owes its existence to the Bermuda-Azores high that occupies the central North Atlantic basin year-round. As we have seen, the anticyclone waxes and wanes seasonally, reaching a maximum intensity in the summer months during the maximum *Hadley cell* intensity and a minimum during the late winter, when the Hadley cell weakens. The position of the Bermuda-Azores high fluctuates seasonally as well, reaching its maximum poleward position during the summer months and its most equatorial location during winter, when the Hadley cell weakens. The clockwise rotation of the ever-present Bermuda-Azores anticyclone imparts considerable shearing force on the waters of the North Atlantic. Warm waters originating in low latitudes flow poleward along the western ocean basin edge near North America, while cooler waters flow equatorward along the eastern basin edge along the coast of Africa, creating the *Canary current*. Because Europe lies poleward of the mean central gyre position, the coldest waters of the Canary current have minimal effect on Europe.

The North Atlantic Drift splits into two distinct currents near the southern coast of England. One part of the current flows southward along the coasts of France, Spain, and Portugal. This water is eventually incorporated into the cooler Canary current. The remaining portion of the North Atlantic Drift flows northward along the west coast of England and Norway, eventually flowing eastward north of the Scandinavian countries and into the Arctic Ocean. The waters are so warm that the area remains ice free even during the coldest winters.

Effect of Mountain Ranges

The second major reason for Europe's mild climate is the position of its mountain ranges (Figure 9.5). The major mountain system of Europe, the Alps, extends along a west-to-east transect. This is a different alignment from the north-south oriented mountain axes of North America. In contrast to North America, European warm air masses originating over the Mediterranean basin are largely confined to the southern regions of the continent. Colder air, originating in higher-latitude polar locations, is primarily confined to the northern regions of the continent, but this air is generally not as frigid as air at comparable latitudes in North America, because of the oceanic influence in Europe. This segregation of dissimilar air masses keeps Europe relatively warm, especially in the southern sections of the continent. The mountains

also have a direct effect on daily weather, especially storms. In contrast to the situation over central North America, European storms are rarely severe, because the mixing of radically dissimilar air masses is almost nonexistent, largely because of the mountain barrier. This is not to say that severe weather does not occur in Europe; rather, the frequency and magnitude of severe weather events are significantly reduced as compared with the volatile North American continent.

The Alps create a regional circulation known as **Föhn winds**, which are similar to the Chinooks of North America. The Föhn winds are initiated when air traveling up the southern windward side of the Alps undergoes adiabatic cooling, usually to the *dewpoint temperature*, causing clouds and precipitation. As the air stream traverses the mountain region and begins to move down the northern leeward side into Germany, adiabatic warming occurs. The warming rate usually exceeds the adiabatic cooling rate on the opposite side of the mountain range, causing a dry, warm blast of air on the leeward side. During winter the Föhn winds may lead to remarkable short-term temperature increases. Although the Föhn winds are important regionally, other European mountain ranges are important for the local winds they generate. These are discussed later in the chapter.

Blocking Anticyclones

Both oceanic and topographic influences play a part in a relatively frequent European phenomenon known as the **blocking anticyclone**. Such anticyclones at the surface (FIGURE 9.6) or blocking ridges aloft originate primarily as a result of the persistent strengthening of the air-sea gyre. Atmospheric “blocks” form from the stalling of Rossby wave ridges over the North Atlantic Ocean and/or Europe. During winter and spring such a situation may occur with the migration of polar outbreaks from the east over northern Europe, in the zone

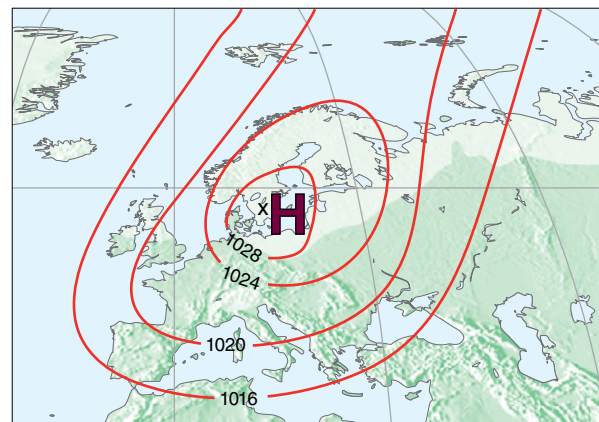


FIGURE 9.6 A blocking anticyclone over Europe.

of polar easterly circulation north of the midlatitudes. During warmer times the situation may develop as the Bermuda-Azores high-pressure cell expands over the North Atlantic and the continent. In either scenario the east-to-west aligned mountains help to maintain the position of the anticyclone.

During blocking events the continent is affected by largely cloudless skies and little chance of precipitation. Approaching midlatitude wave cyclones either stall on the westward flanks of the blocking anticyclone or are forced to skirt the periphery of the blocking system. As a result, storm tracks are displaced either northward or southward of central Europe. Drought, heat waves, cold waves, and severe pollution events are common surface features beneath the blocking anticyclone or ridge, depending on the season and location of occurrence. Subsiding air associated with the blocking high decreases cloud formation by restricting vertical motions in the atmosphere, leading to drought. Extreme cold may result in winter as Arctic air remains stationary over a location. During warmer times the same situation can lead to a heat wave as the clear skies allow extreme amounts of *insolation* reaching the surface while clouds and precipitation are suppressed. Subsidence may also trap pollutants near the surface. These situations periodically but profoundly affect the European climate.

► Climatic Setting of Asia

General Characteristics

A primary climatic attribute of Asia is continentality. Asia is the largest continent on Earth, spanning 160 degrees of longitude (FIGURE 9.7). The high-latitude interior of the continent is as far removed from major sources of water as occurs on the planet. This continentality promotes climates that vary extensively from

season to season. The lowest temperatures recorded in the northern hemisphere have occurred in Asia. One would probably assume the polar area to be the coldest, but the cold extremes in the oceanic north polar region are not as cold as the most extreme temperature in inland Siberia. Even though the polar region is frozen throughout much of the year, the underlying ocean can still impart somewhat of a moderating effect on the climate by acting as an energy source. The Asian land mass holds no such energy reservoir, resulting in extreme cold during the winter months. The cold air supports the *Siberian high*—a strong, thermally driven anticyclone. Development of the Siberian high in winter led to the highest surface air pressure ever recorded when on December 31, 1968, a sea-level equivalent pressure of 1083.8 mb was recorded at Agata, Siberia.

Summer months are marked by a strongly opposite circulation as the Asian interior heats appreciably under long days and abundant solar energy receipt. Large water bodies are too distant to store and tie up energy in latent heat, leaving the interior with an abundant sensible heat supply, which is manifested through high temperatures. The average annual temperature range in a given year across Asia may reach 60 C° (108 F°), the strongest continental influence on Earth.

The size of the Asian continent also subjects it to a wide array of climatic types, including every category in the Köppen-Geiger climate classification system. But overall, the continent is dominated by dry climates, due to the extensive continentality of the interior. *Microthermal* (“D”) climates are also widespread at these high latitudes. Tropical climates are found in the southern parts of the continent. Of those, most are associated with the east and south **Asian monsoons**—the seasonal reversal of continental-scale circulation.

Monsoonal Effects

A **monsoon** is defined as a seasonal reversal of wind that occurs because of a seesaw of atmospheric pressure between the Asian interior and the Indian and North Pacific Oceans. During winter, continentality causes the Asian interior to cool significantly, supporting the Siberian high by chilling the overlying air. Winter is also characterized by relatively low pressure over the Indian Ocean and associated water bodies such as the Arabian Sea and the Bay of Bengal, along with the western tropical Pacific Ocean. This occurs as water bodies retain heat in appreciable quantities. The warmer ocean surfaces heat the overlying atmosphere, thereby supporting lower atmospheric pressures. Because atmospheric mass is transferred from areas of high pressure to areas of lower pressure, surface air in winter circulates from the continental interior toward the tropical oceans even

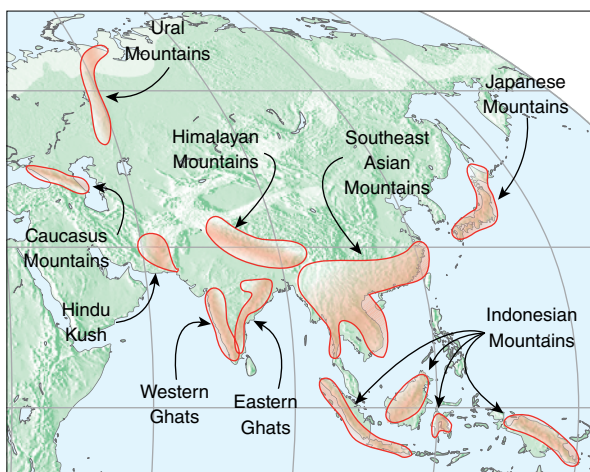


FIGURE 9.7 Selected physiographic features of Asia.

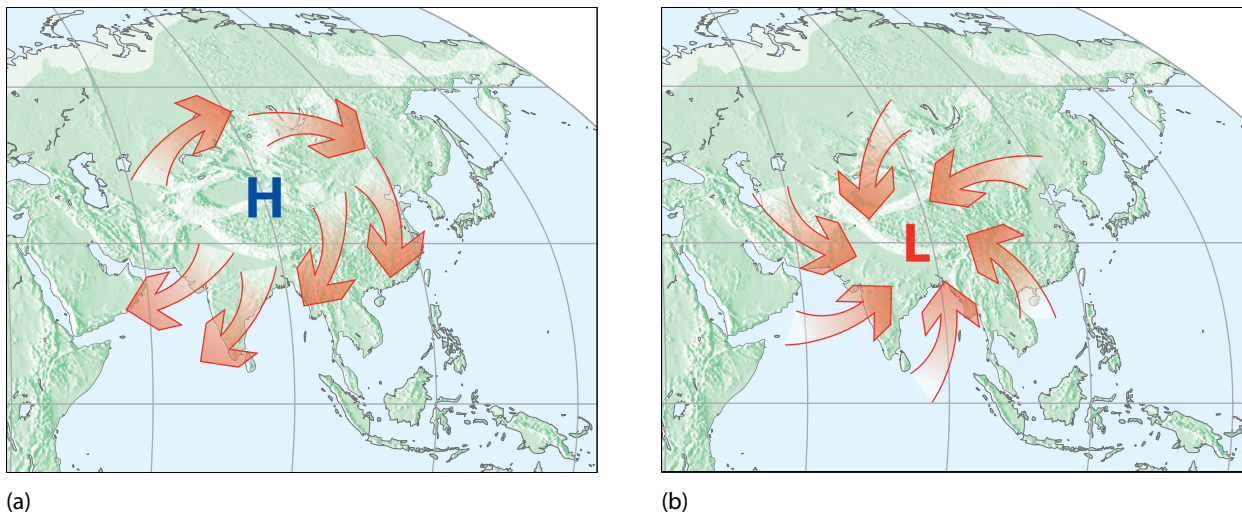


FIGURE 9.8 (a) The Asian winter monsoon. (b) The Asian summer monsoon.

after Coriolis deflection (**FIGURE 9.8a**). Not surprisingly, this air is typically cold and dry. As long as this subsiding airflow persists, little precipitation occurs over most of Asia.

During summer the pressures seesaw in an opposite manner, as the Asian land mass heats in the absence of major water bodies. This surface heating causes the development of a surface-based **thermal low** called the *Tibetan low*. Conversely, the Indian and North Pacific Oceans are relatively cool in summer compared with the heated continent. The cooler air at the ocean surface supports generally higher atmospheric pressures. The resultant airflow over the continent is from the ocean to the continent even after Coriolis deflection (**FIGURE 9.8b**). This flow is manifested as the **southwesterly monsoon** of South Asia. Because this air is warm and moist, it promotes the development of clouds and precipitation over Asia.

Precipitation is further enhanced by orographic uplift over the high plateau that comprises the bulk of the Indian subcontinent and over the Himalayan mountain range. Areas on the windward (or southern, in this case) side of the Himalayas have some of the highest precipitation totals on Earth. Cherrapunji, India, holds the world record for the most precipitation recorded in a single month (929.99 cm, or 366.14 in) and year, when 2646 cm (1042 in) of rain was recorded from 1860 to 1861. This excessive annual precipitation total, which equals 26.5 m (87 ft) of water, is even more impressive in that the vast majority of the precipitation occurred over the course of only about 4 months.

Because the summer phase of the Asian monsoon can produce remarkable precipitation totals, some people assume that the word “monsoon” indicates a

type of storm system. Few remember that the monsoon also induces a distinct dry period that spans roughly half the year.

Effect of Mountain Ranges

Another physical characteristic of Asia that imparts a significant climatic influence are the Himalayas and the Hindu Kush (**Figure 9.7**). We just saw that these mountain chains (particularly the Himalayas) promote very impressive precipitation totals on the windward side, especially during summer. The mountains also help to create and maintain the dry interior of Asia through a **rain shadow effect**—the dryness experienced on the leeward side of a mountain, after the moisture and precipitation is left on the windward side, leaving sinking air that warms adiabatically on the leeward side. As air is warmed its **relative humidity** drops, discouraging cloud formation on the leeward side of the mountain barrier. Because winds are persistent throughout the course of the year, the Tibetan Plateau on the northern side of the Himalayas has a **True Desert (BW) climate**. This situation also causes the dry western interior of North America and several other deserts throughout the world. The rain shadow effect is enhanced in Asia by the extreme height of the Himalayas and the size of the land mass, because most of the moisture in air moving over the continent from a surrounding water body will surely be wrung out long before it reaches the continental interior. The Gobi Desert, which dominates the interior of Asia, is one of the driest locations on Earth.

The east–west orientation of the Himalayas and adjacent Tibetan Plateau also causes the *polar front jet stream* to split into two branches in winter—one branch

north of the mountains and the other to their south. The northern jet's position fluctuates wildly, but the southern jet consistently flows over northern India and then curves northward over southern China and Japan. In summer the southern branch of the jet generally disappears and the onshore southwesterly monsoon tends to dominate regions south of northern China.

Other mountain ranges exert important impacts in other parts of Asia. The mountain spines of the Japanese and Philippine Islands cause significant orographic impacts. The complicated topography of southeast Asia also causes a vast array of microclimates. Finally, the eastern and western Ghats of southern India create important variations and impacts on local climates.

Effect of Coastal Zones on Climate

Some 30% of the world's tropical cyclones occur in the western Pacific Basin of the northern hemisphere, making this by far the most active tropical cyclone region in the world. Many of these storms strike the mainland, from southern Japan southward along the Chinese and Vietnamese coast. Others traverse the Philippines and Taiwan. The northern Indian Ocean is also a high tropical cyclone formation area. Low-lying coastal regions combine with dense human populations to produce the deadliest tropical cyclone landfall region on Earth.

The two branches of the winter polar front jet merge over central China, where an upper-level *trough* is favored due to persistent baroclinicity. This trough tends to be anchored in place because of the sharp temperature gradients that exist between the continent and the ocean. The associated trough-to-ridge side of the Rossby wave occurs over coastal China and Japan, making it a favored zone for extratropical cyclogenesis. This is true particularly because of moisture enhancement from the adjacent East China Sea and other bodies of water in addition to the steep thermal gradient between the continent and ocean surfaces. These storms move across the Pacific Basin and occlude near the western coast of North America.

► Regional Climatology

For the sake of simplicity, our investigation of specific climatic types concentrates on the Köppen-Geiger system because it is the most widely recognized climatic classification system in use today. Because tropical (A) climates within North America and Asia are discussed elsewhere in the text (Chapter 10), our discussion of the regional climates of the extratropical northern hemisphere begins with dry (B) climates.

B—Arid Climates

Geographic Extent

As discussed, dry climates can be defined as those in which *potential evapotranspiration* routinely exceeds precipitation. Dry climates occupy much of the western United States and a small section of adjacent interior western Canada, along with all of interior Asia. They are far less prevalent in Europe, with the Asian B climates spilling over into extreme southern Russia, the southern Ukraine, and local isolated pockets in interior Spain (see world map of Köppen-Geiger climate types [Figure 8.1]). On a global basis, B climates occupy more than 27% of Earth's land area, the most of any of the five major Köppen-Geiger categories. Also, B climates occupy almost 20% of the world's ocean area.

One subcategory of B climates is the drier, or True Desert (BW) climate. In North America the BW climate is centered on the southwestern United States, adjacent northern Mexico, and nearby waters. The BW regions of Asia are far more extensive and exist in three major areas: (1) the Gobi Desert of north-central China and south-central Mongolia; (2) the Aral Sea area, encompassing southern Kazakhstan and most of Uzbekistan and Turkmenistan; and (3) a large swath of southwestern Asia (popularly known as the Middle East) from the Arabian Peninsula across much of Iran, most of Pakistan, extreme western India, and adjacent waters. This latter region extends westward to include nearly all of northern Africa and the eastern subtropical North Atlantic Ocean.

The second type of B climate is the semiarid, or **Steppe (BS) climate**. This type generally surrounds the True Desert core for all BW regions noted above. Steppes are regarded as transition regions—*deficits* are too persistent and long to support forested landscapes, yet the climate is not sufficiently arid to be considered a true desert. Annual variability in precipitation and potential evapotranspiration can cause a given location in a BS climate to be sufficiently humid to be classified as a nonarid climate in one year but sufficiently arid to be classified as a True Desert in the next year. Long-term averages suggest that these regions are semiarid, but they are by no means consistently semiarid every year.

The North American steppe is generally bordered by the western mountain ranges such as the Cascades and Sierra Nevada on the west and the eastern Great Plains region on the east. The steppe extends from southern Alberta southward to include parts of Mexico south of the BW region. In Asia the steppe is extensive through the southwestern and central areas of the continent. Most of western China, along with sizable sections of Mongolia, Kazakhstan, Afghanistan, and Iran, fall into this category. These climates occur despite the **summer monsoon**

circulation regime, as the mountain chains induce a rain shadow effect across the region.

Forcing Mechanisms

The aridity in B climates is caused by only a few climatic forcing mechanisms that act singularly or in some combination. Many dry regions are roughly centered along the 30° line of latitude, a region characterized by subsiding air associated with the subtropical anticyclones on the poleward edge of the Hadley cell. Other desert regions are located on the western portion of continents, near the cold eastern ocean basin currents. Many of the tropical and southern hemisphere deserts (described elsewhere in the text) fall into this category. This oceanic thermal influence reinforces the subtropical anticyclone through persistent atmospheric stability and associated high-pressure characteristics. Subsidence induced by the anticyclone suppresses cloud formation even with adequate water vapor content. Another factor is the rain shadow influence that was described earlier. Finally, the distance to a significant moisture source in continental regions such as central Asia can create B climates.

BW—True Desert

The True Desert (BW) portions of extratropical North America and Asia are subdivided into **Subtropical Hot Desert (BWh)** and **Midlatitude Cold Desert (BWk)** in the Köppen-Geiger classification system. In general, the lower-latitude deserts carry the BWh designation, while the higher-latitude areas are classified as BWk, but this pattern can be disrupted by high elevation or by cooling in subtropical areas from cold ocean currents.

Thermal Characteristics

Temperatures in True Desert areas fluctuate considerably on both daily and seasonal time scales. Daytime summer temperatures may be exceedingly high, while nocturnal temperatures may be cool. This wide range is caused by the characteristic low humidity levels, because the primary *greenhouse gas* in the atmosphere—water vapor—is deficient. When few clouds and water vapor molecules are present to absorb or reflect insolation during the daytime hours, most insolation is transmitted to the surface as *direct radiation* and is converted to sensible heat. Because little surface water exists to be evaporated (which ties up energy in latent form), very high temperatures are possible. Sinking, or subsidence, in the subtropical latitudes at the poleward (sinking) side of the Hadley cell reinforces the tendency for hot, dry conditions, because air aloft that sinks usually contains

little water vapor and warms adiabatically on its descent. The result is an enhancement of the dry, predominantly clear conditions and an even greater likelihood that incoming radiant energy will reach the surface.

The shortwave energy absorbed by the surface is stored and then reradiated as longwave energy from the surface to the atmosphere. At night, little atmospheric water vapor is available to absorb and reradiate longwave energy back down to the surface. The clear nights allow longwave radiation to escape to space readily, resulting in significant radiational cooling of the surface and the near-surface atmosphere. Extreme diurnal temperature ranges are normal because of this weakened local *greenhouse effect*.

BWh Climates

Average summer monthly temperatures may exceed 38°C (100°F) for many Subtropical Hot Desert locations as daily maximum temperatures frequently climb to 44°C (110°F) or more. In fact, the world record for highest temperature occurred when a temperature of 57°C (134°F) was observed at what is now Furnace Creek Ranch in Death Valley, California, on July 13, 1913. Winters are cool, with average monthly temperatures in January and February perhaps near 10°C (50°F). Vast differences between summer and winter lead to high annual temperature ranges, but in many locations the diurnal temperature range exceeds the annual range in mean monthly temperatures throughout the year.

Representative examples of BWh climates in the northern hemisphere's extratropics are at Phoenix, Arizona, and Las Vegas, Nevada. **FIGURES 9.9a** and **9.10a** show *climographs* for these cities, revealing several features of the temperature climatology. First, insolation is intense in summer. Second, the climograph shows that the diurnal and annual temperature ranges are also high. **FIGURES 9.9b** and **9.10b** show mean monthly *water balance diagrams* for Phoenix and Las Vegas. The high radiation receipt causes temperatures and atmospheric demand for water to be so high that large deficits prevail throughout most of the year.

BWk Climates

Midlatitude Cold Desert (BWk) climates are more extensive than BWh in the extratropical regions of the northern hemisphere, because high-latitude and/or nocturnal radiational cooling permits annual mean temperatures in many desert regions to dip below the 18°C (64°F) threshold—the boundary between BWh and BWk. Nevertheless, both BW climates share common features of high surface radiation receipt (especially in summer), high potential evapotranspiration, and little cloudiness and precipitation. Although summer

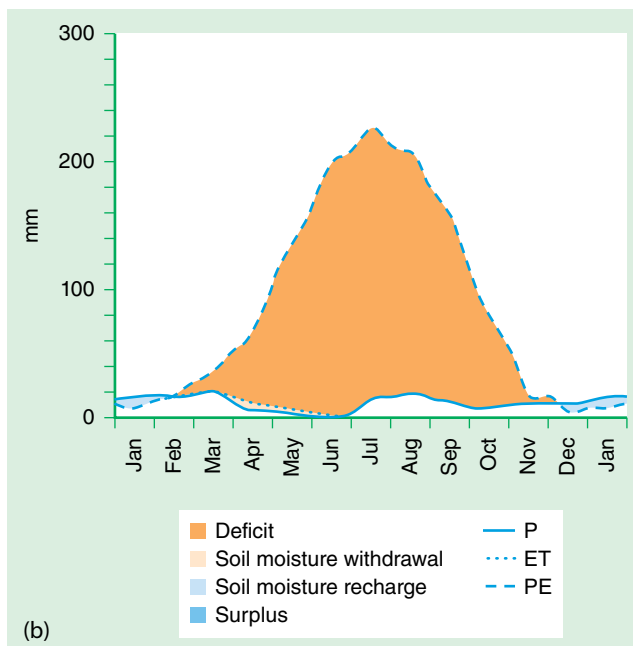
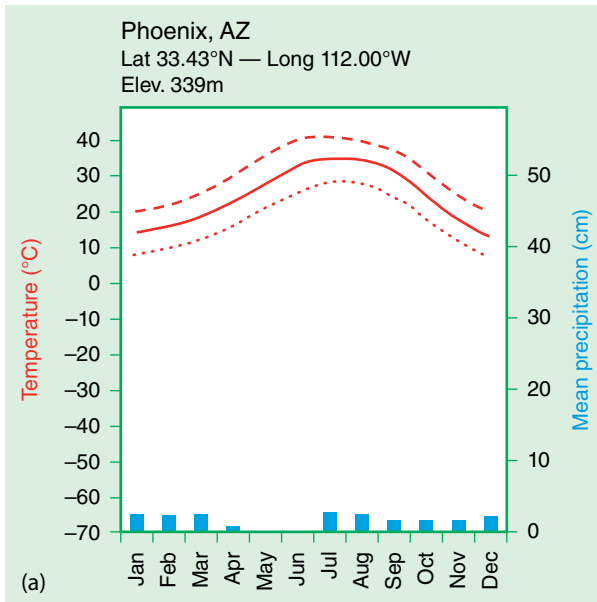


FIGURE 9.9 (a) Climograph for Phoenix, Arizona (BWh climate). Average annual temperature is 22.7°C (72.8°F) and average annual precipitation is 21.1 cm (8 in). (b) Water balance diagram for Phoenix, Arizona.

(a) Source of Temperature and Precipitation Data: 1981–2010 data from <https://www.ncdc.noaa.gov/data-access/land-based-station-data/land-based-datasets/climate-normals/1981-2010-normals-data>. Source of Radiation Data: National Solar Radiation Database, 1961–1990 data from <http://rredc.nrel.gov/solar>. (b) Modified with permission using Web/WIMP version 1.01 implemented by K. Matsuura, C. Willmott, and D. Legates at the University of Delaware, 2003.

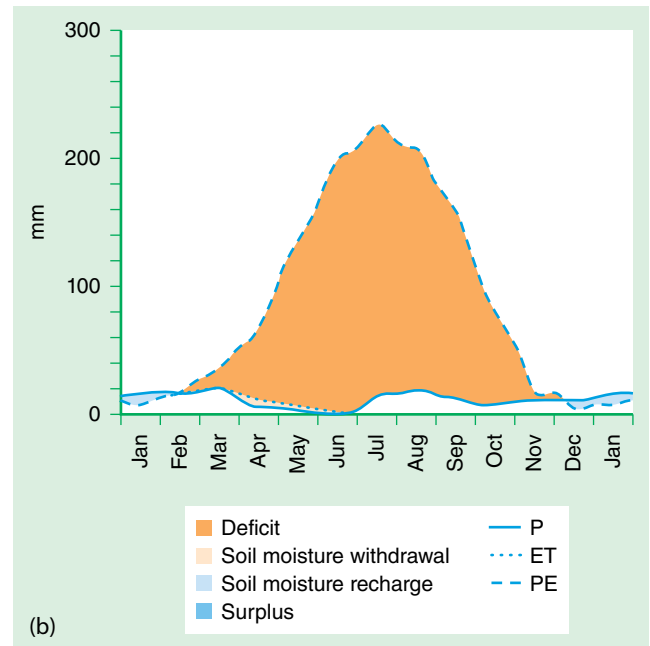
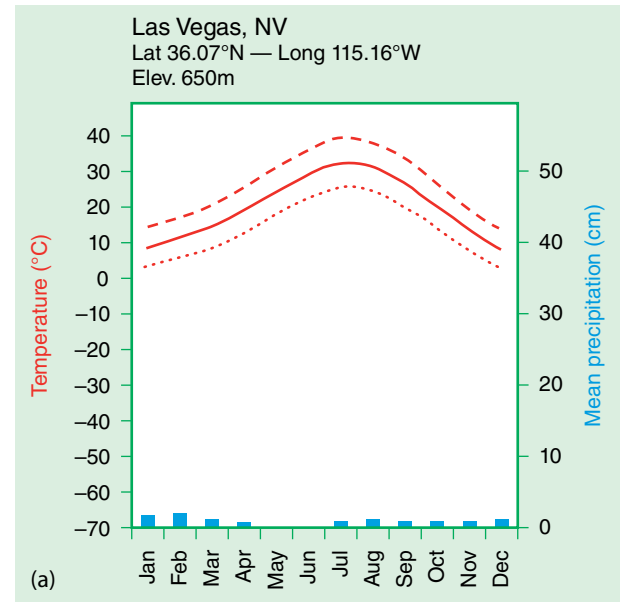


FIGURE 9.10 (a) Climograph for Las Vegas, Nevada (BWh climate). Average annual temperature is 20.1°C (68.1°F) and average annual precipitation is 11.4 cm (4.5 in). (b) Water balance diagram for Las Vegas, Nevada.

(a) Data from National Centers for Environmental Information. (b) Modified with permission using Web/WIMP version 1.01 implemented by K. Matsuura, C. Willmott, and D. Legates at the University of Delaware, 2003.

temperatures are similar, winter temperatures are lower in a midlatitude desert than in a subtropical desert. Locations with BWk climates typically experience greater annual temperature ranges than subtropical deserts. The decreased energy (and, therefore, potential evapotranspiration) totals in BWk climates may partially offset the effect of small precipitation totals in local water balances, thereby producing smaller deficits than in comparable BWh climates.

Moisture Characteristics. Although precipitation totals are small, both BWh and BWk climates tend to experience more frequent, abundant, and intense precipitation during the warmest months. At that time of year precipitation is triggered by the extreme heat that increases the environmental lapse rate, thereby destabilizing the atmosphere and promoting vertical motion of surface air. This causes the development of a thermal low, as discussed previously. In Asia the summer thermal low triggers the impressive monsoonal rains of that continent, but, as we have seen, little moisture is advected as far inland as the Gobi Desert area. Furthermore, the region receives little moisture from migratory midlatitude wave cyclones passing through the region because of the vast distances from upwind moisture sources in the midlatitude westerlies. The climograph for Hami, China (FIGURE 9.11a), reveals low average precipitation totals. FIGURE 9.11b shows that deficits in Hami are high throughout the year in this dry, desolate location with frigid winters. Similar onshore airflow occurs in association with the other major BWk region in Asia—the Aral Sea region—where precipitation increases slightly in late spring and early summer because of the development of the thermal low.

The North American summertime thermal low is far less extensive and influential than that in Asia. Nevertheless, low-level heating induces rising motion centered over Arizona. This causes the *advection* of surrounding surface air from the Gulf of California and the Gulf of Mexico, carrying some moisture with it. This air sweeps into the region, converges in the area of the thermal low, and rises. The rising motions cause the development of cumulonimbus clouds and some rainfall, giving Phoenix a slight late summer precipitation peak (Figure 9.9a), but the peak is not as distinct as in most BWk regions. The thermal low typically reaches its maximum intensity around August. This precipitation characteristic has caused some to refer to this phenomenon as the **North American summer monsoon**.

The BWk climate in North America is represented by Albuquerque, New Mexico. The climograph (FIGURE 9.12a) again suggests abundant summer radiation, wide diurnal and annual temperature ranges, and low precipitation

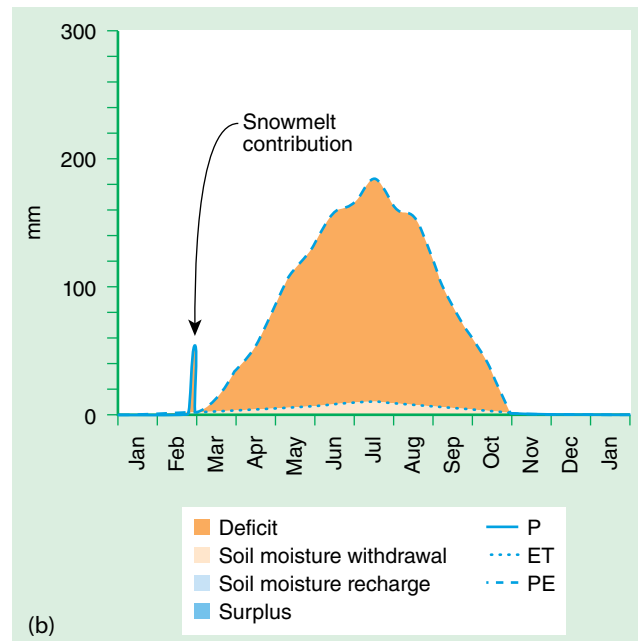
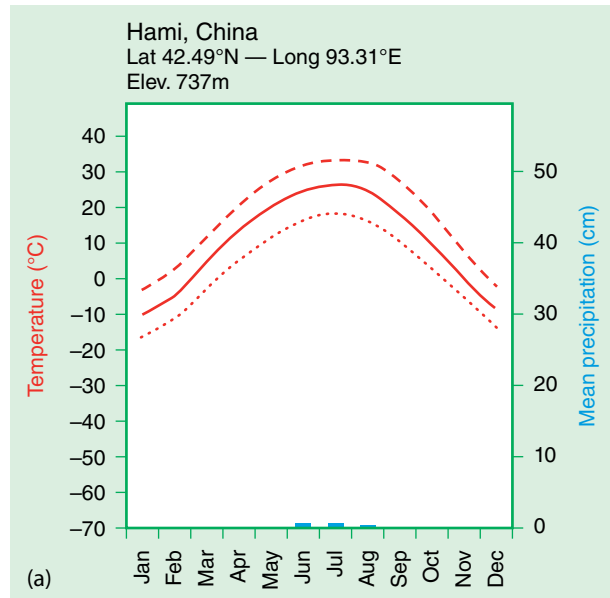


FIGURE 9.11 (a) Climograph for Hami, China (BWk climate). Average annual temperature is 9.9°C (49.8°F) and average annual precipitation is 3.6 cm (1.4 in). (b) Water balance diagram for Hami, China.

(a) Data from National Centers for Environmental Information. (b) Modified with permission using Web/WIMP version 1.01 implemented by K. Matsuura, C. Willmott, and D. Legates at the University of Delaware, 2003.

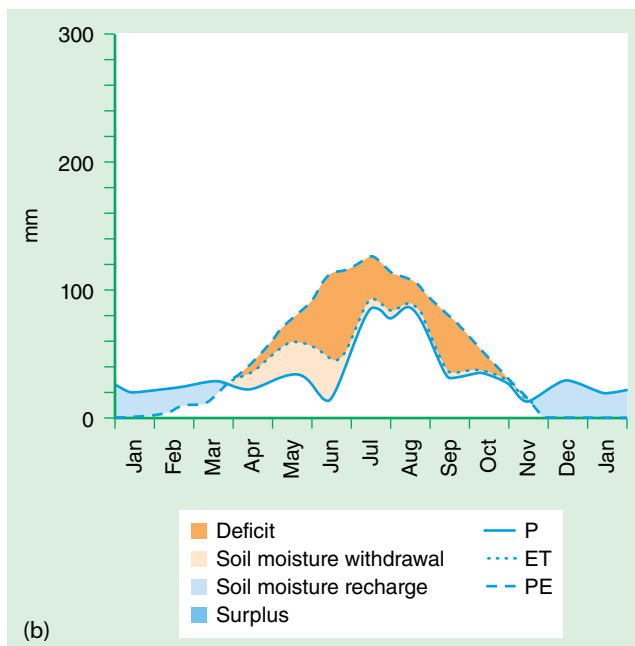
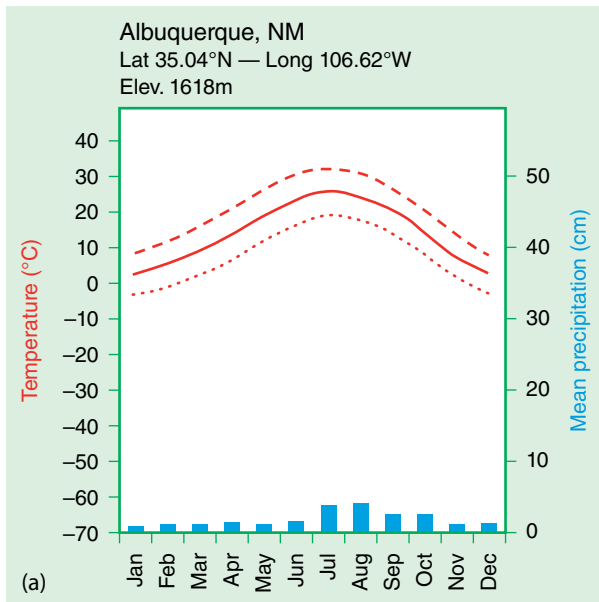


FIGURE 9.12 (a) Climograph for Albuquerque, New Mexico (BWk climate). Average annual temperature is 13.8°C (56.8°F) and average annual precipitation is 24.1 cm (9.5 in). (b) Water balance diagram for Albuquerque, New Mexico.

(a) Data from National Centers for Environmental Information. (b) Modified with permission using Web/WIMP version 1.01 implemented by K. Matsuura, C. Willmott, and D. Legates at the University of Delaware, 2003.

totals with a peak in late summer. **FIGURE 9.12b** shows that the precipitation peak is too small to eliminate moisture deficits. Nevertheless, in contrast to the BWk region in Asia, represented by Hami, the summer precipitation in southwestern North America and cooling effect of high elevation do reduce the deficit despite the copious energy availability for evaporating water in late summer.

Although the North American monsoon region experiences pronounced precipitation seasonality, it differs from a true monsoon, which is characterized by a distinct seasonal reversal of prevailing surface winds. No such situation occurs in the southwestern United States and adjacent northern Mexico. During the cool season, rain and snow are generated by occasional migratory frontal cyclones that sweep through the region. Precipitation totals associated with these storm systems are generally low. Interannual variability of precipitation is high, because many years may pass with virtually no precipitation, but a few other years experience much-above-normal precipitation. Much of this variability is tied to upper-atmospheric flow changes induced by El Niño events. Monthly and annual precipitation averages may be somewhat misleading and unrepresentative of most years.

BS—Steppe

The North American Steppes occur because of the increasing distance from the clockwise advection of moist air by the Bermuda-Azores high and because of a rain shadow produced by Pacific coastal mountain ranges. Steppe regions of the interior of Asia exist primarily because of continentality, in regions located far from major water sources such as the North Atlantic Ocean, the Mediterranean Sea, and the Indian Ocean, but equivalent climates also occur over the subtropical oceans themselves (see again the world map of climatic types). Mountains further deprive the terrestrial regions of moisture through rain shadow effects. These eastern Steppe areas are true transition zones adjacent to the harsher and drier Gobi Desert core of central Asia and the deserts of southwest Asia. Iberian Peninsula (Spain) Steppe regions exist predominantly from rain shadow influences induced by the Pyrenees and Cantabrian Mountains to the north and the Betic Cordillera to the south.

In all these regions, annual precipitation totals—between 25 and 76 cm (10 and 30 in) on average—exceed those of a True Desert. Higher precipitation totals result in the proliferation of Steppe grasses that become more widespread, thicker, and taller with distance from the True Desert core. The grasslands give way to forests at the *ecotone* with the nonarid climatic zones.

Thermal Characteristics. Steppe climates are subdivided into **Hot Steppe (BSH) climates** and **Cold Steppe (BSk) climates**, with the boundary again being the 18°C (64°F) annual mean temperature *isotherm*. In the extratropical northern hemisphere, BSh climates are rare. Two examples are the United States–Mexican border region (represented by Tucson, Arizona) and much of Iraq (represented by Baghdad, Iraq; FIGURES 9.13a and 9.14a, respectively). In addition, some BSh climates are found in sections of southern Iran and India, particularly in low elevations, and in small sections of the Mediterranean basin. Elsewhere, winter temperatures are low enough to qualify extratropical northern hemisphere BS climates as BSk. The BSk climate is prevalent across North America and Asia.

Temperatures in Cold Steppe climates are similar to those in Midlatitude Cold Deserts except that they exhibit less pronounced seasonality. Both annual and diurnal temperature ranges are smaller than in Midlatitude Cold Deserts, as can be seen in the climographs for Lubbock, Texas (FIGURE 9.15a), Cedar City, Utah (FIGURE 9.16a), Boise, Idaho (FIGURE 9.17a), Calgary, Alberta (FIGURE 9.18a), and Rapid City, South Dakota (at the ecotone, FIGURE 9.19a). Similar temperature characteristics are evident by comparing the Asian sites of Baghdad (BSH climate, with average annual temperature of 22.3°C [72.2°F], Figure 9.14a), and Tashkent, Uzbekistan (BSk climate, with average annual temperature of 14.7°C [58.4°F], FIGURE 9.20a).

Moisture Characteristics. Precipitation totals typically reach a maximum during winter for steppe locations at higher latitudes, because of the more frequent passage of migratory midlatitude wave cyclones in winter—Boise and Tashkent provide excellent examples. As the climographs show, the diurnal temperature range increases in summer and decreases in winter, as the clear summer skies allow for much radiation receipt by day and rapid losses at night. On the equatorward side of the True Desert, precipitation totals tend to increase during the summer season when convective thunderstorm activity is greater and when the Intertropical Convergence Zone makes its nearest approach to the region.

The slightly reduced energy levels associated with the lower temperatures in winter generally eliminate the deficits in soil moisture during those months. A comparison of the surface water balance figures (FIGURES 9.13b through 9.20b) reveals that lower temperatures in higher-latitude Steppe climates produce more winter *surplus* than in locations farther equatorward. Although Baghdad experiences only 15.7 cm (6.2 in) of precipitation

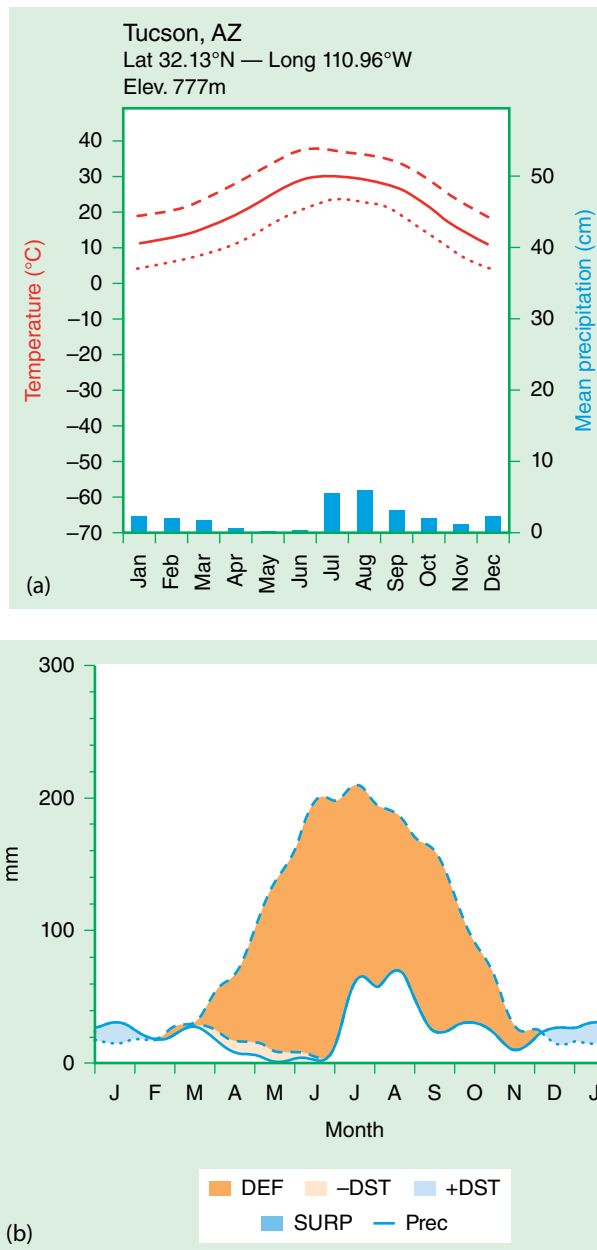


FIGURE 9.13 (a) Climograph for Tucson, Arizona (BSH climate). Average annual temperature is 20.4°C (68.7°F) and average annual precipitation is 30.9 cm (12.2 in). (b) Water balance diagram for Tucson, Arizona.

(a) Data from National Centers for Environmental Information. (b) Modified with permission using Web/WIMP version 1.01 implemented by K. Matsuura, C. Willmott, and D. Legates at the University of Delaware, 2003.

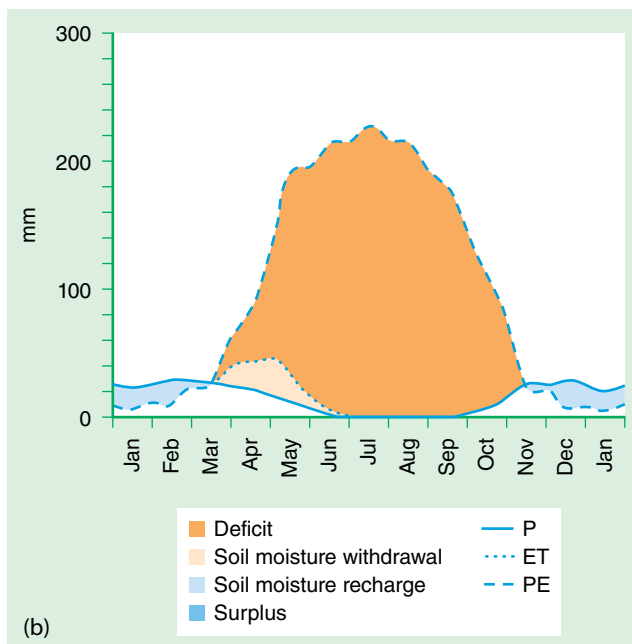
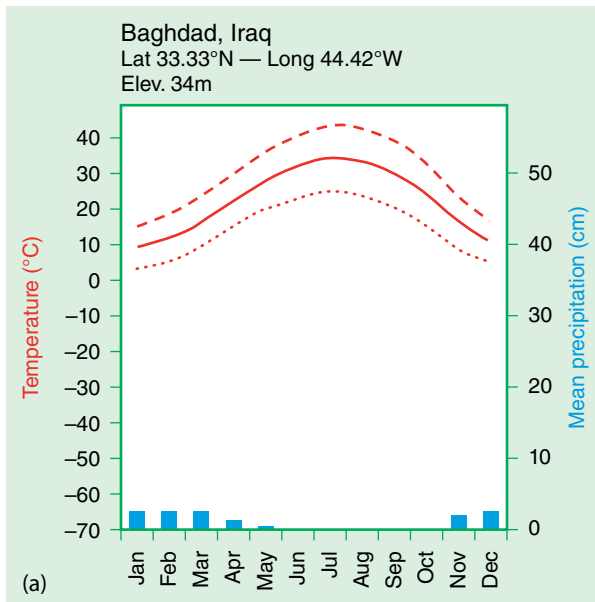


FIGURE 9.14 (a) Climograph for Baghdad, Iraq (BSH climate). Average annual temperature is 22.3°C (72.2°F) and average annual precipitation is 15.7 cm (6.2 in). (b) Water balance diagram for Baghdad, Iraq.

(a) Data from National Centers for Environmental Information. (b) Modified with permission using Web/WIMP version 1.01 implemented by K. Matsuura, C. Willmott, and D. Legates at the University of Delaware, 2003.

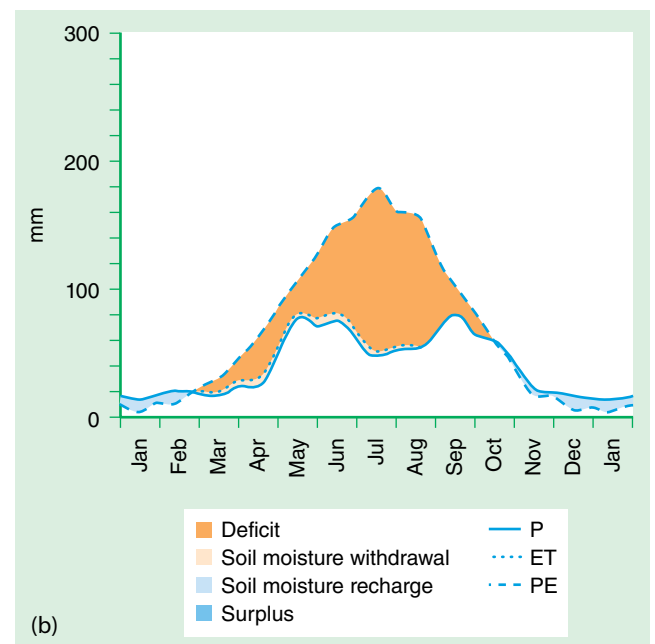
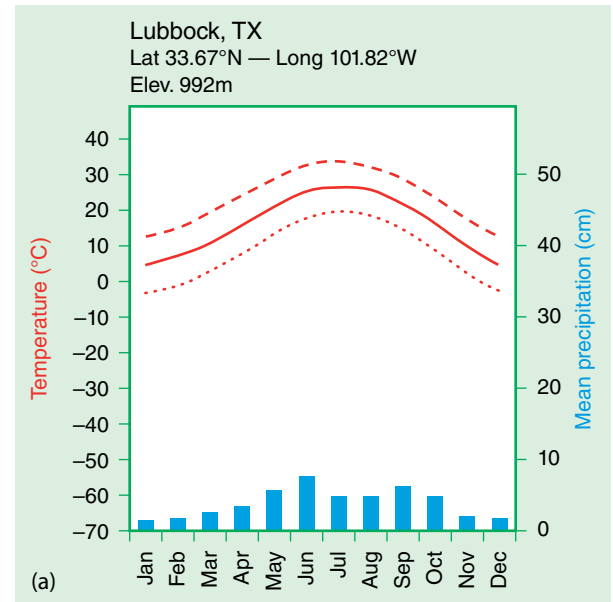


FIGURE 9.15 (a) Climograph for Lubbock, Texas (BSk climate). Average annual temperature is 15.4°C (59.7°F) and average annual precipitation is 47.5 cm (18.7 in). (b) Water balance diagram for Lubbock, Texas.

(a) Data from National Centers for Environmental Information. (b) Modified with permission using Web/WIMP version 1.01 implemented by K. Matsuura, C. Willmott, and D. Legates at the University of Delaware, 2003.

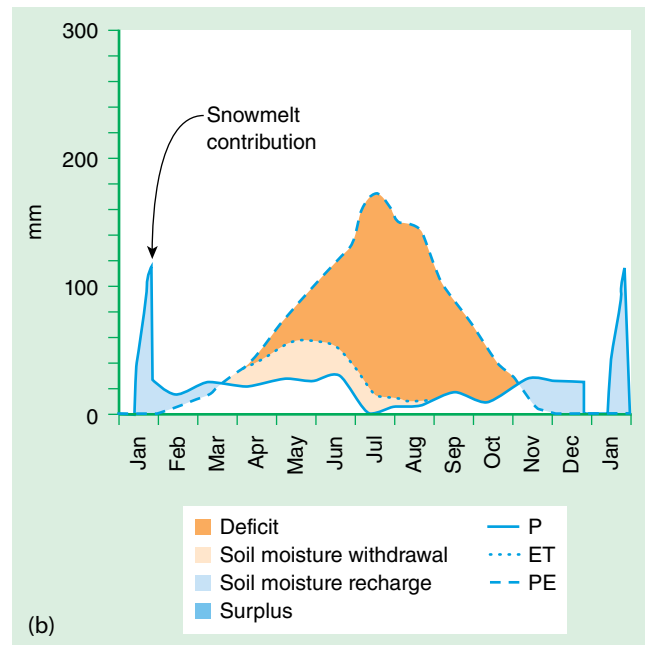
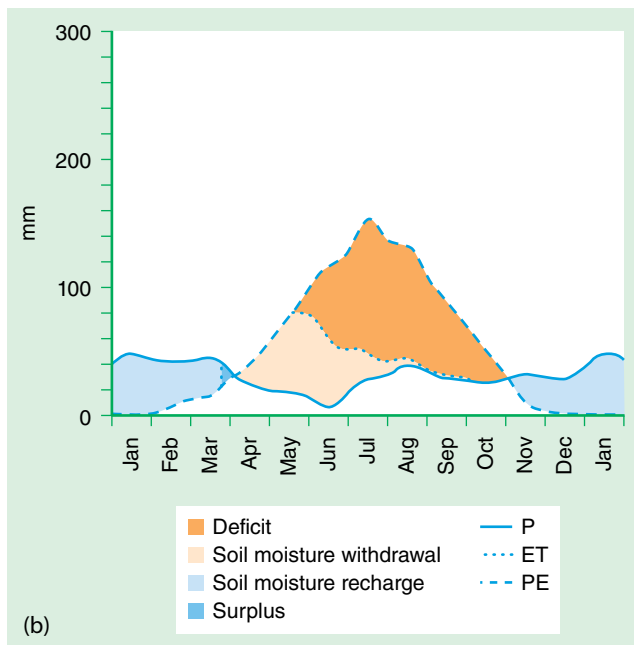
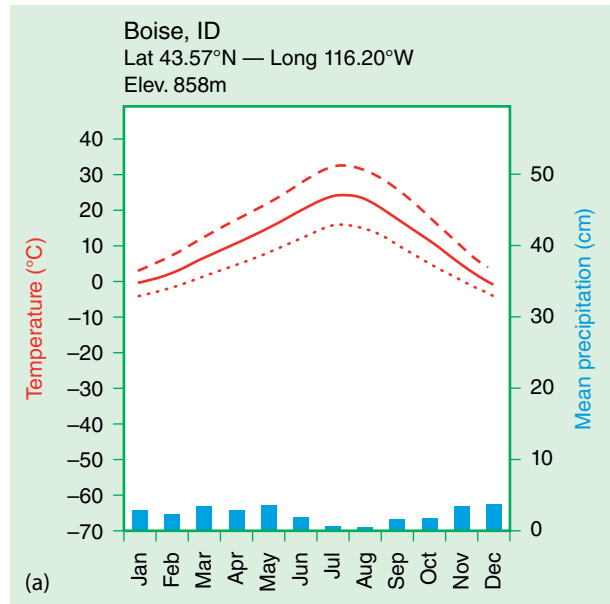
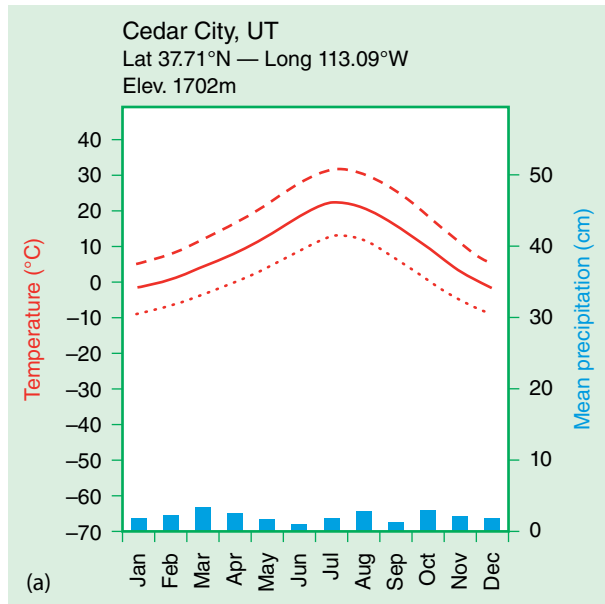


FIGURE 9.16 (a) Climograph for Cedar City, Utah (BSk climate). Average annual temperature is 10.3°C (50.5°F) and average annual precipitation is 29.0 cm (11.4 in). (b) Water balance diagram for Cedar City, Utah.

(a) Data from National Centers for Environmental Information. (b) Modified with permission using Web/WIMP version 1.01 implemented by K. Matsuura, C. Willmott, and D. Legates at the University of Delaware, 2003.

FIGURE 9.17 (a) Climograph for Boise, Idaho (BSk climate). Average annual temperature is 9.7°C (49.4°F) and average annual precipitation is 31.0 cm (12.2 in). (b) Water balance diagram for Boise, Idaho.

(a) Data from National Centers for Environmental Information. (b) Modified with permission using Web/WIMP version 1.01 implemented by K. Matsuura, C. Willmott, and D. Legates at the University of Delaware, 2003.

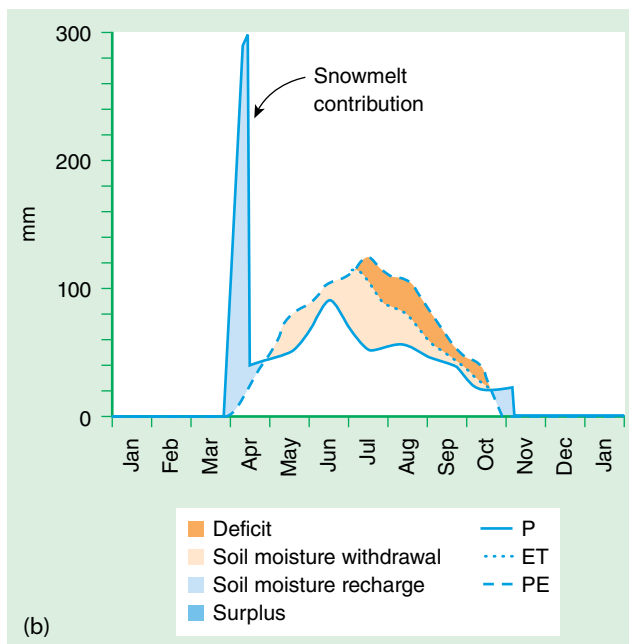
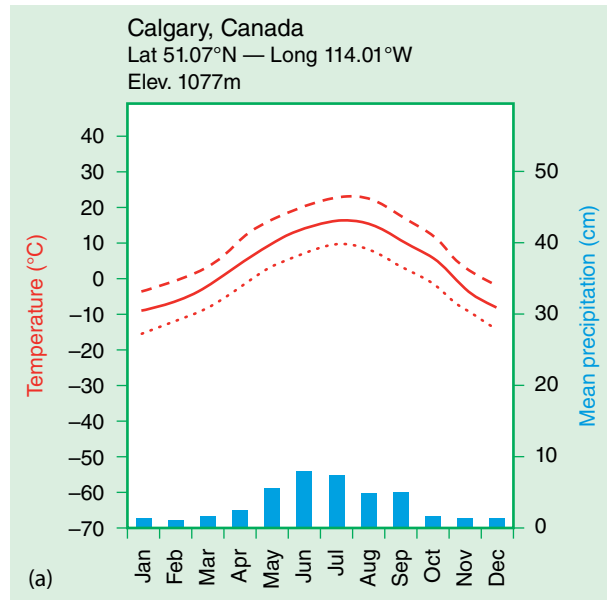


FIGURE 9.18 (a) Climograph for Calgary, Canada (BSk climate). Average annual temperature is 9.7°C (49.4°F) and average annual precipitation is 31.0 cm (12.2 in). (b) Water balance diagram for Calgary, Alberta.

(a) Data from National Centers for Environmental Information. (b) Modified with permission using Web/WIMP version 1.01 implemented by K. Matsuura, C. Willmott, and D. Legates at the University of Delaware, 2003.

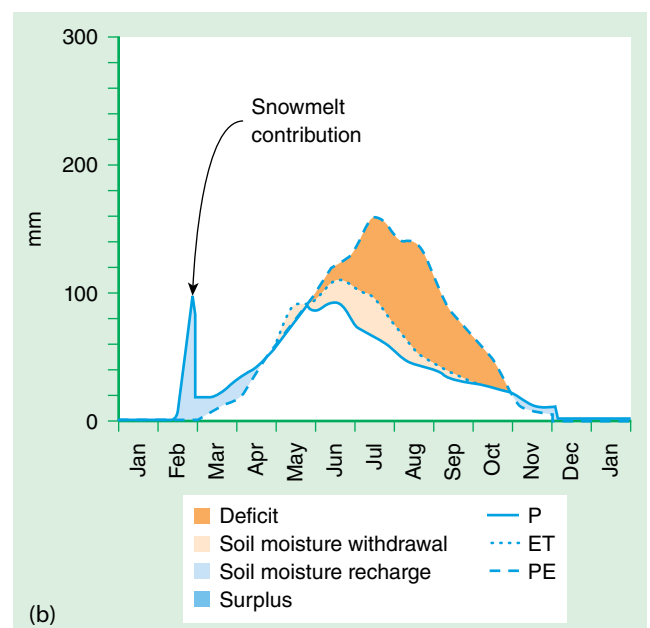
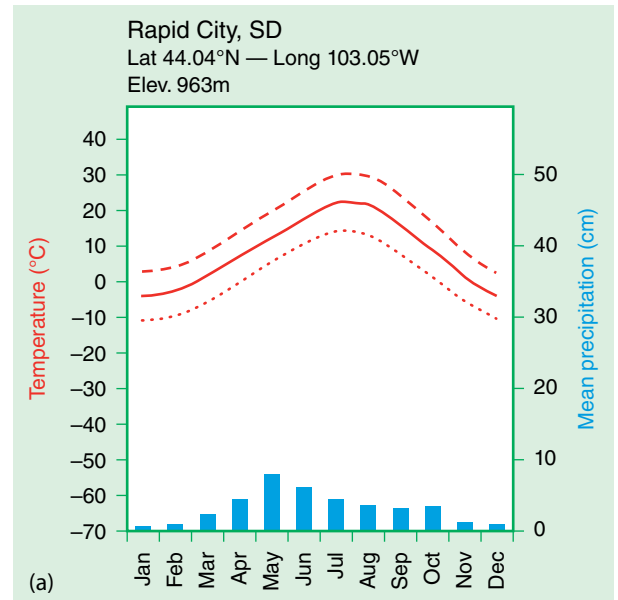


FIGURE 9.19 (a) Climograph for Rapid City, South Dakota (BSk climate). Average annual temperature is 8.1°C (46.6°F) and average annual precipitation is 42.3 cm (16.6 in). (b) Water balance diagram for Rapid City, South Dakota.

(a) Data from National Centers for Environmental Information. (b) Modified with permission using Web/WIMP version 1.01 implemented by K. Matsuura, C. Willmott, and D. Legates at the University of Delaware, 2003.

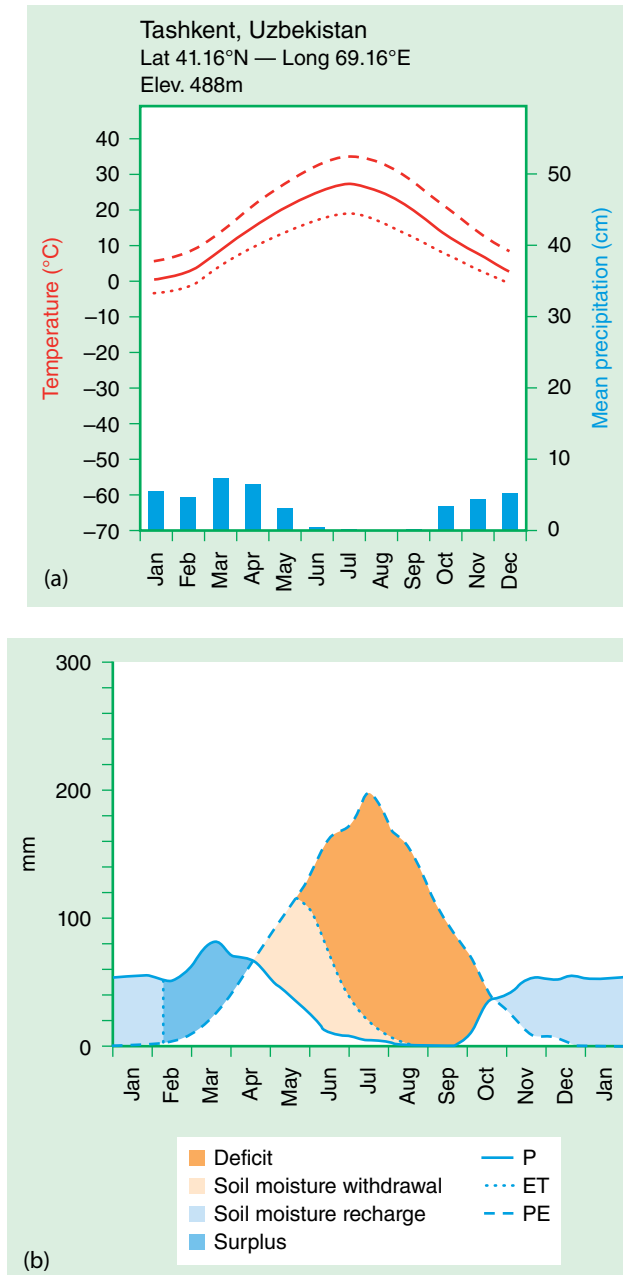


FIGURE 9.20 (a) Climograph for Tashkent, Uzbekistan (BSk climate). Average annual temperature is 14.7°C (58.4°F) and average annual precipitation is 37.5 cm (14.8 in). (b) Water balance diagram for Tashkent, Uzbekistan.

(a) Data from National Centers for Environmental Information. (b) Modified with permission using Web/WIMP version 1.01 implemented by K. Matsuura, C. Willmott, and D. Legates at the University of Delaware, 2003.

annually and Tashkent receives only 37.5 cm (14.8 in), the more equatorward site, Baghdad, shows far more deficit and less surplus (Figures 9.14b and 9.20b, respectively).

C—Mesothermal Climates

Primarily because they are found in the most heavily populated parts of China and India (see world map of Köppen-Geiger climate types), the “C” (or *mesothermal*) family of climates is home to more of the world’s people than any other of the Köppen-Geiger categories. These climates are supportive of intense human activity because of their long growing season, mild winters, and moderate to abundant moisture. Four major types of C climates exist: Humid Subtropical, Subtropical Dry Winter, Mediterranean, and Marine West Coast.

Cfa—Humid Subtropical

The **Humid Subtropical (Cfa) climates** have long, hot summers, relatively mild winters, and abundant precipitation with a relatively even distribution of precipitation across all months. In North America this climatic type occurs through nearly all of the U.S. South, from central Texas to the middle Atlantic coast. Relatively small sections of the ocean basins fall into this climatic type, as the moderating effect of the ocean suppresses summer high temperatures. Cfa climates also dominate southeastern China, Taiwan, and southern Japan. The region is sandwiched between the tropical climates of extreme southeastern Asia and the Highland and more severe midlatitude climates to the north.

Thermal Characteristics. In both North America and Asia the Cfa climate is associated with a *maritime effect* from warm ocean (or Gulf of Mexico) waters. This is especially true of North America, where the clockwise flow of the Bermuda-Azores high pumps mT air far inland. Summers are normally hot, long, and continuous, featuring average temperatures of perhaps 26–28°C (79–82°F) with high relative humidity values. High humidity in conjunction with high temperatures produces sultry, oppressive weather with a high *heat index*. Daily maximum temperatures typically approach 35°C (95°F) during the summer months, with extreme temperatures near 39°C (102°F) for many locations. Such conditions are discernible in climographs for several locations in North America, including Baton Rouge, Louisiana (**FIGURE 9.21a**), Little Rock, Arkansas (**FIGURE 9.22a**), Raleigh-Durham, North Carolina (**FIGURE 9.23a**), and Richmond, Virginia (**FIGURE 9.24a**). A representative example in Asia is Tokyo, Japan (**FIGURE 9.25a**). Notice

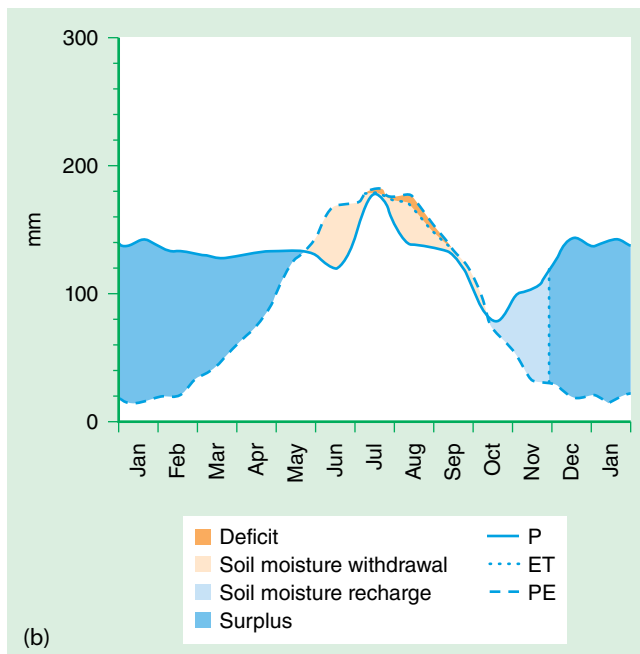
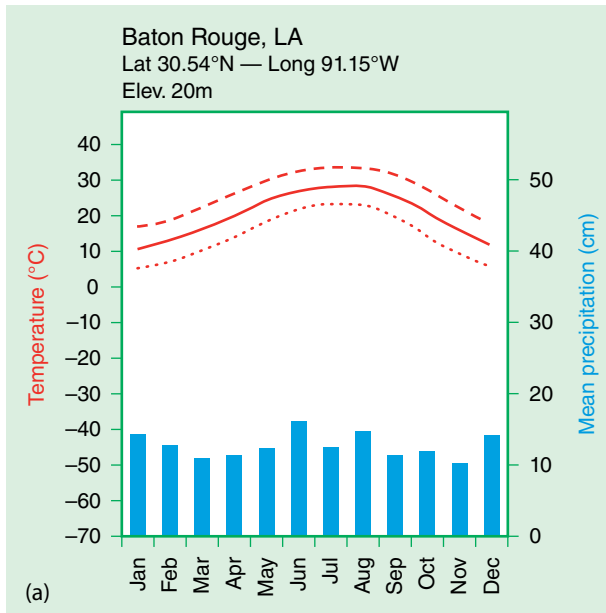


FIGURE 9.21 (a) Climograph for Baton Rouge, Louisiana (Cfa climate). Average annual temperature is 19.4°C (67.0°F) and average annual precipitation is 160.2 cm (63.1 in). (b) Water balance diagram for Baton Rouge, Louisiana.

(a) Data from National Centers for Environmental Information. (b) Modified with permission using Web/WIMP version 1.01 implemented by K. Matsuura, C. Willmott, and D. Legates at the University of Delaware, 2003.

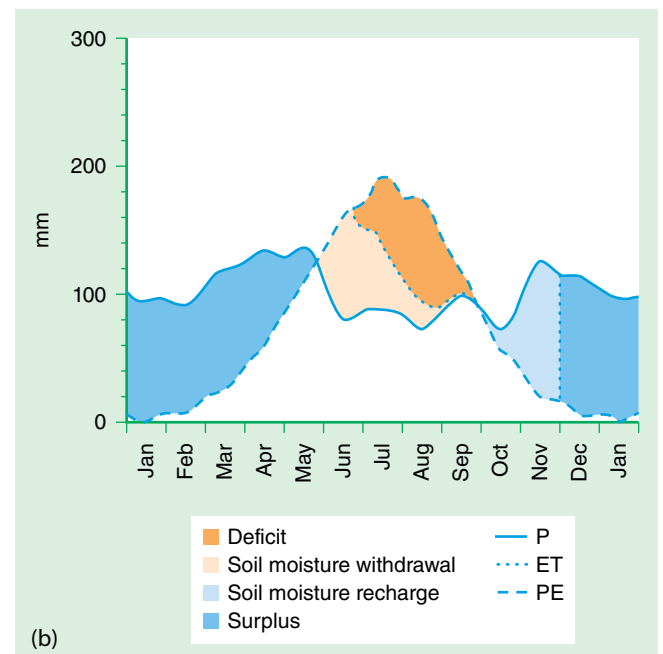
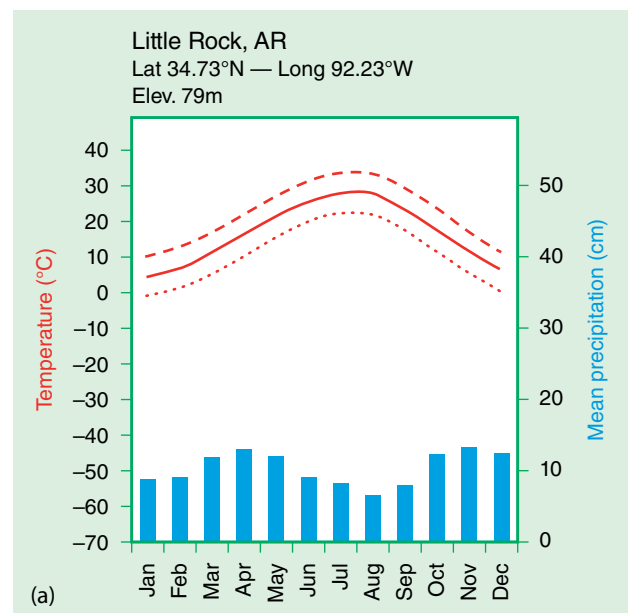


FIGURE 9.22 (a) Climograph for Little Rock, Arkansas (Cfa climate). Average annual temperature is 16.7°C (62.1°F) and average annual precipitation is 129.4 cm (50.9 in). (b) Water balance diagram for Little Rock, Arkansas.

(a) Data from National Centers for Environmental Information. (b) Modified with permission using Web/WIMP version 1.01 implemented by K. Matsuura, C. Willmott, and D. Legates at the University of Delaware, 2003.

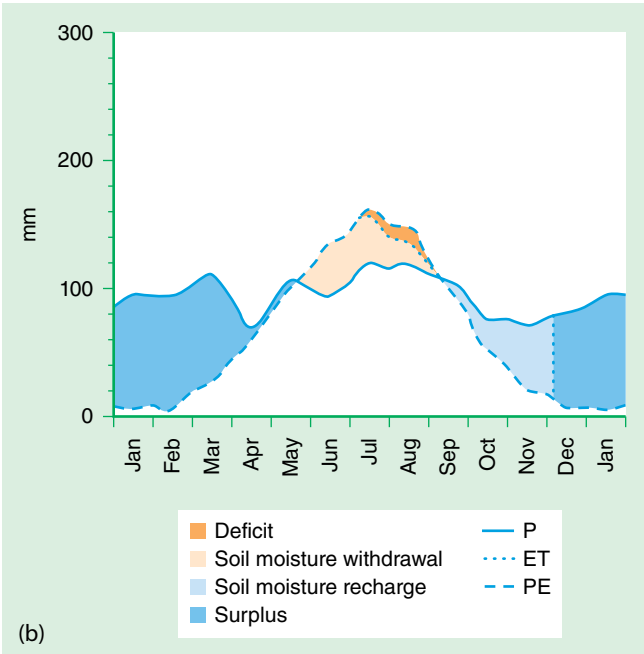
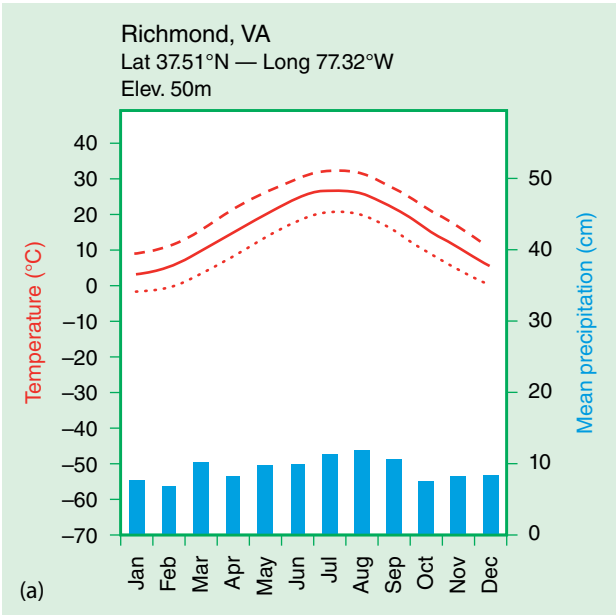
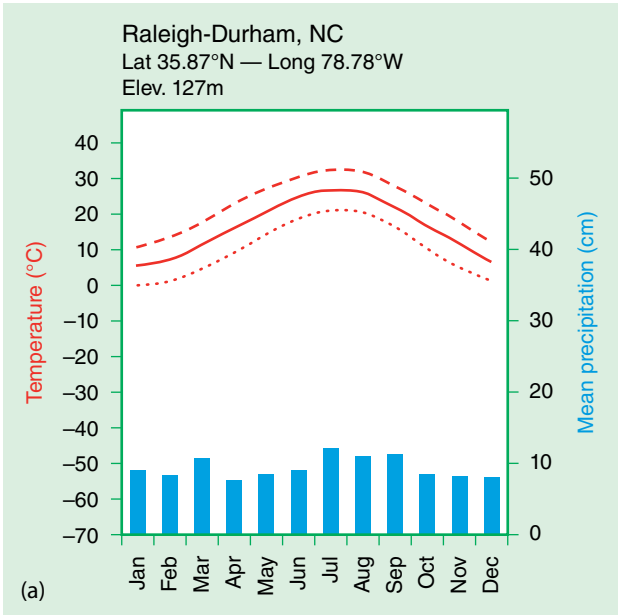


FIGURE 9.23 (a) Climograph for Raleigh-Durham, North Carolina (Cfa climate). Average annual temperature is 15.3°C (59.6°F) and average annual precipitation is 109.3 cm (43.1 in). (b) Water balance diagram for Raleigh, North Carolina.

(a) Data from National Centers for Environmental Information. (b) Modified with permission using Web/WIMP version 1.01 implemented by K. Matsuura, C. Willmott, and D. Legates at the University of Delaware, 2003.

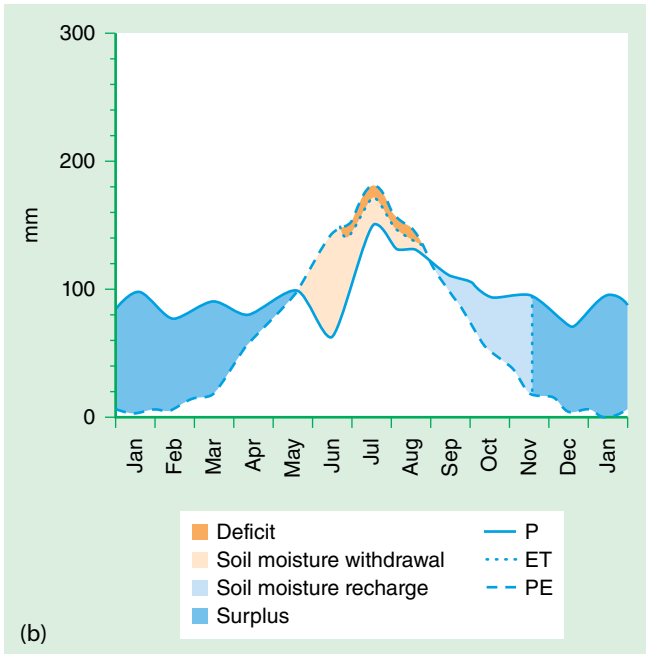


FIGURE 9.24 (a) Climograph for Richmond, Virginia (Cfa climate). Average annual temperature is 14.2°C (57.6°F) and average annual precipitation is 111.5 cm (43.9 in). (b) Water balance diagram for Richmond, Virginia.

(a) Data from National Centers for Environmental Information. (b) Modified with permission using Web/WIMP version 1.01 implemented by K. Matsuura, C. Willmott, and D. Legates at the University of Delaware, 2003.

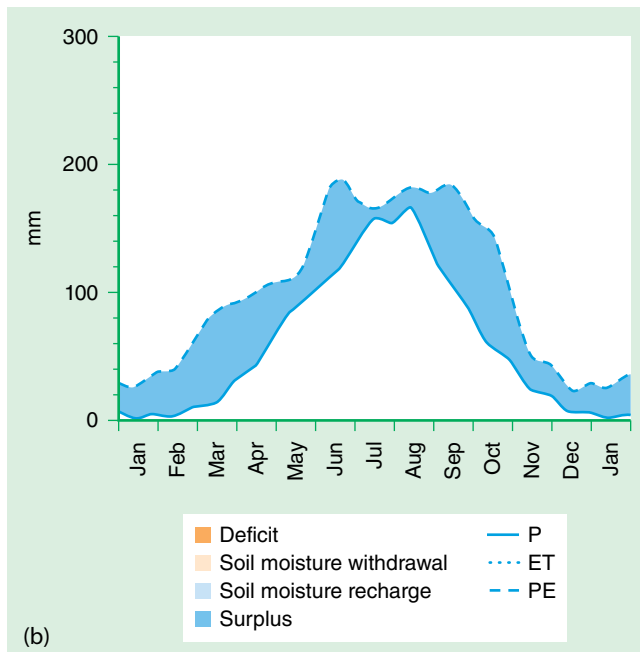
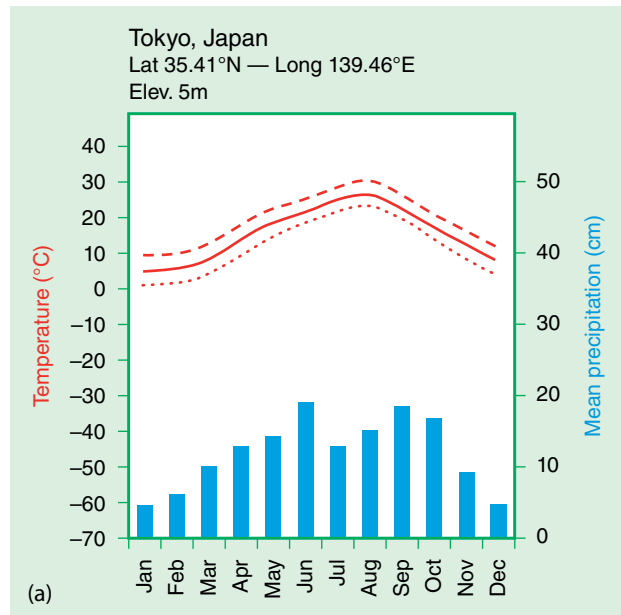


FIGURE 9.25 (a) Climograph for Tokyo, Japan (Cfa climate). Average annual temperature is 14.5°C (58.1°F) and average annual precipitation is 151.9 cm (59.8 in). (b) Water balance diagram for Tokyo, Japan.

(a) Data from National Centers for Environmental Information. (b) Modified with permission using Web/WIMP version 1.01 implemented by K. Matsuura, C. Willmott, and D. Legates at the University of Delaware, 2003.

the moderating effect on coastal sites such as Baton Rouge, Raleigh, Richmond, and Tokyo.

Freezing temperatures are generally not uncommon. The coldest month on average is January, with an average temperature of perhaps 10°C (50°F) in the mildest Cfa regions and only slightly above 0°C (32°F) in the harshest. January is also generally the month of the most frequent freezes, with freezes occurring later in the season nearest to the coasts. Winter in the true sense of the word does exist, but cold weather is interrupted by frequent warmer periods. Extreme cold occurs occasionally.

Moisture Characteristics. Precipitation is generally evenly distributed throughout the year, averaging 102 to 152 cm (40 to 60 in) annually. High-magnitude precipitation events are relatively common, with most associated with convective thunderstorms that can occur on summer afternoons as a result of diurnal heating of the land surface. The water balance diagrams for the North American sites (**FIGURES 9.21b through 9.24b**) show relatively small summer deficits, with higher deficits inland, such as at Little Rock. Convective precipitation is sometimes too intense and short-lived to allow sufficient *infiltration* into the soil. Some Cfa climates are subject to fairly lengthy intervals between summer precipitation events. Wilting vegetation is fairly common even though the monthly precipitation totals may suggest a humid environment. For Tokyo (**FIGURE 9.25b**), the summer monsoon prevents climatological deficits from occurring.

Frontal cyclones are the most common precipitation-forcing mechanism during winter and spring as the polar front jet stream reaches its farthest equatorial position during those seasons.

The frequency of frontal cyclones also increases during those times as the latitudinal thermal gradient is maximized. The steeper thermal gradient triggers greater Rossby wave amplitude and increased storm frequencies and magnitudes to equalize energy inequalities across the latitudes. Moderate reductions in precipitation usually occur in October and November because those months fall within the transition season between the dominance of two main precipitation-forcing mechanisms: afternoon *convection* in the warm season and midlatitude wave cyclones in the cold season. As with tropical climates, the tropical cyclone remains an important source of summer and autumn precipitation, particularly in east Asia. Although destructive, tropical cyclones have some benefit to the regional water balance inland, especially during the somewhat drier autumn season.

Cwa—Subtropical Dry Winter

In Asia a distinct summer monsoon influence is present. If the monsoon season provides an even more distinct increase in summer precipitation than is seen at locations such as Tokyo, it is classified as a **Humid Subtropical Winter Dry (Cwa) climate**. By definition, in this climatic type the month with the highest mean precipitation has at least 10 times the average precipitation as the driest winter month. Cwa climates are among the wettest on Earth in the summer season, especially if the monsoonal rains are augmented by orographic uplift. The Cwa climate is found along an extensive portion of northern India, extending into southeast Asia, but with virtually no area over ocean basins. Two examples of locations with a Cwa climate are Hong Kong, China (FIGURES 9.26a), and New Delhi, India (FIGURES 9.27a).

Thermal Characteristics. Daily maximum temperatures during winter may average near 21°C (70°F) for Cwa locations, while summer temperatures generally peak between 35°C and 43°C (95°F and 110°F). These high temperatures are usually much higher than those found in the Cwb zones. The climograph of New Delhi (Figure 9.27a) illustrates this concept. The highest average monthly temperatures occur in May and June, just before the onset of the summer monsoonal rains. Cloud cover associated with the monsoon suppresses daily maximum temperatures during the middle of summer.

Moisture Characteristics. Extremely high seasonal precipitation totals are recorded within some Cwa climate zones. The seasonality of monthly precipitation totals of Cherrapunji, in northeast India, exemplifies the monsoonal moisture pulse within this region, but a strong *orographic effect* on the normal monsoon-influenced precipitation regime makes these totals atypical compared with most monsoonal locations. The climograph for New Delhi is much more representative of a Cwa climate, with annual precipitation totals below 100 cm (40 in). The associated water balance diagram indicates strong soil moisture deficits in the Cwa location during the dry spring.

Csa, Csb—Mediterranean

Possibly the most identifiable climate in Europe and likely the most enjoyable climatic type in the world is the **Mediterranean climate**. Like Humid Subtropical climates, temperatures are warm to hot in summer and mild in winter. Unlike Humid Subtropical climates, however, Mediterranean climates are characterized by distinct dryness in summer and a relatively wet

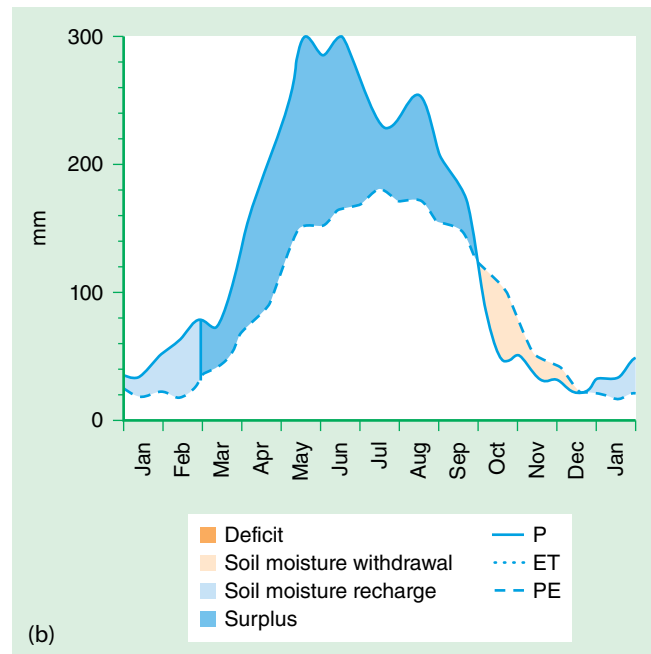
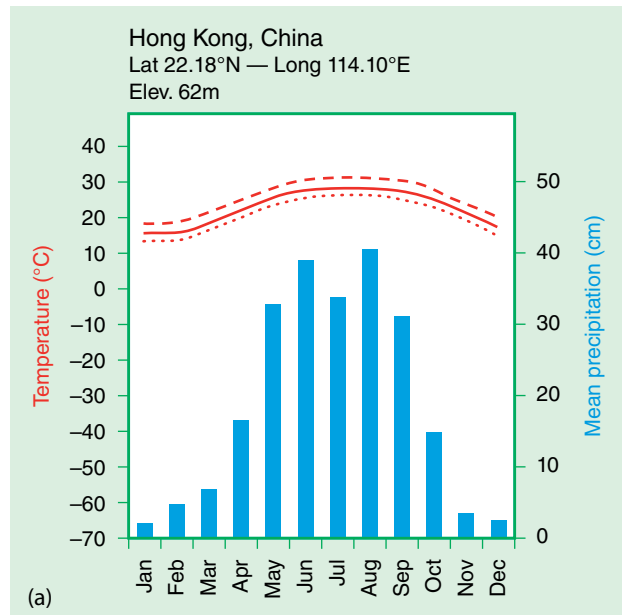


FIGURE 9.26 (a) Climograph for Hong Kong, China (Cwa climate). Average annual temperature is 23.7°C (74.6°F) and average annual precipitation is 218.7 cm (86.1 in). (b) Water balance diagram for Hong Kong, China.

(a) Data from National Centers for Environmental Information. (b) Modified with permission using Web/WIMP version 1.01 implemented by K. Matsuura, C. Willmott, and D. Legates at the University of Delaware, 2003.

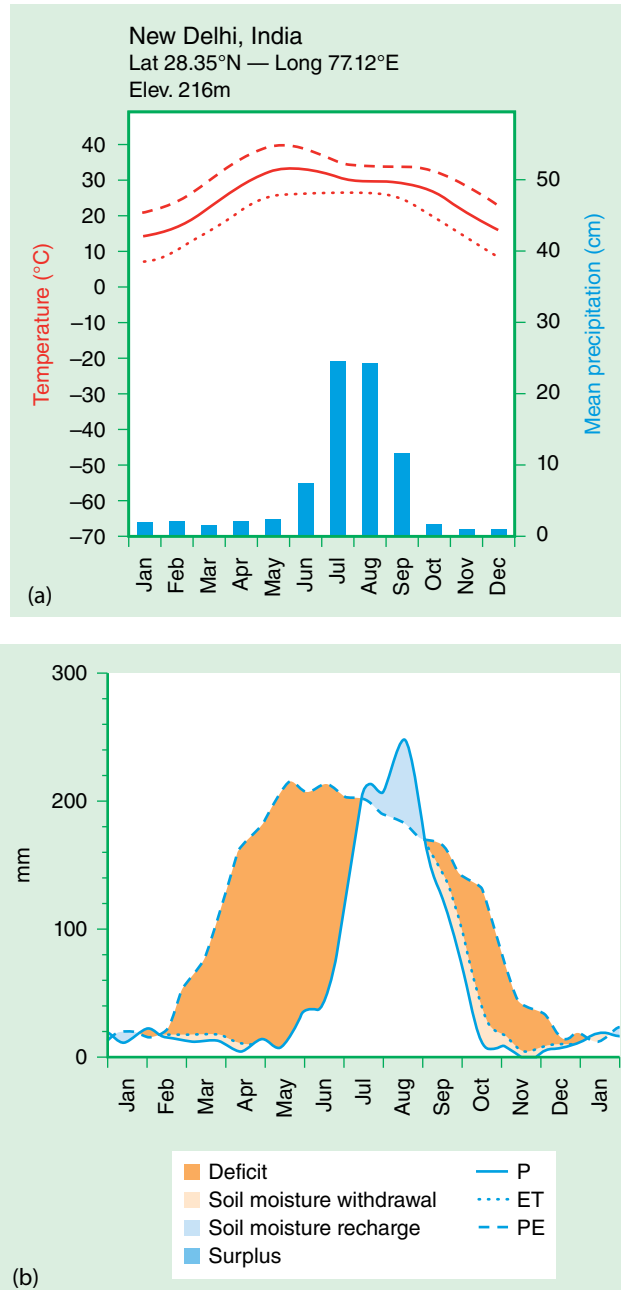


FIGURE 9.27 (a) Climograph for New Delhi, India (Cwa climate). Average annual temperature is 25.0°C (77.1°F) and average annual precipitation is 70.6 cm (27.8 in). (b) Water balance diagram for New Delhi, India.

(a) Data from National Centers for Environmental Information. (b) Modified with permission using Web/WIMP version 1.01 implemented by K. Matsuura, C. Willmott, and D. Legates at the University of Delaware, 2003.

winter. The agricultural landscape of locations with Csa and Csb climates is distinct, because only certain types of crops can thrive in such an environment of extreme aridity in the warm season. Any other crops grown must bring a sufficiently high price to make irrigation feasible. Perhaps the crop that best indicates the presence of a Mediterranean climate is the olive, but others such as artichokes, figs, and certain varieties of grape are also well suited to this distinctive climate. As a result, the customary food and drink in cultures of the regions having Mediterranean climates include olive oil, artichokes, figs, and grapes for wine production.

This climate is found in southern Spain, southern France, Italy, and Greece, and parts of the remainder of the crescent around the Mediterranean Sea (see world map of Köppen-Geiger climate types). It also is found along the western edges of continents in the lower midlatitudes. Mediterranean climates in North America are limited to coastal California, Oregon, and Washington, but a substantial section of the adjacent Pacific Ocean falls into this climatic type. Asia has no large regions that meet the climate classification criteria for Mediterranean type climates except for parts of Turkey, Syria, Lebanon, Israel, Palestine, Jordan, and Iran.

Two associated features encourage sinking atmospheric motions on the eastern sides of the subtropical anticyclones (and, therefore, the western sides of continents) where Mediterranean climates are found. First, the adjacent cold surface ocean currents stabilize the atmosphere, and perhaps even generate a temperature inversion. By contrast, the warm currents on the western sides of the subtropical anticyclones (east sides of continents) destabilize and energize storm systems associated with the Humid Subtropical climates.

Second, sinking motion at subtropical latitudes is more prevalent on the west coasts of continents than east coasts because the eastern sides of the subtropical anticyclones support surface divergence, which draws in subsiding air from aloft. By contrast, the western sides of the subtropical anticyclones support surface convergence, which augments rising motion. In other words, the effect of the subtropical high tilts with height, such that sinking motion occurs down to the surface on the eastern sides (western sides of continents), but only occurs aloft (in fulfillment of the tendency for sinking motion by the general circulation) on the western sides of the anticyclones.

To see why this is the case, we can invoke the **gradient wind equation**, which specifies motion in curved flow, such as around the subtropical anticyclones. The wind

speed in gradient flow (V_G) relates to the *geostrophic wind* (V_g ; i.e., flow with no curved *isohypses*) as:

$$V_G = \frac{2V_g}{1 + \sqrt{1 + \frac{4V_g}{fr}}}$$

where f is the *Coriolis parameter* ($2\Omega \sin \phi$), and r is the radius of curvature of the flow. Smaller r values represent “tighter-turning” flow. Notice from the gradient wind equation that if r is infinite (i.e., if it has no curvature at all), $V_G = V_g$. Positive values of r are used for counterclockwise flow and negative r values represent clockwise flow.

The gradient wind equation suggests that for a negative r (because air moves clockwise around the subtropical anticyclone in the northern hemisphere), the term inside the radical must be less than 1, so the overall denominator in the equation will be less than 2. Because 2 divided by a number less than 2 is greater than 1, V_G is bigger than V_g for a given pressure gradient, for clockwise (anticyclonic in the northern hemisphere) flow. Air flows faster around ridges (which have clockwise flow in the northern hemisphere) than around troughs *if pressure/isohypse gradients are equal*, but pressure gradients around ridges and anticyclones are generally much weaker than those around troughs and cyclones.

Furthermore, for a given pressure gradient at the poleward side of the subtropical anticyclone, f is relatively large. This causes the $4V_g/fr$ term to be nearer to zero than at the equatorward side (but negative), which means that the term inside the radical will be 1 minus a very small number, and the entire denominator will be almost 2. Thus, at the poleward side of the high, V_G is only slightly larger than V_g . But at the equatorward side, where f is a negative number near zero, the $4V_g/fr$ term is more negative. This causes the term inside the radical to be 1 minus a bigger number, and the entire denominator will be much lower than 2. Thus, at the equatorward side of the high, V_G is much larger than V_g . So the gradient wind is larger as air flows around the equatorward side of the high and smaller as it moves clockwise around the polar side of the high. This difference in gradient wind at the surface causes divergence on the eastern sides of the subtropical anticyclones (western sides of continents) and a stable atmosphere and surface convergence on the western side (FIGURE 9.28).

Thermal Characteristics. The warmer subcategory of Cs climates is the **Mediterranean Hot Summer (Csa) climate**, which has the warmest month with an average temperature exceeding 22°C (72°F). The

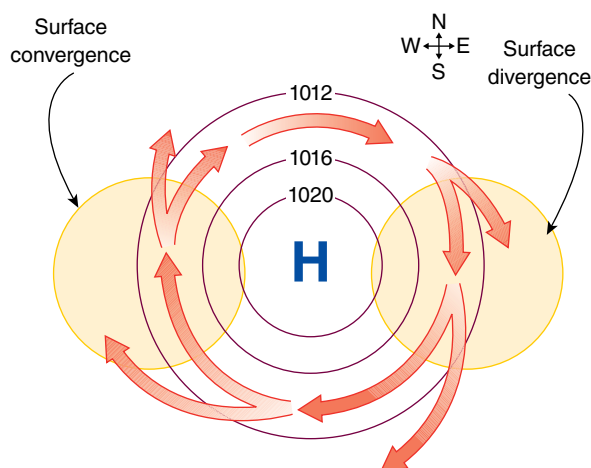


FIGURE 9.28 Surface convergence and divergence associated with flow around a subtropical anticyclone. Of course, in the “real world,” the pressure gradient will be altered in association with the changes in wind speed.

Mediterranean Warm Summer (Csb) climate is characterized by a warmest month averaging below 22°C (72°F). In general, these milder summer temperatures occur near the coast and at higher elevations, with Csa climates becoming more dominant farther inland. Summer coastal temperatures are typically in the range of 21–27°C (70–80°F), while inland locations may have daily highs near 38°C (100°F).

Radiation and temperature seasonality in Mediterranean climates in North America are represented by three California sites: Long Beach (FIGURE 9.29a), where summer temperatures are just high enough to be classified as Csa; Sacramento (FIGURE 9.30a), a warmer inland location; and the Csb coastal site of Santa Maria (FIGURE 9.31a).

Summer temperatures in Mediterranean Europe are moderated by the maritime effect as inlets of the Mediterranean Sea give a large surface area of maritime-influenced lands. Representative examples of Mediterranean climates in Europe are shown by Rome, Italy, with a Csa climate (FIGURE 9.32a), and Faro, Portugal, with a Csb climate (FIGURE 9.33a).

Monthly average winter temperatures in most Mediterranean climates may approximate 10°C (50°F), while summer averages may approach 27°C (80°F) with daytime highs significantly higher. During the winter months inland temperatures may dip below freezing, while coastal locations, moderated by the relative ocean warmth, have mean temperatures that remain in the 10–16°C (50–61°F) range. Fogs are common, especially in winter, as air moving onshore is chilled to its dewpoint temperature by the cold ocean currents. These **advection fogs** generally increase the minimum temperatures in the early morning hours but delay the warming of the surface as morning progresses.

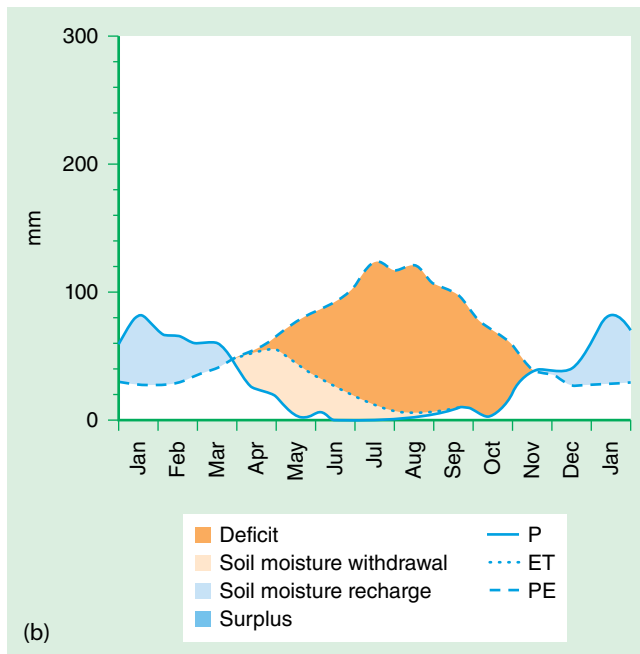
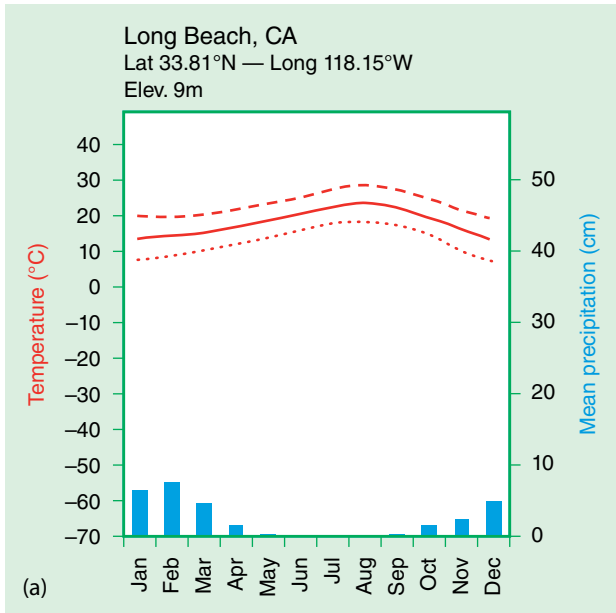
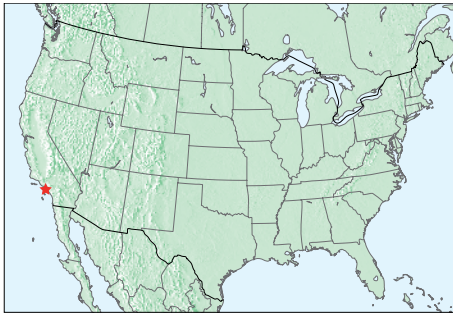


FIGURE 9.29 (a) Climograph for Long Beach, California (Csa climate). Average annual temperature is 18.5°C (65.3°F) and average annual precipitation is 32.9 cm (12.9 in). (b) Water balance diagram for Long Beach, California.

(a) Data from National Centers for Environmental Information. (b) Modified with permission using Web/WIMP version 1.01 implemented by K. Matsuura, C. Willmott, and D. Legates at the University of Delaware, 2003.

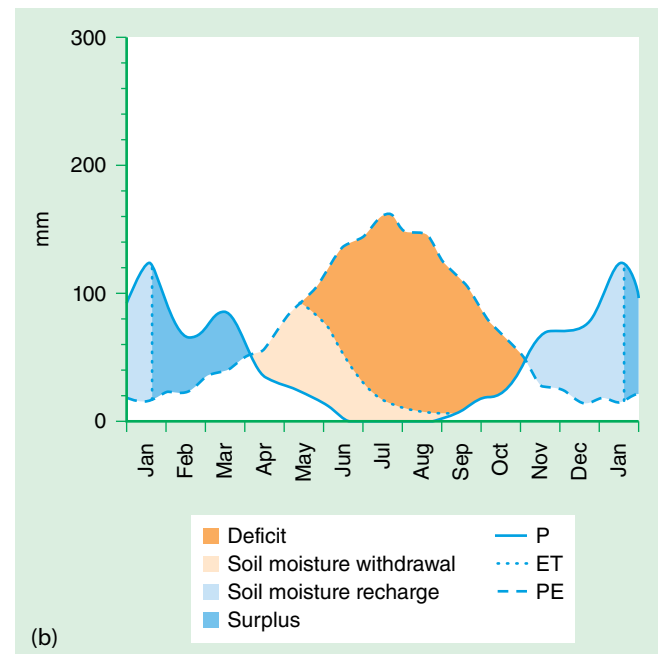
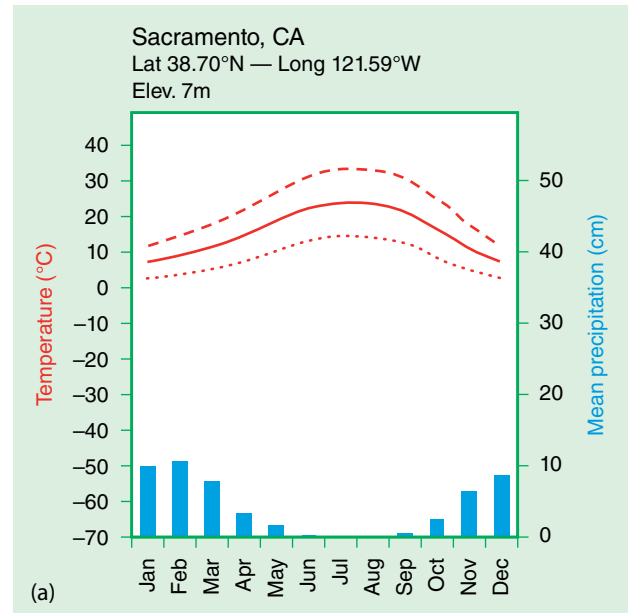
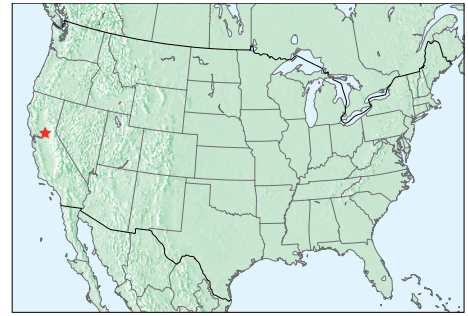


FIGURE 9.30 (a) Climograph for Sacramento, California (Csa climate). Average annual temperature is 16.2°C (61.1°F) and average annual precipitation is 45.5 cm (17.9 in). (b) Water balance diagram for Sacramento, California.

(a) Data from National Centers for Environmental Information. (b) Modified with permission using Web/WIMP version 1.01 implemented by K. Matsuura, C. Willmott, and D. Legates at the University of Delaware, 2003.

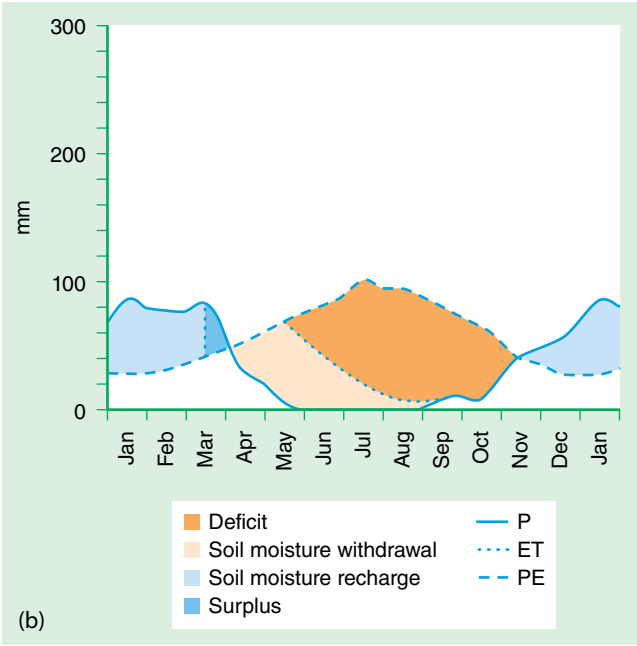
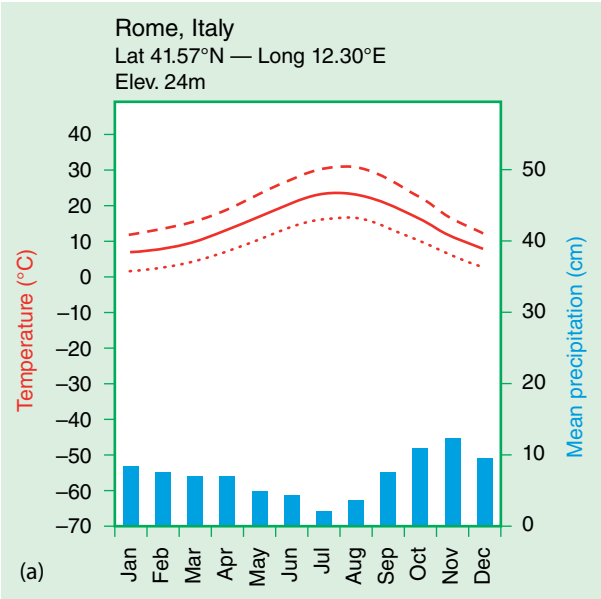
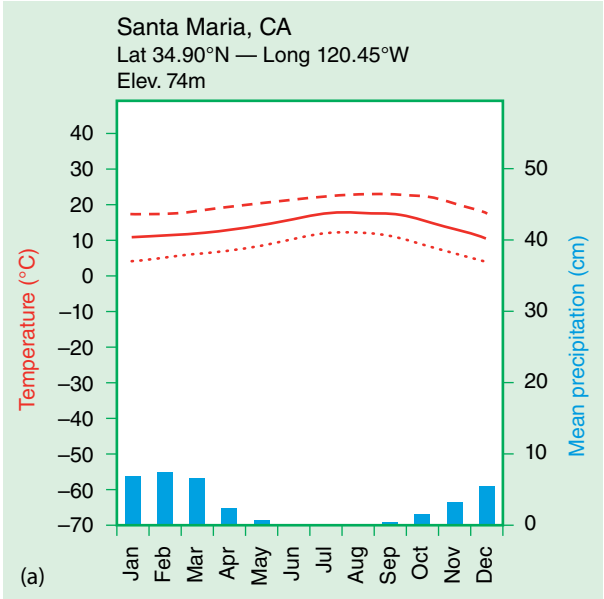
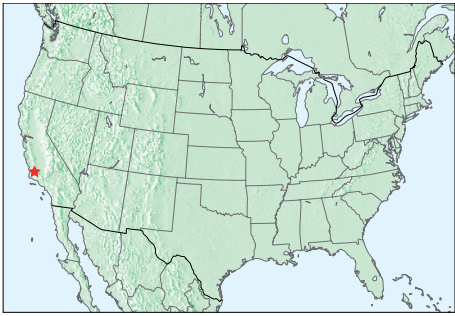


FIGURE 9.31 (a) Climograph for Santa Maria, California (Csb climate). Average annual temperature is 14.3°C (57.7°F) and average annual precipitation is 35.6 cm (14.0 in). (b) Water balance diagram for Santa Maria, California.

(a) Data from National Centers for Environmental Information. (b) Modified with permission using Web/WIMP version 1.01 implemented by K. Matsuura, C. Willmott, and D. Legates at the University of Delaware, 2003.

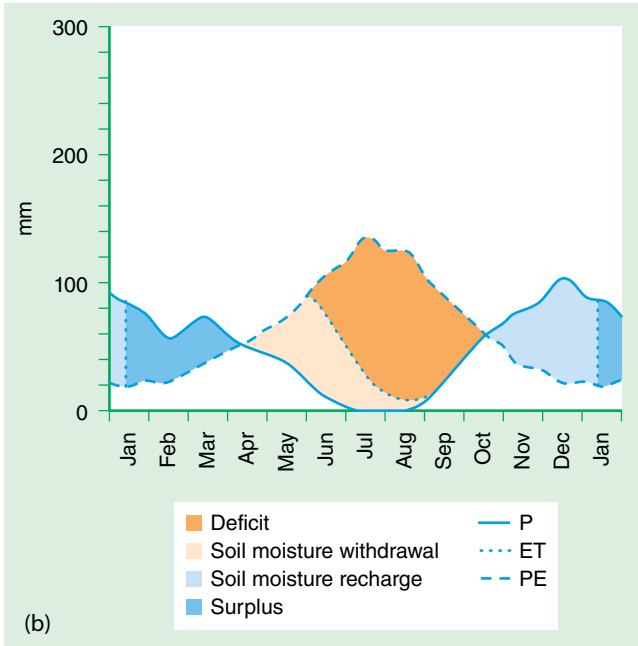


FIGURE 9.32 (a) Climograph for Rome, Italy (Csa climate). Average annual temperature is 15.5°C (60.0°F) and average annual precipitation is 80.3 cm (31.6 in). (b) Water balance diagram for Rome, Italy.

(a) Data from National Centers for Environmental Information. (b) Modified with permission using Web/WIMP version 1.01 implemented by K. Matsuura, C. Willmott, and D. Legates at the University of Delaware, 2003.

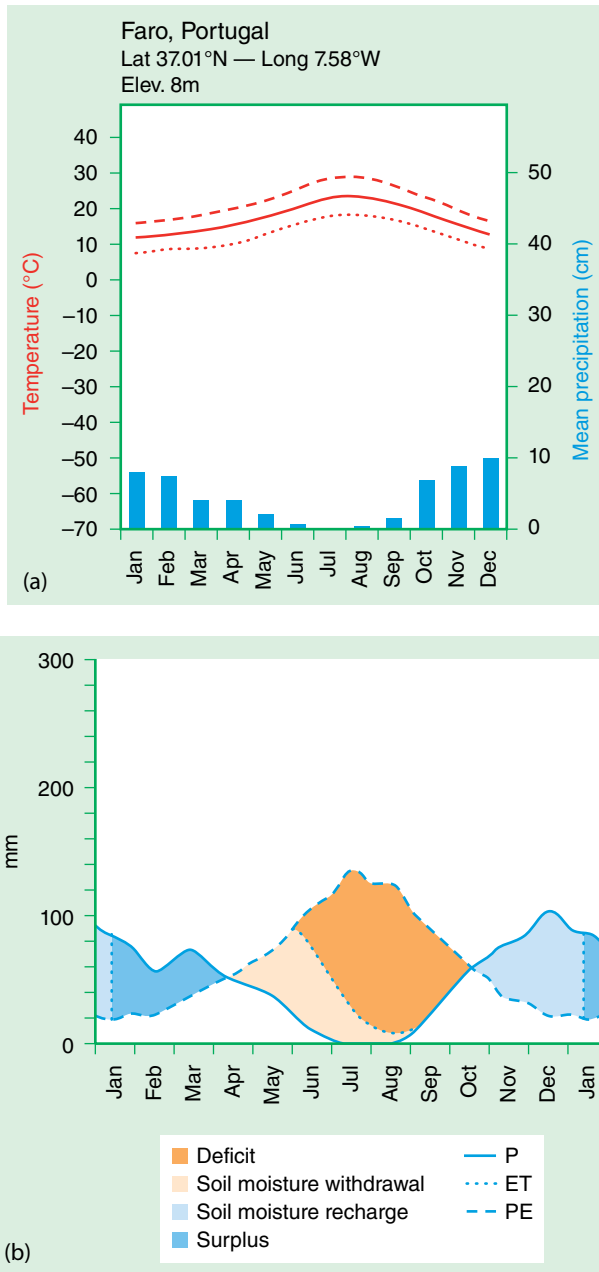


FIGURE 9.33 (a) Climograph for Faro, Portugal (Csb climate). Average annual temperature is 17.4°C (63.3°F) and average annual precipitation is 52.8 cm (20.8 in). (b) Water balance diagram for Faro, Portugal.

(a) Data from National Centers for Environmental Information. (b) Modified with permission using Web/WIMP version 1.01 implemented by K. Matsuura, C. Willmott, and D. Legates at the University of Delaware, 2003.

Moisture Characteristics. The onset of the summer drought occurs as the subtropical anticyclones expand and move poleward, along with the Hadley cells. These subtropical anticyclones then approach the midlatitude west coasts of continents. Along with the cold ocean currents, the subsidence side of the anticyclone suppresses rising motion that might otherwise support precipitation-producing mechanisms.

Summer deficits in North America are induced by the presence of the semipermanent subtropical anticyclone that dominates the central North Pacific Ocean. During the warm season this Hawaiian high becomes particularly well established, especially along the eastern edge of the ocean basin where the cold California current helps to stabilize the overlying atmosphere. During winter the anticyclone weakens and migrates equatorward, allowing for the passage of migratory frontal cyclones embedded in the polar front jet stream flow. The frequency and magnitude of these storm systems are variable. Some winters may be relatively dry, while others produce copious precipitation totals. In general, precipitation increases with latitude in both the Csa and the Csb types because poleward areas are more affected by midlatitude wave cyclones and their trailing cold fronts that traverse the region.

In the case of Europe, high pressure builds over the Mediterranean Sea as summer approaches. In this area the high may be viewed as being an extension of the Bermuda-Azores high that dominates the North Atlantic basin during summer. The polar front jet stream, which follows the upper atmospheric boundary between cold air and much warmer air, typically induces much of the precipitation falling on Europe and other midlatitude locations. It retreats north of the Alps in summer as the *polar cell* and *circumpolar vortex* contract and the subtropical anticyclone expands. As a result, summer precipitation caused by midlatitude wave cyclones embedded within the jet stream is confined to northern and central Europe. Occasional rainfall does occur in Mediterranean Europe as a result of surface heat-induced convective thunderstorms, and these regions are generally wetter in summer than their North American counterparts. Likewise, a comparison of the water balance diagrams for the five cities (**FIGURES 9.29b through 9.33b**) suggests that deficits are somewhat smaller and less prominent in Europe's Mediterranean climates than in those of North America.

During winter, cold polar air builds in higher latitudes and expands toward lower latitudes. In Europe the polar front jet advances southward, ultimately positioning itself south of the Alps and over the Mediterranean basin. In these instances cyclogenesis is common over the warm waters of the Mediterranean Sea, as the warm surface

destabilizes the overlying atmosphere. Midlatitude wave cyclones provide the area with rainfall throughout the winter. Even with these precipitating mechanisms in place, however, annual rainfall amounts are relatively low, ranging from 25 to 89 cm (10 to 35 in).

Cfb, Cfc—Marine West Coast

The **Marine West Coast climate** occupies the coastal strip of North America north of Mediterranean climates along the Pacific coast, from Washington through Alaska (see world map of Köppen-Geiger climate types). The maritime effect does not extend to the leeward sides of the coastal mountains, however, so the **Marine West Coast Warm Summer (Cfb) climate** and the **Marine West Coast Cool Summer (Cfc) climate** occupy a relatively narrow zone in North America. However, this climate type occupies almost 24% of the world ocean basins, including the vast majority of the middle and high latitudes of both the North Pacific and North Atlantic. The climatic type is also found prominently throughout western Europe, from northern Spain through France, the British Isles, the Low Countries, Germany, Poland, much of the Balkans and central Europe, and southern Scandinavia. The European Cfb climatic type is extensive because of the prevalence of the warm North Atlantic Drift and the east–west alignment of the Alps, which allows for the penetration of mP air deep into the continental interior via the global midlatitude westerlies, pushed eastward by the circulation around the southern side of the Icelandic low. Winds and storms that traverse this region from west to east carry the ocean-moderated winds far inland.

Thermal Characteristics. As mentioned above, Marine West Coast temperatures in both North America and Europe are mild considering the latitude of the regions, as the moderating effects of the sea are transported inland. In Europe, in addition to the North Atlantic Drift, the North Sea and Baltic Sea also reinforce the moderating influence of this climatic type through much of Europe. As “C” climates, they are characterized by average monthly temperatures above freezing for all months. Daily and annual temperature ranges are also suppressed by persistent cloud cover virtually year-round.

Mean monthly temperatures in the warmest month rarely exceed 24°C (75°F), while annual averages are typically between 8 and 13°C (46 and 55°F). Monthly averages during winter remain above 0°C (32°F), and daily winter minima rarely dip below −7°C (20°F). Extreme temperatures do occur, but they are rare. North America’s Marine West Coast Warm Summer region is represented by Seattle (**FIGURE 9.34a**), while

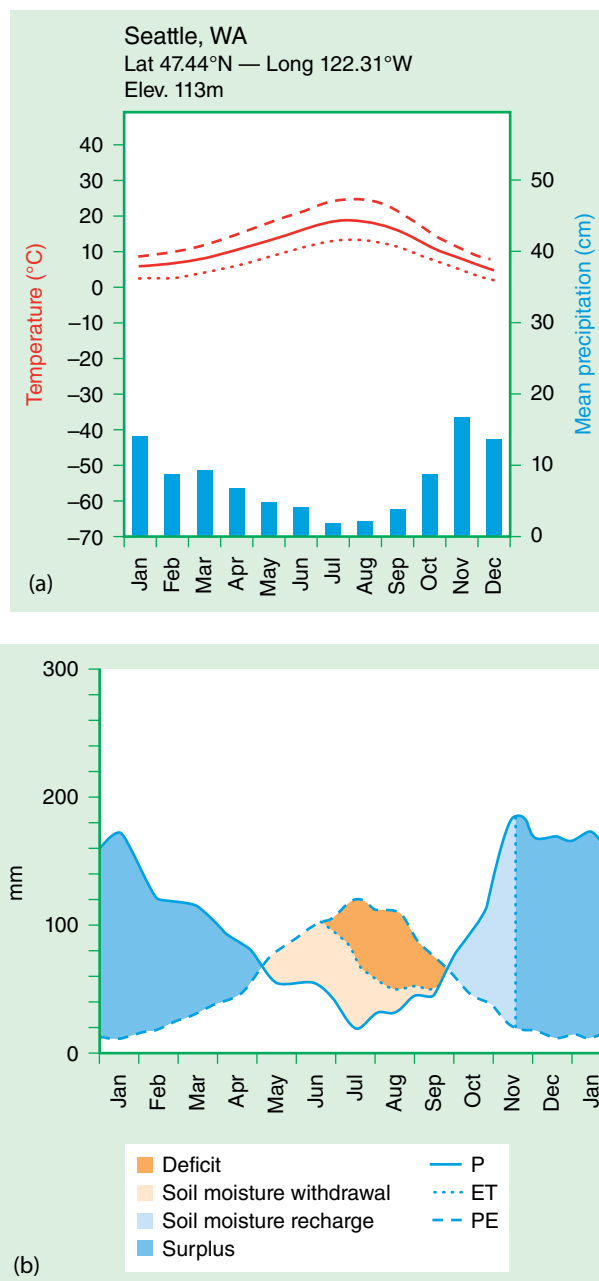
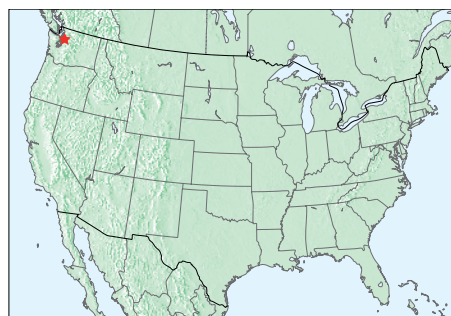


FIGURE 9.34 (a) Climograph for Seattle, Washington (Cfb climate). Average annual temperature is 11.3°C (52.3°F) and average annual precipitation is 94.2 cm (37.1 in). (b) Water balance diagram for Seattle, Washington.

(a) Data from National Centers for Environmental Information. (b) Modified with permission using Web/WIMP version 1.01 implemented by K. Matsuura, C. Willmott, and D. Legates at the University of Delaware, 2003.

Manchester, England (FIGURE 9.35a), and Berlin, Germany (FIGURE 9.36a), characterize the European Cfb climate.

Increasing continentality can be seen in the Berlin climograph, as compared with that of Manchester, as the two cities are at nearly the same latitude. Berlin falls just inside the transition zone between the “C” and “D” climatic boundaries. Manchester is especially influenced by the effects of the ocean both in the annual cycle and in the daily cycle, as the temperature range remains small.

The Cfc climate is distinguished from Cfb by its cooler summer, with only 1 to 3 months having average temperatures above 10°C (50°F). This climatic type is rare on land surfaces, because locations with so few warm months are likely to have at least 1 month with a temperature below freezing and, therefore, fall into the “D” climate regime. Southern Iceland is the largest continuous land mass containing Marine West Coast Cool Summer climates on Earth, and Reykjavik’s climograph is representative of the climatic type (FIGURE 9.37a). However, Cfc climates are much more prevalent over the ocean surfaces, as the moderating marine influence of the sea makes higher latitude oceanic areas cool enough in summer but yet not so cold in winter to be classified in this climate type.

Moisture Characteristics. As is shown in Figures 9.34a through 9.37a, precipitation is evenly distributed through all months of the year in Cfb and Cfc climates. Midlatitude wave cyclones embedded within the polar front jet stream traverse the region nearly year-round and produce precipitation at least every few days. Annual precipitation typically ranges between 75 and 125 cm (30 and 50 in) for most locations, but much higher totals may be common in highland areas.

Many assume that these climates receive higher precipitation totals, but the typically light intensity of precipitation maintains surprisingly low annual totals. Vertical motions are usually forced by a frontal boundary and/or orographic effect without being accompanied by strong convective instability. Furthermore, the contrast between air masses is generally too weak to support vigorous uplift and intense precipitation. The result is abundant, horizontally oriented *stratiform clouds* and relatively few vertically oriented *cumuliform clouds*, and relatively little severe weather. Marine West Coast climates have a high percentage of days with precipitation. Maritime polar air masses originating over the North Pacific and North Atlantic Oceans are generally cool and wet, and they are associated with frontal cyclones that undergo **west-coast occlusion** over western North America and Europe. **Occlusions** represent the decaying phase of a midlatitude wave cyclone’s life cycle. A west-coast occlusion occurs with general warm front characteristics (gentle

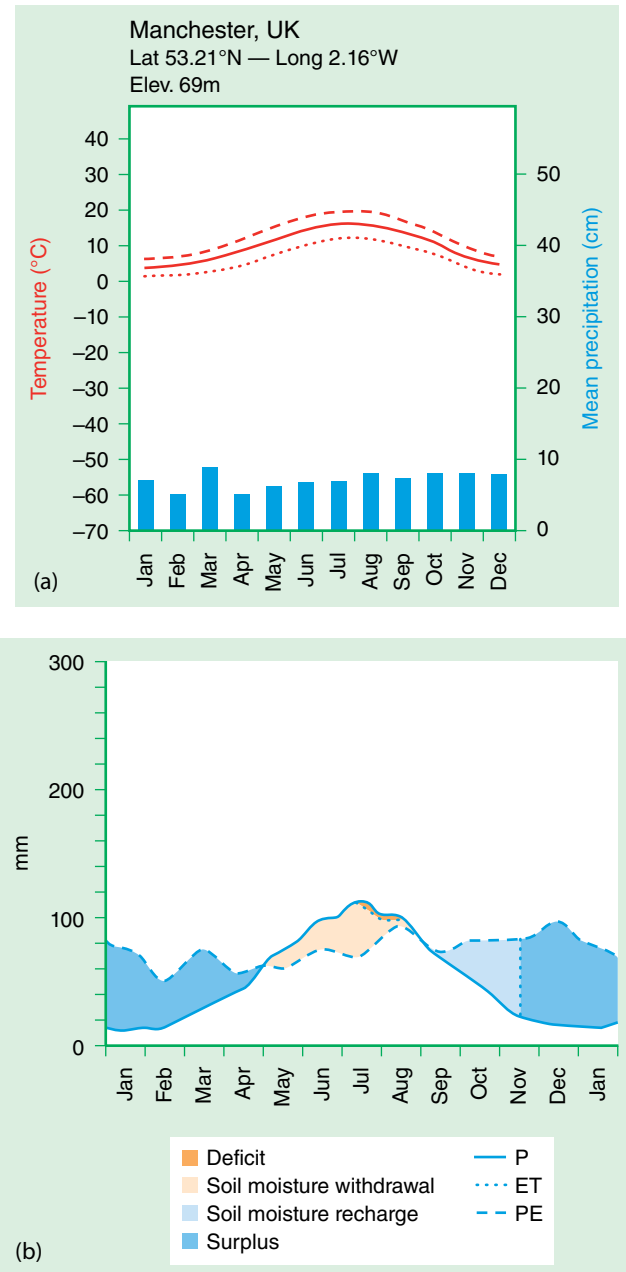


FIGURE 9.35 (a) Climograph for Manchester, United Kingdom (Cfb climate). Average annual temperature is 9.5°C (49.1°F) and average annual precipitation is 89.9 cm (35.4 in). (b) Water balance diagram for Manchester, United Kingdom.

(a) Data from National Centers for Environmental Information. (b) Modified with permission using Web/WIMP version 1.01 implemented by K. Matsuura, C. Willmott, and D. Legates at the University of Delaware, 2003.



Berlin, Germany
Lat 52.28°N — Long 13.18°E
Elev. 58m

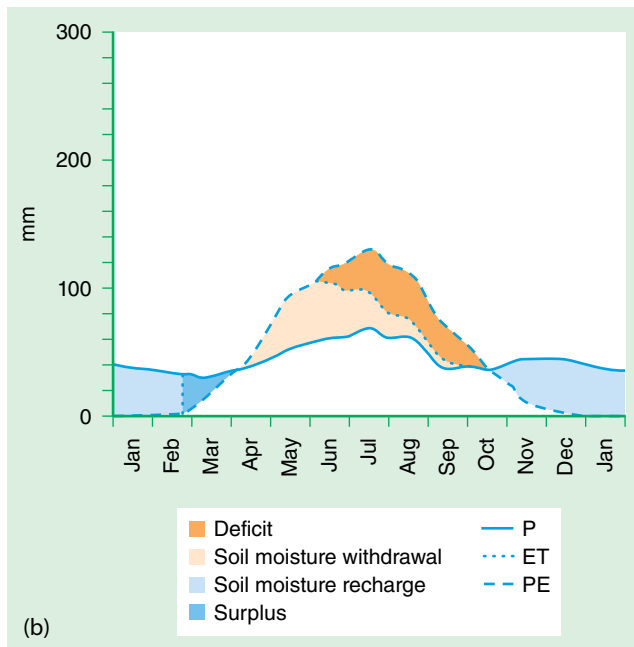
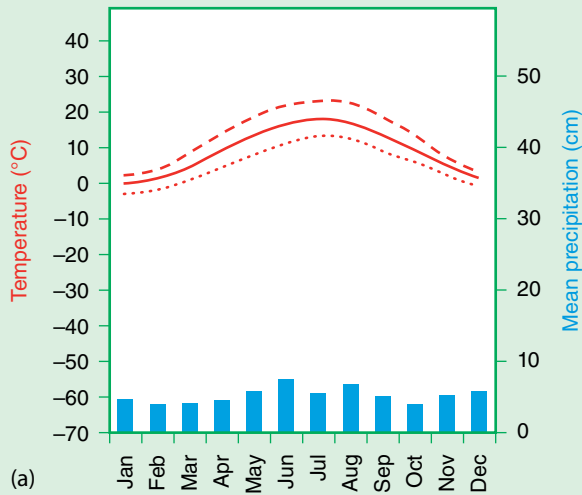


FIGURE 9.36 (a) Climograph for Berlin, Germany (Cfb climate). Average annual temperature is 8.8°C (47.9°F) and average annual precipitation is 58.4 cm (23.0 in). (b) Water balance diagram for Berlin, Germany.

(a) Data from National Centers for Environmental Information. (b) Modified with permission using Web/WIMP version 1.01 implemented by K. Matsuura, C. Willmott, and D. Legates at the University of Delaware, 2003.



Reykjavik, Iceland
Lat 64.08°N — Long 21.54°W
Elev. 61m

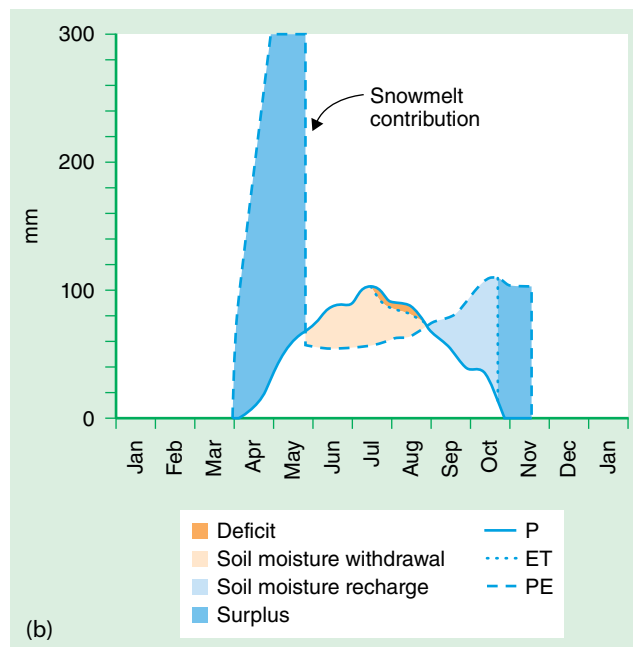
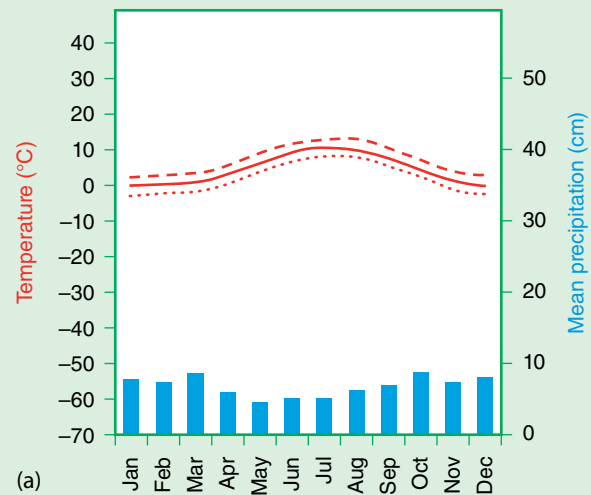


FIGURE 9.37 (a) Climograph for Reykjavik, Iceland (Cfc climate). Average annual temperature is 4.4°C (39.8°F) and average annual precipitation is 82.0 cm (32.3 in). (b) Water balance diagram for Reykjavik, Iceland.

(a) Data from National Centers for Environmental Information. (b) Modified with permission using Web/WIMP version 1.01 implemented by K. Matsuura, C. Willmott, and D. Legates at the University of Delaware, 2003.

uplift of moist cool air, stratiform clouds, and drizzle) induced by the movement of maritime air intruding upon continental air as the system moves inland. This type of occlusion is different from an **east-coast occlusion**, which occurs on the eastern sides of continents. East-coast occlusions are characterized by cold, dry air masses invading warmer, wetter maritime air. In east-coast occlusions, stronger vertical lift occurs, which can induce cumulonimbus cloud development and heavier precipitation, similar to the passage of a cold front.

Snow is uncommon in many Cfb and Cfc locations but common in interior areas or locations with considerable topographical relief. Farther inland, in higher elevations, more impressive annual precipitation totals may occur with local orographic enrichment, with some locations exceeding 250 cm (100 in), similar to tropical rain forest totals. These precipitation totals support the coniferous forests of the Pacific Northwest region. In North America a slight autumn maximum occurs with seasonal shift of the mean jet stream, while a minimum occurs during the summer months. In general, though, there is a relatively even distribution of monthly precipitation. The associated water balance diagrams for the Cfb and Cfc sites also reflect the effects of abundant precipitation and low input energy amounts, because only a minimal summer water balance deficit, if any, occurs (**FIGURES 9.34b through 9.37b**).

D—Microthermal Midlatitude Climates

Dfa, Dfb, Dwa, Dwb—Humid Continental

The **Humid Continental (Dfa, Dfb) climates** extend through the central to east-central portion of the North American continent between the Great Plains and the Atlantic Ocean south of Lake Superior (see world map of Köppen-Geiger climate types). They occur north of the Cfa climatic type and east of the BSk region. In Europe the Dfa region is small, but the Dfb region is vast, extending in a wide swath from Scandinavia and eastern Europe (Baltic nations, Belarus, and Ukraine) to south-central Asia (central Russia and northern Kazakhstan). Small areas of Dfa and Dfb occur in northern Japan and adjacent waters. The climatic regime is similar to the Humid Subtropical climate except that temperatures and precipitation totals are generally lower. Northeastern China, adjacent Russia, and much of the Korean Peninsula experience the **Humid Continental Winter Dry (Dwa, Dwb)** forms of these climates.

Thermal Characteristics. Summer temperatures are considered “hot” (Dfa, Dwa) in the southern parts of the Humid Continental climates, particularly in

the continental interior, and “warm” (Dfb, Dwb) on the northern sides. The 22°C (72°F) isotherm for the warmest month separates the Dfa/Dwa from the Dfb/Dwb. Continentality causes extreme seasonal fluctuations because much of the region is far removed from the moderating effects of large water bodies. Even coastal areas such as New England and eastern China have few moderating effects from the ocean because the midlatitude westerlies carry prevailing winds, influenced by continentality, from west to east. The Great Lakes do provide a bit of moderating influence and a delayed onset of the seasons over the adjacent leeward lands.

In summer when high solar angles prevail, the land heats quickly as sensible heating increases at the expense of latent heating. Low solar angles and the reduction in daylight hours in winter cause little surface heating. The distance from large water bodies upwind augments warming and/or chilling of the land masses and the overlying air, depending on the season. Many locations in this climatic zone have summertime maximum temperatures of 27–29°C (81–84°F), while monthly winter averages dip below –10 to –1°C (14 to 30°F).

Because the Dfa climatic type is so widespread in eastern North America, several examples are shown via climographs to depict within-group variability. Des Moines, Iowa (**FIGURE 9.38a**), Columbus, Ohio (**FIGURE 9.39a**), and Erie, Pennsylvania (**FIGURE 9.40a**) all illustrate features of the Dfa climate. The Dfb type is represented by Duluth, Minnesota (**FIGURE 9.41a**), Caribou, Maine (**FIGURE 9.42a**), and Ottawa, Ontario (**FIGURE 9.43a**).

A special case of Dfb also occurs in the area surrounding Elkins, West Virginia (**FIGURE 9.44a**), because the high elevation causes winter temperatures to fall below the freezing level and prevents summer temperatures from reaching an average of 22°C (72°F), despite its relatively low latitude and despite the fact that the map of world climates cannot show enough detail at this scale to reveal the Dfb climate at Elkins. Notice that Elkins is unique among the Dfb climates shown here because its insolation is even slightly higher than that for the Dfa climates described earlier.

The Eurasian Humid Continental climate is represented by a Dfb climate at Minsk, Belarus (**FIGURE 9.45a**), and Moscow, Russia (**FIGURE 9.46a**). Winter dry versions are represented by Beijing, China’s Dwa climate (**FIGURE 9.47a**), and by a Dwb type at Vladivostok, Russia (**FIGURE 9.48a**).

Moisture Characteristics. Precipitation in all Dfa and Dfb climates is well distributed throughout the year, but a slight maximum generally occurs during the summer

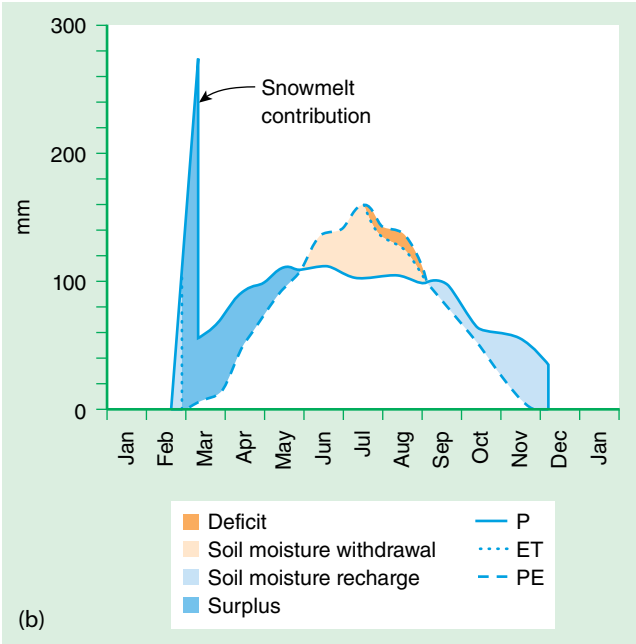
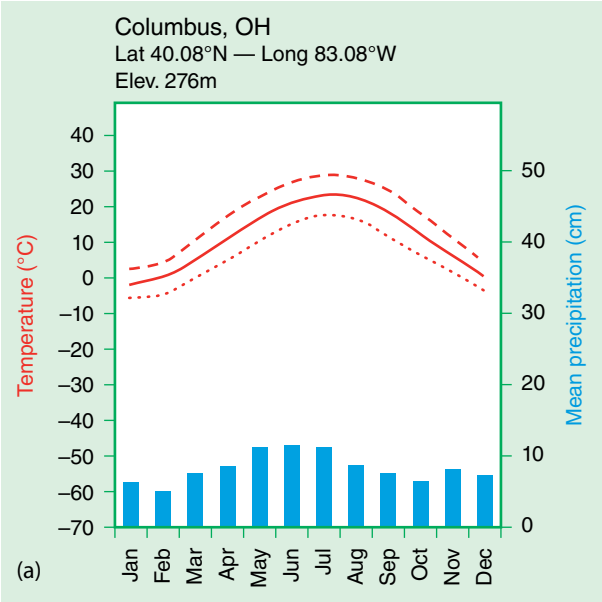
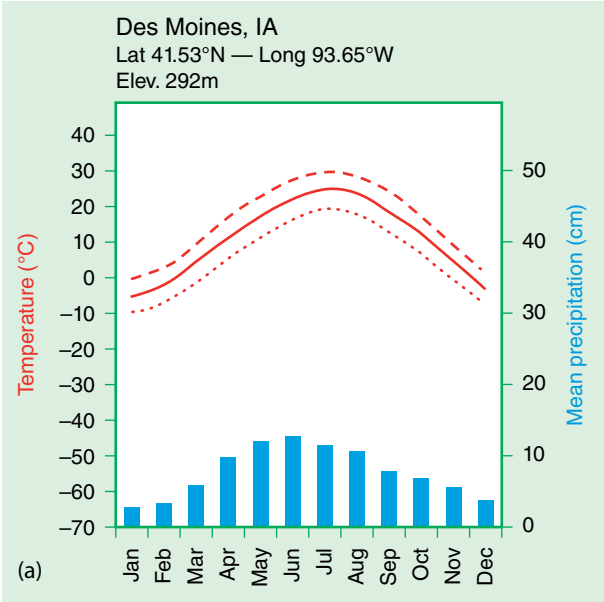


FIGURE 9.38 (a) Climograph for Des Moines, Iowa (Dfa climate). Average annual temperature is 10.0°C (50.0°F) and average annual precipitation is 88.2 cm (34.7 in). (b) Water balance diagram for Des Moines, Iowa.

(a) Data from National Centers for Environmental Information. (b) Modified with permission using Web/WIMP version 1.01 implemented by K. Matsuura, C. Willmott, and D. Legates at the University of Delaware, 2003.

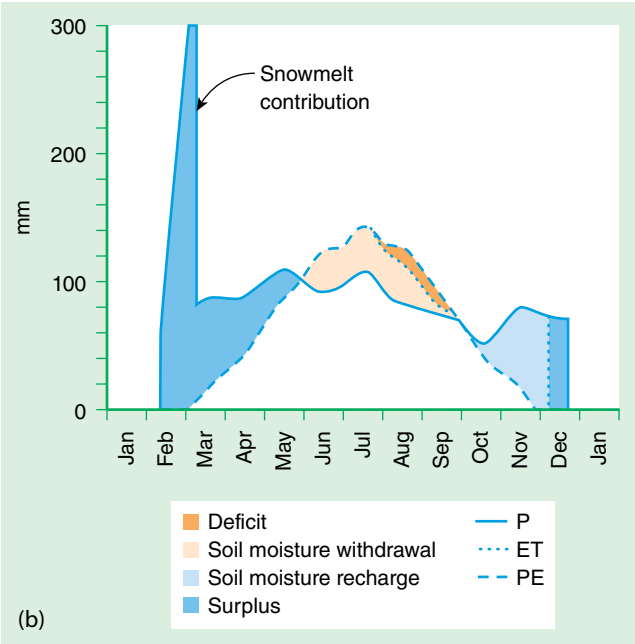


FIGURE 9.39 (a) Climograph for Columbus, Ohio (Dfa climate). Average annual temperature is 11.6°C (52.9°F) and average annual precipitation is 97.8 cm (38.5 in). (b) Water balance diagram for Columbus, Ohio.

(a) Data from National Centers for Environmental Information. (b) Modified with permission using Web/WIMP version 1.01 implemented by K. Matsuura, C. Willmott, and D. Legates at the University of Delaware, 2003.

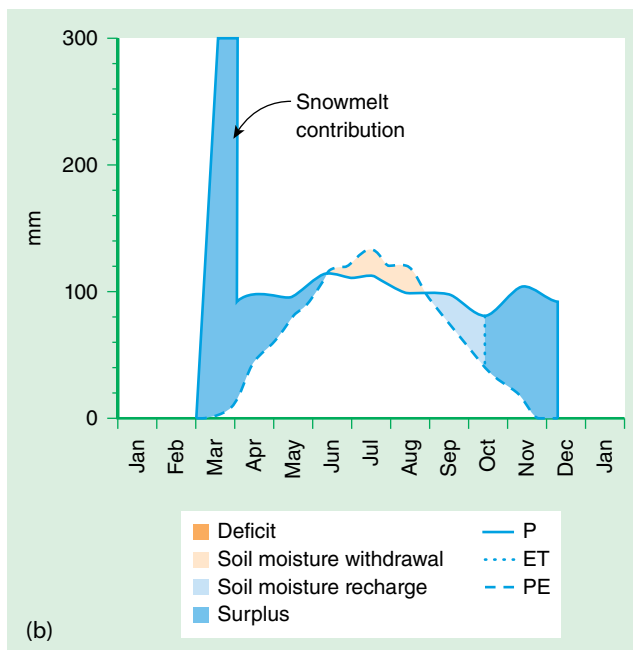
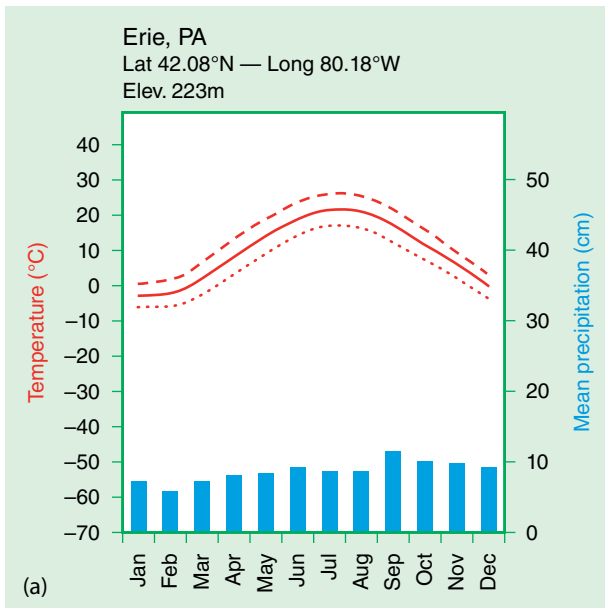


FIGURE 9.40 (a) Climograph for Erie, Pennsylvania (Dfa climate). Average annual temperature is 10.0°C (50.0°F) and average annual precipitation is 108.6 cm (42.8 in). (b) Water balance diagram for Erie, Pennsylvania.

(a) Data from National Centers for Environmental Information. (b) Modified with permission using Web/WIMP version 1.01 implemented by K. Matsuura, C. Willmott, and D. Legates at the University of Delaware, 2003.

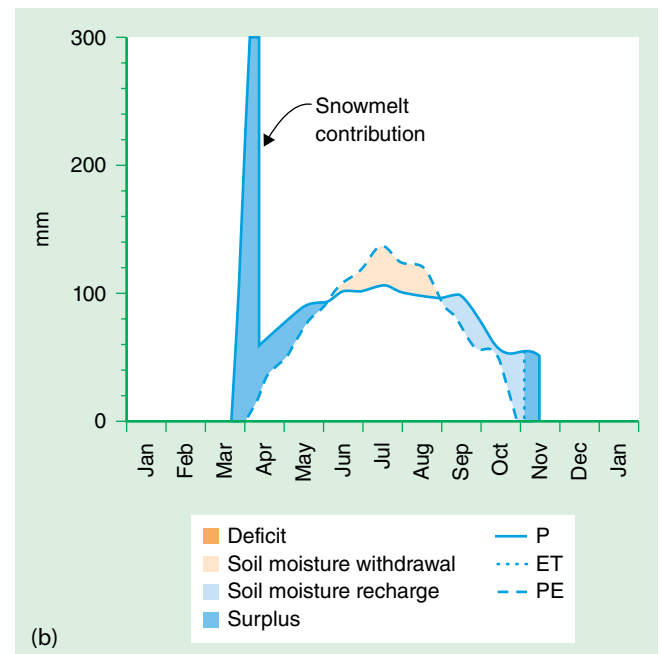
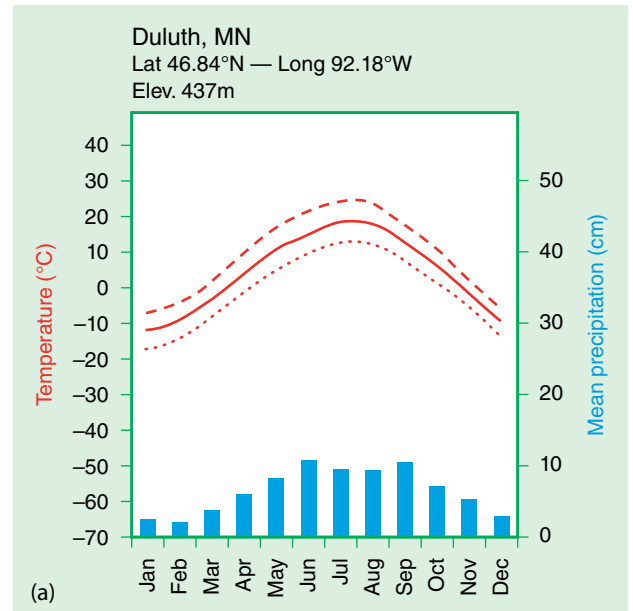


FIGURE 9.41 (a) Climograph for Duluth, Minnesota (Dfb climate). Average annual temperature is 3.9°C (39.1°F) and average annual precipitation is 78.7 cm (31.0 in). (b) Water balance diagram for Duluth, Minnesota.

(a) Data from National Centers for Environmental Information. (b) Modified with permission using Web/WIMP version 1.01 implemented by K. Matsuura, C. Willmott, and D. Legates at the University of Delaware, 2003.

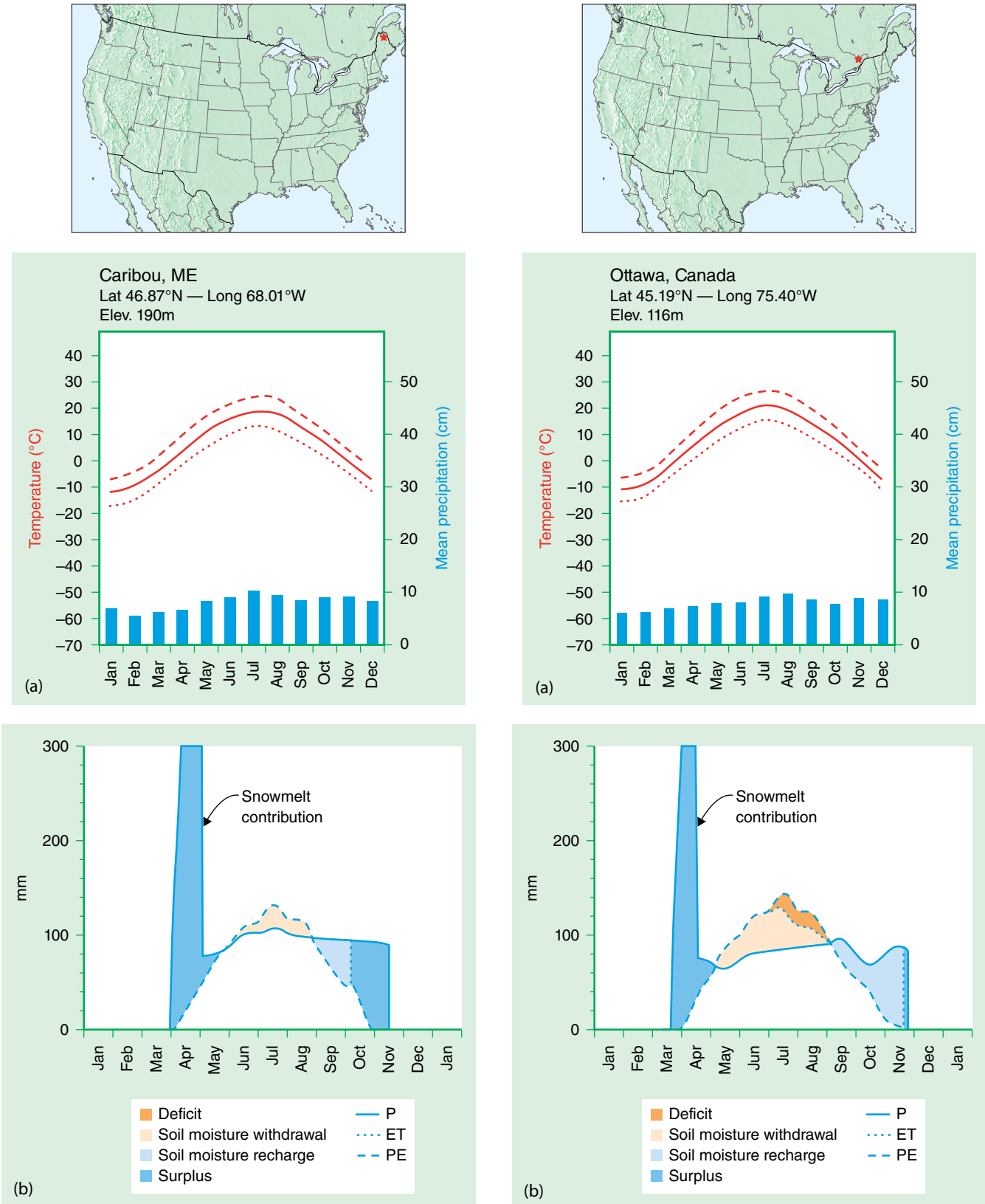


FIGURE 9.42 (a) Climograph for Caribou, Maine (Dfb climate). Average annual temperature is 4.0°C (39.2°F) and average annual precipitation is 95.1 cm (37.4 in). (b) Water balance diagram for Caribou, Maine.

(a) Data from National Centers for Environmental Information. (b) Modified with permission using Web/WIMP version 1.01 implemented by K. Matsuura, C. Willmott, and D. Legates at the University of Delaware, 2003.

FIGURE 9.43 (a) Climograph for Ottawa, Canada (Dfb climate). Average annual temperature is 6.1°C (43.0°F) and average annual precipitation is 87.9 cm (34.6 in). (b) Water balance diagram for Ottawa, Canada.

(a) Data from National Centers for Environmental Information. (b) Modified with permission using Web/WIMP version 1.01 implemented by K. Matsuura, C. Willmott, and D. Legates at the University of Delaware, 2003.

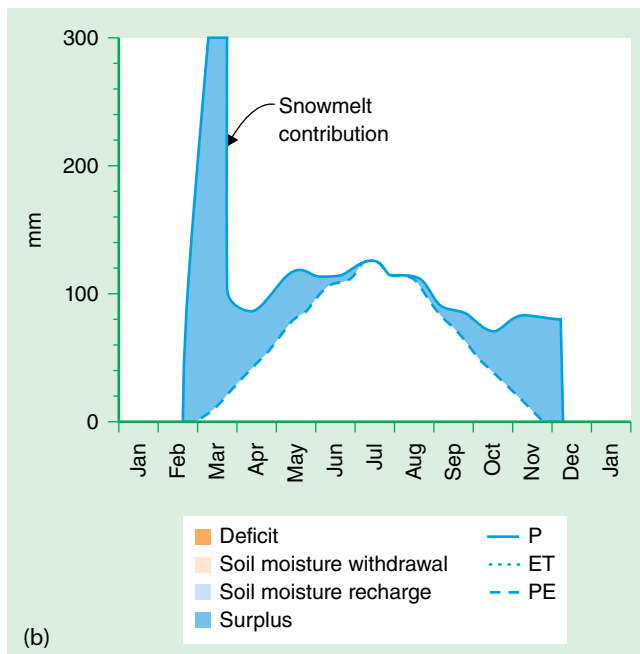
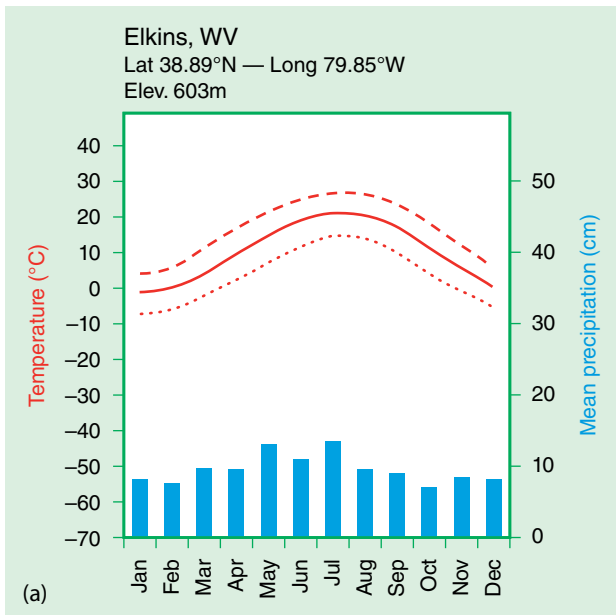


FIGURE 9.44 (a) Climograph for Elkins, West Virginia (Dfb climate). Average annual temperature is 9.9°C (49.8°F) and average annual precipitation is 117.1 cm (46.1 in). (b) Water balance diagram for Elkins, West Virginia.

(a) Data from National Centers for Environmental Information. (b) Modified with permission using Web/WIMP version 1.01 implemented by K. Matsuura, C. Willmott, and D. Legates at the University of Delaware, 2003.

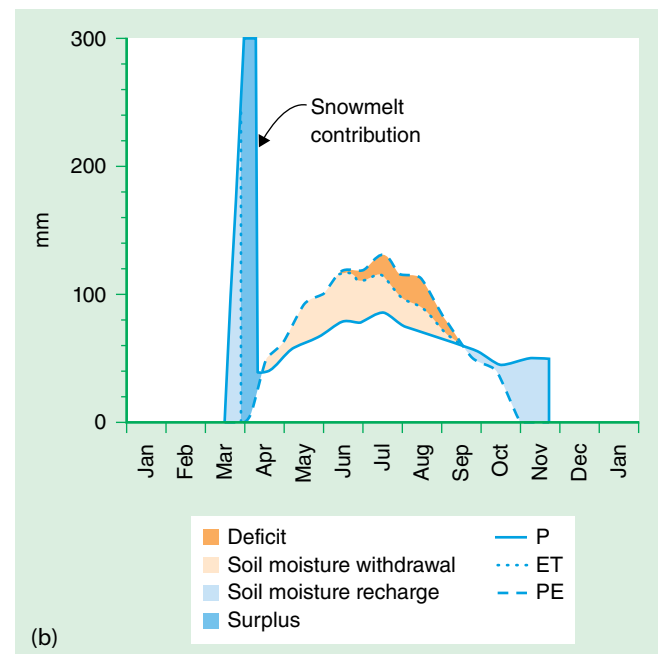
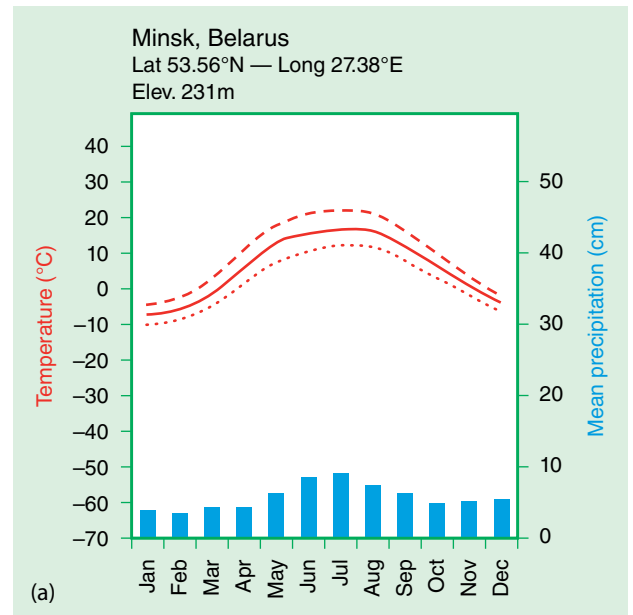


FIGURE 9.45 (a) Climograph for Minsk, Belarus (Dfb climate). Average annual temperature is 6.0°C (42.8°F) and average annual precipitation is 67.8 cm (26.7 in). (b) Water balance diagram for Minsk, Belarus.

(a) Data from National Centers for Environmental Information. (b) Modified with permission using Web/WIMP version 1.01 implemented by K. Matsuura, C. Willmott, and D. Legates at the University of Delaware, 2003.

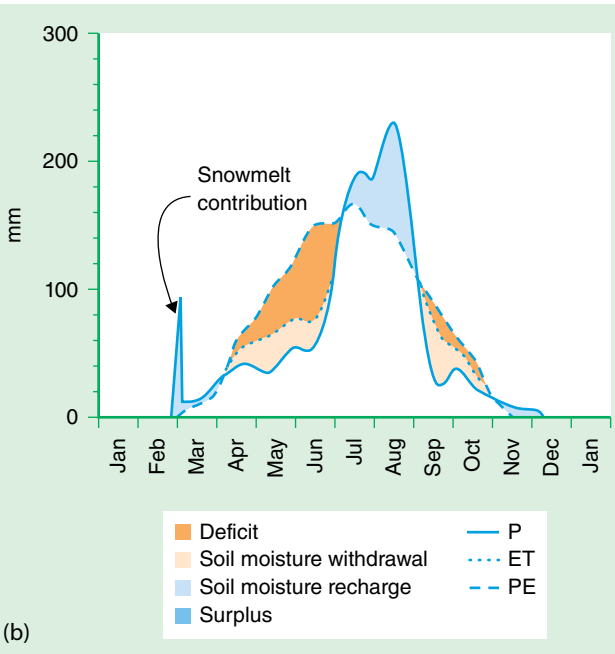
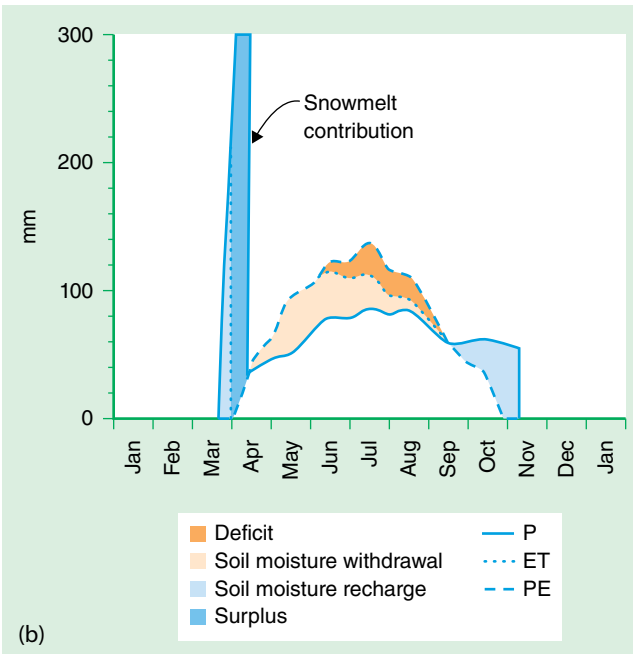
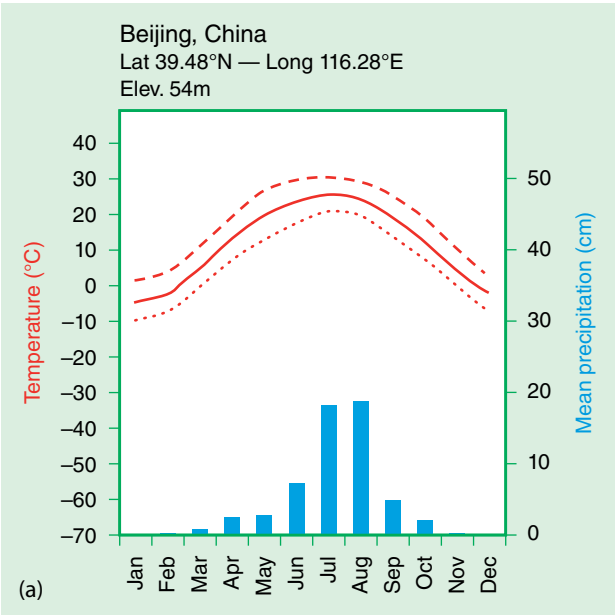
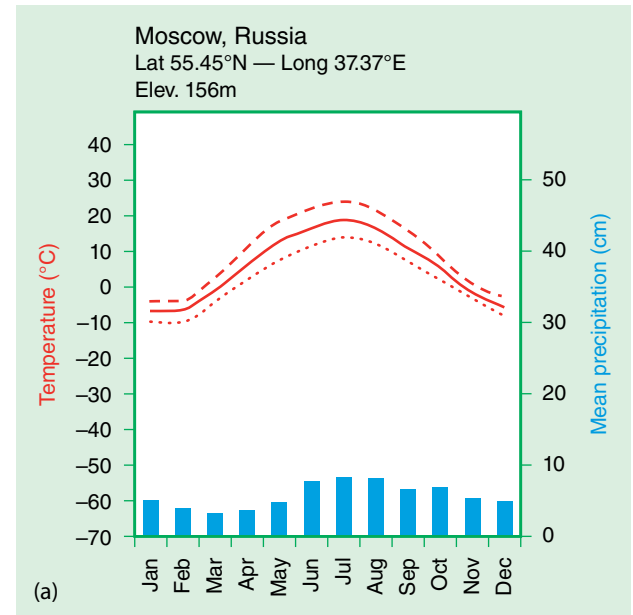


FIGURE 9.46 (a) Climograph for Moscow, Russia (Dfb climate). Average annual temperature is 4.3°C (39.8°F) and average annual precipitation is 59.9 cm (23.6 in). (b) Water balance diagram for Moscow, Russia.

(a) Data from National Centers for Environmental Information. (b) Modified with permission using Web/WIMP version 1.01 implemented by K. Matsuura, C. Willmott, and D. Legates at the University of Delaware, 2003.

FIGURE 9.47 (a) Climograph for Beijing, China (Dwa climate). Average annual temperature is 11.7°C (53.1°F) and average annual precipitation is 63.0 cm (24.8 in). (b) Water balance diagram for Beijing, China.

(a) Data from National Centers for Environmental Information. (b) Modified with permission using Web/WIMP version 1.01 implemented by K. Matsuura, C. Willmott, and D. Legates at the University of Delaware, 2003.

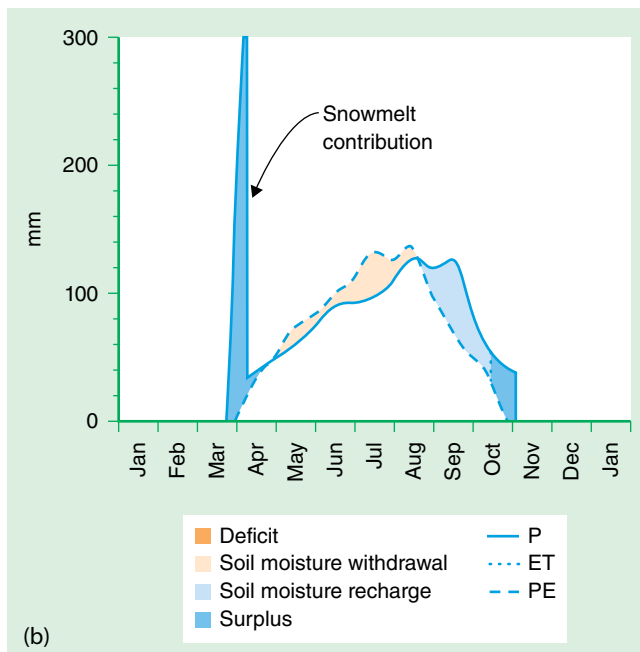
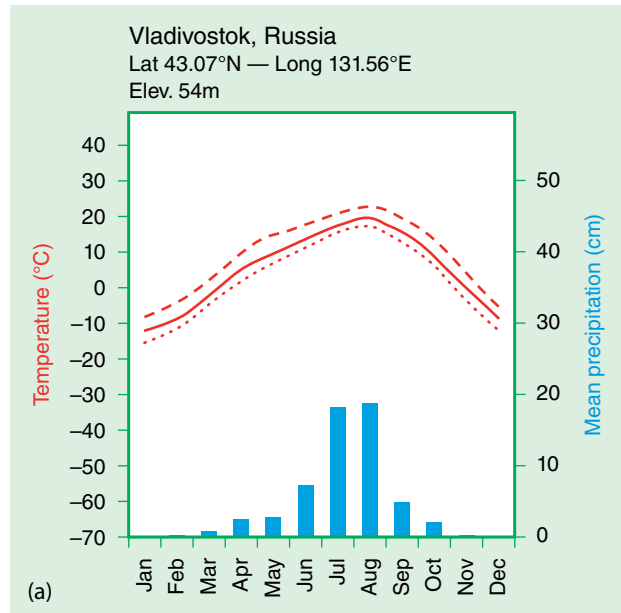


FIGURE 9.48 (a) Climograph for Vladivostok, Russia (Dwb climate). Average annual temperature is 4.4°C (39.9°F) and average annual precipitation is 74.4 cm (29.3 in). (b) Water balance diagram for Vladivostok, Russia.

(a) Data from National Centers for Environmental Information. (b) Modified with permission using Web/WIMP version 1.01 implemented by K. Matsuura, C. Willmott, and D. Legates at the University of Delaware, 2003.

months for locations that are inland or upwind from major water bodies. For example, a summer precipitation peak is obvious in the climograph for Des Moines, Iowa (Figure 9.38a). Adjacent to the Great Lakes the relative warmth of the lakes in winter destabilizes the atmosphere as cold cP and A air masses cross over them. As a result, winter precipitation is as abundant, or even more abundant, than summer precipitation in such locations. The climograph for Erie (Figure 9.40a) shows this lake effect moisture. Much of this winter precipitation occurs in the form of lake effect snow.

Precipitation in both North America and Eurasia is largely generated by migratory frontal cyclone passage during all seasons except summer, when convective thunderstorm activity becomes more important. Like Humid Subtropical areas, the summer convective storms are controlled by intense surface heating that initiates high *evapotranspiration* rates. Advection of moisture from the Gulf of Mexico, the North Atlantic, and the North Pacific Ocean, largely provided by strengthening of the Bermuda-Azores and Hawaiian high pressure systems, is of great importance to summer precipitation. Some summer precipitation is initiated by weak, quick-moving migratory frontal systems. Summer frontal cyclones often track north of the U.S.–Canadian border as the circumpolar vortex retreats poleward, but their trailing cold fronts provide precipitation and temporary relief from fairly high summer temperatures and high humidity values in southern Canada and the northern United States. Annual precipitation totals are usually between 51 and 102 cm (20 and 40 in), with wetter regions occurring nearer to the oceans and drier regions existing farther toward the continental interiors. In the Dwa and Dwb climates less than 30% of the precipitation occurs in winter. In Asia the dry monsoon season and associated Siberian high suppress precipitation.

Water balance diagrams for all the Humid Continental climates (**FIGURES 9.38b through 9.48b**), as well as all climatic types poleward of Dfa/Dwa, have missing data in winter, which results from the storage of water in the form of snow. As spring approaches, snowmelt produces abundant water at the surface, much of which fell as snow months before. This phenomenon is depicted by the prominent spike in surplus, with the spikes occurring later in the spring as temperature decreases. The surface water balances in general suggest that mean deficits are small or nonexistent in Humid Continental climates. The largest deficit occurs at Beijing (Figure 9.47b), at the end of the dry monsoon season and also after the wet monsoon season ends (but while the Sun is still high in the sky and days are still relatively long). Notably, at Elkins, West Virginia (Figure 9.44b), no soil moisture deficit is apparent in the mean monthly data.

Dfc—Subarctic

The **Subarctic (Dfc, Dwc, Dwd) climates** exist poleward of Humid Continental climatic regions (see world map of Köppen-Geiger climate types). All Subarctic areas in North America receive similar precipitation totals year-round and, therefore, no Dwc and Dwd types are found. There, the Dfc region covers more than half of Alaska and Canada and adjacent sections of the North Pacific Ocean and Hudson Bay. The vegetation in this North American region is typically referred to as the *boreal forest*—an area dominated by extensive, slow-growing coniferous forest. In Europe the Subarctic climate is found in the sparsely inhabited northern Scandinavia, while in Asia the four Subarctic types dominate the northern interior tier of the continent (see world map of Köppen-Geiger climate types). Vegetation in the Asian Subarctic climatic zone is termed the **taiga**, the equivalent Russian term for the North American boreal forest. The Dfc climatic type is the third-most extensive on the terrestrial Earth, falling behind only one of the tropical types to be discussed in Chapter 10 and the BWh climate.

Thermal Characteristics. Summer temperatures are lower than those of the Humid Continental climatic region. Winter temperatures are generally far below those of the adjacent climate, with subfreezing average monthly temperatures a common occurrence. Extreme seasonality of temperatures occurs with the annual temperature range may be as high as 60°C (108°F). The highest annual temperature range on Earth occurs at Oymyakon, Siberia, where the range is 64°C (115°F).

The lowest temperature ever recorded in the northern hemisphere occurred within this climatic zone at two Siberian locations: Verkhoyansk and Oimekon. On February 6, 1922, the mercury plummeted at these locations to -68°C (-90°F). In some Subarctic locations the average temperature may remain below freezing for up to 7 months. The mean temperature of the coldest month may approach -38°C (-36°F) for some locations. The transition seasons of autumn and spring are relatively short in comparison with the length of summer and winter, with winter being extremely long. Average summer temperatures show a dramatic reversal with monthly averages perhaps approaching 20°C (68°F).

Climographs representing Dfc climates are shown for the coastal locations of Cold Bay, Alaska (FIGURE 9.49a), Kotzebue, Alaska (FIGURE 9.50a), and Murmansk, Russia (FIGURE 9.51a). Inland Dfc sites shown include Fairbanks, Alaska (FIGURE 9.52a), Yellowknife, Northwest Territories (FIGURE 9.53a), and Moosonee, Ontario (FIGURE 9.54a). Dwc, the dry winter equivalent, is represented by Tura, Russia (FIGURE 9.55a).

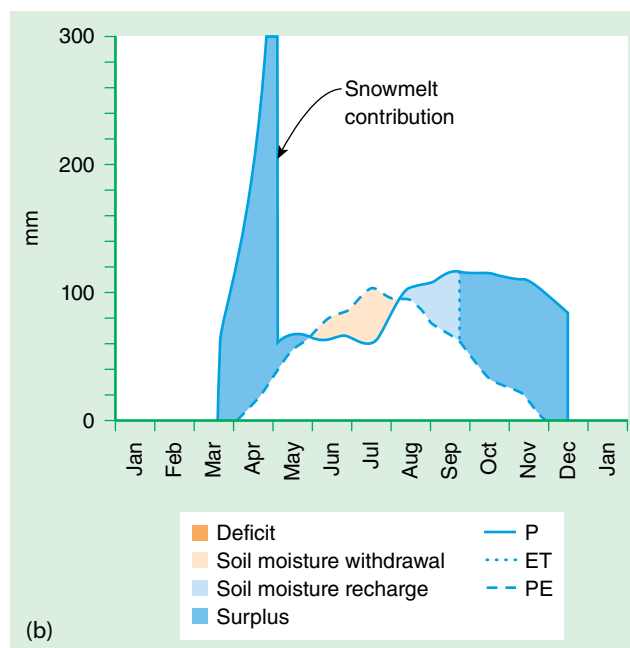
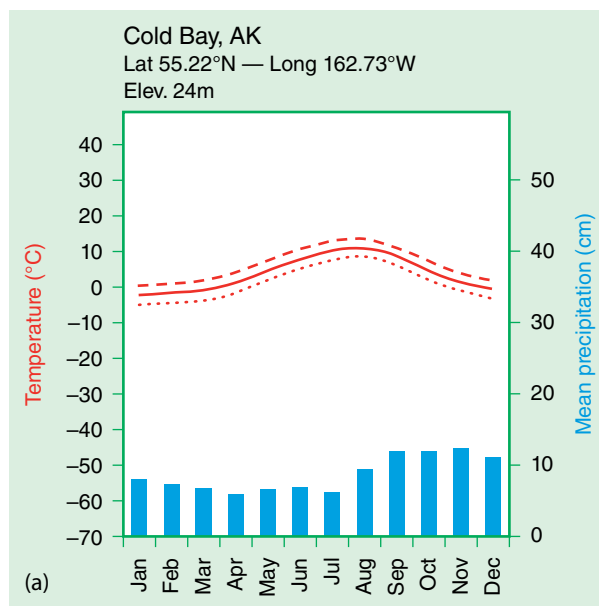


FIGURE 9.49 (a) Climograph for Cold Bay, Alaska (Dfc climate). Average annual temperature is 3.6°C (38.4°F) and average annual precipitation is 102.3 cm (40.3 in). (b) Water balance diagram for Cold Bay, Alaska.

(a) Data from National Centers for Environmental Information. (b) Modified with permission using Web/WIMP version 1.01 implemented by K. Matsuura, C. Willmott, and D. Legates at the University of Delaware, 2003.

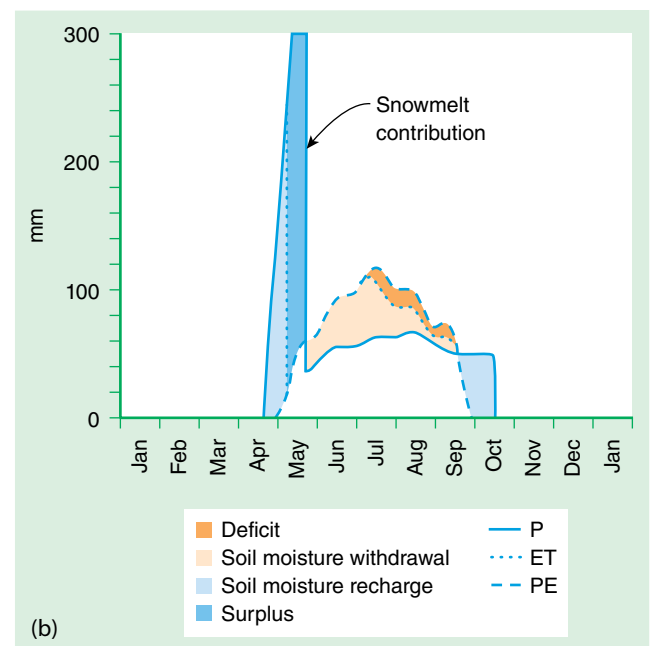
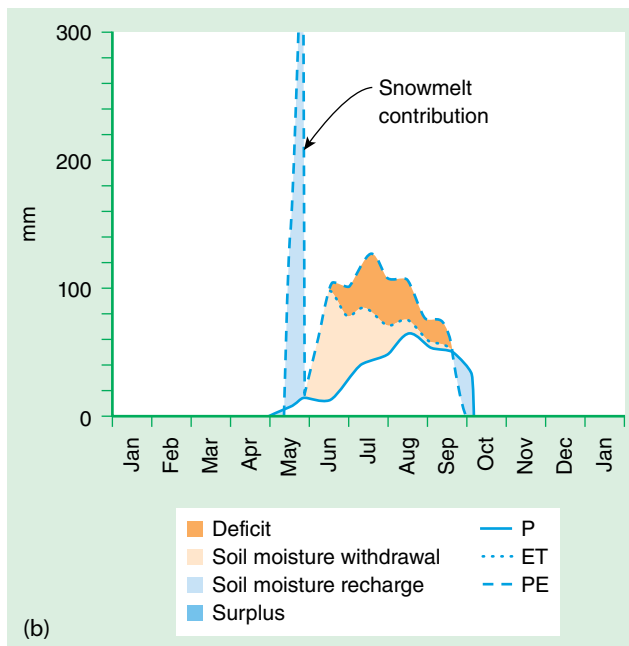
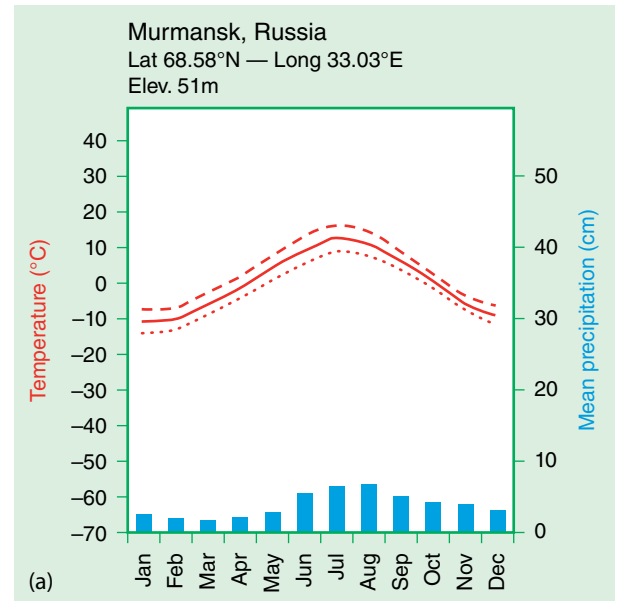
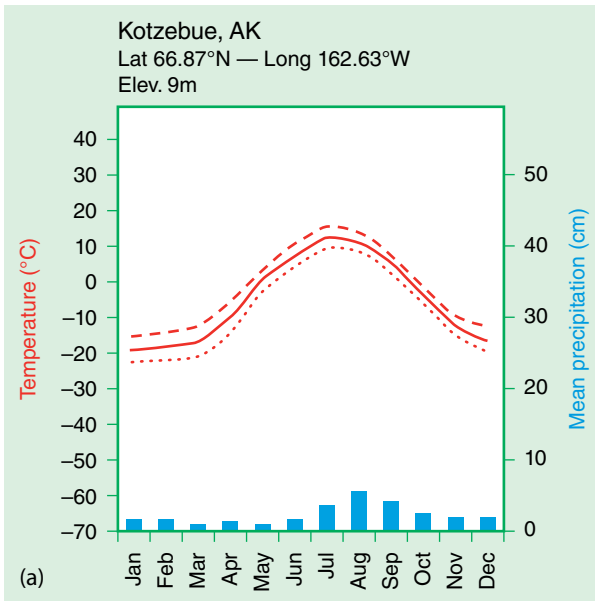


FIGURE 9.50 (a) Climograph for Kotzebue, Alaska (Dfc climate). Average annual temperature is -5.7°C (21.8°F) and average annual precipitation is 25.5 cm (10.1 in). (b) Water balance diagram for Kotzebue, Alaska.

(a) Data from National Centers for Environmental Information. (b) Modified with permission using Web/WIMP version 1.01 implemented by K. Matsuura, C. Willmott, and D. Legates at the University of Delaware, 2003.

FIGURE 9.51 (a) Climograph for Murmansk, Russia (Dfc climate). Average annual temperature is 0.3°C (32.5°F) and average annual precipitation is 41.4 cm (16.2 in). (b) Water balance diagram for Murmansk, Russia.

(a) Data from National Centers for Environmental Information. (b) Modified with permission using Web/WIMP version 1.01 implemented by K. Matsuura, C. Willmott, and D. Legates at the University of Delaware, 2003.

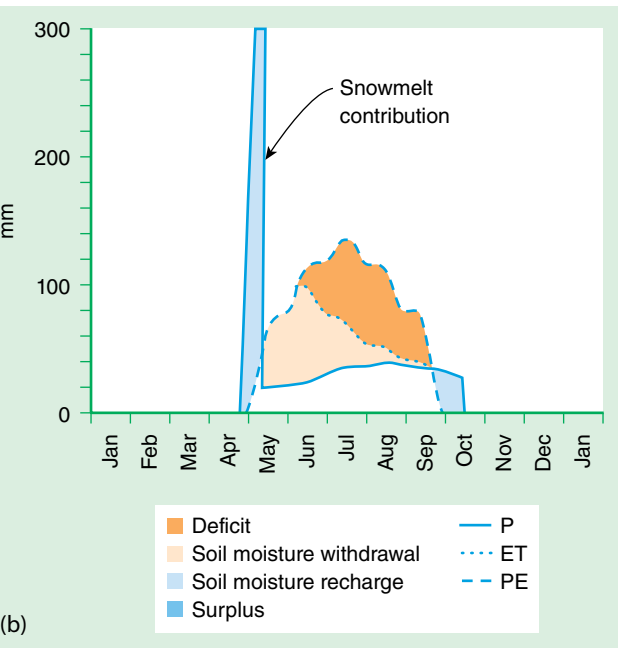
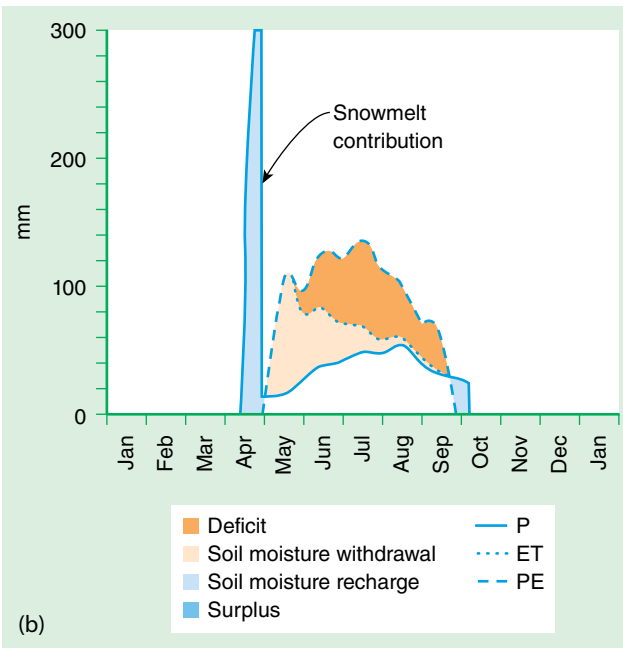
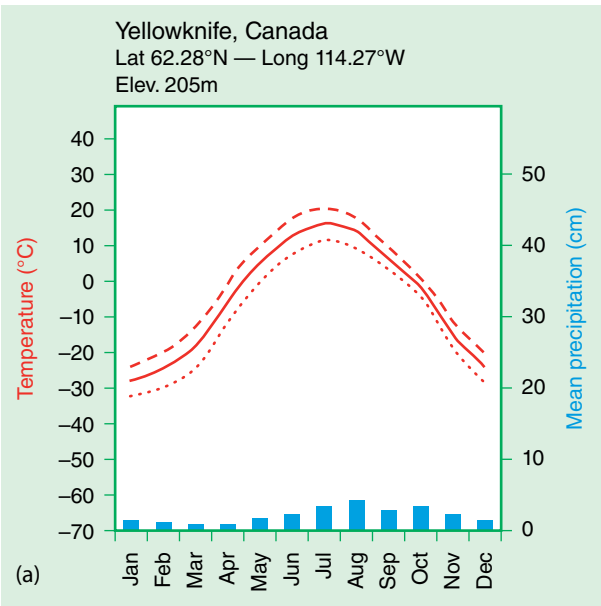
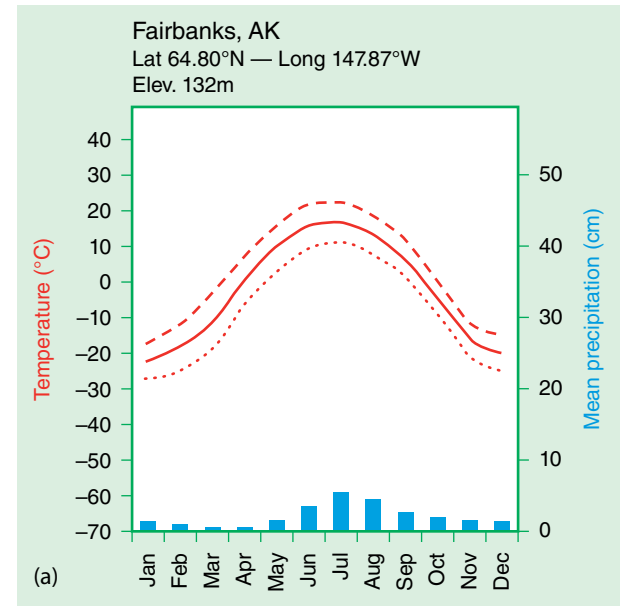


FIGURE 9.52 (a) Climograph for Fairbanks, Alaska (Dfc climate). Average annual temperature is -2.9°C (26.7°F) and average annual precipitation is 26.3 cm (10.3 in). (b) Water balance diagram for Fairbanks, Alaska.

(a) Data from National Centers for Environmental Information. (b) Modified with permission using Web/WIMP version 1.01 implemented by K. Matsuura, C. Willmott, and D. Legates at the University of Delaware, 2003.

FIGURE 9.53 (a) Climograph for Yellowknife, Northwest Territories, Canada (Dfc climate). Average annual temperature is -4.7°C (23.5°F) and average annual precipitation is 25.7 cm (10.1 in). (b) Water balance diagram for Yellowknife, Northwest Territories, Canada.

(a) Data from National Centers for Environmental Information. (b) Modified with permission using Web/WIMP version 1.01 implemented by K. Matsuura, C. Willmott, and D. Legates at the University of Delaware, 2003.

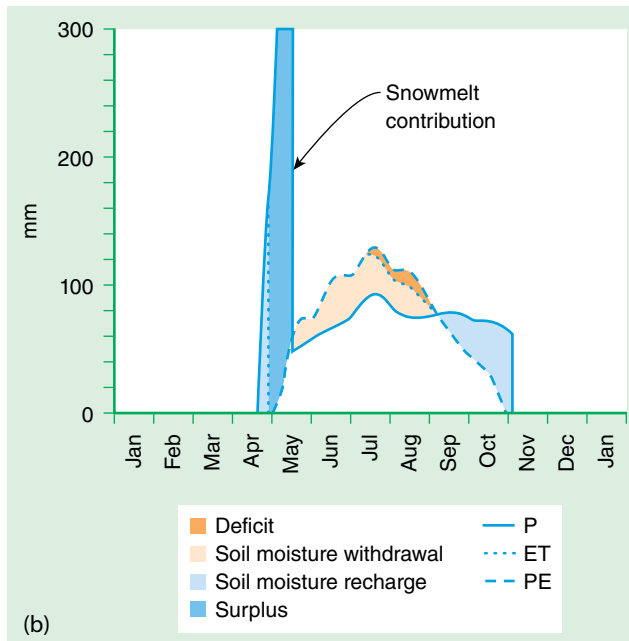
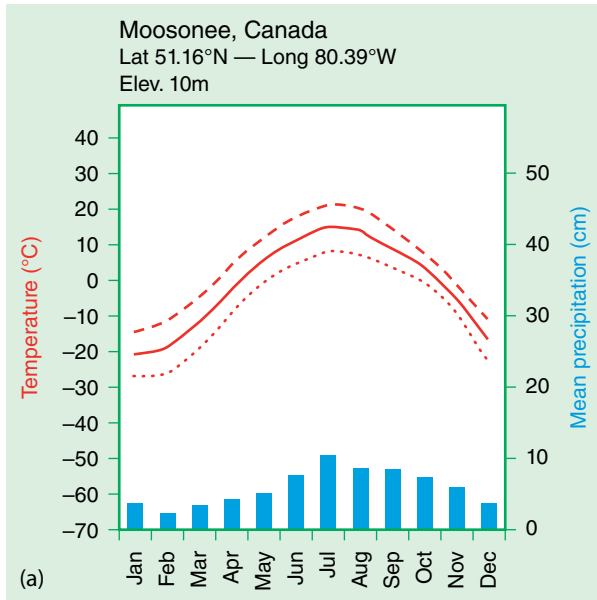


FIGURE 9.54 (a) Climograph for Moosonee, Canada (Dfc climate). Average annual temperature is -1.1°C (30.1°F) and average annual precipitation is 66.3 cm (26.1 in). (b) Water balance diagram for Moosonee, Ontario.

(a) Data from National Centers for Environmental Information. (b) Modified with permission using Web/WIMP version 1.01 implemented by K. Matsuura, C. Willmott, and D. Legates at the University of Delaware, 2003.

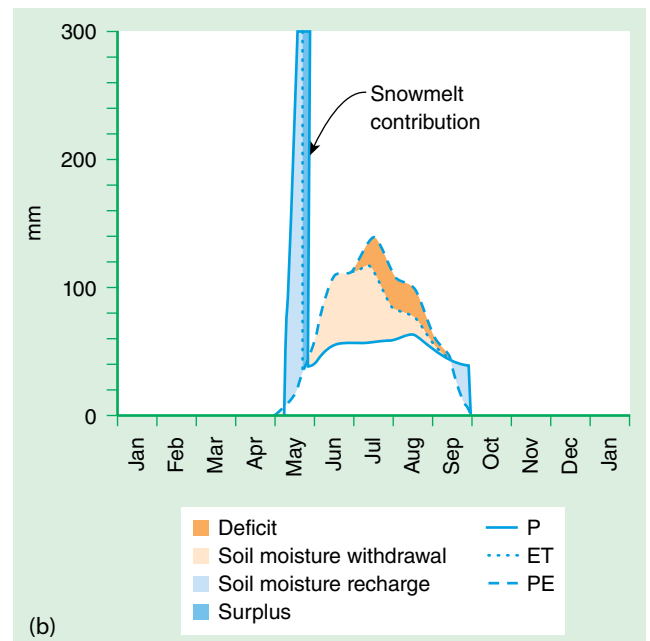
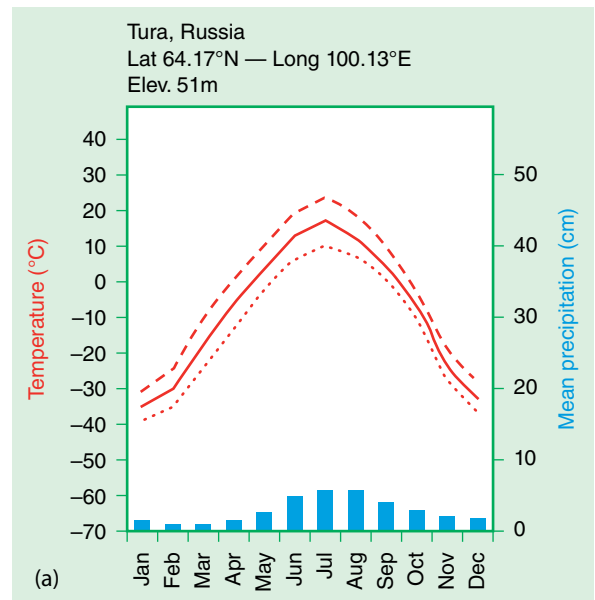


FIGURE 9.55 (a) Climograph for Tura, Russia (Dwc). Average annual temperature is -9.2°C (15.4°F) and average annual precipitation is 33.3 cm (13.1 in). (b) Water balance diagram for Tura, Russia.

(a) Data from National Centers for Environmental Information. (b) Modified with permission using Web/WIMP version 1.01 implemented by K. Matsuura, C. Willmott, and D. Legates at the University of Delaware, 2003.

Moisture Characteristics. Annual precipitation amounts are typically 12 to 50 cm (5 to 20 in) per year. These sparse totals are not surprising, because little moisture is present in such cold air, even at saturation. Summer precipitation maxima are pronounced in most locations, while winter remains dry and cold. Warm-season precipitation is primarily frontally induced, because convection is not strong enough to produce much precipitation, even in summer, and summer is the only time when reasonable air mass contrast is present.

Despite the low precipitation totals, the low amounts of available energy for evapotranspiration generally allow for sufficient soil moisture to support the boreal forests. Moisture also remains frozen in the ground as *permafrost* for extensive periods. Fairly impressive snow depths are common in some areas because an interannual accumulation may result from incomplete melting during the short summers. When temperatures rise suitably for evaporation to occur, the lost moisture is partially replaced through precipitation, but typically this water input is insufficient to offset soil moisture deficits (FIGURES 9.49b through 9.55b).

E—Polar Climates

ET—Tundra

The first of the **Polar climates** is the **Tundra (ET) climate**, which exists poleward of the Subarctic climate. The boreal and taiga forests of North America, Europe, and Asia terminate at the 10°C isotherm for the warmest summer month. This isotherm represents the *treeline*—the border between the Subarctic and Tundra (ET) climates. The ET climate in North America is found in the highest latitudinal locations of Alaska and the Canadian territories. European Tundra is limited to the extreme northern strip of the continent—namely, northern Iceland, Scandinavia, and Russia. The Asian Tundra climate extends through northern Russia to the Kamchatka Peninsula of eastern Russia (see world map of Köppen-Geiger climate types, Figure 8.1).

The Tundra climatic type is named for tundra vegetation, which consists of stunted low-growing flowering plants, bushes, shrubs, lichens, and mosses. Low temperatures combine with low Sun angles and a short period of extensive day lengths to produce specially adapted vegetation types. The low-growing lichens, mosses, and shrubs undergo rapid growth cycles once temperatures climb above freezing. The plants flower almost immediately in the presence of above freezing temperatures, ensuring the propagation of the species.

Thermal Characteristics. Because of the high latitude, winter temperatures are extremely low. The Sun

shines for only a few hours each day, if at all. Even in summer significant beam depletion, low solar angles, and high *albedo* combine to keep temperatures relatively low even in the presence of a nearly constant influx of solar radiation. Resulting summer temperatures remain only slightly above freezing on average. Because freezes may occur in any month of the year, the growing season is effectively nonexistent, but in some locations summer temperatures may become relatively warm over short periods.

During winter all soil is frozen, but in summer the layers above the permafrost thaw. This may create a saturated environment, as liquid water is prohibited from penetrating into the frozen subsurface. Floods can occur because of this and/or the combination of ice dams blocking stream paths into the Arctic Ocean. The latter occurs during spring thaw, with most rivers draining northward toward the Arctic Ocean where the river mouths remain frozen long after the main river body (which lies southward) thaws. The surrounding region thaws as well, leading to a high volume of water moving northward toward an ice-blocked river. Permafrost also leads to complications in construction. Local heating of concrete, for example, may melt permafrost below it, leading to foundation failure of buildings and roads.

Moisture Characteristics. Because of the extreme cold, precipitation is sparse, with annual totals below 25 cm (10 in) and most locations receiving less than 13 cm (5 in). Although some precipitation typically falls in every month, a distinct warm-season maximum is discernible. FIGURE 9.56a shows this feature in the climograph for Thule Air Force Base, Greenland. Snow remains at the surface for long periods, with some areas receiving little melting from year to year. Most locations usually see spring water surpluses in conjunction with low evapotranspiration rates, increasing precipitation, and melting snow (FIGURE 9.56b).

EF—Ice Cap

The final Köppen-Geiger category is the **Ice Cap (EF) climate**. This climate is found in the northern hemisphere extratropics only in interior Greenland. The moderating presence of the Arctic Ocean prevents these climates from existing in Eurasia. Significant sea ice does accumulate throughout the Arctic Ocean region, except along the Scandinavian coast, which is warmed by the North Atlantic Drift.

In the EF climate, ice covers the ground throughout the year as mean monthly temperatures remain below freezing in every month. Cold, dense air forms above the Greenland ice cap and spills toward lower coastal elevations, ensuring frigid temperatures even near the

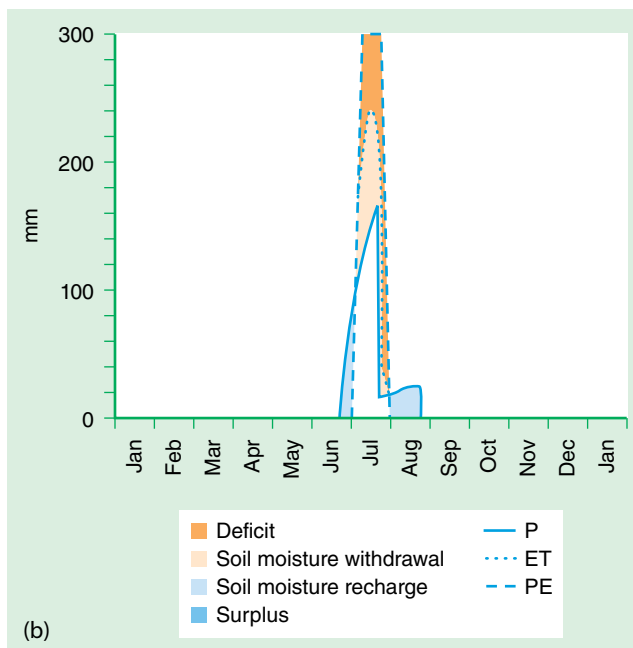
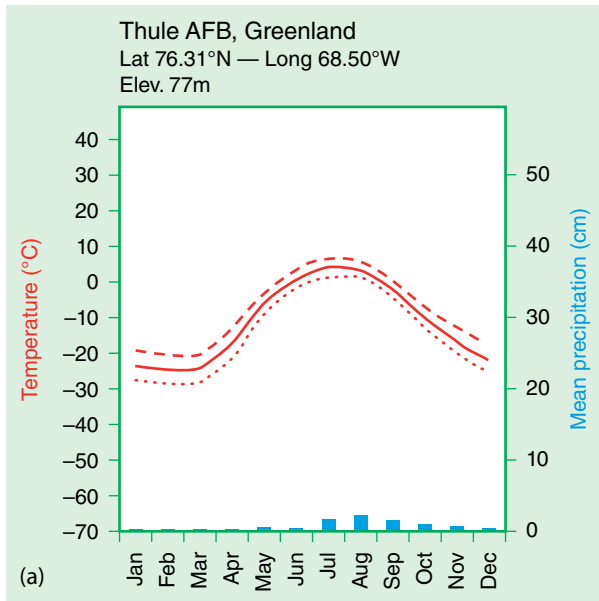


FIGURE 9.56 (a) Climograph for Thule AFB, Greenland (ET climate). Average annual temperature is -11.6°C (11.1°F) and average annual precipitation is 10.2 cm (4.0 in). (b) Water balance diagram for Thule AFB, Greenland.

(a) Data from National Centers for Environmental Information. (b) Modified with permission using Web/WIMP version 1.01 implemented by K. Matsuura, C. Willmott, and D. Legates at the University of Delaware, 2003.

ocean. These **katabatic winds** are especially prominent at night when the air adjacent to the surface increases in density as it undergoes radiative cooling. The region receives very little precipitation, because the extreme cold induces sinking motions in the atmosphere and the saturation vapor pressure is so low in such cold conditions. The little precipitation that does occur is mainly limited to late summer and autumn during the times of highest temperatures. Annual average precipitation is typically less than 12 cm (5 in). The notion of this region being one of raging blizzards is extremely exaggerated. Instead, ice cap growth largely occurs through the *deposition* of atmospheric water vapor directly onto the surface (termed **riming**) in the presence of very low temperatures. This growth is approximately balanced by the slow downslope motion of the ice and its subsequent calving off into the ocean. This climatic type is treated more extensively elsewhere in the text.

H—Highland Climates

Mountainous areas have local climatic characteristics that do not allow them to be classified neatly into one of the climatic types discussed previously. Local-scale elevation changes—**vertical zonation**—create such vast differences in climates that it is impossible to categorize them on a planetary scale of analysis or to depict them on the global map of climate types in Figure 8.1. Such zones can be classified as **Highland (H) climates**, a catch-all category. The progression of climatic zones with height largely mimics the progression of latitudinal climatic zones. For instance, a high mountain near the equator likely has a tropical climate regime and associated vegetation at the base, and then progresses through C, D, and finally E climatic zones and associated vegetation, ascending toward an ice-capped (EF) pinnacle.

In North America, Highland climates exist mainly along the spine of the Rocky Mountains from Alaska through Canada and into the western United States and Mexico (see world map of Köppen-Geiger climate types). Another area of Highland climates exists in the coastal mountains of Alaska and western Canada, extends through the Cascade Mountains of the Pacific Northwest, and finally terminates at the southern portion of the Sierra Nevada of California. In Europe, Highland climates prevail through the central Alps region, centered in Switzerland. The Scottish Highlands and dissected areas of Scandinavia have Highland climates as well. Asia contains the greatest expanse of Highland climates on Earth, centered on the massive Himalayan range and the adjacent Tibetan Plateau. Extending from this zone are the western mountain extensions of the Pamirs, the Hindu Kush, and the Tien Shan mountain ranges. Other significant mountain ranges such as the

Caucasus, the Zagros, and the highlands of Japan also have regions with radical climatic contrasts across small spatial zones.

Local differences in slope, orientation, and elevation make specific categorization of these regions problematic. Vegetation in extratropical H climates, particularly at higher elevations, often is largely limited to equator-facing slopes, because of the prevalence of afternoon sunlight in the southern sky (in the northern hemisphere). Low-latitude mountain regions experience different insolation characteristics than high-latitude mountain areas because the Sun shines on north-facing slopes at one time of year and south-facing slopes at the opposite time of year. However, both extratropical and tropical highland regions support complicated local climate features.

Of particular note in Highland climates is the development of **wind channeling**—the constriction of mountain-induced winds that triggers a velocity increase. In addition, high elevations combine with abundant radiational cooling to create cold, dense air masses over the mountains. The dense air is pulled to lower elevations by gravity through the process of **cold air drainage**. This triggers the development of a katabatic wind, or **mountain wind**, similar to the katabatic winds that form over the ice sheets in EF climates. During winter the downslope-moving katabatic winds are common, especially during the early morning when diurnal cooling is maximized. Mountains may channel these winds through narrow canyons. Katabatic winds are most prevalent under regional high pressure conditions that allow the cold air pools to form under relatively clear skies over the high elevations. The air pools may be as thick as 600 m (2000 ft) and may affect large regions of surrounding plains and valleys. Although adiabatic warming occurs as the air pool descends, the warming is generally not significant enough to offset the chilling effects of the air pool. This movement leads to rapid reductions in air temperature over the affected areas.

A significant katabatic wind in the Adriatic region of Europe is the **bora wind**, which forms in the Balkan highlands and spills toward lower elevations through gaps in the Dinaric Alps toward the Adriatic Sea. The word “katabatic” is derived from the Greek word “*katabasis*,” which refers to an army marching toward a coast, much as the wind spills out of the highlands and progresses toward the sea. The word “bora” is derived from “*Boreas*,” the god of the north wind in Greek mythology. The bora also may be induced when a cyclone occurs over the Ionian Sea region, resulting in a counterclockwise circulation that leads to the funneling of air through the Strait of Otranto between the “heel” of Italy and Albania. Such a situation may lead to treacherous water conditions in the Ionian Sea.

Another significant European katabatic wind is the **meltemi**, which is also associated with the Balkan region. This wind develops when high pressure occurs over the Balkan region near Hungary and a cyclonic center lies to the southeast near or over Turkey. The circulation characteristics of each pressure system combine to produce an offshore wind blowing over the Aegean Sea. Such a synoptic situation usually occurs during the summer when a thermal low develops over Turkey.

The **mistral wind** that affects the Rhone River valley of France is perhaps the best-known katabatic wind system in Europe. The wind flows directly from the Alps and spills through the Rhone valley toward Marseilles, where it spreads along the Mediterranean coast of France. Note that the katabatic winds detailed above differ from Föhn winds—warm, dry winds that affect the regions north of the Alps, mainly Germany.

The winter monsoon in Asia is technically a katabatic wind, as much of the offshore airflow that affects the southern portions of Asia stems from cold air flowing down from the high Tibetan plateau. Other than the monsoonal system itself, the most prominent Asian katabatic wind is the **oroshi wind** of Japan, an equivalent of the European bora.

► Summary

Climates in the extratropical sections of North America and Eurasia are influenced by semipermanent pressure features, ocean currents, topography, continentality, and water bodies. The geography of Central North America is more supportive of severe weather than any other broad location on earth. Other important features of the North American climate include the low-level jet and cyclogenetic regions on the leeward sides of the Rocky Mountains and along the Gulf of Mexico and Atlantic coasts. The Alps of Europe prevent the interaction of the coldest and warmest air masses. The size of the Asian land mass allows for a seasonal shift in circulation known as the Asian Monsoon, and the Himalayas of Asia alter the position of the polar front jet stream and create a strong orographic effect on that continent.

The factors noted above, along with others, produce a wide variety of climates in the extratropical northern hemisphere. True Desert climates are generally located in the southwestern United States and adjacent northern Mexico, along with several zones within a wide swath of Asia from the Red Sea to central China. Semiarid Steppe climates surround the True Deserts and occupy a much more sizable area in western North America than the True Deserts. Most of these True Deserts and Semiarid Steppes are classified as “cold” in the extratropical part

of the world. Sinking air from the poleward edge of the Hadley cell, along with continentality and rain shadow effects, are largely responsible for the aridity. Arid and semiarid climates exist over substantial portions of the subtropical oceans as well.

Mesothermal climates in the extratropical northern hemisphere are also widespread. These areas include the Humid Subtropical climates of the southeastern United States, eastern China, southern Japan, and the winter-dry variety in parts of south Asia. Return flow of warm, humid air around subtropical highs, abundant annual precipitation, and occasional winter cold weather outbreaks characterize this climate. Mediterranean climates persist in coastal southern California and the area surrounding the Mediterranean Sea. These are characterized by very dry summers and wet winters, due to the seasonal influence of the subsidence side of the subtropical highs. Finally, the Marine West Coast climates are found in Pacific coastal North America, northwestern Europe, and substantial sections of the middle- and high-latitude ocean basins. These well-watered, mild summer and mild

winter climates are influenced strongly by the frequent passage of midlatitude wave cyclones.

Microthermal climates occupy vast expanses of northern North America and Eurasia. The Humid Continental type occurs from the Ohio River northward into southern Canada, east of the semiarid climates; in a wide area from eastern Europe toward central Russia; and in northeastern China and the adjacent Russian Far East. Summers are warm to hot, while winters are long, cold, and uninterrupted. An even harsher climate is the Subarctic type, which sees shorter summers and less precipitation than the Humid Continental climates.

Polar climates are found along the northern fringes of the northern hemisphere. Tundra climates may have a freeze in any month of the year, while the Ice Cap type of polar climate sees an average temperature below freezing in every month of the year. Finally, Highland climates exhibit tremendous climatic variety in short lateral distances. The topography in these climates gives rise to several well-known wind systems of local and regional importance.

Key Terms

<i>Advection</i>	<i>Coriolis effect</i>	<i>Hadley cell</i>
<i>Advection fog</i>	<i>Coriolis parameter</i>	<i>Hawaiian high</i>
<i>Air mass</i>	<i>Cumuliform cloud</i>	<i>Heat index</i>
<i>Albedo</i>	<i>Cumulonimbus cloud</i>	<i>Highland (H) climate</i>
<i>Alberta clipper</i>	<i>Cyclogenesis</i>	<i>Hot Steppe (BSh) climate</i>
<i>Anticyclone</i>	<i>Cyclone</i>	<i>Humid Continental (Dfa, Dfb) climate</i>
<i>Arctic (A) air mass</i>	<i>Deficit</i>	<i>Humid Continental Winter Dry (Dwa, Dwb) climate</i>
<i>Arctic Circle</i>	<i>Deposition</i>	<i>Humid Subtropical (Cfa) climate</i>
<i>Asian monsoon</i>	<i>Dewpoint temperature</i>	<i>Humid Subtropical Winter Dry (Cwa) climate</i>
<i>Baroclinicity</i>	<i>Direct radiation</i>	<i>Hurricane</i>
<i>Bermuda-Azores high</i>	<i>Dixie Alley</i>	<i>Ice Cap (EF) climate</i>
<i>Blocking anticyclone</i>	<i>Dryline</i>	<i>Icelandic low</i>
<i>Bora wind</i>	<i>East-coast occlusion</i>	<i>Infiltration</i>
<i>Boreal forest</i>	<i>Ecotone</i>	<i>Insolation</i>
<i>California current</i>	<i>El Niño</i>	<i>International date line</i>
<i>Canary current</i>	<i>Environmental lapse rate</i>	<i>Isohyse</i>
<i>Chinook wind</i>	<i>Evaporation</i>	<i>Isotherm</i>
<i>Circumpolar vortex</i>	<i>Evapotranspiration</i>	<i>Katabatic wind</i>
<i>Climograph</i>	<i>Föhn wind</i>	<i>Labrador current</i>
<i>Cold air damming</i>	<i>Geopotential height</i>	<i>Lake effect snow</i>
<i>Cold air drainage</i>	<i>Geostrophic wind (V_g)</i>	<i>Latent heat</i>
<i>Cold front</i>	<i>Gradient wind equation</i>	<i>Latitude</i>
<i>Cold Steppe (BSk) climate</i>	<i>Greenhouse effect</i>	<i>Leeward</i>
<i>Colorado wave cyclone</i>	<i>Greenhouse gas</i>	<i>Longitude</i>
<i>Continental polar (cP) air mass</i>	<i>Gulf Coast cyclone</i>	<i>Longwave radiation</i>
<i>Continental tropical (cT) air mass</i>	<i>Gulf Stream</i>	
<i>Continentality</i>	<i>Gust front</i>	
<i>Convection</i>	<i>Gyre</i>	

Loop current	<i>North Equatorial current</i>	Subarctic (Dfc, Dwc, Dwd) climate
Low-level jet (LLJ) stream	<i>Occluded front</i>	Subtropical Hot Desert (BWh) climate
Marine West Coast climate	Occlusion	Summer monsoon
Marine West Coast Cool Summer (Cfc) climate	<i>Orographic effect</i>	Superstorm
Marine West Coast Warm Summer (Cfb) climate	Oroshi wind	<i>Surface boundary layer</i>
<i>Maritime effect</i>	Outflow boundary	<i>Surface water balance</i>
<i>Maritime polar (mP) air mass</i>	<i>Permafrost</i>	<i>Surplus</i>
<i>Maritime tropical (mT) air mass</i>	Pineapple Express	Taiga
Mediterranean climate	<i>Polar cell</i>	<i>Temperature inversion</i>
Mediterranean Hot Summer (Csa) climate	Polar climate	Thermal low
Mediterranean Warm Summer (Csb) climate	<i>Polar front jet stream</i>	<i>Tibetan low</i>
Meltemi wind	<i>Positive vorticity</i>	Tornado Alley
<i>Mesothermal</i>	<i>Potential evapotranspiration</i>	<i>Treeline</i>
<i>Microthermal</i>	<i>Potential vorticity</i>	<i>Tropical cyclone</i>
Midlatitude Cold Desert (BWk) climate	Rain shadow effect	<i>Trough</i>
<i>Midlatitude wave cyclone</i>	Relative humidity	True Desert (BW) climate
<i>Midlatitude westerlies</i>	<i>Ridge</i>	Tundra (ET) climate
Mistral wind	Riming	<i>Unsaturated adiabatic lapse rate</i>
Monsoon	<i>Rosby wave</i>	<i>Unstable atmosphere</i>
Mountain wind	Santa Ana wind	<i>Vertical wind shear</i>
Nor'easter	<i>Sensible heat</i>	Vertical zonation
North American summer monsoon	<i>Shortwave radiation</i>	<i>Water balance diagram</i>
<i>North Atlantic Drift</i>	<i>Siberian high</i>	West-coast occlusion
	<i>Source region</i>	Wind channeling
	Southwesterly monsoon	<i>Windward</i>
	Squall line	
	<i>Stability</i>	
	Steppe (BS) climate	
	<i>Stratiform cloud</i>	

Terms in italics have appeared in at least one previous chapter.

Review Questions

- How does the alignment of mountains affect the climates of North America and Europe?
- What role does the low-level jet stream play in the climate of North America?
- What is Tornado Alley and why does it exist?
- Discuss the oceanic circulation regime responsible for the creation of the North Atlantic Drift.
- Describe the importance of the North Atlantic Drift for the climate of Europe.
- Compare/contrast the role of continentality in North America and Asia.
- Why doesn't Europe have a significant continental effect?
- What is a monsoon?
- Discuss the influence of the Himalayan mountain range on precipitation in Asia.
- Discuss the similarities and differences between Desert and Steppe climates.
- Discuss the various climatic causes of arid climates.
- Compare and contrast Mediterranean and Marine West Coast climate regions.
- Why do Mediterranean climates exist?
- Why are Marine West Coast climates so warm for their latitudinal locations?
- Compare and contrast microthermal and mesothermal climatic regimes.
- Discuss the characteristics of the transition from the Subarctic climate to the Tundra and then Ice Cap climates.
- Why is the growth of tundra vegetation stunted?
- Explain why Highland climates constitute a specific climate regime.
- Detail the katabatic and regional mountain winds of each of the continents discussed in this chapter.

Questions for Thought

1. Discuss katabatic wind formation and how these winds differ from mountain-induced winds such as the Chinooks.
2. Review the energy balance diagrams for Dfa and Dfb stations shown in Figures 9.38 through 9.43. What factors govern the difference between insolation receipt at Dfa versus Dfb stations?
3. Identify the climatic type in your hometown and find a town on another continent that has the most similar climatic regime as your town. Why are the climatic regimes so similar?



CHAPTER 10

Tropical and Southern Hemisphere Climates

CHAPTER AT A GLANCE

- Contrasts Between Extratropical and Tropical Atmospheric Behavior
- Contrasts Between Northern and Southern Hemisphere Atmospheric Behavior
- Climatic Setting of Africa
 - General Characteristics
 - Intertropical Convergence Zone
 - Air Mass and General Circulation Influences
- Indian Ocean Dipole
- Climatic Setting of Australia and Oceania
 - General Characteristics
 - El Niño–Southern Oscillation Influences
 - South Pacific Convergence Zone
 - Madden-Julian Oscillation
 - Quasi-Biennial Oscillation
- Climatic Setting of Latin America
 - ENSO Contributions
- Climatic Setting of Antarctica
- Regional Climates
 - A—Tropical Climates
 - B—Arid Climates
 - C—Mesothermal Climates
 - E—Polar Climates
 - H—Highland Climates
- Summary
- Key Terms
- Review Questions
- Questions for Thought

► Contrasts Between Extratropical and Tropical Atmospheric Behavior

This chapter examines the climatic types of the tropics and the southern hemisphere. Atmospheric features in these regions differ markedly from those in the northern hemisphere extratropics. Annual temperature ranges are small in the tropics because day length and Sun angle vary little throughout the year. Also, the *Coriolis effect* is minimal there because its magnitude is proportional to *latitude*. The weakness of the Coriolis effect causes air to flow according to different rules than in the extratropics. Outside the tropics *geostrophic balance* resulting from an equilibrium between the *pressure gradient force* and the Coriolis effect occurs far above the surface, where *friction* is negligible. Flow in the tropics cannot be assumed to be geostrophic and winds cannot be inferred as being parallel to the *isohypses* (lines of constant *geopotential height*). Instead, **streamline analysis** must be used to deduce winds in the tropics.

Furthermore, little or no *air mass* contrast is present in the tropics because cold air masses cannot penetrate to such low latitudes. Tropical storm systems cannot originate from the juxtaposition of cold and warm air masses, and *fronts* are nonexistent, at least in the form that they appear in the midlatitudes. In general, broad-scale tropical weather and climate are much less predictable than in the midlatitudes, where climates are largely controlled by broad-scale, upper-atmospheric interactions and *Rossby waves* mix warm air of tropical origin with cold air of polar origin. The resulting flow patterns govern where and when midlatitude storms or clear skies occur. The dynamics involved have been worked out mathematically, and fairly accurate short-term predictions are possible in the midlatitudes. By contrast, the tropics have little similar overriding upper-air forcing. Instead, climate is largely influenced by local and/or regional factors related to daily heating of the surface. This introduces a level of daily variability that is experienced in the midlatitudes only during the summer season, if at all. Still, some broad-scale factors control and contribute to elements of the tropical climatic landscape.

There are only three ways for a tropical air parcel to rise so that it can cool to the *dewpoint temperature* and produce a cloud that might generate precipitation. Local instability can cause **convective precipitation**, uplift associated with topography can cause an *orographic effect*, and two streams of air might collide to produce *horizontal convergence*, which results in uplift after the collision. In the latter case horizontal convergence may also result from two near-surface air streams moving

laterally in the same direction but at different speeds. The faster-moving parcel could “catch up with” the slower-moving parcel, thereby causing horizontal convergence. Regardless of whether precipitation results from *convection*, the orographic effect, or convergence, the energy that is derived to fuel storms in the tropics must be enormous because the lack of air mass contrast gives no mechanism for producing the dynamic lows that are produced in the middle and high latitudes.

Tropical climates also differ from extratropical climates in the orientation of *ridges* and *troughs*. In the northern hemisphere’s midlatitudes, ridges—elongated zones of high pressure—in Rossby waves are areas where isohypses bulge toward the north, because higher pressure associated with *subtropical anticyclones* is to the south. By contrast, ridges in the northern hemisphere tropics appear as southward “dips” in **easterly waves** in the *northeast trade winds* (FIGURE 10.1a) because the elongation of the effect of the subtropical anticyclones extends from the north.

Likewise, any elongated area of low pressure is a trough. In the northern hemisphere’s midlatitudes, the lower pressure aloft is always associated with the *subpolar lows* to the north, rather than to the south as in the tropics, where the *Intertropical Convergence Zone* (ITCZ) provides the low pressure. This causes troughs to appear as “dips” southward in the northern hemisphere’s midlatitude Rossby waves but “bulges” northward in the northern hemisphere’s tropical easterly waves. The latter, often called **inverted troughs** in the tropics, represent *tropical cyclone* genesis areas.

► Contrasts Between Northern and Southern Hemisphere Atmospheric Behavior

Southern hemisphere climates are distinct from northern hemisphere climates in several important ways. First, the overwhelming dominance of water surface in the southern hemisphere limits the effectiveness of continental air masses and allows ocean currents to redistribute energy effectively between the tropics and the South Polar latitudes. Second, the seasons are inverted from the time of the year when they occur in the northern hemisphere. Because Earth is nearest to the Sun (*perihelion*) during the southern hemisphere’s summer and farthest from the Sun (*aphelion*) during the southern hemisphere’s winter, summer should be a bit warmer and winter should be a bit colder in the southern hemisphere than would otherwise be expected. However, this is not the case due to the moderating effects

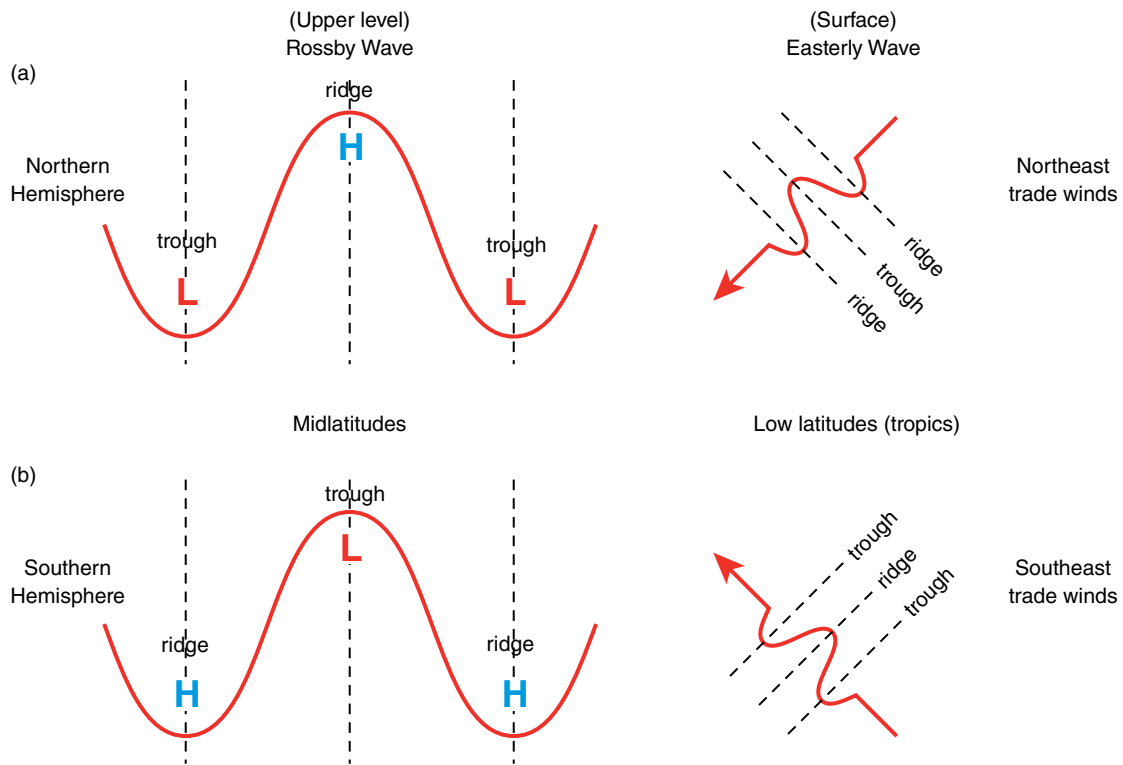


FIGURE 10.1 Rossby waves and easterly waves.

of water. In addition, the leftward (rather than rightward) deflection of the Coriolis effect causes secondary circulation features (i.e., *cyclones* and *anticyclones*) to spin in opposite directions than expected in the northern hemisphere. Finally, Rossby wave ridges in the midlatitude southern hemisphere actually appear the same as troughs in the northern hemisphere (**FIGURE 10.1b**). In the southern hemisphere's midlatitudes the lower pressure associated with the subpolar lows is to the south (rather than to the north as in the northern hemisphere), so southern hemispheric troughs are similar in appearance to northern hemispheric ridges. In both hemispheres the same relationships hold as troughs dip equatorward and ridges bulge poleward.

This chapter describes and explains the tropical and southern hemisphere climates of the world, including climates of Africa, South America, Australia, the islands of the western equatorial Pacific Ocean, and Antarctica. The primary physical causes for the climates of each continent are discussed before investigating the specific Köppen-Geiger climatic regions for these areas.

► Climatic Setting of Africa

General Characteristics

The African continent straddles the tropics, extending poleward to approximately 35° of latitude in both

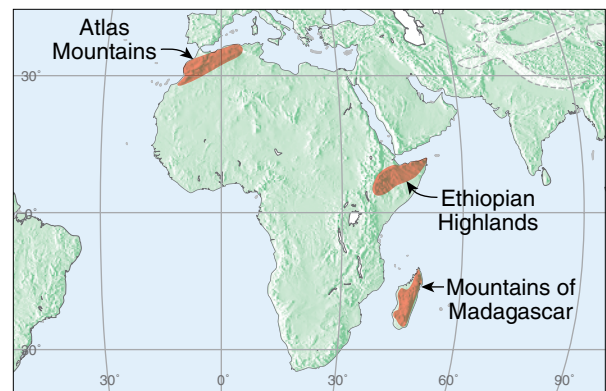


FIGURE 10.2 Selected physiographic features of Africa.

hemispheres (**FIGURE 10.2**). The northern edge of the continent lies at the latitudinal equivalent of Virginia and southern Japan, whereas the southernmost extent lies at similar latitudes to southern Australia and central Argentina. Because of the shape of the continent, there is more than twice as much land area in the northern hemisphere than in the southern hemisphere. The popular notion of Africa as an exclusively equatorial or southern hemisphere continent is inaccurate.

Intertropical Convergence Zone

Tropical influences, particularly the ITCZ, are important to the climatic setting of much of the continent. The

ITCZ is a region of convergence between the northeast trades and the *southeast trade winds*. It largely follows, but lags behind, the vertical rays of the Sun as it migrates between the *Tropic of Cancer* and *Tropic of Capricorn* through the course of the year. Afternoon convection from the high solar angles and the resultant surface heating destabilize the atmosphere and augment the lifting due to convergence.

The ITCZ does not migrate uniformly across African latitudes through the course of the year as the direct rays of the Sun shift seasonally. Instead, there is a high degree of variability in the timing and motions through the year. This variability affects regional climates in that “summer” rains may be delayed or completely diminished for some areas for any given year, leading to extended drought conditions and the associated environmental and social stresses.

The ITCZ affects more than just the amount of rainfall in a given region; it also contributes directly to the associated thermal characteristics. During the “high-sun” period (summer), there is more energy in the environment as compared with other times. The nearly unbroken area of afternoon convection and convective thunderstorms along the ITCZ not only produce much-needed rainfall, but they also shade the surface from the otherwise high input of *insolation*. If the ITCZ moves abnormally slowly and fails to reach a particular area at the climatological average time of year, greater amounts of surface energy are received, leading to increased *evapotranspiration* and stress on the local or regional ecosystem.

In such times, affected areas may have local vegetation cover denuded by human and animal activities. Such a situation changes the local *surface water balance*, usually by decreasing the percentage of precipitation that goes into soil moisture recharge and evapotranspiration back to the atmosphere, and increasing the percentage that becomes *runoff*. If vegetation removal is extensive enough, the regional water balance also may change in a similar fashion. These hydroclimatological changes may lead to expansion of the drier climates adjacent to those that experience rainfall from the ITCZ. Such *desertification* of a region may cascade to even more severe water balance changes on the regional level. A *positive feedback system* may occur, where interactions between the surface and the overlying atmosphere actually reinforce the original circulation that caused the drought, potentially leading to further changes in the domain of the ITCZ. If this occurs, then the desert “permanently” expands over a previously wetter region. This notion was expressed succinctly by climatologist Michael Glantz in the title of his book, *Drought Follows the Plow*.

Desertification caused by natural regional drought in combination with *anthropogenic* land cover changes

occurred in recent decades in the *Sahel* region on the southern edge of the Sahara desert (discussed in Chapter 9). Once vegetation was eliminated in the Sahel, there was less evapotranspiration into the regional atmosphere, leading to a net decrease in cloud formation. This led to expansion of the nearby desert (desertification) into the normally wetter steppe region with a resulting increase in dependency on humanitarian relief aid among the indigenous population. Despite worldwide aid, the region continues to be one plagued by famine, disease, and water shortages.

Air Mass and General Circulation Influences

Africa is affected largely by tropical and equatorial air masses. *Continental tropical (cT) air masses* are dominant in the northern third of the continent and in other smaller patches, particularly in southwestern Africa. *Maritime tropical (mT)* and *Equatorial (E)* air masses tend to be most influential in coastal Africa, especially south of the equator, and also in equatorial Africa. *Midlatitude westerlies* exert a role in the extreme northern and southern latitudes in winter.

The influence of the subtropical anticyclones is strong. Because of the latitudinal extent of Africa, significant portions of the continent fall under the influence of the subtropical anticyclones in both hemispheres. Subtropical anticyclones sit over ocean basins to the northwest, southwest, and southeast of the continent. Of these, the *South Atlantic high* is most persistent. The counterclockwise rotation around this southern hemisphere semipermanent anticyclone produces the **Benguela current**—a cold ocean current that runs along the southwestern coast of Africa. This current persists year-round and causes the convection associated with the ITCZ off Africa’s west coast to remain displaced to the north, in the northern hemisphere through the year. It also stabilizes the atmosphere, creating a *temperature inversion* and dry conditions in adjacent southwestern Africa. The counterclockwise circulation around the *Indian Ocean high* brings the **Aghulas current**—warm equatorial water—to the southeastern African coast. The clockwise flow around the *Bermuda-Azores high* in the northern hemisphere advects cold water southward in the form of the *Canary current* to northwestern coastal Africa, stabilizing the atmosphere and supporting dry conditions in Morocco and adjacent lands.

Much of northern and southern Africa falls under the influence of these high pressure zones. However, the northeastern quadrant of Africa is not influenced by a subtropical anticyclone. Rather, the hot, dry conditions of the Arabian Peninsula are advected toward Africa by the northeast trade winds. These conditions are reinforced by

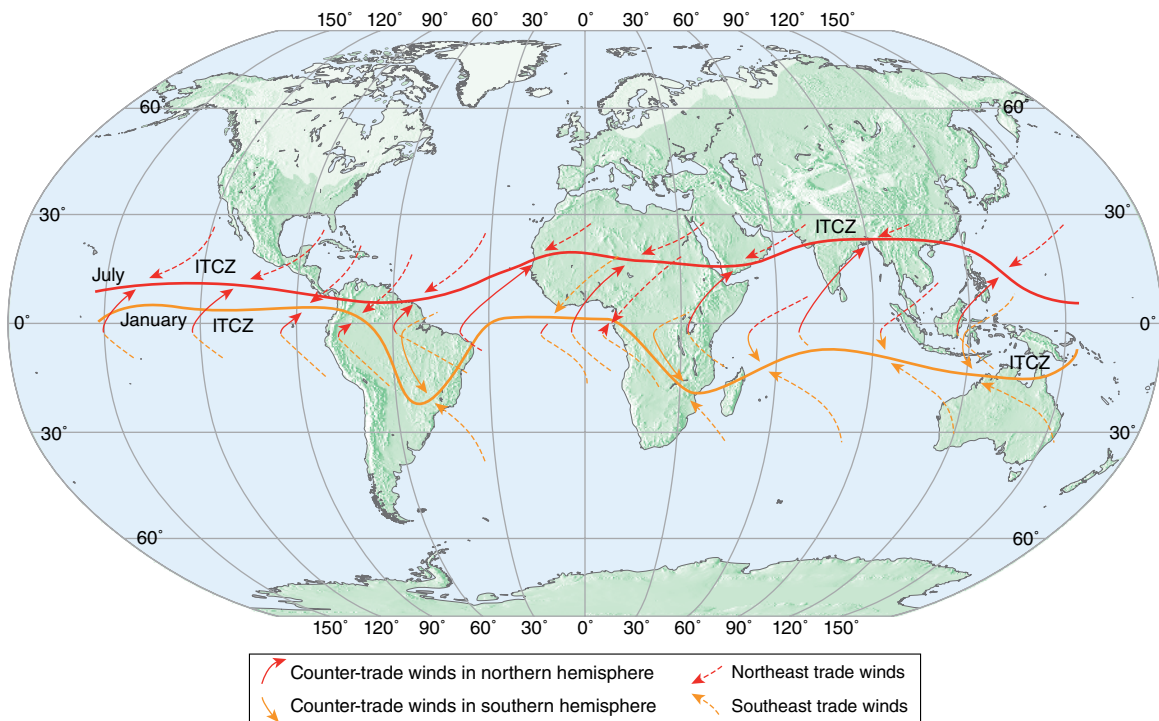


FIGURE 10.3 Counter-trade winds.

strong atmospheric stability around the Horn of Africa (Somalia) by the effect of the *Ekman spiral* as surface waters are deflected offshore and replaced by *upwelling* of colder waters from beneath the surface. In northwestern Africa the northeast trade winds are known as the **Harmattan winds**. These winds can sometimes be especially persistent in blowing dry Saharan air southwestward, resulting in hazy conditions over western coastal Africa, particularly along the Gulf of Guinea region, and they can even occasionally deliver dust and sand to the Caribbean and northern South America.

The Sahara Desert—the largest desert on Earth—dominates northern Africa, spanning approximately 65° of longitude and 20° of latitude. The deserts of southwestern Asia, such as the Arabian Desert and the Rub-al-Khali, are extensions of the Sahara. The lack of Saharan precipitation and cloud cover makes the Sahara among the most inhospitable places on Earth. The region also is arguably the hottest on Earth. The deserts of the southern hemisphere are only slightly less brutal. Harsh conditions exist in the Kalahari Desert, which occupies much of Botswana, Namibia, Zambia, and the Republic of South Africa. Still, permanent, although largely nomadic, populations have found ways to adapt to these harsh conditions.

When the *solar declination* is in the northern hemisphere (as it is from the *vernal equinox* through the *autumnal equinox*), the trade winds generally converge at the ITCZ north of the equator. When the southeast trade winds cross the equator on their trek to the ITCZ, they are influenced by a rightward (rather than leftward) Coriolis deflection. They, therefore, become southwesterly

rather than southeasterly winds, and they are termed **counter-trade winds** (FIGURE 10.3). These southwesterly counter-trades offer some respite from the heat in the Sahel and southern Sahara region, because they can push the oppressively hot cT air masses back toward the northeast. Likewise, when the solar declination is in the southern hemisphere, the northeast and southeast trade winds generally converge in the southern hemisphere at the ITCZ's position at that point in the year. As this happens the northeast trades change direction after crossing into the southern hemisphere to become northwesterly counter-trades.

Another important circulation feature is the **Turkana jet stream**—a low-level (generally from about the 950- to 650-mb level) jet stream that exists between the Ethiopian and East African highlands. Taking its name from the nearby Lake Turkana basin, this easterly or southeasterly jet peaks in intensity between February and March. Although most of Africa is devoid of high mountains, the orography of this section of Africa is most important in the development of the jet. The highlands constrict flow through the region, forcing *wind channeling* as air speed increases when flow is confined. Jet speeds vary diurnally, with the strongest winds occurring during the morning and the weakest winds in the afternoon. The jet is partly responsible for dry conditions over the Lake Turkana basin, as the jet inhibits the development of mesoscale cyclonic circulations over the region.

The Turkana jet differs from the **East African low-level jet**, which is also influenced by regional orography.

The East African jet develops during the daytime hours across the East African coastline. Airflow is directed inland from east to west toward an active convection zone governed by surface heating. The jet is responsible for water vapor *fluxes* and resultant precipitation across East Africa.

The influences of the broader-scale monsoonal flow regime and thermal and frictional forcing factors are also important across the region. The monsoon circulation triggers the **Somali jet**, also known as the **Findlater jet**, another important feature of the tropical circulation in Asia. This low-level jet provides southwesterly flow paralleling the Somali coast, in association with the summer *Asian monsoon* system, advecting moisture into south Asia. Later in the summer monsoon season, the Somali jet and the entire *southwesterly monsoon* give way to the southeasterly flow over much of south and southeast Asia caused by the clockwise flow around the *Hawaiian high*.

► Indian Ocean Dipole

Recurring sea surface temperature **anomalies**—departures from the expected atmospheric conditions—are felt in the tropical and subtropical Indian Ocean and in adjacent lands, including eastern Africa. In the “positive phase” of this **Indian Ocean Dipole (IOD)**, water temperatures are abnormally warm in the western Indian Ocean, near Somalia in what is known as “the Horn” of eastern Africa. Precipitation in this region is normally sparse, but positive IOD events are linked with much wetter than normal conditions in Africa’s Horn. At the same time that waters are warmer than normal near Africa’s Horn, surface water temperatures are abnormally cold in the eastern Indian Ocean, near Indonesia and Australia, where drought conditions prevail. The positive IOD tends to occur, at least to some extent, in concert with *El Niño–Southern Oscillation (ENSO)*–related variability. As discussed in another part of this text, an *El Niño*, also known as a warm-ENSO event, refers to a shifting of warm equatorial waters from the western equatorial Pacific Ocean to the eastern equatorial Pacific. The “cold anomaly” area near Indonesia and Australia during the positive IOD phase often, but not always, coincides with cold anomalies in the same general area during *El Niño* events. However, the positive IOD does not always coincide with the warm-ENSO phase; sometimes the positive IOD pattern even occurs during *La Niña* events, which are characterized by warm temperature anomalies in the east Indian Ocean near Indonesia and Australia. The fact that the southwest-to-northeast flow of moist air during the summer monsoon tracks over water that is warmer than normal near the Horn of Africa during

the positive phase of the IOD means that the positive IOD also tends to be associated with more abundant than average monsoon rainfall in India.

Conditions during the “negative” phase of IOD are the opposite—colder than normal water temperatures in the western Indian Ocean near Somalia, with warmer than normal conditions near Indonesia and Australia. The negative IOD usually brings drought to the Horn of Africa and adjacent lands, and the colder ocean temperatures may reduce monsoon rainfall in south Asia or delay its onset.

► Climatic Setting of Australia and Oceania

The Australian continent is the largest island in a region collectively known as **Oceania** (FIGURE 10.4). The western portion of this region is sometimes called the **Maritime Continent**—the southeastern continuation of the Asian land mass, including Australia and the thousands of smaller islands occupying the southwestern Pacific Ocean basin. These islands include those that make up Indonesia, the Philippines, and Papua New Guinea. Oceania also includes the many island chains elsewhere in the tropical western Pacific basin, including those comprising Melanesia, Micronesia, and Polynesia (the latter of which includes the Hawaiian Islands). For simplicity, the term “Oceania” is used to refer to all islands extending from the southeast Asian mainland except Australia and New Zealand. Much of the region was once connected to southeast Asia during the last **glacial advance**, approximately 18,000 years

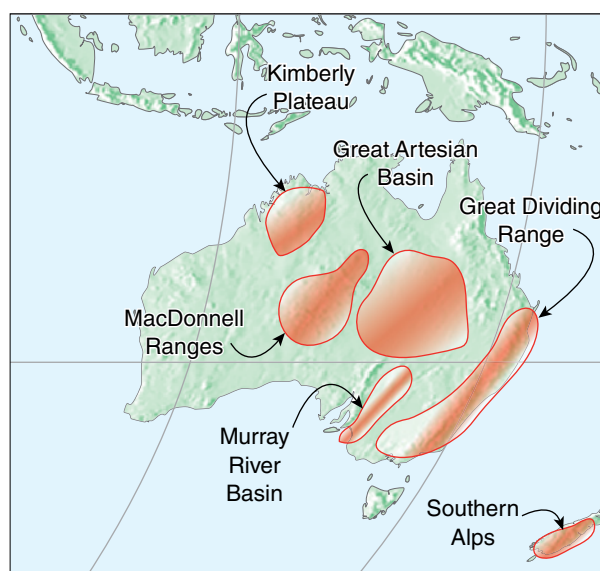


FIGURE 10.4 Selected physiographic features of Australia and New Zealand.

ago. During that time sea levels were low enough to expose land bridges between many of the islands.

General Characteristics

Most of the climatic landscape in this part of the world falls into only two major climatic types: tropical and dry. Virtually all of Oceania is classified under the heading of tropical climates, whereas most of Australia is defined as being dry, and New Zealand is largely *mesothermal*. As in Africa, seasonal migration of the ITCZ plays an integral role in the tropical climates. In this region of the world the position of the ITCZ is influenced by the development of the Asian monsoon and determines moisture anomalies, both intra- and interannually.

Some regions of Oceania, however, receive only minimal seasonal temperature and precipitation variation. This is especially true of regions lying along or near the equator. Precipitation in these locations is forced by thermal characteristics and the development of afternoon thunderstorms. Many areas in this region receive precipitation on most days in the year.

El Niño–Southern Oscillation Influences

The greatest single cause of climatic variability in this region is the ENSO event. A similar but less intense shift in ocean waters is caused annually during the transition between northern hemisphere summer–southern hemisphere winter to northern hemisphere winter–southern hemisphere summer. The transition to winter causes a weakening of the Hawaiian high and the *South Pacific high*, which weakens the trade winds.

Normally, the equatorial trade wind flow is responsible for pushing warm equatorial waters from the eastern Pacific basin to the west, leading to the normal pile-up of warm water off the eastern coasts of Australia and Oceania. This warm-water accumulation induces low sea-level pressure and low-level atmospheric instability, triggering diurnal thunderstorms through this region of Oceania and northern Australia. Sea levels in the west are normally about 20 cm (8 in) higher than in the eastern equatorial Pacific. The higher sea levels remain intact as long as the trade wind flow is sufficient enough to push water from east to west. When the trades weaken during the normal seasonal transition, some of this warm water migrates back toward the eastern Pacific basin. This slight weakening is typical in northern hemisphere autumn.

Approximately every 3 to 7 years a warm-ENSO event occurs in association with a massive reduction in the strength of the trade wind flow. During these times warm water migrates back eastward in autumn. This flow induces significant changes in the overlying

atmosphere in both the western and the eastern equatorial regions. The normally warm western basin waters with low atmospheric pressures and abundant convective thunderstorms give way to greater atmospheric *stability* and higher pressure in the western tropical Pacific Ocean. The low atmospheric pressure and convective activity follow the warm surface waters eastward. This brings precipitation to the central and perhaps even the eastern tropical Pacific basin, where higher atmospheric pressures forced by cold oceanic upwelling usually occur. In short, a warm-ENSO event reverses the normal atmospheric pressures and winds in the tropical Pacific basin. The atmospheric “seesaw” in sea-level pressures between the tropical western and eastern Pacific Ocean is the *Southern Oscillation*.

Australia and Oceania are influenced directly by the frequency and severity of warm-ENSO events. The normally wet regions of the western equatorial Pacific (as well as much of monsoonal Asia) become drought-ridden, whereas the normally dry eastern Pacific basin experiences abundant precipitation. These conditions normally last between 8 and 12 months, but longer periods have occurred. Significant environmental stress occurs through eastern Australia and most of Oceania during warm-ENSO events, as the tropical ecosystems depend on a high amount of precipitation during each month of the year.

FIGURE 10.5a shows the winter/spring mean precipitation anomalies for Australia during the 12 strongest warm-ENSO events on record. Most of eastern Australia is significantly drier than normal during such periods. The northern reaches of Australia are normally dry during the winter/spring time period, partly mitigating the impact of a warm-ENSO event. The ENSO influence in northern Australia is felt more during the summer months, as **FIGURE 10.5b** indicates. Water shortages in the entire region can become a problem during these events, particularly on small islands where available fresh water consists solely of recent local precipitation.

Australia/Oceania is also directly affected by La Niña or cold-ENSO conditions. La Niña is a strengthening of the “normal” atmospheric and oceanic circulation conditions. The normally wet areas of northern Australia and virtually all of Oceania become wetter as regions in the eastern Pacific become even drier. **FIGURE 10.6** shows precipitation anomalies for Australia during the cold-ENSO winter/spring months. Figure 10.6 indicates that virtually all of eastern Australia and especially the northern tip become exceedingly wet during La Niña. The region of positive precipitation anomalies extends northward into the bulk of Oceania.

The environmental stress of El Niño and La Niña is significant across the region. This area may be viewed as one of “feast or famine” regarding precipitation. Both extreme phases stress the physical environment

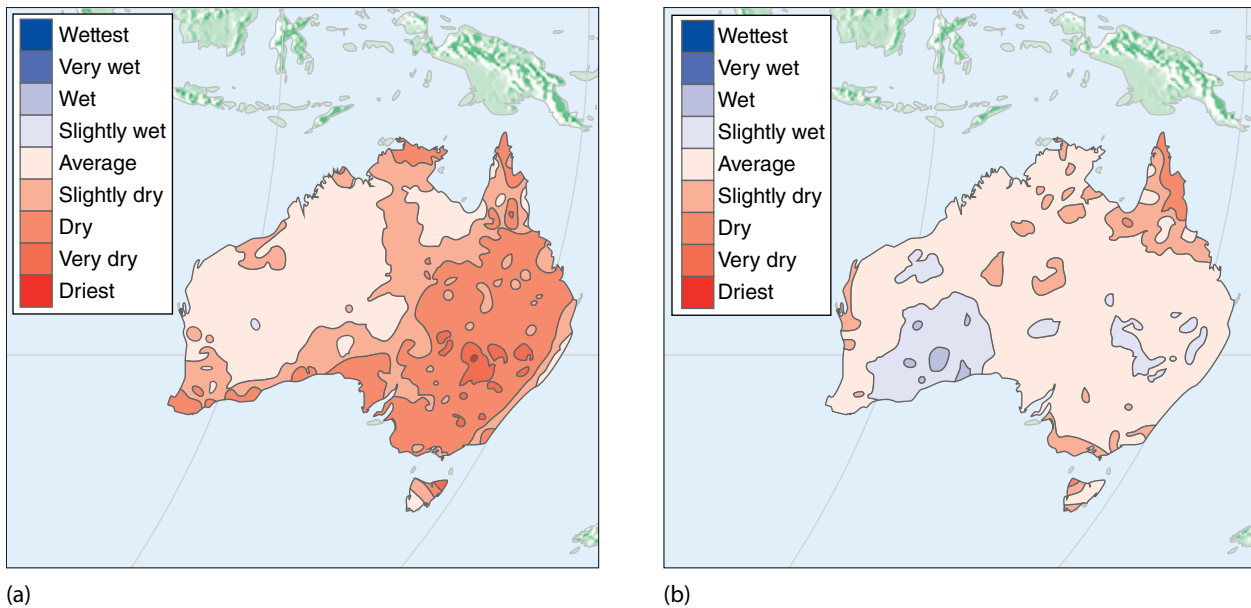


FIGURE 10.5 (a) Winter/spring mean precipitation anomalies during warm-ENSO years. (b) Summer mean rainfall anomalies during warm-ENSO years.

Data from The Australian National Climatic Centre, Bureau of Meteorology, Melbourne, Victoria, Australia.

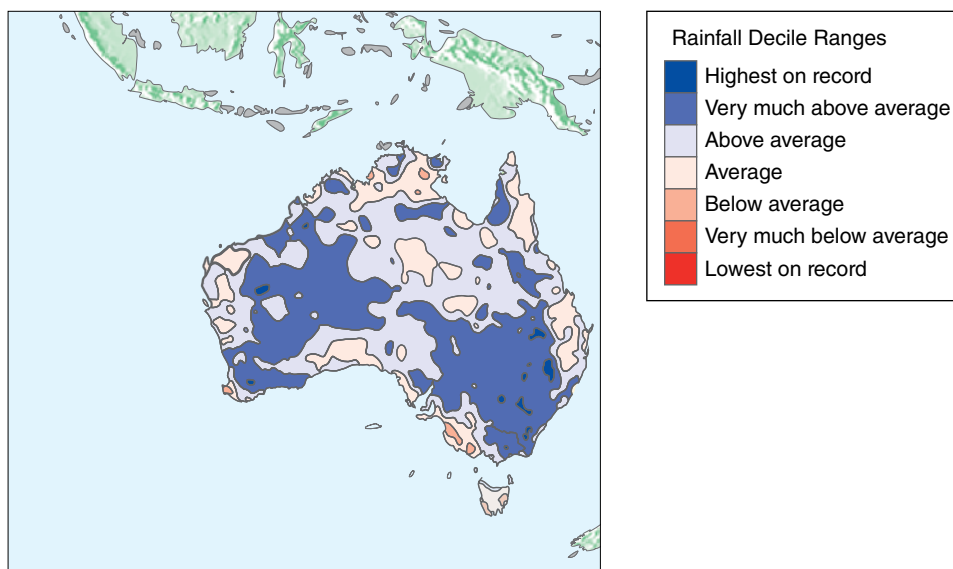


FIGURE 10.6 Winter/spring precipitation anomalies during cold-ENSO years.

Data from The Australian National Climatic Centre, Bureau of Meteorology, Melbourne, Victoria, Australia.

and human activities. The ENSO influence extends to drought and fire, which occur across broad areas during the drier warm-ENSO periods, and severe thunderstorms, increased tropical cyclone activity, and floods, which occur largely in association with cold-ENSO events.

The “flip side” of events indicates the “good” manifestations of the extreme climatic reversals. The Australians often view every situation with an eye toward both “bad” and “good” (or “flip side”) inspection. Drought may be viewed as being detrimental for farmers, but it may also be seen as advantageous for owners of beach resorts.

El Niño and La Niña events offer many opportunities for flip-side viewpoints.

South Pacific Convergence Zone

The **South Pacific Convergence Zone (SPCZ)** is another important contributor to the climatic setting of Australia and Oceania. The SPCZ is an offshoot of the ITCZ, generally oriented in a northwest–southeast alignment or perhaps a north–south alignment (**FIGURE 10.7**), and it is most active during the summer months when surface

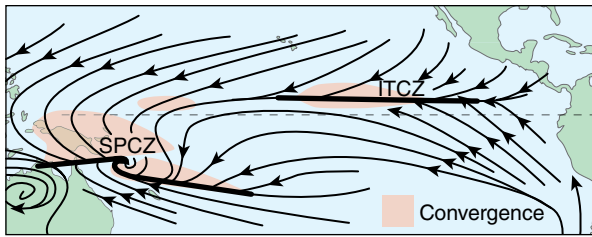


FIGURE 10.7 The South Pacific Convergence Zone.

Data from C. S. Ramage. In: Barry, R. G. and R. J. Chorley (Eds.), *Atmosphere, Weather, and Climate* (8th ed.). New York: Routledge.

heating is maximized. Its band of convection is approximately 200 to 400 km (125 to 250 mi) wide, stretching from the ITCZ near the Solomon Islands to the region of Fiji, Samoa, Tonga, and islands southeastward. Like the ITCZ, diurnal cloud cover and afternoon and early evening precipitation are abundant.

The SPCZ forms as a convergence zone between the South Pacific high and the frequent anticyclones that tend to remain in place over or near Australia. Because both of these anticyclones are in the southern hemisphere, they support counterclockwise-rotating air around them. The SPCZ is formed where the weak southwesterly or southerly flow from the eastern side of an Australian anticyclone meets with the strong northeasterly or northerly flow around the western side of the South Pacific high. Because of variability in both strength and position of the two anticyclones that form the convergence zone, the SPCZ itself may fluctuate in orientation from northwest–southeast to north–south, with the northern part acting almost as a “hinge” with more “swinging” on the southern side. It also varies in its longitudinal location. The position where the SPCZ meets the ITCZ is generally a zone of maximum convection, and it usually occurs in the western tropical Pacific near Indonesia.

Migrations of the SPCZ affect the moisture regimes across the eastern regions of Oceania. A significant shift in the position of the SPCZ occurred during the late 1970s, coincident with a major climatic adjustment throughout North America and the Pacific. The broad-scale circulation shift caused higher surface temperatures in most regions globally and an increase in the frequency and magnitude of warm-ENSO events. The SPCZ typically migrates northeastward during warm-ENSO events and toward the southwest during cold-ENSO events. It is a primary region for the development of South Pacific tropical cyclones, particularly beyond about 5° of latitude south of the equator, where the Coriolis effect increases sufficiently to allow for rotating winds around a low-pressure core.

Madden-Julian Oscillation

Another important contributor to the climates of Oceania and coastal Australia is the **Madden-Julian**

Oscillation (MJO), a phenomenon that explains many of the intra-annual fluctuations in tropical climate. The MJO often is referred to as the **30–60 Day Oscillation** or the **40–50 Day Oscillation** because of the time scales on which it generally operates, with some variability present in the timing of the oscillation. The MJO involves a band of cloudiness and precipitation traveling from west to east across the tropical oceans, sandwiched between bands of suppressed cloudiness and precipitation. Upper- and lower-level winds and sea surface temperatures undergo fluctuations with the presence or absence of the associated convections. Because clouds are involved, the MJO is usually investigated using *longwave radiation* data detected by satellites. Variations in outgoing longwave radiation—terrestrial radiation escaping to space—are proportional to the amount of cloud cover in a region because clouds hinder the loss of terrestrial radiation to space.

The eastward-propagating outgoing longwave radiation anomalies across the tropical Indian and Pacific Ocean recur at a 30- to 60-day interval at a given tropical location. Whenever a band of convective cloudiness rolls through a region, precipitation peaks occur. Between convection bands there are periods of low precipitation. Winds are directed toward the MJO-related convective area from the east and west. Once inside the convective area, convergence increases the uplift of air, triggering thunderstorm development. A region of increasing convection occurs in advance of the main convection zone (between the thunderstorms at the convection zone and the clear skies at the suppressed convection zone) as greater amounts of *evaporation* enhance low-level instability and low-level moisture storage, both resulting from increased insolation in the suppressed convection region. This typically occurs east of the convection zone. The wave then propagates eastward over the enhanced convection zone that then becomes the primary area of convection. The progression then develops anew and the line continues its eastward propagation.

The MJO may be thought of as being a regional-scale version of the air–sea interactions that drive El Niño events. In warm-ENSO events, eastward-propagating convection areas are driven by the movement of warm-water *equatorial Kelvin waves*. The warm surfaces trigger overlying convective thunderstorms that move eastward. MJO propagation is analogous because the clear skies of the suppressed convection zone allow sea surface temperatures to increase in advance of the line of thunderstorms (the convection zone). This creates the enhanced convection zone (which is still marked by clear skies). The line of thunderstorms then migrates toward this area of enhanced convection just as the convection areas migrate along with an equatorial Kelvin wave associated with a warm-ENSO event. The MJO

completes its cycle of wave propagation over a 30- to 60-day period, at which point the cycle begins anew.

Because the MJO involves the continuous migration of a convective zone, it introduces a large-scale overriding climatic forcing mechanism to the affected tropics. Knowledge of the MJO leads to forecasts of increased or decreased convective thunderstorm development for particular regions and is therefore an important climatic component for much of Oceania. Such short-term precipitation oscillations are superimposed on larger-scale phenomena such as monsoon rains and ENSO-induced precipitation anomalies. The MJO may either dampen or intensify the precipitation anomaly produced by the larger-scale phenomena. For instance, the MJO convective zone mitigates La Niña-influenced droughts in western Oceania.

Quasi-Biennial Oscillation

Another circulation feature important to tropical climates is the **Quasi-Biennial Oscillation (QBO)**. Before the use of radiosonde balloons, satellites, and other modern data-gathering tools, little was known about upper-atmospheric motions, particularly in the tropics. During the late 1800s it was assumed that winds in the equatorial *stratosphere* blew from east to west. This assumption was supported by observation of the east-to-west drift of the dust cloud ejected into the stratosphere on August 27, 1883, by the eruption of the **Krakatau** volcano in Indonesia—the largest in modern times. The dust cloud encircled the planet over the low latitudes in only 13 days. These stratospheric winds were then named the **Krakatau easterlies**.

In 1908 data balloons launched above Lake Victoria in Africa recorded westerly winds in the equatorial stratosphere, a finding that contradicted the previous assumption that the Krakatau easterlies prevail unobstructed. The winds are known as the **Berson westerlies**. The nature of these Berson westerlies in the equatorial stratosphere was not resolved until the early 1960s, when it was discovered that stratospheric winds above the equator oscillate in direction with a period of about 26 months. This oscillation of the equatorial zonal stratospheric wind flow came to be known as the QBO.

Further investigations revealed that winds associated with the easterly or westerly phase of the QBO propagate downward from the upper levels of the stratosphere at a rate of about 1 km per month until they reach the tropical *tropopause*. At that point they weaken and the opposite phase is initiated, with westerly (or easterly) winds in the upper stratosphere propagating downward slowly over a period of several months. The winds in the easterly phase of the QBO are approximately twice as strong as those in the westerly phase. A complete

explanation of the cause of this oscillation has not yet been found.

The effects of the QBO are numerous. In addition to mixing gases, including *ozone*, throughout the otherwise-stagnant stratosphere, the QBO also combines with ENSO to influence east Asian monsoon precipitation. Its variation has also been linked to Sahelian precipitation totals. The strongest influence of the QBO is related to tropical cyclone activity in the western Pacific, the western Indian, and the North Atlantic basins. Pacific tropical cyclone activity increases in the westerly phase of the QBO, whereas activity in the western Indian Ocean basin increases with the easterly phase. Increases in *hurricane* activity in the North Atlantic are linked to the westerly QBO phase, with strong decreases in the easterly phase. One reason for the unprecedented 2005 North Atlantic hurricane season was that the QBO was in a strong westerly phase. This combined with high sea surface temperatures across the tropical North Atlantic, the Caribbean, and the Gulf of Mexico to produce a record-setting 28 named tropical cyclones, including 15 hurricanes.

► Climatic Setting of Latin America

The northernmost point in Latin America is in the northern hemisphere subtropics, with the poleward tip of South America extending to approximately 55°S latitude (**FIGURE 10.8**). Because of the shape of the



FIGURE 10.8 Selected physiographic features of Latin America.

continent, the bulk lies within the tropics, with only a tiny strip approaching the high latitudes.

Perhaps the most striking feature of the physiography of Latin America is the western cordillera, from the Sierra Madre Occidental in Mexico along the entire western edge of Central America and continuing as the Andes Mountains of South America. The Andes run the length of western South America from the Llano Highlands of Venezuela and Colombia to southern Chile, covering most of Ecuador and a significant portion of both Peru and Bolivia.

East of the Andes are lowlands across most of Latin America. These include the Central Valley of Mexico, the vast Amazon basin that dominates the continental interior of South America, and the grasslands known as the Pampas and the Patagonian Highlands of Argentina. The eastern side of Mexico and parts of Brazil, particularly the southeast, are elevated, though the Sierra Madre Oriental and the Brazilian Highlands are not as high, steep, or continuous as the western mountains. In parts of Central America the Occidental and Oriental essentially continue as a central highland region.

Of the mountain features, the Andes exert by far the greatest influence on climate. They act as a barrier to moderating air masses of Pacific origin and also prevent the trade winds from advecting moisture to the west coast of South America. The mountains combine with the cold *Humboldt (Peru) current* off the western coast to keep the atmosphere stable. Such conditions promote clear skies and dry conditions through the narrow coastal band.

The Atacama Desert of southern Peru and northern Chile is arguably the driest desert on Earth. Entire ecosystems there have evolved around the prevalence of fog, the only moisture source through much of the coastal zone. *Advection fogs* are frequent and persistent along this region, forming as warm, moist air blows across the waters of the South Pacific Ocean. Just before reaching the coast, the air blows over the cold Humboldt (Peru) current. Combining waters originating from relatively high latitudes near Antarctica with coastal upwelling resulting from Ekman transport creates an ocean surface that is cold enough to chill air passing over it to the dewpoint temperature. The resultant fog blows inland where plants and animals are adept at catching the fog droplets. For instance, spiders string webs between vegetation such that the webbing catches and collects water droplets that then converge into small holes created by the repeated dripping onto the soil. Plants then grow around the hole, taking advantage of the water source that nourishes the immediate area.

A cold surface ocean current also exists off the west coast of North America—the California current. This feature does not affect the west coast of Mexico and

Central America significantly, because the coastline curves away from the *gyre* in the northern tropical Pacific Ocean. This contrasts with the shape of the South American western coastline, which conforms closely to the South Pacific *gyre*.

Despite its interior location, the Amazon basin acts as a primary moisture source for a large segment of South America. Abundant heat energy combines with efficient soil and biomass moisture storage to create a very humid atmosphere. Water evapotranspires throughout the day, increasing local water vapor content in the atmosphere. By the afternoon cumulus cloud development becomes extensive enough to create copious precipitation. This system is sometimes termed the *rain machine* because such a high percentage of the local rainfall is recycled continuously from local moisture sources. Additional water is advected into the continent by the trade winds and some arrives as meltwater from snowpack in the high Andes Mountains. Local water also runs out to sea via the extensive fluvial network.

Significant disruption of the rain machine occurs through agricultural and other developmental practices. *Deforestation* of the Amazon basin is a primary concern for several reasons, including its influence on climate. This largest region of rain forest on Earth acts as the “lungs” of the atmosphere by supplying the global atmosphere with oxygen from *photosynthesis*. It is also feared that decreases in the forest extent will cause a fundamental change in the regional atmospheric moisture balance. Decreasing moisture in the region will subject the area to higher temperatures, which will lead to increased drying. Some believe that deforestation may one day lead to a South American landscape that resembles the extensive deserts of northern Africa.

ENSO Contributions

Like most tropical regions the greatest source of climatic variability is caused by El Niño and La Niña events. The migration of a warm water pool from the western to the eastern equatorial Pacific during warm-ENSO (i.e., El Niño) events displaces the cold surface waters along the western edge of South America. The warm water pool overrides the colder waters because of its decreased density. In addition, the warm water pool causes a deepening near the coast of the *thermocline*—the boundary between cold water in the deep ocean and much warmer water near the ocean surface. Although coastal upwelling still occurs during warm-ENSO events due to the Ekman transport, this water is much warmer than normal and the upwelling does not penetrate all the way up to the surface. The result is that the horizontal and vertical sea surface temperature regimes are fundamentally changed along much of the western South American coastline.

The impact of such a change is profound. First, ecosystem balance is altered, as the indigenous ecosystem largely depends on the existence of upwelling of nutrient-rich cold water. Warming of the sea surface and a net decrease in nutrients fundamentally change the regional oceanic food chain. Second, the increased sea surface temperatures destabilize the overlying atmosphere, leading to low-pressure anomalies that induce clouds and precipitation in a normally stable, clear, and dry environment. The positive precipitation anomalies wreak havoc on local ecosystems. Flooding and mudslides are commonplace throughout western South America during warm-ENSO events.

The El Niño impact carries to other regions as well. Displacement of the usual high pressure over western South America causes a displacement of atmospheric flow across the tropics, including the area over the Amazon Basin. The typically low atmospheric pressure of the Amazon Basin gives way to much higher pressures,

clearer skies, and reduced precipitation during warm-ENSO events. Because of the high temperatures, the basin depends on frequent and heavy daily rainfall totals to avoid a *deficit*. Without diurnal thunderstorms the region may desiccate quickly. The resulting ENSO-induced drought causes considerable stress on the ecosystem.

La Niña events also cause environmental stresses throughout South America. The anomalously cold waters off the western coast of the continent cause unusually dry conditions (even in environments that are normally dry) through the western regions. Over Amazonia the opposite occurs, with heavy afternoon rains.

► Climatic Setting of Antarctica

Antarctica is the fifth-largest continent on Earth. Because it sits over the South Pole (FIGURE 10.9), it is characterized by very low temperatures and high winds. Rapid

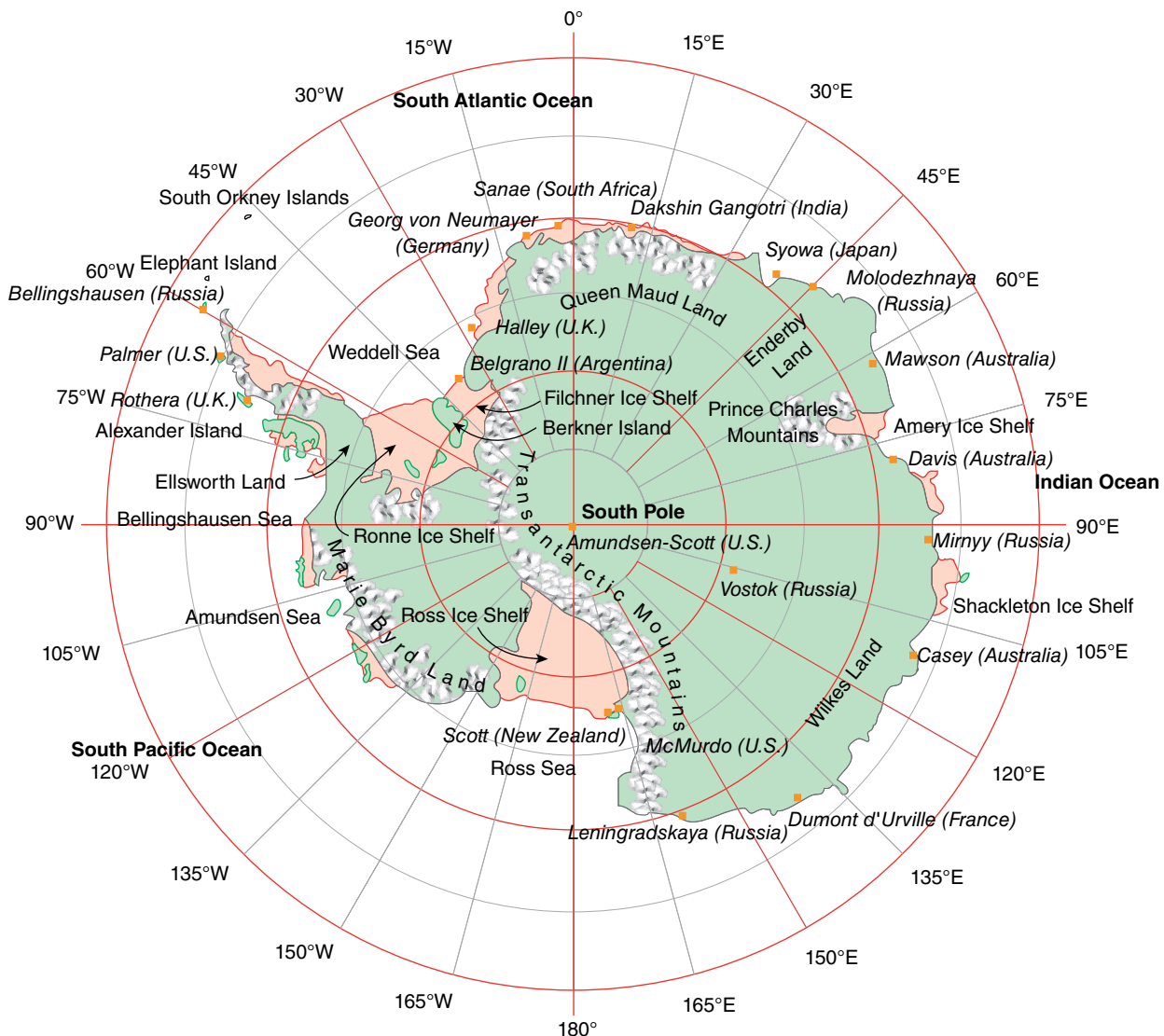


FIGURE 10.9 Selected physiographic features of Antarctica.

changes in weather occur near the coastal fringes, but the interior is marked by persistent cold. The region is the coldest on Earth, being far colder than its Arctic counterpart. The reason is that the Arctic is composed of ocean waters that retain some heat energy for transfer to the overlying atmosphere, even in winter when the Arctic Ocean's surface is frozen.

Not only is Antarctica affected by high latitudes, but it is also strongly influenced by *continentality* and high elevations. Despite its relatively modest high point (the Vinson Massif) of 4897 m (16,066 ft), the mean elevation of 2200 m (7200 ft) far exceeds that of any other continent. Such high elevations lead to low temperatures and low atmospheric pressures. At an elevation of 2800 m (9200 ft), the South Pole has an average surface pressure of only 680 mb. Ironically, though, the continent also contains the lowest point on Earth that is not under seawater. The Bentley Subglacial Trench extends 2555 m (8382 ft) below sea level and is currently locked beneath an extensive ice sheet.

Not surprisingly, the high latitudes, continental influence, and high elevations combine to produce extremely cold conditions. The lowest temperature ever recorded on Earth, -89°C (-129°F), occurred at Vostok, Antarctica, on July 21, 1983. The highest average summer temperatures are around -7°C (20°F), whereas winter temperatures for much of the continent may hover around or below -34°C (-30°F).

A noticeable precipitation gradient exists between coastal locations and the interior. At coastlines, not only is more moisture present in the warmer coastal air, but the air mass contrast is likely to be greater, as relatively warmer maritime air masses interact with the bitter cold continental air masses. The extreme low temperatures in the continental interior dictate that *vapor pressures* are low, even at saturation. Blizzards and **whiteouts**—atmospheric conditions that cause the sky to blend with the snow-covered surface, eliminating the horizon—are common, but they mainly occur from blowing ice, not newly precipitated snow. All clouds are *stratiform* in nature because vertically oriented clouds are impossible given the low energy amounts for uplift.

Antarctica is studied extensively for its potential role in anthropogenic *global warming*, for two major reasons. First, the high latitudes of the continent are intriguing because modeling studies of the impacts of human-influenced global warming show that most of the global warming signal is concentrated at relatively high latitudes—the *Arctic amplification*. Slight warming produces melting, exposing bare soil, thereby decreasing the *albedo* and allowing further warming to occur in a positive feedback system. Second, the continent is overlain with a huge continental ice sheet that has increased *ablation* during warmer climatic conditions,

thereby contributing to global—or **eustatic**—sea level increases.

Less than 5% of the continent is ice-free, with the ice-free portions being small coastal locations, islands, and some mountain areas. The present ice sheet is similar in size and thickness to that which covered North America at the peak of the *Wisconsin Glacial Phase* 18,000 years ago. The region of East Antarctica is covered by a layer of ice that is 4000 m (13,000 ft) thick. This ice sheet is so large that liquid lakes have formed beneath it in some locations. These lakes are composed of basal meltwater formed from the friction between the moving ice sheet and the continental bedrock. The largest is Lake Vostok, which lies approximately 4 km (2.5 mi) beneath the Vostok Research Station in East Antarctica (see Figure 10.9). Lake Vostok is approximately 280 by 60 km (174 by 36 mi) and is 500 m (1600 ft) deep.

Two major coastal indentations occur in the Ross Sea, which opens to the Pacific Ocean, and the Weddell Sea, which opens to the Atlantic Ocean. Both seas are covered by extensive ice shelves, with the Ross Sea covered by the **Ross Ice Shelf** and the Weddell Sea covered by the **Ronne Ice Shelf** and the **Filchner Ice Shelf** (see Figure 10.9). The shelves are between 180 and 1220 m (600 and 4000 ft) thick. Ablation rates in this region are studied extensively as possible indicators of global warming. Sea level increases resulting from melting of these shelves would inundate vast coastal zones of the present-day continents. It must be noted that the ice shelves are distinct from the seasonal sea ice that forms around the continent during the cold season. However, the health of the ice shelves is related to the number of icebergs that typically form as ice chunks calve off of the edge of the shelves.

Considerable variation occurs in Antarctic temperatures, but a notable warming trend has been recorded in recent years. Most of the warming has occurred near the coast, whereas interior temperatures have remained stable. No appreciable temperature change has occurred at the South Pole since the 1970s, but some coastal locations have warmed at a rate of about three times higher than the global average.

There is some correlation between temperatures at the South Pole and the Southern Oscillation, but the correlations are evident only by lagging the temperatures by 1 year. After lagging, the correlation is statistically significant. It therefore takes about a year for the anomalies produced by the Southern Oscillation to have an influence on temperatures at the South Pole. This suggests at least some degree of large-scale forcing on continental interior temperature variation. More recent research has linked temperature variation in nonpolar areas to the Southern Oscillation.

► Regional Climates

A—Tropical Climates

Tropical (A) climates occur throughout Southeast Asia, Indonesia, most of Bangladesh and southern India, northern Australia, Oceania, Central Africa, most of Central America and southern Mexico, the Caribbean Sea, most of South America, and a broad belt of low-latitude ocean basins (see world map of Köppen-Geiger climate types). The southern tip of Florida is also classified as tropical.

Tropical Rain Forest (Af) and Tropical Monsoon (Am) climates dominate throughout most of the equatorial tropics, over both land and ocean. Af is the world's most common climatic type over oceans. The Tropical Monsoon (Am) climate is found mainly along coastal margins and in larger sections of Brazil, with extensive areas of the tropical oceans. Inland areas, as well as substantial parts of oceans, particularly those located several degrees of latitude from the equator and affected by seasonal wind shifts, are classified as **Tropical Savanna (Aw) climates**. The “winter” dry season that characterizes Aw climates marks a transition between the wet tropical climates and the drier climates of interior poleward locations. In Asia these climates are caused by the monsoonal wind shift associated with the development of the *Siberian high* during winter and the *thermal low* during summer.

Af—Tropical Rain Forest

Tropical Rain Forest climates are characterized by persistent hot, humid, and rainy conditions year-round. The climatic type is mainly associated with low-elevation areas bounded by higher topographical regions and equatorial ocean basins. The Af climate also exists in somewhat higher latitudes, where warm ocean currents and year-round precipitation from the equatorward edges of midlatitude wave cyclones occur, such as in the western subtropical Atlantic Ocean. The main distinguishing feature of this climate is a lack of seasonality. In the tropics, neither day lengths nor the amount of insolation receipt at a given time of day over the course of the year changes significantly. Unlike other tropical climates, pronounced seasonal pulses of higher rainfall are absent in most Af climates. Slight seasonal variations in precipitation do occur in some locations, as shown in the climographs of Af locations discussed elsewhere in the text.

Thermal Characteristics. By definition, in tropical climates the coldest month must have an average temperature over 18°C (64°F). In Af climates the diurnal range in temperature, typically about 8 to 10 C° (14 to 18 F°), is much greater than the annual range in mean

monthly temperature, which may be as small as 2 to 3 C° (3 to 5 F°).

Despite the generally sultry conditions, daily maximum temperatures are often much lower than may be expected, with temperatures rarely exceeding 32°C (90°F) at most Af locations. Extensive cloud cover and abundant late afternoon precipitation explain these temperature maxima. Remember that insolation peaks at solar noon, but this energy receipt does not produce a temperature peak at that time. Instead, a lag of 3 to 4 hours occurs between maximum solar reception and maximum air temperatures, because abundant insolation continues to be absorbed at Earth's surface for several hours after solar noon. Longwave radiant energy is continuously emitted to the atmosphere, which absorbs some wavelengths of radiation, resulting in surface air temperature increases for as long as the shortwave and longwave radiation gained by the surface exceeds the longwave radiation emitted to the atmosphere.

The abundant thermal energy combines with high humidity values to generate convective thunderstorms that peak during the time of maximum air temperature. The *cumuliform clouds* then cool the area by shading the surface from additional solar energy receipt and by precipitation generated from the thunderstorms. This precipitation cools the surface as the water evaporates, thus transferring energy from the surface to the atmosphere as *latent heat*. Less energy is left as *sensible heat* at the surface, reducing air temperatures.

Nocturnal temperatures in Af climate regions are also consistently high because so much water exists in the atmosphere. This leads to an enhanced local *greenhouse effect*, which allows for emission of longwave radiation back toward the surface by water vapor and/or cloud cover. Nighttime temperatures are usually in the twenties Celsius (seventies Fahrenheit), and they again show remarkable consistency through the year.

Temperature and precipitation consistency throughout the year promotes the widest **biodiversity** of life forms of any climate because the limitations to growth are minimized. However, competition, predation, and disease limit the number of individuals of any species present. If you were to list every species found in an area of 1 km² of tropical rain forest, the list would be extensive, but only a few individuals of each species would likely be present.

Moisture Characteristics. The “classic” Af precipitation regime is shown by the *climographs* of Hilo, Hawaii (**FIGURE 10.10a**), and Singapore, Singapore (**FIGURE 10.11a**). Seasonal variations in precipitation are more notable in the climographs of Colombo, Sri Lanka (**FIGURE 10.12a**), and Belize City, Belize (**FIGURE 10.13a**). Even stronger seasonality is present in the precipitation regime of Manaus, Brazil (**FIGURE 10.14a**), which is not

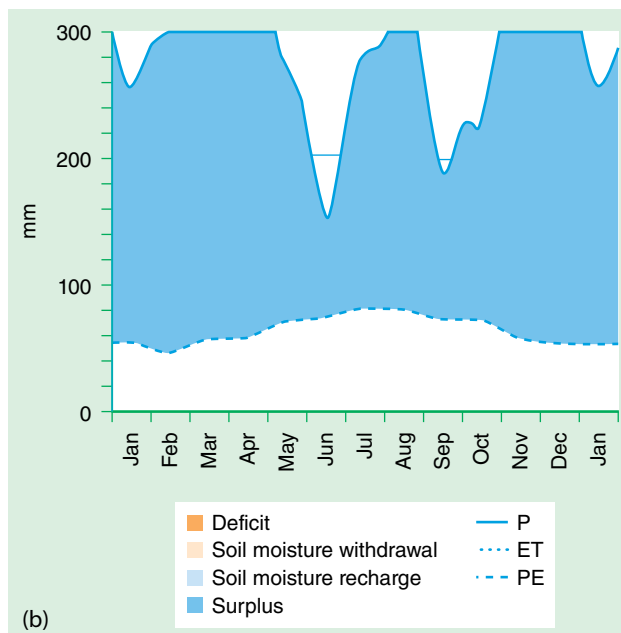
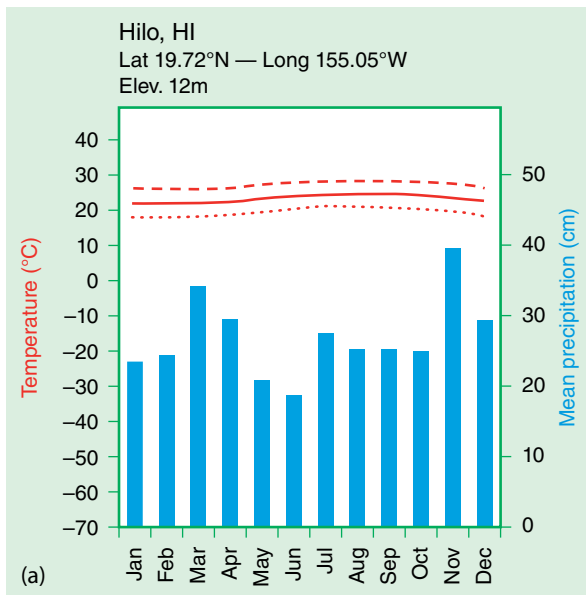


FIGURE 10.10 (a) Climograph for Hilo, Hawaii (Af climate). Average annual temperature is 23.3°C (73.9°F) and average annual precipitation is 320.7 cm (126.3 in). (b) Water balance diagram for Hilo, Hawaii.

(a) Data from National Centers for Environmental Information. (b) Modified with permission using Web/WIMP version 1.01 implemented by K. Matsuura, C. Willmott, and D. Legates at the University of Delaware, 2003.

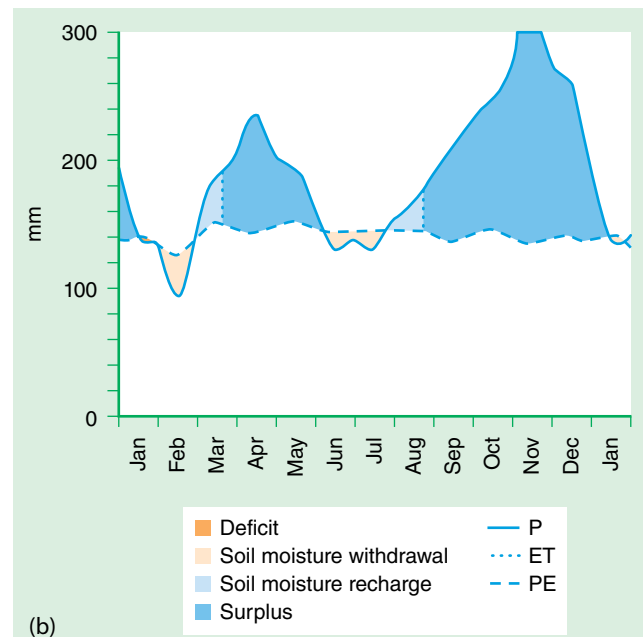
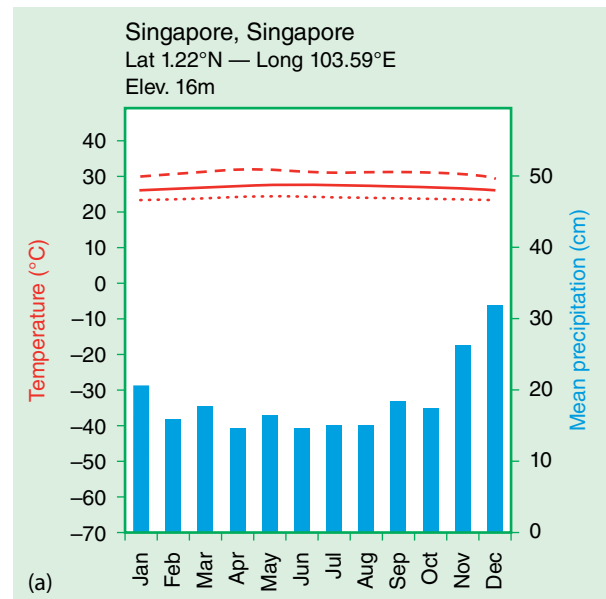


FIGURE 10.11 (a) Climograph for Singapore, Singapore (Af climate). Average annual temperature is 27.1°C (80.8°F) and average annual precipitation is 226.8 cm (89.3 in). (b) Water balance diagram for Singapore, Singapore.

(a) Data from National Centers for Environmental Information. (b) Modified with permission using Web/WIMP version 1.01 implemented by K. Matsuura, C. Willmott, and D. Legates at the University of Delaware, 2003.

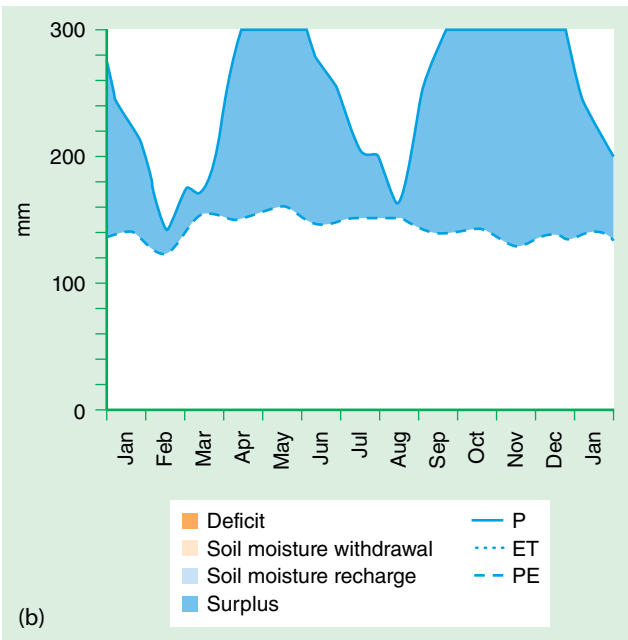
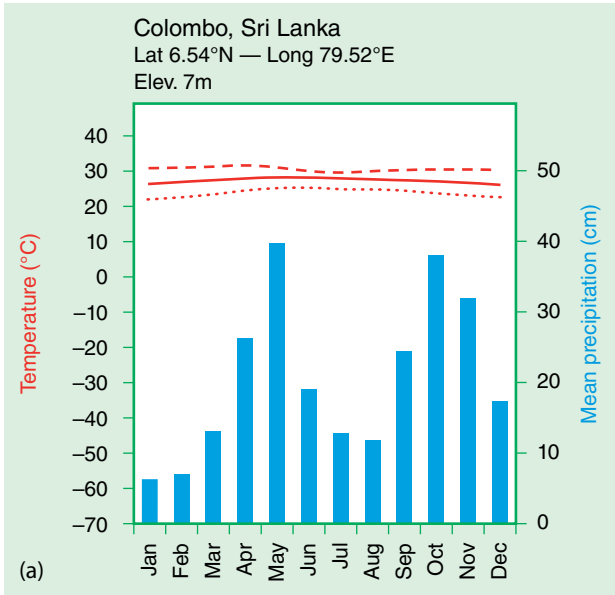
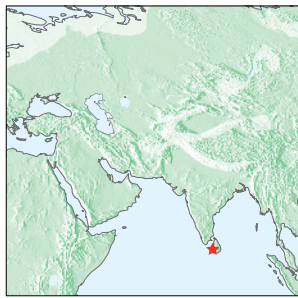


FIGURE 10.12 (a) Climograph for Colombo, Sri Lanka (Af climate). Average annual temperature is 27.8°C (82.0°F) and average annual precipitation is 223.8 cm (88.1 in). (b) Water balance diagram for Colombo, Sri Lanka.

(a) Data from National Centers for Environmental Information. (b) Modified with permission using Web/WIMP version 1.01 implemented by K. Matsuura, C. Willmott, and D. Legates at the University of Delaware, 2003.

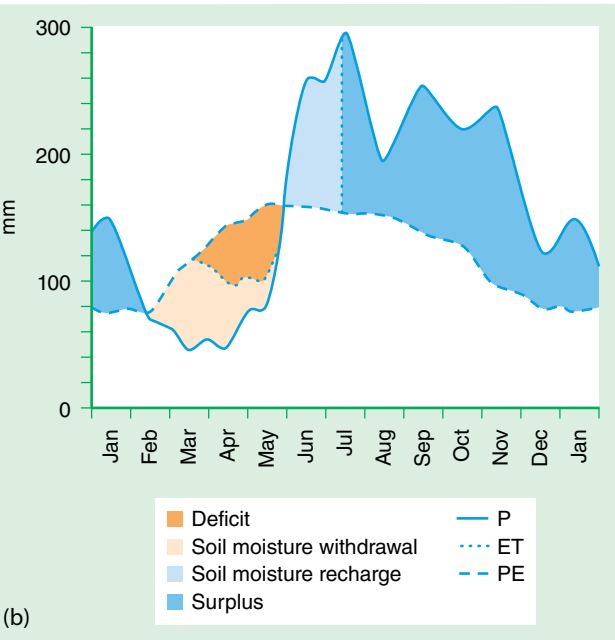
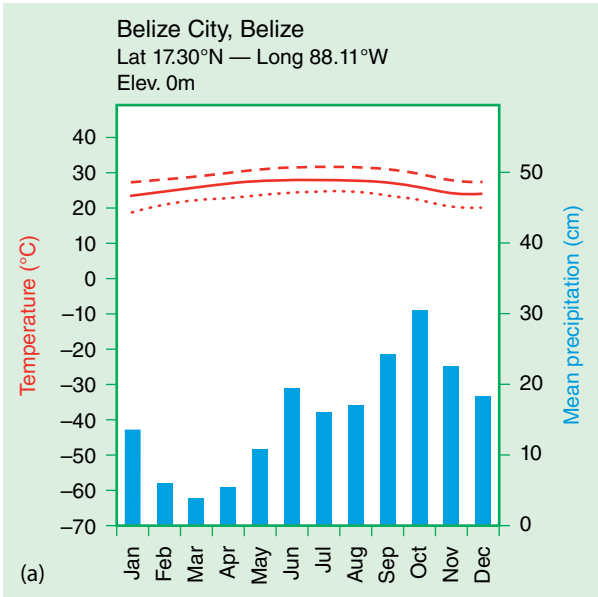


FIGURE 10.13 (a) Climograph for Belize City, Belize (Af climate). Average annual temperature is 26.4°C (79.5°F) and average annual precipitation is 181.9 cm (71.6 in). (b) Water balance diagram for Belize City, Belize.

(a) Data from National Centers for Environmental Information. (b) Modified with permission using Web/WIMP version 1.01 implemented by K. Matsuura, C. Willmott, and D. Legates at the University of Delaware, 2003.

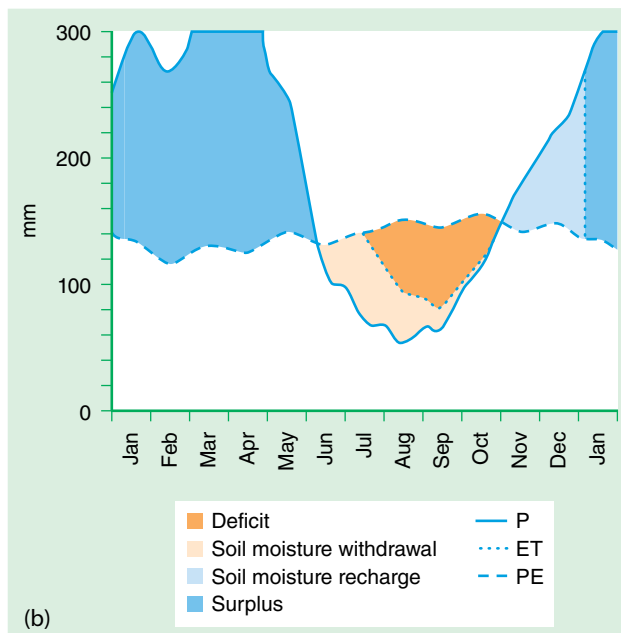
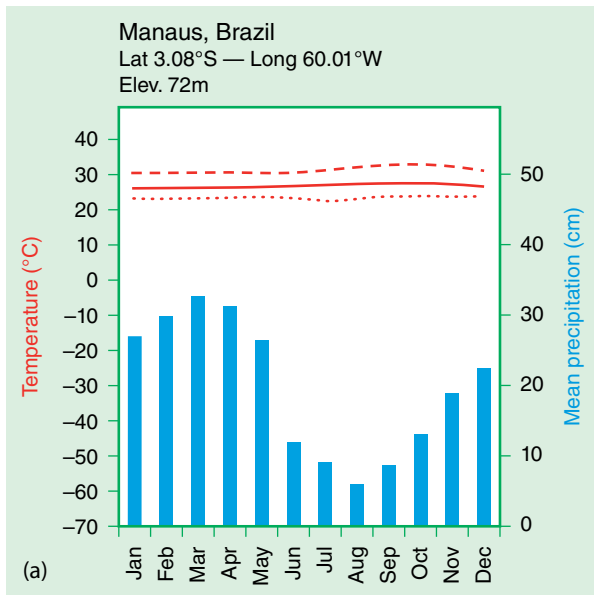


FIGURE 10.14 (a) Climograph for Manaus, Brazil (Af climate). Average annual temperature is 27.9°C (82.2°F) and average annual precipitation is 181.1 cm (71.3 in). (b) Water balance diagram for Manaus, Brazil.

(a) Data from National Centers for Environmental Information. (b) Modified with permission using Web/WIMP version 1.01 implemented by K. Matsuura, C. Willmott, and D. Legates at the University of Delaware, 2003.

as wet from June through September when the ITCZ migrates to the northern hemisphere.

Precipitation is abundant, with annual totals over 200 cm (80 in) for most locations, but amounts vary considerably, ranging from annual mean lows of about 150 cm (60 in) to over 1000 cm (400 in). Precipitation is tied to the development of afternoon convective thunderstorms along the ITCZ, and can be augmented locally by topography, low-level jet streams, or reduced seasonal migration of the ITCZ away from the area. During summer the superheated continent of Asia, and the associated Tibetan low, draws the ITCZ up to its farthest poleward location—to nearly 30°N latitude. Convergence of the trade winds (or counter-trades) associated with the ITCZ typically enhances thunderstorm activity during that time, leading to pronounced summertime peaks in precipitation.

Topography also can exert a significant impact on precipitation in Af regions. High-elevation regions enhance precipitation totals. The cooling in high elevations also results in greater cloud and fog cover. This is especially true for most Caribbean islands, which typically have volcanic mountain cores. The resulting orographic effect creates islands that are dominated by Af climates on the *windward* side (as in Hilo, Hawaii) and much drier climatic types on the *leeward* side.

Another important component of the precipitation regime of Af climates is the tropical cyclone. These storms—called **typhoons** in the western tropical North Pacific Ocean and simply cyclones in the Indian Ocean and tropical South Pacific Ocean—are normally stronger and more frequent than their North Atlantic Ocean hurricane counterparts. The lowest sea level pressure on Earth was recorded over the North Pacific Ocean during Typhoon Tip when on October 12, 1979, the internal pressure dipped to 870 mb. Most people correctly view tropical cyclones as being harbingers of destruction, but these systems are also integral to the water balance maintenance for many locations. Given the high evapotranspiration rates associated with these lush, low-latitude locations, vegetation stress may occur with only a few dry days. Tropical cyclones help replenish moisture shortfalls.

As expected, the surface water balance at Af climates shows few, if any, deficits. Hilo (**FIGURE 10.10b**) and Colombo (**FIGURE 10.12b**) have no signs of significant soil moisture shortage throughout an average year. Hilo is on the windward side of the northeast trade winds and receives orographic enhancement of precipitation year-round. In the case of Colombo, the Asian monsoon suppresses precipitation in winter, but not to the extent of reducing precipitation below the rate of *potential evapotranspiration*. Precipitation also decreases in

late summer when the ITCZ is displaced northward of Colombo, but precipitation nevertheless manages to exceed potential evapotranspiration. Some soil moisture decrease (but no deficit) is characteristic of Singapore (FIGURE 10.11b), and brief deficit occurs in both Belize City (FIGURE 10.13b) and Manaus (FIGURE 10.14b) at the end of the dry season. The deficits are not sufficiently long or intense enough to classify these cities outside of the Tropical Rain Forest climate, even though they are near the edge of the climatic zone, but some years may show climatic conditions that are more characteristic of climates other than Af climates.

Am—Tropical Monsoon

Tropical Monsoon (Am) climates differ from Tropical Rain Forest areas only in that they exhibit a short dry season on a climatological average. Because of the consistency of temperatures, this dry season constitutes the only real seasonal variation in climate. This climatic type may be considered as being a transition between the Tropical Rain Forest and the Tropical Savanna (Aw), because general characteristics fall between those two climatic types. The Am climate is present in South and Southeast Asia and parts of Oceania, the Caribbean, South America, and in ocean basins (usually) poleward of Af and Am climates.

The climatic region is usually found along coastal areas that receive persistent onshore winds for most, but not all, of the year. For a short period each year the trade winds may not advect moist air into these regions. In Am climates of Asia a winter dry season is typical because of the effects of the Asian monsoon, but in many locations, such as the Caribbean, this climate may be found in locations without a true monsoonal wind shift. In such cases, onshore flow regimes wax and wane seasonally along with the intensity of the subtropical anticyclones. “Weak” periods in the subtropical anticyclones cause a short transitional dry season as the trade winds flowing out of the anticyclones subside. This period is then followed by a **trade surge** in moisture-laden air, inducing a precipitation peak.

Thermal Characteristics. Temperatures are similar to those of the Af climate, with mean monthly averages exceeding 18°C (64°F) in each month. The primary temperature difference between the two climatic types involves the annual variation in temperature. Monsoon climates tend to be more variable in this regard, because of the influence of the dry season. During dry times the lack of afternoon cloud cover allows for higher daily temperature maxima, whereas enhancement of nocturnal cooling occurs due to the dampened local greenhouse effect. Because the ITCZ

typically dominates the summer season, the annual temperature peak (and heightened diurnal variability) usually occurs just before that time, during late spring.

Moisture Characteristics. Precipitation amounts vary from location to location, but the general rule is that a distinct dry season occurs just before a notable wet-season peak in precipitation. This pattern is evident in the climographs for this climatic type (FIGURES 10.15a, 10.16a, and 10.17a). The Asian monsoon system produces a brief winter dry period in Manila, Philippines, and Dhaka, Bangladesh, whereas the southerly displacement of the trade winds and weakening of the Bermuda-Azores high leaves Tegucigalpa, Honduras, relatively dry in winter. Tropical cyclones provide moisture in late summer and autumn at all three sites.

Precipitation totals are similar to those of the Af climatic type, resulting in similar rain forest ecosystems. Although the short dry season does occur, local water supplies are seldom fully depleted, and the rain forests receive adequate water through soil moisture storage. The ITCZ typically produces the distinct summer precipitation peak for most locations. Other times are marked by lighter rainfall amounts as compared with the Af climate zone. In some cases, the drier months produce water balance deficits, particularly toward the end of the dry season, as indicated in the associated *water balance diagrams* (FIGURES 10.15b through 10.17b).

Aw—Tropical Savanna

Tropical Savanna (Aw) climates occur in regions poleward of Af and Am climatic types. The most extensive of the tropical climates over land, the Aw climate is characterized by distinct wet and dry seasons of approximately equal length. The Aw dry season is typically longer and more severe than that associated with the Am climate. During the low-precipitation season insolation remains high, and therefore potential evapotranspiration rates are high. The result is a desiccated environment for several months.

The distinct dry season creates a landscape with far fewer trees than in the other tropical climates. Instead of rain forest, the regional vegetation is dominated by tall savanna grasses that grow through the wet season and become dormant during the dry season. Trees do exist, particularly along areas of local moisture accumulation, but the canopy is not closed, as in a forested environment. Instead, a “park-like” environment exists—the type of landscape that would be seen on a safari. A typical tree of this climatic type is the **acacia** (FIGURE 10.18). These trees tend to grow “outward” rather than upward because there is no competition for sunlight from adjacent trees. This form allows giraffes to eat leaves from a large part of the tree.

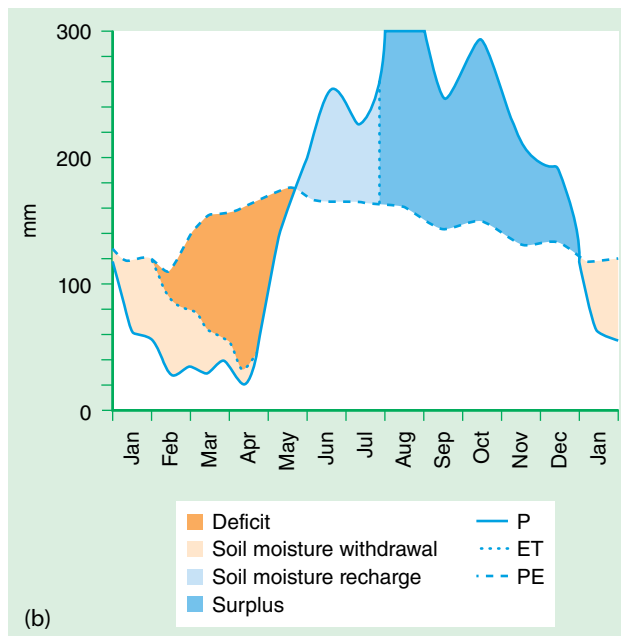
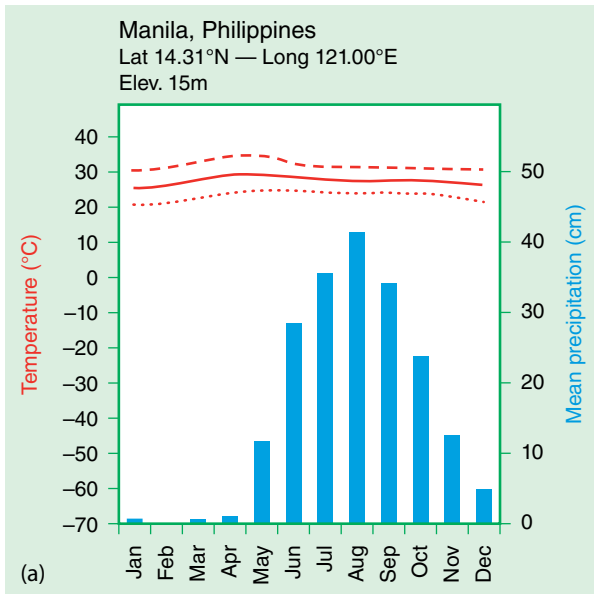


FIGURE 10.15 (a) Climograph for Manila, Philippines (Am climate). Average annual temperature is 27.5°C (81.5°F) and average annual precipitation is 197.4 cm (77.7 in). (b) Water balance diagram for Manila, Philippines.

(a) Data from National Centers for Environmental Information. (b) Modified with permission using Web/WIMP version 1.01 implemented by K. Matsuura, C. Willmott, and D. Legates at the University of Delaware, 2003.

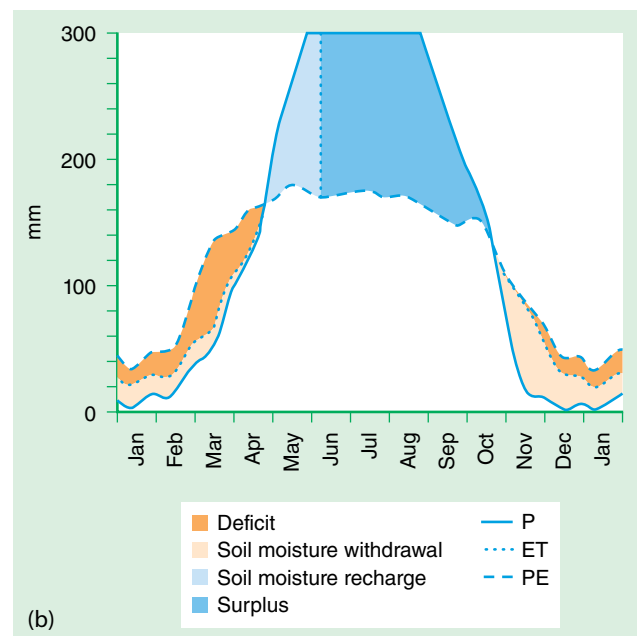
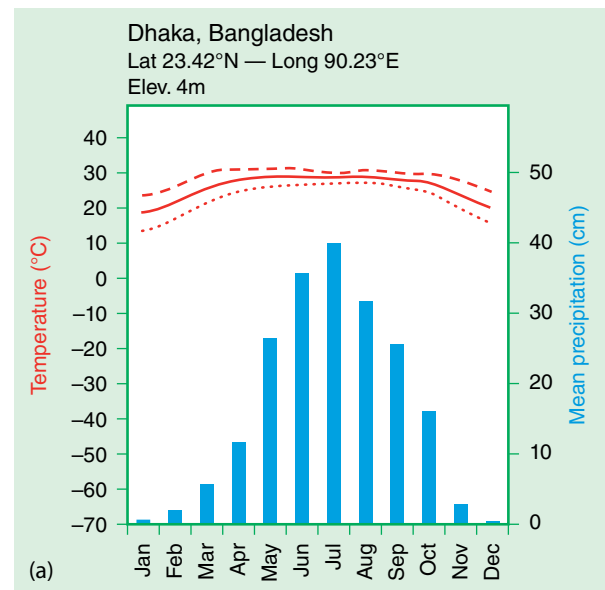


FIGURE 10.16 (a) Climograph for Dhaka, Bangladesh (Am climate). Average annual temperature is 25.8°C (78.5°F) and average annual precipitation is 199.9 cm (78.7 in). (b) Water balance diagram for Dhaka, Bangladesh.

(a) Data from National Centers for Environmental Information. (b) Modified with permission using Web/WIMP version 1.01 implemented by K. Matsuura, C. Willmott, and D. Legates at the University of Delaware, 2003.

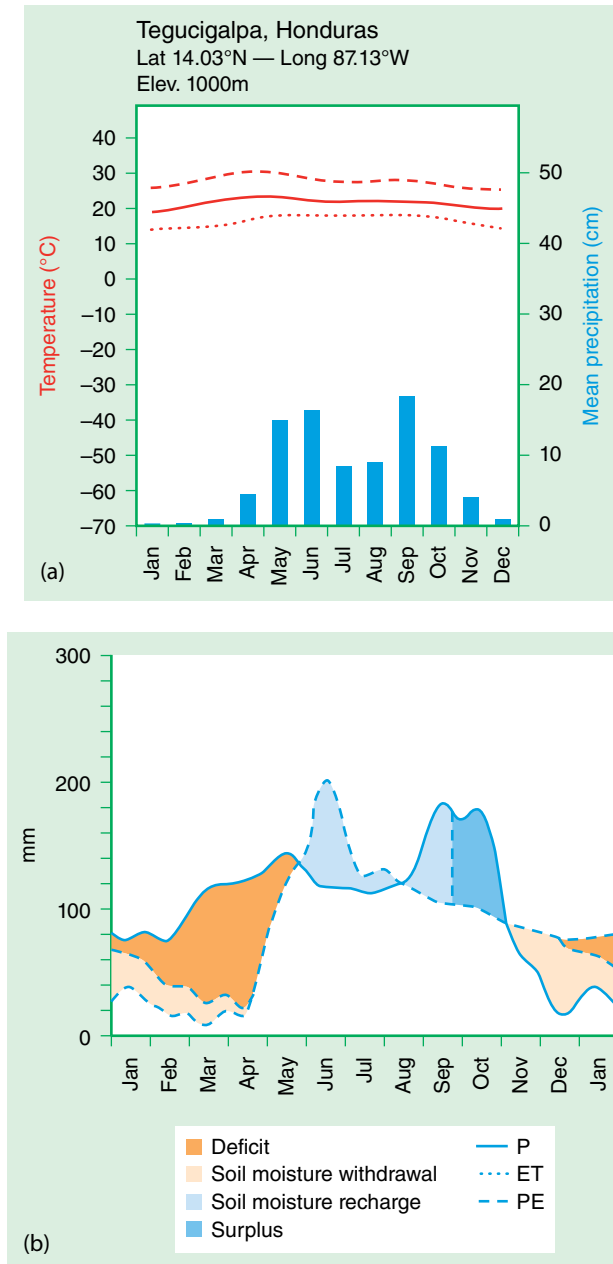


FIGURE 10.17 (a) Climograph for Tegucigalpa, Honduras (Am climate). Average annual temperature is 22.3°C (72.2°F) and average annual precipitation is 90.7 cm (35.7 in). (b) Water balance diagram for Tegucigalpa, Honduras.

(a) Data from National Centers for Environmental Information. (b) Modified with permission using Web/WIMP version 1.01 implemented by K. Matsuura, C. Willmott, and D. Legates at the University of Delaware, 2003.

Many anthropologists believe that the Aw climate provided the optimal environment for the survival and proliferation of early hominids. Disease would be less problematic, and predators would be seen more easily in this environment than in a rain forest environment;



FIGURE 10.18 An acacia tree with surrounding savanna grasses.

© vega bogaerts/Shutterstock, Inc.

early humans could have fled into one of the sporadic trees to avoid predators. Standing on two legs, rather than four, and walking upright was necessary to see over the tall grasses, leading to the development of permanent bipedal locomotion. Furthermore, some anthropologists suggest that the hair on our heads and eyebrows evolved as protection from the high solar angles in Aw climates for early humans, when they began to walk on two legs through the savanna grasses.

Thermal Characteristics. Despite the fact that tropical climates are characterized by an absence of winter, temperatures in Aw climates show more annual variation than the other tropical climates, largely the result of strong differences in cloud cover and humidity between the wet and dry seasons. This climatic type also supports higher diurnal temperature variations with higher daily maximum air temperatures and lower minima than the other tropical climates. The diurnal range peaks during the dry season. This may be seen in the climographs for selected locations having Aw climates (**FIGURES 10.19a** through **10.26a**). In general, temperature maxima may push into the thirties Celsius (upper nineties Fahrenheit), or even near 38°C (100°F), whereas minima may dip into the teens Celsius (fifties Fahrenheit). Monthly means are typically between 19 and 28°C (66 and 82°F).

Moisture Characteristics. Precipitation in Aw climates is largely driven by the ITCZ and the influence of the large-scale monsoonal wind shift for these regions. During the high-sun “summer” period the ITCZ approaches, increasing the chance of convective precipitation. The dry season occurs during the low-sun “winter” as the ITCZ migrates into the opposite hemisphere. Particularly in Asia, the low-sun “winter” period is characterized by relatively dry

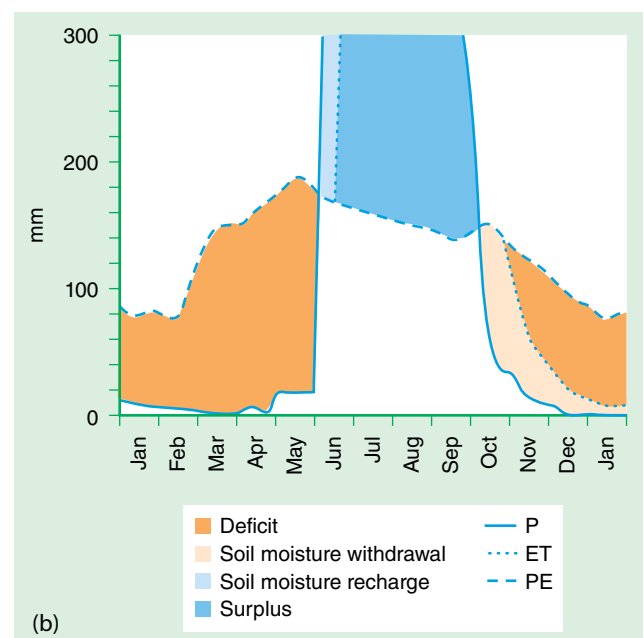
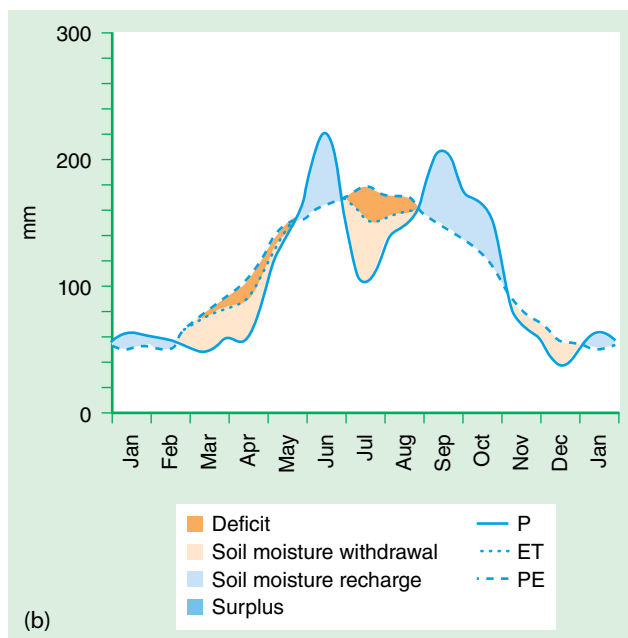
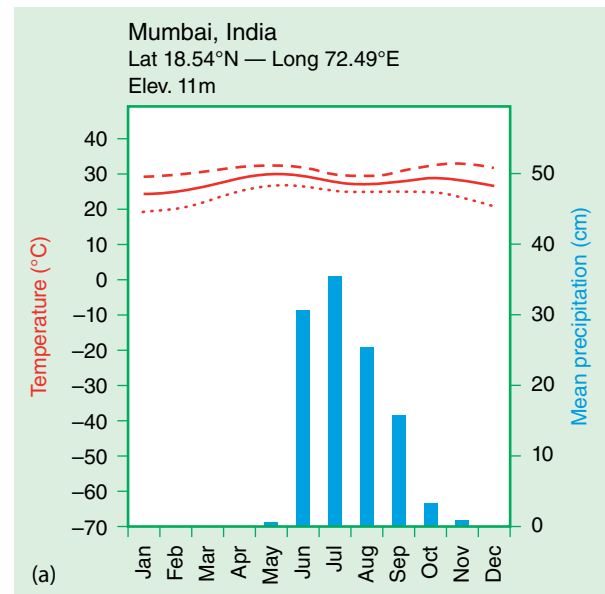
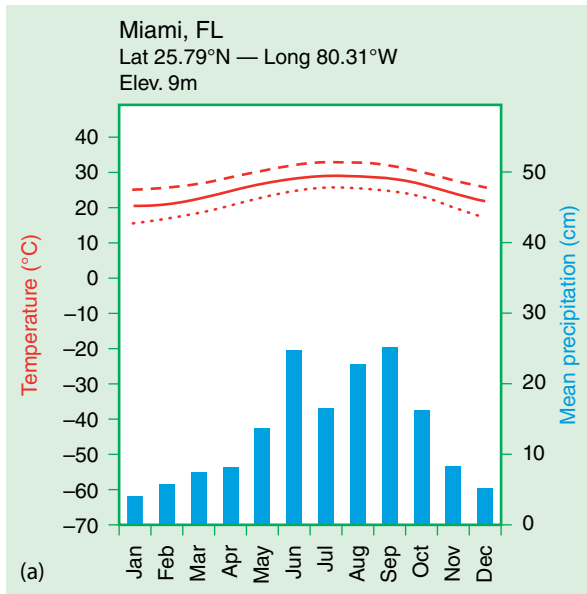


FIGURE 10.19 Climograph for Miami, Florida (Aw climate). (a) Average annual temperature is 24.8°C (76.7°F) and average annual precipitation is 148.7 cm (58.5 in). (b) Water balance diagram for Miami, Florida.

(a) Data from National Centers for Environmental Information. (b) Modified with permission using Web/WIMP version 1.01 implemented by K. Matsuura, C. Willmott, and D. Legates at the University of Delaware, 2003.

FIGURE 10.20 (a) Climograph for Mumbai, India (Aw climate). Average annual temperature is 27.2°C (81.0°F) and average annual precipitation is 216.7 cm (85.3 in). (b) Water balance diagram for Mumbai, India.

(a) Data from National Centers for Environmental Information. (b) Modified with permission using Web/WIMP version 1.01 implemented by K. Matsuura, C. Willmott, and D. Legates at the University of Delaware, 2003.

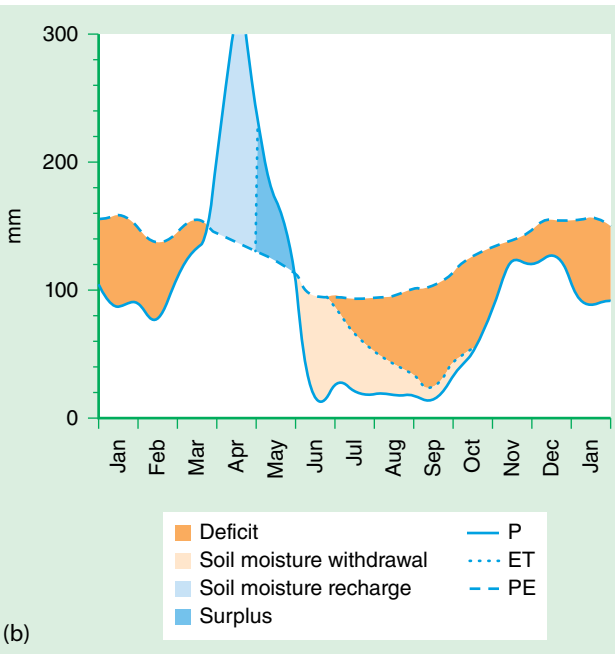
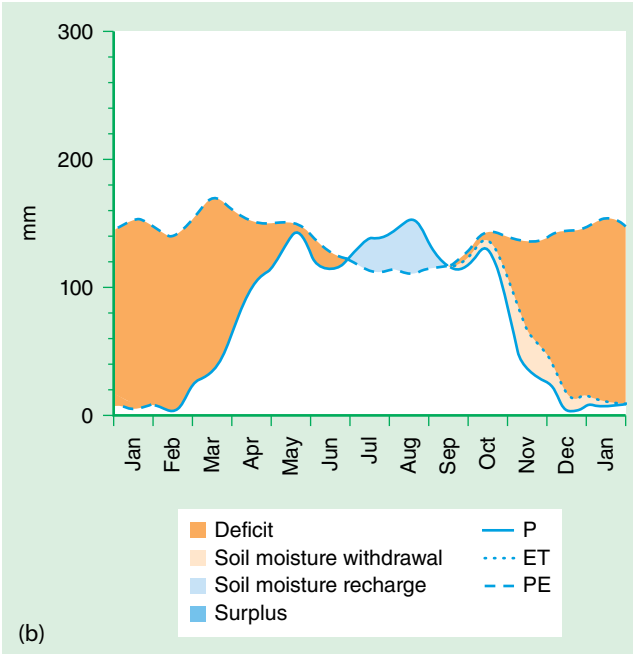
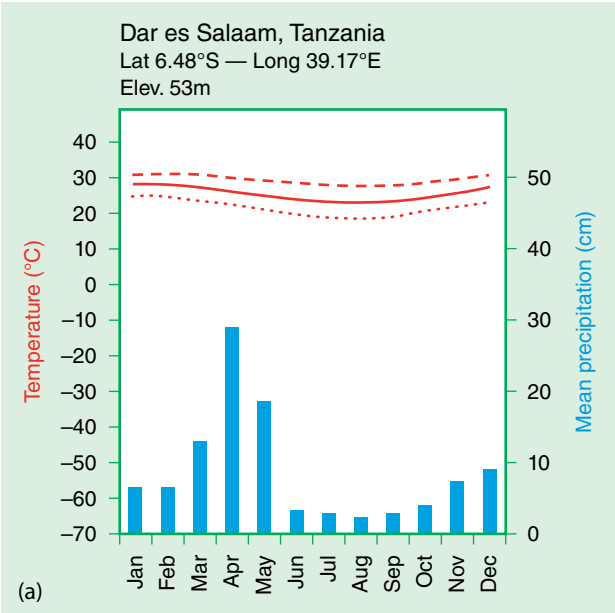
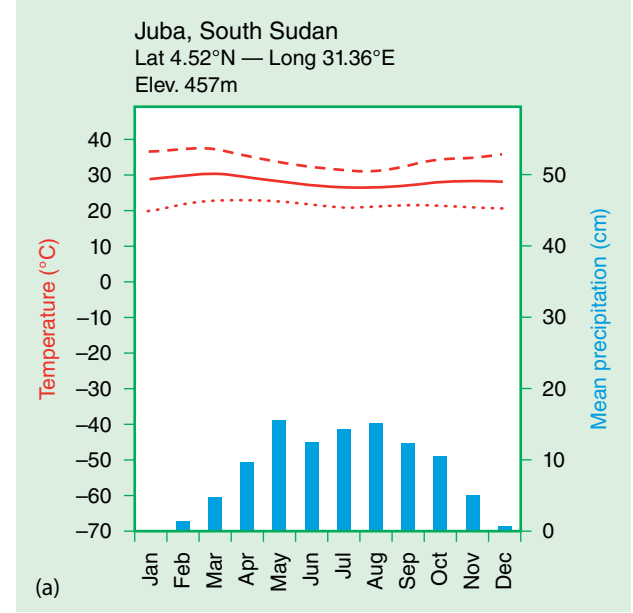


FIGURE 10.21 (a) Climograph for Juba, South Sudan (Aw climate). Average annual temperature is 26.4°C (79.5°F) and average annual precipitation is 97.0 cm (38.2 in). (b) Water balance diagram for Juba, South Sudan.

(a) Data from National Centers for Environmental Information. (b) Modified with permission using Web/WIMP version 1.01 implemented by K. Matsuura, C. Willmott, and D. Legates at the University of Delaware, 2003.

FIGURE 10.22 (a) Climograph for Dar es Salaam, Tanzania (Aw climate). Average annual temperature is 25.8°C (78.5°F) and average annual precipitation is 105.4 cm (41.5 in). (b) Water balance diagram for Dar es Salaam, Tanzania.

(a) Data from National Centers for Environmental Information. (b) Modified with permission using Web/WIMP version 1.01 implemented by K. Matsuura, C. Willmott, and D. Legates at the University of Delaware, 2003.

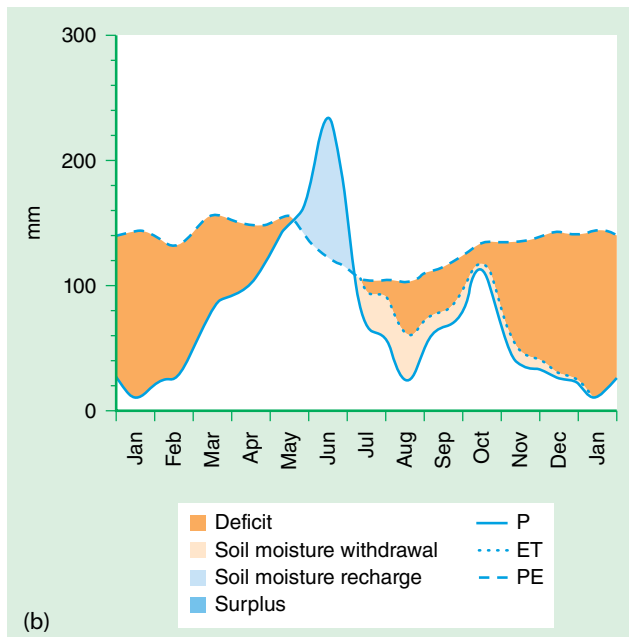
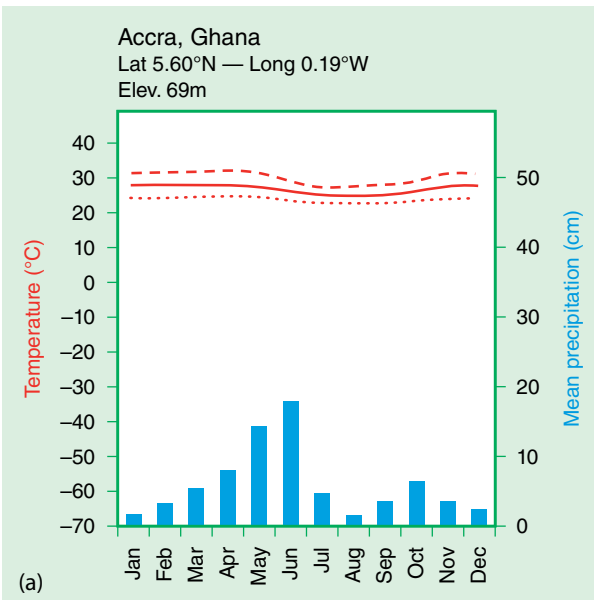


FIGURE 10.23 (a) Climograph for Accra, Ghana (Aw climate). Average annual temperature is 27.2°C (80.9°F) and average annual precipitation is 74.9 cm (29.5 in). (b) Water balance diagram for Accra, Ghana.

(a) Data from National Centers for Environmental Information. (b) Modified with permission using Web/WIMP version 1.01 implemented by K. Matsuura, C. Willmott, and D. Legates at the University of Delaware, 2003.

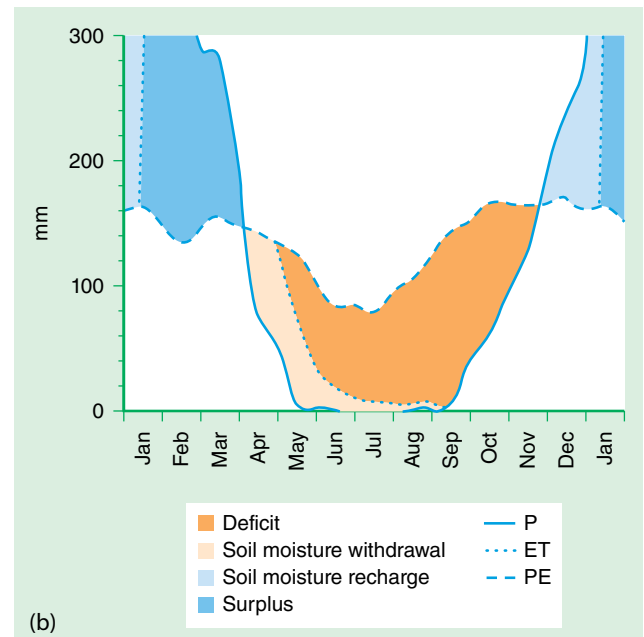
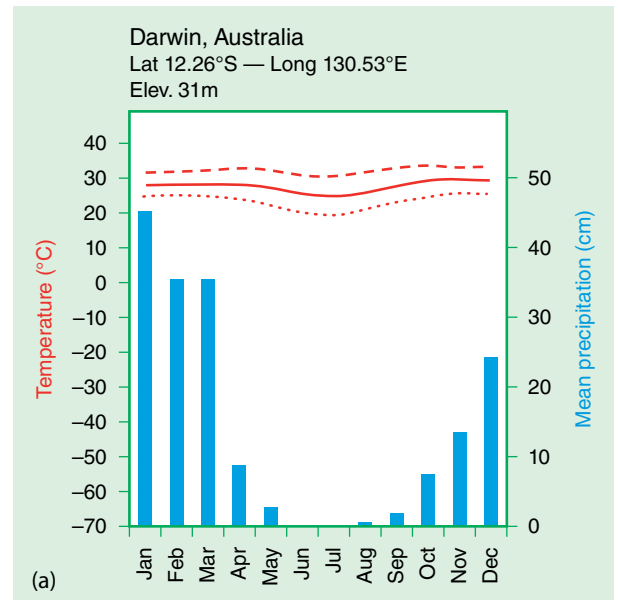


FIGURE 10.24 (a) Climograph for Darwin, Australia (Aw climate). Average annual temperature is 27.8°C (82.0°F) and average annual precipitation is 157.2 cm (61.9 in). (b) Water balance diagram for Darwin, Australia.

(a) Data from National Centers for Environmental Information. (b) Modified with permission using Web/WIMP version 1.01 implemented by K. Matsuura, C. Willmott, and D. Legates at the University of Delaware, 2003.

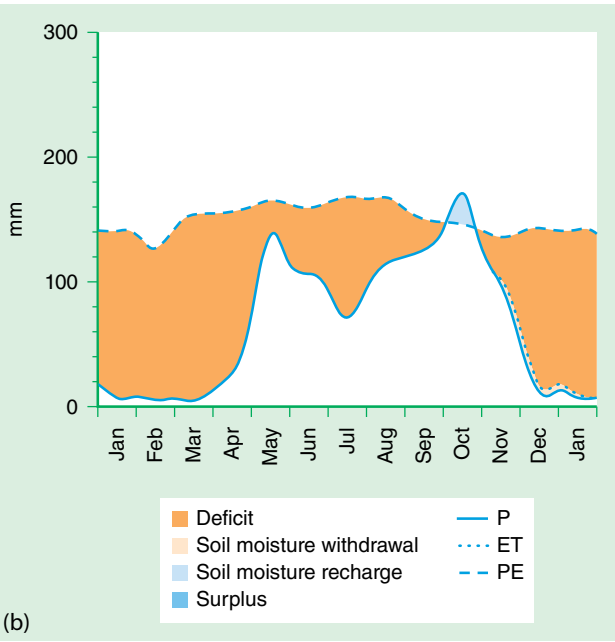
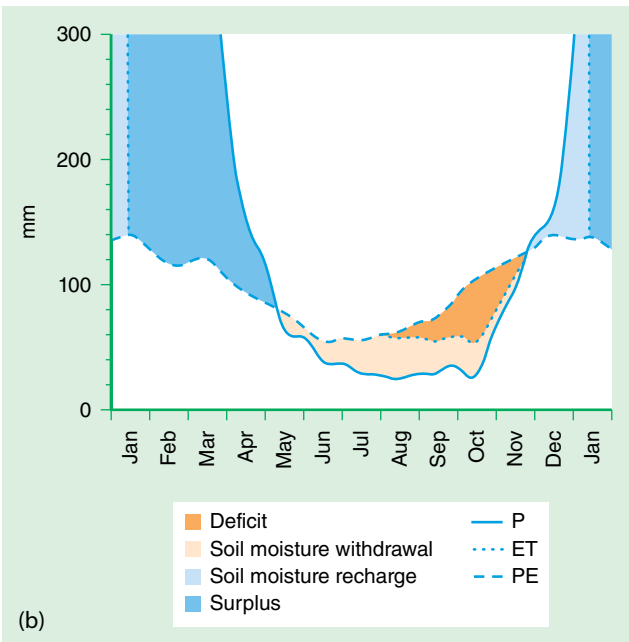
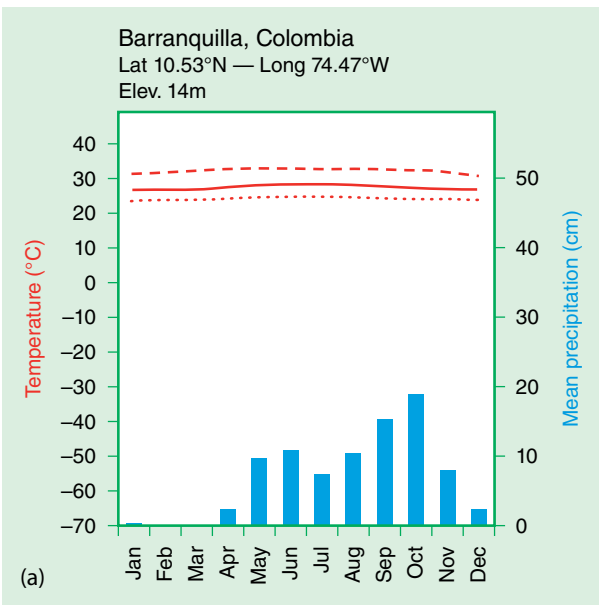
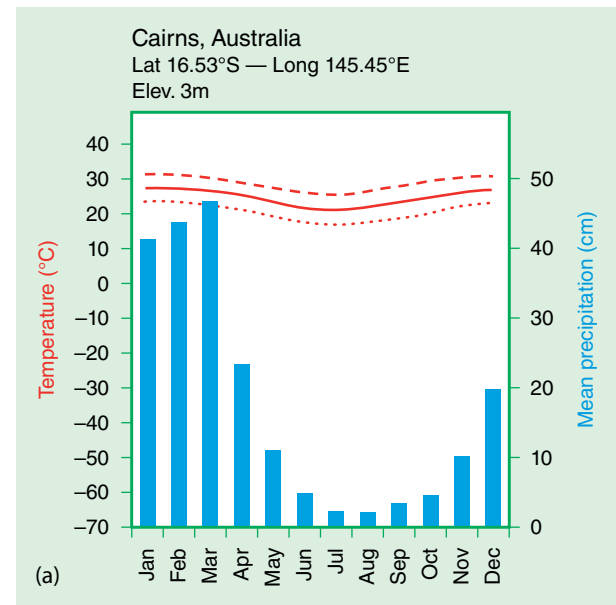


FIGURE 10.25 (a) Climograph for Cairns, Australia (Aw climate). Average annual temperature is 24.7°C (76.5°F) and average annual precipitation is 198.4 cm (78.1 in). (b) Water balance diagram for Cairns, Australia.

(a) Data from National Centers for Environmental Information. (b) Modified with permission using Web/WIMP version 1.01 implemented by K. Matsuura, C. Willmott, and D. Legates at the University of Delaware, 2003.

FIGURE 10.26 (a) Climograph for Barranquilla, Colombia (Aw climate). Average annual temperature is 27.9°C (82.3°F) and average annual precipitation is 85.9 cm (33.8 in). (b) Water balance diagram for Barranquilla, Colombia.

(a) Data from National Centers for Environmental Information. (b) Modified with permission using Web/WIMP version 1.01 implemented by K. Matsuura, C. Willmott, and D. Legates at the University of Delaware, 2003.

offshore airflow from the monsoon, which decreases the chances of cloud and precipitation development. Some African and northern Australian locations experience less-pronounced monsoon-like shifts.

Annual precipitation totals typically fall between 75 and 175 cm (30 and 70 in). Many locations have two distinct precipitation maxima, once when the ITCZ traverses the region on its poleward migration and again when it migrates equatorward. Poleward edges of the Aw climatic zone typically display a single precipitation maximum because the ITCZ generates abundant precipitation over the region at only one time during the year.

Tropical savanna locations are drier than the more equatorial regions, with some months receiving virtually no precipitation. These poleward areas may be thought of as transition zones between the low-latitude rain forests and the much drier higher-latitude continental interiors. Because ITCZ migration is variable, annual precipitation totals show a high degree of interannual variability. Extreme variability is also evident in the intra-annual precipitation totals, which may fluctuate between intense flooding and prolonged drought during the same year.

The distinct dry season combines with high energy and temperatures to produce significant soil moisture deficits during that time, as noted in the associated water balance diagrams (FIGURES 10.19b through 10.26b). The Asian monsoon influence is particularly evident in the water balance diagram for Mumbai, India (Figure 10.20b). During summer, the local water balance indicates strong *surpluses* despite higher energy values. This stems from the overabundance of ITCZ and monsoon-influenced precipitation. Soil moisture decreases rapidly after the onset of the dry season. Accra, Ghana (Figure 10.23b) is affected by the *West African monsoon system*.

B—Arid Climates

The dry regions that fall within the scope of this chapter are the most extensive on Earth. The largest single dry region on the planet is centered in the Sahara Desert, which extends latitudinally across northern Africa and into the adjacent Atlantic Ocean. An eastward extension of the Sahara spills into southwestern Asia, from the Arabian Peninsula into Syria, Iraq, Iran, Afghanistan, Pakistan, and western India (see world map of Köppen-Geiger climate types). Other dry regions of note include most of southern Africa, the bulk of Australia, the western fringe of South America, and large adjacent marine areas.

BW—True Desert

Most of the *True Desert (BW)* climates covered in this chapter are classified as the *Subtropical Desert (BWh)*

climate, because of the relatively low latitudes of the regions. The only region of the *Midlatitude Cold Desert (BWk)* climate exists in southern Chile as part of the Atacama Desert. The Sahara Desert dominates the BWh zone through northern Africa, encompassing over 8.6 million km² (3.3 million mi²). The desert stretches 4000 km (2500 mi) from east to west and between 1200 and 2000 km (750 and 1250 mi) north to south, or about the size of the conterminous United States.

Although the Sahara region is the hottest large region on the planet, and obviously one of the driest, this was not always the case. The desert began to form only about 3 million years ago. Before that time, the region was lush, supporting a wide variety of plants and animals.

Contrary to popular belief, the Sahara is not a vast expanse of sand dunes. Only about 25% of the region is classified as sand dunes. Instead, most of the Sahara consists of gravelly plains, rocky plateaus, and mountains. Still, single dunes may become enormous; the Libyan Erg dune is approximately the size of France. The desert landscape is spotted with many small oases that support freshwater springs and vegetation. Collectively, about 200,000 km² (77,000 mi²) of the region are oases. Over the centuries, nomadic people have learned the shortest routes between these areas. Of the 2.5 million people of many different groups who inhabit the region, the Tuareg are perhaps the most notable for their adaptation to the dry central desert core, as they established efficient trade routes and adapted the camel to assist in nomadic desert life.

Most of the region receives an average of less than 7 cm (3 in) of precipitation per year. Average precipitation totals may be misleading, because a substantial amount of rain may occur at one time, with little or none returning for months or even years. Several years of below-average precipitation may be needed to offset only a single year of above-average precipitation. Paradoxically, more people are believed to die from drowning in the Sahara than from thirst because of the nature of the individual rainfall events, which are typically convective thunderstorms that produce copious downpours.

Another broad desert region exists across the bulk of Australia and westward into the subtropical Indian basin. Perhaps the most famous Australian desert is the Great Sandy Desert, which occupies the northwestern interior. The continental core may be subdivided into the Great Artesian Basin, which occupies the northeastern interior; the Great Victoria Desert, which spans the southern interior; the Gibson Desert in the southwest; the Simpson Desert in the central interior; and the Great Sandy Desert in the northwest. All regions are actually part of one large, dry landscape. Other names for the dry interior include the popular Outback, the Dead Heart, and simply The Desert. All these names

conjure images of a barren, life-devoid landscape even though the region, like most deserts, abounds with specially-adapted plants and animals. Like the Sahara Desert, the deserts of Australia are marked by high temperatures. The Australian desert exists for the same primary reason that the Sahara exists—high atmospheric pressure and sinking air from the persistent influence of global subtropical anticyclones that extend across a latitudinal zone centered at 30° in both hemispheres.

The deserts of southern Africa also fall under the influence of this zone of high atmospheric pressure. The most famous desert in this region is the Kalahari, which is centered in Botswana. Other influences such as the cold Benguela current off the western coast of the continent and the *rain shadow effect* combine with the normally high atmospheric pressures to keep the regions dry. The Namib and Atacama deserts of Africa and South America, respectively, are examples of cold current-induced deserts.

The Atacama Desert extends through approximately 32° of latitude southward from near the equator. The desert begins in Peru and extends through much of the length of Chile, with the bulk of the area overlying the adjacent Pacific. As noted previously, the Atacama is the driest desert on Earth because of a combination of the cold Humboldt current and the nearby Andes Mountains that limits the *advection* of warm and moist air masses originating in the Amazon basin through the western coastal plain of South America. A rain shadow effect, therefore, helps to create the desert through blockage of the easterly trade wind flow across the low latitudes, whereas the mountains trap the cooler oceanic air on their western side, ensuring stable atmospheric conditions. On the eastern side of the mountains, moisture is effectively wrung out of the air by the orographic influence, marking the western edge of the Amazon rain forest. A further influence is provided by a temperature inversion again triggered by the nearby mountains. Cold air drainage from the higher altitudes effectively caps the lower atmosphere, stabilizing the region and reducing the possibility of cloud formation. The higher-latitude regions of the Atacama are classified as BWk because of lower annual average temperatures than the lower-latitude regions.

Thermal Characteristics. Temperatures in the BWh regions are the highest on Earth, due to clear skies and high solar angles. Most regions display a fairly wide annual range in the monthly mean temperature. The diurnal range of temperatures is considerable, because of the low atmospheric moisture content. This decreases the local greenhouse effect, allowing for efficient radiational cooling of the surface at night.

As the climographs for representative locations indicate (FIGURES 10.27a through 10.29a), the lower-latitude

locations show more monthly consistency in average temperatures than poleward locations. The climographs also show that the BWh climates experience a greater daily range in temperatures than locations in A climates.

Moisture Characteristics. Despite the low precipitation, some locations may be humid. For example, a region that records high average annual humidity is located around the Red Sea. The dampness results from a combination of high energy amounts for evaporation and a nearby water source (the sea). The dryness results from the lack of a precipitation-generating mechanism rather than a lack of atmospheric moisture.

Rainfall does occur in even the driest locations, but much is required to overcome the physical and atmospheric barriers that inhibit the precipitation-generating mechanisms in True Desert environments. BW areas display a wide range in the amount and timing of precipitation. The one unifying factor is that the totals are low and that most years have even less rainfall than average.

Virtually all these locations receive only sporadic precipitation events. As the climographs show, total annual precipitation tends to be below 10 cm (4 in) for most locations, although some locations may receive as much as 20 cm (8 in) of annual rainfall. The low precipitation amounts combine with high energy inputs to produce large water balance deficits, as depicted in the associated water balance diagrams (FIGURES 10.27b through 10.29b).

BS—Steppe

As with the True Desert locations, the *Steppe (BS) climates* of the tropics and southern hemisphere are vast. Steppe regions exist poleward of the True Desert cores. This zone represents a transition region between the deserts and the wetter climates. Steppe areas occur in a narrow coastal band on the northwest side of the Sahara Desert, through southwestern Asia, along a narrow band of the interior plateau of India, in a circular ring around the core of Australia, around the Kalahari Desert in southern Africa, the interior of southern South America, and in the Sahel region that lies south of the Sahara. Over the oceans, the Steppe areas also tend to occur on the periphery of the True Desert climates.

Thermal Characteristics. Mogadishu, Somalia (FIGURE 10.30a), is classified as a *Hot Steppe (BSH) climate*. The temperature profile indicates a small annual average range because of the moderating influence of the ocean and relatively consistently high sun angles year-round in this low-latitude city. A more representative temperature profile is indicated by the climograph

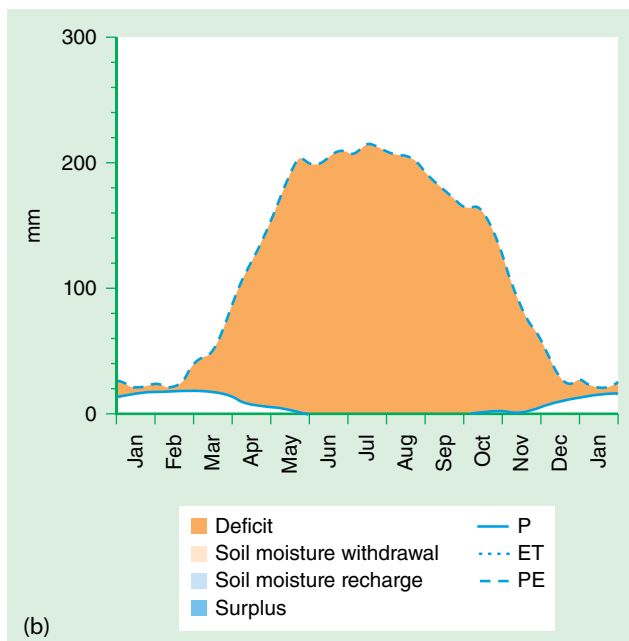
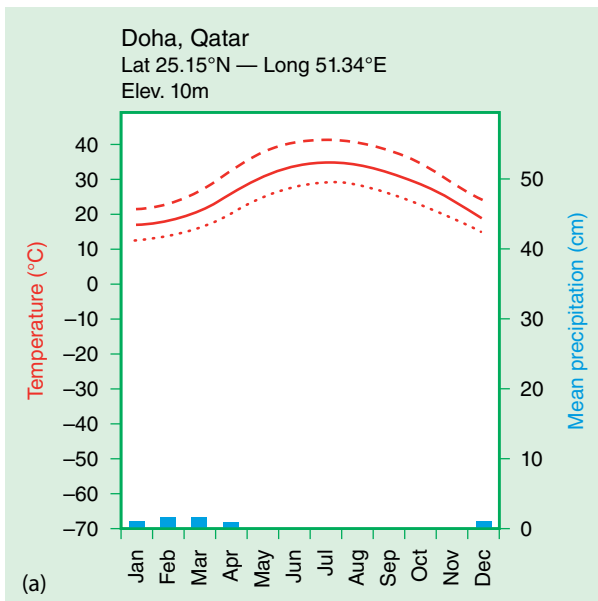


FIGURE 10.27 (a) Climograph for Doha, Qatar (BWh climate). Average annual temperature is 27.1°C (80.8°F) and average annual precipitation is 8.1 cm (3.2 in). (b) Water balance diagram for Doha, Qatar.

(a) Data from National Centers for Environmental Information. (b) Modified with permission using Web/WIMP version 1.01 implemented by K. Matsuura, C. Willmott, and D. Legates at the University of Delaware, 2003.

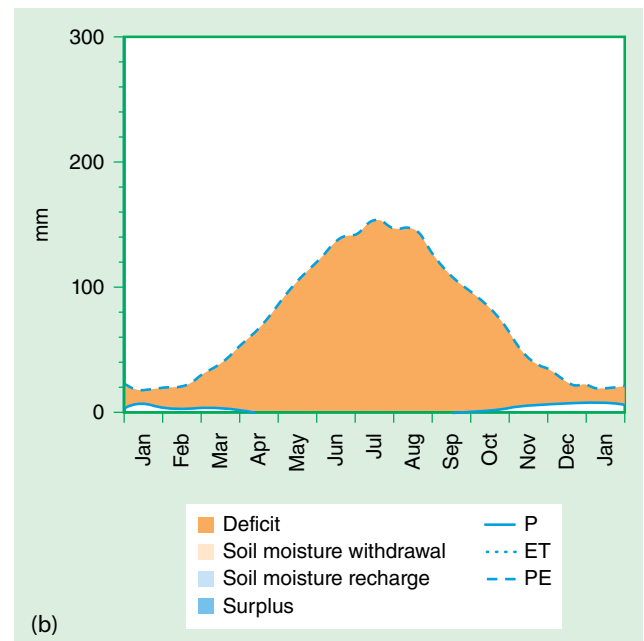
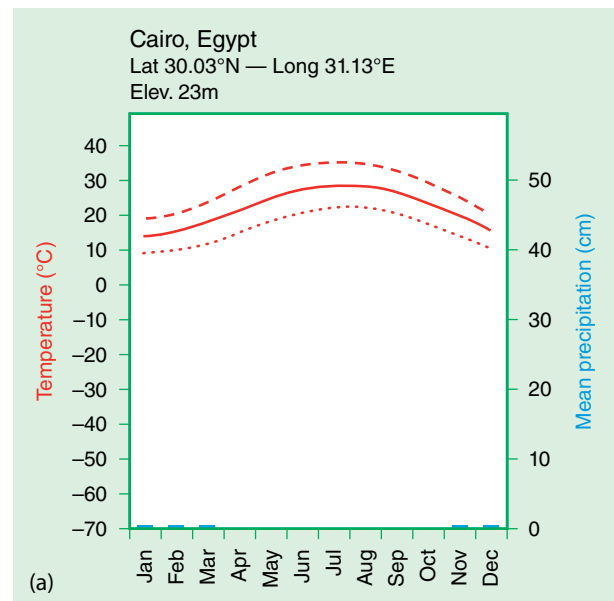


FIGURE 10.28 (a) Climograph for Cairo, Egypt (BWh climate). Average annual temperature is 21.7°C (71.0°F) and average annual precipitation is 2.3 cm (0.9 in). (b) Water balance diagram for Cairo, Egypt.

(a) Data from National Centers for Environmental Information. (b) Modified with permission using Web/WIMP version 1.01 implemented by K. Matsuura, C. Willmott, and D. Legates at the University of Delaware, 2003.

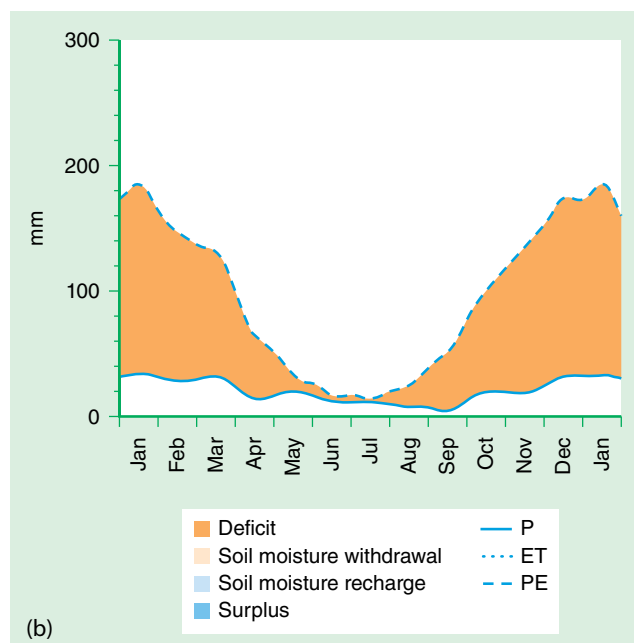
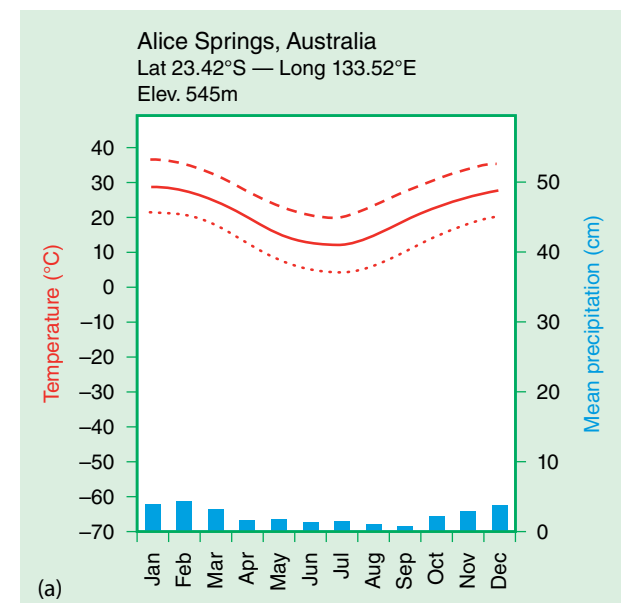


FIGURE 10.29 (a) Climograph for Alice Springs, Australia (BWh climate). Average annual temperature is 20.8°C (69.3°F) and average annual precipitation is 28.7 cm (11.3 in). (b) Water balance diagram for Alice Springs, Australia.

(a) Data from National Centers for Environmental Information. (b) Modified with permission using Web/WIMP version 1.01 implemented by K. Matsuura, C. Willmott, and D. Legates at the University of Delaware, 2003.

of Broome, Australia (**FIGURE 10.31a**), which shows a wider annual temperature range and distinct seasonality in monthly average temperatures. The *Cold Steppe (BSk) climate* in the southern hemisphere is largely restricted to midlatitude Argentina.

Moisture Characteristics. Precipitation in the steppe, although relatively low, is higher than True Desert locations. Furthermore, a distinct seasonality of precipitation is normally noticeable. Such is the case with both of the locations depicted in the climographs. Precipitation in the low-latitude Steppe is largely driven by seasonal passage of the ITCZ, which triggers daily afternoon and evening thunderstorms. Like the True Desert, there is a wide range in monthly precipitation totals across the years. The water balance diagrams (**FIGURES 10.30b** and **10.31b**) indicate severe soil moisture deficits throughout the year, but some surpluses may exist if a distinct wet season occurs.

C—Mesothermal Climates

Climates classified as mesothermal in the part of the world covered by this chapter are limited (see world map of Köppen-Geiger climate types). Only a sparse amount of land exists at the appropriate southern hemisphere latitudes. The eastern and southern coasts of Australia and all of New Zealand carry mesothermal climate designations. In addition, only parts of the extreme coastal zones of southern and northern Africa and southeastern and southwestern sections of South America have mesothermal climates.

Cfa—Humid Subtropical

The *Humid Subtropical (Cfa) climates* comprise a large percentage of the area of mesothermal climate regions of the southern hemisphere. These climates are found along an extensive region of subtropical eastern Brazil, Uruguay, and Argentina and in a small section of the central eastern coast of Australia.

Thermal Characteristics. Like their extratropical northern hemisphere counterparts, Cfa climates have hot summers and moderate winter temperatures. Average monthly means typically peak in the latter portion of summer (January or February), with averages hovering around 25 to 29°C (77 to 84°F). Daily maxima over 35°C (95°F) are common in summer. Cfa areas are also humid, but generally not as humid as in the southeastern United States. Nevertheless, summertime conditions are generally uncomfortable. Temperatures during winter may be comfortable, with averages near 10 to 15°C (50

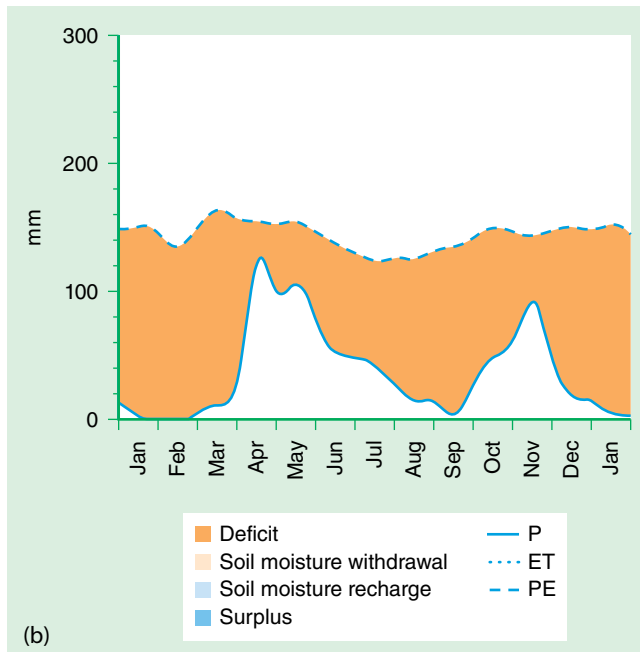
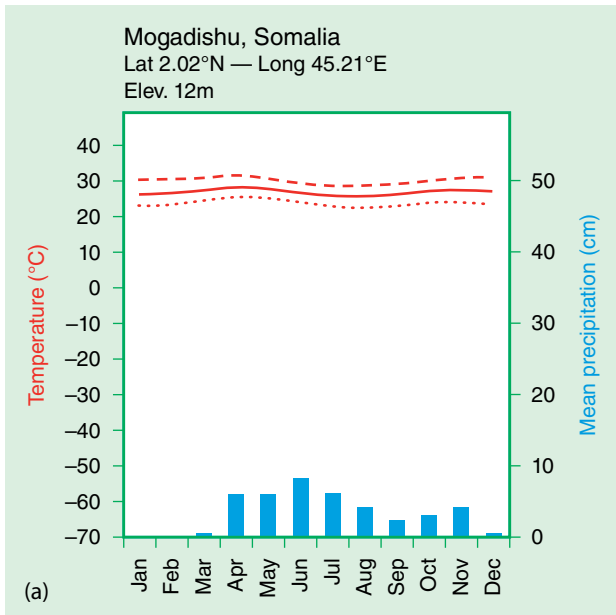


FIGURE 10.30 (a) Climograph for Mogadishu, Somalia (BSH climate). Average annual temperature is 27.7°C (81.9°F) and average annual precipitation is 41.1 cm (16.2 in). (b) Water balance diagram for Mogadishu, Somalia.

(a) Data from National Centers for Environmental Information. (b) Modified with permission using Web/WIMP version 1.01 implemented by K. Matsuura, C. Willmott, and D. Legates at the University of Delaware, 2003.

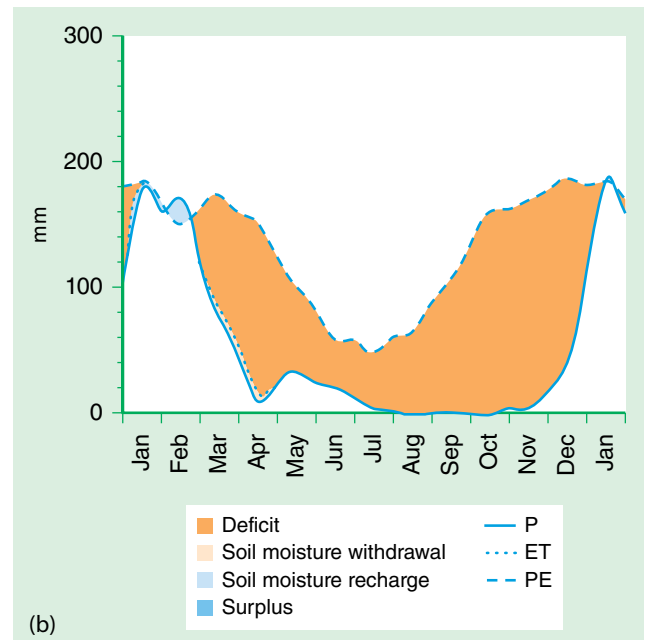
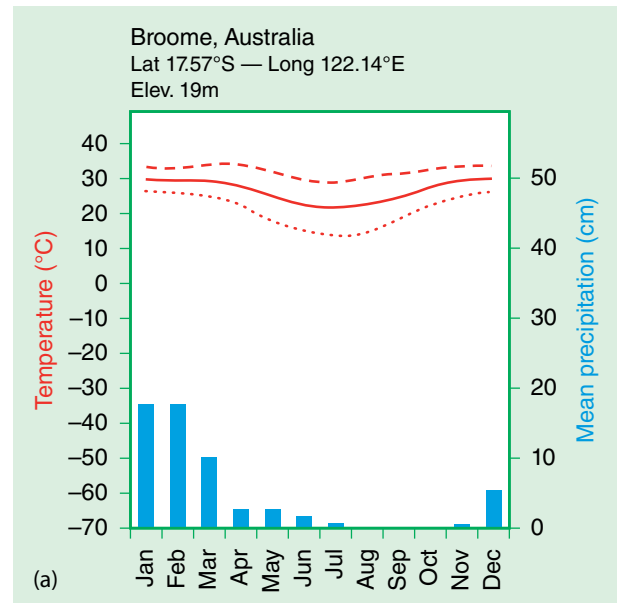


FIGURE 10.31 (a) Climograph for Broome, Australia (BSH climate). Average annual temperature is 26.5°C (79.8°F) and average annual precipitation is 57.9 cm (22.8 in). (b) Water balance diagram for Broome, Australia.

(a) Data from National Centers for Environmental Information. (b) Modified with permission using Web/WIMP version 1.01 implemented by K. Matsuura, C. Willmott, and D. Legates at the University of Delaware, 2003.

to 59°F). The annual temperature range is reflected in the associated climographs of Brisbane, Australia (FIGURE 10.32a), and Buenos Aires, Argentina (FIGURE 10.33a).

Moisture Characteristics. Precipitation is distributed relatively evenly throughout the year. Some regional variation does occur in monthly precipitation amounts, but there is no discernible dry season. A wide range of annual averages may be present, from about 50 cm (20 in) to over 180 cm (70 in). Most precipitation falling during the cool season is caused by the passage of frontal cyclones embedded within the global westerly wind flow, whereas summer precipitation is normally associated with sporadic convective thunderstorm activity.

About 12% of the world's tropical cyclones occur in the South Indian Ocean, approximately the same number as in the South Pacific. Interestingly, virtually no tropical cyclones occur in the South Atlantic Ocean, leaving eastern South America immune to their devastation. One exception occurred in April 2005, leading some to speculate on whether global warming was the culprit. But the absence of any subsequent storms since 2005 tends to suggest that the phenomenon was merely a singular, unusual event.

Large water balance deficits in the southern hemisphere's Cfa climates are uncommon, although they do occur. Periodically substantial surpluses of surface water are more common, occurring during the cooler winter season (FIGURES 10.32b and 10.33b).

Cwa—Subtropical Dry Winter

The *Humid Subtropical Winter Dry (Cwa) climate* is represented in the tropics and southern hemisphere in small sections of South America and Australia and a larger section of inland southern Africa. Dryness in winter is associated with the migration of the ITCZ away from the region, with winter temperatures too cool to remain in the tropical category. A representative example is Lusaka, Zambia (FIGURE 10.34a). Water balance deficits are common in winter (FIGURE 10.34b).

Csa, Csb—Mediterranean

As discussed elsewhere in the text, *Mediterranean climates* are generally found along the western coasts of continents in the midlatitudes. Coastal northwestern Africa falls into this category. The Mediterranean climatic type is also found along the southern coast of Australia, the southwestern tip of southern Africa, and central Chile west of the Andes.

Thermal Characteristics. Like similar areas in North America and Europe, Mediterranean climates are marked by pleasant temperature regimes. Temperatures seldom remain uncomfortably hot or cold for long periods, although uncomfortable extremes may occur for short periods of time. In the *Mediterranean Hot Summer (Csa) climate*, daily maximum temperatures may spike above 38°C (100°F). The cold ocean currents associated with the *Mediterranean Warm Summer (Csb) climate* keep summer average temperatures below 22°C (72°F). For Mediterranean climates in general, annual temperature ranges usually fall between a moderate 7 and 21°C (44 and 70°F). Winter mean monthly temperatures rarely fall below about 4°C (40°F). The Csa regime is represented by Perth, Australia (FIGURE 10.35a), whereas Cape Town, South Africa (FIGURE 10.36a), and Santiago, Chile (FIGURE 10.37a), are typical examples of Csb climates.

Moisture Characteristics. Precipitation in Mediterranean climates is largely a winter phenomenon, when the regions are influenced by the passage of midlatitude frontal systems. Summer convection typically forces whatever small precipitation totals occur during warmer times. Precipitation totals are normally between 50 and 70 cm (20 and 30 in) for most locations. Given the fact that the period of highest temperatures (summer) coincides with the driest time of the year, it is no surprise that soil moisture deficits are common in December through February (FIGURES 10.35b through 10.37b). The water balance profile leads to stunted natural vegetation types, as most plant growth occurs during the time of year with the lowest input of solar radiation.

Cfb, Cfc—Marine West Coast

The *Marine West Coast Warm Summer (Cfb) climates* are found poleward of Humid Subtropical (Cfa) climates. Paradoxically, the Marine West Coast climate is not restricted to the west coasts of continents in the southern hemisphere. In addition to its location on the western coasts of midlatitude Chile and Argentina, the Cfb climate occurs along the southeastern coast of Australia, in virtually all of Tasmania and New Zealand, and along a small sliver of southern Africa (discussed in Chapter 9). In addition, the climate occurs along scattered coastal (or near coastal) locations of southern Brazil and Argentina. A broad, continuous belt of Marine West Coast climate occurs over the midlatitude southern hemisphere ocean, with the cool summer variety (Cfc) represented in the southern hemisphere only over the oceans.

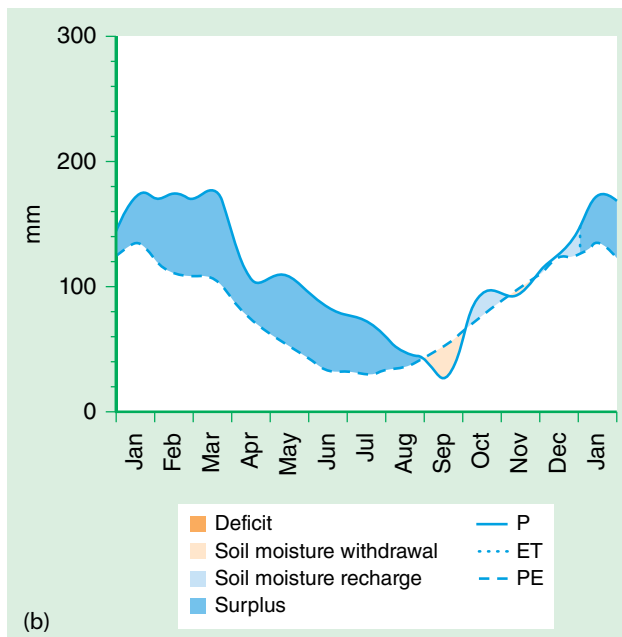
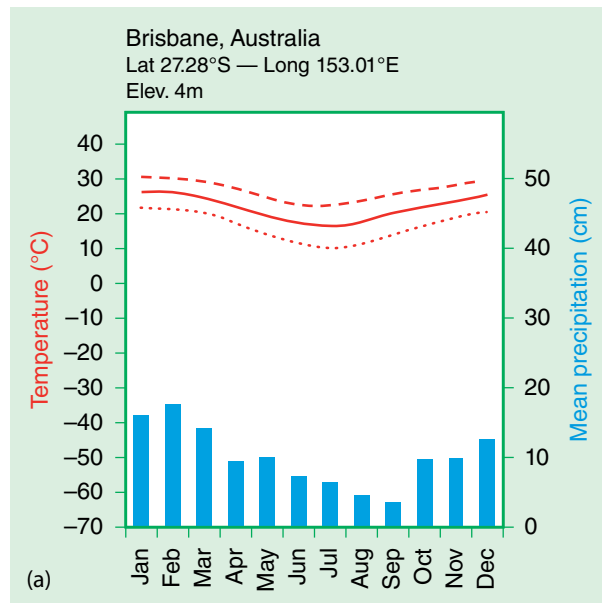


FIGURE 10.32 (a) Climograph for Brisbane, Australia (Cfa climate). Average annual temperature is 20.6°C (69.1°F) and average annual precipitation is 119.6 cm (47.1 in). (b) Water balance diagram for Brisbane, Australia.

(a) Data from National Centers for Environmental Information. (b) Modified with permission using Web/WIMP version 1.01 implemented by K. Matsuura, C. Willmott, and D. Legates at the University of Delaware, 2003.

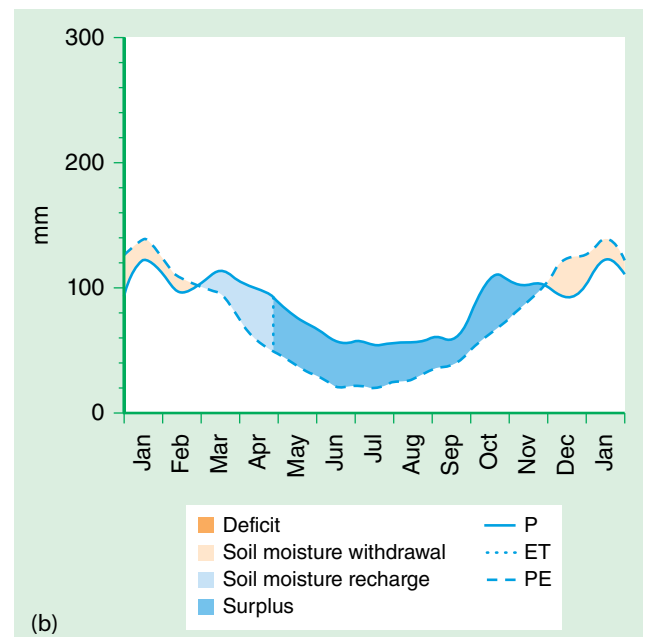
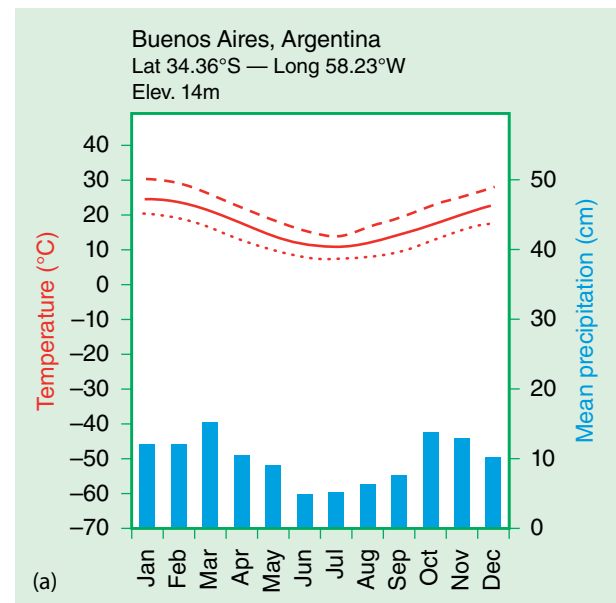


FIGURE 10.33 (a) Climograph for Buenos Aires, Argentina (Cfa climate). Average annual temperature is 16.5°C (61.7°F) and average annual precipitation is 98.0 cm (38.6 in). (b) Water balance diagram for Buenos Aires, Argentina.

(a) Data from National Centers for Environmental Information. (b) Modified with permission using Web/WIMP version 1.01 implemented by K. Matsuura, C. Willmott, and D. Legates at the University of Delaware, 2003.

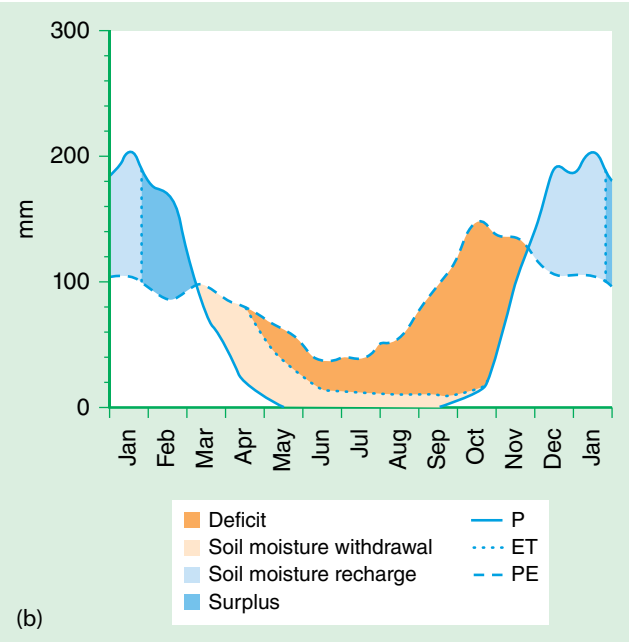
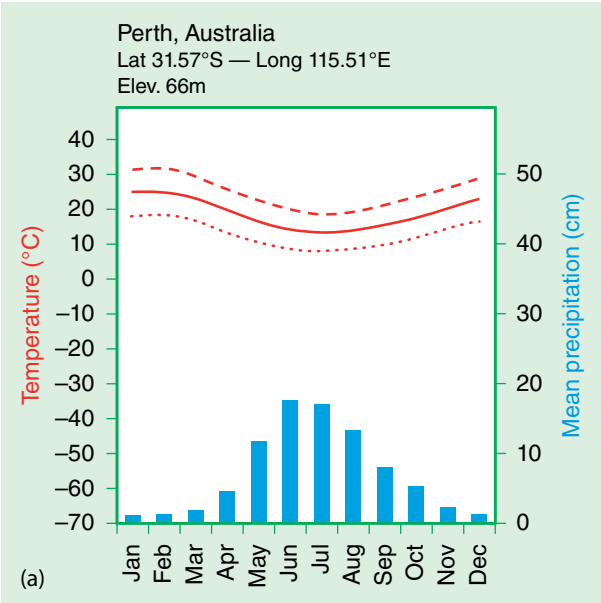
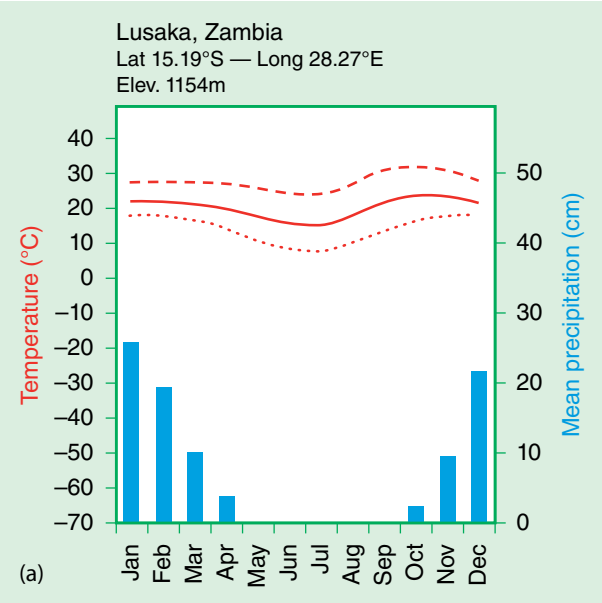


FIGURE 10.34 (a) Climograph for Lusaka, Zambia (Cwa climate). Average annual temperature is 20.6°C (69.0°F) and average annual precipitation is 81.8 cm (32.2 in). (b) Water balance diagram for Lusaka, Zambia.

(a) Data from National Centers for Environmental Information. (b) Modified with permission using Web/WIMP version 1.01 implemented by K. Matsuura, C. Willmott, and D. Legates at the University of Delaware, 2003.

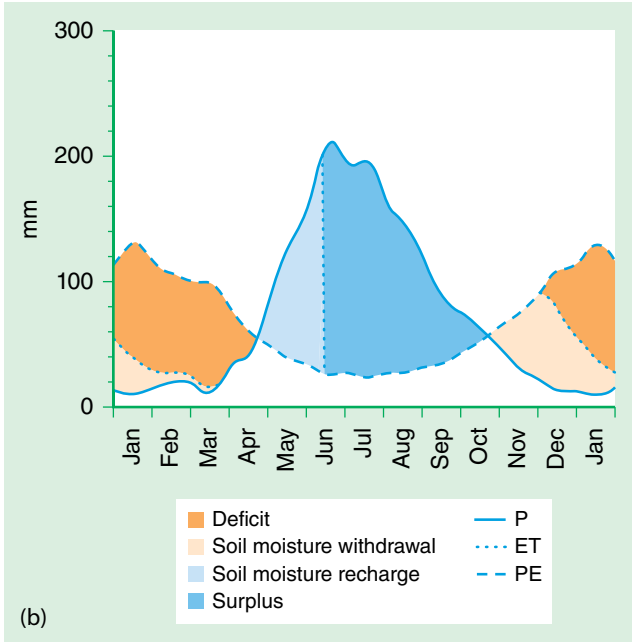


FIGURE 10.35 (a) Climograph for Perth, Australia (Csa climate). Average annual temperature is 18.0°C (64.4°F) and average annual precipitation is 79.8 cm (31.4 in). (b) Water balance diagram for Perth, Australia.

(a) Data from National Centers for Environmental Information. (b) Modified with permission using Web/WIMP version 1.01 implemented by K. Matsuura, C. Willmott, and D. Legates at the University of Delaware, 2003.

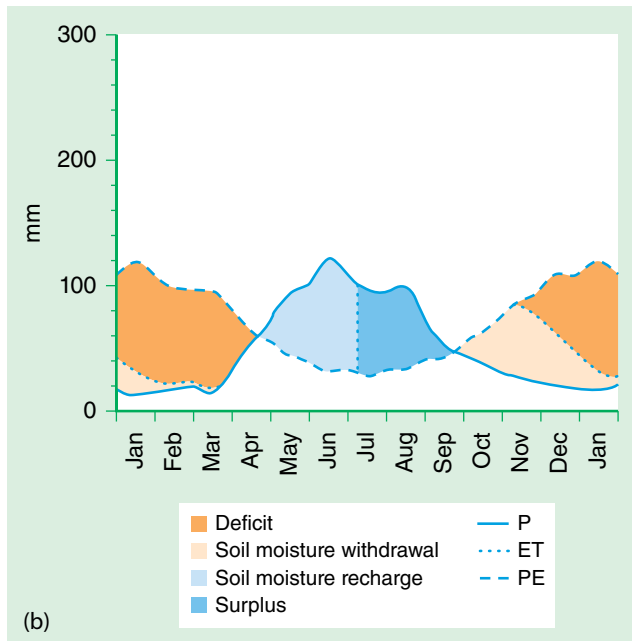
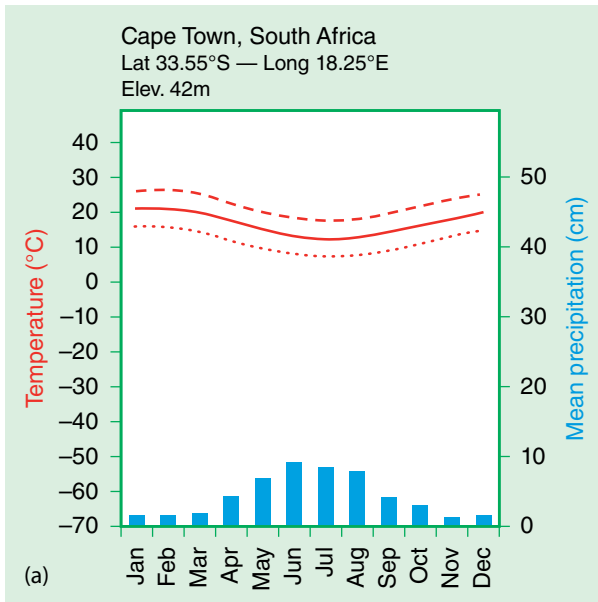


FIGURE 10.36 (a) Climograph for Cape Town, South Africa (Csb climate). Average annual temperature is 17.6°C (63.7°F) and average annual precipitation is 61.2 cm (24.1 in). (b) Water balance diagram for Cape Town, South Africa.

(a) Data from National Centers for Environmental Information. (b) Modified with permission using Web/WIMP version 1.01 implemented by K. Matsuura, C. Willmott, and D. Legates at the University of Delaware, 2003.

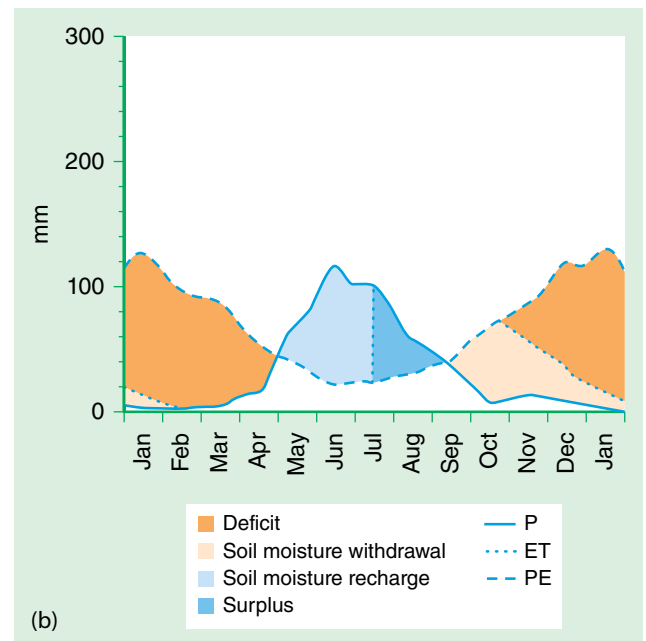
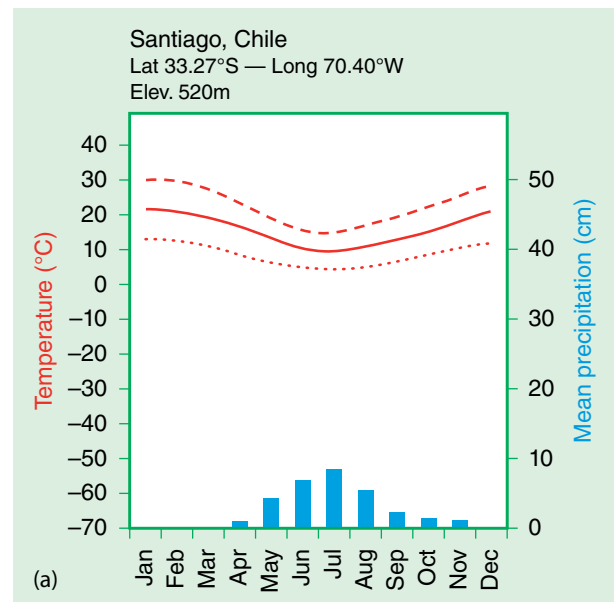


FIGURE 10.37 (a) Climograph for Santiago, Chile (Csb climate). Average annual temperature is 14.6°C (58.3°F) and average annual precipitation is 33.8 cm (13.3 in). (b) Water balance diagram for Santiago, Chile.

(a) Data from National Centers for Environmental Information. (b) Modified with permission using Web/WIMP version 1.01 implemented by K. Matsuura, C. Willmott, and D. Legates at the University of Delaware, 2003.

Thermal Characteristics. The Cfb climate is distinguished from Cfa climates by the magnitude of summer heating. Cfb regions are somewhat cooler, with the coolest month averaging below 22°C (72°F) and average daily maxima usually below 27°C (80°F). Monthly averages during summer are typically around 15 to 20°C (59 to 68°F), whereas winter months dip to approximately 0 to 10°C (32 to 50°F). Christchurch, New Zealand (FIGURE 10.38a), provides an example of the annual cycle of temperature in these climates.

Moisture Characteristics. As in northern hemisphere Cfb climates, precipitation is ample year-round, but summer tends to be drier than winter because the subtropical highs are sufficiently near to suppress large precipitation totals (FIGURE 10.38b). Cfb climates in New Zealand are affected strongly by orographic enhancement and suppression of precipitation on the windward and leeward sides and (respectively) of the Southern Alps range that runs perpendicular to the westerlies.

A variant of the Marine West Coast climate is the **Marine Dry Winter (Cwb) climate**. This climate is rare in the northern hemisphere; instead, it is more common in southeastern Africa and small parts of Brazil and Madagascar (although the part in Madagascar is too small to appear in the world map of climate types). The climographs of Pretoria, South Africa (FIGURE 10.39a), and Antananarivo, Madagascar (FIGURE 10.40a), show distinct winter dry periods, in stark contrast to the adjacent Mediterranean climates. Precipitation in Cwb locations is forced primarily by summertime convection associated with surface heating. The water balance diagrams for Pretoria (FIGURE 10.39b) and Antananarivo (FIGURE 10.40b) show smaller deficits than occur in a Cwa climate because of the cooler summer.

E—Polar Climates

Because of the lack of high-latitude land surfaces in the southern hemisphere, D climates do not exist over land, but they are fairly extensive over the high-latitude southern hemisphere ocean. *Polar climates* encompass all of Antarctica and the southernmost tip of South America, known as Tierra del Fuego (see world map of Köppen-Geiger climate types). The two types of E climates are discussed below.

ET—Tundra

The *Tundra (ET) climates* of the southern hemisphere are limited in extent because of the general absence of land masses at the latitudes in which tundra vegetation thrives. Tundra exists only on the Antarctic Peninsula extending from Ellsworth Land, Antarctica, and on

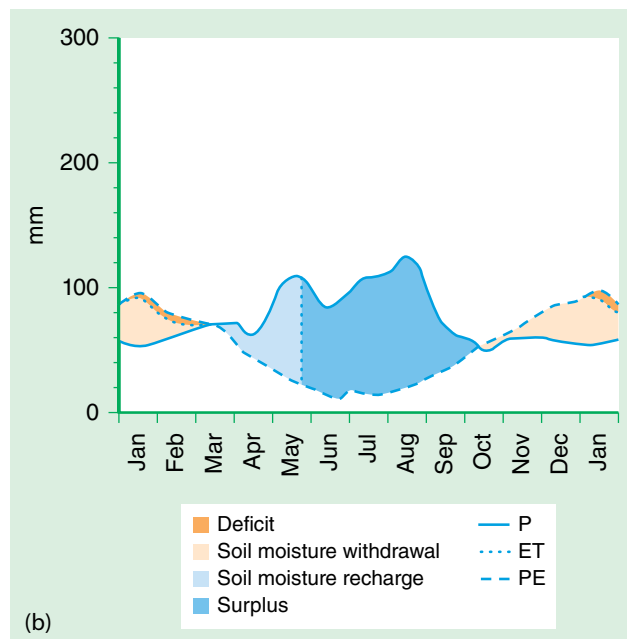
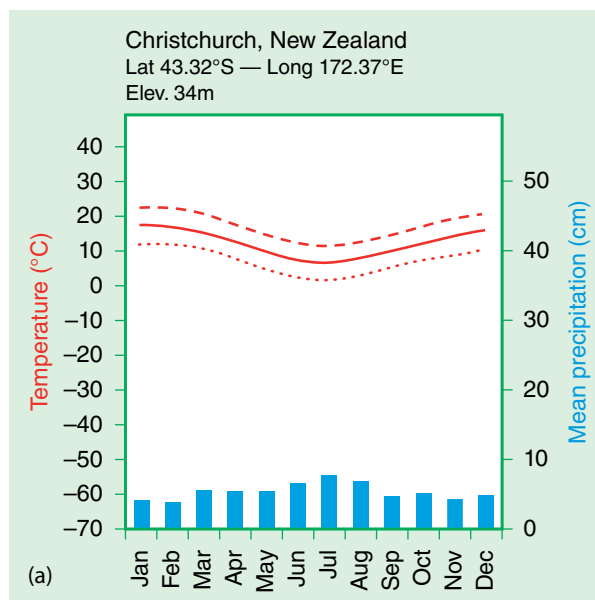


FIGURE 10.38 (a) Climograph for Christchurch, New Zealand (Cfb climate). Average annual temperature is 11.6°C (52.8°F) and average annual precipitation is 65.3 cm (25.7 in). (b) Water balance diagram for Christchurch, New Zealand.

(a) Data from National Centers for Environmental Information. (b) Modified with permission using Web/WIMP version 1.01 implemented by K. Matsuura, C. Willmott, and D. Legates at the University of Delaware, 2003.

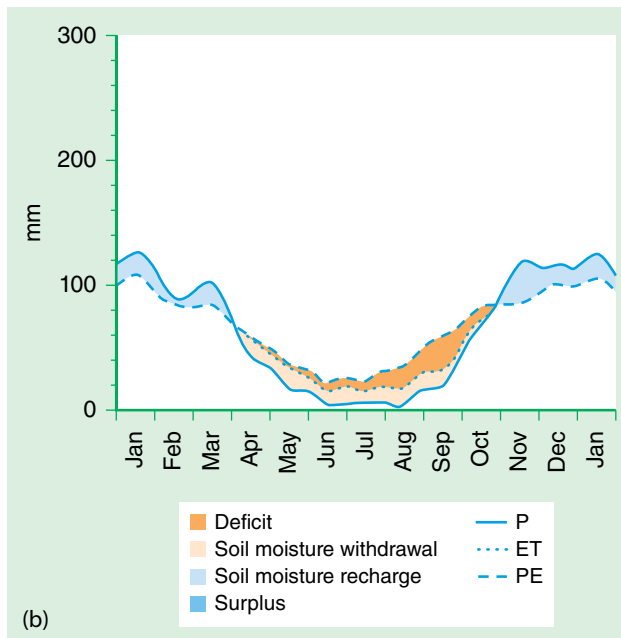
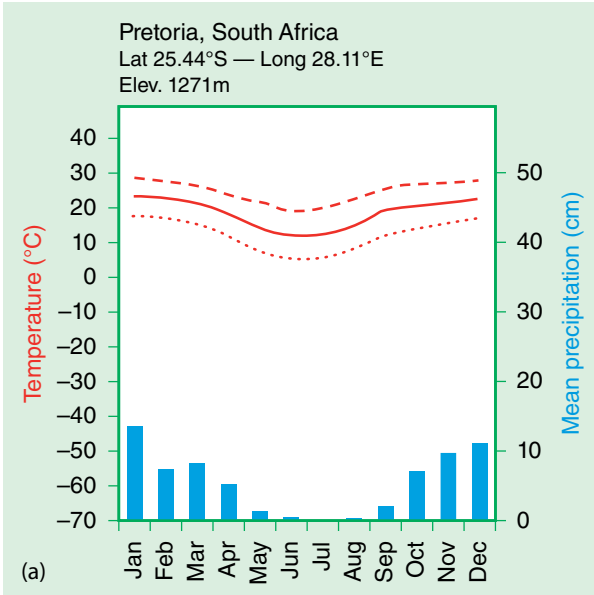


FIGURE 10.39 (a) Climograph for Pretoria, South Africa (Cwb climate). Average annual temperature is 19.0°C (66.2°F) and average annual precipitation is 70.9 cm (27.9 in). (b) Water balance diagram for Pretoria, South Africa.

(a) Data from National Centers for Environmental Information. (b) Modified with permission using Web/WIMP version 1.01 implemented by K. Matsuura, C. Willmott, and D. Legates at the University of Delaware, 2003.

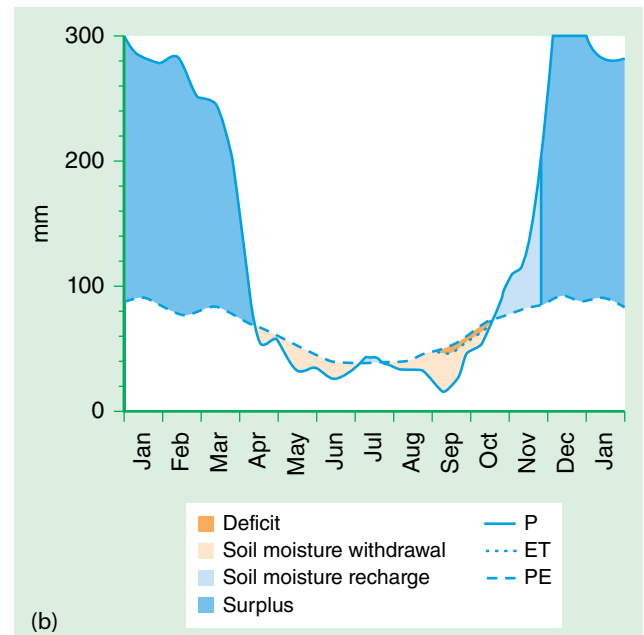
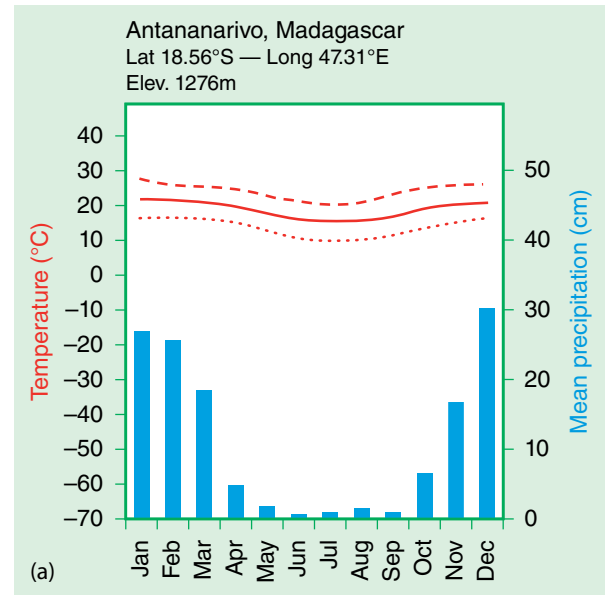


FIGURE 10.40 (a) Climograph for Antananarivo, Madagascar (Cwb climate). Average annual temperature is 19.0°C (66.2°F) and average annual precipitation is 136.1 cm (53.6 in). (b) Water balance diagram for Antananarivo, Madagascar.

(a) Data from National Centers for Environmental Information. (b) Modified with permission using Web/WIMP version 1.01 implemented by K. Matsuura, C. Willmott, and D. Legates at the University of Delaware, 2003.

some of the ice-free islands surrounding Antarctica. These locations have the most moderate climates of the Antarctic continent, because the Antarctic Peninsula represents the farthest equatorward position of Antarctica, pushing to nearly 60°S latitude, just south of the South American coast.

The small ice-free region abounds with marine-adapted life, as do the many ice-free islands of the region. Life persists because of the abundant nutrient supplies in the cold ocean waters. Many scientists regard this region as being the basis of the entire oceanic food chain because it includes a source of phytoplankton and zooplankton for much of the world ocean.

The stability of this food chain is of particular concern to many scientists, because both *phytoplankton* and **zooplankton** are susceptible to excessive amounts of *ultraviolet radiation*. The high latitudes of the southern hemisphere are impacted by the development of a seasonal ozone hole. The hole forms during winter in part as a result of the development of the *circumpolar vortex* over the cold Antarctic continent. The circumpolar vortex limits advection across the latitudes, effectively trapping gases over the continental *troposphere* and stratosphere through the cold season. Ozone amounts decrease naturally under these conditions, because the sunlight required for ozone production is absent during the long high-latitude winter.

At the same time, however, humans have accelerated the growth of the hole through the production of *chlorofluorocarbons* that react with the oxygen atoms that would otherwise produce ozone. These gases also become trapped over Antarctica during winter. This has led to a net increase in the size of the ozone hole in addition to the extension of its existence into the spring months. This is problematic considering that ultraviolet radiation is incoming during a time when ozone molecules in the stratosphere are absent. Increases in surface ultraviolet radiation have led to decreases in the production of phytoplankton and zooplankton in the oceans, damaging the ecosystem. For example, some changes in the DNA of icefish (an Antarctic fish lacking hemoglobin), and the animals that feed on those plants and animals, have already been linked to changes in ultraviolet radiation receipt. Most Earth and environmental scientists agree that if this trend continues, the entire oceanic food chain will be adversely affected. The good news is that global stratospheric ozone concentrations have increased recently as a result of the worldwide ban on CFC production that took effect in 2000.

Thermal Characteristics. As with the northern hemisphere's Tundra climates, temperatures are low throughout the year, but they do reach above the freezing point for a short time during the summer. An explosion of life occurs

during this "warm" period. To be classified as a Tundra climate, the average temperature of the warmest month must be between 0°C (32°F) and 10°C (50°F), which in the southern hemisphere occurs only on the sliver of land that comprises the Antarctic Peninsula. The highest temperature ever recorded on Antarctica, approximately 15°C (58°F), occurred at Esperanza, at 63°S latitude.

Moisture Characteristics. Precipitation is slight, with totals typically being 25 cm (10 in) or less. Precipitation is almost exclusively a summer phenomenon in this region given the extensive cold. Summer is the only season when appreciable amounts of water vapor are present in the air.

EF—Ice Cap

About 98% of Antarctica has an *Ice Cap (EF) climate*. The continental ice sheet is the largest on the planet, averaging approximately 5 km (3 mi) in thickness over an area equivalent in size to the conterminous United States. The floating Ross, Ronne, and Filchner Ice Shelves increase the area of the continent by 11%.

Katabatic winds are a prominent feature of the Antarctic climate, given the high altitude of the land mass. Like Greenland, the katabatic winds originate over the continental ice sheet where air chills and spreads toward the low-elevation coastal locations. The extreme winds, blowing across the featureless ice sheet in a low-friction environment, reduce the **wind-chill factor**—a contrived "temperature" that indexes human comfort by taking both temperature and wind speed into account. The low wind-chill factor makes for even harsher conditions for living creatures than would exist through low temperatures alone. Not surprisingly, the average wind speed is the highest for any continent. High winds cause frequent blizzards of blowing ice and snow. Because of the physical geography of the continent, the area of unimpeded ocean surrounding the land mass produces the most violent seas on Earth. These can be especially treacherous during storms.

Thermal Characteristics. The extreme cold results from the high latitude of the continent. The latitude effect combines with the large land mass to produce a significant continentality effect. However, even mean summer temperatures remain below freezing, due to the latitude and resultant low solar angles. January temperatures for most inland areas average below −18°C (0°F).

Moisture Characteristics. Because of the size of the land mass and higher latitude, Antarctica is much colder and drier than Greenland. The extremely low saturation vapor pressure of such cold air causes the continent to have the lowest *specific humidity* on Earth. The extreme

dryness is noticeable in the climographs of McMurdo Research Station (FIGURE 10.41) and the South Pole (FIGURE 10.42), the latter of which indicates only a trace of summer (February) average monthly precipitation. Annual precipitation totals throughout the continental areas are less than 4 cm (2 in). An occasional cyclonic storm may affect the ice cap region of the continent after formation over the southern oceans. In general, *riming*—the *deposition* of water vapor directly onto the ice surface—leads to subsequent ice accumulation, which is balanced by the slow, downward migration, and subsequent calving off of ice at the coasts. In recent years the rate of accumulation is believed to be less than the rate of calving. Water balance plots are not included for these sites, because they are meaningless in such environments.

H—Highland Climates

Highland (H) climates are scarcer in the regions covered in this chapter than they are in the midlatitude northern hemisphere. Still, even though they are too localized to

appear on global climatic maps, such as Figure 8.1, highland regions occur in Ethiopia in east-central Africa, the core of the Indonesian island of Borneo, and the spine of the western cordillera of North and Central America, continuing through the Andes mountain chain in western South America. The latter represents, by far, the most extensive highland influence. Highland climates are marked by *vertical zonation* in the climatic regimes, along with radically variable climatic conditions across short spaces. The climographs for Mexico City, Mexico (FIGURE 10.43a), Quito, Ecuador (FIGURE 10.44a), and Arequipa, Peru (FIGURE 10.45a), show the temperature and precipitation variability normally associated with highland influences. Although these regions show little variation in temperature, due to relatively low latitudes and nearly constant energy receipt through the year, the locations vary widely in precipitation. Comparison of resultant water balances (FIGURES 10.43b through 10.45b) reflects such differences, with Mexico City and Quito having large surpluses and Arequipa experiencing massive deficits.

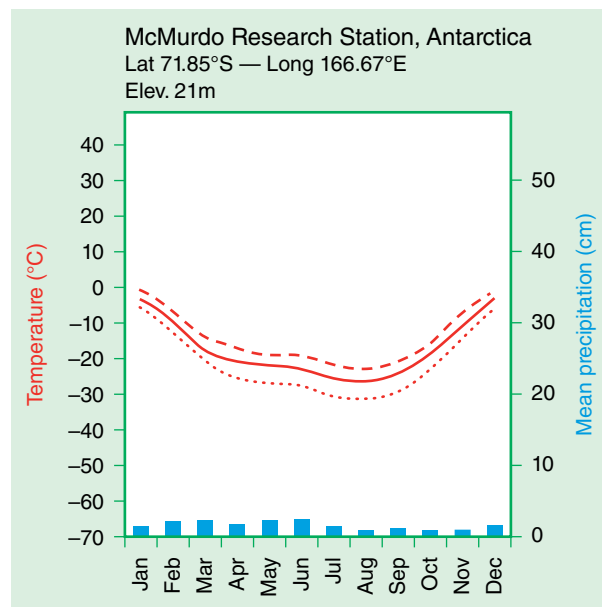
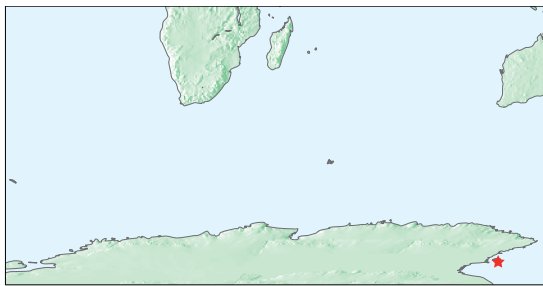


FIGURE 10.41 Climograph for McMurdo Research Station, Antarctica (EF climate). Average annual temperature is -17.2°C (1.1°F) and average annual precipitation is 19.1 cm (7.5 in).

Data from National Centers for Environmental Information.

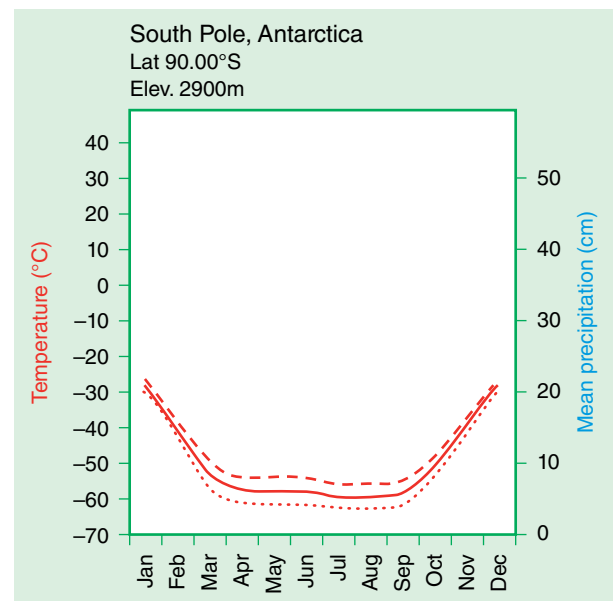
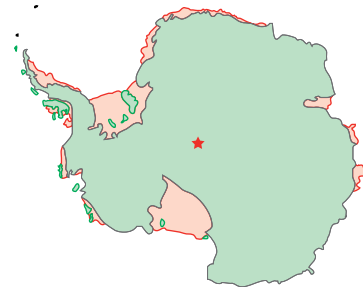


FIGURE 10.42 Climograph for South Pole, Antarctica (EF climate). Average annual temperature is -49.4°C (-56.9°F) and average annual precipitation is 0.3 cm (0.1 in).

Data from National Centers for Environmental Information.

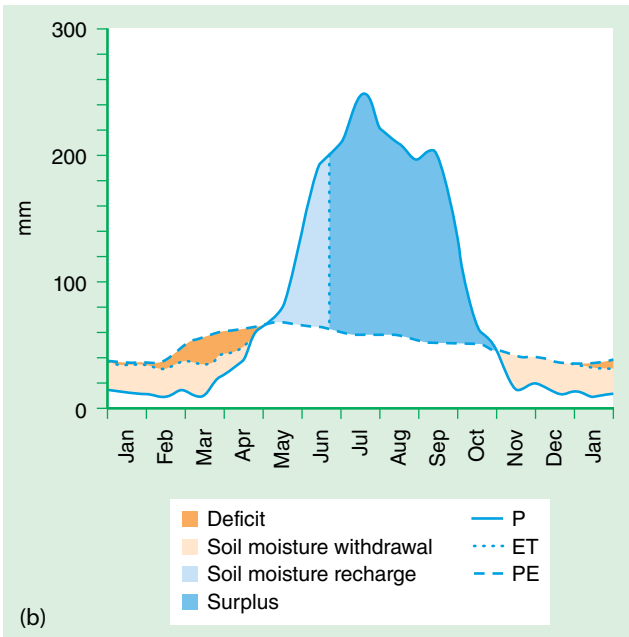
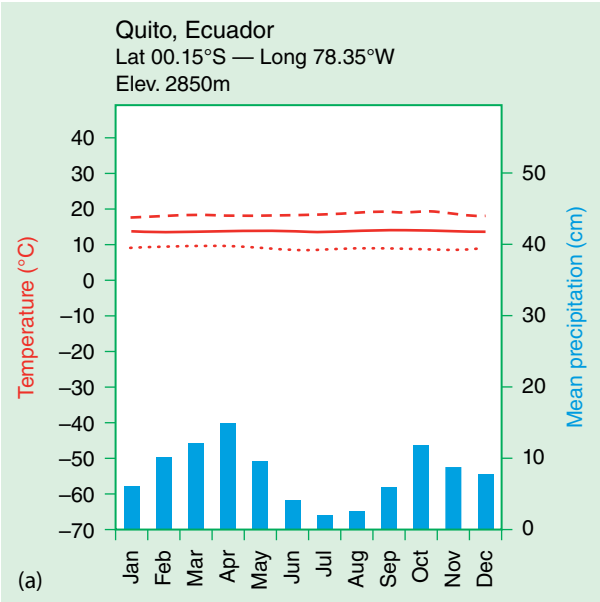
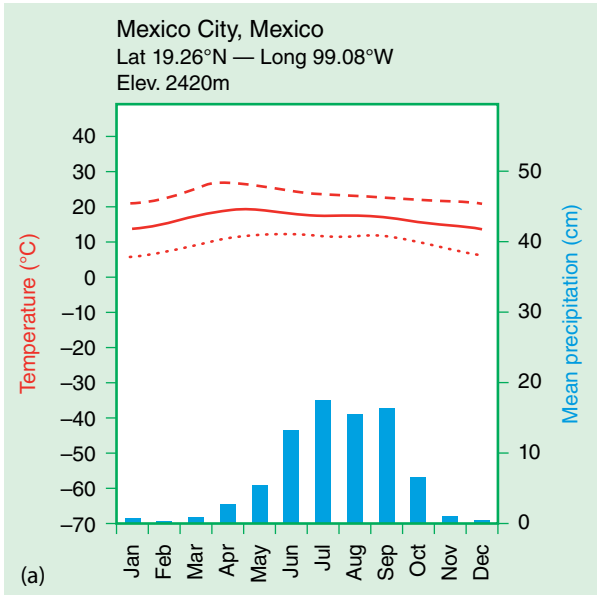


FIGURE 10.43 (a) Climograph for Mexico City, Mexico (H climate). Average annual temperature is 17.1°C (62.7°F) and average annual precipitation is 62.7 cm (24.7 in). (b) Water balance diagram for Mexico City, Mexico.

(a) Data from National Centers for Environmental Information. (b) Modified with permission using Web/WIMP version 1.01 implemented by K. Matsuura, C. Willmott, and D. Legates at the University of Delaware, 2003.

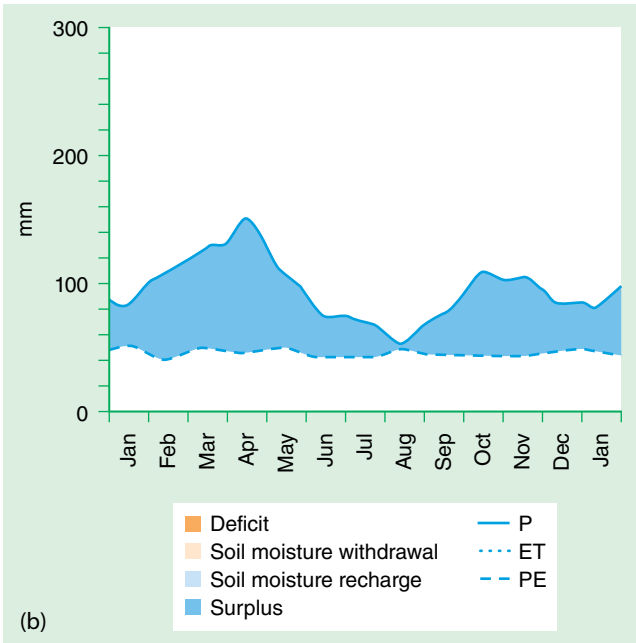


FIGURE 10.44 (a) Climograph for Quito, Ecuador (H climate). Average annual temperature is 14.5°C (58.1°F) and average annual precipitation is 120.9 cm (47.6 in). (b) Water balance diagram for Quito, Ecuador.

(a) Data from National Centers for Environmental Information. (b) Modified with permission using Web/WIMP version 1.01 implemented by K. Matsuura, C. Willmott, and D. Legates at the University of Delaware, 2003.

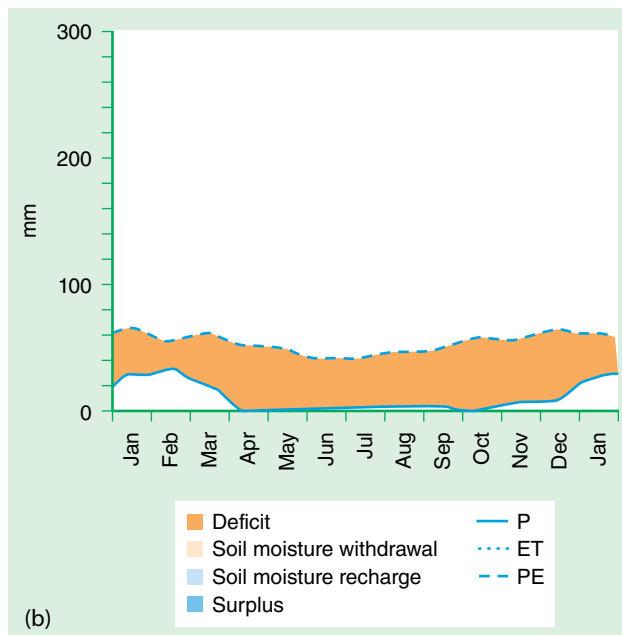
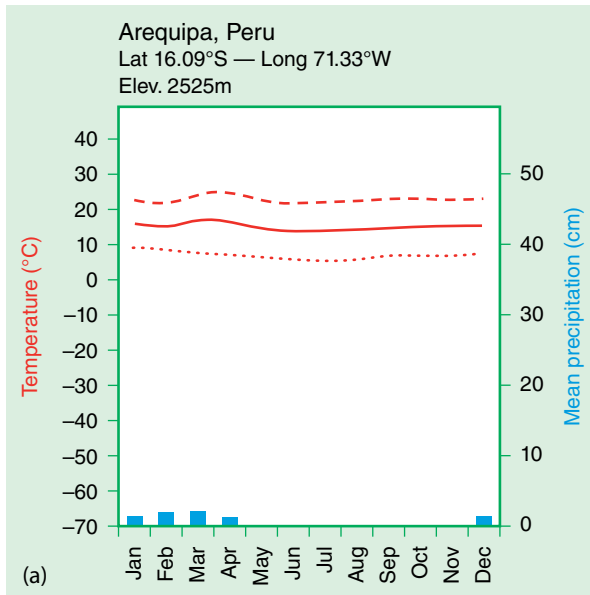


FIGURE 10.45 (a) Climograph for Arequipa, Peru (H climate). Average annual temperature is 15.0°C (58.9°F) and average annual precipitation is 9.7 cm (3.8 in). (b) Water balance diagram for Arequipa, Peru.

(a) Data from National Centers for Environmental Information. (b) Modified with permission using Web/WIMP version 1.01 implemented by K. Matsuura, C. Willmott, and D. Legates at the University of Delaware, 2003.

Summary

This chapter details the causes of regional climate variations for Africa, Oceania, South America, and Antarctica. The daunting array of regions is linked by similar climate forcings, because most of the regions exist in tropical and subtropical latitudes. Specifically, the ITCZ influences many of the climatic variations present throughout all the regions except Antarctica. Migration of the ITCZ triggers high-Sun precipitation through the affected regions, whereas associated afternoon cloud cover influences regional temperatures. The annual migration of the ITCZ causes variations in both temperature and precipitation, mainly across savanna grasslands that separate drier Steppe and True Desert regions from wetter Tropical Rain Forest or Tropical Monsoon regions. These transition zones are of particular concern, given their fragility. Long-term water shortages in these regions contribute, along with human activities, to desertification of the region. In Oceania the position of the SPCZ, an extension of the ITCZ in the South Pacific Ocean, provides another source of moisture variability.

Another common link for most of the areas discussed in this chapter is the influence of warm- and cold-ENSO events. Because ENSO forces large-scale atmospheric and oceanic changes through the tropics, most tropical regions are affected directly. Most locations see an “opposite” climate regime during warm-ENSO events from what is considered “normal.” For instance, an El Niño event usually triggers drought through northern and eastern Australia, southeastern Asia, the Amazon, equatorial Africa, and Oceania, while at the same time causing copious precipitation in western South America, eastern Africa, and western Australia.

Further commonalities for many locations include influences of the subtropical anticyclonic pressure systems embedded over each ocean basin and centered near the 30° latitude area. The subtropical highs are responsible for sinking atmospheric motions leading, at least in part, to the dry regions of Africa (both northern and southern subtropics of the continent), Australia, and South America and adjacent ocean basins. Another commonality involves the MJO, a 30- to 60-day oscillation of progressing lines of convection through the Indian and Pacific Oceans. The QBO also affects tropical latitudes with a diverse array of interactions, including precipitation variability in Southeast Asia, monsoonal variations, Sahelian precipitation, and tropical cyclone activity in the Pacific, Indian, and North Atlantic basins. A final link involves cold ocean currents, which stabilize the atmospheres of western continental coasts and contribute to the formation of deserts in western Africa, Australia, and South America, and adjacent oceans.

The only region that does not share these causes of climate variation is Antarctica. The geographical isolation of this high-latitude continent, along with the presence of an extensive ice sheet and high elevation, causes different forcing features to dominate there. Very little precipitation occurs in Antarctica because

of the extremely low temperatures and the related low saturation vapor pressure of that cold air. Instead, the region is marked by extreme katabatic winds that blow existing ice and snow downslope. New ice accumulation comes primarily through riming of water vapor directly upon the cold surface.

Key Terms

30–60 Day Oscillation	<i>El Niño–Southern Oscillation</i>	<i>Leeward</i>
40–50 Day Oscillation	(ENSO) event	<i>Longitude</i>
<i>Ablation</i>	<i>Equatorial (E) air mass</i>	<i>Longwave radiation</i>
<i>Acacia</i>	<i>Equatorial Kelvin wave</i>	<i>Madden-Julian Oscillation (MJO)</i>
<i>Advection</i>	<i>Eustatic</i>	<i>Marine Dry Winter (Cwb)</i>
<i>Advection fog</i>	<i>Evaporation</i>	climate
<i>Aghulas current</i>	<i>Evapotranspiration</i>	<i>Marine West Coast Warm</i>
<i>Air mass</i>	<i>Filchner Ice Shelf</i>	<i>Summer (Cfb) climate</i>
<i>Albedo</i>	<i>Findlater jet</i>	<i>Maritime Continent</i>
<i>Anomaly</i>	<i>Flux</i>	<i>Maritime tropical (mT) air mass</i>
<i>Anthropogenic</i>	<i>Friction</i>	<i>Mediterranean climate</i>
<i>Anticyclone</i>	<i>Front</i>	<i>Mediterranean Hot Summer</i>
<i>Aphelion</i>	<i>Geopotential height</i>	(Csa) climate
<i>Arctic amplification</i>	<i>Geostrophic balance</i>	<i>Mediterranean Warm Summer</i>
<i>Asian monsoon</i>	<i>Glacial advance</i>	(Csb) climate
<i>Autumnal equinox</i>	<i>Global warming</i>	<i>Mesothermal</i>
<i>Benguela current</i>	<i>Greenhouse effect</i>	<i>Midlatitude Cold Desert (BWk)</i>
<i>Bermuda-Azores high</i>	<i>Gyre</i>	climate
<i>Berson westerlies</i>	<i>Harmattan winds</i>	<i>Midlatitude westerlies</i>
<i>Biodiversity</i>	<i>Hawaiian high</i>	<i>Northeast trade winds</i>
<i>Canary current</i>	<i>Highland (H) climate</i>	<i>Oceania</i>
<i>Chlorofluorocarbon</i>	<i>Horizontal convergence</i>	<i>Orographic effect</i>
<i>Circumpolar vortex</i>	<i>Hot Steppe (BSh) climate</i>	<i>Ozone</i>
<i>Climograph</i>	<i>Humboldt (Peru) current</i>	<i>Perihelion</i>
<i>Cold Steppe (BSk) climate</i>	<i>Humid Subtropical (Cfa) climate</i>	<i>Photosynthesis</i>
<i>Continental tropical (cT) air mass</i>	<i>Humid Subtropical Winter Dry</i>	<i>Phytoplankton</i>
<i>Continentality</i>	(Cwa) climate	<i>Polar climate</i>
<i>Convection</i>	<i>Hurricane</i>	<i>Positive feedback system</i>
<i>Convective precipitation</i>	<i>Ice Cap (EF) climate</i>	<i>Potential evapotranspiration</i>
<i>Coriolis effect</i>	<i>Indian Ocean Dipole (IOD)</i>	<i>Pressure gradient force</i>
<i>Counter-trade winds</i>	<i>Indian Ocean high</i>	<i>Quasi-biennial oscillation (QBO)</i>
<i>Cumuliform cloud</i>	<i>Insolation</i>	<i>Rain machine</i>
<i>Cyclone</i>	<i>Intertropical Convergence Zone</i>	<i>Rain shadow effect</i>
<i>Deficit</i>	(ITCZ)	<i>Ridge</i>
<i>Deforestation</i>	<i>Inverted trough</i>	<i>Riming</i>
<i>Deposition</i>	<i>Isohypse</i>	<i>Ronne Ice Shelf</i>
<i>Desertification</i>	<i>Katabatic winds</i>	<i>Ross Ice Shelf</i>
<i>Dewpoint temperature</i>	<i>Krakatau</i>	<i>Rossby wave</i>
<i>East African low-level jet</i>	<i>Krakatau easterlies</i>	<i>Runoff</i>
<i>Easterly wave</i>	<i>La Niña</i>	<i>Sahel</i>
<i>Ekman spiral</i>	<i>Latent heat</i>	<i>Sensible heat</i>
<i>El Niño</i>	<i>Latitude</i>	<i>Siberian high</i>

<i>Soil moisture recharge</i>	<i>Subtropical Desert (BWh) climate</i>	<i>Tundra (ET) climate</i>
<i>Solar declination</i>	<i>Surface water balance</i>	<i>Turkana jet stream</i>
<i>Somali jet</i>	<i>Surplus</i>	<i>Typhoon</i>
<i>South Atlantic high</i>	<i>Temperature inversion</i>	<i>Ultraviolet radiation</i>
<i>South Pacific Convergence Zone (SPCZ)</i>	<i>Thermal low</i>	<i>Upwelling</i>
<i>South Pacific high</i>	<i>Thermocline</i>	<i>Vapor pressure</i>
<i>Southeast trade winds</i>	<i>Trade surge</i>	<i>Vernal equinox</i>
<i>Southern Oscillation</i>	<i>Tropic of Cancer</i>	<i>Vertical zonation</i>
<i>Southwesterly monsoon</i>	<i>Tropic of Capricorn</i>	<i>Water balance diagram</i>
<i>Specific humidity</i>	<i>Tropical (A) climate</i>	<i>West African monsoon system</i>
<i>Stability</i>	<i>Tropical cyclone</i>	<i>Whiteout</i>
<i>Steppe (BS) climate</i>	<i>Tropical Monsoon (Am) climate</i>	<i>Wind channeling</i>
<i>Stratiform cloud</i>	<i>Tropical Rain Forest (Af) climate</i>	<i>Wind-chill factor</i>
<i>Stratosphere</i>	<i>Tropical Savanna (Aw) climate</i>	<i>Windward</i>
<i>Streamline analysis</i>	<i>Tropopause</i>	<i>Wisconsin Glacial Phase</i>
<i>Subpolar low</i>	<i>Troposphere</i>	<i>Zooplankton</i>
<i>Subtropical anticyclone</i>	<i>Trough</i>	
	<i>True Desert (BW) climate</i>	

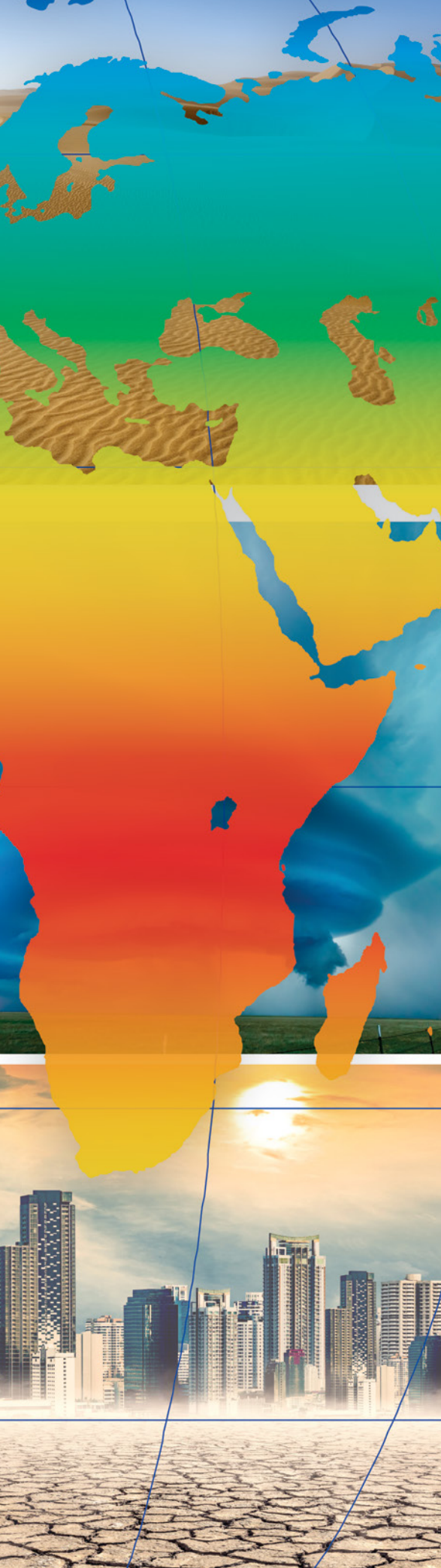
Terms in italics have appeared in at least one previous chapter.

Review Questions

- Discuss the importance of the ITCZ as a climatic control throughout the tropical regions discussed in this chapter.
- How does the SPCZ influence the climate of Oceania?
- Discuss the importance and impacts of ENSO on each of the regions discussed in this chapter.
- How does the Madden-Julian Oscillation form and propagate over time? What are the climatic contributions of the MJO in affected regions?
- Discuss the importance and ramifications of the QBO on tropical climates.
- Detail the impacts of the subtropical anticyclones on the regions covered in this chapter.
- What is the contribution of cold ocean currents to the climatic landscape of the associated regions?
- Discuss the recycling of environmental water in the rain forest regions.
- Discuss recent changes in Alpine glaciers to changes in the Antarctic ice sheet. Are the changes consistent?
- Why is it important to monitor the ice shelves extending from the Antarctic land mass?
- Detail important aspects of the Tropical Rain Forest climatic type.
- Discuss Tropical Monsoon climates.
- Why are Tropical Savanna regions considered climatic transition zones?
- Why are deserts so extensive throughout the regions covered in this chapter?
- What factors contribute to desertification in Steppe climate areas?
- Discuss the causes of mesothermal climates in the associated regions.
- Why are there no “D” climates in the regions associated with this chapter?
- Why is stratospheric ozone so important to the high-latitude regions of the southern hemisphere?

Questions for Thought

- After studying the chapters discussing climates around the world, discuss the climatic accuracies and inaccuracies portrayed in three popular movies. Would the plot of the movie have changed if the climates had been portrayed more accurately?
- Assume that a 7000-m (23,000-ft) mountain suddenly appears at your current location. Using the normal environmental lapse rate, calculate the vertical average temperature from your current elevation to the mountain peak. Based on that temperature, calculate which climatic zones would appear on the mountain, and where they would be located both vertically and horizontally (assuming shading influences, etc.).



PART 4

Climates Through Time

CHAPTER 11 Climatic Change and Variability: A Paleoclimatic Overview

- Climatic Changes in Geological History
- How Do We Know What We Know About Past Climatic Changes?
- Natural Causes of Climatic Change and Variability
- Summary
- Key Terms
- Review Questions
- Questions for Thought

CHAPTER 12 Modern Climatic Change

- Global Warming
- Atmospheric Pollution
- Classifying Air Pollutants
- Reactions and Attitudes to Climatic Change
- Summary
- Key Terms
- Review Questions
- Questions for Thought

CHAPTER 13 Linking Spatial and Temporal Aspects of Climate Through Quantitative Methods

- Computerized Climate Models
- Seven Basic Equations
- Statistical Techniques
- Atmospheric Teleconnections
- Summary
- Key Terms
- Review Questions
- Questions for Thought



CHAPTER 11

Climatic Change and Variability: A Paleoclimatic Overview

CHAPTER AT A GLANCE

- Climatic Changes in Geological History
 - Temperature
 - Ice Ages and Sea Level
 - Recent Trends
- How Do We Know What We Know About Past Climatic Changes?
 - Basic Principles
 - Radiometric Dating
 - Lithospheric and Cryospheric Evidence
 - Biological Evidence
 - Historical Data
 - Converging Proxy Evidence
- Natural Causes of Climatic Change and Variability
 - Continental Drift and Landforms
 - Milankovitch Cycles
 - Volcanic Activity
 - Variations in Solar Output
 - El Niño–Southern Oscillation Events
- Summary
- Key Terms
- Review Questions
- Questions for Thought

Climatology is about much more than just the average weather conditions over a long period of time. Climatology considers both average conditions and variability as well as *extremes*, long-term trends, and impacts of atmospheric conditions. In general, the greatest impacts occur during periods of extremes, and these extremes may provide evidence of climatic change or climatic variability.

Temporal climatic changes and variability may take many forms (FIGURE 11.1). **Random variability** (sometimes referred to as **noise**) occurs when an atmospheric variable undergoes fluctuations that do not appear to be caused systematically. Fluctuation, therefore, does not repeat at a distinct interval and is considered unimportant. **Periodic variability** takes the form of an abnormality that recurs with some relatively constant regularity. **Variability changes** may or may not involve a change in mean but include a temporal drift to larger or smaller variability about the mean.

More permanent changes include **temporal trends**, which are represented by a slow, temporal drift toward an increasing or decreasing mean in some atmospheric variable. **Step changes** involve a sudden shift to a different mean, with no slow drift toward that mean. Of course, random or periodic variability or variability change may be superimposed on any change. It also is important to note that the variability and changes need not be toward increases, as shown in Figure 11.1. Decreasing values of some atmospheric variable are just as likely to occur.

Regardless of the form of climatic variability or change, more than just the atmosphere is involved. Instead, the entire climate system is impacted by atmospheric variability and changes because the system undergoes exchanges of energy, moisture, or *momentum* (which may change in abundance) among the atmosphere, *hydrosphere*, *lithosphere*, *biosphere*, and *cryosphere*. Climatic changes do not occur in isolation.

The form of temporal change and variability being experienced can be complicated and confusing, not only because *anomalies*—observations that do not match the general prevailing trend—may obscure the pattern but also because several different forms of change and variability may exist simultaneously. Trends and cycles can be superimposed on other trends and cycles operating at longer or shorter time scales.

Another complicating effect of temporal climatic change is that the prevailing definition of “change” has itself changed over the last few decades. In the 1960s climatic change was largely used to refer to what we would now call “climatic variability”—that is, climatic inconsistencies or anomalies. In the 1970s climatic change generally connoted long-term changes, perhaps on the

order of thousands of years. The prevailing idea was that climatic change existed on time scales that were too long to be noticed during the course of a human lifetime.

In the 1980s the meaning of climatic change again shifted, this time to refer to differences in 30-year averaging periods. Traditionally, climatologists have used data sets of 30 years, terminating at the end of the last full decade. For example, for discussing annual average temperature anomalies from 2001 through 2010, the 30-year averaging period for comparison was 1971–2000, and from 2011 through the present, the 1981–2010 interval is used. Thus, climatic change came to refer to differences in atmospheric variables from one 30-year period to another, such as the 1951–1980 period versus the 1961–1990 period, even though this comparison of “normals” may indicate short-term variability trends rather than long-term climatic change.

By the 1990s climatic change came to imply that humans were having an impact, whether through the combustion of *fossil fuels*, *deforestation*, land use change, or deliberate attempts to alter the climate directly or through some combination of one or more anthropogenic causes.

Since the turn of the century, climatic change continues to imply a human influence, but with the realization that this human influence can occur on much shorter time scales than previously believed. In this light, climatic change is sometimes even seen as the difference within averaging periods rather than the differences between them.

Despite all the connotations about climatic change that have prevailed since the 1960s, the notion that climate varies is a relatively new one. Before 1900, even professional climatologists largely failed to recognize that climates change, and before the 1960s little thought was given among the general public to the idea that climates change. Even today, climate is erroneously assumed by many in the general public to be static. Yet even among people who recognize that climate varies, many do not realize that climatic variation and change can affect them in their lifetimes, despite the current prevailing theme in the scientific community that human impact on climate, across short time scales, is real. As a result, change and variability are all too often overlooked in environmental planning and hazard mitigation.

In many ways the distinction between climatic variability and climatic change has been blurred in recent years, and it is often impossible to detect whether we are experiencing variability or change as we live through the phenomena. This reality complicates the formulation of policy to deal with the phenomena. For example, should we enact long-term policy that would be necessary if the recent trend in active Atlantic *hurricane* seasons

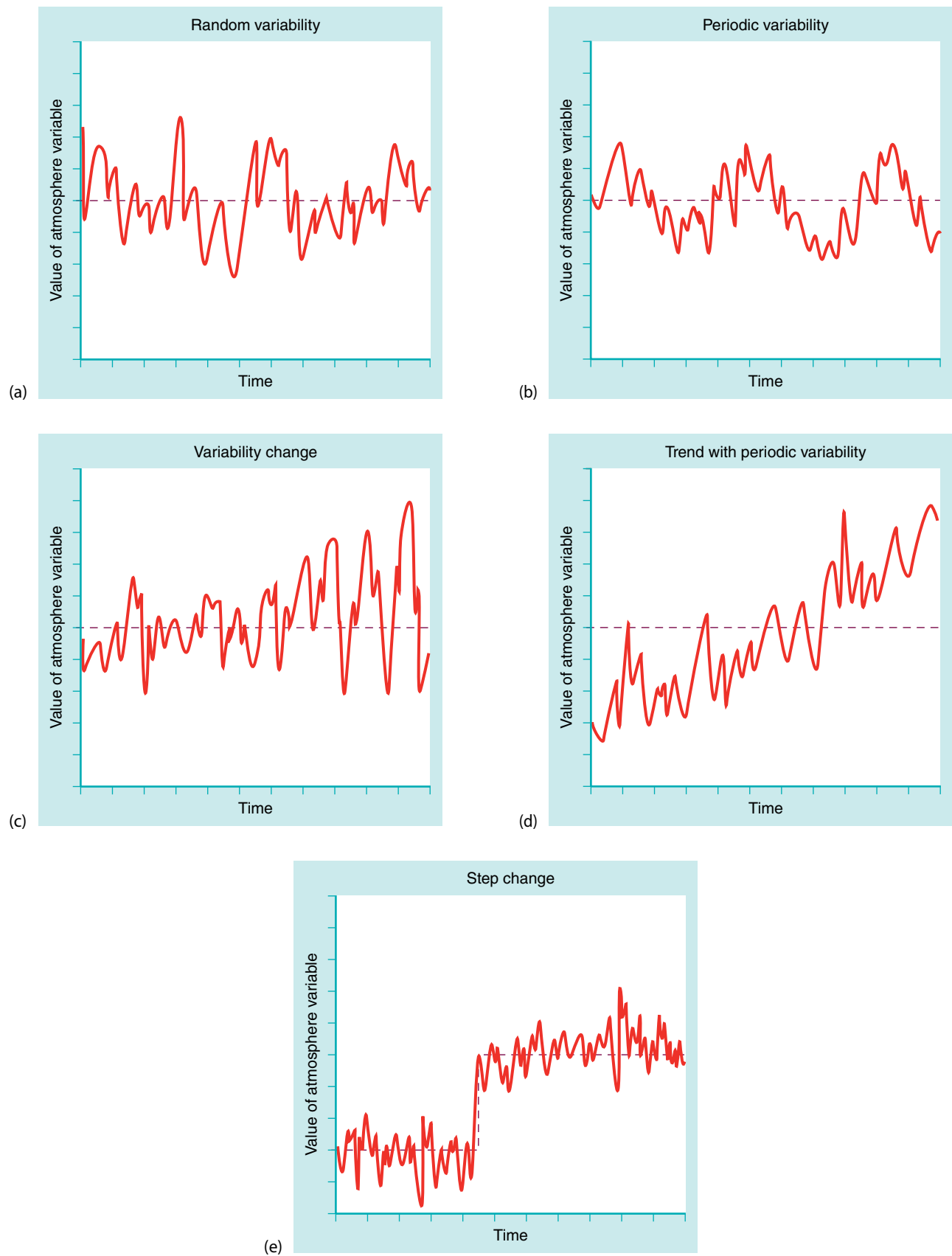


FIGURE 11.1 Many forms of temporal climatic changes and variability: (a) random variability, (b) periodic variability, (c) variability change, (d) trend with random variability embedded, and (e) step change with random variability embedded.

continues unless we believe that increased Atlantic hurricane activity is a long-term reality? Or, should we just “ride it out” until Atlantic hurricanes become less frequent and intense once again?

Both formal and informal policy is often dictated by the persistence of an anomaly. For example, people are usually more willing to help victims of climatic variability, such as a flood, than they would be to help victims who have repeatedly been hit by the same type of disaster. This persistence of the anomaly also affects how we experience variability and change. Variability is experienced as uncharacteristically intense floods, hurricane frequency, heat waves, and other individual extreme events. But change is experienced more insidiously, as the barely noticeable shifting of agricultural and bioclimatic zones, increasingly more extreme events than usual occurring over time, and so forth. In reality, however, the two are intertwined. If an uncharacteristically intense flood, hurricane, or heat wave occurs after many years of barely noticeable climatic trends, such as toward gradually rising waters behind a dam, slow sea level rise, or slight increases in moisture stresses, the impact of the extreme event may be magnified greatly.

We are probably more vulnerable to the effects of extreme events related to climatic variability and change than we once were. More people than ever before are living in “fringe” areas such as fluvial and coastal floodplains and in arid environments. We may not be as vulnerable to minor fluctuations and changes, however, because of the introduction of hybrid crops and improved science and technology for warning the public about potential dangers. But again, if the two types of changes are intertwined, increased immunity to the former may only set us up for increased vulnerability to the latter.

► Climatic Changes in Geological History

Temperature

Converging lines of scientific evidence show that Earth is approximately 4.6 billion years old and the oldest terrestrial rocks identified are approximately 4.3 billion years old. Although it is difficult to identify changes in climate across such an incomprehensibly long period of time, little evidence has been found to suggest that the average global temperature was ever below freezing or above a few tens of degrees above today’s average temperatures. It is more likely that Earth’s average temperature has remained within an even smaller range (about 15 C° [27 F°]), although some evidence to the contrary is present.

Scientific evidence suggests that in Earth’s early history, solar output was about 25% to 30% less than present because of the predictable pattern of stellar evolution that the Sun has undergone. Yet no conclusive evidence suggests that Earth was much colder when the Sun was emitting less energy. This *faint young Sun paradox* remains a topic of wide-ranging geoscientific research today. It is currently believed that *methanogens*—a family of anaerobic bacteria that produces *methane* (CH₄)—may have allowed for an accumulation of atmospheric CH₄. This methane would have absorbed terrestrial *longwave radiation* and reradiated it back downward effectively as *counter-radiation*, enhancing the *greenhouse effect* and keeping Earth relatively warm even while the Sun was emitting less radiation. This hypothesis is supported by the fact that, molecule for molecule, methane is a far more effective greenhouse gas than carbon dioxide (CO₂). This hypothesis is supported by processes observed on Titan—Saturn’s largest moon—which displays characteristics similar to early Earth and has an abundance of CH₄ in its atmosphere. For this reason scientists are eager to probe Titan for signs of life, specifically methanogens. A problem with current explanations for the faint young Sun paradox is that the atmospheric residence time of CH₄ is short, so even when it was abundant in the atmosphere its role as a greenhouse gas may not have been as important as many scientists suggest.

The methanogens are thought to have been intolerant to atmospheric oxygen, which became more abundant after the onset of *photosynthesis* some 3 billion years ago. As a result, just as the Sun began emitting more energy to Earth, the increasing oxygen concentration would have killed the methanogens, making CH₄ less abundant as a *greenhouse gas* and causing Earth’s atmosphere to become less effective as a greenhouse system. At times, the weakening of the greenhouse effect may have overshadowed the consequences of increasing solar intensity. It is suggested that the global demise of the methanogens may have caused Earth’s first global *ice age*—any period in geological history in which ice exists continuously for a sustained period of time over some section of Earth. Furthermore, “pulses” of methanogen demise may have triggered other ice ages.

Regardless of whether the methanogen explanation becomes accepted nearly universally, most of geological history is believed to have been dominated by somewhat higher temperatures than exist today. Furthermore, there is no convincing scientific evidence for widespread glaciation for at least the first half of Earth’s existence. Instead, a sequence of relatively low temperatures and intermittent glaciations has been identified in the geological record, beginning at about 2.5 billion years ago—about halfway through Earth’s existence—coinciding with the arrival of abundant atmospheric oxygen.

This first known major ice age occurred at the beginning of the **Proterozoic Eon**, the last broad division of geological time before the current one—the **Phanerozoic Eon** (FIGURE 11.2). **Eons** are subdivided into **eras**, which are subdivided into **periods**. The

early Proterozoic (2.3 billion years ago) ice age was also the time of the first mass extinction event on Earth. Called the **Great Oxygenation Event**, it was caused by the rapid buildup of diatomic oxygen due to the proliferation of cyanobacteria, the first photosynthetic

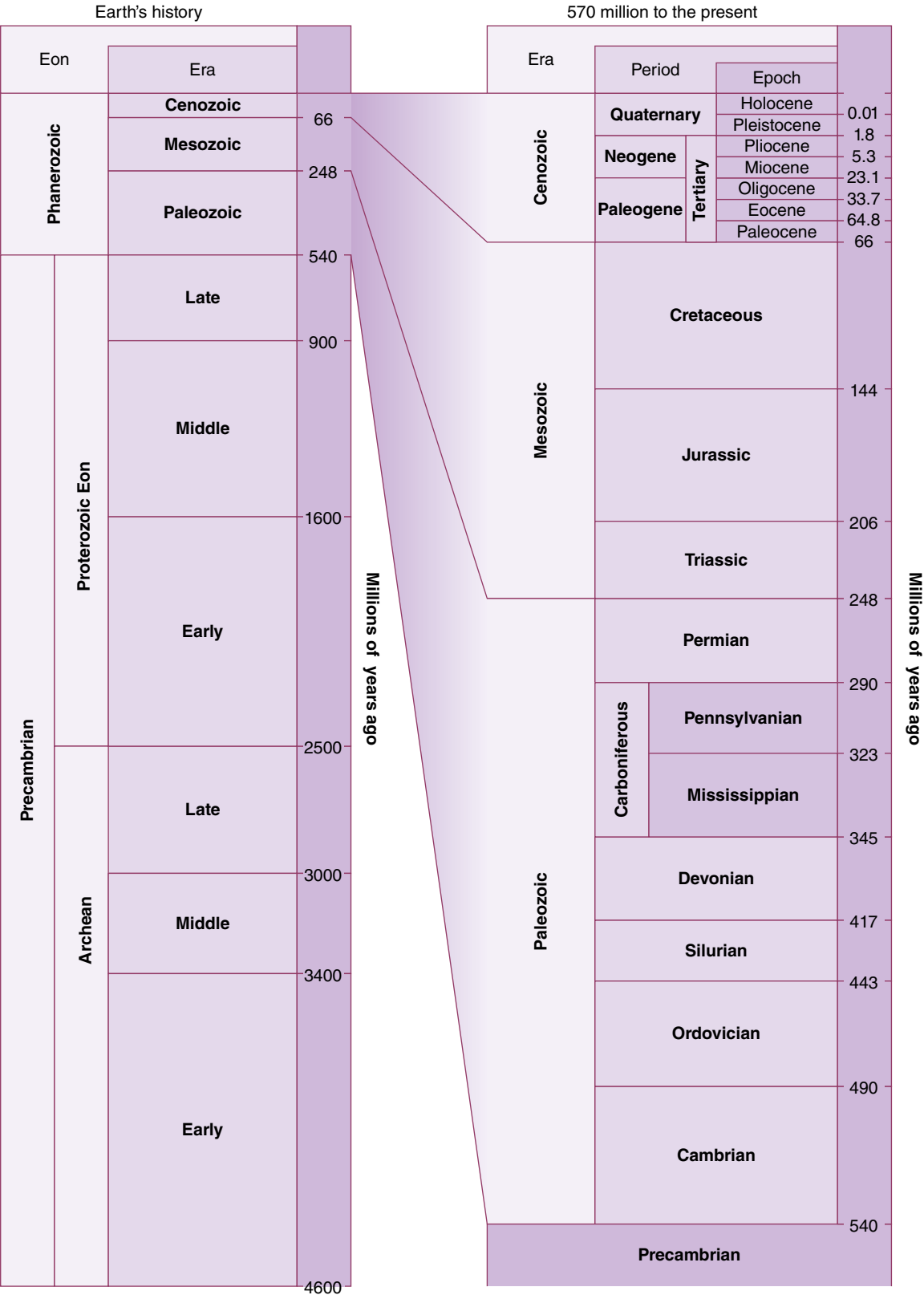


FIGURE 11.2 The geologic time scale.

organism. Cyanobacteria combined with microbial mats of oxygen to produce microbes that caused abrupt changes in atmospheric composition. This led to the demise of the anaerobic organisms that comprised the most abundant life forms on the planet.

Evidence indicates that the most impressive ice age may have occurred in the **Cryogenian Period** of 800 to 600 million years ago at the end of the Proterozoic Eon. Some geological evidence indicates that the presence of large land masses near the poles during this period may have caused the removal of CO₂ from the atmosphere in the rock-forming (sedimentary) processes, thereby weakening the greenhouse effect and triggering a massive ice age. Proponents of this **Snowball Earth hypothesis** assert that conditions were so cold during the Cryogenian Period that ice even existed toward the equatorial land masses and oceans. Although evidence of glacial conditions during this period has been found globally, little convincing evidence of the subsequent warming after such a massive freeze has been identified. Snowball Earth remains a topic of intense research. The end of the Cryogenian glaciation marked the beginning of the Phanerozoic Eon—characterized by the renewed warmth that coincided with the evolution of fish, shellfish, and many other species. This time is known as the **Cambrian Explosion**. CO₂ concentrations during earlier times in Earth history, such as during the Cambrian Explosion, are likely to have been much greater than today's values, perhaps by 25 times. But the values are impossible to estimate, even by using ice cores or other modern techniques.

A third glaciation occurred about 460 to 430 million years ago, mostly during the **Ordovician Period** of the **Paleozoic Era** of the Phanerozoic Eon. Although the Ordovician glaciation was relatively short-lived and minor, it resulted in massive extinctions on the planet. The **Ordovician-Silurian extinction event** was the second largest of the five major extinction events in Earth's history. Perhaps 60% of all marine genera and almost 85% of all marine species went extinct. No single cause of the event has been found, but volcanism, carbon sequestration in sedimentary rocks, and gamma radiation from a nearby hypernova are some proposed causes that, individually or in combination, could have created inhospitable planetary conditions.

The end of this glaciation was followed by warmer, ice-free conditions through the next hundred million years or so (shown in Figure 11.2 as the late Silurian and the Devonian Periods of the Paleozoic Era within the current Phanerozoic Eon). The late Devonian was the time of the next major extinction event. The exact timing of this event is unclear, including whether the event was a single event or as many as seven events

spread over about 25 million years. It is clear that the event was largely exclusive to marine life. Causes are unknown at present, but leading hypotheses center on ocean anoxia triggered by a cooling atmosphere and/or increased oceanic volcanism. The Late Devonian extinction was followed by the **Carboniferous** (often subdivided into the **Mississippian** and **Pennsylvanian**) **Period** and the further evolution of terrestrial plants, insects, trees, and finally amphibians that appeared and evolved to more complex forms.

From about 320 to 250 million years ago, Gondwana, the southern portion of the supercontinent **Pangaea**, was vastly glaciated due to the position of that area in the high latitudes of the southern hemisphere. Conditions there during this **Gondwanan Ice Age** contrasted with those near the equator, on lands that are now North America and Europe. The warmth of these then-tropical lands led to the explosions of biodiversity that mark the Carboniferous and **Permian Periods**. But at the same time, the Gondwanan Ice Age also corresponds with major extinctions that separate the Paleozoic Era from the subsequent, warmer **Mesozoic Era**. These extinctions are sometimes referred to as the **Great Dying**.

The Great Dying ended the Permian Period, leading to the **Triassic Period**. The Great Dying was the largest known extinction, with up to 96% of all marine species and 70% of all terrestrial vertebrate species becoming extinct. It is also the only extinction event known to have triggered extinctions of insects and other invertebrate species. Evidence suggests three separate events, with the causes linked to a large asteroid impact, or **bolide**, and widespread volcanism. The volcanism is thought to be associated with flood basalts, including the **Siberian Traps event**, that was the largest known volcanism in Earth history. Another cause seems to be related to an enhanced greenhouse effect triggered by rapid CH₄ release from warming permafrost or increases in methanogens triggered by earlier climate changes of other causes.

The warmth of the Mesozoic, which may have had 5 to 10 times more atmospheric CO₂ than today, coincided with the development of large reptiles, particularly the dinosaurs, as well as birds, small mammals, and the **angiosperms** (flowering plants). Marine life in the Mesozoic persisted because abundant oceanic carbonates and bicarbonates could neutralize the extra carbonic acid produced under increased atmospheric CO₂ conditions. The extra carbonates and bicarbonates are presumed to have existed in the oceans because of the enhanced rates of weathering, resulting from an enhanced *global hydrologic cycle* energized by the warm greenhouse conditions. The difference between those times and the CO₂ increases seen today is the rate of change. It is believed that today's atmospheric

CO₂ concentrations are increasing too quickly to allow an enhanced hydrologic cycle to weather enough additional carbonate and bicarbonate production to buffer marine life from the effects of the enhanced CO₂. Ocean acidification from excess carbonic acid is quickly increasing in the world ocean, which is detrimental to many marine organisms, especially coral. It has recently been estimated that as much as 90% of the Great Barrier Reef has been “bleached” by recent increases in carbonic acid. Similarly, the increased ocean acidification during the Mesozoic is thought to have been the primary cause of the Triassic-Jurassic mass extinction event. This led directly to the age of the dinosaurs, as nondinosaurian reptiles and large amphibians went extinct. Evidence supports the notion that increased volcanic activity due to the initial breakup of Pangaea spurred the hyperhydrologic cycle by altering atmospheric gas content.

The Mesozoic Era ended suddenly around 66 million years ago with the **K-T extinction**, which derives its name from the German abbreviations for the **Cretaceous** (abbreviated “K”) **Period** of the Mesozoic Era and the succeeding **Tertiary Period**, which began the **Cenozoic Era**—the present era of geological time. In recent years, geoscientists have begun to replace the use of the term “Tertiary Period” with the **Paleogene Period** (66 million to 23 million years ago) and the **Neogene Period** (23 million to 2 million years ago). So in the most recent literature, use of the term “K-T

extinction” is being replaced by **Cretaceous-Paleogene (K-Pg) extinction event**. Prevailing theory suggests that 66 million years ago a comet or bolide that struck Earth near the tip of the Yucatan Peninsula of Mexico, produced massive heat, dust, chemical changes, and volcanic activity that impacted the atmosphere and caused the extinction of perhaps 85% of the species on Earth, including all large mammals and dinosaurs.

Because “permanent” ice exists on Earth today (in the ice sheets of Greenland and Antarctica, along with numerous mountain glaciers), we are currently in another ice age in geological history. This ice age, which may have begun as far back as 40 to 50 million years ago in the Tertiary Period of the Cenozoic Era, began to intensify at around 1.8 million years ago—coinciding with the beginning of the **Quaternary Period** of the Cenozoic Era. The large mammals had largely evolved before the onset of this ice age, but some, such as the giant woolly mammoth and saber toothed cat (*Smilodon*), did not survive.

Ice ages are subdivided into **glacial phases**—intervals when the “permanent” ice is displaced equatorward and downslope—and **interglacial phases**—intervals when the ice retreats poleward and upslope. In general, glacial phases appear to develop slowly and irregularly, and they may persist for perhaps 50,000 to 150,000 years. By contrast, interglacial phases arrive relatively suddenly and tend to exist for shorter time intervals of only 8000 to 12,000 years (**TABLE 11.1**). Because the

TABLE 11.1 Major Glacial and Interglacial Phases within the Pleistocene Ice Age

Name of the Phase*	Approximate Number of Years Before Present (in thousands)	Deposits That Provide the Phase
Holocene Interglacial	< 9	
Wisconsin Glacial	9–70	
Sangamon Interglacial	70–130	Sangamon County, Illinois
Illinoian Glacial	130–180	
Yarmouth Interglacial	180–230	Yarmouth, Nova Scotia
Kansan Glacial	230–300	
Aftonian Interglacial	300–330	Afton, Iowa
Nebraskan Glacial	330–480	

*Different names are used (for all phases except Holocene Interglacial) in northern Europe, Alpine Europe, Britain, eastern Europe, and other parts of the world to correspond with major lines of evidence for the phases found in other locations.

global annual average temperature may vary by perhaps only about 5 C° (9 F°) between glacial and interglacial phases, concern exists that Earth could easily slip into a step change generating a new set of mean conditions, particularly if *positive feedback systems* and human interference are involved.

Currently, we are in an interglacial phase, because the “permanent” ice is currently retreating and confined to polar and high altitude areas. The present *Holocene Interglacial Phase* (named for the geological **epoch** that coincides with this interglacial phase) began around 9000 years ago, with abrupt warming that coincided with the first attempts at human agriculture.

Before the onset of the Holocene Interglacial Phase, the *Wisconsin Glacial Phase* in the *Pleistocene Epoch* peaked at approximately 18,000 years ago, when “permanent” ice covered most of North America north of the Ohio River and extended across the pole to cover much of Europe and Asia. The Wisconsin Glacial Phase and subsequent Holocene Interglacial Phase left numerous signs of their presence on the landscape in the form of glacial landforms. This extensive glacial phase obliterated many of the signs of previous glacial–interglacial sequences (Table 11.1). Some of the more prominent resulting landforms include the final formation phase of the Great Lakes, Martha’s Vineyard, Long Island, the Finger Lakes region of New York, and Yosemite Valley in California.

Ice Ages and Sea Level

During glacial phases and ice ages in general, worldwide sea level falls as more of the global water is stored in the cryosphere in the form of continental ice sheets. During the Wisconsin Glacial Phase, *eustatic* sea level was as much as 170 m (550 ft) below today’s level, exposing large sections of the continental shelves (**FIGURE 11.3a**). At that time the Bering Strait was a land bridge between Asia and North America. Mongoloid traits of Native Americans suggest that the ancestors of the Native American population migrated to the Americas via this land bridge. Many of the islands that comprise the *Maritime Continent* were also connected during that time.

As Pleistocene ice melted during the *Holocene Epoch* (also sometimes referred to as the *Anthropocene Epoch*), eustatic sea level rose, drowning low-lying coastal plains and reducing the slopes of major rivers as they flowed to sea. This caused the deposition of sediments from these rivers, forming vast deltaic land masses and coastal plains through the Holocene. For example, the southernmost part of the Mississippi River valley was formed over the last 10,000 years as conditions warmed, ice melted, and the Mississippi River flooded

over into its floodplain and the Gulf of Mexico. Other ice-melt remnants include the drowned river valleys that comprise Chesapeake Bay and the St. Lawrence Seaway and Great Salt Lake, which is a **pluvial lake**—an isolated lake that existed in much greater size in the past, when conditions were colder and/or wetter than today. A common misconception concerning glaciation sea level adjustment is that sea ice displaces the same amount of water as its liquid equivalent (according to **Archimedes’ Principle**), so its formation and melting do not contribute to sea level changes. In reality, because fresh water is less dense than saltwater, freshwater sea ice occupies a greater volume than an equal mass of seawater in which it floats. The melting of all current freshwater sea ice alone, therefore, would add about 4 cm (1.5 in) to global sea level, according to recent research. This total does not include the much greater amounts of sea level increase from meltwater of continental ice sheets and glaciers. On the other hand, increased precipitation under global warming scenarios could actually increase sea ice extent, according to other recent research by scientists at the University of Maryland.

If all of the world’s current cryosphere were to melt, then sea level would rise by about 67 m (220 ft), and substantial areas of the coastal plains would be flooded worldwide. Even if only the East Antarctic Ice Sheet melted, large areas of the coastal zone would be flooded (**FIGURE 11.3b**). Smaller sea level increases, such as the 5-m (17-ft) increase expected if the West Antarctic Ice Sheet melted, would be problematic as well (**FIGURE 11.3c**). **FIGURE 11.4** depicts the impacts of such sea level increase on coastal Florida.

Some places in Scandinavia and Alaska that were covered by substantial depths of ice during the Wisconsin Glacial Phase are now rising, or rebounding, because of the release of the tremendous pressure/weight of the ice that has been removed recently in geological time. In such places sea level is not currently rising relative to the land as elsewhere in the world. Instead, the **isostatic rebound** (rising continental crust) occurs mainly along such coastal locations in Scandinavia and Alaska. Due to the abundance of major coastal cities and recent coastal development, sea level changes affect the well-being of a sizable share of Earth’s population. In addition, marine ecological systems are affected directly by sea level changes, and changes in the extent of inland seas affect other species.

Recent Trends

Following the peak in the Wisconsin Glacial Phase 18,000 years ago, a period of rapid warming began. Termed the **Bolling-Allerod interstadial**, this warm

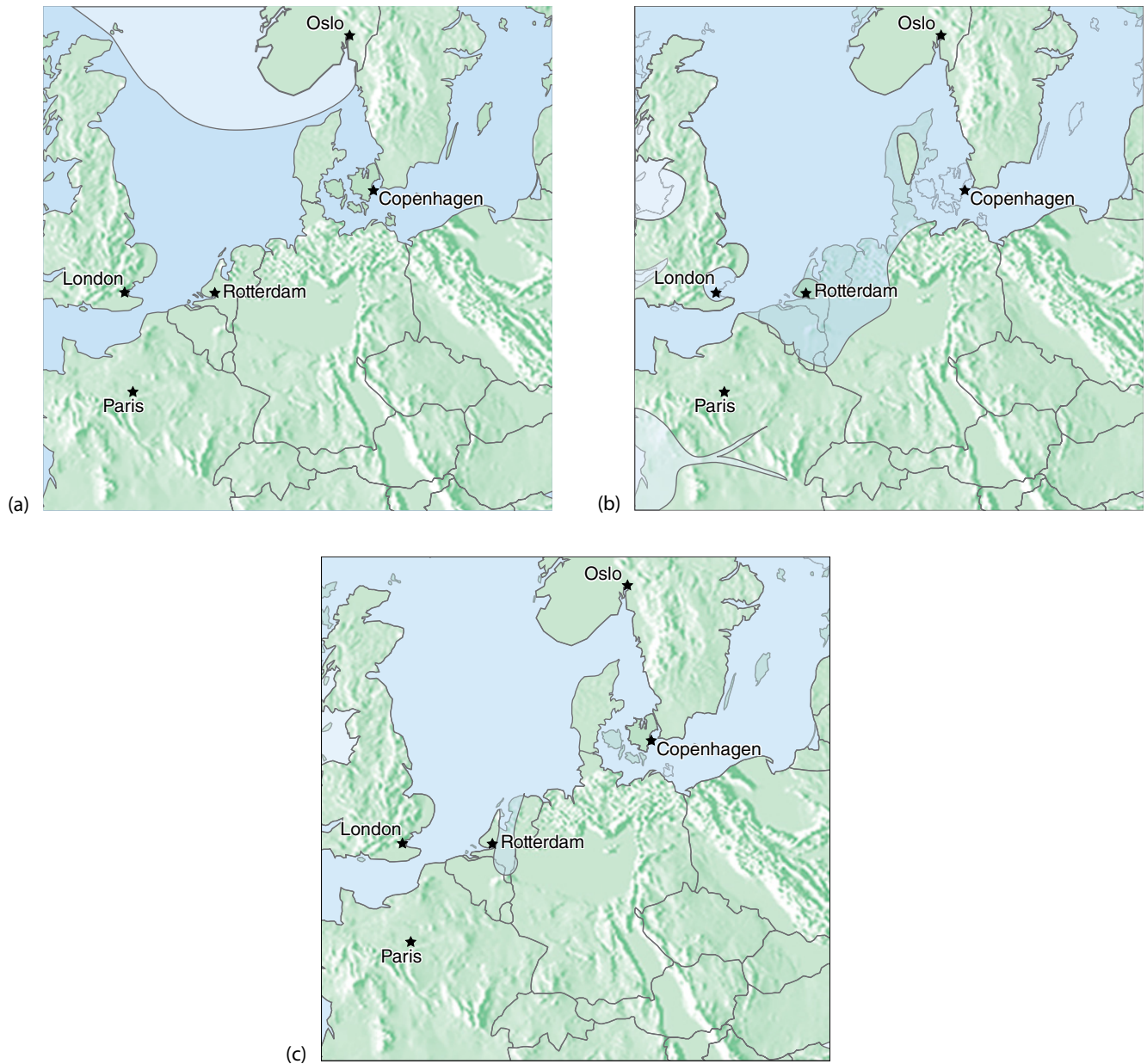


FIGURE 11.3 Impacts of sea level changes on coastlines in northwestern Europe. (a) Coastline approximately 20,000 years ago, during Wisconsin glacial advance; (b) coastline if the East Antarctic Ice Sheet melted, causing a 50-meter (170-foot) sea level increase; (c) coastline if West Antarctic Ice Sheet melted, causing a 7-meter (22-foot) sea level increase.

Data from "Water World," William Haxby, Lamont-Doherty Earth Observatory, for PBS, NOVA website. www.pbs.org/wgbh/warming/waterworld.

period signified the onset of the Holocene Interglacial Phase. A brief but sudden and notable "lapse" back to cold conditions followed from about 14,000 to 11,200 (or 10,100 according to some) years ago. This cold phase is termed the **Younger Dryas**, though Europeans term it the **Loch Lomond Stadial**. The Younger Dryas is named after the dryas, a herbaceous **tundra** plant whose pollen grains in sediment and ice layers identified its chronological occurrence. Its name also distinguishes it from the Older Dryas, a less-impressive geological phase that occurred previously. It is thought that the Younger

Dryas was caused, ironically, by the melting ice, as the still-cold meltwaters from the retreating North American **Laurentide Ice Sheet** drained into the warmer North Atlantic Ocean. This is thought to have caused an extensive cold freshwater lens in the North Atlantic that significantly altered *thermohaline circulation* and triggered a positive feedback loop into the atmosphere, strengthening and expanding the *circumpolar vortex*, and leading to renewed cooling over much of North America and Europe. Much research is being invested in determining whether the Younger Dryas was a true

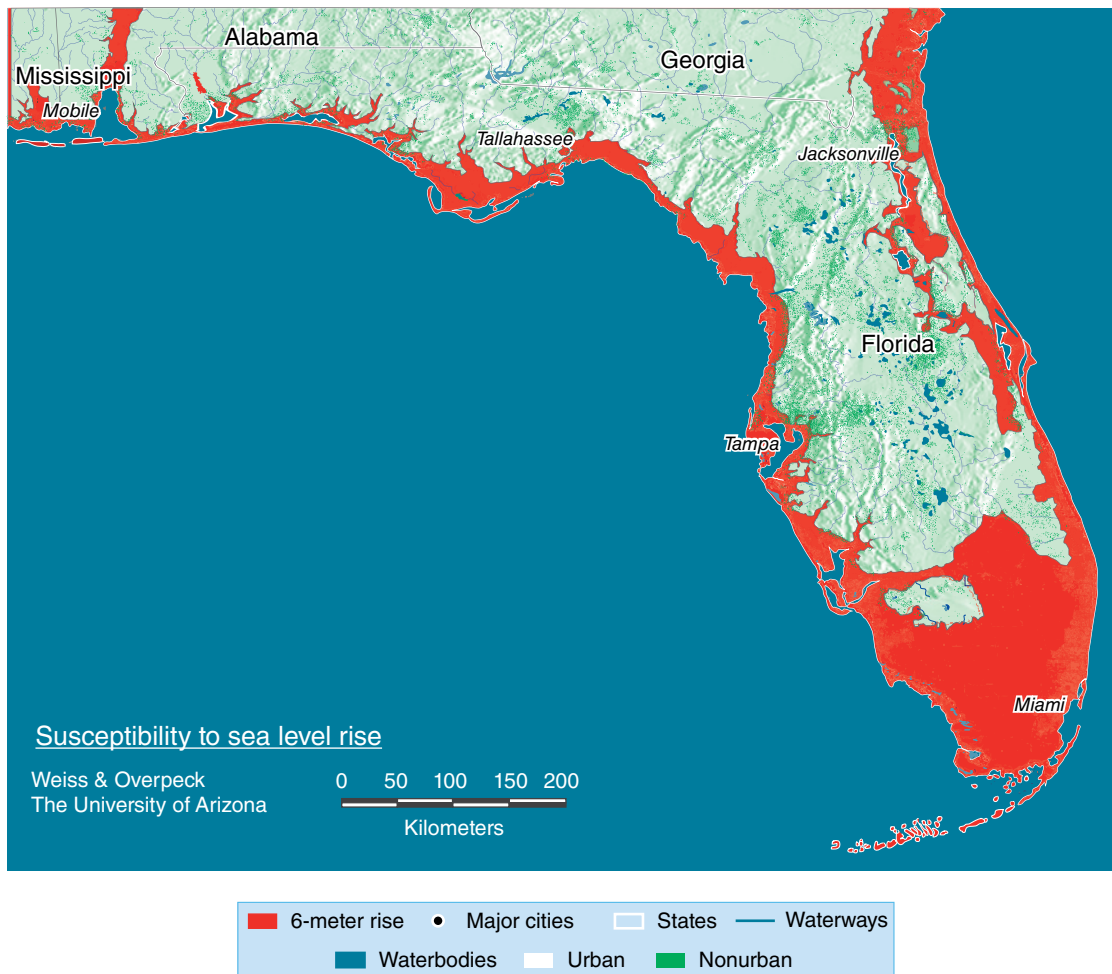


FIGURE 11.4 Effect of a 6-meter sea level rise on Florida.

Courtesy of Jeremy Weiss and Jonathan Overpeck, University of Arizona.

global event, with most now at least agreeing that its influence did extend worldwide. Regardless of its geographical extent, the Younger Dryas is important because it provides concrete evidence that rapid changes in climate have occurred in the past. Presumably, they could also occur in the future.

After the cold conditions associated with the Younger Dryas, the **Pre-Boreal warm interval** ensued. The **Boreal cold interval** followed, lasting from 9100 to 8000 years ago. A warming phase known as the **Hypsithermal** ensued culminating between 8000 and 5000 years ago. During the Hypsithermal, global average temperatures are thought to have been approximately 2 C° (4 F°) above today's levels. Gradual cooling during the **Sub-Boreal cold interval** followed the Hypsithermal, with a desiccation of the areas now covered by desert in southwestern Asia and northern Africa. The **Sub-Atlantic warm interval** followed, lasting until today, albeit with small fluctuations in temperature superimposed.

By AD 500 a cooler and stormier period began in Europe—the Dark Ages. This period came to an end in approximately AD 900, when a warm interval known as the **Medieval Warm Period (MWP)**, also known as the

Little Climatic Optimum, began. It was during that time that the Vikings expanded their empire as ice-free sea lanes to Greenland and the North American coast opened. During the MWP, crops in Europe grew farther north and higher in elevation than the same crops are known to grow now. **Paleoclimatologists**—scientists who study climates of the preinstrumental record—disagree about whether global temperatures in the MWP were higher than today's values.

From approximately 1450 to 1850 the **Little Ice Age (LIA)** occurred. The LIA is an unfortunately named phenomenon because it does not connote the idea that “ice ages” last for millions of years. During the LIA streams in Europe that do not freeze today were observed to freeze regularly. Likewise, the notorious winter at Valley Forge for General Washington and his troops seems to have been more severe than winters experienced today. Another example of the impact of the LIA was the “Year without a Summer” of 1816, in which frosts occurred in every month of the year in New England—an unrealistic phenomenon today. It must be noted that the Year without a Summer followed the massive eruption of **Tambora**, an Indonesian volcano that exacerbated

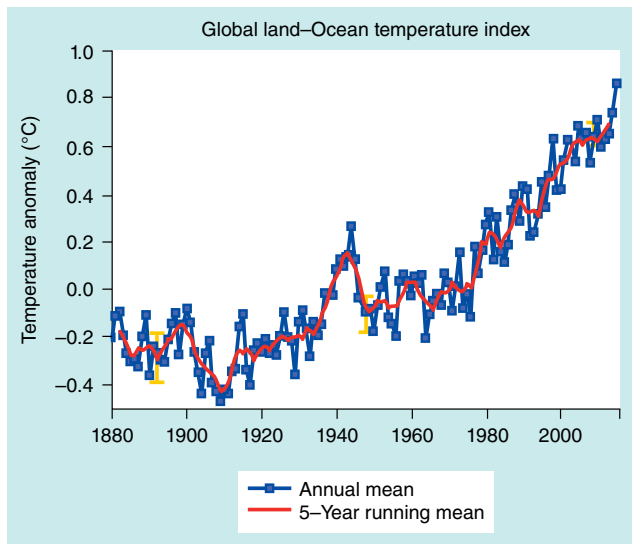


FIGURE 11.5 Global mean annual average temperature since 1880. Anomalies are calculated from the 1951–1980 mean temperature.

From NASA Goddard Institute for Space Studies (http://data.giss.nasa.gov/gistemp/graphs_v3/fig_A2.gif).

the resulting temperature decrease by spreading a huge dust plume through the *stratosphere*. Considerable debate exists about whether all these occurrences were parts of the same truly global phenomenon.

The end of the LIA largely coincides with the onset of formal instrumental records from at least some parts of Earth. Three major global climatic periods can be identified from these modern records (**FIGURE 11.5**). Warming occurred from the late 1800s to about 1945, and then a short but distinct period of cooling was apparent from 1945 to about 1980. Abrupt warming occurred since 1980. Most notably, data from the National Centers for Environmental Information show that every year since 2001 had a global temperature that was at least 0.43 C° (0.78 F°) above the 1901–2000 mean, and that July 2016 was the 15th consecutive warmest month on record globally. An estimated global sea level rise of approximately 15 cm (6 in) has accompanied the warming of the past century. This amount may seem small, but on small islands and coastal zones with little topography, small increases in sea level can produce large increases in beach erosion, saltwater intrusion into fresh or brackish streams, ecosystem disruption, and coastline loss. Some signs in the last 15 years had suggested that the rate of warming had begun to slow, with the extremely warm El Niño year of 1998 perhaps skewing the subsequent trend toward a leveling. However, the intense El Niño event of 2014–2016 caused another increase, and may be skewing the curve for the post-1998 part of the record, as shown in Figure 11.5. Earth's climate is generally believed to be more rigorous in modern times, with greater extremes of heat and cold than during most times in the last 500 million years of geological history.

► How Do We Know What We Know About Past Climatic Changes?

As noted above, formal meteorological records go back only to the mid- to late-1800s. Data from upper-level, balloon-based *radiosondes* extend back only to the mid-1900s, and reliable satellite data exist only as far into the past as the 1970s. Nevertheless, paleoclimatologists can make inferences about climatic conditions into the distant geological past. These estimates are made using *proxy evidence* to ascertain climatic conditions of the past and assess the timing and magnitude of climatic change or variability. These clues are hidden in the geological, geophysical, biological, chemical, and historical record. This section reviews some of the major lines of proxy evidence and how they are used.

Basic Principles

All scientific techniques for paleoclimatic reconstruction rely on some basic principles. First, a preponderance of evidence is used to reach conclusions about the climate of a particular place at a particular time in the past. No single study can provide results with enough certainty to lead to any firm conclusions. Our knowledge of *paleoclimatology* is the result of the majority of conclusions from dozens to thousands of independent scientific research studies spanning numerous scientific disciplines. A corollary to this idea is that no single research manuscript could be used to refute the preponderance of evidence.

All scientific techniques for paleoclimatic reconstruction rely on the **Principle of Uniformitarianism**. This axiom states that the processes that occurred in the past are the same ones that occur in the present, at similar rates. Any evidence (such as vegetation types or soil types) that would accompany a certain climatic type today would be assumed to suggest the same kind of climate at the time in the past when similar evidence existed. The Principle of Uniformitarianism also assumes that the same environmental conditions required by a given species today were also favorable for similar species in the past. The Principle of Uniformitarianism, therefore, states that the present is the key to the past.

The opposite of uniformitarianism is **catastrophism**—the belief that changes do not occur uniformly but will instead reshape Earth's environment in a step change in only a short time geologically. Catastrophic changes certainly do occur in nature, as they did during Hurricane Katrina in 2005, and they can be helpful in providing clues to the timing and forcing mechanisms of paleoclimatic

change. For example, **paleotempestology**—the science of identifying signatures of ancient storms primarily from sediment records—has been used to infer changes in the atmospheric circulation patterns.

Catastrophic events also can complicate our understanding of the paleoclimate record, because evolutionary processes would not necessarily have time to provide a signature of the increasingly stressful or favorable changes that were undergone by organisms in such a short period of geological time. As a result, catastrophism can leave an unresolved discontinuity in the puzzle of climatic change. A good example of catastrophism in the paleoclimate record is the sudden disappearance of any evidence of living dinosaurs after the K-T extinction. We have seen no convincing evidence that the dinosaurs disappeared slowly in geological time. Instead, the bolide that obliterated the dinosaurs may have also destroyed signs of whether climatic changes occurring up to the time of the bolide were favorable to their existence. It must be noted that most uniformitarian views include, and account for, catastrophic elements.

Radiometric Dating

For most scientific forms of paleoclimatological evidence, **radiometric dating** is used to determine the time at which the evidence was preserved. Radiometric dating is based on the principle of **radioactive decay**—the rate at which spontaneous nuclear disintegration of certain (usually rare) **isotopes** of certain elements occurs. Isotopes are different varieties of the same element, usually having the same number of protons but different numbers of neutrons from each other. Protons and/or neutrons spontaneously leave the nuclei of radioactive elements at precisely known rates. When protons leave, the **parent isotope** changes into a different element, resulting in a **daughter isotope**. The inevitable release of energy in the decay process (in fulfillment of the *first law of thermodynamics*) can be detected by a **Geiger counter**.

To determine the age of a sample, the amount of parent isotope remaining is compared with the amount of resulting daughter isotope. The amounts of each isotope are found by using **mass spectrometry**—instrumental laboratory techniques that can determine the chemical composition of a substance. The rate of decay of each radioactive element is known, and the amount of daughter isotope can be used to infer the amount of time since the rock containing the radioactive element formed. The **half-life** of a radioactive element is the amount of time required for one-half of the parent atoms to decay into daughter product. Because radioactive decay occurs independently of temperature, pressure, or any other known variable, it is a useful tool in providing relatively precise dates of paleoclimatological evidence.

Dozens of radioactive elements are useful for radiometric dating. Some elements are used more commonly than others for a variety of reasons, such as relative abundance and convenience of half-life for measuring time on geological time scales. Half of a sample of uranium-238 (U_{238} , so-named because the sum of protons and neutrons—the **atomic mass**—is 238) decays radioactively to its daughter product, lead-206 (Pb_{206}), in 4.46 billion years. All of the Pb_{206} in a given rock or mineral sample can be inferred to have been U_{238} at the time that the rock solidified. Thus, the ratio of the amount of parent isotope present to the original amount of parent isotope can be deduced. This ratio can be used along with the known half-life to determine the time elapsed since the sample formed. Specifically,

$$\text{Time elapsed} = - \frac{\ln \left(\frac{\text{Number of atoms of parent isotope remaining}}{\text{Original number of atoms of parent isotope}} \right)}{\ln 2} \times \text{Half-life}$$

where \ln is the natural logarithmic function. So, for example, if a rock sample containing evidence of paleoclimatic activity has radioactive elements in that sample with 90% U_{238} and 10% Pb_{206} , then the equation above tells us that the climate regime identified by the sample must have occurred at about 678 million years ago because,

$$- \frac{\ln \left(\frac{90}{100} \right)}{\frac{0.693147}{4.46 \times 10^9 \text{ years}}} = 6.78 \times 10^8 \text{ years}$$

Another element commonly used in radiometric dating in the geosciences is a rare, radioactive form of potassium-40 (K_{40}), which has the same atomic mass as nonradioactive K_{40} . The radioactive K_{40} decays in a different manner—when one of its protons becomes a neutron, its nucleus changes from 19 protons and 21 neutrons to 18 protons and 22 neutrons. With 18 protons, the daughter isotope becomes argon instead of potassium, even though its atomic mass remains 40. The half-life of this radioactive decay is approximately 1.3 billion years.

Although U_{238} and K_{40} are both useful for many types of radioactive dating, their long half-lives present a cumbersome problem for relatively recent evidence. Nearly all the parent material of these radioactive elements would remain present if the sample were formed only a few thousands of years ago, and the error in determining the tiny fraction of daughter material may

be far too large to date such a recent sample accurately. Radioactive isotopes that have relatively short half-lives are more useful for relatively young samples.

A commonly used isotope with such a short half-life is C_{14} , with a half-life of approximately 5730 years. C_{14} is an extremely rare isotope, with six protons and eight neutrons, whereas most natural carbon (C_{12}) has six protons and six neutrons. Because carbon is used by all living things, it exists in the same concentration in living tissue as in the atmosphere at the time it was ingested. Although the rare C_{14} immediately begins to decay in living tissue, it is continually being replaced by more C_{14} that is being added to the biomass or body of the organism, so a living organism maintains the same ratio of C_{14} to C_{12} . Upon death, the organism ceases to assimilate carbon and the radioactive isotope decays. Radioactive dating can then be used to determine the amount of time since death. Because the amount of C_{14} becomes too small to detect after approximately 10 half-lives, radiocarbon dating is useful only for dating items of origin in the Holocene and late Pleistocene Epochs (the last 50,000 to 60,000 years). But this range provides useful chronologies for many types of paleoclimatic evidence as well as applications in archaeology, hydrology, oceanography, biochemistry, sedimentology, and a host of other disciplines.

Radiometric dating techniques have strong advantages, because they are the only **absolute dating** techniques that go back farther in geological history than a few hundred years. As such, we rely heavily on them for what we know about the geological past. The technique is also scientifically solid if it can be assumed that the rock or mineral is in a “closed system,” meaning that radioactive parent or daughter isotopes are not brought in from other sources during the time that the originally formed radioactive isotopes are decaying. Some argue that we do not know for certain whether the rate of decay is truly independent of all other factors, by drawing in arguments that some poorly understood processes have not been shown for certain to leave half-lives unaffected. But the overwhelming preponderance of scientific evidence indicates that radiometric dating is a valid, reliable, and precise technique.

Lithospheric and Cryospheric Evidence

If geological samples are not dated radiometrically, the *relative* (rather than *absolute*) ages of various samples in sedimentary rock can be estimated based on the **principle of superposition**—an axiom stating that older evidence is found successively lower in sedimentary rock layers. This **relative dating** of evidence is far simpler and less expensive than absolute dating techniques, but it is less precise.

A related concept is **cross-cutting relationships**—the notion that igneous rock (rock formed from solidifying magma) formations cross-cut (exude into) preexisting sedimentary rock layers. Because the igneous rock cuts through the sedimentary rocks, we know that the sedimentary rock layers must be older than the igneous intrusions. Cross-cutting can be used as both a relative dating technique and an absolute dating technique if samples of the igneous rock layer are subjected to precise radiometric dating techniques.

Relic landforms can also suggest features of past climates. For example, the minerals comprising the breathtaking layers along the walls of the Grand Canyon in Arizona (**FIGURE 11.6**) provide evidence that the region experienced alternating periods of being exposed above the ocean and being submerged below it; some of these features are related to climatic changes. Another example is provided by pluvial lakes. The Great Salt Lake is merely a remnant of the much larger pluvial Lake Bonneville, which formed from melting glaciers associated with the Wisconsin Glacial Phase approximately 18,000 years ago. The *evaporation* of Lake Bonneville left behind the salt flats surrounding the Great Salt Lake that are used for automobile racing today, providing convincing evidence of a very different paleoclimate. Likewise, environmental features in now-arid locations that required humid conditions for their formation, such as Carlsbad Caverns in New Mexico and petrified forests such as those found in Arizona, provide further evidence of past climatic change.

Glaciers provide many other forms of physical evidence. Their formation, motion, and *ablation* leave behind erosional and depositional landforms or features that provide geological hints of their presence in the past. These include glacial **moraines**, which are large piles of unsorted rock and soil debris deposited by a glacier; **rock striations**, which are grooves cut into bedrock by rocks embedded within the base of moving glaciers; and deposits of **loess**, a soil formed by the grinding of rocks by glaciers into a fine, powdery consistency.

More direct evidence of the past presence of glaciers can also be found. For example, **glacial erratics** provide clues that glaciations occurred in Earth's past. Erratics are rocks that differ in composition from the surrounding geology, suggesting that a glacier must have moved the rock to its present location from somewhere near other rocks similar to its composition (**FIGURE 11.7**). Erratics can also provide clues on the movement of glaciers. Evidence of a glacier's advance equatorward and/or downslope suggests a period that was cooling and/or becoming wetter. Likewise, signs of glacial retreat poleward and/or upslope suggest that the climate was warming and/or drying. In some cases



FIGURE 11.6 The colorful walls of the Grand Canyon are the result of differences in the mineral composition of the rock. Many of these contrasts are attributable to the differences in marine versus continental deposition, as oceans covered this region at various times in geologic history.

© Chelsea/Shutterstock, Inc.



FIGURE 11.7 A periglacial landscape in southeastern Ohio: Hocking Hills State Park.

Courtesy of RG Johnson/NPS

the discrepancy between local soils and vegetation characteristic of colder climates and the warmer regional climate present in their locations today can give hints of a past climate to which the local environment has not yet adjusted. These situations are especially

common where the surface is shaded (particularly during summer afternoons) or in high elevations, and the microclimate has not yet had time to respond to the sudden warming since the end of the LIA, or even since the Wisconsin Glacial Phase.

Geological and glacial evidence can be advantageous to paleoclimatologists because of the availability of clues extending back several hundred million years. In fact, geological records provide our only reliable glimpse into Earth's distant past. Although evidence directly produced by glaciers does not occur for such an extended portion of geological history, glaciers do provide clear clues about paleoclimates for recently glaciated areas.

Major limitations of geological and glacial evidence also exist. Convincing geological evidence of paleoclimates is difficult to find, as it is often buried deeply or obliterated over time, sometimes by more recent glaciers. Furthermore, it can be a major challenge to date such ancient occurrences radiometrically because little of the parent isotope may remain or some other process may have introduced parent or daughter isotopes after the evidence in question was produced.

In the case of direct glacial evidence, major parts of Earth that have not been glaciated in the Pleistocene Epoch cannot be searched for clues. This complicates the identification of paleoclimates in tropical and many midlatitude locations as well as at all oceanic locations. In addition, glacial evidence can lead to questions of why the glacier existed. Was it because of the low temperature, wetter conditions, or some combination of the two? Finally, the remnants of glaciations before the Pleistocene are largely erased by more recent glacial episodes, restricting the evidence toward those latter events.

Evidence of climatic change can also come from existing ice. Clues about the paleochemistry of the atmosphere are preserved within air bubbles trapped in ice when the ice formed. To identify these clues, deep holes can be drilled into the ice sheets in Greenland and Antarctica, and the **ice cores** can be sampled subsequently in a laboratory. Variations in the ratio of a rare but natural and stable oxygen isotope—oxygen-18 ($\delta^{18}\text{O}$, pronounced “del-oh-18”)—to “normal” oxygen ($\delta^{16}\text{O}$) in the ice layers can reveal clues about the temperature of Earth. Oxygen-18 contains 8 protons and 10 neutrons, rather than 8 protons and 8 neutrons as in “normal” oxygen-16 ($\delta^{16}\text{O}$). Oxygen-16 is nearly a thousand times more common than $\delta^{18}\text{O}$, but relatively more $\delta^{18}\text{O}$ is present in air trapped in polar ice cores when the global temperature is high. The reason for this feature is that during warm periods the high amount of energy available for evaporation allows the heavier $\delta^{18}\text{O}$ a greater opportunity to be evaporated than normal, on a global average basis. This $\delta^{18}\text{O}$ is then advected toward the polar regions, where it is trapped in air bubbles as ice forms. The ratio of $\delta^{18}\text{O}$ to $\delta^{16}\text{O}$ is even lower than usual during cold periods in geological history, because the decrease in evaporation leaves more of the heavy $\delta^{18}\text{O}$ in the ocean.

Ice cores also provide our only reliable evidence for the concentration of atmospheric CO_2 in the pre-instrumental record. The Vostok ice core from the Russian research station near the geographical center of Antarctica contained trapped samples of air from about 160,000 years ago. It was found that atmospheric CO_2 levels ranged from 180 to over 290 parts per million before the Industrial Revolution (compared with over 407 parts per million today, and rising by a few parts per million per year!). The Vostok core also revealed that periods of higher atmospheric CO_2 concentrations tend to correspond to the warmer interglacial periods, and lower CO_2 concentrations are linked to glacial advances.

A major advantage of ice core data is the scientific soundness of this technique. Another advantage lies in its ability to provide a reliable record of climatic change dating back several hundred thousand years, though this is still only a short period of geologic time. A shortcoming is that it is difficult and expensive to obtain cores from the Greenland or Antarctic ice sheets.

A different type of cryospheric evidence is provided by *varves*, which are annual sets of silt and clay layers deposited on the bottoms of lakes and ponds that freeze in winter and thaw in summer. In a frozen lake only fine suspended clay can be deposited—the winter varve—because the surface ice prevents other materials from penetrating into the lake. When thawing begins in spring, fresh water and coarse sediments that had been deposited on the ice surface sink to the lake bottom—the summer varve. Varve thickness can be related to climatic fluctuations. An abnormally thick summer varve may represent a longer freeze-free period. Lakes beneath glaciers do not have summer varves because of the necessity for annual freezing and thawing. A series of “missing” years in the dating of the sediments, therefore, identifies a time during which a glacier existed over the water body. Unlike any of the other techniques discussed to this point, varves offer the advantage of an annual record. The most extensive record of varves is a German data set that extends back about 23,000 years. Very recent research suggests that the Green River formation in Colorado, Utah, and Wyoming may contain varves that record 20 million years of geologic history. However, there is considerable debate about whether these are truly annual sediments or whether they represent the work of turbidity currents at a much smaller time scale.

The long-term action of falling droplets in caves leaves mineral deposits called **speleothems**, which can also be used as a climate proxy. Speleothems take a variety of forms with the most common being stalactites and stalagmites. Speleothems are particularly good climate proxies as they provide a wide array of climate clues such as precipitation and temperature

and contain oxygen and carbon isotopes for providing further evidence of environmental conditions. They are easily and accurately radiometrically dated to time periods of over one-half million years.

Another source of proxy evidence from the lithosphere comes from the thousands of **boreholes** around the Earth at which temperature is measured at depth. The boreholes themselves have been drilled for a variety of reasons, such as mineral exploration, but the temperatures measured in them at various depths can provide clues about surface air temperature. Because *conduction* is such a slow mechanism of heat transfer, boreholes can provide indications of air temperatures back to hundreds of years. However, adjustments must be made to account for the effects of geothermal heating before a borehole-derived air temperature estimate can be made.

Biological Evidence

Fossils

Biological evidence for climatic changes in geological history takes several forms. First, fossilized rock allows paleoscientists to infer the climatic conditions that existed at the time (as determined by radiometric dating) and place that the fossil was formed. The Principle of Uniformitarianism allows us to assume that the same conditions that support organisms similar to the fossilized organism must have existed when the fossil formed.

Certain specific forms of life provide especially useful clues about Earth's climatic history. These include microfossils produced by **foraminifera**, known as marine protista. During times of warm oceans, some species of foraminifera tend to have more individuals whose shells developed with a coiling on the right side (**dextral**). On the other hand, during times of colder oceanic conditions left-coiling (**sinistral**) individuals are more common. By mapping the percentage of dextral and sinistral individuals over space and dating the samples, the sequence of past oceanic temperature distribution can be deduced. In addition, marine microfossils can provide clues about the salinity of the oceans, which is related to the energy and water budgets of the atmosphere. Furthermore, because foraminifera are so abundant, their shells are believed to represent a significant sink for atmospheric carbon and may play a role in the regulation of atmospheric CO₂, thereby providing evidence for the strength of the greenhouse effect at various times in geological history.

The composition of the exoskeletons of other fossilized microscopic marine organisms also provides clues about ancient atmospheric temperature. Specifically, the ratio of oxygen isotopes reveals the temperature distribution at the time when the shell was formed,

as part of the same process that causes differences in isotope ratios in ice cores. During warm periods in geological history, tropical evaporation is especially intense. The ratio of $\delta^{18}\text{O}$ to $\delta^{16}\text{O}$ in microfossils in the tropical oceans is, therefore, lower than in cold periods, because the heavier $\delta^{18}\text{O}$ can be evaporated more easily than at cooler times. In contrast, as we saw previously, the $\delta^{18}\text{O}$ to $\delta^{16}\text{O}$ ratio is higher in polar ice cores during warm periods as winds in the general circulation carry the oxygen poleward. By contrast, colder periods allow for more “selectivity” in evaporation, causing the heavier $\delta^{18}\text{O}$ to be less likely to be evaporated in the same proportion. Cold periods are identified by a relatively high concentration of $\delta^{18}\text{O}$ in tropical marine microfossils and a simultaneous relatively low concentration of $\delta^{18}\text{O}$ in air bubbles trapped in polar ice cores.

The use of microfossils for a paleoclimatic signature has several benefits. These techniques are scientifically sound and can give reasonably accurate records of climatic change dating back at least 400,000 to 500,000 years—enough to identify previous glacial and interglacial sequences. A major disadvantage of using oceanic microfossil evidence is that the sampling area must be in remote areas to minimize the possibility of transport from other areas.

Palynology

Palynology is the scientific study of pollen and spores. **Angiosperms** and **gymnosperms**—cone-bearing vegetation that does not have seeds enclosed within an ovary—produce pollen grains, and lower plants produce spores. Because pollen and spores are especially resistant to decay and have different characteristics for different species, the presence of pollen and spores can reveal the natural vegetation types during the time that the pollen was produced. Lakes are especially useful catchment basins for pollen and spores because once they reach the water surface, they settle down to the lake bottom. Coring and radiocarbon dating can identify a temporal sequence of pollen/spore types. Some of the changes in the accumulation of pollen and spores are attributable to climatic changes, and they can give scientifically valid clues about Holocene paleoclimates.

Some complications are present in palynological analysis. Because plant species and even individuals of the same species differ markedly in the amount of pollen or spores produced, it is difficult to generalize about whether a certain amount found is indicative of the abundance of that type of vegetation. So, for example, if a small amount of grass pollen is found, it is unclear whether abundant grasslands existed far away and a small amount of its pollen drifted to the site or if a small amount of the grass was present near the site. In

arid areas pollen and spores are dispersed far from the source, but in rainy areas they remain nearby. Again, it is tenuous to ascertain whether a small amount of grass pollen present may indicate that the environment was too humid to advect more of the grass pollen from the source to the location where it was found. Nevertheless, palynology is a useful tool that can provide important information about the paleoclimatic conditions, including circulation (unlike most of the other techniques), especially when used in combination with other types of paleoclimatic evidence.

Dendroclimatology

The characteristics of a tree's annual growth rings can give clues about the climate during the year when that ring was produced. Because tree rings from the early years of living trees can be matched with the rings from the late living years of dead trees, which can in turn be correlated with rings from trees that lived even earlier, **dendroclimatology** can provide climatic evidence dating back hundreds or even thousands of years. Like varves, dendroclimatology offers the advantage of an annual and even a subannual record. Dendroclimatological analysis has been especially useful in precipitation and streamflow reconstructions.

Dendroclimatology also has its complications. First, other factors besides climate influence the growth of tree rings. These factors include the age, health, and species of a tree as well as characteristics of the soil such as nutrient availability and the availability of groundwater. An additional challenge is that the climatic features that the tree ring is indicating may be unclear. For example, if a particular tree shows a series of abnormally narrow rings and it can be assumed that climate produced the stress indicated by the rings, what climatic features limited the growth of the tree? Possibilities may include high summer temperatures, low winter temperatures, lack of precipitation, extreme severe weather events, or recurring periods of minor disturbing events.

A few research groups around the world, most notably at the University of Arizona, have amassed libraries of tree samples for dendroclimatological analyses. The best samples are from trees under stress, because many forms of stress are climate related. Because the features of tree rings are species dependent, dendroclimatologists must understand the characteristics of each tree species sampled, just as palynologists must have great expertise in identifying the species that produced the pollen or spores in a sample.

Other Sources of Biological Evidence

Several other forms of biological proxy evidence exist. For example, analysis of the proportion of calcium

carbonate (CaCO_3) generated from exoskeletons in marine sediments can provide clues about ancient ocean temperatures. Dissolution of CaCO_3 is more rapid in warmer conditions than in colder conditions. The distribution of CaCO_3 remaining in a sediment sample can, therefore, suggest past thermal conditions where the sample was found.

Likewise, when water temperatures exceed 32°C (90°F) for extended periods of time and/or ocean acidification occurs, algae on coral reefs die (which eventually causes the death of the reef because the energy provided by the algae is lost). The coral then appears white or “bleached.” Coral reefs thus can provide evidence of changes in temperature, particularly if the reef is in a “fringe” area of the ocean where temperature could be a limiting factor to its health.

Finally, fluctuations in the *treeline* also provide proxy evidence of climatic change. When climate is cooling, the “line” separating the zone in which trees can survive from the zone in which trees cannot survive moves equatorward and downslope. When the climate is warming, the treeline moves poleward and upslope. Identification of past forested landscapes is relatively straightforward and evidence is abundant. The poleward (or upslope) movement of trees is quicker during warming periods than is the equatorward (or downslope) movement during cooling periods, however, so the timing of the climatic change may be tricky to discern. Furthermore, the location of a treeline does not necessarily index climatic conditions, as climate may not be the only factor involved in treeline fluctuations.

Historical Data

Historical data refer to written information about climate, but they do not include formal meteorological records. Diaries, ship logs, newspaper accounts, and other sources can provide at least some climatic information. Some of these writings directly pertain to atmospheric phenomena. For example, heat waves, floods, hurricanes, and snowfall totals often may be described in historical records. Other types of written records may be directly or indirectly related to weather and climate, such as observations of animal migrations, agricultural and fisheries yields, and the dates of the flowering of various types of trees.

A major advantage of historical data is the abundance of evidence for recent times. A disadvantage is that the results are not usually quantified, so it can be difficult to ascertain meaning. To alleviate this problem, historians often quantify written observations through **content analysis**—an objective method of converting text into discrete categories to infer climatic conditions. For example, if someone says that it is “very cold this

winter,” what does that mean? “Very cold” may mean different things to different people. Recurring patterns of text, however, can be used to glean more meaningful information that can be used to estimate climatic conditions in the historical past.

Converging Proxy Evidence

Paleoclimatological reconstruction requires a wide variety of expertise. Geologists, glaciologists, geochemists, oceanographers, botanists, paleontologists, vulcanologists, foresters, sedimentologists, and historians have all contributed significantly to our understanding of paleoclimates. Because of the inherent difficulty and contradictions in the geological, biological, biochemical, and historical records, the converging evidence from several of the proxy data sources must be used before reaching a firm conclusion. Nevertheless, when the limitations of the various techniques are recognized and conclusions are drawn cautiously, the use of proxy evidence can provide a clear picture of the climates of the past, especially when many forms of proxy evidence converge toward the same conclusions.

► Natural Causes of Climatic Change and Variability

Several geological, astronomical, solar, and oceanographic mechanisms are known to contribute to climatic change and variability, on time scales ranging from millions of years to a few months. This section details the most well-known natural forcing mechanisms, beginning with those that operate at the longest time scales and proceeding to those that operate at the shortest.

Continental Drift and Landforms

Earth’s crustal plates are slowly but constantly moving. Over millions of years this slow drift has moved continents great distances. During times in geological history when continents straddle the polar areas (as they do now), the continents cool far more easily than when water is located over the poles. This tendency has global climatic implications, as the bitter cold polar land masses provide a positive feedback system whereby small amounts of ice and snow cause more reflection (higher *albedo*) of *insolation*, which enhances global cooling. Eventually, ice sheets develop on terrestrial polar locations.

It has been suggested that continental position may explain the ice age/non-ice age sequences. The aggregation of land masses over the South Pole may have led to the Gondwanan Ice Age of the late Paleozoic. Likewise, the present ice age may be attributable to the presence of



FIGURE 11.8 The Bering Strait nearly cuts off the flow of water between the Pacific Ocean and the Arctic Ocean.

Antarctica at the South Pole and the large land masses surrounding the high-latitude Arctic Ocean.

Even without the direct influence of continental positions on ice sheets, the positions of continents can affect ocean circulation (and therefore temperature) to a significant extent. When ocean currents are allowed to mix tropical waters with the colder waters of the high latitudes (such as the *Gulf Stream/North Atlantic Drift* today), ice sheets are less likely to form. In contrast, when continents are positioned so as to hinder the low-latitude waters from mixing with the high-latitude waters (as occurs between Siberia and Alaska today), ice sheets are more likely to form (**FIGURE 11.8**).

Continental position can affect ocean temperatures in other ways, too. Merely 3 million years ago the Isthmus of Panama had not yet connected North America to South America, and warm tropical waters streamed between the Caribbean Sea and the Pacific Ocean. This likely impeded the cold currents in the eastern Pacific and probably influenced atmospheric circulation, including paleohurricanes. Current prevailing thought is that the formation of the isthmus is likely to have strengthened the Gulf Stream/North Atlantic Drift and intensified the global thermohaline circulation by keeping the Atlantic much more saline than the Pacific. Such changes may have initially promoted warming by moving tropical waters poleward in the Atlantic, but later may have eventually contributed to cooling as the additional moisture *advection* toward the North Pole began to precipitate and build ice sheets. Some have speculated that this process could have triggered the present ice age.

In addition to the positions of continents on Earth, the positions of mountainous regions on Earth can be important producers of climatic change. During periods after **orogeny**—the process by which mountains form—more of Earth’s surface area has sufficiently high elevations to produce colder conditions. Once the cold conditions occur, the presence of snow and ice once again reinforces the cold by reflecting more insolation,

setting up a positive feedback system. Mountain uplift can also affect the synoptic-scale atmospheric circulation, which can in turn alter climates. For example, the presence of the Himalayan Mountains affects Asian precipitation and jet stream circulation. Because of the conservation of *potential vorticity*, winds that approach north–south mountain ranges from the west are likely to encourage the formation of longwave ridges upstream and over the mountain ranges and longwave troughs downstream from the mountains. The amplification of such a ridge–trough configuration caused by the mountains can spill cold air equatorward to a greater extent than would occur if the mountain range did not exist or was lower in elevation. In today's environment, for example, Arkansas is probably colder than it would be without the Rocky Mountains to induce an upper-level ridge that spills cold air on the eastern side of the ridge axis (i.e., its ridge-to-trough side).

Milankovitch Cycles

In the early 1900s the Serbian astronomer Milutin Milankovitch calculated several cyclical changes in Earth's orbit around the Sun, axial tilt, and axial orientation. He postulated that these **Milankovitch cycles** that operate on the order of tens of thousands of years may be responsible for cycles in climate, including glacial and interglacial sequences. Milankovitch identified three specific cycles: (1) eccentricity, (2) tilt, and (3) precession of the equinoxes.

Eccentricity

One cycle is in the **eccentricity**—circularity—of Earth's orbit around the Sun. Earth's orbit is not centered on the Sun, and the amount of eccentricity varies over time. At one extreme of the eccentricity cycle, the Sun is at almost the exact center of Earth's orbit. At the other extreme, Earth is approximately 11% closer to the Sun at *perihelion*—the day of the year when Earth reaches its closest distance to the Sun—than at its opposite position 6 months later—*aphelion*. Eccentricity gradually changes from a more circular to a more elliptical orbit, with a periodicity of approximately 95,000 years.

Presently, we are in a period of relatively low eccentricity. At perihelion, which falls on or about January 3, Earth is approximately 3% closer to the Sun than at aphelion, which falls on or about July 4. Because the **inverse square law** states that the intensity of radiation received by a body is inversely proportional to the square of the distance between the emitting and receiving body, this difference in distance results in Earth receiving about 7% less insolation in July than it does in January. The fact that July is a summer month in the northern hemisphere implies that eccentricity is not the major

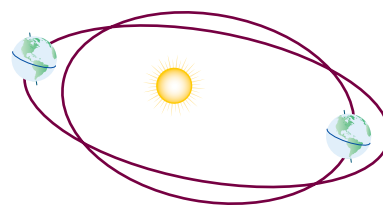


FIGURE 11.9 The eccentricity of Earth's orbit changes over time.

cause for the seasons. The cycle of eccentricity (acting alone) implies that northern hemisphere summers may be moderated more significantly than they would be if the orbital eccentricity were higher at this point in geological history.

Periods of low eccentricity are more likely to coincide with glacial periods within ice ages on Earth, whereas periods of high eccentricity are more likely to be linked to interglacial phases. To understand why, it is important to note that summer temperatures are perhaps a more important determinant than winter temperatures of whether ice is expanded equatorward or retreated poleward. Within an ice age, winters will certainly be cold enough for ice to exist over a relatively large portion of Earth's surface. But the degree to which summer is warm enough to melt the ice is the more important question in determining whether the ice age is characterized by a glacial or an interglacial phase. A more eccentric orbit changes the length of seasons in each hemisphere by changing the length of time between the vernal and autumnal equinoxes (**FIGURE 11.9**). This would provide for longer summers (and shorter winters) in one hemisphere, thereby providing more opportunity for ice to melt in that hemisphere year-round. Furthermore, periods of higher eccentricity place one of the hemispheres much closer to the Sun during the summer. Such a situation makes it difficult for ice to persist throughout the year in that hemisphere. Apparently, these effects tend to be sufficient to offset the tendency in the opposite hemisphere for a longer winter and shorter summer, regardless of which hemisphere contains more land. The result, assuming that all other factors are equal, is a colder Earth under more circular orbital conditions.

Tilt

We have already seen that Earth's axis is tilted from the vertical by 23.5° (**FIGURE 11.10**) and that this angle of tilt does not change through the course of the year. Milankovitch noted, however, that in reality on geological time scales the tilt does slowly change in a cyclical fashion, from a minimum of about 21.8° from the vertical to a maximum of about 24.4° from the

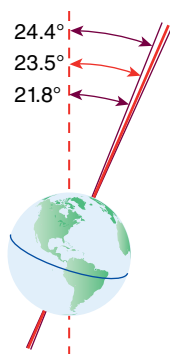


FIGURE 11.10 Variation in tilt of the Earth's axis.

vertical. The periodicity of this Milankovitch cycle is approximately 44,000 years.

This cycle implies that the *Tropic of Cancer* and *Tropic of Capricorn*, which are currently at 23.5°N and 23.5°S latitude, respectively, vary from about 21.8° latitude to about 24.4° latitude. The Tropics of Cancer and Capricorn are significant because they represent the most poleward extent that the *solar declination* can reach at some point throughout the year. On or about June 21, Earth is positioned in its orbit such that the northern hemisphere is tilted toward the Sun to its maximal extent (even though the north polar axis itself remains pointed at Polaris, the North Star, year-round). At the same time the southern polar axis is maximally tilted away from the Sun. Likewise, on or around December 22, Earth's position in its orbit is such that the northern hemisphere is maximally tilted away from the Sun (and the southern hemisphere is maximally tilted toward the Sun).

The cyclical changes in the angle of tilt affect the amount of summer to winter contrast in heating, and, therefore, seasonality. The smaller the tilt, the closer to the equator the Sun's direct rays remain throughout the year. In periods of geological history when the tilt is relatively small, summers in middle and high latitudes are cooler (all other factors being equal) but winters are milder because the solar declination is not so far away in the opposite hemisphere. A smaller tilt is associated with less seasonal temperature variation between summer and winter in middle and high latitudes. Such a situation encourages glaciation (assuming that all other factors are equal) because, as stated earlier, cooler summers tend to support glaciation in the high latitudes to a greater extent than relatively mild winters (which will be below freezing even when they are "mild").

By contrast, periods of high tilt allow the Sun's direct rays to penetrate farther poleward than average. This causes summer temperatures to be high, because the solar declination approaches the midlatitudes more

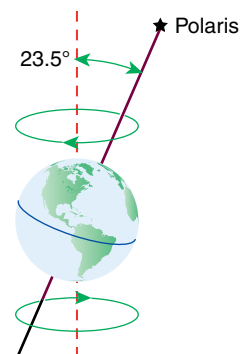


FIGURE 11.11 The precession, or wobble, of Earth on its axis.

closely. But it also causes cold winters, when the solar declination is farther away in the opposite hemisphere.

Precession of the Equinoxes

The final Milankovitch cycle refers to **precession**—the changes in the direction that Earth's axis points (but not the angle—which represents tilt). Earth's axis wobbles like a spinning top because Earth is not a perfect sphere (FIGURE 11.11). Precession refers to this gyrating type of motion. The axis points in a varying direction about the same angle of tilt (although, as we just saw, the tilt simultaneously undergoes cyclical changes) over time, with a periodicity of approximately 23,000 years. This implies that Earth will not always point to our present north star, Polaris. In fact, 11,500 years from now the north star will be Vega, but by that time this book's author will not be here to enjoy his newfound fame.

A progressive change in the dates of the solstices, equinoxes, perihelion, and aphelion occurs because of this Milankovitch cycle and because Earth's elliptical orbit itself is rotating. In 23,000 years the northern hemisphere's summer solstice will again occur on or about June 21. Because 23,000 years is required to advance the cycle by 365 days, we can say that about 63 years are required to advance the cycle by 1 day. In other words, the dates of the solstices, equinoxes, perihelion, and aphelion all change by a little more than 1 day per human lifetime.

This cycle also implies that in about 11,500 years Earth will experience perihelion in July and aphelion in January. Obviously, if Earth is closest to the Sun at the same time that a hemisphere is experiencing summer, that hemisphere could be expected to become hotter. This tendency is particularly true if the summer hemisphere has abundant land surfaces. At this point in geological history, the hemisphere that has most of the land happens to be farthest from the Sun when it is tilted toward the Sun. Summers in the northern hemisphere are milder than they would be if the axis were positioned so that December 22 was its summer solstice, because in that case the northern hemisphere would be pointing toward

the Sun near the same time of year that it experiences perihelion. The same situation also applies to winter cooling for the northern hemisphere.

Combined Effects of the Milankovitch Cycles

It has been proposed that when all three of the above factors are in phase, such that they all point to a warmer or colder Earth, the apexes of the glacial–interglacial sequence seem to be reached. The high latitudes may be the key in regulating the thermal conditions associated with these sequences. Most climatologists believe that tropical areas do not show the climatic fluctuations nearly as much as higher latitudes (i.e., *Arctic amplification*) because changes in the cycles do not affect solar radiation receipt much in those areas. The Milankovitch cycle hypothesis has been disputed in recent years, but it does provide a viable explanation for some types of long-term climatic changes and periodicities.

Volcanic Activity

Earth undergoes intervals of relatively frequent volcanic activity and other intervals of less frequent volcanic eruptions. The uneven frequency of volcanic activity through geological time may be explained by differences in the number and strength of **subduction zones**—locations where a denser crustal plate is displaced beneath an adjacent less-dense plate through tectonic forces driven by interior geological processes. As a plate subducts, partial melting of the subducted plate, the overlying plate, or both occurs to form **magma**—molten rock material beneath Earth's surface. The buoyant fluid rises through the overlying plate, and if the surface is reached a volcano is born. Volcanism can also occur where two crustal plates are spreading apart and magma rises from beneath the surface to fill in the “missing” land.

Atmospheric CO₂ is produced in volcanic eruptions, and it is eventually removed from the atmosphere primarily by absorption and sequestration in oceanic sedimentary rocks. Periods of active volcanism may enhance the greenhouse effect by contributing CO₂ to the atmosphere, leading Earth into an ice-free period, and the slow removal of that CO₂ may allow for the onset of an ice age. Similarly, a drop in the production rate of CO₂ by a relative lack of volcanism might reduce the atmospheric greenhouse effect and lead to lower temperatures. The Gondwanan Ice Age may have begun when the moving continental plates first assembled in Pangaea and then underwent a readjustment period before drifting apart again. Perhaps during the readjustment period the production of CO₂ dropped during a period

of infrequent and weak volcanism along subduction zones, leading to cooling.

Other paleoclimatological evidence suggests that temperature trends may precede trends in CO₂. In other words, CO₂ may respond to temperature variation rather than cause it. One explanation for this sequence is that the solubility of CO₂ in oceans is inversely proportional to ocean temperature. So a slight increase in temperature would result in less CO₂ dissolved in the ocean, and a higher concentration of atmospheric CO₂. However, because the rate at which CO₂ increases are occurring today are apparently much greater than at any time in the geologic past, as far as we know, the role of CO₂ solubility in the oceans in mitigating today's warming is unclear. A related complication is the slow response of oceans to atmospheric temperature changes; the changes in atmospheric CO₂ caused by changes in oceanic assimilation may occur decades or even centuries after the atmospheric temperature change occurred. The entire process is complicated, and the suggestion that increasing CO₂ is an effect rather than a cause of global warming remains controversial today.

Paradoxically, on shorter time scales the high concentrations of dust ejected during periods of intense and frequent volcanism may diminish radiant energy reaching the surface, cooling the climate. In severe eruptions, dust can be ejected into the stratosphere and remain suspended for a year or more. Increased particulates can also alter global atmospheric circulation patterns, resulting in a higher frequency of unusual and extreme weather events.

Several examples in addition to that of the “Year without a Summer” presented earlier suggest that volcanism is an agent of short-term “global cooling” and a culprit of severe and unusual weather. With the possible but unlikely exception of Eyjafjallajökull in Iceland, which erupted in Spring 2010, the most noteworthy example of a volcanic eruption during the period of accurately measured meteorological data that led to surface cooling was **Mount Pinatubo**, which erupted in the Philippines on June 15, 1991. Pinatubo's eruption blasted more than 1.8×10^{10} kg (20 million tons) of SO₂ and ash into the atmosphere. The vertical column of ejected material was measured at 19 km (12 mi) high during the eruption, producing a VEI (Volcanic Explosivity Index, see Chapter 4) of 6. The resulting stratospheric SO₂ plume spread rather evenly across the globe over time, leading to an estimated global surface temperature decline of 0.5 °C (0.9 °F) for 2 years after the eruption. Mount Pinatubo's eruption may have been related to some of the unusual weather experienced in the United States in 1992 and 1993. Specifically, heavy rainfall preceded the catastrophic flood on the upper Mississippi River, a very heavy snow event occurred on the Atlantic coast of the

United States, and other unusual weather events were recorded around the world. Those were the 2 coolest years globally of the last 20.

Other volcanic eruptions during the instrumental period of record confirm that volcanoes can impact climate and human endeavors globally. Eyjafjallajökull's fallout was modest by comparison to Mount Pinatubo's, but its impacts were felt heavily. Air traffic in northern Europe was grounded for 8 days, with subsequent intermittent shutdowns over parts of Europe thereafter. The eruption of **El Chichón** in Mexico in 1982 may have contributed to the unusual global weather of 1982 and 1983, capped by one of the strongest *El Niño* episodes in the meteorological record. Atmospheric extremes included severe drought in South Asia, southern Africa, and Australia, with heavy rains and flooding in the U.S. Gulf Coast and western South America.

Prior to the period of accurate weather data collection, several volcanic eruptions are noteworthy. The 1815 eruption of Tambora in Sumbawa, Indonesia, is regarded as the largest in modern history, as it ejected an estimated 50 km^3 (12 mi^3) of magma and an astonishing $1.8 \times 10^{11} \text{ kg}$ (200 million tons) of SO_2 into the atmosphere. The VEI 7 eruption led to the widely regarded “Year without a Summer” in 1816. Global surface air temperatures are believed to have decreased by 0.4 to 0.7°C (0.7 to 1.3°F) during the year after the eruption.

The eruption of *Krakatau* in 1883, also in Indonesia, is thought to have nearly rivaled Tambora in explosiveness with a VEI of 6. The eruption is believed to have killed up to 40,000 people, and it ejected ash and dust as high as 12 km (7 mi) above the surface as most of Rakata Island disappeared. In total, 20 km^3 (5 mi^3) of material were ejected into the atmosphere, making Krakatau about 20 times as destructive as the **Mount St. Helens** eruption of May 18, 1980. With less ejecta, global temperatures apparently were not affected as significantly as by Tambora. The eruption did cause spectacular sunsets for over 70% of the globe over a time period of 3 years.

Another notable eruption was the 1783 **Laki Fissure** eruption in Iceland, which lasted 8 months and was responsible for devastating much of the human and animal population of Iceland. It is estimated that 14 km^3 (3.4 mi^3) of basalt was ejected. In addition, more than $9.1 \times 10^{10} \text{ kg}$ (100 million tons) of SO_2 were emitted, leading to an estimated 1°C (1.8°F) temperature drop for the northern hemisphere.

Some geoscientists believe that the most catastrophic eruption occurred on **Mount Toba** in Sumatra approximately 71,000 years ago. This eruption may have been so cataclysmic that it may have accelerated the onset of the last **glacial advance**. Global climates may have changed so much that massive extinctions and population declines would have occurred in many plant, animal,

and human populations across the globe. In fact, the event may have caused an evolutionary **bottleneck** in humans—a significant drop in population that triggers rapid genetic divergence in surviving individuals, with today's *Homo sapiens* replacing Neanderthals and *Homo floresiensis* (the hobbits) in southeast Asia. The human bottleneck would have allowed for subsequent rapid proliferation of genetic differences through small populations, as opposed to being washed out of much larger populations. Many geologists fear a future “supereruption” like Mount Toba, with Yellowstone National Park being one candidate as the site for such an eruption.

Variations in Solar Output

Solar output seems like a straightforward factor as a cause of climatic variability and change. It is generally assumed that increased solar output is associated with a warmer climate. Many assumptions about the effects of the Milankovitch cycles rely on this supposition. As we have seen with the faint young Sun paradox, however, reduced solar output does not always lead to colder conditions because other factors may compensate.

There is even some evidence to suggest that an inverse relationship between solar output and temperature could exist. With increased insolation, more latitudinal temperature differences would occur, because increases in heating in the tropics would be *relatively* greater than at the poles—in direct contrast to the notion of Arctic amplification. A wider disparity in radiation receipt would occur than we see today. This increased energy gradient would cause stronger circulation with more vigorous contrast between tropical and polar *air masses*. This increased air mass contrast, along with the additional evaporation from a warmer tropical ocean, would create more precipitation. Some of this extra precipitation would be in the form of high-latitude snow and ice, which would increase the albedo of the surface. With higher albedo, a greater percentage of the Sun's energy would be reflected from the surface, thereby causing colder polar conditions even with greater input of solar energy. This scenario indicates that it is dangerous to oversimplify a problem; the climate system is complicated.

Like volcanism, variations in solar output can cause both long-term changes over geological history and short-term variability. The Sun experiences small short-term fluctuations in output associated with **sunspots**—huge magnetic storms that appear as darker regions on the Sun's surface, varying in number and intensity over time. The sunspots themselves are “cooler” locations on the Sun's surface, but poorly understood reactions above the sunspots more than offset this tendency for lower solar output. Maximum sunspots imply increased solar energy and recur on average every 11 years (**FIGURE 11.12**). The

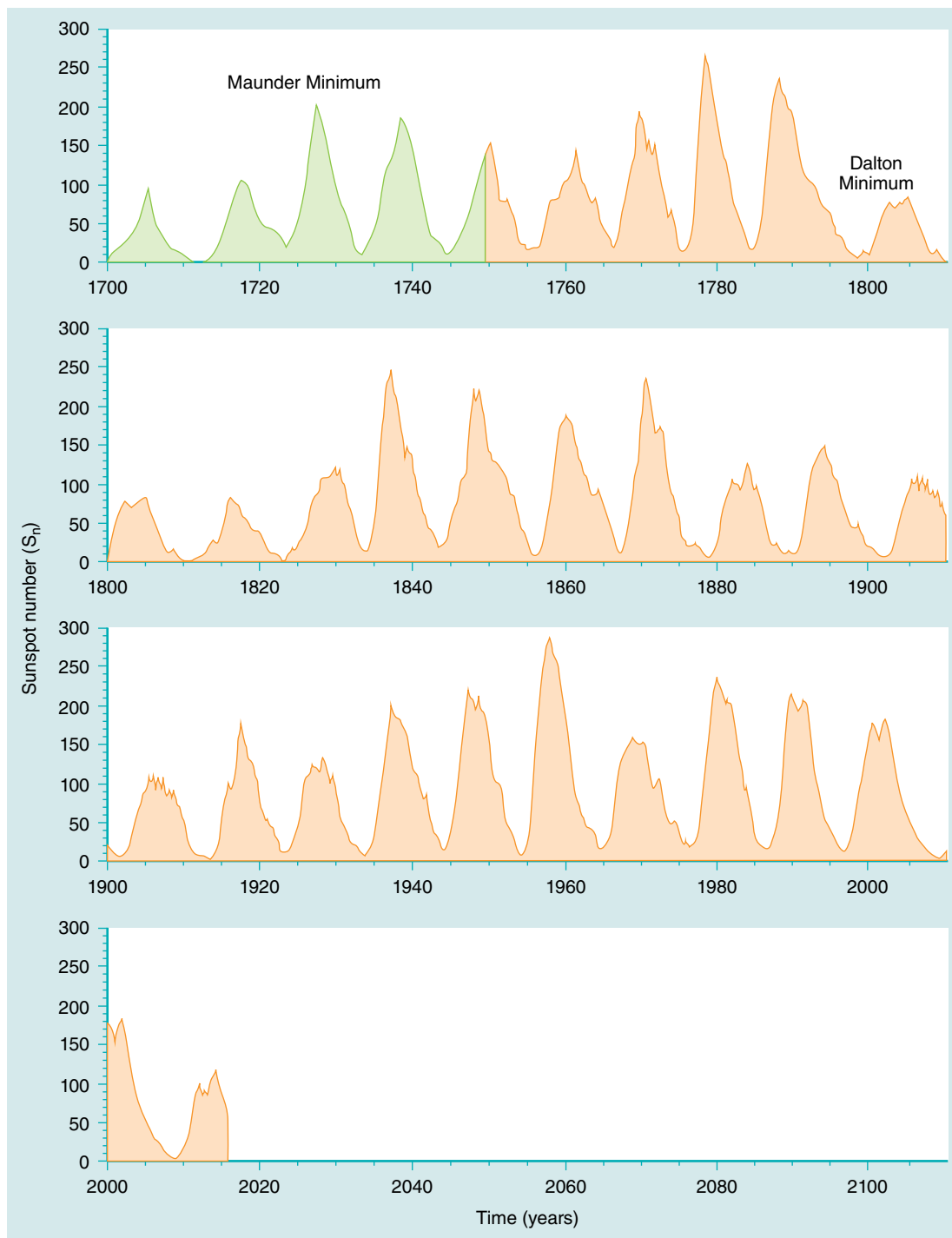


FIGURE 11.12 Number of sunspots observed since the late Maunder Minimum.

SILSO graphics (<http://sidc.be/silso>) Royal Observatory of Belgium.

Sun's equivalent of the *Coriolis effect*—the differential rate of rotation with latitude—is believed to cause the sunspot cycle by altering the solar magnetic field. Every 22 years or so, the Sun's magnetic field reverses during a period of minimum sunspots. The maximum part of the cycle was last reached in 2012–2013. According to NASA scientists, the peak of 67 sunspots (as of May 2013) in this cycle (the 24th officially observed sunspot

cycle) would rank Cycle #24 as the weakest since 1906, unless subsequent months in 2013 surpass the total. The last solar magnetic field reversal was in 2001.

Solar activity indicated by sunspots correlates with some aspects of climate. Supporting evidence includes the fact that few sunspots were observed to exist from about 1645 to 1715 during the **Maunder Minimum** and from 1796 to 1830 in the **Dalton Minimum**. These

periods correspond to the peak and end of the LIA, respectively. This period corresponds to the peak of the LIA. Additionally, droughts in the Great Plains seem to recur on an approximately 22-year cycle, including the Dust Bowl years of the mid-1930s, the mid-1950s (when drought was actually more severe than in the Dust Bowl years), the mid-1970s, and the severe drought of 1995 and 1996 on the southern plains. Are severe droughts of the last few years the beginning of the next phase? Regardless, correlations between sunspot cycles and climate are tenuous at best. A more formidable argument can be made that longer-term changes in solar output drive climatic changes.

El Niño–Southern Oscillation Events

As discussed previously, El Niño, *La Niña*, and the associated *teleconnection*—the *Southern Oscillation*—can have drastic consequences near both the tropical Pacific core of activity and around the globe. El Niño–Southern Oscillation (ENSO) affects the midlatitude atmospheric circulation systems because the shearing motion associated with circulation at the poleward edges of the *Hadley cells* alters midlatitude circulation. Oceanic circulation is also altered in the Pacific.

Impacts may be far-reaching during El Niño. For instance, *monsoon* circulations tend to weaken around the world, and Atlantic *tropical cyclone* activity tends to

be suppressed because of the abnormally strong westerly winds, which shear off the tops of developing tropical cyclones. Other specific important impacts from ENSO have been discussed previously. In general, the effects of El Niño vary according to the strength of the episode. During an El Niño event an area may even experience flooding one time and drought the next.

Because El Niño and La Niña events usually persist for approximately 6 to 18 months and recur every 3 to 7 years on average (FIGURE 11.13), an individual event can hardly be said to bring about climatic change. Instead, ENSO is a producer of climatic variability. Some evidence, however, suggests that the frequency of ENSO events may have changed over long time scales. If true, then ENSO could be a producer of both short-term climatic variability and long-term climatic changes.

Other mechanisms producing climatic change and variability may also be important. One feature in particular is the *quasi-biennial oscillation* (QBO)—a periodic reversal of the equatorial stratospheric winds between westerly and easterly, with a cycle of approximately 26 months. Although the QBO is known to be related to Atlantic tropical cyclone frequency, the *Asian monsoon*, and winter temperature variability in the northern hemisphere, a precise cause–effect relationship has not been established with confidence. Similarly, its influence on other features of the climate system may exist but is poorly understood at this time.

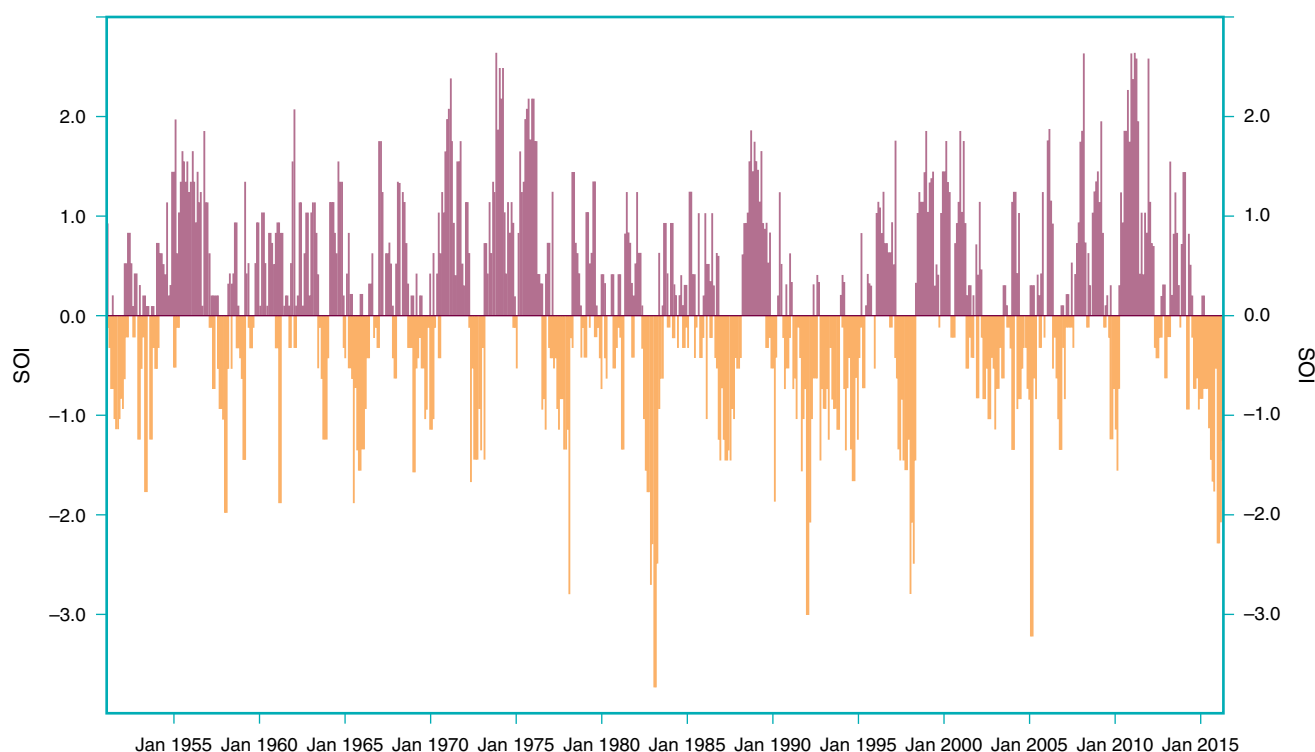


FIGURE 11.13 Southern Oscillation Index (SOI), 1950–2015.

Data from NOAA/Earth System Research Laboratory/Climate Diagnostics Center/Climate Indices Plotting Page. <http://www.cdc.noaa.gov/ClimateIndices>.

► Summary

Climates vary and change through time, as have people's perceptions of what constitutes climatic variability and change. This complicates the establishment of policy related to climate, because climatic variability and change mean different things to different people. Our best scientific evidence suggests that the climate has fluctuated significantly but within a reasonable range of the present temperature, despite the evidence that the solar output was significantly lower in the early part of geological history.

Ice ages are periods of approximately 50 million years when "permanent" ice exists somewhere on Earth's surface. No credible scientific evidence for ice ages in the first half of Earth's 4.6 billion years has been identified. Since that time, at least five ice ages have occurred, with several hundred million years separating major ice ages. The present ice age may have begun as far back as 40 to 50 million years ago, but it escalated in intensity over the last 1.8 million years. Ice ages are subdivided into glacial phases—when ice extends equatorward—and shorter interglacial phases—when the ice retreats but is not absent. We are currently in an interglacial phase of an ice age—a rather unusual time in geological history. During periods when ice is abundant, sea level decreases as more of the global water budget is stored in the cryosphere. Rising sea levels are a concern if Earth continues to warm.

The Wisconsin Glacial Phase represents the most recent glacial advance, when at its peak 18,000 years ago large ice sheets covered North America approximately north of the Ohio River. Abrupt warming occurred after that point, except for a few significant cooling periods. Most notably, the Younger Dryas represented rapid and pronounced cooling, perhaps on a global scale, and showed that the onset of climatic change can occur relatively quickly. Since the Younger Dryas, warming has generally resumed, with the Hypsithermal having

been even warmer than today's climate. In more recent times the cold conditions during the Little Ice Age have been followed by warming from the latter part of the 1800s to about 1945, cooling from 1945 to about 1980, and abrupt and significant warming since 1980.

Various forms of proxy evidence are used to provide information about Earth's paleoclimates dating back hundreds of millions of years. The time at which such evidence was formed can be ascertained by using radiometric dating techniques that rely on the constant rate of decay of radioactive elements within a rock sample. Geological evidence allows for estimates to be made in Earth's most distant past, with glacial, ice core, speleothems, and some forms of biological evidence such as oceanic microfossils allowing for estimates dating back hundreds of thousands of years. Other forms of biological evidence, including pollen, tree rings, treeline fluctuations, and coral, can provide information dating back thousands of years, but with more detail in the record. Sediments in the form of varves can also provide evidence from the past several thousand years with an annual record. Historical records round out the sources of data for paleoclimatic reconstruction, providing evidence over the past several centuries.

Several natural mechanisms have been identified as possible contributors to climatic change and variability. At the broadest time scales, continental drift and mountain-building episodes have been proposed as major causes. Cycles in the orbital and axial features of Earth, known as Milankovitch cycles, are believed to cause changes on time scales of tens of thousands of years because of their role in regulating the range in Earth-Sun distance throughout the year, the range of latitudes that can experience the Sun's direct rays, and the time of year when the solstices occur. Variations in volcanic activity and solar output can cause both short-term variability and long-term changes. Finally, short-term events such as ENSO and perhaps the quasi-biennial oscillation may cause climatic variability on seasonal to biennial time scales.

Key Terms

Ablation
Absolute dating
Advection
Air mass
Albedo
Angiosperm
Anomaly
Anthropocene Epoch
Aphelion

Archimedes' principle
Arctic amplification
Asian monsoon
Atomic mass
Biosphere
Bolide
Bolling-Allerod interstadial
Boreal cold interval
Borehole

Bottleneck
Cambrian Explosion
Carboniferous
Catastrophism
Cenozoic Era
Circumpolar vortex
Conduction
Content analysis
Coriolis effect

Counter-radiation	Isostatic rebound	Phanerozoic Eon
Cretaceous-Paleogene (K-Pg) extinction event	Isotope	<i>Photosynthesis</i>
Cretaceous Period	K-T extinction	<i>Pleistocene Epoch</i>
Cross-cutting relationships	<i>Krakatau</i>	Pluvial lake
Cryogenian Period	Laki Fissure	<i>Positive feedback system</i>
<i>Cryosphere</i>	<i>La Niña</i>	<i>Potential vorticity</i>
Dalton Minimum	Laurentide Ice Sheet	Pre-Boreal warm interval
Daughter isotope	<i>Lithosphere</i>	Precession
<i>Deforestation</i>	Little Climatic Optimum	Principle of superposition
Dendroclimatology	Little Ice Age (LIA)	Principle of Uniformitarianism
Dextral	Loch Lomond Stadial	Proterozoic Eon
Eccentricity	Loess	<i>Proxy evidence</i>
El Chichón	<i>Longwave radiation</i>	<i>Quasi-biennial oscillation (QBO)</i>
<i>El Niño</i>	Magma	Quaternary Period
Eon	<i>Maritime Continent</i>	Radioactive decay
Epoch	Mass spectrometry	Radiometric dating
Era	Maunder Minimum	<i>Radiosonde</i>
<i>Eustatic</i>	Medieval Warm Period (MWP)	Random variability
<i>Evaporation</i>	Mesozoic Era	Relative dating
<i>Extreme</i>	<i>Methane</i>	Rock striations
<i>Faint young Sun paradox</i>	<i>Methanogen</i>	Siberian Traps event
<i>First law of thermodynamics</i>	Milankovitch cycle	Sinistral
Foraminifera	Mississippian Period	Snowball Earth hypothesis
<i>Fossil fuel</i>	<i>Momentum</i>	<i>Solar declination</i>
Geiger counter	<i>Monsoon</i>	<i>Southern Oscillation</i>
<i>Glacial advance</i>	Moraine	Speleothem
Glacial erratic	Mount Pinatubo	Step change
Glacial phase	Mount St. Helens	<i>Stratosphere</i>
<i>Global hydrologic cycle</i>	Mount Toba	Sub-Atlantic warm interval
Gondwanan Ice Age	Neogene Period	Sub-Boreal cold interval
Great Dying	Noise	Subduction zone
Great Oxygenation Event	<i>North Atlantic Drift</i>	Sunspot
<i>Greenhouse effect</i>	Ordovician Period	Tambora
<i>Greenhouse gas</i>	Ordovician-Silurian extinction event	<i>Teleconnection</i>
<i>Gulf Stream</i>	Orogeny	Temporal trend
Gymnosperm	Paleoclimatologists	Tertiary Period
<i>Hadley cell</i>	<i>Paleoclimatology</i>	<i>Thermohaline circulation</i>
Half-life	Paleogene Period	<i>Treeline</i>
<i>Holocene Epoch</i>	Paleotempestology	Triassic Period
<i>Holocene Interglacial Phase</i>	Paleozoic Era	<i>Tropic of Cancer</i>
<i>Hurricane</i>	Palynology	<i>Tropic of Capricorn</i>
<i>Hydrosphere</i>	Pangaea	<i>Tropical cyclone</i>
Hypsithermal	Parent isotope	Tundra
<i>Ice age</i>	Pennsylvanian Period	Variability change
Ice core	<i>Perihelion</i>	<i>Varve</i>
<i>Insolation</i>	Period	<i>Wisconsin Glacial Phase</i>
<i>Interglacial phase</i>	Periodic variability	Younger Dryas
Inverse square law	Permian Period	

Terms in italics have appeared in at least one previous chapter.

Review Questions

- Describe the different forms that climatic variability and climatic change can take in a data set.
- How has the meaning of climatic change evolved since the 1960s?
- What are the major ice ages that are known to have affected Earth? When did they occur?
- What theory prevails regarding the cause of the K-T extinction?
- How can melting sea ice contribute to global sea level rise?
- What is the significance of the Younger Dryas?
- Describe the sequence of global climatic conditions since the Younger Dryas.
- How does radiometric dating work?
- Name three radioactive elements that can be used in radiometric dating and describe their uses.
- What are the advantages and disadvantages of using glacial evidence as a sign of climatic changes?
- Contrast the ratio of $\delta^{18}\text{O}$ to $\delta^{16}\text{O}$ in tropical marine microfossils and polar ice cores. Why does this difference occur?
- What are varves and how are they used to identify climatic changes? What pitfalls exist in the use of varve data?
- What are the advantages and disadvantages of using dendroclimatological evidence for identifying climatic change?
- What is the purpose of content analysis?
- What explanations exist for the formation of ice ages in geological history?
- How is eccentricity affected by the inverse square law?
- How does the tilt of Earth's axis vary through time, and how is this assumed to cause climatic changes?
- Why do the dates of the equinoxes and solstices change throughout geological time?
- How is volcanism a cause of both climatic cooling and climatic warming?
- Discuss the role of volcanism on the primordial atmosphere.
- Discuss the role of volcanism relative to short-term and long-term climatic change and variability.
- How might increased solar output result in a decrease in global temperatures?
- How does ENSO alter the extratropical atmospheric circulation?

Questions for Thought

- If you filled a glass with ice and then poured water into the glass until it was flush with the rim of the glass, would water spill over the edge of the glass when the ice melted? Would the water level decrease when the ice melted? Why?
- What would be the resulting climatic conditions for both hemispheres given a hypothetical highly eccentric orbital variation of 20%, an increased tilt to 25° from vertical, and a reversal of the current perihelion/aphelion?
- You are working for a research institution that is trying to ascertain climatic changes 250 to 500 million years ago. What data sets would you examine and what analytical methods would you use? Explain why you would use them.
- You are now working to ascertain climatic changes that occurred over the past 25,000 years. Again, what data and methods would you use, and why?
- You are now attempting to ascertain recent climatic changes over the past 250 years. What types of data would you examine (assume no access to instrumental records), what methods would you use, and why?
- Compare the 2004 through 2016 Atlantic hurricane seasons using available information online. How are our perceptions of climate variability influenced by the locations where hurricanes strike?



CHAPTER 12

Modern Climatic Change

CHAPTER AT A GLANCE

- Global Warming
 - Greenhouse Effect
 - Greenhouse Gases
 - Urban Heat Island
 - Direct and Indirect Effects of Global Warming
 - Global Warming: The Great Debate
- Atmospheric Pollution
 - Global Dimming
 - Atmospheric Factors Affecting Pollution Concentrations
 - Air Quality Legislation in the United States
- Classifying Air Pollutants
 - By Response
 - By Source
- Reactions and Attitudes to Climatic Change
 - Prevention
 - Mitigation
 - Adaptation
 - Continued Research
- Summary
- Key Terms
- Review Questions
- Questions for Thought

Although natural climatic changes have occurred throughout geological history, not all forcing mechanisms for climatic change are natural. As we have seen, humans exert a tremendous influence on their environment, including its climate, through

land-use changes, and also through activities contributing to *deforestation* and *desertification*.

This chapter investigates some of the most significant *anthropogenic* mechanisms that contribute to climatic change on the planetary scale. Two of these mechanisms

(the anthropogenic *greenhouse effect* and the *urban heat island*) lead to warming and are considered to be irreversible—or more-or-less permanent at least on human time scales—in that they are believed to cause climatic change rather than climatic variability. The third mechanism (atmospheric pollution) may lead to cooling and may be reversible. Because the greatest human impact has occurred in the last century, evidence for these changes comes mostly from formal meteorological records rather than from *proxy evidence*.

The nature of the material in this chapter is controversial in that scientists tend to disagree on the degree of impact that humans have on their environment. Additional controversy arises because so much is at stake. Domestic and international policy hinges on the degree of significance associated with the problem of anthropogenic climatic change—a topic that has become the central issue not only in climatology but also in all Earth and environmental sciences over the last 25 years.

► Global Warming

Greenhouse Effect

As we have seen, the greenhouse effect is a natural process that can be intensified by human activity. The greenhouse effect occurs as certain atmospheric gases absorb *long-wave* (terrestrial) *radiation* and hinder its transmission from Earth’s surface to space. The portion of this energy emitted downward back toward the surface, known as *counter-radiation*, is responsible for keeping Earth warmer than it would be if there were no greenhouse effect. It is

tempting to think of *greenhouse gases* as simply reflecting the longwave radiation back to the surface, but in reality the gases absorb the energy and then reemit energy in all directions, as does any object with a temperature above *absolute zero*. This process was first described by the Swedish chemist Svante Arrhenius in 1896.

The term “greenhouse effect” was chosen because a greenhouse operates in a somewhat similar manner. *Shortwave radiation* from the Sun can enter a greenhouse easier than longwave energy can escape it, making the air inside the greenhouse much warmer than it would be if the greenhouse did not exist. A similar process occurs when the inside of a car is superheated while sitting in the Sun. The analogy between the “real” atmosphere and a greenhouse breaks down when *advection* and *convection* are considered. In the “real” atmosphere, the atmospheric circulation tends to mix warmer air with colder air, both horizontally and vertically. In a greenhouse the warmed air cannot mix with colder air outside the greenhouse. The greenhouse heats by suppressing advection and convection, holding energy in place inside the structure. Of course, no such suppression exists in the real atmosphere, but the analogy remains. In the real atmosphere greenhouse gases decrease longwave radiation losses from Earth’s surface to space, which significantly raises the average surface temperature.

Greenhouse Gases

Water Vapor

Several gases play a major role in the greenhouse effect (**TABLE 12.1**). Water vapor is by far the most abundant and

TABLE 12.1 Wavelengths at Which Greenhouse Gases Absorb and Emit Radiation Under Cloudless Conditions	
Wavelength	Primary Greenhouse Gas
4–5 μm	CO ₂
5–8 μm	H ₂ O vapor (nearly complete at 5–6 μm)
8–13 μm	Atmospheric window—some H ₂ O vapor absorption and a narrow but strong O ₃ absorption band between 9.4 and 9.8 μm
10 μm	Peak emission of energy from Earth and atmosphere*
13–17 μm	O ₂ —strong band
17–24 μm	O ₂ and H ₂ O vapor but partially transparent
> 24 μm	H ₂ O vapor (complete)

Under an overcast sky, atmospheric emission/absorption is augmented, primarily in the 8- to 13-μm “window.”

*Note that Earth emits the greatest amount of energy at a wavelength of about 10 μm.

important greenhouse gas. It varies greatly in concentration across Earth, from nearly 0% of the mass of the lower atmosphere (near the poles in winter, where temperatures are too low to allow much water to exist as a vapor, even at saturation) to about 4% (in tropical oceanic areas) of the lower atmosphere. Water vapor is particularly effective at absorbing longwave radiation from Earth's surface at *wavelengths* between 5 and 8 *micrometers* (μm) and at wavelengths above 17 μm (Table 12.1). When cloud cover increases, water vapor and liquid water behave as effective greenhouse “traps” at all wavelengths at which any substantial terrestrial energy is radiated. By contrast, a lack of atmospheric moisture causes temperatures to decrease more at night than during times when water vapor is more abundant. This is because less atmospheric *absorption* can occur under such circumstances, particularly through the **atmospheric window** of 8 to 13 μm , where Earth emits its maximum amount of radiation. It just so happens that few gases absorb radiation effectively in the wavelengths of the atmospheric window.

Even though water is the most abundant greenhouse gas, it is mentioned little regarding the problem of anthropogenic greenhouse warming because the atmosphere is efficient at ridding itself of excess water vapor via the precipitation process. Humans only play a small role in the global water cycle.

Carbon Dioxide

The second-most abundant greenhouse gas is carbon dioxide (CO_2), which accounts for only about 0.0407% of the atmosphere, as of 2016, with the concentration

increasing slightly each year. This means that only 407 molecules out of every million in the atmosphere are CO_2 . Although this concentration hardly seems significant, CO_2 has a disproportionately large influence on temperature regulation of Earth. Chemical analysis of air bubbles trapped in *ice cores* tells us that this concentration has increased from about 0.0280% in 1860—just the blink of an eye in geological time. The abrupt increase in concentration has occurred since the onset of large-scale combustion of *fossil fuels*—primarily coal, oil, and natural gas—since the beginning of the Industrial Revolution in the late eighteenth century. The discovery of new technologies of extracting fossil fuels, such as hydrologic fracturing (also known as “hydrofracking” or simply “fracking”) is leading some to believe that the fossil fuel combustion will experience an upgrowth for the foreseeable future. Nevertheless, U.S. emission of CO_2 decreased by 7.9% from 1990 to 2009, according to the U.S. Energy Information Administration. The extent to which this decline is related to decreased domestic heating needs because of recent warmer-than-normal winters is a matter of debate.

Carbon dioxide composes by far the largest share of anthropogenic greenhouse gas emissions in the United States and in the world, with fossil fuels contributing the vast majority of CO_2 emissions (**FIGURE 12.1**). The concentration is projected to grow to 0.060% by 2050. According to computer models, this concentration would produce a globally averaged temperature increase of 1.5 to 3.5 $^\circ\text{C}$ (2.7 to 6.3 $^\circ\text{F}$; **FIGURE 12.2**). A worst-case scenario puts the amount of warming equal to that experienced since the *Wisconsin Glacial Phase* but in a drastically shorter period of time.

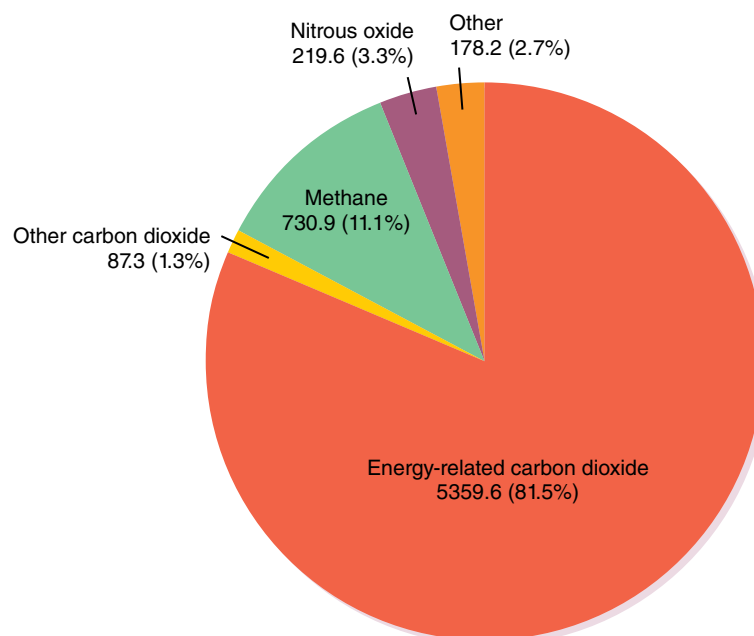


FIGURE 12.1 U.S. anthropogenic greenhouse gas emissions by gas, 2009 (million metric tons of carbon equivalent).

Data from Energy Information Administration. *Emissions of Greenhouse Gases in the United States, 2009*. Washington, DC: 2011.

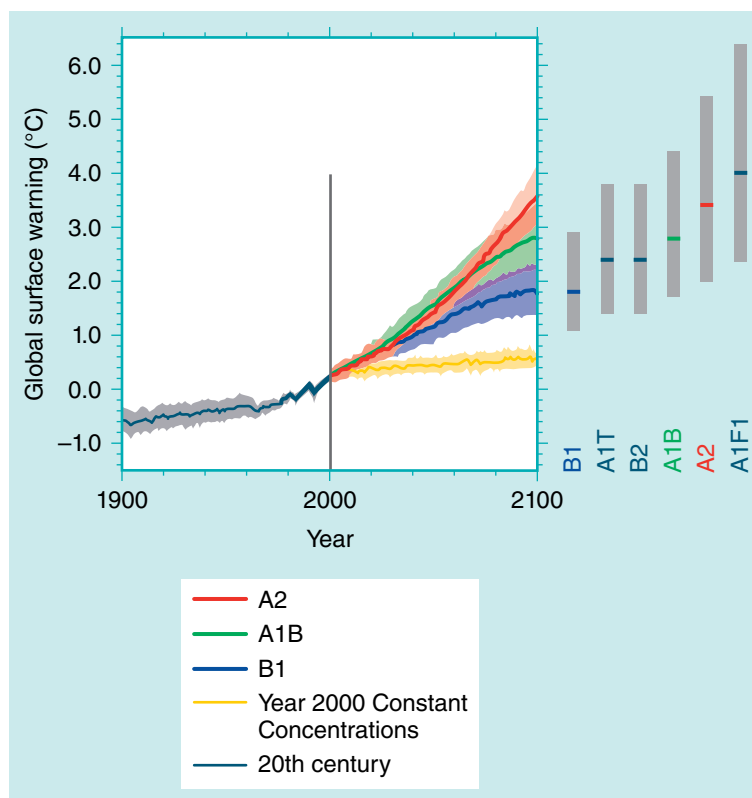


FIGURE 12.2 Global temperature curve, historical and projected. A1B, A1F1, A2, B1, and B2 equal projected CO₂ emission scenarios.

Figure SPM.5 from the report "Projections of Future Changes in Climate" published by IPCC. Reproduced with permission from Intergovernmental Panel on Climate Change (IPCC). https://www.ipcc.ch/publications_and_data/ar4/wg1/en/spmsspmp-projections.html

Fossil fuel emission is the only significant source of atmospheric CO₂ that is primarily non-natural (discussed in Chapter 2). Although the combustion of wood and other organic matter for heating is not natural and emits CO₂ to the atmosphere, it is not considered a major source because the material being burned already removed CO₂ from the atmosphere in a relatively short time during its life cycle. So, little net long-term addition of atmospheric CO₂ from this combustion occurs, unless there is large-scale deforestation of old-growth forests. By comparison, the carbon stored in fossil fuels had been sequestered for millions of years beneath the surface until the CO₂ was released in the combustion process. Natural sources of atmospheric CO₂ include the decomposition of organisms, plant and animal respiration, and some oceanic processes.

Several important CO₂ *sinks*—mechanisms that remove more CO₂ from the atmosphere than they emit to it—are noteworthy. On geological time scales sedimentary rock formation is by far the largest sink. But because this process of **lithification** requires extraordinarily long time periods to remove CO₂ from the atmosphere effectively, we will not consider this to be an important process for mitigating the anthropogenic greenhouse effect.

On human time scales the oceans represent the largest sink. Oceans provide a tremendous *reservoir* in the global

carbon cycle, with 52 times as much carbon as the atmosphere and 19 times as much as in the combined *biosphere* and soils at any given time. Marine phytoplankton take in atmospheric CO₂ and subsequently release carbon in the form of calcium carbonate (CaCO₃) that eventually sinks to the ocean floor, where it is sequestered indefinitely through the lithification of sedimentary rocks. This process is estimated to reduce atmospheric CO₂ concentrations by one-third of what they would be otherwise.

Some researchers have suggested that fertilizing the ocean surface with iron sulfate will allow marine phytoplankton to reproduce rapidly and remove even more atmospheric CO₂, thereby curtailing *global warming*. Even the removal of all atmospheric CO₂ would result in an increase in the ocean storage of less than 2%. But the removal of all atmospheric CO₂ would be catastrophic. Notwithstanding the fact that without any atmospheric CO₂ Earth would cool greatly, CO₂ combines with water to produce **carbonic acid (H₂CO₃)**, a weak acid that is useful in weathering rock and forming soils. But if “enhanced” biological processes in the oceans could remove only the extraneous CO₂ that was released through human activities, a large part of the global warming problem might be solved. Of course, the negative impacts that may result from such a fertilization program have prevented the idea from being implemented. Moreover, experiments have

shown results suggesting that this “solution” would be unsuccessful on broad spatial and temporal scales, as the CO_2 tends to be taken up but then released rather quickly. Regardless of whether such a plan to remove atmospheric CO_2 is ever carried out, researchers are currently working to achieve a better understanding of the ocean’s capacity to store atmospheric CO_2 .

Other atmospheric CO_2 sinks are minor compared with the oceans. Soil is believed to be the second-most important sink on human time scales. Soils sequester atmospheric carbon largely through their containment of partially decomposed organic matter known as **humus**. Although the total amount of potential storage of carbon in soil is unknown, with improved management practices, soils have the capability to sequester more carbon than at present. As improved soil conservation practices gain higher acceptance for their own merits, soils are anticipated to, at least slightly, mitigate the problem of increasing atmospheric CO_2 .

The third important sink for anthropogenic CO_2 is the nonsoil component of the terrestrial biosphere. Actively growing vegetation absorbs CO_2 during *photosynthesis*, and it stores carbon in its biomass as it continues to grow. But because only 30% of Earth’s surface is land and only 30% of that total is covered by forests, the biosphere is a far smaller sink than the ocean and slightly smaller than the soils. Within the biosphere the most critical region for CO_2 sequestration is the tropical rain forest, and these areas are disappearing, largely because of human-related deforestation and desertification. Some evidence even suggests that replanting new forests initially acts as a local source of atmospheric CO_2 because carbon tied in the soil is released to the atmosphere. Other evidence suggests that the effect of deforestation

may be somewhat offset by the more rapid growth of replanted forests because of the nourishing effect of the extra atmospheric CO_2 . Outside the rainforest region, seasonal changes in vegetative cover render CO_2 fixation by the biosphere less effective in winter, even if the environment becomes more favorable for forest growth under global warming scenarios.

Methane

Until recently, *methane* (CH_4) was assumed to play a relatively minor role in the greenhouse effect because its concentration in the atmosphere is only 1.85 parts per million (ppm). But recent research suggests that it is much more important than previously believed because each CH_4 molecule acts as a far more effective absorber of terrestrial radiation than an individual CO_2 molecule. In addition, CH_4 -emitting bacteria, called *methanogens*, are increasingly recognized for their role in maintaining Earth’s early “thermostat.” Furthermore, CH_4 is seen as being an important player in the anthropogenic greenhouse effect because, like CO_2 , its concentration has increased substantially since the Industrial Revolution. Ice core analysis suggests that atmospheric CH_4 concentrations changed little over the last 160,000-year period, remaining near 0.8 ppm, until experiencing an abrupt rise in the last 200 years. This increase is far more rapid than the increase in atmospheric CO_2 .

The details of the global CH_4 budget have been understood only for the last two decades. Methane is released to the atmosphere through several processes (FIGURE 12.3), especially through **anaerobic** decomposition—the breakdown of organic matter in the absence of oxygen. Anaerobic decomposition occurs readily in

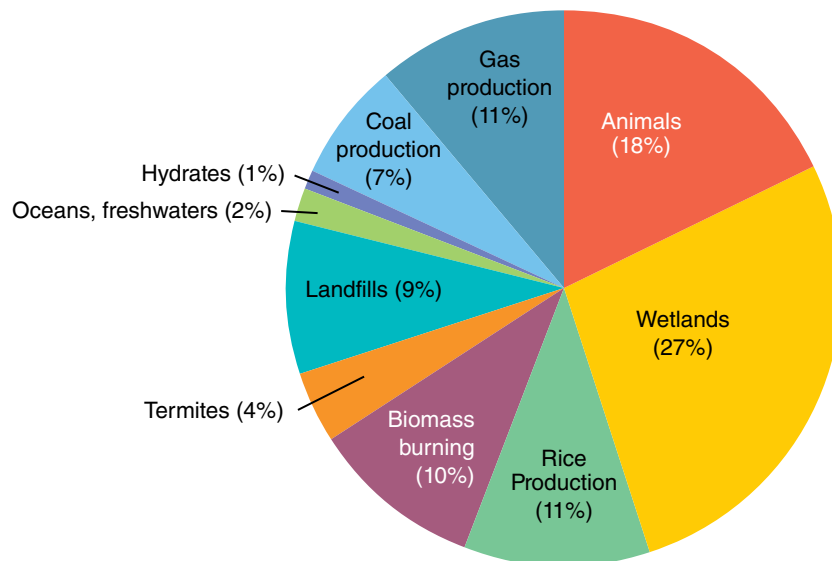


FIGURE 12.3 Sources of net global emission of atmospheric methane.

Data from Mikaloff Fletcher, S. E., Tans, P. P., Bruhwiler, L. M., Miller, J. B., & Heimann, M. (2004). “ CH_4 sources estimated from atmospheric observations of CH_4 and its C-13/C-12 isotopic ratios: 1. Inverse modeling of source processes.” *Global Biogeochemical Cycles*, 78(4). UCLA. Retrieved from <http://escholarship.org/uc/item/7f1m946gq>.

waterlogged environments. On a global basis, about 27% of the atmospheric CH_4 comes naturally from wetlands, including bogs, *tundra*, and swamps, where methane-producing bacteria thrive in the rich organic matter and poor oxygen content. The next leading source, at about 22% of the total, is from the bacteria present in the anaerobic digestive process of animals, particularly ruminants such as cattle and certain species of termites. Livestock emit 18% of the atmospheric CH_4 , with termites alone emitting another 4%. Although other animals also emit CH_4 , the total is thought to be insignificant. A third major source (11%) of CH_4 is from the flooding of rice fields, where certain types of bacteria thrive. Biomass burning, landfills, fossil fuel combustion, and biological oceanic processes are believed to account for most of the rest of the atmospheric CH_4 .

Two other sources of methane worthy of mention are fracking and **methane hydrates**, which together comprise only a small percentage of atmospheric CH_4 today but may be much more substantial sources in the future. Methane hydrates are frozen lattices of water molecules surrounding CH_4 molecules. These solids are found extensively worldwide throughout ocean sediments and deep underground in polar regions. Methane hydrates are so abundant that some believe these provide far more energy potential than the world's known reserves of coal, oil, and natural gas combined. Methane is released from the hydrates naturally with changes in temperature, pressure, salt concentrations, and other factors, but to date no method of extracting the CH_4 safely, efficiently, and economically for energy consumption has been devised. If such methods are developed, far more rapid increases in atmospheric CH_4 would occur.

Other Greenhouse Gases

Other greenhouse gases are thought to play minor roles in the anthropogenic greenhouse effect. **Nitrous oxide (N_2O)** is a non-natural greenhouse gas that contributes a tiny percentage to the anthropogenic effect. It is released to the atmosphere primarily through the combustion of fossil fuels and industrial and agricultural activities. Also, various types of **fluorocarbons** are emitted to the atmosphere by industrial activities. Although miniscule in concentration, they are extremely efficient absorbers of terrestrial energy. Other gases such as **carbon monoxide (CO)** and various types of **nitrogen oxides (NO_x)** other than N_2O can influence chemical cycles in the atmosphere that affect the concentrations of greenhouse gases.

Trends in Greenhouse Gas Emissions

Greenhouse gas emissions are increasing for several reasons. First, sources of CO_2 , CH_4 , N_2O , and fluorocarbons continue to increase worldwide, despite the

ratification of the **Kyoto Treaty** in 1997, which sought to limit emissions of these gases by seven of the eight leading industrial nations of the world (the United States being the exception). Second, large-scale deforestation is decreasing an important CO_2 sink. Finally, the conversion of mature forests to younger forests results in a reduced overall reservoir for carbon in the biosphere, even though the rate of carbon fixation by younger trees is faster than for mature trees.

Within the last few years, the People's Republic of China passed the United States as the leading producer of greenhouse gases, with nearly 28% of the emissions compared with about 16% for the United States. Chinese output is predicted to increase over the foreseeable future along with that of other newly industrializing countries such as India and Brazil, with a continued decrease predicted for the United States. According to the U.S. Energy Information Administration, U.S. emissions are economically efficient, with emissions per dollar of gross national product below the world average and far below the developing world's average (**FIGURE 12.4**). Fossil fuel consumption within the United States tends to be concentrated in regions of highest population and nearest to the deposits, with coal emissions concentrated in the Appalachian states and northern Plains and oil and gas in the Gulf Coast region (**FIGURE 12.5a–c**). On a per capita basis (**FIGURE 12.5d**), the highest energy-consuming

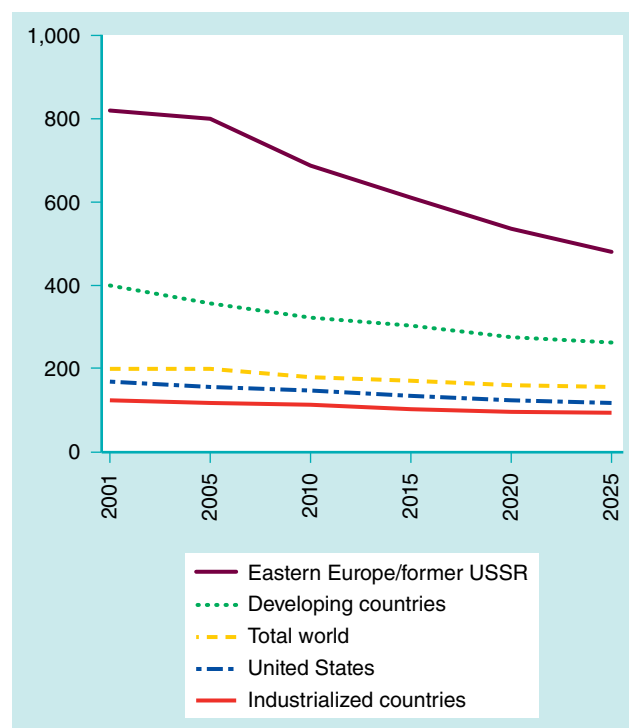


FIGURE 12.4 Current and projected carbon emissions standardized by gross national product (metric tons per million dollars).

Data from International Energy Outlook, 2003. Energy Information Administration.

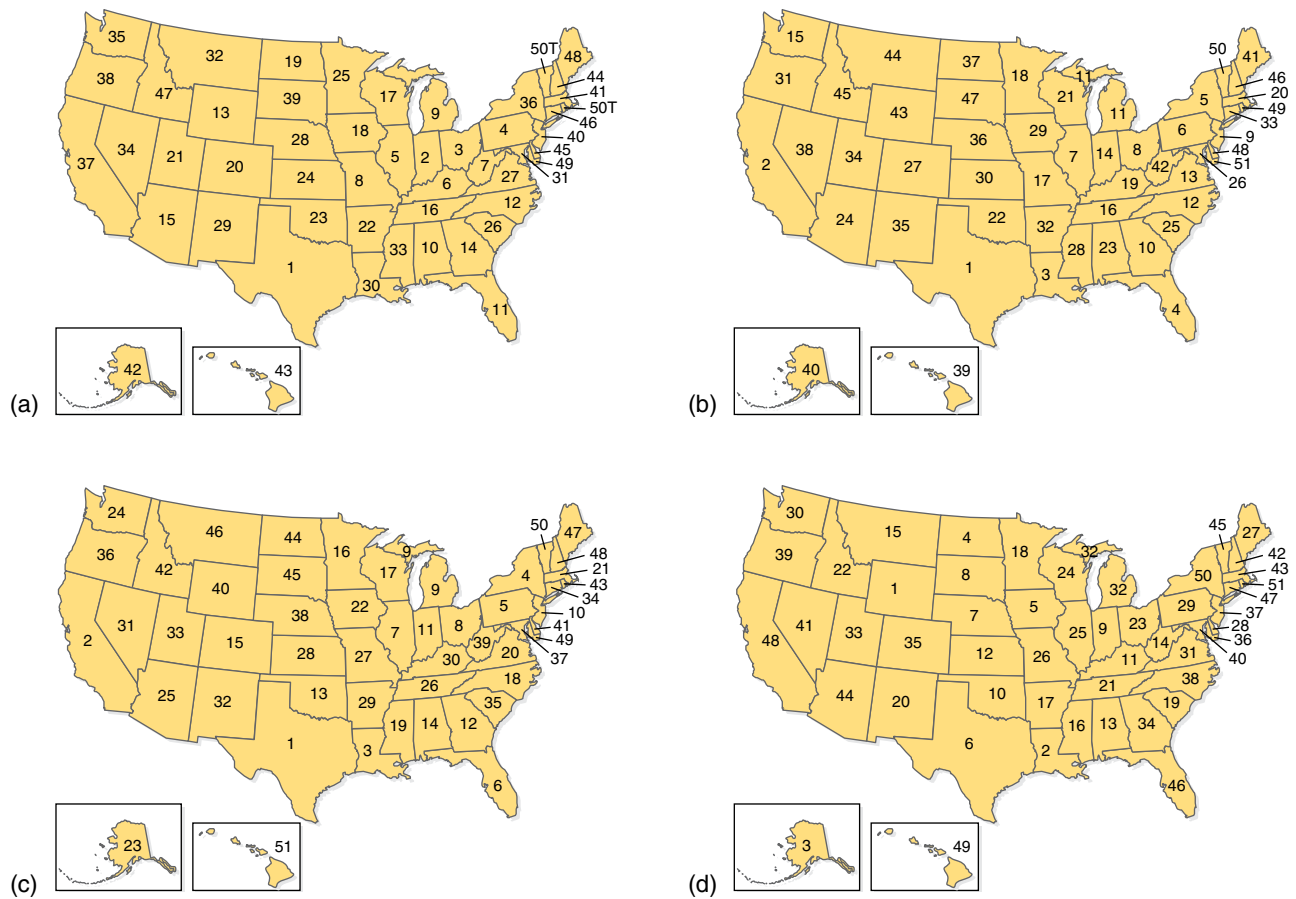


FIGURE 12.5 Fossil fuel emissions ranked by state. (a) Estimated total consumption by coal, 2014. (b) Estimated total consumption by petroleum, 2014. (c) Estimated total consumption by natural gas, 2014. (d) Total consumption from coal, petroleum, and natural gas, per capita, 2013.

Data from U.S. Energy Information Administration. http://www.eia.gov/state/seds/sep_sum/html/pdf/rank_use_source.pdf and <https://www.eia.gov/state/rankings/>. Accessed July 2016.

states tend to be energy-producing states, presumably as carbon-emitting industries locate nearby to make use of the inexpensive fuel.

Urban Heat Island

A second anthropogenic cause of climatic change also contributes to global warming. This effect is associated with urbanization. Cities are generally 1 to 5°C (2 to 9°F) warmer than the surrounding countryside, for several reasons. First, the urban environment has less evaporation and *transpiration* (*evapotranspiration*) of water from soil and plants than rural areas because of the relatively sparse vegetation found in urban areas. This leaves more available energy for *sensible heat* and less shading by trees. Urban rainfall is more likely to become *runoff* immediately after a rainstorm rather than lingering near the surface, and this also causes relatively less latent heating and more sensible heating to occur in the urban area than in the surrounding area.

Additionally, the buildings and streets themselves are composed of materials that are conducive to extra

storage of energy during the daytime and reemission of that stored energy at night, thereby delaying the cooling of urban areas. Materials such as concrete, asphalt, and brick have greater **heat capacity** and **thermal conductivity** than moist, open soil and vegetation. Heat capacity refers to the amount of energy that would need to be added to a unit volume of a substance to raise its temperature by 1 K in the *Kelvin temperature scale*. The units of heat capacity are $\text{Joules m}^{-3} \text{K}^{-1}$. This term is related to *specific heat*, except that specific heat refers to the amount of heat needed to increase a unit mass (not volume) by 1 K. Thermal conductivity refers to the number of Watts of power required to increase the temperature at a point 1 m into the ground by 1 K. The units of thermal conductivity are $\text{W m}^{-1} \text{K}^{-1}$. Heat capacity and thermal conductivity of urban materials allow them to have an ability to absorb a tremendous amount of heat and also conduct that heat (energy) more readily than materials such as open soil. In warm climates without air conditioning systems, building walls tend to be thick enough to absorb the high quantities of afternoon heat without allowing the heat to penetrate

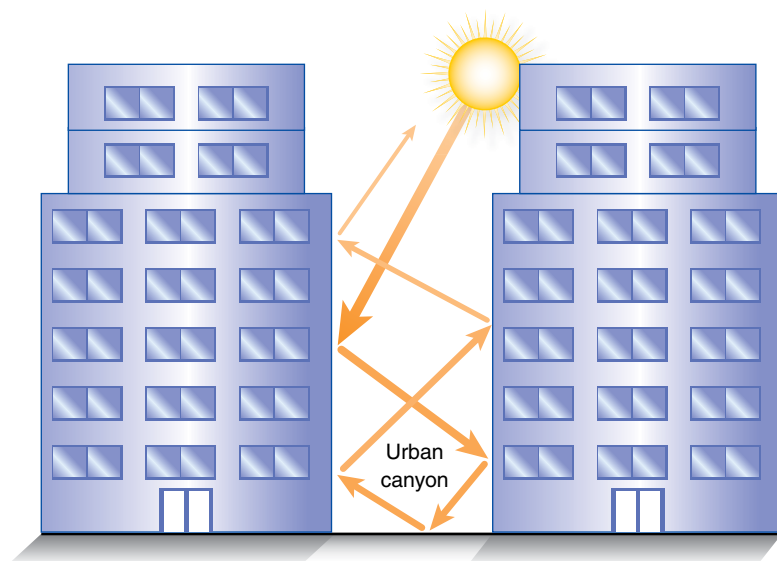


FIGURE 12.6 Effect of building geometry on the urban heat island.

to the interior part of the building. Yet the conductivity must be high enough to allow that heat to flow back outward from the walls during the nocturnal hours. This “building material” effect is a major contributor to the urban heat island at night. The dark and irregular surfaces of buildings also have an impact on retaining heat. Vertical walls permit multiple reflections of *insolation* (FIGURE 12.6) and delay and reduce the amount of insolation reflected back toward space. This increases the energy available to heat the air over cities.

A final reason for the heat island is that urban areas have greater amounts of waste heat released to the atmosphere than rural areas, because of the intense concentration of human activity. This energy includes that used for industrial and domestic purposes, transportation, heating, and illumination. Any object with a light or a motor releases waste heat. Even air conditioning units give off waste heat to the atmosphere!

The urban heat island tends to be magnified under certain conditions. The effect is greatest for large cities that are surrounded by rural areas or are near oceans. The heat island usually becomes more prominent under clear skies rather than under cloudy conditions because clear skies allow more longwave energy to escape from rural terrain, but urban-produced **smog** (a combination of smoke and fog), fog, and cloud cover still prevent some longwave energy from escaping to space over the city unimpeded. Finally, the heat island is best developed under calm conditions. Stronger winds hinder longwave energy from escaping to space over the surrounding rural area because as the radiation encounters more matter from the atmosphere advected by the wind, there is an increased chance of it being absorbed by the matter. The presence of storms or strong pressure gradients

diminishes the heat island effect because of the winds associated with them.

Diurnally, the urban heat island usually reaches its magnitude in late evening. At that time of day the industrial, transportation, and domestic waste heat from the day’s activities have already warmed the atmosphere. By late evening this extra energy is supplemented by the *conduction* of stored energy in the concrete and walls of buildings to the ambient air. Sometimes the extra warmth at night decreases the atmospheric *stability* to such an extent that a nocturnal *temperature inversion* is prevented from forming locally. Such a scenario allows for a deeper mixing layer over the city and more vertical distance for pollution to be dispersed.

Cities also typically display other climatic contrasts with their surrounding rural environments. *Relative humidity* tends to be reduced in urban environments. Although this modification is partially caused by the increased urban temperatures—recall that temperature and relative humidity are inversely related—part of the difference is also caused by the relative lack of transpiration and evaporation in the urban environment. Although relative humidity is generally decreased, fogs are still common in cities because of the city’s abundance of **hygroscopic nuclei**. These are solid *aerosols* that act as such efficient *condensation nuclei*—encouraging the conversion of water vapor to liquid water around them—that fog can occur even at relative humidities far below 100%.

Winds are also modified in urban areas. Prevailing winds are lighter than in surrounding rural areas, because buildings act as obstructions and increase *friction*. By contrast, local winds within the city are often strong, as a *wind channeling effect* around and between buildings—the

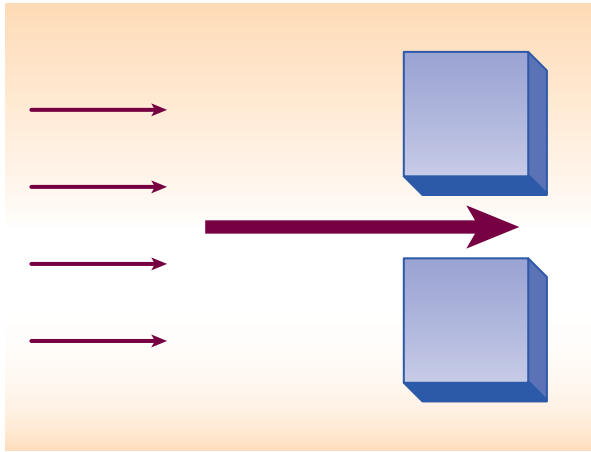


FIGURE 12.7 Effect of channeling in the urban canyon on wind speed.

so-called **urban canyon**—can create locally windy conditions. **FIGURE 12.7** shows this channeling effect. As rural winds enter the urban environment, they get “squeezed” by the buildings such that the surface area upon which their force is applied must decrease. When the winds become funneled into a smaller area, the wind speed must increase to compensate for the “squeezing.”

Studies of precipitation enhancement by urban areas are somewhat inconclusive. Most suggest that cities cause an increase in rainfall downwind—perhaps up to 10%. It is difficult to attribute the precipitation enhancement to the urban area, however, because of the nonquantifiable influence of topographical sites, distance to water bodies, and other factors.

Interestingly, a “negative” urban heat island signal may exist in small, isolated pockets, such as in irrigated deserts and golf courses in arid lands. This occurs as land cover change provides shade, but also, especially because of the increase in *latent heat* and decrease in sensible heat, as a percentage of the local energy budget.

Direct and Indirect Effects of Global Warming

The last three decades are the warmest in the instrumental record and likely the warmest in the last 1400 years (**FIGURE 12.8**). Even more important, the rate of recent warming is unprecedented in long-term proxy records, except when major disruptions to the global energy balance occurred, such as by a *bolide* or significant volcanism. Remotely sensed data from satellites, available globally since 1979, largely confirm this warming reported independently from surface weather stations.

Effects of the warming are evident in several ways. The most obvious is in *ablation* and melting of ice over much of the planet. Increased air temperatures cause melting and *sublimation* in the *cryosphere*. Such melting

decreases the *albedo* of polar regions as darker surfaces replace the snow and ice, exacerbating the situation in a *positive feedback system*, known as *Arctic amplification*. By far the largest contiguous masses of ice are in the polar ice caps and ice sheets. Those over both Greenland and West Antarctica have not only been shrinking over the last 30 years, but, ominously, the rates of ablation have generally been increasing over that time. However, the same is not true of the third ice sheet—the East Antarctic—where ice has been accumulating in recent decades for other reasons. In addition to ablation of the ice caps/ice sheets, melting of Arctic sea ice is also of great concern. The rate of melting of Arctic sea ice has increased in recent years. Again, however, the Antarctic sea ice has not shown similar melting, but is instead accumulating in some places, but any melting is of concern because of its effect on the planetary albedo. Melting is more easily observable in the much smaller but more easily observed masses of ice in the form of continental glaciers. The majority of continental glaciers have been shrinking over the last several decades.

Effects in the oceans are also evident. The meltwater and the warming itself have induced observable sea level increases. The oceans expand slightly in volume as the *density* of the ocean waters decreases under warming conditions. This factor alone is estimated to contribute perhaps 25% of the sea level rise that we are seeing. When combined with the effect of the addition of meltwater, sea level is expected to rise more substantially in the next century. Since 1900, a 1- to 2-mm year⁻¹ (7 in or 18 cm) sea level rise has occurred, with the rate of increase over the past decade being more than double that of the mean from 1900 to 2000. The increase from the peak of the Wisconsin Glacial Phase until 1900 is estimated to have been about 0.1 to 0.2 mm year⁻¹, for a total of 270 cm (106 in). Continued sea level rise could endanger coastal cities, increase coastal erosion problems, and cause *saltwater intrusion* in coastal zones. The increased temperatures also cause increased heat storage in the oceans. One observable effect of this heat storage is in coral bleaching, which is also impacted by ocean acidification that is exacerbated by increases in CO₂ concentrations.

Global Warming: The Great Debate

Mainstream Perspective

Few climate scientists today question that the Earth–ocean–atmosphere system has displayed a significant warming trend over the last century. According to a 2016 survey of 4091 members of the American Meteorological Society, 96% of the respondents believe that climate change is happening, with 58% of those answering that they are “extremely sure” that it is happening.

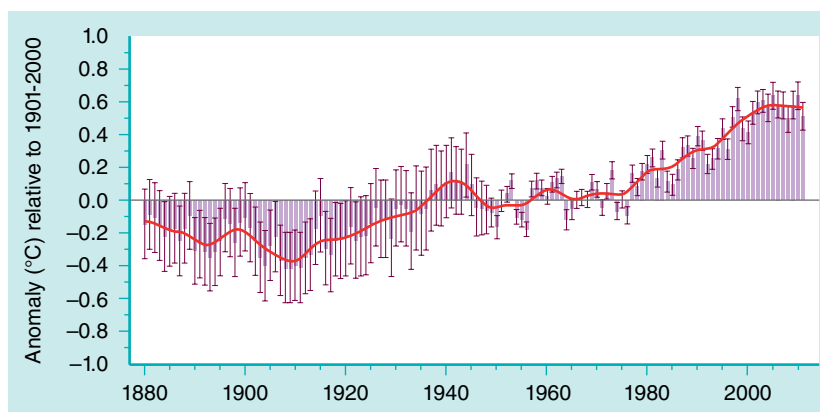


FIGURE 12.8 Global Jan–Dec mean temperature anomalies by year, relative to 1901–2000 average.

Data from NOAA.

There is somewhat less certainty among mainstream scientists about the cause and the severity of the problem. The same survey found that among those who believe that climate change has occurred in the last century, 29% think that the change in the last 50 years is caused largely or entirely (81% to 100%) by human activity, whereas 38% believe that it is caused mostly (60% to 80%) by human activity and 14% responded that the change is caused more or less equally by human activity and natural events. Of the 17% of respondents who reported that their opinion/position on climate change has changed in the past 5 years, 87% feel more convinced that human-caused climate change is happening, whereas the other 13% feel less convinced that human-induced climate change is occurring. Among the 74% of respondents who believe that the climate in their area has changed over the past 50 years, 36% of these answered that the changes have been primarily harmful, with 2% claiming that they have been exclusively harmful. Several valid assertions are used by the mainstream scientists to support their position that warming is of concern and is largely anthropogenic in nature.

First, those who are concerned about global warming note that experiments demonstrate that greenhouse gases are efficient absorbers and radiators of energy of the relevant wavelengths. We know from ice cores and the instrumental record that we are increasing carbon dioxide gas emissions by nearly 32 billion tons annually. Because of that evidence, most scientists see no reason to doubt the problem is real. Likewise, the indisputable fact that urban surfaces and waste heat cause warming, combined with the increase in urbanization over time, give these scientists even more evidence to conclude that the warming trend is tied closely to human activities.

Second, mainstream climate scientists, including many of the survey respondents, point to their observations as

evidence for change. They note, for example, that glaciers around the world have experienced a net poleward and uphill retreat, that *permafrost* is melting in many areas, that sea level is rising, bird migration patterns are changing, and many other observable impacts of a changing climate. They see the human impact of increasing CO₂ concentrations and other human activities as the most likely culprit.

And third, many climate scientists note that the effects of global warming are possibly detrimental and are largely unknown. Unlike a chemistry experiment, there is no laboratory for analyzing possible effects, finding the “answer,” and using the result to establish policy. Instead, Earth itself is the “laboratory,” and we have to live with the result of the experiment, regardless of its outcome. Along these same lines, it is noteworthy that the effects of the “experiment” will linger perhaps for generations even if fossil fuel combustion and other greenhouse gas emissions were to end immediately. Any further delay in addressing the problem will cause even more drastic impacts. This argument implies that the more-developed nations in the world should be the leaders in establishing policy to curtail global warming because climatic conditions in the world up to this point have coincided with prosperity for them.

Finally, those who are concerned about global warming assert that we should be moving toward a world where fossil fuels are phased out, regardless of whether global warming is a problem. Fossil fuels represent a nonrenewable resource, whereas other sources of energy such as solar power, hydropower, and wind power are renewable. The pollutants emitted into the atmosphere by fossil fuels bring environmental, epidemiological, and economic consequences, but the renewable sources of energy listed above cause no such problems. Additionally, fossil fuels are distributed unevenly and lead to international geopolitical tensions, whereas the

renewable sources of energy are more evenly distributed and potentially more accessible to more of the world's people, especially as technological developments reduce the cost of constructing such power-generating facilities. Proponents of this argument note that if global warming is the catalyst for changes in energy policy that lead us to more sustainable, inexpensive, and environmentally friendly sources of energy, then so be it.

Skeptical Perspective

The results of the survey confirm that fewer American Meteorological Society members believe that global warming is a less serious problem. While some 36% of the 74% who have observed climatic changes in their area feel that the impacts have been approximately equally mixed between beneficial and harmful, only 4% reported that the impacts in their area have been primarily beneficial, with zero respondents finding that the impacts have been exclusively beneficial. These “skeptical” scientists, along with the 1% who don't believe that climate change is happening, would claim that some statements purported by the more central view are unrealistic and sensationalized. Though most climate scientists disagree with the skeptical perspective, the argument is an important, healthy, and central theme in the development of any scientific body of knowledge. Such skepticism has led to greater depth of research into climatic systems, the development of better climatic simulation computer models, and ultimately a heightened insight into the interrelationships of the Earth–ocean–atmosphere system. Healthy debate therefore has an important place in science, including climatology.

One popular “skeptical” argument is that there are too many uncertainties to establish drastic changes in policy. For example, we do not know whether *negative feedback systems* might curtail the warming. Proponents of this viewpoint might suggest that increased temperature would likely cause increased evaporation, which then would cause increased *condensation* and cloud cover. This extra cloudiness may then decrease the amount of shortwave energy reaching Earth's surface, thereby keeping temperatures within a reasonable range of normal conditions. A similar kind of negative feedback prevents temperatures in tropical rainforests from rising too high. Another possible negative feedback system is the potentially increasing role of the oceans as a CO₂ sink, through both natural and anthropogenic enhancement. This mechanism is seen by the skeptics as offering hope for solving the problem before it becomes more serious.

Skeptics also suggest that even if negative feedbacks do not curtail the process, the warming may simply be part of a larger natural cycle that will swing back toward

cooling again sometime in the future. They also feel that much of the observed warming of the past century may simply be part of the natural cycle that pulled Earth out of the *Little Ice Age* and the Wisconsin Glacial Phase. Finally, they note that a 1% change in the natural solar output could cause more climatic change than all anthropogenic effects combined.

The skeptical view of the global warming problem also includes the notion that higher temperatures may provide more potential benefits than costs. For instance, agriculture may become more efficient if warming lengthens the growing season, particularly if the warming is concentrated at night (when killing frosts would occur at the beginning and end of the growing season). Furthermore, the extra CO₂ released by fossil fuel emissions is shown to be favorable to the development of many of the world's major crops, because additional carbon acts as a fertilizer. Higher temperatures may also cause fewer economic losses in some other industries such as transportation, tourism, and recreation.

Another source of doubt regarding the global warming problem involves the data. Skeptics wonder whether data biases may be providing a misleading impression of the amount of warming that has occurred. Specifically, they point to the fact that the reliable long-term weather stations upon which the global temperature curve is calculated are overwhelmingly biased toward land-based sites (only 30% of Earth's surface) in the developed world (less than 20% of Earth's land surface). Although the curves shown in Figures 12.2 and 12.8 suggest that sudden warming has occurred over the last 120 years, changes in monitoring procedures and instrumentation have caused concerns among some that the data may be at least somewhat biased. Concern is also generated by the fact that many stations became closer to urbanized areas as the urban areas grew over time. The skeptics claim that the “global” temperature record may be created as an average of a series of locally enhanced increasing urban heat island signals. Skeptics also note that although Arctic polar ice is shrinking alarmingly rapidly, data suggest that the Antarctic sea ice extent reached an all-time peak (measured since 1978) in September 2014. A more egregious data issue involves accusations from both sides that scientists on the other side have manipulated the data sets and hidden results that do not support their agenda.

Another concern with the data record involves the global cooling trend shown from about 1945 to approximately 1980. The skeptics point out that this cooling should not have occurred if emission of greenhouse gases is to blame. This period corresponds to the time when the world's industrial output increased tremendously after World War II, with little or no concern for the environmental impacts of the smokestack industries.

Skeptics claim that either the data record is flawed or negative feedbacks must have occurred that suppressed the warming at that time. If negative feedbacks or other compensating factors did occur, similar feedbacks or phenomena may curtail future warming.

Some of the skeptics' points about the data have been refuted. For example, some research indicates that at least some of the Antarctic sea ice increase is, ironically, a result of warming. A warmer midlatitude atmosphere strengthens the *midlatitude westerlies* and *circumpolar vortex* adjacent to Antarctica. This enhances ocean waves that break and freeze more quickly than calmer waters on the Antarctic shore. Another explanation is that increased freshwater resulting from Antarctic ice sheet ablation and melting contributes to warming by overriding the denser saltwater in the Southern Ocean and decreasing vertical thermal mixing. The lens of fresher water also freezes at a higher temperature than saltier water, thereby keeping albedos lower than they would otherwise be.

The Bottom Line Regarding the Debate

Most atmospheric scientists support the notion that anthropogenic influences have, and are, significantly impacting the climate system. But the degree to which people are contributing to the problem is not known. Our understanding of the anthropogenic global warming problem has been strengthened by examining issues expounded upon by the skeptics. This has probably led to more realistic assessments of future climatic conditions, because many past assessments predicted unrealistically large increases in global temperatures and resulting impacts. Unfortunately, some on both sides of the debate still use these unrealistic assessments in public forums in an attempt to advance political agendas.

The Fifth Assessment Report (AR5) of the **Intergovernmental Panel on Climate Change (IPCC)** was released in 2014. AR5 includes much stronger language than previous reports, confirming human influences on the climate system and the growing impacts throughout the Earth–ocean–atmosphere system. The documents detail the science and socioeconomic impacts associated with climate change and possible policy strategies for addressing the issue.

But there are still many unresolved anthropogenic global warming issues among scientists regarding how societies should implement policy related to the issues. One seemingly fair approach is for climatologists and other Earth and environmental scientists to assess the costs and benefits of human activities contributing to global warming. A “business as usual” approach should only be taken to environmental problems if the benefit exceeds the cost. A complicating factor is that the “cost” of our activities is often inherently nonquantifiable, as

in the case of human health and mortality. In addition, there are often “hidden costs”—costs that we are unaware of until after they occur. As climatologists and other environmental scientists expand their knowledge of the climate system, these hidden costs may be understood better. Finally, the issue is complicated by the fact that the costs and benefits will not occur evenly across Earth, so some nations have more at stake than others. The nature of the warming and whether it will occur primarily in one part of Earth or another, the distribution of warming in the seasonal and daily cycles, and the “side effects” of the warming must be understood better.

► Atmospheric Pollution

The anthropogenic greenhouse effect and the urban heat island are both non-natural phenomena that lead to surface warming. Likewise, both are considered to be permanent in that their effects cannot be reversed easily on human time scales. Other anthropogenic impacts on climate do not cause significant warming and are not necessarily permanent. For instance, aside from its other effects, polluting the atmosphere allows more insolation to be reflected and scattered back out to space before it reaches Earth. Pollution may be masking the thermal effects of increased greenhouse gas emissions to some extent. But atmospheric pollution is not necessarily a permanent feature of the atmosphere.

An extreme example of the effect of atmospheric pollutants would occur in a **nuclear winter**—the hypothesis that a large-scale detonation of nuclear weapons could create enough soot to effectively prevent insolation from reaching much of Earth's surface for up to several years. Global temperatures could be reduced by as much as 20 C° (36 F°) in the process. Such a notion is similar to the theory that the dinosaurs and many other creatures may have succumbed to the *K-T extinction* (also known as the *Cretaceous–Paleogene extinction event*) 65 million years ago because an asteroid or comet struck Earth. The impact is believed to have stirred up enough dust in the atmosphere to reflect most of the insolation for some time, thereby damaging the food supply of the organisms that became extinct.

Recent calculations of the climatic impacts of nuclear winter suggest a less drastic scenario than the one originally developed in the early 1980s, in part because of improvements in atmospheric models that allow for oceanic exchange of energy with the atmosphere. The term **nuclear autumn** has been used in recent years to describe this somewhat less catastrophic version of a nuclear winter. Although considerable debate still exists on whether the effects would last for weeks, months, or years, there is no debate regarding the notion that the climatic effects would be devastating.

Global Dimming

Perhaps the biggest “secret” among major anthropogenic climatic change issues is that of **global dimming**—the observed decreasing trend in insolation striking Earth over recent decades. Estimates generally suggest that a 2% to 3% rate of decrease in insolation occurred each decade from about 1961 through 1990. Interestingly, recent research suggests that the trend toward dimming has reversed since the 1990s. If so, then the extent to which this “global brightening” may be contributing to the recent observed warming poses an interesting question.

The global dimming phenomenon received little acceptance from many climatologists until recently, in part because the dimming seemed to contradict the observed increase in global temperatures during the 1980s. It is now widely believed that the decreasing trend in shortwave radiation receipt between 1961 and 1990 is real and that increasing atmospheric pollution and aerosols from 1961 through 1990 caused at least some of this trend. The additional global cloud cover resulting from the increasing condensation nuclei from pollution and aerosols seems to have reflected an increasing amount of insolation over that period. The result was a suppression of daytime high temperatures, somewhat offsetting the warming effects of greenhouse gas emissions and the urban heat island. This pollution may also partially explain the global cooling trend from about 1945 through 1980. Alternately, temperature may continue to climb in some cases even under increasing pollutants because cloud cover from pollution and aerosols may increase nocturnal temperatures by impeding longwave radiation loss to space. In the days after September 11, 2001, studies showed that the absence of jet contrails (condensation trails) associated with the grounding of all U.S. flights was linked with an increase in the daily temperature ranges (the difference between maximum and minimum temperature) of approximately 1 C° (2 F°) in the United States. These results support the notion that aerosols, including jet contrails, have been masking the effects of global warming, at least during the daylight hours, and perhaps reducing the diurnal temperature range.

The implication is that pollution abatement in the last 15 to 20 years may be at least partially responsible for the reversal of the global dimming trend. This may mean that as skies around the world become less polluted, the effect of greenhouse gas emissions may magnify. The amount of magnification is unclear and the potential for renewed global dimming from additional pollution in rapidly expanding economies in the developing world exists.

Although many effects of atmospheric pollution are global, most of the direct effects are primarily local or

regional. It is important to examine the major causes, types, distribution, and effects of atmospheric pollution.

Atmospheric Factors Affecting Pollution Concentrations

Several atmospheric factors affect the magnitude of the air pollution problem. First, atmospheric stability is an important consideration. During times when the atmosphere is stable, vertical motion in the atmosphere is suppressed, and air pollution remains near the source. Dispersion of atmospheric pollution occurs more easily when the atmosphere is unstable, because *unstable atmospheres* are associated with rising motions of *adiabatically* moving parcels of air.

Because *anticyclones* are often associated with a *stable atmosphere*, they are linked to poor dispersion capability and poor air quality. A particularly good example of anticyclonic effects on stability occurs in the case of the eastern sides of the *subtropical anticyclones*, where a strong sinking motion occurs, largely because the cold ocean currents on the eastern sides provide strong temperature inversions and stable atmospheres. The California coast is one example of a place affected by these conditions. In summer the nearby *Hawaiian high* strengthens and expands over the region, partially supported by the cold *California current*, which provides for a persistent inversion near the coast. The coastal mountain ranges also contribute by confining sinking motions in the atmosphere to the coastal zone, where more than 20 million southern Californians live. Automobile exhaust and other pollutants are also confined to this narrow zone. Even the afternoon onshore breezes provide little relief because the coastal mountains prevent eastward dispersion of pollutants. In winter the Hawaiian high weakens, shrinks, and migrates southward with the direct rays of the Sun, and California is affected more by *midlatitude wave cyclones* that provide rainfall and relief from the poor air quality through enhanced vertical and horizontal mixing. *Cyclones*, then, often facilitate dispersal of pollutants, both because of the upward motion characteristic of unstable atmospheres that often accompanies cyclones and also because of the characteristically strong pressure gradients (and, therefore, winds) associated with storminess.

A second atmospheric factor that affects air pollution is wind. Obviously, windy conditions disperse atmospheric pollutants and dilute them with distance. But strong winds may cause pollution problems farther downwind from the pollution source. For example, Canadians often state that pollution generated in the midwestern United States drifts in the westerlies toward Ontario, Quebec, and the Maritime Provinces. Air pollution does not respect international borders.

A final important atmospheric factor is insolation. Although solar radiation may seem to be harmless, it can trigger chemical reactions that produce poor air quality in a form known as **photochemical smog**. Sunlight can cause preexisting pollutants that are only somewhat harmful to be transformed into more dangerous pollutants. Again, California provides an effective example of the problem of photochemical pollution. Recall that much of California has a *Mediterranean climate*—characterized by sunny summers. The abundant sunshine in summer combines with the stability associated with the eastern side of the Hawaiian high to make photochemical pollution particularly troublesome.

Atmospheric dispersion modelers use principles of atmospheric stability, radiation, and dynamics to forecast the days on which air quality is likely to be a problem. By understanding such principles, an appropriate balance can be reached such that the benefit of human activities (e.g., industry, economic development, transportation) can be achieved for the minimal cost (i.e., air quality problems).

Air Quality Legislation in the United States

Before 1955 no federal laws governing air quality existed in the United States. Instead, air pollution was regulated only at the state and local levels. This meant that one community might have had drastically different air quality standards from a community nearby. Of course, this also meant that pollution from a community that did not regulate air quality could drift to a nearby community without any recourse from the federal government.

In 1955 Congress passed the **Air Pollution Control Act**, which was the first attempt at federal oversight in the United States. But this legislation proved more effective in making people aware that air pollution is a problem than it was in solving the problem. The **Clean Air Act of 1963**, with several subsequent amendments, became the first major effective legislation for regulating air quality and monitoring both stationary sources, such as power plants, and mobile sources, such as automobiles.

One amendment that was monumental in its influence was the **Clean Air Act of 1970**, passed during the Nixon administration. The Clean Air Act has been modified several times since 1970, most notably in 1977 and 1990. One of the most sweeping reforms created by the Clean Air Act of 1970 was the creation of a new federal agency called the **Environmental Protection Agency (EPA)**. The EPA was required to generate a list of **criteria pollutants**—those that are sufficiently widespread and dangerous in the United States that they must be monitored at the federal level. The EPA was also required to determine the **National Air Quality Standards (NAQS)** of those criteria pollutants. The

NAQS determined the “acceptable” concentration of each pollutant (in ppm of the atmospheric molecules). Obviously, this was a difficult job because the same concentration that may be harmless for most of the population may be life-threatening to an elderly person, a newborn infant, or a person with existing respiratory disease.

In 1971 the EPA produced the list of criteria pollutants. The list focused on sulfur oxides (SO_x), carbon monoxide (CO), *particulates* (a family of tiny suspended solid aerosols), lead, nitrogen oxides (NO_x)—**nitric oxide (NO)** and **nitrogen dioxide (NO_2)** in particular—and photochemical oxidants (primarily **tropospheric ozone**). Any areas that persistently exceed the NAQS of a pollutant are said to be **nonattainment zones**. Today, concentrations of all criteria pollutants have been reduced sharply in the United States, including in most nonattainment zones, in large part because of the success of the EPA’s guidance over the years. It is important to note that the EPA makes no attempt to set standards on pollutants that are not widespread nationwide, regardless of their danger. The decision on whether to allow obscure pollutants to be emitted into the air is left to the local and state governments, even if they are dangerous.

► Classifying Air Pollutants

By Response

Threshold pollutants are contaminants not known to be harmful in sufficiently small concentrations but that elicit a response after the concentration exceeds a particular threshold. Such pollutants may be considered to have a concentration–response curve like those shown in **FIGURE 12.9a**. Note that the vertical line in this figure represents the threshold concentration. All criteria pollutants except one—tropospheric ozone—are considered to be threshold pollutants. **Nonthreshold pollutants** evoke a response as soon as they exist at any concentration, meaning that the threshold concentration would be 0 ppm. Some examples of concentration–response curves for nonthreshold pollutants are shown in **FIGURE 12.9b**. The only criteria pollutant that is a nonthreshold pollutant is tropospheric ozone.

Before a decision is to be made about whether a pollution-generating facility is to be allowed to move into a community, several questions relating to the response need to be addressed. First, is the pollutant to be released a threshold or nonthreshold pollutant, and if it is a threshold pollutant, what is the threshold concentration? Second, will the emission of the pollutant exceed this threshold? Third, does the concentration–response curve look more like the exponential curve

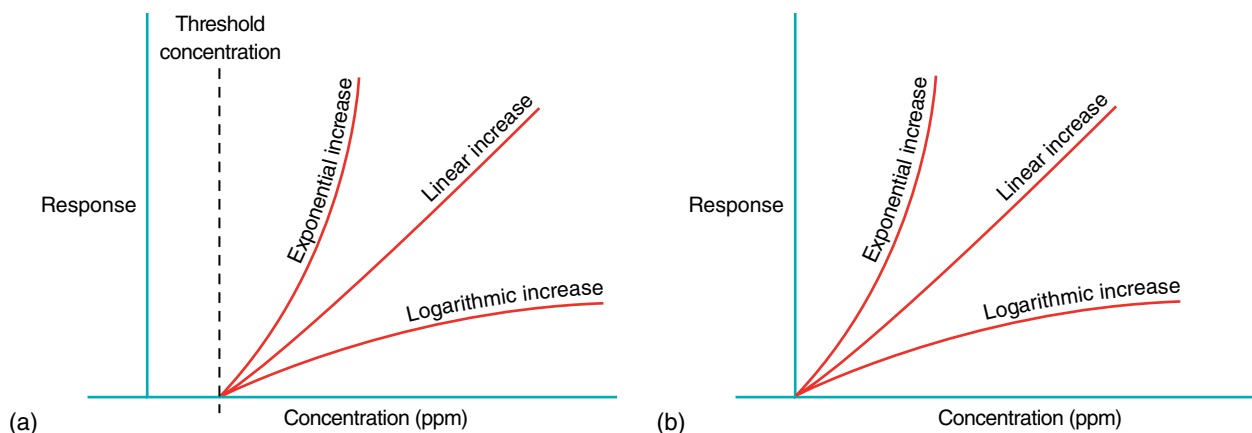


FIGURE 12.9 An example of a concentration–response curve for (a) threshold pollutant and (b) nonthreshold pollutant.

or the logarithmic curve in Figures 12.9a and 12.9b? Finally, what is the response? For example, if the concentration to be emitted does not exceed the threshold, or if the response increases only slightly with increased concentrations and the response is only a minor ailment, then perhaps the benefit of the factory or other emitting source may exceed the cost. If the threshold concentration is to be exceeded greatly and the response increases considerably with increased concentrations, and if the response is a serious illness, then the benefit probably would not exceed the cost. Unfortunately, scientists cannot always be certain about the nature of the threshold concentration or the response.

By Source

Primary Pollutants

We can also classify pollutants by the mechanism by which they appear in the atmosphere. **Primary pollutants** are those solids, liquids, or gases emitted directly by human activities. In general, solids and liquids are “washed out” of the atmosphere by precipitation more easily than gases. Among the criteria pollutants, all except tropospheric ozone and some types of SO_x and particulates are primary.

Each of the primary criteria pollutants has impacts that can be harmful to humans, animals, and plants. Because the United States is the largest producer of pollution, we focus on pollutants and trends in that country.

Sulfur Oxides It has been estimated that about half of the global atmospheric SO_x emissions are emitted naturally. In industrialized areas, however, most atmospheric SO_x is anthropogenic in origin, resulting primarily from fossil fuel combustion. Diesel fuel combustion, steel mills, and oil refineries are particularly large producers of atmospheric SO_x . Of the three

major types of fossil fuels, coal releases far more SO_x per energy unit than oil, and oil releases far more than natural gas.

The most prevalent and dangerous form of SO_x is SO_2 . As illustrated in **FIGURE 12.10**, U.S. counties in nonattainment of SO_2 standards are confined to small, widespread sections of the Midwestern U.S. and urban areas elsewhere. SO_2 tends to destroy plant hormones, stunting growth and reducing reproduction rates. As a result, the economic cost to agriculture and forestry in areas with high atmospheric SO_2 content can be significant. As we see shortly, SO_x can also have important impacts on creating **secondary pollutants**, through the generation of acid precipitation, which impacts vegetation and groundwater.

Humans are also impacted directly by SO_2 . Excessive exposure to SO_2 is associated with respiratory illnesses, including asthma, bronchitis, emphysema, and lung cancer. It is unclear whether SO_2 can cause these illnesses or whether it only accelerates and intensifies these respiratory problems, but sharp increases in respiratory disease have been recorded over the past century in industrialized regions.

Carbon Monoxide Carbon monoxide (CO) is a dangerous pollutant even in miniscule concentrations, and even to healthy people. Most CO is produced by automobiles. Like monatomic oxygen, CO is unstable in the free atmosphere, so when it is emitted it immediately attempts to bond with another atom or molecule. This may hinder the ability of hemoglobin—a protein in red blood cells—to deliver O_2 to body organs and tissues because inhaled CO may outcompete hemoglobin for this oxygen, thereby starving the brain, heart, and other organs of oxygen.

Perhaps you have walked briskly in a downtown area of a major city and felt tired unusually quickly. It is likely that in that situation the sleepy sensation occurred

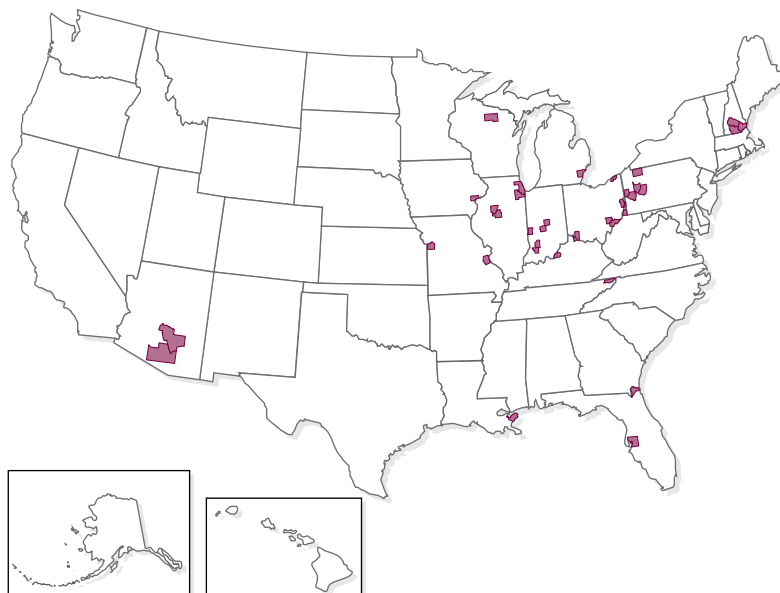


FIGURE 12.10 Nonattainment areas for SO₂ in the United States as of June 2016.

Modified from *The Green Book: Non-Attainment Areas for Criteria Pollutants*. U.S. EPA/Office of Air Quality Planning and Standards. <https://www3.epa.gov/airquality/greenbook/tbcs.html#AZ>.

because your brain was receiving a bit less oxygen than usual after you inhaled CO. Malfunctioning furnaces can release CO to a sealed-up home in winter, causing fatalities. Another means of inhaling CO is through smoking. Only one county, in southern Nevada, is currently not in compliance with the U.S. EPA CO standard.

Particulates Two major classes of particulates have been recognized by the EPA. **PM₁₀** is the category of particulates with diameters of less than 10 μm, whereas **PM_{2.5}** (also known as **fine particles**) refers to those particulates that have diameters smaller than 2.5 μm. Recent research suggests that even though PM₁₀ can be harmful, PM_{2.5} is of particular concern, because cilia in the bronchiole airways have great difficulty in removing it from the human body. These cilia normally move larger foreign substances, including inhaled pollutants and large bacteria, upward to the throat, where they can be expelled from the body via the digestive system. Particulates are believed to cause health problems in people with heart and lung disease. They also reduce visibility and can disrupt the balance of nutrients in soils when they settle to the ground. Finally, they damage buildings and monuments by abrasion as they continuously strike these surfaces.

Although many particulates enter the atmosphere via natural processes, some of these solid and liquid aerosols are emitted directly from vehicles, soil plowing, wood burning, and other human activities that generate dust. Other anthropogenic particulates arrive indirectly when fuel combustion combines with water vapor

and sunlight. PM_{2.5} nonattainment areas are mostly in California (**FIGURE 12.11**).

Lead Lead was listed as a criteria pollutant in 1978, and since that time it has been rapidly phased out of the atmosphere in the United States. Formerly an ingredient in gasoline and paints, it was shown to be linked to numerous brain and neurological disorders (collectively termed **plumbism**), and has been known to harm fish and wildlife. Today, the primary non-natural source of lead in the atmosphere is metal processing plants. Although concentrations are still high near smelters and incinerators, lead is no longer a widespread problem in the United States. As of December 2010 only two counties in the United States—one in Montana and one in Missouri—were in nonattainment of the lead standard.

Nitrogen Oxides Nitrogen oxides are produced naturally through various processes, including bacterial action in the soil, lightning strikes, and volcanic eruptions, but they are also produced by fossil fuel combustion and forest fires (the latter of which may be natural or human induced). Automobile exhaust is an important component of NO_x emissions in heavily populated areas. With the attainment of the standard in four counties surrounding Los Angeles, however, all counties in the United States are currently in attainment for NO_x.

As a primary pollutant, NO_x is harmful because of its ability to erode away objects in contact with it, such as building stone, tombstones, and lungs. As we

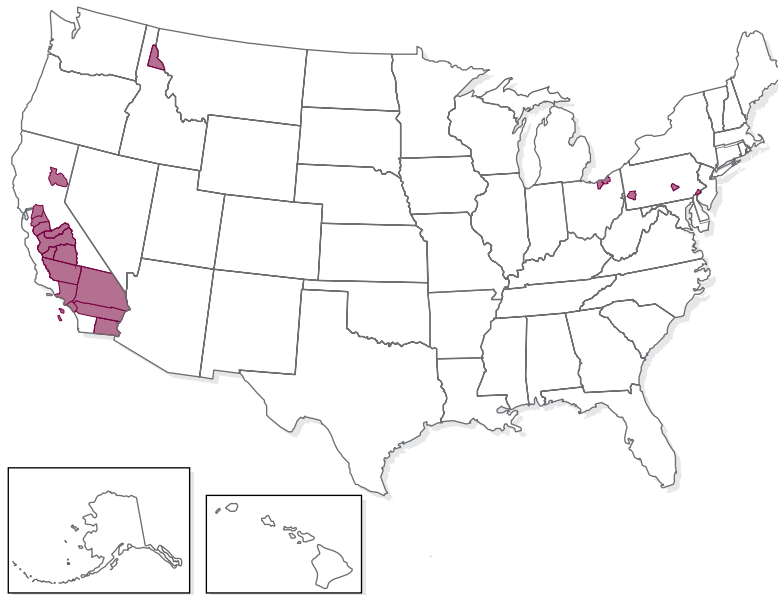


FIGURE 12.11 Nonattainment areas for $PM_{2.5}$ in the United States as of June 2016.

Courtesy of EPA. <https://www3.epa.gov/airquality/greenbook/kbcs.html#CA>.

saw earlier in this chapter, one form of NO_x —nitrous oxide—is a minor greenhouse gas. Nitrogen oxides are also associated with poor visibility. The most serious impacts of NO_x tend to be associated with its role as a secondary pollutant because of its ability to react with other substances to produce different photochemical pollutants. These are presented shortly in the discussion of secondary pollution and acid precipitation.

Secondary Pollutants

Secondary pollutants arrive in the atmosphere as a byproduct of chemical reactions between primary pollutants and other matter or energy in the atmosphere. Two primary pollutants can interact to create another pollutant, which may be even more hazardous than the two original primary pollutants combined.

Industrial Smog One type of secondary pollutant is **industrial smog** (sometimes known as **gray smog**). Industrial smog results from chemical reactions between two primary pollutants—*sulfur dioxide* (SO_2) and particulates—particularly in the presence of fog. The biggest danger of industrial smog is that the particles are too small to be removed by cilia, making them quite damaging to the respiratory system.

Perhaps the most widely recognized industrial smog episode in the United States occurred in Donora, Pennsylvania, a small industrial town nestled in a narrow, steep valley. On October 30, 1948, 17 people perished after an especially persistent anticyclone produced a strong temperature inversion while SO_2 and particulates continued to be released into the atmosphere

by local industrial activities. Limited vertical mixing in the stable atmosphere caused lethal point source pollution concentrations. Such an event, when deadly concentrations of a pollutant build near the emitter, is termed a **fumigation event**.

A far more deadly fumigation event occurred in London in December 1952, when death rates were over three times the normal rate for a period of 3 weeks of persistently stable atmospheric conditions. Over 2000 deaths were associated with this event that saw dense coal smoke combining with fog to produce smog. The fear of other deadly episodes helped to inspire the first federal clean air legislation in the United States.

Photochemical Smog A second family of secondary pollutants is termed photochemical smog (sometimes known as **brown smog**), which results when sunlight triggers a chemical reaction that creates pollution. These complicated reactions occur relatively easily in the presence of nitrogen oxides, **hydrocarbons**, and oxygen. Unlike industrial smog, photochemical smog usually occurs in relatively dry air.

One type of photochemical smog involves the *photodissociation* of NO_2 into NO and O in the presence of sunlight. Because monatomic oxygen is unstable in the atmosphere, it is likely to bond with a diatomic (O_2) molecule (which comprises 21% of the mass of the dry atmosphere) to form tropospheric ozone (O_3). Although this O_3 is chemically identical to the O_3 that protects us from harmful *ultraviolet radiation* in the *stratosphere*, O_3 near the ground is toxic. This feature is exemplified by the EPA's snappy rhyme about O_3 —"good up high,

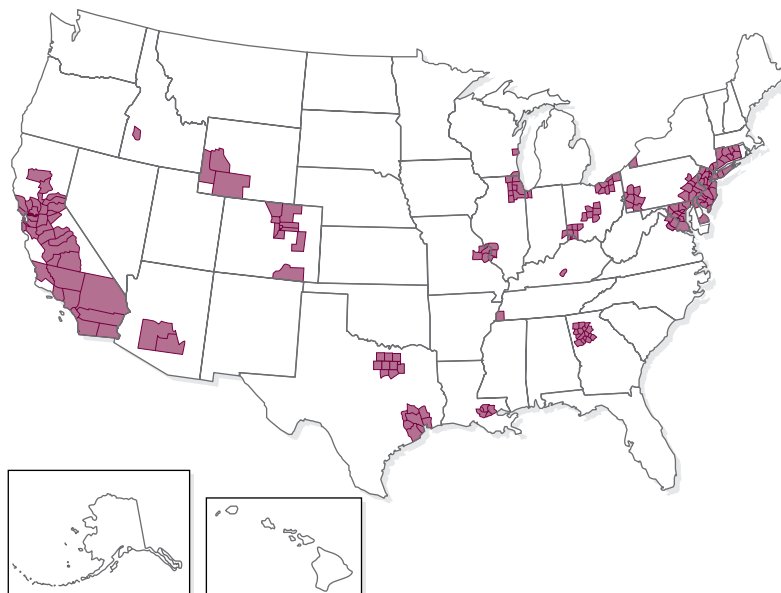


FIGURE 12.12 Nonattainment areas for ozone in the United States as of June 2016.

Courtesy of EPA. <https://www3.epa.gov/airquality/greenbook/hnacs.html#AZ>.

bad nearby.” The NO from the photodissociated NO₂ may then combine with certain hydrocarbons in a series of complicated reactions to form a family of secondary pollutants called **peroxyacetyl nitrates**.

Like NO₂, O₃ is known for wearing away objects in contact with it. These objects may include leaf cuticles, building stone, and human lungs. No conclusive evidence exists to blame O₃ for causing respiratory illness, but it is evident that O₃ worsens existing respiratory problems. Plants and trees that have been affected by O₃ are more susceptible to disease and insect infestation. When trees on slopes succumb to the disease or infestation, the slope becomes more susceptible to mudslides. In California, this problem has resulted in the construction of huge and expensive debris basins to protect homes in adjacent valleys. Any cost–benefit analysis for pollution must include hidden costs such as the purchase, installation, and maintenance of these basins. Further hidden costs are associated with degradation of the natural environment. Hydrocarbons are important in the production of some types of photochemical smog, including peroxyacetyl nitrates, and they also act as O₃ precursor compounds (a substance that must already be in place in the environment before a following chemical reaction can occur). They consist of a wide variety of chemicals, including some familiar ones such as benzene, formaldehyde, and methyl chloroform. Some hydrocarbons, such as isoprene, are emitted directly into the atmosphere naturally by vegetation; a familiar result is the hazy color that gives the Smoky Mountains their name. Some hydrocarbons are emitted by human activities as primary pollutants during fuel combustion

(particularly by automobiles) and in the use of solvents, paints, and other industrial products.

Currently, many U.S. counties exceed the EPA’s standard for O₃ (**FIGURE 12.12**). One reason for the violations is that the EPA’s requirements are becoming more stringent over time as more is learned about the harmful effects of O₃ rather than by an actual deterioration of the air quality. The counties in most serious violation of the standard are concentrated along the northeast coast, California, western Lake Michigan coast, and some urban/industrial areas in the Sunbelt and Midwest.

Acid Precipitation A third family of secondary pollutants is **acid precipitation**, which occurs when certain primary pollutants are deposited on the surface. Though far less common than acid rainfall, **acid fog** is a much more dangerous phenomenon, because of the potential for humans and animals to breathe the acidic concoction. Although all precipitation is naturally acidic due to the incorporation of CO₂ into falling precipitation, precipitation exceeding natural values of acidity are primarily anthropogenic in origin (although some natural processes, such as volcanic eruptions, may create acid precipitation, they are infrequent). The most common form of acid precipitation results from the emission of SO₂ in humid environments. When SO₂ reacts with water, it produces H₂SO₃, which can then react with oxygen to produce **sulfuric acid (H₂SO₄)**, which is corrosive. As we saw earlier, coal combustion releases SO₂ to the atmosphere, and because most early coal-intensive industries in the United States and western Europe

were located in humid environments, this form of acid precipitation has been a major problem historically.

Another type of acid precipitation results through complicated processes involving reactions between NO_x and water to form **nitric acid (HNO_3)**, another corrosive acid. This form of acid precipitation is more problematic in the “freeway cities” of the southern and western United States. It is important to note that either H_2SO_4 or HNO_3 can reach the surface through precipitation—or **wet deposition**—or the SO_2 and NO_x may reach the surface and interact with soil water to produce the acids in a **dry deposition** process.

The good news is that acid precipitation has not been as severe a problem in the United States as was initially anticipated. This outcome is similar to that for many other pollutants that were initially forecasted to increase in concentration far more than has actually occurred. The fact that air quality is generally improving in the United States, and in several other parts of the world, is a testament to the success of the EPA and other organizations in improving air quality. Additional engineering developments have also allowed us to increase the benefit of pollution-generating machines while reducing the environmental cost.

► Reactions and Attitudes to Climatic Change

Many of the human-induced forcing mechanisms discussed above cause global climatic change by shifting prominent atmospheric circulation features, which create different impacts across space. They may cause a warming trend in one location and a cooling trend in another. At this time the complexity of the climate system prohibits us from understanding all the potential impacts. Even so, several strategies can be used in policies designed to deal with the threat of climatic change. These include prevention, mitigation, and adaptation.

Prevention

The tactics designed to reduce a potential threat are referred to as **prevention**. One technique of prevention in the global warming debate is to prevent (or at least minimize) the emission of greenhouse gases. The most recent significant attempt at prevention of global warming was the Kyoto Treaty that was signed by over 150 nations and took effect in February 2005. This agreement requires that the wealthy nations contributing most of the world's greenhouse gases reduce their collective greenhouse gas emissions to 5.2% below the 1990 levels. Each nation has a target reduction under

the treaty. Although several of the world's most industrialized nations must reduce their emissions, some (such as Russia) are currently below their emissions quota; these nations may sell the rights to emit greenhouse gases to others that cannot meet their quota. This idea may be used by countries, states, cities, and industrial companies in a “**cap and trade**” policy. Although some may view “cap and trade” as a tax on economic development, others feel that such a policy is the only realistic means of holding or reducing emissions across the global economic landscape.

The United States refused to ratify the Kyoto treaty for two major reasons: (1) It would create too much risk of economic instability in the United States, especially considering the fact that the economic impacts of global warming and of cuts to fossil fuel emissions are not clearly understood, and (2) it does not require fossil fuel emissions cuts from 14 of the top 20 fossil fuel-emitting nations, including developing nations such as China, Brazil, and India, which are all projected to be producing a greater share of the world's fossil fuel emissions than the United States within 25 to 30 years. Indeed, by some accounts, China has already passed the United States as the world's leading emitter of fossil fuels. Currently, other than the United States, Australia is the largest economic power to refuse to ratify the treaty.

In July 2005 the United States entered into a plan to reduce human-based climatic change with five other nations (Australia, India, Japan, China, and South Korea). This plan focuses more on the development of clean energy sources instead of capping emissions, as in the Kyoto Treaty. The United States also signed a non-legally-binding agreement to reduce CO_2 emissions that was drafted at the 2009 Copenhagen Summit, but the outcomes of that conference are widely considered to have been a disappointment by many environmentalists.

Mitigation

The attempts to decrease the risk associated with a threat, rather than decreasing the threat itself, are referred to as **mitigation**. Whereas prevention strategies attempt to eliminate or reduce the problem of global warming, mitigation might involve building sea walls to combat the risk of coastal land loss from sea level rise resulting from global warming. Or mitigation may involve the introduction of new hybrid crops that would be more resistant to extreme weather variations caused by global warming. Or perhaps mitigation may simply involve purchasing fans for senior citizens to reduce their risk of death during a hot summer. Although mitigation strategies may be successful, they are sometimes criticized for being expensive and not “getting to the root of the problem.”

Adaptation

A strategy that involves simply living with a threat and the consequences associated with the threat is referred to as **adaptation**. It follows a “business as usual” approach, despite the problem at hand. The advantage of adaptation is that the preparation cost is zero, but the obvious disadvantage is that after the damage occurs, the full brunt of the impact must be borne. People living in *hurricane*- or earthquake-prone areas practice adaptation as a strategy for dealing with the problems. Until recently, the world had largely used an adaptation strategy in dealing with global warming.

Continued Research

For complicated environmental problems, such as global warming, policy must be enacted even while the problem is only partially understood. Regardless of whether prevention, mitigation, or adaptation strategies (or some combination of the three) are used, research on such problems must continue. Sometimes, the policy must be changed as research reveals more about the nature and impact of the problem. Not surprisingly, the general public becomes impatient when policy must be changed in response to the increased knowledge.

Research can take one of two forms, or some combination of the two. First, the modeling approach involves the generation of mathematical equations to predict the future severity of the problem. For example, complicated computerized climate models are used to predict the future climate under different magnitudes and rates of the input of CO₂ into the atmosphere. Unfortunately, different models project different results for temperature and especially precipitation for similar locations. In some cases even the sign of the change in a predicted variable is opposite that indicated by other models. For example, one model may predict future desertification for a location, whereas another indicates above-normal precipitation for the same location and time. These inaccuracies are largely confined to regional or local spatial scales, but modeled results at larger scales are more uniform. All major models suggest that global warming will continue and will have potentially destructive impacts. Policymakers must decide whether this model output warrants serious action. Many policymakers are now answering “yes” to this question.

Alternatively, the **empirical approach** involves the use of climatic data to uncover historical trends in variables and relationships between variables. This approach is advantageous because high-quality data represent actual observed conditions rather than a hypothetical, derived condition that may or may not actually happen. It is dangerous and generally inappropriate to extrapolate trends in atmospheric variables out

into the future, however, especially if the mechanism causing the trend in the variable being studied is not fully understood. For example, during the 1970s some scientists were discussing future cooling trends as evidenced by the prevalence of severe winters and cooler-than-normal summers. This climatic trend quickly reversed itself in the 1980s. Simple extrapolation of any trend is unwarranted, because positive feedbacks could cause an acceleration of the observed trend, whereas negative feedbacks could cause a data-driven trend to reverse itself at some point in the future.

In reality, both modeling and empirical approaches should be, and are, used to facilitate understanding. For example, climate models use empirical data to handle some processes for which our understanding of the physics is poor. The modeling and empirical approaches can complement each other or at least provide a “cross-check” to determine the degree of confidence of results from either approach.

Summary

The last century has seen substantial climatic changes, with human activities being considered by most climate scientists to be a culprit. Two broad categories of activities have led to a global warming effect on climate over the past century. First, the release of certain gases, particularly carbon dioxide, methane, and nitrous oxide, as a result of human activities has intensified the natural process of retention of longwave radiation near Earth’s surface—the greenhouse effect. Oceans, soils, and vegetation effectively remove the most important anthropogenic greenhouse gas—carbon dioxide—from the atmosphere, but the rate of removal is being exceeded by the rate of production. The measurable warming over the past century potentially caused by this anthropogenic greenhouse effect is expected to continue and have major consequences. Some of these anticipated consequences include rising sea levels, melting in the cryosphere, circulation shifts, and shifts in agricultural and bioclimatic zones.

A major activity that contributes to warming on a local as well as possibly a regional level is urbanization. Local heating in urban areas is enhanced by the increased retention and slow release of heat in construction materials and streets. The lack of vegetation and surface water storage in urban areas also intensifies this urban heat island by causing a proportionately higher amount of surface energy to be used for sensible heating, while less latent heating occurs compared with rural areas. Finally, waste heat generated by domestic and industrial activities also contributes to this urban heat island. At least some of this excess energy adds

to local- as well as regional-scale heating. The degree to which urban-derived energy infiltrates upward in scale to exacerbate the global-scale warming is not yet fully understood.

Although climatologists generally agree that a global warming trend is present in the climatic record over the past century, the cause and importance of this trend is still debated by some. Most believe that global warming should be curtailed because the trend is reliably measurable. They contend that the effects are real and may be disastrous, and that further delay will magnify the problems even more. They suggest that greenhouse gas emissions should be reduced regardless of their impact on the greenhouse effect. Some, however, believe there is too much uncertainty about the causes and impacts of the warming, feedbacks that may reverse the trend, and the data revealing the warming to enact strict and drastic policy to limit greenhouse gas emissions.

Some anthropogenic problems may be offsetting global warming. In particular, air pollution may reduce the amount of insolation incident on Earth's surface, thereby cooling the planet. An observed global dimming from 1961 to 1990 supports this notion and suggests that the impacts of greenhouse gas emissions may have been masked during this time by the reflection and scattering of some daytime shortwave radiation to space. On the other hand, recent evidence suggests that the dimming trend may have reversed itself in recent years.

Atmospheric stability, wind, and sunshine all govern the severity of pollution episodes. Stable atmospheres allow less pollution dispersal than unstable atmospheres. Windy conditions disperse and dilute pollutants, but light winds can cause pollution to drift long distances from its source. Sunshine can trigger the formation of photochemical pollutants such as ozone and peroxyacetyl nitrates, particularly when in the presence of hydrocarbons.

Landmark legislation on federal air quality in the United States occurred with the passage of the Clean Air Act of 1970. This legislation required that a newly created Environmental Protection Agency (EPA) create a list of widespread problematic pollutants, known as criteria pollutants, and set standards on acceptable concentrations of these pollutants. The criteria pollutants were sulfur oxides, carbon monoxide, particulates, lead, nitrogen oxides, and photochemical oxidants (primarily tropospheric ozone). Although localized concentrations of obscure pollutants may be hazardous, concentrations of all criteria pollutants have decreased in the past 35 years nationally.

Pollutants can be categorized by response and by source. Threshold pollutants elicit a response (whether it be respiratory illness, decreased crop yield, or any other type of impact) only after a certain threshold concentration is exceeded. Nonthreshold pollutants elicit a response as soon as they exist in any concentration. The source of primary pollutants is direct emission by human activities. Most criteria pollutants are primary pollutants. Secondary pollutants arrive in the atmosphere as a result of chemical reactions between primary pollutants or between a primary pollutant and some other matter or energy, such as water or sunshine. Three forms of secondary pollutants are industrial smog, photochemical smog, and acid precipitation.

Policy enacted in response to climatic change takes similar forms to reactions to other forms of hazard or crisis. Prevention measures seek to eliminate a threat. Mitigation strategies are aimed at minimizing the impact of a threat. Adaptation policies are designed to cope with a threat and its possible consequences. Regardless of which strategy or strategies are used in dealing with the hazard posed by anthropogenic climatic change, continued research to understand the problem and its potential impacts is critical to minimizing impacts to human health and the environment.

Key Terms

Absolute zero

Absorption

Acid fog

Acid precipitation

Adaptation

Adiabatically

Advection

Aerosol

Air Pollution Control Act

Albedo

Anaerobic

Anthropogenic

Anticyclone

Arctic amplification

Atmospheric window

Biosphere

Brown smog

California current

“Cap and trade” policy

Carbon monoxide (CO)

Carbonic acid (H₂CO₃)

Circumpolar vortex

Clean Air Act of 1963

Clean Air Act of 1970

Condensation

Condensation nuclei

Conduction

<i>Convection</i>	<i>Kelvin temperature scale</i>	<i>Positive feedback system</i>
<i>Counter-radiation</i>	<i>K-T extinction</i>	<i>Prevention</i>
<i>Cretaceous-Paleogene extinction event</i>	<i>Kyoto Treaty</i>	<i>Primary pollutant</i>
<i>Criteria pollutant</i>	<i>Latent heat</i>	<i>Proxy evidence</i>
<i>Cryosphere</i>	<i>Lithification</i>	<i>Relative humidity</i>
<i>Cyclone</i>	<i>Little Ice Age</i>	<i>Reservoir</i>
<i>Deforestation</i>	<i>Longwave radiation</i>	<i>Respiration</i>
<i>Density</i>	<i>Medieval Warm Period</i>	<i>Runoff</i>
<i>Desertification</i>	<i>Mediterranean climate</i>	<i>Saltwater intrusion</i>
<i>Dry deposition</i>	<i>Methane</i>	<i>Secondary pollutant</i>
<i>Empirical approach</i>	<i>Methane hydrates</i>	<i>Sensible heat</i>
<i>Environmental Protection Agency (EPA)</i>	<i>Methanogen</i>	<i>Shortwave radiation</i>
<i>Evaporation</i>	<i>Micrometer</i>	<i>Sink</i>
<i>Evapotranspiration</i>	<i>Midlatitude wave cyclone</i>	<i>Smog</i>
<i>Fine particles</i>	<i>Midlatitude westerlies</i>	<i>Specific heat</i>
<i>Fluorocarbon</i>	<i>Mitigation</i>	<i>Stability</i>
<i>Fossil fuel</i>	<i>National Air Quality Standards (NAQS)</i>	<i>Stable atmosphere</i>
<i>Friction</i>	<i>National Oceanic and Atmospheric Administration (NOAA)</i>	<i>Stratosphere</i>
<i>Fumigation event</i>	<i>Negative feedback system</i>	<i>Sublimation</i>
<i>Global dimming</i>	<i>Nitric acid (HNO₃)</i>	<i>Subtropical anticyclone</i>
<i>Global warming</i>	<i>Nitric oxide (NO)</i>	<i>Sulfur dioxide (SO₂)</i>
<i>Gray smog</i>	<i>Nitrogen dioxide (NO₂)</i>	<i>Sulfuric acid (H₂SO₄)</i>
<i>Greenhouse effect</i>	<i>Nitrogen oxide (NO_x)</i>	<i>Temperature inversion</i>
<i>Greenhouse gas</i>	<i>Nitrous oxide (N₂O)</i>	<i>Thermal conductivity</i>
<i>Hawaiian high</i>	<i>Nonattainment zone</i>	<i>Threshold pollutant</i>
<i>Heat capacity</i>	<i>Nonthreshold pollutant</i>	<i>Transpiration</i>
<i>Humus</i>	<i>Nuclear autumn</i>	<i>Tropical cyclone</i>
<i>Hurricane</i>	<i>Nuclear winter</i>	<i>Tropospheric ozone</i>
<i>Hydrocarbon</i>	<i>Particulates</i>	<i>Tundra</i>
<i>Hygroscopic nuclei</i>	<i>Peroxyacetyl nitrate</i>	<i>Ultraviolet radiation</i>
<i>Ice core</i>	<i>Photochemical smog</i>	<i>Unstable atmosphere</i>
<i>Industrial smog</i>	<i>Photodissociation</i>	<i>Urban canyon</i>
<i>Insolation</i>	<i>Photosynthesis</i>	<i>Urban heat island</i>
<i>Intergovernmental Panel on Climate Change (IPCC)</i>	<i>Plumbism</i>	<i>Wavelength</i>
<i>Joule</i>	<i>PM_{2.5}</i>	<i>Wet deposition</i>
	<i>PM₁₀</i>	<i>Wind channeling</i>
		<i>Wisconsin Glacial Phase</i>

Terms in italics have appeared in at least one previous chapter.

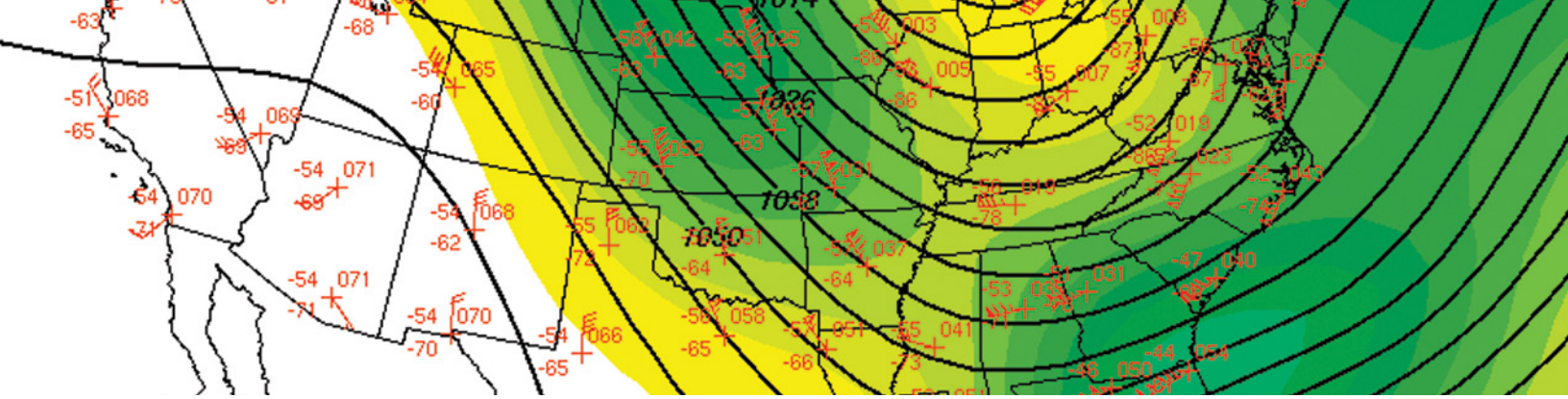
Review Questions

1. Why is anthropogenic climatic change an important issue in contemporary climatology?
2. How does the greenhouse effect work and why is it not solely a natural process?
3. What similarities and differences exist between the heating in the lower atmosphere in the greenhouse effect and the heating of the inside of an actual greenhouse?
4. What is the most abundant greenhouse gas and at what wavelengths is it most effective?
5. What are the sources and sinks of atmospheric carbon dioxide?
6. What are the sources of atmospheric methane?
7. What are methane hydrates and what role do they play in atmospheric methane concentrations?
8. What country is the world's leading emitter of greenhouse gases, and which are projected to be the leading countries in the future?
9. How might positive feedback systems in polar regions accelerate global warming?

10. Why are urban areas warmer than their surrounding rural environments?
11. Other than increased temperatures, what climatological differences exist between cities and their surrounding rural environments?
12. What are the major arguments that environmentalists use to defend their position that the anthropogenic greenhouse effect is a major problem that must be solved?
13. What arguments do skeptics give to justify their position that the anthropogenic greenhouse effect is not as serious as some would suggest?
14. What factors are assumed to have caused global dimming and why has the global dimming trend apparently reversed in recent years?
15. What did studies of the atmosphere in the absence of jet contrails reveal about global dimming in the days after September 11, 2001?
16. How does atmospheric stability affect pollution concentrations?
17. What factors cause California to have severe problems from photochemical pollution?
18. Why was the National Air Quality Standard for criteria pollutants difficult to determine?
19. What are the criteria pollutants? Of these, which are primary pollutants?
20. What are the major anthropogenic sources of atmospheric sulfur oxides?
21. What danger does carbon monoxide pose if inhaled?
22. What are the primary classes of particulates? Of these, which is the more harmful class? Why?
23. How does industrial smog form?
24. How does tropospheric ozone form?
25. What primary pollutants are the major contributors to acid rain, and how does the distribution of these pollutants differ?
26. What are the advantages and disadvantages of mitigation as a strategy in combating anthropogenic climatic change?

Questions for Thought

1. Compare and contrast the history of federal environmental legislation and/or the national federal agency that governs air quality in a country other than the United States to the history and development of U.S. air quality legislation by the EPA.
2. The text discussed prevention, mitigation, and adaptation as strategies to deal with the effects of global climatic change. Think of examples of each of these three strategies in dealing with another threat besides climatic change. Some examples include earthquake risk, bioterrorism, and floodplain development.
3. Other than the topics discussed in this chapter (anthropogenic greenhouse effect, urban heat island, pollution, nuclear winter/autumn, and global dimming), what human activities contribute to altering local and regional climatic environments?
4. Watch the 2006 movie *An Inconvenient Truth*. Does this film portray the global warming problem accurately? Why or why not?



CHAPTER 13

Linking Spatial and Temporal Aspects of Climate Through Quantitative Methods

CHAPTER AT A GLANCE

- Computerized Climate Models
 - Types of GCMs
 - Representing the Earth–Ocean–Atmosphere System in GCMs
 - Data for GCMs
- Seven Basic Equations
 - Navier-Stokes Equations of Motion
 - Thermodynamic Energy Equation
 - Moisture Conservation Equation
 - Continuity Equation
 - Equation of State
 - Similarities and Differences Between GCMs and Weather Forecasting Models
 - Limitations of Model Results
- Statistical Techniques
- Atmospheric Teleconnections
 - Extratropical Teleconnections in the Pacific: The Pacific Decadal Oscillation
 - Extratropical Teleconnections in the Atlantic Ocean
 - Teleconnections over North America
- Summary
- Key Terms
- Review Questions
- Questions for Thought

Elsewhere in the text we focused on the processes that contribute to climate. Other chapters synthesized the information about climatic processes by describing how those processes act to produce climates that vary spatially across Earth. Here we present the variability and changes known to occur in climates across time because of natural and *anthropogenic* processes. The purpose of this chapter is to describe the major mathematical tools available to climatologists to assess the differences in climates across space and time simultaneously. These extremely powerful and important tools represent the state of the art in modern climatology.

► Computerized Climate Models

Computer models are important for simulating atmospheric processes. Some models may serve their purpose quite satisfactorily even though they may be simple. For example, a *surface water balance* model may provide useful information on the impact of a forecasted precipitation event on the hydrology and soil moisture of a particular location. Or an **energy balance model** might be useful for estimating the changes in *insolation* if the solar output were increased or decreased by a certain percentage, or if the *Milankovitch cycles* changed Earth's orbital *eccentricity* or direction or degree of tilt on its axis.

Other climate models are by necessity more complicated. Some models attempt to predict the motion of storms or other patterns of atmospheric behavior through **analog forecasting**—identifying cases from the past and assuming that the atmosphere will behave in an analogous way in a similar situation in the future. Of course, analog models require abundant and accurate historical data to be useful.

Other, more complicated models generally involve the prediction of the global atmospheric circulation based on dynamic conditions rather than by analog comparisons. These models usually operate at the planetary scale because the behavior of the atmosphere is inherently “continuous” around the world, such that processes occurring in one location will be felt elsewhere. These types of models are collectively known as **general circulation models (GCMs)**.

Several research groups around the world are leaders in the generation of GCMs. In the United States the National Aeronautics and Space Administration's Geophysical Fluid Dynamics Laboratory (and associated scientists at Princeton University) and the Goddard Institute of Space Sciences are both world leaders. Other leading institutions include the Hadley Centre (United Kingdom), the Max Planck Institute for Meteorology (Germany), the Canadian Climate Centre, the Japanese

Meteorological Agency, and the Australian Bureau of Meteorology. In recent years several other nations have developed their own GCMs, partially in response to an increased need to understand potential impacts of global climatic change on their territories.

A critical feature of any GCM is the **resolution**, an attribute that refers to the coarseness, or precision, of observations over space (**spatial resolution**) and time (**temporal resolution**). Spatial resolution is reminiscent of pixels on a computer monitor or digital image. Finer spatial resolution provides more pixels per unit area or volume and more detail in the model output across space, but at the expense of a higher number of calculations and greater data handling capacity. It is tempting to consider spatial resolution in only two-dimensional space, but actually GCMs must consider spatial resolution in three dimensions. A GCM that divides the atmosphere into small three-dimensional “boxes” simulates the behavior of the atmosphere in greater spatial detail than one that uses larger boxes. A typical GCM may have a spatial resolution of perhaps $2 \times 2^\circ$ of *latitude* and *longitude*, or, because the lines of longitude converge toward the poles, an equally spaced grid may have a spatial resolution of perhaps 300×300 km (185×185 mi), with perhaps 30 vertical levels.

Temporal resolution refers to the degree of detail in time that a model attempts to forecast. For example, does the model attempt to forecast hourly or daily temperatures (as weather forecasting models may) or monthly, seasonal, annual, or even decadal mean temperatures only (as GCMs may attempt)? A related concept is the **time step**—the length of time into the future that is forecasted by each “run” of the model. If you were asked to forecast your university football team's record 5 years from now, you might proceed by forecasting its record next year. Then you might base your forecast of the following year's record on an assumption that what you predicted this year actually did occur. Then you might proceed, 1 year at a time, until you reached the 5-year forecast. In this example your time step is 1 year.

Similarly, a weather forecasting model that uses a time step of 5 minutes makes a forecast for 5 minutes into the future, then uses that model output as the input for the next 5-minute forecast, and so on. The model is run **iteratively**—that is, over and over again—to a forecasting period such as 24 hours. Smaller time steps require more calculations but perhaps provide better accuracy than longer time steps. Regardless, for the model to be of any use, the time step must be small enough to allow for any disturbance (even those that travel fastest) to appear within the domain of analysis. If a fast-traveling wave can enter the “real world” and then leave it in less time than the time step, the model could never “catch” this feature and take its effects into account.

Types of GCMs

Atmospheric general circulation models consider only those processes that occur in the atmosphere. At short time scales, these may provide adequate simulation of atmospheric motion, so atmospheric GCMs may be adequate for weather forecasting purposes. These may not be applicable for climatological applications, however, because of the importance of the interactions between the atmosphere and the *lithosphere, hydrosphere, cryosphere, and biosphere* at longer time scales. Climatological forecasting models usually require more sophistication, as we see later in this chapter.

Like atmospheric GCMs, **oceanic general circulation models** simulate circulation, but in this case the circulation remains in the hydrosphere. The same equations govern motion in the ocean as in the atmosphere, because both media are fluids, but oceanic circulation is complicated by the fact that the circulation is confined to the ocean basins rather than being “free” to circulate anywhere as the atmosphere does. Furthermore, ocean circulation involves a fluid that is 800 times denser than the fluid circulating in the atmosphere. Assumptions that can be made for the atmosphere cannot be made for the ocean, and vice versa, because the higher *density* of the oceans causes a much longer reaction time to changing forces than in air.

Coupled atmosphere–ocean general circulation models include an ability to simulate not only the circulations of both the atmosphere and the ocean but also the feedbacks and energy transfer between those two fluids. Some crude atmosphere–ocean GCMs may treat the ocean as a **swamp model**—a computerized model in which the water is assumed to have a different *albedo* than land but no capability to store heat. A more advanced type of approach uses a **slab model**, in which a constant depth and ability to store heat are assumed. Nevertheless, even these models may not provide the most reliable projections of climatic change and its impacts. Other atmosphere–ocean GCMs include far more detailed calculations involving physical processes, feedbacks, and energy exchanges. Some may even include mechanisms for accounting for changes to the global *carbon cycle*, but these details come at the expense of spatial and temporal resolution. Spatial resolution of a few hundred kilometers is a reasonable goal in such sophisticated models.

Often the spatial and/or temporal resolution of GCM output is too coarse to be very useful for *prevention, mitigation, or adaptation* strategies for dealing with climate change and its impacts. In such cases, **downscaling** is necessary to generate finer-scale model output than a GCM provides. **Spatial downscaling** refers to modeling at a finer spatial scale than a GCM provides, and **temporal downscaling** refers to the generation

of model output at a finer temporal scale than a GCM produces. Nevertheless, in practice, the finest temporal resolution (i.e., time step) possible is generally chosen based on computing power, and “downscaling” usually implies “spatial downscaling.”

One type of downscaling relies on the use of models that incorporate the same or similar physically based equations as GCMs, but at a finer spatial resolution. In such cases output from a global-scale GCM is used as input to a **regional climate model (RCM)**. Such **dynamic downscaling** techniques zoom in on the particular region of interest and contain greater spatial resolution because the geographical area of interest is smaller. Specifically, RCMs may contain a spatial resolution as small as 20 km (13 mi). This feature enables them to mimic the effects of local surface features and short waves in the atmosphere better than global-scale GCMs. Because of the increasing likelihood of errors magnifying over time when only a small region is represented in the model, however, RCMs are usually restricted to simulate climates of the near future (perhaps a few decades at most). The **National Center for Atmospheric Research (NCAR)** and Penn State University collaborated to produce an RCM called the MM5 (Mesoscale Model version 5) model that is run for the eastern United States. Another popular model for downscaling applications is the **Weather Research and Forecasting (WRF) model**, produced by the University Corporation for Atmospheric Research (UCAR), which is the research arm of NCAR.

As an alternative to dynamical downscaling via RCMs, climatologists may derive statistical relationships between GCM output and atmospheric conditions at a finer grid scale than the GCM can provide to improve upon the resolution of current GCMs. For example, if a GCM outputs a temperature of 10°C in 2100 for a 200 × 200 km surface area, **statistical downscaling** may fine-tune that projection for different land covers within that surface area based on derived statistical relationships between temperature and land cover.

Temporal downscaling projects output at one temporal scale to a finer temporal scale using statistical relationships. For example, if a GCM outputs the annual temperature in 2050, temporal downscaling techniques might be used to resolve that projection down to the monthly level. In some cases output may even be temporally downscaled to the daily or subdaily level, particularly for projections with shorter lead times.

Representing the Earth–Ocean–Atmosphere System in GCMs

Two major families of GCMs can be identified based on the strategy used for modeling geophysical processes.

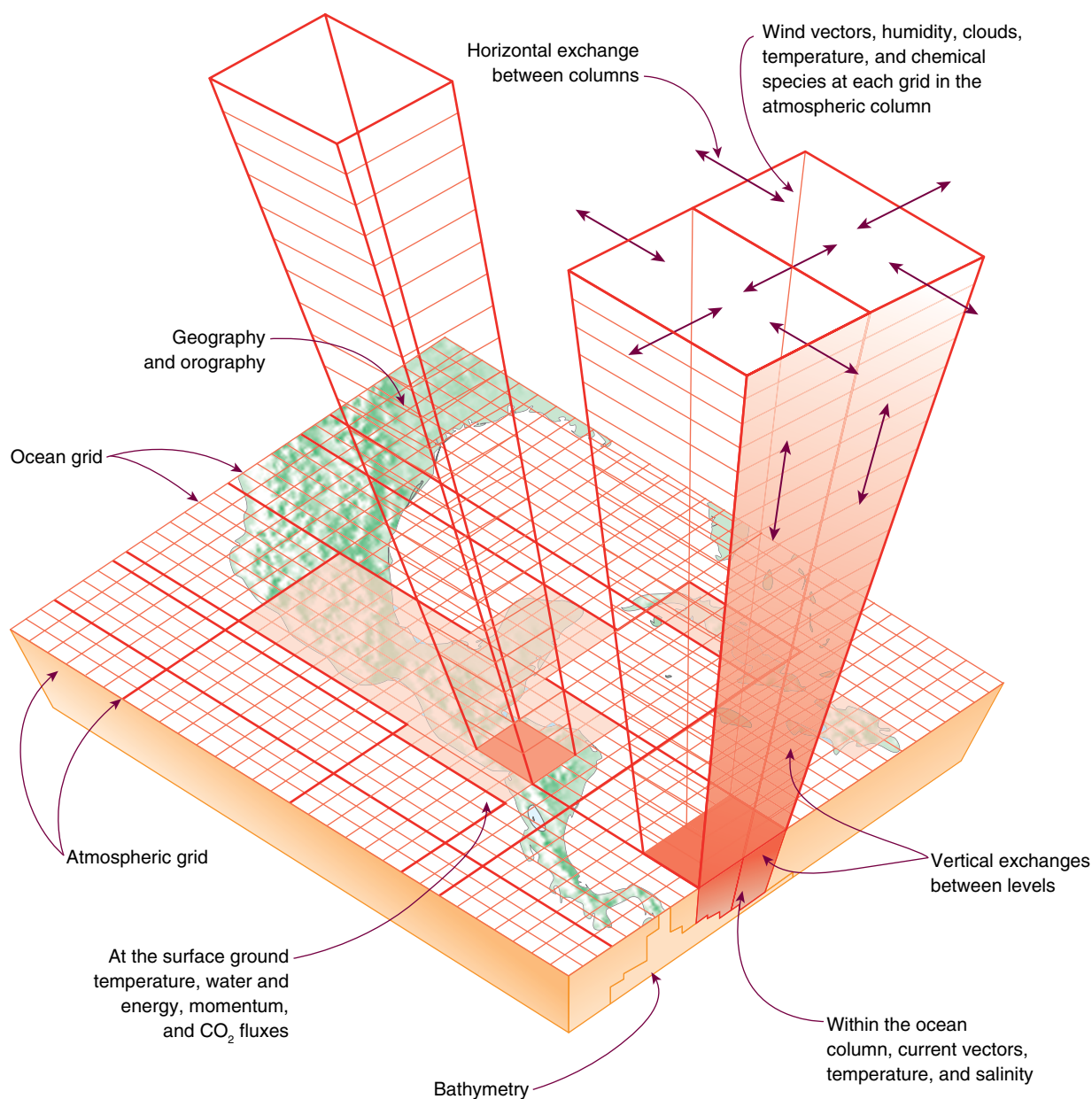


FIGURE 13.1 Schematic of a gridpoint model.

Data from McGuffie, K., & Henderson-Sellers, A. A. (2005). *Climate Modeling Primer*. 3rd ed. New York: John Wiley & Sons.

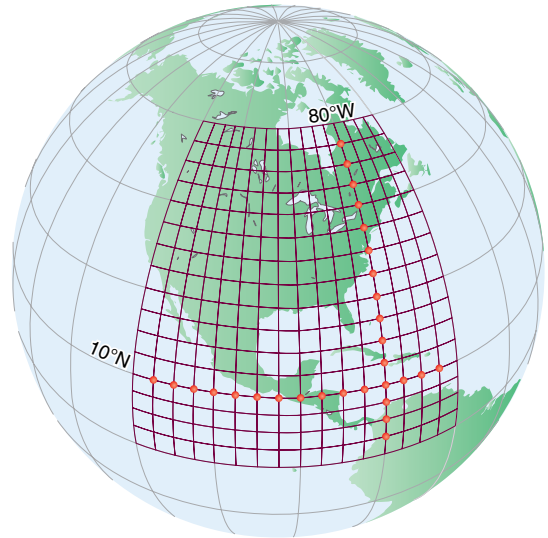
Gridpoint models represent atmospheric phenomena by dividing Earth into equidistant points with imaginary three-dimensional “boxes” centered on those points representing the smallest area in the atmosphere for which motion can be calculated by the model (FIGURE 13.1). The data at those points are interpolated from available atmospheric data and observations. The models are then run by using **finite differencing**—a technique that determines the values of the atmospheric variables at some point into the future. These procedures calculate the value of each atmospheric variable at a gridpoint based on the rate of *advection* of calculated values at each adjacent point, including the points above and below the point of interest.

Spectral models adopt the strategy of expressing atmospheric motion in terms of a series of waves. A schematic of the process of applying spectral techniques is shown in FIGURE 13.2. In spectral methods the collected data are interpolated to a grid system with multiple vertical layers, as they are in gridpoint models. Once the gridded variables are collected, each variable is plotted by latitude and (separately) by longitude, for a grid of latitude and longitude lines that are as fine as the spatial resolution of the model. For example, for 80°W longitude each value of temperature is plotted from the South Pole to the North Pole, with latitude along the *x*-axis and temperature along the *y*-axis. Mathematical techniques are then used to identify curves that approach

1. Data collected at several altitudes for a given variable (e.g., temperature) are quality controlled...

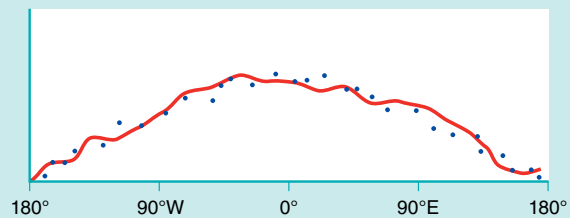


2. and then interpolated to a grid system with multiple layers.

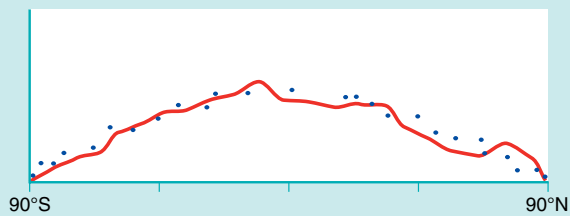


3. The data at each latitude and longitude line are plotted at each vertical level, and the spectral transformation plots the curve that fits the distribution best.

At 10°N Latitude, for height 1

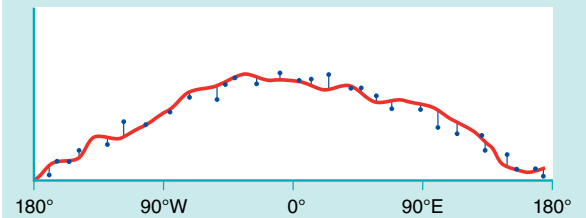


At 80°W Longitude, for height 1

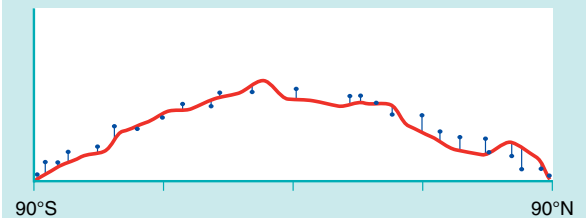


4. The data points are shifted to meet the graphs generated by the spectral transformation, at all latitude and longitude lines.

At 10°N Latitude, for height 1



At 80°W Longitude, for height 1



5. Fluxes are then computed in three-dimensional space, as in the gridpoint models.

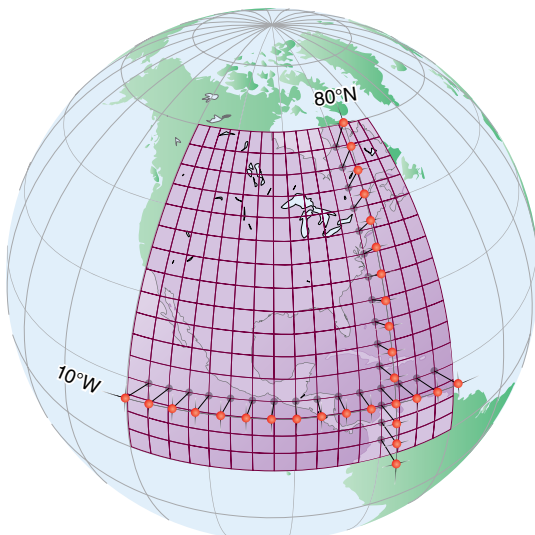


FIGURE 13.2 Schematic of a spectral model.

Data from McGuffie, K., & Henderson-Sellers, A. A. (2005). *Climate Modeling Primer*. 3rd ed. New York: John Wiley & Sons.

as many of the points in the graph as possible, so that the temperature distribution from the South Pole to the North Pole along the 80°W meridian of longitude can be expressed mathematically. After the mathematical expression of the distribution of all variables at all vertical levels, the “results” of the forecast at the time step of interest are projected back to the gridded “data” for input to the next iteration of the model.

The primary advantage of spectral techniques is the representation of atmospheric motion as wavelike, which is a good assumption in the real world. Any motion that occurs on one side of Earth “connects” after that motion propagates around the world back toward the original location. Spectral analysis lends itself well to mimicking this type of atmospheric process. Even in spectral analysis, however, vertical transfers of energy, matter, and *momentum* are still calculated as they are in gridpoint models.

Data for GCMs

Because meteorological data are not collected at equally spaced locations around Earth (except in the case of satellite data), the data at the network of gridpoints are most likely to be interpolated computationally using spatial interpolation methods from the available, collected data. Therefore, the data that are input into the gridpoint models are likely to be generated rather than actually observed. Of course, any errors present in the data generation process would appear in the model even before any forecasting calculations were made. Note that because upper-air observations are far more sparse than surface-based observations, the upper-air data must be interpolated based on far fewer “actual” data points than at the surface. But because upper-level observations are affected less by the land cover and local conditions, the sparse network of points is less problematic than a lack of adequate data at the surface.

► Seven Basic Equations

All weather and climate result from three fundamental entities: motion (both horizontal and vertical), energy, and moisture. Without any of these three, weather and climate do not exist. Any attempt to simulate the behavior of the atmosphere dynamically must include a representation of the fundamental equations that govern motion, energy, and moisture in the atmosphere. Seven equations accomplish this task. These equations are a set of nonlinear, partial differential equations. To gain an appreciation for the complexity of solving such equations simultaneously, imagine a system of two equations with only two unknowns, such as the following:

$$\begin{cases} 2x + 7y = 23 \\ x + 2y = 10 \end{cases}$$

The solution of this system of equations is simple, because both are linear (i.e., the variables do not have exponents other than 1) and because there are only two unknowns.

By contrast, each of the *seven* basic equations is tied together and must be solved simultaneously. To solve seven nonlinear partial differential equations simultaneously is an incredibly intensive computational task. Indeed, no branch of mathematics has yet been invented to accomplish this task efficiently. Instead, the equations must be solved iteratively, repeatedly “guessing” the solution and using each guess to focus in on the solution.

Navier-Stokes Equations of Motion

All GCMs and all weather forecasting models use the seven basic equations (in some form) to analyze and forecast atmospheric flow and behavior. The first three equations are collectively known as the *Navier-Stokes equations of motion*, named after Claude Navier, a French physicist whose equations for vibrational motion were generalized by several scientists, including Sir George Stokes, for use in a wide variety of applications. If you studied calculus you may remember Stokes’ theorem, an important principle in three-dimensional vector calculus. Stokes was interested in the mathematics of motion, and his work has been applied to all areas of fluid mechanics, including large-scale ocean circulation, hydrodynamics, aerodynamics, and atmospheric circulation.

One of the Navier-Stokes equations governs velocity in the west-to-east direction (the positive u direction), another is for south-to-north velocity (positive v), and the third is for down-to-up velocity (positive w). East-to-west, north-to-south, and up-to-down velocities are simply represented as the negative u , v , and w directions, respectively. Thus, all motion (advection and *convection*) can be described by some combination of the u , v , and w equations. The equations themselves describe the rate of change of u , v , and w over time at each gridpoint, and the rate of change of a velocity over time is actually acceleration. The first Navier-Stokes equation may be written in the form of **EQUATION 13.1**, in which the symbols in the first five terms are simply read as

EQUATION 13.1

$$\frac{\partial u}{\partial t} = -u \frac{\partial u}{\partial x} - v \frac{\partial u}{\partial y} - w \frac{\partial u}{\partial z} - \alpha \frac{\partial p}{\partial x} + f_v + F_x$$

1 2 3 4 5 6 7

“the partial derivative of (*variable in the numerator*) with respect to (*variable in the denominator*).” The “partial derivative” is the rate of change of the variable in the numerator over the variable in the denominator, *while holding the effect of all of other variables constant*. For example, term 1 in Equation 13.1 is expressed as the rate of change of west-to-east component of wind velocity (u) over time (an acceleration) at the gridpoint of interest, expressing *how much has the west-to-east component of wind changed since the last observation at this gridpoint?* Notice that because time is in the denominator, this equation has forecasting implications—how much has u changed at this point since the last time step?

The terms on the right side of the equation represent the factors that can influence the rate of change in u over time. Terms 2 and 3 represent the rate of advection of u in the west-east (x) and south-north (y) directions, respectively. As the wind velocity (u and v , respectively) increases, the rate of advection increases. Terms 2 and 3 also show that as the gradient of wind speed increases (in the x and y directions, respectively), the rate of advection increases because of the tendency to equal out imbalances of energy, matter, and momentum. Similarly, term 4 shows the vertical transfer (through convection) of u in the down-to-up (z) direction.

Term 5 describes the effect of the west-east *pressure gradient force*, where α is the **specific volume** (the reciprocal of density)—the amount of space occupied by a solid, liquid, or gas divided by its mass. The pressure gradient force only matters in the x direction because only the change in u with respect to time is sought in this equation. Term 6 represents the *Coriolis effect*, whereby the *Coriolis parameter* is

$$f = 2\Omega \sin \phi$$

with Ω representing the angular velocity of Earth ($7.27 \times 10^{-5} \text{ s}^{-1}$) and ϕ expressing the latitude. Finally, F_x in term 7 represents the impact of *friction* in the x -direction. Friction is difficult to quantify, so different models treat the effect of friction differently.

Likewise, the second Navier-Stokes equation can be expressed as shown in **EQUATION 13.2**. This equation differs from the first equation because it determines the rate of change of the v component of atmospheric

EQUATION 13.2

$$\frac{\partial v}{\partial t} = -u \frac{\partial v}{\partial x} - v \frac{\partial v}{\partial y} - w \frac{\partial v}{\partial z} - \alpha \frac{\partial p}{\partial y} + fu + F_y$$

1 2 3 4 5 6 7

velocity over time. Correspondingly, the terms on the right side of the equation are modified to reflect this change.

The third Navier-Stokes equation is for vertical motion (**EQUATION 13.3**). Interestingly, in the vertical direction, the Coriolis term (term 6) contains a cosine function rather than the sine function as in the first two equations. This is because the Coriolis effect depends slightly on vertical motion (rather than just latitude), but this is such a small term compared with the others that it can usually be ignored (except when analyzing the acceleration in the vertical direction). Additionally, note the presence of the gravity term (term 8). Unlike in the first two equations, gravity must be considered when evaluating vertical motion.

Several of the terms in the third Navier-Stokes equation are very small compared with the others, particularly for motion at the *synoptic scale* and *planetary scale*. Terms 5 and 8 tend to dominate, because for broad-scale atmospheric motion w does not change much in the x , y , or z directions—the air moves horizontally to a much greater extent than vertically—and because the Coriolis and frictional terms are minimal. As a result, for ease and speed of calculation, the small terms are often ignored. The third Navier-Stokes equation for vertical motion is often simplified to,

$$-\alpha \frac{\partial p}{\partial z} = g$$

This simplified form is the *hydrostatic equation* that was discussed previously. It expresses the balance between the upward-directed pressure gradient force (i.e., the buoyancy term) and the downward-directed gravitational force. The negative sign is necessary because *pressure* decreases as height (z) increases.

Simply stated, the hydrostatic equation shows that buoyancy and gravity are the two major factors that

EQUATION 13.3

$$\frac{\partial w}{\partial t} = -u \frac{\partial w}{\partial x} - v \frac{\partial w}{\partial y} - w \frac{\partial w}{\partial z} - \alpha \frac{\partial p}{\partial z} + (2\Omega \cos \phi)u + F_z - g$$

1 2 3 4 5 6 7 8

govern vertical motion. Of course, in some cases where vertical acceleration is important—for example, in local-scale thunderstorms or in situations where advection of w is important—the atmosphere is not behaving as a hydrostatic fluid and the neglect of the six terms in the “full” Navier-Stokes equation for w is unacceptable. It is no surprise, then, that *local-scale* thunderstorms, which have significant vertical acceleration, are difficult or impossible to predict precisely. Broad-scale numerical models generally do not have adequate input data, computational power, and spatial/temporal resolution to allow for the full consideration of all of the terms in the third Navier-Stokes equation.

Likewise, the first two equations of motion may also be simplified to include only those terms that tend to dominate. The advection terms (i.e., those terms that govern the rate of change of the velocity terms u , v , and w across space) are often much smaller (particularly for synoptic and planetary scales of motion) than the effects of acceleration, the pressure gradient force, the Coriolis effect, and friction. This simplification reduces the first two equations to:

$$\begin{aligned}\frac{\partial u}{\partial t} &= -\alpha \frac{\partial p}{\partial x} + f_v + F_x \text{ and} \\ \frac{\partial v}{\partial t} &= -\alpha \frac{\partial p}{\partial y} + f_u + F_y\end{aligned}$$

Collectively, these two equations and the hydrostatic equation are termed the **primitive equations of motion**. If a model is described as “primitive,” it assumes that there is no advection of wind velocity in the west–east, south–north, or down–up direction. The benefit of such a simplification is that computational resources can be devoted toward improving the temporal and/or spatial resolution but at a cost of providing a cruder representation of the atmospheric flow. Local atmospheric flow may be modeled poorly when making the assumptions required to use the primitive equations, particularly in disturbed weather.

Thermodynamic Energy Equation

The fourth of the seven basic equations is the **thermodynamic energy equation**. It expresses the sum of the **internal energy** of the individual molecules comprising the atmosphere and the *kinetic energy* that drives the synoptic- and planetary-scale motion (i.e., the wind). The internal energy is the “thermo” part of the term—temperature actually represents the internal energy present in matter. Kinetic energy is the “dynamic” part of the term.

The temperature in this and other equations is always represented using the *Kelvin temperature scale*.

The reason for this is that only in the Kelvin system is internal energy proportional to the temperature (i.e., doubling the Kelvin temperature of something means that the internal energy is doubled). This is not true in the Celsius or Fahrenheit scale—when the temperature increases from 10 to 20°C, the energy content of the air does not double. Likewise, 0 K—*absolute zero*—actually represents the situation in which zero internal energy exists and all molecular motion ceases, unlike the situation for 0°C or 0°F.

The “thermo” part of the equation can occur through either **diabatic** or *adiabatic* heating/cooling. Diabatic heating of the atmosphere at a gridpoint refers to heating with an energy change and comes from outside sources, such as insolation, *latent heat*, or *sensible heat* in the boundary layer. The diabatic heating changes each minute of the day, as the solar angle changes, cloud cover increases or decreases, and water changes phase. A small time step therefore is necessary to capture the changes in diabatic heating effectively.

As we saw previously, adiabatic heating/cooling—a process without an energy exchange—comes from expanding/contracting motion as an air parcel rises/sinks. In the case of heating (either diabatically, adiabatically, or some combination of the two), the internal energy of the molecules, and, therefore, the temperature, increases at the gridpoint. Likewise, cooling the atmosphere (either diabatically or adiabatically, or both) decreases molecular speed and decreases the internal energy component of the total thermodynamic energy.

The “dynamic” part of the equation occurs through advection of energy from elsewhere (different x , y , and z coordinates). These terms are reminiscent of those in the Navier-Stokes equations of motion. The complete thermodynamic energy equation can be expressed as shown in **EQUATION 13.4**. In this equation term 1 expresses the rate of change of temperature over time at a gridpoint. This is an important quantity because once we know how much temperature change exists at a point for some time step into the future we can then use that temperature to calculate the energy that exists to fuel further vertical and horizontal motion in the atmosphere even farther into the future. Term 2 represents a diabatic heating term, where q is the heat (or energy) added (in *Joules kg⁻¹*) and C_p is the **specific heat at constant pressure** for air (1005 J kg⁻¹ K⁻¹). The latter

EQUATION 13.4

$\frac{\partial T}{\partial t}$	$= \frac{1}{C_p} \frac{dq}{dt}$	$+ \frac{\alpha}{C_p} \frac{\partial p}{\partial t}$	$- u \frac{\partial T}{\partial x}$	$- v \frac{\partial T}{\partial y}$	$- w \frac{\partial T}{\partial z}$
1	2	3	4	5	6

quantity refers to the number of Joules of heat/energy that must be added to 1 kg of a substance (in this case, air) to raise its temperature by 1 C° (or 1 K). Heat is gained or lost continuously, as the solar angle changes or clouds move in front of the Sun at a point.

The third term represents the rate of temperature change due to adiabatic vertical motion, with α representing specific volume. The units of α are in $\text{m}^3 \text{kg}^{-1}$ (volume divided by mass). Pressure (p) has units of Pascals (Pa, which is force divided by area), and Newton's second law states that force can be expressed in units of mass times acceleration. Pressure, therefore, really has fundamental units of mass times acceleration divided by area, or $\text{kg m s}^{-2} \text{m}^{-2}$, or $\text{kg m}^{-1} \text{s}^{-2}$. This gives term 3 units of K s^{-1} . You can verify these units at the end of this chapter in the Questions for Thought section. The last three terms represent the advection of temperature in the west–east (x), south–north (y), and down–up (z) directions, respectively.

Moisture Conservation Equation

The fifth of the basic equations in all GCMs is the **moisture conservation equation**. Atmospheric moisture is usually represented by *specific humidity*, which is normally abbreviated as q , but here we use m because q is also usually used to represent the heat (energy) added in the thermodynamic energy equation. The moisture conservation equation states that the change in moisture content at a gridpoint is equal to the sum of the contribution of moisture via advection and the contribution via phase changes. One form is shown in **EQUATION 13.5**.

The first term is the temporal rate of change of moisture (represented by specific humidity). The second, third, and fourth terms represent the advection of specific humidity in the west–east, south–north, and down–up directions, respectively. Finally, term 5 denotes changes of moisture caused by phase changes, such as *evaporation*, which would add moisture to the air. Often, this term is difficult to quantify. When the physics governing certain processes (such as friction or phase changes) cannot be quantified easily, models sometimes represent such effects with **parameterizations**—statistically based “fudge factors” that are used when the precise equations to simulate the process are either unknown

or impossible to include because the input data are not available to solve those equations.

Continuity Equation

The **continuity equation**, sometimes known as the **mass conservation equation**, is another vital component of all GCMs and weather forecasting models. Total mass must be conserved (i.e., remain constant) in any model, because the *first law of thermodynamics* states that energy must be conserved. Because energy is related to matter according to Einstein's theory of relativity, mass must also be explained. The amount of mass entering any three-dimensional box centered on a gridpoint must be balanced by the amount of mass leaving adjacent boxes to enter the box. Likewise, the amount of mass leaving the imaginary box of interest must be balanced by mass entering adjacent boxes from it.

In the atmospheric sciences mass is an inconvenient variable to measure and monitor. When a “box” of the atmosphere is considered, volume becomes the variable of interest, because the atmosphere is a compressible fluid whose volume changes when mass changes. It is convenient to divide all quantities in an equation by mass. Notice that entities such as C_p tend to have units of mass in the denominator ($\text{J kg}^{-1} \text{K}^{-1}$), because the quantity has been divided by mass. In the continuity equation it is convenient to believe that the volume divided by the mass must be conserved. But volume divided by mass is simply the reciprocal of density. Thus, one form of the continuity equation states that the temporal rate of change of density in the atmosphere is produced by some combination of advection of more (or less) density from the west–east, south–north, and down–up direction and by **velocity convergence**—the pile-up of atmospheric density (or mass) from the west–east, south–north, and down–up directions.

To understand velocity convergence better, imagine the box of air in the atmosphere again, as shown in **FIGURE 13.3a**. If more air enters the box than leaves it from a particular direction, because the air flowing into the box is moving faster than the air leaving the box, velocity convergence is occurring. Even if advection does not bring in air of different density, if more air of the same density is approaching the gridpoint than is moving away from it, the density of the air in the box must increase.

Of course, it is also possible that more mass (or density) could be leaving the box than is entering (from one or more directions), even if advection is not changing the density of the air approaching the box. Such a situation is termed **velocity divergence** (**FIGURE 13.3b**). When velocity convergence or divergence occurs at a gridpoint, the extra (or reduced) mass (or

EQUATION 13.5

$$\begin{array}{cccccc} \frac{\partial m}{\partial t} & = & -u \frac{\partial m}{\partial x} & - & v \frac{\partial m}{\partial y} & - & w \frac{\partial m}{\partial z} & + & S \\ 1 & & 2 & & 3 & & 4 & & 5 \end{array}$$

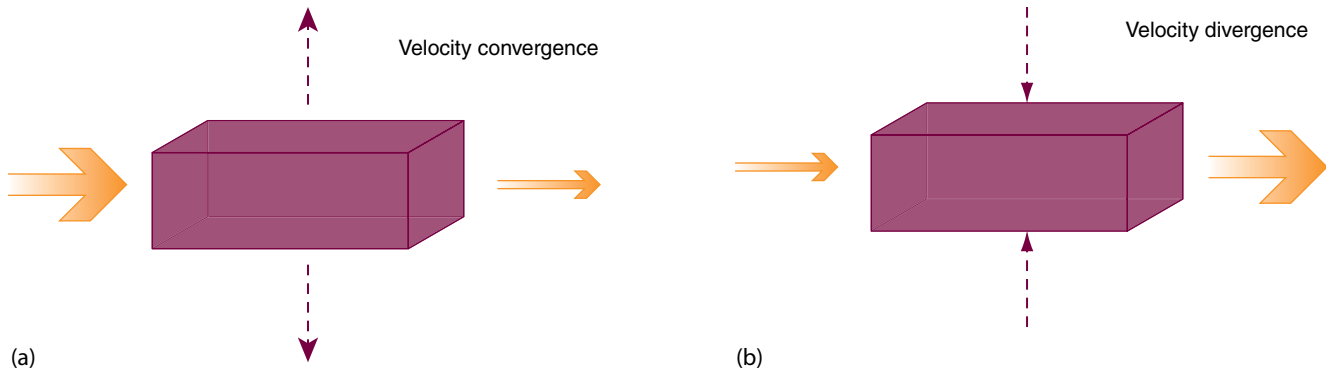


FIGURE 13.3 Velocity (a) convergence and (b) divergence.

EQUATION 13.6

$\frac{\partial \rho}{\partial t}$	$= -u \frac{\partial \rho}{\partial x}$	$- v \frac{\partial \rho}{\partial y}$	$- w \frac{\partial \rho}{\partial z}$	$- \rho \frac{\partial u}{\partial x}$	$- \rho \frac{\partial v}{\partial y}$	$- \rho \frac{\partial w}{\partial z}$
1	2	3	4	5	6	7

density) affects all of the first four equations (including the calculation of the rate of motion in the x -, y -, and z -directions and the rate of temperature change). This is because density is represented by its reciprocal, specific volume (α), in each of these equations. The extra mass also affects moisture conservation because specific humidity is a function of mass. As we are about to see, the extra mass also affects the final result of the other basic equations.

Quantitatively, the continuity equation can be expressed as shown in **EQUATION 13.6**, where the first term represents the rate of change of density from one time interval to the next. Terms 2 through 4 represent the advection of density in the west–east and south–north, and convection in the down–up directions, respectively. Terms 5 through 7 represent the velocity convergence/divergence in the same three directions.

In most analyses at synoptic (or larger) scales, the velocity convergence/divergence terms far exceed the advection terms. It is relatively unusual to find a situation in which air of significantly different density moves into a place from a broad area. But it is not so unusual to have air piling up or spreading out at a location. At *mesoscales* and local scales both the advection and the convergence/divergence components can be important. For example, when a strong frontal boundary is present, density advection becomes more important. In convective thunderstorms, local convergence/divergence as well as advection of air with great density differences—whether they occur between colder versus warmer, or wetter versus drier air—can create even greater effects of local convergence.

Equation of State

The final equation is also the simplest. It is the “glue” that binds the other equations because it relates pressure, density (or specific volume), and temperature. All of the previous six equations (except the moisture conservation equation) explicitly express either temperature, density, or pressure. Even the moisture conservation equation implicitly expresses these quantities in its parameterization of moisture transfer via phase changes. All three quantities, however, are represented separately in those equations despite the fact that they are all related to each other. The *equation of state*, also known as the *ideal gas law*, expresses the relationship between these three fundamental entities so that they can be used in the other equations.

As we saw previously, the equation of state for dry air is,

$$P \propto R_d T$$

where R_d is the dry gas constant ($287 \text{ J kg}^{-1} \text{ K}^{-1}$). In this equation pressure is expressed in Pascals and temperature is expressed in the Kelvin temperature scale to make the units cancel. When dealing with moist air (i.e., air with any water vapor in it), a few adjustments must be made. The pressure and density would then represent the sum of that due to dry air and that caused by water vapor. R_d must then be adjusted to take the moisture into account. This adjustment creates the **equation of state for moist air**, which is expressed as,

$$P \propto \frac{R_d \left(1 + \frac{r}{\epsilon} \right)}{1 + r} T$$

where r is the **mixing ratio**—a *dimensionless quantity* expressing the ratio of the mass of water vapor present in the air to the mass of dry air—and ϵ is the dimensionless ratio of the molecular weight of water vapor to the molecular weight of dry air (0.622). The mixing ratio is closely related to specific humidity (m) by,

$$m = \frac{r}{r + 1}$$

Furthermore, m itself is a dimensionless quantity that can be derived based on known quantities by using:

$$m = \frac{e\varepsilon}{p}$$

Vapor pressure (e) can be calculated from *dewpoint temperature* by using a variant of the *Clausius-Clapeyron equation*:

$$e = 611 \text{ Pa} \exp \left(\frac{L_v M_v}{R^*} \left(\frac{1}{273\text{K}} - \frac{1}{T_d} \right) \right)$$

where L_v is the latent heat of condensation ($2.5008 \times 10^6 \text{ J kg}^{-1}$), M_v is the molecular weight of water vapor ($0.018015 \text{ kg mol}^{-1}$), R^* is the universal gas constant ($8.314 \text{ J mol}^{-1} \text{ K}^{-1}$), and T_d is dewpoint temperature in Kelvins. It should be noted that over an ice surface, L_v is substituted by the latent heat of sublimation (L_s , or $2.8345 \times 10^6 \text{ J kg}^{-1}$ at 0°C).

The terms multiplied by R_d in the equation of state for moist air are sometimes lumped together to form a new quantity called **virtual temperature (T_v)**, where,

$$T_v = \left(\frac{1 + \frac{r}{\varepsilon}}{1 + r} \right) T$$

to give

$$P\alpha = R_d T_v$$

Virtual temperature is the temperature that dry air would have if its pressure and volume were equal to that of a sample of moist air. Because moist air adds pressure (i.e., vapor pressure) and pressure is directly proportional to temperature (according to the equations of state for dry and moist air), T_v cannot be less than T .

Similarities and Differences Between GCMs and Weather Forecasting Models

Weather forecasting models and GCMs are similar in many ways but different in others. Both types of models use the same general equations to simulate atmospheric motion and energy, moisture, and momentum exchanges, because the same physical processes affect the circulation of the atmosphere whether it is at “weather” or “climate” time scales. The most fundamental differences between GCMs and weather forecasting models involve the difference in temporal scale. Unlike a weather forecasting model,

a GCM would not attempt to project the temperature of a specific day, even if prediction of daily conditions could somehow be made accurately to the distant future. Similarly, because of the longer distance of the prediction, the time step in GCMs is generally longer than that for weather forecasting models. A typical time step on GCMs may range perhaps from half a day to a month, compared with only a few minutes for a weather forecasting model.

The importance of accuracy during **initialization**—the setting of initial conditions in a model in preparation for a forecast—is also somewhat relaxed in GCMs. Of course, some errors in initial conditions can magnify over time to create dubious model output. To understand this better, imagine an arrow that hits within a bullseye but is only slightly off from dead center at a target 25 m away. Although a bullseye occurred on a close target, the same arrow might be several centimeters away from the center of a target located 50 m away even when the archer aimed the arrow in the exact same manner. The same shot extended to a target located 100 m away may miss the target completely. This example demonstrates that even a tiny error embedded in a model magnifies in time (as did the arrow) to produce unrealistic results (i.e., miss the target completely). Meteorologist Edward Lorenz named this magnification of errors the **butterfly effect**, a theory based on the idea that a butterfly that flaps its wings in one part of the world could create a tiny perturbation that could cause a chain of magnified events that ultimately alters the planetary-scale atmospheric flow. This idea is at the core of **chaos theory**, which suggests an inherent lack of predictability (sometimes known as a **dynamic instability**) in some systems despite the fact that an order underlies them.

Another fundamental difference is the importance of representing interactions and feedbacks between the atmosphere and the lithosphere, hydrosphere, and biosphere. At meteorological time scales such influences are often negligible compared with other errors that result from erroneous input data, poor parameterization techniques, and/or poorly understood physical processes, but these interactions and feedbacks can be extremely important over longer time periods. For example, a weather forecasting model would not need to consider increased *desertification* in the *Sahel* in predicting differences between tomorrow’s weather and today’s in the United States; likewise, increased *deforestation* at distant locations by tomorrow would be inconsequential for weather prediction. If a GCM is to be run to simulate the climate in 2100, however, the effects of Sahelian desertification and deforestation between now and 2100 must be considered because over such long periods of time it is likely to influence global circulation.

Limitations of Model Results

Regardless of how elaborate a model is, how fine its resolution is, whether it is designed for weather or climate forecasting applications, and the extent to which it is physically based, statistically based, or some combination of the two, there are limitations on the conclusions that can be drawn from its output. First and foremost, it is important to remember that model output cannot be presumed to be accurate in all (or perhaps not even in most) cases. Like any other computer-based model, weather and climate models can be incorrect. Moreover, even the “agreement” of multiple forecasting models cannot be used as direct evidence for the accuracy of the forecasted weather or climate feature, because the models may share similar or the same components—particularly the seven basic equations. Users of model output must also remember that the spatial and temporal resolution output by a given model cannot be assumed to transfer to other spatial or temporal scales, especially if robust downscaling techniques have not been employed. Similarly, model output of one variable cannot be used as evidence for similar trends in other variables, even if those variables are closely related to each other. For example, if a model predicts warming by 3 C° over the next 100 years at a given place of interest, a researcher cannot use this result to conclude that a species that could have tolerated a 4 C° temperature increase will still be extant in that area in 100 years. This is because the model forecasted average temperature only, and changes in precipitation or other atmospheric variables, such as a greater temperature range, could have caused the species to die out. Furthermore, changing extreme climatic conditions (such as length of growing season, number of freeze events, etc.) could cause impacts that remain undetected by models that forecast average conditions only. In general, even though atmospheric models are among the most useful tool that atmospheric scientists can provide to policymakers and society, it is important that users are judicious and cautious in the interpretation of model results.

► Statistical Techniques

In addition to the mathematical methods in GCMs, climatologists use a number of statistical methodologies. Several of these are simple statistical methods that are used across the spectrum of natural and social sciences. These are not discussed here because they are addressed in introductory statistics textbooks. Modern climatic analysis includes other, more advanced statistical techniques that can be useful. For example, *eigenvector analysis* provides a useful suite of information because these techniques are the only ones that

allow for simultaneous examination of variability and changes in climate across space and time.

As we saw previously, it is useful to keep in mind that in climatological data sets, three entities are usually present: (1) atmospheric variables (such as temperature, precipitation, pressure), (2) spatial variables (e.g., weather stations), and (3) temporal variables (e.g., months since 1900). If any one of these three entities contains only one variable, eigenvector analysis can identify relationships between the other two sets of variables simultaneously. In analyses of synoptic circulation, only one atmospheric variable, *geopotential height* or sea level pressure, is usually necessary, because geopotential height or pressure gradients cause atmospheric motion in response to the height or pressure differences represented. Synoptic analysis can often use eigenvector techniques to identify spatiotemporal variability and change in one aspect of climate, such as 500-mb heights.

Although the nuances of the differences between each eigenvector technique listed below are not addressed here, the methods all share some common characteristics. A data set is assembled that contains variables representing the two varying entities under consideration (e.g., months from 1900 through 2010 along the rows and weather stations along the columns) for only one variable of the third entity (sea level pressure, for example). The eigenvector technique then uses matrix algebraic procedures to transform that matrix of data (in this case the weather stations vs. months) into two other matrices. The first of these matrices has the first entity's variables (in this example, the set of all weather stations in the study area) along the rows and the *loading* for each eigenvector along the columns. The first eigenvector explains the maximum amount of variance in the data set, and each loading on that eigenvector describes how strongly the particular observation (each weather station, in this example) is represented by that eigenvector. The total sum of the loadings for all eigenvectors must equal the number of observations (in this case, weather stations) and is termed the *eigenvalue*. So if the data set contains 27 weather stations, then the sum of the eigenvalues for each eigenvector must be 27. The first eigenvector always has the highest eigenvalue, the second has the second-highest eigenvalue, and so on.

If the variable in the loadings matrix is a spatial variable (as in this example), then the loadings for each *component* can be shown using isoline maps. These maps reveal the spatial component to the explained variance. In our example, a loadings map for the first component reveals the geographical areas where variability in sea level pressure is highest during the 1900–2010 period.

In addition to the loadings matrix, a second output matrix is produced. That matrix contains the second

entity's variables (in this example, all monthly weather observations) along the rows. Each variable has a *score* for each eigenvalue, which indicates the magnitude of the influence on the explained variability on that eigenvector (mapped by the loadings matrix) during each time unit of the time series. We can examine the trends over time for the scores in that eigenvector to determine whether the influence has increased or decreased temporally. Furthermore, scores for the eigenvectors, which represent a time series for a particular component, may be correlated against some other phenomenon's time series. This correlation could then be used to reach a conclusion about the relationship between the flow pattern represented by the mapped isolines of loadings for a given eigenvector and the environmental variable, such as dissolved oxygen content in Lake Champlain over time. Which atmospheric flow pattern is coincident with the most oxygenated water in Lake Champlain? Which is associated with the lowest?

Two main variants of eigenvector analysis have been used in climatological studies. The first is *principal components analysis*, which is also essentially the same as two techniques known as singular value decomposition and empirical orthogonal function analysis. A slight variant is **common factor analysis**. Although both techniques work on the same basic principles described above, the principal components analysis model has proved to be the favorite in most climatological applications. The reason is that the matrix transformations in principal components analysis assume no underlying uniqueness among the variables. In other words, nothing unique at weather station A makes station A's data differ from that at station B. Because all stations are influenced by the same Sun, with the same atmospheric composition, the same physical laws, and the same interactions with other "spheres," this assumption is reasonable. By contrast, the common factor analysis model tends to be preferred in social scientific research when dealing with human subjects, because it allows for some "unique" element to contribute to the data. For example, one person may have had a unique life experience that made her answers on a survey differ from the results that would be expected for another female in her peer group.

Eigenvector analysis, and particularly principal components analysis, has been used in *synoptic climatology* to delineate the major modes of variability in the atmospheric flow. This application is useful because atmospheric flow is known to be associated with a wide range of other variables. Because flow patterns are represented by the geographical distribution of geopotential height or pressure, the mapped loadings reveal the locations where geopotential height (or pressure) varies the most. And when the scores matrix is compared with some other environmental impact,

we get a picture of where and when the pressure (and, therefore, the circulation) feature is occurring, and an assessment of the impact of that circulation feature on the environmental problem of interest.

► Atmospheric Teleconnections

Collectively, results of eigenvector-based studies (and other studies that were not based on eigenvector analysis) identified the major **atmospheric teleconnections**—the correlations or "seesaws" in geopotential height or sea-level pressure patterns across a large area. Because the total atmospheric mass is conserved, increases in one location (i.e., higher pressure) must be compensated elsewhere by equal decreases in mass (i.e., lower pressure). Geopotential height or pressure anomalies in certain geographical locations tend to act in tandem—when geopotential height or pressure is abnormally high in one location, it is abnormally low simultaneously in the other, teleconnected location. The seesaw or set of *action centers* is the teleconnection, and the teleconnection can be a source of important regional- to planetary-scale climate impacts. It is, therefore, important to identify these teleconnections. Because the three important tropical climatological phenomena—the *Indian Ocean Dipole*, *Southern Oscillation* (SO), *Madden-Julian Oscillation*, and *Quasi-biennial Oscillation*—were discussed elsewhere in the text for their role in shaping low-latitude climates, we consider only extratropical teleconnections here.

Extratropical Teleconnections in the Pacific: The Pacific Decadal Oscillation

In 1996 fisheries scientist Steven Hare and other scientists, including Nathan Mantua, noticed a climatic oscillation that seemed to be associated with periods of productive and nonproductive years in the Alaskan salmon industry. This discovery led to the description of the *Pacific Decadal Oscillation* (PDO). Like the *El Niño* phase of the SO (FIGURE 13.4), the "positive" or "warm" phase of the PDO is characterized by a periodic warming of the tropical central and eastern Pacific Ocean (FIGURE 13.5a). This warming tends to propagate northward along coastal North America, weakening the cold *California current*, but unlike the SO this warming accompanies abnormally low sea surface temperatures in the north central Pacific Ocean, in the vicinity of the *Aleutian low*. During this "positive" or "warm" phase of the PDO, westerly winds on the southern end of the Aleutian low are stronger than usual (Figure 13.5a).

During the "negative" or "cool" phase of the PDO the opposite conditions occur (FIGURE 13.5b). Waters in

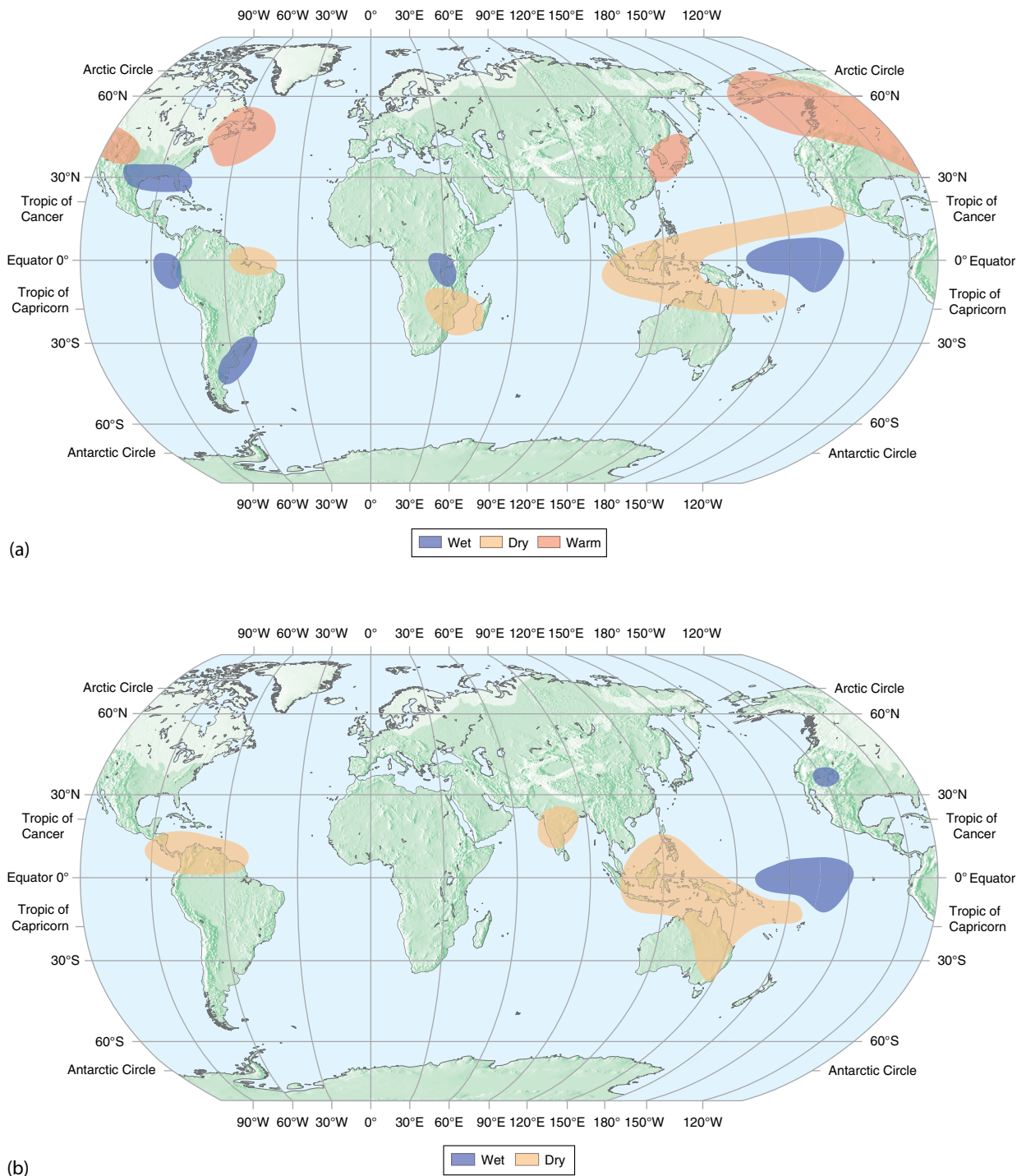


FIGURE 13.4 Impacts of El Niño phase of the Southern Oscillation in (a) January and (b) July.

Modified from *Global Consequences of El Niño: Impacts of El Niño and Benefits of El Niño Prediction*. El Niño Theme Page, NOAA, <http://www.pmel.noaa.gov/tao/elnino/impacts.html>.

the tropical central and eastern Pacific are anomalously cold (as in the *La Niña* phase of the SO), and these cold waters tend to propagate poleward along the west coast of the Americas, leaving the cold currents even colder than usual. At the same time, warm waters tend to exist in the northern central and western Pacific Ocean, and the Aleutian low is weakened.

The PDO, then, is similar to the SO, but with two major exceptions. First, the primary “signature” of the

PDO is apparent not only in the tropical Pacific but also in the extratropical North Pacific Ocean. Second, the PDO fluctuates much more slowly than the SO. A PDO regime may last 20 to 30 years, during which one phase of the oscillation tends to dominate, whereas the SO fluctuates back and forth over periods of 3 to 7 years. During times when the SO and the PDO both favor the same conditions (i.e., a “warm phase” or a “cold phase” in the central and eastern tropical Pacific), the

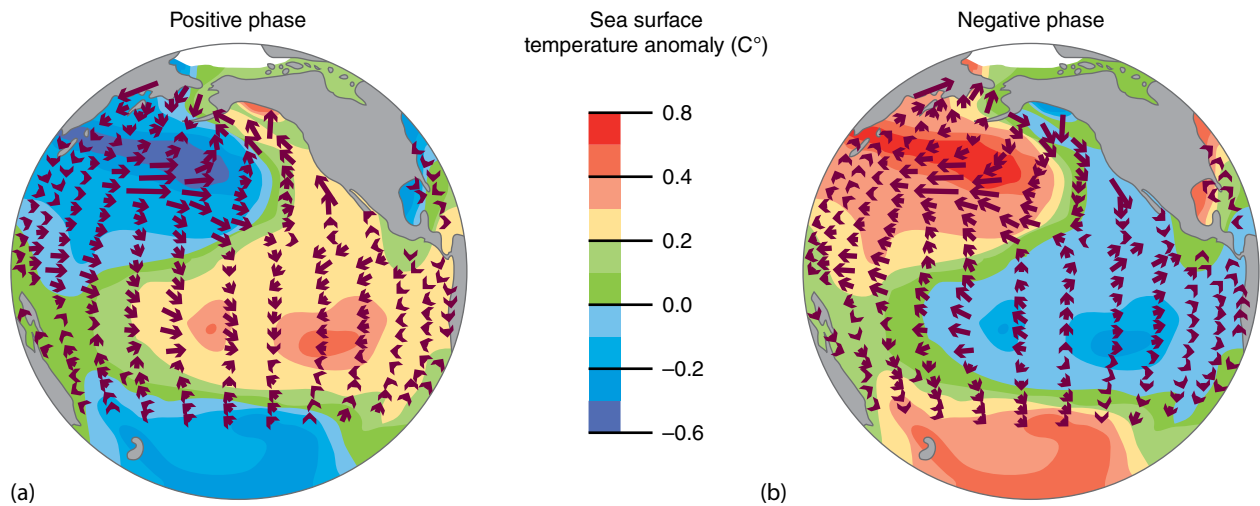


FIGURE 13.5 Comparison of sea surface temperature anomalies during the (a) positive and (b) negative phases of the Pacific Decadal Oscillation. Wind vectors show the surface wind anomalies.

Modified from Nathan Mantua at the University of Washington's Joint Institute for the Study of the Atmosphere and Oceans.

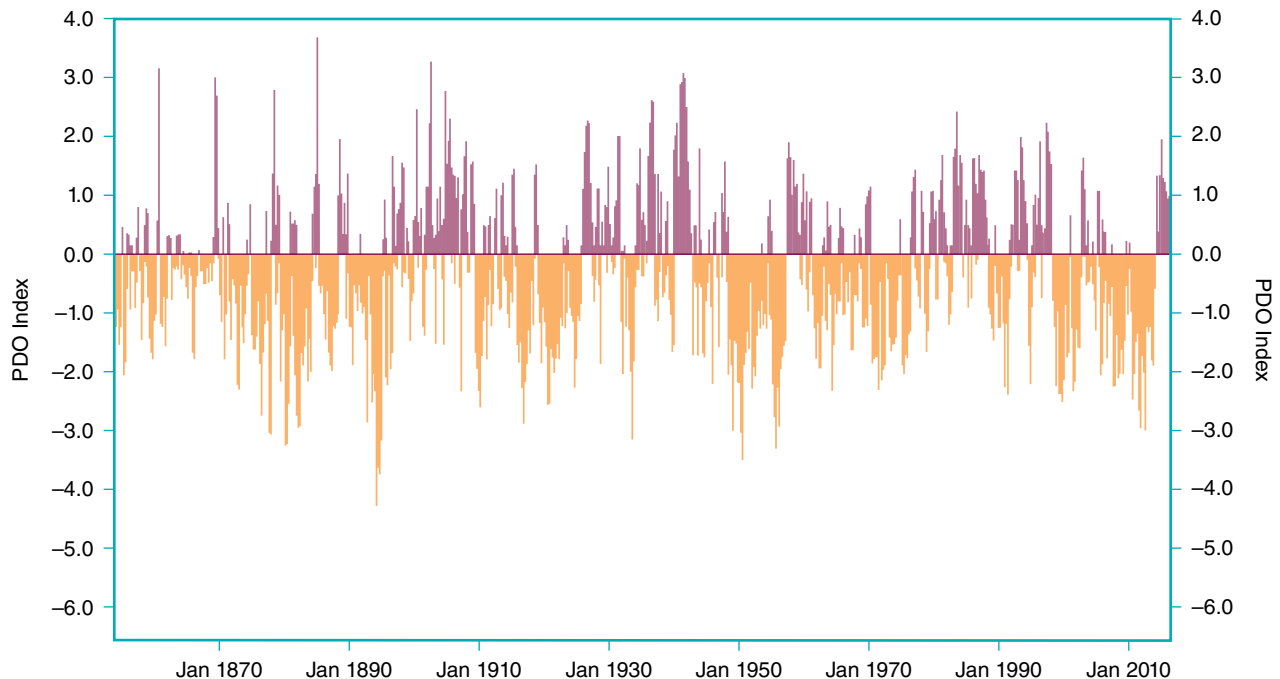


FIGURE 13.6 Time series of the monthly Pacific Decadal Oscillation (PDO) Index.

Courtesy of National Climatic Data Center/NESDIS/NOAA.

impacts tend to be magnified. When one of these Pacific teleconnections is in the “warm” phase and the other is in the “cold” phase, the effects tend to be dampened.

The PDO has undergone a few major “regime shifts” over the last 120 years (**FIGURE 13.6**). From 1925 to about 1946 warm-phase conditions were prevalent. Cold-phase conditions dominated from 1947 until 1976, when the warm phase reemerged. The period since 1999 is somewhat uncertain, as both warm- and cold-phase conditions have shown some signs of dominance, but since 2008 the cold phase seems to be in place. Recent

research suggests that the PDO may be a 20th- and 21st-century phenomenon.

Extratropical Teleconnections in the Atlantic Ocean

Atlantic Multidecadal Oscillation

A phenomenon related to the PDO exists in the North Atlantic Ocean basin. The **Atlantic Multidecadal Oscillation (AMO)** refers to a cycling of warm and cold surface waters over time scales ranging from about 15

to 30 years. But the Atlantic Ocean is not large enough to develop a seesaw pattern in sea surface temperatures as well as in the Pacific. Variations in the AMO impact climate in various ways. For example, the AMO is largely responsible for the cyclical nature of *tropical cyclone* frequency and intensity in the basin. Currently, the AMO is in a warm phase, and the associated high sea surface temperatures contributed to the unprecedented (at least in the instrumental period of record) characteristics of the 2005 Atlantic hurricane season when a record number of tropical cyclones occurred. Additionally, intensities were anomalously high for many of the 2005 storms, particularly Hurricanes Katrina, Rita, and Wilma. Although some point to global warming factors as the cause of the 2005 Atlantic hurricane season, the fact that some of the more recent North Atlantic hurricane seasons were relatively quiet indicates that many factors combine to determine hurricane frequencies and associated intensities.

North Atlantic Oscillation

In addition to the AMO, two teleconnections in the Atlantic Ocean cause well-known impacts on weather and climate in North America and Europe. Of these, the first to be identified was the **North Atlantic Oscillation (NAO)**, a seesaw in pressure patterns between the *Bermuda-Azores high* and the *Icelandic low*. At times the sea level pressure associated with the Bermuda-Azores high is even higher than usual, while at the same time the central pressures of the Icelandic low are even lower than usual. This scenario is called the positive phase of the NAO.

During the NAO's positive phase, the pressure gradient from south to north across the midlatitude North Atlantic Ocean is strong. Because the Bermuda-Azores high is a warm-cored high and the Icelandic low is a cold-cored low, the pressure features associated with these two systems persist vertically in the atmosphere to great heights (FIGURE 13.7). Upper-level latitudinal pressure gradients across the midlatitude North Atlantic Ocean are also strong during the positive phase of the NAO. This causes strong zonal geostrophic winds and strong westerlies across the Atlantic.

At other times the seesaw is “tilted” in the opposite direction. During these periods the Bermuda-Azores high has central pressures that are not as high as usual, while simultaneously the low pressure associated with the Icelandic low is not as low as usual. This scenario is termed the negative NAO pattern. During times of a negative NAO the westerly circulation across the midlatitude North Atlantic Ocean is weak, with *ridges* and *troughs* more likely to appear (in a *meridional flow* pattern). Unlike the SO no rhythmic pattern in the

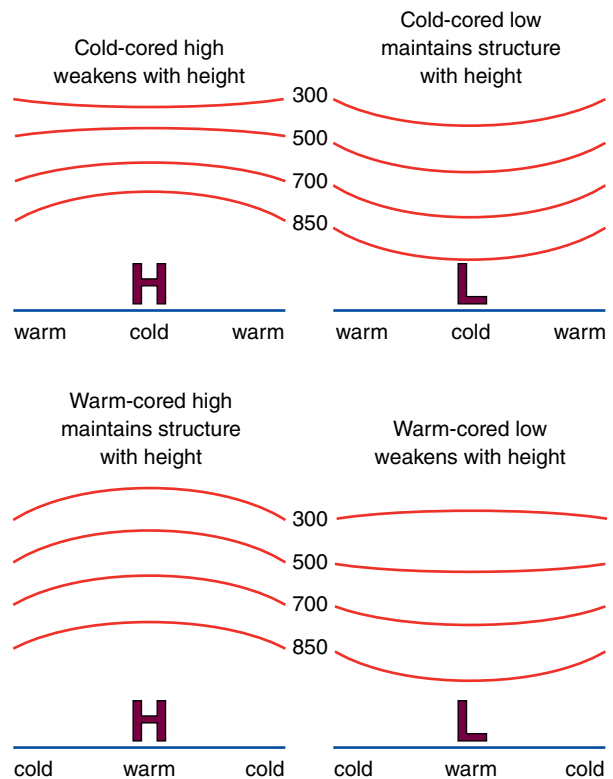


FIGURE 13.7 Vertical structure of cold-cored anticyclones, cold-cored cyclones, warm-cored anticyclones, and warm-cored cyclones. The surface pressure values work with the thermal structure of the surface. A high-pressure area at the surface will appear as a “dome” in the constant pressure field above it, while a low-pressure system will appear as a “bowl” in the constant pressure field above it. However, the thermal structure may eventually overcome this near-surface pressure pattern. Warm-cored systems cause the pressure level to bulge upward and cold-cored systems cause the pressure height to be deflected downward, in fulfillment of the hydrostatic equation. The result is the pressure pattern shown here for the various pressure/thermal combinations.

duration of positive and negative NAO patterns has been observed.

One of the first to observe the NAO was Sir Gilbert Walker, the namesake of the *Walker circulation*—the atmospheric flow associated with the SO. Walker noticed that during times when Iceland was warmer than normal, Greenland tended to be colder than normal, and vice versa. We now know that these observations were caused by the strengthening and weakening of the Icelandic low (FIGURE 13.8). A strong Icelandic low (positive NAO) would advect warm air and near-surface water toward Iceland at the same time that polar air and water were being pulled toward the east coast of Greenland. Some have wondered whether the settlement of “Greenland” may have occurred during a

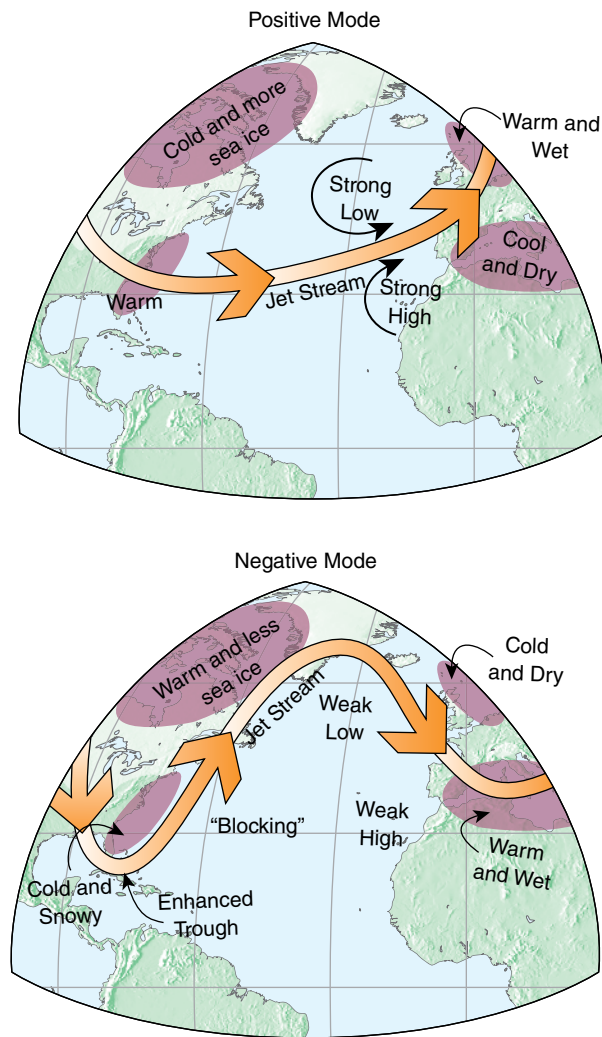


FIGURE 13.8 The North Atlantic Oscillation.

negative NAO period. Such conditions would have been associated with a relatively weak Icelandic low, which would have allowed warmer-than-normal conditions to persist over Greenland while below-normal air and water temperatures affected Iceland (Figure 13.8).

The impacts of the NAO are strong, particularly in winter, for Europe and the Mediterranean Basin. Positive NAO winters usually bring dry conditions to southern Europe and mild, wet conditions to northern Europe, coincident with the primary storm track. Some impacts are also felt in eastern North America. For example, positive NAO winters are usually mild and wet in New England with relatively warm waters in the adjacent Atlantic Ocean, as the strengthened westerlies discourage the southward movement of bitter cold air toward the region and tropical moisture can penetrate farther north than usual. By contrast, negative NAO winters usually see more *continental polar* (cP) air masses with less precipitation over eastern North America and northern Europe, as the ridge-to-trough sides of the

Rossby waves tend to spill cold air southward. Atlantic waters are generally colder than normal in the Atlantic Ocean adjacent to North America during these times.

Arctic Oscillation (Northern Annular Mode)

In 1998 meteorologists David Thompson and John Wallace used eigenvector analysis to reveal the presence of a NAO-like oscillation in which the seesaw in pressure exists throughout most of the troposphere between the north polar region and the midlatitudes. The NAO is considered by some to be the regional expression of this hemispheric-scale phenomenon termed the **Arctic Oscillation (AO)** or the **Northern Annular mode**, as it is sometimes known. In one phase (the “warm” or “positive” phase), the AO is characterized by lower-than-normal pressure in the polar region and above-normal pressure around 45°N. This results in a strengthening and “tightening” of the *circumpolar vortex*. By contrast, the opposite phase (the “cold” or “negative” phase) of the seesaw is associated with relatively high pressure at the North Pole and relatively low pressure at the midlatitudes. This results in a weakening of the circumpolar vortex.

The “warmth” in the positive phase results from the weakened surface pressure gradients that allow relatively warm water from the subtropical oceans to propagate northward. At the same time, relatively strong polar westerly winds exist aloft in the “warm” phase because the lower pressure at the poles drives a strong pressure gradient aloft over the *polar cell* (where surface *polar easterlies* occur). These strong upper-level polar westerlies tend to prevent air masses of Arctic origin from penetrating far to the south. As a result, conditions in midlatitude North America and Eurasia tend to be warmer than normal when the AO is in its positive phase. Storm tracks are usually farther north than normal because the region where cold air and warm air meet retreats poleward. Subtropical locations then tend to be warmer and drier than normal, and the *trade winds* blow over a larger region and are often strengthened, without as much nearby influence of midlatitude circulation features.

In the “cold” or “negative” phase of the AO, different conditions prevail. The abnormally high sea level pressure at the pole causes an expansion of the circumpolar vortex, which tends to push the warm water away from polar regions. At the same time, the relatively high geopotential heights aloft over the pole act to weaken the normal westerlies aloft over the polar easterlies. This is because high pressure exists to the right of the flow in the northern hemisphere, thereby working against the normal westerly circulation aloft in the polar cell. With

the weaker westerlies aloft and an expanded circumpolar vortex, Arctic air can spill southward relatively easily. This results in colder-than-normal conditions in midlatitude North America and Eurasia and storm tracks that are displaced southward. Subtropical locations tend to be cooler and wetter than normal, and the tropical trade winds are weakened as midlatitude circulation features are displaced anomalously equatorward.

The AO moves from a dominant positive phase to a dominant negative phase and back again over long time periods. The periodicity is far longer than the fluctuations associated with the NAO. Therefore, some have considered the relationship between the NAO and the AO to be similar to that between the SO and the PDO in that the two teleconnection pairs show similar behavior but operate on different time scales. It has been said that Adolph Hitler decided to invade Russia in 1941 because he did not believe Russia could experience a third consecutive bitterly cold winter, thereby ensuring that his army could continue the invasion successfully through the winter. As it turned out, the onset of a period of cold-phase dominance of the AO caused a miscalculation in Hitler's thinking. The cold phase also dominated the 1960s and 1970s, whereas the 1980s and 1990s saw mostly warm-phase conditions. Some recent signs point to the return of cold-phase conditions, but it is too early to tell whether a true phase change has occurred.

Teleconnections over North America

Pacific-North American Pattern

The **Pacific-North American (PNA) pattern** has regional importance for North American weather and climate. This teleconnection represents the oscillation between geopotential height in the midtroposphere of northwestern North America, with opposing heights upwind in the northern Pacific and downwind in the southeastern United States. The PNA index is positive when the midtropospheric ridge is amplified over western North America and a concurrent trough is amplified over the eastern United States (**FIGURE 13.9**). Likewise, the PNA pattern is said to be in its negative mode when the ridge–trough pair over midlatitude North America is deamplified (**zonal flow**), or even inverted, with a trough over western North America and a ridge over the east. The PNA pattern describes the condition of the Rossby wave flow across midlatitude North America.

The PNA pattern is known to exert a major impact on atmospheric variability in the United States. In its positive mode the southeastern United States tends to be colder than normal because it lies on the poleward side of the *polar front jet stream*, which dips southward in the trough situated over the eastern United States.



FIGURE 13.9 The Pacific-North American teleconnection pattern.

Source: Vega, A. J. (1994). *The Influence of Regional Scale Circulation on Precipitation Variability in the Southern United States*. A dissertation submitted to the Faculty of Louisiana State University, Department of Geography and Anthropology, 300 pp.

Simultaneously, the northwestern states are warmer than normal, and they lie south of the polar front wave train, beneath the ridge. In the negative mode the Northwest is colder than normal, whereas the Southeast is relatively warm. The PNA pattern is also associated with a more complicated, but still distinguishable, set of precipitation conditions across the United States. For example, the Ohio Valley often experiences wetter-than-normal conditions during negative PNA periods, particularly in winter and spring, as midlatitude storms form and track along the nearby cold–warm boundary.

Summary

Contemporary climatology is quantitative and analytical, and the current trend is toward an increasing emphasis on quantitative and analytical methods. Aside from basic statistical techniques that have become commonplace across the natural and social sciences, two broad families of quantitative techniques can be recognized in climatology. The first involves mathematical methods that are used in numerical models of atmospheric behavior. Some of these models may be simple, but they may serve their purpose adequately. Other numerical models are inherently more complex because they are designed to simulate and predict atmospheric dynamics and thermodynamics at the planetary scale. These general circulation models are the most sophisticated tools available to predict atmospheric motion at climatological time scales. They may be designed to simulate atmospheric or oceanic motion exclusively,

or they may be “coupled” to incorporate exchanges of energy, matter, and momentum between the atmosphere and the ocean, land, and ice surface that may be important at climatological time scales. Output from GCMs can be used as input to a more focused analysis of a particular region through either further dynamical modeling or a downscaling of the results. The input data are projected to a grid, and the GCMs may run by making calculations at each gridpoint and basing forecasts on the conditions at adjacent gridpoints. These models are relying increasingly on spectral techniques in which atmospheric motion is represented as a series of sinusoidal waves rather than through exclusive use of gridpoint representations. Several research groups around the world have developed and are continually updating GCMs to make use of increasing computational power, better surface observations, and improvements in our understanding of the physics behind the processes influencing the atmosphere.

GCMs are similar to weather forecasting models in that they contain seven basic equations governing

atmospheric behavior: the three Navier-Stokes equations of motion, the thermodynamic energy equation, the moisture conservation equation, the continuity equation, and the equation of state. GCMs differ from weather forecasting models in that a longer time step is used for each successive projection, initial conditions are less important, and representation of interactions and feedbacks between the atmosphere and the hydrosphere, lithosphere, cryosphere, and biosphere is emphasized.

Statistical methods also have been used extensively in climatology to provide information about both spatial and temporal variability in climates simultaneously. In this regard eigenvector techniques have been especially useful. Such techniques have revealed various atmospheric teleconnection patterns that exert a significant influence on a wide array of atmospheric and environmental features at time scales from weeks to decades. These teleconnections include the Southern Oscillation, Madden-Julian Oscillation, Pacific Decadal Oscillation, North Atlantic Oscillation, Arctic Oscillation, and Pacific-North American pattern.

Key Terms

Absolute zero
Action center
Adaptation
Adiabatic
Advection
Albedo
Aleutian low
Analog forecasting
Anthropogenic
Arctic Oscillation (AO)
Atlantic Multidecadal Oscillation (AMO)
Atmospheric general circulation model
Atmospheric teleconnections
Bermuda-Azores high
Biosphere
Butterfly effect
California current
Carbon cycle
Chaos theory
Circumpolar vortex
Clausius-Clapeyron equation
Common factor analysis
Component
Continental polar (cP) air mass
Continuity equation

Convection
Coriolis effect
Coriolis parameter
Coupled atmosphere-ocean general circulation model
Cryosphere
Deforestation
Density
Desertification
Dewpoint temperature
Diabatic
Dimensionless quantity
Downscaling
Dynamic downscaling
Dynamic instability
Eccentricity
Eigenvalue
Eigenvector analysis
El Niño
Energy balance model
Equation of state
Equation of state for moist air
Evaporation
Finite differencing
First law of thermodynamics
Friction
General circulation model (GCM)

Geopotential height
Gridpoint model
Hydrosphere
Hydrostatic equation
Icelandic low
Ideal gas law
Indian Ocean Dipole
Initialization
Insolation
Internal energy
Iterative
Joule
Kelvin temperature scale
Kinetic energy
La Niña
Latent heat
Latitude
Lithosphere
Loading
Local-scale
Longitude
Madden-Julian Oscillation
Mass conservation equation
Meridional flow
Mesoscale
Milankovitch cycle
Mitigation

Mixing ratio	<i>Pressure</i>	Spectral model
Moisture conservation equation	<i>Pressure gradient force</i>	<i>Statistical downscaling</i>
<i>Momentum</i>	<i>Prevention</i>	<i>Surface water balance</i>
National Center for Atmospheric Research (NCAR)	Primitive equations of motion	Swamp model
<i>Navier-Stokes equations of motion</i>	<i>Principal components analysis</i>	<i>Synoptic climatology</i>
<i>Newton's second law</i>	<i>Quasi-biennial Oscillation</i>	<i>Synoptic scale</i>
North Atlantic Oscillation (NAO)	Regional climate model (RCM)	Temporal downscaling
Northern Annular mode	Resolution	Temporal resolution
Oceanic general circulation model	<i>Ridge</i>	Thermodynamic energy equation
<i>Pacific Decadal Oscillation (PDO)</i>	<i>Rosby wave</i>	Time step
Pacific-North American (PNA) pattern	<i>Sahel</i>	<i>Trade winds</i>
Parameterization	<i>Score</i>	<i>Tropical cyclone</i>
<i>Pascal</i>	<i>Sensible heat</i>	<i>Trough</i>
<i>Planetary scale</i>	Slab model	Velocity convergence
<i>Polar cell</i>	<i>Southern Oscillation</i>	Velocity divergence
<i>Polar easterlies</i>	Spatial downscaling	Virtual temperature (T_v)
<i>Polar front jet stream</i>	Spatial resolution	<i>Walker circulation</i>
	Specific heat at constant pressure	Weather Research and Forecasting (WRF) model
	<i>Specific humidity</i>	Zonal flow
	Specific volume	

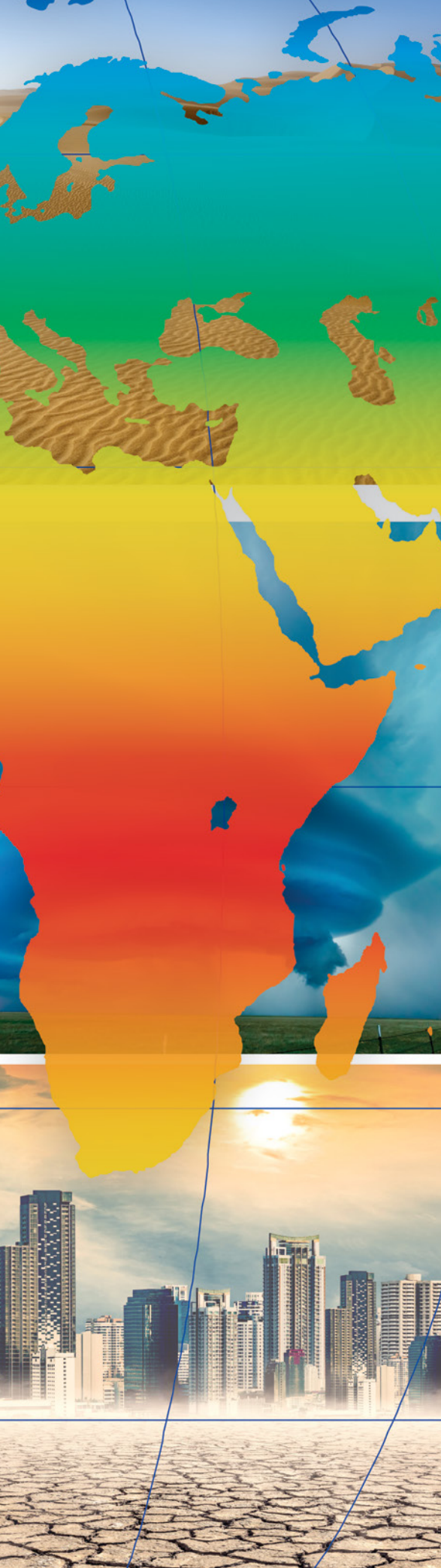
Terms in italics have appeared in at least one previous chapter.

Review Questions

1. What are the advantages and disadvantages of increasing the spatial and temporal resolution in a GCM?
2. What is a “coupled” GCM?
3. Why is downscaling sometimes necessary when evaluating GCM output?
4. What is the main advantage of a spectral model over a gridpoint model?
5. What are the primitive equations of motion and what is their purpose?
6. What two kinds of energy are represented as components of the thermodynamic energy equation?
7. What is the difference between diabatic and adiabatic heating?
8. What is the purpose of the continuity equation?
9. What is virtual temperature?
10. Are initial conditions more important in weather forecasting models or in GCMs? Why?
11. What is the primary advantage of using eigenvector techniques to identify climatic patterns?
12. Why is principal components analysis generally preferred over common factor analysis in climatological studies?
13. Compare and contrast the Pacific Decadal Oscillation and the Southern Oscillation.
14. What impact does the Pacific-North American teleconnection have on North American climate?

Questions for Thought

1. Verify that the units cancel to the appropriate units in each of the seven basic equations that appear in all GCMs.
2. Why are numerical models of atmospheric motion sometimes inaccurate even though the equations representing the atmospheric dynamics and thermodynamics involved are known?
3. Find and use some form of climatic data (such as temperature) for a town, along with teleconnection indices posted online, to examine the influence of one of the teleconnections described in this chapter on the local climate.



PART 5

Relationships Between Climate and Other Endeavors

CHAPTER 14 Applied Climatology, Climate Impacts, and Climatic Data

- Climate Impacts
- Climatological Data Sources
- Summary
- Key Terms
- Review Questions
- Questions for Thought

CHAPTER 15 Future of Climatology

- Relationship Between Climatology and Meteorology
- Interdisciplinary Work with Other Scientists
- Interaction Between Climate Scientists and Nonscientific Professionals
- Improved Atmospheric Data Availability and Display
- Climatology as Part of the Ultimate Goal of Sustainability
- Summary
- Key Terms
- Review Questions
- Questions for Thought





CHAPTER 14

Applied Climatology, Climate Impacts, and Climatic Data

CHAPTER AT A GLANCE

- Climate Impacts
 - Impacts on Natural Systems
 - Impacts on Societal Systems
 - Impacts on Human Health and Comfort
 - Climate Vulnerability, Adaptability, and Resilience
- Climatological Data Sources
 - Data Collection Agencies
 - Primary Versus Secondary Data
 - Secondary Data Sources for Applied Synoptic and Dynamic Climatological Studies
 - Secondary Sources for Applied Studies of the Climate System
 - Secondary Sources Well Suited to Studies in Paleoclimatology and Climate Change
 - Secondary Sources Well Suited to Studies in Physical Climatology
- Summary
- Key Terms
- Review Questions
- Questions for Thought

In each of the previous chapters, climatology has been discussed from a “process” approach. Emphasis was placed on the factors that cause climates to be the way they are, from the *microscale* to the *planetary* scale. The first chapters concentrated on the processes themselves. Then the spatial distributions of climates resulting from those processes were described, and temporal variability and changes in the climates resulting

from those factors were reviewed. Finally, analytical and quantitative methods of identifying patterns resulting from those processes were presented.

This chapter takes a completely different perspective. It examines the *effects* of climate rather than the *causes*. For example, imagine that a 5-cm (2-in) rainstorm occurred over a 3-hour period. A hydroclimatologist or a synoptic, dynamic, or tropical climatologist may be

concerned with the atmospheric conditions that caused the event to occur. However, it is also perfectly legitimate to wonder not why the event occurred, but why it is important and determine its impact. How often do events of such magnitude occur at this location within a 3-hour period at this time of year? What impact did the event have on the local corn crop?

Applied climatology is the study of the effects of climate on natural and social systems. These effects range from the direct to the indirect. Both numerical and statistical models can be used to estimate these effects. Output from climate models can undergo *downscaling* to provide more localized estimates of the modeled conditions. The model output can then be used to plan and prepare accordingly for impacts in various sectors of society.

A different approach to the assessment of impacts is to examine the relationship between “actual” past atmospheric conditions and observed features of the natural or social systems that climate is believed to impact. According to this *empirical approach*, climatic data are used to uncover historical trends. The scope of applied climatology, then, includes the impacts and applications of atmospheric data (either modeled or measured) to address practical research questions that fall outside of the atmospheric sciences.

The applied climatologist may also use these data to estimate atmospheric conditions at some specific time of interest in the past. For example, a legal consultant may need to know whether the Sun was positioned in the line of sight of a traffic light at the time of a traffic accident. An entomologist may want to determine whether atmospheric conditions may have played a role in the migration of a certain insect pest during a period of time. An engineer may be interested in the frequency that 5 cm (2 in) of precipitation falls within a 3-hour period at a location, because a culvert may need to be designed to withstand frequent flooding. An architect may need to know the weight of snow that can be expected to accumulate on a roof, so that it may be designed accordingly. A technician working with a scientific instrument may need to know the atmospheric pressure at a certain location and time so that a sensitive piece of equipment can be calibrated accurately. A farmer may want to understand the climatological *surface water balance* in a location before deciding whether to plant a certain crop that may need to be irrigated. These are just a few of the many types of questions that applied climatologists address.

In some cases data sources are available to answer the question at hand, but a more likely scenario is that no formal data exist for the place and time necessary. In such cases the applied climatologist must act as a

detective by trying to determine the most likely conditions at the time of interest. Sometimes this detective work may involve the spatial interpolation of data at nearby (or sometimes not-so-nearby) places, when the location of interest does not have a weather station. At other times a nearby station may exist, but it may not measure the variable that is needed, which means that the applied climatologist may need to make an educated guess based on the data that are available. Finally, in some cases the variable of interest is measured at a nearby site, but the data may be missing on a day or on a series of days. In that case the applied climatologist may estimate the values on the days with missing observations. In short, the applied climatologist must be able to supply the most appropriate data, or at least provide reliable estimates when “actual” data do not exist. Applied climatologists are often called to give expert testimony in court, both to provide their best assessment of the atmospheric conditions at the time of interest and to comment on the reliability of the data upon which their opinions are based.

This chapter begins by presenting specific examples of the impacts of climate on various components of the natural environment and sectors of the economy. It then examines some sources of climatological data for use in applied climatological problems and discusses some of the applications and limitations of certain types of data.

► Climate Impacts

Few entities affect the array of natural and social systems to the extent that climate does. **Primary climate impacts** are natural or social systems affected most directly by climate, and **secondary climate impacts** are those affected only indirectly. In reality, some effects fall somewhere between primary and secondary, but for simplicity we consider all impacts to be either “primary” or “secondary.” Both types of impacts occur in natural and human systems.

Impacts on Natural Systems

Processes in the atmosphere are inherently tied to those in the *cryosphere*, *hydrosphere*, *biosphere*, and *lithosphere*. These systems influence the climate system, which is also impacted by processes occurring in all the other “spheres” through many interrelated feedback loops. Despite continual interaction between the “spheres,” climate may be appropriately considered to be the most overriding influence on the natural environment.

Perhaps the most direct impact of climate is felt in the cryosphere. Snow- and ice-covered surfaces reflect as much as 90% of the *shortwave radiation* incident upon

them. Relatively modest changes in polar temperatures can, therefore, melt ice or freeze water. As was discussed previously, these changes alter *albedo*. The changes, however, tend to magnify over time, because small increases in albedo make further cooling more likely, as more snow and ice can exist in the reinforced cooler conditions. Slight increases in temperature likewise melt an amount of the cryosphere, which decreases polar albedo and allows further warming to take place as the snow and ice are replaced by darker surfaces. These changes—known as the *Arctic amplification*—represent a *positive feedback system* because relatively small impacts magnify over time.

In the hydrosphere, temperature and precipitation directly affect the amount, seasonality, and distribution of water available at the surface—the surface water balance. Changes to the global climate system inherently affect water on Earth's surface because *evapotranspiration* is the only variable that appears in both the energy balance and the water balance equations. Changes in energy input at the surface, therefore, inherently change the water balance. These primary impacts of climate cause direct impacts in human systems, such as agriculture, fisheries, recreation, and environmental planning.

The hydrosphere is also affected by increases or decreases in salinity resulting from changes to the input of fresh water at the surface. These salinity changes can then affect the biosphere directly by impacting fisheries, coastal vegetation, and coastal and marine ecosystem productivity. In addition, changes to the atmosphere impact the deep-water circulation in the oceans by altering the conveyor belt that is part of the *thermohaline circulation* described elsewhere in the text.

Within the biosphere, climatological impacts are felt in numerous other ways. Effects of predator–prey relationships, disease and insect infestations, and ecosystem stability are inherently tied to climatic conditions. Magnitude and timing of precipitation affect all these ecological features, winds affect pollen distribution and dispersal, and solar radiation relates to rates of *photosynthesis* and ecosystem productivity.

Climatological impacts are felt directly in the lithosphere. The field of climatic geomorphology is emerging as an important and interesting area of research inquiry. Most notably the field investigates how temperature and moisture affect rates of weathering, soil formation, and subsurface freeze–thaw. Precipitation events, glaciers, and winds also shape landforms, and coastal landforms are shaped by both acute events such as individual storms and the chronic process of everyday weather phenomena. And at both short and long time scales, volcanic activity causes feedbacks on climate. These regions are likely topics of climatic geomorphology research.

Impacts on Societal Systems

Climate affects some societal systems in a primary manner and others to a secondary extent. The most direct impact may be on agriculture. The intensity, magnitude, duration, and timing of precipitation; the length of time between the last spring frost and the first autumn frost (the **growing season**); the severity of storms; and temperature all impact agriculture directly. These factors affect agricultural commodities and futures, and many commodities brokerage firms provide advice and assess weather-related risk for the agricultural sector.

Climate also affects many forms of recreation. The ski industry, for example, relies on subfreezing temperatures and snowfall. In many cases perception of climate is as important as the climate itself. For example, during active periods of *hurricane* activity, tourist activity may decrease, both from the meteorological event itself and from the climatological perception. Eight hurricanes hit Florida between August 2004 and October 2005 (Charley, Frances, Ivan, Jeanne, Dennis, Katrina, Tammy, and Wilma), and for several years thereafter tourism was affected so detrimentally that the surging economy in the Gulf region was interrupted. How many more hurricanes will strike before the collective mindset of vacationers begins to remove Florida from their late summer and early autumn travel plans? By contrast, since Wilma, the continental U.S. underwent its longest period since 1900 without a landfalling hurricane having winds exceeding 178 km hr^{-1} (110 mi hr^{-1}). But perception remains the key, as few Americans are aware of this “lull,” especially after the destruction of Hurricane Ike in 2008 and Hurricane/Superstorm Irene in 2012. These storms brought winds at landfall of only 178 km hr^{-1} (110 mi hr^{-1}) and 140 km hr^{-1} (85 mi hr^{-1}), respectively.

Transportation is another societal sector directly affected by climate. Extreme events play an even greater role in creating impacts to the transportation industry than to other sectors. A snowier-than-usual winter will exhaust the budget of municipalities for snow removal before the end of the snow season, and impacts will thereafter be even greater. In other cases forecasts of heavy snow that never materialize can also be very costly, because municipal workers who are held for overtime have no work to do. This is an especially difficult problem in heavily populated areas that experience occasional strong winter snowstorms. In the northeastern United States, for example, *nor'easters* that track up the Atlantic coast may dump 45 cm (18 in) of snow on Boston, New York, or Philadelphia. But a slightly more eastward track may provide no snow at all for these cities. In this case an incorrect forecast can be very costly. The American

architect/inventor/engineer Buckminster Fuller believed that the construction of a large geodesic dome over midtown Manhattan would pay for itself after only 10 years from the savings in snow removal alone.

Climate also affects energy supply and demand directly. Power companies must often buy additional power from other companies during unseasonably cold winters and hot summers in their service areas. In general, the farther in advance such purchases are made, the lower the cost of the power. Consulting climatologists are employed to provide long-lead climatic forecasts to minimize additional expense to their companies. Climatologists are also consulted to determine feasibility of solar and wind power. The United Kingdom is the leader in offshore wind farms, with more coming onto the energy grid in the near future and others in the planning stages. While the United States is not mentioned in the list of top 25 wind farms, in 2011 the government released plans for a major push toward constructing several along the Delaware, New Jersey, and Virginia coasts. Some recent evidence suggests that coastal winds may be sufficiently strong and persistent to provide for a reasonable share of the nation's energy needs in the near future, especially if the turbines are tall. Another area of wind power development is the northern Great Plains of the United States. This region has been called the "Saudi Arabia of wind power" by many environmentalists.

The insurance and risk management industry is also directly tied to weather and climate. Two major factors contribute to increasing risks to life and property caused by weather and climate. First, more people are living in areas vulnerable to atmospheric (and other) natural hazards now than ever before. Development along hurricane-prone coastlines and construction in floodplains provide two examples of this increasing hazard. It is well known that the bulk of hurricane storm surge damage occurs within 100 m (330 ft) of the high tide mark, yet development within that zone has accelerated in recent decades.

Second, a major concern is that global climatic change will cause more severe weather events and more chronic climatic problems (and, therefore, higher insurance premiums), particularly until people can adapt better to the changing environmental conditions. The insurance industry is adjusting its strategies to cope with climate change–related claims, but few companies have adopted comprehensive plans. Risk management trading (typically structured as a "climate contract" or "derivative" and operating on the principle of an insurance policy) has mushroomed into a major industry with the recognition that weather/climate may affect as much as 70% of all business activity. These transactions provide assistance when weather conditions

exceed certain thresholds that cause hardship for the contracted business.

Secondary societal impacts are felt in numerous sectors. For example, animal and human health and food prices are a result of both primary atmospheric influences on agriculture and other nonatmospheric factors. Likewise, economic and political conditions can be affected indirectly by climate, particularly in smaller political units that might be overwhelmed by extreme weather and climate events. In his book, *The Little Ice Age*, Brian Fagan argues that the shortage of grain and bread in the 1780s was one factor that contributed to the timing of the French Revolution. Even sectors such as fashion, art, and literature have been linked indirectly to atmospheric features.

Impacts on Human Health and Comfort

Atmospheric conditions exert a primary impact on many types of bacteria, viruses, and vector-borne diseases. Extremes of heat and cold cause numerous deaths each year. Recent research by climatologists at Arizona State University suggests that databases vary widely in reporting the total number of heat- and cold-related deaths in the United States, depending on, among other factors, the method of determining whether or not a death was considered to be a result of atmospheric conditions. Regardless, it appears that heat waves may cause more massive weather mortality events than cold waves. On the other hand, cold waves are more likely to cause a larger number of isolated deaths—people stranded alone in a deadly situation—and on the whole, these deaths seem to make cold weather more deadly than hot weather, even if increased severity of diseases from cold weather is not included. It is feared that long-term climatic change will increasingly threaten human health. For example, global warming may already be causing the mosquito-borne dengue fever and other diseases to spread to locations beyond their traditional tropical domains.

Climate Vulnerability, Adaptability, and Resilience

Extreme weather and climate events such as floods, tropical cyclones, severe winter storms, tornadoes, and droughts can be considered a **hazard** if they have the potential to threaten and endanger the surrounding natural environment and adversely affect the health, safety, welfare, and property of the human environment. Climate change can be a hazard, both because of the extreme events it may support and because of its potential impacts through nonextreme events. No place is immune to hazards, and most places are prone to the effects of many different types of hazards. A disaster is an occurrence of a hazard that

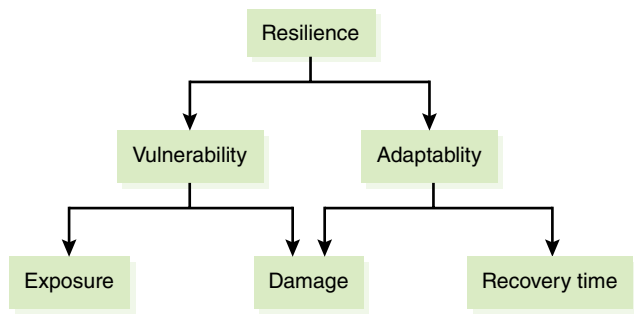


FIGURE 14.1 Schematic of the Resilience Inference Measurement (RIM) model.

causes such drastic impacts to the human environment that the community must receive assistance from other communities in order to recover.

One aspect of climate impacts that has received significant attention in recent years is **vulnerability**, **adaptability**, and **resilience** to weather and climate disasters. Lam et al. (2012) has identified a set of relationships between these variables in the **Resilience Inference Measurement (RIM) model** (FIGURE 14.1).

Vulnerability can be defined as the degree to which a community is threatened by the effects of a disaster, including a weather event or climate change. What makes communities vulnerable to the impacts of natural hazards, including climatic hazards? Exposure to severe hazards is the most obvious factor, but frequency of exposure does not necessarily correlate with vulnerability. If a community is exposed to the same hazard above some base frequency threshold, experience and preparation tend to reduce the vulnerability and increase the adaptability to the hazard. For example, a community that experiences an ice storm an average of once every 2 years might be considered to be more vulnerable to this hazard than one that experiences an ice storm once every 5 years, and that community might be more vulnerable to ice storms than a third community which experiences the hazard an average of once every 10 years. However, communities that experience an ice storm more often than once every 2 years may be increasingly less vulnerable to this hazard if they have infrastructure and budgets in place to clear roads of ice, trim tree limbs near power lines, and care for the most dependent members of society during power failures. But at even more frequent thresholds, the vulnerability may then begin to increase again just based on the sheer number of events of which some are bound to cause excessive damage (whether in terms of loss of life and/or economic losses) even among the most prepared communities. In the RIM model, vulnerability is defined as the ratio of damage from a particular hazard relative to the amount of exposure to that same hazard by a community. Communities that suffer extreme losses

even over relatively small exposure would have a high vulnerability to that hazard.

In the RIM model, adaptability is defined as the ratio of damage to recovery time in a community for a given hazard. Recovery time can be defined in many ways, such as the amount of time required for a population or employment rates to return to predisaster levels. A community that has required only a short recovery time relative to the amount of damage sustained from an extreme weather or climate event would be said to have shown high adaptability. Such a community would have buffered itself from the effect of the hazard.

The ratio of a community's adaptability to vulnerability for a given hazard defines the resilience to that hazard. Resilience is generally built through both policies and planning that reduce both the recovery time and the damage, thereby increasing adaptability and decreasing vulnerability simultaneously, even if exposure to the hazard increases.

The vulnerability, adaptability, and resilience of a given community may differ substantially by hazard and may change substantially over time. Despite the fact that climates are always changing, the biggest changes to vulnerability, adaptability, and resilience are likely to occur as a result of human interventions rather than natural ones. A well-prepared community can enhance its resilience substantially in a relatively short time. Applied climatologists interact with social scientists and community planners in an effort to enhance resilience.

► Climatological Data Sources

Data Collection Agencies

Compared with most other regions of the world, the United States is well served by historical records of climatological data. This has been attributed to the need to keep accurate records so that settlers would know what to expect from a relatively unfamiliar environment. Weather records in the 1700s and 1800s were kept by the more educated professionals such as surgeons, statesmen, and engineers. The **Federal Weather Service** was established by Congress as a component of the U.S. Army in 1870, then moved in 1891 to the U.S. Department of Agriculture and renamed the **United States Weather Bureau**. In 1940, in response to the increasing needs of weather data in the transportation and newly evolving aviation industry, the Weather Bureau was moved to the Department of Commerce. The demands on the Weather Bureau became so heavy that in 1970, coincident with the 100th anniversary of organized reporting, forecasting, and dissemination of atmospheric data to the public, the U.S. Weather Bureau was renamed the National Weather Service. The *National Weather Service*

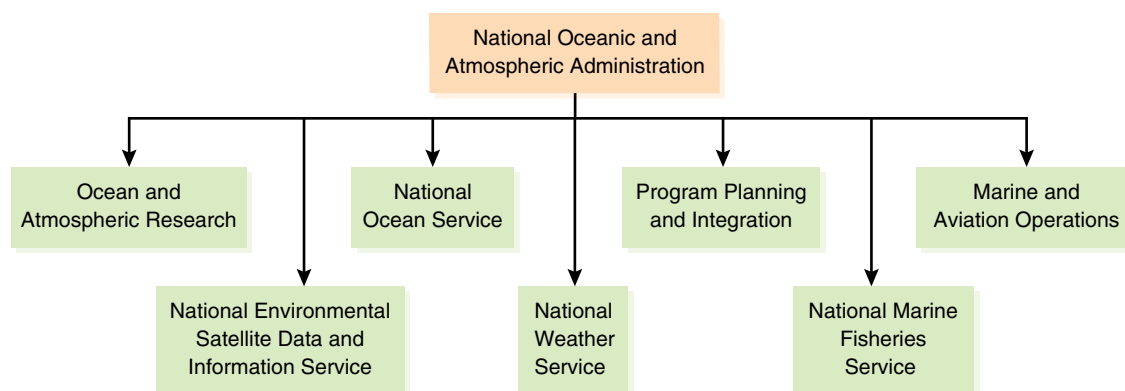


FIGURE 14.2 Simplified organizational chart for the National Oceanic and Atmospheric Administration.

Courtesy of NOAA/Workforce Management Office.

was established as a branch of the *National Oceanic and Atmospheric Administration* (NOAA), a new agency that oversaw other organizations as well, whose missions ranged from fisheries management to environmental data collection to oversight of the newly launched weather satellite program (**FIGURE 14.2**). NOAA grew quickly, as its budget tripled in its first 10 years of existence. From the beginning its mission has been to protect life and property and to recognize the integrative aspects of the Earth–ocean–atmosphere system.

The data collection arm of what is now NOAA is the **National Environmental Satellite, Data, and Information Service (NESDIS)**, headquartered in Silver Spring, Maryland. Within NESDIS are 11 offices that collect geophysical data of all types. These include the **National Centers for Environmental Information (NCEI)**, which is headquartered in Asheville, North Carolina. NCEI was formed in 1951 (even predating NOAA, but before 2015 was known as National Climatic Data Center) when several offices were merged. Today, NCEI archives weather data obtained by National Weather Service, Military Services, Federal Aviation Administration, U.S. Coast Guard, and voluntary observers.

With the increasing collection, availability, and demand for atmospheric data over the years, many additions and improvements to the NCEI program have been made. For instance, nearly every U.S. state has a State Climatologist who is responsible for the archival and dissemination of atmospheric data to the public and private sectors for climatological applications. In some states the **State Climatology Program** is funded more heavily than in others, so the scope of the program varies widely from state to state. In addition, six **Regional Climate Centers** distributed around the United States specialize in the archiving and dissemination of atmospheric data and monitor atmospheric events in their respective regions. These were established in the 1980s as a result of the passage in 1978 of the **National Climate Program Act**, which greatly increased the scope and

mission of atmospheric data collection and archiving in the United States. Demand for data from NCEI and other sources has increased tremendously in recent years, coinciding with the growth of the applied climatology industry as well as the additional sources of data for the United States and world from agencies outside of NOAA. Areas of coverage for National Weather Service and NOAA climate services are shown in **FIGURE 14.3**.

Recent climatological studies have benefited from the widespread availability of data. Most data are now accessible via the Internet, with many data sets provided free of charge or for only a nominal fee. This ease of availability has increased the number of independent studies on climate, leading to a heightened understanding of climatic processes.

Primary Versus Secondary Data

Primary data are defined as data collected by an investigator using thermometers, *radiometers*, moisture sensors, or other equipment in the field. **Secondary data** are data used by researchers after being collected, quality controlled, and compiled elsewhere, usually in digital format. Because of the nature of this research, those working at *local scales* and microscale, such as boundary layer climatologists, are more likely than synoptic and dynamic climatologists to use primary data. Likewise, synopticians and dynamicists are more likely to use secondary data sources. Primary data can be collected using methods such as those described in an earlier chapter. Some important secondary sources are discussed below. No attempt is made here to describe all major sources of secondary data—there are many!

Secondary Data Sources for Applied Synoptic and Dynamic Climatological Studies

In recent years the availability of high-quality climatological data sets for research has blossomed. The

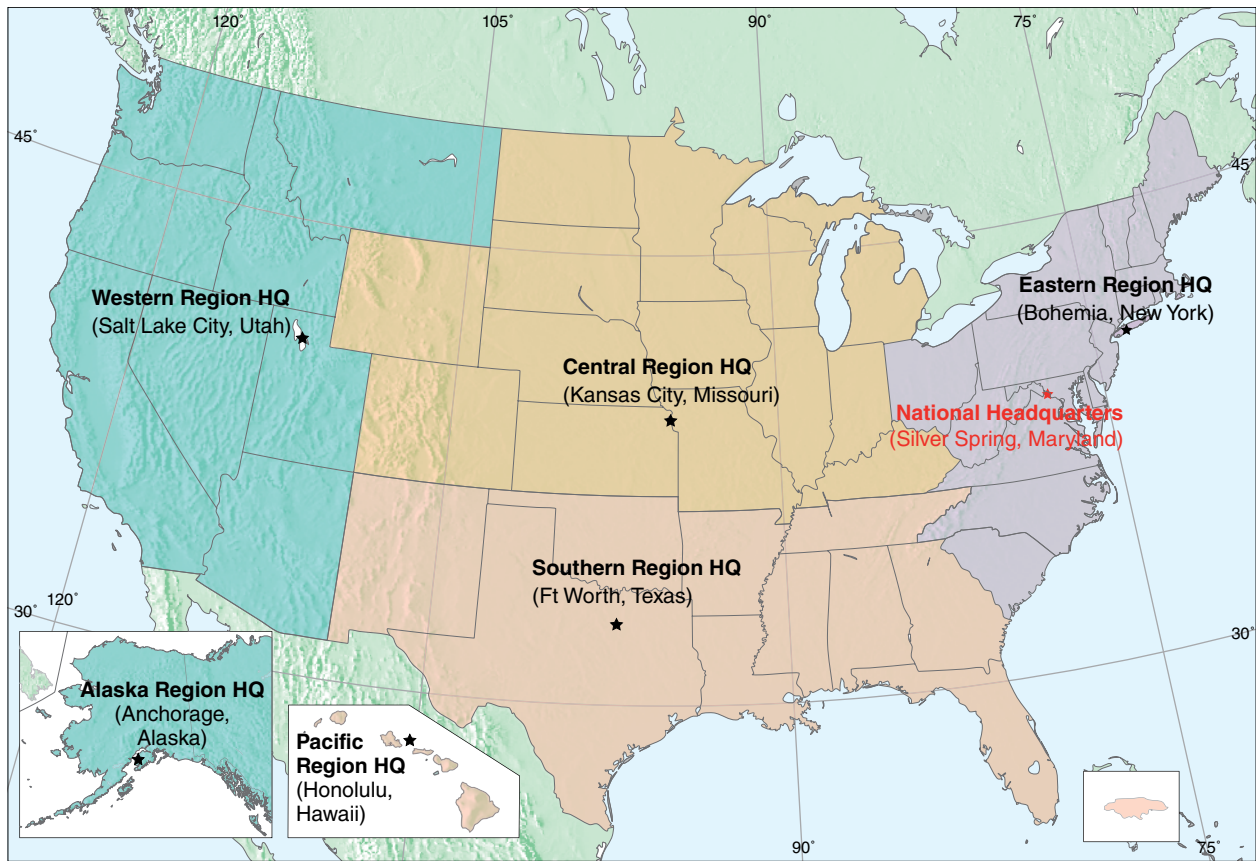


FIGURE 14.3 Areas of coverage for National Weather Service and NOAA climate services regions.

Modified from NOAA/NESDIS/National Centers for Environmental Information/Regional Climate Centers.

reanalysis data set produced by the *National Center for Atmospheric Research* in cooperation with the **National Centers for Environmental Prediction** is among the most widely used resources of global climatic data for dynamic and synoptic studies. The “reanalysis” involves the compilation and assimilation of observed data from a wide variety of sources, such as surface meteorological stations, buoys, satellites, aircraft, and ships, into a single data set for each variable analyzed. This collection of data sets, interpolated to a grid, provides a multitude of atmospheric variables at several vertical levels in the atmosphere. Much of these data are available on the Internet at four observation times per day, back to 1948. Other data are aggregated into daily or monthly totals.

In the United States NCEI/NOAA produces several publications on an ongoing basis that provide atmospheric data on the Internet and also in paper form. A particularly useful monthly publication is **Climatological Data (CD)**, which is produced for each state and contains a monthly summary of statewide areally weighted precipitation for that month, along with both means and extremes of temperature and the locations and dates during which the extremes occurred. It also provides these data and more for all official monitoring stations around the state of interest (**TABLE 14.1**). At the end of the

year **Climatological Data: Annual Summary (CDAS)** also is published for each state. Although CDAS does not replicate the daily data that were already published in each month’s CD for that year, it does report monthly totals for each month in that year and annual compilation statistics (**TABLE 14.2**). In general, if monthly data are required, CDAS provides a “shortcut” in analyzing station data.

For more detailed information, NCEI/NOAA provides other resources. For example, **Local Climatological Data (LCD)** is published monthly for more than 270 sites around the United States and Pacific Islands. All large cities and many smaller cities are represented in this publication. An advantage of LCD is that it provides some data with temporal resolution as high as every 3 hours rather than just the daily data included in CD. Furthermore, LCD provides additional variables. **TABLE 14.3** shows the data that are available in that resource. The disadvantage of LCD is that it is available for far fewer sites than CD provides. In general, if data are needed at a particular site, LCD should be used if available for that site or for a nearby city, if data are required for variables that are not reported by CD, and/or if higher temporal resolution is necessary. On the other hand, if no LCD exists near the site of interest

TABLE 14.1 Information Contained in *Climatological Data*

Section	Data Included
Statewide summary	Monthly precipitation total compared against other years Temperature and precipitation extremes for the month
Monthly station and divisional temperature	Average daily maxima and minima Monthly mean and departure from normal Extreme high and low and date of occurrence Heating and cooling degree days Number of days with maximum $\geq 90^{\circ}\text{F}$ or $\leq 32^{\circ}\text{F}$ Number of days with minimum $\leq 32^{\circ}\text{F}$ or $\leq 0^{\circ}\text{F}$
Monthly station and divisional precipitation	Monthly total and departure from normal Greatest day and date of occurrence Snowfall total Maximum snowfall depth on ground and date of occurrence Number of days with snowfall of ≥ 0.10 , 0.50 , or 1.00 in.
Daily station and divisional information	Precipitation Temperature Soil temperature Pan evaporation Wind (accumulated daily totals, measured in miles on an "odometer")
Station index	Identifying index number Climate division County Latitude/longitude Elevation Time of observation Observer name or company/agency name Reference notes Map of state with stations labeled

TABLE 14.2 Information Contained in *Climatological Data: Annual Summary*

Section	Data Included
Statewide summary	Line graph of statewide annual precipitation plotted against that of other years in the historical record
Station and divisional precipitation	Monthly total and departure from normal
Average station and divisional temperature	Monthly average and departure from normal Date of last spring minimum at or below 16°F , 20°F , 24°F , 28°F , and 32°F and temperature Date of first autumn minimum at or below 32°F , 28°F , 24°F , 20°F , and 16°F , and temperature Number of consecutive days between dates with temperatures at or below 16°F , 20°F , 24°F , 28°F , and 32°F (if less than 365)
Other	Monthly and seasonal cooling degree days* Monthly average soil temperatures and extremes Monthly total pan evaporation (in inches) and wind movement (in miles)

*Monthly and seasonal heating degree days are contained in the July issue of *Climatological Data*.

TABLE 14.3 Information Contained in *Local Climatological Data*

Section	Data Included
Daily totals	Temperatures: maximum, minimum, average, departure from normal Average daily dewpoint temperature Average daily wet bulb temperature Heating and cooling degree days Type of weather observed; rain, drizzle, thunderstorms, haze, fog, dust storms, tornadoes, blowing snow, etc. Snow/ice depth and water equivalent (at a fixed time each day) Average station pressure, and adjusted sea-level pressure Mean wind speed, resultant direction Maximum 5-second and 2-minute wind speed and direction Monthly averages/totals Visibility in miles Sunrise and sunset times
Hourly precipitation	Precipitation totals ending each hour Maximum 5-, 10-, 15-, 20-, 30-, 45-, 60-, 80-, 100-, 120-, 150-, and 180-minute precipitation total and date of occurrence
Observations at 3-hourly intervals	Sky cover (clear, scattered, broken, overcast) Cloud ceiling height Visibility Type of weather observed; rain, drizzle, thunderstorms, haze, fog, dust storms, tornadoes, blowing snow, etc. Temperature, dewpoint temperature, wet bulb temperature Relative humidity Wind speed and direction Station pressure and adjusted sea-level pressure

or if high spatial resolution of data that are provided by CD is required, then CD is used.

For occasions when 3-hourly data do not provide sufficient temporal resolution to solve the problem at hand, surface data collected on an hourly basis can be used. Such hourly data are available from NCEI or the regional climate centers for more than 500 stations around the United States and 12,000 stations worldwide via the **surface airways observations**. Many, but certainly not all, of the surface airways sites in the United States are also sites published in LCD. These data usually include the variables shown in **TABLE 14.4**.

Precipitation may vary tremendously in small spatial and temporal periods and is a factor in many applied climatological problems. NOAA's **Hourly Precipitation Data (HPD)** is another publication designed to provide precipitation data at temporal and spatial resolution as fine as possible. Like CD, HPD is also published monthly by state. A typical state may have approximately one HPD site for every two counties, on average. The specific precipitation data types available in HPD are described in **TABLE 14.5**. Among the most widely used information

TABLE 14.4 Data Available Through Surface Airways Observations

- Wind speed and direction
- Ceiling height
- Horizontal visibility
- Sky cover
- Altimeter setting
- Station pressure
- Sea level pressure
- Air temperature
- Wet bulb temperature
- Dewpoint temperature
- Relative humidity
- Solar radiation
- Present weather conditions (e.g., snow, thunderstorm, haze)

in HPD is that which relates to the maximum intensity of precipitation to fall within specific time durations. To document such heavy precipitation events and severe weather, **Storm Data** is a monthly publication that

TABLE 14.5 Information Contained in <i>Hourly Precipitation Data</i>	
Section	Data Included
Daily precipitation totals by station	Precipitation by station, including the type of gauge used
Hourly precipitation totals by station	Precipitation totals at each hour, ending on the hour
Monthly precipitation maxima by station	Maximum for measurement periods of 15, 30, and 45 minutes and 1, 2, 3, 6, 12, and 24 hours, with the date and time of occurrence

provides a chronological summary, by state, of severe and unusual weather that occurred during that month, including data on the storm trajectories, damage, and casualties resulting from each event.

A final important secondary data source for the United States is NOAA’s *Daily Synoptic Series*, a booklet of seven daily surface and 500-mb weather maps. Applied climatologists can often use these to determine the most likely time of passage of a frontal system or to provide other clues that might identify the most likely time that a temperature or precipitation event occurred, when using daily data.

NCEI offers a variety of other products that are not described in detail here. A few examples include global climatological normals, engineering weather data, archived hourly radar images of the United States, rainfall frequency atlas of the United States for various durations and magnitudes of precipitation events, and satellite imagery of significant weather events in the past.

The **World Meteorological Organization (WMO)** of the United Nations also dispenses a variety of climatological data products for use in large-scale synoptic and dynamic climatological studies, including some of the same data sets produced by NOAA/NESDIS/NCEI. Other data sets in the WMO archives are contributed by organizations around the world, such as the U.K.’s Hadley Centre and the German and Japanese Weather Services.

Considerations Regarding Instrumentation Used

One important consideration when using *HPD* is the type of rain gauge used at the station of interest. Although the **standard nonrecording rain gauge** is used at



FIGURE 14.4 Fischer Porter rain gauge.
Courtesy of Robert V. Rohli.

most of the 13,000 precipitation gauges in the United States (including all of the sites reported in *CD*), hourly stations must have more sophisticated equipment for measuring rain automatically. In most of the United States two types of gauges are most prevalent for hourly recordings.

The **Fischer-Porter rain gauge** (FIGURE 14.4) is a 1.52-m (5-ft) tall tube with a 0.6-m (2-ft) diameter. This type of gauge reports precipitation collected in a bucket based on the water’s weight. Every 15 minutes a special tape is punched mechanically to report a running total of the precipitation (in tenths of an inch) since the bucket was emptied. Network connections allow instant access to the data.

An important consideration of the Fischer-Porter gauge is that it is only precise to 2.5 mm (0.10 in) of precipitation. In other words, 2.5 mm (0.10 in) of rainfall must occur before any rainfall is reported. This can be problematic for some applications. For instance, many rainfall-related traffic accidents occur in the first few minutes of precipitation because the slight dampening causes roads to become slick from oils previously deposited on the roadway. After several minutes of moderate precipitation, the oils are washed from the road, making them somewhat safer. If precipitation data are needed to determine whether rain may have played a role in an automobile accident, the time of precipitation onset may not be readily apparent

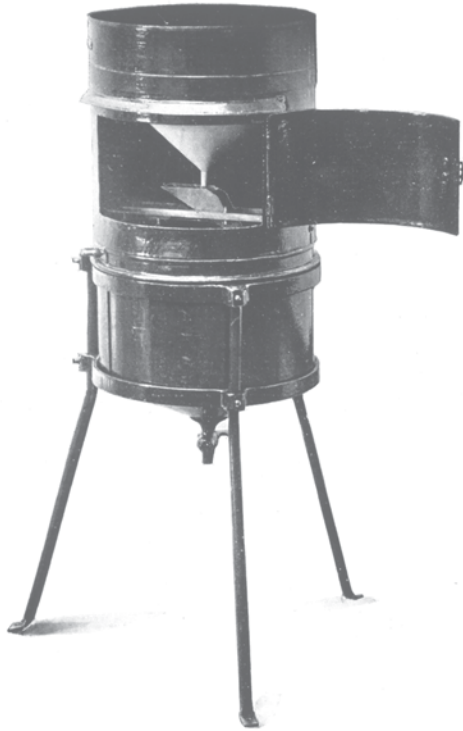


FIGURE 14.5 A tipping bucket rain gauge.

Courtesy of Sean Linehan, NOS, NGS/NOAA.

from the Fischer-Porter readings, because a significant amount of time may be required for as much as 2.5 mm (0.10 in) to be accumulated. Furthermore, some light rain showers may go totally unreported. Likewise, if an amount of less than 2.5 mm (0.10 in) accumulates in the gauge, a precipitation total of 2.5 mm (0.10 in) will be reported relatively quickly after the beginning of the next rain shower (which may occur days later) because some precipitation will have accumulated in the gauge from the previous shower. For these reasons readings from Fischer-Porter gauges should be interpreted with caution, particularly in certain applications.

The other common type of automated precipitation recorder is the **tipping bucket rain gauge**, an instrument consisting of two small buckets that alternate in the collection of precipitation (**FIGURE 14.5**). When .25 mm (0.01 in) of precipitation occurs, the active bucket dumps its water while the other bucket quickly moves into its place to begin collecting the precipitation. The number of “tips” is monitored electronically to provide a continuous measure of precipitation. The tipping bucket gauge is advantageous in that it measures with precision of 0.25 mm (0.01 in), but a major disadvantage is that some precipitation is not “captured” in the brief moment when the buckets are alternating. This *undercatch* can be significant during heavy rainstorms. Problems related to undercatch in standard nonrecording rain gauges were described with surface water balance elsewhere in the text (Chapter 6).

In addition to precipitation, temperature data are also routinely collected and reported at some 5000 “official” stations around the United States and published in secondary data sources such as *CD* and *LCD*. Because data at most stations are collected by volunteers and are not automated (i.e., computerized) stations, the thermometers and/or precipitation gauges are only checked once daily. For this, a special type of instrument, called a **maximum/minimum thermometer**, is used. Although there are several varieties of maximum/minimum thermometers, the basic principle is that the instrument leaves a mark at the highest temperature that had occurred since the last resetting of the instrument. Likewise, the base of the mercury allows for the lowest temperature since the last resetting to be reported. At a designated time each day, the observer notes the maximum and minimum temperatures and then resets the instrument, usually by twirling it. The maximum/minimum thermometers are necessary to avoid having to ask volunteers to check their thermometers at multiple times of the day and night; with this instrument at least the high and low temperatures for the previous 24 hours can be noted.

Time of Observation

When using data collected daily by maximum/minimum thermometers or by standard nonrecording rain gauges, the time of observation is a critical consideration and is reported in *CD*. To illustrate how the time of observation can influence the data set, imagine a station that reports at 3:00 pm. Because 3:00 pm is near the typical time of maximum temperature for the day, it is possible that on a hot day the temperature at 2:59 pm was 37°C (99°F) and was the high temperature for the day. When the observer notes the maximum temperature at 3:00 pm, she reports the temperature that occurred at 2:59 pm, and then she resets the instrument. At 3:01 pm the temperature is still likely to be 37°C (99°F), but this temperature is not counted until the following calendar day. So even though only one day with a 37°C temperature may have occurred, *CD* may report it as two separate days of high temperatures of 37°C. In cases of heat waves, afternoon-reporting stations thus are likely to “double-count” the maximum temperatures.

The opposite situation can occur for morning-reporting stations. For example, if a station’s time of observation is 7:00 AM, a cold wave that occurred on a single morning could be reported in the daily data as having two “days” with low temperatures hovering at the temperature of the single cold day.

This situation is known as **time of observation bias**. Many stations in the United States have changed from afternoon-reporting to morning-reporting stations over the past 40 to 50 years, because more of the

general population is employed during the afternoon hours and has less time at home to monitor weather conditions. The bias toward lower temperatures has, therefore, increased over time. The fact that temperatures have risen substantially in the last 30 years, despite this general trend toward more morning-reporting stations, provides further evidence that the observed warming is significant.

Time of observation is also critical when analyzing daily precipitation data. It is important to remember that a “daily” precipitation total really refers to the 24-hour total terminating at the time of observation on the calendar day that the precipitation is reported. Precipitation reported on a certain day at a morning-reporting station is likely to have fallen on the previous calendar day, particularly in places and times of the year when afternoon *convective precipitation* supplies a large proportion of the precipitation. No adjustment of temperature or daily precipitation totals is made before publication to account for the “most likely” time of the precipitation or the high or low temperatures—it is up to the applied climatologist to determine the most likely time/day that a temperature or precipitation event occurred. This could be achieved by comparing the data of interest with data measured at a nearby site that reports at intervals of 1 or 3 hours, such as *HPD* or *LCD*.

Other Variables

Although most variables reported in the various secondary data sources are self-explanatory, a few need additional explanation. One such set is the “degree-day” variables—a concept that can be used to extract additional meaning from the daily temperature data for specific applications. For example, in energy applications the **heating degree-day (HDD)** can be used to index the amount of energy needed to heat or cool a building. Heating is usually assumed to be required when the daily mean temperature of a location is 18°C (65°F) or below. Each degree of daily mean temperature below this base is counted as one HDD. For example, if the maximum temperature on a given day was 22°C (70°F) and the minimum temperature was 10°C (50°F), 2 Celsius or 5 Fahrenheit HDDs would have accumulated on that day because the average temperature was 16°C (60°F). Monthly and seasonal cumulative totals of HDDs for the heating season (usually considered to be July 1 through June 30, in the northern hemisphere) are published in *CD* and *LCD*. Energy planners devise mathematical relationships between HDDs and energy consumption, and long-lead seasonal climatic outlooks are used to estimate energy demands for the upcoming season.

Likewise, the **cooling degree-day (CDD)** operates on the same principle as the HDD, but it is used

to identify the energy demand for cooling a building whenever the daily mean temperature exceeds the base of 18°C (65°F). So for instance, if the maximum and minimum temperatures were 32°C (90°F) and 20°C (68°F), respectively, on a given day, then 8 Celsius or 14 Fahrenheit CDDs were accumulated. Because cooling is generally not necessary in the winter months, in the northern hemisphere the CDD season is generally considered to run from January 1 through December 31. In reality, however, factors other than temperature may determine energy consumption, including cultural behavior and meteorological factors. For example, many consumers in the southern United States tend to use their air conditioners on some days even when daily temperatures fall below 18°C (65°F) because humidity and/or lack of wind might lead to discomfort if they opened their windows. HDDs and CDDs are published in *CD*, *CDAS*, and *LCD*.

For agricultural applications of temperature data, a similar concept is the **growing degree-day (GDD)**, a variable that is accumulated for each degree that the daily mean temperature exceeds some base value. The base value is determined experimentally, varies by crop, and is the theoretical minimum daily temperature required to provide enough energy for that crop to grow. For example, a typical base value for alfalfa is 5°C (41°F). On a given day, if the high temperature is 18°C (64°F) and the minimum temperature is 4°C (39°F), then 6 Celsius GDDs are accumulated. If the daily mean temperature falls below the threshold, then 0 GDDs are accumulated. It is impossible to have “negative” GDDs, just as it is impossible to accumulate negative HDDs or CDDs. Because each crop theoretically requires a certain number of GDDs before harvest, a running total of GDDs for a growing season tells a farmer whether the crop is on schedule to be harvested on time. Of course, the GDD concept assumes that other conditions are met adequately, such as precipitation totals and timing, protection from disease, and nutrient availability.

A related agricultural application is the **crop heat unit (CHU)**, which actually calculates two values: One base temperature is for the daily minimum temperature and the other is for the daily maximum temperature. As for HDDs, CDDs, and GDDs, if the daily minimum and/or maximum temperature is below the base, zero CHUs are accumulated for that calculation, and for each degree above the base, 1 CHU is reported for that calculation. The daily maximum temperature also has an “optimal” temperature, which is the temperature at which maximum growth occurs for a given crop. If the daily maximum temperature exceeds this optimal temperature, the CHU for the daily maximum begins to fall. The total CHU for the day is simply the mean of the CHU calculation for the minimum and maximum

temperatures on that day. Although the CHU is not published in the sources described above, it is used more commonly in Canada.

Wind data are often tricky to decipher in secondary data sources. In *LCD* wind is reported in tens of degrees using 360° compass headings from north. Thus, a wind direction reported as “9” represents winds coming from 90°—an easterly wind (i.e., wind blowing from east to west). Likewise, “18” (i.e., 180°) represents a southerly wind, “27” (270°) is a westerly wind, and “30” (300°) would be a wind from the west-northwest. In this notation, “0” is usually reserved for a calm wind (which, by definition, has no direction) and “36” (360°) is used for a northerly wind. In some applications wind speed and direction are transformed into west–east and south–north vector components—*u* and *v*, as described in the earlier discussion of the *Navier-Stokes equations of motion*.

Some secondary sources report wind according to the **Beaufort wind scale**, a simple observation-based scale that measures wind in units of 0 to 12 “Beauforts,” which convey information about the estimated effect of the wind’s force rather than the wind speed itself. In this system, “0” represents calm winds and “12” corresponds to hurricane-force winds, as shown in **TABLE 14.6**. Beauforts are typically used in situations where direct wind measurements are not feasible, such as on the ocean, in military combat zones, and in remote terrain.

Secondary Sources for Applied Studies of the Climate System

Because of the local nature of the processes, secondary data sources for analyzing vegetation–climate relationships are more difficult to find. Usually, the researcher must use instrumentation to gather primary data but some secondary data sources are available. For example, the **Long-term Ecological Research (LTER) Program**, which began in 1980, provides bioclimatological data (along with other environmental information such as hydrological measurements, soil composition and quality, land-use change, and even demographic data) for 26 sites across North America, the Caribbean, and Antarctica (**FIGURE 14.6**). These data reveal information about surface–atmosphere interactions of climatological importance, including broad-scale trace gas composition, which would be difficult to monitor without such a sophisticated network of sensors. Similarly, the **AmeriFlux** program began in 1996 as part of a wider network of stations, including **EuroFlux**. These stations provide data on energy, matter, and *momentum* exchanges in the biosphere, with a particular emphasis placed on carbon *fluxes*. The AmeriFlux and EuroFlux stations are shown in **FIGURES 14.7** and **14.8**, respectively.

Other agencies collect, maintain, and archive cryospheric and hydrologic data of interest to climatologists. For example, a major clearinghouse for cryospheric data, including snow cover, glaciers, continental ice sheets, avalanches, permafrost, and sea ice, is located in Boulder, Colorado, at the **National Snow and Ice Data Center**. This agency was formed in 1982 as a means of consolidating operations from several preexisting locations. The **National Data Buoy Center**, located at Stennis Space Center in Mississippi, is responsible for dispatching and maintaining a network of buoys and coastal stations around North America and in some other parts of the world that collect atmospheric data. The **Global Energy and Water Cycle Experiment (GEWEX)**, under the auspices of the **World Climate Research Programme**, provides data on fluxes of energy, water, and momentum between the surface and atmosphere, both on land and in the oceans. The goal is to support improvements in the forecasting of global and regional climatic change.

Secondary Sources Well Suited to Studies in Paleoclimatology and Climate Change

An often-used source of data well suited to global change detection as well as atmospheric composition, *fossil fuel* consumption, and the carbon cycle, is provided by the **Carbon Dioxide Information Analysis Center (CDIAC)** at Oak Ridge National Laboratory in Tennessee. CDIAC also produces the global **Historical Climatology Network**—a set of mean monthly temperatures, precipitation, and sea level pressure for thousands of stations worldwide for time periods of up to 50 years. The U.S. component of this data set consists of daily and monthly records. A major advantage of the HCN over *CD* and other sources is that much effort has been invested in ensuring that only high-quality, accurate data are included and that station moves are minimized.

The **World Data Center for Paleoclimatology**, headquartered in Boulder, Colorado, is a branch of NCEI that acts as a repository for paleoclimatological data sets from thousands of locations worldwide. These data include both historical and proxy sources described in Chapter 11. Researchers who are willing to share their findings with the public contribute the data.

Secondary Sources Well Suited to Studies in Physical Climatology

Although the LTER, GEWEX, and CDIAC projects provide free global data on atmospheric gas concentrations, other data sets are widely used for other types of studies in physical climatology. For instance, the **Global Hydrology Center** of the **National Aeronautics**

TABLE 14.6 Beaufort Wind Scale, for Use at Sea and on Land

Class	Speed (mph)	WMO Classification	Appearance on Sea Surface	Appearance on Land Surface
0	0–1	Calm	Smooth and mirror-like	Calm, smoke rises vertically
1	1–3	Light air	Scaly ripples, no foam crests direction, still wind vanes	Smoke drift indicates wind
2	4–7	Light breeze	Small wavelets, crests glassy, no breaking	Wind felt on face, leaves rustle, lanes begin to move
3	8–12	Gentle breeze	Large wavelets, crests begin to break, scattered whitecaps	Leaves and small twigs constantly moving, light flags extended
4	13–18	Moderate breeze	Small waves 1–4 ft becoming longer, numerous whitecaps	Dust, leaves, and loose paper lifted, small tree branches move
5	19–24	Fresh breeze	Moderate waves 4–8 ft taking longer form, many whitecaps, some spray	Small trees in leaf begin to sway
6	25–31	Strong breeze	Larger waves 8–13 ft, whitecaps common, more spray	Larger tree branches moving, whistling in wires
7	32–38	Near gale	Sea heaps up, waves 13–20 ft, white foam streaks off breakers	Whole trees moving, resistance felt walking against wind
8	39–46	Gale	Moderately high (13–20 ft) waves of greater length, edges of crests begin to break into spindrift, foam blown in streaks	Whole trees in motion, resistance felt walking against wind
9	47–54	Strong gale	High waves (20 ft), sea begins to roll, dense streaks of foam, spray may reduce visibility	Slight structural damage occurs, slate blows off roofs
10	55–63	Storm	Very high waves (20–30 ft) with overhanging crests, sea white with densely blown foam, heavy rolling, lowered visibility	Seldom experienced on land, trees broken or uprooted, “considerable structural damage”
11	64–72	Violent storm	Exceptionally high (30–45 ft) waves, foam patches cover sea, visibility more reduced	
12	73+	Hurricane	Air filled with foam, waves over 45 ft, sea completely white with driving spray, visibility greatly reduced	

Data from National Weather Storm Prediction Center, NOAA. www.spc.noaa.gov/faq/tornado/beaufort.html. Accessed April 2013.

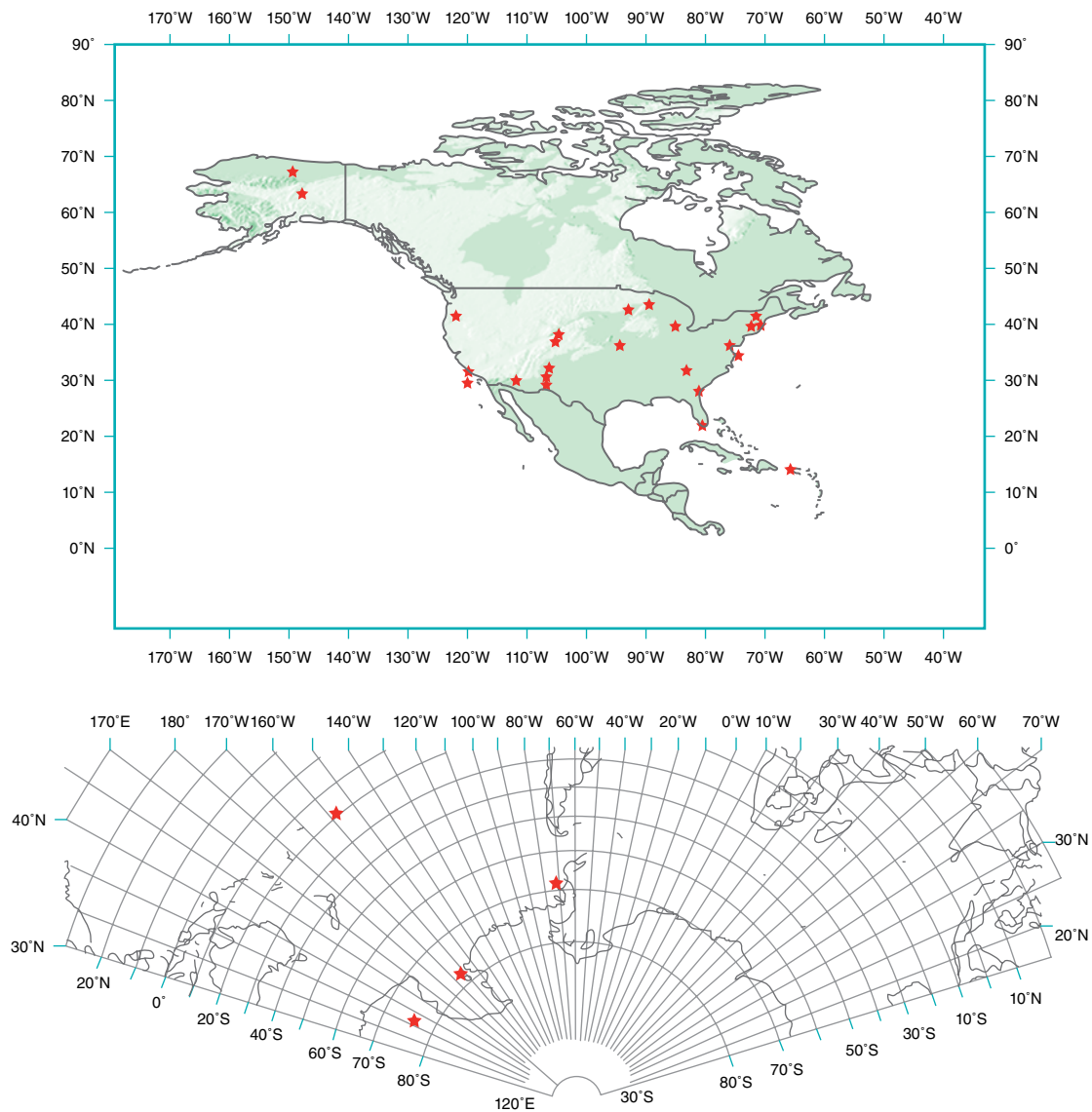


FIGURE 14.6 Long-term Ecological Research Stations.



FIGURE 14.7 AmeriFlux research stations.

Courtesy of AmeriFlux, Oak Ridge National Laboratories, U.S. Department of Energy.



FIGURE 14.8 EuroFlux research stations.

and Space Administration provides a wide array of satellite-based observations for climatological research, including such variables as lightning strikes, aerosol loadings, and data for studies of cloud formation and physics. NOAA's **Climate Monitoring and Diagnostics Laboratory** maintains data related to stratospheric ozone

concentrations and other atmospheric phenomena. The U.S. Department of Energy's **Renewable Resource Data Center** provides *insolation* and wind data for a series of sites around the United States.

► Summary

Applied climatology investigates the impacts of climate on other phenomena. Although computer models can be used to estimate these impacts, empirical (historical data-driven) approaches are also important. Applied climatologists must be knowledgeable about both the available data sources and any shortcomings in answering the research question at hand. They must also be adept at making educated guesses about the condition of the atmosphere in cases when formal, reliable atmospheric data are unavailable.

Primary impacts of climate include those systems that climate affects directly, whereas secondary impacts are felt only indirectly. Both types of impacts occur in both natural and social systems and also affect human health. Some sectors that are influenced in a primary manner include agriculture, vegetation, hazards, insurance, water resources, recreation, energy supply and demand, construction, and transportation. Secondary

impacts include food supply and cost, political and economic stability, and health.

Several sources of data assist applied climatologists. In the United States most of these data are supplied by federal agencies that fall within the Department of Commerce, and much of these data are available online. Other data are being supplied by non-Department of Commerce agencies, as satellite and ecological data become more widely available.

Most of the data available are provided in a self-explanatory format, but a few important variables may need additional explanation. An understanding of the strengths and possible limitations of the type of rain gauge used may be an important factor in some applied climatological investigations. Likewise, the time of observation may be important in reconstructing events using data from daily-reporting stations. Finally, it is important to note that wind data are often supplied in vector format, with the direction listed in tens of degrees using a 360° compass heading. For energy and agricultural applications, the degree-day and crop growth unit concepts are also important. Several data sources for studies on the relationships between the atmosphere and the other “spheres,” along with paleoclimates and physical climatology, are also available.

Key Terms

Adaptability

Albedo

AmeriFlux

Applied climatology

Arctic amplification

Beaufort wind scale

Biosphere

Carbon Dioxide Information

Analysis Center (CDIAC)

Climate Monitoring and

Diagnostics Laboratory

Climatological Data (CD)

*Climatological Data: Annual
Summary (CDAS)*

Convective precipitation

Cooling degree-day (CDD)

Crop heat unit (CHU)

Cryosphere

Daily Synoptic Series

Downscaling

Empirical approach

EuroFlux

Evapotranspiration

Federal Weather Service

Fischer-Porter rain gauge

Flux

Fossil fuel

Global Energy and Water Cycle

Experiment (GEWEX)

Global Hydrology Center

Growing degree-day (GDD)

Growing season

Hazard

Heating degree-day (HDD)

Historical Climatology Network

Hourly Precipitation Data (HPD)

Hurricane

Hydrosphere

Insolation

Lithosphere

Local Climatological Data (LCD)

Local scale

Long-term Ecological Research

(LTER) Program

Maximum/minimum
thermometer

Microscale

Momentum

National Aeronautics and Space
Administration

*National Center for Atmospheric
Research*

National Centers for
Environmental Information
(NCEI)

National Centers for
Environmental Prediction
National Climate Program Act

National Data Buoy Center

National Environmental Satellite,
Data, and Information Service
(NESDIS)

*National Oceanic and
Atmospheric Administration
(NOAA)*

National Snow and Ice Data Center
National Weather Service
Navier-Stokes equations of motion
Nor'easter
Photosynthesis
Planetary scale
Positive feedback system
 Primary climate impact
 Primary data
Radiometer
 Reanalysis data set
 Regional Climate Center

Renewable Resource Data Center
 Resilience
 Resilience Inference
 Measurement (RIM) model
 Secondary climate impact
 Secondary data
Shortwave radiation
 Standard nonrecording rain gauge
 State Climatology Program
Storm Data
 Surface airways observation
Surface water balance

Thermohaline circulation
 Time of observation bias
 Tipping bucket rain gauge
Undercatch
 United States Weather Bureau
 Vulnerability
 World Climate Research Programme
 World Data Center for Paleoclimatology
 World Meteorological Organization (WMO)

Terms in italics have appeared in at least one previous chapter.

Review Questions

- How does the empirical approach differ from the modeling approach in solving atmospheric problems?
- The text compares applied climatologists to detectives. In what way do you believe this comparison is valid?
- Name five social or economic sectors of activity that are affected by climate and determine whether these impacts are primary or secondary.
- How does the total of heat-related deaths compare with that of cold-related deaths in the United States?
- How does a hazard differ from a disaster?
- What are vulnerability, adaptability, and resilience to a hazard?
- What is the main advantage of the National Center for Atmospheric Research reanalysis data set?
- What advantages do *HPD* provide that are not provided by *LCD*?
- How does a Fischer-Porter rain gauge work? What caveats should be heeded when using Fischer-Porter data? Why?
- Why is the time of observation a critical variable in applied climatological analysis?
- What is a cooling degree-day and why is it an important variable?
- What is the difference between a crop heat unit and a growing degree-day?
- What are the advantages and disadvantages of using the Beaufort wind scale?
- A traffic accident occurred on the corner of Final and Exam Streets at a particular day and time. What sources would you consult to identify the weather conditions at that place and time?
- Name three data sets that you might recommend to a friend who is doing research on long-term changes in atmospheric carbon dioxide.

Questions for Thought

- Select a type of hazard that is experienced in your hometown and acquire data that allow you to assess your community's vulnerability, adaptability, and resilience to that hazard relative to that of a nearby community of comparable size.
- A homeowner calls you, a climatologist at the Greater Good Environmental Consulting Company, because he believes there may be a crack in the foundation of his built-in swimming pool. He indicates that it seems to him the water is disappearing from the pool faster than it should be, given that it is April. Using what you learned, how would you go about determining whether he is justified in his accusation that the construction work was faulty?
- To what extent do you agree with the following statement: "Applied climatology represents the best hope for climatologists to provide a contribution to knowledge to others outside the field"?
- How would you go about finding out the last day when hail fell in your hometown?





CHAPTER 15

Future of Climatology

CHAPTER AT A GLANCE

- Relationship Between Climatology and Meteorology
- Interdisciplinary Work with Other Scientists
- Interaction Between Climate Scientists and Nonscientific Professionals
- Improved Atmospheric Data Availability and Display
 - ▶ Recognition of the Possibility for Rapid Climate Change
- Climatology as Part of the Ultimate Goal of Sustainability
- Summary
- Key Terms
- Review Questions
- Questions for Thought

Our understanding of atmospheric processes, models to simulate those processes, and data that show the results of those processes, as described throughout this text, has propelled climatology to a position of respect among the natural sciences. But what trends and challenges will characterize climatology in the coming years? What lines of inquiry will be pursued? Which ideas about Earth's climate system will be debated? This chapter offers some perspectives on possible answers to these questions.

▶ Relationship Between Climatology and Meteorology

In the years ahead we can expect that the distinction between the traditionally defined domains of climatology

and meteorology will continue to blur. Well-trained climatologists will increasingly be expected to have an understanding of the physical principles usually taught in meteorology courses. These perspectives include a firm grounding in dynamic, synoptic, and physical meteorology. Likewise, well-trained meteorologists will benefit from the broad and integrative perspective traditionally offered by climatology courses. The result is a cross-fertilization of ideas that strengthens both of the atmospheric sciences. Both climatologists and meteorologists will also benefit increasingly from a background in social sciences, environmental science, and public policy.

The recent upgrade of the *National Oceanic and Atmospheric Administration's* (NOAA's) primary model for weather prediction, the Global Forecast System (GFS), with grid resolution improving from 27 km

to 13 km, will allow for meteorological forecasts to become more abundant, precise, and accurate out to longer lead times. The **Climate Prediction Center (CPC)** within NOAA's *National Weather Service*, has become an increasingly important office, producing temperature and precipitation forecast products in such intervals as 8 to 14 days, 1 month, and 3 months. The 3-month outlooks are currently available with lead times out to 15 months into the future. Currently, these products forecast either “above normal,” “near normal,” or “below normal” conditions across the United States. As the quality, quantity, specificity, and lead times for such outlooks continue to improve with advances in technology and knowledge of the science of the climate system, the distinction between meteorology and climatology will continue to blur.

► Interdisciplinary Work with Other Scientists

Climatologists will increasingly find themselves as parts of interdisciplinary teams whose goal is to solve complex climate-related problems. Already, paleoclimatological research has reached this interdisciplinary sphere. As we saw previously, biological, geological, geochemical, and historical evidence is often used in tandem to decipher climates of the past, and the interpretation of such evidence requires expertise in a range of disciplines. In addition, the increased emphasis on interactions between the atmosphere and various other physical “spheres,” such as Earth–ocean–atmosphere interactions and feedbacks, will necessitate increasing interdisciplinary work between climatologists and oceanographers, vulcanologists, geophysicists, biological scientists, and geochemists. In short, climatology will move closer to the “hub” of scientific environmental analysis and take on more of an all-encompassing (holistic) scientific perspective. This is logical because climate is the most fundamental limiting factor in the environment. This “coming of age” means that climatologists will “see the forest through the trees” while the other natural scientists focus more specifically on “seeing the trees” in examining the relationship between climate and their specialization.

Attention to these interactions between the various spheres of the Earth–ocean–atmosphere system will be focused increasingly on interactions between processes at various scales. This concept has been described as a “cascade of linkages” by climatologist Werner Terjung over 30 years ago. One manifestation of this cascade is the trend toward understanding the influence of global atmospheric *teleconnections* on local, near-surface atmospheric features, the *surface water balance*, and

circulations that impact the climate system to produce distinctive local and regional climates. Others are the generation of regional climate models to simulate impacts of the broad-scale atmospheric circulation and the use of climatic data sources to quantify this impact in a local area. In the future, climate models will have increasingly finer resolution, and replacement of *down-scaling* techniques at a given scale with model output at that scale is inevitable. Climatology is certainly a part of the Information Age!

► Interaction Between Climate Scientists and Nonscientific Professionals

As the human influence on global climate becomes even more indisputable, climate scientists not only will collaborate with other natural scientists but also will interact increasingly with policymakers, social scientists, and the mass media. Policymakers will come under increased pressure to make decisions based on sound science. Versatile specialists who have a background in both climate science and climate policy will be in increasing demand in both the political and environmental consulting arenas and at local, regional, national, and international levels. At the local and regional levels, climate consultants will increasingly work with urban and regional planners and representatives of local industry to ensure greater efficiency in energy use, resource expenditures, and compliance with federal clean air standards.

In the United States and many other parts of the world, emission regulations are becoming stricter over time as technology allows for improved energy efficiency and alternative sources of energy as a means of curtailing anthropogenic *global warming* and enhancing the local quality of life. An improved understanding of the climate system allows for increasing the benefits of industry while reducing the cost of that industry in terms of environmental impact. Likewise, improved understanding of the local climate system will aid in design, engineering, and agricultural applications. These **greening initiatives** are currently being set in place to mitigate future environmental problems. In the national and international spheres, efforts to understand climatic change through modeling and the *empirical approach* will guide policy designed to prevent, mitigate, and adapt to those changes.

Future national and international debate will focus on devising fair and efficient means of ensuring a safe global atmospheric environment while minimizing economic costs. Professional climatologists, such as those who participate in the *Intergovernmental Panel*

on *Climate Change* sanctioned by the United Nations and the *World Meteorological Organization*, will play a central role in these discussions. The strengthening link between climate science and policy will also have repercussions in climatology because of the increased interactions between climatologists and social scientists. The realization that human behavior is likely to affect and be affected by climate will draw such attention. Climatic implications on energy consumption, migration patterns, recreation, disaster planning and management, and political and agricultural systems are only a few of the areas that are likely to receive increasing attention.

As a result of increased awareness of the importance of climate, climatologists are appearing in the local and national media more and more over time. For example, seasonal hurricane forecasts by researchers at Colorado State University generate much public interest. Other documentaries and movies about climatologists have been made in recent years. And many national television newscasts now include climate-related news stories.

► Improved Atmospheric Data Availability and Display

The increasing availability of high-quality atmospheric data for general use will continue to revolutionize the study of climate. Already, atmospheric data are more widely available free of charge than at any previous time. Similarly, other digital data pertaining to the climate system, such as **Normalized Difference Vegetation Index**, which represents the greenness of vegetation measured remotely to give a fast indication of the biophysical response to dryness, are also now readily available. These newly available data sets will facilitate the study of climate by the private sector and by researchers outside of the major research institutions around the world. Furthermore, as future satellite-derived data sets reach lengths of a few decades, new climatic cycles and phenomena will be discovered. In the coming years the influence of sophisticated techniques for analysis and display in climatology will become even stronger. Powerful statistical and other quantitative techniques will continue to characterize the study of climate. Included among these is the increasing implementation of the techniques of **artificial neural networks**—a method of modeling processes computationally in a manner analogous to the processing of information by the human brain, with simultaneous calculations and an ability to “learn” from previously discovered relationships between variables. These statistical methods are especially well-suited to climatology because they can be used to model feedbacks and nonlinear processes—two important and complex features of climate that we have

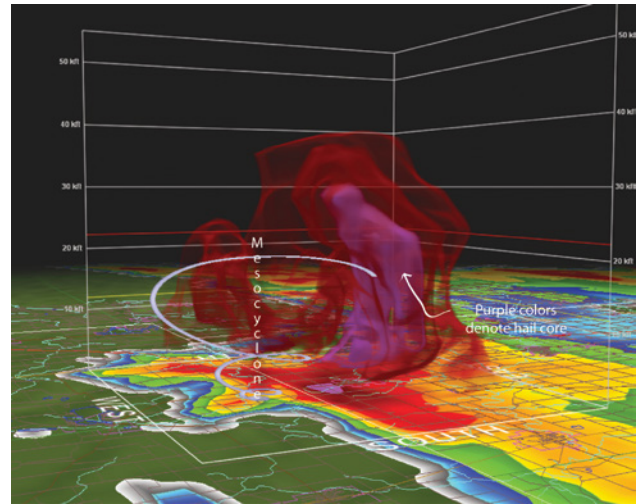


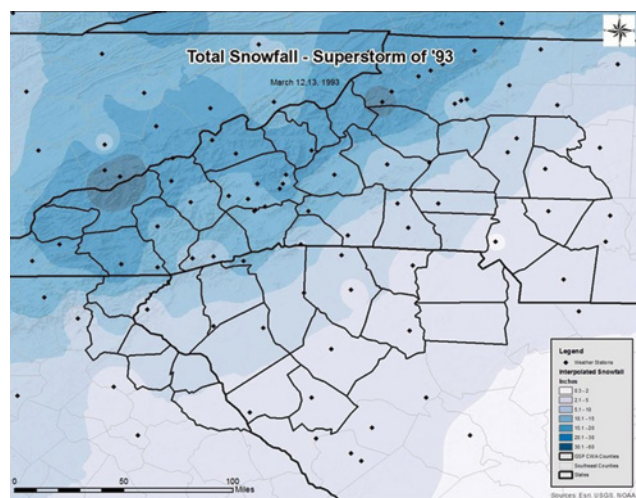
FIGURE 15.1 Three-dimensional Doppler radar image of a developing thunderstorm mesocyclone with hail formation.

Courtesy of the National Weather Service. Retrieved from: https://www.weather.gov/lsx/20070726_supercell.

seen throughout this text. They are also used increasingly in *statistical downscaling* in climate models.

Visualization—a tool of increasing importance for displaying data in climatology—has traditionally referred to the use of maps and other graphics, but in recent years the scope of visualization has broadened with advances in mapping and display technology. For instance, three-dimensional maps showing temperature or pressure surfaces, or rotating updrafts as in **FIGURE 15.1**, are now common. Also, animations that show hurricane structure, pollution *advection*, and other phenomena across space and time simultaneously have revolutionized the way that we can convey information in climatology. Because climate inherently varies across both space and time, the trend toward the increasing use of visualization techniques is likely to continue.

Other tools that will be used with rapidly increasing frequency in climatology involve *geographic information systems (GIS)*—the use of computer hardware and software to assemble, store, update, analyze, and display spatial information and to link nonspatial information to the spatial features. Although some applications may use GIS only for mapping (visualization), GIS can also be used for many more powerful analytical purposes. For example, GIS can measure areas of enclosed polygons, distances between points, or optimal routes on a road map. If you have ever used map websites on the Internet or a phone/electronic device application to find a location, you have already used a GIS. GIS can also be used to provide accurate and high-resolution surface and topographic information, two critical controls in climatic processes, as well as interpolations of point-based observations (**FIGURE 15.2**). As data become more widely available and digital file sizes become more manageable by improvements in technology, an increased need for GIS to analyze those



At the broadest scale, Earth itself operates in a sustainable manner. Nutrients are continuously recycled through biological, chemical, physical, and geological processes over time. All healthy ecosystems exist in a sustainable manner. Humans are the only animals whose practices at broad spatial and temporal scales have impeded the attainment of a sustainable Earth. It is increasingly recognized that humans cannot continue to exist in a nonsustainable lifestyle.

Because business and industry produce so much human-related waste, it is important that those sectors seek to become involved in sustainable practices. The notion of sustainable industry practices led to the **Triple Bottom Line (TBL) concept**. Before the concept of sustainability gained acceptance, the bottom line simply meant economic gain. If a company was profitable, the mission was complete. The TBL concept underscores the importance of not only economic performance (the first bottom line) but also social (second bottom line) and environmental (third bottom line) performance, primarily for the company's own benefit. TBL practices show greater respect for all living things (including humans) as well as the wise management of resources.

Many companies have used the TBL approach to maximize economic performance. For example, a farmer who pays for crop waste to be carried to landfills by a waste removal provider is not running her business in a sustainable fashion. A more sustainable, TBL-based approach involves selling the crop waste to a composting company, which can then use it in the production of an organic fertilizer, or selling the waste directly to other farmers, who can either compost it into fertilizer or use it directly as feedstock. The sustainable practice turns an expense into a money-making venture while simultaneously reducing the amount of material dumped into landfills. Likewise, increased efficiency in automating the acquisition and interpretation of remote sensing imagery in real-time now allows crop dusters to adjust fertilizer applications on the fly, sometimes within seconds. Improved knowledge of the atmospheric dispersion properties on a given day for a given particle size, nozzle size, and application height might allow the same cropduster to spray pesticides only onto the intended crops, with no excess spilling over into a nearby school or subdivision. These examples maximize profits (economic gain) while minimizing health risks (social gain) and protecting the environment (environmental gain).

As an additional advantage, companies can enjoy financial benefit resulting from increasing the public-perceived good will by advertising their "green" practices that minimize their "carbon footprint," because society

is placing increasing value on green initiatives. As public pressures mount, such practices are becoming required of many industries. Lists are now generated which rank major companies and industries according to their levels of "greenness."

Though the TBL approach is becoming increasingly accepted and mastered within the free market system without government interference, the government sector often guides the path toward sustainability, not only through legislation and education but also through direct practice. For example, universities may mandate that only recycled paper be purchased—a practice that requires paper companies to shift their practices to accommodate the demand for recycled products. Government agencies may also require vendors to meet some threshold regarding the generation of waste. Companies vying for government contracts are then forced to reduce waste or face not being hired for the projects. One path to sustainability could involve even more incentives. For example, a government could require that a minimum of 20% of the energy needs of its vendors be provided through renewable sources. Such an incentive would spur the development of solar, wind, geothermal, and other potential energy industries. These energy sources would then become increasingly feasible for public consumption. The resulting decrease in reliance on fossil fuels for energy production would lead to less overall waste and environmental degradation and a trajectory toward sustainability. Such practices would streamline the production of goods and services that are in demand, making the involved industries more profitable, but free market-directed sustainability is the ideal solution.

The ultimate goal of improving the human condition could be achieved by evolving to an entirely sustainable state of existence. Implementation of policy in support of sound climate science should support this goal. Only in a truly sustainable global environment will the ecosystems that further support the human condition be preserved. Technology has progressed to a point whereby true sustainability is possible. We are currently awaiting the proper implementation incentives. Unfortunately, all too often political agendas—rather than science—interfere with optimizing the balance between economic, social, and environmental considerations. Earth and environmental scientists, including climatologists, are far better qualified than politicians to make the difficult (and often unquantifiable) decisions about how to achieve that balance. Sustainability is the *only* path to ensure the long-term health of the only planetary body known to be capable of supporting life, and climatologists should take their rightful place in its pursuit.

► Summary

Climatology will continue to be a vibrant, interesting, and integrative field of inquiry in the foreseeable future. Its importance beyond simply understanding climate “for its own sake” is already being recognized and appreciated by meteorologists and other scientists as well as non-scientists. Improved data quality and availability, along

with improvements in model resolution and increasing use of quantitative methods, will allow climatologists to play an expanding role in understanding the Earth–ocean–atmosphere system and its relationship to human activities. Most importantly, climatologists should contribute toward the goal of achieving sustainability—the only goal that would ensure that continued habitability of our planet into the distant future.

Key Terms

Advection

Anthropogenic

Artificial neural network

Climate Prediction Center (CPC)

Downscaling

Empirical approach

Geographic information

systems (GIS)

Global warming

Greening initiatives

Interglacial phase

Intergovernmental Panel on

Climate Change

National Oceanic and

Atmospheric Administration

National Weather Service

Normalized Difference

Vegetation Index

Positive feedback system

Statistical downscaling

Surface water balance

Sustainability

Teleconnection

Thermohaline circulation

Triple Bottom Line (TBL)

concept

Visualization

World Meteorological

Organization

Terms in italics have appeared in at least one previous chapter.

Review Questions

1. The text suggests that climatology will become increasingly interdisciplinary in the future. Is this an advantage or a disadvantage for the future of climatology? Why?
2. How does the “systems” approach to the study of climate affect the way that climatologists of the future will need to be trained?
3. What advantages do artificial neural networks offer for the study of climate?
4. What advantages do geographic information systems offer for climatologists?

Questions for Thought

1. Imagine yourself applying for a job as a climatologist with the World Health Organization upon graduation. What kinds of skills would you like to be able to tell the interviewer you have acquired?
2. Think back to the types of proxy evidence for paleoclimates that were discussed earlier in the book. Name as many different types of scientists as you can that would participate in each of those types of investigations.
3. What kinds of future changes might occur in higher education and in society in general that would make climatology a more important or less important topic of study?
4. Pick a topic from this book that evokes particular interest to you. What universities specialize in this topic? What scientists are the leading experts in the topic? Are they all from the same discipline? How are their perspectives similar, and how are they different? How does the national science foundation in your home country fund research on that topic? What do you anticipate to be the next great breakthrough in the topic of your interest? Why?



Glossary

Note: Numbers in parentheses indicate chapters in which the term was used.

A

30–60 Day Oscillation See Madden-Julian Oscillation.

40–50 Day Oscillation See Madden-Julian Oscillation.

Ablation The combined effect of melting and sublimation that causes a glacier to retreat. (4, 10, 11)

Absolute dating Any means of assessing the age (in number of years since formation) of rocks, sediments, or fossils by radiometric techniques. (11)

Absolute humidity The mass of water vapor per cubic meter of air. (5)

Absolute vorticity The spin of a body that results from the combined effect of relative vorticity and planetary vorticity. (7, 8)

Absolute zero The theoretical temperature at which all molecular motion ceases and no internal energy is present. (3, 5, 12, 13)

Absorption The process by which radiant energy is retained by matter and converted to internal energy of that matter. (5, 12)

Acacia A type of spiny tree that is characteristic of Tropical Savanna climates. (10)

Accumulated potential water loss In a decreasing availability water balance model, a running total of the $P - PE$ value, used to decrease the modeled loss of water from soil with increasing cumulative aridity. (6)

Accumulation The expansion of a glacier due to the effect of precipitation, condensation, and deposition. (4)

Acid fog A secondary pollutant formed when a primary pollutant interacts with fog droplets to produce a chemical change. (12)

Acid precipitation A secondary pollutant formed when certain primary pollutants interact with water from precipitation, either before or after the precipitation reaches the surface. (12)

Action center A pair of locations where ridging and troughing or pressure anomalies of opposite sign frequently occur simultaneously. (7, 13)

Adaptability The ratio of damage to recovery time in a community for a given hazard or type of hazard. (14)

Adaptation A strategy for dealing with climate change that refers to simply living with the threat and the consequences associated with the threat. (12, 13)

Adiabat A plot on a thermodynamic diagram that shows the temperature profile of an adiabatically moving air parcel at a given place and time. (5)

Adiabatic motion A type of thermodynamic process that occurs without any gain or loss of energy from outside the system. (5, 9, 12, 13)

Adret slope The side of a mountain that is exposed to sunlight. (3)

Advection A type of convection characterized by the horizontal transfer of matter and/or energy. (3, 4, 5, 6, 8, 9, 10, 11, 12, 13, 15)

Advection fog A type of fog that occurs when air flows across a colder surface and is chilled to its dewpoint temperature from below. (9, 10)

Aerosol A tiny suspended solid or liquid particle in the air, including soot, volcanic ash, soil particles, salt crystals, and fog and cloud droplets. (2, 3, 4, 5, 7, 12)

Aghulas current A warm, surface ocean current of the subtropical Indian Ocean that moves southward along the southeastern coast of Africa, guided by the winds on the western side of the Indian Ocean anticyclone. (10)

Agricultural climatology The branch of bioclimatology concerned with the impact of atmospheric properties and processes on living things of economic value, including crops and livestock. (1)

Air mass A body of air that is relatively uniform in its characteristics for distances of hundreds to thousands of square kilometers. (8, 9, 10, 11)

Air Pollution Control Act The 1955 legislation that represented the first attempt at federal oversight of air quality in the United States. (12)

Albedo The ratio of the shortwave energy reflected from a mass divided by the total shortwave energy incident on that mass. (4, 5, 7, 9, 10, 11, 12, 13, 14)

Alberta clipper A midlatitude wave cyclone with cyclogenesis on the eastern side of the Canadian Rockies and a generally east–northeastward track. (9)

Aleutian low The semipermanent subpolar low pressure system over the north Pacific Ocean. (7, 13)

AmeriFlux A network of stations, funded by the U.S. Department of Energy and other federal agencies that provides data on energy, matter, and momentum exchanges in the biosphere, with particular emphasis placed on carbon fluxes. (14)

Amplitude The degree of meridionality of a Rossby or other type of wave. (4, 7)

Anaerobic Any process that occurs in the absence of oxygen. (12)

Analemma A graph in the general shape of a figure eight that shows the equation of time adjustment as a function of solar declination. (5)

Analog forecasting Predicting atmospheric behavior based on the outcome of a similar synoptic situation in the past. (13)

Angiosperm A flowering plant. (11)

Anomaly A departure from the expected atmospheric conditions at a place. (10, 11)

Antarctic Bottom Water (AABW) The deepest global ocean current, circumnavigating Antarctica in all the southern oceans and leading to the Atlantic Deep Water. (4)

Antarctic Circle The 66.5°S parallel of latitude; the most equatorward latitude that experiences 24 consecutive hours of daylight on the December solstice and 24 consecutive hours of night on the June solstice. (3)

Antarctic Deep Water (ADW) A moderately deep and salty part of the global ocean conveyor belt originating near Antarctica that flows northward and upward, eventually flowing beneath the North Atlantic Deep Water. (4)

Antarctic Intermediate Water (AAIW) Part of the global ocean conveyor belt that flows northward beneath South Atlantic and South Pacific waters and above the North Atlantic Deep Water until it converges with northern ocean currents. (4)

Anthropocene Epoch Another name for the Holocene Epoch. (4, 11)

Anthropogenic Human induced. (4, 10, 12, 13, 15)

Anti-CLAW hypothesis The idea that increased stable stratification of the oceans under atmospheric warming could contribute to an acceleration of the warming (i.e., encourage a positive feedback). (4)

Anticyclone Any enclosed area of relatively high pressure, rotating generally clockwise in the northern hemisphere and counterclockwise in the southern hemisphere. (3, 7, 9, 10, 12)

Aphelion The day on which Earth is at its farthest orbital extent from the Sun, corresponding approximately to July 4. (3, 10, 11)

Applied climatology The subfield of climatology concerned with the effects and impacts of climate on various sectors, such as agriculture, forestry, architecture, insurance, engineering, health, and transportation. (1, 14)

Archimedes' principle The notion that the buoyancy of any mass immersed in a fluid is equal to the weight of the fluid that the mass displaces. (11)

Arctic (A) air mass A body of air that is relatively uniform in its very cold and very dry characteristics for hundreds or thousands of square kilometers, emanating from high-latitude source regions that are either inland or over sea ice. (8, 9)

Arctic amplification The notion that polar areas are more sensitive to positive feedbacks that accelerate global warming than tropical areas. (4, 10, 11, 12, 14)

Arctic Circle The 66.5°N parallel of latitude; the most equatorward latitude that experiences 24 consecutive hours of daylight on the June solstice and 24 consecutive hours of night on the December solstice. (3, 5, 9)

Arctic Oscillation (AO) A teleconnection in which pressure anomalies seesaw between the polar region and around 45°N, resulting in variability of the circumpolar vortex, also known as the Northern Annular Mode. (13)

Artificial neural network A method of modeling processes in a manner analogous to the processing of information by the human brain, with simultaneous calculations and an ability to “learn” from previously discovered relationships between variables. (15)

Asian monsoon The seasonal reversal of continental-scale circulation between offshore and onshore in Asia, caused by the winter dominance of the Siberian high and the summer dominance of a thermally driven low-pressure system over southern Asia. (9, 10, 11)

Atlantic Multidecadal Oscillation A cycling of warm and cold surface waters over time scales ranging from about 15 to 30 years. (13)

Atmosphere The thin layer of gases suspended above the surface of a celestial body. (1, 2, 4)

Atmospheric teleconnections The correlations in geopotential height or sea-level pressure patterns across a large area. (13)

Atmospheric general circulation model A complicated computer-based model that simulates and/or predicts global atmospheric circulation based on dynamic conditions but that does not take processes from the hydrosphere, lithosphere, biosphere, or cryosphere into account. (13)

Atmospheric window The range of the electromagnetic spectrum from about 8 to 13 micrometers, in which the atmospheric absorption of terrestrial radiation occurs only when water vapor is abundant. (5, 12)

Atomic mass The total mass of an atom, essentially equal (in atomic mass units) to the sum of protons and neutrons contained in that atom. (11)

Attenuation The depletion of the solar rays as they pass through the atmosphere through the combined effect of absorption and scattering by atmospheric particles. (3, 5, 7)

Autumnal equinox The day of the year midway between the summer and winter solstices, when the solar declination is at the equator, neither hemisphere is tilted toward or away from the Sun, and day length is 12 hours over the entire Earth; currently corresponds roughly to September 22 (the September equinox) for a northern hemisphere observer and March 21 (the March equinox) for a southern hemisphere observer. (3, 10)

Axial tilt The angle between the vertical and Earth's axis; corresponds approximately to 23.5° currently in geological history. (3)

Azimuth angle A coordinate indicating the number of degrees that the Sun's position deviates laterally from true north relative to the observer, ranging from 0° to 360°, with 180° representing a position in the southern sky. (5)

Azores high See Bermuda-Azores high.

B

Backing A counterclockwise change in wind direction with increasing height. (3)

Baroclinic zone Any region (at the surface or aloft) where warm air is laterally adjacent to much colder air. (7)

Baroclinicity The intermixing of radically different air masses. (7, 9)

Beam spreading The dilution of the rays of incoming solar radiation as they penetrate the atmosphere and reach the surface at an oblique angle, as in the high latitudes or near sunrise/sunset. (3, 7)

Beaufort wind scale A simple scale from 0 to 12, based on the observed effect of wind's force rather than the wind speed itself. (14)

Benguela current A cold, surface ocean current of the South Atlantic Ocean that moves northward along the southwestern coast of Africa, guided by the winds on the eastern side of the South Atlantic high. (10)

Bergeron Climatic Classification System A genetic climatic categorization of climate at a place, determined by the frequency with which it is dominated by certain types of weather. (8)

Bermuda-Azores high The semipermanent subtropical high-pressure system over the North Atlantic Ocean. (7, 9, 10, 13)

Bernoulli effect A phenomenon whereby an increase in wind speed above a friction-generating object causes a decrease in air pressure on one side of that object; allows lift of airplanes and undercatch in rain gauges. (6)

Berson westerlies Lower-stratospheric winds that blow from west to east as one phase of the Quasi-Biennial Oscillation. (10)

Bioclimatology The subfield of climatology concerned with the relationship between atmospheric properties and processes and the well-being of humans and other life forms. (1)

Biodiversity The variety in life forms found in a location. (10)

Biome A natural vegetation community. (8)

Biosphere The component of the Earth-ocean-atmosphere system containing life, including parts of the atmosphere, hydrosphere, and lithosphere. (1, 2, 4, 5, 11, 12, 13, 14)

Biotemperature In the Holdridge Life Zones Climatic Classification System, an adjusted temperature that considers temperatures below freezing or above 30°C to provide no contribution to the proliferation of life (i.e., to have a biotemperature of zero) because plants will be dormant whether the temperature is freezing, far below freezing, or above 30°C. (8)

Blaney-Criddle model A simple method of estimating monthly evapotranspiration as a function of a crop-specific coefficient, monthly mean temperature, and monthly percentage of daytime hours of the year. (6)

Blocking anticyclone The positioning of a surface anticyclone or ridge, or an upper-level ridge over the same location for a period of many days, resulting in an extended period of synoptic-scale subsidence and clear, dry conditions. (9)

Bolide A meteor. (11)

Bolling-Allerod interstadial The interval of time immediately following the Last Glacial Maximum, characterized by abrupt global warming. (11)

Bora wind Winds forming in the Balkan highlands and spilling toward lower elevations through gaps in the Dinaric Alps toward the Adriatic Sea. (9)

Boreal cold interval The globally cold phase that immediately followed the Pre-Boreal warm interval. (11)

Boreal forest The extensive, slow-growing coniferous forest of subarctic climates of North America and Eurasia. (4, 9)

Borehole A hole drilled into the ground in which temperature can be measured and used to infer air temperature at some point in the past. (11)

Bottleneck A significant drop in population that triggers rapid genetic divergence in surviving individuals. (11)

Boundary-layer climatology The subfield of climatology concerned with atmospheric properties and exchanges of energy, matter, and momentum in the near-surface atmosphere. (1)

Brown smog See Photochemical smog.

Budyko Climatic Classification System A method of categorizing climates based on the ratio of energy received to energy required to evaporate local precipitation. (8)

Budyko ratio In the Budyko Climatic Classification System, the ratio of net radiation received to the energy required to evaporate a unit volume of local precipitation; a ratio of 1.0 separates dry from humid climates. (8)

Buoyancy The tendency of a fluid to float on top of a denser fluid. (5)

Butterfly effect The magnification of errors over time as described by chaos theory caused by erroneous or unknown initial conditions. (13)

C

California current A cold ocean current of the eastern North Pacific Ocean that moves southward near the west coast of North America, guided by the winds on the eastern side of the Pacific high. (4, 9, 12, 13)

Cambrian Explosion The time in the beginning of the Paleozoic Era characterized by the rapid evolution of species in response to a warming climate. (11)

Canary current A cold, surface ocean current of the North Atlantic Ocean that moves southward along the northwestern coast of Africa, guided by the winds of the eastern side of the Bermuda-Azores high. (4, 9, 10)

Cap and trade policy A policy that limits total carbon dioxide emissions to the atmosphere by companies or nations, but allows the sale of “carbon credits” from companies or nations that emit less carbon dioxide than their imposed quota to companies or nations that emit more carbon dioxide than their quota allows. (12)

Carbon cycle The continuous movement of carbon through the Earth–ocean–atmosphere system. (2, 13)

Carbon Dioxide Information Analysis Center (CDIAC) An agency within the U.S. Department of Energy that produces the often-used global Historical Climatology Network and disseminates data related to atmospheric composition, fossil fuel consumption, and the carbon cycle. (14)

Carbon monoxide (CO) A colorless, odorless gas monitored by the U.S. Environmental Protection Agency as a criteria pollutant. (12)

Carbonic acid (H_2CO_3) A weak acid formed by the bonding of carbon dioxide and water. (12)

Carboniferous The period of geologic time in the Paleozoic Era from about 290 to 345 million years ago; subdivided into the Pennsylvanian and Mississippian. (11)

Catastrophism The notion that cataclysmic events reshape Earth’s environment to a greater extent than gradual, persistent forces. (11)

Cenozoic Era The present era of geological time, which began with the K-T extinction approximately 65 million years ago and contains the Tertiary and Quaternary Periods. (11)

Centrifugal acceleration (CA) An apparent acceleration directed radially outward from the center of curvature in a rotating system, caused by the inertia of the rotating mass. (3, 5)

Chaos theory An idea suggesting an inherent lack of predictability in some systems despite the fact that an order underlies them because small occurrences that may be difficult or impossible to model can create large impacts to apparently unrelated phenomena. (13)

Charles’ Law The property of an ideal gas that temperature and density are inversely related if pressure is held constant. (2)

Chimú floods Ancient periodic flooding in the Moche Valley of Peru, believed to be linked to extreme El Niño events. (4)

Chinook wind A warm, dry wind caused as air descends the leeward sides of the western mountain ranges in North America (except southern California). (9)

Chlorofluorocarbon (CFC) A family of compounds consisting of carbon, hydrogen, oxygen, and fluorine that are used for various domestic and industrial purposes; these compounds bond with monatomic oxygen in the atmosphere, thereby preventing the formation of ozone, and also act as minor greenhouse gases. (2, 10)

Circle of illumination The imaginary line, as viewed from space, that separates the illuminated and dark halves of Earth at any given time. (3)

Circumpolar vortex An area of strong winds aloft encircling the hemisphere and surrounding the high surface atmospheric pressures with low geopotential heights aloft that form over the poles. (7, 9, 10, 12, 13)

Class A Evaporation Pan An instrument used for measuring evaporation, consisting of a metal pan 4 ft in diameter that sits on a short wooden platform and is exposed to the elements. (5)

Clausius-Clapeyron equation The equation that expresses saturation vapor pressure as a function of temperature. (5, 6, 13)

CLAW hypothesis The idea that increased emission of dimethyl sulfides to the atmosphere by increasing phytoplankton growth could regulate the warming that may have allowed phytoplankton population growth to occur. (4)

Clean Air Act of 1963 The first major effective legislation in the United States for regulating air quality and monitoring both stationary pollution sources, such as power plants, and mobile pollution sources, such as automobiles. (12)

Clean Air Act of 1970 Sweeping legislation that created the Environmental Protection Agency and required it to identify criteria pollutants to be monitored, determine the National Air Quality Standards of those criteria pollutants, and set up state-level environmental protection agencies in each state. (12)

Climate The long-term, overall state of the atmosphere at a given place, both at the surface and aloft, including not only the mean conditions but also variability and seasonality of those conditions and factors that cause those conditions. (1)

Climate division A subset of a state of the United States into which point-based climatic data are aggregated for analysis and display. (6)

Climate Monitoring and Diagnostics Laboratory An agency within the U.S. National Oceanic and Atmospheric Administration that maintains data related to stratospheric ozone concentrations and other atmospheric phenomena. (14)

Climate Prediction Center (CPC) The office within the federal National Weather Service (NWS) and National Oceanic and Atmospheric Administration (NOAA) that generates products and information for describing and predicting climatic variation on time scales from weeks to years, with the intent of reducing the risk and increasing resilience to the effects of climate on society. (15)

Climatological Data (CD) A monthly publication of the National Climatic Data Center for each state that contains a monthly summary of statewide precipitation for that month, along with both means and extremes of temperature, as well as other daily data for all official monitoring stations in the state. (14)

Climatological Data Annual Summary (CDAS) A monthly publication from the National Oceanic and Atmospheric Administration for each state that contains monthly totals by site in that state for each month in that year, as well as annual compilation statistics. (14)

Climatology The scientific study of climate; the branch of the atmospheric sciences that analyzes the long-term state of the atmosphere, explains the causes of those conditions, and forecasts possible changes in those conditions at seasonal time scales and beyond. (1)

Climograph A representation of the monthly mean temperature (using a line) and precipitation (using bars) for each month of the year at a place. (8, 9, 10)

Cloud seeding The intentional introduction of substances into the atmosphere in an attempt to cause or enhance precipitation. (1)

Cluster analysis A quantitative technique in which the scores resulting from an eigenvector analysis are grouped together based on their position in n -dimensional space, where n is the number of components derived by the analysis. (8)

Coastal Kelvin wave Poleward-moving ocean waves along the western coast of the Americas, resulting from the splitting of the eastward-moving equatorial Kelvin wave at the coast. (4)

Co-kriging A variant of kriging in which spatial interpolation can be performed by considering the effect of other variables on the spatial interpolation of the variable being mapped using a kriging procedure. (6)

Cold air damming A condition whereby low-level cold air becomes trapped as a midlatitude surface anticyclone or cyclone forces surface air toward a mountain range, often along the eastern sides of both the Rocky and the Appalachian mountains when synoptic-scale systems track eastward. (9)

Cold air drainage Any situation in which cold, dense air is pulled to lower elevations by gravity. (9)

Cold front A narrow zone separating two air mass types in which the colder air mass is actively displacing the warmer air mass. (8, 9)

Cold Steppe (BSk) climate A semiarid climate in which the mean annual temperature is below 18°C (64°F). (9, 10)

Colorado wave cyclone A midlatitude wave cyclone with cyclogenesis on the eastern side of the Rockies in the vicinity of Colorado and tracking generally northeastward. (9)

Common factor analysis A type of eigenvector analysis that assumes some underlying uniqueness among the variables that contributes to the eigenvector. (13)

Common Water (CW) The deepest large-scale component of the global ocean circulation in the Pacific Ocean, originating near Antarctica as a branch of the Antarctic Bottom Water. (4)

Component A mode of variability in a data set revealed in principal components analysis or another form of eigenvector analysis, analogous to a regression line in bivariate regression analysis. (8, 13)

Condensation The phase change of water molecules from a gaseous to a liquid state. (2, 4, 5, 6, 12)

Condensation nuclei Solid aerosols that encourage the conversion of water vapor to liquid water around them. (4, 12)

Conditional instability An atmospheric condition in which rising motion is encouraged if the atmosphere is saturated but discouraged if the atmosphere is unsaturated. (5)

Conduction The transfer of energy by one molecule to another molecule touching it, and then to the next molecule, etc. (2, 5, 11, 12)

Confluence The horizontal convergence of air streams moving in the same direction at a given altitude. (7)

Conservation of angular momentum The property of curved motion that states that the product of mass, velocity, and radius of curvature is constant. (7)

Constant absolute vorticity trajectory The characteristic movement of air in a manner such that the total amount of vorticity is conserved, resulting in the wavelike shape of Rossby wave flow across the midlatitudes. (7)

Constant gas A component of the atmosphere that maintains its concentration across space and time. (2)

Content analysis An objective method of converting qualitative text into discrete categories for inferring climatic conditions from historical writings. (11)

Continental polar (cP) air mass A body of air that is relatively uniform in its cold and dry characteristics for hundreds or thousands of square kilometers, emanating from inland, high-latitude source regions. (8, 9, 13)

Continental tropical (cT) air mass A body of air that is relatively uniform in its hot and dry characteristics for hundreds or thousands of square kilometers, emanating from inland, low-latitude source regions. (8, 9, 10)

Continentality The degree to which a location is distant from a large body of water. (3, 4, 7, 9, 10)

Continuity equation The equation found in all general circulation models and weather forecasting models, also known as the *mass conservation equation*, that ensures that the amount of mass entering any imaginary three-dimensional “box” centered on a gridpoint must be balanced by the amount of mass leaving adjacent boxes to enter the box of interest. Likewise, the amount of mass leaving the imaginary box of interest must be balanced by mass entering adjacent boxes from it. (13)

Convection The vertical transfer of matter and the energy that accompanies it through a fluid. (2, 3, 4, 5, 7, 9, 10, 12, 13)

Convective precipitation Precipitation resulting from atmospheric instability, particularly on warm, sunny afternoons; associated with cumuliform cloudiness. (10, 14)

Cooling degree-day (CDD) An index of the amount of cooling that is required for human comfort in a building; 1 CDD is accumulated for each degree that the daily mean temperature rises above the base temperature of 65°F (18°C). (14)

Coriolis effect (CE) An apparent deflective force that causes moving objects to appear to be deflected to the right in the northern hemisphere and to the left in the southern hemisphere, resulting from the rotation of Earth. (3, 4, 5, 7, 9, 10, 11, 13)

Coriolis parameter The product of twice the angular velocity of Earth and the sine of the latitude; proportional to the magnitude of the Coriolis deflection, it represents the magnitude of planetary vorticity. (7, 9, 13)

Counter-radiation Longwave radiation emitted by the atmosphere downward to the surface. (5, 11, 12)

Counter-trade winds Surface winds immediately north of the equator that blow from southwest to northeast, and immediately south of the equator that blow from northwest to southeast, resulting from Coriolis deflection in the opposite direction from the trade winds as the air crosses the equator. (10)

Coupled atmosphere–ocean general circulation model A complicated computer-based model that simulates and/or predicts global atmospheric and oceanic circulation based on dynamical conditions, including effects of feedbacks and energy transfer between these fluids. (13)

Crest The magnitude of peak streamflow following a precipitation event, expressed either as the water height in the stream or as the volume of stream discharge. (6)

Cretaceous–Paleogene (K–Pg) extinction event A mass extinction at the end of the Mesozoic Era; also known as the *K–T extinction*. (11)

Cretaceous Period The last period in the Mesozoic Era, terminating about 65 million years ago with the K–T extinction. (11)

Criteria pollutant Pollutants that are deemed to be sufficiently widespread and dangerous in the United States that they should be monitored at the federal level by the Environmental Protection Agency; includes sulfur oxides, carbon monoxide, particulates, lead, nitrogen oxides, and photochemical oxidants. (12)

Crop heat unit (CHU) An index of the exposure of crops to the warmth required for growth, commonly used in Canada; for each degree above the base (for both minimum and maximum daily temperature), 1 CHU is reported for that calculation, but for each degree that the maximum temperature surpasses the optimal temperature, 1 CHU is lost. (14)

Crop Moisture Index (CMI) A water balance–based measure of drought severity in which moisture in the uppermost layers is emphasized, for suitability in many agricultural applications. (6)

Cross-cutting relationships A principle used in relative dating techniques that any igneous rock formation must be younger than sedimentary rock layers through which it cross-cuts. (11)

Cryogenian Period The last period of the Proterozoic Eon, from about 800 to 600 million years ago, which coincided with perhaps the most impressive glaciation in geological history. (11)

Cryosphere The component of the Earth–ocean–atmosphere system comprising frozen water in all its forms (glaciers, sea ice, surface ice, permafrost, and snow) seasonally or “permanently.” (1, 4, 5, 6, 11, 12, 13, 14)

Cumuliform cloud A set of liquid droplets and ice suspended in the atmosphere oriented vertically, characterized by localized cloudiness and perhaps short periods of relatively intense precipitation. (8, 9, 10)

Cumulonimbus cloud A set of liquid droplets and ice suspended in the atmosphere oriented vertically in very unstable atmospheric conditions; severe weather clouds. (8, 9)

Cyclogenesis The beginning stage of storm formation. (7, 9)

Cyclone Any enclosed area of relatively low pressure, rotating generally counterclockwise in the northern hemisphere and clockwise in the southern hemisphere. (3, 4, 7, 8, 9, 10, 12)

D

Daily mean temperature The average temperature at a given place over the course of a day, calculated simply by averaging the maximum and minimum temperature for that day. (1)

Daily Synoptic Series A booklet of seven daily surface and 500-mb weather maps, produced and circulated by the U.S. National Oceanic and Atmospheric Administration. (14)

Dalton Minimum The interval from about 1796 to about 1830 when fewer than normal sunspots were reported. (11)

Daughter isotope The form of an element that remains after the radioactive decay of the parent isotope. (11)

December solstice The day of the year when the solar declination is at the Tropic of Capricorn, the northern hemisphere is tilted maximally away from the Sun, the southern hemisphere is tilted maximally toward the Sun, and day length is minimized in the northern hemisphere and maximized in the southern hemisphere; currently corresponds to December 22 and the winter solstice for a northern hemisphere observer and the summer solstice for a southern hemisphere observer. (3)

Decreasing availability water balance model A method of accounting for water in the Earth–ocean–atmosphere system at a location over a period of time; assumes that as soil-moisture withdrawal increases, the water becomes increasingly more difficult to be moved upward via evapotranspiration. (6)

Deficit (D) The amount of water (in centimeters or inches of equivalent precipitation) needed by the atmosphere over a given time period but not supplied to the atmosphere either through precipitation or soil moisture withdrawal. (6, 8, 9, 10)

Deforestation The systematic and widespread clearing of forested landscapes. (4, 6, 10, 11, 12, 13)

Dendroclimatology The science of using annual tree rings to infer paleoclimates. (11)

Density A physical property of matter represented by the ratio of mass to volume. (2, 5, 7, 12, 13)

Deposition The transformation of water molecules from a gaseous state directly to a solid state. (4, 5, 6, 9, 10)

Depression storage Water that is stored in puddles, gutters, and other natural or human-made “depressions” on the landscape. (6)

Desertification The conversion of a climate toward increasing aridity, either through natural or anthropogenic causes. (4, 10, 12, 13)

Dewpoint temperature (T_d) The temperature at which saturation occurs at a given place and time. (5, 6, 9, 10, 13)

Dextral An individual of a species of foraminifera whose shell developed with a coiling on the right side, thereby suggesting that the ocean was relatively warm at the time that the individual lived. (11)

Diabatic A type of heating or cooling that occurs from external sources through energy exchange in fulfillment of the second law of thermodynamics; includes solar radiation, latent heating or cooling, and sensible heating in the boundary layer. (13)

Diffluence The horizontal spreading of air streams moving in the same direction at a given altitude. (7)

Diffuse radiation Solar radiation that is scattered in the atmosphere down to the surface. (5)

Diffusion The process by which molecules spread and intermix as a function of their kinetic energy of motion in compliance with the second law of thermodynamics.

Dimensionless quantity A ratio or constant that has no units associated with it. (5, 13)

Dimethyl sulfide A compound emitted by phytoplankton that can act as condensation nuclei in the atmosphere. (4)

Direct radiation Solar radiation that is neither absorbed, scattered, nor reflected in the atmosphere but is instead transmitted to Earth's surface. (5, 9)

Dixie Alley The region of high tornado frequencies from Texas to Florida. (9)

Doldrums A nickname given to the belt of calm winds between the northeast trades and southeast trades. (7)

Downdraft A local downward rush of air associated with a cumulonimbus cloud. (3)

Downscaling The process of using statistical or mathematical techniques to derive a finer spatial and/or temporal scale than is output by a general circulation model. (13, 14, 15)

Downwelling An oceanic condition commonly found on the western sides of ocean basins in which surface airflow pushes water against a coastline, forcing it to sink. (4)

Dry deposition A process by which acid precipitation is produced only after the precipitation reaches the surface and interacts with soil water to produce the acids. (12)

Dryline The line of contact between a maritime tropical air mass and a continental tropical air mass in the warm sector of a midlatitude wave cyclone. (9)

Dryness index (DI) In the Thornthwaite Climatic Classification System, the ratio of deficit to potential evapotranspiration in the surface water balance at a location. (8)

Dust Veil Index (DVI) A scale used to estimate the total amount of particulate matter in the atmosphere based on surface air temperatures and the amount of solar radiation reaching the surface. (4)

Dynamic climatology The physics of broad-scale atmospheric motion at long time scales. (1)

Dynamic downscaling The process of focusing computing resources on a smaller spatial scale to use knowledge of the dynamics of weather systems to derive a finer spatial and/or temporal scale than is output by a general circulation model. (13)

Dynamic instability An inherent lack of predictability in a complicated process, despite the presence of order within that process. (13)

E

East African low-level jet A fast-moving river of east-to-west-flowing air that develops during the daytime hours across the East African coastline. (10)

East-coast occlusion An occluded front characterized by a cold, dry air mass moving into warmer, wetter maritime air, inducing strong vertical lift, cumulonimbus cloud development, and heavy precipitation, similar to the case of a cold front. (9)

Easterly wave A “kink” in the trade wind flow that represents a location where low pressure associated with the Intertropical Convergence Zone can extend slightly farther poleward than elsewhere. (10)

Eccentricity The degree to which Earth's orbit deviates from being circular at any given time in geological history. (11, 13)

Ecotone A transition zone between two biomes. (8, 9)

Eddy covariance The measurement of turbulent fluxes of energy, matter, and momentum based on measured covariance of fluctuations between vertical wind velocity (for vertical fluxes) and changes in temperature, specific humidity, and horizontal wind speed, respectively. (5)

Eigenvalue In eigenvector analysis, the total variance accounted for by a component. (8, 13)

Eigenvector analysis A family of quantitative techniques based on algebraic transformation of a data matrix to allow for relationships between two different sets of variables to be analyzed simultaneously; in climatology, these techniques are most often used for the simultaneous examination of variability and changes in climate across space and time. (8, 13)

Ekman spiral The idealized depiction of the change in wind vector with height in the atmosphere, or the flow vector in the oceanic boundary layer, caused by changes in the impact of friction and Coriolis deflection with distance from the surface. (3, 4, 5, 10)

El Chichón A volcano that erupted in southern Mexico in 1982. (11)

Electromagnetic spectrum The full assemblage of all possible wavelengths of energy of the form that advances as disturbances in electrical and/or magnetic fields. (2, 5)

El Niño An oceanic phenomenon during which the normal accumulation of warm tropical waters in the western tropical Pacific migrates eastward, resulting in a decrease in the upwelling of cold water along the tropical South American coast. (4, 9, 10, 11, 13)

El Niño–Southern Oscillation (ENSO) event The combined oceanic and atmospheric alterations that result from the migration of warm tropical waters from the western to the eastern tropical Pacific Ocean. (4, 10)

Empirical approach The use of climatic data to uncover historical trends in variables and relationships between variables. (12, 14, 15)

Empirical Bayesian kriging A spatial analytic technique that allows multiple variograms to be created for subsets of the data during modeling instead of assuming that a singular variogram fits the entire surface. (6)

Empirical climatic classification system Any method of categorizing climates based on the data that represent the effects of the forcing mechanisms rather than the causes of the climates. (8)

Energy balance The relationship between the radiant flux received at the surface and the convective and conductive fluxes. (5)

Energy balance model A representation of the (usually global) availability of energy to account for effects of changes to inputs, reservoirs, or surface features such as global cloud cover, soil moisture, or deforestation. (13)

Environmental lapse rate (γ) The rate at which temperature decreases with increasing height in a static atmosphere; the global annual average is 6.5 °C/km but varies widely across space and time. (2, 5, 9)

Environmental Protection Agency The office of the U.S. government created by the Clean Air Act of 1970, designed to promote healthy environmental conditions in the United States. (12)

Eon The broadest division of geological time, lasting for hundreds of millions or billions of years. (11)

Epoch A unit of geological time within a period. (11)

Equal availability water balance model A method of accounting for water in the Earth–ocean–atmosphere system at a location over a period of time, by assuming that soil water is equally available to be evapotranspired regardless of the amount of storage in the soil. (6)

Equation of state The relationship of pressure to temperature and density (or specific volume) in an ideal gas; also known as the *ideal gas law*. (3, 5, 7, 13)

Equation of state for moist air The relationship of pressure to temperature and density (or specific volume) in an ideal gas, when the effect of water vapor in the air is taken into account. (13)

Equation of time An adjustment made when computing solar time from zone mean time to account for the slight variations in Earth's orbital velocity throughout the year; a function of time of year. (5)

Equatorial (E) air mass A body of air that is relatively uniform in its very warm and moist characteristics for hundreds or thousands of kilometers, emanating from low-latitude, oceanic source regions. (8, 10)

Equatorial Kelvin wave A near-surface wave that propagates from west to east across the tropical Pacific Ocean, particularly during El Niño events, in opposition to the normal trade wind–induced waves. (4, 10)

Equatorial Rossby wave A near-surface wave that propagates from east to west across the tropical Pacific Ocean

in response to the equatorial Kelvin wave, signaling the demise of an El Niño event. (4)

Equilibrium line The line at which the rate of accumulation equals the rate of ablation in a glacier. (4)

Equinox A day on which 12 hours of daylight occur worldwide; corresponds approximately to March 21 and September 22. (5)

Era The broadest division of geological time within an eon. (11)

Eukaryote Multicelled organisms that evolved in Earth's early ocean and released carbon dioxide to the atmosphere through fermentation. (2)

EuroFlux A network of stations established in 1995 that provides data on energy, matter, and momentum exchanges in the biosphere across a wide range of climatic types in Europe, with particular emphasis placed on carbon fluxes. (14)

Eustatic Globally uniform, as in sea level. (10, 11)

Evaporation The transformation of water molecules from a liquid to a gaseous state directly, without being routed through vegetation in the process. (1, 2, 3, 4, 5, 6, 7, 8, 9, 10, 11, 12, 13)

Evapotranspiration (ET) The movement of water from the soil to the atmosphere either directly or after moving upward through vegetation. (5, 6, 8, 9, 10, 12, 14)

Extreme An unusually high or low value of a measured atmospheric feature at a given place and time. (1, 8, 11)

F

Faint young Sun paradox The apparent contradiction that solar output was weaker early in Earth's history than today, despite the lack of convincing evidence that the Earth was ever significantly colder than today. (2, 11)

Federal Weather Service The forerunner of the National Weather Service in the United States, established in 1870 as a component of the U.S. Army. (14)

Fermentation The process by which simple organisms acquire energy through the breakdown of food in the absence of oxygen, releasing carbon dioxide to the atmosphere. (2)

Fick's law The principle that the flux of any entity is proportional to the gradient of that entity in the fluid through which the flux occurs. (5)

Field capacity In the surface water balance, the maximum amount of precipitated water (in centimeters of equivalent precipitation) capable of being held in a soil against the force of gravity; also known as *soil moisture storage capacity*. (6)

Filchner Ice Shelf One of two thick, vast sheets of ice protruding from Antarctica into the Weddell Sea, which opens to the Atlantic Ocean. (10)

Findlater jet See Somali jet.

Fine particles See PM_{2.5}.

Finite differencing In computer models, a technique for calculating the value of each atmospheric variable at a gridpoint based on the calculated values at each adjacent point (including the points above and below the point of interest). (13)

First law of thermodynamics The principle that energy can never be simply created or destroyed in nature; it may only change from one form to another. (5, 11, 13)

Fischer-Porter rain gauge An instrument that collects precipitation in a bucket, measures it based on the water's weight, and punches a special tape mechanically every 15 minutes to report a running total of the precipitation (in tenths of an inch) since the bucket was emptied. (14)

Fluorocarbon A family of chemicals emitted to the atmosphere by industrial activities; although very minute in concentration, an extremely efficient absorber of terrestrial energy. (12)

Flux A flow. (2, 3, 5, 6, 10, 14)

Föhn wind Warm, dry winds caused when air flows down the leeward side of the Alps and undergoes adiabatic warming. (9)

Foraminifera An order of mostly marine protozoans that can provide evidence of paleoclimatic conditions. (11)

Forced convection See Mechanical turbulence.

Fossil fuel Hydrocarbon deposit (primarily in the form of coal, oil, and natural gas) derived from formerly living matter that releases carbon dioxide, methane, and other compounds to the atmosphere when burned. (2, 4, 11, 12, 14)

Free atmosphere The layer above the transition layer of the troposphere beginning at approximately 1 km above the surface; characterized by the negligible impact of friction. (3, 5)

Free convection See Thermal turbulence.

Frequency The rate of occurrence of a particular phenomenon at a particular place over a long period of time. (1)

Friction A force caused by one body resisting the forward motion of an adjacent mass. (1, 3, 5, 10, 12, 13)

Frigid Zone The area of Earth having the coldest climatic type in the climatic classification system of the ancient Greeks. (8)

Front A narrow zone between two air masses with distinct temperature and moisture conditions. (8, 10)

Frostpoint temperature The temperature to which the air would have to be cooled for saturation to be reached and frost to form at a given place and time. (5)

Fumigation event A situation that exists when limited vertical mixing and a highly stable atmosphere cause deadly concentrations of a pollutant to accumulate near the emission source. (12)

G

Geiger counter An instrument for detecting and measuring radioactivity. (11)

General circulation The interconnected mechanisms by which energy is transferred across the atmosphere at the planetary scale. (7)

General circulation model (GCM) Any complicated computer-based model that simulates and/or predicts global atmospheric circulation based on dynamic conditions. (13)

Genetic climatic classification system Any method of categorizing climates based on the causes of the climates rather than the data that represent the effects of the forcing mechanisms. (8)

Geographic information systems (GIS) Computer hardware and software used to assemble, store, update, analyze, and display spatial information and to link nonspatial information to the spatial features. (6, 15)

Geopotential height The altitude (in meters above sea level) of a given pressure surface over a particular location at a certain time. (7, 8, 9, 10, 13)

Geostrophic balance An equilibrium established between the pressure gradient force and the Coriolis effect, when the effects of other forces such as friction are negligible; results in air flowing parallel to isobars with higher pressure to the right of the flow in the northern hemisphere and to the left of the flow in the southern hemisphere. (3, 5, 7, 10)

Geostrophic flow In the oceans, the flow resulting from a balance between the tendency of the Coriolis effect (manifested as the Ekman spiral) and gravity. (4)

Geostrophic wind The airflow that results when the pressure gradient force balances the Coriolis effect and other forces are negligible; results in air flowing parallel to isobars. (3, 9)

Glacial advance Any time during an ice age when "permanent" ice is migrating equatorward and downslope. (10, 11)

Glacial erratic A rock that differs in composition from the surrounding geology, suggesting that a glacier must have moved the rock from a location near other rocks similar to its composition to its present location. (11)

Glacial phase Any interval of time within an ice age characterized by an equatorward and downslope displacement of ice. (11, 12)

Global dimming The long-term, slight decrease in solar radiation striking Earth's surface in the latter part of the twentieth century. (12)

Global Energy and Water Cycle Experiment (GEWEX) An initiative as part of the World Climate Research Programme that promotes an improved understanding of the global energy and hydrologic budgets by providing data on fluxes of energy, water, and momentum between the surface and the atmosphere, both on land and in the ocean. (14)

Global hydrologic cycle The constant cycling of water (in all of its forms) throughout the Earth-ocean-atmosphere system. (1, 6, 11)

Global Hydrology Center A U.S. agency within the National Aeronautics and Space Administration that provides a wide array of satellite-based observations for climatological research, including such variables as lightning strikes, aerosol loadings, and data for studies of cloud formation and physics. (14)

Global warming Irreversible increases in Earth's surface atmospheric temperatures caused by increasing greenhouse gas concentrations. (4, 10, 12, 15)

Global water balance equation The expression of precipitation as the sum of evapotranspiration and runoff. (6)

Gondwanan Ice Age The period of “permanent” ice on Earth’s surface at the end of the Paleozoic Era, occurring after the breakup of Pangaea. (11)

Gradient Richardson number (Ri) An index for describing the relative importance of thermal and mechanical turbulence and for assessing atmospheric stability in the local, near-surface atmosphere. (5)

Gradient wind equation The equation that relates the speed of air moving in curved flow to geostrophic wind speed. (9)

Gray smog See Industrial smog.

Great Dying The mass extinction that occurred at the end of the Paleozoic Era. (11)

Great Oxygenation Event The first known major mass extinction event; caused by the buildup of atmospheric oxygen by cyanobacteria, which caused the demise of oxygen-intolerant life. (11)

Greenhouse effect The phenomenon by which Earth’s lower atmosphere is warmed by the presence of gases that absorb longwave radiation from the Earth and emit radiation downward to the Earth. (2, 4, 9, 10, 11, 12)

Greenhouse gas An atmospheric pollutant that contributes to the greenhouse effect by enhancing the efficiency of absorption of longwave radiation emitted from the surface and reemitting radiation back downward effectively as counter-radiation. (2, 4, 9, 11, 12)

Greening initiatives The use of improved technology and understanding of the Earth–ocean–atmosphere system to enhance the quality of the environment. (15)

Gridpoint model A representation of circulation created by dividing Earth into equidistant points with imaginary three-dimensional “boxes” centered on those points representing the smallest area in the atmosphere for which motion can be calculated. (13)

Gridpoint technique A spatial analytic method for converting point data to areal data, in which an artificial grid is superimposed over the study region, point totals are calculated for each of the resulting gridpoints based on an inverse-distance-weighted function of the value at each of the known stations, and the mean of the derived values represents the areal mean. (6)

Groundwater Water stored below the soil layer. (6)

Growing degree-day (GDD) An index of the exposure of crops to the warmth required for growth; one unit is accumulated for each degree that the daily mean temperature exceeds the theoretical minimum daily temperature required to provide enough energy for that crop to grow. (14)

Growing season The interval of time between the last spring frost and the first autumn frost. (14)

Guard cell A cell on a leaf that works as part of a pair to control the opening of a stomate. (5, 6)

Gulf Coast cyclone A midlatitude wave cyclone with cyclogenesis in the northwestern Gulf of Mexico and a general northeastward track. (9)

Gulf Stream A warm ocean current flowing northward along the eastern coast of North America and becoming the North Atlantic Drift near northwestern Europe. (3, 4, 9, 11)

Gust front See Outflow boundary.

Gymnosperm Plants such as conifers that do not have seeds enclosed within an ovary. (11)

Gyre A circular current in the near-surface ocean, caused by a coupling of the atmospheric and surface oceanic circulation around a subtropical anticyclone. (4, 7, 9, 10)

H

Hadley cell A convection cell, with rising motion near the equator at the Intertropical Convergence Zone and sinking motion near 30° latitude in each hemisphere, most prominent at the longitude experiencing diurnal heating at any given time. (7, 9, 11)

Half-life The amount of time required for one-half of the parent atoms to decay into daughter product in a radioactive element. (11)

Harmattan winds Northeasterly surface winds that blow hot, dry, Sahara Desert winds toward the Gulf of Guinea region in association with the northeast trade winds. (10)

Hawaiian high The semipermanent subtropical high-pressure system over the northern subtropical Pacific Ocean; also known as the *North Pacific high*. (7, 9, 10, 12)

Hazard An event with the potential to threaten and endanger the surrounding natural environment and adversely affect the health, safety, welfare, and property of the human environment. (14)

Heat capacity The amount of heat (energy) necessary to be added to a unit volume of a substance to raise its temperature by one Kelvin; distinguished from specific heat by the fact that specific heat refers to a unit mass rather than a unit volume. (12)

Heat index A contrived “temperature” based on how the temperature “feels” for people by taking into account the ease with which evaporative cooling can occur. (3, 9)

Heating degree-day (HDD) A variable that indexes the amount of heating that is required for human comfort in a building; 1 HDD is accumulated for each degree that the daily mean temperature falls below the base temperature of 65°F (18°C). (14)

Heterosphere The layer of the atmosphere corresponding to the thermosphere, characterized by a layering of gases according to density. (2)

Highland (H) climate In the Köppen system, a climate type in rugged terrain characterized by great climatic contrasts across space caused by elevation differences. (9, 10)

Historical Climatology Network A data set of mean monthly temperature, precipitation, and sea level pressure for thousands of stations worldwide for time periods of up to 50 years. (14)

Holdridge Life Zones Climatic Classification System A global categorization system of climate, most commonly

used in tropical areas, that incorporates annual precipitation and the derived PE-to-precipitation ratio. (8)

Holocene Epoch The current epoch of geological time; embedded within the Quaternary Period, corresponding to the current interglacial phase and the last 10,000 years. (4, 11)

Holocene Interglacial Phase The most recent time in geological history, consisting of the last 9000 years, comprising the vast majority of the Holocene Epoch, characterized by the poleward and upslope retreat of the “permanent” ice on Earth’s surface. (4, 11)

Homosphere The layer of the atmosphere corresponding to the troposphere, stratosphere, and mesosphere where atmospheric gases are continuously mixed by winds. (2)

Horizontal convergence The collision of two streams of air moving laterally in opposite directions, or from the same direction but with one stream moving faster and “catching up with” the other. (10)

Horse latitudes Generic term for the latitudinal belt around 30°N and 30°S. (7)

Hot Steppe (BSH) climate A semiarid climate in which the mean annual temperature is above 18°C (64°F). (9, 10)

Hourly Precipitation Data (HPD) A publication issued monthly by the U.S. National Oceanic and Atmospheric Administration that provides hourly precipitation data for sites in each state, along with the maximum intensity of precipitation to fall within specific time durations during that month. (14)

Human bioclimatology The study of the relationship between people and the atmospheric environment immediately surrounding them and affecting their health, comfort, and performance. (1)

Humboldt (Peru) current A cold, surface ocean current of the South Pacific Ocean that moves northward along the coast of South America, guided by the winds of the eastern side of the South Pacific high. (4, 10)

Humid Continental (Dfa, Dfb) climate In the Köppen system, a climatic type of the midlatitudes generally found inland and on the east coasts of continents, characterized by warm to hot summers, cold winters, and wet conditions year-round. (9)

Humid Continental (Dwa, Dwb) Winter Dry climate In the Köppen system, a climatic type of the midlatitudes generally found inland and on the east coasts of continents, characterized by warm to hot summers, cold winters, and wet conditions only in the warm season. (9)

Humid Subtropical (Cfa) climate In the Köppen system, a climatic type of the near-tropical midlatitudes characterized by hot summers, mild winters, and wet conditions year-round. (9, 10)

Humid Subtropical Winter Dry (Cwa) climate In the Köppen system, a climatic type of the near-tropical midlatitudes characterized by hot summers, mild winters, and wet conditions except in the cold months. (9, 10)

Humidity index (HI) In the Thornthwaite Climatic Classification System, the ratio of monthly surplus to potential

evapotranspiration in the monthly surface water balance at a location. (8)

Humus Partially decomposed organic matter in soil. (12)

Hurricane Regional name given to the strongest type of tropical cyclone in the Atlantic Ocean basin. (9, 10, 11, 12, 14)

Hybrid climatic classification technique Any method of climatic categorization in which investigator-identified “prototype” atmospheric circulation patterns are used as input into an automated cluster analysis, so that other maps can be matched automatically to the prototype map that they most resemble. (8)

Hydrocarbon A type of compound that contains only hydrogen and carbon. (12)

Hydroclimatology The study of the interaction between the atmosphere and near-surface water at long time scales; the atmospheric component of the global hydrologic cycle. (1)

Hydrosphere The component of the Earth–ocean–atmosphere system consisting of liquid water, including the oceans, groundwater, surface streams and lakes, atmospheric water, and soil water. (1, 2, 4, 5, 6, 11, 13, 14)

Hydrostatic equation The equation that relates changes in pressure to changes in height and density in an atmosphere characterized by hydrostatic equilibrium. (5, 13)

Hydrostatic equilibrium A balance between the downward-directed gravitational force and the upward-directed buoyancy force in the atmosphere. (2, 3)

Hygrometer An instrument that measures relative humidity. (5)

Hygroscopic nuclei Solid aerosols that act as very efficient condensation nuclei. (12)

Hypsithermal A period of time from about 8000 to 5000 years ago, characterized by global average temperatures that were perhaps 2 C° (4 F°) above today’s levels. (11)

I

Ice age Any time in geological history during which ice exists continuously for a long period of time over some section of Earth. (4, 11)

Ice Cap (EF) climate In the Köppen system, a climatic type of the high latitudes characterized by mean temperatures below freezing in every month of the year. (9, 10)

Ice core A sample drilled into an ice surface and brought to a laboratory for subsequent analysis of composition of air bubbles, pollen grains, and other proxy evidence of paleoclimates. (11, 12)

Icelandic low The semipermanent subpolar low-pressure system over the North Atlantic Ocean. (7, 9, 13)

Ideal gas law See Equation of state.

Indian Ocean Dipole A set of sea surface temperature anomalies in which warmer than normal conditions occur in the western Indian Ocean near Somalia while cold temperature anomalies occur simultaneously in the eastern

Indian Ocean near Indonesia and Australia, or vice versa. (10, 13)

Indian Ocean high The subtropical anticyclone of the Indian Ocean. (7, 10)

Industrial smog A secondary pollutant that results from chemical reactions between sulfur dioxide (SO₂) and particulates; also known as *gray smog* and *London smog*. (12)

Inertia The property of matter that causes it to retain its velocity (or lack thereof) until acted upon by a force. (3)

Inertial period The length of time required for a fluid's inertia to be balanced by the Coriolis effect. (3)

Infiltration The downward movement of water from the surface into the soil and plant rooting zone. (6, 9)

Initialization The setting of initial conditions in a model in preparation for a forecast. (13)

Insolation Incoming solar (shortwave) radiation; radiation emitted by the Sun and intercepted by the Earth–ocean–atmosphere system. (2, 3, 4, 5, 6, 7, 9, 10, 11, 12, 13, 14)

Interception Water held on surfaces other than the soil, such as tree leaves and rooftops, until it eventually evaporates. (6)

Interglacial phase Any interval of several thousand years within an ice age when “permanent” ice is present but not very extensive on Earth's surface. (4, 11, 15)

Intergovernmental Panel on Climate Change An international group sanctioned by the United Nations and the World Meteorological Organization to address issues and policies related to global climate change. (12, 15)

Internal energy The capacity for individual molecules to move. (13)

International date line The imaginary zigzagging line roughly corresponding to the 180° meridian of longitude; by international agreement, calendars are advanced by one calendar day when moving westward across this line and calendars are set backward one day when moving eastward across the line. (5, 9)

Intertropical Convergence Zone (ITCZ) The belt of low surface pressure around the equatorial region of Earth, caused by rising motion in the general circulation. (7, 10)

Inverse square law The axiom stating that the intensity of radiation received by a body is inversely proportional to the square of the distance between the emitting and the receiving body. (11)

Inverted trough An elongated zone of low pressure in the tropics that extends poleward (in either hemisphere). (10)

Isobar A line on a map that connects locations having the same atmospheric pressure. (3)

Isohyet A line on a map that connects locations having the same precipitation total over a given period of time. (6)

Isohyetal method A spatial analytic method for converting point data to areal data, in which isolines are drawn based on the point data and the mean value between each isoline is weighted by the percentage of area enclosed between those isolines to determine the overall areal mean value. (6)

Isohypse On upper-level atmospheric maps, a line connecting locations having the same geopotential height. (7, 9, 10)

Isostatic rebound A local rising in continental crust as a reaction to the weight of ice being removed; results in a decrease in local sea level. (11)

Isotherm A line on a map that connects locations having the same temperature. (3, 6, 7, 9)

Isothermal layer Any zone in the atmosphere in which temperature changes relatively little with height, as in the lower stratosphere. (2)

Isotope A form of an element having the same number of protons but different numbers of neutrons from another form of that element. (11)

Iterative Involving repetition, as in the repetitive automated calculation of solutions to a set of differential equations until one is found. (13)

J

Jet streak The region of greatest wind speed within a jet stream. (7)

Jet stream A fast-moving river of air that moves generally from west to east across the upper troposphere. (4, 7)

Joule The metric unit of energy or work, equivalent to 1 kilogram times 1 square meter divided by 1 squared second. (3, 5, 6, 12, 13)

June solstice The day of the year when the solar declination is at the Tropic of Cancer, the northern hemisphere is tilted maximally toward the Sun, the southern hemisphere is tilted maximally away the Sun, and day length is maximized in the northern hemisphere and minimized in the southern hemisphere; currently corresponds to June 21 and the “summer solstice” for a northern hemisphere observer and the “winter solstice” for a southern hemisphere observer. (3)

K

K-T extinction A relatively sudden mass elimination of approximately 85% of the species existing on Earth that occurred about 65 million years ago. (11, 12)

Katabatic wind A local circulation in which air moves downslope, typically at night when the air adjacent to the surface increases in density as it cools; also known as *mountain wind*. (9, 10)

Keeling curve The graph of increasing atmospheric carbon dioxide through time, measured continuously since 1957 at the Mauna Loa Observatory in Hawaii. (2)

Keetch-Byram Drought Index A measure of moisture conditions designed to assess the risk of fire potential by examining the relationship of evapotranspiration to precipitation in the organic matter on a forest floor and in the uppermost soil layers. (6)

Kelvin temperature scale A direct system of representing the internal energy content of matter by maintaining proportionality between temperature and internal energy. (3, 5, 6, 7, 12, 13)

Kinetic energy Energy possessed by a body as a consequence of the motion of that body (rather than the molecular motion of individual particles within that body). (3, 5, 7, 13)

Köppen Climatic Classification System An empirical method of categorizing climates so that they correspond to major biomes, based on monthly temperature and precipitation data and the seasonality of those data. (8)

Krakatau A volcano in Indonesia that erupted in 1883, causing massive damage and fatalities. (10, 11)

Krakatau easterlies Lower-stratospheric winds that blow from east to west as one phase of the Quasi-Biennial Oscillation. (10)

Kriging A geostatistical technique that allows for the estimation of data at a point based on values across adjacent points while also taking into account the degree of uncertainty and variability in the spatial distribution of the data. (6)

Kyoto Treaty An international agreement that requires wealthy nations contributing most of the world's greenhouse gases to reduce their collective greenhouse gas emissions to 5.2% below the 1990 levels. (12)

L

Labrador current A cold surface ocean current that moves southward along Canada's Atlantic coast. (9)

Lake effect snow Snow that forms immediately downwind of a large lake, with totals enhanced by the moisture and atmospheric instability provided by the lake. (3, 9)

Laki Fissure A volcano that erupted in Iceland in 1783, causing devastating impacts. (11)

Lamb Weather Types A climatic classification system based on the position of a location relative to a midlatitude wave cyclone, designed for application in the British Isles. (8)

Laminar layer The few millimeters of the atmosphere nearest to the surface or elements on the surface, such as crops, trees, buildings, or waves on the sea. (5)

La Niña An oceanic phenomenon during which the normal accumulation of warm tropical waters in the western tropical Pacific is even more exaggerated than usual, associated with a strengthening of the trade winds and Walker circulation, and an increase in the upwelling of cold water along the tropical South American coast. (4, 10, 11, 13)

Lapse rate A rate of change of temperature with height. (5)

Latent energy (heat) Radiant energy that evaporates water in the Earth-ocean-atmosphere system rather than heating the atmosphere or surface. (3, 4, 8, 9, 10, 12, 13)

Latent heat flux See Turbulent flux of latent heat.

Latitude A set of imaginary lines that runs east-west and measures distances north or south of the equator; 0° latitude corresponds to the equator, with 90°N and 90°S corresponding to the North and South Poles, respectively. (3, 4, 5, 6, 7, 8, 9, 10, 13)

Laurentide Ice Sheet The large mass of ice that occupied most of northern North America during the Quaternary glacial advances. (11)

Leeward Downwind; the side of a topographic feature facing away from the wind. (3, 7, 8, 9, 10)

Level of nondivergence The height in the atmosphere at which neither convergence nor divergence is occurring, despite having convergence above it and divergence below it (or vice versa). (7)

Lifting condensation level The height in the atmosphere at which the air becomes saturated and an adiabatically rising air parcel no longer cools at the unsaturated adiabatic lapse rate but begins cooling instead at the saturated adiabatic lapse rate; corresponds to a cloud base. (5)

Lithification The process by which sedimentary rock is formed from compaction and cementing together of unconsolidated sediments. (12)

Lithosphere The uppermost part of the solid Earth, from the surface to approximately 100 km of depth; the solid-Earth component of the Earth-ocean-atmosphere system. (1, 2, 4, 5, 6, 11, 13, 14)

Little Climatic Optimum (LCO) The period from about AD 900 to about 1450, characterized by relatively warm conditions in Europe; also known as the *Medieval Warm Period*. (11, 12)

Little Ice Age (LIA) The period from approximately AD 1450 to 1850, characterized by colder global conditions than at present. (11, 12)

Loading In eigenvector analysis, a coefficient that is proportional to the degree to which the eigenvector model represents the variability in each observation of one set of variables collectively for all observations in another set of variables simultaneously; in climatology, the loadings often represent the correlation between a component and the atmospheric variable of interest at each station in the data set, collectively across all times of observation. (8, 13)

Local apparent time See Solar time.

Local Climatological Data (LCD) A monthly publication of the National Climatic Data Center of the National Oceanic and Atmospheric Administration for about 270 sites around the United States; contains data with temporal resolution as high as every 3 hours and data for more variables than *Climatological Data* provides. (14)

Local scale A spatial scale of analysis between about 0.5 and 5 km (0.3 and 3 mi), including atmospheric phenomena that generally persist from a few minutes to a few hours. (1, 13, 14)

Loch Lomond Stadial The European name for the Younger Dryas. (11)

Loess A fine, angular-grained soil or wind-blown deposit formed by the grinding of glaciers against bare rock until it forms a powdery consistency. (11)

Logarithmic wind profile The theoretical variation of wind speed with height under neutral stability conditions, in which wind speed varies linearly with the natural logarithm of height. (5)

Longitude A set of imaginary lines that runs north–south and measures distances east or west of the prime meridian; 0° longitude corresponds to the prime meridian, and 180° corresponds approximately to the international date line. (3, 5, 7, 9, 10, 13)

Long-term Ecological Research (LTER) Program An initiative that collects and disseminates bioclimatological data (along with other environmental information such as hydrological measurements, soil composition and quality, land-use change, and even demographic data) for 26 sites across North America, the Caribbean, and Antarctica. (14)

Long wave See Rossby wave.

Longwave radiation Electromagnetic radiation at wavelengths greater than 4.0 micrometers, generally considered in the atmospheric sciences to be synonymous with radiation emitted by Earth and the atmosphere. (5, 9, 10, 11, 12)

Loop current A surface ocean circulation that branches away from the Gulf Stream into the Gulf of Mexico immediately west of the Florida peninsula. (9)

Low-level jet stream (LLJ) A river of air at approximately the 800- to 900-mb level, moving northward from the western Gulf of Mexico at perhaps 40 to 110 km hr⁻¹ (25 to 70 mi hr⁻¹). (9)

Lysimeter An instrument that is installed underground and weighs the soil and vegetation on top of it to measure volumetric water content. (5, 6)

M

Madden-Julian Oscillation (MJO) A system of continual intra-annual variations of upper- and lower-level winds, sea surface temperatures, and associated cloudiness and precipitation in the tropical Pacific Ocean. (10, 13)

Magma Molten rock material beneath Earth's surface. (11)

March equinox The day of the year midway between the December and June solstices, when the solar declination is at the equator, neither hemisphere is tilted toward or away from the Sun, and day length is 12 hours over the entire Earth; currently corresponds roughly to March 21. (3)

Marine Dry Winter (Cwb) climate A variant of the Marine West Coast climate found in a small area of southeastern Africa and Madagascar, characterized by warm summers, mild winters, and abundant precipitation except in winter. (10)

Marine West Coast climate In the Köppen system, a climatic type of the mid to high latitudes characterized by warm to mild summers, cool winters, and wet conditions year-round. (9)

Marine West Coast Cool Summer (Cfc) climate A Marine West Coast climate with only 1 to 3 months having average temperatures above 10°C (50°F). (9)

Marine West Coast Warm Summer (Cfb) climate A Marine West Coast climate with more than 3 months having average temperatures above 10°C (50°F). (9, 10)

Maritime Continent Australia and the islands southeast of continental Asia, including Indonesia, the Philippines, New Guinea, and thousands of other islands occupying the tropical and southwestern Pacific Ocean basin. (4, 10, 11)

Maritime effect A moderating influence on temperature by bodies of water, caused primarily by the high specific heat of water, circulation within water, relatively high transparency of water, and latent heating over water bodies. (3, 4, 9)

Maritime polar (mP) air mass A body of air that is relatively uniform in its cool and humid characteristics for hundreds or thousands of square kilometers, emanating from high-latitude oceanic source regions. (8, 9)

Maritime tropical (mT) air mass A body of air that is relatively uniform in its warm and humid characteristics for hundreds or thousands of square kilometers, emanating from low-latitude oceanic source regions. (8, 9, 10)

Mass conservation equation See Continuity equation.

Mass spectrometry An instrumental laboratory technique that can determine the chemical composition of a substance. (11)

Maunder Minimum The interval of time from about AD 1645 to 1715 in which few sunspots were observed. (11)

Maximum/minimum thermometer A special type of instrument that measures temperature by leaving a mark at the highest temperature that had occurred since the last resetting of the instrument and having the base of the mercury sit at the lowest temperature since the last resetting. (14)

Mean free path The distance that an atom or molecule must travel in the atmosphere before encountering another atom or molecule. (2)

Mechanical turbulence Microscale convective motion resulting from vertical gradients of horizontal momentum. (5)

Medieval Warm Period See Little Climatic Optimum.

Mediterranean (Cs) climate In the Köppen system, a climatic type of the midlatitudes characterized by dry and warm to hot summers and by mild, wet winters. (9, 10, 12)

Mediterranean Hot Summer (Csa) climate In the Köppen system, a Mediterranean climate characterized by a warmest month averaging above 22°C (72°F). (9, 10)

Mediterranean Warm Summer (Csb) climate In the Köppen system, a Mediterranean climate characterized by a warmest month averaging below 22°C (72°F). (9, 10)

Meltemi wind A katabatic wind system that develops when high pressure occurs over the Balkan region near Hungary and a cyclonic center lies to the southeast near or over Turkey, resulting in an offshore wind blowing over the Aegean Sea. (9)

Meridional flow Rossby waves with high amplitudes (i.e., pronounced ridges and troughs), characterized by strong north–south and south–north components of atmospheric motion. (7, 13)

Mesopause The boundary separating the mesosphere from the thermosphere. (2)

Mesoscale A spatial scale of analysis between about 5 and 100 km (3 and 60 mi), including atmospheric phenomena that typically persist from a few hours to a few days. (1, 13)

Mesosphere A layer of the atmosphere in which temperature decreases with height, from about 48 to 80 km (29 to 50 mi) above the surface. (2)

Mesothermal Any of the mild, midlatitude climatic types in the Köppen classification system, including Humid Subtropical, Mediterranean, Marine West Coast, and Marine Dry Weather climates. (8, 9, 10)

Mesozoic Era The era of geological time with generally warm conditions, beginning at the end of major extinctions associated with the Gondwanan Ice Age approximately 250 million years ago and ending with the K-T extinction about 65 million years ago. (11)

Meteorology The scientific study of weather; the atmospheric science that analyzes the properties and causes of atmospheric conditions at a specific place and time. (1)

Methane (CH₄) A compound consisting of one atom of carbon and four of hydrogen that acts as a greenhouse gas despite a very low atmospheric concentration. (2, 4, 11, 12)

Methane hydrates Frozen lattices of water molecules surrounding CH₄ molecules. (12)

Methanogen Any of various bacteria that are intolerant of atmospheric oxygen and give off methane. (2, 11, 12)

Micrometer One millionth of a meter, represented by μm . (2, 12)

Microscale A spatial scale of analysis smaller than about 0.5 km (0.3 mi), including atmospheric phenomena that typically persist from a few seconds to a few hours. (1, 5, 13, 14)

Microthermal Either of the cold, midlatitude climatic types in the Köppen classification system, including Humid Continental and Subarctic. (8, 9)

Midlatitude Cold Desert (BWk) climate In the Köppen system, a climatic type characterized by potential evapotranspiration that far exceeds precipitation and a climatological mean annual temperature that is below 18°C (64°F). (9, 10)

Midlatitude (frontal) wave cyclone The largest storm systems on the planet, consisting of a low-pressure center with cyclonic circulation and fronts extending from that low-pressure center. (3, 8, 9, 12)

Midlatitude westerlies The prevailing general circulation feature over the middle latitudes in both hemispheres, both at the surface and aloft, in which flow occurs primarily from west to east. (7, 9, 10, 12)

Milankovitch cycle Any of the three axial and orbital variations (eccentricity, precession, tilt) that cause Earth's climate to vary on time scales of thousands of years. (11, 13)

Millibar A unit of pressure in the metric system equivalent to 100 Pascals; average sea level pressure is 1013.25 mb. (3, 5)

Mississippian Period A period in the latter part of the Paleozoic Era largely within the Gondwanan Ice Age, from about 350 to 325 million years ago. (11)

Mistral wind Air that flows downslope from the Alps and spills though the Rhone Valley, where it spreads along the Mediterranean coast of France. (9)

Mitigation A strategy for dealing with climate change that attempts to decrease the risk associated with the threat rather than decreasing the threat itself. (12, 13)

Mixing ratio The dimensionless ratio of the mass of water vapor present in the air to the mass of dry air. (13)

Moisture conservation equation The equation in general circulation models that expresses the change in moisture content at a gridpoint as the sum of the contribution of moisture via advection and the contribution via phase changes. (13)

Moisture index (MI) In the Thornthwaite Climatic Classification System, a variable calculated as the ratio of the difference between total surplus and deficit to potential evapotranspiration at a location. (8)

Momentum A property of a body in motion equivalent to the product of mass and velocity. (1, 3, 4, 5, 7, 11, 13, 14)

Monsoon A seasonal reversal of wind caused by synoptic-scale pressure changes, often accompanied by seasonal changes in moisture. (9, 11)

Moraine A large pile of rock and soil debris deposited by a glacier. (11)

Mountain wind See Katabatic wind.

Mount Pinatubo A volcano in the Philippines that erupted on June 15, 1991, and has been linked to a temporary reduction in subsequent global temperatures. (11)

Mount St. Helens A volcano in the state of Washington that had a catastrophic eruption on May 18, 1980. (11)

Mount Toba A volcano that erupted in Sumatra about 71,000 years ago, accelerating the last glacial advance. (11)

Muller Weather Types A climatic classification system based on the position of a location relative to a midlatitude wave cyclone, designed for application on the U.S. Gulf Coast. (8)

Multivariate ENSO Index A representation of the intensity of an El Niño or La Niña episode that uses a combination of many other variables, including sea level pressure, sea surface temperatures, wind vectors, and cloud cover. (4)

N

National Aeronautics and Space Administration (NASA) An independent agency of the federal government that oversees the U.S. space flight program. (14)

National Air Quality Standards (NAQS) The maximum concentration of a pollutant (in parts per million of the atmospheric molecules) that is deemed by the U.S. Environmental Protection Agency to be acceptable. (12)

National Center for Atmospheric Research (NCAR) A federally funded research center in Boulder, Colorado, that provides research opportunities and data, including the re-analysis data set. (13, 14)

National Centers for Environmental Information (NCEI) A U.S. federal agency within the National Environmental Satellite, Data, and Information Service (NESDIS), within National Oceanic and Atmospheric Administration (NOAA), that archives and disseminates atmospheric data. (14)

National Centers for Environmental Prediction (NCEP) A branch of the U.S. National Weather Service that provides specialized forecasts through nine offices, including the Climate Prediction Center, Hydrometeorological Prediction Center, Aviation Weather Center, Tropical Prediction Center, and Storm Prediction Center. (14)

National Climate Program Act The 1978 legislation that greatly increased the scope and mission of atmospheric data collection and archiving in the United States and included the establishment of the Regional Climate Centers. (14)

National Data Buoy Center (NDBC) A U.S. federal agency within the National Oceanic and Atmospheric Administration that is responsible for dispatching and maintaining a network of buoys and coastal stations around North America and in some other parts of the world that collect atmospheric data. (14)

National Environmental Satellite, Data, and Information Service (NESDIS) The office within the National Oceanic and Atmospheric Administration in the United States that collects and disseminates atmospheric and other geophysical data. (14)

National Oceanic and Atmospheric Administration (NOAA) The federal agency in the United States that includes the National Weather Service in addition to managing the nation's fisheries, and collecting and disseminating environmental data. (6, 12, 14, 15)

National Snow and Ice Data Center (NSIDC) A U.S. federally funded center that provides cryospheric data, including snow cover, glaciers, continental ice sheets, avalanches, permafrost, and sea ice. (14)

National Weather Service The present federal agency that oversees government-sponsored weather forecasting in the United States, established in 1970 when the U.S. Weather Bureau was renamed and moved to the Department of Commerce. (1, 3, 5, 6, 14, 15)

Navier-Stokes equations of motion The three equations found in all general circulation models that express motion in the west–east, south–north, and down–up directions. (3, 13, 14)

Nebula A vast cloud of interstellar dust, from which stars and planets form. (2)

Negative feedback system An input to a system that decreases the likelihood of further changes of the same type to the system. (4, 12)

Negative vorticity Rotation that is clockwise in the northern hemisphere or counterclockwise in the southern hemisphere; anticyclonic rotation. (7)

Neogene Period The interval of geologic time between 23.1 million years ago and 1.8 million years ago. (11)

Net radiation (Q^*) The difference between radiant energy absorbed by matter and that emitted by matter. (5, 6, 8)

Neutral atmosphere An atmospheric condition in which the buoyancy force balances the gravitational force, and a hypothetical air parcel will neither rise nor sink once a lifting force is removed. (5)

Newton (N) The metric unit of force. (3)

Newton's laws of motion The physical laws that govern flow upon which the Navier-Stokes equations are based. (3)

Newton's second law of motion The notion that force on a moving body can be expressed as the product of mass and acceleration. (2, 7, 13)

Niño 3.4 Index A representation of the intensity of an El Niño or La Niña episode based on sea surface temperatures in the region of the tropical Pacific Ocean bounded by 120°W–170°W and 5°S–5°N. (4)

Nitric acid (HNO_3) A very strong acid formed by complicated processes involving interactions between nitrogen oxides and water. (12)

Nitric oxide (NO) A type of nitrogen oxide photodissociated from NO_2 in the presence of ultraviolet radiation in the troposphere; monitored by the U.S. Environmental Protection Agency as a criteria pollutant. (12)

Nitrogen dioxide (NO_2) A type of nitrogen oxide that is noted for wearing away objects in contact with it; monitored by the U.S. Environmental Protection Agency as a criteria pollutant. (12)

Nitrogen oxide (NO_x) Any compound formed by the bonding of a nitrogen atom with one or more atoms of oxygen; monitored by the U.S. Environmental Protection Agency as a criteria pollutant. (12)

Nitrous oxide (N_2O) A non-natural greenhouse gas that contributes a tiny percentage to the anthropogenic effect. (12)

Noise See Random variability.

Nonattainment zone Any area that persistently exceeds the satisfactory concentration threshold of a pollutant. (12)

Nonthreshold pollutant A contaminant that evokes a response as soon as it exists at any concentration. (12)

Nor'easter A midlatitude wave cyclone with cyclogenesis over the mid-Atlantic coast near Cape Hatteras and a generally north–northeastward track in the Atlantic Ocean. (9, 14)

Northern Annular mode See Arctic Oscillation.

Normal The average measurement of an atmospheric feature at a given place and time. (1, 8)

Normalized Difference Vegetation Index A representation of the greenness of vegetation measured via remote sensing techniques to give an indication of the biophysical response to dryness on the landscape.

North American summer monsoon The tendency for onshore flow associated with a thermal low centered over Arizona in summer, resulting in more precipitation in late summer than in the rest of the year. (9)

North Atlantic Deep Water (NADW) A part of the global ocean conveyor belt originating from the remnant of the

North Atlantic Drift; flows southward near the coast of North America in the Atlantic Ocean and eventually above the Antarctic Deep Water. (4)

North Atlantic Drift The northernmost part of the Gulf Stream current; moderates the climate of northwestern Europe. (3, 4, 9, 11)

North Atlantic Oscillation (NAO) A teleconnection in which pressure patterns seesaw between the Bermuda-Azores high and the Icelandic low. (13)

North Equatorial current An east-to-west flow of surface water in the northern hemisphere immediately north of the equator. (4, 9)

North Pacific high See Hawaiian high.

North Pacific Intermediate Water (NPIW) A part of the global ocean conveyor belt in the Pacific Ocean that overlies the Pacific Subarctic Water. (4)

Northeast trade winds The dominant surface circulation pattern in the tropical northern hemisphere, with consistent winds blowing from northeast to southwest. (4, 7, 10)

Nuclear autumn A somewhat less dramatic scenario than “nuclear winter” of the impact of large-scale detonation of nuclear weapons on the Earth–ocean–atmosphere system. (12)

Nuclear fusion A process in star formation in which lighter elements (principally hydrogen) are converted into heavier elements (primarily helium). (2)

Nuclear winter The notion that a widespread detonation of nuclear weapons could create so much soot that it would effectively block the Sun’s energy from reaching much of Earth’s surface for up to several years, leading to widespread surface cooling. (12)

O

Occluded front A surface front that results in the late stage of a midlatitude wave cyclone’s life cycle after the cold front has overtaken the warm front; results in warm sector being wedged upward between cold air behind the cold front and cool air ahead of the warm front. (8, 9)

Occlusion The process by which a cold front overtakes a warm front in a midlatitude wave cyclone. (9)

Oceania A broad geographic region of the Pacific Ocean, including the Maritime Continent (except for Australia) and the islands comprising Melanesia, Micronesia, and Polynesia. (10)

Oceanic general circulation model A complicated computer-based model that simulates and/or predicts global hydrospheric circulation based on dynamic conditions. (13)

Oort cloud A collection of icy comets, dust, and debris surrounding the outer edges of our solar system. (2)

Optical air mass The ratio of the distance of the path length of a beam of insolation to the minimum distance (perpendicular to the surface) that it could possibly have to travel to reach the surface. (5)

Ordovician Period A period of geological time from about 490 through 440 million years ago, within the Paleozoic Era,

during which a massive extinction coincided with a major but short-lived glaciation. (11)

Ordovician-Silurian extinction event The third major mass extinction and second greatest in intensity, occurring from approximately 460 to 430 million years ago. (11)

Orogeny The process by which mountains form. (11)

Orographic effect The enhancement of precipitation on the windward sides of slopes. (3, 6, 9, 10)

Oroshi wind A katabatic wind system in Japan, similar to the bora of Europe. (9)

Outflow boundary A line of contact between a cold downdraft that hits the surface in a thunderstorm and warmer air in advance of the system. (9)

Outgassing The release of gases from the lithosphere to the atmosphere—for example, as through volcanic activity. (2, 4)

Ozone (O₃) A molecule containing three oxygen atoms that absorbs ultraviolet radiation in the stratosphere but represents a toxic pollutant to humans in the troposphere. (2, 10)

P

Pacific Decadal Oscillation (PDO) A teleconnection in sea surface temperatures of the north Pacific Ocean, with the action centers located in the tropical central to eastern Pacific and the northwestern Pacific. (4, 13)

Pacific-North American (PNA) pattern A teleconnection that represents the oscillation between geopotential height in the midtroposphere of northwestern North America, with opposing heights upwind in the northern Pacific and downwind in the southeastern United States. (13)

Pacific Subarctic Water (PSW) Part of the deep water conveyor belt emanating from the Common Water and moving northward in the Pacific Ocean. (4)

Paleoclimatologist A scientist who studies climates of the preinstrumental period. (11)

Paleoclimatology The scientific study of climates of the preinstrumental period and the causal mechanisms that produced those climates. (1, 11)

Paleogene Period The interval of geologic time between 66 million years ago and 12.1 million years ago. (11)

Paleotempestology The science of identifying signatures of ancient storms primarily from sediment records. (11)

Paleozoic Era The first era within the current Phanerozoic Eon, lasting from about 540 to 250 million years ago, beginning with the first fish and shellfish and ending with the massive Permian extinction. (11)

Palmer Drought Severity Index (PDSI) A water balance–based measure of drought severity in which relatively deep soil-moisture conditions are emphasized, for assessing long-term moisture conditions. (6)

Palmer Hydrological Drought Index A water balance–based measure of drought severity used for even longer-term analysis than the Palmer Drought Severity Index, used to assess conditions relating to groundwater availability and reservoir supplies. (6)

Palynology The scientific study of pollen, particularly as an indicator of paleoenvironmental conditions. (11)

Pan adjustment coefficient A factor used to adjust measured Class A pan evaporation downward to provide an estimate of potential evapotranspiration. (5)

Pangaea The supercontinent that existed during the late Paleozoic Era. (11)

Parallelism The property of Earth's axis of remaining tilted at the same fixed angle throughout its revolution about the Sun. (3)

Parameterization A statistically based "correction factor" used when the precise equations to simulate a process are either unknown or impossible to include in a model because the input data are not available to solve the equation. (13)

Parent isotope The form of an element that exists before radioactive decay begins. (11)

Particulates A criteria pollutant monitored by the U.S. Environmental Protection Agency consisting of a family of tiny suspended solid aerosols. (4, 12)

Pascal A metric unit of pressure equal to one Newton per square meter. (3, 5, 7, 13)

Path length The distance through the atmosphere that a ray of insolation travels. (3, 5)

Penman-Monteith equation A theoretical, physically based method of computing potential evapotranspiration, requiring the measurement of net radiation, substrate heat flux, vapor pressure (or some humidity measurement that can be converted to vapor pressure), temperature, and resistance. (6)

Pennsylvanian Period A period in the latter part of the Paleozoic Era following the Mississippian Period and largely within the Gondwanan Ice Age, from about 325 to 300 million years ago. (11)

Percolation The gradual downward movement of water through the lithosphere to replenish the groundwater supply. (6)

Perihelion The day on which Earth is at its nearest distance from the Sun, corresponding approximately to January 3. (3, 10, 11)

Period The largest subdivision of geological time within an era, usually lasting tens of millions of years. (11)

Periodic variability A fluctuation from the mean of any atmospheric variable that recurs with some relatively constant regularity. (11)

Permafrost Permanently frozen subsoil. (4, 9)

Permeability The property that describes the ability of water to flow through soil (or rock, in the case of groundwater recharge). (6)

Permian Period The last period in the Paleozoic Era, at the end of the Gondwanan Ice Age, from about 300 to 250 million years ago, coinciding with perhaps the most complete mass extinction other than the one occurring presently. (11)

Peroxyacetyl nitrate A family of secondary pollutants formed when nitric oxide from photodissociated nitrogen dioxide combines with volatile organic compounds. (12)

Peru current See Humboldt current.

Phanerozoic Eon The current eon of geological time, beginning approximately 540 million years ago with the beginning of the Paleozoic Era and the evolution of the first fish and shellfish. (11)

Photochemical smog A secondary pollutant formed when sunlight interacts with a primary pollutant, triggering a chemical change; also known as *brown smog*. (12)

Photodissociation The splitting apart of molecules caused by exposure to radiation. (2, 12)

Photosynthesis The process by which green plants use sunlight to synthesize food. (2, 4, 5, 10, 11, 12, 14)

Physical climatology The study of the nature of atmospheric energy and matter at long time scales. (1)

Phytoplankton Aquatic microorganisms that derive their energy from photosynthesis. (4, 10)

Pineapple Express A type of midlatitude wave cyclone moving from near Hawaii across California, common during El Niño winters. (9)

Plane of the ecliptic The imaginary plane bisecting Earth and the Sun, on which Earth and other planets revolve about the Sun. (3)

Planetary albedo The component of solar radiation reaching the top of Earth's atmosphere reflected by cloud tops, scattered by atmospheric particles back to space, or reflected from the surface all the way out to space. (5)

Planetary boundary layer The lowest 500 to 1000 meters of the atmosphere, including the laminar, roughness, and transition layers. (5)

Planetary scale The broadest spatial scale of climatological analysis, including phenomena on the order of 10,000 to 40,000 km (6,000 to 24,000 mi) and persisting from weeks to months. (1, 5, 13, 14)

Planetary vorticity The spin acquired by a body as a consequence of its location on another rotating body, such as Earth. (7)

Planetesimal Small celestial bodies of condensed debris moving over wildly eccentric orbits about the Sun during the formation of the solar system. (2)

Pleistocene Epoch The interval of geological time from about 1.8 million years ago until about 10,000 years ago. (4, 11)

Plumbism Any brain or neurological disorder caused by lead poisoning. (12)

Pluvial lake An ancient lake that existed in a wetter and/or colder period than today. (11)

PM_{2.5} The category of particulates with diameters less than 2.5 μm ; also known as *fine particles*. (12)

PM₁₀ The category of particulates with diameters less than 10 μm . (12)

Polar cell The feature of the general circulation from the pole to about 60° latitude, including the polar high, surface polar easterlies, subpolar lows, and upper-level westerlies in each hemisphere. (7, 9, 13)

Polar climate The coldest of the broad categories of climate types in the Köppen system. (9, 10)

Polar easterlies The prevailing general circulation feature from the pole to about 60° latitude in both hemispheres at the surface, in which flow occurs primarily from east to west. (7, 13)

Polar front The boundary between cold, dense, polar air and warm, less dense, tropical air. (7)

Polar front jet stream A large river of fast-moving air in the upper troposphere over the midlatitudes in each hemisphere that transports energy and moisture via the Rossby waves; exists at zones where cold air is adjacent to much warmer air. (4, 7, 9, 13)

Polar high The semipermanent surface anticyclone that sits over or near the North and South Poles. (7)

Porosity The ratio of the volume of all subsurface pore spaces in soil or rock to the volume of the whole. (6)

Positive feedback system An input that creates change to a system in such a way that additional, similar changes in the system occur as a result. (4, 10, 11, 12, 14, 15)

Positive vorticity Rotation that is counterclockwise in the northern hemisphere or clockwise in the southern hemisphere; cyclonic rotation. (7, 9)

Potential evapotranspiration (PE) The maximum amount of evapotranspiration that would occur at a place over a given time if water were not a limiting factor. (5, 6, 8, 9, 10)

Potential temperature The temperature that a parcel of air would have if moved dry adiabatically from its height in the atmosphere to the 1000-mb level. If the lapse rate of potential temperature is positive, the atmosphere is stable; if it is negative, the atmosphere is unstable. (5)

Potential vorticity The ratio of the sum of relative vorticity and planetary vorticity to the height of a column of mass; tends to remain constant. (7, 9, 11)

Pre-Boreal warm interval A globally warm phase that immediately followed the Younger Dryas. (11)

Precession The direction of Earth's axial tilt at any given time in geological history. (11)

Precipitable water The depth of water (in centimeters) in a column of atmosphere if all water molecules in that column condensed and precipitated. (6)

Pressure The amount of force exerted on a given area. (1, 3, 13)

Pressure gradient force (PGF) The force that initiates movement of air from areas of higher pressure to areas of lower pressure at right angles to the isobars, in fulfillment of the second law of thermodynamics. (3, 5, 7, 10, 13)

Prevention A strategy for dealing with climate change that implements tactics designed to reduce the threat. (12, 13)

Primary climate impact A natural or social system that is affected most directly by climate. (14)

Primary data Data collected by an investigator using thermometers, radiometers, moisture sensors, or other equipment in the field. (14)

Primary pollutant Any contaminant that enters the atmosphere as a direct emission by human activities. (12)

Prime meridian The meridian of longitude that runs through Greenwich, England, and corresponds to 0° longitude. (3)

Primitive equations of motion A simplification of the Navier-Stokes equations of motion in which acceleration of motion in the west-east, south-north, and down-up directions is assumed to be zero. (13)

Principal components analysis (PCA) The type of eigenvector technique most often used in climatology. (8, 13)

Principal meridian The lines of longitude spaced evenly at 15° intervals, beginning at 0° (the prime meridian), along which zone mean time corresponds to solar time. (5)

Principle of Superposition The axiom that older geological materials will be found successively lower in sedimentary rock layers than younger materials; used in most relative dating techniques. (11)

Principle of Uniformitarianism The axiom that the processes that occurred in the past are the same ones that occur in the present, at the same rates, and that the same environmental conditions required by a given species today were also favorable for that or similar species in the past. (11)

Prokaryote Single-celled ancestors of bacteria and blue-green algae that existed in Earth's primordial ocean. (2)

Proterozoic Eon The eon of geological time prior to the current eon, lasting from approximately 2.5 billion years ago to approximately 550 million years ago. (11)

Proxy evidence Indirect clues about past climatic conditions, used when direct measurements are not available; includes geological, biological, geophysical, and historical clues. (1, 11, 12)

Pyranometer A type of radiometer that measures the flux of shortwave radiant energy. (5)

Pyrgometer A type of radiometer that measures the flux of longwave radiant energy. (5)

Pyrradiometer A type of radiometer that measures the combined flux of longwave and shortwave radiant energy. (5)

Q

Quasi-Biennial Oscillation (QBO) A continual reversal of wind direction in the lower stratosphere with an average period of 26 months, alternating between the Krakatau easterlies and the Berson westerlies. (10, 11, 13)

Quaternary Period The current period of geological history, encompassing the last 1.8 million years and coinciding with the intensification of the present ice age. (11)

R

Radiant energy Radiation transmitted by means of electromagnetic waves. (3)

Radiation balance equation The expression of net radiation as the sum of the net shortwave radiant energy at the surface and the net longwave radiant energy at the surface. (5)

Radioactive decay The rate at which spontaneous nuclear disintegration of certain isotopes of certain elements occurs. (11)

Radiometer Any instrument that measures the intensity of radiation (in Watts) over a unit area (in square meters) of the surface. (5, 14)

Radiometric dating A laboratory technique used to determine the approximate age of a specimen, based on the principle of radioactive decay. (11)

Radiosonde An instrument package that ascends with a weather balloon and measures the vertical profile of atmospheric properties such as temperature, humidity, wind speed and direction, and pressure. (5, 11)

Rain machine Nickname given to tropical rain forest climates where a large percentage of the evaporated and transpired water falls locally as precipitation. (4, 10)

Rain shadow effect The dryness experienced on the leeward side of a mountain, both because the moisture and precipitation is left on the windward side where the air ascends the slope and because of the adiabatic warming associated with descending air on the leeward side. (9, 10)

Random variability A fluctuation from the mean of any atmospheric variable that does not appear to be caused systematically; also known as *noise*. (11)

Reanalysis dataset A widely used source of global climatic data for dynamic and synoptic studies produced by the U.S. National Center for Atmospheric Research and the National Centers for Environmental Prediction. (14)

Reflection A change of direction of a beam of radiant energy that is not scattered in a multitude of different directions. (5)

Refraction The bending of light when it encounters a medium of different density. (3)

Regional Climate Center One of the six offices distributed around the United States that specializes in the archiving and dissemination of climatic data and monitoring weather and climate events in their respective regions. (14)

Regional climate model (RCM) A representation of circulation that zooms in on the particular region of interest and usually contains much greater spatial resolution than general circulation models because the geographical area of interest is smaller. (13)

Regional climatology A description of the climate of a particular part of Earth's surface, sometimes including an explanation of the processes generating that climate. (1)

Regression line A line drawn across a scatterplot of data points designed to pass as closely as possible to as many points as possible, so as to minimize the squared sum of the distances between each point and the line in the *y* direction. (8)

Relative dating Any means of assessing the age of rocks, sediments, or fossils only in comparison with (i.e., younger

than or older than) that of some other rock, sediment, or fossil based on the Principle of Superposition. (11)

Relative humidity The ratio of vapor pressure divided by saturation vapor pressure. (5, 6, 9, 12)

Relative vorticity The spin of a body that occurs because the object itself is turning rather than because the object on which it rests is turning. (7)

Renewable Resource Data Center An agency within the U.S. Department of Commerce that provides solar radiation and wind data for a series of sites around the United States. (14)

Reservoir A component of a system that effectively stores matter and/or energy for a certain period of time, after which it allows for the movement of that matter and/or energy to another component of the system. (2, 6, 12)

Residence time The mean length of time that an individual molecule remains suspended in the atmosphere. (2, 6)

Residual The variance in a data set that remains unexplained by a regression line or a component. (8)

Resilience The ratio of a community's adaptability to vulnerability to a given hazard. (14)

Resilience Inference Measurement (RIM) model A conceptual framework that relates exposure to a hazard, and damage and required recovery time from that hazard. (14)

Resistance A component of force exerted by air that works parallel and in the opposite direction to the turbulent flux; in general, relatively high during times of static stability and lower during times of static instability. (6)

Resolution The sharpness of observations either in space or time. (13)

Respiration An energy-production process in which living organisms take in oxygen, oxidize organic molecules, and release carbon dioxide. (2, 3, 12)

Revolution The path of a planet around the Sun; one complete Earth revolution requires approximately 365.25 days. (3)

Ridge Any elongated area of high atmospheric pressure on a map. (4, 7, 8, 9, 10, 13)

Riming The deposition of water vapor directly onto a solid surface. (9, 10)

Rock striation A groove cut into bedrock by rocks embedded within the base of moving glaciers. (11)

Ronne Ice Shelf One of two thick, vast sheets of ice protruding from Antarctica into the Weddell Sea, which opens to the Atlantic Ocean. (10)

Ross Ice Shelf A thick, vast sheet of ice protruding from Antarctica into the Ross Sea, which opens to the Pacific Ocean. (10)

Rossby wave Upper-tropospheric, midlatitude waves with wavelengths of hundreds to thousands of kilometers. (7, 8, 9, 10, 13)

Rotation The spin of a body on its axis; one complete rotation of Earth requires approximately 24 hours. (3, 5)

Roughness layer A layer of very strong mechanical turbulence above the laminar layer, extending to approximately 50 to 100 m above Earth's surface. (5)

Roughness length The height above Earth's surface at which the air theoretically begins to move laterally in the logarithmic wind profile. (5)

Runoff Precipitated water that runs downhill to feed streams. (6, 10, 12)

S

Sahel A semiarid area of north central Africa south of the Sahara Desert, where widespread desertification has occurred in the last 30 years. (4, 10, 13)

Saltwater intrusion Movement of saltwater upstream into a freshwater estuary or stream. (6, 12)

Santa Ana wind A warm, dry wind resulting from descent of air on leeward sides of the mountains of southern California. (9)

Sargasso Sea The region of the North Atlantic Ocean where the Bermuda-Azores high is located. (7)

Saturated adiabatic lapse rate The rate of decrease of temperature as an adiabatically moving air parcel with a relative humidity at 100% rises; always less than 10 °C/km. (5)

Saturation vapor pressure (e_s) The atmospheric pressure exerted by water vapor when the air is at saturation. (5, 6, 7)

Scattering The deflection of electromagnetic radiation is in various directions upon interacting with matter in the atmosphere. (5)

Score In eigenvector analysis, a coefficient that is proportional to the degree to which the eigenvector model represents the variability in each observation of one set of variables collectively for all observations in another set of variables in the data set simultaneously; in climatology, it is common for the scores matrix to represent the relationship between each component and each time of observation, collectively across all stations simultaneously. (8, 13)

Scree plot A graph depicting the eigenvalue for each successive component or factor in eigenvector analysis. (8)

Second law of thermodynamics The fundamental principle that energy moves from areas of higher concentration to areas of lower concentration, with the result that disorder, or entropy, increases in a system. (2, 3, 7)

Secondary circulation A smaller circulation feature that is embedded within the larger general circulation, such as a midlatitude wave cyclone or migratory anticyclone. (7, 8)

Secondary climate impact A natural or social system that is affected only indirectly by climate. (14)

Secondary data Data used by researchers after being collected, quality-controlled, and compiled elsewhere, usually in digital format. (14)

Secondary pollutant A contaminant that arrives in the atmosphere as a byproduct of a chemical reaction between primary pollutants and/or other matter or energy in the atmosphere. (12)

Sensible energy (heat) Radiant energy that heats the Earth-ocean-atmosphere system rather than evaporates water. (3, 4, 7, 9, 10, 12, 13)

Sensible heat flux See Turbulent flux of sensible heat.

September equinox The day of the year midway between the June and December solstices when the solar declination is at the equator, neither hemisphere is tilted toward or away from the Sun, and day length is 12 hours over the entire Earth; currently corresponds roughly to September 22. (3)

Shearing stress See Vertical flux of horizontal momentum.

Shortwave radiation Electromagnetic radiation at wavelengths shorter than 4.0 μm , usually considered synonymous with radiation emitted by the Sun. (2, 5, 9, 12, 14)

Siberian high The strong surface anticyclone that persists through winter over the high latitudes of continental Asia. (7, 9, 10)

Siberian Traps event The largest known volcanism in Earth history, characterized by major flood basalts in present-day Siberia; a possible explanation for the Great Dying. (11)

Siderite An iron carbonate (FeCO_3) mineral that would have formed in relic soils if past atmospheric CO_2 concentrations had been substantially higher than today's. (2)

Sinistral An individual of a species of foraminifera whose shell developed with a coiling on the left side, thereby suggesting that the ocean was relatively cold at the time that the individual lived. (11)

Sink A route or mechanism by which matter or energy is removed from circulation in a system by being held in a reservoir for an extended period of time. (2, 4, 12)

Skew T-Log P Diagram A type of thermodynamic diagram that shows temperature on lines slanted upward emanating from the x -axis and the logarithm of pressure along the y -axis. (5)

Slab model A computer model in which water is assumed to have a different albedo than land and a constant depth and ability to store heat. (13)

Slash and burn agriculture A type of migratory farming in which forests are continually cleared and burned. (4)

Smog A combination of smoke and fog. (12)

Snowball Earth hypothesis The controversial idea that conditions were so cold during the Cryogenian Period that ice even existed toward the equatorial land masses and oceans. (11)

Soil heat flux plate An instrument for measuring the substrate heat flux. (5)

Soil moisture recharge In the surface water balance, the amount of precipitated water (in centimeters or inches of equivalent precipitation) during a given time period that replenishes the storage in the soil. (6, 10)

Soil moisture storage capacity See Field capacity.

Soil moisture withdrawal In the surface water balance, the amount of soil water (in centimeters or inches of equivalent precipitation) used by the atmosphere during a given time period to fulfill or partially fulfill the atmospheric demand. (6)

Solar declination The parallel of latitude on which the direct rays of the Sun fall on a given day; varies between the Tropic of Cancer and the Tropic of Capricorn throughout the year. (1, 3, 5, 7, 10)

Solar noon The time when the Sun is at its highest point in the sky for that day at that location. (3, 5, 7)

Solar time The “true” time at a location based on the location’s position with respect to the Sun; incorporates the zone mean adjustment and equation of time adjustment; also known as *local apparent time*. (5)

Solar wind Radioactive particles from the Sun moving through space at the speed of light. (2)

Somali jet A low-level, fast-moving river of air that provides southwesterly flow paralleling the Somali coast and advects moisture into southern Asia in association with the Asian summer monsoon system; also known as the *Findlater jet*. (10)

Source area Locations in the ocean near the surface that provide water to the depths. (4)

Source region The place where an air mass forms and obtains its characteristics. (8, 9)

South Atlantic high The semipermanent anticyclone in the subtropical South Atlantic Ocean. (7, 10)

South Pacific Convergence Zone (SPCZ) A band of convection, most active during the summer months when surface heating is maximized, that branches southward or southeastward from the Intertropical Convergence Zone in the western South Pacific Ocean. (10)

South Pacific high The semipermanent anticyclone in the subtropical South Pacific Ocean. (7, 10)

Southeast trade winds The dominant surface circulation pattern in the tropical southern hemisphere, with consistent winds blowing from southeast to northwest. (4, 7, 10)

Southern Oscillation A seesaw effect (teleconnection) of surface atmospheric pressure between the eastern and western equatorial Pacific Ocean in which higher-than-normal pressure in one of these two regions is coincident with lower-than-normal pressure in the other. (4, 10, 11, 13)

Southern Oscillation Index (SOI) A measure of the condition of the Southern Oscillation at a given time, derived from sea level pressure differences between the eastern Pacific (represented by Tahiti) and western Pacific (represented by Darwin, Australia); positive values represent La Niña conditions, whereas negative values represent El Niño conditions. (4)

Southwesterly monsoon The continental-scale, prevailing surface airflow over much of Asia in summer, characterized by onshore flow. (9, 10)

Spatial downscaling The process of deriving a statistical relationship between general circulation model output and atmospheric conditions at a finer grid scale than the general circulation model can provide. (13)

Spatial resolution The distance between observations of a variable at a given location. (13)

Spatial Synoptic Classification System An automated method of categorizing climates in which eigenvector

analysis is conducted on atmospheric variables over time at a single site, the analysis is repeated for many other sites, and locations where similar characteristics of the atmosphere tend to occur simultaneously are clustered in the same category. (8)

Specific heat The amount of heat (energy) required to raise the temperature of a 1 g mass by 1 °C or 1 K; distinguished from heat capacity by the fact that heat capacity refers to a unit volume rather than a unit mass. (3, 7, 12)

Specific heat at constant pressure The amount of energy that must be added to 1 kg of a substance (in this case, air) to raise its temperature by 1 °C (or 1 K) assuming that pressure does not change; approximately equivalent to 1005 J kg⁻¹ K⁻¹. (13)

Specific humidity The ratio of the mass of moist air to the total mass of the air. (5, 10, 13)

Specific volume The amount of space occupied by a solid, liquid, or gas divided by its mass; the reciprocal of density. (13)

Spectral model A general circulation model that expresses motion in terms of a series of waves. (13)

Speleothem Mineral deposits in caves that often form large and unusual formations that can be used in climatic reconstruction. (11)

Squall line A line of thunderstorms within the warm sector of a midlatitude cyclone in advance of a cold front. (9)

Stability A condition of the local atmosphere at a given place and time that describes the likelihood of a hypothetical parcel of air to rise or sink spontaneously. (5, 6, 7, 9, 10, 12)

Stable atmosphere An atmospheric condition in which rising motion is suppressed because the relevant adiabatic lapse rate exceeds the environmental lapse rate, thereby making the hypothetical adiabatically moving air parcel cooler than its surrounding environment and decreasing its buoyancy. (4, 5, 12)

Stable stratification Any situation in which colder waters underlie warmer water; analogous to a temperature inversion in the ocean. (4, 8)

Standard nonrecording rain gauge The nonautomated instrument for measuring rainfall that is used at the vast majority of the 13,000 precipitation gauges in the United States, including all sites reported in *Climatological Data*. (14)

State Climatology Program Offices in each U.S. state that are responsible for the archiving and dissemination of current and historical atmospheric data from that state to the public and private sectors. (14)

Stationary front A narrow zone separating two air mass types in which neither is actively displacing the other at a given time. (8)

Statistical downscaling The process of using statistical relationships between various land cover types and model output to produce a finer spatial resolution than that which a general circulation model offers. (13, 15)

Step change An abrupt shift to a different mean, without a slow “drift” toward that mean. (11)

Steppe (BS) climate In the Köppen system, a climatic type characterized by potential evapotranspiration that moderately exceeds precipitation. (8, 9, 10)

Stomate A tiny pore in leaf tissue, through which transpiration occurs. (5, 6)

Stommel model A simplified model of the general circulation of the deep ocean. (4)

Storm Data A monthly publication by the National Climatic Data Center of the National Oceanic and Atmospheric Administration that provides a chronological summary, by U.S. state, of severe and unusual weather that occurred in that month, including data on storm trajectories, damage, and casualties resulting from each event. (14)

Stratiform cloud A set of liquid droplets or ice crystals suspended in the atmosphere oriented in a horizontal sheet, characterized by widespread cloudiness and perhaps long periods of precipitation of weak or moderate intensity. (8, 9, 10)

Stratopause The thin layer of the atmosphere separating the stratosphere from the mesosphere. (2)

Stratosphere The layer of the atmosphere between the troposphere and mesosphere, containing the ozone layer and characterized by a temperature inversion; begins at approximately 8 to 20 km (5 to 13 mi) above the surface and extends to approximately 48 km (29 mi) above the surface. (2, 4, 10, 11, 12)

Streamline analysis A form of atmospheric analysis that uses lines to represent the flow at any given time and level of the atmosphere. (10)

Sub-Atlantic warm interval The relatively warm period that followed the Sub-Boreal cold interval, largely persisting to today. (11)

Sub-Boreal cold interval A time of gradual global cooling that followed the Hypsithermal. (11)

Subarctic (Dfc, Dwc, Dwd) climate In the Köppen system, a climatic type of the high latitudes characterized by at least one month with a climatological mean temperature above 10°C (50°F) but with extremely cold winters, very high annual temperature ranges, and adequate moisture. (9)

Subduction zone A location where a crustal plate is displaced beneath an adjacent, less-dense plate. (11)

Sublimation The transformation of water molecules from a solid directly to a gaseous state. (4, 5, 12)

Subpolar low An area of semipermanently low surface pressure centered on the oceans at about 60° latitude in each hemisphere. (7, 10)

Substrate heat flux (Q_G) The flow of energy from the surface into the ground (and vice versa) via conduction. (5, 6)

Subtropical anticyclone A semipermanent surface high-pressure cell at latitudes of approximately 20° to 30° in each hemisphere over the oceans. (4, 7, 8, 10, 12)

Subtropical Hot Desert (BWh) climate In the Köppen system, a climatic type characterized by potential evapotranspiration that far exceeds precipitation and a climatological mean temperature above 18°C (64°F). (9, 10)

Subtropical jet stream A large river of fast-moving air generally from west-to-east in the upper troposphere near 30° latitude in each hemisphere; exists because of the increasing Coriolis deflection of accelerating poleward-moving air as angular momentum is conserved. (4, 7)

Sulfur dioxide (SO_2) A colorless, irritating gas that is emitted from volcanic eruptions and combustion of fossil fuel. (4, 12)

Sulfuric acid (H_2SO_4) A very corrosive acid that forms when sulfur dioxide (SO_2) reacts with water to produce H_2SO_3 (sulfurous acid), which can then react with oxygen to form H_2SO_4 . (12)

Summer monsoon The continental-scale circulation feature, particularly in Asia, whereby surface air moves inland because of a thermally driven low-pressure area over the continent. (9)

Summer solstice The day of the year when the solar declination is at its farthest poleward extent in the observer's hemisphere, the observer's hemisphere is tilted maximally toward the Sun, and day length is maximized in the observer's hemisphere; currently corresponds to June 21 for a northern hemisphere observer and December 22 for a southern hemisphere observer. (3, 5)

Summer thermal efficiency concentration In the Thornthwaite Climatic Classification System, the ratio of potential evapotranspiration in the summer months to total annual potential evapotranspiration at a location. (8)

Sun path diagram A graph that shows the position in the Sun using zenith and azimuth angles, relative to an observer at a given parallel of latitude, throughout the course of a day and year. (5)

Sunspot A huge magnetic storm that appears as a darker region on the Sun's surface, varying in number and intensity over time. (11)

Superstorm Any extremely large and destructive storm (cyclone), particularly those that involve the merger of a tropical cyclone with a midlatitude wave cyclone. (9)

Surface airways observation A collection of hourly atmospheric data for more than 500 stations around the United States and 12,000 stations worldwide. (14)

Surface boundary layer (SBL) The lowest 100 or so meters of the troposphere, characterized by constant fluxes of energy, matter, and momentum with height (not across space) at a given instant in time; includes the laminar and roughness layers. (5, 9)

Surface tension The attraction of molecules to each other within water. (6)

Surface water balance The representation of the hydrological cycle at a local scale, accounting for the input, output, and storage of water and interactions with available surface energy and moisture. (6, 8, 9, 10, 13, 14, 15)

Surplus In the surface water balance, the amount of water (in centimeters of equivalent precipitation) that is supplied to the surface as precipitation in a given time period in excess of that which can be evapotranspired or stored in the soil. (6, 8, 9, 10)

Sustainability Development without depleting resources or degrading the environment to an extent that would compromise the ability of future generations to meet their own needs. (15)

Swamp model A computer model in which water is assumed to have a different albedo from land but no capability to store heat. (13)

Synoptic climatology The study of the relationship between regional-scale atmospheric circulation and environmental features at the surface. (1, 13)

Synoptic scale A spatial scale of analysis between about 100 and 10,000 km (60 and 6000 mi), including atmospheric phenomena that typically persist from days to weeks. (1, 13)

T

Taiga The Russian term for the boreal forest. (9)

Tambora An Indonesian volcano that erupted in 1815 and is alleged to have caused the “Year without a Summer” of 1816. (11)

Teleconnection A set of locations that tend to have a “seesaw” pattern of pressure and ridging/troughing with each other at some height in the troposphere. (7, 11, 15)

Temperate Zone The area of Earth having a moderate climatic type in the climatic classification system of the ancient Greeks. (8)

Temperature inversion Any situation in which the temperature of the static atmosphere increases as height increases. (2, 5, 9, 10, 12)

Temporal downscaling The process of projecting output from a general circulation model at one temporal scale to a finer temporal scale using statistical relationships. (13)

Temporal resolution The amount of time between observations of a variable at a given location. (13)

Temporal trend A slow drift over time toward an increasing or decreasing mean in some atmospheric variable. (11)

Tertiary Period The first of two periods in the Cenozoic Era, from about 65 million years ago until about 2 million years ago. (11)

Thermal conductivity The ability of a solid to allow heat (energy) to propagate through it; the number of watts per square meter of energy required to raise the temperature at a point 1 meter into the ground by 1 K. (12)

Thermal efficiency index (T/ET) In the Thornthwaite Climatic Classification System, the ratio of temperature to calculated evapotranspiration; increasing values represent increasingly arid climates. (8)

Thermal low Any area of relatively low surface pressure because of the ascent of relatively warm air. (9, 10)

Thermal turbulence Microscale convective motion resulting from unstable atmospheric conditions. (5)

Thermocline The boundary between relatively warm surface waters and colder deep waters. (4, 10)

Thermodynamic diagram Any type of graph that shows a vertical profile of various meteorological variables and can assist with the determination of stability conditions. (5)

Thermodynamic energy equation The equation that expresses the rate of change of temperature over time as the sum of the diabatic heating, adiabatic temperature change due to vertical motion, and temperature advection. (13)

Thermohaline circulation The global, three-dimensional oceanic circulation system that results from inequalities of heat and salinity across large distances. (3, 4, 11, 14, 15)

Thermohaline current Any of the various subcomponents of the global thermohaline circulation. (4)

Thermosphere The highest layer of the atmosphere, beginning at approximately 80 km (50 mi) above Earth's surface and gradually extending to outer space. (2)

Thiessen polygon method A spatial analytic method for converting point data to areal data in which perpendicular bisectors for the lines connecting each adjacent station in the study area are connected, and the percentage of the total area enclosed within each resulting subarea is calculated so that the point-based totals can be weighted by these percentages to determine an overall areal mean value. (6)

Thornthwaite Climatic Classification System A method of categorizing climate types based on the interplay between temperature and moisture as represented by the surface water balance. (8)

Thornthwaite potential evapotranspiration A set of empirical equations based only on the temperature and latitude used to estimate the maximum combined amount of evaporation and transpiration of the location of interest. (6)

Threshold pollutant A contaminant that is not known to be harmful in sufficiently small concentrations but that elicits a response after the concentration exceeds a particular threshold. (12)

Tibetan Low A semipermanent zone of low pressure that occurs over south-central Asia and is especially prominent in summer. (7, 9)

Time of observation bias The bias in weather records caused by a permanent change in the meteorological observing station's official time at which observations are measured and recorded. (1, 14)

Time step The length of time into the future that is forecasted by each “run” of a computer model. (13)

Time zone A longitudinally based region across Earth's surface theoretically centered on a principal meridian, in which, by convention, clocks are set to the same time. (3, 5)

Tipping bucket rain gauge An instrument for the automated measurement and recording of precipitation consisting of two small buckets that alternate in the collection of precipitation. (14)

Tornado Alley The swath from south-central Canada southward through central Texas where tornado frequency is the highest on Earth. (9)

Torrid Zone The area of Earth having the warmest climatic type in the climatic classification system of the ancient Greeks. (8)

Trade surge A sudden strengthening in the trade winds that resumes the flow of moisture inland and the wet season in tropical monsoon climates. (10)

Trade winds The dominant near-surface atmospheric circulation systems between the subtropical and equatorial latitudes in each hemisphere, consisting of the northeast trades, southeast trades, and counter-trade winds. (4, 13)

Transition layer The layer in the lower troposphere that extends from the top of the surface boundary layer to approximately 500 to 1000 m above the surface, characterized by strong turbulent fluxes and also a notable decrease in friction with height. (5)

Transpiration The process by which vegetation loses water from its leaf surface that had moved from the soil through its roots and stem. (4, 5, 6, 8, 12)

Transverse wind shear The shearing motions that result from variations in horizontal wind speed across a horizontal surface. (7)

Treeline The line that separates the subarctic from the polar climates, either latitudinally or altitudinally, in the Köppen system. (8, 9, 11)

Triassic Period The duration of geologic time from about 248 to 206 million years ago, at the beginning of the Mesozoic Era, characterized by generally warm conditions. (11)

Triple Bottom Line (TBL) concept The doctrine that social and environmental performance must be considered in addition to economic performance in assessing corporate success. (15)

Tropic of Cancer The 23.5°N parallel of latitude; represents the solar declination on the June solstice—the most poleward extent of the solar declination in the northern hemisphere. (3, 7, 10, 11)

Tropic of Capricorn The 23.5°S parallel of latitude; represents the solar declination on the December solstice—the most poleward extent of the solar declination in the southern hemisphere. (3, 7, 10, 11)

Tropical (A) climate In the Köppen system, any climatic type in which the mean monthly temperature of the coldest month exceeds 18°C (64°F) and moisture is generally adequate through at least half of the year; includes tropical rain forest, tropical monsoon, and tropical savanna climates. (10)

Tropical cyclone Any storm of tropical origin. (3, 9, 10, 11, 12, 13)

Tropical Monsoon (Am) climate In the Köppen system, a climatic type in which the coldest month has a mean temperature above 18°C (64°F) and a short dry season. (10)

Tropical Rain Forest (Af) climate In the Köppen system, a climatic type in which the coldest month has a mean temperature above 18°C (64°F) and precipitation generally exceeds potential evapotranspiration year-round. (10)

Tropical Savanna (Aw) climate In the Köppen system, a climatic type in which the coldest month has a mean temperature above 18°C (64°F), abundant precipitation exists in the high-sun season, and deficits dominate the low-sun season. (10)

Tropopause The boundary separating the troposphere and the stratosphere. (2, 5, 7, 10)

Troposphere The lowest 8 to 20 km of the atmosphere, characterized by temperatures that usually decrease with height, abundant convection, most of the atmosphere's mass, and nearly all of the atmosphere's water—the weather and climate layer. (2, 3, 5, 7, 10)

Tropospheric ozone A secondary, nonthreshold pollutant formed primarily by photodissociation of NO₂ in the presence of ultraviolet radiation that seeps into the troposphere; monitored by the U.S. Environmental Protection Agency as a criteria pollutant. (12)

Trough Any elongated area of low atmospheric pressure on a map. (4, 7, 9, 10, 13)

True Desert (BW) climate In the Köppen system, a climatic type characterized by potential evapotranspiration that far exceeds precipitation in most months. (9, 10)

Tundra Any of various types of polar shrubs and successively shorter polar vegetation. (11, 12)

Tundra (ET) climate In the Köppen system, a climatic type of the high latitudes characterized by mean monthly temperature below 10°C (50°F) in each month but with at least one month having a climatological mean temperature above freezing. (8, 9, 10)

Turbulence Any irregular fluctuation of flow in a fluid. (5, 8)

Turbulent flux of latent heat (latent heat flux) The convective transport of energy absorbed during evaporation and sublimation, usually from the surface upward. (5)

Turbulent flux of sensible heat (sensible heat flux) The convective transport of energy that can be felt as heat, usually from the surface upward. (5)

Turc method A procedure for estimating daily evapotranspiration as a function of mean daily temperature, incoming shortwave radiation, and a humidity-based value. (6)

Turkana jet stream An easterly or southeasterly low-level, fast-moving river of air that exists between the Ethiopian and East African highlands, peaking in intensity between February and March. (10)

Typhoon Regional name given to the strongest type of tropical cyclone in the western Pacific Ocean. (10)

U

Ubac slope The side of a mountain that is not exposed to direct sunlight. (3)

Ultraviolet (UV) radiation Electromagnetic radiation having wavelengths between approximately 0.005 and 0.4 micrometers. (2, 10, 12)

Undercatch The reduced measurement of precipitation in a rain gauge compared with actual precipitation fallen, as a result of factors such as the lateral wind movement across the top of the gauge, water remaining on the side of the tube rather than at the bottom, and evaporation from inside the tube. (6, 14)

United States Weather Bureau The forerunner of the National Weather Service, established in 1891 when the Federal Weather Bureau was renamed and moved to the U.S. Department of Agriculture. (14)

Unsaturated adiabatic lapse rate (UALR) The rate of change of temperature as an adiabatically moving air parcel with a relative humidity below 100% rises or sinks; always $10\text{ }^{\circ}\text{C}/\text{km}$. (5, 9)

Unstable atmosphere An atmospheric condition in which rising motion occurs because the environmental lapse rate exceeds the relevant adiabatic lapse rate, thereby making the hypothetical adiabatically moving air parcel warmer than its surrounding environment and increasing its buoyancy. (4, 5, 9, 12)

Updraft An upward thrust of air in an unstable atmosphere, mainly associated with cumuliiform clouds. (3)

Upwelling An ascending current of usually cold water caused by the advection of surface waters. (3, 4, 10)

Urban canyon The narrow zone between buildings in an intensely urbanized area. (12)

Urban heat island An isolated zone of relatively high temperatures in built-up areas; caused by the lack of vegetation, decreased evaporative cooling, waste heat from domestic and industrial processes, and thermal properties of construction materials. (1, 3, 4, 12)

V

Vapor pressure (e) The contribution of the total atmospheric pressure exerted by water vapor molecules. (5, 6, 10)

Variable gas A component of the atmosphere that varies in its concentration across space and/or time. (2)

Variability change A temporal drift to larger or smaller fluctuations about the mean value of an atmospheric variable, with or without a change in the mean. (11)

Variogram A graph used in kriging that express the relationship between distance between any two points in the study area and the squared variation between them in the variable being estimated. (6)

Varve An annual set of layers of silt and clay deposited on the bottoms of lakes and ponds that freeze in winter and thaw in summer, thereby giving proxy evidence of the length of the frost-free season. (1, 11)

Veering A clockwise change in wind direction with increasing height. (3)

Velocity convergence A situation in which more mass is entering an imaginary “box” of atmosphere than is leaving (from one or more directions); accounted for by the *continuity equation*. (13)

Velocity divergence A situation in which more mass is leaving an imaginary “box” of atmosphere than is entering (from one or more directions); accounted for by the *continuity equation*. (13)

Vernal equinox The day of the year midway between the winter and summer solstices, when the solar declination is at the equator, neither hemisphere is tilted toward or away from the Sun, and day length is 12 hours over the entire Earth; currently corresponds roughly to March 21 (the March equinox) for a northern hemisphere observer

and September 22 (the September equinox) for a southern hemisphere observer. (3, 10)

Vertical flux of horizontal momentum (shearing stress) The downward propagation of horizontal momentum caused by vertical wind shear. (5)

Vertical wind shear The change in horizontal wind speed and/or direction with height. (5, 9)

Vertical zonation Climatic variety caused by local-scale elevation differences. (9, 10)

Virtual temperature The temperature that dry air would have if its pressure and volume were equal to a sample of moist air; always greater than or equal to temperature. (13)

Visualization Any graphical technique that uses sequences of maps to show spatial features across time. (15)

Vog Volcanic smog. (4)

Volcanic Explosivity Index (VEI) A scale between 1 and 8 used to describe the magnitude, intensity, dispersion, and destructiveness of individual volcanic events. (4)

Vorticity The rotation or spin of any object. (7)

Vulnerability The ratio of damage from a particular hazard to the amount of exposure to that same hazard for a community. (14)

W

Walker circulation The “normal” atmospheric circulation system in the equatorial Pacific Ocean, characterized by high surface pressure and concurrent sinking motion in the east and relatively low surface pressure and concurrent rising motion in the west, with easterly trade winds at the surface and westerlies aloft. (4, 13)

Warm front A narrow zone separating two air mass types in which the warmer air mass is actively displacing the colder air mass. (8)

Warm sector The wedge-shaped area of a midlatitude wave cyclone between the cold front and the warm front. (8)

Water balance diagram A graph that shows the amounts of potential evapotranspiration, precipitation, soil moisture recharge, soil moisture withdrawal, surplus, and deficit for a particular place over a particular period of time. (6, 9, 10)

Wavelength The distance between two successive crests or ridges in any wave. (2, 5, 7, 12)

Weather The overall instantaneous condition of the atmosphere at a certain place and time. (1)

Weather Research and Forecasting (WRF) model A popular model for spatial and temporal downscaling applications, produced by the University Corporation for Atmospheric Research (UCAR). (13)

West African monsoon system A seasonal reversal of winds in tropical western Africa. (10)

West-coast occlusion An occluded front associated with the movement of maritime air intruding upon continental air as the system migrates inland in the midlatitude

westerlies; characterized by conditions similar to a warm front, with gentle uplift of moist cool air, stratiform clouds, and drizzle. (9)

Western-boundary intensification Any very deep, fast-moving western ocean basin current, such as the Gulf Stream. (4)

Wet bulb depression The difference between the dry bulb temperature and the wet bulb temperature when measuring relative humidity. (6)

Wet deposition A situation in which acid precipitation is produced by reactions between precipitation and primary pollutants before the falling precipitation reaches the surface. (12)

Whiteout An atmospheric condition caused primarily by wind-blown ice that makes the sky appear to blend with the snow-covered surface, eliminating the horizon. (10)

Wilting point The minimum amount of water (in centimeters or inches of precipitation equivalent) that is necessary in the rooting zone to allow extraction by plants. (6)

Wind Air in motion; the transfer of atmospheric mass from one location to another. (1, 3)

Wind channeling The constriction of air as it flows between narrow obstructions, triggering a velocity increase. (9, 10, 12)

Wind-chill factor A contrived “temperature” that represents human comfort by taking both temperature and wind speed into account. (10)

Windward Upwind; the side of a mountain facing the wind. (3, 9, 10)

Winter solstice The day of the year when the solar declination is at its farthest poleward extent in the opposite hemisphere, the observer’s hemisphere is tilted maximally away from the Sun, and day length is minimized in the observer’s hemisphere; currently corresponds to December 22 for a northern hemisphere observer and June 21 for a southern hemisphere observer. (3, 5)

Wisconsin Glacial Phase The last major glacial advance, peaking at about 18,000 years ago. (4, 10, 11, 12)

World Climate Research Programme (WCRP) An initiative sponsored by the World Meteorological Organization

to address climatic research questions, especially those that promote the successful prediction of global and regional climatic variations. (14)

World Data Center for Paleoclimatology A branch of the U.S. National Climatic Data Center that acts as a repository for paleoclimatological data sets at thousands of locations worldwide. (14)

World Meteorological Organization (WMO) An agency of the United Nations that dispenses a variety of climatological data products for use in synoptic and dynamic climatological studies, in addition to promoting the protection of the international atmospheric environment and protecting people from atmospheric hazards. (14, 15)

Y

Younger Dryas A brief but abrupt and notable “lapse” back to cold conditions after the ice had retreated following the last glacial maximum, lasting from about 13,000 years to 11,500 years before the present time; known as the *Loch Lomond Stadial* in Europe. (11)

Z

Zenith angle A coordinate indicating the number of degrees that the Sun is located away from the vertical relative to an observer’s location, ranging from 0° to 90°. (5)

Zonal flow Rossby waves with low amplitudes (i.e., deamplified ridges and troughs), characterized by strong west-east and weak south-north and north-south components of atmospheric motion. (7, 13)

Zone mean time A commonly used system of time-keeping in which the “clock time” at a location is synchronized across a range of longitudes so no adjustment is necessary except when crossing from one time zone to another. (5)

Zooplankton Microscopic marine animals that drift in ocean currents. (10)



Index

Note: Page numbers followed by *f* or *t* indicate material in figures or tables, respectively.

A

- ablation, 285, 309
 - in Antarctica, 241
 - snow/ice, 74
- absolute dating, 285
- absolute humidity, 95
- absolute vorticity, 145, 172
- absolute zero, 34, 302
 - radiation and, 91
 - thermodynamic energy equation and, 332
- absorption, 82, 303
- acacia trees, 246, 248*f*
- acceleration, 12
- Accra, Ghana, 253
 - climograph for, 251*f*
 - water balance diagram for, 251*f*
- accumulated potential water loss, 125
- accumulation, snow/ice, 73
- acid fog, 318
- acid precipitation, 318–319
- action centers, 146, 337
- adaptability, 350–351
 - defined, 351
- adaptation, 320, 327
- adiabat, 100
- adiabatic heating, 332
- adiabatic lapse rate
 - saturated, 99, 100*f*
 - unsaturated, 98, 100*f*, 183
- adiabatic motion, 98
- adiabatically, 313
- “adjustment” time, 125
- adret slope, 46
- advection, 32, 54, 192, 290, 302, 328, 330, 367
 - in air masses, 171
 - in baroclinic zones, 147, 148*f*
 - fogs, 204, 239
 - pollution, 367
 - radiation and, 91
 - water flux via, 108–109, 108*f*
- aerosols, 11, 70
 - general circulation of, 132
 - in global dimming, 313
 - hygroscopic nuclei, 308
 - indices of, 71
- insolation
 - absorbed by, 90
 - scattered by, 27
 - from volcanic activity, 70
- Africa
 - climatic setting of, 231–234
 - desertification in, 73, 73*f*
 - Marine West Coast climates in, 262
 - physiographic features of, 231*f*
 - temperature range in, 48
- Aghulas current, 232
- agricultural climatology, 7
- agriculture
 - climate impacts on, 349
 - in deforestation, 72
 - droughts and, 232
 - insolation levels and, 81
 - slash and burn, 72
 - temperature data and, 358
- Agung, Indonesia, eruption, 71*t*
- air masses, 169–171, 170*f*, 170*t*, 294
 - in African climates, 232–234
 - Rocky Mountains and, 183
 - in tropical atmospheres, 290
- air pollution, 313–314. *See also* pollution
 - classification of pollutants in, 314–319
- Air Pollution Control Act (1955), 314
- air quality legislation, 314
- airflow
 - baroclinicity, 147
 - convergence and divergence in, 147–148, 148*f*
 - in cyclones and anticyclones, 42–44, 42–44*f*
 - diffluence and confluence in, 148–149, 149*f*
 - meridional, 142, 143*f*
 - over mountainous terrain, 146–147, 148*f*
 - upper-level, 142–153
- Alaska
 - Subarctic climate in, 218
 - Tundra climates in, 222
 - volcanic activity in, 70, 71*t*
- albedo, 290, 309, 327, 349
 - in Antarctica, 241
 - definition of, 71, 90
 - desertification and, 73
- ice and, 74
- planetary, 90
- polar cells and, 134
- in Tundra climates, 222
- values for surfaces, 90*t*
- volcanic activity and, 71
- Alberta clippers, 183, 184
- Albuquerque, New Mexico
 - climate in, 192–193
 - climograph for, 192, 193*f*
 - water balance diagram for, 192, 193*f*
- Aleutian Islands
 - latitude of, 180
 - volcanic activity in, 70
- Aleutian low, 141, 337
- Alice Springs, Australia
 - climograph for, 256*f*
 - water balance diagram for, 256*f*
- Alps, 186
 - Highland climates in, 223
 - Mediterranean climates and, 207
- altitude
 - geopotential height and, 136
 - temperature and, 46
- Am climates. *See* Tropical Monsoon climates
- Amazon basin
 - Atacama Desert and, 254
 - climatic effects of, 238*f*, 239
 - deforestation of, 239
 - in ENSO events, 65
 - orographic influences of, 254
 - runoff in, 109
- American Meteorological Society, 309, 311
- AmeriFlux program, 359, 361*f*
- ammonia (NH₃), 17
- AMO. *See* Atlantic Multidecadal Oscillation
- amplitude
 - jet stream, 67
 - of upper-level airflow, 142
- anaerobic decomposition, 305–306
- analemma, 87, 87*f*
- analog forecasting, 326
- Andes Mountains, 238*f*, 239, 254
- angiosperms, 278, 288
- angular momentum, conservation of, 135
- animal migrations, 67, 289

- annual climatic normals, 274
- Annular mode, 341–342
- anomalies, 233
 - climatic change and, 274–276
- Antananarivo, Madagascar
 - climograph for, 263*f*
 - water balance diagram for, 263*f*
- Antarctic Bottom Water, 58
- Antarctic Circle, day length in, 31
- Antarctic Deep Water, 58
- Antarctic Intermediate Water, 58
- Antarctic sea ice, 309, 311, 312
- Antarctica
 - climatic setting of, 240–241
 - Ice Cap climate in, 264–265
 - ice sheet melting in, 74, 279, 281*f*
 - July isotherms in, 47, 48*f*
 - permanent ice in, 74
 - physiographic features of, 240*f*
 - Polar climate in, 262, 264
 - temperature range in, 48
- Anthropocene Epoch, 74, 280
- anthropogenic changes, 368
 - adaptation to, 320
 - in Africa, 232
 - in Antarctica, 241
 - atmospheric pollution. *See* atmospheric pollution
 - carbon cycle, 14
 - climate modification, 5, 8–9, 274
 - continued research on, 320
 - deforestation and desertification, 71–73
 - global dimming, 313
 - global warming. *See* global warming
 - mitigation of, 319
 - prevention of, 319
 - rapid climate change and, 368
 - reactions and attitudes to, 319–320
 - sustainability and, 368–369
 - variable gases concentrations, 15–16
- anthropogenic processes, 326
- anti-CLAW hypothesis, 70
- anticyclones, 132, 232, 237, 313
 - airflow in, 42–44, 42–44*f*
 - blocking, 186–187, 186*f*
 - definition of, 43
 - Mediterranean climates and, 207
 - negative vorticity in, 143
 - permanent, 139
 - ridges compared with, 142–143
 - as secondary circulations, 172
 - semipermanent subtropical, 45
 - subtropical, 54
- AO. *See* Arctic Oscillation
- aphelion, 28, 230
 - orbit eccentricity and, 291
 - precession and, 292*f*
- applied climatologists, 351
- applied climatology, 7, 347–362
 - on climate impacts, 348–351
 - data sources in, 351–362
- definition of, 348
- scope of, 348
- secondary sources for, 359
- Arabian Desert, 233
- Arabian Peninsula, 232, 253
- Arabian Sea, 187
- Aral Sea, 189, 192
- Archimedes' Principle, 280
- architecture, 81–82, 82*f*
- Arctic (A) air masses, 170, 180
- Arctic amplification, 75, 241, 293, 309, 349
- Arctic Circle, 180
 - day length in, 30–31
 - Sun path diagram for, 86
- Arctic Ocean, 75, 222
- Arctic Oscillation (AO), 341–342
- Arctic polar ice, 311
- Arctic sea ice, melting of, 309
- Arequipa, Peru
 - climograph for, 267*f*
 - water balance diagram for, 267*f*
- argon (Ar), 12, 13, 13*t*
- arid (B) climates
 - forcing mechanisms in, 190
 - geographic extent of, 189–190
 - Midlatitude Cold Desert, 190, 192–193
 - northern hemisphere, 189–198
 - southern hemisphere, 253–256
 - steppe, 189, 193–198, 254, 256
 - Subtropical Hot Desert, 190
 - True Desert, 190, 253–254
- arid climatic classification, 159, 162
- Arizona, humidity in, 33
- Arizona State University, 350
- artificial neural networks, 367
- Asia
 - climatic setting of, 187–189
 - coastal zones in, 189
 - continentality effects in, 33, 141
 - general characteristics of, 187
 - Highland climates in, 223
 - Humid Subtropical (Cfa) climates in, 198
 - January isotherms in, 47, 48*f*
 - July isotherms in, 47, 48*f*
 - Mediterranean climate in, 203
 - mountain ranges in, 188–189
 - steppe climates in, 189, 254
 - taiga in, 218
 - temperature range in, 48
 - Tundra climates in, 222
- Asian monsoons, 187–188, 245–246
 - in Africa, 234
 - in India, 253
 - katabatic winds in, 224
 - QBO in, 238
 - quasi-biennial oscillation in, 296
 - Subtropical Dry Winter climates and, 202
- Atacama Desert, 55, 62, 239, 253, 254
- Atlantic hurricane season, 340
- Atlantic Multidecadal Oscillation (AMO), 339–340
- Atlantic Ocean
 - circulation in, 56
 - currents in, 45
 - extratropical teleconnections in, 339–342, 340*f*, 341*f*, 342*f*
 - geostrophic flow in, 56
 - hurricane season in, 238
 - North America, climate effects of, 180
 - as source area, 58
 - subtropical anticyclones in, 133
 - thermohaline currents in, 58
 - tropical cyclones in, 258
- atmosphere, 11–21, 54
 - carbon cycle and, 13–15
 - composition of, 13–16, 70
 - constant and variable gases in, 15–16
 - definition of, 3
 - faint young Sun paradox and, 16–17
 - free, 41
 - interactions with other “spheres,” 4*t*
 - local
 - moisture in, 93–97
 - stability in, 99–102
 - mass of, 12
 - neutral, 98
 - origin of, 12–13
 - path length in, 27, 27*f*
 - stable, 54–55
 - structure of, 17–21, 18*f*
 - unstable, 55, 181
- atmospheric data, availability and display, 367–368, 367*f*, 368*f*
- atmospheric dispersion modelers, 314
- atmospheric effect, 54–55
- atmospheric general circulation models, 327
- atmospheric moisture, 95, 104
- atmospheric pollution, 312–314
 - air quality legislation in United States, 314
 - atmospheric factors affect pollution concentrations, 313–314
 - classification, 314–319
 - global dimming, 313
- atmospheric stability, 98–99, 111
 - assessing, 99–102
- atmospheric statics, 97–102
- atmospheric teleconnections, 337–342
- atmospheric waves, 143
- atmospheric window, 91, 302*t*, 303
- atomic mass, 284
- attenuation, 26, 82, 134
- aurora australis*, 20
- aurora borealis*, 20, 20*f*
- Australia
 - arid climates in, 253
 - Bureau of Meteorology, 326
 - climatic setting of, 234–238
 - deserts in, 253–254

Australia (*continued*)

- El Niño–Southern Oscillation events
 - in, 62, 64, 235–236
 - general characteristics of, 235
 - Madden–Julian Oscillation, 237–238
 - mesothermal climates in, 256, 258
 - physiographic features of, 234*f*
 - steppe climates in, 254
 - subtropical dry winter climate in, 258
 - temperature range in, 48
- autumnal equinox, 31
- Aw climates. *See* Tropical Savanna climates
- axial precession, 292
- axial tilt, 28–29, 29*f*, 291–292, 292*f*
- day length and, 28–32
- azimuth angle, 83, 83*f*

B

- backing process, 42
- Baghdad, Iraq
 - climograph for, 195*f*
 - water balance diagram for, 195*f*
- Baltic Sea, 208
- baroclinic zones, 147, 148*f*
- polar front jet stream and, 149–151
- baroclinicity, 147, 148*f*
- in Asia, 189
- in North America, 180
- barometers, 36, 36*f*
- Barranquilla, Colombia
 - climograph for, 252*f*
 - water balance diagram for, 252*f*
- bathtubs, water flow in, 40
- Baton Rouge, Louisiana
 - climograph for, 199*f*
 - monthly water balance in, 124–125, 124*t*
 - water balance diagram for, 199*f*
- Bay of Bengal, 187
- beam spreading, 27, 134
- Beaufort wind scale, 359, 360*t*
- Beijing, China
 - climograph for, 216*f*
 - water balance diagram for, 216*f*
- Belize City, Belize
 - climograph for, 244*f*
 - water balance diagram for, 244*f*
- Benguela current, 232
- Bentley Subglacial Trench, Antarctica, 240
- Bergeron Climatic Classification System, 168
- Bergeron, Tor, 168
- Bering Strait, 280, 290*f*
- Berlin, Germany
 - climograph for, 210*f*
 - water balance diagram for, 210*f*
- Bermuda–Azores high, 134, 139, 140*f*
- effects of Africa, 232
- Mediterranean climates and, 207
- North Atlantic Oscillation and, 340
- Rocky Mountains and, 183
- Bernoulli effect, 118
- Berson westerlies, 238
- between-group variability, 158, 176
- bias, in data, 9
- bioclimatology, 7
- biodiversity, 242
- biological evidence
 - of climate change, 288–289
 - sources of, 289
- biomes, 159
- biosphere, 54, 80, 274, 304, 327
- applied climatology on, 349
- in atmosphere evolution, 13
- as carbon reservoir, 14
- definition of, 3
- interactions with atmosphere, 4*t*
- biotemperature, 166
- Bjerknes, Jacob, 60, 169
- Blaney–Criddle model, 114
- Blaney, H. F., 114
- “Blizzard of the Century” (1993), 185
- blocking anticyclones, 186–187, 186*f*
- Bogotá, Colombia, climatic
 - classification of, 157
- boiling point, 46
- Boise, Idaho
 - climograph for, 196*f*
 - water balance diagram for, 196*f*
- bolide, 278, 284, 309
- Bolling–Allerød interstadial, 280–281
- bora winds, 224
- boreal cold interval, 282
- boreal forests, 72, 218, 222
- boreholes, 288
- bottleneck, 294
- boundary layer climatologists, 352
- boundary-layer climatology, 6, 7
- Brazil, rain forest destruction in, 72. *See also* Amazon basin
- Brazilian Highlands, 238*f*, 239
- “break in slope,” scree plot with, 176, 176*f*
- Brisbane, Australia
 - climograph for, 257*f*
 - water balance diagram for, 257*f*
- broad-scale numerical models, 332
- bromine, 19
- Broome, Australia
 - climograph of, 257*f*
 - water balance diagram, 257*f*
- brown smog, 317
- Brundtland Commission, 368
- BS climates. *See* steppe climates
- BSh climates. *See* Hot Steppe climates
- BSk climates. *See* Cold Steppe climates
- Budyko Climatic Classification System, 167
- Budyko, M. I., 167
- Budyko ratio, 167
- Buenos Aires, Argentina
 - climograph for, 259*f*
 - water balance diagram for, 259*f*
- “bulls-eye” effect, 120

buoyancy

- of atmosphere, 11, 18
 - hydrostatic equation and, 97
- buoys, 359
- butterfly effect, 335
- BW climates. *See* True Desert climates
- BWh climates. *See* Subtropical Desert climates
- BWk climates. *See* Midlatitude Cold Desert climates

C

- CA. *See* centrifugal acceleration
- Cairns, Australia
 - climograph for, 252*f*
 - water balance diagram for, 252*f*
- Cairo, Egypt
 - climatic classification of, 157
 - climograph for, 255*f*
 - water balance diagram for, 255*f*
- calcium carbonate (CaCO₃), 289, 304
- Calgary, Canada
 - climograph for, 197*f*
 - water balance diagram for, 197*f*
- California current, 67, 185, 239, 313, 337
- California, photochemical pollution
 - in, 318
- Cambrian Explosion, 278
- Canada
 - ice pack in, 74
 - ocean current effects on, 46
 - Subarctic climate in, 218
- Canadian Climate Centre, 326
- Canary current, 56, 186, 232
- western-boundary intensification
 - and, 57, 57*f*
- Cantabrian Mountains, 193
- cap and trade policy, 319
- Cape Town, South Africa
 - climograph for, 261*f*
 - forcing mechanisms in, 168
 - water balance diagram for, 261*f*
- carbon cycle, 13–15, 327
- carbon dioxide (CO₂), 12, 13
- in atmosphere composition, 13, 13*t*, 16*t*
- emission trends in, 306, 306*f*
- global warming skeptics on, 309
- as greenhouse gas, 303–305, 303*f*, 304*f*
- ice core data on, 287
- increase in atmospheric quantity, 14–15
- rain forests and, 72
- reservoirs of, 14, 14*f*
- sinks for, 14, 304
- U.S. emissions of, 303
- as variable gas, 16, 16*t*
- volcanic activity, 70, 293
- Carbon Dioxide Information Analysis Center (CDIAC), 359

- carbon monoxide (CO), 16, 16*t*, 306, 315–316
- carbon sinks, 72
- carbonic acid (H₂CO₃), 304
- carboniferous, 278
- Caribou, Maine
 - climograph for, 214*f*
 - water balance diagram for, 214*f*
- Carlsbad Caverns, New Mexico, 285
- Cascade Mountains, 168, 169*f*, 189
 - Highland climates in, 223
- cascade of linkages, 366
- catastrophism, 283, 284
- CD. *See* Climatological Data
- CDAS. *See* Climatological Data: Annual Summary
- CDD. *See* cooling degree-day
- CDIAC. *See* Carbon Dioxide Information Analysis Center
- CE. *See* Coriolis effect
- Cedar City, Utah
 - climograph for, 196*f*
 - water balance diagram for, 196*f*
- Cenozoic Era, 277*f*, 279
- Central America, rain forest destruction in, 72
- centrifugal acceleration (CA), 40
 - in free atmosphere, 81
 - friction and, 40–41
- Cfa climates. *See* Humid Subtropical climates
- Cfb climates. *See* Marine West Coast Warm Summer climates
- CFCs. *See* chlorofluorocarbons
- chaos theory, 335
- Charles' law, 18
- Cherrapunji, India, rainfall record in, 188, 202
- Chesapeake Bay, 280
- Chile, maritime effects on, 55
- Chimú Floods, 62
- China
 - cyclones, 189
 - greenhouse gas emissions in, 306
 - mesothermal climates in, 198
 - steppe climate in, 189
- Chinook winds, 183
- chlorine, 19
- chlorofluorocarbons (CFCs), 16, 19, 264
- Christchurch, New Zealand
 - climograph for, 262*f*
 - water balance diagram for, 262*f*
- CHU. *See* crop heat unit
- Cincinnati, Ohio, time zone of, 87
- circle of illumination, 28, 29*f*, 30*f*
- circulation, 33–46
 - cyclones and anticyclones in, 42–44
 - general, 132–153
 - oceanic, 44–46, 54–59
 - pressure in, 34–36, 35*f*
 - prototype patterns of, 176
 - secondary, 132
 - Sun as driver of, 81–82
 - thermohaline, 45
 - vertical motion in, 41–42
 - Walker, 60–61, 61*f*
 - wind in, 36–41
- circumpolar vortex, 149, 150*f*, 264, 281, 312, 341
- Class A Evaporation Pan, 96, 96*f*
- classification
 - climatic, 157–177
 - ineffective, 158
 - uses of, 157–158
- Clausius-Clapeyron equation, 94, 113, 335
- CLAW hypothesis, 70
- Clean Air Act
 - 1963, 314
 - 1970, 314
- climate
 - controls on, 25–50
 - definition of, 5
 - divisions, 126
 - human health and comfort, 350
 - impacts of, 348–351
 - latitude effects on, 26*f*, 28
 - longitude effects on, 26, 26*f*
 - natural systems, 348–349
 - records and statistics of, 7–9
 - regionalization of, 158
 - societal systems, 349–350
- Climate Monitoring and Diagnostics Laboratory, 361
- Climate Prediction Center (CPC), 126, 127, 366
- climate scientists, and nonscientific professionals, 366–367
- climate system, 25–50
 - circulation, 33–46
 - continentality in, 32–33, 32*f*
 - cryospheric changes and, 73–75
 - deforestation and desertification and, 71–73
 - effects on, 54–75
 - energy in, 81–93
 - latitude in, 26–28, 26*f*
 - local features in, 46–47
 - ocean circulation in, 54–59
 - spatial and seasonal variation in, 47–48
 - topography in, 46
 - volcanic activity and, 70–71
- climate vulnerability, 350–351
- climatic boundaries, 114
- climatic change and variability, 274–296
 - continental drift and landforms in, 290–291
 - definition of, 274, 275*f*, 276
 - in geological history, 276–283
 - information sources on historical, 289–290
 - lithospheric and cryospheric evidence of, 285–288
 - Milankovitch cycles and, 291–293
 - natural causes of, 290–296
 - radiometric dating and, 284–285
 - rapid, recognition of, 368
 - secondary sources on, 359
- climatic classification, 157–177
 - air masses and fronts in, 169–171
 - classical age of, 159–167
 - early attempts at, 158–159
 - genetic, 167–173
 - local and regional, 173, 173*f*
 - quantitative analysis to derive, 174–176
- climatic sites, 25–26, 28
- climatic situation, 26
- Climatological Data (CD), 353, 354*t*, 355, 356
- Climatological Data: Annual Summary (CDAS), 353, 354*t*
- climatologists, 4, 5, 327, 365, 366–367, 368, 369
- climatology
 - applied. *See* applied climatology
 - definition of, 3
 - derivation of word, 4
 - future of, 365–370
 - holistic perspective of, 5–6
 - improved atmospheric data and display in, 367–368
 - interdisciplinary work in, 366
 - meteorology and, 4–6, 365–366
 - records and statistics, 7–9
 - regional, 189–224
 - scales in, 6
 - subfields of, 6–7
 - sustainability and, 368–369
- climographs
 - for Accra, Ghana, 251*f*
 - for Albuquerque, New Mexico, 192, 193*f*
 - for Alice Springs, Australia, 256*f*
 - for Antananarivo, Madagascar, 263*f*
 - for Arequipa, Peru, 267*f*
 - for Baghdad, Iraq, 195*f*
 - for Barranquilla, Colombia, 252*f*
 - for Baton Rouge, Louisiana, 199*f*
 - for Beijing, China, 216*f*
 - for Belize City, Belize, 244*f*
 - for Berlin, Germany, 210*f*
 - for Boise, Idaho, 196*f*
 - for Brisbane, Australia, 259*f*
 - for Broome, Australia, 257*f*
 - for Buenos Aires, Argentina, 259*f*
 - for Cairns, Australia, 252*f*
 - for Calgary, Canada, 197*f*
 - for Cape Town, South Africa, 261*f*
 - for Caribou, Maine, 214*f*
 - for Cedar City, Utah, 196*f*
 - for Christchurch, New Zealand, 262*f*
 - for Cold Bay, Alaska, 218*f*
 - for Colombo, Sri Lanka, 244*f*
 - for Columbus, Ohio, 212*f*
 - for Dar es Salaam, Tanzania, 250*f*
 - for Darwin, Australia, 251*f*
 - for Des Moines, Iowa, 212*f*
 - for Dhaka, Bangladesh, 247*f*

climographs (*continued*)

- for Doha, Qatar, 255*f*
- for Duluth, Minnesota, 213*f*
- for Elkins, West Virginia, 215*f*
- for Erie, Pennsylvania, 213*f*
- for Fairbanks, Alaska, 220*f*
- for Faro, Portugal, 207*f*
- for Hami, China, 192, 192*f*
- for Hilo, Hawaii, 243*f*
- for Hong Kong, China, 202*f*
- for Juba, Sudan, 250*f*
- for Kotzebue, Alaska, 219*f*
- for Las Vegas, Nevada, 191*f*
- for Little Rock, Arkansas, 199*f*
- for Long Beach, California, 205*f*
- for Lubbock, Texas, 195*f*
- for Lusaka, Zambia, 260*f*
- for Manaus, Brazil, 245*f*
- for Manchester, England, 209*f*
- for Manila, Philippines, 247*f*
- for McMurdo Research Station, Antarctica, 265*f*
- for Mexico City, Mexico, 266*f*
- for Miami, Florida, 249*f*
- for Minsk, Belarus, 215*f*
- for Mogadishu, Somalia, 257*f*
- for Moosonee, Canada, 221*f*
- for Moscow, Russia, 216*f*
- for Mumbai, India, 249*f*
- for Murmansk, Russia, 219*f*
- for New Delhi, India, 202, 203*f*
- for Ottawa, Canada, 214*f*
- for Perth, Australia, 260*f*
- for Phoenix, Arizona, 191*f*
- for Pretoria, South Africa, 263*f*
- for Quito, Ecuador, 266*f*
- for Raleigh-Durham, North Carolina, 200*f*
- for Rapid City, South Dakota, 197*f*
- for Reno, Nevada, 168, 169*f*
- for Reykjavik, Iceland, 210*f*
- for Richmond, Virginia, 200*f*
- for Rome, Italy, 206*f*
- for Sacramento, California, 205*f*
- for Santa Maria, California, 206*f*
- for Santiago, Chile, 261*f*
- for Seattle, Washington, 208*f*
- for Singapore, Singapore, 243*f*
- for South Pole, 265*f*
- for Tashkent, Uzbekistan, 198*f*
- for Tegucigalpa, Honduras, 248
- for Thule Air Force Base, Greenland, 223*f*
- for Tokyo, Japan, 201*f*
- for Tucson, Arizona, 194*f*
- for Tura, Russia, 221*f*
- for Vladivostok, Russia, 217*f*
- for Yellowknife, Canada, 220*f*

clock time, 86

clouds

- front types and, 171
- generation of, 33
- insolation and, 33
- as liquid aerosols, 12

- seeding, 7
- in temperature variations, 33
- cluster analysis, 175–176, 176*f*
- CMI. *See* Crop Moisture Index
- co-kriging, 120
- coastal Kelvin waves, 64
- cold air
 - damming, 183
 - drainage, 224
- Cold Bay, Alaska
 - climograph for, 218*f*
 - water balance diagram for, 218*f*
- cold-ENSO events. *See* La Niña
- cold fronts, 171, 171*f*, 180
- Cold Steppe (BSk) climates, 194, 256
- Colombo, Sri Lanka
 - climograph for, 244*f*
 - water balance diagram for, 244*f*
- Colorado wave cyclones, 183
- Columbus, Ohio
 - climograph for, 212*f*
 - water balance diagram for, 212*f*
- common factor analysis, 174, 337
- Common Water, 58
- components, 174, 336
- computerized climate models, 326–330
- concentration-response curve, 315*f*
- condensation, 69, 92, 107, 311
 - in atmosphere formation, 13
 - lifting level of, 100
- condensation nuclei, 70, 308
- conditional instability, 99
- conduction, 18, 92, 288, 308
- confluence, 148–149, 149*f*
- conservation of angular momentum, 135
- constant absolute vorticity trajectory, 145–146, 145*f*
- constant gases, 15–16
- content analysis, 289
- continental drift, 290–291
- continental glaciers, 309
- continental polar (cP) air masses, 170, 341
 - in North America, 180
- continental tropical (cT) air masses, 170
 - in Africa, 232
 - tornado formation in, 181
- continentality, 32–33, 32*f*, 54, 180
 - in Antarctica, 241
 - in Asia, 187
 - over Asian continent, 141
 - definition of, 32
 - latitude and, 47
 - in North America, 180
 - seasonality and, 48
- continuity equation, 333–334
- convection, 32, 230, 302, 330
 - cell, 132, 132*f*
 - in cloud formation, 33
 - continentality and, 32
 - in deep ocean thermohaline currents, 57
 - definition of, 18
 - forced, 103
 - free, 102

- in general circulation, 132, 132*f*
- in troposphere, 80
- in turbulent fluxes, 92
- convective fluxes, 92
- convective precipitation, 290, 358
- convective thunderstorms, 334
- convergence, 147–148, 148*f*. *See also* South Pacific Convergence Zone (SPCZ)
 - horizontal, 230
 - velocity, 333, 334*f*
- cooling degree-day (CDD), 358
- coral reefs, 289
- Coriolis effect (CE), 38–40, 81, 295, 331
 - in Asian monsoons, 187–188
 - constant absolute vorticity trajectory and, 146
 - in convergence and divergence, 147
 - on cyclones and anticyclones, 42, 43
 - downwelling and, 56
 - friction and, 41
 - in general circulation, 133
 - low-level jet stream and, 182
 - northern vs. southern hemisphere, 230–231
 - on ocean surface currents, 54
 - in oceanic circulation, 45
 - polar cells and, 134
 - on polar front jet stream, 149
 - SPCZ and, 237
 - in surface wind systems, 134
 - in tropical atmospheres, 230
 - in upper-level winds, 135
 - vorticity and, 143
- Coriolis parameter, 143, 204, 331
- counter-radiation, 91, 276, 302
- counter-trade winds, 233, 233*f*
- coupled atmosphere–ocean general circulation models, 327
- cP air masses. *See* continental polar air masses
- crest, streamflow, 123
- Cretaceous–Paleogene (K–Pg) extinction event, 279, 312
- cretaceous period, 277*f*, 279
- Criddle, W. D., 114
- criteria pollutants, 314
- crop heat unit (CHU), 358
- Crop Moisture Index (CMI), 127, 128*f*
- cross-cutting relationships, 285
- Cryogenian Period, 278
- cryosphere, 80, 274, 309, 327
 - applied climatology on, 348–349
 - climate change and, 73–75
 - definition of, 3
 - evidence of climatic change in, 285–288
 - feedbacks in, 74–75
 - interactions with atmosphere, 4*t*
 - solid water in, 108
- Csa. *See* Mediterranean Hot Summer climates
- Csb. *See* Mediterranean Warm Summer climates

cumuliform clouds, 171, 209, 242
 cumulonimbus clouds, 171, 181
 currents. *See* oceans, currents
 Cwb climates. *See* Marine Dry Winter climates
 cyanobacteria, 278
 cyclogenesis, 230
 in Africa, 232
 in Asia, 189
 in Mediterranean climates, 207
 mountains and, 147
 polar lows and, 141
 Rocky Mountains in, 183
 Rossby waves in, 145
 in tropical climates, 230, 231
 cyclones, 42–43, 132, 169, 313
 airflow patterns in, 42, 42*f*, 43
 definition of, 42
 divergence and convergence in, 147, 148*f*
 Gulf Coast, 185
 in Humid Continental climates, 217
 in North America, 181
 surface, 145
 troughs compared with, 143
 vorticity in, 143

D

daily mean temperature, 7–8
Daily Synoptic Series, 356
 Dalton Minimum, 295
 dams, 73
 Dar es Salaam, Tanzania
 climograph for, 250*f*
 water balance diagram for, 250*f*
 Darwin, Australia, 62
 climograph for, 251*f*
 water balance diagram for, 251*f*
 data collection, 41
 agencies in, 351–352
 in general circulation models, 330
 on global warming, 311–312
 instrumentation in, 356–357, 356*f*, 357*f*
 other variables in, 358–359
 primary vs. secondary data in, 352
 time of observation and, 357–358
 data sets, 274
 data sources, 351–362
 daughter isotope, 284
 day length
 Hipparchus on, 158
 isotherms and, 47
 latitude and, 28, 31
 polar cells and, 141
 revolution, rotation, and tilt in, 29–32
 December solstice, 31
 decreasing availability water balance model, 125
 deficits, water, 122, 164, 240
 in steppe climates, 189
 in Tropical Rain Forest climates, 245

deflection. *See* Coriolis effect (CE)
 deforestation, 71–73, 109, 274, 301, 335
 Andes Mountains, 239
 definition of, 71
 degree-days, 358
 dendroclimatology, 289
 density, 17, 35, 95, 134, 309, 327
 height and, 45
 hydrostatic equation and, 97
 deposition, 73, 92, 107, 265
 in Ice Cap climates, 223
 lapse rate and, 99
 depression, 36, 56
 storage, 122
 Des Moines, Iowa
 climograph for, 212*f*, 217
 water balance diagram for, 212*f*
 desert climates, 16. *See also* arid (B) climates; True Desert (BW) climates
 desertification, 71–73, 301, 335
 in Africa, 232
 definition of, 72
 in South America, 239
 developing countries, weather data collection, 9
 Devonian Periods, 278
 dewpoint temperature (T_d), 94, 335
 air temperature and, 114
 in Europe, 186
 in tropical atmospheres, 230
 dextral individuals, 288
 Dhaka, Bangladesh
 climograph for, 247*f*
 water balance diagram for, 247*f*
 DI. *See* dryness index
 diabatic heating, 332
 diatomic nitrogen (N_2), 13
 diatomic oxygen (O_2), 13, 13*t*, 19
 diffluence, 148–149, 149*f*
 diffuse radiation, 91
 diffusion, 14
 dimensionless quantity, 95, 334
 dimethyl sulfide (DMS), 70
 dimming, global, 313
 dinosaurs, 279, 284, 312
 direct radiation, 91, 190
 disaster, 350–351
 divergence, 147–148, 148*f*
 velocity, 333–334, 334*f*
 Dixie Alley, 181
 DMS. *See* dimethyl sulfide
 Doha, Qatar
 climograph for, 255*f*
 water balance diagram for, 255*f*
 doldrums, 135
 domestic waste, 368
 downdrafts, 42
 downscaling, 327, 348, 366
 downwelling, 56
Drought Follows the Plow (Glantz), 232
 droughts, 114
 deficits and, 122
 desertification and, 73

from ENSO events, 65, 68
 indices of, 126–128, 127–129*f*
 in Latin America, 240
 in Mediterranean climates, 207
 solar output and, 296
 transpiration rates in, 95
 dry climates, 162*t*, 163, 165*t*
 dry deposition, 319
 dryline, 181
 dryness index (DI), 164
 Duluth, Minnesota
 climograph for, 213*f*
 water balance diagram for, 213*f*
 Dust Bowl, 296
 Dust Veil Index, 71
 dynamic climatology, 7
 secondary data sources for, 352–359
 dynamic downscaling, 327
 dynamic instability, 335

E

Earth
 age of, 276
 axial precession of, 292
 axial tilt of, 28–29, 29*f*, 291
 circulation on nonrotating, 132–133, 132*f*
 curvature, path length and, 27–28, 27*f*
 eccentricity in orbit of, 291, 291*f*
 gravity of, 12
 magnetic field of, 20
 mass of, 12
 orbit changes of, 291
 radiation by, 91
 revolution of, 28–32, 30*f*
 rotation of, 28
 Earth–ocean–atmosphere system, 69, 309, 311, 312
 carbon cycle in, 13–15
 in general circulation models, 327–330, 328*f*, 329*f*
 global hydrologic cycle in, 108
 temperature regulation in, 14, 16–17
 zones in, 3
 Earth–Sun relationships, 28–32
 axial tilt, 28–29, 29*f*
 combined effect of revolution, rotation, and tilt, 29–32
 revolution, 28
 East African low-level jet, 233–234
 East Antarctic Ice Sheet, 75, 280, 281*f*
 east-coast occlusions, 211
 easterly waves, 230, 231*f*
 eccentricity, 291, 291*f*, 326
 economic gain, 369
 ecotone, 159, 163, 193
 eddy covariance, 97
 EF climates. *See* Ice Cap climates
 eigenvalues, 176, 336
 eigenvector analysis, 174–175, 175*f*, 336–337

- Ekman spiral, 45, 45*f*, 47, 81, 82*f*
 in Africa, 232
 downwelling and, 56
 geostrophic balance and, 56, 56*f*
 ocean surface currents and, 54
 upwelling and, 55
- Ekman, Walfrid, 45
- El Chichón, Mexico, eruption, 71*t*, 294
- El Niño, 234
 atmospheric consequences of, 64
 characteristics of, 63–64, 64*f*, 65*f*
 definition of, 60–61
 global climate anomalies, 66*f*
 global effects of, 65–67, 67*t*
 historical data on, 62–63, 63*t*
 impacts of, 337, 338*f*
 MJO compared with, 237
 in North American summer monsoon, 193
 ocean response to, 64*f*
 precipitation and, 67, 68
 Rocky Mountains and, 183
 volcanic activity and, 294
- El Niño–Southern Oscillation (ENSO)
 event, 59–70, 234
 in Australia and Oceania, 235–236
 climatic change from, 296, 296*f*
 cryospheric effects of, 75
 effects on U.S., 67–68
 global climate anomalies, 66*f*
 global effects of, 65–67, 67*t*
 global warming and, 69
 historical observations of, 62–63, 63*t*
 in Latin America, 239–240
 QBO in, 238
 SPCZ and, 237
 Walker circulation in, 60–61, 61*f*
- electromagnetic spectrum, 19, 91
- elevation
 pressure and, 36
 pressure gradient force and, 37–38
- Elkins, West Virginia, 211, 217
 climograph for, 215*f*
 water balance diagram for, 215*f*
- ELR. *See* environmental lapse rate
- empirical approach, 320, 348, 366
- empirical Bayesian kriging, 120
- empirical climatic classification system, 167
- empirical orthogonal function analysis, 174
- energy
 climate effects of, 350
 in climate system, 81–93
 general circulation and, 132
 kinetic. *See* kinetic energy
 measuring radiant, 87, 89
 momentum flux, 102
 radiation balance and, 90–92
 Sun as source of, 81–87
 thermal and mechanical turbulence and Richardson number and, 102–103
 thermodynamic equation for, 332–333
 turbulent fluxes and, 92
- energy balance, 93
- energy balance equation, 93, 110
- energy balance model, 326
- ENSO event. *See* El Niño–Southern Oscillation event
- environmental gain, 369
- environmental lapse rate (ELR), 18, 80, 185
- environmental planning, 8, 274
- Environmental Protection Agency (EPA), 314
- eons, 277
- EPA. *See* Environmental Protection Agency
- epoch, 280
- equal availability water balance models, 125
- equation of state, 35, 151, 334–335
 hydrostatic equation and, 97
 for moist air, 334
- equation of time, 86, 88–89*t*, 88*f*
- equator, 47
 atmosphere thickness at, 18
 axial tilt and, 29
 day length at, 29, 32
 geopotential height at, 136, 137*f*
 latitude of, 26
 ocean salinity at, 58
- equatorial (E) air masses, 170, 232
- equatorial Kelvin waves, 64, 67, 237
- equatorial Rossby wave, 64
- equilibrium, hydrostatic, 11
- equilibrium line, 74
- equinoxes
 autumnal, 31
 precession of, 292–293, 292*f*
 Sun path diagrams and, 83
 vernal, 31
- eras, 277
- Erie, Pennsylvania
 climograph for, 213*f*
 water balance diagram for, 213*f*
- erratics, glacial, 285
- ET. *See* evapotranspiration
- eukaryotes, 13
- Eurasian Humid Continental climate, 211
- EuroFlux, 359, 361*f*
- Europe
 blocking anticyclones, 186–187, 186*f*
 climatic setting of, 185–187
 deforestation in, 72
 Humid Continental climates in, 211
 Marine West Coast climate in, 208
 Mediterranean climate in, 202, 207
 mountain ranges in, 186
 North Atlantic Oscillation and, 340–341
 ocean current effects on, 46, 185–186
 physiographic features of, 185*f*
 sea level changes and, 281*f*
 Tundra climates in, 222
- eustatic sea levels, 241, 280
- evaporation, 7, 33, 58, 107, 164, 183, 237, 307, 308, 311, 333
 altitude and, 46
 cooling from, 33
 desertification and, 73
 eddy covariance, 97
 estimation, 114
 of Lake Bonneville, 285
 on land vs. water, 137
 latent heat in, 92
 pans, 96, 96*f*, 111
 radiant energy conversion in, 33
 in rain gauges, 118
 water vapor and, 15
- evapotranspiration (ET), 95–96, 108, 163, 232, 307, 349
 in global water balance equation, 109
 measuring, 96–97
 potential, 96
 in surface water balance, 112*f*, 113*f*, 114
 water flux via, 108–109, 108*f*
- extinction, 72, 279, 284
- extratropical northern hemisphere climates, 180–225
 Europe, 185–187
 regional climatology, 189–224
- extremes, 274
 definition of, 5
 regionalization and, 158
- Eyjafjallajökull, Iceland, eruption, 71*t*, 135, 293, 294
- ## F
- Fagan, Brian, 350
- faint young Sun paradox, 16–17, 276
- Fairbanks, Alaska
 climograph for, 220*f*
 water balance diagram for, 220*f*
- famines
 desertification and, 73
 from ENSO events, 67
- Faro, Portugal
 climograph for, 207*f*
 water balance diagram for, 207*f*
- Federal Weather Service, 350
- feedback systems
 negative, 75, 311
 positive, 74, 232, 280, 309, 349, 368
- fermentation, 13
- Fick's law, 81, 102
- field capacity, 121
- Fifth Assessment Report (AR5), 312
- Filchner Ice Shelf, 241
- Findlater jet, 234
- fine particles, 316
- Finger Lakes Region, New York, 280
- finite differencing, 328
- first law of thermodynamics, 94, 284, 333

Fischer-Porter rain gauge, 356–357, 356f
 fish migrations, 67
 floods, 222
 climate change and, 276
 in Latin America, 240
 Florida, sea level changes and, 280, 282f
 fluorocarbons, 306
 flux, 14, 32, 359
 convective, 92
 energy balance and, 93
 Fick's law, 81
 latent heat, 81, 92
 local, of matter, 93–97
 momentum, 102
 sensible heat, 81, 92
 substrate heat, 92–93
 turbulent, 81, 92, 92f
 of water, 108–109, 108f
 foams, 19
 Föhn winds, 186
 fog, 184
 acid, 318
 advection, 204, 239
 foraminifera, 288
 forced convection, 103
 forcing mechanisms, 190
 Antarctic, 241
 in arid climates, 190
 classification systems based on, 168
 forests
 boreal, 218
 carbon dioxide sequestration in, 305
 40–50 Day Oscillation, 237
 fossil fuels, 14, 274, 310, 359
 carbon dioxide from, 303–304
 climate effects of, 72
 emission, 304, 306–307
 Kyoto Treaty on, 306
 U.S. consumption of, 306, 307f
 fossils, 288
 fracking, 303
 free atmosphere, 41, 80, 81
 free convection, 102
 freezing, 107
 French Revolution, 350
 Freon, 19
 frequencies, definition of, 5
 fresh water, 108
 friction, 6, 80, 230, 308, 331
 on cyclones and anticyclones, 42
 free atmosphere layer, 81
 in oceanic circulation, 45
 wind and, 40–41
 friction-free zone, 41
 Frigid Zone, 158
 frontal wave cyclones, 42, 201
 fronts, 230
 air masses and, 169–171, 170f, 170t
 classification of, 171–173, 171f, 172f
 cold, 171, 171f
 definition of, 171f
 occluded, 172–173, 172f, 183
 stationary, 171, 171f
 warm, 171, 171f

frostpoint temperature, 94
 fudge factors, 333
 Fuller, Buckminster, 350
 fumigation event, 317

G

Galileo, 159
 gases, 12
 compression of atmospheric, 18
 constant, 15–16
 greenhouse, 17
 ideal, 18
 noble, 12
 variable, 15–16, 16t
 from volcanic activity, 70
 GCMs. *See* general circulation models
 GDD. *See* growing degree-day
 Geiger counter, 284
 Geiger, Rudolf, 159–164
 general circulation, 132–153
 in African climates, 232–234
 definition of, 132
 Hadley cells in, 133–134, 133f, 138–140
 idealized, on rotating planet, 133–137
 land–water contrasts in, 137–138
 midlatitude features in, 142
 over mountainous terrain, 146–147, 147f
 of nonrotating Earth, 132–133, 133f
 observed surface patterns in, 137–141
 polar cells in, 134, 139–141
 subtropical anticyclones in, 138–139, 140f
 upper-level airflow in, 142–153
 general circulation models (GCMs), 326–327, 330
 basic equations for, 330–336
 data for, 330
 Earth–ocean–atmosphere system in, 327–330, 328f, 329f
 types of, 327
 and weather forecasting models, 335
 genetic classification system, 168
 genetic climatic classifications, 167–173
 geographic information system (GIS), 118, 367–368
 geologic time scale, 277f
 geological history, 276–283
 evidence of climatic change in, 285–290
 Geophysical Fluid Dynamics Laboratory, 326
 geopotential height, 136, 137f, 174, 230, 336
 equatorial, 153
 low-level jet stream and, 182
 mean, in northern hemisphere, 151, 152f, 153
 polar front jet stream and, 151

geostrophic balance, 43, 230
 in free atmosphere, 81
 isohypses and, 149
 in tropical atmospheres, 230
 geostrophic flow, 56, 57f
 geostrophic wind, 43, 204
 GEWEX. *See* Global Energy and Water Cycle Experiment
 Ghats mountains, 189
 Gibson Desert, 253
 GIS. *See* geographic information systems
 glacial advance, 73–74, 234, 294
 glacial erratics, 285
 glacial phases, 279, 279t
 glaciation, 16
 axial tilt changes and, 291–292, 292f
 Milankovitch cycles and, 291–293
 glaciers, 73, 285, 287
 Glantz, Michael, 232
 global dimming, 313
 Global Energy and Water Cycle Experiment (GEWEX), 359
 Global Forecast System (GFS), 365–366
 global hydrologic cycle, 7, 107–129, 108f, 278
 surface water balance in, 110–124
 Global Hydrology Center, 359
 global mean annual average, 283f
 global temperature curve, 304f
 global warming, 59, 302–312, 366
 adaptation to, 320
 in Antarctica, 241
 bottom line regarding debate, 312
 continued research on, 320
 deep-water conveyor and, 59
 direct and indirect effects of, 309, 310f
 ENSO events and, 69
 great debate, 309–312
 greenhouse effect in, 302
 greenhouse gases. *See* greenhouse gases
 health impacts of, 350
 mainstream perspective, 309–311
 mitigation of, 319
 ocean fertilization and, 304
 policymaking on, 366
 prevention of, 319
 skeptical perspective on, 311–312
 urban heat island in, 307–309, 308f
 global water balance equation, 109
 Gobi Desert, 188, 189, 192, 193
 Goddard Institute of Space Sciences, 326
 Gondwanan Ice Age, 278, 290, 293
 governmental policies, 8
 cap and trade, 319
 gradient Richardson number (Ri), 103
 gradient wind equation, 203
 Grand Canyon, 285, 286f
 gravity
 hydrostatic equation and, 97
 vertical motion and, 41

- gray smog, 317
 grazing, in desertification, 72
 Great Artesian Basin, 253
 Great Barrier Reef, 279
 great dying, 278
 Great Lakes
 climate effects on, 183–184
 formation of, 280
 in Humid Continental climates,
 211, 217
 lake effect snows around, 47, 47f
 Great Oxygenation Event, 277
 Great Salt Lake, 280, 285
 Great Sandy Desert, 253
 Great Victoria Desert, 253
 Green River, 287
 greenhouse effect, 15, 69, 190. *See also*
 global warming
 faint young Sun paradox and, 17
 fossil evidence of, 288
 global temperature curve and, 304f
 in global warming, 302
 methanogens in, 276
 in Tropical Rain Forests, 242
 greenhouse gases, 17, 190, 276,
 302–307, 302t
 carbon dioxide, 303–305, 303f, 304f
 carbon monoxide, 306
 emission trends in, 306–307
 fluorocarbon, 306
 in global warming, 69, 302
 methane, 305–306, 305f
 nitrogen oxides, 306
 nitrous oxide, 306
 snow cover and, 74
 water vapor, 302–303
 wavelengths absorbed and
 emitted by, 302–303, 302t
 greening initiatives, 366
 Greenland, 264
 latitude of, 180
 North Atlantic Oscillation and,
 340–341
 permanent ice in, 74
 Viking colonization of, 282
 Greenwich, England, 26
 gridpoint models, 328, 328f, 329f, 330
 gridpoint technique, 119–120, 119f
 groundwater, 108
 drought indices and, 127
 percolation and, 109
 growing degree-day (GDD), 358
 growing season, 349
 guard cells, 95, 125
 Gulf Coast cyclones, 185
 Gulf of Mexico
 climate effects of, 180, 182
 ENSO events and, 68
 Loop current and, 185
 Muller Weather Types for, 173, 173f
 Gulf Stream, 46, 56, 290
 continental drift and, 290
 deep-water thermohaline currents
 and, 58
 European climate effects of, 185
 in North American climate, 184
 western-boundary intensification in,
 57, 57f
 gust fronts, 181
 gymnosperms, 288
 gyres, 54, 147, 186, 239
- ## H
- H climates. *See* Highland climates
 Hadley cells, 133–134, 133f, 296
 in Europe, 186
 ITCZ and, 138, 138f, 139f
 locations and strength of features in,
 138–139
 upper-level winds in, 135, 136f
 Hadley Centre (United Kingdom), 326
 Hadley, George, 132
 half-life of radioactive element, 284
 Hami, China
 climograph for, 192, 192f
 water balance diagram for,
 192, 192f
 Hancock County, Illinois, precipitation
 measurement in, 118, 119f
 Harmattan winds, 232
 Hawaiian high, 139, 140f, 185, 313
 Africa and, 234
 Mediterranean climate and, 207
 hazard, 350–351
 assessment, 8
 mitigation, 274
 HDD. *See* heating degree-day
 heat capacity, 307
 heat index, 33
 heating degree-day (HDD), 358
 helium, 12, 15
 heterosphere, 21
 HI. *See* humidity index
 Highland (H) climates, 223–224,
 265–267
 highland climatic classification, 162t
 Hilo, Hawaii
 climograph for, 243f
 water balance diagram for, 243f
 Himalayan Mountains
 in Asian monsoons, 188–189
 Highland climates in, 223
 Hindu Kush, 188, 223
 Hipparchus, 158
 Historical Climatology Network, 359
 historical data, 289–290
 Hitler, Adolph, 342
 HMS Bounty, 135
 Hocking Hills State Park, 286f
 Holdridge, L. R., 166
 Holdridge Life Zones Climatic
 Classification System, 166,
 167f, 168f
 Holocene Epoch, 74, 280
 Holocene Interglacial Phase, 74, 279t,
 280, 281
 hominids, 248
 Homo floresiensis, 294
 Homo sapiens, 294
 homosphere, 20
 Hong Kong, China
 climograph for, 202f
 water balance diagram for, 202f
 horizontal convergence, 230
 Horn, Lyle, 159
 horse latitudes, 133
 Hot Steppe (BSh) climates, 194,
 194f, 254
Hourly Precipitation Data (HPD),
 355, 356t
 human bioclimatology, 7
 human health and comfort, 350
 human. *See* anthropogenic changes
 Humboldt (Peru) current, 55, 239
 Humid Continental (Dfa, Dfb) climates,
 211–217
 Humid Continental Winter Dry
 (Dwa, Dwb) climates, 211
 Humid Subtropical (Cfa) climates,
 198–201, 258
 Humid Subtropical Winter Dry (Cwa)
 climates, 202, 258
 humidity, 33
 absolute, 95
 ocean surface currents and, 55
 polar front jet stream and, 150–151
 Red Sea area, 16, 254
 relative, calculation, 93
 specific, 95
 thermodynamic diagrams and, 100
 humidity index (HI), 164
 humus, 305
 Hurricane Katrina, 180, 185
 Hurricane Wilma, 185
 hurricanes
 active periods of, 349
 Atlantic season of, 185, 274, 276
 greenhouse gases and, 320
 historical data on, 289
 La Niña and, 68
 QBO and, 238
 hybrid climatic classification
 techniques, 176
 hydrocarbons, 317, 318
 hydroclimatology, 7
 hydrofracking, 303
 hydrogen, 12, 16, 16t
 nuclear fusion of, 16
 as variable gas, 16, 16t
 hydrologic cycles, global, 107–129.
 See also moisture; water
 hydrosphere, 54, 80, 274, 326
 applied climatology on, 349
 in atmosphere evolution, 13
 definition of, 3
 global warming and, 59
 interactions with atmosphere, 4t
 moisture movement through, 107
 hydrostatic equation, 331–332
 statics and, 97–98

- hydrostatic equilibrium, 11, 41
 - hygrometer, 95
 - hygroscopic nuclei, 308
 - hypsithermal, 282
- I**
- Iberian Peninsula Steppe, 194
 - ice
 - caps, 309
 - cores, 287, 288, 303, 305, 310
 - dams, 222
 - on Earth's surface, 73–74
 - evidence of climatic change in, 287
 - permanent, 74
 - planetary, 74
 - polar cells and, 134
 - sheet, 309
 - shelves, 241
 - ice ages, 16, 17, 276, 279
 - definition of, 74
 - glacial phases in, 279, 279*t*
 - interglacial phases in, 279–280, 279*t*
 - Little, 282–283
 - methanogens and, 277, 278
 - orbit eccentricity and, 291
 - sea level changes and, 280
 - Ice Cap (EF) climates, 159, 162*t*, 222, 264–265
 - icefish, 264
 - Iceland
 - currents near, 45
 - Marine West Coast climate in, 208, 209
 - North Atlantic Oscillation and, 340–341
 - Tundra climates in, 222
 - volcanic activity in, 135
 - volcanic eruptions in, 71*t*
 - Icelandic low, 141, 185, 340–341
 - ideal gas law, 35, 151, 334
 - ideal gases, 18, 35
 - India
 - greenhouse gas emissions in, 306
 - mesothermal climates in, 198
 - steppe climates in, 254
 - Indian Ocean
 - currents to, 45
 - ENSO events in, 66
 - monsoons in, 187
 - thermohaline currents in, 58, 59
 - tropical cyclones in, 258
 - Indian Ocean Dipole (IOD), 234, 337
 - Indian Ocean high, 139, 140*f*, 232
 - indices
 - of aerosols, 71
 - drought, 126–128, 127–129*f*
 - dryness, 164
 - humidity, 164
 - moisture, 164, 165*t*
 - thermal efficiency, 164
 - Indonesia
 - downwelling around, 56
 - rain forest destruction in, 72
 - Industrial Revolution, 14, 72, 303
 - industrial smog, 317
 - inertia, 40
 - inertial period, 40
 - infiltration, 109, 201
 - initialization, 335
 - insolation, 70, 290, 308, 326, 362
 - aerosol indices and, 71
 - in Africa, 232
 - and agriculture, 81
 - albedo values and, 90, 90*t*
 - circulation and, 33
 - clouds and, 33
 - continentality and, 33
 - definition of, 17
 - in Europe, 187
 - evaporation and, 94
 - ice and, 74
 - in land vs. water, 137
 - latitude and, 26, 27*f*
 - pollution concentrations and, 312, 314
 - potential evapotranspiration and, 111
 - rotation, tilt, and revolution effects on, 31
 - surface temperatures and, 17
 - wavelengths in, 19
 - instrumentation, in data collection, 356–357, 356*f*, 357*f*
 - insurance, 350
 - interception, 123
 - interdisciplinary work, 366
 - interglacial phases, 74, 279, 279*t*, 368
 - Milankovitch cycles and, 291–293
 - orbit eccentricity and, 291
 - rapid climate change and, 368
 - Intergovernmental Panel on Climate Change (IPCC), 312, 367
 - internal energy, 332
 - international date line, 86, 180
 - Intertropical Convergence Zone (ITCZ), 135, 138, 138*f*, 139*f*, 230
 - in Africa, 231–232
 - in general circulation, 142
 - global view of, 138*f*
 - low pressure from, 231
 - migration of, 138, 139*f*
 - in Tropical Rain Forest climates, 245
 - in Tropical Savanna climates, 248, 253
 - inverse square law, 291
 - inverted troughs, 230
 - IOD. *See* Indian Ocean Dipole
 - irrigation, 73
 - isobars
 - definition of, 36
 - mean surface, in semipermanent surface pressure cells, 140*f*
 - isohyetal method, 118–120, 119*f*
 - isohyets, 118, 119*f*, 120
 - isohypses, 149, 150*f*, 204
 - isostatic rebound, 280
 - isothermal layer, 19
 - isotherms, 47, 147
 - definition of, 47
 - in July, 47, 48*f*
 - isotopes, 284
 - ITCZ. *See* Intertropical Convergence Zone
 - iterative models, 326
- J**
- Japan
 - cyclones in, 189
 - Humid Subtropical (Cfa) climates in, 198
 - Meteorological Agency, 326
 - mountain effects in, 189
 - oroshi in, 224
 - jet streak, 149, 150*f*
 - jet streams
 - definition of, 67
 - ENSO events and, 67
 - Findlater, 234
 - Pacific-North American pattern and, 342
 - snowfall and, 74
 - Somali, 234
 - transverse wind shear and, 144, 144*f*
 - Turkana, 233
 - Joules, 35, 94, 307
 - Juba, Sudan
 - climograph for, 250*f*
 - water balance diagram for, 250*f*
 - June solstice, 30, 31
- K**
- K-T extinction, 279, 284, 312
 - Kalahari Desert, 233, 254
 - steppe climates in, 254
 - Kalkstein, Laurence, 174
 - katabatic winds, 223, 264
 - Katmai, Alaska, eruption, 71*t*
 - Keeling, Charles, 15
 - Keeling curve, 15, 15*f*
 - Keetch-Byram Drought Index, 127–128, 128*f*
 - Kelvin temperature scale, 35, 94, 113, 151, 307, 332
 - Kelvin waves
 - coastal, 64, 67
 - equatorial, 64, 67
 - Kilauea, Hawaii, volcanic activity in, 70
 - kinetic energy, 34, 92
 - geopotential height and, 136
 - thermodynamic energy equation and, 332
 - Köppen Climatic Classification System, 159
 - modified, 161–164
 - Köppen, Vladimir, 159–164

Köppen–Geiger climate system, 159,
160–161*f*
in Asia, 189
climatic types of, 163*t*
first-order subdivisions in, 159, 162*t*
second-order subdivisions in,
159, 162*t*
third-order subdivisions in, 159, 162*t*
Thornthwaite system compared with,
166, 166*f*
Kotzebue, Alaska
climograph for, 219*f*
water balance diagram for, 219*f*
Krakatau, 238, 294
Krakatau easterlies, 238
Krakatau, Indonesia, eruption, 71*t*
kriging, 120
krypton, 15
Kuala Lumpur, Malaysia, climatic
classification of, 157
Kyoto Treaty (1997), 306, 319

L

La Niña, 60, 234. *See also* El Niño–Southern Oscillation (ENSO) event
in Australia and Oceania,
235–236, 236*f*
characteristics of, 64–65
climatic change from, 296
global effects of, 67
in Latin America, 240
MJO and, 238
ocean response to, 65*f*
Pacific Decadal Oscillation and, 69
phase of, 338
precipitation and, 68
Labrador current, 184
Lake Bonneville, 285
lake effect snows, 47, 184, 217
Lake Vostok, 241
Laki Fissure, 294
Lamb Weather Types, 173, 173*f*
laminar layer, 80, 80*f*, 81
land use, 72–73
landforms, change in, 290–291
Landsberg, Helmut, 169
land–water contrasts, 137–138,
184–185
lapse rate, 98
environmental, 18, 80, 185
saturated adiabatic, 99, 100*f*
unsaturated adiabatic, 98, 100*f*, 183
Las Vegas, Nevada
climate of, 190
climograph for, 191*f*
Late Devonian extinction, 278
latent energy, 33, 72
latent heat, 172, 242, 309, 332
of vaporization, 110
latent heat flux (Q_E), 81, 92, 107
Latin America. *See* South America
latitude, 26–28, 54, 80, 230, 326
atmospheric circulation and, 34
centrifugal acceleration and, 40
climate effects of, 28
combined effects of revolution,
rotation, and tilt on, 29–32
Coriolis effect and, 38–40
in Europe, 185–187
general circulation, 132
horse, 133
lines of, 26*f*
in North America, 180
oceanic circulation and, 45
polar, 158
potential evapotranspiration, 111
pressure, 6
rotational speed and, 40
Sun path diagrams, 83
Laurentide Ice Sheet, 281
laws of motion, 45
LCD. *See* Local Climatological Data
LCO. *See* Little Climatic Optimum
lead, 316
leeward areas, 33
continentiality in, 33
of mountain ranges, 168
potential vorticity in, 146, 147*f*
precipitation in, 46
Rocky Mountain, 183
in Tropical Rain Forest climates, 245
Legates, David, 118
legislation, on air quality, 314
level of nondivergence, 145
LIA. *See* Little Ice Age
Libyan Erg dune, 253
lifting condensation level, 100
lithification, 304
lithosphere, 54, 80, 274, 288, 326
applied climatology on, 349
in atmosphere evolution, 13
definition of, 3
evidence of climatic change in,
285–288
interactions with atmosphere, 4*t*
water percolation through, 109
Little Climatic Optimum (LCO), 282
Little Ice Age (LIA), 282–283, 311
Little Ice Age, The (Fagan), 350
Little Rock, Arkansas
climograph for, 199*f*
water balance diagram for, 199*f*
livestock, methane from, 306
loadings, 174, 175, 175*f*, 336
local apparent time, 87
local atmosphere
advantage and disadvantage of, 353
assessing stability in, 99–102
moisture in, 93–97
Local Climatological Data (LCD), 353,
355, 355*t*
local features, 46–47
local scale, 6, 352
local-scale thunderstorms, 332
local vertical, 38, 39*f*
Loch Lomond Stadial, 281
loess, 285
logarithmic wind profile, 103, 103*f*
London smog event (1952), 317
Long Beach, California
climograph for, 205*f*
water balance diagram for, 205*f*
Long-term Ecological Research (LTER)
Program, 359, 361*f*
long waves, 143
longitude, 26, 26*f*, 233, 326
international date line and, 180
low pressure belt, 132
in North America, 180
rotation of Earth and, 28
Sun path diagram, 83
longwave radiation, 80, 237, 276, 302
low-level jet stream and, 182, 182*f*
from the Earth, 91
Loop current, 185
Lorenz, Edward, 335
low-level jet streams
East African, 233–234
in North American climate, 182
LTER Program. *See* Long-term
Ecological Research Program
Lubbock, Texas
climograph for, 195*f*
water balance diagram for, 195*f*
Lusaka, Zambia, 258
climograph for, 260*f*
water balance diagram for, 260*f*
lysimeters, 96, 96*f*, 111

M

Madagascar, drought in, 66
Madden-Julian Oscillation (MJO),
237–238, 337, 343
magma, 293
magnetic fields, 20
Manaus, Brazil
climograph for, 245*f*
water balance diagram for, 245*f*
Manchester, England
climograph for, 209*f*
water balance diagram for, 209*f*
Manila, Philippines
climograph for, 247*f*
water balance diagram for, 247*f*
March equinox, 31
Marine Dry Winter (Cwb) climates, 262
Marine West Coast (Cfb, Cfc) climates,
208–211
Marine West Coast Cool Summer (Cfc)
climates, 208–211
Marine West Coast Warm Summer (Cfb)
climates, 208–211, 258, 262
Maritime Continent, 56, 61, 234, 280
maritime effects, 32, 198
latitude and, 47
ocean surface currents and, 55
upwelling in, 45

- maritime polar (mP) air masses, 170, 185
- maritime tropical (mT) air masses, 170
 - in Africa, 232
 - in North America, 180
- Martha's Vineyard, formation of, 280
- mass, 34
 - advection, 55–57
 - height and, 46
- mass conservation equation, 333
- mass spectrometry, 284
- Massachusetts Institute of Technology, 34
- Mather, John, 125
- matter
 - general circulation of, 132
 - local flux of, 93–97
- Mauna Loa, Hawaii, 15
- Maunder Minimum, 295
- Max Planck Institute for Meteorology (Germany), 326
- maximum/minimum thermometer, 357
- McMurdo Research Station, Antarctica,
 - climograph for, 265f
- mean free path, 21
- mechanical turbulence, 80–81, 102–103
- Medieval Warm Period (MWP), 282
- Mediterranean (Csa, Csb) climates, 202–208, 258, 314
- Mediterranean Hot Summer (Csa)
 - climates, 204, 258
- Mediterranean Warm Summer (Csb)
 - climates, 204, 258
- meltemi, 224
- melting, 309
 - process, 92
- mercury in barometers, 36, 36f
- meridians, principal, 86. *See also*
 - longitude
- meridional flow, 142
 - pattern, 340
 - vorticity in, 146
- mesopause, 20
- mesoscale, 6, 334
 - convective complexes, 6
 - convective systems, 6
- Mesoscale Model version 5 (MM5)
 - model, 327
- mesosphere, 20
- mesothermal (C) climates
 - in Australia and Oceania, 235
 - classification of, 159, 162, 162t
 - Humid Subtropical, 198–201, 256, 258
 - Marine West Coast, 208–211, 258, 262
 - Mediterranean, 202–208, 258
 - northern hemisphere, 198–211
 - southern hemisphere, 256, 258–262
 - subtropical dry winter, 258
- Mesozoic Era, 278
 - marine life in, 278
- meteorologists, 4–5, 365
- meteorology and climatology, 4–6, 365–366
- methane (CH₄), 13, 72, 276
 - in global warming, 305–306, 305f
 - hydrates, 306
 - from methanogens, 17
 - as variable gas, 16, 16t
- methanogens, 17, 276, 305
- Mexico City, Mexico
 - climograph for, 266f
 - water balance diagram for, 266f
- MI. *See* moisture index
- Miami, Florida
 - climograph for, 249f
 - water balance diagram for, 249f
- microfossils, 288
- micrometers, 19, 303
- microscale, 6, 80, 347
- microthermal climatic classification, 159, 162, 162t, 187
- Microthermal Midlatitude (D) climates, 211–217
 - Subarctic, 218–222
- Middle East, 189
- Midlatitude Cold Desert (BWk) climates, 190, 192–193, 192f, 253
- midlatitudes
 - climatic classification of, 162–163
 - cold climatic classification, 159
 - mild climatic classification, 159
 - northern hemisphere, 180
 - prevailing wind in, 34
 - as source regions, 170
 - surface features in, 142
 - upper-level winds in, 136–137, 137f
 - wave cyclones, 42, 313
 - fronts in, 171f, 172
 - in Marine West Coast climates, 209
 - Mediterranean climates and, 207
 - in North America, 180
 - Rocky Mountains and, 183
 - westerlies, 312
 - in Africa, 232
 - definition of, 135
 - in North America, 180
- midoceanic ridges, 70
- Milankovitch cycles, 291–293, 326
- Milankovitch, Milutin, 291
- millibar (mb), 36, 94
- Minsk, Belarus
 - climograph for, 215f
 - water balance diagram for, 215f
- Mississippi River, 109
 - formation of, 280
 - saltwater intrusion in, 123
 - surplus and runoff, 123
 - volcanic activity and, 293–294
- Mississippian period, 277f, 278
- mistral winds, 224
- mitigation, 319, 327
- mixing ratio, 334
- MJO. *See* Madden-Julian Oscillation
- MM5 model. *See* Mesoscale Model version 5 model
- modern climatic changes, 301–320
- Mogadishu, Somalia, 254
 - climograph for, 257f
 - water balance diagram for, 257f
- moisture
 - in air mass classification, 169–170, 170t
 - anomalies, 235
 - and atmospheric statics, 97–102
 - in Australia and Oceania, 235
 - conservation equation, 333
 - in Desert climates, 188, 192–193
 - in Humid Continental climates, 211, 217
 - in Humid Subtropical climates, 201, 258
 - in Ice Cap climates, 264–265
 - in local atmosphere, 93–97
 - in Marine West Coast climates, 209–211, 262
 - in Mediterranean climates, 207–208, 258
 - in Polar climates, 264
 - in steppe climates, 194, 198, 256
 - in Subarctic climates, 222
 - in Subtropical Dry Winter climates, 202
 - in surface boundary layer, 95–96
 - of Thornthwaite Classification System, 165t
 - in Tropical Monsoon climates, 246
 - in Tropical Rain Forest climates, 242–246
 - in Tropical Savanna climates, 248, 253
 - in True Desert climates, 254
 - in Tundra climates, 222
- moisture index (MI), 164, 165t
- momentum, 6, 69, 80, 274, 330, 359
 - of air, 42
 - conservation of angular, 135
 - flux in, 102
 - general circulation of, 132
 - in oceanic circulation, 44–45
- Mongolia, steppe climate in, 189
- monsoons, 296
 - Asian, 187–188
 - definition of, 187
 - effects of Asia, 187–188
 - summer, 189–190
 - west African monsoon system, 253
- Moon, 12
- Moosonee, Canada
 - climograph for, 221f
 - water balance diagram for, 221f
- moraines, 285
- Moscow, Russia
 - climograph for, 216f
 - water balance diagram for, 216f
- motion
 - Navier-Stokes equations of, 41, 330–332, 359
 - Newton's laws of, 44
 - Newton's second law of, 12
 - primitive equations of, 332

Mount Pinatubo, Philippines, eruption, 71*t*, 293

Mount St. Helens, 294

Mount Toba, 294

mountains

- airflow over, 146–147, 147*f*
- in Asian climate, 188–189
- in Asian monsoons, 188–189
- in European climate, 186
- formation of, 290–291
- glacier retreat in, 74
- in North American climate, 183
- uplift, 291
- winds, 224

mudslides, 67, 114, 240

Mullen, George, 17

Muller Weather Types, 173, 173*f*

Multivariate ENSO Index, 62

Mumbai, India

- climograph for, 249*f*
- water balance diagram for, 249*f*

Murmansk, Russia, 46

- climograph for, 219*f*
- water balance diagram for, 219*f*

N

Namib Desert, 254

NAO. *See* North Atlantic Oscillation

National Aeronautics and Space Administration (NASA), 326, 359, 361

National Air Quality Standards (NQA), 314

National Center for Atmospheric Research (NCAR), 326, 327, 353

National Centers for Environmental Information (NCEI), 283, 352, 353, 356, 359

National Centers for Environmental Prediction, 353

National Climate Program Act, 352

National Climatic Data Center (NCDC), 352

National Data Buoy Center, 359

National Environmental Satellite, Data, and Information Service (NESDIS), 352, 356

National Oceanic and Atmospheric Administration (NOAA), 123, 352, 353, 353*f*, 355, 356, 365–366

- organizational chart for, 352*f*

National Snow and Ice Data Center, 359

National Weather Service, 5, 41, 99, 351–352, 353*f*, 366

- evapotranspiration measurement by, 96
- water balance models used by, 123, 123*f*

Native Americans, migration of, 280

natural systems, climate impacts on, 348–349

Navier-Stokes equations of motion, 41, 330–332, 359

NCDC. *See* National Climatic Data Center

near-surface troposphere, 80–81

nebula, 12, 12*f*

negative feedback systems, 69, 311

negative vorticity, 143

Neogene period, 279

neon, 12, 15

NESDIS. *See* National Environmental Satellite, Data, and Information Service

net radiation (Q^*), 90, 93, 110

- in Budyko Climatic Classification System, 167
- potential evapotranspiration and, 113

neutral atmosphere, 98

- potential temperature, 101
- Richardson number in, 103

Nevada, anticyclones in, 183

New Delhi, India

- climograph for, 202, 203*f*
- water balance diagram for, 203*f*

New Orleans, Louisiana, zone mean time in, 86

New York, ocean current effects on, 46

New Zealand

- Marine West Coast climates in, 258, 262
- mesothermal climates in, 256

Newton (N), 36

Newton's laws of motion, 44

Newton's second law of motion, 12, 134, 333

Niño 3.4 Index, 62, 62–63*f*

nitric acid (HNO_3), 319

nitric oxide (NO), 314

nitrogen

- atmospheric composition of, 13*t*
- as constant gas, 15
- diatomic (N_2), 13

nitrogen dioxide (NO_2), 314

nitrogen oxides (NO_x), 306, 316–317

nitrous oxide (N_2O), 16, 16*t*, 306, 317

NOAA. *See* National Oceanic and Atmospheric Administration

noble gases, 12

noise, 274

nonattainment zone, 314

nonscientific professionals, and climate scientists, interaction between, 366–367

nonthreshold pollutants, 314, 315*f*

nor'easters, 180, 184, 349

Normalized Difference Vegetation Index, 367

normals

- annual climatic, 274
- definition of, 5
- regionalization and, 158

North America

- air motion over, 151
- average annual snowfall in, 117*f*
- boreal forest in, 218
- climatic setting of, 180–185
- deforestation in, 72
- Gulf of Mexico effects on, 180, 182
- Highland climates in, 223
- Humid Continental climates in, 211
- Humid Subtropical (Cfa) climates in, 198
- Marine West Coast climate in, 208
- Mediterranean climate in, 203, 204, 207
- mountain ranges in, 182–183
- physiographic features of, 180*f*
- teleconnections over, 342, 342*f*
- temperature range in, 48
- Tundra climates in, 222

North American Steppes, 189, 193

North American summer monsoon, 192

North Atlantic Deep Water, 58

North Atlantic Drift, 46, 56, 290

- continental drift and, 290
- European climate effects of, 185–186
- Ice Cap climates and, 222
- in Marine West Coast climates, 208

North Atlantic Ocean, 281

North Atlantic Oscillation (NAO), 340–341, 340*f*, 341*f*

North Equatorial current, 56, 61, 186

North Pacific high, 139, 140*f*

North Pacific Intermediate Water, 58

North Pole

- geopotential height at, 137, 137*f*
- latitude of, 26
- rotation viewed from, 28
- surface wind systems in, 135

North Sea, 208

North Star, 29

northeast trade winds, 61, 230

- in Africa, 232
- easterly waves in, 230, 231*f*
- in surface wind systems, 134

Northern Annular mode, 341

northern hemisphere

- atmospheric behavior in, 230–231
- climates, 180–225
- Europe, 185–187
- regional, 189–224
- Coriolis effect in, 39
- cyclone and anticyclone airflow in, 42, 42–44*f*
- day length in, 29–31
- Ekman spiral in, 45, 45*f*
- extratropical climates in, 180–225
- January isotherms in, 47, 48*f*
- mean geopotential height in, 151, 152*f*, 153
- ocean surface currents in, 54, 55

northern lights, 20

Norway, ocean current effects on, 46

NQA. *See* National Air Quality Standards

nuclear autumn, 312
 nuclear fusion, 12, 16
 nuclear winter, 312
 nutrients, 369

O

oases, 253
 occluded fronts, 172–173, 172*f*, 183
 occlusions, 209
 Oceania, 234
 climatic setting of, 234–238
 ENSO events in, 235–236
 general characteristics of, 235
 MJO in, 237–238
 physiographic features of, 234*f*
 QBO in, 238
 oceanic circulation, 44–46
 oceanic general circulation models, 327
 oceanic Rossby waves, 64
 oceans. *See also* continentality
 acidification, 279
 advection in, 32
 as carbon reservoirs, 13–14, 304
 circulation in, 44–46, 54–59
 in climate system, 32–33
 climatic feedbacks in, 69–70
 convection in, 33
 currents
 in circulation, 54–59
 deep ocean thermohaline, 57–59
 in European climate, 185–186
 in North American climate, 184–185
 salinity inequalities and, 45
 surface, 54–57, 54*f*
 upwelling, downwelling, and mass advection in, 55–57
 pressure in, 35
 reservoirs, 108
 surface temperatures of, 9
 upwelling in, 45
 water transparency in, 32–33
 Oimekon, Siberia, 218
 Oort cloud, 12
 optical air mass, 82
 orbit changes, 291
 Ordovician period, 278
 Ordovician-Silurian extinction event, 278
 Orion Nebula, 12*f*
 orogeny, 290
 orographic effects, 46, 230
 in Asian monsoons, 189
 precipitation measurement and, 120
 in Subtropical Dry Winter, 202
 in tropical climates, 230
 in Tropical Rain Forest climates, 245
 oroshi wind, 224
 Ottawa, Canada
 climograph for, 214*f*
 water balance diagram for, 214*f*

Outback, 253
 outflow boundary, 181
 outgassing, 13, 70
 oxygen
 as constant gas, 15
 deep-water conveyor movement of, 59
 diatomic (O_2), 13, 13*t*, 19
 historical changes in levels of, 276, 277, 278
 methanogens and, 17
 rain forests and, 72
 oxygen-16, 287
 oxygen-18, 287
 Oymyakon, Siberia, temperature range in, 218
 ozone (O_3), 13, 238
 layer, 13
 ozone hole, 264
 processes in, 19–20
 photochemical smog and, 317
 polar climates and, 264
 production and dissociation of, 19
 as variable gas, 16, 16*t*

P

Pacific Decadal Oscillation (PDO), 69
 ENSO events and, 69
 teleconnections in, 337–339, 339*f*
 Pacific-North American (PNA) pattern, 342, 342*f*
 Pacific Ocean
 extratropical teleconnections in, 337–339, 338*f*, 339*f*
 monsoons in, 187
 as source area, 58
 Southern Oscillation Index and, 62
 thermohaline currents in, 58, 59
 trade winds, 60
 tropical cyclones in, 258
 Pacific Subarctic Water, 58
 paleoclimatological evidence, 293
 paleoclimatological reconstruction, 290
 paleoclimatologists, 282
 paleoclimatology, 7, 283. *See also* climatic change and variability
 secondary sources on, 359
 Paleogene Period, 279
 paleotempestology, 284
 Paleozoic Era, 278
 Palmer Drought Severity Index (PDSI), 126–128, 127*f*
 Palmer Hydrological Drought Index, 127
 palynology, 288–289
 pan adjustment coefficient, 96
 Pangaea, 278, 279, 293
 parallelism, 28–29
 parallels, 26. *See also* latitude
 Paramenides, 158
 parameterizations, 333
 parent isotope, 284

particulates, 71, 314, 316, 317*f*
 Pascals (Pa), 36, 94, 151
 path length, 27, 27*f*, 82
 PCA. *See* principal components analysis
 PDO. *See* Pacific Decadal Oscillation
 PDSI. *See* Palmer Drought Severity Index
 PE. *See* potential evapotranspiration
 pendulum day, 40
 Penman, H. L., 113, 114
 Penman-Monteith equation, 113
 Pennsylvanian period, 277*f*, 278
 percolation, 109
 perihelion, 28, 230
 orbit eccentricity and, 291
 precession and, 292–293, 292*f*
 periodic variability, 274, 275*f*
 periods, 277, 278
 permafrost, 72, 222, 310
 permeability, 122
 Permian periods, 277*f*, 278
 peroxyacetyl nitrates, 318
 perspiration, 95
 Perth, Australia
 climograph for, 260*f*
 water balance diagram, 260*f*
 Peru, 55
 current, 55, 239
 ENSO events in, 62
 PGF. *See* pressure gradient force
 Phanerozoic Eon, 277
 Philippines
 cyclones in, 189
 Maritime Continent, 56
 mountain effects in, 189
 volcanic activity in, 71*t*
 Phoenix, Arizona
 climate of, 190
 climograph for, 191*f*
 photochemical smog, 314, 317–318, 318*f*
 photodissociation, 19, 317
 photosynthesis, 13, 70, 81, 276, 349
 Amazon basin in, 239
 in atmosphere formation, 13
 carbon dioxide in, 305
 ozone layer and, 19
 in rain forests, 72
 physical climatology, 7
 secondary sources on, 359, 361–362
 phytoplankton, 70, 264
 Pineapple Express, 183
 plane of the ecliptic, 28, 29*f*
 planetary albedo, 90
 planetary boundary layer, 81
 planetary scale, 6, 80, 326, 331, 347
 of climatic classification, 158
 planetary-scale, waves of motion, 132
 planetary vorticity (f), 143
 planetary wind systems, 134–137, 136*f*, 137*f*
 planetesimals, 12
 Pleistocene Epoch, 74, 280, 285, 287

plumbism, 316
 pluvial lake, 280
 PM₁₀ particulates, 316
 PM_{2.5} particulates, 316, 317f
 PNA pattern. *See* Pacific-North American pattern
 polar (E) climates, 222–223
 Ice Cap, 159, 222–223, 264–265
 Tundra, 159, 222, 262, 264
 polar cells, 134, 341
 locations and strength of features in, 139–141
 upper-level winds in, 135–136, 136f
 polar climatic classification, 159, 162t, 163
 polar easterlies, 135, 341
 polar front, 141
 jet stream, 67, 68, 149–151, 150f
 Himalayas and, 188
 Pacific-North American pattern and, 342
 polar highs, 134
 polar jet stream, 74
 polar regions
 molecular kinetic energy at, 136
 water vapor in, 16
 polar vortex. *See* polar high
 Polaris, 29
 pollen, 288–289
 pollutants, classification of air, 314–319
 pollution, 312
 air quality legislation and, 314
 atmospheric, 312–314
 classification of air pollutants, 314–319
 climate influences of, 47
 factors affecting, 313–314
 in global dimming, 313
 smog, 308
 porosity, 121
 positive feedback systems, 69, 74, 280, 309, 368
 cryospheric, 232
 natural system impacts and, 349
 greenhouse gases and, 309
 positive phase of NAO, 340
 positive vorticity, 143
 Rocky Mountains and, 183
 potential evapotranspiration (PE), 96, 189, 246
 global annual average of, 111, 112f, 113f
 Holdridge method of calculating, 167
 measuring, 111, 113
 moisture index and, 164, 165t
 Penman-Monteith equation for, 113
 in surface water balance, 111, 112f, 113f
 Thornthwaite, 111, 112f, 113f, 164
 unadjusted, 112
 U.S. annual average of, 111, 112f, 113f
 in water balance diagrams, 126, 126f

potential temperature, 101–102, 102f
 potential vorticity, 146, 147f, 291
 Rocky Mountains and, 183
 pre-boreal warm interval, 282
 precession, 292–293, 292f
 precipitable water, 108
 precipitation
 annual average throughout the world, 116f
 annual North America, 115f
 in Antarctica, 241
 in anticyclones, 43
 in Asian monsoons, 188
 in Australia and Oceania, 235, 236f, 237
 cloud thickness and, 171
 cooling by, 33
 ENSO events and, 62, 68
 instrumentation in measuring, 356–357, 356f, 357f
 ITCZ in, 142
 measurement of, 115–116, 116f, 118f
 in rain forests, 72
 spatial analysis of, 118–119, 119f
 in surface water balance, 114–120
 thermohaline currents and, 57–58
 topography and, 46
 undercatch of, 118, 357
 urban heat islands and, 309
 water vapor levels and, 16
 pressure, 34–36, 35f, 331
 centrifugal acceleration and, 40
 cyclones and anticyclones and, 42–44
 in deep ocean thermohaline currents, 57
 definition of, 34
 high, 36
 isobars, 36
 low, 36
 mean surface, in semipermanent surface pressure cells, 140f
 notations for, 36
 Southern Oscillation Index of, 62
 pressure gradient force (PGF), 37–38, 38f, 41, 81, 230, 331
 in surface wind systems, 134
 vertical motion and, 41
 Pretoria, South Africa
 climograph for, 263f
 water balance diagram for, 263f
 prevention, 327
 of global warming, 319
 primary climate impacts, 348
 primary data, 352
 primary pollutants, 315–317
 prime meridian, 26
 primitive equations of motion, 332
 principal components analysis (PCA), 174, 337
 principal meridians, 86, 87f
 principle of superposition, 285
 Principle of Uniformitarianism, 283
 prokaryotes, 13

Proterozoic Eon, 277
 prototype atmospheric circulation patterns, 176
 proxy evidence, 7, 283, 290, 297, 302
 pyranometer, 89
 Pyrenees, 193
 pyrgeometer, 89
 pyrradiometer, 89

Q

QBO. *See* quasi-biennial oscillation
 quantitative analysis, 174–176
 cluster, 175–176, 176f
 eigenvector, 174–175, 175f
 hybrid techniques for, 176
 quantitative methods, 326–342
 atmospheric teleconnections and, 337–342
 basic equations in, 330–336
 computerized climate models, 326–330
 statistical techniques, 336–337
 quasi-biennial oscillation (QBO), 238, 296, 337
 quaternary period, 277f, 279
 Quito, Ecuador
 climograph for, 266f
 water balance diagram for, 266f

R

radar-derived precipitation data, 118
 radiant energy, 33
 measuring, 87, 89
 radiation
 and absolute zero, 91
 and advection, 91
 atmospheric window for, 302t, 303
 balance equation, 91
 balance of, 90–92
 counter-, 91
 diffuse, 91
 direct, 91
 longwave. *See* longwave radiation
 net, 90
 path length of, 27, 27f
 shortwave. *See* shortwave radiation
 ultraviolet, 13
 wavelengths of, 19, 80
 radioactive decay, 284
 radiometers, 87, 352
 radiometric dating, 284–285
 techniques, 285
 radiosondes, 99, 283
 rain forests. *See* tropical rain forests
 rain gauges, 115, 116f, 117
 Fischer-Porter, 356–357, 356f
 standard nonrecording, 356
 tipping bucket, 357, 357f
 type of, 356–357
 rain machine, 72, 239

- rain shadow effects, 188, 193
 - Atacama Desert, 254
 - in steppe climates, 193
 - Raleigh-Durham, North Carolina
 - climograph for, 200f
 - water balance diagram for, 200f
 - random variability, 274, 275f
 - Rapid City, South Dakota
 - climograph for, 197f
 - water balance diagram for, 197f
 - RCM. *See* regional climate model
 - reanalysis data set, 353
 - recovery time, defined, 351
 - recreation, 349
 - recycling, 367
 - Red Sea, 16, 254
 - reflection, radiation balance and, 90.
 - See also* albedo
 - refraction, 31
 - Regional Climate Centers, 352
 - regional climate model (RCM), 327
 - regional climatology, 7, 189–224
 - regionalization of climate, 158
 - regression lines, 175, 175f
 - relative dating, 285
 - relative humidity, 93, 95, 308
 - around Asian mountains, 188
 - wet bulb depression and, 113
 - relative vorticity, 143
 - relativity, theory of, 35
 - relic landforms, 285
 - Renewable Resource Data Center, 362
 - Reno, Nevada
 - climograph for, 168, 169f
 - forcing mechanisms in, 168
 - research, on global warming, 320
 - reservoirs, 13–14, 73, 108, 304
 - residence time, 13, 108
 - of carbon, 14
 - of constant gases, 15
 - of variable gases, 15
 - residuals, 175
 - resilience, 350–351
 - defined, 351
 - Resilience Inference Measurement (RIM) model, 351, 351f
 - resistance, potential evapotranspiration and, 113
 - resolution, 326, 336
 - respiration, 13, 304
 - revolution, 28
 - of Earth, 28
 - Reykjavik, Iceland
 - climograph for, 210f
 - water balance diagram for, 210f
 - Richardson number, 102–103
 - Richmond, Virginia
 - climograph for, 200f
 - water balance diagram for, 200f
 - ridges, 67, 143–145, 230, 342
 - constant absolute vorticity trajectory and, 145, 146
 - in energy balance, 143
 - ENSO events and, 67
 - mountains and, 291
 - negative vorticity in, 143
 - over North America, 151
 - northern vs. southern hemisphere, 231
 - Rocky Mountains and, 183
 - in tropical atmospheres, 230
 - upper-level, 172
 - riming, 223, 265
 - risk management industry, 350
 - River Forecast Centers, 123, 123f
 - robust downscaling techniques, 336
 - rock striations, 285
 - Rocky Mountains, 183, 223
 - Rome, Italy
 - climograph for, 206f
 - water balance diagram for, 206f
 - Ronne Ice Shelf, 241
 - Ross Ice Shelf, 241
 - Ross Sea, 241
 - Rossby, Carl, 143, 145
 - Rossby waves, 143, 230, 341, 342
 - action centers in, 146
 - air mass transfer by, 171
 - constant absolute vorticity trajectory, 145f, 146
 - cyclogenesis in, 145
 - diffluence and confluence in, 148–149, 149f
 - divergence and convergence in, 147–148, 148f
 - equatorial, 64
 - mean patterns of, 15f, 151, 153
 - northern vs. southern hemisphere, 231
 - Rocky Mountains and, 183
 - in tropical atmospheres, 230, 231f
 - vorticity of, 143–145, 144f
 - rotation of Earth, 28, 86
 - Coriolis effect and, 38–40
 - vorticity and, 143
 - roughness layer, 80, 80f, 81
 - roughness length, 103
 - Rub-al-Khali, 233
 - runoff, 109, 123, 123f, 307
 - in Africa, 232
 - global distribution of, 109, 110f, 111f
 - rural areas, weather data collection in, 9
- S**
- Sacramento, California
 - climograph for, 205f
 - water balance diagram for, 205f
 - Sagan, Carl, 17
 - Sahara Desert, 73, 233
 - arid climate in, 253–254
 - steppe climate around, 254
 - Sahel, 335
 - desertification in, 73, 73f, 232
 - steppe climates in, 254
 - salinity
 - ocean currents and, 45
 - thermohaline currents and, 57–59
 - saltwater intrusion, 123, 309
 - San Diego, California
 - forcing mechanisms in, 168
 - Sun angle in, 28
 - San Francisco, California
 - continentality effects on, 32, 32f, 33, 34
 - maritime effect in, 34
 - sand dunes, 253
 - Santa Ana winds, 183
 - Santa Maria
 - California
 - climograph for, 206f
 - water balance diagram for, 206f
 - Guatemala, eruption, 71t
 - Santiago, Chile
 - climograph for, 261f
 - water balance diagram for, 261f
 - Sargasso Sea, 134
 - satellite monitoring and recording,
 - global warming skeptics on, 311–312
 - saturated adiabatic lapse rate (Gs), 99, 100f
 - saturation vapor pressure (e_s), 93, 94f, 108, 150
 - SBL. *See* surface boundary layer
 - scales in climatology, 6
 - scattering, 82, 90
 - scores, 174, 175, 337
 - scree plots, 176, 176f
 - sea level
 - in Antarctica, 241
 - El Niño and, 62
 - eustatic, 241
 - ice ages and, 280
 - ice sheet melting and, 280, 281f
 - La Niña and, 65, 65f
 - pressure at, 35, 36
 - sea surface, 60, 61, 63
 - sea surface temperatures (SSTs),
 - El Niño and, 61, 62
 - seasonality
 - axial tilt changes and, 292
 - carbon dioxide cycles and, 15
 - Earth–Sun relationships in, 28–32
 - in North America, 180
 - northern vs. southern hemisphere, 230–231
 - prevailing winds and, 34
 - of surface pressure features, 141
 - temperature variation and, 47–48, 48f, 49f
 - tropical, 26
 - Seattle, Washington
 - climograph for, 208f
 - water balance diagram for, 208f
 - second law of thermodynamics, 11, 34, 36, 132

- secondary circulations, 132, 142–153
 anticyclones, 173
 cyclones, 145, 173
 midlatitude wave cyclones as, 173
 northern vs. southern hemisphere, 231
 Rossby waves, 142–153
- secondary climate impacts, 348
- secondary data, 352
- secondary pollutants, 315, 317–319
- sedimentary rock, 13, 14, 285, 304
- semiarid climate, 162, 162*t*
- semiarid regions, 159
 desertification of, 73
 northern hemisphere, 189
- semipermanent high-pressure cells, 139, 140*f*
- sensible energy, 33, 72
- sensible heat, 242, 307, 332
- sensible heat flux (QH), 81, 92
 potential evapotranspiration and, 113
- sensible heating, 134
- Seoul, South Korea, climatic classification of, 157
- September equinox, 31
- severe weather. *See also* cyclogenesis
 in Europe, 186
 in North America, 180–182, 180*f*
- shearing stress, 81
- Sheridan, Scott, 174
- ship logs, weather data in, 63, 289
- shortwave radiation, 19, 80, 348–349
 global budget of, 90, 90*f*
 greenhouse effect and, 302
 in low-level jet stream formation, 182
 radiation balance and, 90
- Siberia
 low temperatures in, 141
 ocean current effects on, 46
 temperature extremes in, 187, 218
- Siberian high, 141, 187, 242
- Siberian Traps event, 278
- siderite (FeCO₃), 17
- Sierra Madre Occidental, 238*f*, 239
- Sierra Madre Oriental, 238*f*, 239
- Sierra Nevada Mountains, 168, 169*f*, 183
 Highland climates in, 223
 steppe climate around, 189
- Simpson Desert, 253
- Singapore, Singapore
 climograph for, 243*f*
 water balance diagram for, 243*f*
- singular value decomposition, 174
- sinistral individuals, 288
- sinks, 72
 carbon dioxide, 14, 304
- skeptics, 311–312
- Skew T–Log P diagram, 100
- slab model, 327
- slash and burn agriculture, 72
- smog, 308
 industrial, 317
 photochemical, 314, 317–318, 318*f*
- snow. *See also* precipitation
 in Antarctica, 264
 gauge, 115, 116*f*
 whiteouts, 241
- snow and snowfall, 116*f*. *See also* precipitation
 average annual global, 118*f*
 average annual North America, 115–117, 117*f*
 in Humid Continental climates, 217
 lake effect, 47, 47*f*
 in Marine West Coast climates, 211
 measuring, 115–117, 117*f*, 118*f*
 polar cells and, 134
- snowball Earth hypothesis, 278
- snowfall, historical data on, 289
- social gain, 369
- societal systems, climate impacts on, 349–350
- SOI. *See* Southern Oscillation Index
- soil
 as carbon reservoir, 14
 in climatic classification, 159
 heat flux plates, 93
 moisture, 253
 recharge, 122, 125, 126, 232
 storage capacity in, 121–122, 121*f*, 122*f*
 withdrawal, 122, 126
 permeability of, 122
 porosity of, 121
 in tropical rain forests, 72
- solar declination, 28, 32
 in Africa, 233
 axial tilt changes and, 292
 ITCZ and, 138
 revolution, rotation, and tilt in, 30
 Sun path diagrams and, 83, 83–85*f*
- solar noon, 31, 32, 86, 132
- solar output, 16–17, 294–296, 295*f*
- solar system, formation of, 13
- solar time, 86–87
- solar wind, 12
- solid aerosols, 11–12, 71
- solstice
 December, 31
 June, 30
 precession and, 292, 292*f*
 summer, 30, 82
 winter, 31, 82
- Somali jet, 234
- source areas, 58
- source regions, 169, 182, 185
- South America
 climatic setting of, 238–240, 238*f*
 ENSO events in, 62, 65
 Humid Subtropical climates in, 258
 rain forest destruction in, 72
 subtropical dry winter climate in, 258
 temperature range in, 48
 upwelling around, 55
- South Atlantic high, 139, 140*f*, 232
- South Equatorial current, 61
- South Pacific Convergence Zone (SPCZ), 236–237, 237*f*
- South Pacific high, 139, 140*f*, 235
- South Pacific subtropical anticyclone, 55
- South Pole, 240–241, 240*f*
 climograph for, 265, 265*f*
 continental drift and, 290
 day length at, 31
 geopotential height at, 137, 137*f*
 latitude of, 26
 surface wind systems in, 135
- southeast trade winds, 61
 in Africa, 232
 in surface wind systems, 134
- southern hemisphere
 atmospheric behavior in, 230–231
 climates
 Africa, 231–234
 Antarctica, 240–241
 Australia and Oceania, 234–238
 Latin America, 238–240
 regional, 242–267
 tropical vs. extratropical, 230
 Coriolis effect in, 39
 day length in, 31
 January isotherms in, 47, 48*f*
 July isotherms in, 47, 48*f*, 49*f*
 ocean surface currents in, 54, 55
- southern lights, 20
- Southern Oscillation (SO), 60, 69, 235, 241
 climatic change from, 296
 impacts of, 337, 338*f*
- Southern Oscillation Index (SOI), 62, 296*f*. *See also* El Niño–Southern Oscillation (ENSO)
 event
- south-westerly monsoons, 188, 234
- spatial analysis methods, 118–119, 119*f*
- spatial downscaling, 327
- spatial resolution, 326
- spatial scales, 80
- Spatial Synoptic Classification System, 174
- SPCZ. *See* South Pacific Convergence Zone
- specific heat, 32, 33*t*, 137, 307
 at constant pressure, 332
- specific humidity, 95, 264, 333, 334
- specific volume, 331
- spectral models, 328, 329*f*
- speleothems, 287
- Spokane, Washington, forcing mechanisms in, 168, 169*f*
- spores, 288–289
- squall lines, 181
- St. Lawrence Seaway, 280
- St. Louis, Missouri, continentality effects on, 32, 32*f*
- stability, 97, 235, 308
 assessing local atmosphere, 99–102
 atmospheric, 98–99, 111
 and hydrostatic equation, 97–102
 low-level atmospheric, 139
 in low-level jet stream, 182

- stable atmosphere, 54–55, 98
 - pollution concentrations in, 313
 - potential temperature in, 101
 - stable stratification, 57
 - of air, 172
 - standard nonrecording rain gauge, 356
 - star formation, 12, 16
 - State Climatology Program, 352
 - statics, atmospheric, 97–102
 - stationary fronts, 171, 171*f*
 - statistical downscaling, 327
 - in climate models, 367
 - statistical techniques, 336–337
 - statistics, 7–9
 - step changes, 274, 275*f*
 - steppe (BS) climates, 162*t*, 163, 164*t*, 189, 193–198, 254, 256
 - stomates, 95, 125
 - Stommel, Henry, 59
 - Stommel model, 59, 59*f*
 - Storm Data*, 355–356
 - storms. *See* cyclogenesis
 - Strait of Otranto, 224
 - stratification, stable, 57, 57*f*
 - stratiform, 241
 - clouds, 171, 209
 - stratopause, 20
 - stratosphere, 19, 70, 71, 238, 283, 317
 - streamline analysis, 230
 - Styrofoam, 19
 - sub-boreal cold interval, 282
 - Subarctic (Dfc, Dwc, Dwd) climates, 218–222
 - subduction zones, 293
 - sublimation, 74, 92, 309
 - subpolar lows, 134, 135, 141, 230
 - substrate heat flux (Q_G), 92–93, 93*f*, 113
 - subtropical anticyclones, 54, 230, 313
 - in Africa, 232
 - in arid climates, 190
 - as forcing mechanisms, 168
 - in general circulation, 138–139, 140*f*
 - Hadley cells and, 133
 - location and strength of, 138–139, 140*f*
 - in Mediterranean climates, 203, 204*f*, 207
 - migration of, 139
 - ocean salinity and, 58
 - ocean surface currents and, 54
 - in surface wind systems, 134
 - Subtropical Desert (BWh) climates, 253
 - Subtropical Dry Winter (Cwa, Cwb) climates, 202, 258
 - Subtropical Hot Desert (BWh) climates, 190
 - subtropical jet stream, 67, 136
 - sulfur, 13
 - sulfur dioxide (SO₂)
 - in industrial smog, 317
 - volcanic activity and, 70
 - sulfur oxides, 315
 - sulfuric acid (H₂SO₄), 318
 - summer monsoons, 189–190
 - Subtropical Dry Winter climates and, 202
 - in Tokyo, 202
 - summer solstice, 30, 82
 - summer thermal efficiency
 - concentration, 164, 165*t*
 - Sun, 13
 - angle effect on building design, 82*f*
 - angle of
 - climate and, 180
 - latitude and, 26–28, 26*f*, 29, 32
 - changes in output from, 16, 276, 291–296
 - Earth–Sun relationships and, 28–32
 - energy from, 81–82
 - faint young Sun paradox and, 16–17
 - ozone layer and, 19
 - path diagram, 83–86, 87*f*
 - radiation emission spectrum of, 91
 - wavelength from, 19, 19*f*
 - sunlight, 314
 - sunspots, 294, 295*f*
 - supereruption, 294
 - superstorm, 180
 - surface airways observations, 355, 355*t*
 - surface boundary layer (SBL), 81
 - in low-level jet stream, 182
 - moisture in, 95–96
 - surface currents, ocean, 54–57, 54*f*
 - surface cyclones, 145
 - surface tension, 121
 - surface water balance, 110–124, 163, 232, 366
 - in Africa, 232
 - applied climatology and, 348
 - deficits in, 122
 - diagrams on, 126, 126*f*
 - droughts indices and, 126–128, 127–129*f*
 - evapotranspiration, 114
 - example of, 124–125, 124*t*
 - Great Lakes in, 184
 - models, 326
 - potential evapotranspiration in, 111–113, 112–113, 112*f*, 113*f*
 - types of, 125–126
 - precipitation in, 114–120
 - snowfall in, 115–117, 116*f*, 117*f*, 118*f*
 - soil moisture storage in, 121–122, 121*f*, 122*f*
 - surplus and runoff, 122–123, 123*f*
 - surplus water, 122, 123*f*
 - in Tropical Rain Forest climates, 245
 - surface weather maps, 36, 37*f*
 - surface wind systems, 134–135
 - surplus water, 122, 123*f*, 164
 - sustainability, 368–369
 - defined, 368
 - swamp
 - drainage of, 73
 - model, 327
 - synoptic analysis, 336
 - synoptic climatology, 7, 337
 - secondary data sources for, 352–355
 - synoptic scale, 6, 331
- ## T
- taiga, 218, 222
 - Taiwan
 - cyclones in, 189
 - Humid Subtropical (Cfa) climates in, 198
 - Tallahassee, Florida, thermodynamic diagram for, 101*f*
 - Tambora, Indonesia, eruption, 71*t*, 282–283, 294
 - Tashkent, Uzbekistan
 - climograph for, 198*f*
 - water balance diagram for, 198*f*
 - Tasmania, 258
 - TBL concept. *See* Triple Bottom Line concept
 - technology, 369
 - Tegucigalpa, Honduras, 24
 - climograph for, 248*f*
 - water balance diagram for, 248*f*
 - teleconnections, 146, 296, 337–342, 366
 - extratropical Atlantic, 339–342, 340*f*, 341*f*, 342*f*
 - extratropical Pacific, 337–339, 338*f*, 339*f*
 - over North America, 342, 342*f*
 - Temperate Zone, 158
 - temperature
 - absolute zero, 34, 91, 302, 332
 - in air mass classification, 169–170, 170*t*
 - altitude and, 46
 - average, 7–8
 - climatic changes in geological history, 276–280
 - clouds and, 34
 - daily mean, 7–8
 - degree-days, 358
 - in Desert climates, 190
 - dewpoint, 94, 114, 230
 - Earth's revolution and, 28
 - extremes of, 8
 - faint young Sun paradox, 16–17
 - fossil evidence on, 288
 - in fronts, 171
 - frostpoint, 94
 - glacial advances and, 73
 - in Humid Continental climates, 211
 - in Humid Subtropical climates, 198–201, 256, 258
 - in Ice Cap climates, 264
 - inversions, 19, 90, 308
 - in Africa, 232
 - in low-level jet stream, 182
 - stratosphere, 20–21
 - thermosphere, 21

- temperature (*continued*)
 Kelvin scale for, 35
 lapse rate of, 98
 in Marine West Coast climates, 208–209, 262
 maximum–minimum calculation of, 8
 in Mediterranean climates, 204, 258
 mesopause, 20
 mesosphere, 20
 normals of, 8
 in Polar climates, 264
 potential, 101–102, 102*f*
 pressure and, 35
 records and statistics on, 7–9
 regionalization of, 173, 174*f*
 saturation vapor pressure and, 93, 94*f*
 seasonality and, 47–48, 48*f*, 49*f*
 solar output and, 294
 in steppe climates, 194, 254, 256
 in Subarctic climates, 218
 in Subtropical Dry Winter climates, 202
 surface, 17
 of Thornthwaite Classification System, 165*t*
 in Tropical Rain Forest climates, 242
 in Tropical Savanna climates, 248
 tropopause, 18
 in True Desert climates, 254
 in Tundra climates, 222
 water, 34
- temporal climatic changes, 274, 275*f*
 temporal downscaling, 327
 temporal resolution, 326
 temporal trends, 274
 Terjung, Werner, 366
 terrestrial radiation, 302
 tertiary period, 277*f*, 279
 thermal conductivity, 307
 thermal efficiency index, 164
 thermal lows, 188, 242
 thermal turbulence, 81, 102–103
 thermoclines, 64, 239
 thermodynamics
 diagrams, 99–101, 100*f*
 energy equation, 332–333
 first law of, 94
 processes, 17–18
 second law of, 11, 34, 36, 132
 thermohaline circulation, 45, 281, 349, 368
 deep ocean, 57–59
 rapid climate change and, 368
 thermohaline currents, 57
 thermometers, 159
 maximum/minimum, 357
 thermosphere, 21
 Thiessen polygon method, 119, 119*f*, 120
 30–60 Day Oscillation, 237
 Thompson, David, 341
 Thornthwaite, C. W., 111, 112*f*, 113*f*, 125, 159, 164–166
 Thornthwaite Climatic Classification System, 159, 164–166, 165*t*, 166*f*
 Köppen system compared with, 166
 Köppen–Geiger climate system compared with, 166*f*
 Thornthwaite potential
 evapotranspiration, 111
 threshold pollutants, 314, 315*f*
 Thule Air Force Base, Greenland
 climograph for, 223*f*
 water balance diagram for, 223*f*
 Tibetan low, 141, 188, 245
 Tibetan Plateau, 188
 Tien Shan mountains, 223–224
 Tierra del Fuego, 262
 time of day, record keeping and, 9
 time of observation bias, 9, 357
 time steps, 326
 time zones, 28, 86, 86*f*
 tipping bucket rain gauge, 357, 357*f*
 Titan, 276
 Tokyo, Japan
 climograph for, 19*f*
 water balance diagram for, 201*f*
 topography, 46
 circulation and, 132
 in North America, 180, 180*f*
 precipitation measurement and, 120
 in Tropical Rain Forest climates, 245
 Tornado Alley, 181, 181*f*
 tornadoes
 centrifugal acceleration in, 40
 as cyclones, 42
 low-level jet stream in, 183
 in North America, 181, 181*f*
 Rocky Mountains and, 183
 Toronto, Ontario, continentality in, 33
 Torricelli, Evangelista, 36, 159
 Torrid Zone, 158
 trade surge, 246
 trade winds, 60, 61
 Arctic Oscillation and, 341
 counter-, 233, 233*f*
 El Niño and, 60
 ITCZ and, 138, 138*f*, 139*f*
 La Niña and, 64, 65*f*
 in Latin America, 239
 northeast, 61, 134, 135, 230, 231*f*, 233
 southeast, 61, 134, 135, 232
 in surface wind systems, 134–135
 in Tropical Rain Forest climates, 245
 Walker circulation and, 63
 transition layer, 80*f*, 81
 transpiration, 72, 95, 107, 164, 307
 transportation, 349
 transverse wind shear, 144, 144*f*
 tree rings, 289
 treeline, 163, 222, 289
 Trewartha, Glenn, 159
 Triassic Period, 278
 Triple Bottom Line (TBL) approach, 369
 Tropic of Cancer, 30, 232
 axial tilt changes and, 292
 ITCZ and, 138
 Tropic of Capricorn, 31, 231
 axial tilt changes and, 292
 ITCZ and, 138
 tropical (A) climates
 in Australia and Oceania, 235
 classification of, 159, 162*t*
 extratropical vs., 230
 southern hemisphere, 242–253
 Tropical Monsoon, 246
 Tropical Rain Forest, 242–246
 Tropical Savanna, 246, 248–253
 tropical cyclones, 42, 296
 in Asia, 189
 Atlantic Ocean, 258
 frequency, 340
 Indian Ocean, 258
 in North America, 180
 Pacific Ocean, 258
 typhoons, 245
 Tropical Monsoon (Am) climates, 246
 Tropical Rain Forest (Af) climates, 242–246
 tropical rain forests
 deforestation of, 72, 239
 diversity in, 72
 soils in, 72
 in Tropical Monsoon climates, 246
 Tropical Savanna (Aw) climates, 242, 246, 248–253
 tropics
 definition of, 32
 net energy surplus in, 137
 seasonality in, 26
 tropopause, 18, 80, 137, 238
 troposphere, 17, 264
 circumpolar vortex and, 264
 cyclones and anticyclones and, 42, 43
 Hadley cells and, 133
 near-surface, 80–81, 80*f*
 properties of, 80
 temperature and altitude in, 46
 tropospheric ozone, 314
 troughs, 143, 342
 convergence and divergence around, 147
 in energy balance, 143
 ENSO events and, 67, 68
 inverted, 230
 mountains and, 291
 over North America, 151
 in tropical atmospheres, 230
 vorticity in, 144, 145
 True Desert (BW) climates, 162*t*, 163–164, 164*t*
 in Asia, 188
 in North America, 190
 northern hemisphere, 188, 190
 southern hemisphere, 253–254
 Tuareg, 253

Tucson, Arizona
 climograph for, 194f
 water balance diagram for, 194f
 Tundra (ET) climates, 159, 162*t*, 222,
 262, 264
 tundra, 306
 plant, 281
 Tura, Russia
 climograph for, 221f
 water balance diagram for, 221f
 turbulence, 80, 169
 mechanical, 80–81, 102–103
 thermal, 81, 102–103
 turbulent flux
 of latent heat, 81
 of sensible heat, 81
 turbulent fluxes, 92
 Turc method, 114
 Turkana jet stream, 233
 Twain, Mark, 34
 Typhoon Tip (1979), 245
 typhoons, 245

U

UALR. *See* unsaturated adiabatic
 lapse rate
 ubac slope, 46
 ultraviolet (UV) radiation, 13, 19–20,
 264, 317
 undercatch, 118, 357
 United States
 air quality, 318, 319
 legislation in, 314
 average annual precipitation
 in, 115f
 ENSO effects on, 67–68
 fossil fuel consumption in,
 306, 307f
 greenhouse gas emissions in, 306
 United States Weather Bureau, 351
 University Corporation for Atmospheric
 Research (UCAR), 327
 unsaturated adiabatic lapse rate (UALR),
 98, 100f, 183
 unstable atmosphere, 55, 181
 atmospheric stability and, 98
 pollution concentrations in, 313
 potential temperature in, 101
 Richardson number in, 103
 updrafts, 42
 upper-level winds, 135–137, 136f, 137f
 baroclinicity, 147, 148f
 constant absolute vorticity trajectory,
 145–146, 145f
 divergence and convergence in,
 147–148, 148f
 vorticity in, 143–145, 144f
 upwelling, 45, 47, 55, 55f, 232
 in La Niña, 64, 65f
 urban canyon, 309, 309f
 urban heat island, 8–9, 47, 73,
 307–309, 308f

urbanization
 desertification and, 73
 global warming skeptics and, 311
 greenhouse effect and, 307–309
 U.S. Department of Energy, 362
 U.S. Energy Information
 Administration, 306
 U.S. Forest Service, 127, 129f
 Utah
 anticyclones in, 183
 baroclinic zone over, 147, 148f
 UV radiation. *See* ultraviolet
 radiation

V

Vancouver, British Columbia, Sun
 angle in, 28
 vapor pressure (*e*), 93, 113, 264
 vaporization, latent heat of, 110
 variability. *See also* climatic change and
 variability
 changes, 274, 275f
 variable gases, 15–16, 16*t*
 variogram, 120
 varves, 7, 287
 veering, 42
 velocity
 convergence, 333, 334f
 divergence, 333–334, 334f
 Navier-Stokes equation for, 330
 Verkhoyansk, Siberia, 218
 vernal equinox, 31, 233
 vertical acceleration, 332
 vertical flux of horizontal
 momentum (τ), 81
 vertical motion, 41–42, 331–332
 vertical wind shear, 103, 181
 vertical zonation, 223, 265
 Vietnam, cyclones in, 189
 Vinson Massif, Antarctica, 241
 virtual temperature (T_v), 335
 visualization, 367
 Vladivostok, Russia
 climograph for, 217f
 water balance diagram for, 217f
 vog, 70
 volcanic activity
 aerosol indices and, 71
 atmosphere composition and,
 12, 70
 climate effects of, 70–71, 293–294
 general effects of, 70–71
 major eruptions, 71*t*
 volcanic eruptions, 135, 293, 294
 Volcanic Explosivity Index (VEI),
 71, 293
 volcanism, 278, 293, 294
 vorticity, 143–145, 144f
 absolute, 145, 172
 jet stream, 151
 negative, 143
 potential, 146, 147f, 291

Vostok ice core, 287
 Vostok Research Station, 241
 vulnerability, 350–351
 defined, 351

W

Walker circulation, 60–62, 61f, 340
 Walker, Gilbert, 60, 340
 Wallace, John, 341
 warm-ENSO events. *See* El Niño
 warm fronts, 171, 171f
 warm sector, 172, 172f
 Washington, DC
 continentality effects on, 32, 32f
 maritime effect in, 34
 thermodynamic diagram for, 100, 100f
 water
 altitude and, 47
 deficits, 122
 depression storage, 122
 fresh, 108
 global distribution of, 108, 109f
 interception, 123
 latent heat flux in, 92
 precipitable, 108
 runoff, 109, 110f, 123, 123f
 in solar system, 13
 surface tension of, 121
 surface water balance, 110–124
 surplus, 123, 123f
 transparency of, 137
 water balance. *See* surface water
 balance
 water balance diagrams, 126, 126f
 for Accra, Ghana, 251f
 for Albuquerque, New Mexico,
 192, 193f
 for Alice Springs, Australia, 256f
 for Antananarivo, Madagascar, 263f
 for Arequipa, Peru, 267f
 for Baghdad, Iraq, 195f
 for Barranquilla, Colombia, 252f
 for Baton Rouge, Louisiana, 199f
 for Beijing, China, 216f
 for Berlin, Germany, 210f
 for Boise, Idaho, 196f
 for Brisbane, Australia, 259f
 for Broome, Australia, 257f
 for Buenos Aires, Argentina, 259f
 for Cairns, Australia, 252f
 for Cairo, Egypt, 255f
 for Calgary, Canada, 197f
 for Cape Town, South Africa, 261f
 for Caribou, Maine, 214f
 for Cedar City, Utah, 196f
 for Christchurch, New Zealand, 262f
 for Cold Bay, Alaska, 218f
 for Colombo, Sri Lanka, 244f
 for Columbus, Ohio, 212f
 for Dallas, Texas, 126, 126f
 for Dar es Salaam, Tanzania, 250f
 for Darwin, Australia, 251f

water balance diagrams (*continued*)

- for Des Moines, Iowa, 212*f*
 - for Dhaka, Bangladesh, 247*f*
 - for Doha, Qatar, 255*f*
 - for Duluth, Minnesota, 213*f*
 - for Elkins, West Virginia, 215*f*
 - for Erie, Pennsylvania, 213*f*
 - for Fairbanks, Alaska, 220*f*
 - for Faro, Portugal, 207*f*
 - for Hami, China, 192*f*
 - for Hilo, Hawaii, 243*f*
 - for Hong Kong, China, 202*f*
 - for Juba, Sudan, 250*f*
 - for Kotzebue, Alaska, 219*f*
 - for Las Vegas, Nevada, 191*f*
 - for Little Rock, Arkansas, 199*f*
 - for Long Beach, California, 205*f*
 - for Lubbock, Texas, 195*f*
 - for Lusaka, Zambia, 260*f*
 - for Manaus, Brazil, 245*f*
 - for Manchester, England, 209*f*
 - for Manila, Philippines, 247*f*
 - for Mexico City, Mexico, 266*f*
 - for Miami, Florida, 249*f*
 - for Minsk, Belarus, 215*f*
 - for Mogadishu, Somalia, 257*f*
 - for Moosonee, Canada, 221*f*
 - for Moscow, Russia, 216*f*
 - for Mumbai, India, 249*f*
 - for Murmansk, Russia, 219*f*
 - for New Delhi, India, 203*f*
 - for Ottawa, Canada, 214*f*
 - for Perth, Australia, 260*f*
 - for Phoenix, Arizona, 191*f*
 - for Pretoria, South Africa, 263*f*
 - for Quito, Ecuador, 266*f*
 - for Raleigh-Durham, North Carolina, 200*f*
 - for Rapid City, South Dakota, 197*f*
 - for Reykjavik, Iceland, 210*f*
 - for Richmond, Virginia, 200*f*
 - for Rome, Italy, 206*f*
 - for Sacramento, California, 205*f*
 - for Santa Maria, California, 206*f*
 - for Santiago, Chile, 261*f*
 - for Seattle, Washington, 208*f*
 - for Singapore, Singapore, 243*f*
 - for Tashkent, Uzbekistan, 198*f*
 - for Tegucigalpa, Honduras, 248*f*
 - for Thule Air Force Base, Greenland, 223*f*
 - for Tokyo, Japan, 201*f*
 - for Tucson, Arizona, 194*f*
 - for Tura, Russia, 221*f*
 - for Vladivostok, Russia, 217*f*
 - for Yellowknife, Canada, 220*f*
- water vapor
- continentiality and, 33
 - deposition of, 73
 - faint young Sun paradox and, 17
 - as greenhouse gas, 302–303
 - riming, 265
 - sublimation of, 74
 - as variable gas, 15, 16, 16*t*

- Watertown, New York, continentality in, 33
- wavelengths, 19, 19*f*, 80, 143, 302*t*, 303.
See also radiation
- for Sun and Earth, 19*f*
- waviness of upper-level airflow, 142
- weather
- accuracy of forecasting, 41
 - data collection, 9
 - definition of, 4
 - forecasting, 5
 - models, 335
 - normals, 5
 - regionalization of, 158
 - sphere, 18
 - stations, 41
 - west-coast occlusions, 209
- Weather Research and Forecasting (WRF) model, 327
- weather sphere. *See* troposphere
- Weddell Sea, 241
- west African monsoon system, 253
- West Antarctic Ice Sheet, 75, 280, 281*f*
- western-boundary intensification, 57, 57*f*
- wet bulb depression, 113
- wet deposition, 319
- wetted perimeter, 118
- whiteouts, 241
- Willmott, Cort, 112
- wilting point, 122
- wind-chill factor, 264
- winds
- Antarctic, 240–241
 - atmosphere stability and, 102–103
 - backing, 42
 - Beaufort scale for, 359, 360*t*
 - belts of, 6
 - bora, 224
 - centrifugal acceleration and, 40
 - channeling, 224, 233
 - effect, 308–309
 - Chinook, 183
 - in climate control, 36–41
 - Coriolis effect and, 38–40
 - data, 359
 - definition of, 36
 - Föhn, 186
 - friction and, 40–41
 - general circulation, 132–153
 - geostrophic, 43, 204
 - Harmattan, 233
 - katabatic, 224, 264
 - katabatic. *See* katabatic winds
 - latent heat flux, 81
 - mistral, 224
 - mountain effects on, 183
 - northeast trade, 61
 - ocean currents and, 46
 - oroshi, 224
 - planetary boundary layer and
 - direction of, 81, 82*f*
 - planetary systems of, 134–137, 136*f*, 137*f*
 - precipitation measurement and, 118

- pressure and generation of, 34–36
 - pressure gradient force and, 37–38, 38*f*
 - prevailing, 34
 - secondary circulations, 132–153
 - shears
 - shearing stress and, 81
 - transverse, 144, 144*f*
 - vertical, 103
 - solar, 12
 - southeast trade, 61
 - surface systems of, 134–135
 - surface vs. upper-level, 41
 - trade, 60, 61
 - upper-level, 135–137, 136*f*
 - in urban canyons, 308–309, 309*f*
 - veering of, 42
- windward areas
- continentality in, 33
 - precipitation in, 46
 - Sierra Nevada Mountains, 183
- windward side in Tropical Rain Forest climates, 245
- winter solstice, 31, 82
- Wisconsin Glacial Phase, 74, 241, 280, 285, 297, 303, 311
- within-group variability, 158, 176
- WMO. *See* World Meteorological Organization
- World Climate Research Programme, 359
- World Data Center for Paleoclimatology, 359
- World Meteorological Organization (WMO), 356, 367

X

- xenon, 15

Y

- Yarnal, Brent, 7
- “Year without a Summer” (1816), 282, 294
- Yellowknife, Canada
- climograph for, 220*f*
 - water balance diagram for, 220*f*
- Yellowstone National Park, 294
- Yosemite Valley, formation of, 280
- Younger Dryas, 281, 282

Z

- zenith angle, 83, 83*f*
- zonal flow, 142, 142*f*, 144*f*, 145
- Pacific-North American pattern and, 342
 - transverse wind shears, 144*f*, 145
 - vorticity in, 144*f*, 145
- zone mean time, 86
- zooplankton, 264